Geological Survey of Canada
Commission géologique du Canada

PAPER
ÉTUDE 84-1A

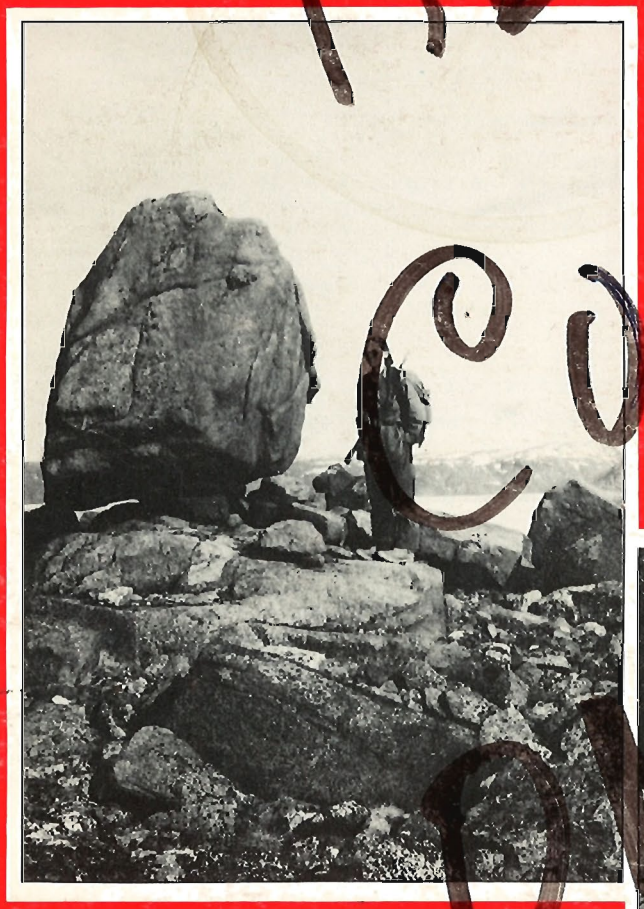

CURRENT RESEARCH

RECHERCHES EN COURS

PART A
PARTIE

1984

Canada

GEOLOGICAL SURVEY
PAPER 84-1A

COMMISSION GÉOLOGIQUE
ÉTUDE 84-1A

CURRENT RESEARCH
PART A

RECHERCHES EN COURS
PARTIE A

1984

Available in Canada through

authorized bookstore agents
and other bookstores

or by mail from

Canadian Government Publishing Centre
Supply and Services Canada
Ottawa, Ontario, Canada K1A 0S9

and from

Geological Survey of Canada
601 Booth Street
Ottawa, Canada K1A 0E8

A deposit copy of this publication is also available
for reference in public libraries across Canada

Cat. No. M44-84/1AE Canada: $15.00
ISBN 0-660-11531-X Other countries: $18.00

Price subject to change without notice

Cover

Left: Perched erratic boulder near Cape Herschel, Ellesmere Island, N.W.T. (GSC 203670-U)

Right: Conducting experimental induced polarization measurements in the GSCs 300 metre test borehole at Bells Corners near Ottawa. (GSC 203575-P)

Geological Survey of Canada – *Commission géologique du Canada*

R.A. PRICE
Director General
Directeur général

J.G. FYLES
Chief Geologist
Géologue en chef

M.J. KEEN
Director, Atlantic Geoscience Centre, Dartmouth, Nova Scotia
Directeur du Centre géoscientifique de l'Atlantique, Dartmouth (Nouvelle-Écosse)

J.A. MAXWELL
Director, Central Laboratories and Technical Services Division
Directeur de la Division des laboratoires centraux et des services techniques

R.G. BLACKADAR
Director, Geological Information Division
Directeur de la Division de l'information géologique

W.W. NASSICHUK
Director, Institute of Sedimentary and Petroleum Geology, Calgary, Alberta
Directeur de l'Institut de géologie sédimentaire et pétrolière, Calgary (Alberta)

J.C. McGLYNN
Director, Precambrian Geology Division
Directeur de la Division de la géologie du Précambrien

A.G. DARNLEY
Director, Resource Geophysics and Geochemistry Division
Directeur de la Division de la géophysique et de la géochimie appliquées

J.S. SCOTT
Director, Terrain Sciences Division
Directeur de la Division de la science des terrains

D.C. FINDLAY
Director, Economic Geology Division
Directeur de la Division de la géologie économique

R.B. CAMPBELL
Director, Cordilleran Geology Division, Vancouver, British Columbia
Directeur de la Division de la géologie de la Cordillère, Vancouver (Colombie-Britannique)

Separates

A limited number of separates of the papers that appear in this volume are available by direct request to the individual authors. The addresses of the Geological Survey of Canada offices follow:

601 Booth Street,
OTTAWA, Ontario
K1A 0E8

Institute of Sedimentary and Petroleum Geology,
3303-33rd Street N.W.,
CALGARY, Alberta
T2L 2A7

Cordilleran Geology Division
100 West Pender Street,
VANCOUVER, B.C.
V6B 1R8

Atlantic Geoscience Centre,
Bedford Institute of Oceanography,
P.O. Box 1006,
DARTMOUTH, N.S.
B2Y 4A2

When no location accompanies an author's name in the title of a paper, the Ottawa address should be used.

Tirés à part

On peut obtenir un nombre limité de "tirés à part" des articles qui paraissent dans cette publication en s'adressant directement à chaque auteur. Les adresses des différents bureaux de la Commission géologique du Canada sont les suivantes:

601, rue Booth
OTTAWA, Ontario
K1A 0E8

Institut de géologie sédimentaire et pétrolière
3303-33rd, St. N.W.,
CALGARY, Alberta
T2L 2A7

Division de la géologie de la Cordillère
100 West Pender Street
VANCOUVER, Colombie-Britannique
V6B 1R8

Centre géoscientifique de l'Atlantique
Institut océanographique de Bedford
B.P. 1006
DARTMOUTH, Nouvelle-Écosse
B2Y 4A2

Lorsque l'adresse de l'auteur ne figure pas sous le titre d'un document, on doit alors utiliser l'adresse d'Ottawa.

SCIENTIFIC AND TECHNICAL REPORTS
RAPPORTS SCIENTIFIQUES ET TECHNIQUES

ECONOMIC GEOLOGY/GÉOLOGIE ÉCONOMIQUE

GEOCHEMISTRY/GÉOCHIMIE

GEOMATHEMATICS/GÉOMATHÉMATIQUES

GEOPHYSICS/GÉOPHYSIQUE

MARINE GEOSCIENCE/ÉTUDES GÉOSCIENTIFIQUES DU MILIEU MARIN

MINERALOGY/MINÉRALOGIE

PALEONTOLOGY/PALÉONTOLOGIE

PETROLOGY/PÉTROLOGIE

QUATERNARY GEOLOGY/GÉOLOGIE DU QUATERNAIRE

Inventory Mapping and Stratigraphic Studies/Inventaire cartographique et stratigraphique

Paleoecology and Geochronology/Paléoécologie et géochronologie

Sedimentology and Geomorphology/Sédimentologie et géomorphologie

REGIONAL GEOLOGY/GÉOLOGIE RÉGIONALE

Appalachian Region/Région des Appalaches

Cordilleran Region/Région de la Cordillère

Precambrian Shield/Bouclier précambrien

Stratigraphy/Stratigraphie

SCIENTIFIC AND TECHNICAL NOTES
NOTES SCIENTIFIQUES ET TECHNIQUES

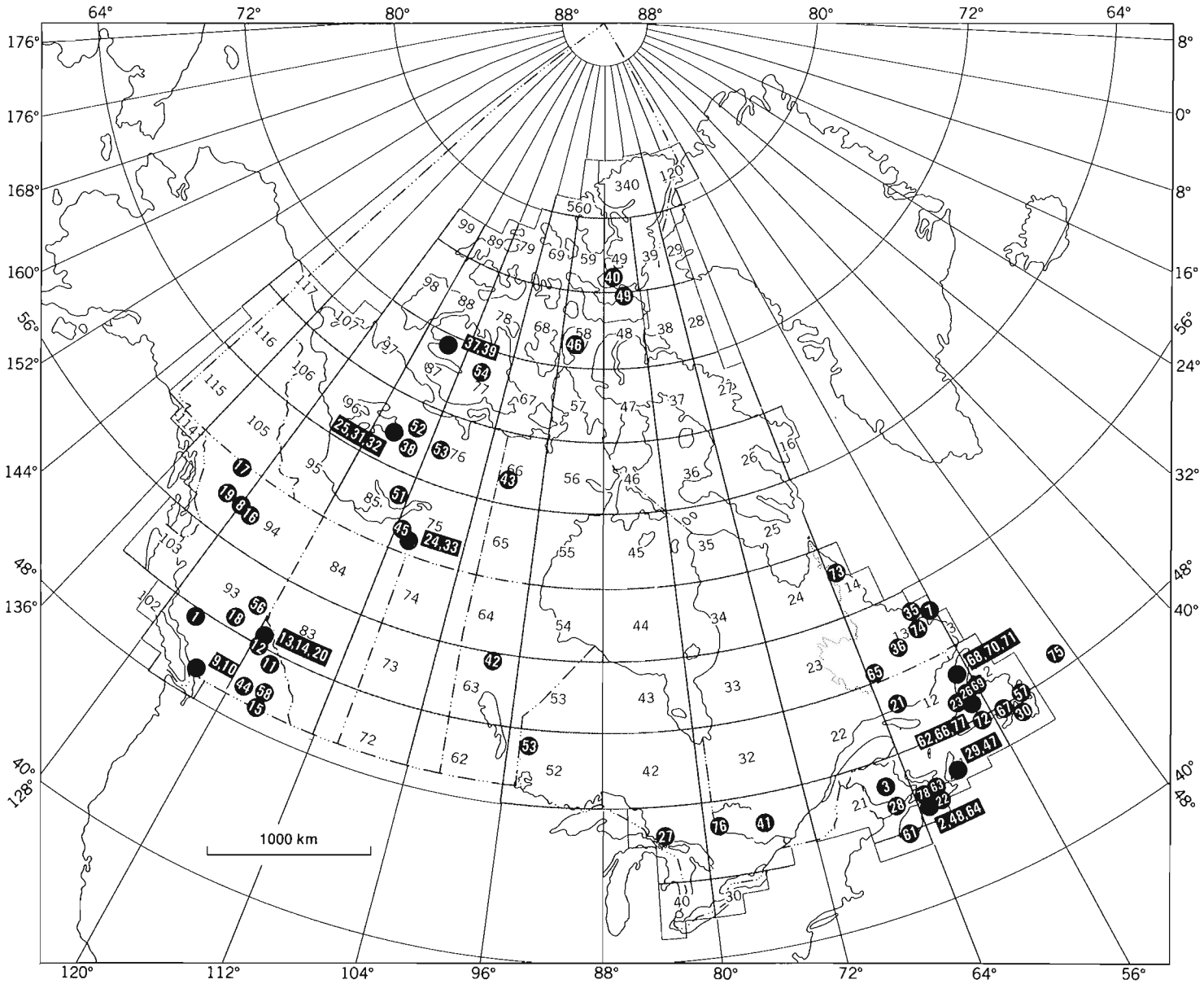

Numbers on index map refer to Scientific and Technical Reports in this volume

1. THE ILGACHUZ RANGE, A PERALKALINE SHIELD VOLCANO IN CENTRAL BRITISH COLUMBIA

Project 770001

J.G. Souther
Cordilleran Geology Division, Vancouver

Souther, J.G., The Ilgachuz Range, a peralkaline shield volcano in central British Columbia; in Current Research, Part A, Geological Survey of Canada, Paper 84-1A, p. 1-10, 1984.

Abstract

The Ilgachuz Range is one of three moderately dissected, late Tertiary shield volcanoes in the east-trending Anahim Volcanic Belt of central British Columbia. It is the product of two pulses of magmatic activity: an early dome and shield-forming stage which culminated in the collapse of a central caldera, and a late-stage effusion of basalt which formed the outer part of the shield. The pile is chemically bimodal, with a pronounced SiO_2 and alkali gap separating oversaturated, peralkaline rocks of the early stage from hawaiite of the late stage. Five new K-Ar dates from the Ilgachuz confirm the progressive decrease in the age of volcanic centres eastward along the Anahim Belt, and support the concept of an easterly migrating hotspot.

Résumé

Le chaînon Ilgachuz est un de trois volcans-boucliers modérément érodés du Tertiaire récent sis dans la zone volcanique d'Anahim à orientation est du centre de la Colombie-Britannique. Il résulte de deux impulsions d'activité magmatique: une phase ancienne de formation du dôme et du bouclier que vient terminer l'effondrement d'une caldera centrale et une effusion récente de basalte, roche dont se compose la partie extérieure du bouclier. L'amas est chimiquement bimodal, avec une lacune prononcée de SiO_2 et d'alcalis qui sépare des roches hyperalcalines sursaturées de la phase ancienne de l'hawaiite produite au cours de la phase récente. Cinq nouvelles dates au K-Ar provenant du chaînon Ilgachuz confirment le rajeunissement progressif des centres volcaniques vers l'est le long de la zone d'Anahim et appuient l'hypothèse selon laquelle un point chaud se déplace vers l'est.

INTRODUCTION

The Ilgachuz Range is one of three moderately dissected, alkaline to peralkaline shield volcanoes that comprise the central part of the Anahim Volcanic Belt. This east-west belt of late Miocene to Recent volcanoes extends from the coast, near Bella Bella, across the Interior Plateau, to the Clearwater area in the Cariboo Highlands (Fig. 1.1). It was first interpreted as a manifestation of crustal flexuring above the northern edge of the downgoing Juan de Fuca plate (Stacey, 1974; Souther, 1977). Subsequent isotopic dating of eruptive centres along the Belt revealed an apparent systematic, easterly decrease in the onset of volcanism from west to east and lead to the concept of an easterly migrating mantle hotspot (Bevier et al., 1979; Rogers, 1981; Rogers and Souther, 1983). The western end of the Belt is defined by subvolcanic plutons (12-14 Ma) and the eastern end by the Clearwater lavas at 0.5 Ma (Hickson and Souther, in press). Activity along the Anahim Belt was thus coeval with eruption of the Chilcotin lavas in the Interior Plateau. Bevier (1983a) showed that these transitional flood basalts erupted from multiple centres along the northwesterly trending axis of the Plateau during two periods of eruptive activity – 2-3 Ma and 6-10 Ma. The Chilcotin lavas are interpreted to be the product of back-arc volcanism above the Juan de Fuca plate (Souther, 1977; Bevier, 1983b).

The present work was undertaken in an attempt to establish the relationship of the Anahim Belt to the surrounding Chilcotin lavas, and to examine in greater detail the geology and petrological history of one of the principal volcanoes in the Belt. This preliminary account is based on the first 12 days of field work in a continuing study.

ROCK CLASSIFICATION

The basalts and trachytes (agpaitic index <1) are classified according to Irvine and Baragar (1971), see Figure 1.2. Oversaturated, peralkaline rocks (A.I. >1), which comprise a major part of the Ilgachuz pile are more difficult to classify. The two most commonly used schemes are normative Q vs Σ normative femics (Macdonald and Bailey, 1973), and Al_2O_3 vs FeO (Macdonald, 1974). Both of these schemes divide the quartz-normative peralkaline rocks into two rhyolitic classes (comendites and pantellerites) and two trachytic classes (comenditic trachyte and pantelleritic trachyte). Most rocks plot in the same field of both diagrams but there are enough exceptions to lead to confusion. Using the normative classification only two of the analyzed Ilgachuz specimens fall within the trachytic class whereas seven specimens from the same suite plot within the trachytic fields of the Al_2O_3 vs FeO diagram (Fig. 1.2). Names used in the following description are based on the normative classification but, as discussed later, the Al_2O_3 vs FeO scheme is probably a better discriminant for the older, more altered rocks.

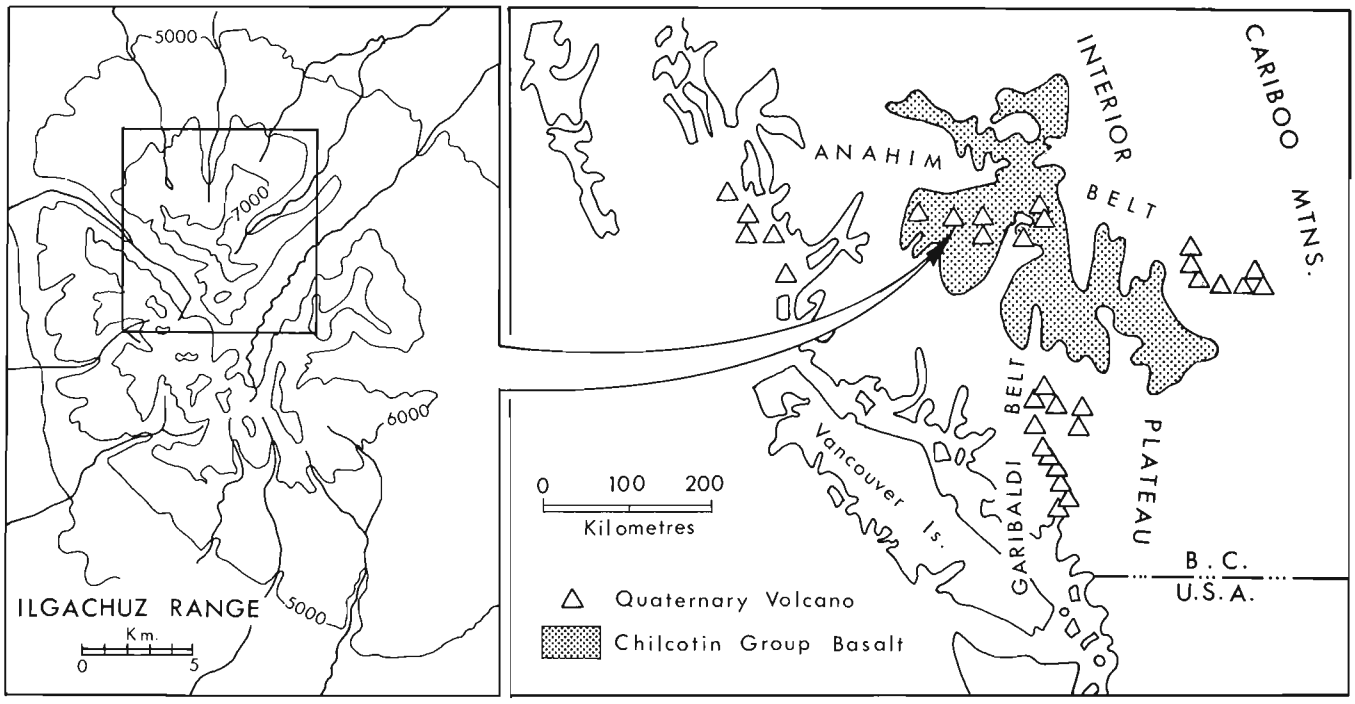

Figure 1.1. *Index map showing the relationship of the Ilgachuz Range to the Anahim Volcanic Belt, and the location of the geological map (Fig. 1.3) within the Range.*

GENERAL GEOLOGY

The Ilgachuz pile has been subdivided into six igneous assemblages (Fig. 1.3), each of which includes intrusive and extrusive phases. The assemblages are distinguished on the basis of their morphology and age relative to construction of the shield and subsequent collapse and filling of a central caldera. Each assemblage may include rocks of several lithologies.

PRECALDERA ASSEMBLAGE

Unit 1

Hydrothermally altered, pale yellow, ochre and red-weathering trachyte and rhyolite flows, breccia and associated intrusions are exposed along the lower slopes of Blue Canyon and Carnlick creeks, and in the south fork of Tanswanket Creek where the assemblage is at least 450 m thick. The internal structure lacks any apparent organization. Discontinuous flow and dome segments are interspersed with chaotic breccia, most of which appears to have been formed by random, post-eruptive fracturing. Primary pyroclastic deposits may also be present but the entire assemblage has been so intensely disturbed and altered that few primary features can be recognized. The eruptive rocks are cut by a profusion of large and small dykes and cupolas that have weathered out to form hoodoo-like ribs and spires, around which hydrothermal alteration is most intense.

Where fractures are widely spaced the intervening rock is relatively unaltered. It is microporphyritic with about 10% phenocrysts of euhedral alkali feldspar from 1 to 3 mm across, sparse phenocrysts of ferrohedenbergite up to 1 mm across and rare, 1-mm granules of opaque oxide. The groundmass consists of a holocrystalline mosaic of stubby alkali feldspar euhedra, interstitial aenigmatite, acmitic pyroxene and arfvedsonite, and a trace of finely disseminated opaque minerals. In some thin sections the aenigmatite and opaque minerals have been altered to hydrous iron-oxide.

The three analyzed specimens from this unit plot in the comenditic trachyte field of the Al_2O_3 vs FeO diagram. This classification is preferred for this unit because iron and aluminum are less affected than the alkalies by post-eruptive alteration.

The Precaldera assemblage is overlain locally by trachyte and rhyolite of the Early Dome-forming Assemblage (units 2 and 3) and, over a wider area, by Ilgachuz comendite (unit 4).

EARLY DOME-FORMING ASSEMBLAGE

This assemblage includes two units: the Blue Canyon rhyolite (unit 2), and the Rich Creek rhyolite (unit 3).

Blue Canyon rhyolite

The Blue Canyon rhyolite is exposed on the ridge between Blue Canyon and Carnlick creeks where it includes three cooling units with a composite thickness of about 150 metres. Each cooling unit rests on about a metre of porphyritic, granular obsidian. Above this relatively thin basal selvage the rock is uniformly massive, commonly with well developed, thick (>1 m) columns. A vertical plug of similar rhyolite cuts through the centre of the pile and is believed to be one of the principal feeders. The lateral extent of the cooling units is not known. Their absence on the north side of Blue Canyon Creek suggests that they formed only small domes or very thick, stubby flows that piled up around a central vent.

Thin sections of Blue Canyon rhyolite show no alteration. Euhedral phenocrysts of alkali feldspar up to 4 mm across form about 15% of the rock. Euhedral ferrohedenbergite crystals are commonly less than 1 mm across and comprise about 5% of the phenocrysts. The groundmass of the holocrystalline rhyolite is a felted intergrowth of very fine alkali feldspar laths, interstitial quartz, and poikilitic acmitic pyroxene, aenigmatite and

minor arfvedsonite. The basal obsidians contain a similar phenocryst population enclosed by a completely vitreous matrix with perlitic cracks.

Rich Creek rhyolite

More than 180 m of light grey to white, white-weathering rhyolite are exposed in upper Rich Creek. The base is a layer of massive obsidian several metres thick. Above this, complexly contorted flow layering grades up into a flaggy rock with pronounced planar flow layering, and finally into massive, slightly feldspar-phyric, pale grey rhyolite in the central and upper part of the pile. The exposures in Rich Creek appear to be part of a single dome at least 2.5 km across. A smaller area of rhyolite exposed in South Tanswanket Creek may be part of the same body.

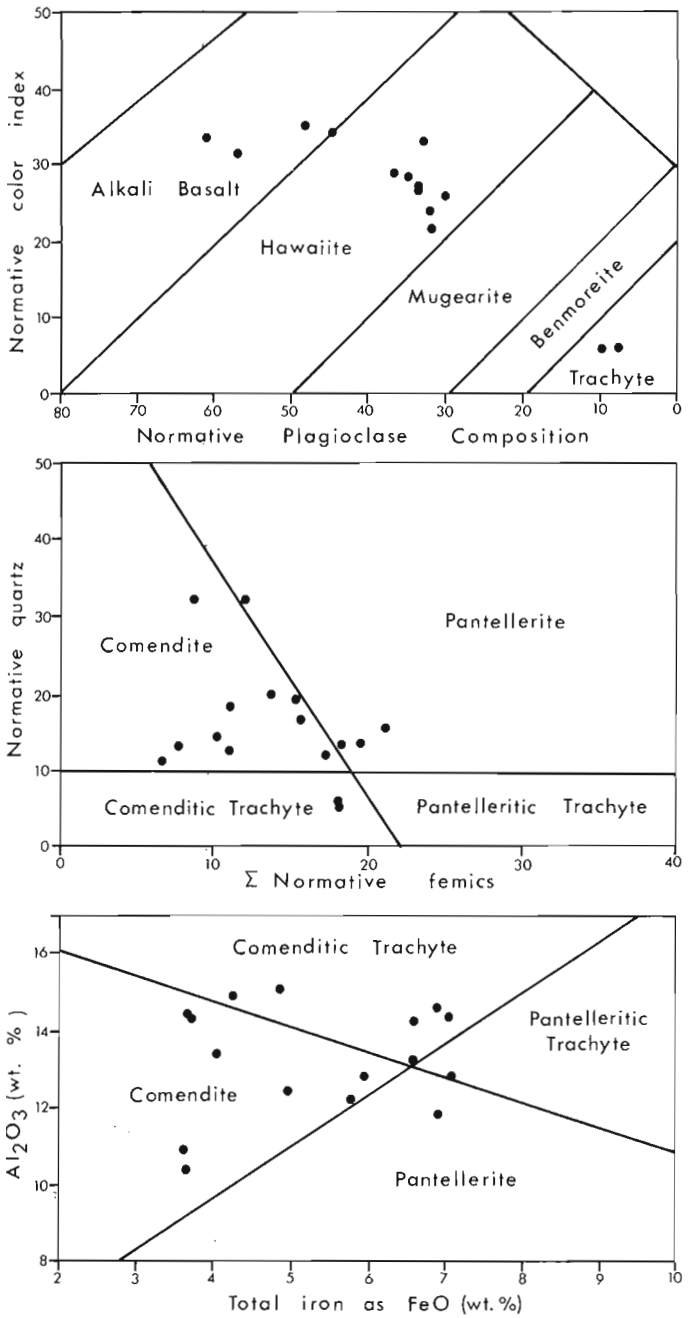

Figure 1.2. *Plot of 30 analyzed Ilgachuz specimens on discriminant diagrams used for classification. Normative Colour Index vs Normative Plagioclase Composition (after Irvine and Baragar, 1971); Normative Quartz vs Σ normative femics (after Macdonald and Bailey, 1973); Al_2O_3 vs FeO (after Macdonald, 1974).*

In thin section the holocrystalline rhyolite is microporphyritic, with sparse phenocrysts of rounded, subhedral alkali feldspar (~1 mm), in a fine grained groundmass of sutured alkali feldspars, locally in myrmekitic intergrowth with quartz. Interstitial acmitic pyroxene, arfvedsonite and a trace of aenigmatite together form less than 2% of the rock. The basal obsidian contains rare, rounded phenocrysts of alkali feldspar up to 1 mm across and acicular microlites, the largest of which are pale green, probably sodic pyroxene.

Both the Blue Canyon rhyolite and Rick Creek rhyolite are overlain disconformably by the Ilgachuz comendite (unit 4).

LATE DOME-FORMING ASSEMBLAGE

Ilgachuz comendite

The Ilgachuz comendite (unit 4) is the most voluminous single map unit in the northern Ilgachuz Range. It comprises scores of overlapping domes, flows, minor pyroclastic breccia, dykes, plugs and cupolas. Individual cooling units range from about 15 m to more than 300 m thick, and the largest unit can be traced for 3 km along South Tanswanket valley. The base commonly comprises a layer of white to pale green ash, porous lapilli, and autobreccia. This unconsolidated layer is overlain by a few metres of glassy flow breccia in which clasts of trachyte have been sintered into a vitroclastic rock with prominent eutaxitic texture. This grades up into green, massive to flaggy, feldspar-phyric comedite which forms the bulk of each cooling unit. The upper surface of most domes and flows is covered with a few metres of porous, pale green flow-top breccia.

Dykes and small cupolas of relatively unaltered green comendite cutting the Precaldera assemblage (unit 1) are believed to be minor intrusive equivalents of the Ilgachuz comendite but no major feeders were discovered.

The Ilgachuz comendite contains from 10 to 25% alkali feldspar phenocrysts in euhedral crystals up to 3 mm across and from 1 to 2% microphenocrysts of euhedral ferrohedenbergite. Rare microphenocrysts of fayalitic olivine are present in some thin sections. They are commonly surrounded by, or in clusters with microphenocrysts of arfvedsonite and aenigmatite (Fig. 1.4a). The groundmass is a holocrystalline mosaic of stout alkali feldspar euhedra, interstitial quartz, and poikilitic arfvedsonite, aenigmatite, acmitic pyroxene, and sparse, finely disseminated opaque oxides.

INTRACALDERA ASSEMBLAGE (UNITS 5, 6, 7)

The three units that comprise this assemblage occupy a caldera, part of which is exposed in the southern part of the mapped area, near the centre of the Ilgachuz Range. The depression in which these units were deposited was at least 2.6 km across and may have been much larger. Its northern boundary truncates the Precaldera and Late Dome-forming assemblages and is overlapped by Postcaldera, Blue Canyon basalt (unit 11). The Intracaldera rocks and younger units of the Early Shield-forming Assemblage are not in contact and their relative age is unknown.

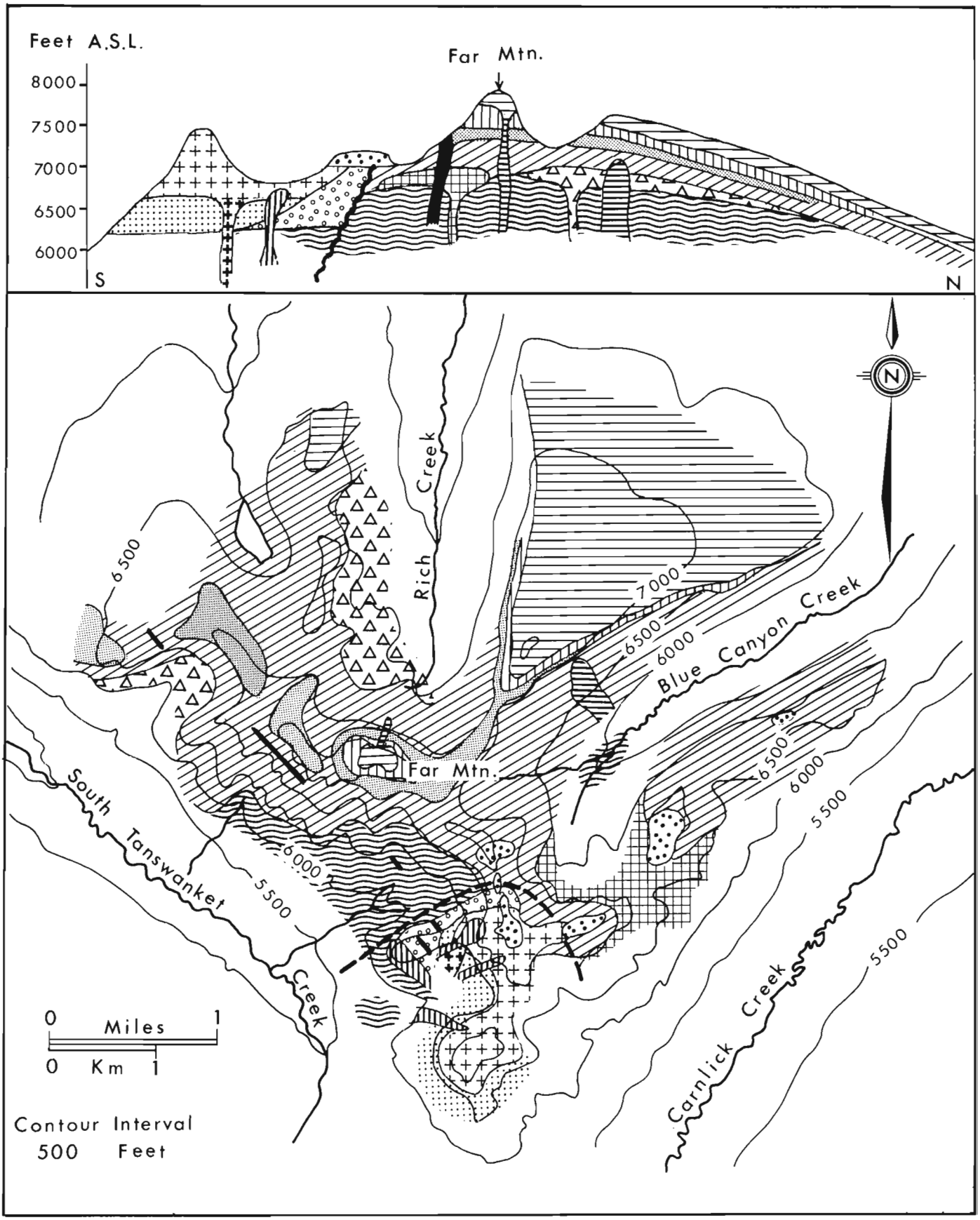
Feet A.S.L.
8000
7500
7000
6500
6000
S
N
Far Mtn.
Rich Creek
Blue Canyon Creek
South Tanswanket Creek
Carnlick Creek
Far Mtn.
6500
7000
6000
5500
0 Miles 1
0 Km 1
Contour Interval
500 Feet

Unit 5

Epiclastic boulder and block deposits form a crudely bedded, steeply south-dipping succession at least 100 m thick along the northern margin of the caldera. The unit laps against truncated flows of the Precaldera and Late Dome-forming assemblages and dips under units 6 and 7 which fill the central part of the caldera depression. It comprises a chaotic, clast-supported and largely unsorted jumble of angular to subrounded comendite and minor basalt clasts. Most of the clasts are less than a metre across but some are as large as three metres.

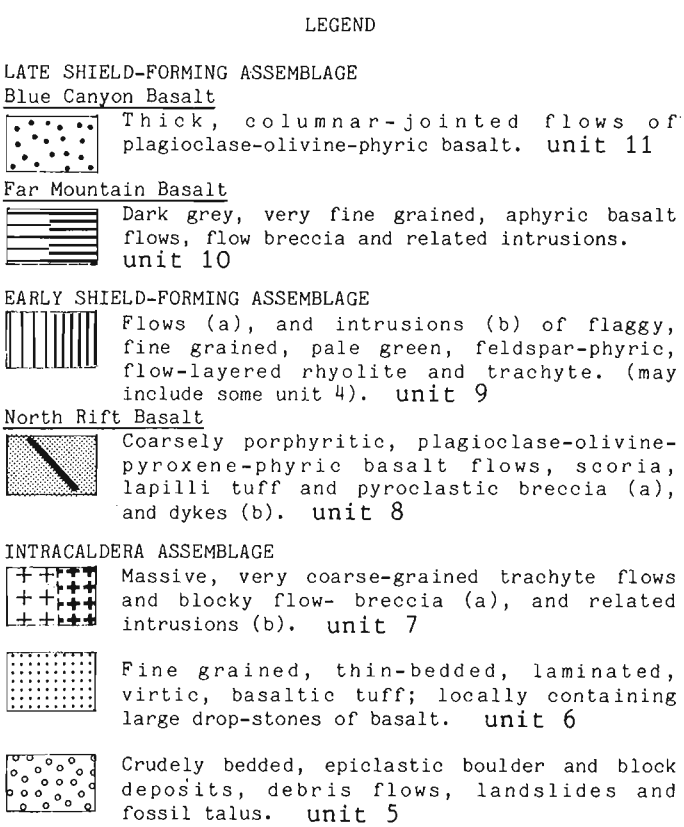

Figure 1.3. *Generalized geological map of the northern Ilgachuz Range and schematic cross-section showing the relative positions of the map units projected onto a north-south plane through Far Mountain.*

Unit 6

Thin bedded, dark grey to black, finely laminated vitric tuff forms a nearly flat-lying succession at least 150 m thick in the central part of the caldera. Its northern edge laps out against the wedge of epiclastic fill (unit 5) and near this contact the fine grained tuff beds contain a few subrounded dropstones of basalt (Fig. 1.5) and comendite up 0.6 m across. Bedding features in the tuff are best seen on weathered surfaces. They resemble the rhythmic light and dark layers of siltstone in a turbidite succession. Normal and reverse grading, minor crossbedding and slump structures are present in various parts of the succession.

In thin section the tuff is seen to comprise about 95% shards of pale yellow, completely vitreous glass, and 5% or less broken feldspar crystals (Fig. 1.4b). Rare lithic grains are from peralkaline trachyte. The shards in most sections have sharp cusps and show no alteration or abrasion, except for slightly rounded grains in some beds. Most of the tuffs are clast supported or have a matrix of very fine, closely packed vitric debris surrounding the larger shards.

The vitric tuff is overlain conformably by trachyte of unit 7.

Unit 7

Coarsely porphyritic trachyte forms the uppermost unit within the caldera (unit 7a). It comprises a single massive cooling unit, probably a ponded flow, at least 240 m thick. The lower 60 to 90 m are coarse autobreccia made up of subrounded clasts (up to 2 m across) of porphyritic trachyte in a granular aggregate of comminuted debris ground from the larger fragments. The autobreccia rests directly on the underlying tuff (unit 6) without an intervening quenched selvage or pyroclastic layer. The top of the breccia grades, within a few metres, to massive trachyte with the same coarsely porphyritic texture as the breccia fragments and a widely spaced, vertical joint set forms sheer cliffs extending to the top of the flow.

A large intrusive mass of this characteristic rock (unit 7b) is exposed near the northern edge of the caldera and probably represents one of the principal conduits. The rock is texturally identical to the flow but has massive, subhorizontal columnar jointing and extends down through the underlying tuff, 120 m below the basal autobreccia. Its nearly vertical northern contact with the underlying bedded tuff is well exposed. The tuff is bleached almost white for about half a metre adjacent to the contact but no quenched selvage formed on the trachyte.

Thin sections show that the trachyte is a nearly pure feldspar rock (Fig. 1.4c). Euhedral alkali feldspar phenocrysts, up to 1 cm across, comprise about 50% of the rock and the holocrystalline, very fine grained groundmass consists almost entirely of stout, closely packed alkali feldspar euhedra. Pale green calcic pyroxene (salite) and an opaque oxide are present as minor phenocryst and groundmass phases. Relatively large apatite crystals are commonly associated with the opaque phenocrysts.

Unit 8 is overlain conformably by remnants of Blue Canyon basalt (unit 11).

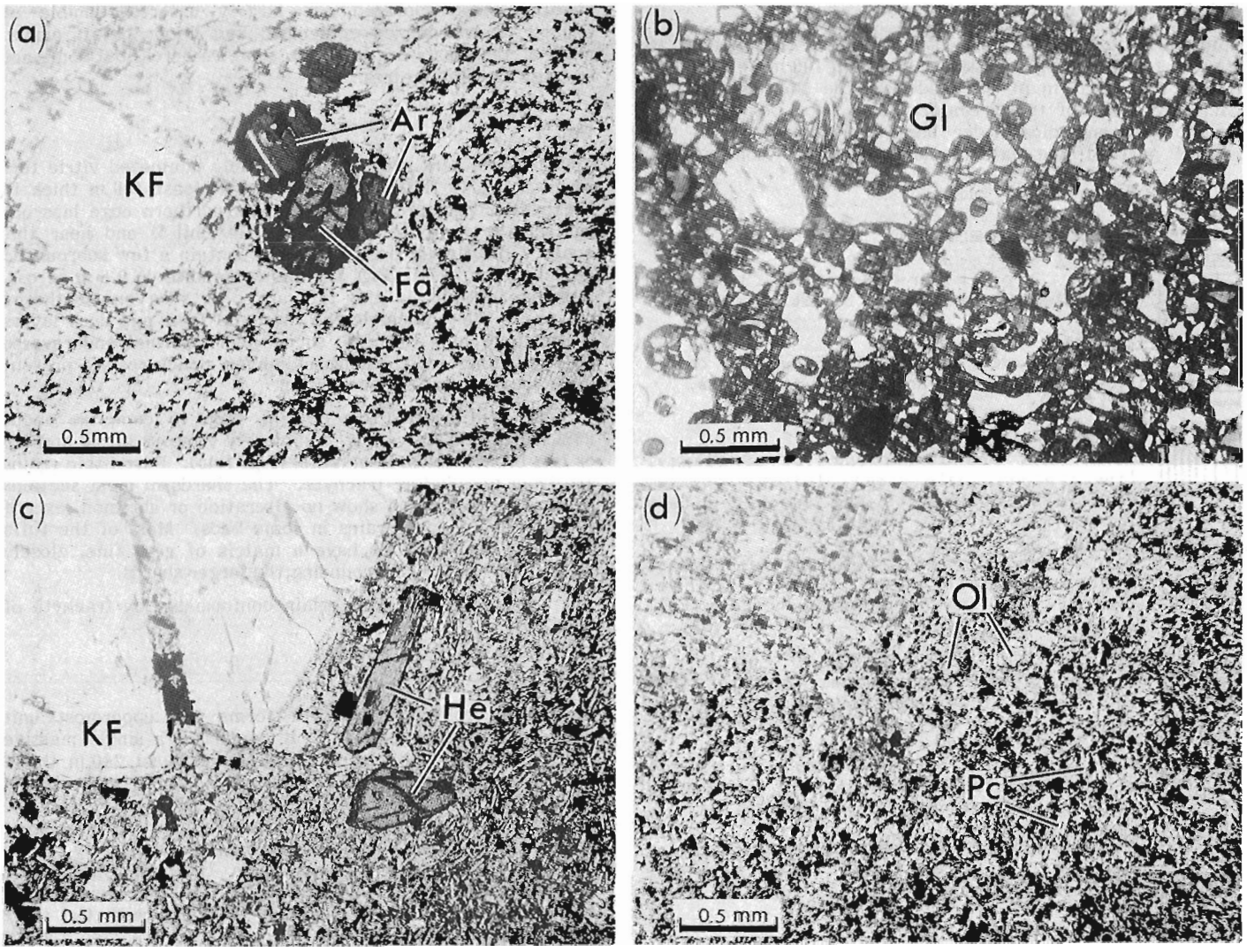

Figure 1.4. *Photomicrographs: (a) porphyritic comendite, unit 4; (b) vitric tuff, unit 6; (c) porphyritic trachyte, unit 7; (d) aphyric hawaiite, unit 10. (Gl-glass, Pc-plagioclase, KF-alkali feldspar, ol-olivine, Fa-fayalite, He-hedenbergite, Ar-arfvedsonite)*

Figure 1.5

Large dropstone of basalt suspended in finely laminated vitric tuff of unit 6.

Figure 1.6

View south across a portion of the North Rift dyke. Flat-topped mountain in background is a remnant of the intracaldera assemblage comprising a massive cap of porphyritic trachyte (unit 7) resting on vitric tuff (unit 6).

EARLY SHIELD-FORMING ASSEMBLAGE (UNITS 8, 9, 10)

The three units that comprise this assemblage are confined to the middle and outer portion of the shield and, with the possible exception of unit 9, they issued from vents that lie well outside the central caldera. The source of the comendite flows on Far Mountain (unit 9a) is not known but they are lithologically similar to, and occupy approximately the same chronological position, as a group of cupolas (unit 9b) that intrude the Intracaldera rocks. The cupolas and flows of unit 9 are tentatively correlated on this basis.

North Rift basalt (unit 8)

Coarsely porphyritic, plagioclase-pyroxene-olivine-phyric basalt forms a nearly flat-lying horizon through the lower part of Far Mountain and prominent, cliff-bounded, flow-remnants on the adjacent plateau. It rests disconformably on an irregular surface of Ilgachuz trachyte (unit 4) and, on Far Mountain, it is overlain conformably by comendite of unit 7. On the west side of Far Mountain the base of the unit is a 30 m layer of gently north-dipping agglutinated basaltic lapilli, bombs and spatter. This is overlain by a series of thin (~1 m) flows interlayered with red, oxidized, proximal scoria. The distal flows on the plateau, which are up to 15 m thick, were probably fed by several coalescing streams of lava.

The principal source of the North Rift basalt is a large, northwesterly trending, vertical dyke which stands as a prominent rib along the slope west of Far Mountain (Fig. 1.6). It is 5 to 10 m thick and is continuously exposed for about 1 km. Discontinuous, thinner segments of this same dyke system define a zone at least 4 km long. The segment west of Far Mountain is exposed about 60 m vertically below the dissected remnants of large pyroclastic cones on the adjacent upper surface of the ridge. It must have been emplaced very close to the surface where reduced confining pressure allowed it to flare out to such a great thickness.

The North Rift basalt contains from 15 to 30% euhedral, complexly zoned plagioclase phenocrysts (~calcic andesine) up to 5 mm across. Olivine, titaniferous salite and opaque oxide phenocrysts together form less than 5% of the rock and are commonly less than 1 mm across. The groundmass is a holocrystalline mosaic of the same minerals plus relatively abundant apatite.

Unit 9

On Far Mountain the North Rift basalt is overlain by a 60 m comendite flow that is assigned to unit 9a. It rests on an unconsolidated, 2-m thick earthy layer of pale yellow ash and pumice. The base of the flow is massive, granular obsidian which grades up through a 3-m welded, vitroclastic layer into flaggy, pale green, feldspar-phyric comendite. Similar, but much more coarsely porphyritic comendite occupies the same stratigraphic position on the flatiron between Rich and Blue Canyon creeks. The largest flow in that section has giant (2.5 m) columns that extend the full 58 m thickness of the flows.

Tabular and irregular cupolas, up to half a kilometre long and numerous smaller dykes and plugs of platy green comendite (unit 9b) intrude the western part of the Intracaldera assemblage. Their selvages are vitreous and, for 1 or 2 m adjacent to contacts, the rock is crowded with deformed, lenticular cognate and accidental clasts which give it a prominent eutaxitic fabric. The interior of the larger bodies is commonly flaggy and has complex columnar jointing. Glass-rimmed apophyses from some of the cupolas extend for several tens of metres into the roof rock and terminate as narrow wedges only a few centimetres across. The extrusive equivalent of these bodies is not known but the cupolas are clearly younger than the Intracaldera assemblage and they are petrographically similar to the shield-forming comendite (unit 9a) with which they are tentatively correlated.

Both intrusive and extrusive phases of unit 9 contain from 15 to 30% euhedral alkali-feldspar phenocrysts and about 2% ferrohedenbergite as small, dark green, euhedral prisms. The coarsely porphyritic, columnar flow between Rich and Blue Canyon creeks contains small, sparse phenocrysts of fayolite. The groundmass in all the sections examined is relatively rich in mafic minerals. It comprises small, interpenetrating crystals of alkali feldspar and both poikilitic and intergranular aenigmatite, arfvedsonite and acmitic pyroxene. No opaque oxide phase is present.

LATE SHIELD-FORMING ASSEMBLAGE (UNITS 10, 11)

This assemblage includes two petrographically distinct basalt units which issued from separate vents after collapse and filling of the central caldera.

Far Mountain basalt (unit 10)

This unit is named for a basalt succession erupted from a vent near the summit of Far Mountain where fine grained, aphyric flows, lightly agglutinated block, bomb and lapilli deposits and small plug domes form the upper 60 to 90 m of the mountain. The conduit system through which they were erupted is exposed on the north face where a sinuous, irregular dyke up to 5 m thick extends up through the underlying rocks and flares into a small plug dome near the summit.

Similar, fine grained, aphyric basalt flows and associated breccia form the upper part of the triangular interfluve between Rich and Blue Canyon creeks. There, the section is about 90 m thick and comprises a succession of light grey, randomly jointed, 2 to 3 m metre thick flows separated by thin layers of scoriaceous, flow-top breccia. A plug of identical aphyric basalt (unit 10b) is exposed in the upper part of Blue Canyon valley. It is probably a related subvolcanic intrusion and may be part of a conduit system that fed another vent.

In thin section the Far Mountain basalt is seen to contain sparse microphenocrysts (~0.2 mm) of subhedral olivine, plagioclase and opaque oxides. The extremely fine grained groundmass is a holocrystalline, intergranular mosaic of anhedral plagioclase, olivine, pyroxene and opaque oxides (Fig. 1.4d). A characteristic feature of these rocks is their uniformly fine grain size and abundance of opaque oxides (~15%) as a microphenocryst and groundmass phase.

Blue Canyon basalt (unit 11)

Remnants of thick, porphyritic basalt flows rest on an irregular erosion surface that cuts across the northern edge of the Intracaldera assemblage onto the adjacent Ilgachuz comendite. Individual cooling units are extremely variable in thickness and appear to have been ponded in depressions. They probably issued from multiple vents near the northern edge of the caldera but no related, proximal pyroclastic deposits were found. Two circular pillars of basalt, one 120 m high, on the ridge between Blue Canyon and Carnlick creeks resemble volcanic necks and may be one of the Blue Canyon basalt eruptive centres.

The Blue Canyon basalt contains about 10% tabular, euhedral phenocrysts of plagioclase up to 3 mm long and less than 2% olivine in small (~0.5 mm) subhedral grains. The groundmass is a holocrystalline mosaic of euhedral plagioclase laths, partly or wholly enclosed by ophitic plates of titaniferous salite, and intergranular olivine and opaque oxides.

CHEMISTRY

Thirty analyses of specimens from the northern Ilgachuz Range are plotted in Figures 1.2 and 1.7, and six representative analyses are listed in Table 1. The suite is strongly bimodal with respect to silica and alkalies, one group comprising mainly undersaturated basalts and the other comprising oversaturated, mostly peralkaline rhyolites and trachytes.

Analyses of basaltic flows and intrusions from units 8, 10, and 11 form a fairly tight cluster in the alkaline field of the alkali-silica diagram (Fig. 1.7) whereas the vitric, basaltic tuff of unit 6 plots in the subalkaline field. This shift is probably due to alkali loss from the very fine grained, glassy tephra during and after its eruption. Almost all of the basalts are nephaline normative hawaiites. The single alkali-olivine basalt specimen is from the base of a thick flow that contains cumulus olivine.

Analyses of the oversaturated rocks (units 1, 2, 3, 4, 7, 9) plot in a small field that straddles the alkaline-subalkaline boundary of the alkali-silica diagram (Fig. 1.7). With the exception of two analyses of trachyte from unit 7, all of these rocks are mildly peralkaline (A.I. 1.1 to 1.4). The composition of the unit 7 trachyte (A.I. ~ 0.9) confirms the petrographic observation that it is a nearly pure alkali feldspar rock.

AGE AND CORRELATION

The eruptive sequence in the Ilgachuz is similar to that in the adjacent Rainbow and Itcha Ranges (Bevier, 1981; Stout and Nicholls, 1983) where the early eruption of oversaturated peralkaline lavas was followed by the effusion of hawaiite. Bevier et al. (1979) reported four K-Ar ages (6.7 to 8.7 Ma) from the Rainbow Range and three (0.8 to 3.2 Ma) from the Itcha Range. Five new dates from the Ilgachuz Range (Table 1.2) have been determined at the University of British Columbia (Armstrong, internal GSC report 64-7926, 1983), two from the Ilgachuz comendite (4.9 ± 0.2 and 5.0 ± 0.2 Ma) and three from the North Rift basalt (5.4 ± 0.2, 5.5 ± 0.2, 5.6 ± 0.2 Ma). This material was

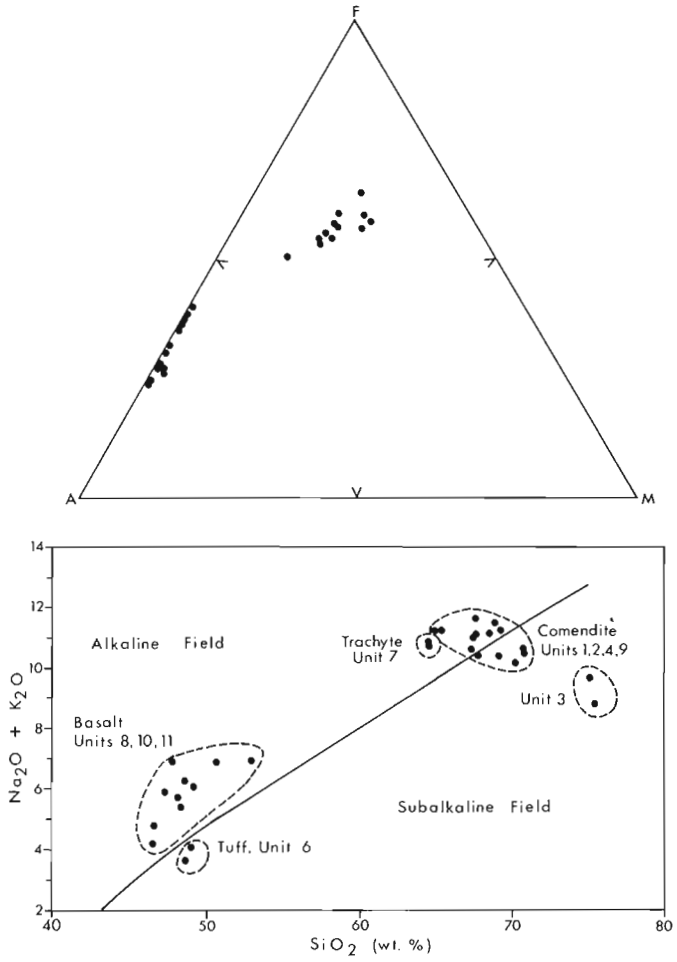

Figure 1.7. Alkalies vs SiO_2 and A-F-M plots of 30 analyses from the northern Ilgachuz Range. Note strongly bimodal distribution.

Table 1.1. Representative major element analyses from the northern Ilgachuz Range

	Hawaiite		Trachyte		Comendite	
	Ilg 26	Ilg 28	Ilg 15	Ilg 16	Ilg 8	Ilg 10
SiO_2	47.48	47.75	64.06	63.62	70.69	69.17
Al_2O_3	16.07	17.60	16.77	16.93	13.41	12.09
Fe_2O_3	5.29	4.29	2.39	2.94	2.14	3.30
FeO	7.74	8.60	2.01	1.29	2.15	2.72
CaO	6.51	6.39	1.96	1.94	0.46	0.54
MgO	4.25	3.84	0.25	0.32	0.20	0.50
Na_2O	4.30	4.86	6.08	5.93	5.63	5.26
K_2O	1.81	2.03	4.75	4.69	5.08	4.81
TiO_2	3.12	2.95	0.58	0.55	0.28	0.03
P_2O_5	0.76	1.00	0.16	0.15	0.02	0.03
MnO	0.21	0.28	0.16	0.11	0.12	0.21
H_2O	2.26	0.51	1.52	2.18	0.78	1.60
Total	99.80	100.06	100.69	100.65	100.78	100.17

(XRF analyses by Chemex Labs Ltd., Vancouver, B.C.)

Table 1.2. Whole rock K-Ar dates from the Ilgachuz Range

Sample	Map Unit	%K	Ar 10^{-6} cc/g	$\%Ar^{40}$	Date Ma
SE250581	4	4.08	0.791	77.4	5.0 ± 0.2
SE2507a81	4	4.12	0.784	80.3	4.9 ± 0.2
SE250381	8	1.30	0.272	55.8	5.4 ± 0.2
SE250481	8	0.84	0.1815	60.3	5.5 ± 0.2
SE2511a81	8	0.96	0.2086	43.4	5.6 ± 0.2

(Age determinations by R.L. Armstrong, University of British Columbia)

collected in 1981, before detailed mapping had established the stratigraphy, and thus is not representative of the entire Ilgachuz succession. However, the close agreement of dates from the precaldera Ilgachuz comendite and the postcaldera North Rift basalt suggests that a large part of the Ilgachuz pile erupted in a relatively short time span, probably no longer than the 1.5 Ma duration of the Rainbow Range eruptive cycle (Bevier, 1981). The Ilgachuz dates are also intermediate between those from the Rainbow and Itcha ranges, providing further evidence for progressive, eastward development of volcanic centres along the Anahim Belt.

DISCUSSION

Construction of the Ilgachuz shield volcano began with the eruption of a large volume of peralkaline rhyolite and trachyte from a cluster of vents near the centre of the range. This first phase of activity culminated with the collapse of a central caldera in which a lake formed prior to the resumption of volcanic activity. The first major eruption following caldera collapse produced about 2 km^3 of vitric, basaltic tephra, probably from a vent within the caldera lake. Soon after the tephra was deposited a massive effusion of coarsely porphyritic trachyte issued from vents within the caldera, filling the remaining depression with a single, thick, ponded flow.

Filling of the caldera was followed by a period of alternating, relatively small eruptions of basalt and rhyolite, and finally by the effusion of a large volume of hawaiite which forms the outer flanks of the shield. Although hawaiite is petrologically the most primitive rock it is clearly the product of a second pulse of magma that could not be parental to the oversaturated rocks in the lower part of the shield.

Oversaturated peralkaline magma is commonly considered to be the product of extensive fractionation of feldspar from moderately alkaline basalt in crustal reservoirs. If this is the origin of peralkaline rocks in the Rainbow, Ilgachuz and Itcha ranges then what was the source of the parent basalt and why did it accumulate in reservoirs along the Anahim Belt? The parent magma may have been comagmatic with alkali basalt of the Chilcotin Group but no peralkaline, or even oversaturated derivatives are associated with Chilcotin eruptive centres elsewhere in the Interior Plateau. The central Anahim belt is clearly related to a deep structure that favoured the accumulation of basaltic magma in large crustal reservoirs. Whether the controlling structure was initiated by the transect of a mantle hotspot (Bevier et al., 1979), by flexuring of the crust over the edge of a subducting plate (Stacey, 1974), or the opening of an incipient zone of extension in response to larger plate motions remains an open question.

The five new K-Ar dates from the Ilgachuz Range are in agreement with the hotspot model but more dates are needed to establish the onset and duration of the magmatic cycle in the Ilgachuz and in the other shields of the Anahim Belt. The chronology of magmatic events along this anomalous volcanic belt through central British Columbia has major implications that must be considered in any model of Late Tertiary tectonic events in the Cordillera.

ACKNOWLEDGMENTS

The writer wishes to thank M.E.K. Souther for assistance in the field.

REFERENCES

Bevier, M.L.
1981: The Rainbow Range, British Columbia: A Miocene peralkaline shield volcano; Journal of Volcanology and Geothermal Research, v. 11, p. 225-251.

1983a: Regional stratigraphy and age of Chilcotin Group basalts, south-central British Columbia; Canadian Journal of Earth Sciences, v. 20, p. 515-524.

1983b: Implications of chemical and isotopic composition for petrogenesis of Chilcotin Group basalts, British Columbia; Journal of Petrology, v. 24, p. 207-226.

Bevier, M.L., Armstrong, R.L., and Souther, J.G.
1979: Miocene peralkaline volcanism in west-central British Columbia – its temporal and plate-tectonics setting; Geology, v. 7, p. 389-392.

Hickson, C.J. and Souther, J.G.
– Late Cenozoic volcanic rocks of the Clearwater-Wells Gray area, British Columbia; Canadian Journal of Earth Sciences. (in press)

Irvine, T.N. and Baragar, W.R.A.
1971: A guide to the chemical classification of the common volcanic rocks; Canadian Journal of Earth Sciences, v. 8, p. 523-548.

Macdonald, R.
1974: Nomenclature and petrochemistry of the peralkaline oversaturated extrusive rocks; Bulletin Volcanologique, v. 38, p. 1-19.

Macdonald, R. and Bailey, D.K.
1973: The chemistry of the peralkaline oversaturated obsidians; United States Geological Survey, Professional Paper 440-N-1, p. 1-37.

Rogers, G.C.
1981: McNaughton Lake seismicity – more evidence for an Anahim hotspot?; Canadian Journal of Earth Sciences, v. 18, p. 826-828.

Rogers, G.C. and Souther, J.G.
1983: Hotspots trace plate movements; Geos, v. 12, p. 10-13.

Souther, J.G.
1977: Volcanism and tectonic environments in the Canadian Cordillera – a second look; in Volcanic Regimes in Canada, ed. W.R.A. Barager, L.C. Coleman, and J.M. Hall; Geological Association of Canada, Special Paper 16, p. 3-24.

Stacey, R.A.
1974: Plate tectonics, volcanism and lithosphere in British Columbia; Nature, v. 250, p. 133-134.

Stout, M.Z. and Nicholls, J.
1983: Origin of the hawaiites from the Itcha Mountain Range, British Columbia; Canadian Mineralogist, v. 21, p. 575-581.

2. COMPOSITION, RANK AND DEPTH OF BURIAL OF TWO NOVA SCOTIA LIGNITE DEPOSITS

Project 680103

P.A. Hacquebard,
Atlantic Geoscience Centre, Dartmouth

Hacquebard, P.A., Composition, rank and depth of burial of two Nova Scotia lignite deposits; in Current Research, Part A, Geological Survey of Canada, Paper 84-1A, p. 11-15, 1984.

Abstract

Borehole intersections of the 2.60 m thick occurrence at Dickie Brook (in Musquodoboit Valley) and the 0.48 m thick deposit at Diogenes Brook (in Central Cape Breton Island) have been logged in detail, and a total of nine interval samples have been examined for proximate chemical analyses, equilibrium moisture content and calorific values. On the "as-received-basis" the moisture and ash contents of the samples varied from 5.02-10.13%, and 8.67-49.85% respectively, while the calorific values ranged from 4862-9951 Btu/lb. However, the equilibrium or "bed" moisture contents are much higher, namely 30.13 and 34.79% for the seam totals, with corresponding "moist, mineral-matter free" calorific values of 8080 and 8303 Btu/lb. This places the coals in the category of lignite "A", according to the A.S.T.M. classification. This rank assignment is supported by the vitrinite reflectance data on five samples, which showed a variation of 0.25-0.33% Ro.

Depth of burial calculations, based on previously established correlations of bed moisture and overburden of German and Alberta lignites and subbituminous coals, gave the following results. For the "clean coal" portion of the Dickie Brook deposit: 762 m; for the Diogenes Brook lignite: 779 m. These figures are supported by the present depth of similar (0.3% Ro) lignite deposits on the Scotian Shelf, which occur at 700-1000 m below the surface. For these deposits the present depth and the maximum amount of burial are regarded as approximately the same.

Résumé

Les intersections des trous de sonde dans la venue du ruisseau Dickie (dans la vallée de la rivière Musquodoboit), dont l'épaisseur est de 2,6 m, et dans le dépôt du ruisseau Diogenes (dans la partie centrale de l'île du Cap-Breton), d'une épaisseur de 0,48 m, ont été enregistrées en détail et neuf échantillons ont été étudiés afin d'en déterminer la composition chimique approximative, la teneur en humidité d'équilibre et les valeurs calorifiques. Les teneurs en humidité et en cendre des échantillons varient respectivement de 5,2 à 10,13 % et de 8,67 à 49,85 %, tandis que les valeurs calorifiques varient de 4 862 à 9 951 Btu/lb. Toutefois, la teneur en humidité d'équilibre totale pour tous les filons est beaucoup plus élevée, soit de 30,13 % et de 34,79 %, tandis que les valeurs calorifiques "humides, sans matières minérales atteignent 8 080 et 8 303 Btu/lb. Ces chiffres indiquent que les charbons appartiennent à la catégorie lignite <<A>>, selon la classification ASTM. La valeur du pouvoir réflecteur de la vitrinite, calculée pour cinq échantillons et variant de 0,25 à 0,33 % Ro, confirme cette classification.

Le calcul de la profondeur d'enfouissement, fondé sur des corrélations déjà établies entre l'humidité du lit et l'épaisseur de la couverture pour les lignites et les charbons subbitumineux allemands et albertains, a donné les résultats suivants: pour la partie de <<charbon épuré>> du gisement du ruisseau Dickie, 762 m; pour la lignite du gisement du ruisseau Diogenes, 779 m. Ces chiffres sont corroborés par la profondeur actuelle, soit entre 700 et 1 000 m sous la surface, des gisements semblables (0,3 % Ro) de lignite du plateau continental de Scotian. Il semble que la profondeur actuelle et la profondeur maximale d'enfouissement sont équivalentes dans le cas de ces gisements.

INTRODUCTION

The presence of Mesozoic lignite in Nova Scotia was first reported in 1959 when material from a clay pit near Shubenacadie was examined for spores and pollen by Hacquebard and Barss (see Stevenson, 1959, p. 35). Subsequent palynological studies indicated an early Cretaceous age and thus proved the existence of Mesozoic sediments in the onshore region of Nova Scotia, several years before they were discovered in the offshore area.

In more recent times the Nova Scotia Department of Mines and Energy has initiated a program to search for additional Mesozoic deposits in the Province and to examine in greater detail those known already. As a result, drilling was carried out on two lignite deposits, one in the Musquodoboit Valley and the other in central Cape Breton Island. From these boreholes the cores were submitted to the author by Mr. John Fowler for detailed logging and coal quality evaluations of the lignite intersections. This report gives the results of this investigation.

LOCATIONS, SEAM SECTIONS AND SAMPLING DATA

Tables 2.1 and 2.2 give the pertinent information regarding the lignite occurrences at Dickie Brook near Middle Musquodoboit, and Diogenes Brook in the vicinity of Whycocomagh. The areal extent of the lignite deposits has not been determined, but in the Musquodoboit Valley the associated clay outcrops for at least 10 km along the river (Stevenson, 1959).

The Dickie Brook intersection is quite substantial and consists of a 2.60 m thick seam that is underlain by a thin (0.25 m thick) bench coal, which occurs 1.10 m below it. The Diogenes Brook intersection is only 0.48 m thick.

COAL COMPOSITION AND RANK

Proximate chemical analyses, as well as calorific values and equilibrium moisture determinations on the nine interval samples from the two boreholes were carried out by the Fuel Research Laboratories of CANMET, partially in Sydney and partially in Ottawa. This work was undertaken through the

Table 2.1. Section and sampling record

Seam: Lignite Depth: 103.20 m
Logged by: P.A. Hacquebard
AGC Dartmouth, N.S.

Borehole: Dickie Bk. #1
Musquodoboit Valley
Nova Scotia

Date: December 7, 1982

Location: 45°04'07"N; 63°06'21"W

Total height (cm)	Interval (cm)	Megascopic description of seam intervals	Samples	
			No.	Thickness (cm)
		Roof: ?		
38	38	Lignite, black, fairly soft, breaks easy	A1	38
60	22	Lignite, dense with conchoidal fracture, very hard	A2	22
63	3	Pyrite nodule (B)		
150	87	Lignite, as in A1, splits easily on bedding plane	C1 C2	44 43
215	65	Lignite, more dense and compact than A1; has more clay associated with it.	D1	65
218	3	Pyrite nodule		
228	10	Lignite, dense, etc. as in A2	D2	10
260	32	Lignite, friable, as in A1	E	32
370	110	Mudstone, carbonaceous (organic), black becoming more silty towards the bottom		
395	25	Lignite, friable, as in A1	F	25
		Pavement: Mudstone, black, silty, grading into grey clay at 470 cm.		

Table 2.2. Section and sampling record

Seam: Lignite Depth: 115.40 m
Logged by: P.A. Hacquebard
AGC Dartmouth, N.S.

Borehole: Diogenes Bk. #1
Cape Breton Is.,
Nova Scotia

Date: December 7, 1982

Location: 45°52.67'N; 61°18.35'W

Total height (cm)	Interval (cm)	Megascopic description of seam intervals	Samples	
			No.	Thickness (cm)
		Roof: ?		
48	48	Clay, dark grey lignite, brownish black, crumbly, not as compact as the Dickie Bk. material, and not as black	1	48
		Pavement: Silt, light grey, followed by white marl		

Table 2.3. Analytical data on two Nova Scotia lignites

Sample No.	Interval thickness cm	- As received basis - Moist.	Ash	Vol. matter	Fixed carbon	Sulphur	Btu/lb	Equil. moist.	Ro max.	Max. burial from equil. moist. in m
DICKIE BROOK, BH. no. 1 (Musquodoboit Valley); lignite at 103.2 m										
A1	38	6.25	47.57	23.91	22.27	1.85	4862	24.69	-	-
A2	22	10.09	8.67	37.18	44.06	2.71	9951	38.90	0.27	-
C1	44	9.29	14.11	34.09	42.51	2.58	9395	34.19	0.29	-
C2	43	9.08	19.94	31.69	39.29	2.17	8620	34.42		-
D1	65	6.51	46.34	23.61	23.54	1.18	5359	27.85	-	-
D2	10	10.13	15.81	35.02	39.04	2.77	9039	36.32	0.33	-
E	32	5.02	49.85	20.49	24.64	3.65	5250	22.12	-	-
F	25	8.22	25.16	30.45	36.17	4.54	8240	29.84	0.30	-
Seam Total	279	7.73	31.83	28.18	32.26	2.41	7170	30.13	0.29	927
Clean coal (A2+C1+ C2+D2)	119	9.43	15.35	33.87	41.35	2.47	9187	35.32	0.30	762
DIOGENES BROOK, BH. no. 1 (Cape Breton Is.); lignite at 115.4 m										
One	48	9.03	20.43	31.14	39.40	9.01	8676	34.79	0.25	779

good offices of Mr. Gary Bonnell of the CANMET laboratory in Sydney. In addition, vitrinite reflectance measurements on five samples were done at the Coal Petrology Laboratory of the Atlantic Geoscience Centre in Dartmouth by Mr. M.P. Avery. The results are shown in Table 2.3.

The Dickie Brook occurrence shows considerable variation in ash content, and although the entire seam averages 31.83%, it is possible to recognize a 1.19 m thick portion of "clean coal" that has only 15.35% ash. The sulphur contents average 2.41 and 2.47%, respectively, and are due largely to the presence of pyrite, of which several large nodules were noted (see Table 2.1).

The apparently high calorific values of this coal, namely 7170 Btu/lb. for the seam total and 9187 Btu/lb. for the "clean coal" portion are due to the dried-out nature of the borehole samples. When considered with their capacity (or equilibrium) moisture contents, the calorific values become reduced to 5430 and 6561 Btu/lb. respectively. This compares with "bed-moisture" Btu values (on as-received-basis) of 5000 for the Onakawana lignite of Northern Ontario, and 6000-7400 for the Saskatchewan lignites.

The Diogenes Brook lignite is very similar in composition, only the sulphur content is extraordinarily high. This is most likely due to the presence of a "local" sulphur nodule in the core, which was not identified separately, as was done in the Dickie Brook section.

In low rank coals the A.S.T.M. classification uses the calorific value as the classifying factor. The respective Btu values, when calculated to the moist mineral-matter free basis are as follows[1]: (1) For the Dickie Brook samples, 8303 for the seam total, and 7888 for the "clean coal" portion; (2) 8080 for the Diogenes Brook material. These calorific values classify the coals as Lignite A, because they possess less than 8300 Btu/lb. (MMMF), which is the upper limit set by the A.S.T.M. for this group. The average reflectance of 0.30% Ro supports this rank assignment.

DEPTH OF BURIAL CALCULATIONS

The coalification process is caused by the actions of pressure, heat and duration of heat. During the early stages of diagenesis it is mainly pressure that advances the degree of coalification. The pressure, caused by the weight (and thickness) of the original overburden causes a loss of moisture content, until the rank of bituminous coal is reached. On the basis of a series of German data, Hacquebard (1977) found that an asymptotic relationship exists between "bed" (or equilibrium) moisture content and depth of burial. This relationship is shown in Figure 2.1, in linear fashion because the bed moisture is plotted in logarithmic scale. The German data have recently been augmented by moisture determinations on subbituminous coals of Alberta by Nurkowski (in press), and the resultant correlation is shown in Figure 2.2. As can be seen, some differences exist between the two curves in the actual correlation of the moisture content and the depth of burial, i.e. in Figure 2.1 a moisture content of 20% correlates with 1500 m of overburden, whereas in Figure 2.2 it correlates with approximately 1400 m. Otherwise, the same relationship is represented; it has been expressed by Nurkowski in the following formula:

$$DOB = \frac{1.865 - \log.MEQ}{0.00046}$$

in which DOB = maximum depth of coal burial; and MEQ = equilibrium moisture content.

[1] Refers to coal containing the original bed moisture (or equilibrium moisture) content, but devoid of mineral matter; the m-m free Btu values, therefore, have been converted from "as received" moisture to "equilibrium" moisture content.

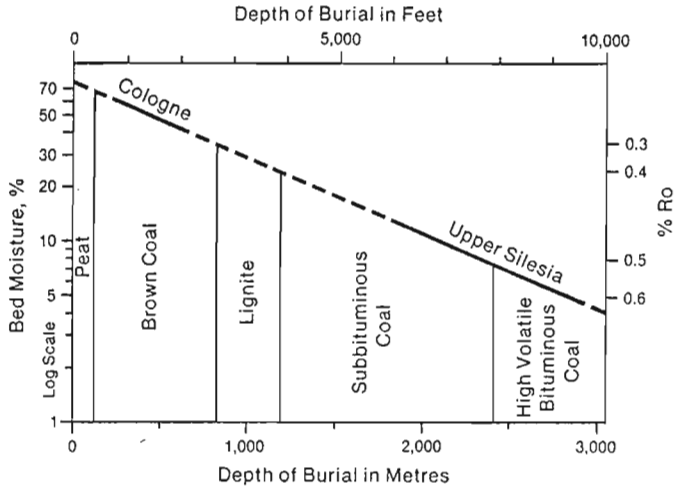

Figure 2.1. *Relationship of moisture content in coal versus original depth to burial (from Hacquebard, 1977).*

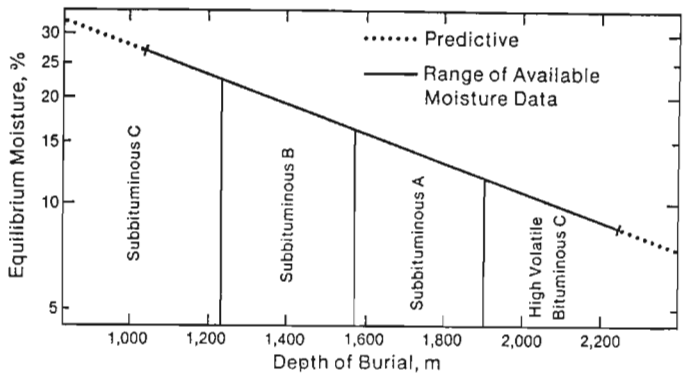

Figure 2.2. *Modification of Hacquebard's (1977) diagram, including the coal ranks as found in the plains of Alberta (Nurkowski, in press).*

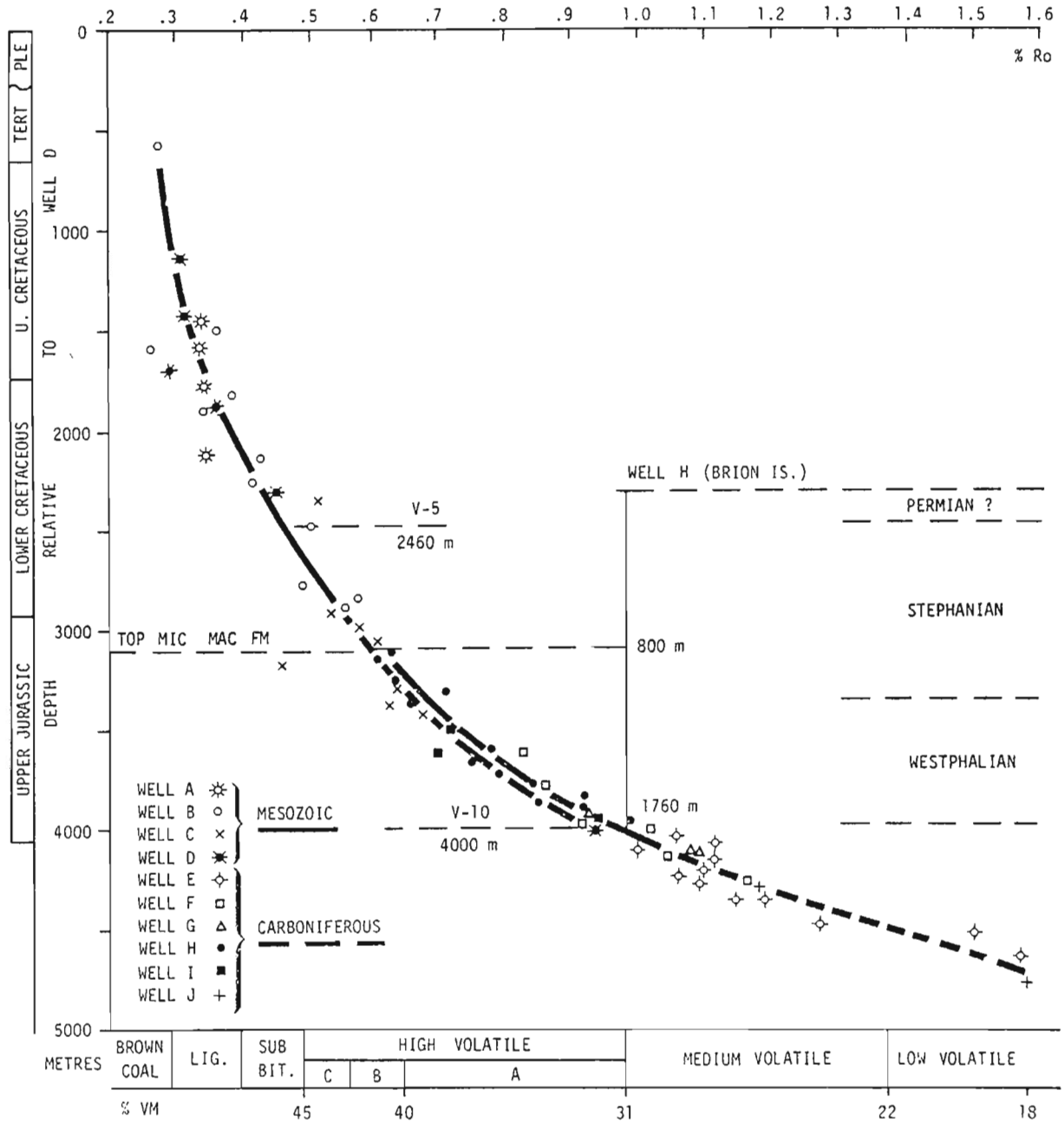

Figure 2.3. *Composite coalification curve of Mesozoic and Carboniferous coal sequences in Maritime region (after Hacquebard, 1975).*

With the aid of this formula the following depth of burial data have been obtained for the Nova Scotia lignites. For Dickie Brook's "seam total": 927 m and for the "clean coal" portion 762 m; while the Diogenes Brook lignite gave a depth of 779 m. The lower figures are preferred, because they refer to lower ash coals and relate more to the coaly substance itself. Therefore, an average depth of burial of 770 m is assumed for the two lignite occurrences referred to.

This figure seems to be reasonable when compared with rank-depth correlations represented by Mesozoic sediments in the offshore region. On the Scotian Shelf a vitrinite reflectance of 0.3% Ro occurs at a depth of between 700 and 1000 m (Fig. 2.3). As there has been but little or no erosion of these sediments, the present depth compares closely to the original depth of burial.

In low rank coals, such as discussed here, the Ro values give only approximate depths, because the rate of change in reflectance is very gradual; but once past 0.6% Ro it increases rapidly and then becomes a more accurate depth indicator. Equilibrium moisture, on the other hand, is immediately affected by the pressure of the overburden and therefore is the most sensitive parameter in low rank coals.

REFERENCES

Hacquebard, P.A.

1975: Pre- and post-deformational coalification and its significance for oil and gas exploration; Centre Nationale Recherche Scientifique, Paris; Collogue International de "Pétrographie organique et potentiel pétrolier", p. 225-241.

1977: Rank of coal as an index of organic metamorphism for oil and gas in Alberta; Chapter 3 of "The origin and migration of petroleum in the Western Canadian Sedimentary Basin, Alberta"; Geological Survey of Canada, Bulletin 262, p. 11-22 and Appendices B and C on p. 119-121.

Nurkowski, J.R.

– Coal quality, coal rank variation and its relation to reconstructed overburden, Upper Cretaceous and Tertiary Plains coals, Alberta, Canada; Alberta Research Council. (in press)

Stevenson, I.M.

1959: Shubenacadie and Kennetcook map-areas, Colchester, Hants and Halifax Counties, Nova Scotia; Geological Survey of Canada, Memoir 302, 86 p.

3. GEOLOGICAL AND GEOTHERMAL EFFECTS ON COAL RANK VARIATIONS IN THE CARBONIFEROUS BASIN OF NEW BRUNSWICK[1]

Project 680102

P.A. Hacquebard and M.P. Avery
Atlantic Geoscience Centre, Dartmouth

Hacquebard, P.A. and Avery, M.P., Geological and geothermal effects on coal rank variations in the Carboniferous Basin of New Brunswick; in Current Research, Part A, Geological Survey of Canada, Paper 84-1A, p. 17-28, 1984.

Abstract

Vitrinite reflectance measurements on 162 coal occurrences within the Carboniferous Basin of New Brunswick form the data base of this investigation. The Ro isopleths, plotted relative to sea level, show a systematic pattern. This pattern, as interpreted by trend-surface analyses, indicates a progressive increase in rank from high volatile "C" bituminous coal in the east, to anthracite in the southwest. It is accompanied by the occurrence of progressively older formations in the same direction, but the rank increase to the level of anthracite cannot be related solely to greater depth of burial and corresponding higher geotemperatures.

The additional heat required for this rank was likely obtained through increased conductivity of the underlying pre-Carboniferous basement rocks. The nature of these rocks was deduced from the Bouguer gravity map, which shows that areas of low gravity, believed to denote igneous rocks, underlie areas of higher coal rank. The high heat flow in these rocks is attested by present day measurements, which in the vicinity of the anthracite occurrence reach the highest value recorded in the Maritime Provinces of Canada.

Other abnormal coalification patterns which occur in the Fredericton Graben are related to tectonism. These are revealed by unusually high birefringence and irregular coalification gradients.

Resume

Le calcul du pouvoir de réflecteur de la vitrinite dans 162 venues de charbon au sein du bassin carbonifère du Nouveau-Brunswick forme la base des données de la présente étude. Les isothermes Ro, tracés relativement au niveau de la mer, donnent une configuration systématique. Cette configuration, interprétée en termes d'analyses tendance-surface, indique qu'il y a accroissement progressif du rang, du charbon bitumineux de catégorie <<C>> à haute teneur en matières volatiles dans l'est, à l'anthracite dans le sud-ouest. En outre, l'âge des formations augmente progressivement dans la même direction; toutefois, l'accroissement du rang jusqu'au niveau de l'anthracite ne peut pas être relié uniquement à une plus grande profondeur d'enfouissement et à des températures géothermales correspondantes plus élevées.

La chaleur additionnelle requise pour atteindre ce rang résulte probablement de la conductivité accrue du socle précarbonifère sous-jacent. La carte des anomalies gravimétriques de Bouguer, qui permet de déduire la nature du socle rocheux, montre que les régions de faible gravité, phénomène susceptible d'indiquer la présence de roches ignées, reposent sous des régions de charbon de rang plus élevé. Des calculs récents montrent l'importance du flux thermique dans ces roches, et établissent qu'aux environs des venues d'anthracite, le flux thermique atteint sa plus haute valeur dans les provinces Maritimes du Canada.

D'autres configurations anormales de houillification trouvées dans le graben de Fredericton sont reliées aux phénomènes de tectonique. En effet, le taux de biréfringence exceptionnellement élevé et les gradients irréguliers de la houillification révèlent l'existence de ces configurations.

INTRODUCTION

This investigation is a follow-up to the New Brunswick coal rank study undertaken by Hacquebard and Donaldson in 1970. At that time only a limited number of samples were available from the large area covered with Carboniferous sediments, which comprises about 26 000 km^2. However, some broad regional trends in coalification became apparent, rather than simply a random rank distribution.

In 1977 a unique opportunity to enlarge on the previous study presented itself with the Carboniferous coal drilling project. This project involved 294 test holes, averaging 122 m in depth, drilled at more or less regular intervals of 8 km across the entire area (Fig. 3.1). It provided a substantial number of additional samples, and although the data base still averages only one sample per 160 km^2 of the Carboniferous cover, it has been possible to correlate the coalification pattern with the geological setting and the natural heat flow distribution of the Basin.

GEOLOGICAL SETTING

The Carboniferous Basin of New Brunswick comprises the Northern Pennsylvanian and Moncton basins, which are separated by the Kingston Uplift which brought Mississippian and older formations to the surface (Fig. 3.1). In both basins late Pennsylvanian platform rocks (Westphalian C to Stephanian age) constitute the final phase of nonmarine Carboniferous sedimentation (Hacquebard, 1972). They consist of red and grey fluvial and fluvial-lacustrine sediments, which contain a few thin isolated coal seams. The uniformity in lithostratigraphy of these sediments makes surface mapping rather difficult, but in general three megacyclothems seem to be represented (Van de Poll, 1970).

Systematic spore investigations carried out by Barss et al. (1963, 1967, 1979) have made it possible to recognize separate biostratigraphic units. Figure 3.2 shows the regional distribution of these units, of which four are identified in the cross-section of Figure 3.3.

[1] Presented at the Tenth International Congress of Carboniferous Stratigraphy and Geology, Madrid, Spain, September 13, 1983.

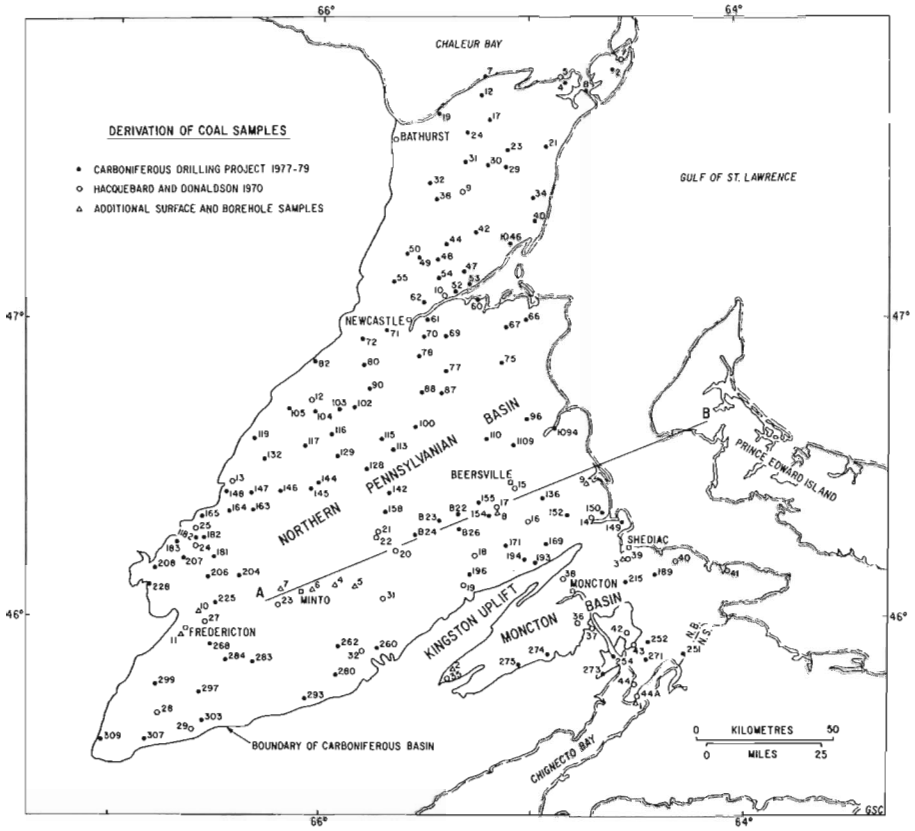

Figure 3.1

Carboniferous Basin of New Brunswick with locations of coal samples. Line A-B refers to cross-section shown in Figure 3.3.

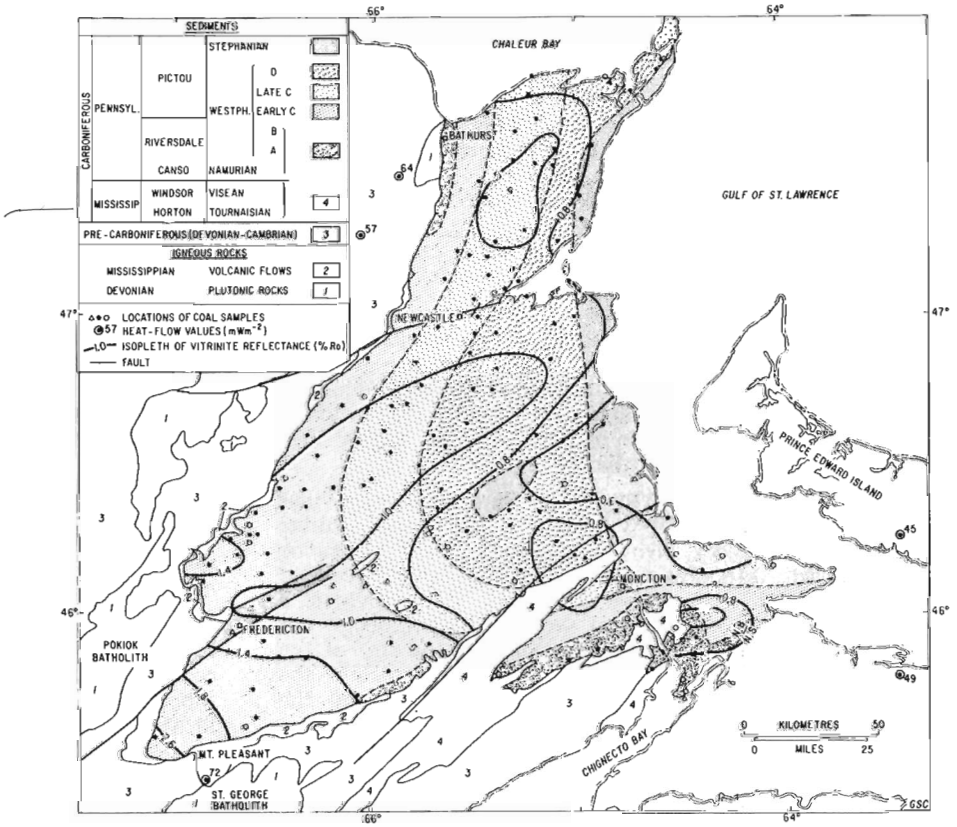

Figure 3.2

Geological age, heat flow data and rank variations.

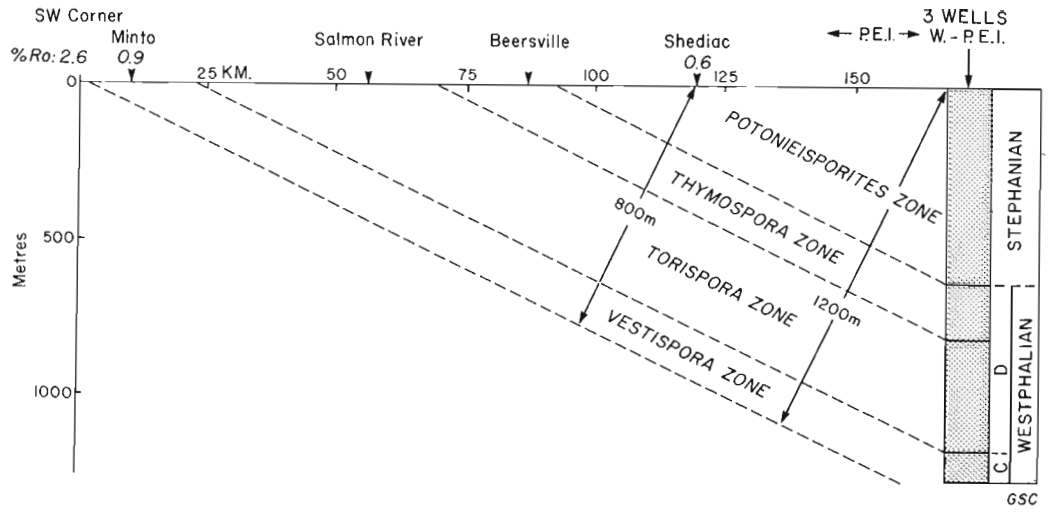

Figure 3.3. Generalized cross-section from Minto to western Prince Edward Island (after Barss et al., 1963) showing relationship between rank and stratigraphy (for geographic position see Fig. 3.1).

The total Carboniferous cover in New Brunswick is less than 2 km thick and rests with marked angular unconformity on a basement of earlier Paleozoic and Precambrian rocks. These earlier sediments were considerably metamorphosed by earth movements and intrusions of granite during the Acadian Orogeny in Devonian time (Gussow, 1953). All igneous rocks of the region predate the coal-bearing measures, with the final intrusive phase occurring during Mississippian time. Volcanic flows of this age are exposed along the SW margin of the Northern Basin, and also protrude through it in at least two locations (Potter et al., 1979; Fig. 3.2, Formation 2).

Much has been learned in recent years about the nature and configuration of the pre-Carboniferous basement complex from interpretation of gravity surveys (Chandra et al., 1980) and some of this information is correlated with the coal rank data in this report.

SAMPLING DATA

A total of 162 samples were examined from three sources: 117 samples from the 1977-79 Carboniferous Drilling Project (Ball et al., 1981), 34 samples from the coal rank study by Hacquebard and Donaldson (1970), and 11 samples of surface outcrops and boreholes acquired from other sources since 1970 (Fig. 3.1, Table 3.1). The samples were taken from thin seams (maximum thickness less than 30 cm), coaly stringers and bark vitrains, which occurred at different depths, ranging from surface exposures to a maximum depth of 248 m. Since surface elevations also varied considerably (from 2-236 m), all rank data were calculated relative to sea level.

The rank was determined for all samples by means of vitrinite reflectance measurements, which provide the most accurate parameter for comparing coalification levels. The maximum reflectance, obtained by rotating the specimen, is used throughout this report.

REGIONAL RANK VARIATIONS

Rank adjustment to sea level datum

As rank is dependent on depth of burial according to Hilt's Law (1873), a standard correction for adjusting the rank data to sea level was required. The general Maritime coalification curve, published by Hacquebard in 1975, has been used for this purpose. It is shown in Figure 3.4A and reveals an asymptotic relationship between coal rank and depth below the surface. When plotted on a semilogarithmic scale (Fig. 3.4B), a linear relationship is represented, which was used to adjust measurements to sea level. Nearly all changes were of minor proportions, the maximum being from 1.25 to 1.4% Ro, caused by a sea level adjustment of 225 m.

It would have been more accurate to have chosen a precise stratigraphic horizon rather than sea level as a standard plane of reference. However, stratigraphic boundaries within the coal measures are poorly defined, and because the regional dip within the Basin is low, the inaccuracies of the sea level adjustments are only minor.

Isoreflectance contours and trend-surface analyses

Figure 3.5 gives the rank changes based on computer-drawn isoreflectance contours. It shows that the variations in coal rank are not randomly distributed, but that a distinct pattern is present. This pattern resembles the one previously depicted by Hacquebard and Donaldson (1970), but because of many more data there are significant changes in detail. The lowest reflectance of 0.6% Ro occurs in the east, and the highest value of 2.6% Ro is present in the SW part of the basin. There appears to be a systematic change between these minimum and maximum values. To determine the nature of this change and verify its significance, the data were subjected to a trend-surface analysis, similar to that described by Kalkreuth (1979) in his coalification study of the Ostsauerland region of West Germany. The analysis was carried out to the 8th degree. The most significant changes occur in the 3rd, 5th, 7th and 8th degree trend-surface maps, which are illustrated in Figure 3.6. Briefly, these computer drawn maps show the following trends:

At the 3rd degree level the general increase in rank from NE to SW is clearly indicated, and the 0.8 contour shows a considerable deflection to the SW.

In the 5th degree map a NE protrusion of the 1.0 contour becomes apparent, and the 0.6 contour is better delineated.

In the 7th degree map the 1.0 contour protrudes even more distinctly to the NE, and the high rank area in the SW becomes better defined.

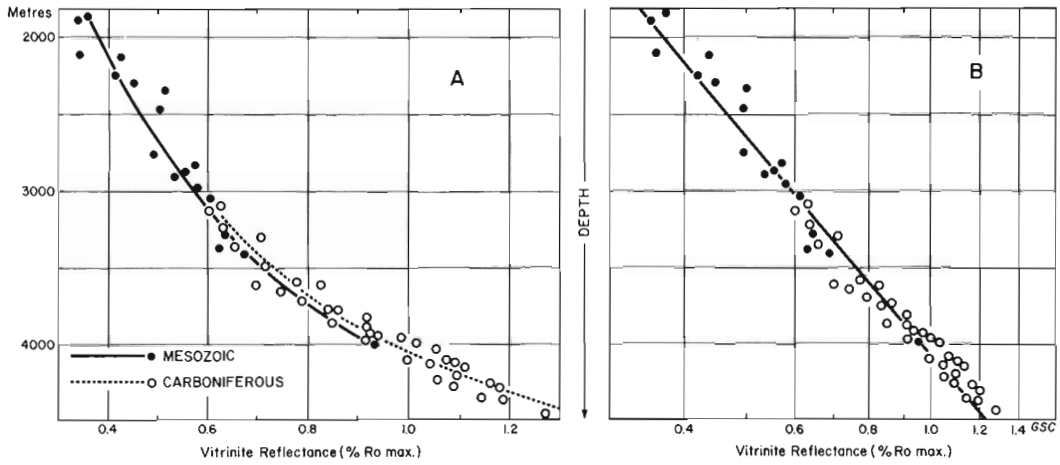

Figure 3.4. General coalification curve for Maritime region (after Hacquebard, 1975).

Finally at the 8th degree level, the picture differs only by the presence of a 1.0 contour area in the extreme SE part of the Basin.

The trend-surface analysis supports the observation that a systematic pattern is represented by the recorded rank changes. However, this pattern is at times obscured by local variations, which may be due to the nature of the samples (bark vitrain versus true coal and degree of weathering) and to inaccuracies in adjustment of rank data to sea level (Fig. 3.4). Therefore a more generalized rank map, incorporating the trends that have been revealed, was constructed (Fig. 3.7). This map forms the basis for interpreting the underlying causes of the regional rank variations.

The coal rank terms of the A.S.T.M. classification are used in Figure 3.7, and the map shows that a progressive increase exists from H.V.-C bituminous coal to anthracite via H.V.-B, H.V.-A, M.V., L.V., and semianthracite, when proceeding from NE to SW. Most striking is the presence of the northerly trending tongue of M.V. coal, which was not revealed in the 1970 study by Hacquebard and Donaldson.

EFFECT OF GEOLOGY ON COAL RANK CHANGES

Relationship with stratigraphy of the coal-bearing measures

The geology of the Carboniferous Basin shown in Figure 3.2 is based essentially on palynological data, acquired originally by Barss et al. (1963), Hamilton (1962), and since 1967 considerably updated by Barss only (see Ball et al., 1981). The Pennsylvanian rocks are divided into five biostratigraphic units, of which the four units belonging to the Pictou Group occupy nearly the entire area. These four units show a distinct NE to SW progression from younger to older zones, which have been named by their most characteristic spores, namely: **Potonieisporites** zone, **Thymospora** zone, **Torispora** zone and **Vestispora** zone (Barss and Hacquebard, 1967; Fig. 3.3).

In Figure 3.2 the rank isopleths (shown in per cent Ro) superimposed on the geology reveal that a broad correlation exists, i.e. the rank in the older formations is generally higher than in the younger formations. This relationship is in accordance with Hilt's Law, because the older formations were more deeply buried than the younger ones. The cross-section of Figure 3.3 illustrates how reliable this correlation may be and to what extent it can be applied regionally. The geographic position of the section is shown in Figure 3.1. It gives the approximate thicknesses of the formations containing the coals, and is based on the spore correlations of the New Brunswick surface rocks with those present in three boreholes drilled in western Prince Edward Island (Barss et al., 1963). The total thickness of the coal-bearing sediments is 1200 m, which at Shediac has become reduced to approximately 800 m, and at Minto to practically zero. The question therefore arises: "Are these differences in thickness sufficient to explain the differences in rank between 0.6% Ro at Shediac, 0.9% Ro at Minto and 2.6% Ro at the SW corner of the Basin?"

By applying these data to the Maritime coalification curve (Fig. 3.8) it is apparent that an additional 800 m of overburden will give an increase in rank from 0.6 to 0.9% Ro; this is exactly the value required to obtain the rank observed at Minto relative to Shediac. Therefore, the western increase in rank as far as Minto can adequately be explained by the stratigraphic relationships. However, since the same stratigraphic interval that occurs at Minto (the **Vestispora** zone) continues over the remainder of the Basin to the SW, the further increase in rank in that direction to 2.6% Ro could hardly be related entirely to older strata of this zone, as they do not exceed 200 m in thickness. If the increase in rank were due to additional overburden of younger strata, then some 2200 m would be needed. This is considered highly unlikely over a distance of less than 100 km in the relatively stable environment of deposition of the New Brunswick platform. A heat source other than that provided by greater depth of burial is therefore required. It may have originated from the igneous rocks that surround the SW corner area and most likely underlie it also (Fig. 3.2).

Relationship with underlying igneous rocks

Figure 3.2 shows that the rocks surrounding the SW corner of the Carboniferous Basin are Mississippian volcanic flows and Devonian plutons of the Pokiok-Mt. Pleasant-St. George batholith system (Ruitenberg et al., 1977). The presence of these rocks underneath the coal measures is indicated by the Bouguer gravity map illustrated in Figure 3.9. This map was prepared by the Department of Natural Resources of New Brunswick (Chandra et al., 1980) and shows the gravity variations in 20 milligals increments. Negative gravity values of -20 milligals and more are interpreted as expressions of igneous rocks, whereas those less than

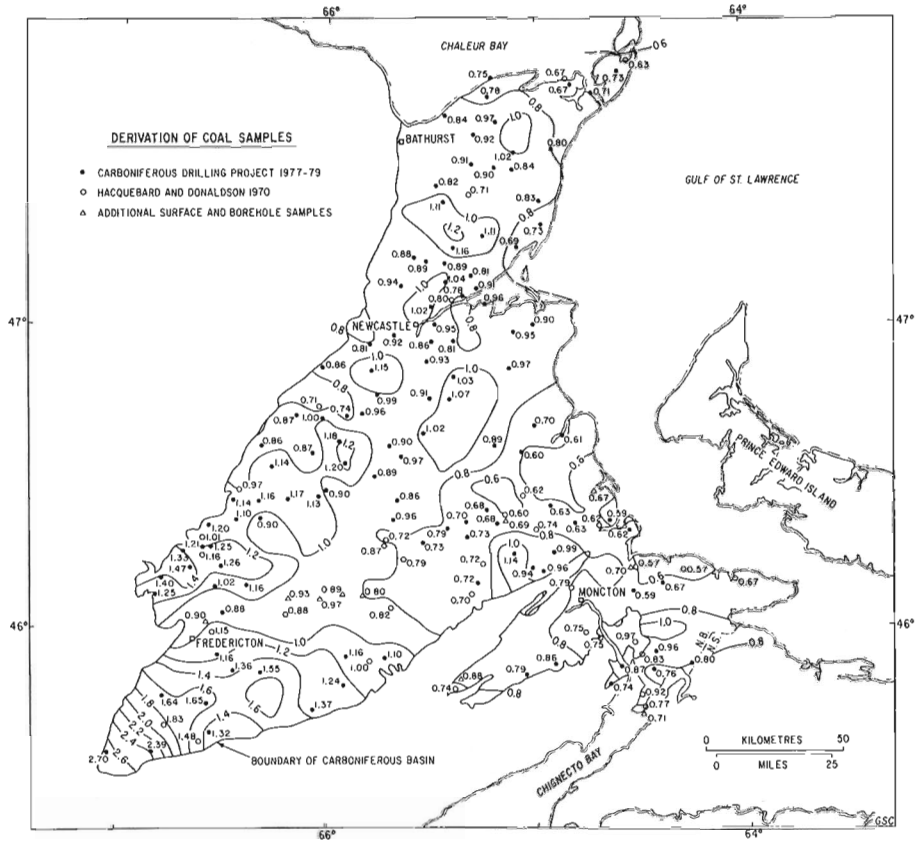

Figure 3.5

Rank variations shown with computer drawn isoreflectance contours (data are given in per cent Ro max.).

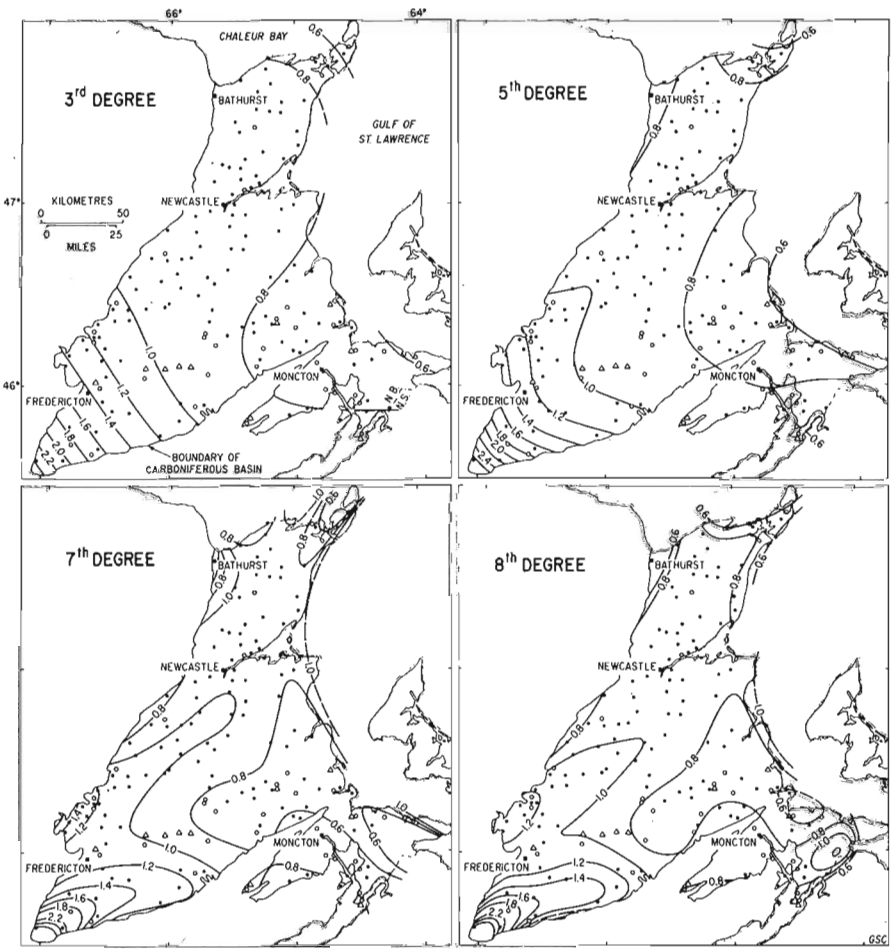

Figure 3.6

Rank variations based on trend-surface analyses, shown at 3rd, 5th, 7th and 8th degree levels.

-20 milligals denote metamorphic and sedimentary sequences. The map indicates that the pre-Carboniferous igneous rocks that border the basin in the SW corner of the area probably occur also underneath it, and may continue past Fredericton in a NE direction. This assumption is supported by the surface exposure of Mississippian lava near Minto (Fig. 3.1, 3.2, Formation 2). Other igneous rocks of the pre-Carboniferous basement complex may occur near Bathurst in the north and in the extreme SE at the border between New Brunswick and Nova Scotia.

The possible effect of the igneous rocks on the variations in coal rank are indicated by the isoreflectance contours which have been superimposed on the gravity map. Areas of higher rank appear to be underlain by igneous rocks or lie in close proximity to them. Since the latter predate the coal measures by a considerable amount of time (they are Devonian and Mississippian in age), direct heating from intrusion or volcanism did not occur, but additional heat flow due to the high conductivity of igneous rocks likely did take place. This view is supported by present day heat flow measurements in the area (Hyndman et al., 1979), which show the highest value (72 mWm^{-2}) at Mt. Pleasant (Fig. 3.2). This compares with values of 57 and 64 south of Bathurst, 45 in central Prince Edward Island, and 49 at Wallace in Nova Scotia.

The progressive increase in heat flow towards the igneous masses appears to offer a better explanation for the occurrence of high rank coals in the SW corner than the 2200 m of additional overburden from younger formations that was mentioned previously.

Tectonic relationships

In the Northern Pennsylvanian Basin of New Brunswick the sediments were laid down under platform conditions and therefore were but little affected by tectonism. The beds are essentially horizontal, showing only a broad regional dip to the NE, resulting in older formations being present towards the SW. The increased coalification that accompanies this trend shows that it is caused by thermal effects related to depth of burial. This coalification therefore was of predeformational origin, although the term has little significance here because no major deformation took place in this region (Hacquebard, 1975).

The only tectonic events of significance are related to faulting. The basin is dissected by numerous NE-trending normal faults, the majority of which are confined to the pre-Carboniferous basement. However, several of these faults were active during and after the deposition of the Carboniferous sediments, notably those that bound the Fredericton Graben. This structure has brought Stephanian sediments of the **Potonieisporites** zone in contact with Westphalian "C" sediments of the **Vestispora** zone, and therefore indicates post-Stephanian movement (Ball et al., 1981; Le Gallais, 1983).

Since significant vertical movements, such as in graben or rift systems, are accompanied by increased and greatly variable heat flows in the sediments, a noticeable effect on the coalification can be expected. This was observed in the Rhine Graben where geothermal variations of 3 to 12°C/100 m caused great changes in the rank of dispersed coaly particles (Teichmüller et al., 1979). Apart from the effects of postdepositional heat flow, stress-related rank changes in close proximity to the major faults were noted also. Similar conditions occur in the sediments of the Fredericton Graben, which have been downfaulted approximately 50 to 150 m (Le Gallais, 1983).

The rank of the Stephanian surface sediments in the Fredericton Graben is considerably above the V-6 level of the corresponding Stephanian sediments that occur in the eastern part of the basin. It varies from V-8 to V-17, and this

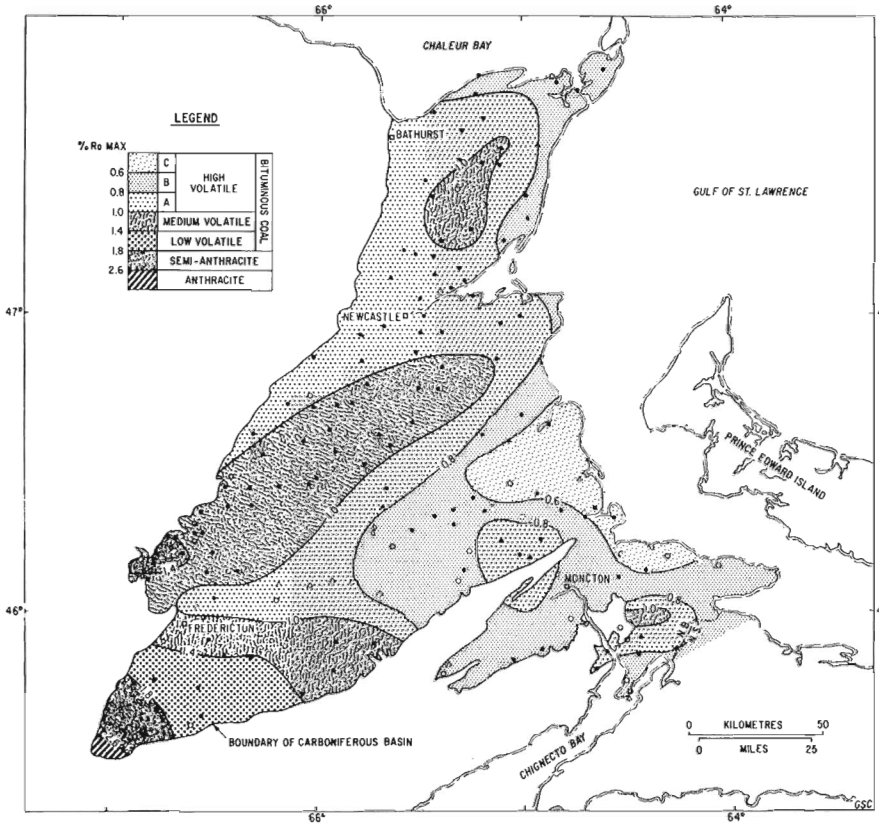

Figure 3.7

Generalized coal rank map of the Carboniferous Basin of New Brunswick.

increased rank is likely due to a secondary coalification that was superimposed on the "predeformational" rank derived from the depth of burial. The secondary rank was the result of the tectonic movement that created the graben.

Variable coalification within the Fredericton Graben is shown by the rank-depth curves of the three wells illustrated in Figure 3.10. These wells are only 12 km apart and show a considerable variation in initial (or surface) rank and in coalification gradient. The latter normally increases with the rank increment because of the asymptotic relationship between rank and depth, but here abnormal gradients were obtained in two of the three wells examined. This is revealed by a comparison with the gradients of similar rank intervals of the Maritime coalification curve.

The gradients for the K.O.G.-No. 3 well are 0.060 and 0.053% Ro/100 m, respectively, indicating that near normal rank conditions prevailed in this well. However, the Marysville No. 2 well shows substantial additional heat flow because its gradient of 0.096 is markedly higher than the 0.072 gradient of the Maritime curve. The results obtained in the SNCL-F-2 well were most unusual; an abnormally low gradient of 0.062 is present, which compares with 0.100% Ro/100 m for the Maritime curve.

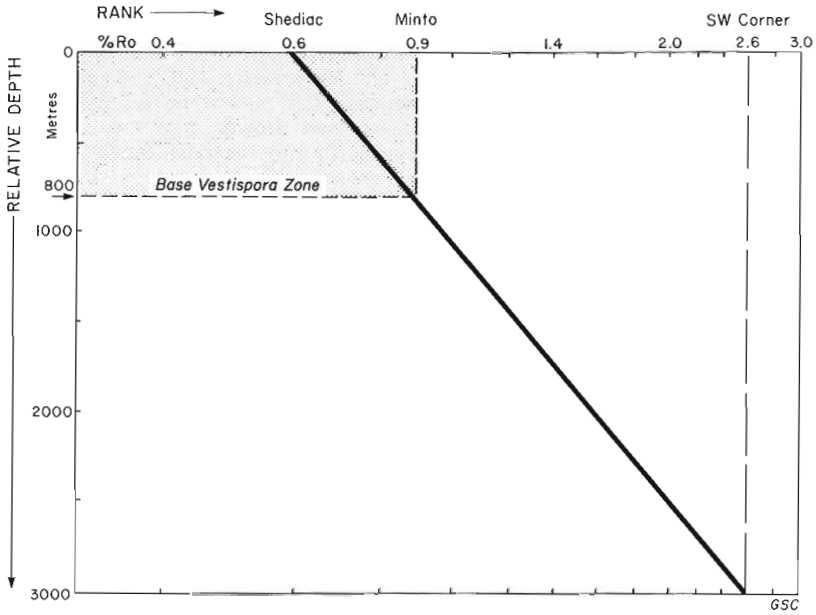

Figure 3.8

Rank-overburden correlations without additional heat source, using Maritime coalification curve.

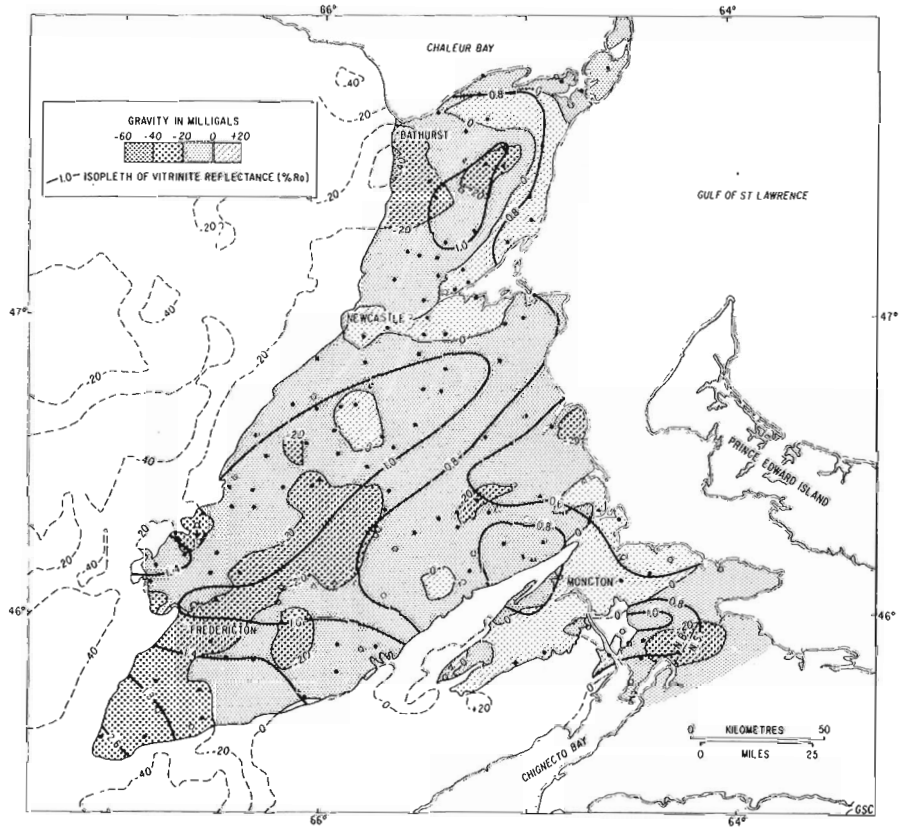

Figure 3.9

Relationship of gravity variations and coal rank.

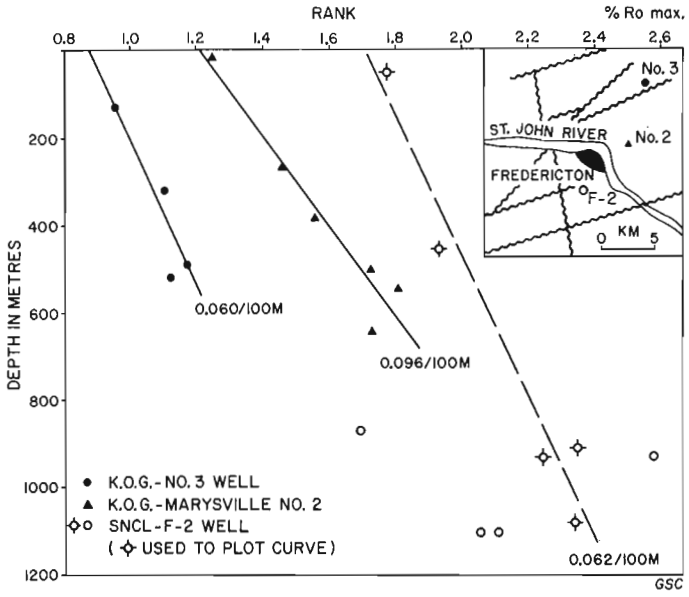

Figure 3.10. *Rank-depth curves of three wells in Fredericton Graben. Inset shows well locations relative to major faults in the area.*

Nine data points were available for the F-2 well and although scattered, show a progression of rank with depth. Five of these points were used to delineate the curve. Apart from these irregularities, all samples showed abnormally high birefringence. With an increase in rank coal becomes anisotropic, reaching complete crystallization in graphite. The degree of anisotropy is shown by the amount of birefringence, which is given by the difference between maximum and minimum reflectance. Birefringence (or bireflectance) increases with rank as can be seen in Figure 3.11, namely from about 0.2% Ro in the high- and medium-volatile bituminous coals of Nova Scotia (V-9 to V-13) to about 0.6% Ro in anthracite of the Münsterland No. 1 well (at V-35; Teichmüller et al., 1979).

In bituminous coals the reflectance anisotropy is essentially uniaxial, but anthracitic vitrinites exhibit biaxial optical properties (Dahme and Mackowsky, 1951). Cook et al. (1972) were able to show that the biaxial optics were the result of tectonic stresses, and Hower and Davis (1981) correlated these properties with the tectonic fabric of the Appalachian Mountains in Pennsylvania.

Figure 3.11 shows that the birefringence measurements of the (biaxial) anthracites of the F-2 well (with Ro max. > 2.05%) are much larger than those recorded in the Münsterland well. In the latter a normal coalification pattern, related to increased heat flux from greater depth of burial, is represented. In the F-2 well, however, tectonic stress from the nearby Hanwell fault is considered the prime agency responsible for the elevated and abnormal coalification that has been encountered.

In the other two wells drilled in the Fredericton Graben more normal birefringence measurements were obtained, and their rank relationships therefore are considered a thermal rather than a stress related phenomenon. In the K.O.G. – No. 3 well the birefringence varied between 0.09 and 0.26% Ro in the range of V-8 to V-12. In the Marysville No. 2 well, which encompasses a rank of V-12 to V-18, it varied between 0.24 and 0.55% Ro.

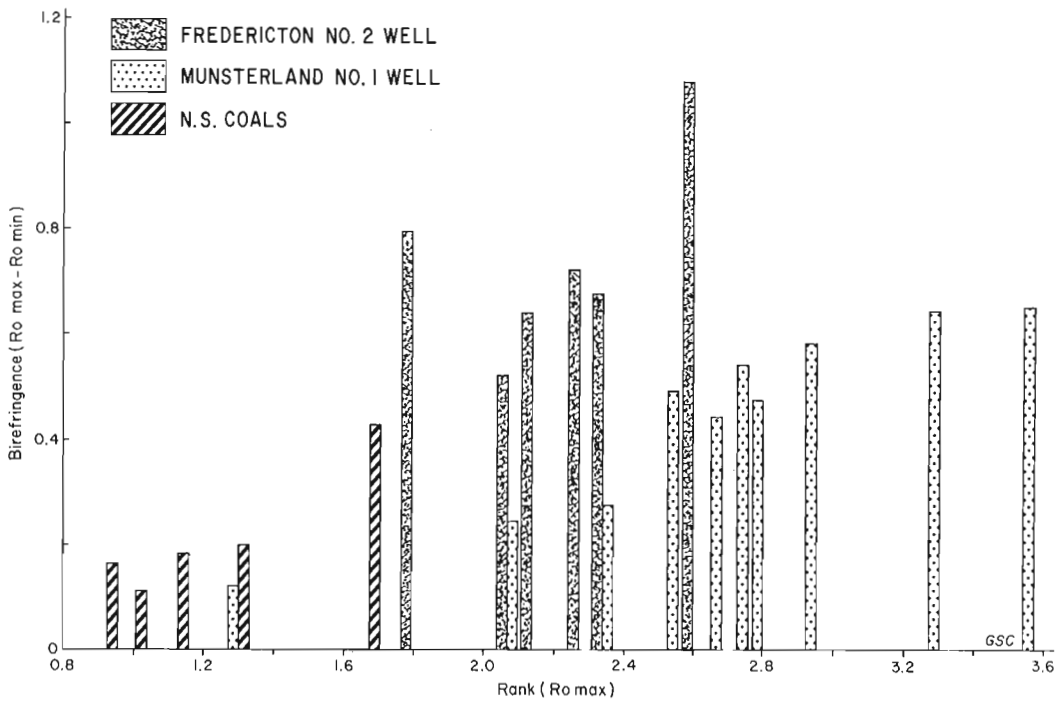

Figure 3.11. *Birefringence of Fredericton No. 2 well coals compared with coals from Nova Scotia and from Münsterland No. 1 well of West Germany (from data of Teichmüller et al., 1979).*

Table 3.1. Record of coal samples used for rank measurements in Carboniferous Basin of New Brunswick

Testhole or reference no.	Location		Elevation (ft)	Depth to coal (ft)	% Ro max	
	Latitude (north)	Longitude (west)			recorded	corrected to sea level
	Samples from Carboniferous Drilling Project 1977-79					
2	47 49 27	64 35 57	68	260	0.75	0.73
4	47 47 25	64 50 19	35	15	0.67	0.67
7	47 48 25	65 12 58	38	80	0.75	0.75
8	47 45 20	64 43 41	3	340	0.75	0.71
12	47 44 51	65 14 06	152	60	0.75	0.76
17	47 39 54	65 11 45	202	140	0.96	0.97
19	47 41 15	65 26 08	65	65	0.84	0.84
21	47 34 38	64 55 28	48	170	0.81	0.80
23	47 34 00	65 06 17	203	330	1.04	1.02
24	47 37 27	65 18 08	272	120	0.90	0.92
29	47 30 44	65 06 58	228	110	0.83	0.84
30	47 31 05	65 12 11	231	360	0.92	0.90
31	47 31 46	65 18 46	347	160	0.88	0.91
32	47 27 42	65 29 07	560	160	0.77	0.82
34	47 24 26	64 59 11	31	50	0.83	0.83
38	47 24 06	65 27 06	512	40	1.03	1.11
40	47 19 37	64 58 46	6	260	0.76	0.73
42	47 17 38	65 15 33	244	280	1.12	1.11
44	47 15 44	65 24 10	304	110	1.13	1.16
47	47 09 49	65 18 51	166	50	0.80	0.81
48	47 12 22	65 26 06	173	300	0.91	0.89
49	47 12 33	65 32 00	352	410	0.90	0.89
50	47 13 22	65 35 19	446	390	0.87	0.88
52	47 07 13	65 17 15	58	30	0.91	0.91
53	47 05 50	65 21 28	63	250	0.80	0.78
54	47 08 36	65 26 18	285	180	1.02	1.04
55	47 07 49	65 39 06	384	300	0.93	0.94
60	47 04 15	65 15 01	23	300	1.00	0.96
61	47 00 12	65 29 24	95	40	0.94	0.95
62	47 03 38	65 30 35	314	190	1.00	1.02
66	47 00 10	65 00 47	49	10	0.89	0.90
67	46 58 44	65 06 39	59	190	0.97	0.95
69	46 56 56	65 23 57	161	200	0.81	0.81
70	46 56 54	65 30 11	125	360	0.89	0.86
71	46 58 15	65 41 09	111	230	0.94	0.92
72	46 56 28	65 47 52	54	200	0.83	0.81
75	46 51 32	65 07 59	190	20	0.95	0.97
77	46 49 52	65 24 03	151	170	1.03	1.03
78	46 52 57	65 32 06	78	375	0.97	0.93
80	46 51 16	65 47 44	164	110	1.14	1.15
82	46 52 10	66 01 39	250	150	0.85	0.86
87	46 45 25	65 25 11	266	270	1.07	1.07
88	46 45 36	65 30 54	200	300	0.92	0.91
90	46 46 29	65 45 51	125	130	0.99	0.99
96	46 40 09	65 00 44	85	30	0.69	0.70
100	46 38 50	65 32 34	295	180	1.00	1.02
102	46 42 43	65 50 44	200	150	0.95	0.96
103	46 42 17	65 54 27	150	340	0.76	0.74
104	46 41 43	66 01 39	405	70	0.95	1.00
105	46 42 22	66 09 10	315	70	0.84	0.87
110	46 36 16	65 12 12	184	80	0.88	0.89
113	46 34 04	65 38 54	197	300	0.99	0.97
115	46 36 12	65 42 29	171	370	0.93	0.90
116	46 37 16	65 56 50	330	150	1.15	1.18
117	46 34 49	66 04 37	320	300	0.87	0.87
119	46 36 18	66 19 11	550	90	0.80	0.86
128	46 30 10	65 46 41	246	390	0.91	0.89

Table 3.1 (cont.)

Testhole or reference no.	Location		Elevation (ft)	Depth to coal (ft)	% Ro max	
	Latitude (north)	Longitude (west)			recorded	corrected to sea level
129	46 32 43	65 55 03	260	130	1.18	1.20
132	46 32 06	66 16 30	435	100	1.08	1.14
136	46 24 16	64 56 01	200	388	0.65	0.63
142	46 25 15	65 40 13	299	244	0.85	0.86
144	46 27 26	66 00 32	270	117	0.88	0.90
145	46 26 35	66 02 44	340	290	1.12	1.13
146	46 25 34	66 11 37	505	150	1.11	1.17
147	46 25 15	66 20 10	450	50	1.09	1.16
148	46 25 32	66 27 10	520	240	1.09	1.14
149	46 19 10	64 33 36	66	385	0.65	0.62
150	46 21 15	64 39 13	62	395	0.62	0.59
152	46 20 46	64 49 17	217	331	0.64	0.63
154	46 20 55	65 11 12	269	284	0.68	0.68
155	46 23 27	65 14 22	259	291	0.68	0.68
158	46 21 33	65 40 57	259	180	0.95	0.96
163	46 22 02	66 19 39	470	180	0.86	0.90
164	46 21 46	66 26 13	540	90	1.03	1.10
165	46 20 32	66 34 07	570	40	1.11	1.20
169	46 15 00	64 55 12	302	250	0.98	0.99
171	46 14 38	65 06 44	243	20	1.10	1.14
181	46 12 24	66 30 40	580	320	1.21	1.26
182	46 16 05	66 33 10	450	120	1.19	1.25
183	46 15 11	66 41 26	620	120	1.28	1.38
189	46 08 41	64 24 22	72	330	0.70	0.67
193	46 11 16	64 58 12	308	107	0.93	0.96
194	46 12 02	65 01 27	351	200	0.92	0.94
196	46 09 01	65 17 10	177	375	0.74	0.72
204	46 08 34	66 23 15	500	40	1.08	1.16
206	46 08 14	66 32 14	470	348	1.00	1.02
207	46 12 02	66 39 25	300	120	1.43	1.47
208	46 10 01	66 47 30	775	40	1.25	1.40
215	46 07 14	64 32 42	95	340	0.61	0.59
225	46 03 08	66 29 56	300	190	0.87	0.88
228	46 06 43	66 49 21	775	53	1.12	1.25
251	45 52 51	64 16 01	125	5	0.79	0.80
252	45 55 16	64 26 22	322	260	0.95	0.96
254	45 52 15	64 35 55	49	200	0.89	0.87
260	45 54 04	65 43 58	130	154	1.10	1.10
262	45 54 32	65 54 44	130	270	1.18	1.16
268	45 54 48	66 31 31	125	260	1.18	1.16
271	45 51 33	64 27 11	289	260	0.76	0.76
273	45 49 03	64 39 04	564	330	0.71	0.74
274	45 52 47	64 55 11	748	240	0.80	0.86
275	45 50 38	65 03 23	568	300	0.76	0.79
280	45 48 46	65 55 21	225	10	1.20	1.24
283	45 51 01	66 19 22	43	90	1.56	1.55
284	45 51 45	66 26 49	25	250	1.41	1.36
293	45 43 49	66 04 15	70	220	1.40	1.37
297	45 45 19	66 34 26	25	199	1.69	1.65
299	45 46 34	66 46 55	375	195	1.60	1.64
303	45 39 24	66 33 25	75	270	1.36	1.32
307	45 35 28	66 49 47	423	235	2.32	2.39
309	45 35 22	67 02 39	510	83	2.53	2.70
1046	47 15 14	65 05 17	159	621	0.74	0.69
1094	46 38 21	64 52 26	30	814	0.69	0.61
1109	46 35 03	65 04 24	98	713	0.66	0.60
1182	46 16 03	66 35 56	530	32	1.12	1.21
B22	46 21 01	65 20 25	261	292	0.70	0.70

Table 3.1 (cont.)

Testhole or reference no.	Location		Elevation (ft)	Depth to coal (ft)	% Ro max	
	Latitude (north)	Longitude (west)			recorded	corrected to sea level
B23	46 19 48	65 25 48	214	249	0.79	0.79
B24	46 16 58	65 32 48	224	60	0.71	0.73
B26	46 18 05	65 20 05	304	256	0.72	0.73
	Samples of Hacquebard & Donaldson (1970, Table II, p. 1159-1160)					
5	47 48 15	64 51 00	0	outcrop	0.67	0.67
7	47 51 45	64 33 00	0	outcrop	0.63	0.63
9	47 25 45	65 19 30	300	outcrop	0.68	0.71
10	47 05 00	65 24 30	0	outcrop	0.80	0.80
12	46 44 00	66 02 45	200	outcrop	0.69	0.71
13	46 27 30	66 25 30	300	outcrop	0.93	0.97
14	46 20 15	64 42 15	50	outcrop	0.62	0.62
15	46 26 15	65 04 00	100	outcrop	0.61	0.62
16	46 19 30	65 00 15	200	outcrop	0.72	0.74
17	46 22 30	65 09 15	200	outcrop	0.58	0.60
18	46 12 45	65 15 30	260	outcrop	0.69	0.72
19	46 06 45	65 18 50	100	outcrop	0.69	0.70
20	46 13 45	65 38 15	200	outcrop	0.77	0.79
21	46 17 30	65 43 15	100	outcrop	0.71	0.72
22	46 16 30	65 43 45	100	outcrop	0.86	0.87
23	46 02 45	66 12 00	100	outcrop	0.87	0.88
24	46 14 30	66 36 00	300	outcrop	1.11	1.16
25	46 18 00	66 36 00	400	outcrop	0.95	1.01
27	45 59 15	66 33 00	115	427	1.20	1.15
28	45 40 45	66 46 15	180	outcrop	1.78	1.83
29	45 37 30	66 36 30	250	outcrop	1.43	1.48
31	46 04 00	65 42 00	175	outcrop	0.80	0.82
32	45 53 30	65 48 00	100	outcrop	0.99	1.00
35	45 48 00	65 23 30	200	outcrop	0.72	0.74
36	45 59 01	64 46 15	300	29	0.72	0.75
37	45 58 00	64 42 00	300	310	0.76	0.76
38	46 08 00	64 50 15	100	outcrop	0.78	0.79
39	46 11 45	64 32 00	10	outcrop	0.57	0.57
40	46 11 20	64 18 30	50	outcrop	0.57	0.57
41	46 09 15	64 03 45	0	outcrop	0.67	0.67
42	45 57 00	64 32 13	25	250	1.00	0.97
43	45 54 30	64 30 30	150	outcrop	0.81	0.83
44	45 46 30	64 30 30	0	outcrop	0.92	0.92
44A	45 44 15	64 29 30	0	outcrop	0.77	0.77
	Additional Surface and Borehole Samples					
1	45 43 00	64 30 00	0	outcrop	0.71	0.71
2	45 50 00	65 22 00	200	outcrop	0.85	0.88
3	46 11 43	64 32 39	50	outcrop	0.69	0.70
4	46 06 45	65 55 30	20	outcrop	0.89	0.89
5	46 06 30	65 49 54	50	outcrop	0.79	0.80
6	46 05 51	66 02 06	125	outcrop	0.95	0.97
7	46 06 00	66 11 21	280	outcrop	0.89	0.93
8	Coalbranch No. 1 well					
	46 21 22	65 09 01	200	285	0.70	0.69
9	Buctouche No. 1 well					
	46 27 01	64 43 24	50	760	0.74	0.67
10	K.O.G. No. 3 well					
	46 01 15	66 35 00	42	420	0.95	0.90
11	SNCL-F-2 well					
	45 56 00	66 39 24	350	161	1.78	1.83

ACKNOWLEDGMENTS

The authors gratefully acknowledge contributions to this paper by the following personnel of the Atlantic Geoscience Centre in Dartmouth, Nova Scotia: G.M. Grant and G. Cook for assisting with the compilation of the diagrams and M.S. Barss and A.C. Grant for their critical review of the manuscript. Sincere thanks are also extended to F.D. Ball, formerly with the Department of Natural Resources of New Brunswick (presently with Three-D Consultants Ltd. in Fredericton, N.B.), who provided the coal samples from the Carboniferous Drilling Project and made available the required geological information. Samples were also provided by C.J. Le Gallais of S.E.R.U. Nucleaire (Canada) Lte, for which we express our appreciation.

REFERENCES

Ball, F.D., Sullivan, R.M., and Peach, A.R.
1981: Carboniferous drilling project; Department of Natural Resources of New Brunswick, Report of Investigation 18, 109 p.

Barss, M.S. and Hacquebard, P.A.
1967: Age and stratigraphy of the Pictou Group in the Maritime Provinces as revealed by fossil spores; Geological Association of Canada, Special Paper 4, p. 267-283.

Barss, M.S., Bujak, J.P., and Williams, G.L.
1979: Palynological zonation and correlation of sixty-seven wells, Eastern Canada; Geological Survey of Canada, Paper 78-24, 118 p.

Barss, M.S., Hacquebard, P.A., and Howie, R.D.
1963: Palynology and stratigraphy of some upper Pennsylvanian and Permian rocks of the Maritime Provinces; Geological Survey of Canada, Paper 63-3, 13 p.

Chandra, J.J., Wallace, J., and Kingston, P.
1980: Bouguer gravity map of New Brunswick; Department of Natural Resources of New Brunswick, Plate 80-43, scale 1:500 000.

Cook, A.C., Murchison, D.G., and Scott, E.
1972: Optically biaxial anthracitic vitrinites; Fuel, v. 51, p. 180-184.

Dahme, A. and Mackowsky, M.T.
1951: Chemisch-physikalische und petrographische Untersuchungen an Kohlen, Koksen und Graphiten; Brennstoff-Chemie, v. 49, p. 11-21, 47-52, 106-110.

Gussow, W.C.
1953: Carboniferous stratigraphy and structural geology of New Brunswick, Canada; American Association of Petroleum Geologists, Bulletin v. 37, p. 1713-1816.

Hacquebard, P.A.
1972: The Carboniferous of Eastern Canada; C.R. 7th Carboniferous Congress, Krefeld 1971, tome I, p. 69-90.

1975: Pre- and postdeformational coalification and its significance for oil and gas exploration; C.N.R.S. Paris, 1973 International Colloquium on: "Pétrographie de la matiére organique des sédiments, etc.", p. 225-241.

Hacquebard, P.A. and Donaldson, J.R.
1970: Coal metamorphism and hydrocarbon potential in the Upper Paleozoic of the Atlantic Provinces, Canada; Canadian Journal of Earth Sciences, v. 7, p. 1139-1163.

Hamilton, J.B.
1962: Correlation of the Pennsylvanian rocks in the western part of the central Pennsylvanian basin of New Brunswick by means of fossil spores; unpublished M.Sc. thesis, University of New Brunswick, Fredericton, N.B., 118 p.

Hilt, C.
1873: Die Beziehungen zwischen der Zusammensetzung und den technischen Eigenschaften der Steinkohlen; Zeitschrift Ver. Deutscher Ingen., Bd. 17, Ht. 4, p. 194-202.

Hower, J.C. and Davis, A.
1981: Vitrinite reflectance anisotropy as a tectonic fabric element; Geology, v. 9, p. 165-168.

Hyndman, R.D., Jessop, A.M., Judge, A.S., and Rankin, D.S.
1979: Heat flow in the Maritime Provinces of Canada; Canadian Journal of Earth Sciences, v. 16, p. 1154-1165.

Kalkreuth, W.
1979: Das Inkohlungsbild des Ostsauerländer Hauptsattels im Rhenoherzynikum mit besonderer Berücksichtigung der Trendflächen-analysen; Fortschritte in der Geologie von Rheinland und Westfallen, v. 27, p. 277-321 (For English review see Hacquebard, P.A., 1980, International Journal of Coal Geology, no. 1, p. 90).

Le Gallais, C.J.
1983: Stratigraphy, sedimentation and basin evolution of the Pictou Group (Pennsylvanian), Oromocto Sub-basin, New Brunswick; unpublished M.Sc. thesis, Department of Geological Sciences, McGill University; Montreal, Quebec, 123 p.

Potter, R.R., Hamilton, J.B., and Davies, J.L.
1979: Geological map of New Brunswick; Department of Natural Resources of New Brunswick, Map no. MCR 29, second edition, scale 1:500 000.

Ruitenberg, A.A., Fyffe, L.R., McCutcheon, S.R.,
St. Peter, C.J., Irrinki, R.R., and Venugopal, D.V.
1977: Evolution of pre-Carboniferous tectono-stratigraphic zones in the New Brunswick Appalachians: Geoscience Canada, no. 4, p. 171-181.

Teichmüller, M., Teichmüller, R., and Weber, K.
1979: Inkohlung und Illitkristallinität. Vergleichende Untersuchungen im Mesozoikum und Paläozoikum von Westfalen; Fortschritte inder Geologie von Rheinland und Westfallen, v. 27, p. 201-276. (For English review see Hacquebard, P.A., 1980, International Journal of Coal Geology, no. 1, p. 89).

Van de Poll, H.W.
1970: Stratigraphical and sedimentological aspects of Pennsylvanian strata in southern New Brunswick; unpublished Ph.D. thesis, University College of Swansea, University of Wales, 199 p.

4. STATISTICAL ANALYSIS OF GRANITE PORE SIZE DISTRIBUTION DATA, LAC DU BONNET BATHOLITH, EASTERN MANITOBA

Project 690038

F.P. Agterberg, T.J. Katsube[1], and S.N. Lew
Economic Geology Division

Agterberg, F.P., Katsube, T.J., and Lew, S.N., Statistical analysis of granite pore size distribution data, Lac du Bonnet batholith, eastern Manitoba; in Current Research, Part A, Geological Survey of Canada, Paper 84-1A, p. 29-38, 1984.

Abstract

Micropores and microfractures in crystalline rocks are of interest in the field of nuclear fuel waste containment due to their radionuclide retardation potential. Mercury porosimetry data for ten drill core samples from the Lac du Bonnet batholith have been statistically analyzed. The porosity is divided into three separate components by using a newly developed trimodal model. The porosity component for the pore size range of 0.025 to 0.063 µm is extracted and is suggested to be linearly related to fracture flexibility. At depths less than 400 m, changes in total porosity are almost entirely due to changes in the porosity of nanopores (pore size less than 0.025 µm).

Résumé

Les micropores et les microfractures dans les roches cristallines présentent beaucoup d' intérêt en ce qui a trait à l'entreposage des déchets nucléaires piusqu'ils pourraient retarder le déplacement des radionuclides. Des données sur la porosité du mercure obtenues de dix carottes prélevées dans le batholite du Lac du Bonnet ont été analysées statistiquement. On a divisé la porosité en trois composantes distinctes au moyen d' un modèle trimodal nouvellement mis au point. La composante de porosité pour les vides de 0,025 à 0,063 µm est calculée et devrait être reliée d'une façon linéaire à la souplesse des fractures. À des profondeurs inférieures à 400 m, les changements dans la porosité totale résultent presque entièrement des changements dans la pososité des nanopores aux dimensions inférieures à 0,025 µm.

INTRODUCTION

An extensive network of micropores and microfractures exists in crystalline rocks (Sprunt and Brace, 1974; Montgomery and Brace, 1975; Simmons and Richter, 1976; Brace, 1977). These micropores and microfractures contribute to the advection of fluids (Brace et al., 1968; Brace, 1980) and the diffusion of ions through crystalline rocks (Gordon, 1945; Bradbury et al., 1980; Skagius and Neretnieks, 1982; Wadden and Katsube, 1982). Micropores and microfractures are of particular interest in the field of nuclear fuel waste containment, due to their potential for absorbing and retarding radionuclides (Neretnieks, 1980; Tang et al., 1980; Grisak and Pickens, 1981; Katsube, 1982) if they dissolve into the groundwater from the waste and migrate along major fractures and fissures.

Quantitative information concerning the network of microcavities such as porosity values for different pore sizes, is obtained through mercury porosimetry (Rootare, 1970). An investigation of the pore size distribution for a suite of granitic rock samples from a Whiteshell nuclear fuel waste management research area (near Lac du Bonnet, Manitoba) suggested the existence of a trimodal distribution of micropores (Katsube, 1981) as shown in Figure 4.1. This distribution provided significant insight into the pore structure of these rocks. However, because of the relative randomness of the porosity values obtained for each pore size, the reliability of the pore size data for individual samples and for pores in the range of 0.025 to 0.063 µm is rather poor. For this reason it has become necessary to develop a method for statistically analyzing the pore size distribution data. This paper presents such a method.

STATISTICAL METHODS FOR DECOMPOSITION OF MIXTURES OF NORMAL DISTRIBUTIONS

The data in Figure 4.1 suggest that the porosity data satisfy a mixture of two or three normal (Gaussian) distributions, when logarithmically (base 10) transformed pore size is plotted in the horizontal direction and porosity in volume per cent in the vertical direction.

Three statistical methods of approach exist for the decomposition of mixtures of normal distributions:

1. Graphical approach using normal or lognormal probability paper (cf. Hald, 1952, p. 152-158);
2. Method of moments (cf. Johnson and Kotz, 1970, p. 89-92); and
3. Nonlinear model of least squares (cf. McCammon, 1969).

Efficient computer programs are in existence for the method of moments (M.W. Clark, 1977) and nonlinear least squares (I. Clark, 1977; Bridges and McCammon, 1980). For the present study we have implemented and used the program GETHEN by M.W. Clark (1977). New computer programs have been prepared for displaying the original data and fitted normal curves on the screen of a Tektronix 4014 terminal and by means of a CALCOMP plotter. Because satisfactory results were obtained by using the method of moments, no attempt has been made to use the other methods. However, a study to compare results obtained by different techniques would be of interest.

At the beginning of GETHEN, unbiased estimates of a number of moments of a population are obtained from sample information using k-statistics. The input consists either of observed data or of data grouped regularly for classes. Sheppard's correction is applied if the data are grouped. The first five moments are needed to estimate the five unknown

[1] Resource Geophysics and Geochemistry Division

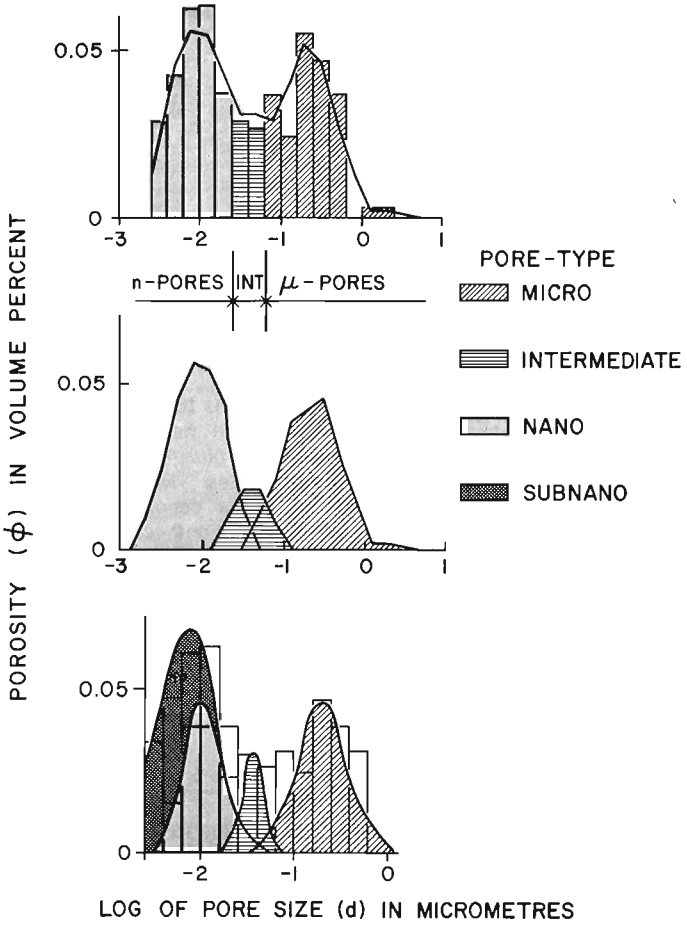

Figure 4.1. *Average pore size distribution of 10 Lac du Bonnet rock samples and groupings of the pore sizes (from Katsube, 1981). Top diagram with original data reveals two distinct pore groups (micropores and nanopores) in the >0.063 and <0.025 μm pore sizes. It also suggest the existence of intermediate pores (0.025-0.063 μm pore size) and subnanopores. The latter would belong to the same probability distribution as the nanopores. This group may be related to alteration.*

coefficients in the probability distribution $f_2(x) = f(x; \mu_1, \sigma_1, \mu_2, \sigma_2, \alpha)$ for a mixture of two normal distributions $N(\mu_1, \sigma_1^2)$ and $N(\mu_2, \sigma_2^2)$ with:

$$f_2(x) = \alpha\, \phi\left(\frac{x - \mu_1}{\sigma_1}\right) + (1 - \alpha)\, \phi\left(\frac{x - \mu_2}{\sigma_2}\right)$$

In these expressions α denotes the proportion of $N(\mu_1, \sigma_1^2)$ in the mixture. Estimation of the five parameters from the first five moments involves the solving of a polynomial equation of the ninth degree as originally derived by Pearson (1894). GETHEN also fits $f_1(x) = f(x; \mu, \sigma)$ for a single normal distribution $N(\mu, \sigma^2)$ by using the first two moments.

Advantages and drawbacks of GETHEN have been listed by M.W. Clark (1977, p. 258). The latter include that this method is not easily extended to more than two components and that there is a small possibility that the numerical technique which is used to solve the nonic equation may not converge. These problems were indeed encountered in some

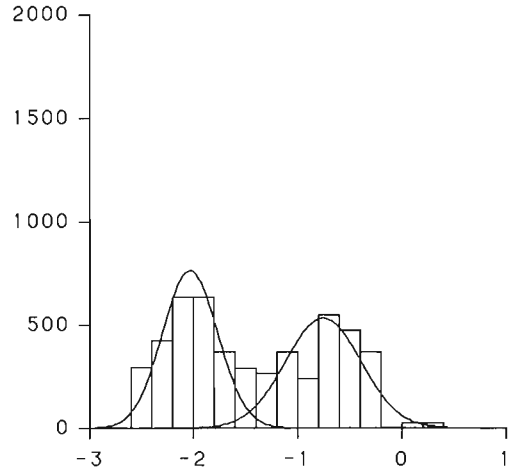

Figure 4.2. *GETHEN solution of two normal distributions for average pore size distribution with statistics of "standard" in Tables 4.1 and 4.2. Note that values on theoretical curves should be added in range of overlap for comparison with observed data. This diagram was constructed automatically on CALCOMP plotter. Horizontal axis is for logarithm (base 10) of pore size in micrometres; vertical axis is for porosity in ppm.*

computer runs performed for our study, but minor modifications of the method could be introduced to obtain approximate solutions in those situations (see later).

A particular problem related to the nature of the data which had to be considered is that the frequency is not given in terms of numbers of observations for specific values or classes but as volume per cent. The data are grouped regularly but numbers of pores per class have not been determined. The measurement error of the mercury porosimetry method employed for obtaining the combined volumes for all pores belonging to specific classes provides a smoothing effect preventing the precise estimation of actual numbers of pores. For the purpose of this discussion, it is assumed that the measured pore volume for a class labelled i is equivalent to n_i "independent" observations and that $n = \sum n_i$ represents the total number of these independent observations. Differences between estimated moments and parameters in the output of GETHEN would result from the use of different k-statistics. Because n, on which the k-statistics depend, is not known, the following empirical approach was taken. The values of n_i were initially set equal to volume in ppm rounded off to the nearest integer value. Other values of n_i were created by dividing these initial values by 10 and 100, respectively, and rounding off. GETHEN was run three times on a representative data set using the different sets of values of n_i. The differences in the resulting parameters were negligibly small and it was decided to use the ppm values for all further work.

Normally, the results of a GETHEN run are evaluated by means of a chi-squared test. For this, the values of n_i must be available. Because this information was lacking, satisfactory goodness-of-fit tests could not be performed on our results. However, each sequence of mercury porosimetry data for a sample can be regarded as a time series. Later in this paper an attempt will be described to address the problems of porosity measurement error and goodness of fit of the components extracted from the data by using methods of time series analysis.

Table 4.1. Mercury porosimetry data used for statistical analysis (cf. Katsube, 1981)

Log_{10} Pore size (in μm)	WN2 24	WN2 85	WN1 138	WN1 160	WN1 223	WN1 245	WN1 303	WN1 345	WN1 385	WN1 410	Ave. (Standard)
-2.6 -2.4	261	1365	0	263	0	0	0	0	526	524	294
-2.4 -2.2	261	1365	0	789	263	526	0	0	526	524	425
-2.2 -2.0	783	819	526	1052	789	789	0	262	789	524	633
-2.0 -1.8	783	1092	789	789	526	526	0	524	789	526	634
-1.8 -1.6	783	819	526	526	263	0	263	262	263	0	370
-1.6 -1.4	261	546	0	526	0	0	263	0	789	524	291
-1.4 -1.2	261	546	0	263	263	263	0	262	526	262	265
-1.2 -1.0	261	546	263	263	526	526	263	0	526	524	370
-1.0 -0.8	261	546	263	0	263	0	263	0	0	786	238
-0.8 -0.6	522	0	526	789	526	526	526	0	0	2096	551
-0.6 -0.4	261	0	789	526	263	526	1052	786	0	524	473
-0.4 -0.2	261	0	263	263	526	526	263	786	263	524	368
-0.2 -0.0	0	0	0	0	0	0	0	0	0	0	0
0.0 -0.2	0	0	0	0	0	0	0	0	263	0	26
0.2 -0.4	0	0	263	0	0	0	0	0	0	0	26
Total (ϕ_T)	4959	7644	4209	6049	4208	4208	2893	2882	5260	7336	4964

Samples came from two boreholes (WN1 and WN2). Sample numbers correspond to depth in metres along borehole. Measurements are given in ppm.

Table 4.2. Parameters (means, standard deviations and proportion of first component) estimated by GETHEN method for decomposition of mixture of two normal distributions

Sample	μ_1	σ_1	μ_2	σ_2	α
WN2- 24	-1.912	0.298	-0.715	0.257	0.636
WN2- 85	-2.238	0.198	-1.327	0.274	0.605
WN1-138	-1.970	0.092	-0.665	0.508	0.358
WN1-160	-2.004	0.262	-0.704	0.250	0.652
WN1-223	-1.963	0.211	-0.703	0.282	0.484
WN1-245	-2.039	0.200	-0.640	0.251	0.490
WN1-303	-1.490	0.183	-0.579	0.152	0.257
WN1-345	-1.829	0.189	-0.423	0.118	0.430
WN1-385	-2.060	0.109	-1.273	0.726	0.466
WN1-410	-2.126	0.261	-0.761	0.250	0.332
Standard	-2.033	0.265	-0.757	0.362	0.512

These results are shown graphically in Figures 4.2 and 4.3. For plotting, the frequencies of the two components were multiplied by $\alpha\phi_T$ and $(1 - \alpha)\phi_T$, respectively.

RESULTS OF GETHEN RUNS

The original mercury porosimetry data for 10 samples from the Lac du Bonnet granite are shown in Table 4.1. The numbers in the last column are averages of those in the preceding ten columns. These averages will be used as a standard to which each of the ten original samples will be compared.

Results of running GETHEN on the eleven data sets of Table 4.1 are shown in Table 4.2 and Figures 4.2 and 4.3. A 2-component solution for WN1-138 could not be obtained immediately because the numerical technique used to solve the nonic equation did not converge. The frequency distribution curve for this sample was smoothed by fitting a cubic spline function (using the IMSL subroutine ICSSCU maintained at the EMR Computer Science Centre). The fitted values differed only slightly from the original measurements, but convergence was now achieved for the numerical technique in GETHEN.

From the results in Table 4.1 and Figure 4.3 it can be seen that a first component (Component 1) with its mean near -2.0 was extracted from nearly all samples. Exceptions are Sample WN2-85 in which the model of two Gaussian curves is not clearly reflected in the original data, and WN1-303 from which Component 1 seems to be missing. Mean and standard deviation of the second component are considerably more variable. This second component may, therefore, be a mixture of two or more other distributions.

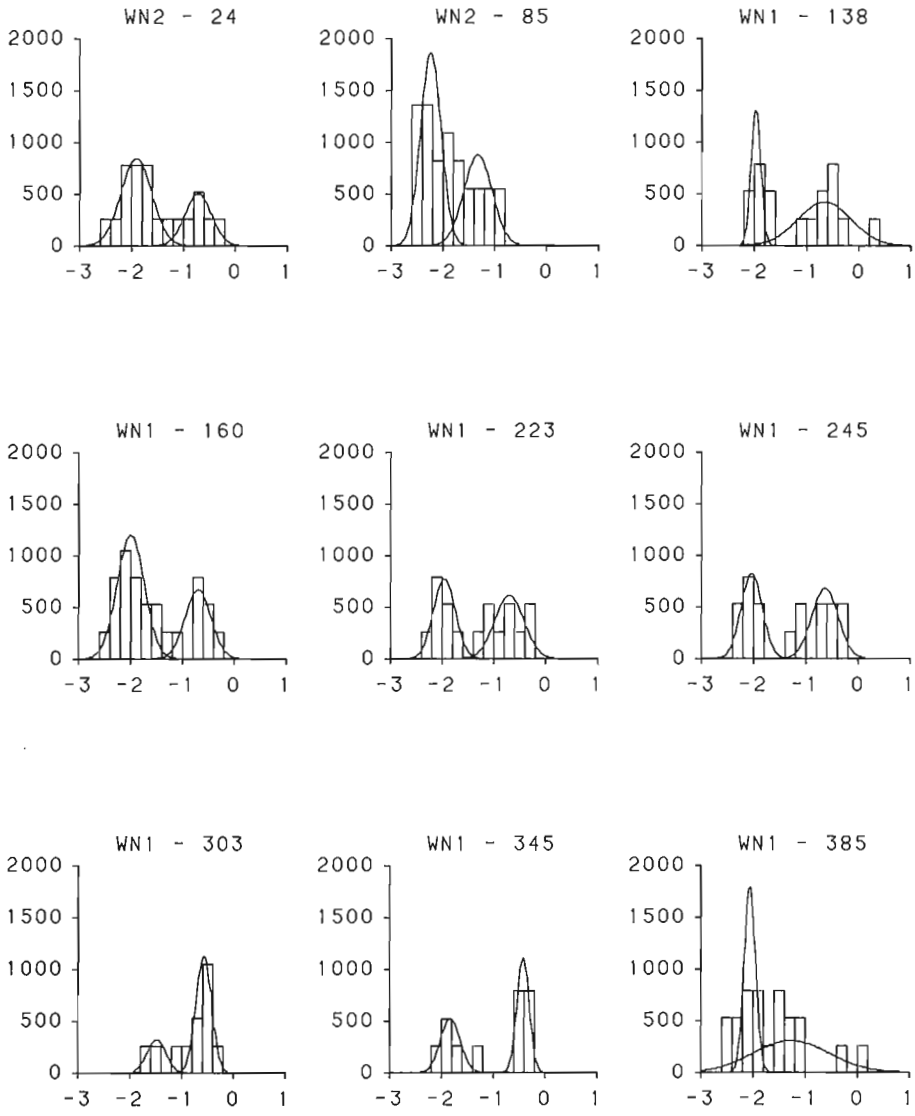

Figure 4.3

GETHEN solutions for 10 individual samples. For statistics, see Tables 4.1 and 4.2. For labels of axes, see caption of Figure 4.2.

In order to test this assumption, the first component shown in Figure 4.2 was extracted from the standard, and the remaining volume per cent values were again processed by means of GETHEN. Initially, the nonic equation could not be solved as for WN1-138 (see before). The instability causing failure of the algorithm to achieve convergence is related to the occurrence of two values greater than 0.0 on the extreme right-hand side of the histogram (Fig. 4.3). Either omission of these two values or smoothing the tail by spline-curve fitting yielded a GETHEN solution. The three components eventually selected are shown in Figure 4.4. Component 2 has mean and standard deviation equal to -1.202 and 0.206. The mean and standard deviation of Component 3 are -0.538 and 0.167, respectively. Although the fit in Figure 4.4 is better than that in Figure 4.3, it should be kept in mind that the parameters of Components 2 and 3 are less well established than those for Component 1. In several of the original samples, Components 2 and 3 are not clearly recognizable.

In Figure 4.4 it can be seen that the lower value tail of Component 2 has practically disappeared at value -1.8. The same applies to Component 3 at value -1.0. Also, the highest value tail of Component 1 has vanished at value -1.0. These properties of the three components can be used for determining their proportions in the ten original samples.

On the basis of Figure 4.4 it can be assumed that the cumulative frequency at value -1.8 constitutes 81.1% of the proportion of Component 1 in each sample. The remainder can be assigned to Components 2 and 3 combined. Suppose that the observed frequencies for classes are reduced by removing the expected frequencies for Component 1. Because the mean and standard deviation of Component 2 are -1.202 and 0.206, it can be estimated that 83.7% of the proportion of Component 2 can be set equal to the cumulative frequency of the remainder at value -1.0. These percentage values (81.1 and 83.7, respectively) were obtained from statistical tables of fractiles for the normal distribution in standard form as applied to Components 1 and 2, respectively. The resulting proportions of the three components in each of the samples are shown in Table 4.3.

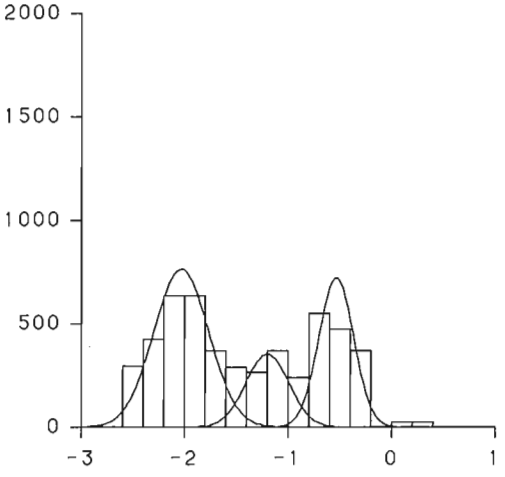

Figure 4.4. *Component 1 (mean = -2.033 and standard deviation = 0.265) was removed from standard and GETHEN solution of two normal distributions obtained for remainder. This gave Component 2 (mean = -1.202; standard deviation = 0.206) and Component 3 (mean = -0.538; standard deviation = 0.167). The result is three separate normal curves for standard. For statistics, see Table 4.3. For labels of axes, see caption of Figure 4.2.*

Figure 4.5 shows how much of each component was identified in each sample by assuming that each of the three components shown in Figure 4.4 is indeed present in each sample.

In general, the fit for Component 1 is excellent in Figure 4.5 and is close to the results obtained for Component 1 in Figure 4.2. Separation of the remainder into two components is clearly justified for some samples, notably WN1-160, WN1-223, WN1-245 and WN1-303. However, in other samples this separation may not be meaningful. Also, spurious results were obtained for some samples; e.g. in WN2-85 where the little peak for Component 3 is due to the single observed value in the -0.8 to -1.0 class.

GOODNESS OF FIT OF TWO- AND THREE-COMPONENT MODEL

The curves in Figures 4.3 and 4.4 can be integrated between class limits and the resulting expected frequencies compared to the observed frequencies. As mentioned at the beginning of this paper, the results of chi-squared tests cannot be interpreted because the frequencies were given in volume per cent and it is not known to how many single "observations" they correspond. Within the range from -3.0 to 1.0, there are 20 classes with width equal to 0.2. The observed values for these classes may be written as y_k, k = 1, 2, ..., n with n = 20. Various statistical models labelled i (i = 0, 1, 2, 3) yield calculated values $\hat{y}_{ik}$ and residuals $\hat{e}_{ik} = y_k - \hat{y}_{ik}$. The sum of squared residuals will be written as $E_i = \sum_{k=1}^{n} \hat{e}_{ik}^2$. The average porosity is 4964 ppm (or 0.4964%). Suppose first (for i = 0) that the frequency distribution is uniform with $\hat{y}_{0k} = \bar{y} = 248.2$. Then, $E_0 = 987{,}097$.

After fitting 1, 2 and 3 Gaussian curves with i = 1, 2, 3, respectively, $E_1 = 550{,}482$; $E_2 = 142{,}720$; and $E_3 = 103{,}985$ are obtained. The ratios $R_i = E_{i-1}/E_i$ for i = 1, 2, 3 satisfy $R_1 = 1.79$, $R_2 = 3.86$, and $R_3 = 1.37$. These ratios are all greater than 1.00 which would correspond to the situation of no improvement in fit. The technique of analysis of variance cannot be applied because appropriate numbers of degrees of freedom are not known.

Suppose that a measurement error of y_k is defined as a random variable without autocorrelation. One definitely would have to stop fitting curves of more complex shapes

Table 4.3. Proportions of three components (as extracted from standard) in individual samples

Sample	Proportions C_1	C_2	C_3	Porosities ϕ_T	ϕ_1	ϕ_2
WN2-24	0.519	0.260	0.221	0.496	0.257	0.129
WN2-85	0.749	0.215	0.036	0.764	0.572	0.164
WN1-138	0.385	0.137	0.478	0.421	0.162	0.058
WN1-160	0.590	0.179	0.231	0.605	0.357	0.108
WN1-223	0.462	0.194	0.344	0.421	0.195	0.081
WN1-245	0.540	0.102	0.358	0.421	0.227	0.043
WN1-303	0.000	0.326	0.674	0.289	0.000	0.094
WN1-345	0.336	0.141	0.523	0.288	0.097	0.040
WN1-385	0.617	0.339	0.044	0.526	0.325	0.178
WN1-410	0.352	0.134	0.514	0.580	0.204	0.078
Standard	0.512	0.184	0.304	0.496	0.254	0.091

The three components are total porosity (ϕ_T), and porosities for Components 1 and 2. Porosities are given in per cent.

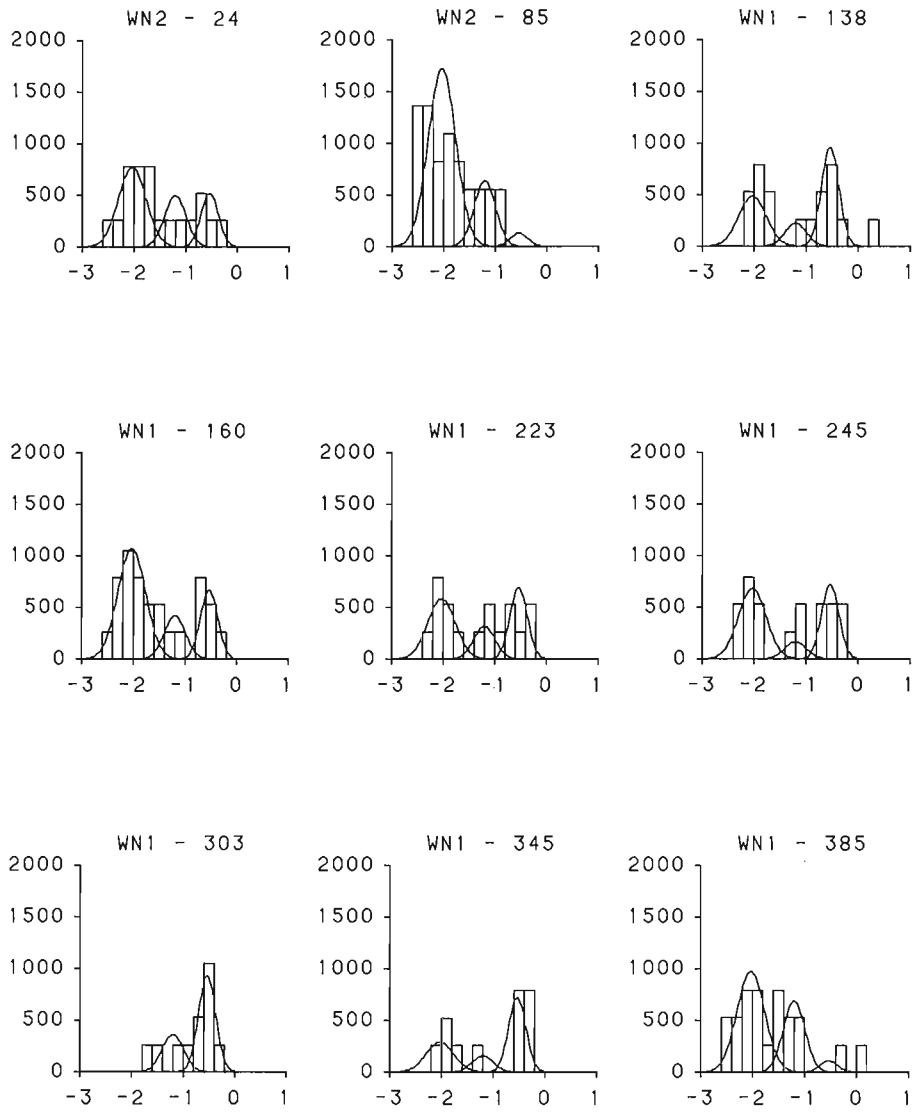

Figure 4.5

Three components for standard (see Fig. 4.4) were extracted from each individual sample according to method described in the text. For corresponding statistics, see Table 4.3. For labels of axes, see caption of Figure 4.2.

when the point of residuals without autocorrelation is reached. The residuals can be tested for serial correlation either by calculating the first serial correlation coefficient:

$$r_{1_i} = \frac{n \sum_{k=1}^{n-1} \hat{e}_{i,k+1} \cdot \hat{e}_{ik}}{(n-1)\, E_i}$$

or the Durbin-Watson statistic:

$$d_i = \sum_{k=1}^{n-1} (\hat{e}_{i,k+1} - \hat{e}_k)^2 / E_i$$

For the first serial correlation coefficient r_{1_i} (i = 0, 1, 2, 3): $r_{10} = 0.75$; $r_{11} = 0.55$; $r_{12} = -0.07$; and $r_{13} = -0.39$. Suppose that these values are compared to zero by using the significance limits for serial correlation coefficients (see e.g. Quenouille, 1952, p. 166). Significance limits for zero autocorrelation are approximately 0.38 and -0.49 for $\alpha = 0.01$ where α represents level of significance. Clearly, r_{10} and r_{11} probably are greater than zero; but r_{12} and r_{13} could be zero. Unfortunately, this test does not help us in deciding whether or not it is justified to proceed from the two-component model of Figure 4.3 to the three-component model of Figure 4.4.

For the Durbin-Watson statistic d_i (i = 0, 1, 2, 3): $d_0 = 0.51$; $d_1 = 0.89$; $d_2 = 2.15$; and $d_3 = 3.78$. When it is attempted to test these values for being indicative of positive autocorrelation, a new problem is encountered: this particular test was developed by Durbin and Watson (1951) for multiple regression of one dependent variable on k' independent variables (k' = 1, 2, ..., 5 in Durbin and Watson's statistical tables). The value of k' is not known because the method of least squares for a linear model was not applied in our study. It may be assumed that approximately k' = 2, for i = 1, and k' = 5 for i = 2. For $\alpha = 0.05$, the tabulated significance limits d_L and d_U of d are approximately 1.10 and 1.54 for k' = 2, and 0.79 and 1.99 for k' = 5. This would indicate significant (non-zero) autocorrelation for d_1, whereas the opposite holds true for d_2.

Table 4.4. Fracture flexibility (ε) and porosity data of granite samples from Lac du Bonnet batholith

		Porosities**			
Sample	ε*	$\phi_{sn,n}$	ϕ_{int}	ϕ_m	ϕ_T
WN2-24	2.31	0.29	0.05	0.16	0.50
WN2-85	2.62	0.55	0.11	0.11	0.76
WN1-138	3.84	0.18	0.00	0.24	0.42
WN1-160	4.54	0.34	0.08	0.18	0.60
WN1-223	3.58	0.18	0.03	0.21	0.42
WN1-245	4.03	0.18	0.03	0.21	0.42
WN1-303	3.62	0.03	0.03	0.24	0.29
WN1-345	3.92	0.10	0.03	0.16	0.29
WN1-385	4.30	0.29	0.13	0.11	0.53
WN1-410	4.37	0.21	0.08	0.29	0.58
	($\times 10^{-4}$)	(%)	(%)	(%)	(%)

* Annor and Katsube (1983)
** Katsube (1981)

$\phi_{sn,n}$, ϕ_{int}, ϕ_m and ϕ_T are the nano- and subnano pore porosity, intermediate pore porosity, micropore porosity and total porosity, respectively.

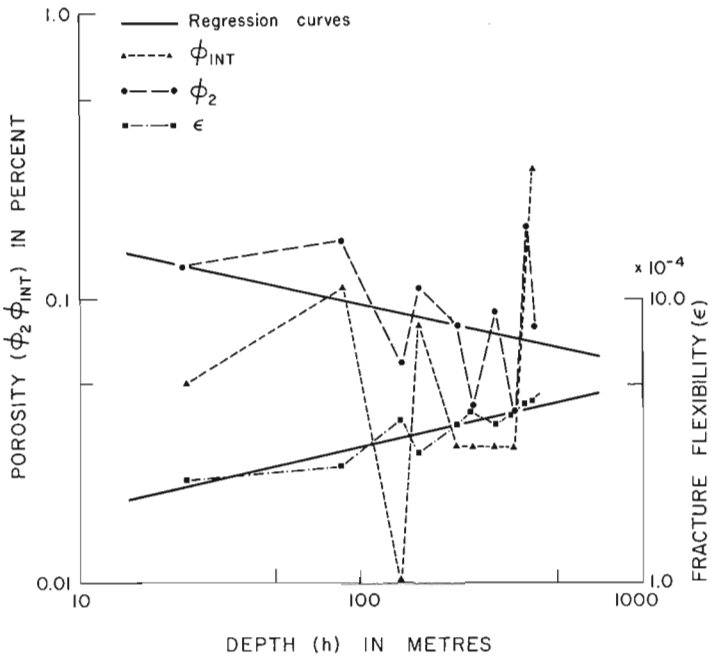

Figure 4.6. Variation with depth (h) for porosities ϕ_2, ϕ_{int} and fracture flexibility ε.

According to the preceding approximate Durbin-Watson test we are therefore justified in fitting two normal distributions but there is no clear-cut reason for fitting three normal distributions. These statistical considerations are in agreement with the evaluations based on visual inspection of the illustrations (Fig. 4.2-4.4) presented earlier. However, it will be demonstrated in the next section that all three components are meaningful by relating them to one another and to other variables (notably depth and fracture flexibility).

APPLICATION TO PORE STRUCTURE STUDIES

The newly developed statistical technique for trimodal distribution analysis will now be applied to previous data (Katsube, 1981) in order to evaluate its significance.

The porosities ϕ_1, ϕ_2 and ϕ_3 can be equated to nano and subnano pore porosity $\phi_{sn,n}$, intermediate pore porosity ϕ_{int} and micropore porosity ϕ_m of the previous work. In the previous work the three porosities were determined on the basis of visually determined boundaries of 0.025 and 0.063 μm. The two sets of porosity data are listed in Table 4.4. Note that there is little difference between the values of ϕ_1 and $\phi_{sn,n}$, but there is a significant difference between ϕ_2 and ϕ_{int}. For example, in samples WN2-223, WN1-245, WN1-303 and WN1-345, ϕ_{int} is 0.03 for all, but ϕ_2 varies between 0 04 to 0 09 The mean value $\bar{\phi}_2$ has increased to 0.09 from $\bar{\phi}_{int} = 0.06$. Changes between ϕ_m and ϕ_3 also exist but are generally not significant compared to those between ϕ_{int} and ϕ_2.

In the previous work (Katsube, 1981), the porosities $\phi_{sn,n}$, ϕ_{int} and ϕ_m were compared with fracture flexibility (ε) and effective porosity (ϕ_E). The parameter ε is determined by a mechanical test and represents the strain at a pressure of 10 MPa (Annor and Katsube, 1983). This strain is affected by the flexibility of the micropores and microfractures. The effective porosity (ϕ_E) is determined by immersion porosity measurements (previously represented by "immersion porosity" ϕ_1), which is based on the mass

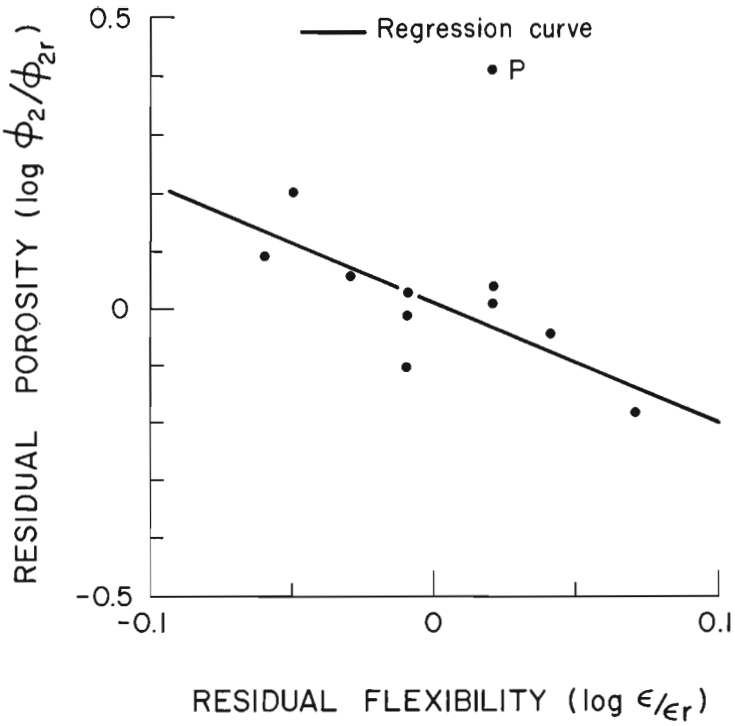

Figure 4.7. Correlation between residuals of porosity $\log_{10}$ (ϕ_2/ϕ_{2r}) and of fracture flexibility $\log_{10}$ (ϵ/ϵ_r).

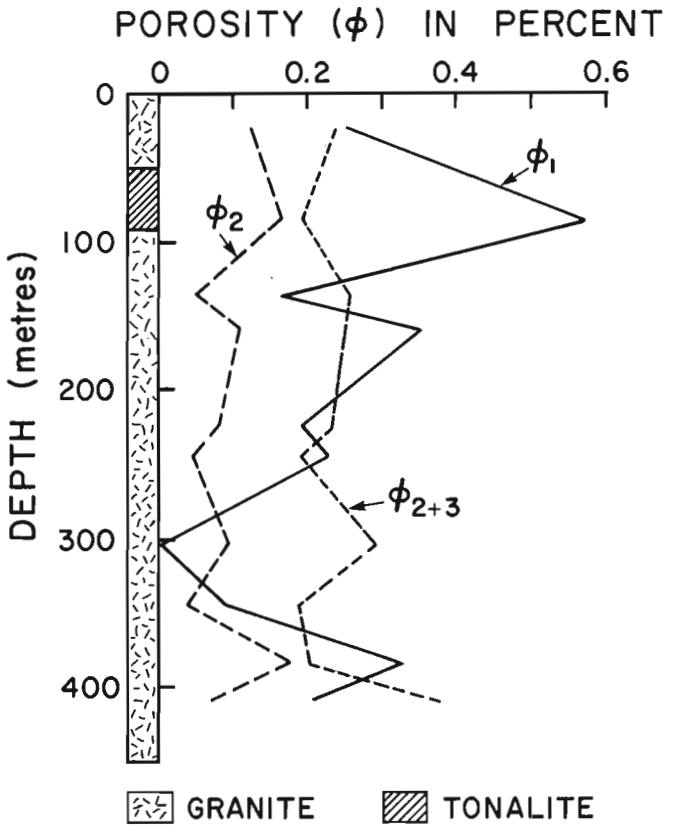

Figure 4.8. Porosities for separate components of Table 4.3 are shown against depth. Note that ϕ_{2+3} remains nearly constant above WN1-410 and that ϕ_1 is variable with a minimum in the vicinity of 300 m.

difference between the rock specimen when water saturated and oven dry. The results of the comparison showed a correlation coefficient (r) of 0.94 and 0.80, respectively. When these three porosities are replaced by ϕ_1, ϕ_2 and ϕ_3 no significant changes in these values are seen. This implies that there is no change in the conclusions reached in previous work, because of replacing the analytical technique.

However, there is a good relationship seen between the variations of ϵ and ϕ_2, which was not noticed when ϵ was related to ϕ_{int}. The variables ϵ, ϕ_2 and ϕ_{int} are plotted against depth (h) in Figure 4.6. There is a general increase of ϵ, and a general decrease of ϕ_2 with depth (h). These general trends are represented by the following regression curves:

$$\epsilon_r = 1.07\ h^{0.23} \qquad (r = 0.91)$$

$$\phi_{2r} = 0.26\ h^{-0.22} \qquad (r = -0.35)$$

The residuals of $\log_{10} \phi_2$ plotted against those of $\log_{10} \epsilon$ are shown in Figure 4.7. The correlation is relatively good (r = -0.85) when the anomalous point "P" (WN1-384) is ignored. No effect of depth on ϕ_{int} is seen, and the correlation between $\log_{10} \phi_{int}$ and $\log_{10} \epsilon$ is not so good (r = -0.68) even if the same point for WN1-384 is ignored.

Porosities ϕ_1, ϕ_2 and ϕ_{2+3} ($\phi_2+\phi_3$) are plotted against depth in Figure 4.8. The variations with depth for ϕ_2 and ϕ_{2+3} are small compared to those of ϕ_1. A very good correlation between the total porosity (ϕ_T) and ϕ_1 is shown in Figure 4.9. Initially, regression lines were obtained, as follows, for the cases where the plot for WN1-410 is included and excluded, respectively:

(includes WN1-410) $\phi_T = 0.27 + 0.86\phi_1$ (r = 0.92)
(excludes WN1-410) $\phi_T = 0.25 + 0.89\phi_1$ (r = 0.98)

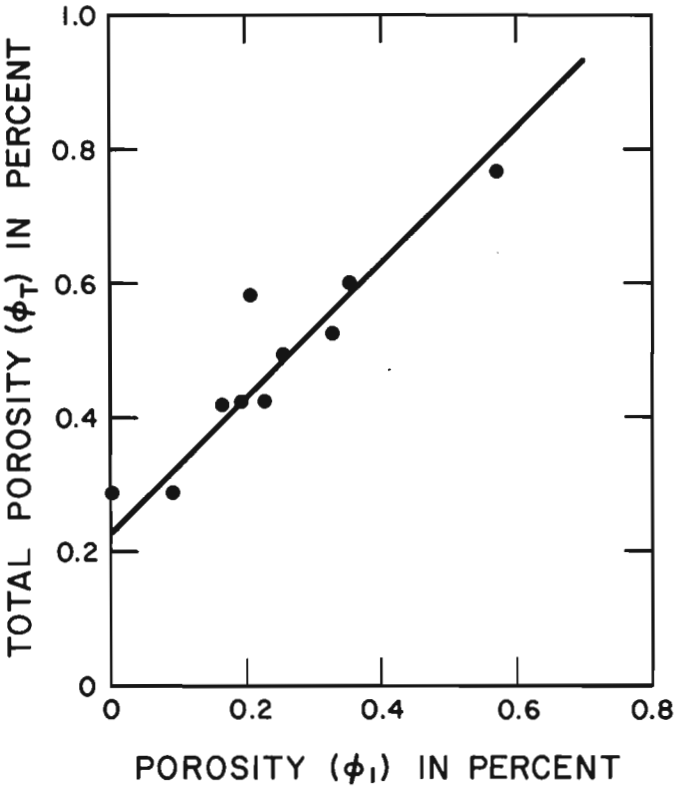

Figure 4.9. Total porosity (ϕ_T) plotted against porosity (ϕ_1) of first component. For statistics, see Table 4.3. Straight line with equation ϕ_T = constant + ϕ_1 was fitted by method of least squares to all values except "outlier" for WN1-410.

This implies that the total porosity (ϕ_T) consists of a constant component of $\phi_2+\phi_3$, and a varying component of ϕ_1. The ϕ_T axis intercept for these regression lines is 0.25-0.27, and the mean value (± standard deviation) of $\phi_2+\phi_3$ is 0.24 ± 0.06. It is interesting that these values are close to 0.29 which is the minimum value of ϕ_E (Katsube, 1981). If ϕ_1 is regressed on ϕ_T, instead of ϕ_T on ϕ_1 as above, lines with a steeper dip are obtained. The straight line plotted in Figure 4.9 has angle of slope equal to 45°. It was obtained by means of the method of least squares forcing the slope to be equal to unity and excluding WN1-410. Then the linear relationship is simply $\phi_T = 0.24 + \phi_1$ where 0.24 is the mean value of $\phi_2 + \phi_3$.

CONCLUSIONS

As a result of a bimodal analysis (GETHEN run) of the mercury porosimetry data, a porosity component with a mean aperture of near 10^{-2} µm was extracted from nearly all 10 samples that were analyzed. Based on these results a new method has been developed to determine the porosities of the three pore groups in a trimodal porosity distribution. When this new method is applied to mercury porosimetry data of 10 granitic rock samples, the results do not necessitate any changes in previously reached conclusions. They show the strength of this method in revealing trends not seen before in areas where porosity data are scarce and sporadic, such as the intermediate pore size range or the range of ϕ_2. This is the pore size range of 0.025 to 0.063 µm. Therefore, this new method shows considerable promise as an advanced technique for analyzing mercury porosimetry data, and should be applied on a routine basis.

Some interesting data regarding pore structure has been obtained. It appears that the variations in ϕ_2 is related to those in fracture flexibility (ε). The total porosity (ϕ_T) which is obtained from the mercury porosimetry, consists of a relatively constant porosity component of pores larger than 0.025 µm, and a considerably variable porosity component of pores smaller than 0.025 µm. The mean value of the relatively constant component is 0.24 ± 0.06% and is close to the value of 0.29% which is the minimum value of the effective porosity for these samples. Determining the reasons for these trends is a worthwhile pursuit for the future.

ACKNOWLEDGMENTS

The authors thank J.B. Percival and J.P. Hume (Geological Survey of Canada) for their comments.

REFERENCES

Annor, A. and Katsube, T.J.
1983: Nonlinear elastic characteristics of granite rock samples from Lac du Bonnet Batholith; in Current Research, Part A, Geological Survey of Canada, Paper 83-1A, p. 411-416.

Brace, W.F.
1977: Permeability from resistivity and pore shape; Journal of Geophysical Research, v. 82, no. 23, p. 3343-3349.

1980: Permeability of crystalline and argillaceous rocks; International Journal of Rock Mechanics, Mining Sciences and Geomechanics Abstracts, v. 17, p. 241-251.

Brace, W.F., Walsh, J.B., and Frangos, W.T.
1968: Permeability of granite under high pressure; Journal of Geophysical Research, v. 73, no. 6, p. 2225-2236.

Bradbury, M.H., Lever, D., and Kinsey, D.
1980: Aqueous phase diffusion in crystalline rock; in Scientific Basis for Nuclear Waste Management V, Volume 11; Elsevier, New York, N.Y., p. 569.

Bridges, N.J. and McCammon, R.B.
1980: DISCRIM: a computer program using an interactive approach to dissect a mixture of normal or lognormal distributions; Computers and Geoscience, v. 6, no. 4, p. 361-396.

Clark, I.
1977: ROKE, a computer program for nonlinear least-squares decomposition of mixtures of distributions; Computers and Geoscience, v. 3, no. 2, p. 245-256.

Clark, M.W.
1977: GETHEN, a computer program for the decomposition of mixtures of two normal distributions by the method of moments; Computers and Geoscience, v. 3, no. 2, p. 257-267; Errata, ibidem, v. 4, no. 4, p. 373-374.

Durbin, J. and Watson, G.S.
1951: Testing for serial correlation in least squares regression; II. Biometrika, v. 38, p. 159-178.

Gordon, A.R.
1945: The diaphram-cell method of measuring diffusion; New York Academy of Sciences, Annals, v. 46, p. 285.

Grisak, G.E. and Pickens, J.F.
1981: An analytical solution for solute transport through fractured media with matrix diffusion; Journal of Hydrology, v. 52, p. 47.

Hald, A.
1952: Statistical Theory and Engineering Applications; Wiley, New York, N.Y., 783 p.

Johnson, N.L. and Kotz, S.
1970: Continuous Univariate Distributions-1; Wiley, New York, N.Y., 300 p.

Katsube, T.J.
1981: Pore structure and pore parameters that control the radionuclide transport in crystalline rocks; Proceedings Technical Program, International Powder and Bulk Solids Handling and Processing, Rosemont, Il1., May 12-14, p. 393-409.

1982: Pore structure parameters of igneous crystalline rocks – their significance for potential radionuclide migration and storage; in Proceedings of the Canadian Nuclear Society; International Conference on Radioactive Waste Management, Winnipeg, Manitoba. Sept. 12-15.

McCammon, R.B.
1969: FORTRAN IV program for nonlinear estimation; Kansas Geological Survey, Computer Contribution, v. 34, 20 p.

Montgomery, C.W. and Brace, W.F.
1975: Micropores in plagioclase; Contributions to Mineralogy and Petrology, v. 52, p. 17-28.

Neretnieks, I.
1980: Diffusion in the rock matrix: an important factor in radionuclide retardation?; Journal of Geophysical Research, v. 85, p. 4379.

Pearson, K.
1894: Contributions to the mathematical theory of evolution; Royal Society of London, Philosophical Transactions, Series A, v. 185, p. 71-110.

Quenouille, M.H.
1952: Associated Measurements; Butterworths, London, England, 242 p.

Rootare, H.M.
1970: A review of mercury porosimetry; Advanced Experimental Techniques in Powder Metallurgy, Plenum, New York, N.Y., p. 225-252.

Simmons, G. and Richter, D.
1976: Microcracks in rocks; in Physics and Chemistry of Minerals and Rocks, ed. R.G.J. Strens; Wiley, New York, N.Y., p. 105-150.

Skagius, K. and Neretnieks, I.
1982: Diffusion in crystalline rocks; in Scientific Basis for Nuclear Waste Management V, Volume 11, p. 509; Elsevier Science Publishing Co., Inc., New York.

Sprunt, E. and Brace, W.F.
1974: Direct observation of microcavities in crystalline rocks; International Journal of Rock Mechanics and Mining Science, v. 11, no. 4, p. 139-150.

Tang, D.H., Frind, E.O., and Sudicky, E.A.
1980: Contaminant transport in fractured porous media. An analytical solution for a single fracture; Water Resources Research, v. 17, p. 555.

Wadden, M.M. and Katsube, T.J.
1982: Radionuclide diffusion in crystalline rocks; Chemical Geology, v. 36, p. 191-214.

5. URANIUM DEPOSIT RESEARCH, 1983

Project 750010

V. Ruzicka and G.M. LeCheminant [1]
Economic Geology Division

Ruzicka, V. and LeCheminant, G.M., Uranium deposit research, 1983; in Current Research, Part A, Geological Survey of Canada, Paper 84-1A, p. 39-51, 1984.

Abstract

Research on uranium deposits in Canada, conducted as a prerequisite for assessment of the Estimated Additional Resources of uranium, revealed that (a) the uranium-gold association in rudites of the Huronian Supergroup preferably occurs in the carbon layers; (b) chloritized ore at the Panel mine, Elliot Lake, Ontario, occurs locally in tectonically disturbed areas in the vicinity of diabase dykes; (c) mineralization in the Black Sturgeon Lake area, Ontario, formed from solutions in structural and lithological traps; (d) the Cigar Lake deposit, Saskatchewan, has two phases of mineralization: monomineralic and polymetallic; (e) mineralization of the JEB (Canoxy Ltd.) deposit is similar to that at McClean Lake; (f) the uranium-carbon assemblage was identified in the Claude deposit, Carswell Structure; and (g) the Otish Mountains area, Quebec, should be considered as a significant uranium-polymetallic metallogenic province.

Résumé

Les travaux de recherche sur les gisements d'uranium au Canada, menés afin d'évaluer les ressources additionnelles estimatives d'uranium, révèlent a) que l'association uranium-or dans les rudites du supergroupe huronien se présente de préférence dans les couches de carbone; b) que le minerai chloritisé à la mine Panel à Elliot Lake, en Ontario, se présente localement dans les zones tectoniquement remaniées aux environs des filons de diabase; c) que la minéralisation dans la région du lac Black Sturgeon, en Ontario, s'est formée à partir de solutions dans des pièges structuraux et lithologiques; d) que le gisement du lac Cigar, en Saskatchewan, comprend deux phases de minéralisation: une phase monominérale et une phase polymétallique; e) que la minéralisation du gisement JEB de la Canoxy Ltd. ressemble à celle du lac McClean; f) que l'assemblage uranium-carbone a été identifié dans le gisement Claude, structure Carswell et g) que la région des monts Otish, au Québec, doit être considérée comme une province métallogénique urano-polymétallique importante.

INTRODUCTION

In spite of declining levels of uranium exploration in Canada over the past three years (exploration expenditures decreased by about 30 per cent annually), more than 200 new occurrences were recorded in the GSC uranium files. Selected key deposits and occurrences from Ontario, Saskatchewan, Quebec, Northwest Territories and Atlantic Canada were studied in detail by the authors. These studies were complementary to assessments of uranium resources conducted on behalf of the EMR Uranium Resource Appraisal Group (EMR Report EP 83-3; Fig. 51a,b). Some results of these studies are presented in this paper.

URANIUM-GOLD MINERALIZATION ASSOCIATED WITH CARBON; MATINENDA FORMATION, ELLIOT LAKE AREA, ONTARIO

Association of uranium and gold with carbon in the Witwatersrand deposits in South Africa has been documented by, among others, Feather and Koen (1975), Hallbauer (1975), Pretorius (1975), Minter (1981), Simpson and Bowles (1981) and Tankard et al. (1982). Uranium in carbonaceous matter from the Huronian Supergroup was reported by Roscoe (1969, 1973), Ruzicka and Steacy (1976), Theis (1979) and Ruzicka (1979, 1981).

Although numerous occurrences of radioactive carbon (commonly called "thucholite") were reported from rocks of the Huronian Supergroup, the quantities are relatively restricted. To better clarify the genesis of Huronian Supergroup carbon, the authors studied samples collected from the Elliot Lake area.

Our observations indicate: (a) several generations of carbon occur in the Huronian, mainly in conglomerates of the Matinenda Formation; (b) the oldest generation of carbon appears to be that deposited during the last phase of upward-fining sedimentary cycles, i.e. in areas of quiescent sedimentation (Ruzicka, 1981); this generation of carbon is usually developed as layers concordant with bedding or as a component in the matrix (Fig. 5.2); (c) younger generations of carbon appear to be remobilized phases of the first generation; they occur as fracture fillings or impregnations of porous rocks commonly discordant to bedding; (d) carbon of the first generation, as observed on samples from Denison mines, Elliot Lake, Ontario, exhibits columnar structure, has sulphur content higher than the younger generations (commonly exceeding 20%) and contains rounded, subrounded and hypidiomorphic to idiomorphic grains of uraninite, monazite, galena, pyrrhotite, and non-particulate gold. D.J. Mossman of Mount Allison University, Sackville, New Brunswick (written communication) studied carbon from the concordant layers in a few samples collected by Ruzicka from Elliot Lake area and found that it contained, in one sample, 1100 ppb Au whereas the underlying sulphide-rich portion without the carbon contained only 94 ppb Au (analyzed by Nuclear Activation Services, Hamilton, Ontario). A layer of carbon about 0.5 cm thick in another sample from the same area contained 2000 ppb Au. Hattori et al. (1981) interpreted some carbon (from the same sample where Mossman detected 1100 ppb Au), using scanning electron microscopic techniques (Fig. 5.3a,b), as having been introduced, post-lithification, along bedding between two sedimentation cycles. The primordial source of this carbon, however, has not been determined and, more evidence is necessary to resolve this problem.

The mineral assemblage in the conglomerate matrix from the upper portion of the Matinenda Formation (from an occurrence at the south shore of Elliot Lake) contains, in addition to auriferous carbon (D.J. Innes, verbal communication), rare-earth-elements-bearing uranothorite (?), large zircons, a Ti-U-Si-Fe phase

[1] Central Laboratories and Technical Services Division

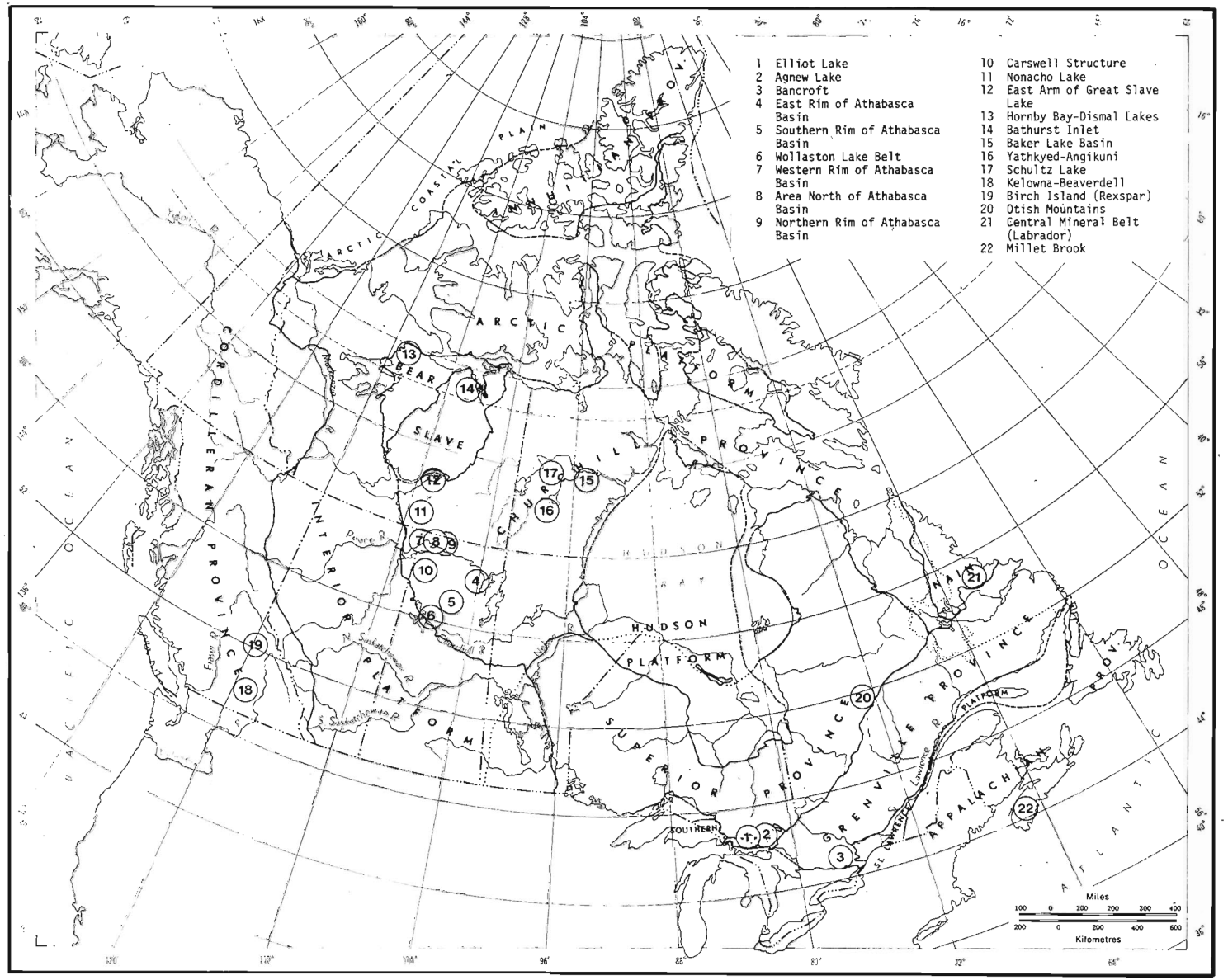

Figure 5.1a. *Uranium resource areas in Canada associated with identified deposits.*

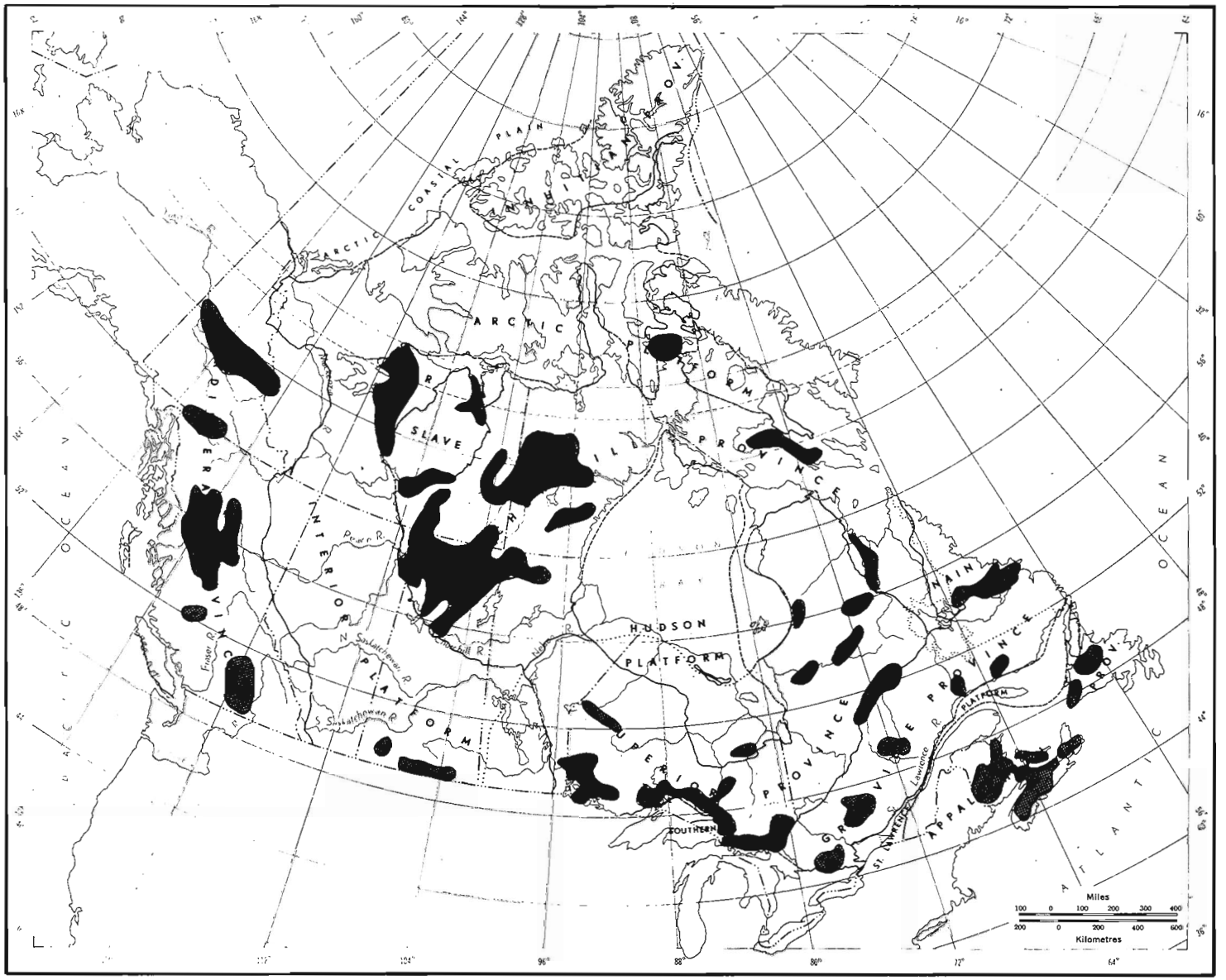

Figure 5.1b. *Areas shown in black indicate prognosticated and speculative uranium resources.*

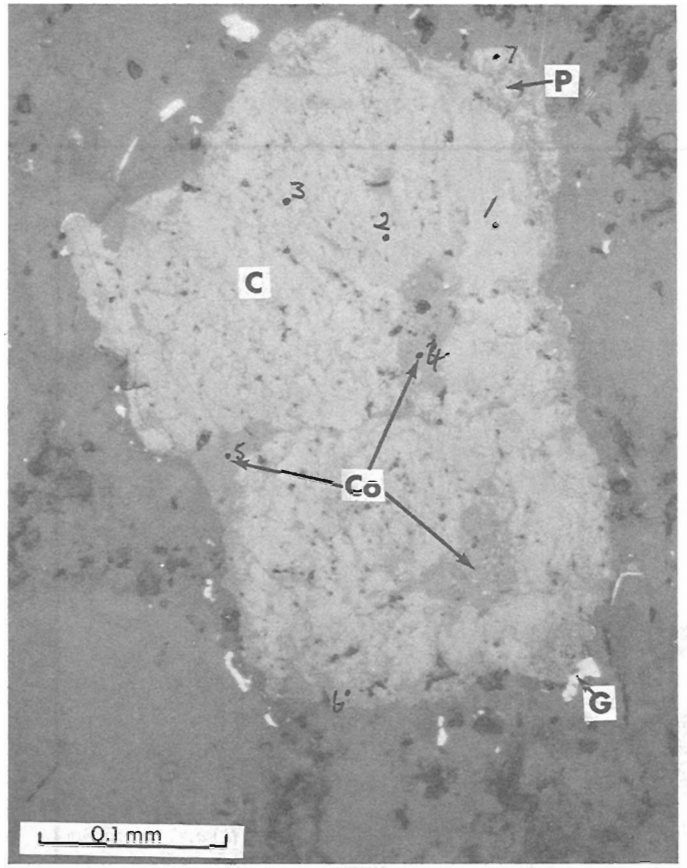

Figure 5.2. *Radioactive carbon ('thucholite') from rocks of the Huronian Supergroup, Quirke 2 mine, Elliot Lake, Ontario; C = carbon containing uranium and sulphur, Co = coffinite, P = pitchblende, G = galena. Photomicrograph, reflected light. Dots with numbers denote microprobe tests.*

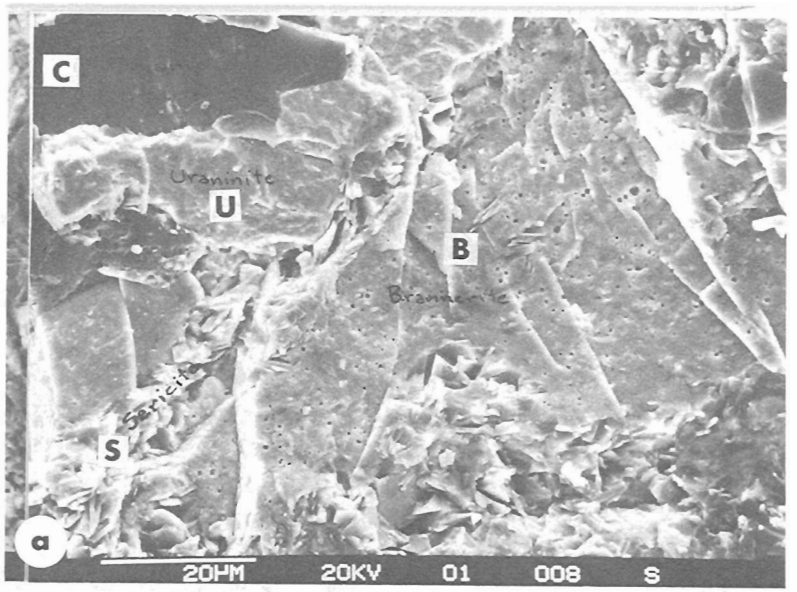

Figure 5.3a. *Carbon (C) associated with uraninite (U), brannerite (B) and sericite (S) from a layer in uraniferous quartz-pebble conglomerate, Denison mine, Elliot Lake, Ontario. Electron photomicrograph by K. Hattori, University of Ottawa. Sample collected by V. Ruzicka.*

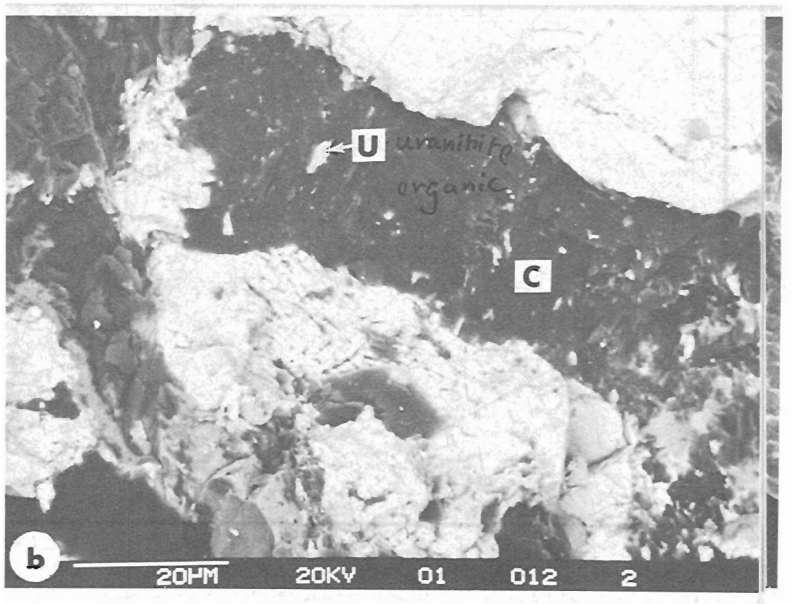

Figure 5.3b. *Carbon (C) containing uraninite (U) from a carbon layer in uraniferous quartz-pebble conglomerate, Denison mine, Elliot Lake, Ontario. Electron photomicrograph by K. Hattori, University of Ottawa. Sample collected by V. Ruzicka.*

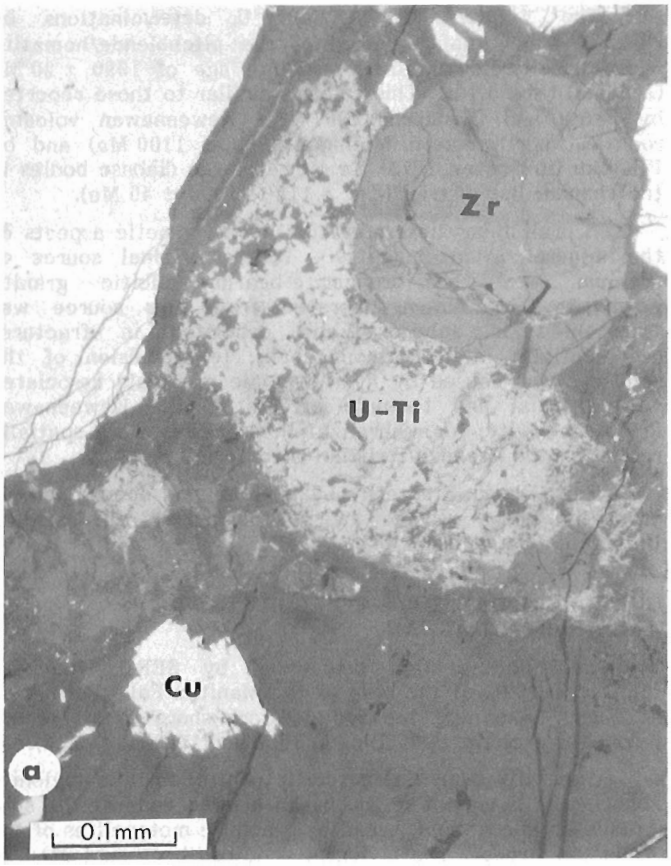

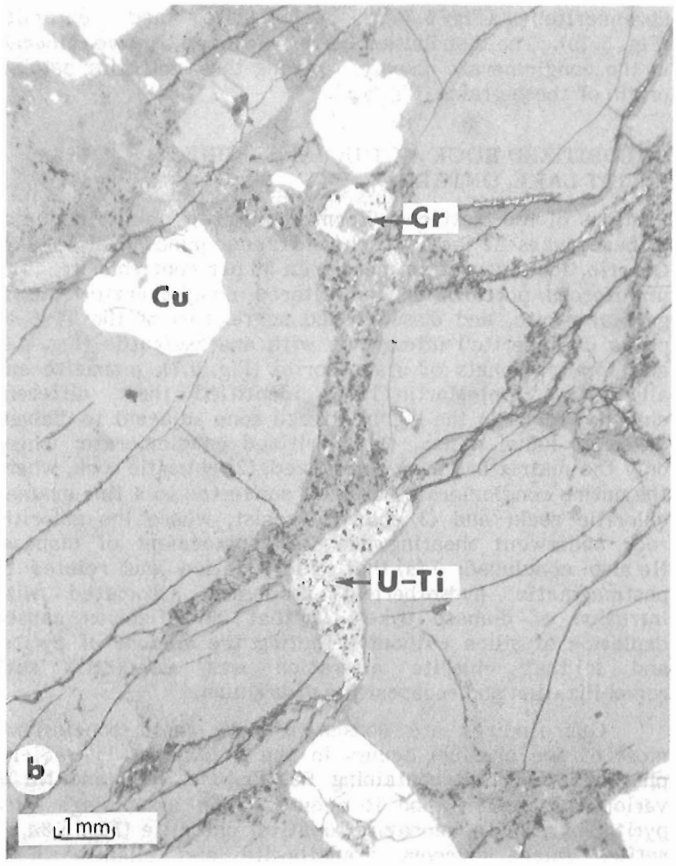

Figure 5.4a,b. *Mineral assemblage in the matrix of the conglomerate from the upper portion of the Matinenda Formation, at the south shore of Elliot Lake, Ontario. Zr = zircon, U-Ti-a Ti-U-Si-Fe phase, Cu = chalcopyrite, Cr = chromite. Photomicrograph, reflected light.*

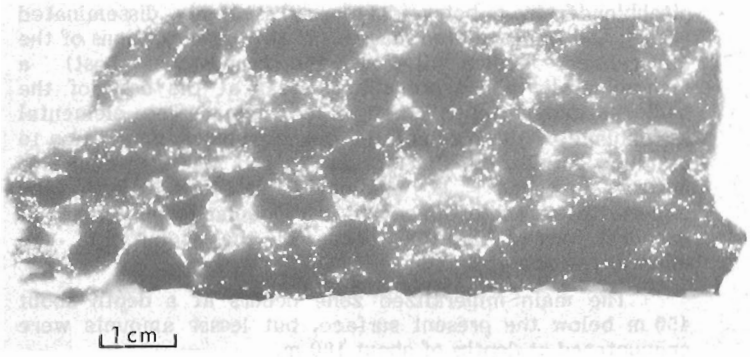

Figure 5.5. *Autoradiograph of a radioactive conglomerate from the south shore of Elliot Lake (Spine Road, Elliot Lake, Ontario. White spots indicate distribution of radioactive minerals.*

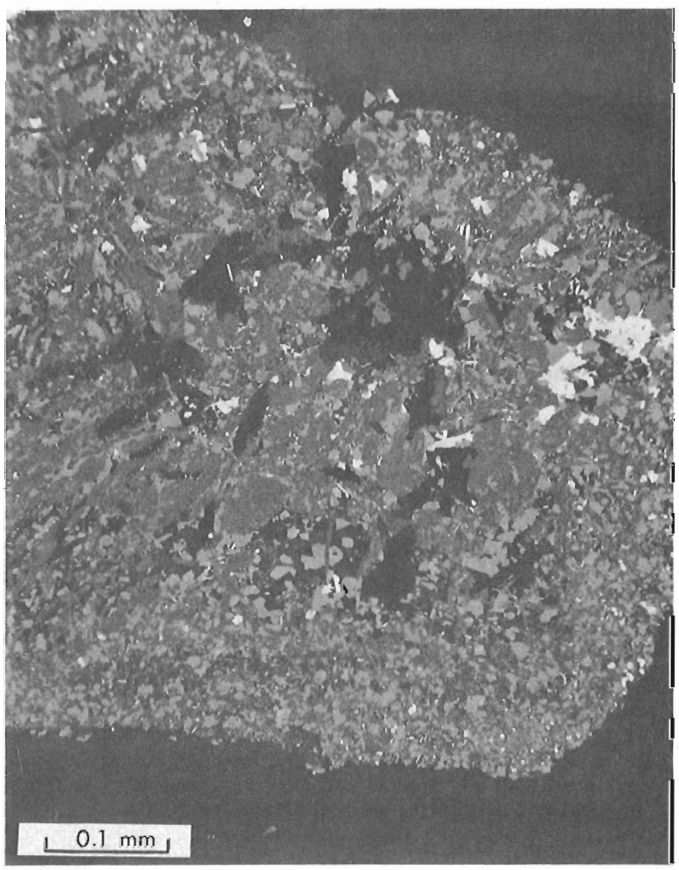

Figure 5.6. *A grain of intergrown Ti-U-Si phase (dark grey) with anatase/rutile (light grey) and galena (white) in quartz-pebble conglomerate from the Panel mine, Elliot Lake, Ontario. Photomicrograph, reflected light.*

('brannerite') (Fig. 5.4a), chalcopyrite and chromite (Fig. 5.4b). The distribution of the most radioactive minerals in the conglomerate displays layering thus indicating detrital origin of these grains (Fig. 5.5).

CHLORITIZED ROCK AT THE PANEL MINE, ELLIOT LAKE, ONTARIO

Portions of the Matinenda Formation in the vicinity of major diabase dykes in the Denison and Panel mines, Elliot Lake, Ontario, locally contain more than 50 per cent chlorite. The uraniferous portions of the altered conglomerate contain galena, pyrite, and disseminated aggregates of the Ti-U-Si phase ('brannerite') intergrown with anatase/rutile (Fig. 5.6) and small amounts of uranothorite (Fig. 5.7), monazite and allanite. Saint-Martin (1983) identified three different chloritic rocks in the highly altered zone adjacent to diabase dykes at Panel mine: (1) chloritized conglomerate, where only the matrix has been chloritized; (2) chloritic rock, where the entire conglomerate has been converted to a fine grained chloritic rock; and (3) chloritic schist, where the chloritic rock underwent shearing due to emplacement of diabase. He also concluded: (a) that chloritization was related to postmagmatic hydrothermal processes associated with intrusion of diabase dykes; (b) that chloritization caused depletion of silica without affecting the amount of pyrite; and (c) that chlorite alteration was associated with remobilization and redeposition of uranium.

Our findings are consistent with these conclusions: most of the uranium occurs in the authigenic Ti-U-Si-Fe phase ('brannerite') containing Pb, Fe, Ce, REE and Nb in various proportions and it occurs in an assemblage with pyrite, pyrrhotite, monazite, apatite, chromite (Fig. 5.8a,b), rutile, galena, zircon, uranothorite and allanite in a chlorite/pyrite matrix. Locally the chlorite grades into biotite. The chloritization is developed only locally, usually in tectonically disturbed portions of the deposits in the vicinity of major diabase dykes.

URANIUM MINERALIZATION IN THE BLACK STURGEON LAKE AREA, ONTARIO

Recent geological mapping in the Lake Nipigon area revealed a new uranium occurrence (Sutcliffe, 1981). J.F. Scott of the Ontario Ministry of Natural Resources, Thunder Bay office, later identified a uranium occurrence east of the Black Sturgeon Lake area, Ontario (Fig. 5.11). This occurrence was further explored by Uranerz Exploration and Mining Limited. The prospect is at present dormant. The geology of the area was described by Coates (1972).

The uranium mineralization occurs mainly as filling in northwesterly trending fractures in Archean (?) ferruginous rocks ('Iron Formation' of Coates) and as disseminations in albitic granite pegmatite. The Helikian Sibley Group rocks, which unconformably overlie the Archean, are exposed about 6 km northwest and 10 km southeast of the uranium occurrence. Diabase sills occur at various levels beneath, within and above the Sibley sedimentary rocks.

Mineralization in the fractures consists essentially of pitchblende, intimately intergrown with hematite. The pitchblende forms veinlets and specks up to a few millimetres wide (Fig. 5.9) and is locally associated with copper mineralization. Brannerite in the albitic granite pegmatite is in discrete grains irregularly distributed in the rock (Fig. 5.10). A whole rock delayed neutron activation analyses of a grab sample from the mineralized ferruginous rock detected 0.74 per cent U and that of a grab sample from the mineralized pegmatite showed 0.06 per cent U.

The $^{206}Pb/^{238}U$, $^{207}Pb/^{235}U$ determinations by Geospec Consultants Limited of the pitchblende/hematite mineralization indicated an absolute age of 1090 ± 20 Ma (2 sigma) (Fig. 5.12). This value is similar to those reported by Faure and Chaudhuri (1967) for Keweenawan volcanic rocks in northwestern Michigan (980 to 1100 Ma) and by Franklin (in Coates, 1972) for Keweenawan diabase bodies in the Thunder Bay district (837 ± 115 to 1080 ± 40 Ma).

A preliminary interpretation of the genetic aspects of the mineralization indicates: (a) the original source of uranium was the brannerite-bearing albitic granite pegmatite; (b) uranium liberated from this source was transported in solutions and deposited in fractures preferentially in ferruginous rocks; (c) propulsion of the solutions was caused by hydrodynamic gradients associated with thermal and tectonic effects of the Keweenawan igneous activity; (d) mineralization processes were spatially related to the Archean/Helikian unconformity.

The Black Sturgeon Lake uranium occurrence is presently being studied by S.V. Thompson at Carleton University, Ottawa.

CIGAR LAKE DEPOSIT, WATERBURY LAKE AREA, SASKATCHEWAN

Uranium mineralization discovered by SERU Nucleaire Limitée in 1981, at the base of the Manitou Falls Formation at Cigar Lake near the southwestern shore of Waterbury Lake, was explored by drilling in 1982 and 1983 (Fig. 5.13).

Mineralization is structurally controlled by a mylonite zone in the basement rocks, by an altered zone at the sub-Athabasca unconformity, and by graphitic metapelites of the Wollaston Group. The mylonite zone has been subjected to faulting and cross faulting. Retrograde metamorphism resulted in extensive clay (kaolinite, illite and chlorite) alteration of the host rocks.

The uranium mineralization consists almost entirely of pitchblende, which occurs in several forms: as massive concentrations, often crosscut by veinlets of younger pitchblende; in a botryoidal form; as finely disseminated grains; and in brecciated masses. In the upper portions of the mineralized bodies (i.e. in the sandstone host) a monomineralic phase prevails whereas at the base of the bodies a polymetallic phase is common. The elemental assemblage of the polymetallic phase includes, in addition to uranium, Ni, Co, Pb, Cu, Mo, As, Zr and Zn. Carbonaceous matter (kerogen?) is commonly associated with the mineralization and often occurs in a globular form. Druses of euhedral quartz crystals occur in the vicinity of the mineralized zone.

The main mineralized zone occurs at a depth about 450 m below the present surface, but lesser amounts were encountered at depths of about 100 m.

JEB URANIUM OCCURRENCE NEAR McCLEAN LAKE, SASKATCHEWAN

As a result of the 1982 winter exploration program on the Wolly property Canadian Occidental Petroleum Limited in partnership with Inco discovered a mineralized zone named 'JEB' about 10 km north of the McClean Lake deposit. The zone was tested by ten drillholes; at a depth of about 90 m five of them intersected uranium mineralization ranging from 0.23% U over a 4.6 m core length to 7.86% U over 7 m. The strike length of the tested mineralization is about 122 m (Canadian Oxy, 1982, Annual Report).

The mineralization of the JEB Zone resembles that of the McClean Lake deposit (Saracoglu et al., 1983). In addition to massive and nodular pitchblende it contains secondary uranium, molybdenum and nickel minerals.

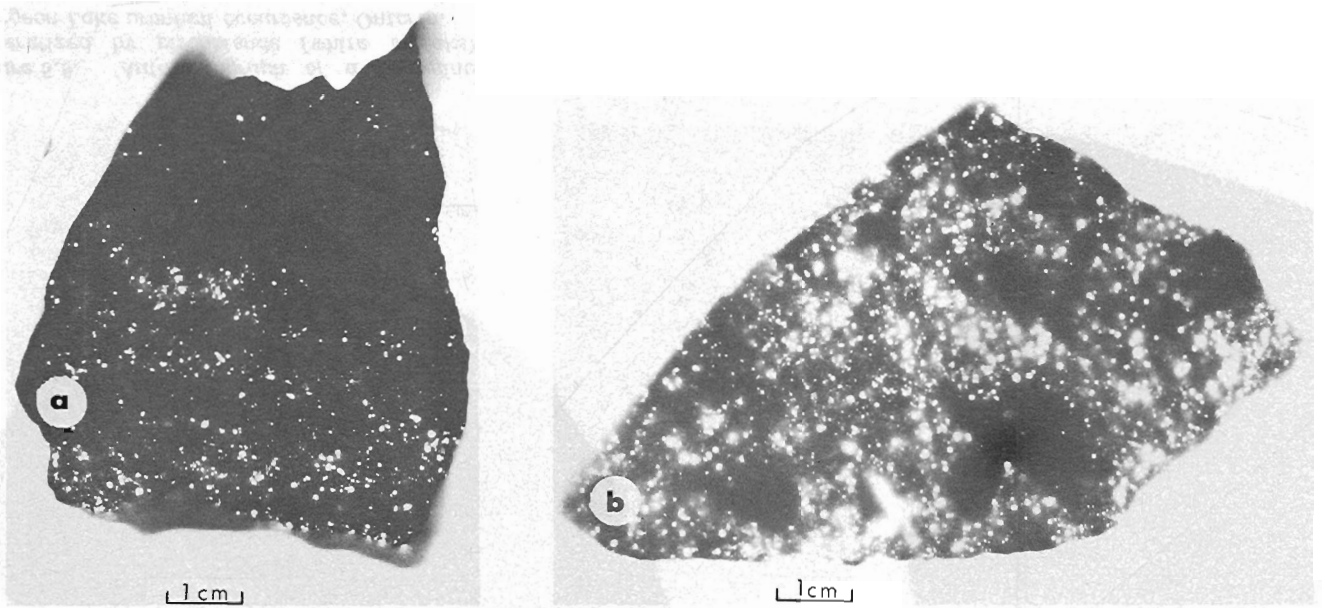

Figure 5.7a,b

Autoradioluxograph of highly chloritized conglomerate from the Panel mine, Elliot Lake, Ontario; the white spots indicate presence of radioactive minerals (uranothorite, uranium-bearing monazite and allanite). (a) about 100 m from the diabase dyke; (b) in the vicinity of the diabase dyke.

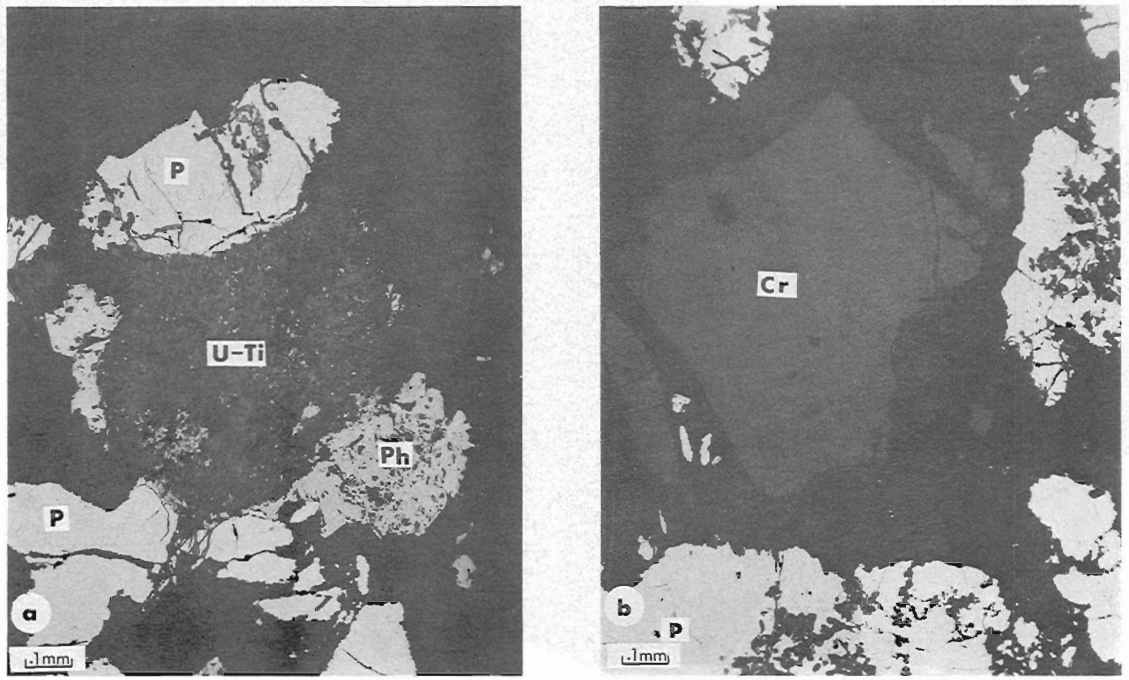

Figure 5.8a,b. *Photomicrographs of a sample from a chloritized conglomerate, Panel mine, Elliot Lake, Ontario. Pyrite (P), pyrrhotite (Ph), Ti-U-Si phase (Ti-U) and chromite (Cr). Reflected light.*

Figure 5.9. *Autoradiograph of a ferruginous rock mineralized by pitchblende (white streaks); Black Sturgeon Lake uranium occurrence, Ontario.*

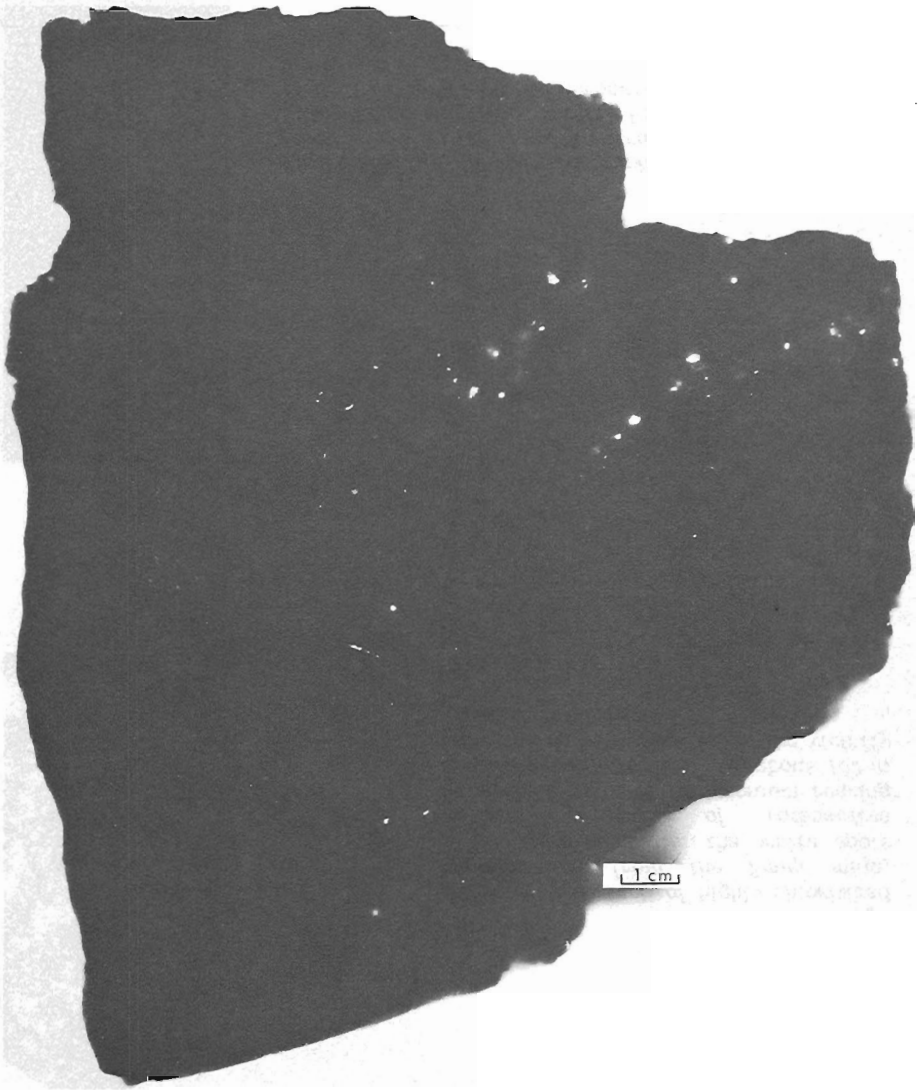

Figure 5.10. *Autoradiograph of an albitic granite pegmatite mineralized by brannerite (white spots); Black Sturgeon Lake uranium occurrence, Ontario.*

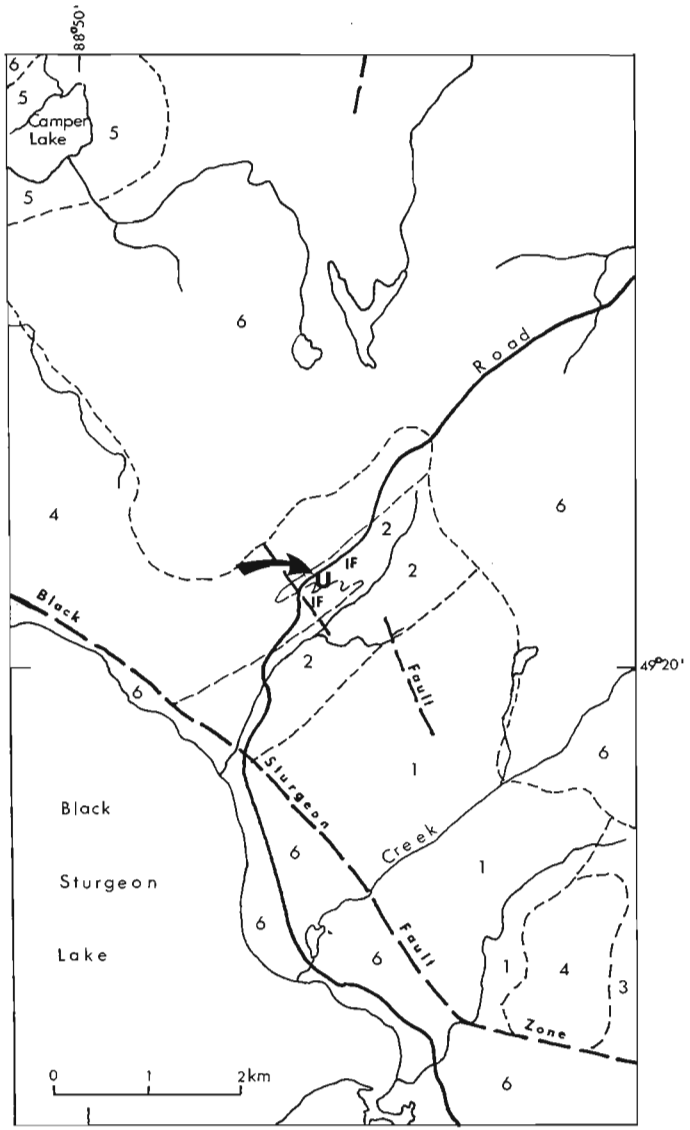

Figure 5.11. *Location of the Black Sturgeon Lake uranium occurrence (U); Archean (1-4): (1) metavolcanics, (2) metasedimentary rocks, (3) migmatite, (4) felsic igneous and metamorphic rocks, IF = Iron Formation; Proterozoic (5,6): (5) Sibley Group rocks, (6) diabase. Geology after Coates (1972).*

Figure 5.12. *Concordia plot of pitchblende mineralization; Black Sturgeon Lake uranium occurrence, Nipigon area, Ontario. Analyses of two samples (A and B).*

Figure 5.13. *Location of the Cigar Lake deposit, Waterbury Lake area, Saskatchewan.*

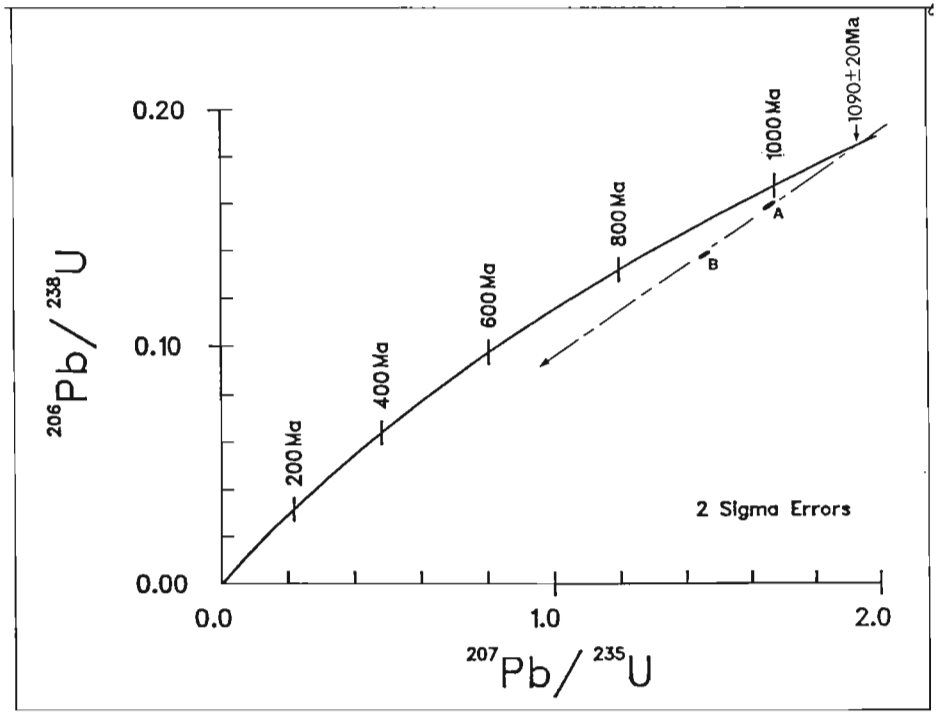

Figure 5.12

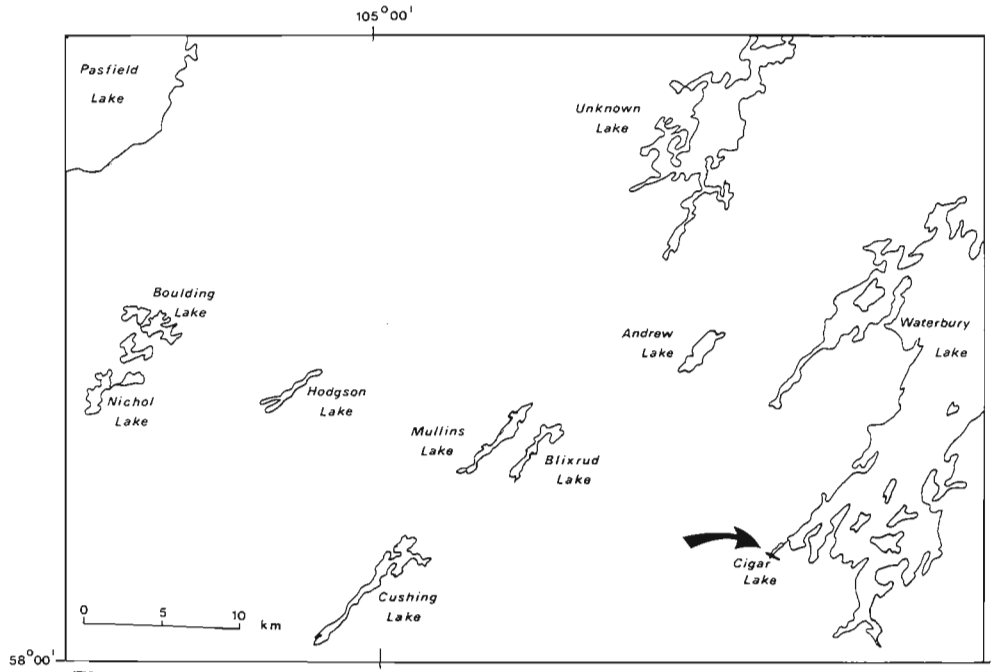

Figure 5.13

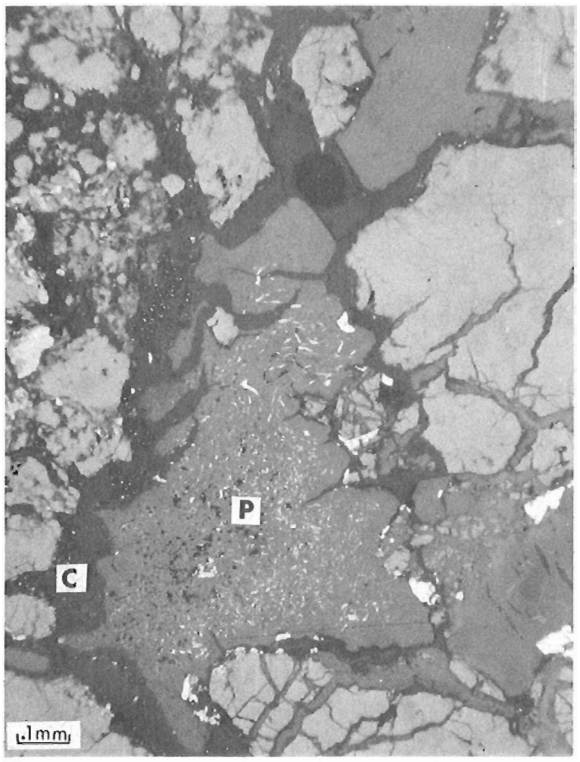

Figure 5.14. Massive pitchblende (P) in a carbon (C) matrix; the pitchblende contains blebs of galena and shards of chalcopyrite. Claude deposit, Carswell Structure, Saskatchewan. Photomicrograph, reflected light.

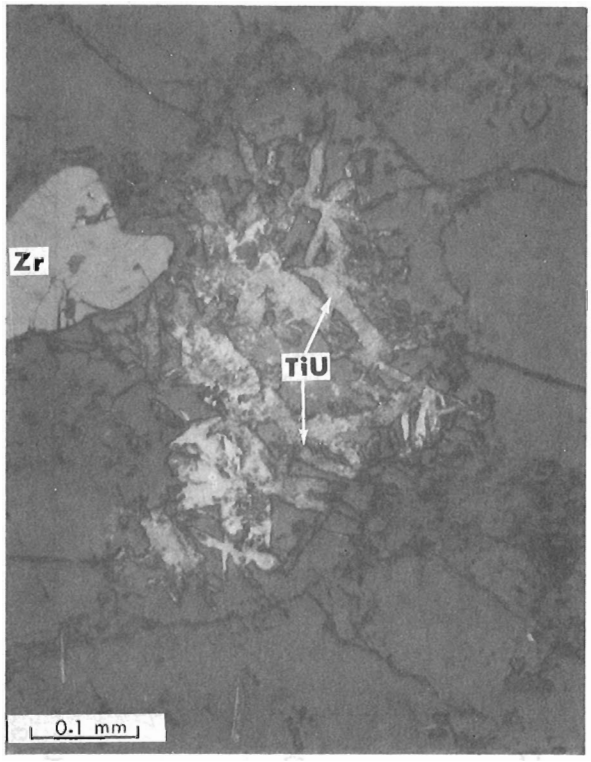

Figure 5.16. Zircon (Zr) and shards of a Ti-U-Si phase (TiU) in quartz from sedimentary rocks of the Indicator Formation, Otish Mountains, Quebec. Photomicrograph, reflected light.

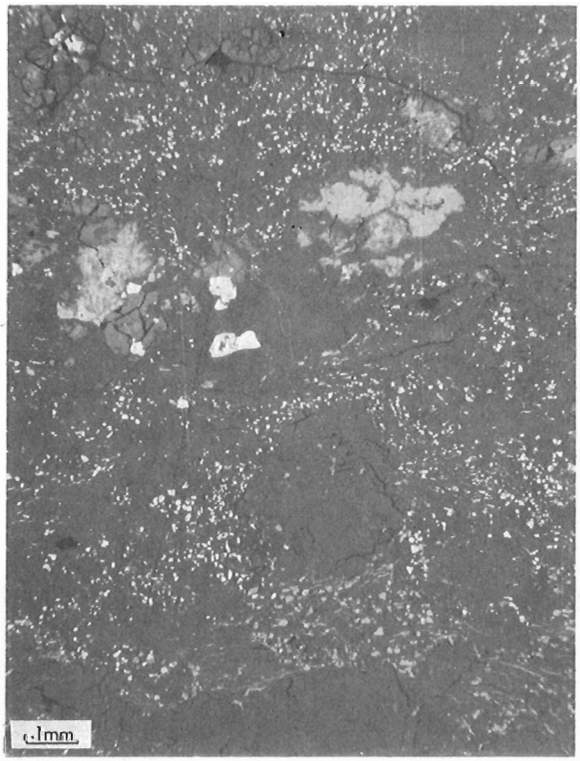

Figure 5.15. Opaque minerals: galena (large white spot), chalcopyrite and sphalerite (small white spots) associated with (diffuse grey) rutile and pitchblende; Claude deposit, Carswell Structure, Saskatchewan. Photomicrograph, reflected light.

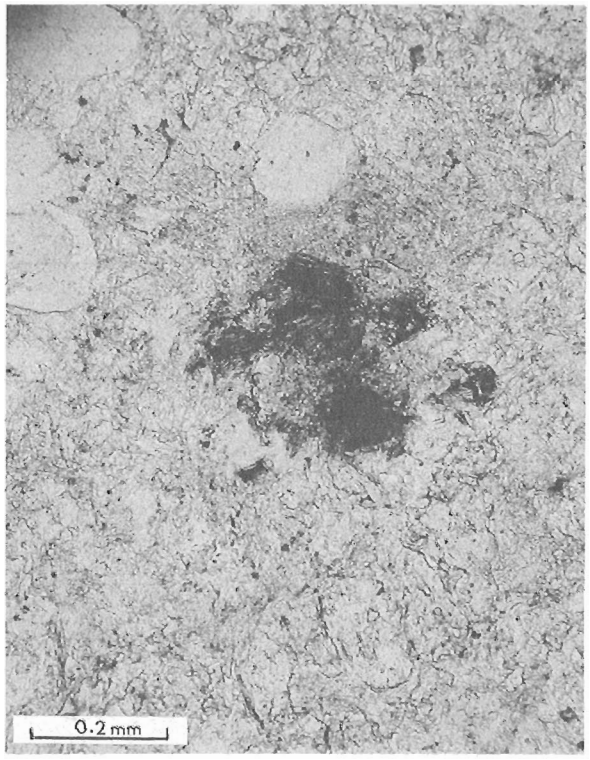

Figure 5.17. Meta-uranocircite (black) within the sericite matrix in quartzite of the Indicator Formation, Otish Mountains, Quebec. Photomicrograph, transmitted light.

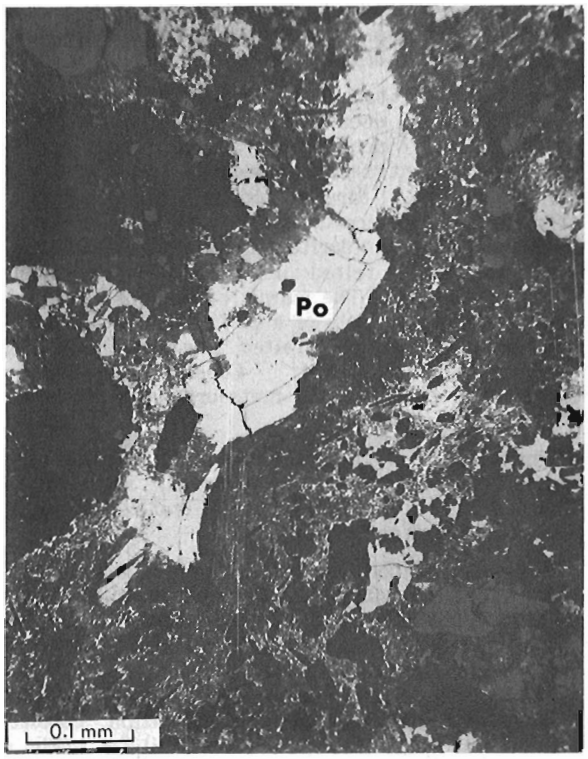

Figure 5.18. Platy crystal (Po) of poubaite $((BiPb)_3(Se\ Te\ S)_4)$ from a carbonate vein associated with gabbro, Otish Mountains area, Quebec. Photomicrograph, transmitted light.

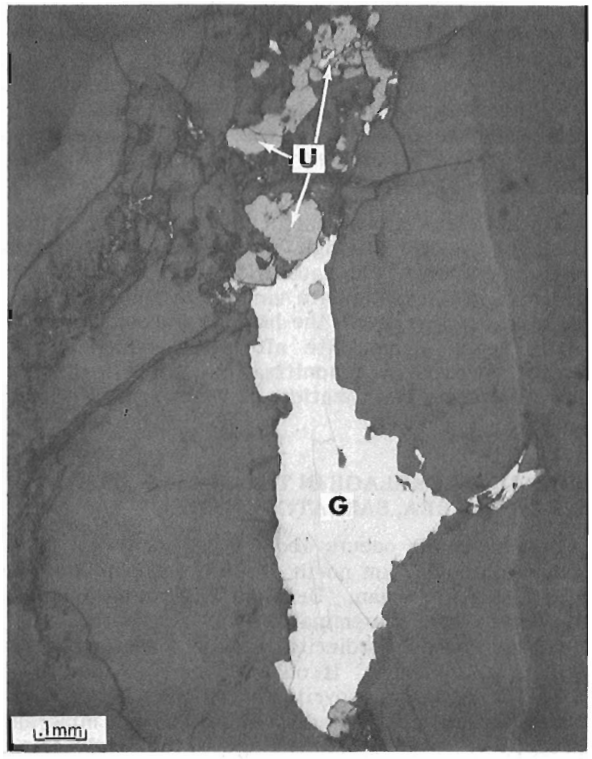

Figure 5.19. Guanajuatite (Bi_2Se_3) – (G) and uraninite (U) from a fracture filling associated with aplitic rocks intruding arkosic conglomerate, Otish Mountains area, Quebec. Photomicrograph, reflected light.

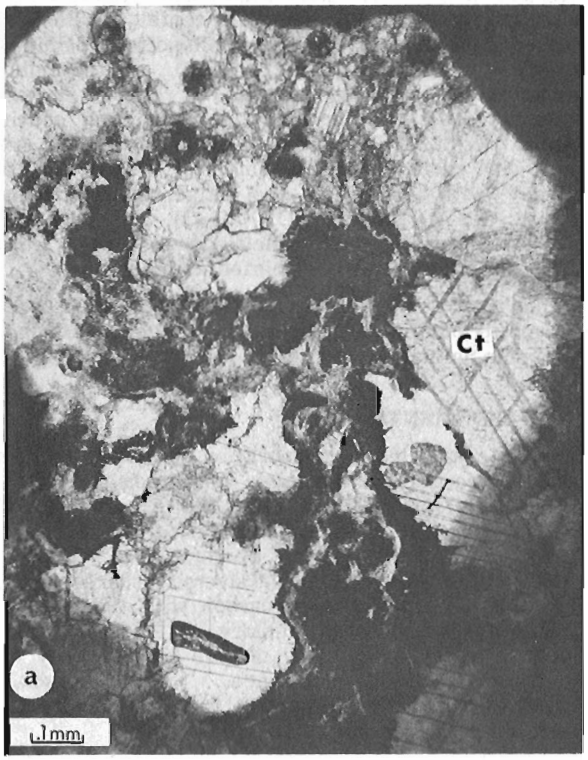

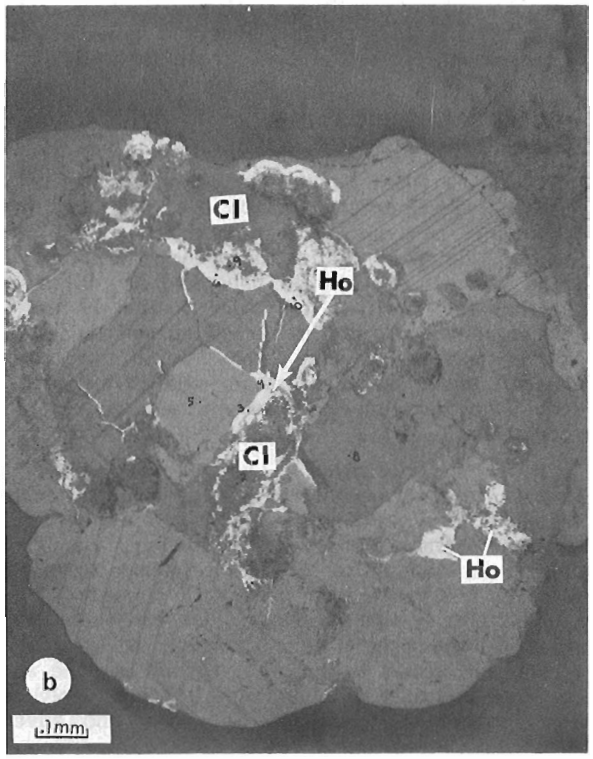

Figure 5.20a,b. Curite (?) ($Pb_2U_5O_{17}\cdot 4H_2O$) (Ct) and hollandite ($BaMn_8O_{16}$) (Ho) associated with clay (Cl) and dolomite (Do) from a carbonate vein associated with rhyolitic rocks intruding quartz-pebble conglomerate, Otish Mountains, Quebec. Photomicrographs, (a) transmitted light, (b) reflected light.

The mineralization is structurally controlled by an east-west trending fault and by the sub-Athabasca unconformity. Although the footwall of the mineralization occurs within the same lithostratigraphic unit as the Dawn Lake deposits (about 5 km to the southwest), the strike of the graphitic semipelite horizon which lithologically controls the mineralization, is about 270° at JEB, in contrast to Dawn Lake where the horizon strikes about 030°.

Toward the mineralized zone basement rocks are increasingly altered through chloritization of the ferromagnesian minerals and saussuritization of the feldspars. Illite occurs in the immediate vicinity of the mineralization. Chlorite is also present in the hanging wall sandstone, where it partly replaces hematite alteration, which in turn is succeeded upwards by limonitization of the matrix, which, farther from the mineralization, contains kaolinite and silica cement.

A MINERAL ASSEMBLAGE IN THE CLAUDE DEPOSIT, CLUFF LAKE AREA, SASKATCHEWAN

The Claude deposit occurs about 3 km northwest of the 'D' orebody and about 2 km north of Cluff Lake in the Carswell Structure, Saskatchewan. Uranium mineralization occurs in veins, lenses and disseminations in feldspathic quartzite enclosed by garnet-cordierite gneiss. The main uranium mineral is pitchblende. It occurs locally in patches along with galena and chalcopyrite in a hydrocarbon (kerogen) matrix (Fig. 5.14). In addition to these minerals the pitchblende-hydrocarbon assemblage is commonly associated with sphalerite, rutile, boltwoodite and Fe-oxides embedded in felted mica and crossed by veins of calcite (Fig. 5.15).

The pitchblende-hydrocarbon assemblage was a common type of mineralization in the now depleted 'D' orebody, which was deposited at the unconformity between the Athabasca Group rocks and the regolithic portion of the basement rocks (Ruzicka, 1975). It is possible that the mineralization in Claude represents roots of an orebody similar to the 'D'.

URANIUM OCCURRENCES IN THE OTISH MOUNTAINS GROUP, QUEBEC

The Proterozoic Otish Mountains Group northeast of Lake Mistassini, Quebec, consists of 100 m of sedimentary rocks unconformably overlying Archean basement rocks. Most of the known uranium mineralization occurs: (a) in association with the Archean/Proterozoic unconformity; (b) in clastic sedimentary rocks within the lower portion of the Group (i.e. in the Indicator Formation); (c) in carbonate rocks within the upper portion of the Group (i.e. in the Peribonca Formation); and (d) in veins associated with intrusive rocks and commonly paragenetically or spatially related to sodic metasomatites.

The mineralization associated with the Archean/Proterozoic unconformity is structurally controlled by this unconformity and intersecting faults and lithologically by Archean volcanic rocks and by reducing facies of the Indicator Formation. The top of the Archean basement and the base of the Proterozoic rocks are strongly altered to clay, chlorite-carbonate and albite. The carbonate occurs as a gangue with the uranium mineralization; this assemblage is, as a rule, surrounded by chlorite; the outer zone contains albite. In addition to uranium, some thorium, molybdenum, niobium, vanadium, titanium, lead, gold and silver are present. The pitchblende is associated with a Ti-U-Si phase ('brannerite') intergrown with or overgrown on rutile/anatase, pyrite, pyrrhotite and uranothorite.

The mineralization in sedimentary rocks of the Indicator Formation occurs as: (i) stratabound syngenetic concentrations; (ii) epigenetic fracture fillings; and (iii) impregnations at redox boundaries usually associated with limonitization. Stratabound mineralization contains uranothorite, pyrite, zircon, apatite and rutile/anatase and galena associated with chlorite. The fracture filling consists of altered plagioclase, felted mica and a bismuth/lead (Bi, Pb (U, Ca, Y)) compound. The matrix of the quartz-microcline arenites commonly consists of a U-Ti-Si phase ('brannerite'), zircon, very fine grained felted muscovite and Fe – or (Ti, Fe) – oxides (Fig. 5.16). Locally the uranium is associated with phosphate in meta-uranocircite ($Ba(UO_2)_2(PO_4)_2 \cdot 8H_2O$) (Fig. 5.17).

Mineralization in the carbonate (mainly dolomite) rocks of the Peribonca Formation contains, in addition to francevillite and pitchblende (Ruzicka and Littlejohn, 1982), chalcocite ('ophitic') and uraninite.

Epigenetic mineralization in veins associated with intrusive rocks and related to sodic metasomatism is common in the Otish Mountains area. Occurrences of this type contain a variety of mineral assemblages. For example, calcite veins in chloritized gabbro contain U ±Bi ±Pb ±Se ±Te ±Cu ±Ti assemblages in various proportions of the elements; the mineralization consists of uraninite, poubaite ($(Bi\ Pb)_3\ (Se\ Te\ S)_4$) – (Fig. 5.18), chalcopyrite, native bismuth and a U-Ti-Si-Pb phase ('brannerite'). Fracture fillings associated with aplitic rocks intruding arkosic conglomerate contain U ±Bi ±Se ±Pb assemblages with uraninite, guanajuatite (Bi_2Se_3) (Fig. 5.19), curite ($Pb_2U_5O_{17} \cdot 4H_2O$) and apatite as the main minerals. Calcite/dolomite veins associated with rhyolitic rocks intruding quartz-pebble conglomerate contain U ±Ba ±Mn ±Pb assemblages with curite and hollandite ($Ba\ Mn_8\ O_{16}$) encrustations around clay (Fig. 5.20a,b). Within albitized shear zones in quartzite intruded by diabase dykes the authigenic matrix of tourmaline, fuchsite and apatite is associated with U ±Ba ±Bi ±Se ±Pb ±Ti elemental assemblages. In addition to an unidentified Fe-U-P phase associated with goethite, the mineralization contains gorceixite ($Ba\ Al_3\ (PO_4)_2\ (OH)_5 \cdot H_2O$) and guanajuatite. Locally the shear zones are silicified and contain goyazite ($Sr\ Al_3\ (PO_4)_2\ (OH)_5 \cdot H_2O$) associated with clay.

Thus the Otish Mountains area should be considered as a significant uranium-polymetallic metallogenic province of the Canadian Shield.

ACKNOWLEDGMENTS

The authors acknowledge co-operation of geologists from the following exploration and mining companies: Amok Ltee, Canoxy Ltd., Denison Mines Ltd., Rio Algom Ltd., SERU Nucleaire Ltee, and Uranerz Exploration and Mining Ltd. Professors K. Hattori of the University of Ottawa and D.J. Mossman of Mount Allison University shared results of their studies on the Huronian carbon with the authors and J.F. Scott of the Ontario Ministry of Natural Resources contributed material and field advice to the study of the Black Sturgeon Lake occurrence. S.V. Thompson, and N. Prasad assisted in the field and J.A. Kerswill was responsible for sample preparation.

REFERENCES

Coates, M.E.
1972: Geology of the Black Sturgeon River Area, District of Thunder Bay; Ontario Department of Mines and Northern Affairs, Geological Report 98.

Faure, G. and Chaudhuri, S.
1967: The geochronology of the Keweenawan rocks of Michigan and the origin of the copper deposits; Report No. 1, Laboratory for Isotope Geology and Geochemistry, Department of Geology, Ohio State University.

Feather, C.E. and Koen, G.M.
1975: The Mineralogy of the Witwatersrand Reefs; Minerals Science and Engineering, v. 7, no. 3, July 1975, p. 189-224.

Hallbauer, D.K.
1975: The Plant Origin of the Witwatersrand 'Carbon'; Minerals Science and Engineering, v. 7, no. 2, April 1975, p. 111-131.

Hattori, K., Campbell, F.A., and Krouse, H.R.
1981: Stable isotope study on uraniferous conglomerate in Elliot Lake (abstract); Geological Association of Canada-Mineralogical Association of Canada – Canadian Geophysical Union Joint Annual Meeting, Calgary, p. A24.

Minter, W.E.
1981: The crossbedded nature of Proterozoic Witwatersrand placers in distal environments and a paleocurrent analysis of the Vaal Reef placer; in Genesis of Uranium and Gold-Bearing Precambrian Quartz-Pebble Conglomerates; United States Geological Survey, Professional Paper 1161-A-BB, p. G1-G9.

Pretorius, D.A.
1975: The depositional environment of the Witwatersrand goldfields: A chronological review of speculations and observations; Minerals Science and Engineering, v. 7, no. 1, January 1975, p. 18-47.

Roscoe, S.M.
1969: Huronian rocks and uraniferous conglomerates; Geological Survey of Canada, Paper 68-40, 205 p.

1973: The Huronian Supergroup, a Paleoaphebian succession showing evidence of atmospheric evolution; in Geological Association of Canada; Special Paper 12, p. 31-47.

Ruzicka, V.
1975: Some metallogenic features of the "D" uranium deposit at Cluff Lake, Saskatchewan; in Report of Activities, Part C, Geological Survey of Canada, Paper 75-1C, p. 279-283.

Ruzicka, V. (cont.)
1979: Uranium and thorium in Canada, 1978; in Current Research, Part A, Geological Survey of Canada, Paper 79-1A, p. 139-155.

1981: Some metallogenic features of the Huronian and Post-Huronian uraniferous conglomerates; in "Genesis of Uranium and Gold-Bearing Precambrian Quartz-Pebble Conglomerates", United States Geological Survey, Professional Paper 1161-V, p. V1-V8.

Ruzicka, V. and Littlejohn, A.L.
1982: Notes on mineralogy of various types of uranium deposits and genetic implications; in Current Research, Part A, Geological Survey of Canada, Paper 82-1A, p. 341-349.

Ruzicka, V. and Steacy, H.R.
1976: Some sedimentary features of conglomeratic uranium ore from Elliot Lake, Ontario; Report of Activities, Part A, Geological Survey of Canada, Paper 76-1A, p. 343-346.

Saint-Martin, M.
1983: The petrology and geochemistry of uraniferous chloritized rocks at Panel mine, Elliot Lake, Ontario; unpublished B.Sc. thesis, University of Ottawa.

Saracoglu, N., Wallis, R.H., Brummer, J.J., and Golightly, J.P.
1983: The McClean uranium deposits, northern Saskatchewan – discovery; The Canadian Mining and Metallurgical Bulletin, April, 1983, p. 1-17.

Simpson, P.R. and Bowles, J.F.W.
1981: Uranium mineralization of the Witwatersrand and Dominion Reef systems; in Genesis of Uranium and Gold-Bearing Quartz-Pebble Conglomerates, United States Geological Survey Professional Paper 1161-A-33, p. R1-R26.

Sutcliffe, R.H.
1981: Geology of the Wabigoon-Quetico Sub-province Boundary in the Lake Nipigon Area, District of Thunder Bay; in Summary of Field Work, 1981 by the Ontario Geological Survey, ed. J. Wood, O.L. White, R.B. Barlow, and A.C. Colvine; Ontario Ministry of Natural Resources, Miscellaneous Paper 100, p. 26.

Tankard, A.J., Jackson, M.P.A., Eriksson, K.A., Hobday, D.K., Hunter, D.R., and Minter, W.E.L.
1982: Crustal Evolution of Southern Africa. The Golden Proterozoic; Springer-Verlag, Berlin, p. 115-150.

Theis, N.J.
1979: Uranium-bearing and associated minerals in their geochemical and sedimentological context, Elliot Lake, Ontario; Geological Survey of Canada, Bulletin 304, 50 p.

6. RADIOACTIVE EQUILIBRIUM STUDIES ON FOUR CANADIAN URANIUM REFERENCE ORES

Project 720084

R.L. Grasty and W. Dyck
Resource Geophysics and Geochemistry Division

Grasty, R.L. and Dyck, W., Radioactive equilibrium studies on four Canadian uranium reference ores; in Current Research, Part A, Geological Survey of Canada, Paper 84-1A, p. 53-56, 1984.

Abstract

Four Canadian uranium reference ores were analyzed for their radium-226 and polonium-210 content. Radium-226 was measured both by gamma-ray spectrometry and by a radon emanation technique. Polonium-210 was determined by alpha-spectrometry.

A comparison of the recommended uranium values with the measured polonium and radium content showed that within the accuracy of the measurements the four ores are in radioactive equilibrium.

Résumé

Quatre minerais d'uranium canadiens ont été analysés relativement à leur teneur en radium 226 et en polonium 210. La teneur en radium 226 a été mesurée au moyen d'un spectromètre à rayons gamma et d'une technique qui permet d'évaluer l'émanation radon, et le contenu en polonium 210, au moyen d'un spectromètre alpha.

Une comparaison des valeurs d'uranium recommandées quant aux teneurs en polonium et en radium mesurées a permis de constater que, compte tenu de la précision possible des mesures, les quatre minerais étaient en équilibre radioactif.

INTRODUCTION

The Canadian Certified Reference Materials Project (CCRMP) offers for sale several uranium and uranium/thorium ore reference materials derived from Canadian ore bodies. A project to provide recommended values for the activities of several nuclides from the uranium-238 decay series in four of these reference materials was recently initiated by the Canada Centre for Mineral and Energy Technology (CANMET). As part of this project, four reference ores, ground to -74 µm, were submitted to the Geological Survey of Canada for the determination of radium-226 and polonium-210. Information on the radon-222 emanation of each powdered ore into air and also into water was obtained at the same time.

The reference ores analyzed, DL-1A, DH-1A, BL-4A and BL-5, are described in CANMET reports by Steger et al. (1981), Faye et al. (1979), Ingles et al. (1977) and Steger and Bowman (1980). DL-1A and DH-1A are principally uraninite and brannerite ores from Elliot Lake, Ontario. BL-4A is a pitchblende ore, and BL-5 is low grade uraninite from Beaverlodge, Saskatchewan. Two batches of each ore were analyzed.

ANALYTICAL PROCEDURES

Determination of polonium-210

For each of the four reference ores, eight 1 g samples (four from each batch) of the powdered ores were first heated to dryness in teflon beakers on a hot plate using successively two 5 ml solutions of concentrated nitric acid followed by two 5 ml solutions of hydrofluoric acid. The final digestion was achieved using two 5 ml solutions of a mixture of three parts of concentrated nitric to two of perchloric acid. Perchloric acid was used in the digestion to destroy any organic matter on which polonium is strongly absorbed. The resulting residue was dissolved with warm 0.5 M hydrochloric acid, transferred to a #14 plastic vial and the volume adjusted to 20 ml with 0.5 M hydrochloric acid. A clean 1.9 cm diameter nickel disc was then placed in the vial which was shaken for 17 hours to plate the polonium-210 in solution onto the disc. The alpha activity of the polonium-210 on both sides of the disc was determined with an Ortec alpha spectrometer system with a 450 mm^2 surface barrier detector. The alpha spectrometer was calibrated using a standard lead-210 solution (#SO/8/5, code RBZ.44) in equilibrium with polonium-210 obtained from Amersham Corporation, Oakville, Ontario. In the calibration procedure 1 g aliquots of the standard solution were added to samples of silica sand and the same procedure followed as described previously.

Determination of radium-226 by emanation

Radium-226 was determined by a radon-222 emanation technique in which the sample is first dissolved in acid and then bottled for sufficient time for the radon-222 to reach equilibrium with the radium in solution. The radon was then degassed into a silver-activated zinc sulphide cell where the alpha activity was measured with a photomultiplier-scaler assembly.

Four 1 g samples of each of the two batches of the reference ores were heated to dryness in a teflon beaker with two 5 ml solutions of concentrated nitric acid followed by two 7 ml solutions of concentrated hydrofluoric acid. Final digestion was carried out overnight using 20 ml of 0.5 M hydrochloric acid. The resulting residue was dissolved in 10 ml of concentrated hydrochloric acid and transferred to a 295 ml glass bottle of the soft-drink type. The bottle was then completely filled with distilled water, capped and stored for about two weeks to allow the radon-222 to approach equilibrium with the radium in solution. In calculating the radium content, a correction factor was incorporated to allow for any disequilibrium between radon and radium. A 130 ml aliquot of the solution was transferred to the radon degassing apparatus and the radon flushed into an evacuated radon cell by slowly bubbling atmospheric air through the solution for four minutes. The gas was then left for three hours to allow the radon to equilibrate with the short-lived alpha emitting decay products polonium-218 and polonium-214. The radon alpha activity in the cell was determined with an alpha scintillation counter. The method was calibrated by sealing two National Bureau of Standards radium-226 solutions (SRM-4955 and SRM-4917) in the standard glass bottles and then following the procedure described previously. A more complete account of the method may be found in Dyck (1969).

Determination of radon-222 emanation into water

Eight 1 g samples of each reference ore (four from each bottle) were placed in the standard 295 ml glass bottles which were then filled with distilled water and capped. The bottles were then stored for about two weeks, to allow the radon to approach equilibrium with the radium, and shaken periodically. Immediately prior to the radon analysis, each bottle was shaken and centrifuged and the clear solution decanted into the degassing apparatus. The radon activity was then measured following the same procedure described for the analysis of radium.

Determination of radium-226 by gamma-ray spectrometry

The radium-226 activity of the reference ores was determined by comparing their gamma-ray spectra with those from three standards of potassium, radium and thorium.

The gamma-ray spectrometer system utilizes two 12.7 x 12.7 cm (5 x 5 inch) lead shielded sodium iodide detectors. Samples being analyzed are sealed in metal cans which are rolled automatically between the two detectors. The multichannel analyzer and the data recording system which records the complete gamma-ray spectrum has been described by Bristow (1979). Gamma-rays from potassium-40, bismuth-214 in the uranium decay series and thallium-208 in the thorium decay series are registered in the following windows:

Potassium-40	1360 - 1560 keV
Bismuth-214	1660 - 1860 keV
Thallium-208	2420 - 3420 keV

The counts in these windows are compared with three standards containing a known amount of radium chloride, thorium nitrate which is now in equilibrium, and potassium carbonate. The radium chloride was obtained from the U.S. National Bureau of Standards and the aged thorium nitrate from the Radiochemical Centre, Amersham, England. Details of the preparation of the standards and the calibration of the spectrometer are described in Grasty et al. (1982).

Due to the large volume of the detectors, the measured gamma-ray spectrum becomes distorted when high concentrations of uranium or thorium are measured. For this reason the three high-activity ores BL-5, BL-4A and DH-1A were blended with known amounts of pure silica to reduce the uranium concentration of the samples to less than 1000 ppm. Two samples weighing approximately 350 g from each of the two batches of each ore were sealed into the laboratory sample containers. These sixteen samples were then analyzed one day after sealing, and again after 26 days when the bismuth-214 had reached equilibrium with the radium-226.

RESULTS

In order to assess the state of equilibrium in the four uranium ores, measurements of the activities of the various decay products are presented in terms of equivalent uranium concentrations which can be compared directly with the chemical uranium concentrations recommended by CANMET. The equivalent uranium concentration, eU, is that concentration of uranium which is calculated from the measured concentration of a decay product of uranium assuming radioactive equilibrium.

The polonium-210 activity of the uranium ores was obtained from a calibration curve of the alpha activity, expressed as Bequerels per gram (Bq/g), of various concentrations of polonium-210 standard solutions.

The polonium activity, P_B, in Bq/g may be converted to equivalent uranium concentration eU, (in g/g) using the relationship

$$P_B = eU \times \frac{0.99275}{238} \times \frac{\log_e 2}{T_{\frac{1}{2}}} \times A$$

where, A is Avogadro's Number (6.02×10^{23}),
$T_{\frac{1}{2}}$ (4.468×10^9y) is the half-life of uranium-238 (Lederer and Shirley, 1978),
0.99273 is the relative abundance of uranium-238 to total uranium and
238 is the atomic weight of uranium-238.

Using these figures we find that

$$1 \text{ ppm eU} = 0.01234\ P_B$$

or $$eU \text{ (ppm)} = 81.01\ P_B \quad (1)$$

The radium determinations were all derived by comparing the activity of the ores with the activity of radium standards containing a known concentration of radium-226. Consequently, the radium results were initially calculated as concentrations (g/g).

The equivalent uranium concentration eU, (g/g) of the ores may be calculated from the radium concentration, Ra-226 (g/g) by the expression:-

$$eU = \frac{\text{Ra-226}}{0.99275} \times \frac{4.468 \times 10^9}{1600} \times \frac{238}{226}$$

where, 1600 is the half-life of radium-226 (Lederer and Shirley, 1978),
226 is the atomic weight of radium-226 and all other values have been explained previously.

If the radium concentration is measured in pico grams/gram and the equivalent uranium is measured in parts per million, this expression reduces to

$$eU \text{ (ppm)} = 2.962 \times \text{Ra-226 (pg/g)} \quad (2)$$

Table 6.1 compares the recommended uranium concentrations with the equivalent uranium determinations calculated using equations (1) and (2). The errors quoted are at the one sigma level and take into consideration the errors in the calibration of the methods as well as errors in the mean of the separate determinations for each sample. The errors in the radium and lead standards have not been included and are quoted by the supplier as ±1.8%.

Table 6.1. Equivalent uranium determinations

Ore	Recommended uranium (ppm)	Po-210 eU (ppm)	Ra-226 by Rn-222 eU (ppm)	Ra-226 by Bi-214 eU (ppm)
DL-1A	116+/-1.5	113+/-3	115+/-2	117+/-2
BL-4A	1248+/-7	1308+/-28	1236+/-22	1300+/-26
DH-1A	2629+/-1.5	2538+/-62	2469+/-33	2642+/-30
BL-5	70900+/-150	73450+/-1815	69600+/-915	72950+/-950

The errors quoted are at the one sigma level and take into consideration the errors in the calibration of the method as well as errors in the mean of separate determinations for each sample.

Errors in the standards have not been included and are quoted by the suppliers as ±1.8%

Table 6.2. Radon emanation efficiency

Ore	Recommended uranium (ppm)	Emanation efficiency (per cent) Into air	Into water
DL-1A	116+/-1.5	3+/-2	15.8+/-0.5
BL-4A	1248+/-7	5+/-3	18.8+/-0.3
DH-1A	2629+/-1.5	6+/-3	33.9+/-0.4
BL-5	70900+/-150	2+/-2	6.5+/-0.2

In Table 6.2 the efficiency of radon-222 emanation into water and into air is shown. The emanation efficiency is defined as the percentage of the total radon produced in the ore that emanates into the water or the air.

The radon emanation into water was determined by comparing the alpha activity of the radon entering the water with the total radon activity of the ores. The radon emanation of the dry material into air was determined by comparing the bismuth-214 gamma-ray activity one day after sealing the ores in the laboratory sample containers with the measurements after the bismuth-214 had reached equilibrium with the radium-226. The difference in bismuth-214 activity between the two measurements results from the radon emanating from the ore. A small correction was made for the minor build-up of the emanating radon that occurred in the one day period before the samples were measured.

The information on radon emanation is provided for those interested in problems that may arise through storing or utilizing these particular ores. The results show that a water saturated ore can lose substantially more radon than one which is dry, as has been noted by other workers (Tanner, 1978).

DISCUSSION AND CONCLUSIONS

The equivalent uranium content of DH-1A by the emanation technique is approximately 5% lower than the recommended uranium content. However, the equivalent uranium concentration by gamma-ray spectrometry shows good agreement with the recommended uranium value, suggesting that radium was lost somewhere in the chemical procedure. This radium loss was partially explained by gamma-ray spectrometric analysis of the undissolved ore residue which showed the presence of a minor amount of radium.

Apart from the radium analyses of ore DH-1A by the radon emanation technique, all the equivalent uranium values are within about two standard deviations of the recommended uranium concentrations. The analytical procedures were therefore unable to detect disequilibrium in any of the four ores anlayzed. For most practical purposes all four ores can be considered to be in equilibrium.

ACKNOWLEDGMENTS

We acknowledge the valuable analytical work carried out by J.C. Pelchat and G.W. Cameron as well as H. Schneeberger, a visiting student from the Federal Republic of Germany.

REFERENCES

Bristow, Q.
1979: A gamma-ray spectrometry system for airborne geological research; in Report of Activities, Part C, Geological Survey of Canada, Paper 79-1C, p. 55-61.

Dyck, W.
1969: Field and laboratory method used by the Geological Survey of Canada in geochemical surveys, no. 10. Radon determination apparatus for geochemical prospecting for uranium; Geological Survey of Canada, Paper 68-21, 30 p.

Faye, G.H., Bowman, W.S., and Sutarno, R.
1979: Uranium ore BL-5 – A certified reference material; CANMET Report 79-4, CANMET, Energy, Mines and Resources Canada, 11 p.

Grasty, R.L., Bristow, Q., Cameron, G.W., Dyck, W., Grant, J.A., and Killeen, P.G.
1982: Primary calibration of a laboratory gamma-ray spectrometer for the measurement of potassium, uranium and thorium; Proceedings of OECD and IAEA Symposium on Uranium Exploration Methods, Paris, p. 699-712.

Ingles, J.C., Sutarno, R., Bowman, W.S., and Faye, G.H.
1977: Radioactive ores DH-1, DL-1, BL-1, BL-2, BL-3 and BL-4 – certified reference materials; CANMET Report 77-64, CANMET, Energy, Mines and Resources Canada, 22 p.

Lederer, C.M. and Shirley, V.S.
1978: Table of Isotopes, 7th Edition; John Wiley & Sons, New York, 1523 p.

Steger, H.F. and Bowman, W.S.
1980: DL-1a: A certified uranium-thorium reference ore, CANMET Report 80-10E, CANMET, Energy, Mines and Resources Canada, 15 p.

Steger, H.F., Bowman, W.S., and Zechanowitsch, G.
1981: DH-1a: A certified uranium-thorium reference ore; CANMET Report 81-11E, CANMET, Energy, Mines and Resources Canada, p. 14.

Tanner, A.B.
1978: Radon migration in the ground: A supplementary review, ed. T.F. Gesell and W.M. Lowder; Proceedings of the Third International Symposium on the Natural Radiation Environment, Houston, Texas; U.S. Department of Commerce, Springfield, Virginia, p. 5-56.

7. LATE QUATERNARY STRATIGRAPHY OF THE INNER LABRADOR SHELF

Project 750038

G. Vilks, I. Hardy, and H.W. Josenhans
Atlantic Geoscience Centre, Dartmouth

Vilks, G., Hardy, I., and Josenhans, H.W., Late Quaternary stratigraphy of the inner Labrador Shelf; in Current Research, Part A, Geological Survey of Canada, Paper 84-1A, p. 57-65, 1984.

Abstract

High resolution HUNTEC Deep Tow profiles of a series of subbasins in Groswater Bay show basal till overlain by a stratified marine deposit. The sediments of six piston cores taken along the seismic profiles are a mixture of clay and sandy-gravelly mud with a thin sandy-gravelly surface layer in shallower localities. Assemblages of benthic foraminifera form three ecostratigraphic zones that have a more distinct lateral continuity across the inner shelf than the corresponding acoustics and lithostratigraphy. The interpretation of these zones and ^{14}C dates of molluscan shells indicate that a late glacial environment of relatively low salinities and fast sedimentation rates terminated at approximately 10 000 BP.

Résumé

Des profils HUNTEC Deep Tow à haute résolution d'une série de sous-bassins dans la baie de Groswater montrent qu'un till basal est sous-jacent à un dépôt marin stratifié. Les sédiments dans six carottes prélevées au moyen d'un appareil à piston le long des profiles séismiques se composent d'un mélange d'argile et de boue sableuse-graveleuse avec une mince couche superficielle sableuse-graveleuse dans les endroits moins profonds. Des assemblages de foraminifères benthiques forment trois zones écostratigraphiques ayant une continuité latérale plus distincte en travers de la plate-forme intérieure que l'acoustique et la lithostratigraphie correspondantes. L'interprétation de ces zones et la datation au C^{14} des coquilles de mollusques indiquent qu'un environnement glaciaire récent de salinité relativement faible et de vitesse de sédimentation rapide a cessé d'exister il ya a environ 10 000 BP.

INTRODUCTION

The Labrador continental shelf south of Groswater Bay appears not to have been glaciated during the Late Wisconsinan. Surface physiography southeast of the Mealy Mountains, southeastern Labrador, shows evidence of a major glacial margin and suggests that the Late Wisconsinan ice margin formed the Paradise Moraine (Fig. 7.1) and continued northward to Groswater Bay northwest of Sandwich Bay (Rogerson, 1977; Fulton and Hodgson, 1979). The extensive outwash deposits between Sandwich Bay and Groswater Bay suggest a major front during deglaciation. Immediately north of Groswater Bay, the terrain lacks any features that mark the presence of a major glacial margin, suggesting that here the Late Wisconsinan maximum may have extended into the sea. High resolution seismic surveys 30 km offshore show a series of tills that flank the depression of the Cartwright Saddle (Fig. 7.1), but these are most likely pre-Late Wisconsinan (Josenhans, 1983).

Faunas in sediment cores from Cartwright Saddle also suggest the absence of an offshore ice sheet during the Late Wisconsinan in this region (Vilks and Mudie, 1978; Vilks, 1980). The inner shelf facing the exposed outwash deposits to the north of Sandwich Bay therefore provides an opportunity to study the proglacial sedimentary and paleo-oceanographic environment throughout the Late Wisconsinan. This report discusses initial results of seismic and sediment studies along a transverse depression crossing the inner Labrador Shelf to the south of Groswater Bay. Seismic, lithological and foraminiferal interpretations are combined to provide a tentative proglacial sedimentary and paleo-oceanographic model for the region.

METHODS

During the **Hudson** Cruise 79018 one of the bathymetric depressions crossing the inner shelf (Fig. 7.1) was surveyed with a HUNTEC Deep Tow high resolution boomer, a 655 cm^3 airgun and a 750 m, 72 kHz sidescan system. On the basis of the seismic profiles, coring sites were established at strategic localities to sample sediments from as many acoustic units as possible. Sediments were taken with a Benthos piston corer, modified Hessler Box corer and Van Veen grab sampler.

Approximately 35 ml of sediment taken at 25 cm intervals from each core were subsampled for foraminifera and sediment grain size. The sieve and pipette method was used for sediment analysis. Foraminifera were extracted from the sediment fraction with grains greater than 0.063 mm in diameter.

SEDIMENT

Regional setting

The Labrador Shelf can be classified into four major physiographic zones: the inner shelf, the marginal channel, the outer shelf and the transverse saddles. The inner shelf is generally shallower than approximately 100 m and extends from coastline to the marginal channel (Fig. 7.1, 7.2). The marginal channel occupies the central part of the Labrador Shelf at a distance of 30-50 km from the coastline and at water depths of approximately 500 m. The outer shelf consists mainly of relatively flat banks with minimum depths close to 140 m. Between the banks the water depth of the transverse saddles ranges from 300-400 m, but in places where the transverse saddles intersect the marginal channel, the water depth can reach 800 m.

The inner and outer shelves were developed on different bedrock types and consequently display many different morphologies (Umpleby, 1979). In contrast to the smooth relief of the outer shelf, which was developed on semi-consolidated Tertiary sandstone and siltstone, the inner shelf has a very uneven relief that reflects the highly variable resistance to weathering of the Precambrian granites and metasediments. The marginal channel follows the contact zone between the two major bedrock types (Grant, 1972).

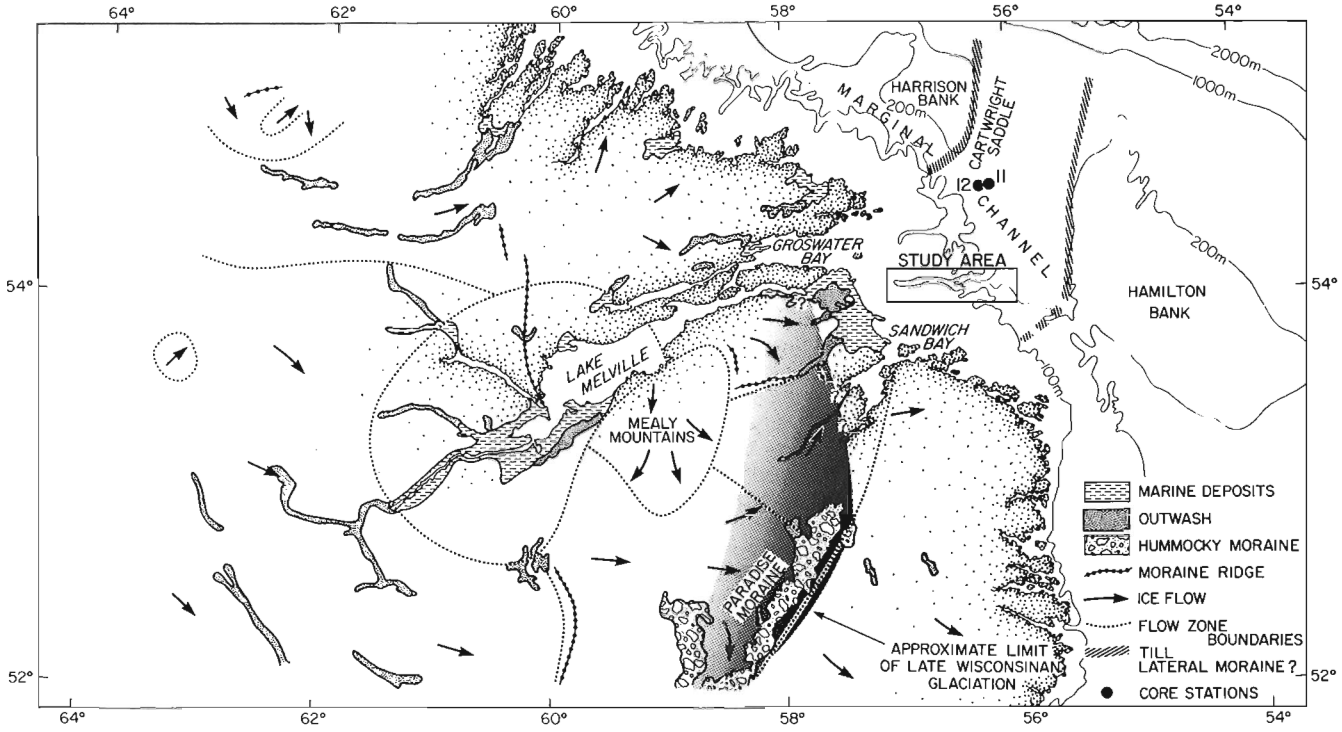

Figure 7.1. *Approximate limit of Late Wisconsinan glaciation ice flow regions, glacial outwash and postglacial marine deposits (after Fulton and Hodgson, 1979). Offshore lateral moraine after Josenhans, 1983.*

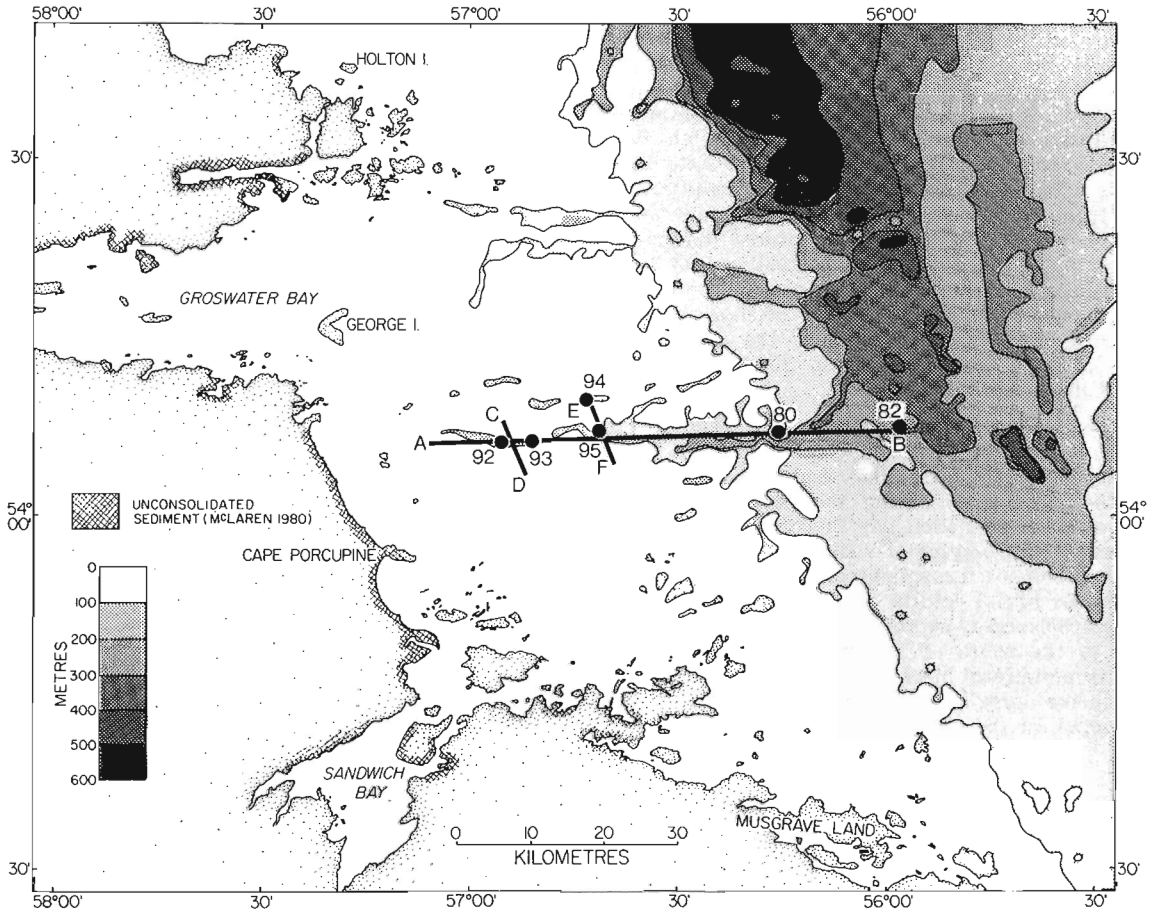

Figure 7.2. *Inner shelf bathymetry, core locations and seismic lines.*

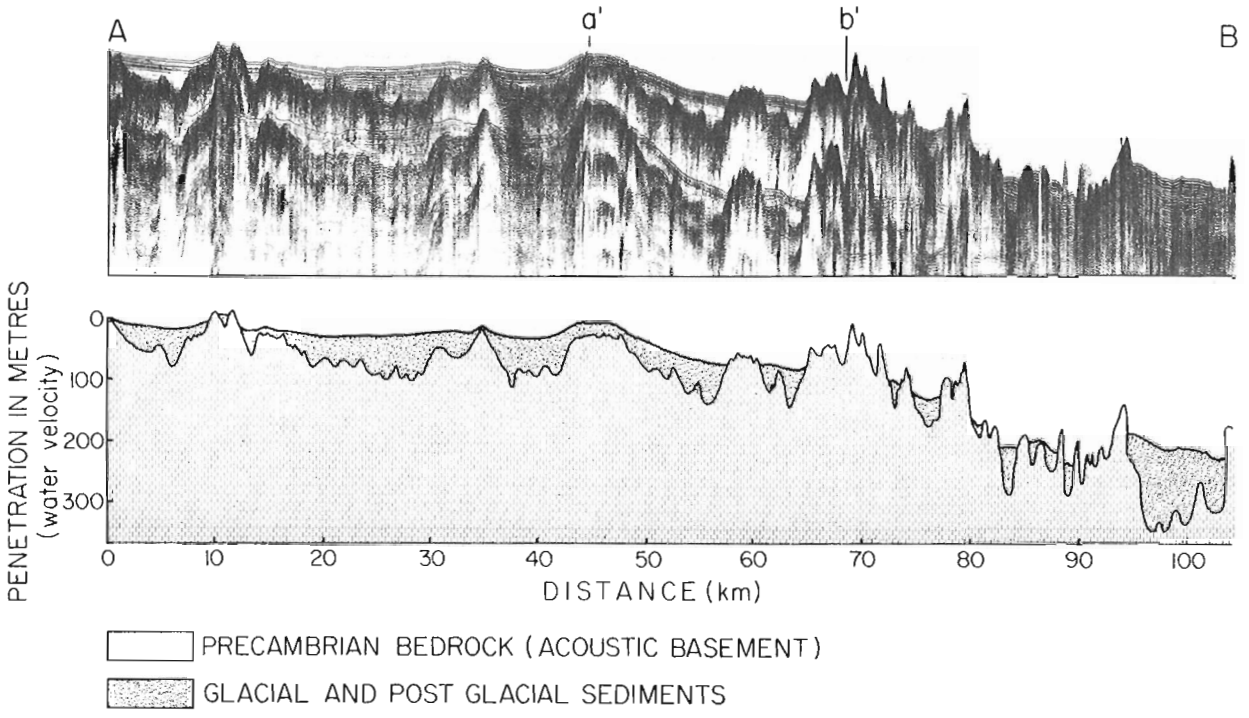

Figure 7.3. *Airgun profile along seismic line A-B; a'-b' is Huntec DTS high resolution profile shown in Figure 7.4.*

The unconsolidated Quaternary deposits of the Labrador Shelf are thickest in basins, but vary from a few metres to 100 m on the banks.

General description of acoustic units

Because of the uneven surface topography, the inner shelf surficial sediments are deposited in more or less isolated basins, where acoustic characteristics of sediment change over a relatively short distance. Consequently, mapping the sediment stratigraphy of the inner shelf requires more closely spaced seismic lines and more accurate navigation when coring the acoustic units than is necessary on the outer shelf (e.g. Josenhans, 1983).

A 655 cm^3 airgun profile which transects the inner shelf (Fig. 7.2 section A-B; Fig. 7.3) illustrates the undulating character of the Precambrian bedrock (acoustic basement) of the inner shelf, and shows the ponded nature of the glacial and postglacial sediments between bedrock highs. Although the section traverses the axis of a major channel (Fig. 7.2), correlation of a consistent stratigraphic assembly between subbasins is not possible. This lack of stratigraphic continuity is shown at a more detailed scale by the Huntec DTS high resolution profile illustrated in Figure 7.4 section a'-b'.

Despite local variability, 4 generalized stratigraphic units are recognized above bedrock on the basis of acoustic character. The oldest, unit I (Fig. 7.5A,B), immediately overlies the acoustic basement and appears as a poorly defined unstratified unit that is generally confined to the basin floors. Unit I is interpreted as glacial till. Unit II is typically well stratified and conformably overlies the till. It could be equivalent to the conformable cover unit defined in the basins of Makkovik Bay, Labrador (Barrie and Piper, 1982) and the conformable acoustic facies 3 in Kaipokok Bay, Labrador (Kontopoulos and Piper, 1982). Unit III is highly stratified and is typically ponded on the basin floors (Fig. 7.6A,B). It is separated from unit II by an unconformity that is conspicuous at coring site 92 because of the angular nonconformity between the reflectors of units II and III. Unit IV represents a veneer of coarse sediments that could be traced from basin floors to slopes and saddles.

General description of lithological units

On the basis of core logs and X-radiographs three major lithological units could be recognized (Fig. 7.7).

Unit 1

A thin veneer of sands and coarser sediments are confined to the surface of cores 93, 94A and 95. In core 92 this coarse unit unconformably overlies sandy gravelly mud at the depth of 1.03 m below surface, and is covered by approximately 90 cm of silty clay. The ^{14}C date of organic carbon at the contact is 5180 ± 330 BP. The surface lithological unit of coarser sediments is not present in cores 80 and 82 and at surface grabs at corresponding localities.

Unit 2

Within the isolated basins these sediments change to a highly bioturbated olive-grey (5 YR 4/2) sandy mud. In core 92 this unit is represented by a sandy gravelly mud that may laterally grade into the olive-grey (5 YR 4/2) muds encountered within the remaining seaward cores. If this assumption is correct, the coarser nearshore sediments give way to finer sediments within the offshore basins. Sediment size analyses show a general grain size increase upcore within these muds, although visually and radiographically the muds appear to be relatively homogeneous and structureless, except for the occasional erratic and sand stringer. Silt and clay ratios also increase towards the surface of cores.

Table 7.1. Major species in zones A, B, and C. The numbers indicate average relative per cents of species occurrence in each zone. **E.exca.f.cla.** = **Elphidium excavatum f. clavata,** WD = water depth

	92 WD 109 m 0-107 cm	93 WD 97 m 0-5 cm	94A WD 95 m 0-5 cm	95 WD 135 m 0-5 cm	80 WD 289 m 0-5 cm	82 WD 335 m 0-5 cm
A	40 S. biformis 8 I. helenae 7 A. cassis 5 R. fusiformis 5 Elphidium sp. 5 R. arctica 4 B. frigida 3 C. reniforme 3 N. labradorica 2 N. auriculata 2 A. gallowayi 2 T. atlantica 1 T. squamata	25 R. arctica 15 S. biformis 9 C. reniforme 9 R. fusiformis 5 I. helenae 5 Elphidium sp. 5 V. fusiformis 5 C. crassimargo 5 A. cassis	27 E. advena 14 Elphidium sp. 11 C. reniforme 10 E. exca.f.cla. 7 B. frigida 7 A. gallowayi	23 I. helenae 21 E. advena 13 Elphidium sp. 11 R. arctica 10 S. biformis 7 C. reniforme 7 E. exca.f.cla. 6 N. labradorica	17 R. fusiformis 16 A. glomerata 16 C. crassimargo 11 C. lobatulus 6 E. advena	47 A. glomerata 25 C. crassimargo 9 S. biformis
	107-250	5-730	5-805	5-360	5-550	5-430
B	51 I. helenae 23 E.exca.f.cla. 12 C. reniforme 5 Elphidium sp.	37 E.exca.f.cla. 35 C. reniforme 20 I. helenae	29 I. helenae 23 B. frigida 22 C. reniforme 20 E.exca.f.cla. 14 Elphidium sp. 3 S. biformis	33 E.exca.f.cla. 29 I. helenae 28 C. reniforme 2 V. fusiformis	33 E.exca.f.cla. 26 C. reniforme 21 V. fusiformis 20 I. helenae 4 P. orbiculare 2 C. lobatulus	31 E.exca.f.cla. 25 C. reniforme 20 I. helenae 11 V. fusiformis
	205-405	730-755	805-830	360-805	550-870	430-555
C	TRACE Pteropoda: L. helicina	TRACE	TRACE	TRACE	TRACE	TRACE

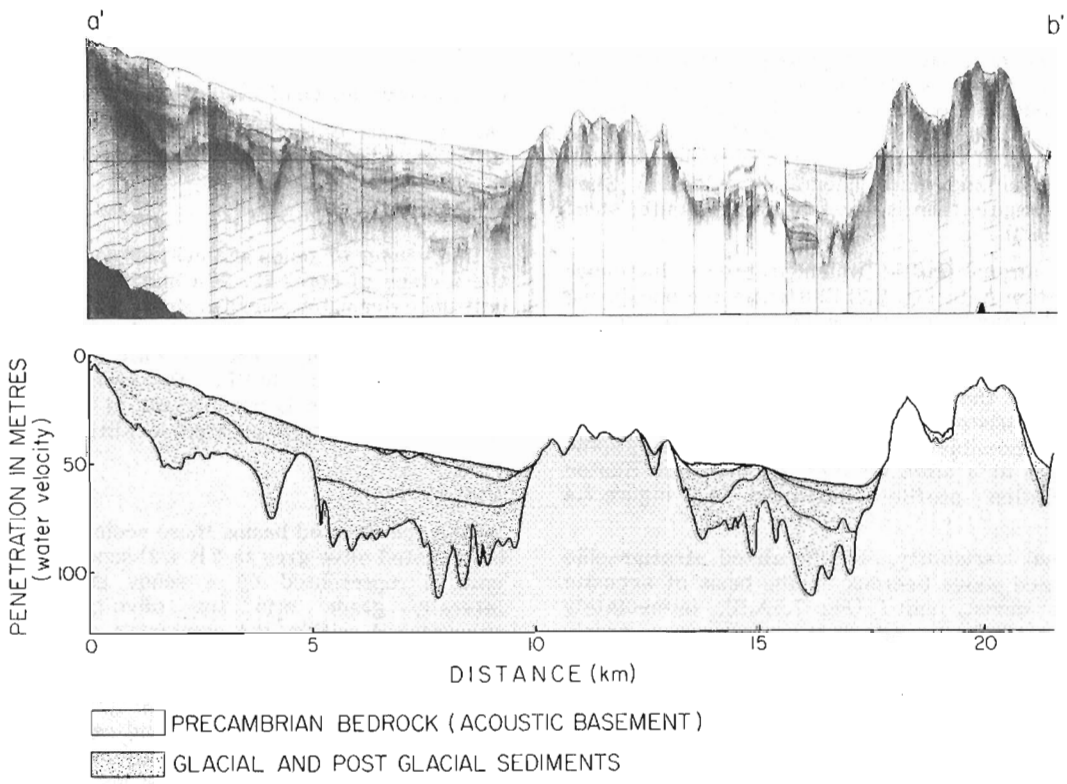

Figure 7.4. *Huntec DTS high resolution profile. See Figure 7.3 for location of line a'-b'.*

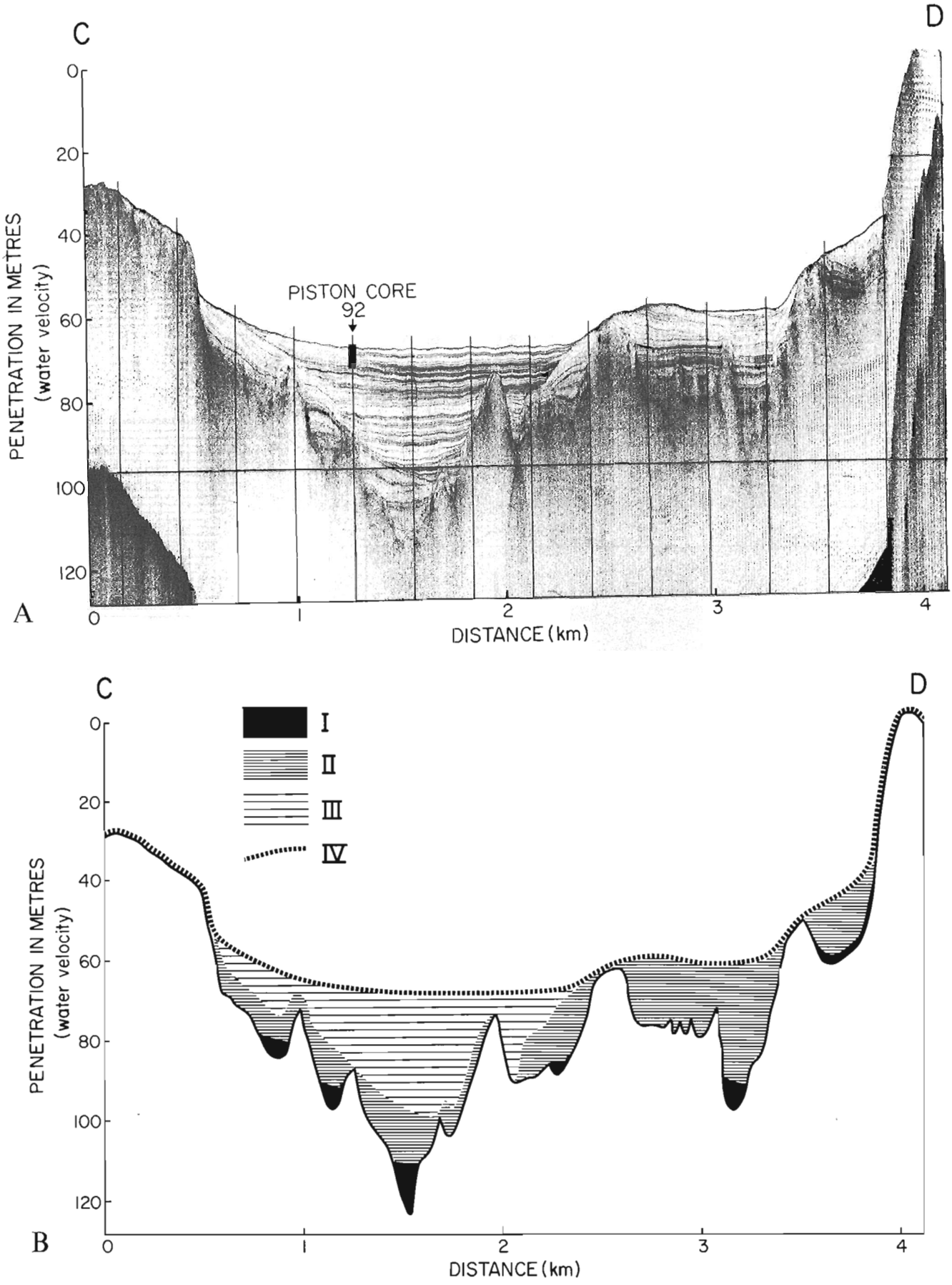

Figure 7.5. *A. Huntec DTS profile along C-D; see Figure 7.2 for location. B. Interpretation of profile E-F.*

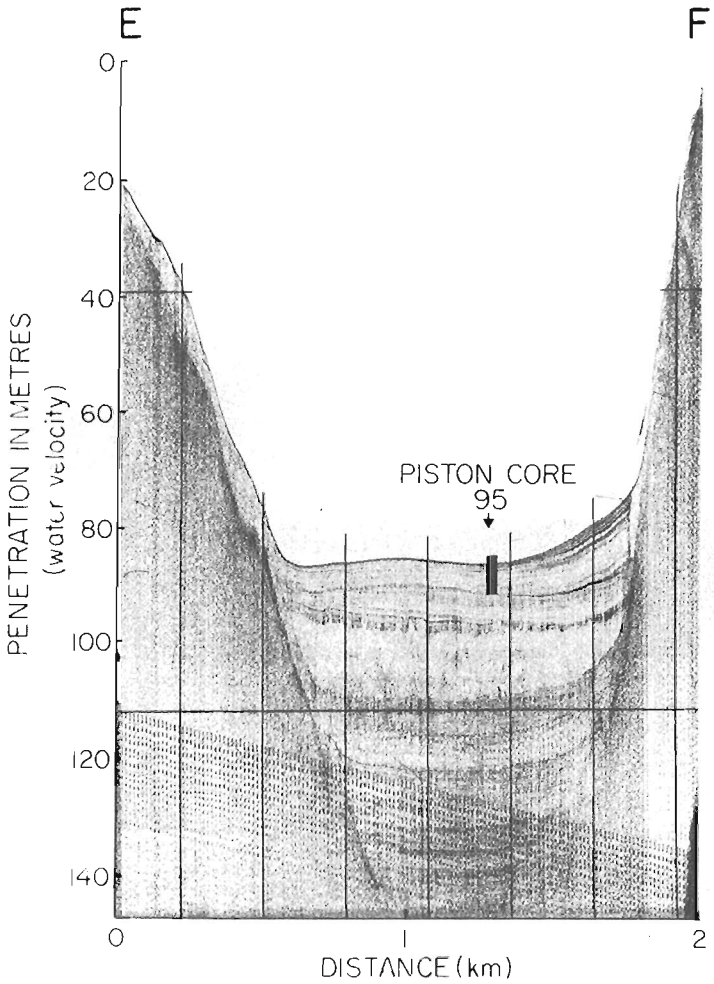

Figure 7.6A. Huntec DTS profile along E-F; see Figure 7.2 for location.

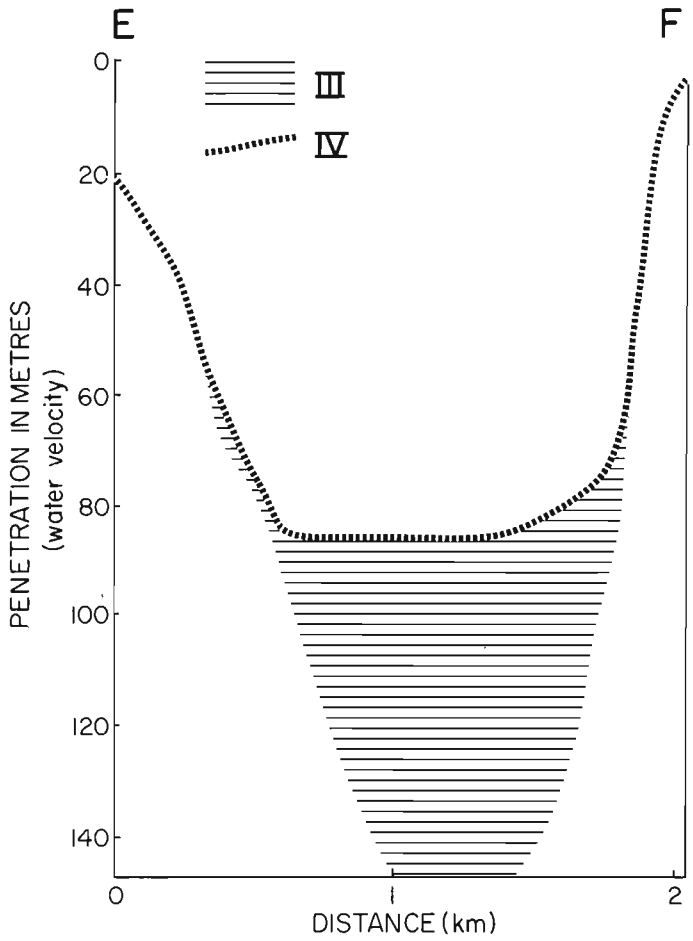

Figure 7.6B. Interpretation of profile E-F.

Unit 3

Towards the bottom of the most seaward core 82, the sandy gravelly mud has different characteristics from the gravelly layers of unit 2; it is a relatively stiff, dark brown (10 YR 4/3), more consolidated unit that may represent the uppermost till deposit of Josenhans (1983).

Biostratigraphy

In each of the six cores three faunal zones could be recognized (Table 7.1): A) surface zone dominated by arenaceous agglutinated species, B) intermediate zone of calcareous foraminifera dominated by **Islandiella helenae** and **Elphidium excavatum** f. **clavata** and C) bottom zone that is barren of foraminifera except for occasional occurrences of highly reworked tests.

Although the arenaceous species are dominant throughout Zone A, there is a change in species content towards offshore. In waters that are shallower than 200 m, the ranking species are **Spiroplectammina biformis, Reophax arctica, Eggerella advena** and **Islandiella helenae.** In waters that are deeper than 250 m the dominant species are **Reophax fusiformis, Adercotryma glomerata** and **Cribrostomoides crassimargo** (Table 7.1).

The arenaceous surface zone appears to be only a few centimetres thick in all the core sites, except at core 92, where the arenaceous species were found to a depth of approximately 107 cm. The thin surface zone was not sampled with the piston corer, which normally looses the surface muds during coring (Vilks et al., 1982). The faunas in Zone A were established by combining the results of Van Veen, box core and trigger core samples, but because of sampling uncertainties, the exact thickness of Zone A could not be established and boundaries shown in Table 7.1 are only approximate.

Zone B is characterized by predominantly calcareous species, which change their order of abundance from core to core in a random fashion, without showing major downcore or spatial trends (see Table 7.1) although a slight reduction in abundance of **I. helenae** and the occurrence of **V. fusiformis** in the offshore cores may indicate a minor biofacies change. Zone B is present throughout most of the cores with a relatively sharp and consistent boundary between Zones A and B. The boundary between B and C, however, is gradual and is defined here on the basis of abundance decreasing to less than one specimen per ml of sediment in Zone C.

The difference between Zones A and B is significant in terms of species number, abundance and diversity (Table 7.2). On the average, Zone A contains more than twice as many species as Zone B, with an average diversity of 2.3 in comparison to 1.4 in Zone B. The lower diversity in Zone B is due to the significantly lower species number, thus the equitabilities do not differ significantly in the two zones.

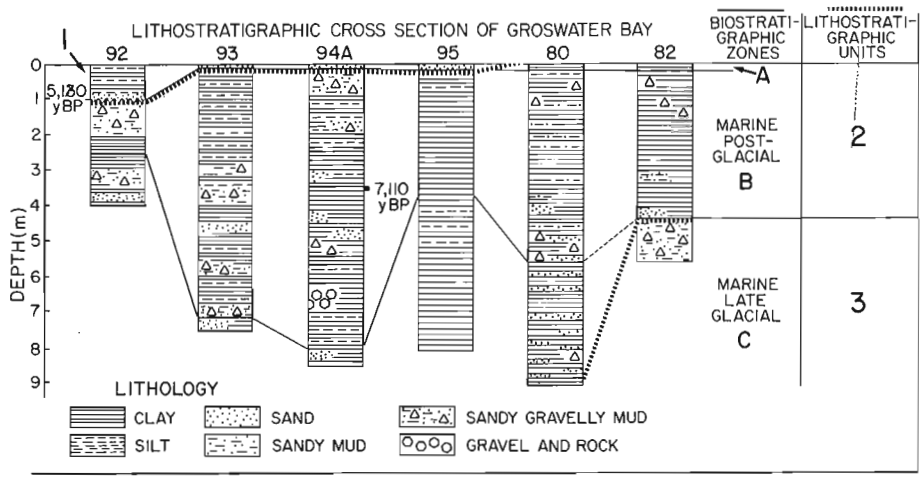

Figure 7.7

Lithostratigraphic units 1, 2, and 3 and biostratigraphic zones A, B and C.

Table 7.2. Comparison of species number between Zones A and B, diversity $H = -\Sigma_{pi} \ln_{pi}$, where pi is proportion of species in sample and equitability $e^{H/S}$, where S is number of species

Species	Tests/ ml	Diversity	Equitability	Zones	Station
16	5.3	2.07	0.52	A	92
9	3.7	1.35	0.40	B	
24	1.7	2.56	0.54	A	93
10	8.4	1.24	0.38	B	
27	5.1	2.45	0.40	A	94A
10	7.4	1.42	0.42	B	
24	4.8	2.37	0.45	A	95
11	33.6	1.36	0.36	B	
27	3.4	2.60	0.50	A	80
8	4.8	1.31	0.56	B	
17	13.1	1.89	0.41	A	82
12	11.5	1.40	0.33	B	
23	5.6	2.32	0.47	A	Averages
10	11.6	1.35	0.40	B	

However, in both zones the equitabilities are low, indicating that in both cases an important contribution to the diversity function is a relatively large number of species occurring in small proportions, i.e. the populations are strongly dominated by a few major species.

Although the average test per ml of sediment in Zone B is twice as high as in Zone A, the Coefficient of Variation (CV = Variance/Mean x 100) in Zone A is 258% and in Zone B 1073%, indicating that the difference in the mean is not significant. Nevertheless, Zone B can be characterized by a much larger variability of foraminiferal abundances.

In core 94A the total organic carbon dates are older than the carbonate carbon dates at the same level (Table 7.3) and in Core 95 downcore organic ^{14}C ages are reversed from 380 cm to surface. It is highly probable that redistribution of organic carbon has taken place mixing carbon of various ages. Sediment reworking is also evident from the truncated structures shown by the high resolution acoustic profiles along the sills and by ponded sediment in the basins. Thus, Fillon et al. (1981) may be correct in maintaining that the shell ^{14}C date in Core 94A is more reliable than the organic ^{14}C date.

To arrive at the most likely age framework for the sediments along the traverse, the ^{14}C dates are used in combination with the foraminiferal zone boundaries, assuming that these boundaries are synchronous over the length of the traverse. In the case of the A-B boundary, the assumption is realistic because of the insignificant onshore-offshore change in faunas, e.g., the A-B change is not basically depth controlled but due to a regional oceanographic change. The B-C boundary most likely is younger at core 92 than the offshore site of core 82.

The organic carbon date of core 92 places the ^{14}C age of the A-B boundary at 5180 BP or younger if the A-B boundary is marked by a hiatus. According to the age of this boundary and the shell date in core 94A the average sedimentation rate in Zone B of core 94A is 182 cm/1000 yr and the age of B-C boundary is 9576 BP or approximately 10 000 BP. Figure 7.7 shows that sedimentation rates in Zone B have varied considerably from basin to basin.

The extrapolated sedimentation rates can be used to suggest possible ages of acoustic units. For example, in core 95 the sedimentation rate in Zone B is 90 cm/1000 yr and assuming that this is a minimum sedimentation rate throughout the sediment column of 40 m, the till (acoustic unit I) was deposited at the most 50 000 BP. Thus the till must be early Wisconsinan rather than pre-Wisconsinan.

Correlation of acoustic, biostratigraphy and lithostratigraphy

The four acoustic units that were recognized signify the changing sedimentary environments through time. The surface unit IV of coarser sediments represents the ongoing sediment reworking and may be correlated to the lithostratigraphic unit 1. The foraminiferal Zone A was sampled with the piston corer only at station 92 where the coarse sediments of lithostratigraphic unit 1 were covered with close to one metre of fine sediments. At the remainder of localities piston core tops did not contain Zone A foraminifera, although they contained sediments of lithostratigraphic unit 1. Therefore, Zone A can only be correlated with a thin surface subunit of unit 1 that was sampled with the surface grabs.

Correlation of cores with acoustics shows that only part of unit III is sampled in the cores. Extrapolated ^{14}C dates and foraminifera in the six cores suggest that the ponded sediments of unit III span the time of the late glacial to postglacial oceanographic environments. It is interesting to note that the B-C boundary of foraminiferal zones is not detected in the acoustic profiles. Units II and I are beyond the reach of the cores and the interpretation entirely depends on the acoustic character of the sediment. The well stratified and conformable unit II may be proglacial to

Table 7.3. ^{14}C dates of cores discussed in this report

Age of sediment				
Core	Interval (cm)	^{14}C age BP	Material	Lab. number
94A	360-366	7 110 ± 240	Mollusc shell	GSC 3125
	350-375	15 330 ± 640	TOC	GSC 3126
92	84.5-103	5 180 ± 330	TOC	GSC 3274
95	118-133	13 900 ± 700	TOC	GSC 2993
	365-380	11 000 ± 440	TOC	GSC 3014
	760-775	20 400 ± 1 650	TOC	GSC 2977

TOC = total organic carbon

subglacial with sediment supplied from suspension in ice margin environment and with limited reworking (Barrie and Piper, 1982). It therefore represents a more proximal glacial environment than unit III when sediment reworking was a major process. It overlies the unstratified till of unit I that may have been deposited directly under glacial ice.

The lithological character of the cores shows a greater facies change towards offshore than change in time, thus, only lithostratigraphic unit 2 could be recognized throughout the six cores. The surface log of coarse sediment of unit 1 is present only on the shallower inner shelf and not on the deeper basins of cores 80 and 82. The sandy-gravelly mud of unit 2 also grades to finer sediment towards offshore. Unit 3 is found only at the bottom of core 82. This dark brown "till like" deposit could represent an extension towards the inner shelf of the upper till of Josenhans, 1983.

The biostratigraphy of the sediments between the cores is established with the correlation of two boundaries: the arenaceous-calcareous boundary between Zones A and B and the sharp reduction in preserved faunas between Zones B and C. The sharpness of the upper boundary associated with the distinctive faunal and lithological change strongly suggests the presence of an unconformity. Zone A-B boundary is very close to the surface, and if the ^{14}C date of the boundary at 5180 BP in core 92 is also true for the other cores, then it appears that very little sediment has been accumulating in the basins during the last 5000 years.

The interpretation of the A-B boundary, however, must be discussed in terms of the preservation of arenaceous foraminifera in subsurface sediment. Vilks et al. (1982) preferred poor preservation of arenaceous tests to explain the absence of arenaceous foraminifera in piston cores at localities where they were abundant in surface grabs. This explanation was based on the experience with deep sea sediments below the carbonate compensation depth where the rich arenaceous faunas in surface sediments are seldom found below surface. It is highly possible that the arenaceous tests are destroyed in areas of slow sedimentation rates in an oxidizing environment due to bacterial action and bioturbating macrobenthos. Thus, the possibility exists that the zone A-B boundary does not signify a faunal change in response to the environment, but poor preservation of arenaceous foraminifera.

Although on the Labrador Shelf a great number of arenaceous tests are destroyed in the bioturbated zone, other evidence would suggest that the A-B boundary does represent a paleo-oceanographic change at about 5000 BP. Firstly, a distinct arenaceous-calcareous change was also documented in Lake Melville piston cores several metres below surface and was dated at 5000 BP (Vilks and Mudie, 1983). Here, fast sedimentation rates would prevent test destruction. Secondly, both in Lake Melville and Labrador Shelf the total number of specimens (including calcareous) per ml of sediment is smaller in the surface arenaceous zone, with the calcareous faunas either totally absent or occurring in smaller numbers than in sediments below. Thirdly, a 100% arenaceous agglutinated fauna was also found in a surface zone of a number of cores collected from the inner Scotian Shelf, and their disappearance was interpreted to signify a paleo-oceanographic change (Scott et al., 1982).

The B-C boundary is gradual and was established within a zone of declining foraminiferal numbers, at a level where the core subsamples persistently contained less than one test/ml sediment. The reduction of tests per sample did not correspond with detectable change in species assemblages or evidence of carbonate dissolution. The preservation of carbonates must have been excellent because of the presence of pteropods in Zone C of core 92. The aragonitic pteropod tests are dissolved more readily than foraminifera in deep sea sediments and are seldom preserved on Labrador Shelf. Zone C, therefore, most likely represents a period of relatively fast sedimentation rates of glaciofluvial material during a period before about 10 000 BP. The B-C boundary is prominent in all the cores across the inner shelf, but it could be diachronous because of the earlier reduction of sediment-rich effluent offshore, away from the source.

SUMMARY OF STRATIGRAPHIC INTERPRETATION

Acoustic stratigraphy and lithostratigraphy provide basic information of major paleosedimentary changes in terms of sediment dynamics and mode of deposition on the inner shelf. Major faunal changes reflect changes in oceanographic setting, and are influenced to a lesser extent by sediment dynamics. Therefore, in the dynamic sedimentary environment of the inner shelf, foraminiferal zones can provide more continuous stratigraphic markers, provided the sedimentary basins are sufficiently open to the sea and do not create localized oceanographic environments.

The acoustic character suggests that the earliest sediments on top of the basement were deposited by ice, and that the glacial sediments are overlain by a sequence of stratified glacial marine or marine deposits. Very little can be said about the oceanographic environment of sediments deeper than can be reached by piston coring.

The oceanographic setting in Zone C at the bottom of the piston cores, was probably governed by glacial runoff that carried high amounts of sediment as indicated by previous studies of Core 95 (Vilks and Wang, 1981). The combined effect of high sedimentation rates and perhaps dilution of the water would account for the reduction of benthos.

At the beginning of Zone B, around 10 000 BP the glacial runoff decreased and the inner shelf Labrador Current became a dominant feature. The **Elphidium excavatum f. clavata, Islandiella helenae** and **Cassidulina reniforme** faunas are characteristically euryhaline species occurring at bottom water salinity ranges between 34.9-30‰, but with high relative abundances only in the 32-33‰ range (Mudie et al., 1983). The marginal marine aspect is also demonstrated by the low species diversities and moderate faunal abundances. The faunas do not show a major change from nearshore to offshore, indicating extensive inner shelf waters at least to the Marginal Channel of the Labrador Shelf.

The high diversity arenaceous faunas of Zone A are difficult to explain. **Spiroplectammina biformis** is the major species in waters shallower than 200 m in inter-island seas of the Queen Elizabeth Islands that are covered with summer ice (Vilks, 1969). The other species are also common in the cold intermediate water of the Gulf of St. Lawrence (Schafer and Cole, 1978). The total assemblage suggests lower water temperatures and may coincide with the appearance of the cold core of the Labrador Current between 50 and 200 m in the water column around 5000 BP.

ACKNOWLEDGMENTS

We are grateful to David J.W. Piper and Peta J. Mudie for their constructive criticism of the manuscript.

REFERENCES

Barrie, C.Q. and Piper, D.J.W.
1982: Late Quaternary marine geology of Makkovik Bay, Labrador; Geological Survey of Canada, Paper 81-17, 37 p.

Fillon, R.H., Hardy, I.A., Wagner, F.J.E., Andrews, J.T., and Josenhans, H.W.
1981: Labrador Shelf: shell and total organic matter ^{14}C date discrepancies; in Current Research, Part B, Geological Survey of Canada, Paper 81-1B, p. 105-111.

Fulton, R.J. and Hodgson, D.A.
1979: Wisconsin glacial retreat, southern Labrador; in Current Research, Part C, Geological Survey of Canada, Paper 79-1C, p. 17-21.

Grant, A.C.
1972: The continental margin off Labrador and eastern Newfoundland – morphology and geology; Canadian Journal of Earth Sciences, v. 9, no. 11, p. 1394-1430.

Josenhans, H.W.
1983: Evidence of pre-late Wisconsinan glaciations on Labrador Shelf – Cartwright Saddle region; Canadian Journal of Earth Sciences, v. 20, no. 2, p. 225-235.

Kontopoulos, N. and Piper, D.J.W.
1982: Late Quaternary stratigraphy and sedimentation, Kaipokok Bay, Labrador; in Current Research, Part B, Geological Survey of Canada, Paper 82-1B, p. 1-6.

Mudie, P.J., Keen, C.E., Hardy, I., and Vilks, G.
1983: Multivariate analysis of benthic foraminifera in seabed samples and Late Quaternary sediment cores, northern Canada; Marine Micropaleontology.

Rogerson, R.J.
1977: Glacial geomorphology and sediments of the Porcupine Strand area, Labrador, Canada; unpublished Ph.D. thesis, MacQuarie University, Eastwood, Sydney, Australia, 277 p.

Scott, D.B., Mudie, P.J., and Vilks, G.
1982: Holocene-Late Wisconsinan paleo-oceanographic events on the Scotian Shelf, Canada; Geological Society of America, Abstracts with Programs, v. 15, no. 7, p. 613.

Schafer, C.T. and Cole, F.E.
1978: Distribution of foraminifera in Chaleur Bay, Gulf of St. Lawrence; Geological Survey of Canada, Paper 77-30, 55 p.

Umpleby, D.C.
1979: Geology of the Labrador Shelf; Geological Survey of Canada, Paper 79-13, 34 p.

Vilks, G.
1969: Recent foraminifera in the Canadian Arctic; Micropaleontology, v. 15, no. 1, p. 35-60.

1980: Postglacial basin sedimentation on Labrador Shelf; Geological Survey of Canada, Paper 78-28, 28 p.

Vilks, G. and Mudie, P.J.
1978: Early deglaciation of the Labrador Shelf; Science, v. 202, p. 1181-1183.

1983: Evidence for postglacial paleo-oceanographic and paleoclimatic changes in Lake Melville, Labrador; Arctic and Alpine Research.

Vilks, G. and Wang, Y.
1981: Surface texture of quartz grains and sedimentary processes on the southeastern Labrador Shelf; in Current Research, Part B, Geological Survey of Canada, Paper 81-1B, p. 55-61.

Vilks, G., Deonarine, B., Wagner, F.J., and Winters, G.V.
1982: Foraminifera and mollusca in surface sediments of southeastern Labrador Shelf; Geological Society of America, Bulletin, v. 93, p. 225-238.

8. LATE TRIASSIC AND JURASSIC MAGMATISM ALONG THE STIKINE ARCH AND THE GEOLOGY OF THE STIKINE BATHOLITH, NORTH-CENTRAL BRITISH COLUMBIA

Project 700047

R.G. Anderson
Cordilleran Geology Division, Vancouver

Anderson, R.G., Late Triassic and Jurassic magmatism along the Stikine Arch and the geology of the Stikine batholith, north-central British Columbia; in Current Research, Part A, Geological Survey of Canada, Paper 84-1A, p. 67-73, 1984.

Abstract

The informally named Stikine batholith is typical of Late Triassic and Jurassic composite intrusions which underlie part of the Stikine Arch and are coeval and, in part, comagmatic with Middle to Upper Triassic Stuhini Group volcanism. Heterogeneous, equigranular or megacrystic, and medium grained leucocratic granite, quartz monzodiorite or diorite, hornblendite or hornblende clinopyroxenite, quartz monzonite or granite and gabbro phases were emplaced sequentially into polydeformed Mississippian to Permian chlorite schist, chert and amphibolite and massive Upper Triassic porphyritic volcanics. A Late Triassic isotopic age (222 ± 10 Ma) is consistent with observed external and interphase intrusive relations. A small, composite mid(?)-Jurassic inrusion crosscuts part of the Late Triassic pluton and volcanics. Lithology, structure, associated subvolcanic dykes, intrusive relations, isotopic age and petrography of Late Triassic phases in the Stikine batholith compare closely with the Triassic plutonic suite of the Hotailuh Batholith 125 km to the west along the Stikine Arch.

Résumé

Le batholite auquel on a officieusement donné le nom de Stikine est caractéristique des intrusions composées du Trias récent et du Jurassique; ces dernières, sous-jacentes à une partie de l'arche de Stikine, sont contemporaines et en partie comagmatiques avec le volcanisme du groupe Stuhini du Trias moyen à supérieur. Des roches hétérogènes, équigranulaires ou macrocristallines composées de granite leucocrate à grains moyens, de monzodiorite quartzique ou de diorite quartzique, de hornblendite ou de clinopyroxénite à hornblende, de monzonite quartzique ou de phases de granite et de gabbro, ont été mises en place les unes après les autres dans des schistes chloriteux, des cherts et des amphibolites mississipiens à permiens polydéformés et des roches volcaniques porphyriques massives du Trias supérieur. L'âge isotopique du Trias récent (222 ± 10 ma), correspond aux relations externes et aux relations intrusives de l'interphase observées. Une petite intrusion composite du Jurassique moyen (?) traverse une partie du pluton et des roches volcaniques du Trias récent. La lithologie, la structure, les filons subvolcaniques conveyes, les liens intrusifs, l'âge isotopique et la pétrographie des phases du Trias récent dans le batholite de Stikine se comparent étroitement à la suite plutonique d'âge triassique du batholite Hotailuh, situé à 125 km à l'ouest le long de l'arche de Stikine.

INTRODUCTION

The easterly-trending Stikine Arch (Fig. 8.1) was the site of Permian to mid-Triassic deformation and metamorphism, localized Middle to Late Triassic magmatism. Subsequently it became the provenance for Early to Middle Jurassic sedimentation in the Whitehorse Trough (Fig. 8.1; Souther and Armstrong, 1966; Souther, 1971, 1977; Bultman, 1979; Tipper, 1978; Anderson, 1983; Read, 1983). Recent studies of the Hotailuh Batholith (Anderson, 1978, 1979, 1980, 1983; Fig. 8.1) showed that a suite of Late Triassic plutons characterized by distinctive lithology, structure, external and interplutonic intrusive relations, associated subvolcanic dykes, isotopic age, petrography and geochemistry could be separated from a Jurassic plutonic suite. The Late Triassic plutons are essentially coeval and, in some cases, comagmatic with the surrounding Middle to Upper Triassic Stuhini Group volcanics (Anderson, 1983; Read, 1983).

The Stikine batholith, north of the Stikine River and 125 km east of the Hotailuh Batholith (Fig. 8.1), was considered to be part of a Late Triassic or Early Jurassic suite of plutons spatially related to volcanics of the Upper Triassic Takla and Jurassic Hazelton groups (Gabrielse, 1977; Thorstad, 1980) and of about the same age (222 ± 10 Ma; Dodds in Wanless et al., 1979, p. 10). The present study indicates close similarity in lithology, structure, intrusive relations and stratigraphic age, geochronometry and petrography between the Late Triassic phases in the Stikine

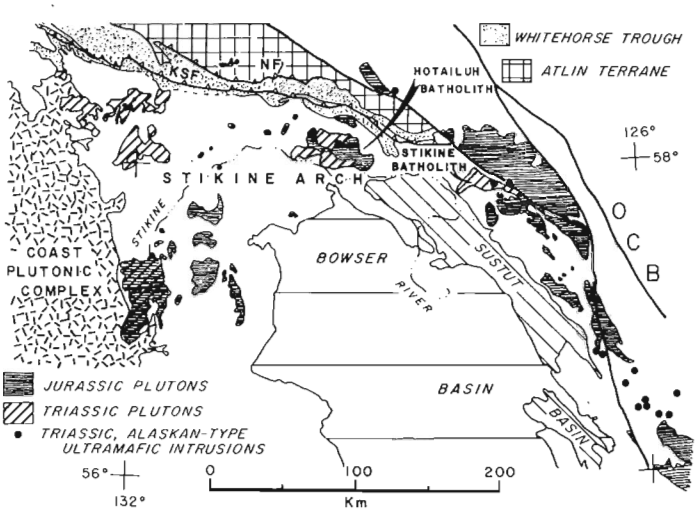

Figure 8.1. Tectonic elements near the Stikine Arch and location of the Stikine batholith and Hotailuh Batholith (modified from Tipper et al., 1981). Abbreviations are: KSF = King Salmon Fault; NF = Nahlin Fault; and OCB = Omineca Crystalline Belt.

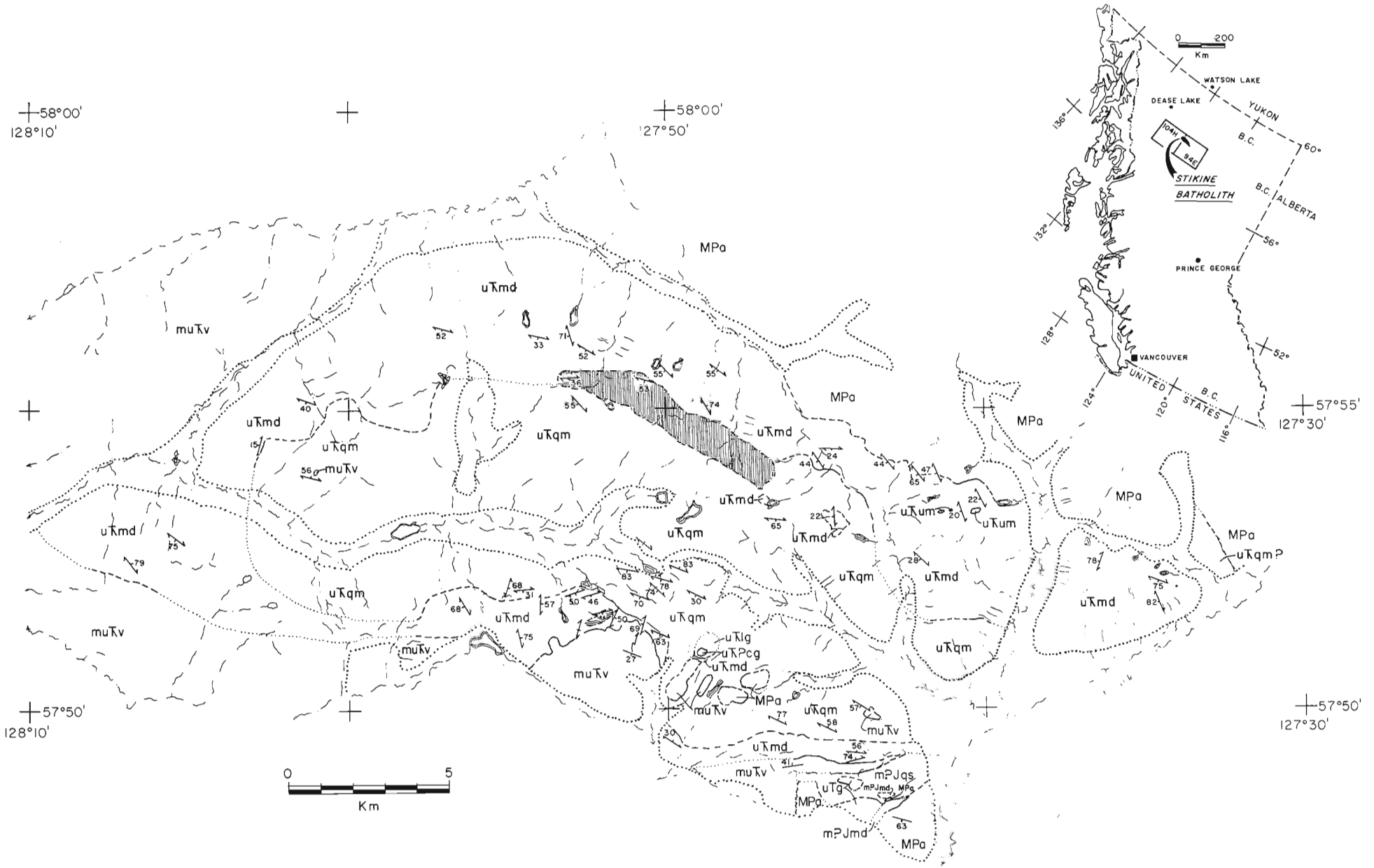

Figure 8.2. *Location (inset map) and geology of the Stikine batholith. Geology of the country rocks modified from Thorstad (1980) and Gabrielse (1977, unpublished information, 1977).*

Legend for Figure 8.2

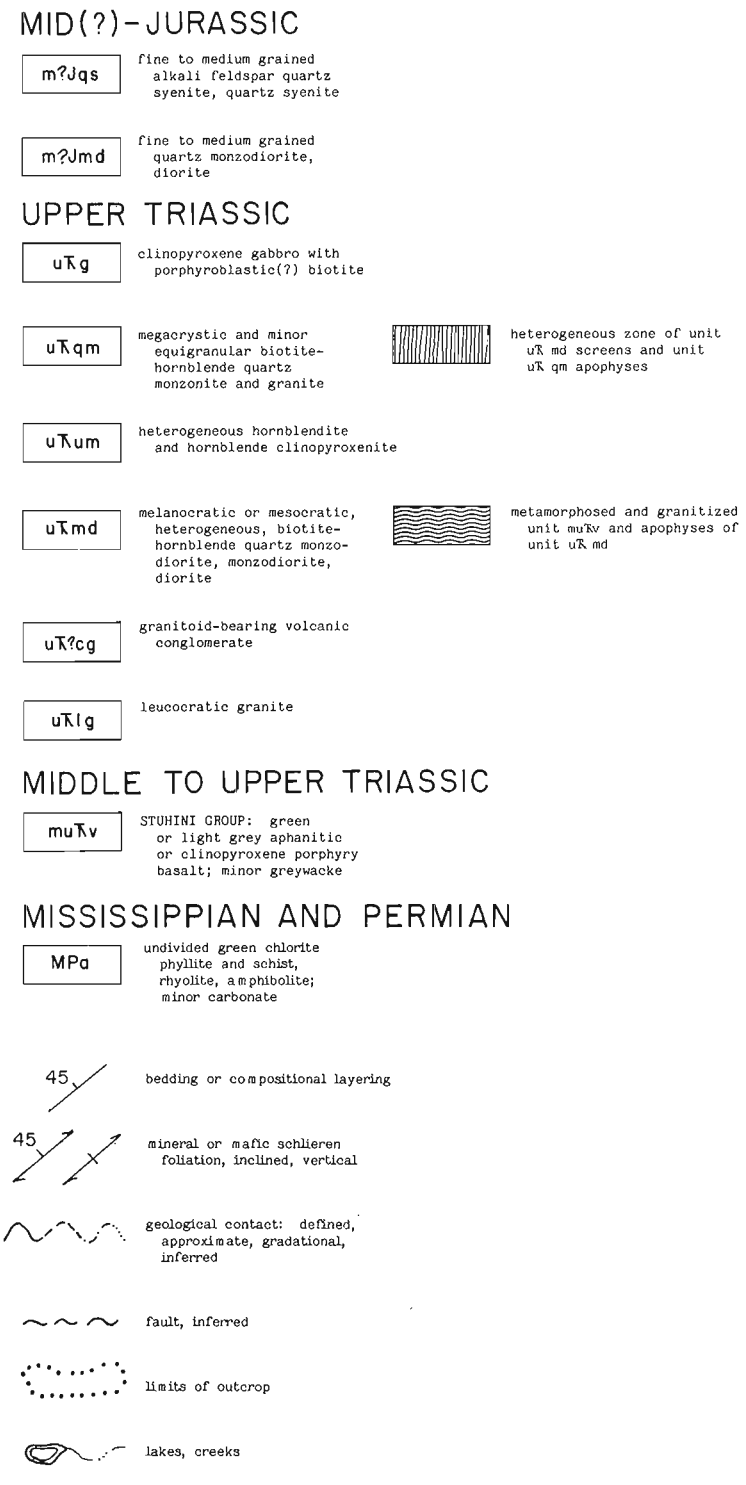

batholith and the Late Triassic plutonic suite of the Hotailuh Batholith. Both have the same relationships with Stuhini Group volcanics and sediments.

GEOLOGY OF THE STIKINE BATHOLITH AND COUNTRY ROCKS

Late Triassic and mid(?)-Jurassic plutons constitute the Stikine batholith (300 km^2 in area) and are distinguished on the bases of lithology, inclusions, structure, intrusive relations, and associated dykes (Fig. 8.2, 8.3). The batholith was emplaced into polydeformed Mississippian to Permian metasediments and metavolcanics (Thorstad, 1980) and massive Middle to Upper Triassic clinopyroxene porphyry volcanics.

Country rocks

Mississippian to Permian greenish grey chlorite phyllite and schist, amphibolite, white weathering, poorly layered rhyolite and minor carbonate (unit MPa, Fig. 8.2; unit Pa of Gabrielse (1977); units 1, 2, 3 and 5 of Thorstad, (1980, Fig. 23.2 and 23.3)) occur as pendants and form the country rock for the batholith along its northeastern and part of its southeastern margins (Fig. 8.2). Locally along the northeastern margin, two phases of folding (refolded folds; see also Thorstad (1980, Fig. 23.4)) were recognized in the amphibolite.

Dark greyish green, massive, uralized clinopyroxene porphyry and aphanitic basalt and minor greywacke of the Middle to Upper Triassic Stuhini Group (unit muTv) are intruded by or included as pendants within units uTmd and uTqm. Metamorphism of the volcanics is characterized by amphibolitization of the mafic groundmass. A distinctive elongate pendant, 200 m wide, consisting of metamorphosed and granitized amphibolite and mafic diorite apophyses parallels part of the southern margin of the batholith (Fig. 8.2). A 100-300 m wide screen of aphanitic basalt separates the extensive Late Triassic and mid(?)-Jurassic phases near the batholith's southeastern margin.

A small outcrop of distinctive granitoid-bearing, massive volcanic conglomerate occurs in the south central part of the batholith (unit uT?cg; Fig. 8.2). The conglomerate appears to overlie nonconformably the leucocratic granite (unit uTlg) along an irregular paleosurface which was subsequently tilted. Unsorted, predominantly matrix-supported, round to subangular common leucocratic granite (similar to unit uTlg), uncommon green clinopyroxene-plagioclase porphyry and rare chlorite schist fragments reach sizes of 1.5 x 1.5 x 0.5 m (average length 5-10 cm) and make up 85-90 per cent of the rock. Poorly sorted greywacke forms the groundmass. Locally, the fragments are crudely imbricated and imply a southerly or southwesterly current direction (uncorrected for poorly known orientation of the conglomerate). Size, shape and lithological similarity of the granitoid fragments to the underlying leucocratic granite suggest a provenance for the fragments close to its present location. The age of the conglomerate and its relationship to surrounding Stuhini Group stratigraphy is not known but it must postdate an episode of clinopyroxene porphyritic basaltic volcanism.

Late Triassic pluton

Five heterogeneous, massive or well foliated, equigranular or megacrystic, medium grained phases make up the Late Triassic pluton in the Stikine batholith (Fig. 8.2).

Pink weathering, massive, siliceous, leucocratic granite (unit uTlg) with sparse biotite underlies a small area (0.5 km^2) in the central part of the batholith. Granitoid-bearing volcanic conglomerate (see above) nonconformably

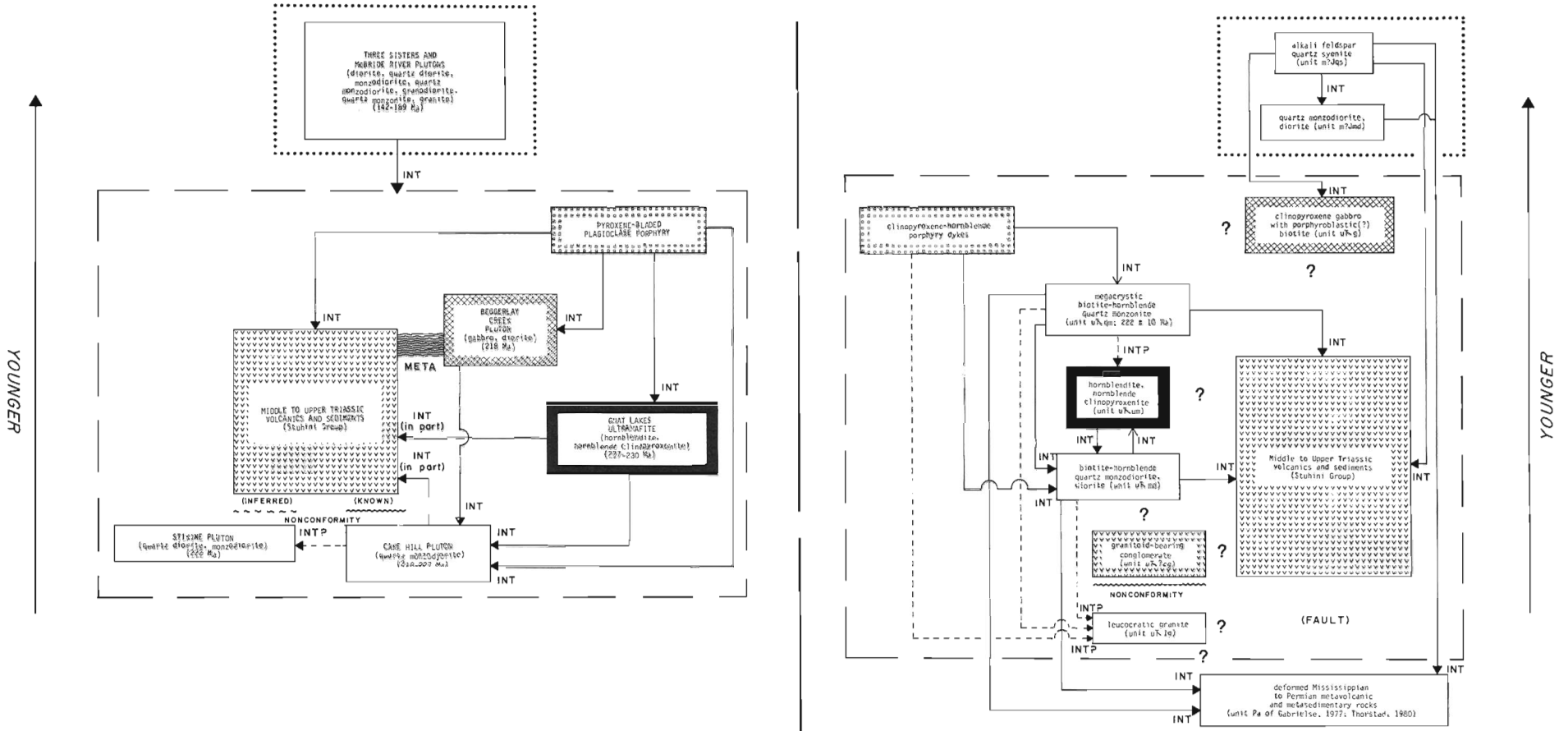

HOTAILUH BATHOLITH

STIKINE BATHOLITH

Arrows lead from intrusion to country rock.
Solid arrowhead indicates most common intrusive relations.
Open arrowhead indicates less common relationship.
Heavy dashed box – Middle and Late Triassic volcano-plutonic units.
Dotted box – Early and Middle Jurassic plutonic suites.

Dashed lines indicate probable but uncertain geological relationships.
Question marks indicate unknown relationships.
INT = intrusive, META = metamorphoses.

Potassium-argon isotopic age for the Stikine batholith taken from Wanless et al. (1979, GSC Paper 78-22, p. 10).
Isotopic ages for the Hotailuh Batholith are summarized in Stevens et al. (1982, p. 4-11) and Anderson et al. (1982).

Figure 8.3. *External, interphase and interplutonic intrusive relations for the Stikine batholith and comparisons with the Late Triassic plutonic suite of the Hotailuh Batholith. Intrusive relations for Late Triassic plutons in the Hotailuh Batholith are modified from Anderson (1979, 1983) and Read (1983, personal communication, 1983).*

overlies the unit along a poorly exposed irregular paleosurface. Instrusive relations are poorly exposed but the leucocratic granite may be intruded by units uTmd and uTgm and by a mafic clinopyroxene-hornblende porphyry dyke.

Melanocratic or mesocratic, commonly well foliated and rarely lineated, heterogeneous biotite-hornblende quartz monzodiorite, monzodiorite and diorite (unit uTmd) form a discontinuous marginal phases in the batholith 0.5-2.5 km wide (134 km^2 in area). Mafic minerals define a steeply dipping, predominantly northwesterly or westerly trending planar fabric. Round or oval mafic inclusions are most common in this phase (1-5 per cent) and consist of medium grained hornblendite or hornblende clinopyroxenite (similar to unit uTum) and fine grained diorite. Unit uTmd is clearly intruded by units uTqm and uTum and aplite, clinopyroxene-hornblende porphyry and aphanitic, mafic dykes. Part of the northeastern contact between units uTmd and uTqm is marked by a heterogeneous zone of quartz monzodiorite screens and pendants (with subhorizontal mineral foliation) and equigranular granite apophyses 700-1200 m wide (Fig. 8.2). Elsewhere, within 100-200 m of this contact, a metasomatic aureole is developed, distinguished by uncommon but widespread alkali feldspar megacrysts in the quartz monzodiorite. The megacrystic quartz monzonite appears to grade into the quartz monzodiorite at these localities. Along some contacts with unit uTum and rarely with unit uTqm, the quartz monzodiorite is apparently remobilized and back-veins the hornblendite.

Unit uTum consits of dark greyish green, massive, heterogeneous, medium grained or medium to coarse grained hornblendite, hornblende clinopyroxenite and minor, mafic hornblende gabbro. It form small (50-200 m^2) round to elliptical plugs in unit uTmd, aligned along a westerly trend. Although not seen in contact with unit uTqm, unit uTum is assumed to be older because the megacrystic unit uTqm contains lithologically similar ultramafic inclusions.

An extensive area (117 km^2) of more felsic rock (unit uTqm) forms the core of the batholith. It is a white or mottled pink and white weathering, massive, foliated or rarely lineated, medium grained, megacrystic or equigranular, biotite-hornblende quartz monzonite or granite. Small (1 cm) squarish, pink alkali feldspar megacrysts make up 1-5 per cent of the rock and locally contain inner concentric zones of fine grained mafic minerals. Equigranular granite is most common near the northern intrusive contacts with unit uTmd. Mineral foliation is faintly to intensely developed, and is steeply dipping and westerly trending. Foliation of the mafic minerals is most common; intensely foliated rocks contain alternating thin lenses of quartz and alkali feldspar. Xenoliths are rare (less than one per cent) and are predominantly medium grained hornblendite or hornblende clinopyroxenite. Aplite, mafic aphanitic and biotite porphyry and rare clinopyroxene-hornblende porphyry dykes intrude unit uTqm.

Unit uTg forms two small oblong bodies (0.85 km^2 in total area) along the southeastern part of the batholith. It is melanocratic, greyish green weathering, massive, seriate, medium grained gabbro characterized by coarse, uralized clinopyroxene and locally, by porphyroblastic(?) biotite. Unit mJqs intrudes and separates unit uTg from other Late Triassic phases in the batholith, but the gabbro phase is included in the Late Triassic pluton on the basis of its grain size, mineralogy and intrusive relations with the mid(?)-Jurassic pluton.

Mid(?)-Jurassic pluton

A small (3.5 km^2), westerly-elongated, massive, equigranular, fine to medium grained, composite mid(?)-Jurassic pluton occurs south of the southeastern margin of the batholith. Heterogeneous, massive, fine grained or fine- to medium-grained, biotite-hornblende quartz monzodiorite and diorite (unit m?Jmd; 0.34 km^2 in area) are intruded by more extensive (3.2 km^2 in area), pink weathering hornblende-biotite alkali feldspar quartz syenite and quartz syenite (unit m?Jqs). The latter phase is also equigranular and fine- to medium-grained, but is more homogeneous than the mafic phase. The clinopyroxene-hornblende porphyry dykes, distinctive of the Late Triassic pluton, were not observed in the mid(?)-Jurassic pluton.

AGE

A single K-Ar isotopic age of 222 ± 10 Ma was determined for hornblende from a sample of unit uTqm (GSC Paper 78-22; Dodds in Wanless et al., 1979, p. 10). Besides this determination, intrusive relations between the Late Triassic pluton and Stuhini Group volcanics (Fig. 8.3), which are known to be Middle to Late Triassic (Souther, 1971; Monger, 1977, 1980; Read, 1983), and intraplutonic intrusive relations suggest a Late Triassic age for most of the batholith. In view of the loose stratigraphic constraints and lack of isotopic dating, the mid(?)-Jurassic age assignment of the younger pluton is made on the basis of lithological similarity to the dated Mount Albert Dease suite (167 ± 6 Ma; Dodds in Wanless et al., 1979, p. 11).

PETROGRAPHY

Accessory minerals zircon, apatite, opaque minerals (magnetite?) and titanite and essential minerals plagioclase, clinopyroxene, hornblende, biotite, quartz and alkali feldspar (in approximate order of crystallization) characterize the extensive Late Triassic phases in the Stikine batholith. Clinopyroxene cores in olive to bluish green hornblende and irregular, calcic (labradorite?) cores in oligoclase or andesine are typical in unit uTmd. Microperthitic, poikilitic alkali feldspar distinguish unit uTqm. Intensely foliated varieties of both phases contain strained biotite, common quartz subgrains and small-scale mortar texture adjacent to bent plagioclase which is aligned with the mafic foliation.

Hornblendite of unit uTum is characterized by optically zoned euhedral hornblende, medium grained apatite and titanite, uncommon, finer grained euhedral clinopyroxene and interstitial, altered plagioclase.

Unit uTg is the most pervasively altered of any phase in the batholith. Uralization of subophitic clinopyroxene, intense sericitization and sausseritization of subhedral or euhedral plagioclase, clots of actinolite(?), chlorite and epidote and late forming, poikiloblastic biotite are characteristic.

Widespread subhedral or euhderal, pale to chocolate brown biotite, which contain rare apatite inclusions, distinguishes the extensive Late Triassic phases (units uTmd and uTqm) in the Stikine batholith from compositionally similar and coeval plutons (i.e. Stikine and Cake Hill plutons) in the Hotialuh Batholith. The petrography of the mafic, Late Triassic phases (units uTum and uTg) in the Stikine batholith is identical with that of the Gnat Lakes ultramafite and Beggerlay Creek pluton, respectively, in the Hotailuh Batholith.

COMPARISONS BETWEEN THE STIKINE AND HOTAILUH BATHOLITHS

There are striking similarities in lithology, structure, intrusive relations, petrography and isotopic age of the Late Triassic and mid(?)-Jurassic plutons in the Stikine and Hotailuh batholith (Fig. 8.3). Nonetheless, type and distribution of some plutons or phases distinguish each batholith.

The Late Triassic plutons in each batholith are most similar. Specifically, the mafic units uTum and uTg of the Stikine batholith are lithologically and petrographically similar to the Gnat Lakes Ultramafite and Beggerlay Creek pluton, respectively, of the Hotailuh Batholith (Anderson, 1978, 1979, 1983). The most extensive plutons or phases in each batholith (units uTmd and uTqm in the Stikine batholith; Stikine and Cake Hill plutons in the Hotailuh Batholith) are dissimilar, especially in the presence of common biotite in the Stikine batholith, but all are characterized by a widespread, moderately to intensely developed, easterly or northwesterly trending mineral foliation. The stikine batholith is characterized by sequential intrusion towards its core and by the extensive, megacrystic biotite-hornblende quartz monzonite.

Relationships between the Late Triassic plutonic suites and surrounding Middle to Upper Triassic Stuhini Group volcanics and sediments are common to both batholiths (Fig. 8.3). Granitoid-bearing volcanic conglomerates, which nonconformably overlie the source for the granitoid detritus, are associated with each batholith. Late Triassic plutons in both areas intrude Middle and (or) Upper Triassic sediments and volcanics (Anderson, 1979; Read, 1983). Mafic, porphyritic basalt dykes with some or all of bladed plagioclase, clinopyroxene and hornblende phenocrysts, characterize both Late Triassic plutonic suites and are absent in the Jurassic plutons. The coeval, spatial and probable comagmatic association of the dykes, hornblendite and hornblende clinopyroxenite intrusions and lithologically similar porphyritic basaltic volcanics of the Stuhini Group is a significant petrogenetic similarity between these plutonic suites.

The K-Ar isotopic age for the megacrystic quartz monzonite is within the 213-230 Ma range of K-Ar isotopic ages determined for the Late Triassic plutonic suite in the Hotailuh Batholith (Anderson in Stevens et al., 1982).

Finally, the association of crudely similar Early to Middle Jurassic composite plutons with the Late Triassic plutonic suites of each batholith and Middle to Late Triassic volcanism indicates a long-lived magmatic history for these areas.

CONCLUSIONS

The Stikine batholith in northwestern Toodoggone River and northeastern Spatsizi map areas consists of composite Late Triassic (222 ± 10 Ma) and mid(?)-Jurassic plutons which intrude Middle to Upper Triassic Stuhini Group volcanics. Distribution and nature of constituent phases and their lithology, structure, inclusions, intrapluton, interpluton, and external intrusive relations, petrography and isotopic age are similar to that for coeval plutonic suites in the Hotailuh Batholith 125 km to west.

Similar late Paleozoic and Mesozoic deformational, metamorphic, volcanic and structural histories may be traced along the easterly strike of the Stikine Arch. Plutonic styles in large Mesozoic plutono-volcanic centres, which underlie parts of the Stikine Arch, are also comparable.

ACKNOWLEDGMENTS

Helicopter access to the area and other logistical support from the Operation Dease field party based at Dease Lake under the direction of Dr. H. Gabrielse and the assistance of A. Arthur, A. Duvadi and J. Steel are gratefully acknowledged.

REFERENCES

Anderson, R.G.
1978: Preliminary report on the Hotailuh Batholith: its distribution, age and contact relationships in the Cry Lake, Spatsizi and Dease Lake map-areas, north-central British Columbia; in Current Research, Part A, Geological Survey of Canada, Paper 78-1A, p. 29-31.

1979: Distribution and emplacement history of plutons within the Hotailuh Batholith in the Cry Lake and Spatsizi map-areas, north-central British Columbia; in Current Research, Part A, Geological Survey of Canada, Paper 79-1A, p. 393-395.

1980: Satellitic stocks, volcanic and sedimentary stratigraphy, and structure around the northern and western margins of the Hotailuh Batholith, north-central British Columbia; in Current Research, Part A, Geological Survey of Canada, Paper 80-1A, p. 37-40.

1983: The geology of the Hotailuh Batholith and surrounding volcanic and sedimentary rocks, north-central British Columbia; unpublished Ph.D. thesis, Carleton University.

Anderson, R.G., Loveridge, W.D., and Sullivan, R.W.
1982: U-Pb isotopic ages of zircon from the Jurassic plutonic suite, Hotailuh Batholith, north-central British Columbia; in Current Research, Part C, Geological Survey of Canada, Paper 82-1C, p. 133-137.

Bultman, T.R.
1979: Geology and tectonic history of the Whitehorse Trough west of Atlin, British Columbia; unpublished Ph.D. thesis, Yale University, 284 p.

Gabrielse, H.
1977: Geology of Toodoggone (NTS 94 E) and Ware (NTS 94 F W/2) map-areas, British Columbia; Geological Survey of Canada, Open File 483.

Monger, J.W.H.
1977: The Triassic Takla Group in McConnell Creek map-area, north-central British Columbia; Geological Survey of Canada, Paper 76-29, 45 p.

1980: Upper Triassic stratigraphy, Dease Lake and Tulsequah map areas, northwestern British Columbia; in Current Research, Part B, Geological Survey of Canada, Paper 80-1B, p. 1-9.

Read, P.B.
1983: Geology, Classy Creek (104 J/2E) and Stikine Canyon (104 J/1W), British Columbia; Geological Survey of Canada, Open File 940.

Souther, J.G.
1971: Geology and mineral deposits of the Tulsequah map-area, British Columbia; Geological Survey of Canada, Memoir 362, 84 p.

1977: Volcanism and tectonic environments in the Canadian Cordillera – a second look; in Volcanic Regimes in Canada, ed. W.R.A. Baragar, I.C. Coleman and J.M. Hall; Geological Association of Canada, Special Paper 16, p. 3-24.

Souther, J.G. and Armstrong, J.E.
1966: North central belt of the Cordillera of British Columbia; in Tectonic History and Mineral Deposits of the Western Cordillera. Canadian Institute of Mining and Metallurgy, Special Volume 8, p. 171-184.

Stevens, R.D., Delabio, R.N., and Lachance, G.R.
1982: Age determinations and geological studies, Geological Survey of Canada, Paper 82-2, p. 4-11.

Thorstad, L.
1980: Upper Paleozoic volcanic and volcaniclastic rocks in northwest Toodoggone map area, British Columbia; in Current Research, Part B, Geological Survey of Canada, Paper 80-1B, p. 207-211.

Tipper, H.W.
1978: Jurassic biostratigraphy, Cry Lake map-area, British Columbia; in Current Research, Part A, Geological Survey of Canada, Paper 78-1A, p. 25-27.

Tipper, H.W., Woodsworth, G.J., and Gabrielse, H.
1981: Tectonic assemblage map of the Canadian Cordillera and adjacent parts of the United States of America; Geological Survey of Canada, Map 1505A.

Wanless, R.K., Stevens, R.D., Lachance, G.R., and Delabio, R.N.
1979: Age determinations and geological studies; Geologial Survey of Canada, Paper 79-2, p. 10.

9. DEVELOPMENT-INDUCED TIDAL FLAT EROSION, FRASER RIVER DELTA, BRITISH COLUMBIA

Project 790006

J.L. Luternauer[1], D. Duggan[1], and M. Hendry[1]
Cordilleran Geology Division, Vancouver

Luternauer, J.L., Duggan, D., and Hendry, M., Development-induced tidal flat erosion, Fraser River Delta, British Columbia; in Current Research, Part A, Geological Survey of Canada, Paper 84-1A, p. 75-80, 1984.

Abstract

Dendritic creeks have eroded part of the ecologically important eelgrass beds at the head of a ship basin lying between causeways on southern Roberts Bank. Preliminary field investigations and airphoto interpretations coupled with data drawn from previous reports suggest (a) focusing of ebb tidal flows by the dredged depression and consequent increase in flow velocities are the direct causes of the erosion, (b) a crest protection wall or dyke built at the head of the basin and across the channels has not stopped channel extension, (c) creeks within an area which were exposed to siltation during dredging operations are more stable than those in an adjacent area floored by cleaner sand and (d) the locus of fastest erosion has migrated, or is migrating, to the eastern side of the vegetated intercauseway area which allows free access of ebbing waters to the open Strait of Georgia.

Résumé

Des cours d'eau dendritiques ont érodé une partie des lits de zostères d'importance écologique à l'amont d'un bassin situé entre des chaussées de la partie sud du banc Roberts. Des études préliminaires sur le terrain et des travaux d'interprétation de photographies aériennes, ainsi que des données prélevées de rapports antérieurs, suggèrent a) que l'érosion résulte directement de la concentration des eaux des marées descendantes par la dépression draguée et de l'augmentation résultante de la vitesse d'écoulement, b) qu'un mur de protection ou levée construit à l'amont du basin et en travers des chenaux n'a pas empêché la prolongation du chenal, c) que les ruisseaux d'une région, envasés durant les travaux de dragage, sont plus stables que ceux d'une région voisine aux lits couverts de sable propre et, d) que le centre de l'érosion la plus rapide s'est déplacé, ou se déplace, vers le côté est de la région entre les chaussées; cette région, couverte de végétation, permet aux eaux descendantes d'atteindre le détroit de Géorgie.

INTRODUCTION

This report presents an appraisal of factors influencing tidal flat erosion at the head of the Roberts Bank Coalport ship basin on the southwestern delta front of the Fraser River (Fig. 9.1, 9.2). This appraisal is based on recently initiated field investigations and previously available reports.

GENERAL BACKGROUND

The Coalport and associated causeway were constructed in 1969 (McKenzie, 1983) northwest of the already present Tsawwassen Ferry Terminal and causeway. Materials for the core of the Coalport complex were extracted from the adjacent seafloor, which was dredged to form a ship basin (Fig. 9.2). This basin lies within 400 m of ecologically valuable eelgrass beds (Fig. 9.2); Beak Consultants Ltd., 1977b; McKenzie, 1983; Wiebe and Moody, 1983) growing on sand and silty sand substrate (Luternauer, 1976, 1980; Beak Consultants Ltd., 1977a). Concentration of ebb-tidal flows by the basin and the consequent apparent increase in flow velocities on the adjacent flats are considered to have caused the denudation of the vegetated area at its head (Beak Consultants Ltd., 1977b). Expansion of the port from 1 to 4 pods was carried out from September 1981 through June 1983 (M. Tarbotton, personal communication, 1983). Thirteen million cubic metres of fill required for this expansion of the terminal area were excavated in the course of enlarging the existing ship basin (Ekstrom, 1983).

A crest protection wall (or c.p.w. about 6 m wide and 0.5 to 1 m high) was placed at the perimeter of the head of the ship basin (Fig. 9.2) in the spring of 1982 in an attempt to restrict the seaward flow of water and sediment through the dendritic tidal channels (Hawley, 1979; Wiebe and Moody, 1983). Some sand excavated to form a shallow 0.5 m trench (Wiebe and Moody, 1983) to hold the riprap boulders

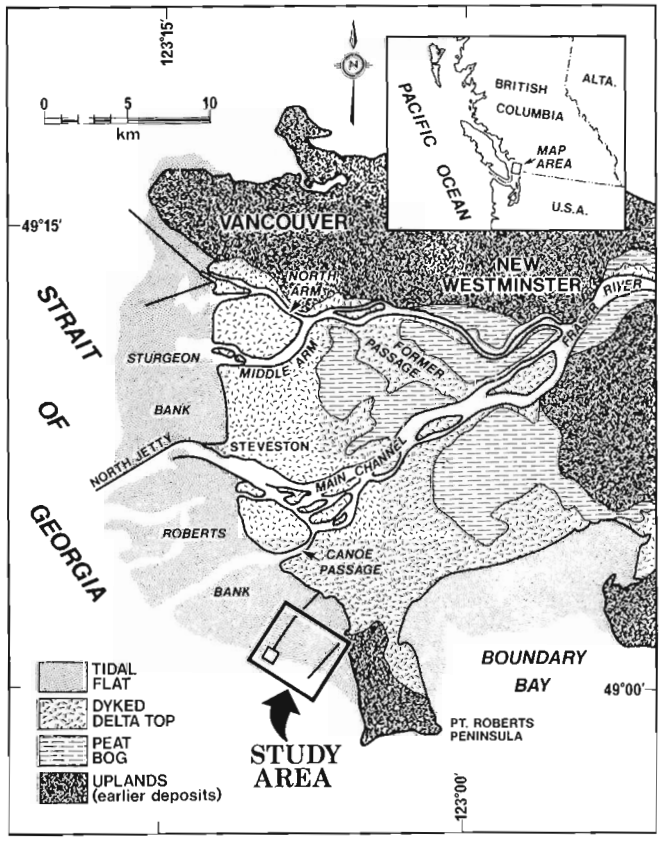

Figure 9.1. *Sedimentary setting and location of study area.*

[1] Pacific Geoscience Centre, Sidney, B.C.

for the c.p.w. was to be dumped in channels on the inshore side of the trench in an attempt to build up the tidal flat surface. As this spoil disposal was performed entirely while the area was submerged (M. Tarbotton, personal communication, 1983), the dumped sand was not all contained within channel margins and some remains as sand mounds or bars among the creeks (Fig. 9.3). Silt also was discharged onto the tidal flat between the c.p.w. and the Coalport causeway between September 1982 and February 1983 during the filling of pod site 4 (Fig. 9.2, 9.4) with the sandier fraction of dredge spoil (M. Tarbotton, personal communication, 1983).

The only previous morphological study of the area is that of M. Hawley (1979) who investigated the stability of the dredged basin. He established, on the basis of a comparison of 1973 and 1979 echo-sounding records, that negligible change had occurred to the side slope angles, location of channel margins and general shape of the basin; and on the basis of the same bathymetric data coupled with 1969 and 1976 airphotos, that channel erosion currently shows no signs of reaching equilibrium and would likely be accelerated should additional dredging and development be undertaken. Hawley (1979) further noted that the construction of a dyke around the head of the ship basin as suggested by Hinton & Associates Ltd. (1977) "would probably stop erosion in the present area," but added that it would "likely result in the development of a new area of erosion elsewhere on the tidal flats". The height of the crest protection wall that finally was erected was kept to a minimum to diminish this effect as much as possible (M. Tarbotton, personal communication, 1983).

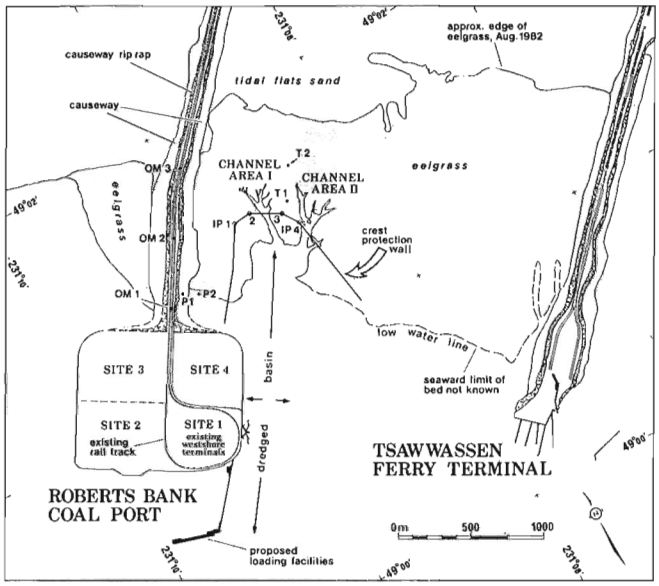

Figure 9.2. *Major features within study area including dendritic channel system at head of dredged ship basin (arrows within basin denote approximate dimension in 1970). OM, P, IP represent survey marker locations. T = navigation towers. Adapted from National Airphoto Library imagery (Roll #A37849) and Swan Wooster Engineering Co. Ltd. blueprint drawings.*

Botanical investigations were performed, concurrently with the geological studies described herein, by P.G. Harrison and associates of the University of British Columbia to establish habitat requirements, growth characteristics and potential for transplantation of eelgrass within the affected area. These studies included creation of a sand bag dam across one of the channels (Fig. 9.3) to slow ebb flows, induce accretion and attempt to establish a locally more favourable environment for eelgrass recolonization.

FIELD AND LABORATORY TECHNIQUES

Field

Channel morphology

Nine representative locations were selected for short and long-term monitoring of channel cross-section changes (four transects in channel area I and five in channel area II). End points of profiles were marked by 6 mm (1/4") "rebar" (iron rod). These were placed 5 to 10 m beyond the channel margin on the adjacent bank to allow for changes in channel width. The rebars, flagged with surveyors tape, are driven about 0.5 m into the sediment and are visible 0.75 to 1.0 m above the exposed tidal flat surface. Elevations were taken at well defined morphological inflection points or at 5 m intervals (whichever distance was shortest) with a Zeiss Auto Level, a rod and a 30 m tape extended between rebars. Back sites used were one of four benchmarks located on the c.p.w. (Fig. 9.3). These measurements were first taken in June then repeated in July and August, 1983. Vertical precision of the measurements is ±5 cm.

Four baselines, defined by three to four rebars each, were established near the heads of several channels to measure headward erosion. These measurements will serve in

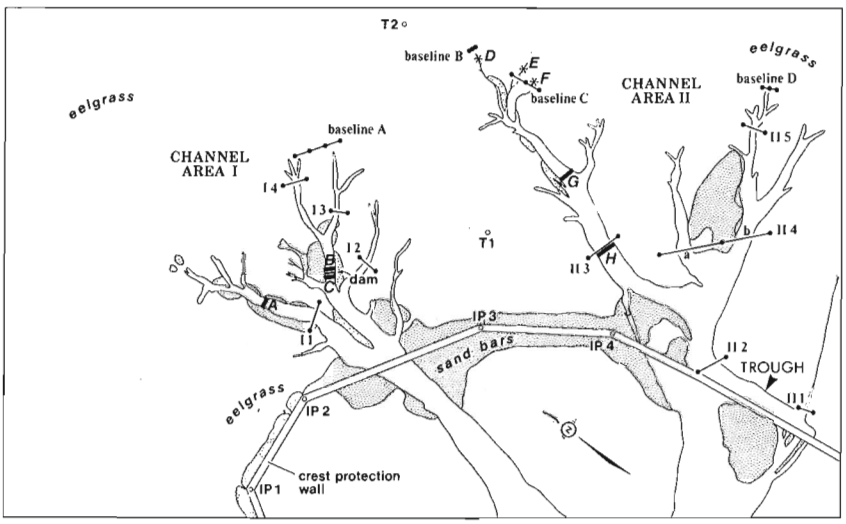

Figure 9.3

Locations of reference (or base) lines at heads of channels, transects where channel profiles were surveyed (thin line connecting dots), transects where flow rates were measured at several sites across channels (heavy line) and where spot checks were made of flow rates at heads of creeks (*). Navigation towers are 250 m apart.

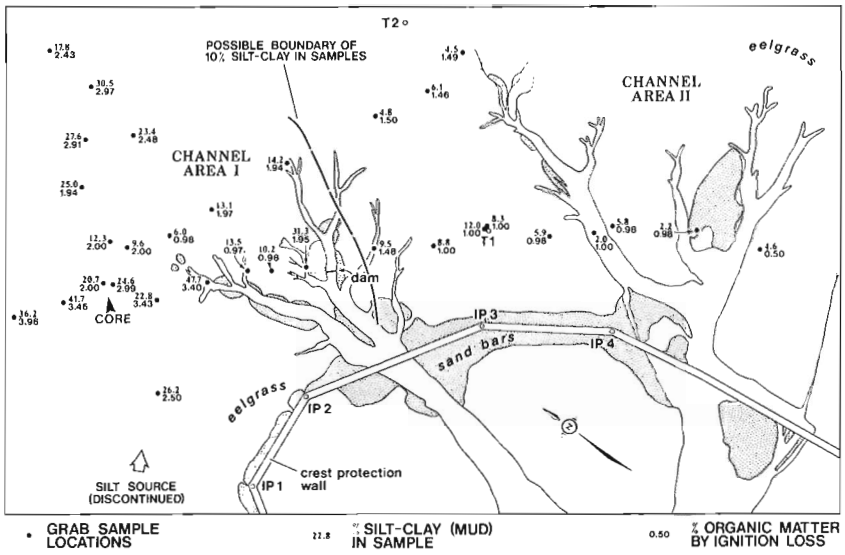

Figure 9.4

Grab sample locations indicating weight per cent mud and organic matter in sampled sediment.

the future as ground truth against which estimates of channel extension calculated from airphotos can be compared and refined.

The locations of the profile transects and baselines were established with a transit-mounted Geodimeter. Positioning accuracy is ±0.1 m.

Sediment distribution

Thirty-four grab samples consisting of a handful of the top 2-3 cm of sediment were collected in the vicinity of the tidal channels (Fig. 9.4). Stations were fixed with a sextant siting (precision ±3 m) on reference stations along the causeway or on the tidal flats. Seven cores 50 to 100 cm long and 7 cm in diameter were collected along the area between the causeway and c.p.w. The purpose of the sampling program was to define the present extent and thickness of the silt layer which accumulated during landfilling operations at pod site 4.

Channel flow metering

A limited initial program to determine flow velocities along selected sites (Fig. 9.3) was performed in August with two OTT C1 meters. For periods of up to 2.5 hr, readings were taken at three to five locations across the channel at 0.4 m of the water depth from the channel floor.

Laboratory

Grain size analysis

Samples were split, washed to remove salt, dried, weighed, wet sieved through a 63 µm sieve and a determination was made of the dry weight proportion of sand and mud. The dry weight per cent organic matter within the sample was determined by weight loss on ignition.

Airphoto analysis

A first estimate of the rate of headward erosion of the channel system was determined by measuring along the centre line of the most westerly of the trunk channels in each of the main areas in 8 photos spanning the years 1969 through 1982. Channel length was measured from the inshore margin of the ship basin which Hawley (1979) established was not retreating significantly. Airphotos also were examined for evidence of new creek development.

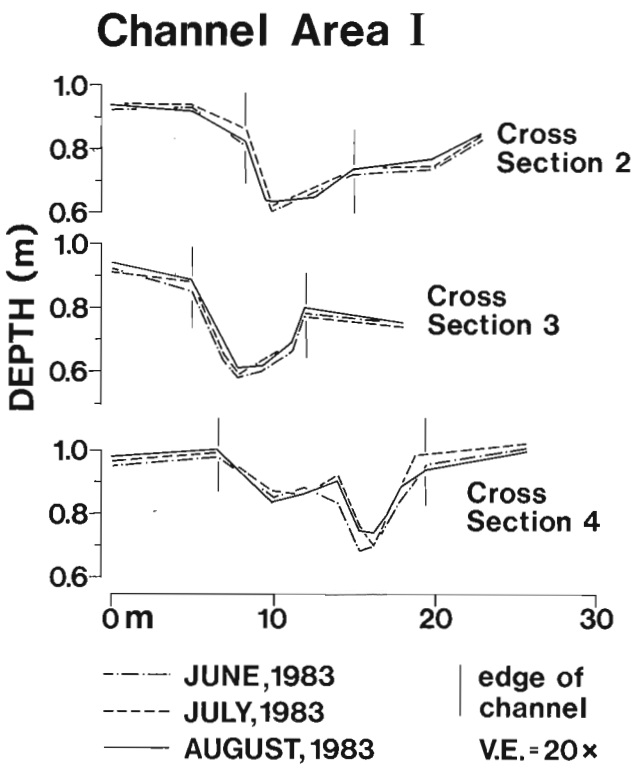

Figure 9.5. *Comparison of channel profiles surveyed in channel area I (Fig. 9.3; profile locations 2, 3, 4).*

RESULTS

Cross-section profiles in channel area I display no significant change during the months for which we have data, whereas those in channel area II fluctuated considerably (Fig. 9.5-9.7). The position of channel heads with respect to baselines were determined in August prior to making precise measurements next summer. Although no rates of advance were determined, it was clear that the narrow channel heads, especially in area II, were vigorously cutting back into the eelgrass beds (Fig. 9.8a). Flows leading to these channels appear to follow well defined streamlines between individual plants and suggest the course of future erosion. Analysis of the grab samples revealed that highest silt and organic

concentrations were found within channel area I. The one analyzed core (location indicated in Figure 9.4) revealed that the silt-rich layer capping the sediment column is approximately 10 cm thick at this site. Of possible significance is that the uppermost 2-3 cm of this section has a somewhat lower (23 vs. 36%) silt content than the remainder. Preliminary compilations of channel flow data indicate that flow rates are highest in channel area II and the highest there, at 78 cm/s, is over twice the threshold velocity for initiation of movement of the local sand (Sternberg, 1971). Measurements of channel extension made from airphotos indicate headward erosion rates range from 100 + m/a shortly after the ship basin was dredged to about 20 m/a or less from the period 1977 through 1981 (Table 9.1; Fig. 9.9). After 1981, when expansion and renewed dredging at the site had begun, erosion rates within both channel areas appear to have increased moderately (a similar rate of increase just in channel area II prior to 1980 cannot be related to development). Airphotos also indicate that the trough in channel area II (Fig. 9.3) has developed since the erection of the c.p.w. The absence of change in trough width from June through August 1983 indicated by our surveys suggests this feature has become stable. It was also noted in the field that (a) the c.p.w. is lower where it crosses a channel, but it is not clear whether this is due to the original riprap conforming to the existing topography or whether the highly turbulent flows crossing the wall have scattered and/or led to settling of the cobbles and boulders (Fig. 9.8b), (b) sand accumulated on the inshore side of the sandbag dam in channel area I during the course of the summer, (c) the present configuration of structures on the tidal flats tends to pond water in the vicinity of channel area I on an ebbing tide.

SUMMARY OF OBSERVATIONS

Measurements of channel extension from airphotos suggest, as Hawley (1979) suspected, that increasing the ship basin increased the rate of tidal channel erosion. Growth of a trough on the eastern side of the crest protection wall coupled with higher flow rates in, and greater instability of, area II channels (although sand is still being transported at least along trunk channels in area I) suggest that even a far less imposing erosion control structure than was originally proposed (Hinton & Associates Ltd., 1977) can shift the locus of fastest erosion. The less rapid headward erosion in area I as compared to area II evident in 1983 may not only reflect the local ponding of ebbing water (which probably has contributed to the greater retention of organic matter) and the shifting of the locus of fastest erosion but also the greater cohesiveness of silty sediments. A follow-up study should establish whether the areal extent and thickness of this silty deposit decreases with time and, if so, whether there is an associated increase in local channel erosion rates. The upward coarsening of the silty sediments capping the analyzed core suggests that some removal of fines has already taken place since the discharge of silt into the area

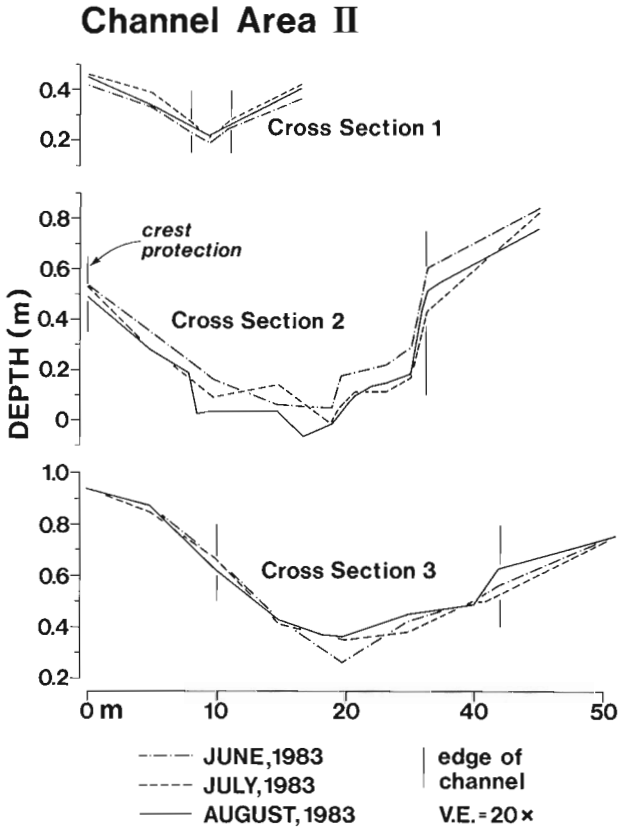

Figure 9.6. Comparison of channel profiles surveyed in channel area II (Fig. 9.3; profile locations 1, 2, 3).

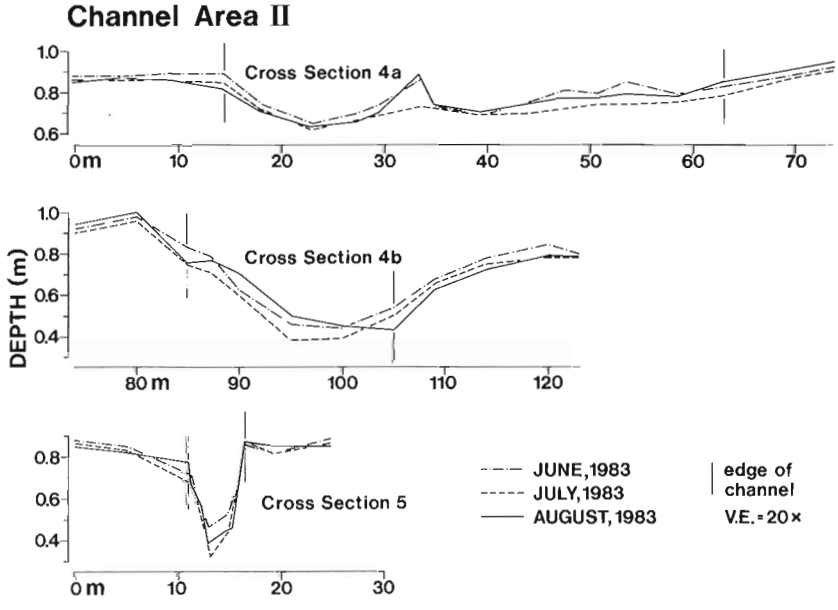

Figure 9.7

Comparison of channel profiles surveyed in channel area II (Fig. 9.3; profile locations 4a, 4b, 5).

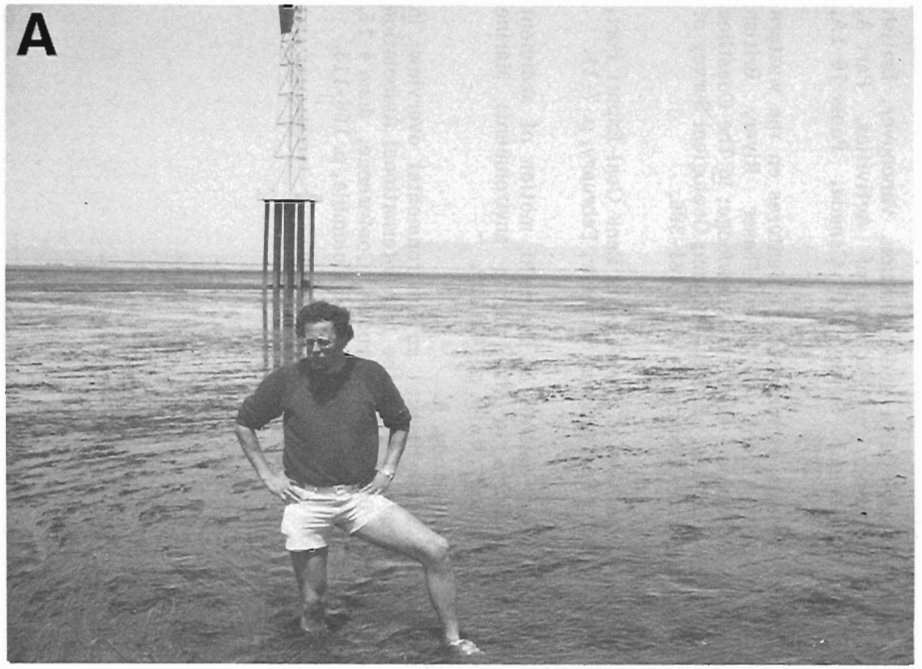

Figure 9.8a. *Right leg is in plunge pool at head of creek in channel area II. Navigation tower #2 is in background.*

Figure 9.8b. *Site where channel area II trunk stream crosses crest protection wall. Looking west towards Coalport.*

Table 9.1. Estimates of channel growth calculated from airphotos

Airphoto			Channel I.		Channel II.	
Year	Roll #	Exposure #	Length (m)	Rate of change ave. (m/a)	Length (m)	Rate of change ave. (m/a)
1969	A37859 1R	71,72	0		0	
				140		104
1970	A37817 1R	331	140		104	
				70		91
1971	A37778 1R	65	210		195	
				42		38
1977	BC79207	139	457		421	
				17		6
1979	A31164	28	491		433	
				18		21
1980	BC5431	218	509		454	
				9		21
1981	BC5471	109	518		475	
				24		37
1982	BC5332	9	542		512	

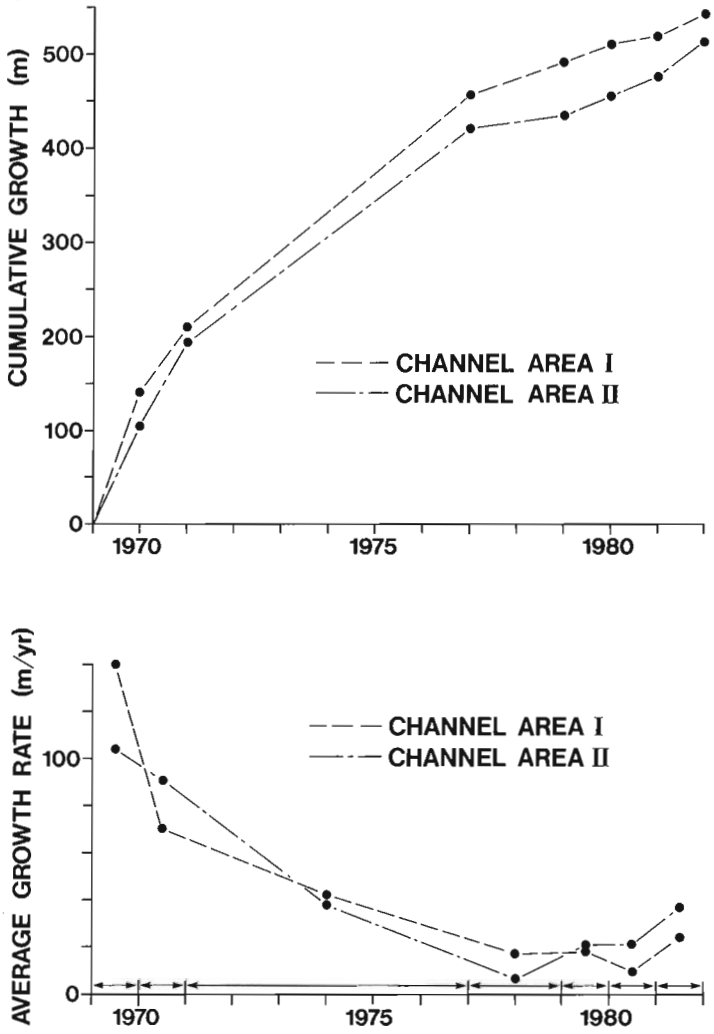

Figure 9.9. *Plots of the historical changes in the growth of the westermost trunk channels within channel area I and II (Fig. 9.3). Double headed arrows along horizontal axis of bottom plot indicate time span for which average rate was calculated.*

was stopped. Comparisons of the areal extent of the devegetated area at the head of the basin in earlier imagery and in new aerial photos obtained this summer by the Port of Vancouver should offer a more rigorous assessment of the response of the drainage system to basin expansion and erection of the present crest protection wall. Establishment of the relationships among water flow, sediment loads and tide level should permit us to estimate the frequency that a grain size is eroded or transported along different parts of the channels. These considerations, coupled with determinations of what flow velocities can be achieved at successively higher levels of the tidal flat, and what sediment type, burrowing organisms and vegetation lie at those levels, may permit construction of a model that will reveal the equilibrium form that the drainage network will assume under the prevailing hydrologic conditons.

ACKNOWLEDGMENTS

Special thanks are due R. Moody (Port of Vancouver), M. Tarbotton (Swan Wooster Engineering Co. Ltd.) and P.G. Harrison (Botany Department, University of British Columbia) for helpful advice and general assistance in the field. Thanks are also due G. Veres, D. Murphy and P. Sawyer (Swan Wooster Engineering Co. Ltd.) for assistance with the surveying. P. McLaren kindly critiqued a draft of the manuscript.

REFERENCES

Beak Consultants Ltd.
1977a: The existing physical environment; in Environmental Impact Assessment of Roberts Bank Port Expansion; National Harbours Board, Port of Vancouver, v. 3 (Appendix A), 91 p.

1977b: The existing biological environment; in Environmental Impact Assessment of Roberts Bank Port Expansion; National Harbours Board, Port of Vancouver, v. 4 (Appendix B), 140 p.

Ekstrom, B.A.
1983: Roberts Bank Port expansion – an engineering overview; in Proceedings of the 13th International Association of Ports and Harbours Conference, June 4-11, 1983, Vancouver, British Columbia, p. 39-55.

Hawley, P.M.
1979: Erosional stability of a dredged burrow pit on southern Roberts Bank, Fraser Delta, B.C.; unpublished B.A.Sc. thesis, University of British Columbia, Vancouver, 65 p.

Hinton, B.R. & Associates Ltd.
1977: Main report; in Environmental Impact Assessment of Roberts Bank Port Expansion; National Harbours Board, Port of Vancouver, 201 p.

Luternauer, J.L.
1976: Fraser Delta sedimentation, Vancouver, British Columbia; in Report of Activities, Part A, Geological Survey of Canada, Paper 76-1A, p. 213-219.

1980: Genesis of morphologic features on the western delta front of the Fraser River, British Columbia – status of knowledge; in The Coastline of Canada, ed. S.B. McCann; Geological Survey of Canada, Paper 80-10, p. 381-396.

McKenzie, W.C.
1983: Expansion of the Roberts Bank Coal Export Port, B.C.; Professional Engineer, February, p. 7-11.

Sternberg, R.W.
1971: Measurements of incipient motion of sediment particles in the marine environment; Marine Geology, v. 10, p. 113-119.

Wiebe, J.D. and Moody, R.
1983: Roberts Bank: an environmental overview; in Proceedings of the 13th International Association of Ports and Harbours Conference, June 4-11, 1983, Vancouver, British Columbia, p. 106-115.

10. THE WHYTECLIFF OIL SPILL, BRITISH COLUMBIA: SEDIMENT TRENDS AND OIL MOVEMENT ON A BEACH

Project 780027

P. McLaren[1]
Cordilleran Geology Division

McLaren, P., The Whytecliff oil spill, British Columbia: sediment trends and oil movement on a beach; in Current Research, Part A, Geological Survey of Canada, Paper 84-1A, p. 81-85, 1984.

Abstract

On January 21, 1983, a small pocket beach north of Vancouver was heavily contaminated with an undetermined amount of Bunker B type oil. Sediment samples taken on February 8 from the high-tide level, the zone of most severe oiling, contained hydrocarbon concentrations ranging from <100 to 9580 ppm. A second group of samples taken on April 16 from the mid-tide level showed that oil concentrations had dropped to below background levels (<100 ppm) with the exception of the north end of the beach where the concentration was 190 ppm.

Although no correlation between grain size parameters and oil concentration in the sediments was found, high concentrations could be predicted on the basis of sediment transport trends. Using the relative changes in mean, sorting and skewness of the grain-size distributions to determine sediment transport directions, oil concentrations were observed to increase significantly in the same directions. The use of sediment trends to predict the pattern of oil movement in the coastal zone appears, therefore, to be a useful criterion for oil-spill contingency planning.

Résumé

Le 21 janvier 1983, une petite plage concave au nord de Vancouver a été sérieusement polluée par une quantité inconnue de mazout lourd de type B. Des échantillons de sédiments prélevés le 8 février du niveau de la marée haute, zone la plus polluée, ont donné des concentrations d'hydrocarbures variant de moins de 100 ppm à 9 580 ppm. Dans une deuxième série d'échantillons prélevés le 16 avril du niveau de la mi-marée, les concentrations de mazout étaient inférieures au niveau de base (<100 ppm) sauf dans l'extrémité nord de la plage, où la concentration était de 190 ppm.

Bien qu'aucune corrélation n'ait été décalé entre les paramètres granulométriques et la concentration d'hydrocarbures dans les sédiments, il est possible de prévoir des concentrations élevées en se fondant sur les directions de transport des sédiments. L'utilisation des changements relatifs de la moyenne, du triage et de l'asymétrie de la répartition granulométrique pour déterminer les directions de transport des sédiments révèle que les concentrations de mazout augmentent beaucoup dans les mêmes directions. L'utilisation des directions de transport en vue de prévoir le mouvement des hydrocarbures dans la zone littorale semble donc être un critère utile pour la planification en phase de déversement.

INTRODUCTION

On January 18, 1983 Bunker B type oil was spilled in Vancouver Harbour, an unknown quantity of which drifted onto the beaches of Whytecliff Park three days later (Fig. 10.1). Although attempts were made to contain the oil with booms (Fig. 10.2), one drifted out of control resulting in the release of thick, sticky oil which covered an intertidal area of about 100 m^2.

Oil was deposited throughout the length of Whyte Cove, which contains a small pocket beach about 200 m long, bounded on the north by a rocky headland and marina pier and on the south by a boulder "tombolo" extending out to Whyte Islet (Fig. 10.1). The beach, composed of sandy gravel is backed by an eroding bluff, some of which is stabilized with concrete. The "tombolo", dry at low tide, was constructed in the 1930s to protect the cove.

At the time of sediment sampling (Feb. 8, 1983) a thick coating of oil was concentrated at the high tide level on nearby bedrock exposures and on the boulders of the south side of the tombolo. In the latter area the intertidal zone was essentially completely covered with oil and sheens were clearly visible on tide pools and on the water table.

By contrast, the north side of the tombolo was relatively clean, probably as a result of large waves which enter Whyte Cove on each passing of the Nanaimo-Horseshoe Bay ferry (every two hours throughout the day). No oil was visible on the beach surface although a sheen was usually present on the water table. The pilings and marina floats at the north end of the cove still contained an abundant oil covering, in spite of extensive cleanup efforts.

The principal purpose in the investigation of the Whytecliff oil spill was to examine the relationship between oil concentration in beach sediments and sediment transport trends as determined by changes in grain size distributions. According to McLaren (1981a), the direction of sediment transport can be ascertained by relative changes in the moment measures of mean, variance (sorting) and skewness which describe grain size distributions. Sediment transport can be inferred if grain size distributions become progressively finer, better sorted and more negatively skewed or coarser, better sorted and more positively skewed[2]. In several papers (McLaren, 1980, 1981b, 1983; McLaren et al., 1981) I have suggested that oil movement in the coastal zone may be predicted by the transport paths determined from sediment trends. The Whytecliff oil spill provided the first opportunity to test this hypothesis.

FIELD METHODS AND DATA PRESENTATION

On February 8, 1983, seven sediment samples were collected at the high tide line, the zone of heaviest oiling (Fig. 10.1). Each sample included about the top 20 cm of beach face and

[1] Pacific Geoscience Centre, P.O. Box 6000, Sidney, B.C. V8L 4B2

[2] Present work on sediment trends has shown that sediments cannot become finer and more positively skewed in the direction of transport, a trend that was described as being possible in McLaren, 1981a.

was kept frozen until analyzed for hydrocarbon content. Total hydrocarbon was measured using standard fluorometric techniques and the sediment was kept for later grain size analysis (Table 10.1). A further six samples were collected from Whytecliff Beach on April 16, 1983, by Fred Beech of the Environmental Protection Service. These samples (locations shown in Fig. 10.1) were taken at mid-tide level and identical analyses were performed on them (Table 10.1).

The grain size analyses show that the beach sediments are predominantly gravel (mean content 67 ± 12 per cent) with an overall mean grain size of -2.08 ± 0.77 Ø (pebble size). No correlation exists between any of the textural parameters and oil concentration. At the time of the first sampling, oil concentrations were highest on the south side of the tombolo, the area protected from waves generated by ferry traffic. In contrast samples 4 and 5 show concentrations that are probably within background levels of hydrocarbon content (<100 ppm; David Hope, Seakem Oceanography, personal communication). The sediments in this area are most exposed to the ferry waves and after 18 days, hydrocarbon contamination was already minimal. However, the remaining beach still contained relatively high concentrations with sample 3 having the greatest amount (Table 10.1).

At the second sampling, 55 days later, both the south side of the tombolo and most of the beach appeared to be clean with the exceptions of sites A and D. The latter, with an oil concentration of 113 ppm, is somewhat suspect because the sample contained a notable amount of organics and the solvent used to extract hydrocarbons did not turn dark in the manner typical of the other oil contaminated samples. Fluorescing plant pigments are probably responsible for the relatively high concentration. Sample A, however, produced an extract that was visibly contaminated with oil indicating that the north end of the beach was still appreciably polluted.

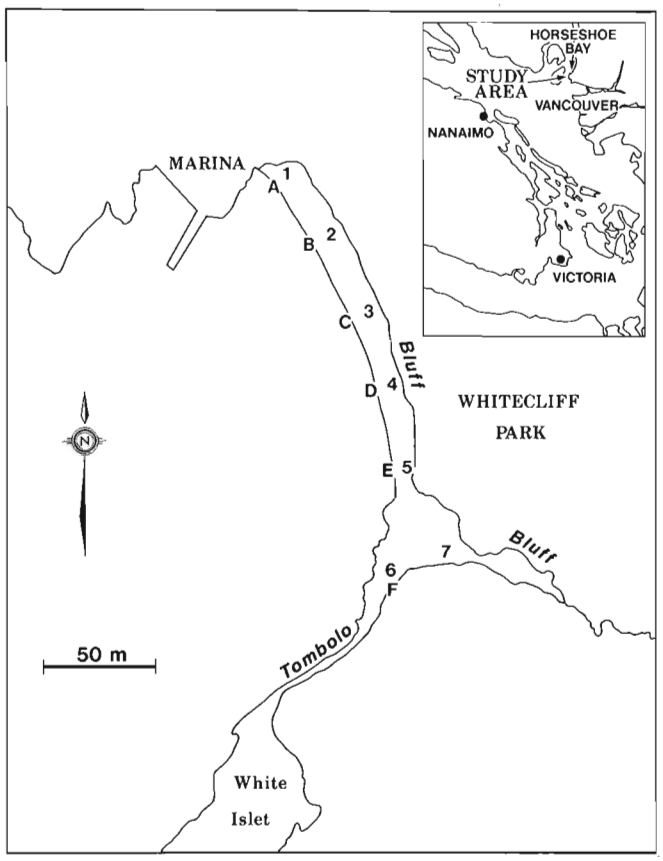

Figure 10.1. Location map and sample locations: samples 1-7 collected on February 8, 1983; samples A-F collected by F. Beech, April 16, 1983.

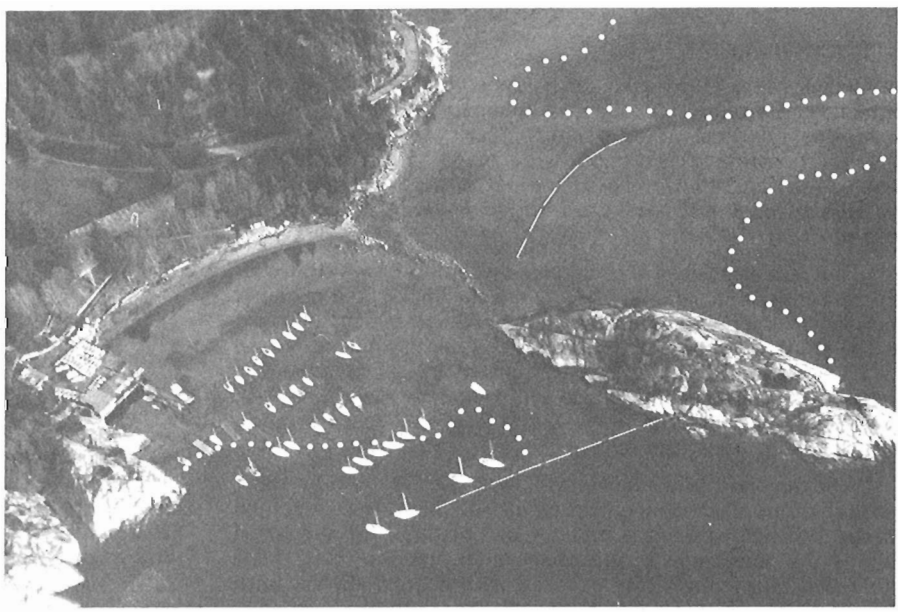

Figure 10.2

Attempted booming operation at Whyte Cove. Dots denote outer limits of the oil slick; dashes indicate locations of booms. (Photo by Fred Beech, Environmental Protection Service).

SEDIMENT DEPOSIT \ SEDIMENT SOURCE	SAMPLE 6	SAMPLE 7
SAMPLE 6		coarser poorer +
SAMPLE 7	finer better −	

Figure 10.3. A sediment trend matrix for tombolo samples 6 and 7. Sample 7 is finer, better sorted and more negatively skewed than sample 6 suggesting that the direction of sediment transport is from 6 to 7. Sample 6 is coarser, more poorly sorted and more positively skewed than sample 7 (the shaded box), a trend which is unacceptable for transport to have occurred from 7 to 6 (see McLaren, 1981a).

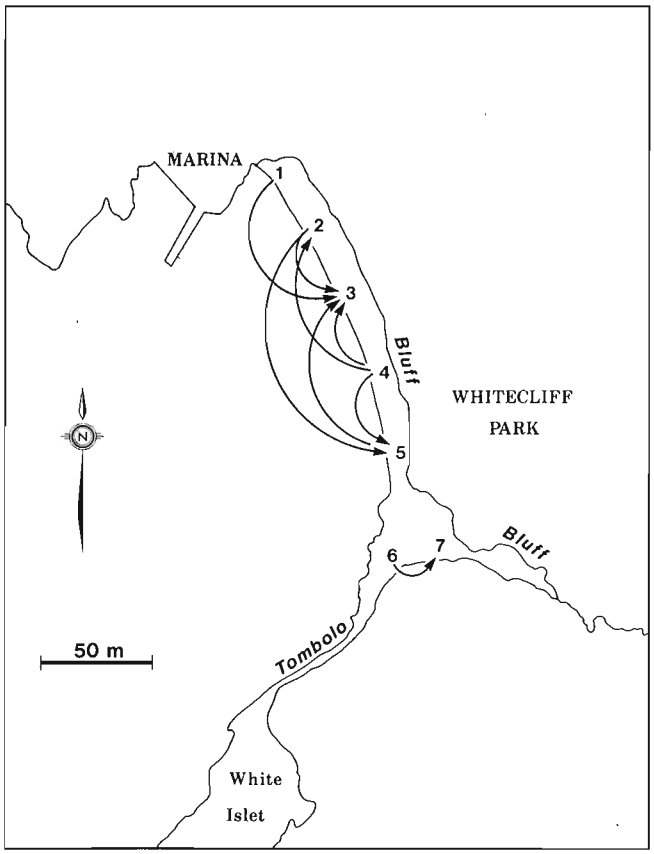

Figure 10.4. Summary of sediment transport directions derived from the February 8, 1983 samples. Arrows indicate possible sediment transport paths based on the sediment trend matrices (Fig. 10.3, 10.5).

SEDIMENT DEPOSIT \ SEDIMENT SOURCE	1	2	3	4	5
1		finer better +	finer poorer −	finer better +	finer better +
2	coarser poorer −		finer poorer −	finer better −	finer poorer −
3	coarser better +	coarser better +		coarser better +	coarser better +
4	coarser poorer −	coarser poorer +	finer poorer −		coarser poorer +
5	coarser poorer −	coarser better +	finer poorer −	finer better −	

Figure 10.5. A sediment trend matrix for high tide beach samples 1 to 5 taken on February 18, 1983. Shaded boxes indicate unacceptable trends; the method of using the matrix is described in the caption to Figure 10.3.

SEDIMENT DEPOSIT \ SEDIMENT SOURCE	A	B	C	D	E
A		coarser better +	finer better +	finer better −	coarser better +
B	finer poorer −		finer poorer −	finer better −	coarser poorer +
C	coarser poorer −	coarser better +		finer better −	coarser better +
D	coarser poorer +	coarser poorer +	coarser poorer +		coarser poorer +
E	finer poorer −	finer. better −	finer poorer −	finer better −	

Figure 10.6. A sediment trend matrix for mid-tide beach samples A-E taken on April 16, 1983. Shaded boxes indicate unacceptable trends; the method of using the matrix is described in the caption to Figure 10.3.

Table 10.1. Oil concentrations and sediment characteristics from beach samples located in Figure 10.3

Sample (location Fig. 10.3)	Oil Concentration ppm(mg/kg)	% Gravel	% Sand	Moment Measures (ϕ) Mean	Sorting	Skewness
Feb. 8, 1983						
1	160	66	34	-2.08	2.45	0.52
2	119	60	40	-2.20	2.63	0.03
3	934	89	10	-3.34	2.01	1.36
4	94	69	30	-2.56	2.67	0.39
5	25	65	33	-2.27	2.62	0.24
6	2130	70	29	-2.40	2.53	0.57
7	9580	60	39	-1.67	2.29	0.21
April 16, 1983						
A	190	79	20	-1.77	1.84	1.00
B	29	55	44	-1.16	2.14	0.22
C	58	85	13	-2.58	1.86	0.89
D	113	76	20	-3.11	3.22	1.13
E	25	54	45	-1.00	1.90	0.02
F	62	48	51	-0.84	2.17	-0.08

SEDIMENT TRENDS

(i) Tombolo

Grain size analyses of samples 6 and 7 on the south side of the tombolo indicate a sediment transport direction from 6 to 7 (Fig. 10.3, 10.4). Given that oil concentrations should increase or accumulate in the direction of transport, the data support this concept with oil concentration values of 2130 ppm at sample 6 and 9580 ppm at sample 7.

(ii) Whytecliff Beach (Feb. 8)

A sediment trend matrix (Fig. 10.5) demonstrates that for the high tide samples all transport paths end at site 3 indicating accumulation of oil may be favoured at this location (Fig. 10.4). The oil concentration data (Table 10.1) confirms that the sediment transport paths have correctly predicted an increased oil concentration level which is nearly an order of magnitude higher than at the other locations.

(iii) Whytecliff Beach (April 16)

Analyses of samples from the middle tide level produced a different set of trends from those collected at the high tide line. The sediment-trend matrix (Fig. 10.6) and the corresponding sediment transport paths (Fig. 10.7) show three southward trends and six northward trends. This is a 2:1 ratio in favour of accepting north as the preferred direction of transport. Sample A contains a significant degree of oil concentration compared to background levels predominating elsewhere (Table 10.1).

CONCLUSIONS

Given that sediments must become either coarser, better sorted and more positively skewed or finer, better sorted and more negatively skewed in the direction of transport, a derived pattern of sediment transport in the coastal zone may be able to predict the movement of oil and hence be an aid for oil-spill contingency planning. The Whytecliff oil spill provided an appropriate opportunity to test this hypothesis. In each of three separate sediment transport patterns (the south side of the tombolo; the high tide line on February 8 and the mid-tide line on April 16), oil concentrations

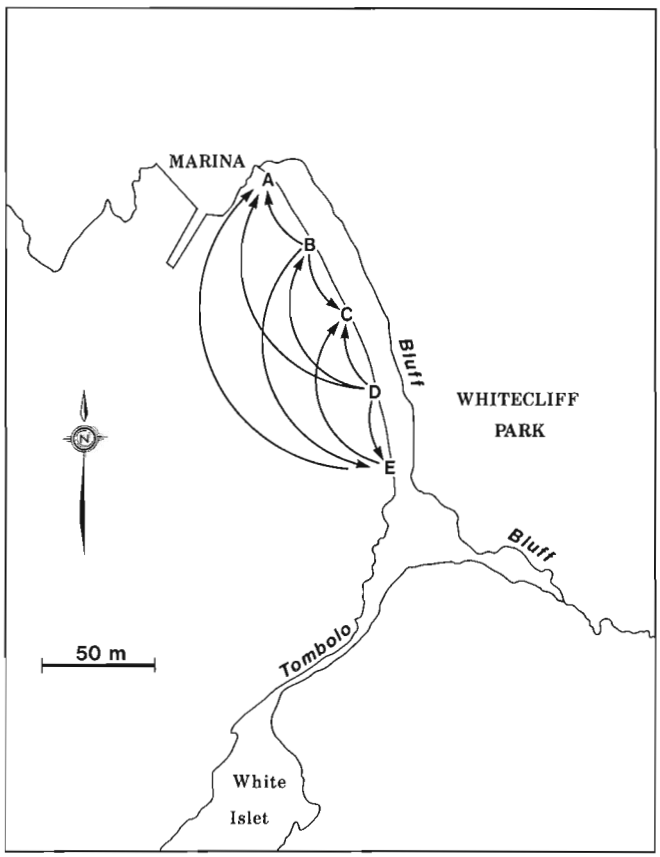

Figure 10.7. Summary of sediment transport directions derived from the April 16, 1983, samples. Arrows indicate possible sediment transport paths based on the sediment trend matrix shown in Figure 10.6.

significantly increased in the direction of transport as determined by a sediment trend analysis. It appears, therefore, that sediment trends can predict with considerable accuracy the pattern of oil movement on a beach and could be a powerful technique in oil-spill contingency planning. For example, the results of the sediment trends indicate clearly that cleanup on the south side of the tombolo should proceed from west to east and on Whytecliffe Beach from south to north to minimize the probability of recontamination.

ACKNOWLEDGMENTS

The writer is indebted to Fred Beech of the Environmental Protection Service for expressing an interest in pursuing this research and for collecting a suite of beach face samples. Kim Conway provided help in the field and David Hope of Seakem carried out the hydrocarbon analyses. The help of Trudie Forbes for the grain size analyses and editorial clarification is gratefully acknowledged.

REFERENCES

McLaren, P.

1980: Trends in sediment distributions: a method to predict oil spill movement in the coastal zone; Spill Technology Newsletter, Environmental Proection Service, Ottawa, v. 5, no. 3, p. 76-87.

1981a: An interpretation of trends in grain size measures; Journal of Sedimentary Petrology, v. 51, no. 2, p. 611-624.

1981b: Coastal geology and oil spills; Episodes, v. 1981, p. 3-8.

1983: Coastal sediments of the Strait of Juan de Fuca: implications for oil spills; in Current Research, Part A, Geological Survey of Canada, Paper 83-1A, p. 241-244.

McLaren, P., Barrie, W.B., and Sempels, J.M.

1981: The coastal morphology and sedimentology of Cape Hatt: implications for the Baffin Island Oil Spill Project (BIOS); in Current Research, Part B, Geological Survey of Canada, Paper 81-1B, p. 153-162.

11. GEOLOGY OF THE BLACKWATER RANGE, BRITISH COLUMBIA

EMR Research Agreement 300-4-83

Filippo Ferri[1] and P.S. Simony[1]
Cordilleran Geology Division, Vancouver

Ferri, F. and Simony, P.S., Geology of the Blackwater Range, British Columbia; in Current Research, Part A, Geological Survey of Canada, Paper 84-1A, p. 87-90, 1984.

Abstract

In the Blackwater Range in the western Rocky Mountains of British Columbia, Hadrynian to Cambrian strata are incorporated within the Porcupine Creek Anticlinorium. These rocks are composed of slates and clastics of the Miette and Gog groups, overlain by argillaceous limestones of the Chancellor Formation. Detailed mapping allowed a further subdivision of the Lower and Middle Chancellor Formation.

The chancellor strata are structurally thickened above the more competent Gog strata within the core of the anticlinorium, and at the level of the Gog Group the anticlinorium narrows southeastward. These factors indicate that a detachment horizon at or above the Gog/Chancellor contact has accommodated the shortening and thickening of the Chancellor strata.

A penetrative, locally crenulated cleavage fans across the anticlinorium. Metamorphism is of lower greenschist grade and is late to posttectonic.

Résumé

En Colombie-Britannique, des couches hadryniennes à cambriennes font partie de l'anticlinorium de Porcupine Creek dans le chaînon Blackwater des Rocheuses occidentales. Ces roches se composent de schistes ardoisiers et de roches clastiques des groupes de Miette et de Gog que recouvrent des calcaires argileux de la formation de Chancellor. La cartographie détaillée a permis de subdiviser encore plus les parties inférieure et moyenne de la formation de Chancellor.

Les couches de la formation de Chancellor sont plus épaisses au-dessus des couches plus compétentes du groupe de Gog au sein du noyau de l'anticlinorium, qui s'amincit vers le sud-est au niveau du groupe de Gog. Ces facteurs indiquent qu'un horizon de décollement au niveau du contact Gog/Chancellor, ou au-dessus de ce dernier, a facilité le raccourcissement et l'épaississement des couches de la formation de Chancellor.

Un clivage pénétrant et localement plissaté s'étend en travers de l'anticlinorium. Le métamorphisme récent à post-tectonique a atteint le degré inférieur du faciès des schistes verts.

INTRODUCTION

During the summer of 1983 the Blackwater Range was mapped at a scale of 1:24 000. This area is located within the western Main Ranges of the Rocky Mountains; approximately 70 km northwest of Golden, British Columbia. It is bounded on the north by Bush Arm of Kinbasket Lake, and on the west by Succour Creek, there occupying the Rocky Mountain Trench. The area is underlain by strata ranging in age from Hadrynian to Middle Cambrian. These rocks were deformed and incorporated into a large fan-shaped structure (termed the Porcupine Creek Anticlinorium (PCA); Price, 1965; Balkwill, 1969) during the major period of east-west contraction in the Canadian Cordillera.

To the north of the study area in the Solitude Range, Wheeler (1963, 1965) and Meilliez (1972) documented the involvement of the Miette Group and Lower Cambrian Gog quartzites in the main structure of the Porcupine Creek Anticlinorium. To the south, however, Gardner (1977) who worked within Upper Cambrian to Ordovician slates and carbonates found that extrapolation of his geological data to depth would not allow the incorporation of the Lower Cambrian quartzites into the Porcupine Creek Anticlinorium. A major detachment zone above the Lower Cambrian quartzites was therefore implied, which in turn required a major change in structural style between the areas northwest and southeast of Blackwater Range.

Investigation of that change in structural style and the documentation of the stratigraphy of the Lower and Middle Chancellor Formation, which previously was investigated only on a reconnaissance scale by Fyles (1960) and Wheeler (1963), are the main aims of this study.

STRATIGRAPHY

Three main groups of rocks are found in the area. In stratigraphic order they are: Miette Group, Gog Group and Lower to Middle Chancellor Formation. These are cut by later mafic sills and dykes. The oldest rocks exposed in the area are Upper Hadrynian in age and belong to the Miette Group. These rocks are confined to the lower slopes, within the core of the Porcupine Creek Anticlinorium, and no reliable stratigraphic thickness is available. The maximum thickness seen is approximately 700 m of primarily greyish green slates with lesser amounts of coarse feldspathic wacke (grit) and silty slates to slaty siltstones. The coarser clastics tend to be discontinuous and may form lenses within the slates as described by Pell and Simony (1981).

Unconformably above the Miette is approximately 1000 m of beds assigned to the Gog Group. These rocks are confined entirely to the timbered slopes, but a section exposed in roadcuts allowed the identification of the Mahto, Mural and McNaughton formations. The Mahto and McNaughton formations are approximately 600 and 300 m thick, respectively. They are composed of quartz-arenites, quartz-wackes, siltstones and lesser amounts of grey-green slates. The McNaughton Formation is distinguished by a basal white to beige quartzite 100 m thick. The Mural Formation is approximately 150 m thick. It includes a 10 m thick white to beige limestone followed by a sequence that is mostly slates and siltstones with lesser amounts of quartzite and carbonate. The Gog in the area is slightly thinner than sections measured to the north in the Solitude Range where Meilliez (1972) recorded minimum values of approximately 1240 m.

[1] Department of Geology and Geophysics, University of Calgary, Calgary, Alberta T2N 1N4

Conformably above the Gog Group is approximately 2100 m of Middle Cambrian Chancellor slates, argillaceous limestone and limestone. The lower, middle and possibly the lowest part of the upper Chancellor have been recognized.

The lower Chancellor has been subdivided into four units: l_1LCh, l_2LCh, mLCh and uLCh. The l_1LCh corresponds to Fyles' (1960) and Wheeler's (1963) Tsar Creek argillite. The remaining lower Chancellor corresponds to Fyles' (1960) Kinbasket Limestone.

The l_1LCh is composed primarily of medium to dark grey slates, with lesser argillaceous limestone found mainly in the middle part of this unit. This thickness of this unit varies greatly. On the western limb of the Porcupine Creek Anticlinorium it is at most 150 m thick, whereas in the core of the anticlinorium it is at last 700 m thick largely as a result of tectonic thickening.

The l_1LCh is 200-240 m thick on the western limb of the Porcupine Creek Anticlinorium, whereas towards the core projection into a cross-section gives a thickness of up to 600 m. The unit has a rough three-fold subdivision: limestone at its base, followed by interlayered medium to dark grey slate, limestone and argillaceous limestone, and then limestone again. The limestone in this unit is a dense medium to dark grey micritic rock with bedding typically 1 to 10 cm thick, although beds up to 7 m thick were seen. These limestone beds are separated by thinner beds of white to beige argillaceous limestone. Layers of carbonate debris flows with clasts of argillaceous limestones occur within the lower limestone.

The mLCh is approximately 240 m thick on the limb but thickens to more than twice this amount in the hinge of the Porcupine Creek Anticlinorium. It is thin bedded (0.5 to 2 cm) dark brown or grey-brown argillaceous limestone with local horizons (<4 m thick) that resemble either l_2LCh or uLCh. Intraformational conglomerate layers of possible debris flow origin are found within it.

The uLCh is at least 450 m thick in the limb of the Porcupine Creek Anticlinorium; its top contact is not recognized in the area. This unit is also an argillaceous limestone but is more calcareous that the mLCh. The limestone layers vary from a greenish creamy grey to dark grey and the dolomitic layers from a rusty brown to white. This unit is distinguished by laminar bedding 2-10 cm thick, typically showing a gradational increase in the concentration of dolomite towards the top of each bed, associated with a noticeable upward fining of the limestone. Although the gradational bedding is not always present or may be

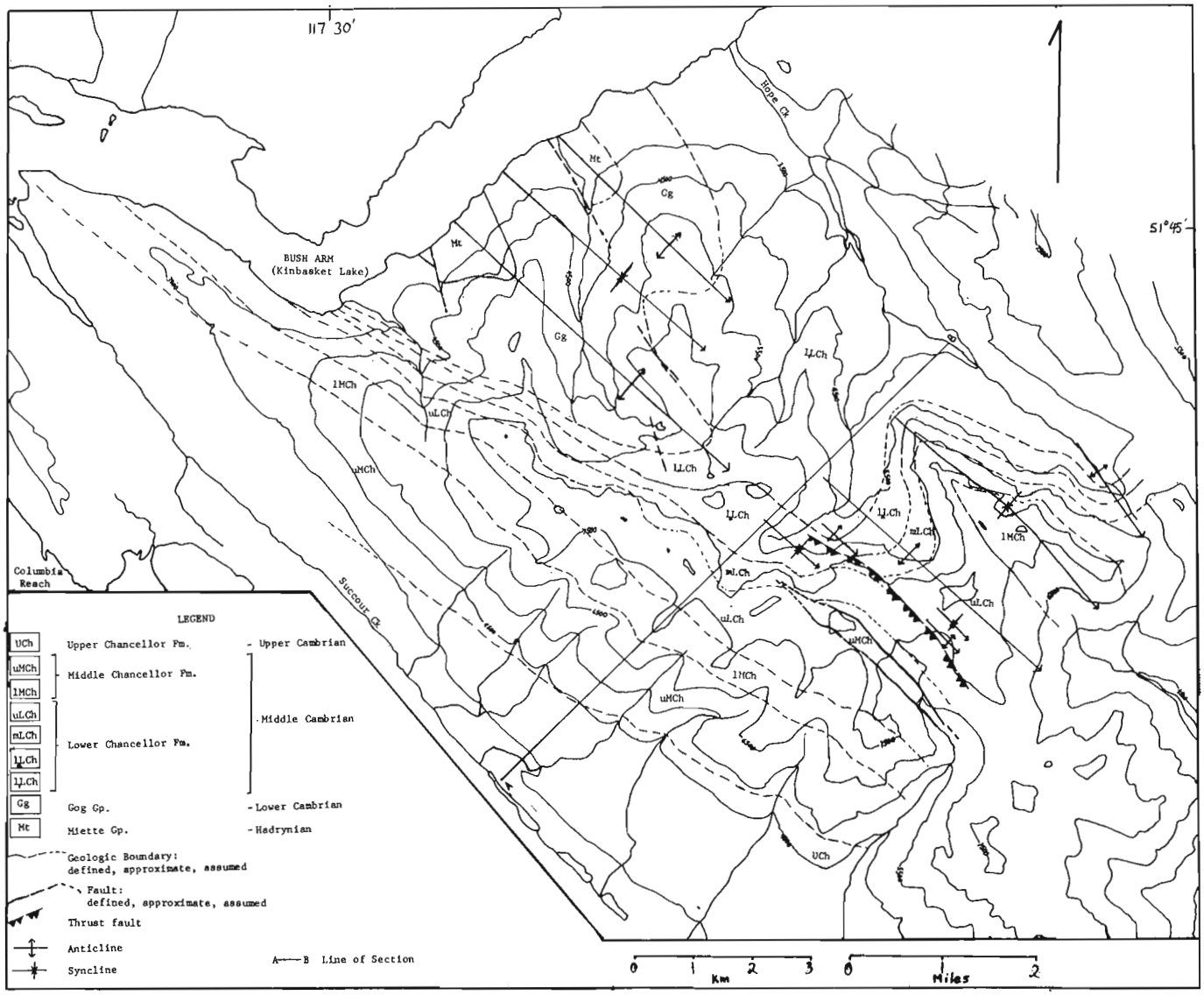

Figure 11.1. *Geological map of the Blackwater Range, British Columbia.*

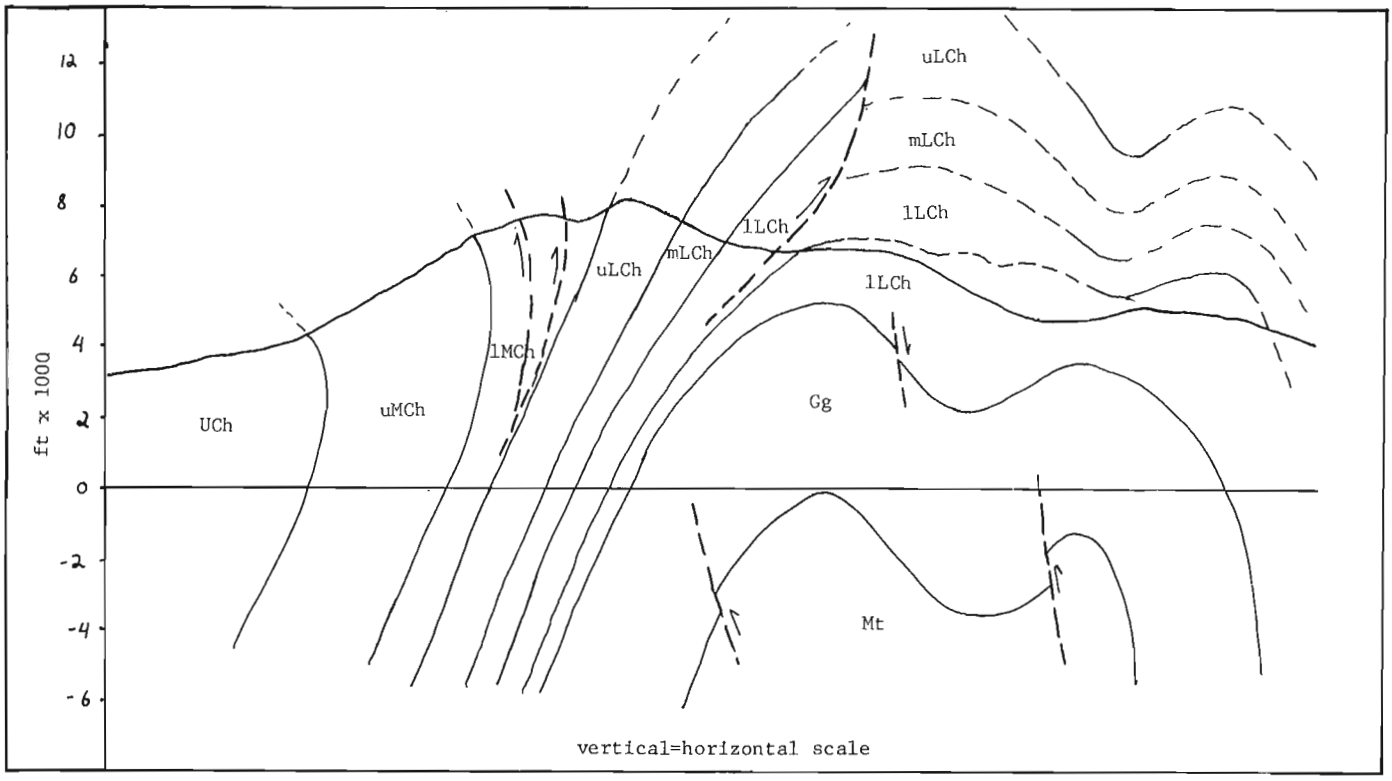

Figure 11.2. *Vertical cross-section through line A-B indicated on Figure 11.1*

very sharp, this unit is distinguishable because it is typically thicker bedded than the mLCh. The mLCh and the uLCh could not be distinguished everywhere, particularly within the core of the anticlinorium.

The Middle Chancellor could be subdivided into only two distinguishable units, here termed lMCh and uMCh. The Middle Chancellor is primarily interbedded grey limestone and dolomitic limestone with lesser amounts of argillaceous limestone and slate.

The lMCh is approximately 300 m thick and consists of grey micritic limestone layers 3-5 cm thick separated by thin (0.50-1 cm) bioturbated dolomitic layers. There are approximately 30-60 m of uLCh strata which are transitional to the lMCh. Some graded limestone conglomerate as well as rare oolitic limestone beds are present.

The uMCh is composed of 1000-1500 m of massive grey limestone or argillaceous limestone and minor slate. This unit is gradational with the lMCh in that lithologies of both units are interlayered with each other in sections 10 to 30 m thick, in a zone 60-120 m thick. The base of the uMCh was taken at the first section of massive grey argillaceous limestone.

The limestone of the uMCh is locally massive, but commonly contains thin discontinuous argillaceous layers that are white to light brown. Thin, oolitic beds are locally present. A distinctive feature of these limestones is the presence of "augen" of medium to coarse calcite. These masses of calcite behaved rigidly during deformation as the bedding was flattened around them. Grey-green slate interbedded with dark grey, micritic limestone, marks the top of this unit.

In the southern portion of the area approximately 150 m of grey-green to maroon slates overlie the uMCh. These slates also contain minor micritic limestone beds and argillaceous limestones. These have been tentatively assigned to the lUCh.

STRUCTURE

The major structure of the area is the southeast-plunging Porcupine Creek Anticlinorium (PCA). On the geological map (Fig. 11.1), the anticlinorium is most clearly outlined by the competent Gog Group. The mean plunge of mesoscopic folds in the area is 15°, with steeper plunges locally within the Chancellor strata. The rocks contain a penetrative cleavage which fans across the Porcupine Creek Anticlinorium; the cleavage dips southwesterly on the eastern limb and changes abruptly to a northeast dip on the western limb of the anticlinorium.

The Porcupine Creek Anticlinorium is flanked on its southwest side by Cambro-Ordovician beds of the McKay Group, a relationship best accounted for by a steeply southwest dipping, west-side-down normal fault along the east wall of the Rocky Mountain Trench.

The cross-section in Figure 11.2 shows that, at the level of the Gog Group, the Porcupine Creek Anticlinorium is in the form of two broad anticlines with an intervening faulted syncline. In southern Solitude Range, northwest of Bush Arm, Meilliez (1972) documented precisely the same shape for the Porcupine Creek Anticlinorium at Gog level. However, in Blackwater Range, the two anticlinal crests, as well as the steep limbs marked by the Gog, are closer together. The angle between the converging fold crest is about 5° and the Porcupine Creek Anticlinorium, at the level of the Gog, narrows down plunge.

In the core of the Porcupine Creek Anticlinorium high angle extension faults lengthen the beds in the Gog Group within which buckle-folding predominates. This is in sharp contrast to the fold style of the argillaceous limestones and calcareous slates of the Chancellor Group which outline folds of nearly "similar" geometry. This can be seen on a large scale in Figure 11.2. The Lower Chancellor stratigraphy is thickened appreciably within the crest of the anticlinorium.

The folds, cleavage and thrust faults appear to be related to a single deformational event, but the cleavage is overprinted on limestone fault breccia that is associated with normal faults which must represent an early extension episode.

Great contrast in mechanical properties between the Chancellor and Gog groups was responsible for the disharmony in folding style and to the development of a detachment zone between them. The thinly laminated and incompetent beds of the lLCh immediately overlying the Gog Group probably played a major role in the development of the detachment zone. The Chancellor beds slid and piled up towards the crest, as the Porcupine Creek Anticlinorium developed. As a result the Chancellor beds are thickened and shortened much more than the Gog strata below the detachment. As the fold, at the Gog level, becomes narrower down plunge (to the southeast) the shortening difference, or disharmony, between the Gog and Chancellor must increase.

On the western limb of the Porcupine Creek Anticlinorium the dips of bedding and cleavage reverse abruptly at or near the contact between unit uLCh and unit lMCh. In some areas along this contact, steep to northeasterly-dipping thrust faults cut upwards through the stratigraphy, suggesting that the more competent lMCh was thickened on a series of imbrecate thrusts over the less competent uLCh, as shown in Figure 11.2. As the western limb steepened during growth of the Porcupine Creek Anticlinorium, bedding and cleavage above the imbricate thrust were rotated through the vertical to become overturned, as presently seen at the surface. However, the beds must become upright and subsequently dip southwest at depth in conformity with the Gog quartzite which must dip southwest on the western limb of the Porcupine Creek Anticlinorium (Fig. 11.2).

The cleavage is penetrative in all rock types and in the more calcareous rocks it is of pressure solution origin. In most areas only one cleavage is present but locally in l_1LCh slates a crenulation cleavage is superimposed on the earlier penetrative cleavage. The crenulation cleavage is thought to have resulted from the rotation of the first cleavage toward parallelism with bedding in the Gog Group as the slates flowed into the hinge zone of the Porcupine Creek Anticlinorium. As this happened the first cleavage reached a critical angle relative to the shortening direction, and a new cleavage developed and produced crenulation of the older cleavage.

METAMORPHISM

The only metamorphic minerals observed were chloritoid, muscovite, chlorite and minor pyrophyllite. Chloritoid in the slates forms porphyroblasts which are poorly aligned with cleavage, indicating that the peak of metamorphism was late to posttectonic. The chlorite and muscovite form fine masses parallel to cleavage, or occur as vein material, and pyrophyllite was noted only as fracture fillings.

REFERENCES

Balkwill, H.R.
1969: Structural analysis of the Western Ranges, Rocky Mountains, near Golden, British Columbia; unpublished Ph.D. thesis, University of Texas at Austin, Austin, Texas.

Fyles, T.J.
1960: Geological reconnaissance of the Columbia River between Bluewater Creek and Mica Creek, British Columbia; British Columbia Minister of Mines, Annual Report 1959, p. 90-105.

Gardner, D.A.
1977: Structural geology and metamorphism of calcareous Lower Paleozoic slates, Blueberry River – Redburn Creek Area, near Golden, British Columbia; unpublished Ph.D. thesis, Queen's University, Kingston, Ontario.

Meilliez, F.
1972: Structure of the Southern Solitude Range, British Columbia; unpublished M.Sc. thesis, The University of Calgary, Calgary, Alberta.

Pell, J. and Simony, P.
1981: Stratigrpahy, structure and metamorphism in the southern Cariboo Mountains, British Columbia; in Current Research, Part A, Geological Survey of Canada, Paper 81-1A, p. 227-330.

Price, R.A.
1965: Golden, east-half, map area (82NE1/2), British Columbia and Alberta; in Report of Activities, Part B, Geological Survey of Canada, Paper 67-1B, p. 88-91.

Wheeler, J.O.
1963: Rogers Pass map-area, British Columbia and Alberta; Geological Survey of Canada, Paper 62-32.

1965: Big Bend map-area, British Columbia; Geological Survey of Canada, Paper 64-32.

12. STRUCTURAL EVOLUTION AND METAMORPHISM OF THE SOUTHERN CARIBOO MOUNTAINS NEAR BLUE RIVER, BRITISH COLUMBIA

EMR Research Agreement 300-04-83

R.G. Dechesne[1], P.S. Simony[1], and E.D. Ghent[1]
Cordilleran Geology Division

Dechesne, R.G., Simony, P.S., and Ghent, E.D., Structural evolution and metamorphism of the southern Cariboo Mountains near Blue River, British Columbia; in Current Research, Part A, Geological Survey of Canada, Paper 84-1A, p. 91-94, 1984.

Abstract

Metasedimentary rocks belonging to the Semipelite-Amphibolite, Middle Marble and Upper Clastic units of the Hadrynian Horsethief Creek Group, were metamorphosed to a Barrovian-type facies series with grade rising from staurolite + kyanite + muscovite + sillimanite in the north, near Thunder River, to sillimanite + K-feldspar with abundant migmatite in the Shuswap Complex south of Blue River. The contrasting styles of metamorphism juxtaposed across the North Thompson normal fault suggest that the fault has a normal, west-side-down motion of several kilometres. The Middle Marble outlines a large, southwest verging phase 1 fold pair refolded by large, northeast verging second phase folds. A thrust fault in the Thunder River valley is associated with these phase 2 folds. A plutonic complex of granite, pegmatite and gneissic quartz diorite intrudes the Hadrynian rocks south of Blue River.

Résumé

Des roches métasédimentaires appartenant aux unités Semipelite-Amphibolite, Middle Marble et Upper Clastic du groupe hadrynien de Horsethief Creek ont été métamorphisées en un faciès de type barrovien; le métamorphisme passe de l'étape de la staurotide + cyanite + muscovite + sillimanite au nord, près de la rivière Thunder, à celle de la sillimanite + feldspath potassique avec des quantités abondantes de migmatite dans le complexe Shuswap au sud de la rivière Blue dans la même province. Les styles contrastants de métamorphisme juxtaposés en travers de la faille normale de North Thompson laissent entendre qu'il y a eu mouvement descendant normal de la lèvre ouest de la faille sur une distance de plusieurs kilomètres. L'unité Middle Marble délimite un grand pli incliné vers le sud-ouest qui a été replié par des gros plis de phase 2 inclinés vers le nord-est. Une faille chevauchante dans la vallée de la rivière Thunder est associée à ces plis de phase 2. Un complexe plutonique de granite, de pegmatite et de diorite quartzique gneissique pénètre les roches hadryniennes au sud de la rivière Blue.

INTRODUCTION

Mapping and sampling along the northern margin of the Shuswap Metamorphic Complex west of the town of Blue River, British Columbia, and south of Thunder River was undertaken during the summers of 1982 and 1983. The area (Fig. 12.1), a portion of the Canoe River Sheet (83 D), had been mapped on a reconnaissance scale by Campbell (1968). The presence of sillimanite was used by Campbell (1968) to differentiate the Shuswap Metamorphic Complex from rocks mapped as Hadrynian metasediments.

The present study, at a scale of 1:24 000, establishes that the Shuswap Metamorphic Complex in this area consists of paragneisses of the upper portions of the Hadrynian Horsethief Creek Group which are cut by quartz diorite, muscovite-biotite granite and muscovite-bearing pegmatite plutons.

STRATIGRAPHY

Three major stratigraphic units are recognized in the area; a unit of semipelite, psammite and amphibolite; a marble; and an overlying unit of semipelite, psammite and pelite with minor grit. These are most reasonably correlated with the Semipelite-Amphibolite, Middle Marble and Upper Clastic divisions of the Hadrynian Horsethief Creek Group identified north of Thunder River by Pell and Simony (1981).

The oldest exposed rocks belong to the Semipelite-Amphibolite unit, which is dominated by interlaminated semipelite, pelite and psammite. The semipelite locally contains hornblende-biotite semipelite beds. Amphibolite is common near the top of the unit and occurs as layers parallel to bedding; these layers range in thickness from a few millimetres to several metres. Thin calcsilicate-bearing marbles are associated with the amphibolite. The total thickness is not exposed, but the upper 1.5 km of the Semipelite-Amphibolite unit is.

Above the Semipelite-Amphibolite unit is the Middle Marble unit, which is 20 to 100 m thick in the study area. The Middle Marble commonly has one or two, 4 to 25 m thick, massive, coarsely crystalline, white marble beds. The remainder of the unit is composed of thin bedded, brown weathering, calcsilicate-bearing marble. Thin calcsilicate amphibolilte and hornblende-biotite semipelite beds are also common.

The overlying Upper Clastic unit is characterized by interbedded semipelite, pelite and psammite. There are also some graded feldspathic grit layers and lenses as well as hornblende-, diopside-, and garnet-bearing calcsilicate lenses. A lateral facies change in the lower part of the unit is telescoped across the Thunder River valley by deformation. On the north side of the valley thick grit beds occur near the base of the Upper Clastic Unit (Pell and Simony, 1982), whereas they are thin and relatively uncommon in the basal layers on the south side of the river. Farther south, granules were found here and there in psammites and semipelites; throughout the rest of the area, no gritty beds were found in the unit. Thus, within the southern part of the study area, the Upper Clastic unit has a marked resemblance to the Semipelite-Amphibolite unit, though the latter has more amphibolite and somewhat less psammite. Pelites of the Upper Clastic Unit tend to be more aluminous, containing abundant sillimanite, whereas pelites of the Semipelite-Amphibolite unit contain only traces of sillimanite except at very high metamorphic grades. The exposed thickness of the Upper Clastic unit is approxiamtely 0.5 km.

[1] Department of Geology and Geophysics, University of Calgary, Calgary, Alberta T2N 1N4

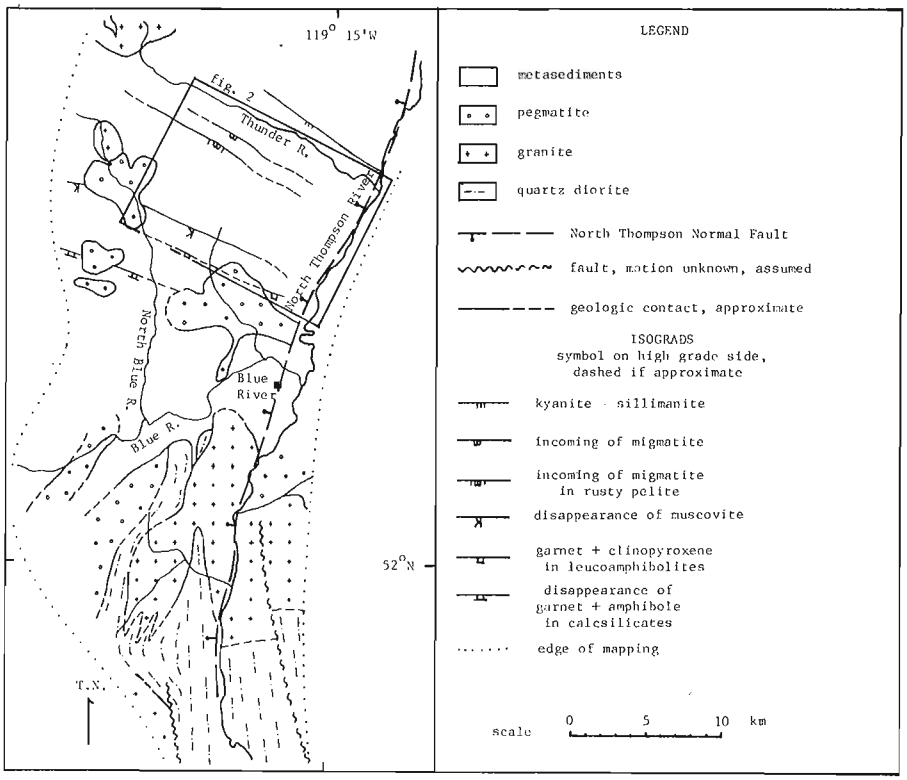

Figure 12.1. Geology of the southern Cariboo Mountains, British Columbia. The position of the kyanite = sillimanite isograd after Pell and Simony (1981).

STRUCTURE

The rocks in the area have undergone three major phases of deformation. The structural relationships, the mesoscopic and microscopic fabrics and the relationship to metamorphism of phase 1 and phase 2 structures are consistent with those described for phase 1 and phase 2, respectively, by Pell and Simony (1982), Raeside and Simony (1983) and Simony et al. (1980).

The structures formed in the first deformation phase are a penetrative foliation in all rock types, small isoclines and large fold pair illustrated in Figure 12.2. The area to the northeast of this fold pair represents a long upper limb of the F_1 anticline with upright stratigraphy and with a number of large assymetric phase 1 mesoscopic folds which indicate the presence of a large phase 1 anticline to the southwest. That anticline is the tight antiform marked F_1 on section A-B and it is followed to the southwest by a synform shown on section A-B as a phase 1 syncline. It is marked by an abundance of phase 1 mesoscopic folds and it cannot be a phase 2 synform and fit the regular succession of phase 2 antiforms and synforms. Prior to phase 2 therefore the megascopic phase 1 fold pair was southwest verging. The phase 1 structures are folded by northeast verging second phase folds that dominate the map pattern and are associated with a foliation, S_2, that grades from a strain-slip cleavage in the north to a penetrative schistosity in the south. Throughout most of the area, the regional foliation is mapped as S_{1+2} because S_1 and S_2 cannot be distinguished where they are subparallel. This approach was also taken by other workers in nearby areas (e.g. Simony et al., 1980). S_1 can be distinguished from S_2 in the hinge zones of phase two folds. These folds range from very tight to open in style. Associated with the second phase folds is a large thrust fault which outcrops in the Thunder River and North Thompson valleys. This thrust puts approximately 1 km of the Semipelite-Amphibolite unit on 1.5 km of Upper Clastic grits and hence has a stratigraphic separation of 2.5 km. The minimum possible dip-slip motion of this fault is 6 km though a dip-slip of at least 8 km is more probable.

Late folding, assigned to the third phase of deformation, followed the regional metamorphic peak. Micas were bent and broken during the formation of the crenulations that characterize this deformational episode. Locally, the crenulations pass into a strain-slip cleavage that is difficult to distinguish from S_2. Thick marble units folded by third phase folds commonly have bedding plane décolements near their contacts. Phase three deformation produces only mesoscopic folds and does not markedly affect the map pattern. Postmetamorphic reactivation and broad folding of the thrust in the Thunder River area may be a large scale manifestation of third phase deformation. Unrecrystallized pseudotachylite and mylonite can be found in the fault zone. The motion, however, could be of the type described above – bedding plane slip during buckle folding. The contrast between the competencies of the massive grit and conglomerate of the Upper Clastic unit and the thin bedded semipelite, pelite and psammite of the structurally overlying Semipelite-Amphibolite unit would certainly allow such disharmony. It is possible that some third phase thrust motion took place as well.

The North Thompson normal fault is the result of late extension. The fault juxtaposes a terrane of relatively low pressure metamorphism on its west side against one of higher pressure on the east. Based on metamorphic arguments, Pell and Simony (1981) suggested that a west-side-down normal motion of at least 4 km had occurred on the fault.

Field mapping in the present study has allowed the tracing of a fault southward from the town of Blue River through crushed and chloritized granite and quartz diorite outcrops (Fig. 12.1). It is possible that this represents the continuation of the North Thompson normal fault. The presence of crushed and slickensided granite near Avola indicates that at least part of the fault system may extend as far south as latitude 51°45'N.

METAMORPHISM

The rocks in the area were metamorphosed to upper amphibolite facies, similar to that of the Barrovian facies series. Metamorphic grade is lowest in the northern portion of the area and increases southward towards the plutonic complex that occurs south of the town of Blue River (Fig. 12.1). The relationship between the plutonic rocks and the metamorphism is unclear.

In the area north of Thunder River, staurolite breakdown occurred just as sillimanite started to form (Pell and Simony, 1981). Temperatures estimated by garnet-biotite geothermometry from the kyanite = sillimanite isograd are approximately 550°C with a corresponding pressure of 450MPa (Pell and Simony, 1981), compared to

about 600°C and 600MPa obtained from the same isograd at Mica Creek (Ghent et al., 1982). The nature and sequence of isograds just east of the North Thompson normal fault is similar to that found at Mica Creek (Pell and Simony, 1981) i.e. a broad staurolite-free upper kyanite zone with abundant migmatite. This contrasts markedly with the spacing of the staurolite breakdown and kyanite = sillimanite isograds west of the fault.

The first appearance of abundant migmatite (Fig. 12.1) in the study area is as much as 3 km south, and hence upgrade, of the kyanite = sillimanite isograd. This is consistent with a lower metamorphic pressure on the west side of the North Thompson normal fault, using the pressure-temperature diagram of Thompson and Tracy (1979). The incoming of migmatite is best seen in biotite + muscovite + garnet pelites and semipelites. The leucosome forms veins many centimetres long parallel to the foliation. Rusty, sillimanite + muscovite pelites first show leucosome development at still higher grade (Fig. 12.1) and then only as 0.5 cm by 2 cm lenses parallel to the foliation; these pelites do not have extensive migmatite until south of Whitewater Creek. This development of leucosome may be due to the breakdown of white mica, but a decrease in the percentage of white mica, and the parallel production of K-feldspar, is only seen south of Cook Creek (Fig. 12.1).

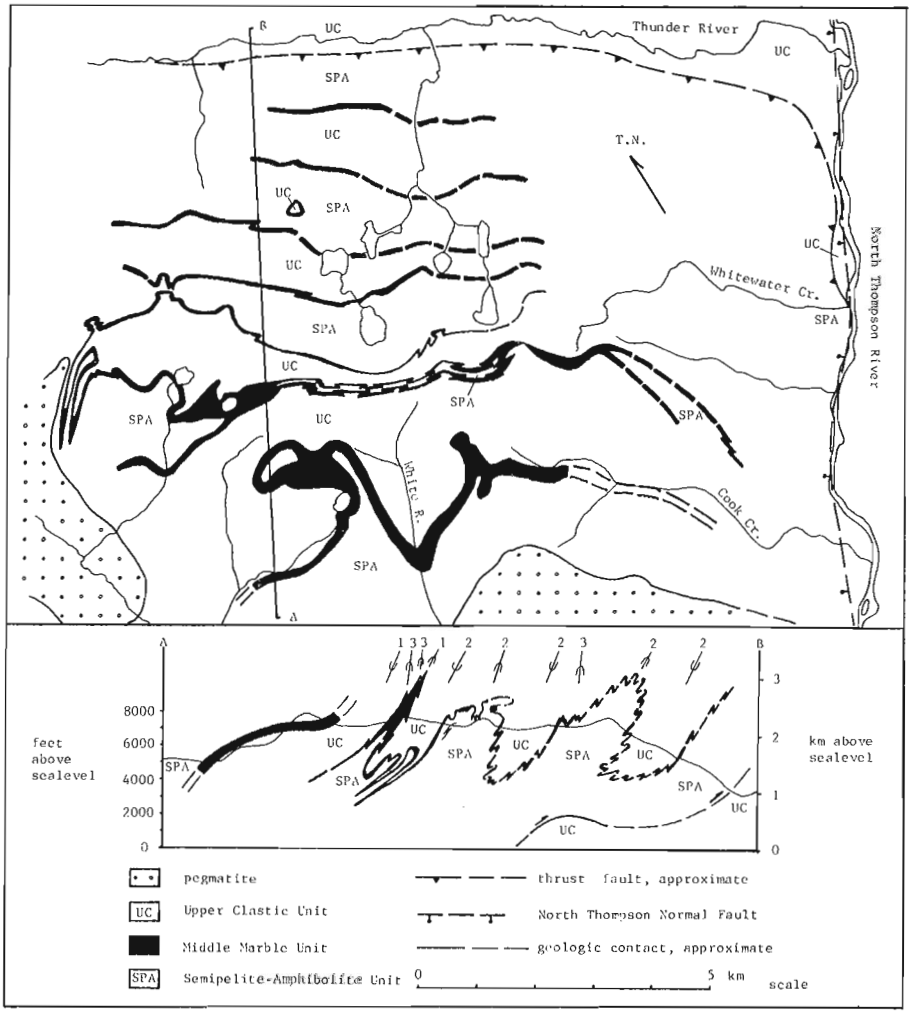

Figure 12.2. *Detailed geologic map and cross-section of the northern portion of the study area. See Figure 12.1 for location.*

Amphibolitic rocks are locally very common and are of three main types: mafic amphibolites, with a composition approximating basalt; leucoamphibolites, with an andesitic composition; and calcsilicate amphibolites, similar to those described by Ghent and de Vries (1972). All three types of amphibolite have the typical hornblende + plagioclase + quartz assemblage, though the hornblende in the calcsilicate amphibolite is actinolitic. Garnet is an essential mineral in the calcsilicate amphibolite and a common accessory in the other amphibolite types. Biotite may occur in all three types. Garnet + clinopyroxene can be found in the calcsilicate amphibolite – even to the exclusion of the amphibole – at the kyanite = sillimanite isograd. Leucoamphibolites contain garnet + clinopyroxene-bearing assemblages south of a line 4 km north of the junction of the White and Blue rivers (Fig. 12.1). Mafic amphibolites nowhere develop garnet + clinopyroxene-bearing assemblages. This is consistent with a lower metamorphic pressure in the present study area than at Mica Creek where garnet + clinopyroxene assemblages in mafic amphibolites are present within 1 km of the kyanite = sillimanite isograd (Ghent et al., 1983). In the calcsilicate rocks the assemblage garnet + amphibole was not seen south of a line just north of the junction of the White and Blue rivers (Fig. 12.1).

SUMMARY

The rocks of the northern portion of the Shuswap Metamorphic Complex have been affected by three phases of folding. Early southwest verging isoclinal folds, perhaps associated with nappe production, were refolded by northeast verging second phase folds associated with a large thrust fault. The postmetamorphic third phase generally produced relatively small folds only and reactivated the phase-two thrust fault. The North Thompson normal fault then dropped the rocks on its west side. The motion on this fault was large enough to juxtapose two terranes of significantly different metamorphic pressures. The relative order and spacing of the staurolite breakdown, incoming of migmatite, kyanite = sillimanite and garnet + clinopyroxene (in mafic amphibolite) isograd suggest a metamorphic pressure difference across the fault of at least 100MPa.

REFERENCES

Campbell, R.B.
1968: Canoe River, British Columbia; Geological Survey of Canada, Map 15-1967.

Ghent, E.D. and de Vries, C.D.S.
1972: Plagioclase-garnet-epidote equilibria in hornblende-plagioclase bearing rocks from the Esplanade Range, British Columbia; Canadian Journal of Earth Sciences, v. 9, p. 618-635.

Ghent, E.D., Knitter, C.C., Raeside, R.P., and Stout, M.Z.
1982: Geothermometry and geobarometry of pelitic rocks, upper kyanite and sillimanite zones, Mica Creek area, British Columbia; Canadian Mineralogist, v. 20, p. 295-305.

Ghent, E.D., Stout, M.Z., and Raeside, R.P.
1983: Plagioclase-clinopyroxene-garnet-quartz equilibria and the geobarometry and geothermometry of garnet amphibolites from Mica Creek, British Columbia; Canadian Journal of Earth Sciences, v. 20, p. 699-706.

Pell, J. and Simony, P.
1981: Stratigraphy, structure, and metamorphism in the Southern Cariboo Mountains, British Columbia; in Current Research, Part A, Geological Survey of Canada, Paper 81-1A, p. 227-230.

Pell, J. and Simony, P. (cont.)
1982: Hadrynian Horsethief Creek Group/Kaza Group correlations in the southern Cariboo Mountains, British Columbia; in Current Research, Part A, Geological Survey of Canada, Paper 82-1A, p. 305-308.

Raeside, R.P. and Simony, P.S.
1983: Stratigraphy and deformational history of the Scrip Nappe, Monashee Mountains, British Columbia; Canadian Journal of Earth Sciences, v. 20, p. 639-650.

Simony, P.S., Ghent, E.D., Craw, D., Mitchell, W., and Robbins, D.B.
1980: Structural and metamorphic evolution of northeast flank of Shuswap Complex, southern Canoe River area, British Columbia; Geological Society of America, Memoir 153, p. 445-461.

Thompson, A.B. and Tracy, R.J.
1979: Model systems for the anatexis of pelitic rocks: II. Facies series melting and reactions in the system $CaO\text{-}KAlO_2\text{-}NaAlO_2\text{-}SiO_2\text{-}H_2O$; Contributions to Mineralogy and Petrology, v. 70, p. 429-438.

13. STRATIGRAPHY OF THE HADRYNIAN KAZA GROUP BETWEEN THE AZURE AND NORTH THOMPSON RIVERS, CARIBOO MOUNTAINS, BRITISH COLUMBIA

EMR Research Agreement 300-04-83

Jennifer Pell[1] and P.S. Simony[1]

Pell, J. and Simony, P.S., Stratigraphy of the Hadrynian Kaza Group between the Azure and North Thompson rivers, Cariboo Mountains, British Columbia; in Current Research, Part A, Geological Survey of Canada, Paper 84-1A, p. 95-98, 1984.

Abstract

A complete section of Hadrynian Kaza Group metasediments was measured between the headwaters of the North Thompson and Azure rivers. The section is 3800 m thick and can be divided into three major units; Lower Kaza pelites and psammites, 700 m; Middle Kaza grits, with thick pelitic intervals, quartzites and carbonates, 1400 m; and Upper Kaza grits, with no pelitic markers, 1700 m. Contacts with both the underlying Middle Marble of the Horsethief Creek Group, and with the overlying Isaac Formation of the Cariboo Group are gradational.

First phase, southwest-verging folds are outlined by Kaza Group strata south of McAndrew Creek. These folds and the associated S_1 cleavage are refolded by upright, northwest-plunging F_2 folds. In the upper Kaza and Isaac Formation west of the Azure River, no F_1 folds, or S_1 cleavage have been developed, indicating that phase one deformation diminishes up section. At higher levels "F_2" folds are the earliest structures.

Résumé

Les auteurs ont mesuré une section complète de métasédiments du groupe hadrynien de Kaza entre les cours supérieurs des rivières Thompson nord et Azure. La section a une épaisseur de 3 800 mètres et se divise en trois unités principales: les pélites et les psammites de la partie inférieure ont une épaisseur de 700 m; les grits de la partie moyenne, d'une épaisseur de 1 400 m, contiennent des intervalles épais de pélites, de quartzites et de carbonates; les grits de la partie supérieure sont dépourvus de repères pélitiques et ont une épaisseur de 1 700 m. Les contacts avec l'unité Middle Marble sous-jacente du groupe de Horsethief Creek et la formation d'Isaac sus-jacente du groupe de Cariboo sont progressifs.

Au sud du ruisseau McAndrew, les couches du groupe de Kaza délimitent des plis de première phase qui sont inclinés vers le sud-ouest. Ces plis et le clivage S_1 associé ont été repliés par des plis droits F_2 qui plongent vers le nord-ouest. À l'ouest de la rivière Azure, il n'y a pas de plis F_1 ni de clivage S_1 dans la partie supérieure du groupe de Kaza et dans la formation d'Isaac et la déformation de phase 1 diminue en montant la section. À des niveaux plus élevés, les plis F_2 sont les premières structures formées.

INTRODUCTION

A complete section of Hadrynian Kaza Group is exposed in the southern Cariboo Mountains of British Columbia between the headwaters of the Azure and the North Thompson rivers (between longitudes 119°35' and 119°50' W, and at latitude 52°35'N). The section was measured by mapping, in detail, three adjacent ridges (west of Azure River, south of McAndrew Creek and north of Stormking Creek) at 1:12 000 scale (Fig. 13.1). Bedding attitude, cleavage-bedding relationships, and stratigraphic tops were determined at 100-300 m intervals, at precisely located stations.

The rocks are complexly deformed and metamorphosed to chlorite, chlorite-biotite, and garnet grades.

Structure

The rocks of the Kaza Group outline folds belonging to two phases of deformation. Second generation (F_2) folds are the major structures within the area mapped. They have vertical to steep northeast or southwest dipping axial planes and, in general, shallow northwest axial plunges (Fig. 13.2). On the ridge south of McAndrew Creek, both in the garnet and the chlorite-biotite zone (Fig. 13.1), S_2, the axial planar fabric related to the F_2 folds, is a weak to moderately well developed crenulation cleavage of an earlier S_1 foliation. West of Azure River, in sub-biotite grade rocks, the foliation axial-planar to "F_2" folds is apparently the earliest fabric; no evidence of a prior "S_1" cleavage was found in rocks of either the Upper Kaza Group or the Isaac Formation.

South of McAndrew Creek, a broad open F_2 synform of simple morphology, the Slide Mountain Synform (Fig. 13.1, 13.2), dominates the structure, and extends parallel to the axial trend some 30 to 40 km to the southeast (Pell and Simony, 1982). A fan axis roughly coincides with the axial trace of the Slide Mountain Synform. On the southwest limb of the synform megascopic F_2 folds have northeast-dipping axial planes, whereas on the northeast limb, axial planes dip steeply southwest. This fanning is more prominent farther to the southeast (Pell and Simony, 1982).

In the core of the Slide Mountain Synform the strata have shallow dips, and abundant graded beds indicate that everywhere the package is upright. On the southwest limb of the synform, a northeast-dipping fault separates this zone of simple structure from one with steeply dipping strata which are frequently overturned, as defined by graded-bedding tops (Fig. 13.2). Bedding/S_2 cleavage relationships indicate that the strata are everywhere upright with respect of F_2 folds; therefore, overturning is a result of F_1 folding, as confirmed by bedding/S_1 cleavage relationships. A series of F_1 folds can be outlined, their sense of vergence indicating that they are parasitic folds on the upright limb of a major southwest-verging nappe. To the southeast (Pell and Simony, 1982), an analogous structure was mapped; however, the F_1 folds in the area are considerably larger, yet still parasitic on the limb of the major structure.

The Upper Kaza Group rocks on McAndrew Ridge project, to the northwest, beneath the Isaac Formation contact. The Isaac apparently was involved only in the F_2 folding; no manifestation of F_1 folds or an S_1 fabric has been noted (see also the 1:250 000 map of Campbell, 1968).

[1] Department of Geology and Geophysics, University of Calgary, Calgary, Alberta T2N 1N4

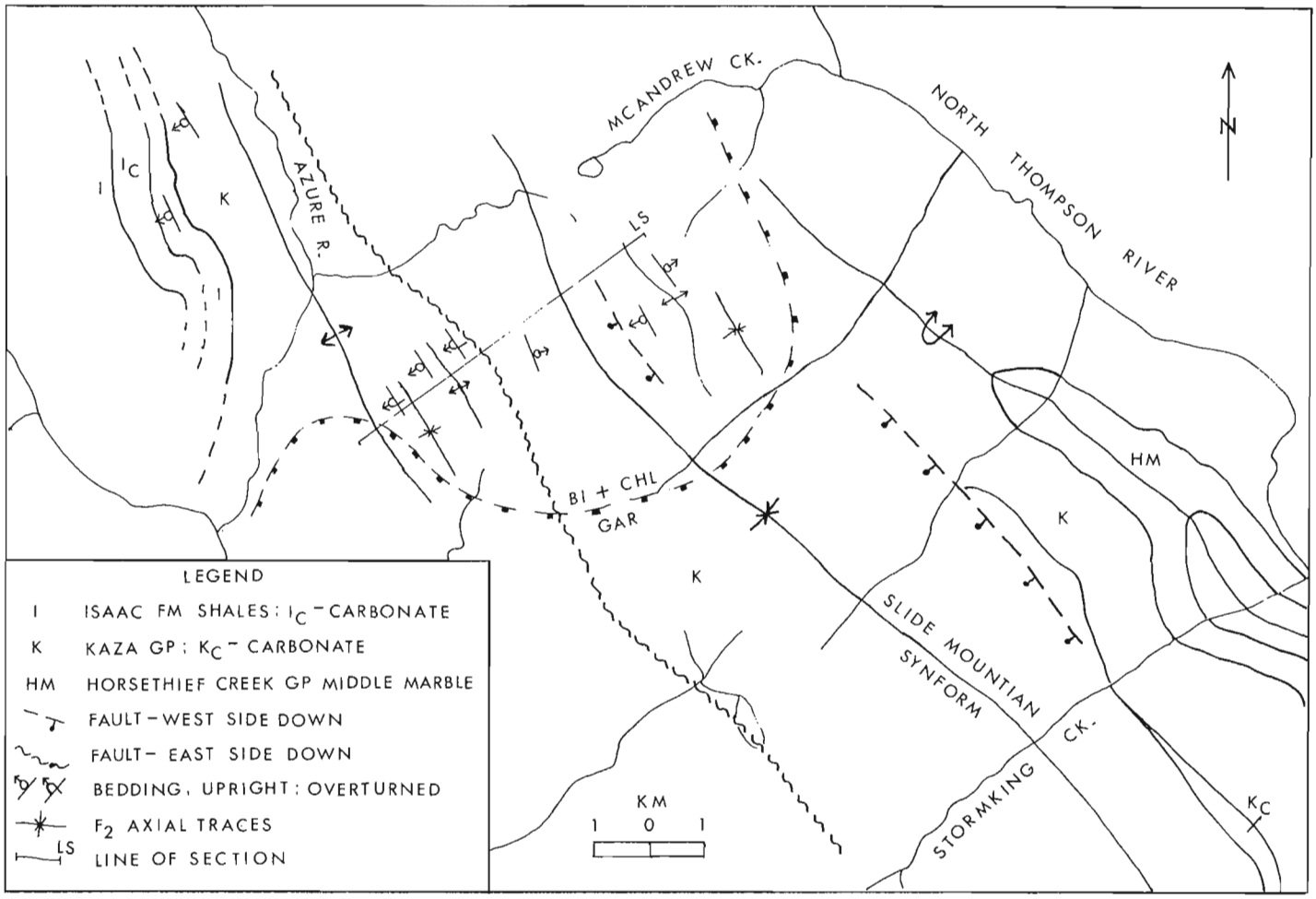

Figure 13.1. *Geology of the Cariboo Mountains between the North Thompson and Azure rivers.*

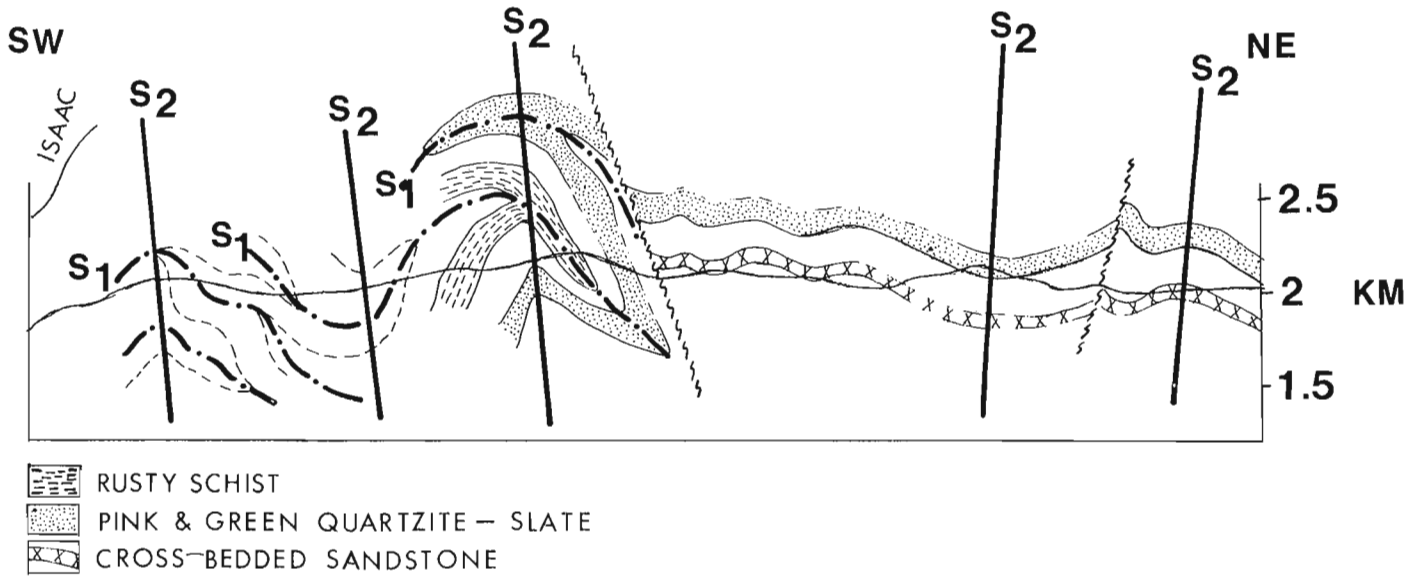

Figure 13.2. *Schematic cross-section. See Figure 13.1 for location of section. Horizontal = vertical scale.*

First phase structures appear to diminish, both in size and importance up section, both structurally and stratigraphically, until at high levels they are nonexistent.

STRATIGRAPHY

The base of the Kaza Group is taken at the top of the Middle Marble division of the Horsethief Creek Group (Pell and Simony, 1982). That contact is gradational, with beds and lenses of grit, pelite, psammite and buff weathering calcareous grit interbedded over a 50 to 100 m interval. The overlying Lower Kaza consists of pelite and psammite interbedded with variable amounts of semipelite, grit and distinctive hornblende-garnet calc-silicate layers and lenses. Distinctly graded grit beds are rare. The Lower Kaza is rather variable in lithology, and its thickness varies between 150 and 1000 m. In our measured section north of Stormking Creek (Fig. 13.1), the Lower Kaza is 700 m thick, and is capped by 5 to 10 m of grey and buff weathering sandy marble (Fig. 13.3). This mappable horizon is present in most, but not all sections.

The Middle Kaza is 1400 m thick and, in our measured section, consists of four distinct units. The lower 870 m (Fig. 13.3) consists of grit-psammite-pelite cycles 30 to 100 m thick, with the base of each cycle marked by coarse graded grit in beds 0.5 to 2 m thick. Locally, some of the cycles are capped by sandy grey and white marble beds 2 to 10 m thick. Hornblende-garnet calc-silicate layers and lenses are associated with psammite in the lower part of this unit.

The next unit consists of 220 m of graded grit and psammite cycles 5 to 10 m thick, "stacked" one on the other, with 5 to 20 m thick pelite layers intervening between some of the cycles. The upper 70 m of this unit are characterized by calcareous, crosslaminated and trough crossbedded sandstone beds and lenses, marking the top of the graded grit-psammite cycles.

The overlying unit is some 150 m thick, and consists of pink quartzite, psammite and pelite interbedded with green laminated pelite. The quartzite beds and distinct colour combine to make this a useful marker.

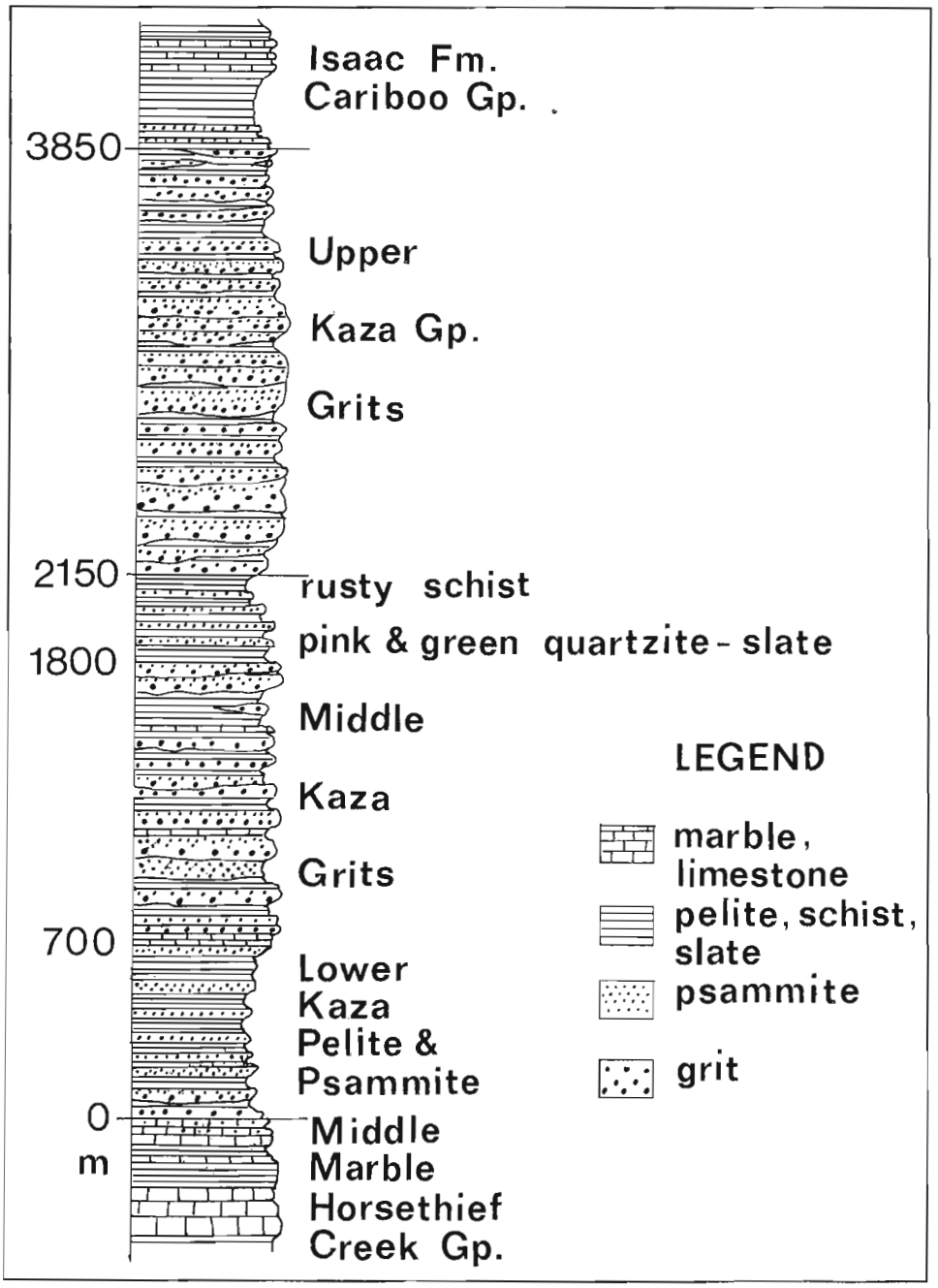

Figure 13.3

Stratigraphic section of the Hadrynian Kaza Group between the North Thompson and Azure rivers.

The Middle Kaza is capped by about 100 m of rusty schist. At its base is orange weathering crosslaminated calcareous psammite, and green, parallel and crosslaminated silty pelite. The overlying rusty zone consists of interbedded calcareous psammite, in 0.2 to 1 m beds, rusty laminated pelites, buff sandy marble, white quartzite, black graphitic and sulphide-rich schist and buff calcareous grit.

The Upper Kaza is grit dominated, and about 1700 m thick (Fig. 13.3). It is distinguished from the Middle Kaza by the absence of distinct, thick pelitic markers and by the complete lack of any carbonate or calc-silicate beds. No markers subdivide this great thickness of grit in which cycles of graded "stacked" grits, grit-psammite, and grit-psammite-pelite occur. Cycles are 5 to 20 m thick, and individual graded grit beds are 0.5 to 1.5 m thick. Coarse grit fills channels at the base of the grit layers, and in these are quartz and feldspar clasts 5 to 15 mm across. Bluish quartz, typical of Hadrynian clastics of the Cordillera, is present, but not abundant. Tabular and deformed pelite "rip-up" clasts are common in the central, poorly graded parts of grit beds. Pelitic beds between the grits and psammites are both parallel and crosslaminated.

The upper 200 m of the Kaza Group are marked by the presence of brownish weathering, dark grey laminated slates. Grit beds are thinner, finer, much less feldspathic, and less abundant upward. The Kaza Group grades into the dark slates, calcareous slates, and thin calcareous sandstones of the lower portion of the Isaac Formation. The top of the Kaza was picked at the top of the highest graded grit sequence.

In our section, 300 m of dark grey to black and brown, calcareous slate, with thin argillaceous and sandy limestone beds which mark the base of the Isaac Formation, are overlain by several hundred metres of dark grey and buff limestone, calcareous slate, limestone conglomerate and limestone breccia beds.

The Middle and Upper Kaza together bear a strong resemblance to the Middle Miette grits of the Rocky Mountains, and our observations would support the correlation of these two grit units, as proposed by Campbell et al. (1973). The Lower Kaza and underlying Horsethief Creek Group would then correlate with the Lower Miette of the Rocky Mountains, as suggested by Pell (1982).

CONCLUSIONS

The Middle and Upper Kaza are probably correlative with the Middle Miette grits of the Rocky Mountains, which they closely resemble. The Lower Kaza, and the underlying Horsethief Creek strata are then correlative with the Lower Miette.

The Kaza strata outline southwest-verging phase one folds, refolded by phase two folds on the southwest limb of the Slide Mountain Synform. Phase one deformation diminishes upward through the Upper Kaza, and is absent in the Isaac.

REFERENCES

Campbell, R.B.
1968: Geology of Canoe River, British Columbia; Geological Survey of Canada, Map 15-1967.

Campbell, R.B., Mountjoy, E.W., and Young, F.G.
1973: Geology of the McBride map area, British Columbia; Geological Survey of Canada, Paper 72-35, 104 p.

Pell, J.
1982: New correlations of Hadrynian strata, southern Canadian Cordillera; Geological Association of Canada, Abstracts, v. 7, p. 73.

Pell, J. and Simony, P.S.
1982: Hadrynian Horsethief Creek Group/Kaza Group correlations in the southern Cariboo Mountains, British Columbia; in Current Research, Part A, Geological Survey of Canada, Paper 82-1A, p. 305-308.

14. BASEMENT GNEISSES AND HADRYNIAN METASEDIMENTS NEAR BULLDOG CREEK, SELWYN RANGE, BRITISH COLUMBIA

EMR Research Agreement 300-04-83

Michael R. McDonough[1] and P.S. Simony[1]
Cordilleran Geology Division, Vancouver

McDonough, M.R. and Simony P.S., Basement gneisses and Hadrynian metasediments near Bulldog Creek, Selwyn Range, British Columbia; in Current Research, Part A, Geological Survey of Canada, Paper 84-1A, p. 99-102, 1984.

Abstract

Two bodies of gneiss occur in the Bulldog Creek area; Bulldog Gneiss consisting of banded paragneiss intruded by leuco-orthogneiss, and Yellowjacket Gneiss, a mass of porphyritic granite deformed to foliated augen gneiss. Bulldog Gneiss, in the core of a phase-2 fold, is in the hanging wall of the Purcell Thrust, whereas the Yellowjacket Gneiss, in the core of a phase-1 fold, is in the footwall of the fault. The gneiss masses form the basement for a facies of the Hadrynian Miette Group that closely resembles the Horsethief Creek Group and stratigraphically underlies Middle Miette grit.

Sillimanite, kyanite and staurolite are found together in a 100 m-wide belt in the footwall of the Purcell Thrust. Metamorphic grade decreases eastward through a kyanite-staurolite zone to the garnet zone.

Résumé

Deux masses de gneiss se présentent dans la région du ruisseau Bulldog, soit le gneiss de Bulldog, composé d'un paragneiss zoné traversé par un orthogneiss leucocrate et le gneiss de Yellowjacket, masse de granite porphyrique déformé en gneiss oeillé feuilleté. Le gneiss de Bulldog, dans le noyau d'un pli de phase 2, se situe dans le toit de la faille chevauchante de Purcell, tandis que le gneiss de Yellowjacket, dans le noyau d'un pli de phase 1, se trouve dans le mur de la faille. Les masses de gneiss forment le socle d'un faciès du groupe hadrynien de Miette qui ressemble étroitement au groupe de Horsethief Creek et qui est sous-jacent au grit de Middle Miette.

De la sillimanite, de la cyanite et de la staurotide se présentent ensemble dans une zone large de 100 mètres dans le mur de la faille chevauchante de Purcell. Le degré de métamorphisme baisse vers l'est en passant d'une zone de cyanite-staurotide à une zone de grenat.

INTRODUCTION

Field work was carried out during the summer of 1983 in the Selwyn Range, in the western Main Ranges of the Rocky Mountains. The study area is centred on Bulldog Creek at latitude 52°40'N, approximately 25 km southeast of Valemount, British Columbia. An area of 130 km^2 was mapped on a scale of 1:24 000. The project is designed to determine the structure and petrological affinities of the Bulldog Gneiss, its tectonic relationship to the adjacent Hadrynian Miette Group metasediments, and the character of amphibolite facies metamorphism involved in the deformation.

Previous work in the Bulldog Creek area includes reconnaissance-scale mapping of the Canoe River Sheet (83D) conducted by Campbell (1968), a detailed study of the Malton Gneiss and related gneiss bodies located east of the Rocky Mountain Trench initiated by Giovanella (1967, 1968), and some geochemical and geochronological work carried out by Chamberlain et al. (1978).

THE GNEISSES

The gneisses in the Bulldog Creek area occur essentially in two masses; the Bulldog Gneiss Complex and the larger, more easterly, Yellowjacket Gneiss. Both are enveloped by metasediments ascribed to the Hadrynian Miette Group.

The Bulldog Gneiss Complex consists of five slices of gneiss and Hadrynian sediment all in the hanging wall of a major thrust. In the field, Bulldog Gneiss can be subdivided into four lithological types. The oldest and most abundant is a banded, fine grained melanocratic to intermediate biotite-rich gneiss, locally with small feldspar augen. A foliation is formed from the planar alignment of biotite flakes. Occasional boudinaged quartzite pods and minor 5-10 cm thick marble bands are indicative of a metasedimentary origin for the biotite-rich gneisses. An increase in strain within the melanocratic gneiss toward the contact with a basal Hadrynian quartzite is evident. Near this contact the paragneiss is strongly banded and has some mylonite layers.

The second most abundant rock type within the Bulldog Gneiss is a granitic lineated leucocratic orthogneiss which contains biotite and minor muscovite, with abundant feldspar augen up to 2 cm long. This leuco-orthogneiss is generally weakly foliated, and is locally massive. It typically exhibits a strong lineation due to elongate feldspar and quartz grains, as well as aligned biotite and muscovite aggregates. Inclusions of melanocratic paragneiss within leuco-orthogneiss indicate that the leucocratic gneiss intruded the paragneiss. Near the fault zones, outcrops of paragneiss and leuco-orthogneiss contain retrograde mineral assemblages which include abundant chlorite and epidote. The presence of relict feldspar porphyroblasts and occasional hornblende aggregates suggests a gneissic origin for such chloritized rocks.

The third rock type is aplite, in dykes which are observed only in association with leucocratic orthogneiss. Thus the aplite dykes probably represent a late stage of orthogneiss intrusion. The aplite dykes are oriented parallel to the dominant foliation (S_1) in the gneiss body, but may have been aligned parallel to S_1 due to inhomogenous simple shear on the margin of the body during F_1 (see Escher et al., 1975).

The fourth Bulldog Gneiss rock type consists of amphibolite dykes and pods, and schistose mafic dykes. These are also typically oriented parallel to S_1, and may have been rotated due to simple shear during F_1. Locally, minor veinlets of mafic schist are observed orthogonal to S_1, suggesting the parallelism of mafic dykes to S_1 is a result of rotation.

[1] Department of Geology and Geophysics, University of Calgary, Calgary, Alberta T2N 1N4

The Yellowjacket Gneiss is a foliated augen orthogneiss which consists of abundant large feldspar augen up to 5 cm across, with subordinate biotite and quartz. This augen gneiss contains a well developed foliation (S_1) which is formed from the alignment of biotite, and a lineation formed from elongation of feldspar and quartz grains. The homogenity of the body and its undeformed nature at depth suggest that the Yellowjacket Gneiss is a pluton.

On Bulldog Ridge (Fig. 14.1), 150 m below the basement-cover contact, Yellowjacket Gneiss is a massive, granoblastic to faintly foliated, medium grained porphyritic granite. Increasing shear strain toward the gneiss body margin is represented by an increasing biotite content within the foliation, and by the presence of quartzofeldspathic mylonitic bands. This shear strain at the orthogneiss-cover contact is suggestive of a basement-cover décollement.

The relative age of Yellowjacket Gneiss with respect to Bulldog Gneiss is uncertain. Yellowjacket Gneiss is not observed to intrude either Bulldog Gneiss or Miette Group metasediments. The basal décollement character of the Yellowjacket Gneiss-Miette Group contact suggests that Yellowjacket Gneiss probably forms part of the pre-Hadrynian basement; however, it could be a pluton as young as Late Jurassic with Miette Group rocks thrust over it.

STRATIGRAPHY

A 50 m thick, fine grained, mylonitic, foliated, muscovitic quartzite unit nonconformably overlies the Bulldog Gneiss. The quartzite is strongly recrystallized, but exhibits bedding surfaces and foliation formed by muscovite flakes aligned parallel to bedding. It is considerably thickened in the core of a large overturned F_2 anticline. This foliated muscovitic quartzite is interpreted as the basal member of the Hadrynian Miette Group (Oke and Simony, 1981; Evenchick, 1982, 1983). The basal quartzite was not observed overlying Yellowjacket Gneiss farther east.

Two to three metres of marble, minor calc-silicate and contorted para-amphibolite are exposed in the core of a large F_2 anticline between the basal quartzite and a stratigraphically overlying grit unit. These grits occur in beds 0.5-1 m thick with interbeds of pelite. Clast size within grit beds ranges up to 2 cm with smoky quartz, quartzite and feldspar clasts contained in a phyllosilicate-rich matrix.

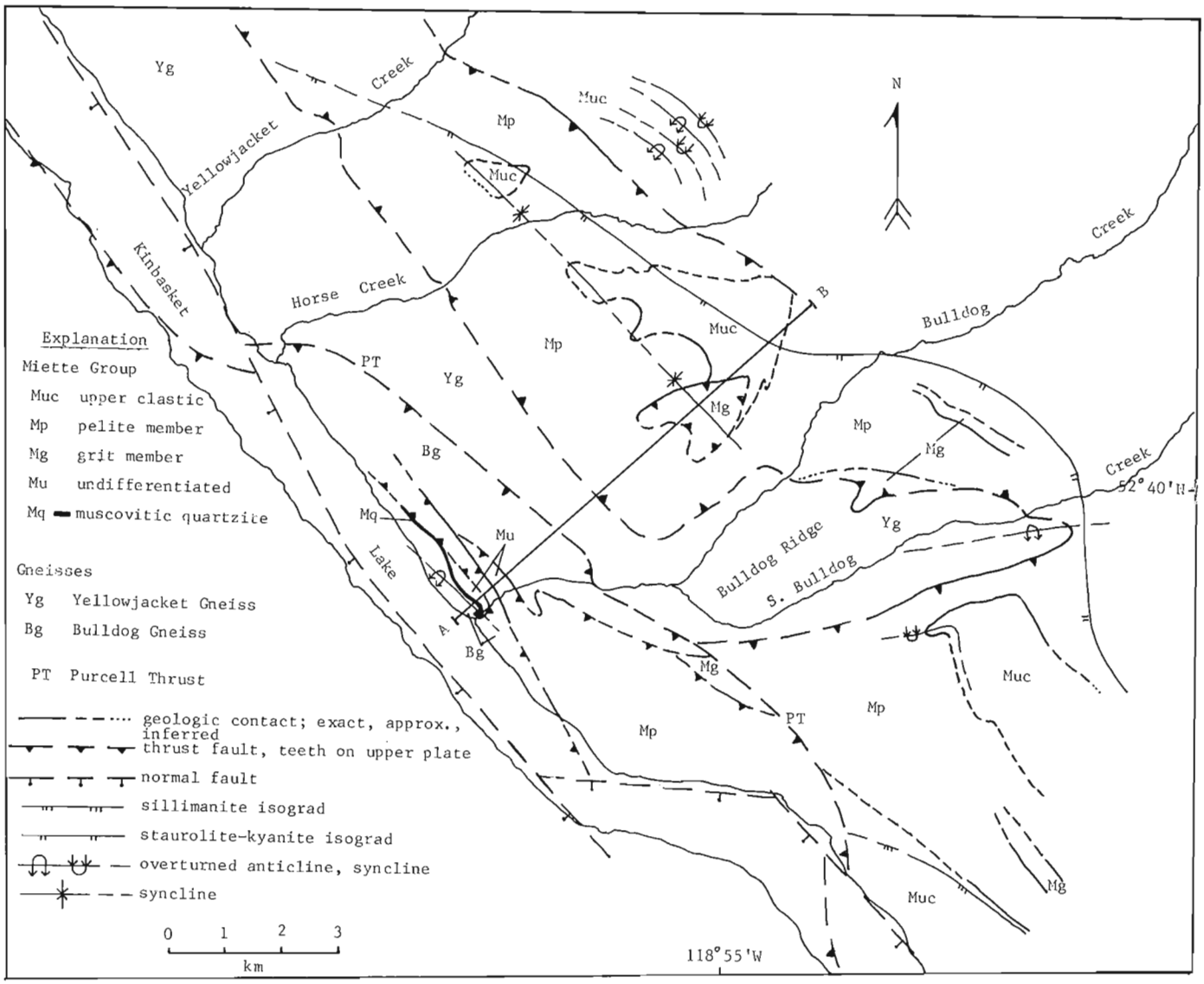

Figure 14.1. *Geological map of Bulldog Creek area.*

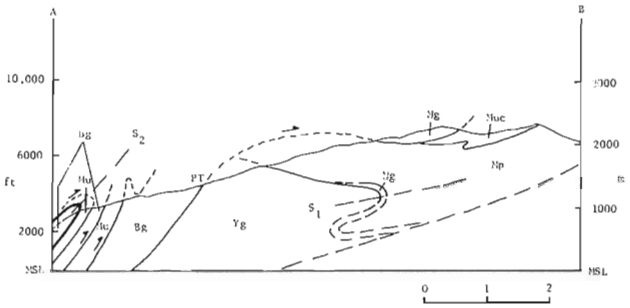

Figure 14.2. *Vertical section AB (1:1); see Figure 14.1 for location and legend.*

The grit unit is approximately 25 m thick and is stratigraphically overlain by 75 m of pelite and interbedded psammite. This stratigraphic succession is quite thin, but appears to be correlative with the lower part of the Horsethief Creek Group on the west side of the Rocky Mountain Trench.

Above the basal décollement on Bulldog Ridge lies a thin and discontinuous unit of grit with interbedded pelite which ranges up to 150 m thick. This is the lower grit unit of the Miette Group. There, vein quartz, quartzite and feldspar clasts up to 3 cm long are recognized within grit beds 0.3-2 m thick. This grit unit may be tectonically thinned, but probably represents depositional pinching out of the lower Miette sequence onto a basement surface which was a topographic high during Hadrynian time. Overlying the lower grit member is an 800-1000 m thick sequence of pelite with interbeds of psammite. This pelite member consists of both coarse grained schist and fine grained phyllite.

Overlying the pelite member is the upper clastic division of the Miette Group (Simony et al., 1980). The upper clastic division consists mainly of pelite with subordinate beds of psammite and grit. The psammites within the upper clastic division contain calc-silicate amphibolite assemblages which are similar to rocks described by Ghent and De Vries (1972) from the Esplanade Range, British Columbia. These grossular-hornblende-epidote-plagioclase-bearing rocks probably had a protolith of sandstone with calcareous cement. Locally, tremolite is observed to coexist with actinolitic hornblende.

The Hadrynian strata of the Miette Group associated with the gneisses in the Bulldog Creek area resemble the stratigraphy described by Oke and Simony (1981) and by Craw (1978) on the west flank of the Rocky Mountains southeast of the Bulldog Creek area. They correlated these strata with the Horsethief Creek Group of the northern Purcell Mountains. The sequence in the Bulldog Creek area is dominated by pelite, the lower grit unit is thin and a continuous marble unit, between the pelite and the overlying upper clastic unit, is lacking. Only in the southeast part of the area does a 3-4 m marble delineate the pelite-upper clastic boundary. The association of calc-silicate amphibolite and grit lenses in a pelitic sequence, typical of the upper clastic unit, suggests correlation of that unit with the base of the Kaza Group in the Cariboo Mountains (Pell and Simony, 1982).

In the northeast part of the area the pelitic sequence, which resembles the Horsethief Creek Group, is clearly stratigraphically overlain by a thick unit of coarse grit having stretched quartz clasts up to 12 cm long interbedded with pelite, which probably correlates with the Middle Miette exposed farther to the east in the Rocky Mountains. The underlying strata, there correlated with the Horsethief Creek Group, would therefore represent a facies of the Lower Miette.

STRUCTURE

Three phases of folding, a set of thrusts and a set of normal faults are superposed within the Bulldog Creek area. First and second phase folds within the Bulldog Gneiss are coaxial, producing mesoscopic, type-III interference patterns (Ramsay, 1962). First phase folds are characterized by northeast-verging isoclines with folded but predominantly southwest-dipping axial planes. No large scale F_1 structures have been observed within the Bulldog Gneiss. Second phase folds in the gneisses are typically tight, northeast-verging, southeast-plunging folds with steeply southwest-dipping axial planes. Third phase folds have not been observed within the gneisses.

The dominant structural feature within the Bulldog Gneiss is a southeast-plunging overturned F_2 anticline cored by gneiss and outlined by basal Hadrynian quartzite. Overturned asymmetric mesoscopic F_2 folds within the slice of gneiss on the overturned east limb of this structure are indicative of emplacement of this slice above the Hadrynian cover of the Bulldog Gneiss prior to F_2. A southwest dipping folded mylonite zone immediately south of Bulldog Creek also suggests the gneiss slice was thrust over the basal Hadrynian units prior to F_2. Mylonite at the Bulldog Gneiss-quartzite contact suggests a detachment between the basement and cover rocks, which was probably last active during F_2.

The Yellowjacket Gneiss lies in the core of a northeast-verging recumbent F_1 anticline. At the southeast contact of the gneiss, Miette Group metasediments are seen to pass underneath the gneiss in the valley of South Bulldog Creek. The metasediments which lie above Yellowjacket Gneiss are deformed into megascopic, northeast-verging recumbent F_1 isoclines. These isoclines involve a minimum of 300 m of strata and exhibit considerable thickening in hinge zones. These large scale F_1 structures plunge southeast in the southern part of the area, and plunge shallowly northwest in the northern part of the study area, with a plunge culmination near Bulldog Ridge.

Second phase folds in the cover rocks are typically open to tight, east-verging folds with an axial planar crenulation cleavage. Locally, a conjugate set of F_2 minor folds and crenulation cleavages exist. The dominant set of F_2 folds trend about 200° while the second set trends about 140°. Second phase folds in the cover rocks east of the Purcell Fault are not coaxial to F_1, and they do not affect the map pattern because they are of a significantly lesser scale than F_1 isoclines. Second phase folds in the cover rocks have the same relationship to metamorphism as F_2 folds in the gneiss bodies. Third phase folds, which are observed to fold S_2 crenulation cleavage, are seen only in the cover rocks.

Thrust faults in the Bulldog Creek area are recognized on the basis of ductile quartzofeldspathic mylonite zones and phacoidal cleavage in pelite. A thrust, which may be the Purcell Fault, emplaces Bulldog Gneiss and metasediments onto Yellowjacket Gneiss and Miette Group rocks. The final stage of motion on the Purcell Thrust postdates F_2, as the mylonite foliation appears to overprint S_1 and small scale F_2 structures. Imbricate faults within the hanging wall of the Purcell Thrust bring up metasediments of the Miette Group. The klippe of Miette grit (Fig. 14.1) may be a klippe of the Purcell Fault. This klippe consists of a number of horses in a southwest dipping thrust duplex structure (Boyer and Elliott, 1982).

Late stage (Tertiary?) normal faulting is probably west-side-down as all observed brittle fault zones dip steeply southwest. Extreme cataclasis and associated retrogression of mineral assemblages postdate all deformation within normal fault zones. Normal faults in the Rocky Mountain Trench are shown to be on the east side of Kinbasket Lake (Fig. 14.1) on the basis of extreme brittle shearing of outcrops along the east side of the lake.

METAMORPHISM

Metamorphic grade in the Bulldog Creek area is recorded by Barrovian index minerals, and ranges from sillimanite grade in the west to garnet grade in the east. Timing of peak metamorphic conditions is documented by Columbian leucosome which has been folded by F_2 in the gneisses as well as in the cover rocks. Sillimanite, kyanite, and staurolite porphyroblasts overgrow S_1 and are folded by F_2 crenulations in aluminous pelites. Therefore, the peak of metamorphism was syn-post deformational to F_1 and predeformational to F_2. Garnets are included within kyanite and staurolite porphyroblasts, indicating that initial garnet growth predated peak metamorphic conditions. The textural relationships and timing of peak metamorphism are similar to those described by Oke (1982) from Hugh Allan Creek area 30 km to the southeast, and by Simony et al. (1980) south of the Malton Gneiss, west of the Rocky Mountain Trench. The textural relationships are consistent with the interpretation that F_2 in the Bulldog Creek area is equivalent to F_3 in the Monashee Mountains.

The sillimanite isograd in the footwall of the Purcell Thrust is a 100 m wide zone where kyanite and porphyroblastic sillimanite coexist. Sillimanite occurs as 2-3 cm-long needles in biotite-rich schist. This isogradic zone also contains staurolite with equilibrium textures, suggesting that pressures and temperatures necessary for staurolite consumption were not attained. Near the staurolite-kyanite isograd, staurolite has been replaced by aggregates of chlorite and quartz.

Many outcrops in the Bulldog Creek area exhibit coarse grained high grade schist with adjacent phyllitic schist which are not in tectonic contact. Such relationships demonstrate the extreme control of bulk composition over the development of metamorphic textures.

CONCLUSIONS

Basement rocks in the Bulldog Creek area are involved in the deformation as two distinct tectonic packages. The Bulldog Gneiss is contained within an overturned F_2 anticline and imbricate slices of the hanging wall of the Purcell Fault. Yellowjacket Gneiss, in the footwall of the Purcell Fault, acts as basement, and is involved in the core of a recumbent F_1 anticline. Mylonite fabric in the Purcell Fault Zone shows the final stage of fault motion to be post-F_2. The Hadrynian strata which envelop the basement gneisses are correlative with the Horsethief Creek Group and stratigraphically underlie the grits of the Middle Miette.

REFERENCES

Boyer, S.E. and Elliot, D.
1982: Thrust systems; American Association of Petroleum Geologists, v. 66, p. 1196-1230.

Campbell, R.B.
1968: Canoe River (83D), British Columbia; Geological Survey of Canada, Map 15-1967.

Chamberlain, V.E., Lambert, R. St. J., and Holland, J.G.
1978: Preliminary subdivisions of the Malton Gneiss Complex, British Columbia; in Current Research, Part A, Geological Survey of Canada, Paper 78-1A, p. 491-492.

Craw, D.
1978: Metamorphism, structure and stratigraphy in the southern Part Ranges, British Columbia; Canadian Journal of Earth Sciences, v. 15, p. 86-98.

Escher, A., Escher, J.C., and Watterson, J.
1975: The reorientation of the Kangamit dike swarm, West Greenland; Canadian Journal of Earth Sciences, v. 12, p. 158-173.

Evenchick, C.A.
1982: Stratigraphy, structure and metamorphism in Deserters Range, Northern Rocky Mountains, British Columbia; in Current Research, Part A, Geological Survey of Canada, Paper 82-1A, p. 325-328.

1983: Nonconformity at the base of Upper Proterozoic Misinchinka Group, Deserters Range, Northern Rocky Mountains; in Current Research, Part A, Geological Survey of Canada, Paper 83-1A, p. 475-476.

Ghent, E.D. and De Vries, C.D.S.
1972: Plagioclase-garnet-epidote equilibria in hornblende-plagioclase-bearing rocks from the Esplanade Range, British Columbia; Canadian Journal of Earth Sciences, v. 9, p. 618-635.

Giovanella, C.A.
1967: Structural relationships of the metamorphic rocks along the Rocky Mountain Trench at Canoe River; in Report of Activities, Part A, Geological Survey of Canada, Paper 67-1A, p. 60-61.

1968: Structural studies of the metamorphic rocks along the Rocky Mountain Trench at Canoe River; in Report of Activities, Part A, Geological Survey of Canada, Paper 68-1A, p. 27-30.

Oke, C.
1982: Basement gneisses at Mt. Blackman, British Columbia; unpublished M.Sc. thesis, University of Calgary, Calgary, Alberta, 123 p.

Oke, C. and Simony, P.S.
1981: Basement gneisses of the western Rocky Mountains, Hugh Allan Creek Area, British Columbia; in Current Research, Part A, Geological Survey of Canada, Paper 81-1A, p. 181-184.

Pell, J. and Simony, P.S.
1982: Hadrynian Horsethief Creek Group/Kaza Group correlations in the southern Cariboo Mountains, British Columbia; in Current Research, Part A, Geological Survey of Canada, Paper 82-1A, p. 305-308.

Ramsay, J.G.
1962: Interference patterns produced by the superposition of folds of similar type; Journal of Geology, v. 70, p. 466-481.

Simony, P.S., Ghent, E.D., Craw, D., Mitchell, W., and Robbins, D.D.
1980: Structural and metamorphic evolution of northeast flank of Shuswap Complex, southern Canoe River area, British Columbia; Geological Society of America, Memoir 153, p. 445-461.

15. THE CHAMPION LAKE FAULT IN THE TRAIL-CASTLEGAR AREA OF SOUTHEASTERN BRITISH COLUMBIA

EMR Research Agreement 300-04-83

C.R. Corbett[1] and P.S. Simony[1]
Cordilleran Geology Division, Vancouver

Corbett, C.R. and Simony, P.S., The Champion Lake Fault in the Trail-Castlegar area of southeastern British Columbia; in Current Research, Part A, Geological Survey of Canada, Paper 84-1A, p. 103-104, 1984.

Abstract

The Champion Lake Fault strikes northward from the east side of Trail, follows the most westerly of the Champion Lakes, and can be traced beyond Castlegar where it turns northeastward. It has a variable eastward dip in the 40 to 80° range; its width is a function of the lithologies through which it cuts. The fault zone is widest (up to 600 m) in the Trail and Bonnington plutons. The dominant lithologies in the fault zone are beccia and microbreccia with chlorite, epidote, quartz, calcite, and hematite. Protomylonite is rare. The juxtaposition of higher and deeper levels of plutons and of stratigraphy cut by the fault suggest a minimum east-side-down displacement of 1-2 km. The Champion Lake Fault cuts mid-Jurassic plutons and some, but not all, members of an Eocene(?) dyke swarm.

Résumé

La faille de Champion Lake se dirige vers le nord à partir du côté est de Trail, suit le lac Champion le plus à l'ouest, et peut être suivie au delà de Castlegar où elle tourne vers le nord-est. Son pendage vers l'est varie de 40° à 80°; sa largeur est fonction des lithologies qu'elle traverse. La zone de faille atteint sa largeur maximale (jusqu'à 600 m) dans les plutons de Trail et de Bonnington. Les lithologies principales de la zone de faille comprennent des brèches et des microbrèches avec de la chlorite, de l'épidote, du quartz, de la calcite et de l'hématite, et quelques rares venues de protomylonite. La juxtaposition de niveaux plus élevés et plus profonds de plutons et de la stratigraphie coupée par la faille suggère qu'il y a eu mouvement descendant de la lèvre est sur au moins un ou deux kilomètres. La faille de Champion Lake traverse des plutons du Jurassique moyen et certains membres, mais pas tous, d'un groupe de filons de l'Éocène(?).

INTRODUCTION

The Champion Lake Fault (CLF) was first mapped by Little (1962) and was interpreted by Simony (1979) as a steeply dipping, west-side-down normal fault hinged at the northern boundary of the Trail Pluton. Extensional faults, particularly on the margins of gneiss complexes, are an intriguing problem in the Columbian Core zone (Read and Brown, 1981). The Champion Lake Fault was therefore re-examined, and during the summer of 1983 the Champion Lake Fault was mapped in detail at a scale of 1:24 000 northward from Trail to beyond Castlegar. It was found to be a northerly striking, steeply-east-dipping, east-side-down normal fault that displaces the Trail and Bonnington plutons.

The Champion Lake Fault (Fig. 15.1) can be traced from Bear Creek, east of Trail, northward through the Trail Pluton, along the western border of Champion Lake Park and the eastern shoreline of First Lake, and along the new Highway 3 that leads northward into Castlegar. At the junction of the Columbia and Kootenay rivers the Champion Lake Fault swings slightly northwestward and passes along the upper slopes of Pass Creek Valley (Fig. 15.1). R. Parrish (personal communication, 1983) has traced the Champion Lake Fault northeastward from this point toward Krestova.

North of the Trail Pluton, the Champion Lake Fault juxtaposes Lower Jurassic volcaniclastic and clastic sediments of the Rossland Group in the hanging wall, with the pre-Carboniferous Trail Gneiss in the footwall. East of Castlegar, the Bonnington Pluton is offset by the fault, and is also juxtaposed against Castlegar and Trail gneiss.

NATURE OF THE CHAMPION LAKE FAULT

In the Castlegar-Trail area the Champion Lake Fault is characterized by brittle deformation; breccias and green, siliceous microbreccias are the dominant rock types within the fault zone. Well developed mylonites are absent but protomylonite zones consisting of elongated quartz and feldspar lenses were noted in a few outcrops.

The Champion Lake Fault varies significantly in width along strike as a function of the lithology of the disrupted rocks. Where the fault juxtaposes Trail Gneiss against the Rossland Group the fault zone is approximately 15 m wide, beyond which the rocks are relatively fresh. In the more competent quartz diorite and granodiorite of the Bonnington Pluton, the Champion Lake Fault consists of a central zone of microbreccia up to 60 m wide, bordered by a peripheral crush zone up to 600 m wide. The Champion Lake Fault continues southward across the Trail Pluton, forming a well crushed zone approximately 600 m wide. Within this crushed zone lenses of green microbreccia are found locally.

Although poor exposure prevents proving an offset of the northern boundary of the Trail Pluton, a sudden and pronounced change of the attitude of the contact across the fault zone may reflect a possible offset. In the hanging wall the trace of the contact of the Trail Pluton "vees" into the valleys and the border phase foliation dips away from the interior of the pluton, indicating that the pluton continues northeastward under a roof of Mesozoic rocks. In the footwall, the border phase dips towards the interior of the pluton, and the outcrop pattern suggests that the Trail Gneiss dips beneath it. The outward dip of the contact east of the Champion Lake Fault probably represents an upper level of the pluton that has been downthrown against a lower level of the pluton that is characterized by the inward dipping contact.

No evidence of faulting or crushing was recognized south of the Trail Pluton. The Champion Lake Fault may therefore be hinged within the Trail Pluton, and the displacement dissipated along several minor fault splays in

[1] Department of Geology and Geophysics, University of Calgary, Calgary, Alberta T2N 1N4

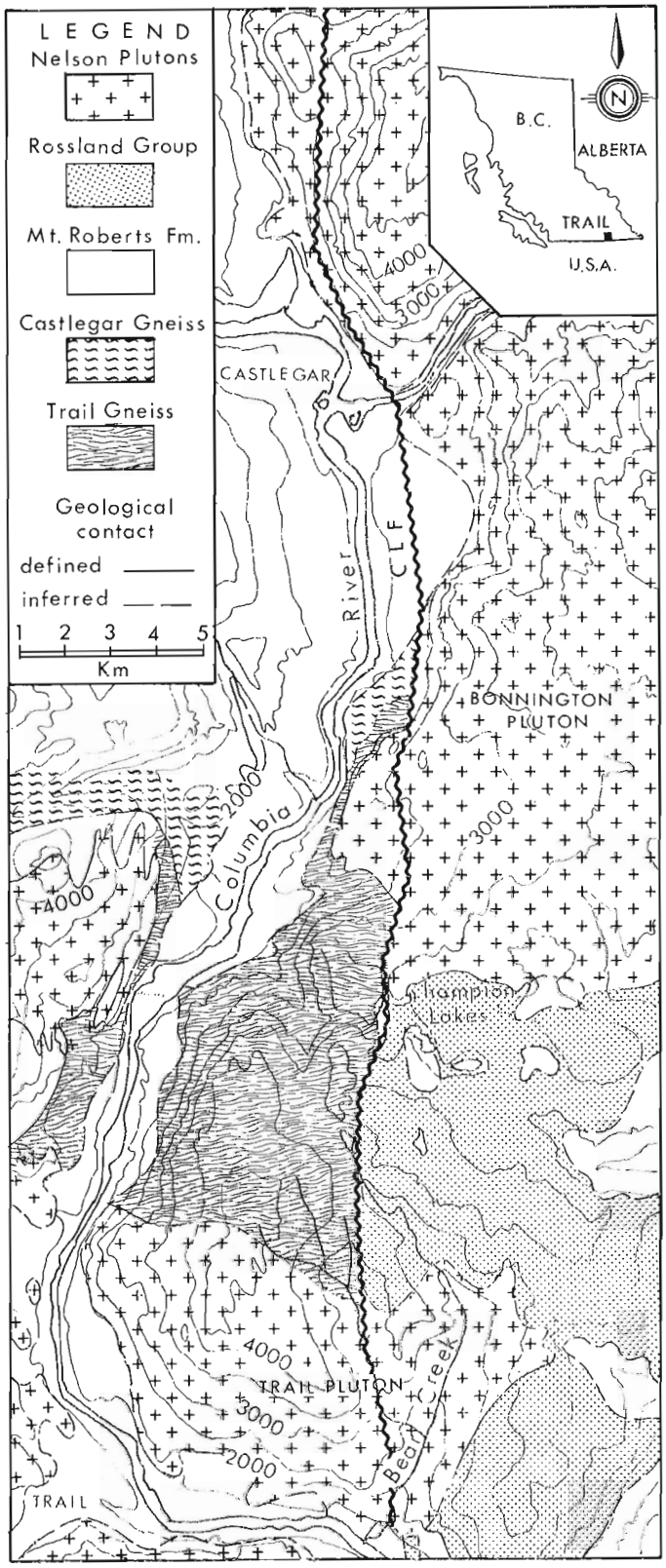

Figure 15.1. *Regional setting of the Champion Lake Fault (CLF), Trail-Castlegar area B.C. (after Little, 1982).*

the crushed zone; or the Champion Lake Fault may continue southward along the Columbia River, but is masked by Pleistocene deposits.

The net slip along the Champion Lake Fault is not known. However, the Bonnington Pluton has a distinctly lineated border phase which is mappable on both sides of the Champion Lake Fault. Using this information in conjunction with the juxtaposition of the higher and lower levels of the Trail Pluton, a minimum east-side-down dip slip of 1-2 km is probable. Such a minimum is also required by the juxtaposition of the Trail Gneiss and Rossland Group strata.

AGE OF FAULTING

The Champion Lake Fault clearly offsets the Bonnington Pluton and clearly produced a crushed zone in, and probably cuts through, the Trail Pluton. The Trail Pluton has been dated as 163 Ma (R.L. Armstrong, personal communication); this restricts the maximum age of faulting to the Middle Jurassic.

Within the Trail Pluton are swarms of Eocene(?) mafic dykes (Little, 1982), and both fresh and crushed dykes can be found in the Champion Lake Fault crush zone. From this ambiguous relationship we infer that faulting may be contemporaneous with the emplacement of the dykes and, therefore, may be Tertiary. The mafic dykes vary in orientation, but generally have a northerly trend and a steep easterly dip. This orientation is consistent with the proposition that the Champion Lake Fault and the dykes are contemporaneous, and that both may be due to the same Tertiary east-west extension at the time of faulting. The attitudes of several hundred protomylonite zones, shear zones, and crush zones along the Champion Lake Fault were also measured. The dominant northerly strike with easterly dips in the range of 40 to 85° is considered to reflect the attitude of the Champion Lake Fault.

Secondary minerals developed in the crushed and sheared zones include chlorite, epidote, calcite, quartz, and, less commonly, hematite. This restricts the pressure and temperature during faulting to greenschist conditions.

REFERENCES

Little, H.W.
1962: Trail map-area, British Columbia; Geological Survey of Canada, Paper 62-5.

1982: Geology of the Rossland-Trail Map Area, British Columbia; Geological Survey of Canada, Paper 79-26.

Read, P.B. and Brown, R.L.
1981: Columbia River Fault zone: southeastern margin of Shuswap and Monashee complexes, southern British Columbia; Canadian Journal of Earth Sciences, v. 18, p. 1127-1145.

Simony, P.S.
1979: Pre-carboniferous basement near Trail, British Columbia; Canadian Journal of Earth Sciences, v. 16, p. 1-11.

16. STRUCTURE AND STRATIGRAPHY IN THE HANGING WALL OF THE SIFTON FAULT, SIFTON RANGES, NORTHERN BRITISH COLUMBIA

Project 700047

C.A. Evenchick[1]
Cordilleran Geology Division, Vancouver

Evenchick, C.A., Structure and stratigraphy in the hanging wall of the Sifton fault, Sifton Ranges, northern British Columbia; in Current Research, Part A, Geological Survey of Canada, Paper 84-1A, p. 105-108, 1984.

Abstract

Rocks in the hanging wall of the Sifton fault comprise an assemblage of quartzite, amphibolite, carbonate and schist of presumed late Proterozoic age overlying basement augen gneiss dated at 1.85 Ga. This assemblage, possibly more than 1000 m thick, is intensely and penetratively deformed above a sole fault that truncates structures in the footwall. A variety of strain indicators suggest a relative southerly movement of the hanging wall rocks in a ductile environment.

Résumé

Les roches dans le toit de la faille de Sifton comprennent un assemblage de quartzite, d'amphibolite, de carbonate et de schiste datant probablement du Protérozïoque récent; ces roches recouvrent un socle formé d'un gneiss oeillé datant de 1,85 milliard d'années. L'assemblage, dont l'épaisseur pourrait être supérieure à 1 000 mètres, est fortement déformé par une faille unique qui coupe les structures dans le mur. Une gamme d'indicateurs de déformations suggèrent qu'il y a eu mouvement relatif vers le sud des roches du toit dans un milieu ductile.

INTRODUCTION

Field studies in the Sifton Ranges, bounded on the east by the Northern Rocky Mountain Trench (Fig. 16.1), were completed in 1983. Particular attention was given to the structural style within the intensely deformed hanging wall assemblage of the Sifton fault and to the relationships of the hanging wall assemblage to the footwall rocks (see Evenchick, 1983 for an account of the footwall stratigraphy).

Lisel Currie and Jennifer O'Brien provided excellent assistance in the field.

SIFTON FAULT

The gently dipping Sifton fault separates a footwall assemblage of recumbently folded metasedimentary rocks, in which stratigraphic units show considerable continuity, from a hanging wall assemblage of intensely and penetratively deformed rocks in which stratigraphic continuity of individual units has been greatly disrupted or obliterated. In essence the hanging wall rocks form a fault zone as much as 1000 m thick, the sole fault of which truncates a broad anticlinorium in the footwall (Fig. 16.2a,b). Structures in the footwall imply tectonic transport with a general east-west orientation, whereas those in the hanging wall, described below, imply a south direction.

STRUCTURE

Rocks in the hanging wall of the Sifton fault have been deformed into a variety of structures indicating intense and pervasive ductile strain. These include the extensive development of ribbon quartz, commonly imparting a cherty texture to the quartzite, strong stretching lineation, shear bands, sheath folds (Fig. 16.3) and widespread anastomosing truncations of units. Strain indicators consistently show a relative north to south tectonic transport of the hanging wall over the footwall.

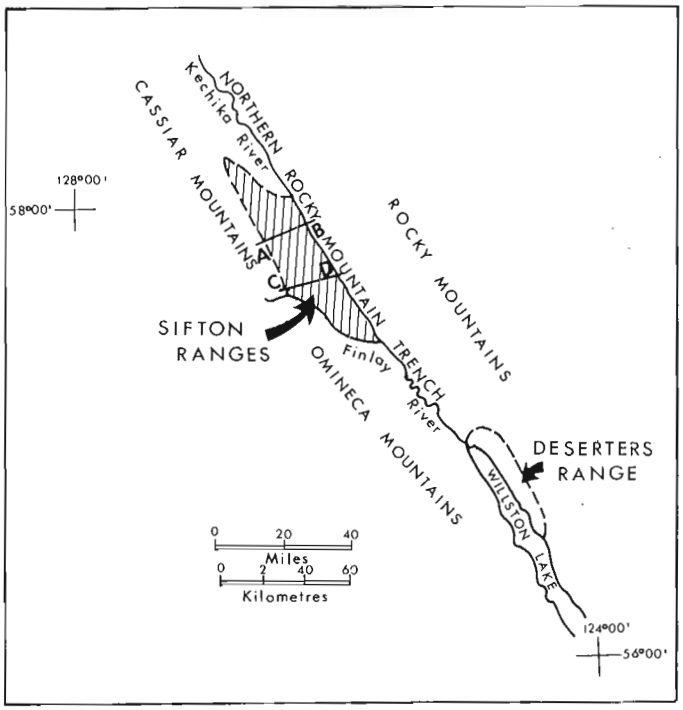

Figure 16.1. *Location map with locations of cross-sections.*

[1] Department of Geological Sciences, Queen's University, Kingston, Ontario

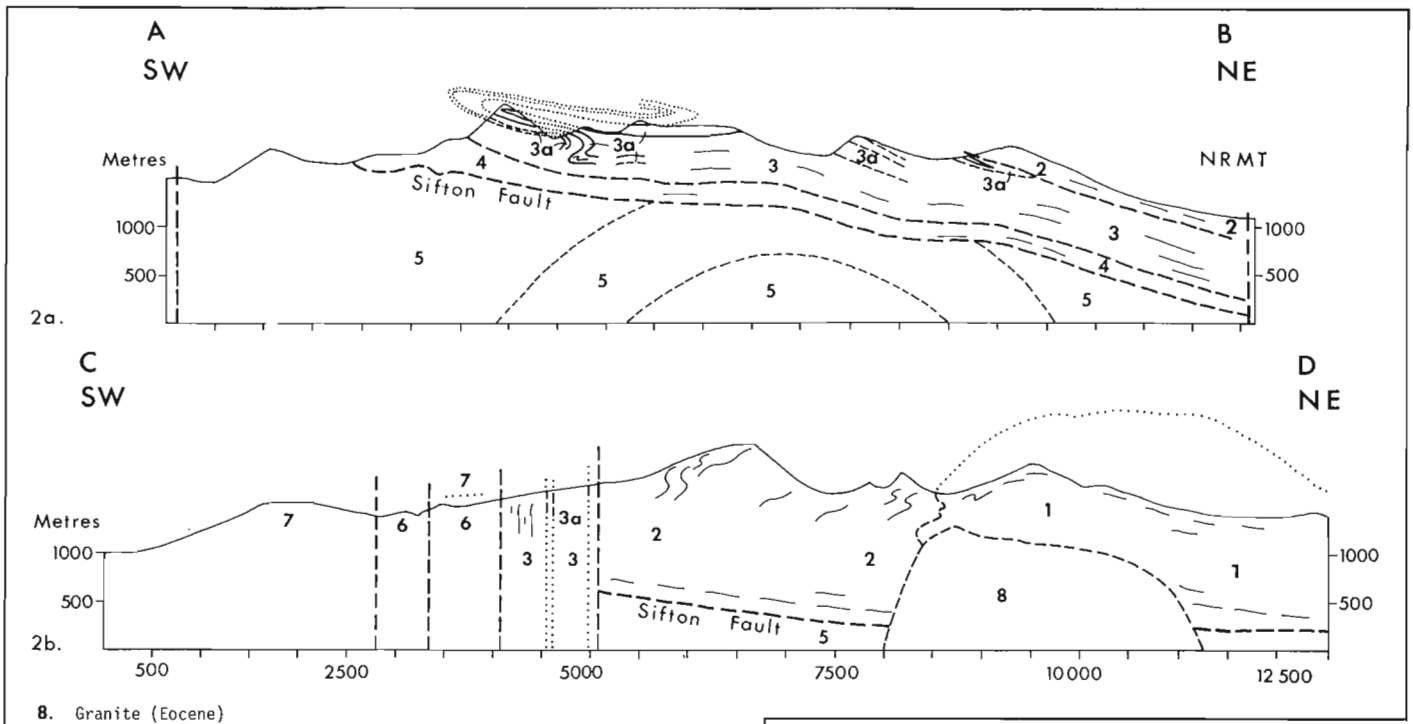

8. Granite (Eocene)
7. Sifton Formation (late Cretaceous to early Tertiary)
6. Kechika Group (Cambro-Ordovician)
5. Footwall rocks of the Sifton Fault (late Proterozoic)
4. wavy retrograded schists (late Proterozoic?)
3. wavy schist, pelitic schist, quartzite, marble(3a) late Proterozoic?)
2. quartzite, feldspathic quartzite, amphibolite (late Proterozoic?)
1. granitoid gneiss and amphibolite (1.85 Ga)

NRMT Northern Rocky Mountain Trench

——— fault

----- geological contact

—— 2 —— form lines

Figure 16.2

Cross-sections in central and southern Sifton Ranges.

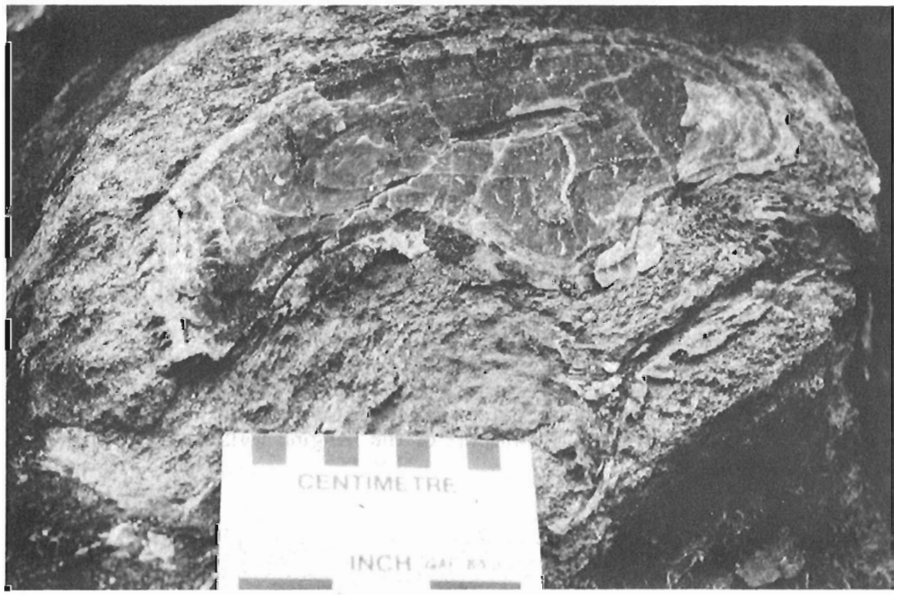

Figure 16.3

Cross-section of a sheath fold approximately perpendicular to the direction of tectonic transport.

Figure 16.4

Typical outcrop of quartzite in unit 2.

STRATIGRAPHY

Although on outcrop scale few stratigraphic units can be followed because of intense shearing, on a map scale the hanging wall can be divided into four fairly distinct lithological units. Structurally above the fault in the northern part of the Sifton Ranges, is a unit of wavy, retrograded schist which is overlain by wavy schist, marble and quartzite in turn structurally overlain by white orthoquartzite, (Fig. 16.4) feldspathic quartzite and amphibolite with rare pelitic schist (Fig. 16.2a). Marbles in the middle member are probably the most useful for showing map-scale structural style in the hanging wall assemblage.

Basement granitoid gneiss farther south forms the core of a gently north-northwestward-plunging anticline (Fig. 16.2b). The gneiss is folded with, and overlain by, the quartzite and amphibolite unit, with no apparent structural break. At the same latitude the structural relationships between units overlying the gneiss are uncertain because of complexities related to late, steeply dipping faults.

The base of the proposed stratigraphic assemblage is a strongly potassic augen orthogneiss and possibly some paragneiss (unit 1) with a U-Pb date on zircons of 1.85 Ga (R. Parrish, personal communication, 1983). The gneiss appears to be overlain by feldspathic quartzite, orthoquartzite and, locally, pelitic schist (unit 2). Both units include boudins and layers of amphibolite. Unit 3, consisting of carbonate and pelitic and psammitic schist, apparently overlies the quartzite of unit 2 and is overlain by schist of unit 4 (Fig. 16.2a). This proposed stratigraphic succession is based on the assumption that movements associated with the Sifton fault have not interleaved the original stratigraphy of the hanging wall. No structures showing stratigraphic tops are preserved.

The overturned stratigraphy shown in Figure 16.2a is likely the result of recumbent folding and related thrusting before, or during, movement on the Sifton fault. The sequence outlined above is similar to that in lower parts of the Windermere Supergroup elsewhere in the Cordillera. Although the possibility that the overturned stratigraphy shown in Figure 16.2a is the result of tectonic stacking cannot be ruled out, field evidence of interleaving of stratigraphy was not seen, nor are boundaries of stratigraphic units more strained that the interiors.

REFERENCE

Evenchick, C.A.

1983: Stratigraphy, structure and metamorphism in the Sifton Ranges, Cassiar Mountains, northern British Columbia; in Current Research, Part A, Geological Survey of Canada, Paper 83-1A, p. 221-227.

17. STRUCTURAL STYLE OF THE SYLVESTER ALLOCHTHON, NORTHEASTERN CRY LAKE MAP AREA, BRITISH COLUMBIA

Project 770016

Tekla Harms[1]
Cordilleran Geology Division, Vancouver

Harms, T., Structural style of the Sylvester Allochthon, northeastern Cry Lake map area, British Columbia; in Current Research, Part A, Geological Survey of Canada, Paper 84-1A, p. 109-112, 1984.

Abstract

The Sylvester Allochton comprises a stack of structurally interleaved fault-bounded slices of an order of magnitude smaller than the terrane itself. The basal Sylvester fault, and faults separating the imbricate slices, are not deformed. In contrast, lithological units within slices show a characteristic suite of penetrative structures; most commonly folds and mullions in chert, and pencil cleavage in argillite. Parallelism of lineations throughout the Sylvester in the study area result in a consistent linear fabric between azimuths 285 and 325°. Thrust faults and folds superimposed upon pre-existing southwest-verging structures in the autochthon immediately below the Sylvester suggest a northeast direction of emplacement of the allochthon.

Résumé

L'allochtone de Sylvester comprend un amas de lames structuralement enchevétrées, limitées par des failles, dont l'ampleur des dimensions est moindre que celle de la formation. La faille basale de Sylvester et d'autres failles qui séparent les lames imbriquées ne sont pas déformées. Par opposition, les unités lithologiques au sein des lames font voir une série caractéristique de structures pénétrantes, notamment des plis et des structures linéaires dans le chert et un clivage produisant des petits fragments allongés dans l'argilite. Le parallélisme des linéations dans l'allochtone dans la région à l'étudie produit une structure et une texture (fabrique) linéaires, continues, qui s'orientent entre 285 et 385°. Des failles chevauchantes et des plis superposés sur des structures déjà existantes inclinées vers le sud-ouest dans l'autochtone sis immédiatement sous la faille de Sylvester suggèrent que l'emplacement de l'allochtone a suivi une orientation nord-est.

INTRODUCTION

Oceanic lithologies of the Sylvester Group, predominantly chert, argillite, basalt, pillow basalt, gabbro, and ultramafic rocks have, since their orginal description (Gabrielse, 1963), been recognized as distinct from the miogeoclinal carbonate and argillite which they overlie. Recent recognition of older-over-younger relationships within assemblages of the Sylvester Group (Gordey et al., 1982) has substantiated reinterpretation of the Sylvester as an allochthonous terrane (Gabrielse and Mansy, 1980). During the 1983 field season, detailed structural mapping, conducted in northeastern Cry Lake map area (Fig. 17.1), concentrated on the internal structure of the Sylvester Allochthon, the nature of its basal, tectonic contact, and on deformation in the autochthonous strata immediately below the allochthon.

BASAL SYLVESTER FAULT

Early recognition of the tectonic nature of the contact between the Sylvester Allochthon and strata of the miogeocline was almost certainly impeded by the undistinguished expression of the sole fault. The Sylvester lies either on the relatively thin upper McDame Group carbonate or, more commonly, on Frasnian-Famennian or undated argillite above the McDame Group. The autochthonous argillite may be tectonically condensed or attenuated, and can be difficult to distinguish from Sylvester Group argillite. the sole fault of the Sylvester Allochthon commonly lies somewhere within a fissile to well-cleaved section of argillite which grades without apparent interruption upward into chert-argillite or basalt-argillite units of the Sylvester, and downward into argillite of the autochthon.

Careful mapping of the basal Sylvester fault shows that, despite the complexity of structures within both allochthonous and autochthonous strata, the fault surface is not deformed. The sole fault has some minor local relief, but this can be attributed to ramping over the autochthon; no evidence exists for folding or thrust faulting that involves both Sylvester and miogeoclinal units. The basal Sylvester fault clearly truncates both mesoscopic and map-scale structures of the autochthon.

STRUCTURAL CHARACTER OF THE ALLOCHTHON

The Sylvester Allochthon comprises a stack of tectonolithological sheets, each bounded by generally planar, and shallow-dipping to subhorizontal faults. Each slice may consist of one lithology (gabbro or banded chert sheets are common), or of a few related or repeated lithologies, such as interlayered basalt/argillite, chert/argillite, and argillite/minor carbonate sequences. The sheets which make up the Sylvester Allochthon are significiantly smaller than the allochthonous terrane itself; slices tectonically pinch out laterally and furthermore, may, be exceedingly thin compared to their areal extent. A distinctively coloured, banded chert which makes up one tectonic slice was traced discontinuously for approximately 15 km along strike. This marker unit is nowhere more than 50-150 m thick. Most Sylvester lithologies are significantly less distinct and more difficult to trace and correlate laterally. Nonetheless, the vertical separation between sheet-bounding faults of the chert unit is typical for the terrane. Structural interleaving of the tectono-lithologic slices results in a "stratigraphy" for the Sylvester which varies widely from place to place. The associated lithologies of the Sylvester Allochthon are clearly

[1] Department of Geosciences, University of Arizona, Tucson, Arizona

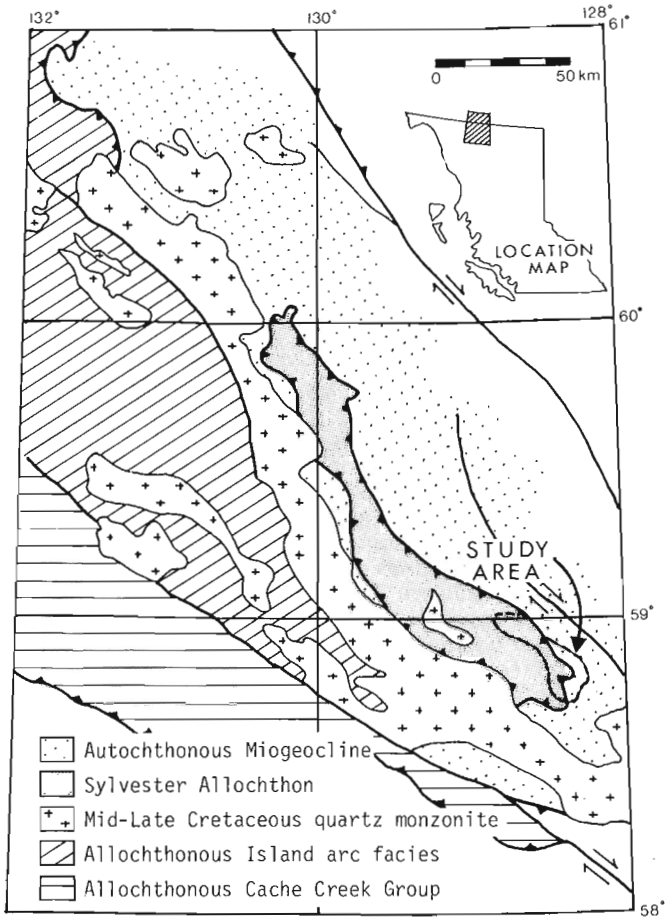

Figure 17.1. *Location and regional geology of study area. Modified from Tipper et al. (1981).*

oceanic in composition. However, gabbroic and basaltic tectonic slices, in a majority of cases, show intrusive relationships with remnants of included chert and argillite. The Sylvester, then, does not appear to be a simple, tectonically dismembered and shuffled ophiolite.

Deformation of the slices which compose the Sylvester Allochthon is unrecognized; sheet boundaries are generally subplanar and lithological units do not appear to be significantly infolded. However, outcrop-scale structures within slices are pervasive. Each of the general lithologies present in the Sylvester appears to have responded to deformation by the development of a characteristic structure or small suite of structures. Sheet-bounding faults are commonly recognized simply as surfaces of disharmony between internal sheet structures. Banded chert units display the most striking mesoscopic structure, and are almost invariably folded into close to tight wave forms, with amplitudes usually of 1-4 m (Fig. 17.2). Both similar and parallel folds are common. In some places, chert beds are sharply mullioned (Fig. 17.3). All cherts examined in the study area have been recrystallized to a fine quartzitic texture, destroying any radiolarian shells which may have existed. In contrast, Sylvester argillite forms massive, nondescript units in which bedding has become completely transposed and obliterated by cleavage, and folds which may have developed in the argillites are unrecognizable. Argillite adjacent to folded chert sheets is separated from them by surfaces of structural disharmony; the two lithologies are not seen infolded. Two oblique cleavages are commonly present in argillite, resulting in strong pencil cleavage as the dominant structural element. Gabbro and basalt are generally massive and although commonly altered to greenstone are not usually foliated. Although mylonitic or cataclastic structures are rarely observed at sheet boundaries, gabbro sheets are commonly cut internally by irregularly distributed very narrow ductile shear zones. These kinds of deformation typify the mesoscopic structural style in the Sylvester. However, one structurally high slice is a penetratively lineated and foliated tectonite. The protolith is as yet undetermined but may be a siliceous argillite.

Figure 17.2

Tight mesoscopic fold train in banded chert of Sylvester Allochthon.

Figure 17.3. *Strongly mullioned banded chert of Sylvester Allochthon.*

In contrast to the structural disharmony and discontinuity which separate tectono-lithologic slices of the Sylvester, all lineations observed in the allochthon have a fairly consistent trend. Pencil cleavage, crenulation cleavage, mullions (Fig. 17.3), fold axes (Fig. 17.2) and mineral elongation in tectonites are subparallel and lie between azimuths 285 and 325°.

STRUCTURAL CHARACTER OF THE AUTOCHTHON

Detailed mapping of mid-Paleozoic carbonate and argillite strata of the autochthon within 1-2 km of the base of the Sylvester revealed considerable structural complexity. The distribution and attitudes of the units cannot immediately be resolved into a simple 3-dimensional geometric pattern. However, clearly defined structures at specific sites demonstrate the following relationships:

i) Autochthonous strata are deformed by a suite of southwest-verging structures, including overturned sequences, asymmetric folds, and thrust faults. (see also Gabrielse and Mansy, 1978, 1980).

ii) Southwest-verging structures of the autochthon are truncated by the uninterrupted base of the Sylvester Allochthon.

iii) As has been suggested in previous studies (Gabrielse and Mansy, 1978, 1980) immediately below the Sylvester, northeast-verging folds and thrust faults are developed (Fig. 17.4). These structures are superimposed upon, and offset southwest-verging structural elements.

Overprinting and superposition of northeast-verging structures on pre-existing southwest-verging structures are thought to be responsible for the complexity of the map pattern of autochthonous units near the Sylvester Allochthon.

KINEMATICS

The pattern of overprinting and the limited distribution of northeast-verging structures in the autochthon below the Sylvester suggests northeasterly emplacement of the allochthon. Streaked grains and distinct elongation of fossils within McDame carbonate immediately beneath the Sylvester, forming a lineation at approximately aximuth 300°, also support this interpretation. Linear fabric

Figure 17.4

Looking NW. NE-verging folds in McDame Group, immediately below basal Sylvester fault (off photo to left).

elements, which are consistent and pervasive throughout the tectonic slices of the Sylvester Allochthon, parallel those in the autochthon (northwest-trending) and are also tentatively interpreted as perpendicular to the direction of transport during deformation. However, whether the formation of the Sylvester lineations is coeval with stacking of imbricate slices and with emplacement of the terrane is equivocal. The vergence of mesoscopic structures (predominantly folds in banded cherts) within Sylvester tectonic sheets is not straightforward. Most of the fold trains observed are kinematically symmetrical; those which are overturned commonly have northeast-dipping axial planes. These data tentatively suggest that tectono-lithologic slices of the Sylvester Allochthon, like the autochthonous strata on which they rest, may have a pre-emplacement history of southwest-verging deformation.

REFERENCES

Gabrielse, H.
1963: McDame map area, British Columbia; Geological Survey of Canada, Memoir 319, 138 p.

Gabrielse, H. and Mansy, J.L.
1978: Structural style in northeast Cry Lake map-area, north-central British Columbia; in Current Research, Part A, Geological Survey of Canada, Paper 78-1A, p. 33-34.

1980: Structural style in northeastern Cry Lake map area, north-central British Columbia; in Current Research, Part A, Geological Survey of Canada, Paper 80-1A, p. 33-35.

Gordey, S.P., Gabrielse, H., and Orchard, M.J.
1982: Stratigraphy and structure of Sylvester Allochthon, southwest McDame map area, northern British Columbia, in Current Research, Part B, Geological Survey of Canada, Paper 82-1B, p. 101-106.

Tipper, H.W., Woodsworth, G.J., and Gabrielse, H.
1981: Tectonic assemblage map of the Canadian Cordillera and adjacent parts of the United States of America; Geological Survey of Canada, Map 1505A.

18. STRATIGRAPHY OF QUESNEL TERRANE NEAR DRAGON LAKE, QUESNEL MAP AREA, CENTRAL BRITISH COLUMBIA

Project 820014

L.C. Struik
Cordilleran Geology Division, Vancouver

Struik, L.C., Stratigraphy of Quesnel Terrane near Dragon Lake, Quesnel map area, central British Columbia; in Current Research, Part A, Geological Survey of Canada, Paper 84-1A, p. 113-116, 1984.

Abstract

A re-examination of an area near Dragon Lake, Quesnel map area, has established that volcanic and sedimentary rock formerly thought to be Cambrian and Lower Jurassic is dominantly Upper Triassic. Lower Jurassic strata are poorly exposed but include basalt, shale, andesite and limestone. The oldest observable Upper Triassic rock is polymictic conglomerate with basaltic and granitoid clasts. Lower Cambrian limestone outcrops in one locality and because its contacts with the surrounding Mesozoic rock of the Quesnel Terrane are not exposed, and therefore no stratigraphic link with the terrane can be made, it is not included in that terrane.

Résumé

Le réexamen d'une région près du lac Dragon, région cartographique de Quesnel, révèle que les roches volcaniques et sédimentaires que l'on croyait dater du Cambrien et du Jurassique inférieur datent principalement du Trias supérieur. Les couches du Jurassique inférieur, mal découvertes, comprennent du basalte, du schiste argileux, de l'andésite et du calcaire. La roche du Trias supérieur la plus ancienne qui soit visible est un conglomérat polygénique à fragments basaltiques et granitoïdes. Un calcaire du Cambrien inférieur affleure à un endroit, mais n'est pas inclus dans le terrain puisque ses contacts avec les roches mésozoïques voisines du terrain de Quesnel n'affleurent pas et qu'il est donc impossible d'établir un lien stratigraphique avec le terrain.

INTRODUCTION

Rock at Dragon Lake near Quesnel (NTS 93B), British Columbia is wholly contained within the Intermontane Belt and is mainly of the Quesnel Terrane (Fig. 18.1). The Quesnel Terrane forms a band through Kamloops and Prince George and is in fault contact to the west and south with Cache Creek Terrane and to the east with Slide Mountain Terrane (Fig. 18.1). The succession consists mostly of Triassic and Jurassic basaltic and andesitic volcaniclastics and fine grained clastic rocks with less mafic volcanic flows, conglomerate and limestone. At Dragon Lake it is composed of Upper Triassic conglomerate, greywacke, shale and limestone; Upper Triassic and Lower Jurassic mafic volcaniclastics; Lower Jurassic(?) basalt tuff and flows(?); and Lower and Middle Jurassic fine grained clastic rock and minor limestone. All strata of the area were previously assigned to the Lower Jurassic or Cambrian (Tipper, 1978).

Anomalous to the Mesozoic rocks that dominate the Intermontane Belt is Lower Cambrian limestone just north of Hallis Lake (Fig. 18.2). Tipper (1978) included it with shale and greywacke now thought to be Triassic. The Cambrian limestone is important because it is either part of a basement to the Quesnel Terrane, an exotic clast, or represents a separate terrane in fault contact as a block, thrust window or klippe. It is shown underlying an easterly thrust Quesnel Terrane by Campbell et al. (1982). None of these alternatives were confirmed, as attempts to determine the contact relationship of the Cambrian limestone with the surrounding Triassic rocks remain frustrated by poor exposure.

STRATIGRAPHY

Cambrian

Represented entirely by limestone, the Lower Cambrian sequence underlies approximately 0.25 km^2 one kilometre north of Hallis Lake. It is bounded on the north and south by Upper Triassic basalt and on the northeast by Lower Jurassic(?) basalt, but contact relations with these rocks are unknown.

The limestone is light grey weathering, grey, and crystalline (0.05 to 0.2 mm) and contains archeocyathids which vary in size from 5 to 50 mm, generally being 10 mm across and which form approximately 2 to 5% of the rock. The fossils were originally identified by A.W. Norris (Tipper, 1978). W.H. Fritz re-examined the original collection and two others collected by the author (GSC loc. 40142, C-102811, C-102812). He concluded that as in North America archeocyathids are known only from the upper part of the Lower Cambrian, the limestone is probably of that age.

Triassic

From oldest to youngest, the Triassic rocks consist of conglomerate, volcaniclastic greywacke, shale, tuff, limestone, calcareous shale and augite porphyry volcaniclastic and flow rocks. The lower part of the assemblage, from the conglomerate to the top of the calcareous shale, appears to be stratigraphically continuous and unconformably overlain by augite porphyry basalt. The lower sequence is exposed along the powerline cut between the Quesnel River and the road passing south of Hallis Lake, as well as along the road and on Dragon Mountain. The augite porphyry basalt occurs in a limited area north of the road. The base of the Triassic sequence is not exposed.

The conglomerate has an olive matrix and is most commonly polymictic. Most of the clasts are basalt, andesite, granodiorite, diorite, and rhyolite; some are quartzite and marble. The basalt clasts are dark grey and purple and generally aphanitic. The quartzite clasts are white, pink or light green with 0.3 to 1.0 mm crystals. Clasts vary from pebbles to large cobbles, the shape from subrounded to rounded with medium to low sphericity and the clast proportion of the total rock ranges from 10 to 40%. Mafic, coarse- to medium-grained volcanic greywacke and felsic tuff form interbeds within the conglomerate sequence exposed along the road up the west side of Dragon Mountain. The tuff is confined to one or possibly two layers but the greywacke beds thicken and increase in number up-section.

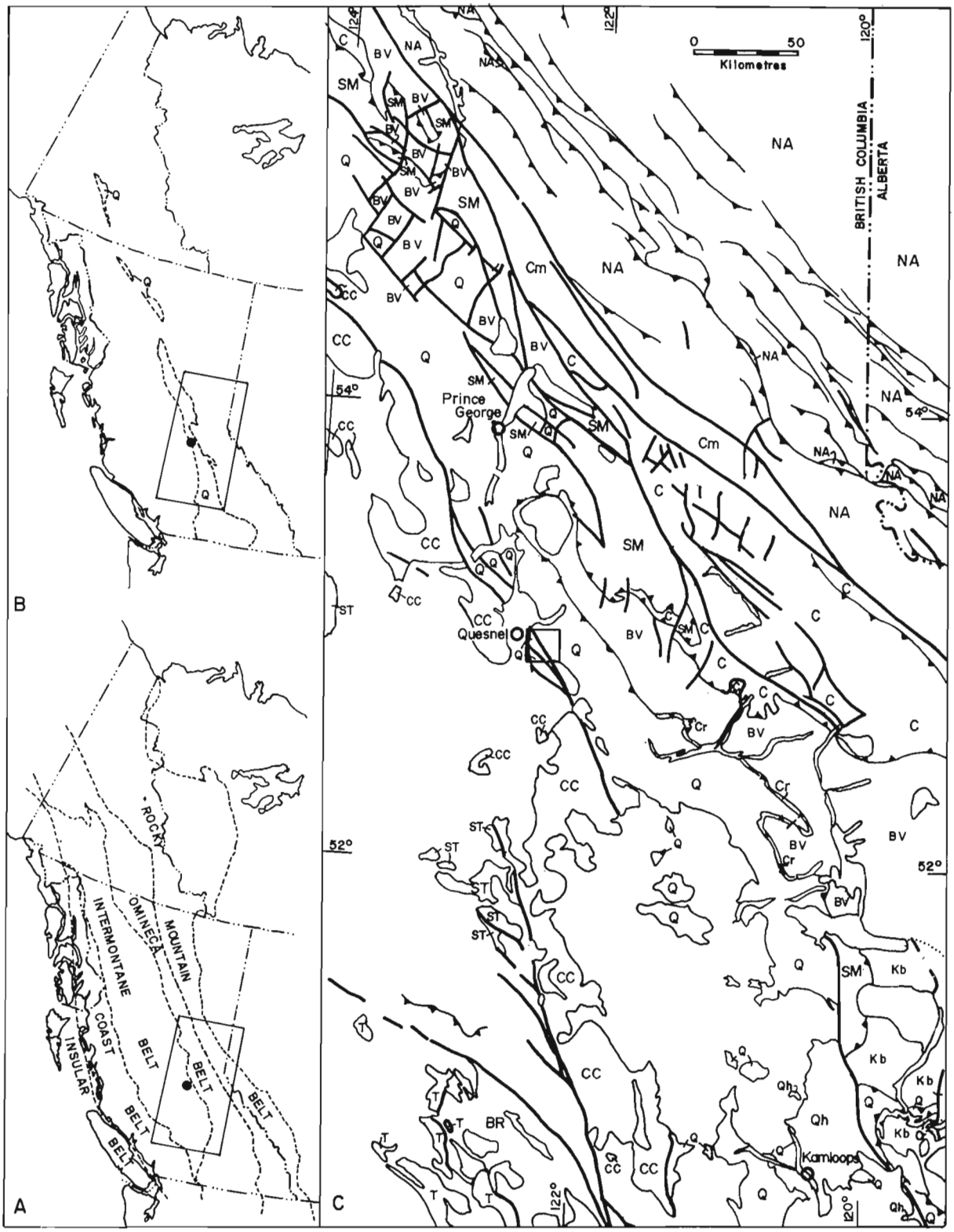

Figure 18.1. *Map 'A' shows the study area (black dot) in relation to the 5 geological belts of the Canadian Cordillera, and map 'B' relates it to the distribution of Quesnel Terrane. Map 'C' (rectangles of 'A' and 'B') locates the study area with respect to some relevant terrane boundaries. Terrane symbols used in Map 'C' are: BR-Bridge River, C-Cariboo, CC-Cache Creek, Cm-McGregor (subdivision of Cariboo Terrane), Kb-Kootenay (southern extension of BV), NA-North American, Q-Quesnel, Qh-Harper Ranch (subdivision of Quesnel), SM-Slide Mountain, ST-Stikinia, T-Tyaughton, BV-Barkerville. Terrane boundaries and names are in part from Monger (personal communication, 1983).*

Where the greywacke dominates the sequence it is interbedded with dark grey argillite and slate. Graded bedding in the greywacke and slate consistently indicates that the beds are right way up and overlie the conglomerate (assuming normal grading). In turn they are overlain by calcareous greywacke and subsequently by limestone. The limestone weathers light grey and varies from medium to dark grey. It is bioclastic containing crinoid, shell and bone fragments and contains greenstone and felsite clasts just south of the microwave towers on Dragon Mountain. Calcareous shale overlies the crinoidal limestone on the road from Dragon Lake to Hallis Lake. The shale is grey and contains bone and shell fragments.

The conglomerate to limestone sequence is thought to be continuous because clasts of the same lithologies appear throughout and most contacts appear to be gradational. The fining of the sequence records gradual but sporadic subsidence after the initial uplift responsible for exposing the source terrane.

The calcareous shale at the top of the sequence has yielded shell impressions identified by H.W. Tipper and E.T. Tozer as Upper Triassic **Halobia** sp. (C-102816). It also contains very poorly preserved bone fragments. It is assumed that the succession represents continuous deposition from lower conglomerate to upper calcareous shale and is thought

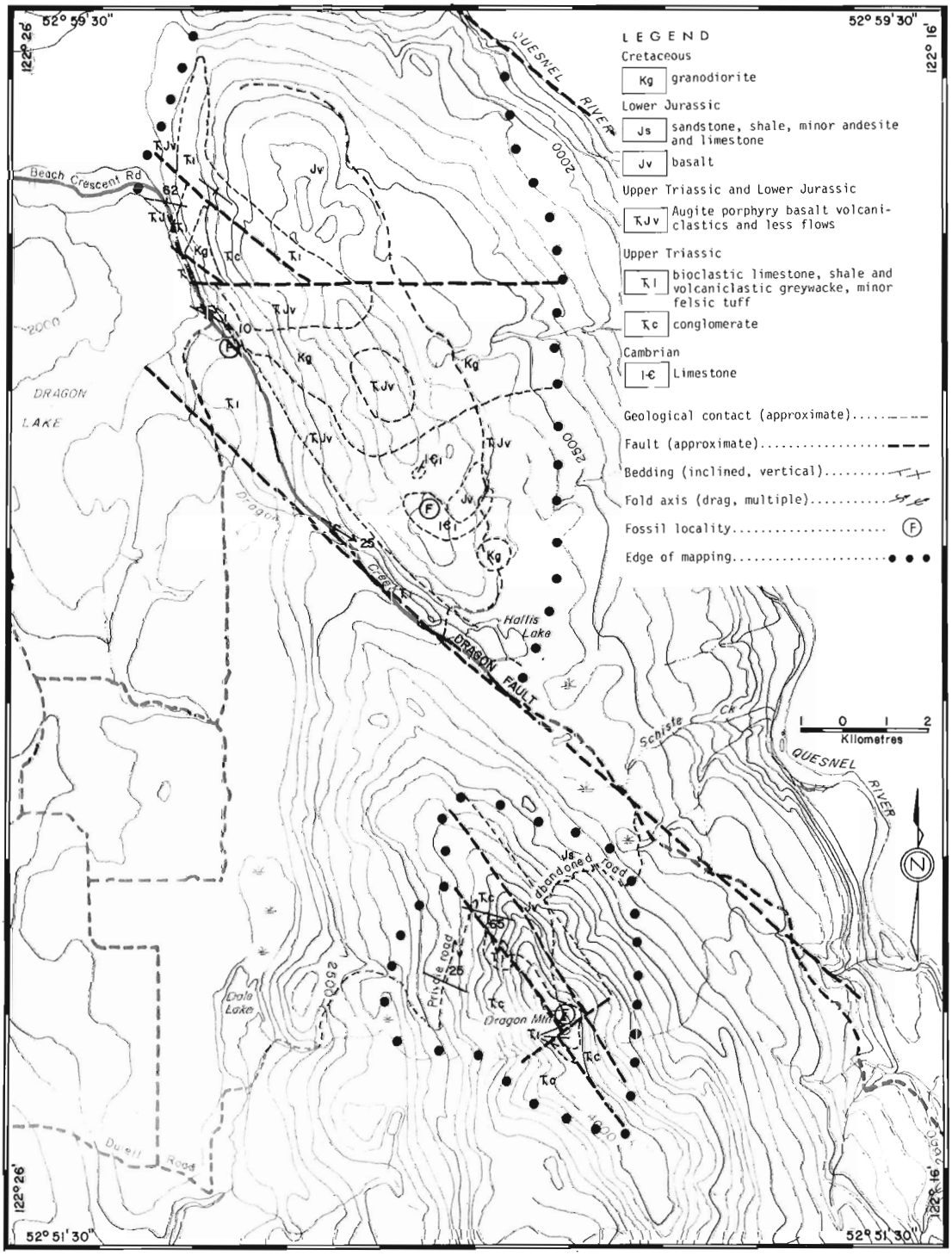

Figure 18.2. *Geological map of the study area. Located in Figure 18.1C.*

to be entirely Upper Triassic. This conclusion contradicts the suggestion by Tipper (1978) that the conglomerate is Lower Jurassic and that its granitoid clasts are derived from the Jurassic granite of Granite Mountain. A further suggestion that some of the clasts are from the Cache Creek Group could not be substantiated though I am not familiar with all the subtleties of that group.

Augite porphyry basalt unconformably overlies the conglomerate to limestone sequence at the **Halobia** fossil locality. Outcrops extend from north of Dragon Lake to Hallis Lake road and consist mostly of volcaniclastic material. The basalt lies on the calcareous shale and laterally on the underlying crinoidal limestone. Some isolated outcrops on the ridge north of Hallis Lake resemble flows and others are agglomerate.

The age of the basalt is locally determined to be Upper Triassic or younger. Similar rocks to the east in Quesnel Lake map area (unit TJb of Campbell, 1978) are thought to be mainly Upper Triassic but may be Lower Jurassic.

Lower Jurassic

From oldest to youngest the Lower Jurassic rocks include basalt, sandstone, limestone, andesite and shale. The basalt is distinguished from the Triassic augite porphyry basalt by its purplish grey colour, lack of phenocrysts and presence of amygdules. The sandstone has no counterpart in the Triassic. The limestone is micritic and apparently unfossiliferous which distinguishes it from the Triassic of Dragon Mountain. The andesite and shale are nondescript and indistinguishable from those of the Triassic.

The basalt is found near the Lower Cambrian limestone north of Hallis Lake and east of Dragon Mountain. Its relationship with other units of the area is obscure and its stratigraphic position is determined by correlation with basalt of the Quesnel Lake map area (unit TJd of Campbell, 1978). It is grey with varying tinges of purple, generally aphanitic and amygdaloidal, locally resembling tuff. In one place it contains minor inclusions (3 cm across) of calcite crystals (0.3 to 1 mm size). The age of the basalt is assumed to be Lower Jurassic, like the age of Campbell's unit TJd.

The sandstone to shale sequence was seen only in isolated outcrops on the abandoned forestry road up the east side of Dragon Mountain and nothing is known of its order of succession or contact relationships. The sandstone is green and brown weathering and contains detrital muscovite. The limestone weathers light grey and is medium to dark grey and micritic. The andesite is olive grey and aphanitic. The shale is grey. This sequence is suspected to overlie the purplish basalt and to be part of a sedimentary unit containing the Lower Jurassic fossils described by Tipper (1978). He found Lower Jurassic fossils at the base of the abandoned forestry road to Dragon Mountain.

INTRUSIVE ROCK

A granodiorite pluton intrudes the Triassic rocks and probably the Lower Jurassic basalt. The suggestion by Tipper (1978) that the pluton may be Cretaceous is well within the confines of the present data.

DISCUSSION

Re-examination of rock near Dragon Lake establishes an Upper Triassic sequence with a base of conglomerate which bears granitoid clasts. The relationship of the conglomerate to tectonic events is unknown. It was formerly considered to be an erosion product from a partly granitoid highland to the south (Tipper, 1978).

Cambrian limestone near Hallis Lake has been an oddity in the context of Quesnel Terrane stratigraphy and remains so, because no contacts are exposed. It has three possible relationships to the Quesnel Terrane; any of which when understood would provide information so far unattained from any other part of the Cordillera. The alternatives are: 1) it is part of the Quesnel Terrane as a basement, 2) it is part of the Quesnel Terrane as a clast included in the Triassic sequence or 3) it is part of a separate terrane in fault contact with the Quesnel Terrane.

As basement to the Quesnel Terrane it would be the oldest known unit and have undergone the same right lateral transcurrent motion (Tipper, 1981) as the terrane. To the south near Kamloops the upper Paleozoic and(?) lowest Mesozoic Harper Range Group (Monger, 1982; Qh, Fig. 18.1) is basement to Quesnel Terrane (J.W.H. Monger, personal communication, 1983) and the lower Cambrian Hallis Lake limestone may be part of that sequence.

As a clast within the sedimentary rock of the Quesnel Terrane the limestone requires an exposed and eroding Lower Cambrian rock in proximity to the terrane during the Triassic. The possibility of such a missing source is strengthened by the necessity of a source (also unrecognized) for the quartzite and granitoid clasts in the Upper Triassic conglomerate of Dragon Mountain (suggestion by R.B. Campbell).

The third possibility, that the Lower Cambrian limestone is faulted against the Quesnel Terrane has three scenarios, where the limestone is part of a terrane that: 1) is overthrust by the Quesnel Terrane and therefore represents a window, 2) that overthrusts the Quesnel Terrane and therefore is a klippe and 3) is a sliver bound by strike-slip faults. In the first scenario the limestone may represent the farthest westward extension of the Barkerville or Cariboo terranes (BV, C, of Fig. 18.1) each of which contains Lower Cambrian limestone. As such it would indicate a minimum 30 km eastward thrusting of the Quesnel Terrane. Such a thrust relationship is proposed by Campbell et al. (1982). The second scenario is considered to be only slightly possible, because the overthrust terrane must be everywhere else eroded. The third scenario requires the limestone to be translated northward from southern Cambrian bearing terranes, but all are far to the east.

Each of the alternatives requires substantial northward translation of the limestone and/or eastward thrusting of Quesnel and possibly adjacent terranes.

REFERENCES

Campbell, R.B.
1978: Quesnel Lake (93A) map area; Geological Survey of Canada, Open File 574.

Campbell, R.B., Mountjoy, E.W., and Struik, L.C.
1982: Structural cross-section through south-central Rocky and Cariboo mountains to the Coast Range; Geological Survey of Canada, Open File 844.

Monger, J.W.H.
1982: Geology of Ashcroft map area, southwestern British Columbia; in Current Research, Part A, Geological Survey of Canada, Paper 82-1A, p. 293-297.

Tipper, H.W.
1978: Northeastern part of Quesnel (93B) map area, British Columbia; in Current Research, Part A, Geological Survey of Canada, Paper 78-1A, p. 67-68.

1981: Offset of an upper Pliensbachian geographic zonation in the North American Cordillera by transcurrent movement; Canadian Journal of Earth Sciences, v. 18, no. 12, p. 1788-1792.

19. LOWER AND MIDDLE JURASSIC SEDIMENTS AND VOLCANICS OF THE SPATSIZI MAP AREA, BRITISH COLUMBIA

Project 750035

P.L. Smith[1], R.C. Thomson[1], and H.W. Tipper
Cordilleran Geology Division, Vancouver

Smith, P.L., Thomson, R.C., and Tipper, H.W., Lower and Middle Jurassic sediments and volcanics of the Spatsizi map area, British Columbia; in Current Research, Part A, Geological Survey of Canada, Paper 84-1A, p. 117-120, 1984.

Abstract

Two correlative sequences, the Toodoggone volcanics and the Spatsizi sediments, are exposed along the northern margin of the Bowser Basin on the southern flank of the Stikine Arch. The volcanics form a roughly arcuate belt that grades abruptly southward into the sediments which are unconformably below Bowser Lake Group rocks in the Bowser Basin. The age of the sequences is Early Pliensbachian to Early Bajocian; all intervening stages are present, at least in part.

Résumé

Deux séquences mises en corrélation, les roches volcaniques Toodoggone et les sédiments Spatsizi, affleurent le long de la marge nord du bassin de Bowser sur le flanc sud de l'arche de Stikine. Les roches volcaniques forment une zone grossièrement arquée qui se transforme brusquement vers le sud en sédiments qui reposent en discordance sous les roches du groupe de Bowser Lake dans le bassin de Bowser. L'âge des séquences varie du Pliensbachien ancien au Bajocien ancien; toutes les étapes intermédiaires sont présentes, du moins en partie.

INTRODUCTION

Earlier geological work in northern British Columbia disclosed the presence of volcanic rocks of a general Early and early Middle Jurassic age (Geological Survey of Canada, 1957; Souther, 1972; Gabrielse et al., 1977). Some of these rocks have been referred to informally as the Toodoggone volcanics but the age, succession, and internal and external structural relations were largely unknown. Work on the volcanics in the Spatsizi map area (104 H) in 1981 and 1983 revealed a new sequence, Early and early Middle Jurassic in age, which is mainly shale and siltstone with minor tuffs and tuffaceous sediments. Previously these strata were included with the overlying Bowser lake Group of late Middle and Upper Jurassic age but diagnostic fossil collections from the sediments and from interbeds within the Toodoggone volcanics have shown the units to be correlative and separated by an angular discordance from the overlying Bowser Lake Group. The biostratigraphy of the abundant fossil fauna of part of these sequences will be the subject of a Master's thesis at the University of British Columbia by Thomson.

TOODOGGONE VOLCANICS

The Toodoggone volcanics were first identified as such in the Toodoggone River map area (94 E) by Carter (1972) and were thought to be of Early Jurassic age mainly because of the similarity to Hazelton Group volcanic formations. Work in adjacent areas has permitted inclusion of volcanic sequences of similar lithology but paleontological evidence has shown these sequences to be Middle Jurassic (Bajocian and Aalenian), Early Jurassic (Pliensbachian and Toarcian), Triassic (Norian), and possibly even Permian or earlier. As a major discordance apparently exists between Norian and Pliensbachian strata and as the intent of the informal term was to include Jurassic rocks, pre-Jurassic sequences are excluded. The term Toodoggone volcanics should be formally defined or abandoned but for the present its informal use is continued. In this report the term refers to a varicoloured group of rhyolitic, andesitic, and basaltic breccias, tuffs, and flows of Middle and Early Jurassic age. They are distributed roughly along the southern margin of the Stikine Arch and form a rim of volcanic rocks around the northern margin of the Bowser Lake Group. Some contemporaneous volcanics, not previously called Toodoggone volcanics, are included here (Fig. 19.1). Interbedded thin sedimentary sequences provide ample fossil faunas to confirm the age of the volcanics in most areas.

The thick sections of volcanic rocks lying south of Cold Fish Lake between Spatsizi River and Cartmel Mountain to the northwest form the bulk of the group in Spatsizi map area and are mainly of Early Pliensbachian age. Southeast of the junction of Stikine and Klappan rivers a small area of Toarcian strata includes volcanic tuff, breccia, and flows; this section is discussed below with the Lower Jurassic Spatsizi sediments. In the Cry Lake map area (104 I) to the north a few Toarcian sections include tuffaceous beds. Bajocian volcanics are known in the Telegraph Creek map area (104 G) west of Iskut River (Souther, 1972), east of Eddontenajon Lake in Spatsizi map area, in southern Cry Lake map area (104 I) (Gabrielse, 1979), and east of Spatsizi River in Spatsizi area. In the Toodoggone River map area (94 E) where the name originated, the age is uncertain but one fossil collection suggests either a Bajocian or Toarcian age, probably the latter, for part of the group. There is no evidence, other than lithologic similarity to the Telkwa Formation of the Hazelton Group (Sinemurian) to suggest that any part of the group is of Sinemurian age. Wherever diagnostic fossil faunas have been found it has been clear that correlation based on lithologic similarity alone is not reliable for any of these volcanic sequences.

SPATSIZI SEDIMENTS

The sedimentary rocks referred to informally as the Spatsizi sediments are correlative with the volcanic rocks described in the foregoing and are of Early Pliensbachian to Early Bajocian age. Although there are abundant hiatuses in most sections, most of the time span is represented by fossil faunas, mainly ammonites. Shale, concretionary shale, siltstone, tuffaceous siltstone, tuff, rare limy lenses, sandstone, rare pebble conglomerate, and local cobble conglomerate lenses make up the sequence but facies changes are common and abrupt. Several sections were measured and studied in detail and two are presented here as typical of the group.

[1] Department of Geological Sciences, University of British Columbia, Vancouver, B.C.

SECTION 1: SOUTHEAST OF JUNCTION OF STIKINE AND KLAPPAN RIVERS (P.L.S.)

In the extreme northwest part of the Eaglenest Range, Jurassic rocks (Fig. 19.2) rest on diorite of uncertain age. The sequence reaches a thickness of nearly 375 m; the upper contact is a thrust fault. There are thin basal conglomerates but the lower third consists predominantly of purple and light green, volcaniclastic siltstone and minor sandstone. The remainder of the section is more coarse grained and resistant, consisting of volcanic breccia, conglomerate, tuff and siltstone yielding a reasonably well preserved ammonite fauna. Lava near the middle of the section is rhyolitic whereas the cap is resistant amygdaloidal and vesicular basalt. Age control on the lower part of the section is poor but the presence of **Weyla** in an arenaceous limestone 100 m above the base indicates an Early Jurassic age. The Toarcian ammonite **Dactylioceras** is abundant in the upper part of the section and the presence of **Harpoceras** s.l. and fragments resembling **Protogrammoceras** indicate a position low in the Toarcian.

SECTION 2: SOUTHWEST OF MT. WILL (R.C.T.)

The Lower and early Middle Jurassic section illustrated (Fig. 19.3) is underlain by rhyolitic Toodoggone flows and overlain by the lowermost strata of the Bowser Lake Group. In the Mt. Will area Lower Pliensbachian siltstone conformably overlies the volcanics but in an area 7 km to the west, Middle Toarcian shale rests unconformably on the volcanics.

Lower Pliensbachian rocks of the section contain a rich and diverse fauna. In addition to the ammonite genera listed in section 2, specimens of the bivalve genus **Weyla** are particularly abundant, as well as several other bivalve and brachiopod genera. Colonial and solitary corals are common in thin limestone beds but bryozoans and echinoids are rare.

The upper Pliensbachian shale unit overlying Lower Pliensbachian siltstone is largely unfossiliferous except for locally developed concretionary horizons and tuffaceous lenses which provide sufficient paleontological control.

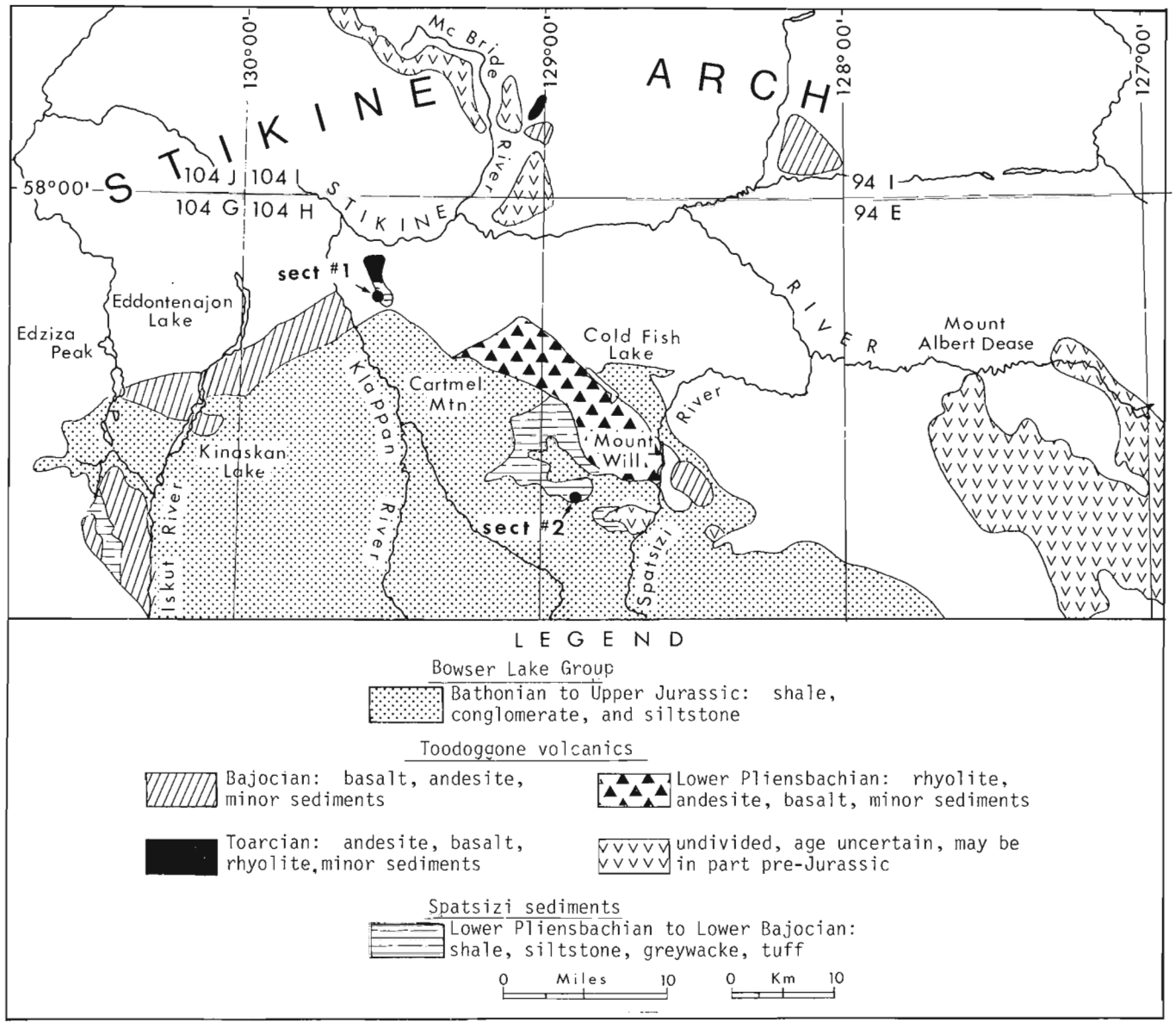

Figure 19.1. Distribution of Lower and lower Middle Jurassic rocks along northern margin of Bowser basin.

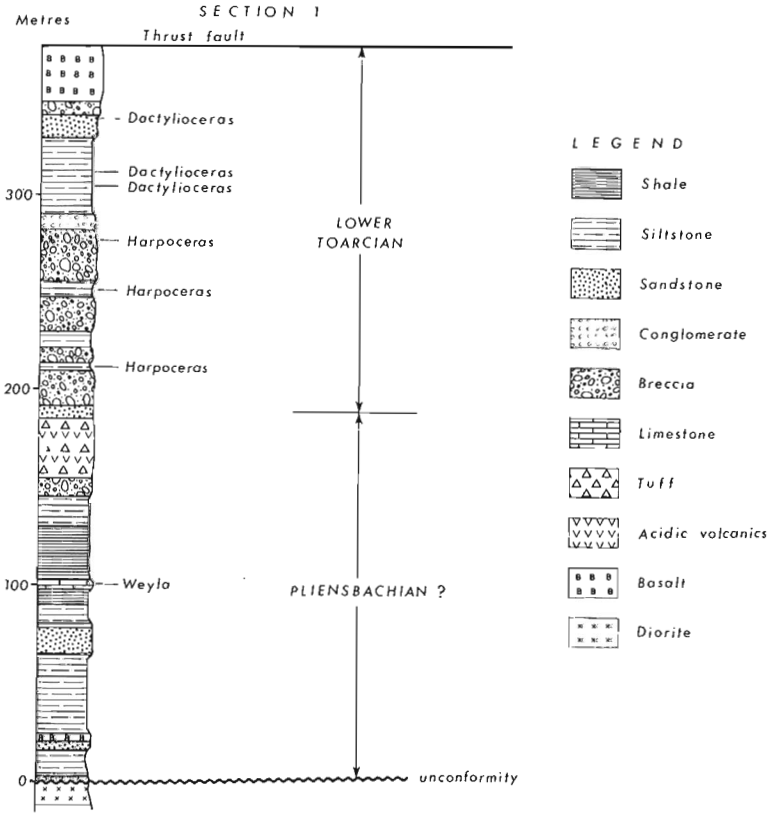

Figure 19.2

Measured section (Section 1) of Lower Toarcian and Pliensbachian(?) volcanics and sediments northwest of Mt. Cartmel.

***Figure 19.3** (below)*

Measured section (Section 2) of Lower Pliensbachian to Lower Bajocian sediments southwest of Mt. Will.

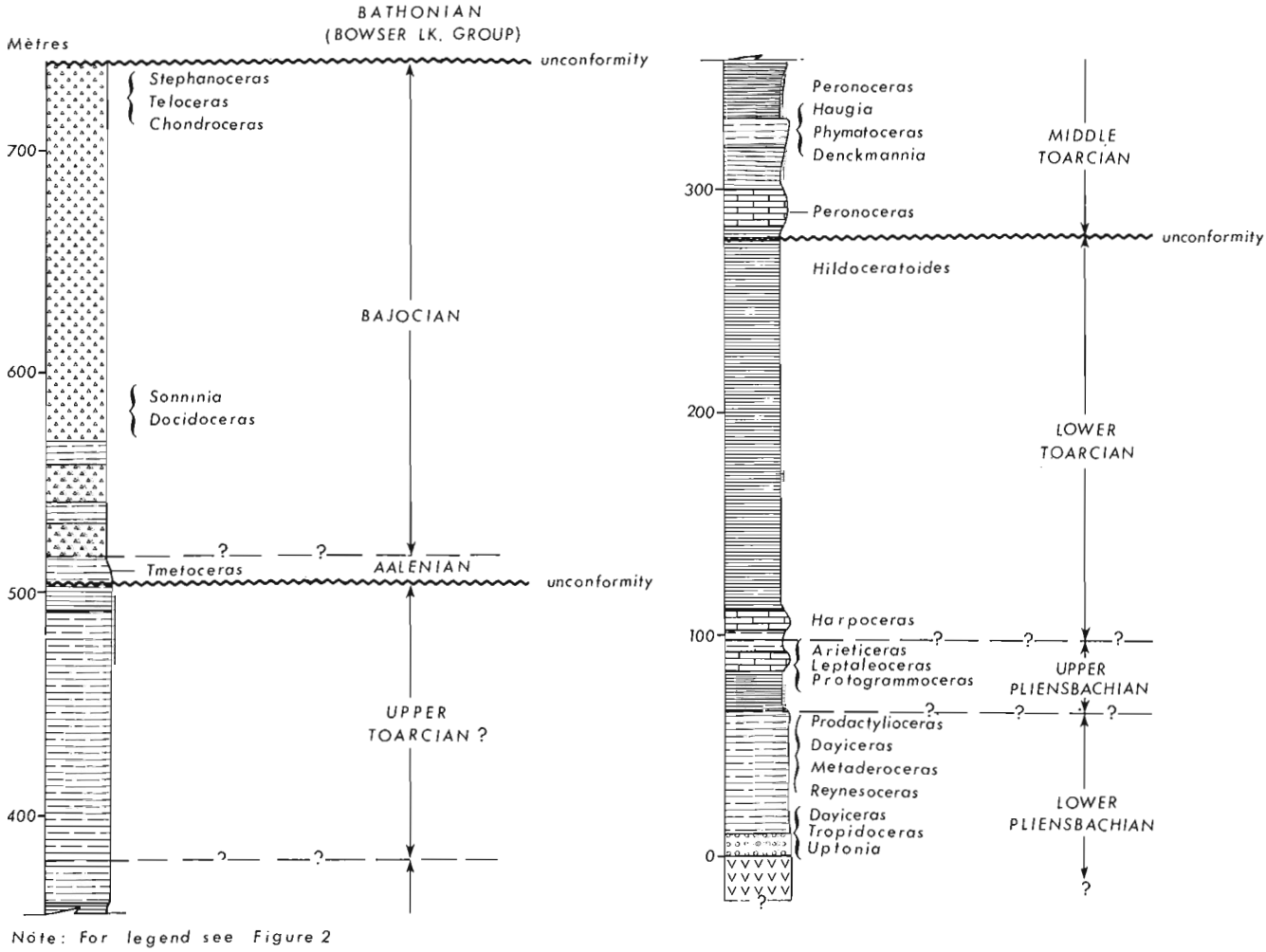

Note: For legend see Figure 2

Two distinct horizons of **Peronceras** were found in the Middle Toarcian; one below and one above the level of **Haugia, Phymatoceras,** and **Denkmannia.** The forms found in the upper horizon are similar to those reported from South America by Hillebrandt and Schmidt-Effing (1981). Throughout the map area the Upper Toarcian siltstone and tuffaceous siltstone unit varies markedly in thickness and is absent in places. Probable Upper Toarcian ammonites were found in correlative sections northwest of the Mt. Will section. The overlying Aalenian beds are thin (probably less than 40-60 m), poorly exposed, and yield only a limited fauna including **Pseudolioceras** and **Tmetoceras** and small bivalves.

The Bajocian stage is represented here by easily recognized, varicoloured, banded tuff and silty tuff. These are unconformably overlain by black shale and pebble conglomerate of the Bowser Lake Group.

RELATION OF THE TOODOGGONE VOLCANICS TO THE SPATSIZI SEDIMENTS

The Spatsizi sediments are correlative with the Toodoggone volcanics and represent a facies change from the volcanic piles that accumulated in an arc oriented more or less east-west near the Stikine River towards a sedimentary basin southeast, south, and southwest of the arc. The times when volcanism was most active can be recognized in most cases, in the sedimentary sequences by the presence of tuff or tuffaceous sediments. Clearly some correlative beds grade from waterlain tuff and breccia to tuffaceous siltstone to shale where beds can be traced from north to south near section 2. Evidence suggests that the distribution of the volcanics shown in Figure 19.1 may represent the main volcanic centres lying on the southerly flank of the east-west oriented Stikine Arch. The tectonic mobility of this arc through time may explain the hiatuses and deformation recorded in the sedimentary record. The sedimentary rocks may extend throughout the Bowser Basin and form a sedimentary base unconformably below the Bowser Lake Group.

REFERENCES

Carter, N.C.
1972: Toodoggone River area; in Geology, Exploration and Mining in British Columbia, 1972; British Columbia Department of Mines and Petroleum Resources, p. 63-70.

Gabrielse, H.
1979: Geology of Cry Lake (104I) map-area; Geological Survey of Canada, Open File 610.

Gabrielse, H., Dodds, C.J., and Mansy, J.L.
1977: Geology of Toodoggone River (94E) and Ware West-half (94F); Geological Survey of Canda, Open File 483.

Gabrielse, H., Wanless, R.K., Armstrong, R.L., and Erdman, L.R.
1980: Isotopic dating of Early Jurassic volcanism and plutonism in north-central British Columbia; in Current Research, Part A, Geological Survey of Canada, Paper 80-1A, p. 27-32.

Geological Survey of Canada
1957: Stikine River area, Cassiar District, British Columbia; Geological Survey of Canada, Map 9-1957.

Hillebrandt, A. von and Schmidt-Effing, R.
1981: Ammoniten aus dem Toarcium (Jura) von Chile (sudamerika); Zitteliana, 6.

Souther, J.G.
1972: Telegraph Creek map-area, British Columbia; Geological Survey of Canada, Paper 71-44.

20. METAMORPHISM, STRUCTURE AND STRATIGRAPHY AROUND THE MOUNT BLACKMAN GNEISS, BRITISH COLUMBIA

EMR Research Agreement 53/04/83

Richard Leonard[1]
Cordilleran Geology Division, Vancouver

Leonard, R., Metamorphism, structure and stratigraphy around the Mount Blackman Gneiss, British Columbia; in Current Research, Part A, Geological Survey of Canada, Paper 84-1A, p. 121-127, 1984.

Abstract

Two distinct stratigraphic sequences of Hadrynian rocks are separated by a major thrust northeast of the Mount Blackman Gneiss, British Columbia. Polydeformed Middle Miette Group grits and phyllites in the footwall underlie polydeformed rocks that belong to older strata tentatively assigned to the Horsethief Creek Group. These rocks, north and east of the gneiss have been metamorphosed to upper amphibolite facies. Postmetamorphic cation exchange is present between different phases where these phases are in contact. Chemical zoning is also present in some phases. Conditions of metamorphism are estimated to have been 580°C at 6.25 kb as suggested by garnet-biotite and garnet-plagioclase-kyanite-quartz equilibria from samples collected north of the gneiss-Horsethief Creek Group contact.

Résumé

Deux séquences stratigraphiques distinctes de roches hadryniennes sont séparées par une faille chevauchante majeure au nord-est du gneiss du mont Blackman, en Colombie-Britannique. Des grès grossiers et des phyllades polydéformés du groupe de Middle Miette dans le mur sont sous-jacents à des roches polydéformées qui appartiennent à des couches plus anciennes provisoirement classées dans le groupe de Horsethief Creek. Ces roches, au nord et à l'est du gneiss, ont été métamorphisées à l'étape supérieure de l'amphibolite. L'échange post-métamorphique de cations a eu lieu entre différentes phases là où elles étaient en contact. Certaines phases font voir un zonation chimique. Le métamorphisme se serait produit à une température de 580°C et à une pression de 6,25 kb, comme l'indiquent les phases d'équilibre grenat-biotite et grenat-plagioclase-cyanite-quartz révélées dans des échantillons prélevés au nord de la zone de contact entre le gneiss et le groupe de Horsethief Creek.

INTRODUCTION

The Archean Mount Blackman Gneiss is located immediately east of Valemount, British Columbia (Fig. 20.1). It is separated from the Malton Gneiss west of the Rocky Mountain Trench by the Purcell fault and an unnamed normal fault. The gneiss is surrounded by metasedimentary rocks that are tentatively assigned to the Horsethief Creek Group which underlies the Miette Group. The gneiss and surrounding supracrustal rocks have been studied on a regional scale by Campbell (1968) and Price and Mountjoy (1970). The basement gneiss itself was studied in more detail by Oke and Simony (1980) and Chamberlain et al. (1978).

In this study, the supracrustal rocks have been examined in more detail and special emphasis has been placed on metamorphism.

GEOLOGICAL SETTING

The Mount Blackman Gneiss is conformably overlain by Hadrynian strata which are tentatively assigned to the Horsethief Creek Group because they differ considerably from Miette Group rocks to the east and resemble Horsethief Creek Group rocks to the southwest. The Horsethief Creek Group is informally divided into an upper and a lower division in the area mapped. The lower division, from base to top, consists of 250 m of muscovitic quartzite, 150 m of pelite and 750 m of grit. The pelite unit consists of interbedded pelite, psammite, minor calc-silicate and minor quartzite. The grit unit consists of thin grits, fine and coarse grained sandstone and pelite; the grits and sandstones form beds up to 1 m thick at intervals of more than 20 m. Sandy and gritty beds make up about 60 per cent of this unit.

The upper division of the Horsethief Creek Group consists predominantly of pelite and is divisible into two sequences. A lower 800 m thick sequence is made up of interbedded pelite, semi-pelite, psammite, calc-silicate and minor grits. Brown and green pelite forms most of the package whereas grits make up about 20 per cent. The grits are crumbly, brown weathering and commonly found in 10 m thick intervals. Southeast of Mount Blackman, a 100-m-thick carbonate unit lies about 530 m above the lower-upper

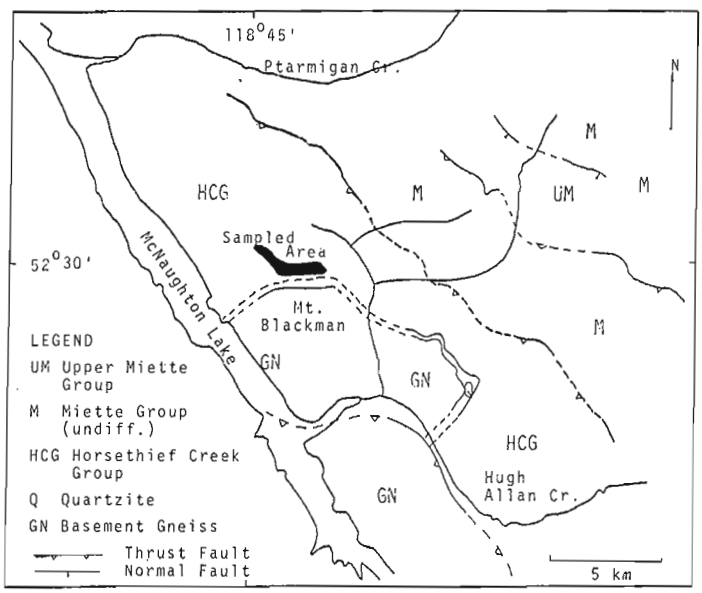

Figure 20.1. *Geology around Mount Blackman, British Columbia.*

[1] Department of Geological Sciences, McGill University, Montreal

Horsethief Creek Group contact. It consists of limestone and calcareous sandstone and laterally is discontinuous. It probably represents an isolated carbonate mass. An upper sequence, more than 275 m thick, of the upper Horsethief Creek Group is made up of pelite, psammite and rare calc-silicate.

The Horsethief Creek Group rocks that surround Mount Blackman have been thrust over Miette Group rocks to the east. This previously unrecognized fault juxtaposes two very different grit and pelite successions. The fault places overturned Horsethief Creek Group rocks over right-side-up Miette Group in the footwall. The strata in the footwall are assigned to the middle and upper Miette Group because they are the same as the Miette Group that outcrops immediately to the east near the head of Ptarmigan and Blackman creeks. The middle Miette consists of grits, pelite and rare calcareous sandstone. Grits make up about 50 to 65 per cent of this succession. Pelites in the middle Miette are commonly brown to greenish grey. The upper Miette Group consists predominantly of pelite, psammite, some quartzite, rare pink calcareous sandstone and rare grits. The pelites of the upper Miette Group are either green and very lustrous or chocolate brown and rusty weathering. The rusty pelites are slightly sandier than the green pelites. The two types of pelite grade laterally into each other.

Supracrustal rocks around Mount Blackman have been affected by three phases of deformation. The first phase is defined by a bedding-parallel foliation which is axial planar to large scale, isoclinal, northeast verging, inclined to recumbent folds. The overturned limbs of these folds are commonly truncated by thrust faults. These faults, commonly folded along with bedding in the same style as the F_1 structures, are probably synchronous with the first phase of deformation. The displacement on these first phase faults may not be as important as that on later high-angle reverse faults because the early faults generally do not juxtapose different stratigraphic sequences. The second phase of deformation is reflected in large scale, broad, upright to slightly inclined folds on the upward-facing limbs of the first phase folds. A strong crenulation cleavage, axial planar to these folds, has the same orientation as that of high-angle reverse faults; thus these faults may be related to the second phase of deformation. The high-angle reverse faults commonly juxtapose different stratigraphic sequences. Structures produced by the third phase of deformation are uncommon. They include warping of limbs and axial planes of second phase folds and kinking of second phase crenulation cleavage, with the kink surface parallel to bedding. Late normal faults occur northeast of Mount Blackman, close to the head of Hugh Allan Creek.

METAMORPHISM

Rocks of the Horsethief Creek Group around Mount Blackman have been metamorphosed to high pressure, upper amphibolite facies. Metamorphic isograds and temperature and pressure conditions are readily determined from the mineral assemblages in this dominantly pelitic succession. The distribution of Mg-Fe between garnet and biotite may be used as a geothermometer (Thompson, 1976; Ferry and Spear, 1978; Pigage and Greenwood, 1982), and the compositions of coexisting garnet and plagioclase in kyanite-bearing assemblages may be used as a geobarometer (Ghent, 1976; Newton and Haselton, 1981).

Mineral assemblages and reactions

Mineral assemblages observed in pelitic rocks of the Horsethief Creek Group around Mount Blackman are:

1. garnet-biotite-chlorite-quartz-muscovite-oxides
2. garnet-staurolite-biotite-quartz-muscovite-oxides
3. staurolite-biotite-kyanite-quartz-muscovite-oxides
4. garnet-biotite-staurolite-kyanite-quartz-muscovite-oxides
5. garnet-biotite-kyanite-quartz-muscovite-oxides
6. garnet-biotite-sillimanite-quartz-muscovite-oxides

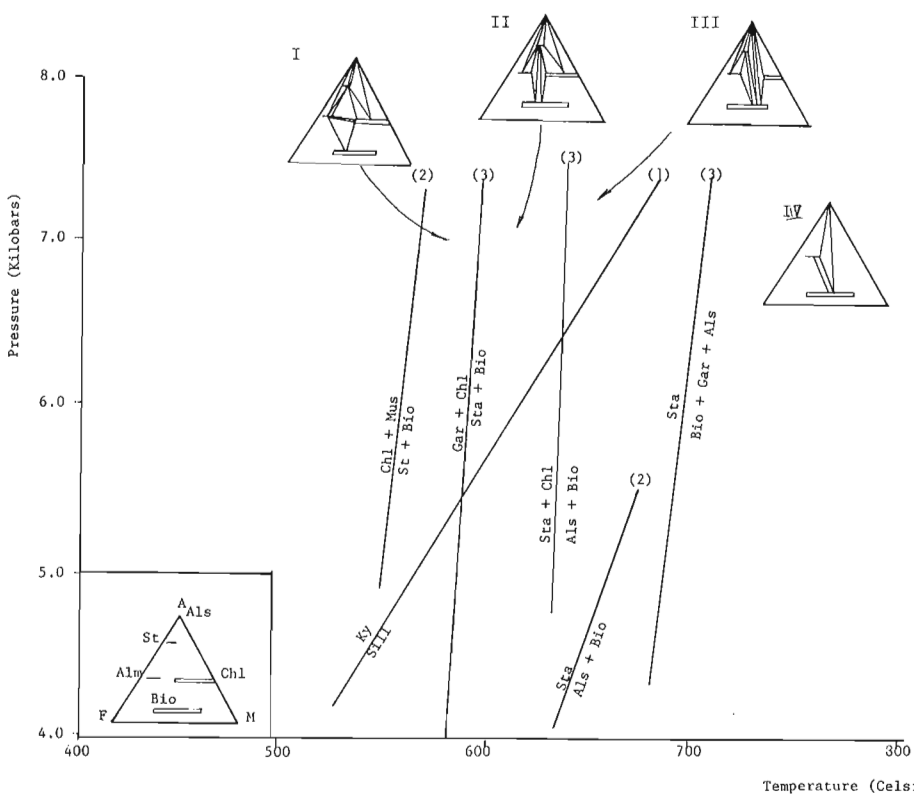

Figure 20.2

Partial petrogenetic grid showing changes in topology as discontinuous metamorphic reactions are crossed. Data from (1) Holdaway (1971), (2) Hoscheck (1969), (3) Thompson (1976).

As shown in Figure 20.2, two discontinuous reactions relate assemblage 1 to assemblages 2 and 3. These are:

$$\text{chlorite} + \text{garnet} \rightleftharpoons \text{staurolite} + \text{biotite} + H_2O$$

followed by

$$\text{staurolite} + \text{chlorite} \rightleftharpoons \text{kyanite} + \text{biotite} + H_2O$$

Assemblages 2 and 3 are related to assemblage 5 through the discontinuous reaction

$$\text{staurolite} \rightleftharpoons \text{garnet} + \text{biotite} + \text{kyanite} + H_2O$$

This reaction is reflected in assemblage 4 which represents an univariant assemblage. Finally, assemblages 5 and 6 are related to each other by the polymorphic transformation

$$\text{kyanite} \rightleftharpoons \text{sillimanite}$$

Mineral chemistry

To obtain estimates of pressure and temperature below, at, and above the staurolite-out reaction, garnet and biotite were analyzed in garnet-staurolite-biotite (below staurolite-out reaction), garnet-staurolite-biotite-kyanite-plagioclase (at staurolite-out reaction) and garnet-biotite-sillimanite (above staurolite-out reaction) assemblages. Plagioclase in garnet-biotite-staurolite-kyanite-plagioclase assemblages was also analyzed.

Thompson (1976) showed that the Mg/Fe ratio of garnet, biotite and staurolite increases with temperature as the staurolite-out reaction is approached and that the Mg/Fe ratio of garnet and biotite decreases with increasing temperature above the staurolite-out reaction. The samples were plotted in order of inferred increasing metamorphic grade using these relationships and the mineral assemblages (Fig. 20.2 to 20.5). Sample A29-5 is interpreted to be the lowest grade sample because it is the only one below the staurolite-out isograd. Sample Sl-8 is the highest grade sample because it is the only one above the staurolite-out reaction. In the case of the other samples, the suspected increase in grade is based on Mg/Fe ratio of garnet and biotite.

Many observations of mineral chemistry suggest that there has been post-metamorphic cation exchange between pairs of minerals that are in contact. For example, isolated garnet grains are more strongly zoned in Mg/Fe ratio than grains in contact with biotite; cores of garnet grains in contact with biotite have a more erratic change in composition with grade than cores of isolated grains; and cores, and rims of isolated garnets have compositions different from those of cores and rims of grains in contact with biotite (Fig. 20.3). Also, biotite grains in contact with garnet are generally poorer in Mg than isolated grains (Fig. 20.5). These observations suggest Mg-Fe exchange between garnet and biotite. Ca exchange seems to have taken place between garnet and plagioclase because garnet grains in contact with plagioclase are less zoned than isolated grains (Fig. 20.4), and rims of plagioclase grains in contact with garnet in lower grade samples are richer in Ca than rims of isolated grains (those surrounded by quartz and muscovite), whereas the converse is true for higher grade rocks. Higher grade rocks show much stronger zoning from core to rim for isolated plagioclase grains than for grains in contact with garnet (Fig. 20.6). The presence of postmetamorphic cation exchange between phases in contact suggests that only compositions of isolated grains should be used for geothermobarometric calculations.

Garnet shows important chemical zoning, with Fe and Mg enrichment, Mg/Fe ratio increase and Ca and Mn depletion towards the rim. Because this zoning is typical of prograde reactions (Tracy et al., 1976; Woodsworth, 1977), only garnet rim compositions should be used in the geothermobarometric calculations. Garnet rims show a smooth increase followed by decrease of Mg/Fe ratio as function of metamorphic grade (Fig. 20.3). Within a given sample, biotite is much more homogeneous than garnet. The Mg/Fe ratio of biotite increases with metamorphic grade and then decreases as the staurolite-out reaction is crossed (Fig. 20.5). Plagioclase found in lower grade samples is less calcic and less strongly zoned than in higher grade samples (Fig. 20.6).

Geothermometry

In this study, three different methods based on the Mg-Fe distribution between garnet and biotite were used to estimate the temperature of metamorphism. One method is from

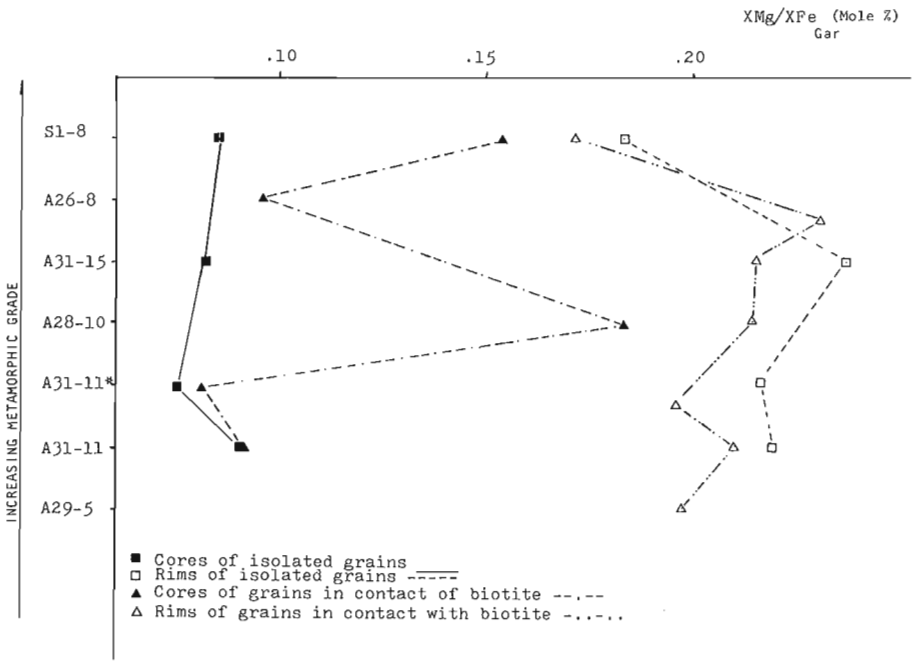

Figure 20.3

Average XMg/XFe ratio of garnet plotted for analyzed samples. Note that garnet cores and rims are plotted separately and that there is a distinction between grains in contact with biotite and isolated grains. Samples are shown in suspected upwards increase in metamorphic grade, based on the increase in Mg/Fe ratio as the staurolite out reaction is approached and decrease after it is passed.

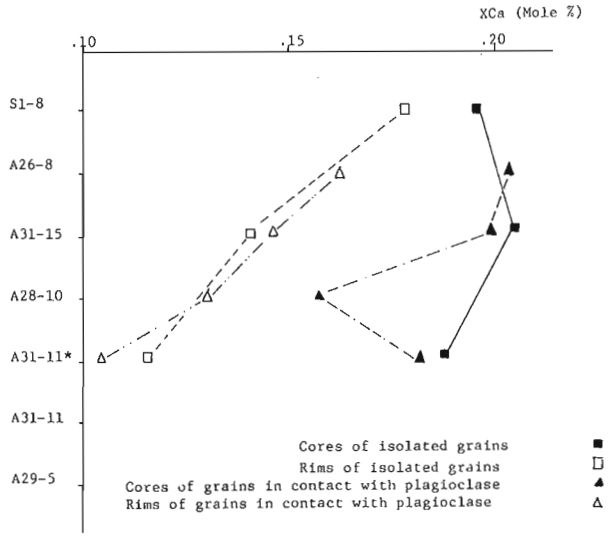

Figure 20.4. Average XCa of garnet plotted for analyzed samples. Note that cores and rims are plotted separately and that there is a distinction between isolated grains and grains in contact with plagioclase.

Thompson (1976) who calibrated values of ln Kd (where $Kd = (XMg/XFe)_{gar} \times (XMg/XFe)_{bio}$) using temperatures obtained from other thermometers. The second is from Ferry and Spear (1978) who experimentally calibrated the partitioning of Mg and Fe between synthetic garnet and biotite. The final method is from Pigage and Greenwood (1982); they applied a correction for the Mn and Ca content of garnet by using symmetrical Margules parameters from Ganguly (1979).

Table 20.1 shows that temperatures obtained from garnet rims are higher than temperatures obtained from garnet cores. Also, temperatures obtained using the Pigage and Greenwood (1982) calibration are higher than both Thompson (1976) and Ferry and Spear (1978) temperatures. Calculations from an average value of Kd (on rims) from Figure 20.7 yield a temperature of 510°C using the Ferry and Spear (1978) calibration, and of 580°C using the Pigage and Greenwood (1982) method.

Geobarometry

Two different geobarometric models may be used with plagioclase-garnet-kyanite-quartz assemblages. These models are based on the breakdown reaction

$$3 \text{ anorthite} \rightleftharpoons \text{grossularite} + 2 \text{ kyanite} + \text{quartz} \qquad (1)$$

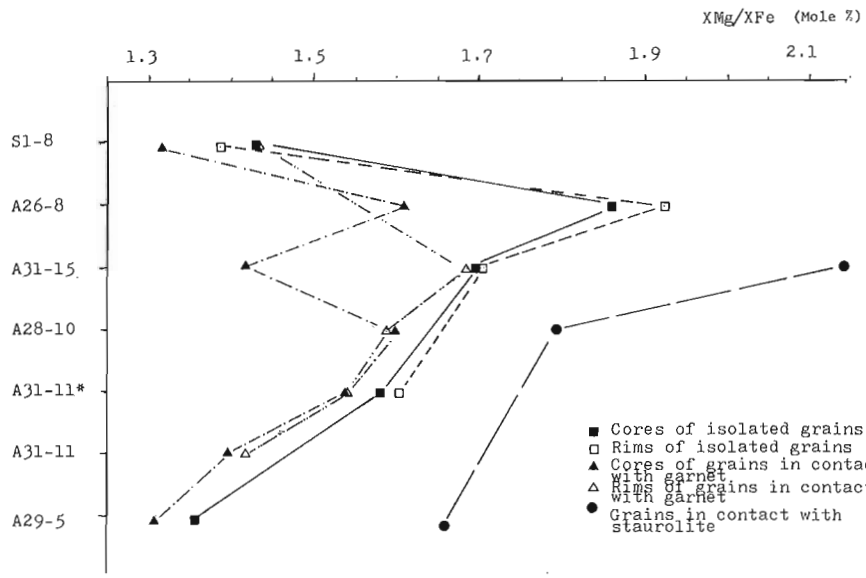

Figure 20.5

Average XMg/XFe ratio of biotite plotted for analyzed samples. Cores and rims are plotted separately and a distinction is made between grains in contact with garnet and isolated grains.

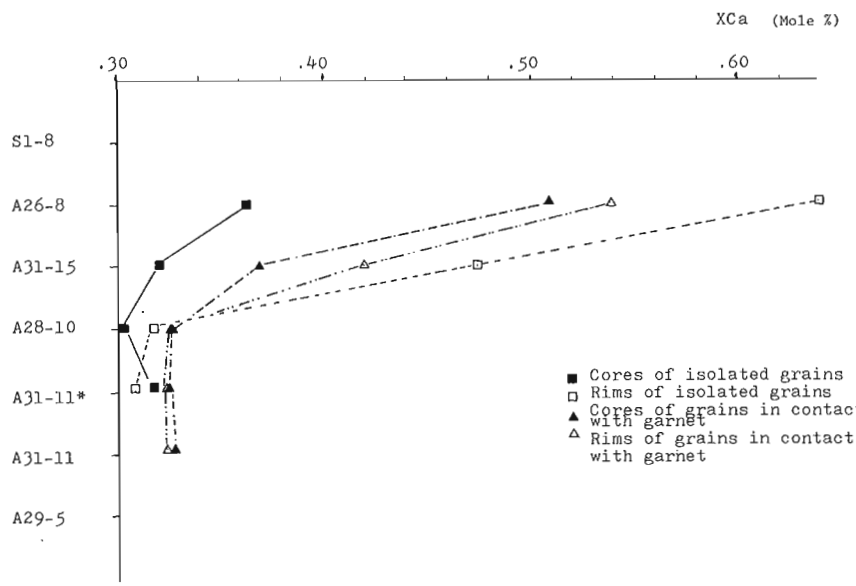

Figure 20.6

Average XCa of plagioclase plotted for analyzed samples. Cores and rims are plotted separately and there is a distinction between isolated grains and grains in contact with garnet.

The two calibrations used are from Ghent (1976) and from Newton and Haselton (1981). In both cases, the activity of anorthite in plagioclase is from Newton et al. (1980) and the activity coefficient of grossularite in garnet is from Newton and Haselton (1981). They used data from Hensen et al. (1975) to estimate the Ca-Mg exchange parameter. In the case of the Newton and Haselton (1981) calibration, data from Goldsmith (1980) were used for the end-member reaction (1). Pressure calculations were made for these two models using each of the three temperature models (Table 20.2). The models yielding the higher temperatures also yield the higher pressures. For a given temperature method, the Newton and Haselton (1981) calibration yields a higher pressure than the Ghent (1976) calibration. This difference never exceeds 300 bars and makes it impossible to choose a preferred method. A representative pressure for the whole suite may be obtained from the slope in Figure 20.8. Pressure calculation using the method of Ferry and Spear (1978) to calculate average temperature (Fig. 20.7) and the $(a_{an}^{pl})^3$ vs a_{gr}^{gar} slope in Figure 20.8, in conjunction with the Newton and Haselton (1981) calibration yields a value of 4.9 kb. A pressure of 6.3 kb is obtained if the same method is used combining the Pigage and Greenwood (1982) method with the Newton and Haselton (1981) calibration. These values are close to the average pressure obtained from the five samples (Table 20.2) using the same models.

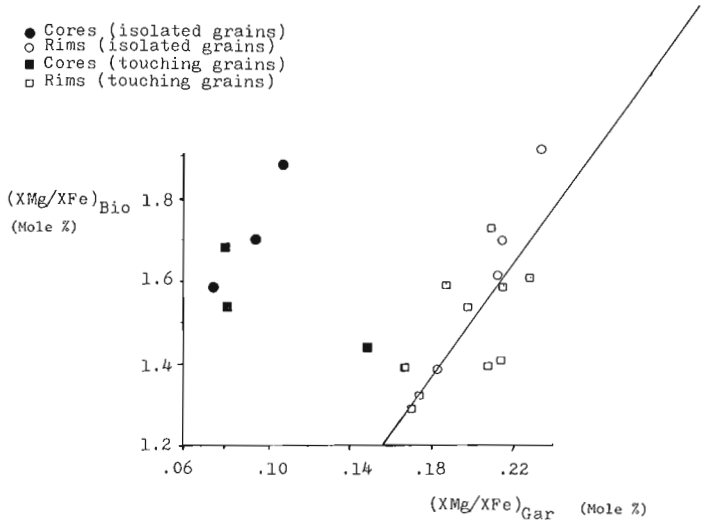

Figure 20.7. *$(XMg/XFe)_{gar}$ vs $(XMg/XFe)_{bio}$ plot. Cores and rims are plotted separately and a distinction is made between isolated grains and grains in contact with each other (garnet-biotite). The line shown passes through the origin and gives an average Kd (inverse of slope) for rims of grains.*

Table 20.1. Garnet, plagioclase and biotite compositions and estimates of temperature

Sample		XMg	XFe	XMn	XCa	T1	T2	T3
A28-10	Gar core	.121	.699	.031	.150	409	443	534
	Gar rim	.149	.708	.011	.132	442	495	576
	Biotite	.508	.319					
	Plagioclase				.309			
A26-8	Gar core	.073	.701	.022	.203	321	324	402
	Gar rim	.155	.667	.015	.163	436	465	556
	Biotite	.545	.283					
	Plagioclase				.640			
A31-15	Gar core	.063	.697	.040	.201	311	298	404
	Gar rim	.165	.694	.000	.141	459	507	584
	Biotite	.520	.305					
	Plagioclase				.476			
A31-11	Gar core	.064	.714	.028	.194	331	328	429
	Gar rim	.161	.733	.004	.102	475	541	604
	Biotite	.481	.338					
	Plagioclase				.314			
A29-5	Gar rim	.156	.788	.007	.049	479	517	546
	Biotite	.468	.346					
SI-8	Gar core	.087	.662	.049	.202	387	414	537
	Gar rim	.124	.675	.022	.179	441	502	597
	Biotite	.472	.345					
A31-11	Gar rim	.157	.722	.005	.116	448	500	563
	Biotite	.519	.322					
	Plagioclase				.313			

T1 calculated from Thompson (1976), T2 calculated from Ferry and Spear (1978), T3 calculated from Pigage and Greenwood (1982).

Table 20.2. Pressure estimates (kb)

Sample	Temperature model	Pressure model 1	2
A28-10	1	3.6	3.9
	2	4.9	5.2
	3	6.8	7.0
A31-15	1	3.5	3.8
	2	4.5	4.8
	3	6.2	6.4
A26-8	1	3.4	3.8
	2	4.0	4.3
	3	5.8	6.1
A31-11	1	3.7	4.0
	2	5.2	5.4
	3	6.6	6.8
A31-11	1	3.4	3.7
	2	4.6	4.9
	3	6.1	6.3

Pressure model	1	Ghent (1976)
	2	Newton and Haselton (1981)
Temperature model	1	Thompson (1976)
	2	Ferry and Spear (1981)
	3	Pigage and Greenwood (1982)

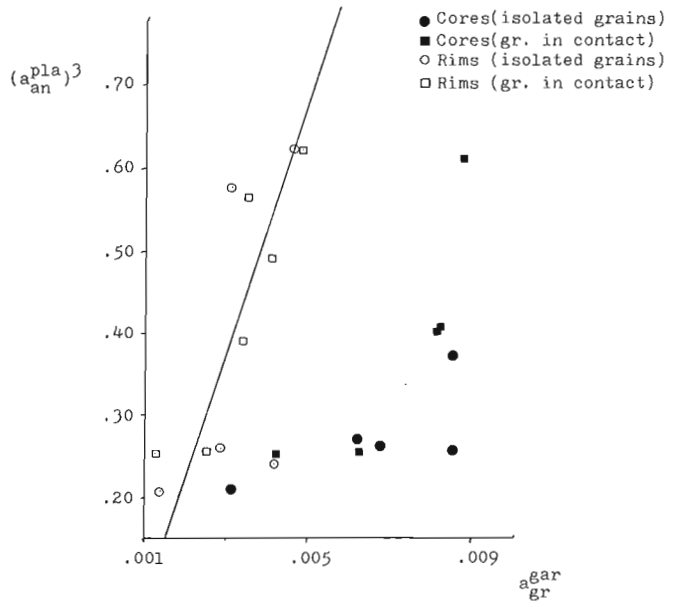

Figure 20.8. *Anorthite activity in plagioclase (cubed) vs grossular activity in garnet plot. Cores and rims are plotted separately and a distinction is made between isolated grains and grains touching each other (garnet-plagioclase). Line shown passes through origin and gives average distribution of Ca between plagioclase and garnet (rims of grains). Inverse of slope is used in pressure calculations.*

FAVOURED METAMORPHIC CONDITIONS ESTIMATE

Since three geothermometric methods and two geobarometric methods have been used, a total of six P-T estimates may be made for each sample. The best thermometer method is judged to be the one whose results correlate best with the mineral assemblages in the analyzed samples. Fortunately, the mineral assemblages in five of the seven samples selected occur on an univariant line (staurolite-out reaction) whose slope is quite steep in P-T space (Carmichael, 1978; Richardson, 1968). The favoured geothermometer is the one that was used by Pigage and Greenwood (1982) because it yields the lowest temperature for the lowest grade sample (A29-5) i.e. the only one below the staurolite-out reaction. This is unlike the Ferry and Spear (1978) method which yields a temperature for sample A29-5 which is above the temperature obtained from samples on the staurolite-out reaction. The favoured thermometer differs from the others because it takes into account the Ca and Mn content of garnet. This may account for its internal consistency. Temperatures obtained from this method (Table 20.1) differ from Richardson's (1968) experimental data, which suggest a temperature of about 700°C from 3 to 9 kb for the Fe end member staurolite-out reaction:

$$\text{Fe staurolite} + \text{quartz} \rightleftharpoons \text{almandine} + \text{sillimanite} + H_2O$$

However, Carmichael (1978) located the staurolite-out reaction in the Mg and Fe bearing system at a much lower temperature (550°C at 4.8 kb). Furthermore, Pigage and Greenwood (1982) concluded that caution should be exercised when using experimental data from the staurolite + quartz breakdown. These calibrations occur at temperatures too high to be consistent with other equilibria such as garnet-biotite-kyanite-sillimanite plus C-O-H gas.

With the a_{gr}^{gar} and a_{an}^{pl} used in this paper, the geobarometers of Ghent (1976) and Newton and Haselton (1981) are in essential agreement, so that the best estimates of the conditions of metamorphism are considered to be 580°C at 6.3 kb (Fig. 20.7, 20.8).

ACKNOWLEDGMENTS

The author is most grateful to E.W. Mountjoy and A. Hynes for their counselling and helpful discussions. The author was supported by a National Science and Engineering Research Council postgraduate scholarship. Financial support for field work and laboratory analyses comes from Dr. Mountjoy's NSERC grant A2128. Research agreement No. 53 with the Department of Energy, Mines and Resources provided partial support during the summer of 1983.

REFERENCES

Campbell, R.B.
1968: Canoe River, British Columbia; Geological Survey of Canada, Map 15-1967.

Carmichael, D.M.
1978: Metamorphic bathozones and bathograds: a measure of the depth of post-metamorphic uplift and erosion on the regional scale; American Journal of Science, v. 278, p. 769-797.

Chamberlain, V.E., Lambert, R.St.J., and Holland, J.G.
1978: Preliminary subdivisions of the Malton Gneiss Complex, British Columbia; in Current Research, Part A, Geological Survey of Canada, Paper 78-1A, p. 491-492.

Ferry, J.M. and Spear, F.S.
1978: Experimental calibration of the partitioning of Fe and Mg between biotite and garnet; Contributions to Mineralogy and Petrology, v. 66, p. 113-117.

Ganguly, J.
1979: Garnet and clinopyroxene solid solutions, and geothermometry based on Fe-Mg distribution coefficient; Geochimica et Cosmochimica Acta, v. 43, p. 1021-1029.

Ghent, E.
1976: Plagioclase-garnet-Al_2SiO_5-quartz: a potential geobarometer-geothermometer; American Mineralogist, v. 61, p. 710-714.

Goldsmith, J.R.
1980: Melting and breakdown reactions of anorthite at high pressures and temperatures; American Mineralogist, v. 65, p. 821-836.

Hensen, B.J., Schmid, R., and Wood, B.J.
1975: Activity-composition relations for pyrope-grossular garnet; Contributions to Mineralogy and Petrology, v. 51, p. 161-166.

Holdaway, M.J.
1971: Stability of andalusite and the aluminum silicate phase diagram; American Journal of Science, v. 271, p. 97-131.

Hoschek, G.
1969: The stability of staurolite and chloritoid and their significance in metamorphism of pelitic rocks; Contributions to Mineralogy and Petrology, v. 22, p. 208-232.

Newton, R.C., Charlu, T.V., and Kleppa, O.J.
1980: Thermochemistry of the high structural state plagioclases; Geochimica et Cosmochimica Acta, v. 44, p. 933-941.

Newton, R.C. and Haselton, H.T.
1981: Thermodynamics of the garnet-plagioclase-Al_2SiO_5-quartz geobarometer; in Thermodynamics of Minerals and Melts, ed. R.C. Newton, A. Navrotsky, and B.J. Wood, Springer-Verlag, New York.

Oke, C. and Simony, P.S.
1980: Basement gneisses of the Western Rocky Mountains, Hugh Allan Creek area, British Columbia; in Current Research, Part A, Geological Survey of Canada, Paper 81-1A, p. 181-184.

Pigage, L.C. and Greenwood, H.J.
1982: Internally consistent estimates of pressure and temperature: the staurolite problem; American Journal of Science, v. 282, p. 943-969.

Price, R.A. and Mountjoy, E.W.
1970: Geologic structure of the Canadian Rocky Mountains between Bow and Athabasca Rivers, a progress report; Geological Association of Canada, Special Paper 6, p. 7-26.

Richardson, S.W.
1968: Staurolite stability in a part of the system Fe-Al-Si-O-H; Journal of Petrology, v. 9, p. 467-488.

Thompson, A.B.
1976: Mineral reactions in pelitic rocks: calculations of some P-T-X (Fe-Mg) phase relations; American Journal of Science, v. 276, p. 425-454.

Tracy, R.J., Robinson, P., and Thompson, A.B.
1976: Garnet composition and zoning in the determination of temperature and pressure of metamorphism, Central Massachusetts; American Mineralogist, v. 61, p. 762-775.

Woodsworth, G.J.
1977: Homogenization of zoned garnets from pelitic schists; Canadian Mineralogist, v. 15, p. 230-242.

21. SELECTED MINERAL ASSOCIATIONS IN RADIOACTIVE AND REE OCCURRENCES IN THE BAIE-JOHAN-BEETZ AREA, QUEBEC: A PROGRESS REPORT

Project 770061

J. Rimsaite
Economic Geology Division

Rimsaite, J., Selected mineral associations in radioactive and REE occurrences in the Baie-Johan-Beetz area, Quebec: a progress report; in Current Research, Part A, Geological Survey of Canada, Paper 84-1A, p. 129-145, 1984.

Abstract

This paper documents results of rapid chemical, spectrographic, scanning electron microscope, semiquantitative energy dispersive spectrometer, and neutron activation analyses for uranium content of minerals and host rocks for the following associations of primary and secondary minerals:

1. *metasediments grading to garnetiferous feldspar pegmatites containing mafic xenoliths;*
2. *fergusonite-bearing pegmatite and rock-forming feldspars and micas;*
3. *biotite-hornblende gneiss hosting white radioactive pegmatites containing titanite, allanite and bastnaesite;*
4. *granite pegmatite containing associations of primary and secondary Pb, Ti, Nb, Th, U and Y minerals;*
5. *syenite pegmatite containing biotite, uraninite, uranothorite, zircon, apatite, allanite, xenotime, monazite, hydroxyl-bastnaesite and secondary amorphous phyllosilicates and U, Zr and REE mineral aggregates.*

Résumé

Le présent rapport présente les résultats d'analyses chimiques rapides, d'analyses spectrographiques, d'analyses au microscope électronique à balayage, d'analyses semiquantitatives au spectromètre fonctionnant selon la technique de la dispersion de l'énergie et d'analyses par activation neutronique effectuées afin de déterminer la teneur en uranium de minéraux et de roches minéralisées pour les associations suivantes de minéraux primaires et secondaires:

1. *métasédiments se transformant en pegmatites à feldspath grenatifère qui renferment des xénolites mafiques;*
2. *pegmatite à fergusonite et feldspaths et micas de roches;*
3. *gneiss à biotite et à hornblende renfermant des pegmatites radioactives blanches qui contiennent de la titanite, de l'allanite et de la bastnaésite;*
4. *pegmatite granitique contenant des associations de minéraux primaires et secondaires de Pb, de Ti, de Nb, de Th, d'U et d'Y;*
5. *pegmatite syénitique contenant de la biotite, de l'uraninite, de l'uranothorite, du zircon, de l'apatite, de l'allanite, de la xénotime, de la monzanite, de la bastnaésite à hydroxyle, des phyllosilicates amorphes secondaires et des aggrégats de minéraux renferment de l'uranium, du zircon et des éléments des terres rares.*

INTRODUCTION

The Baie-Johan-Beetz area and adjacent region north of the Gulf of St. Lawrence and within the Grenville structural province contain several occurrences of radioactive and rare-earth element (REE)-bearing mineral associations (Blais, 1956; Sharma and Franconi, 1970; Cameron-Schimann, 1978; Rose, 1979; Rimsaite, 1981a). The radioactive and REE mineralization occurs in granitoid pegmatites of Blais' (1956) unit 11 and Cooper's (1957) unit 4. Blais (1956) distinguished the following petrographic units in the area between Baie Quétachou and Costebelle Lake, east of Baie-Johan-Beetz: 1: banded granitic gneiss; 2: augen gneiss; 3: quartzite of Wakeham group; 4: schists of sedimentary origin; 5: pyroxene gabbro and amphibolite; 6: hornblende gabbro; 7: schistose and altered gabbro; 8: gneissic biotite granite; 9: pink granite; 10: granite porphyry; 11: muscovite pegmatite, and 12: unconsolidated deposits. Caron Lake fault, indicated by signs of hydrothermal alteration, separates granite and augen gneisses in the Costebelle Lake area on the east from the Wakeham quartzites of lower metamorphic grade to the west of the fault. Cooper (1957) mapped eight units corresponding to those of Blais (1956) in the Baie-Johan-Beetz area: S-1: micaceous quartzite; S-2: grey quartzite; and S-3: migmatite of the Wakeham group; unit 1: gabbro and derivatives (units 5, 6, 7 of Blais, 1956); unit 2: gneissic granite; unit 3: biotite granite; unit 4: pegmatite; and swamp, clay, sand. To the author's knowledge, no isotopic dating has been performed to determine age relationships between the above units. Pegmatites are commonly intruded along the contact between metagabbro sheets and granitoid rocks. White radioactive pegmatites occur in swampy areas underlain by quartzites. Pink granite pegmatites associated with biotite granite are also radioactive, whereas vast areas of grey and pink pegmatites associated with gabbro and other mafic rocks, rarely show uranium concentrations in excess of 50 ppm. The pegmatites differ in grain size, in the frequency, shape and size of gabbroic and metasedimentary xenoliths, and in their degree of differentiation from oligoclase-rich, through microcline, albite, quartz to cleavelandite-rich varieties (Rimsaite, 1981a, 1982a). Lead/uranium and Pb/Pb isotopic ratios from selected pegmatitic minerals indicated a minimum age of 1000 Ma for redistribution of radioactive and radiogenic elements (Rimsaite, 1982a, Fig. 3.5b).

This report documents results of new rapid chemical, spectrographic, scanning electron microscope (SEM), semiquantitative energy dispersive spectrometer (EDS) and neutron activation (NA) analyses for U and Th of mineral and rock specimens collected in 1978, 1979 and 1980 in an area between Baie-Johan-Beetz, Costebelle Lake and Baie Pontbriand. Chemical changes during alteration of diverse

Table 21.1. Partial chemical analyses of selected rocks and minerals from Baie-Johan-Beetz area, Quebec*

	Quartzite, gneiss, pegmatite, xenoliths from Gull Island area (1-5)					Costebelle Lake – Baie Pontbriand (6-12)							Baie Quétachou (13-15)			Grandroy Deposit (16-19)**			
	1	2	3	4	5	6	7	8	9	10	11	12	13	14	15	16	17***	18	19***
SiO_2 %	70.9	72.5	47.2	75.5	34.8	44.7	46.1	44.2	38.4	46.1	74.3	75.2	75.4	46.3	66.2	63.8	62.	35.5	60.
TiO_2	0.1	0.1	2.4	0.1	3.5	2.7	1.3	0.9	1.9	1.7	0.0	0.0	0.0	0.3	0.0	0.3		2.5	
Al_2O_3	14.0	15.5	17.1	13.4	15.1	15.0	16.6	9.9	14.5	14.4	14.5	14.2	14.9	33.8	19.4	19.6	20.	16.3	19.
Cr_2O_3	0.0	0.0	0.0	0.0	0.0	0.0	0.0	0.1	0.0	0.1	0.0	0.0	0.0	0.0	0.0	0.0		0.0	
Fe_2O_3	0.2	0.1	2.9	0.3	9.3	3.6	1.8	3.9	1.6	2.6	0.2	0.0	0.4	3.0	0.0	1.1	0.0	9.3	0.0
FeO	4.7	0.9	10.2	0.6	19.1	10.7	9.9	12.6	15.2	9.1	0.1	0.6	0.4	0.5	0.3	1.5	0.3	14.9	1.7
MnO	2.7	0.2	0.2	0.1	0.8	0.3	0.2	0.3	0.2	0.2	0.0	0.0	0.4	0.0	0.0	0.1		0.9	
MgO	0.3	0.0	4.7	0.2	5.1	7.8	8.6	11.2	13.9	8.1	0.3	0.2	0.1	0.3	0.0	0.9		6.6	
CaO	0.7	0.9	9.2	1.0	0.2	8.3	6.2	12.0	0.9	9.5	0.6	1.9	0.6	0.1	0.7	2.4	2.	0.5	2.
Na_2O	4.6	6.4	3.4	5.4	0.0	2.8	2.4	1.6	0.2	2.6	3.0	3.7	5.4	0.9	6.6	7.4	8.	0.0	7.
K_2O	0.6	2.1	1.1	1.7	5.9	1.4	4.1	1.1	8.8	2.0	7.0	3.0	1.9	10.3	6.5	1.6	1.	7.8	1.
H_2O	0.4	0.3	0.9	0.2	5.2	2.5	2.1	1.4	3.6	1.9	0.3	0.0	0.3	4.4	0.0	0.5	0.5	3.6	0.8
Cl	0.03	0.03	0.05	0.03	0.14	0.04	0.04	0.03	0.04	0.03	0.02	0.01	0.02	0.01	0.02	0.01	0.02	0.04	0.03
F	0.02	0.01	0.04	0.01	0.28	0.11	0.78	0.76	1.50	0.24	0.01	0.01	0.02	0.11	0.01	0.09	0.05	0.57	0.06
P_2O_5	0.01	0.03	0.35	0.03	0.03	0.35	0.06	0.03	0.08	0.35	0.03	0.02	0.11	0.04	0.14	0.11		0.38	
CO_2	0.5	0.2	0.1	0.2	0.8	0.00	0.5	0.1	0.3	0.7	0.1	0.1	0.2	0.00	0.1	0.1		0.3	
S	0.01	0.00	0.02	0.02	0.13	0.04	0.0	0.08	0.27	0.08	0.03	0.06	0.01	0.08	0.06	0.06		0.09	
Ba	0.01	0.00	0.04	0.00	0.01	0.04	0.03	0.01	0.07	0.01	0.04	0.01	0.00	0.00	0.00	0.01		0.03	
Rb	0.01	0.03	0.01	0.01	0.19	0.01	0.04	0.00	0.26	0.01	0.03	0.01	0.02	0.20	0.04	0.02		0.15	
Sr	0.01	0.01	0.04	0.01	0.00	0.02	0.01	0.00	0.00	0.01	0.01	0.01	0.00	0.00	0.01	0.01		0.00	
Zn	0.01	0.01	0.01	0.01	0.08	0.01	0.01	0.03	0.09	0.01	0.00	0.00	0.00	0.00	0.08	0.00		0.06	
Zr	0.02	0.02	0.01	0.00	0.01	0.02	0.01	0.01	0.00	0.02	0.01	0.01	0.00	0.00	0.00	0.00		0.12	
U ppm	10	45	1	23	237	1	7	2	3	14	18	538	5	1	3	2440	14600	4460	27700
Th ppm	11	23	1	16	140	2	2	1	1	4	18	15	1	1	1	300	1100	630	2100
U/Th	1	2	1	1.4	1.7	0.5	3.5	2	3	3.1	1	36	5	1	3	8.1	13.3	7	13.2

* Chemical and spectrographic analyses by the staff of the Central Laboratories and Technical Services Division, Geological Survey of Canada. Uranium (ppm) determined by neutron activation analysis by Atomic Energy of Canada Ltd. Thorium (ppm) determined by X-ray Assay Laboratories Limited (NA method, detection limit 1 ppm).

** For sample locations see Fig. 17.1 in Rimsaite (1981a). See Appendix 1 for description of samples.

*** Estimates only due to unusual composition (U-rich samples).

minerals and accompanied leaching of radionuclides recorded in SEM micrographs and in EDS spectra, are discussed for the following associations of primary and secondary REE, radioactive and rock-forming minerals and their host rocks:

1. metasediments grading to garnetiferous feldspar pegmatites containing mafic xenoliths;
2. fergusonite-bearing pegmatite and rock-forming feldspars and micas;
3. biotite-hornblende gneiss hosting white radioactive pegmatites containing titanite, allanite and bastnaesite;
4. granite pegmatite containing associations of primary and secondary Pb, Ti, Nb, Th, U and Y minerals;
5. syenite pegmatite containing biotite, uraninite, uranothorite, zircon, apatite, allanite, xenotime, monazite, hydroxyl-bastnaesite and secondary amorphous phyllosilicates and U, Zr and REE mineral aggregates.

Calculated atomic percentages of ion exchange during replacement of primary minerals by secondary mineral aggregates indentified by X-ray diffraction (XRD, Rimsaite, 1982c) have been substantiated and documented here by actual semiquantitative SEM-EDS analyses of the same minerals (Tables 21.2, 21.3).

Paragenesis and alterations of radioactive and REE minerals studied in Baie-Johan-Beetz area have been compared with those reported for mineral deposits in Scandinavia (Nordenskiøld, 1868; Broegger, 1890; Sverdrup et al., 1959), Southern Europe (Maksimovic and Panto, 1978) and U.S.S.R. (Semenov et al., 1961; Dorfman and Senderova, 1964; Kupriyanova et al., 1964; Gerasimovsky et al., 1966; Pyatenko, 1966).

This study has been based on 57 analyses (Tables 21.1, 21.2, 21.3). In contrast, Russian geologists had many more analyses, amongst Russian workers, Gerasimovsky et al. (1966) based their conclusions on 3000 analyses of 67 elements and Ronov et al. (1967), who studies redistribution of REE and separation of Ce from light REE during weathering, had as many as 30 000 analyses.

Acknowledgments

I gratefully acknowledge the following analytical support: neutron activation analyses for U by the Atomic Energy of Canada Limited and for Th by the X-ray Assay Laboratories Limited; chemical and spectrographic analyses by the staff of the Analytical Chemistry Section Geological Survey of Canada; and X-ray identification of minerals by A.C. Roberts and scanning electron microscope and semiquantitative energy dispersive spectrometer analyses by D.A. Walker and G.J. Pringle all of the Geological Survey of Canada.

METASEDIMENTS GRADING TO GARNETIFEROUS FELDSPAR PEGMATITES CONTAINING MAFIC XENOLITHS

A vast area east of Baie-Johan-Beetz, including Gull Island, consists predominantly of peristerite-rich pegmatites which contain relicts of metasediments and of adjacent metagabbro. Peristerite crystals are fresh lamellar albitic oligoclase antiperthite which vary in colour from bluish grey to pink and strongly reflect light from the cleavage planes thus appearing like mirrors on a sunny day. In addition to peristerite, pegmatite contains local segregations of quartzite and garnet, the latter accounting for higher Fe and Mn contents in the spessartite-bearing portions of the rock (analysis 1, Table 21.1). The pegmatite also contains local concentrations of coarse biotite flakes, radiating crystals of tourmaline and allanite, and interstitial microcline and muscovite. The biotite is iron rich, partly altered to chlorite, and overgrown by muscovite, sericite and calcite. Garnet is crystallized in muscovite rims and is partly replaced by sericite. Other accessory minerals are apatite, titanite, zircon, magnetite and epidote. Unidentified radioactive mineral aggregates coat biotite flakes and are surrounded by pleochroic haloes. The radioactive titaniferous inclusions and crusts in biotite account for 237 ppm U and 140 ppm Th in the biotite concentrate (analyses 2 and 4: pegmatite, 5: biotite, Table 21.1).

Quartz and alkali feldspars penetrate metagabbro adjacent to pegmatite thus producing a patchy black and white rock resembling dalmationite. The metasomatically altered metagabbro consists mainly of green hornblende and less abundant biotite and magnetite which crystallized around white feldspathic patches. Metagabbro contains accessory apatite, epidote, Ti oxides and zircon (analysis 3, Table 21.1). Pegmatites associated with metagabbro are dry, leucocratic and contain less than 50 ppm U thus resembling dry feldspar pegmatites to the north on Turgeon Lake (Rimsaite, 1981a, Fig. 17.1, locality "B").

FERGUSONITE-BEARING PEGMATITE AND ROCK-FORMING FELDSPARS AND MICA

Specimens of fergusonite-bearing pegmatite were collected in a feldspar quarry on the north shore of Baie Quétachou, east of Baie-Johan-Beetz. The pegmatite consists mainly of white cleavelandite crystals which are intergrown with quartz, K-feldspar and muscovite, and locally contains biotite, spessartite (Mn-garnet) and/or large grains of fergusonite-polycrase-samarskite. The latter is amorphous to X-rays and produced a fergusonite-polycrase-like pattern only after heating (XRD = 65245, 65254). Energy dispersive spectra of the fergusonite showed the following element lines listed in order of decreasing intensities: Nb, Y, Ta, U, Th, Ti, Si, Al, Ca, Fe, Ce, Pb (Rimsaite, 1982c, Fig. 31.8h). This cleavelandite pegmatite contains abundant white mica which postdates crystallization of, and replaces along with calcite, all other minerals and substitutes for K-feldspar in antiperthitic blebs in cleavelandite-antiperthite. The muscovite is relatively rich in hydroxyl and poor in fluorine (analysis 14, Table 21.1), thus indicating low temperature of postmagmatic crystallization during a hydrothermal stage. Gerasimovsky (1964) discussed the relationship between the evolution stages of a pegmatite, the temperature of crystallization and the fluorine content in hydroxyl-bearing minerals. According to that author, the fluorine content in minerals decreases with decreasing temperature of crystallization and fluorine-bearing species which crystallized at higher temperature recrystallize to fluorine-poor species at the lower temperature of postmagmatic crystallization. The cleavelandite-pegmatite north of Baie Quétachou represents a late stage of magmatic crystallization and of postmagmatic hydrothermal crystallization (late hydroxyl-muscovite and sericite). The pegmatite contains 5 ppm U and 1 ppm Th, accounted for by samarskite-fergusonite. Concentrates of muscovite and of cleavelandite-K-feldspar intergrowths contain less U than the whole rock (analyses 15, 16, 17, Table 21.1).

BIOTITE-HORNBLENDE GNEISS HOSTING WHITE RADIOACTIVE PEGMATITES CONTAINING TITANITE, ALLANITE AND BASTNAESITE

White radioactive pegmatites underlain by biotite-hornblende gneisses occur in swampy areas north of Baie Pontbriand. Rocks exposed along the shoreline at low tide in Baie Pontbriand are red oxidized pegmatites interbanded with sheets of metagabbro (analysis 6, Table 21.1). The metagabbro consists of recrystallized euhedral hornblende crystals and less abundant biotite, plagioclase, accessory

Table 21.2. Distribution and relative abundance of radioactive and rare earth elements in primary and secondary U, Th, Pb, Ti, Nb, Y minerals and replacing phyllosilicates*

	Uranothorite and uraninite and their alteration products							Associations of U, Th, Pb, Ti, Nb, Y minerals											
	1	2	3	4	5	6	7	8	9	10	11	12	13	14	15	16	17	18	19
SiO_2 %	12.4	0.9	0.4	5.1	11.6	-	9.0	18.4	0.4	0.6	1.3	-	7.4	34.6	13.3	1.7	6.4	6.9	22.7
P_2O_5	2.7	-	-	0.5	0.9	-	1.7	2.7	-	1.8	-	-	-	-	1.4	-	3.4	6.0	-
SO_3	1.0	-	-	-	-	-	-	13.7	6.4	20.8	10.0	-	-	-	-	-	1.0	-	-
TiO_2	0.7	-	-	-	-	-	1.0	0.3	-	0.7	2.0	94.2	37.4	0.5	-	25.4	46.1	23.4	17.4
Nb_2O_3	-	-	-	-	-	-	-	-	-	-	-	1.5	3.1	0.2	-	17.7	0.8	1.4	-
Al_2O_3	1.1	1.1	-	0.4	0.4	-	4.9	2.6	-	-	0.4	-	-	21.8	1.1	1.1	1.5	1.5	8.7
FeO**	1.0	0.5	0.9	4.6	3.8	1.0	40.	6.9	0.3	0.3	0.8	1.5	2.4	14.5	2.3	5.7	5.4	4.6	33.0
MgO	-	-	-	-	-	-	0.3	-	-	-	0.4	-	-	11.4		-	-	-	4.6
CaO	0.3	0.3	1.9	1.7	3.6	-	0.3	0.5	3.1	1.4	1.4	-	-	-	0.8	2.0	1.7	3.4	0.3
Other	-	-	Mn	-	Cr,Mn	-	-	-	K	-	-	-	-	Mn	Ba,Cr	-	-	-	-
Y_2O_3	3.6	1.8	4.1	2.0	1.0	4.8	2.8	4.1	-	0.5	2.3	0.9	10.5	1.0	20.3	13.0	9.7	14.5	-
Yb_2O_3	-	-	-	-	-	-	-	-	-	-	-	-	-	-	2.1	-	-	-	-
Gd_2O_3	-	-	-	-	-	-	-	-	-	-	-	-	-	-	0.7	-	-	-	-
Dy_2O_3	0.7	-	-	-	-	-	-	-	-	-	-	-	-	-	1.8	-	-	-	-
Ho_2O_3	-	-	-	-	-	-	-	-	-	-	-	-	-	-	0.7	-	-	-	-
Er_2O_3	-	-	-	-	-	-	-	-	-	-	-	-	-	-	2.5	-	-	-	-
La_2O_3	0.7	-	-	-	-	-	-	-	-	-	-	-	-	-	-	-	-	-	-
Ce_2O_3	2.7	-	-	1.5	-	-	-	-	-	-	-	-	-	-	-	-	-	-	-
Nd_2O_3	2.1	-	-	-	-	-	-	-	-	-	-	-	-	-	-	-	-	-	-
PbO	-	10.6	8.6	6.3	3.0	8.4	4.1	23.8	16.0	41.0	19.9	-	-	-	0.4	-	1.7	1.1	-
ThO_2	42.6	8.4	6.2	13.9	3.2	3.9	3.2	6.2	-	5.5	16.9	-	4.3	-	14.6	3.2	3.9	5.0	-
UO_2	12.5	72.8	68.9	48.6	61.2	70.5	25.8	21.0	-	17.0	28.7	-	31.0	0.7	26.0	16.7	15.4	21.7	-
U/Th	0.3	8.9	11.1	3.6	19.1	18.0	8.0	3.4	-	3.1	1.7	-	7.2	-	1.77	5.0	4.5	4.3	-
Pb/U	-	0.15	0.12	0.13	0.05	0.12	0.16	1.13	-	2.4	0.69	-	-	-	0.02	-	0.11	0.05	-
Pb/Th	-	1.2	1.4	0.45	0.93	2.2	1.3	3.8	-	7.5	1.18	-	-	-	0.03	-	0.44	0.2	-

* Semiquantitative SEM-EDS analysis by G.J. Pringle on spectra collected by D.A. Walker at the SEM Laboratory, Geological Survey of Canada. See Appendix 2 for description of samples.

** Total iron reported as FeO.

titanite, magnetite, apatite and zircon. Plagioclase crystals have altered to sericite in the centre and biotite has been chloritized. The metagabbro and amphibolite contain only 1 ppm U and apparently did not contribute to the formation of radioactive occurrences in the area.

Biotite-hornblende gneiss is made up of mafic hornblende and/or biotite bands which contain abundant accessory minerals such as titanite, anatase, apatite, zircon and monazite all in a groundmass of plagioclase and quartz (analysis 7, Table 21.1). The hornblende and biotite from the gneiss contain more iron and less fluorine than biotite and hornblende from migmatite in the Bancroft area (analyses 8 and 9, Table 21.1 and analyses 11 and 12 in Rimsaite, 1982a, Table 3.1).

White pegmatite underlain by hornblende-biotite gneiss resembles white radioactive pegmatites in swampy areas in occurrence "E", west of Baie-Johan-Beetz (Rimsaite, 1981a, Table 17.1, analyses 8, 9), the main difference being the absence of hornblende, more prominent differentiation into microcline, albite, biotite and quartz-rich phases and higher radioactivity of the pegmatite in occurrence "E". The pegmatite north of Baie-Pontbriand also exhibits evidence of differentiation during the sequence of crystallization and locally mirrors mineralogical composition of the underlying gneiss. It contains portions enriched in plagioclase, in microcline and in hornblende-biotite intergrowths. The microcline-rich portions contain less uranium and lower U/Th ratio than pegmatite portions which contain similar proportions of plagioclase and microcline. Fine grained uranyl-bearing mineral aggregates which produce yellow stain on the white pegmatite account for 538 ppm U and for the high U/Th ratio of 36, whereas allanite accounts for 15-18 ppm Th in the pegmatite (analyses 10, 11, 12, Table 21.1). Allanite occurs in hornblende-biotite-rich patches. Biotite bands and streaks grade into titanite which in turn grades into allanite and bastnaesite. The allanite and bastnaesite crystallize late in the sequence of crystallization of the pegmatite and account for the presence of REE. Similar associations of allanite anf F-bearing REE carbonates have been described by Nordenskiöld (1868) for the type locality in Bastnäs, Sweden. Broegger (1890) who studied evolution of REE-bearing pegmatites reported concentrations of trivalent and of oxidized quadrivalent cerium in analyses of F-REE-carbonates which formed as overgrowths on eudidymite following crystallization of zeolites during the hydrothermal phase of crystallization. Oftedal (1929) studied the crystal structure of bastnaesite which also crystallized during a late stage of crystallization as overgrowths and replacements of fluocerite. In the above examples, REE carbonates have crystallized from postmagmatic hydrothermal solutions as overgrowths and replacements of REE-bearing and other accessory minerals.

GRANITE PEGMATITE CONTAINING ASSOCIATIONS OF PRIMARY AND SECONDARY Pb, Ti, Nb, Th, U AND Y MINERALS

Granite pegmatites associated with syenite were studied in radioactive occurrences "A", "D", "E" and in the Grandroy Deposit (Rimsaite, 1981a, Fig. 17.1, rock analyses 24, 25, 26, 27, 28, Table 17.2). Granite pegmatites are made up mainly of neosome microcline and variable proportions of quartz which invade and replace plagioclase-rich syenitic paleosome portions of a pegmatite. The content of silica, alumina, sodium, calcium, potasisum, iron and magnesium vary depending on proportions of microcline, quartz, remant plagioclase, type and amount of xenoliths and alterations (Rimsaite, 1981a, 1982a). Radioactive and REE minerals crystallized either within paleosome palgioclase grains, at the boundary between plagioclase and quartz, adjacent to biotite or in neosome portions of the rock. Mineralogical and chemical compositions of ore and accessory minerals depend on the environment and sequence of crystallization, thus xenotime, monazite, uraninite, uranothorite, zircon and apatite mineral association in remnants of plagioclase-rich paleosome (Fig. 21.1) has crystallized earlier than uraninite crystals surrounded by muscovite rims which crystallized in fractures of neosome quartz. Therefore several types of mineral associations can be found in a pegmatite which is made up of older (paleosome) and younger (neosome) portions (Rimsaite, 1980a, 1980b, 1983b). Furthermore, postmagmatic hydrothermal alterations and weathering may contribute to the diversity of associations of primary and secondary minerals.

Chemical changes and trends resulting from natural alteration and replacements of primary minerals by secondary mineral aggregates, were previously documented by X-ray diffraction (Rimsaite, 1982c). Tables 21.2 and 21.3 present semiquantitative SEM-EDS analyses and U/Th, Pb/U and Pb/Th ratios which illustrate the relative mobility, enrichment and depletion of these elements. They thus

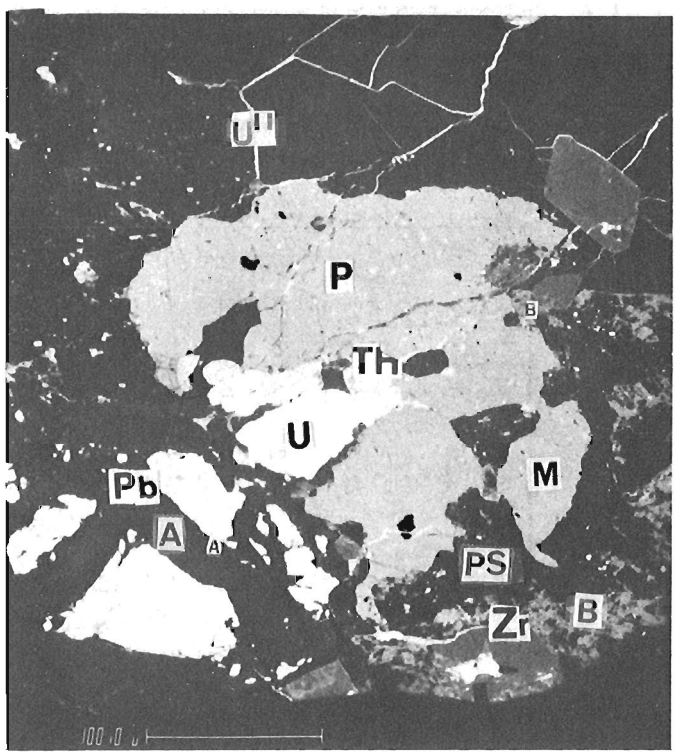

Figure 21.1. *Association of primary and secondary U, Th, REE, P, Pb and Zr minerals. Xenotime and monazite (phosphates, P, M) are intergrown with uraninite (U), uranothorite (Th), galena (Pb) and zircon (Zr). Monazite (M) has altered to amorphous and poorly-crystalline aggregates of bastnaesite-hydroxyl bastnaesite (B, XRD = 65197, 65246) which have been replaced by phyllosilicates (PS) of chlorite group, glauconite-celadonite, sericite and montmorillonite (XRD = 65164, 65163, 65185) and by disordered goethite (XRD = 65164). Galena (Pb, white) has been replaced by anglesite (A, black, XRD = 65246) along the fractures. Secondary uranium minerals (U^{II}), mainly kasolite, uranophane and phosphuranylite (XRD = 65248, 65250, 60159) crystallize in fractures and interstices forming white bands (GSC 203577-R). Figure 21.8 illustrates secondary U minerals in high power electron micrographs and their EDS (Energy dispersive spectra. Element lines are listed in order of decreasing intensities).*

Table 21.3. Distribution and relative abundance of radioactive and rare earth elements in primary and secondary P, REE, Zr, U, Th, Pb minerals and crusts*

	Phosphates, zircon and their alteration products							Pseudomorphous replacements of uraninite and crusts											
	1	2	3	4	5	6	7	8	9	10	11	12	13	14	15	16	17	18	19
SiO_2 %	-	3.4	1.3	6.0	30.0	32.1	9.6	8.6	13.3	16.7	10.3	18.0	13.3	1.3	-	-	9.8	8.1	5.6
P_2O_5	36.6	13.3	26.1	-	-	-	6.9	-	1.7	2.5	-	-	-	-	-	-	-	-	0.9
SO_3	-	-	-	-	-	-	tr	0.9	0.9	1.0	-	-	-	-	-	1.5	tr	-	-
TiO_2	-	-	-	-	-	-	-	-	-	-	-	-	1.3	-	-	-	31.3	0.3	20.0
Al_2O_3	-	-	-	3.0	17.8	-	1.1	2.7	1.5	3.0	-	-	2.6	0.4	-	0.8	0.8	3.4	1.1
Cr_2O_3	-	-	-	-	-	-	-	-	-	0.9	-	-	0.9	0.9	-	-	-	0.9	-
FeO**	-	-	-	-	17.3	0.5	0.3	22.2	3.1	13.2	0.8	0.5	7.0	4.1	0.3	-	8.3	8.5	1.8
MgO	-	-	-	-	12.6	-	-	-	-	-	-	-	0.7	-	-	-	-	0.7	-
MnO	-	-	-	-	0.3	-	-	-	-	-	-	-	-	-	-	-	-	-	-
CuO	-	-	-	-	0.5	-	-	1.2	-	-	-	-	-	-	3.6	1.8	-	-	-
ZnO	-	-	-	-	0.7	-	-	-	-	-	-	-	-	-	0.7	-	-	-	-
CaO	-	2.2	tr	3.0	tr	0.1	17.5	0.3	0.3	0.6	4.2	5.6	-	0.8	-	1.4	0.3	0.3	0.8
BaO	-	-	-	-	-	-	-	-	-	-	-	-	-	2.7	-	-	-	1.8	-
Na_2O	-	-	-	-	-	-	-	1.1	0.8	-	-	-	-	-	-	-	-	-	-
K_2O	-	0.2	-	0.5	tr	-	-	-	0.2	-	-	-	-	-	-	-	0.5	-	0.5
ZrO_2	-	-	-	-	-	64.0	12.4	6.5	15.9	18.4	-	-	-	-	-	-	-	-	-
HfO_2	-	-	-	-	-	2.1	-	-	1.3	1.1	-	-	-	-	-	-	-	-	-
Cl	-	-	-	-	-	-	-	0.2	0.4	-	-	-	-	-	-	-	-	-	-
Y_2O_3	45.0	17.5	-	-	-	-	1.0	2.5	4.3	3.0	-	-	-	-	2.0	3.6	4.6	-	3.6
Yb_2O_3	5.2	3.9	-	-	-	-	-	-	-	-	-	-	-	-	0.7	-	-	-	-
Gd_2O_3	2.1	-	-	-	-	-	0.2	1.2	-	-	-	-	-	-	0.5	0.7	0.6	-	-
Dy_2O_3	3.7	-	-	-	-	-	0.6	-	-	-	-	-	-	-	1.1	-	-	-	-
Ho_2O_3	0.7	-	-	-	-	-	-	-	-	-	-	-	-	-	-	-	-	-	-
Er_2O_3	2.5	1.4	-	-	-	-	-	1.1	1.4	-	-	-	-	-	0.2	-	-	-	-
Tb_2O_3	0.5	-	-	-	-	-	-	-	-	-	-	-	-	-	-	-	-	-	-
Tm_2O_3	0.5	0.7	-	-	-	-	-	-	-	-	-	-	-	-	-	-	-	-	-
Lu_2O_3	0.7	-	-	-	-	-	-	-	-	-	-	-	-	-	-	-	-	-	-
La_2O_3	-	-	14.3	13.6	-	-	0.7	-	-	-	-	-	-	-	0.2	-	-	-	-
Ce_2O_3	-	-	28.5	28.2	-	-	1.7	0.7	1.0	-	-	-	-	-	-	0.7	1.7	-	1.2
Pr_2O_3	-	-	2.6	2.3	-	-	0.2	-	-	-	-	-	-	-	-	0.2	-	-	-
Nd_2O_3	-	-	10.5	9.1	-	-	0.7	0.7	1.2	-	-	-	-	-	0.5	2.6	0.9	-	0.7
Sm_2O_3	-	-	2.3	-	-	-	0.2	-	0.5	-	-	-	-	-	-	1.2	-	-	-
PbO	-	1.3	-	0.9	-	-	0.2	0.4	-	-	3.0	0.2	27.9	18.1	4.1	-	7.8	16.2	1.9
ThO_2	-	1.6	4.3	1.8	-	-	13.2	0.9	1.8	12.3	4.1	0.7	-	0.2	tr	2.7	2.2	-	3.6
UO_2	-	38.2	-	0.5	0.9	-	5.0	20.0	31.4	19.9	64.9	58.3	36.7	61.4	0.2	23.1	21.8	44.2	38.9
U/Th	-	24.0	-	0.28	-	-	0.38	22.2	17.4	1.62	15.8	83.3	-	307.	-	8.6	9.9	-	10.8
Pb/U	-	0.04	-	1.80	-	-	0.04	0.02	-	-	0.05	0.01	0.76	0.3	20.5	-	0.36	0.36	0.05
Pb/Th	-	0.8	-	0.50	-	-	0.02	0.44	-	-	0.73	0.24	-	90.5	-	-	3.54	-	0.53

* Semiquantitative SEM-EDS analysis by G.J. Pringle on spectra collected by D.A. Walker at the SEM Laboratory, Geological Survey of Canada. See Appendix 3 for description of samples.

** Total iron reported as FeO.

supplement the earlier calculated atomic proportions of liberated ions given in Rimsaite, 1982c, Tables 31.1, 31.2). In order to distinguish between the effects of sequence and environment of crystallization on various types of alteration and reactions between adjacent minerals in complex mineral assemblages, the following discussion has been subdivided into subsections dealing with alterations of U, Th, Pb minerals, with U and Ti minerals, and with Ti, Nb, Y pyrochlore-like minerals.

Primary Th and U minerals, their pseudomorphous replacements and alteration

Radioactive occurrences in Baie-Johan-Beetz area commonly contain more uranium than thorium (Rimsaite, 1981a, Table 17.2). Thorium is present in uranothorite, in the structure of uraninite and as uranothorite phase replacing uraninite (analyses 1 and 4, Table 21.2; Rimsaite, 1980a, Fig. 38.1, 38.3). Uraninite grains analyzed contain 8.4 to 3.9% Th in their structure, depending on the availability of Th and on the sequence (and thus temperature) of crystallization. Uraninite containing more Th (8.4%) has crystallized in association with monazite, xenotime and uranothorite in plagioclase paleosome adjacent to biotite. Uraninite having an intermediate Th content (5-6%) has crystallized either in plagioclase paleosome altered to sericite or in fractured quartz in muscovite rims. Muscovite represents late stages of magmatic crystallization and initial phases of hydrothermal alteration. Uraninite having the lowest Th content in the structure (3.9% Th) is associated with pyrochlore and crystallized in prominent chlorite/serpentine rims during an advanced hydrothermal phase of crystallization in altered rocks in which biotite has been almost entirely replaced by chlorite and feldspar by sericite (analyses 2, 3, 6, Table 21.2, Fig. 21.1, 21.2). When a Th-Si phase replaces part of uraninite, the uranium content and U/Th ratio in the replaced portion markedly decrease (analysis 4, Table 21.2; Rimsaite, 1982a, Table 3.2). Phyllosilicate rims on uraninite commonly have U-rich spots and outer rims which contain less Pb and Th than the host uraninite (analyses 3 and 5, Table 21.2).

Lead is the natural decay product of uranium and thorium. The chemical lead/uranium ratio has been used to estimate approximate age of uranium mineralization using Pb and U values obtained on fresh grains of uraninite (Cameron-Schimann, 1978). However, lead is one of the most mobile elements during alteration of uraninite and it follows two opposite trends, namely that of enrichment or of depletion compared with the host (Pb/U and Pb/Th ratios in Tables 21.2 and 21.3).

Replacements of uraninite by Pb-rich phases are common in the Baie-Johan-Beetz area and have been studied on samples from occurrences "AB", "D", "E" and from the Grandroy Deposit (Rimsaite, 1981a, Fig. 17.1, 17.3A-E, 17.4C). The Pb-rich pseudomorphs after uraninite include oxides (unnamed $PbUO_4$), hydrated oxides (unnamed $Pb_2U_5O_{17}{\cdot}3H_2O$), uranyl silicates, kasolite, Fe-rich gummite, galena, anglesite and hydrocarbons (analyses 7, 8, 9, 10, 11, Table 21.2; analyses 13, 14, 15, 16, Table 21.3; Rimsaite, 1982c, Table 31.1). The pseudomorphous replacement of uraninite by Pb-rich phases and the destruction of the replacing phases took place in a series of the following steps: (1) uraninite was replaced by galena which in turn was oxidized to anglesite; (2) through action of CO_2-bearing groundwater, anglesite was pseudomorphously replaced by cerussite which in turn altered to a Pb-bearing carbonaceous substance containing low concentration of heavy cations, thus giving low totals on SEM-EDS analyses (analyses 9, 10, 11, Table 21.2; analyses 14, 15, 16, Table 21.3). Most grains of the altered uraninite retain remnants of the successive alteration products. However, most of the alteration

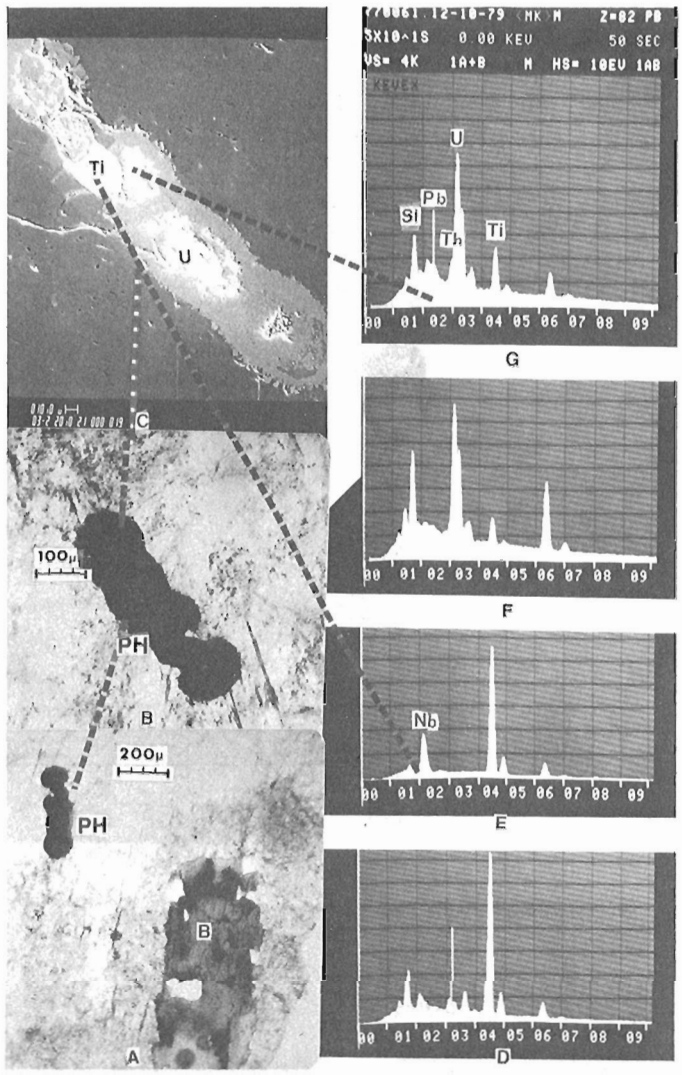

A – Photomicrograph of altered biotite (B) and chain of attached phyllosilicate rims (PH) which contain black pleochroic haloes enclosing uraninite, rutile and complex U-Ti grains.

B – Chain of Fe-rich phyllosilicates (PH), enlarged from "A".

C – BEI (Backscattered electron images) of the Fe-rich phyllosilicate rims (grey, XRD = 65201: chlorite-serpentine) which enclose Ti and U minerals illustrated in a photomicrograph "B".

D – EDS of Ti-rich grains in "C" (Ti>Si>Nb = Ca>Fe =U).

E – EDS of niobian rutile in "C" (Ti>Nb>Fe>Si, XRD = 65231: rutile, anatase, chlorite).

F – EDS of Fe-bearing coffinite-like minerals associated with uraninite (U) and Ti-oxides (Ti) in "C" (U>Si>Fe>Ti = Al, Ca).

G – EDS of U-Si-Ti-bearing grains in "C" which are probably reaction products between altered niobian anatase and uraninite (XRD = 65236). EDS element line intensities: U>Si>Ti>Th>Nb>Pb>Ca = Fe.

Figure 21.2. *Association of uranium and titanium-niobium minerals enclosed in altered biotite and/or in Fe-rich silicate rims (GSC 203577-W).*

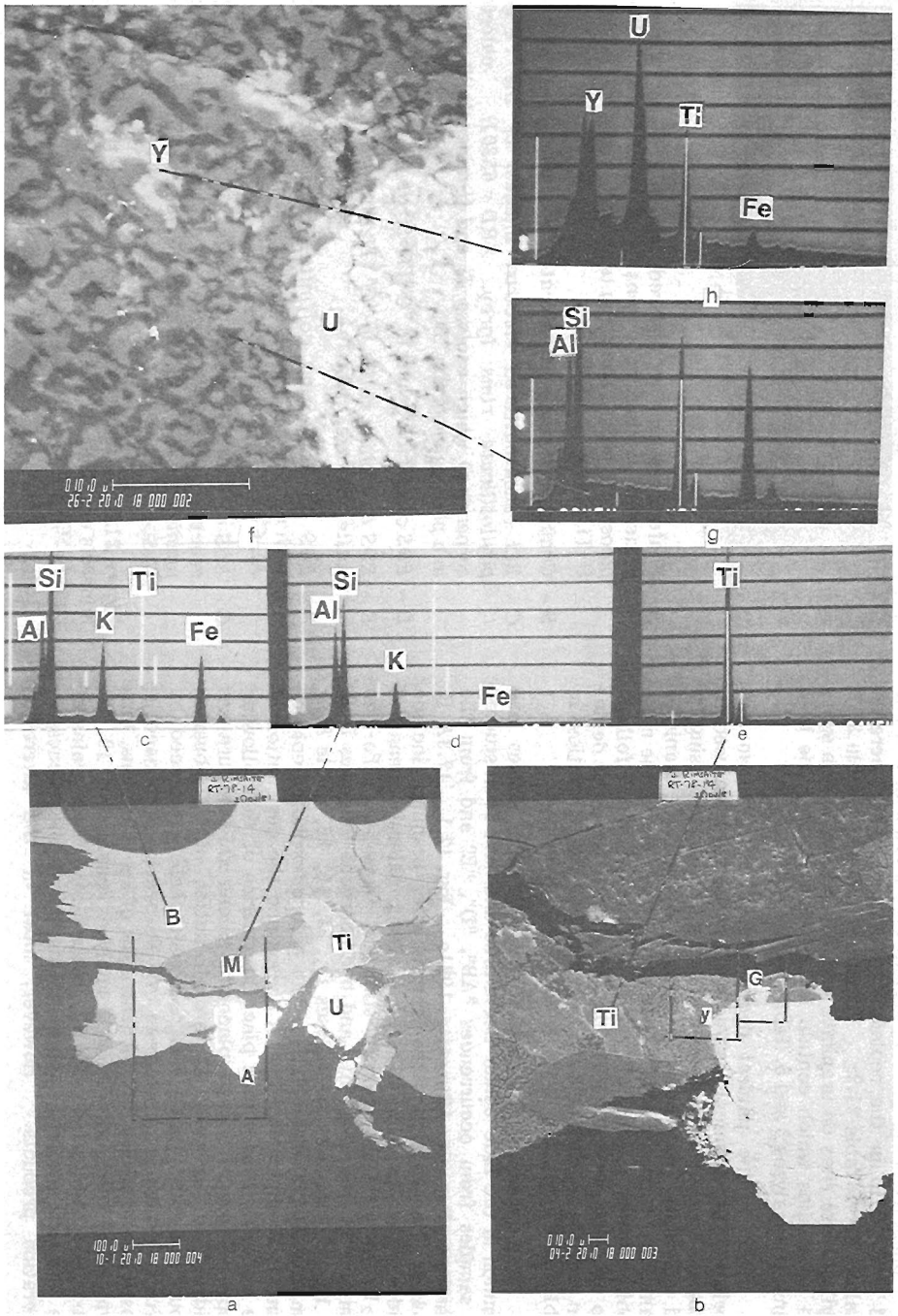
Y
U
f
U
Y
Ti
Fe
h
Si
Al
g
Si
Al
Ti
K
Fe
c
Si
Al
K
Fe
Ti
d
e
B
M
Ti
U
A
a
Ti
C
y
b

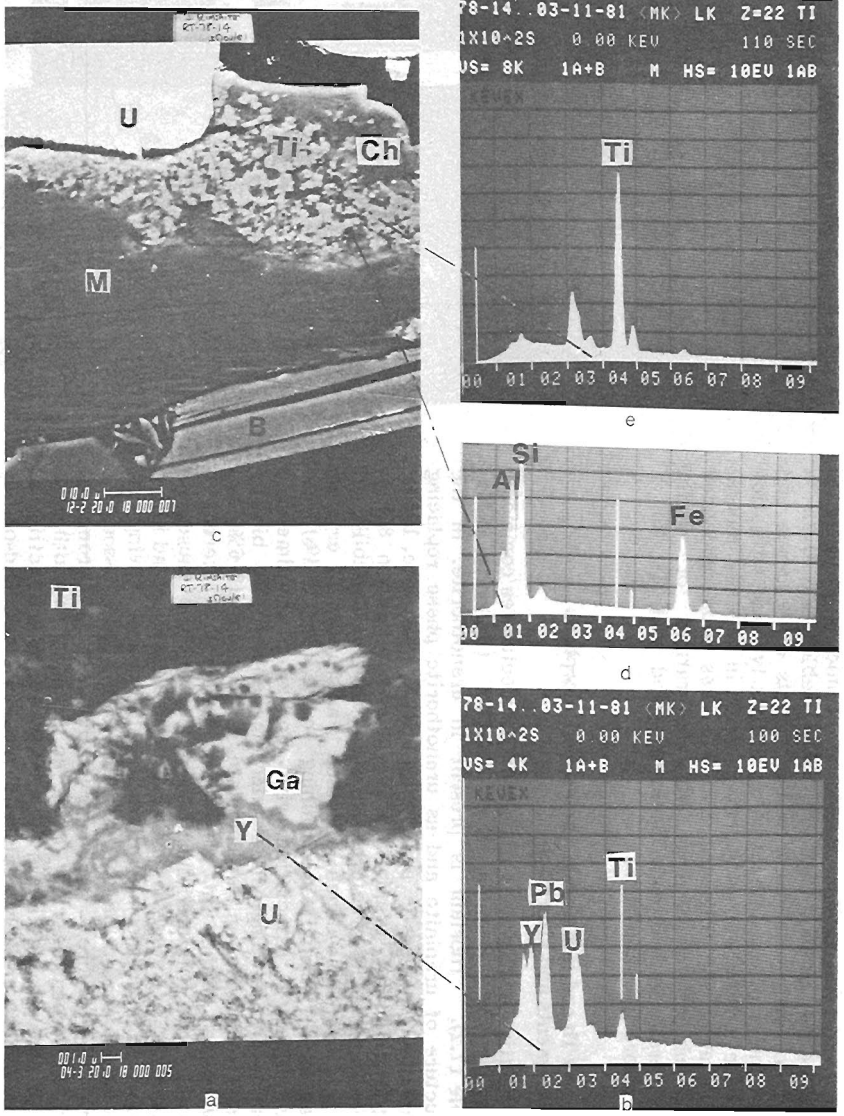
U
Ti
Ch
M
B
c
78-14..03-11-81 (MK) LK Z=22 TI
1X10^2S 0.00 KEV 110 SEC
VS= 8K 1A+B M HS= 10EV 1AB
Ti
00 01 02 03 04 05 06 07 08 09
e
Si
Al
Fe
00 01 02 03 04 05 06 07 08 09
d
Ti
Ga
Y
U
a
78-14..03-11-81 (MK) LK Z=22 TI
1X10^2S 0.00 KEV 100 SEC
VS= 4K 1A+B M HS= 10EV 1AB
Pb
Y
U
Ti
00 01 02 03 04 05 06 07 08 09
b

a – *BEI of intergrowths of biotite (B), muscovite (M), altered Ti oxides (Ti) and uraninite (U).*

b – *Enlarged portion "A" from "a" with marked areas "y" and "G" for further magnification of contact zones between uraninite and Ti oxides in "f" and in Figure 21.4.*

c – *EDS of biotite in "a" (Si>Al≥K≥Fe>Mg).*

d – *EDS of muscovite in "a" (Si≥Al>K>Fe).*

e – *EDS of rutile and anatase in "a" and "b" (Ti).*

f – *Enlarged portion "y" from "b" showing a contact between uraninite (U) and Ti oxide (mottled grey) which contains patches of unidentified Y-bearing mineral aggregates (Y, pale grey).*

g – *EDS of altered Ti oxide in "f" (Si≥Ti≥Al≥Fe).*

h – *EDS of Y-bearing mineral aggregates in "f" (U>Y = Si≥Ti>Fe).*

Figure 21.3. *Association of U, Ti, Y minerals in phyllosilicates (GSC 203724-H,F).*

a – *BEI of yttrian contact zone (Y) between uraninite (U) and a rim of galena (Ga) in altered Ti oxide (Ti).*

b – *EDS of yttrian phase in "a" (Pb>Y = U≥Si≥Ti>Fe).*

c – *BEI of remnant Ti oxides (Ti) partly replaced by chlorite (Ch) in muscovite (M) adjacent to uraninite (U) and biotite (B).*

d – *EDS of chlorite in "c" (Si≥Al>Fe>Mg). Note high peak of Al inferring that the Al-rich chlorite has formed from muscovite.*

e – *EDS of remnant Ti oxide which apparently reacted with adjacent uraninite (Ti>U).*

Figure 21.4. *Enlarged portion "G" from Fig. 21.3b showing yttrian contact zone between uraninite and Ti oxide which has been corroded and partly replaced by chlorite (GSC 203724-K). Table 21.2 presents semiquantitative analyses of the minerals.*

products are amorphous to X-rays and have been identified in their back scattered electron micrographs by different shades of grey and in their changing EDS spectra (Rimsaite, 1981a, Fig. 17.3; 1982c, Fig. 31.2). Similar trends of alteration of oxidized galena have been discussed by Dorfman and Senderova (1964), and carbonaceous alteration products retaining some REE have been described by Kupriyanova et al. (1964) who studied alterations in a molybdenum deposit which contained monazite, allanite and pyrochlore in addition to molybdenite.

An opposite alteration trend of uraninite which resulted in Pb-poor alteration products took place during advanced stages of hydration when uraninite and kasolite have been replaced by coffinite and ultimately by uranophane aggregates (analyses 11, 12, Table 21.3). During pseudomorphous replacement by uranophane, uraninite loses about 10% U and almost its entire Th and Pb contents. The ultimate weathering products of surficial alteration are Si-Al clays where all radioactive elements have been removed from the weathered portions of a deposit (Rimsaite, 1982d).

Associations of primary and secondary U, Ti and Y minerals

Uraninite grains intergrown with ilmenite, rutile, anatase or titanite commonly crystallize in or adjacent to micas (Fig. 21.3, 21.4; Rimsaite, 1982a, Fig. 3.3a,b; 1983a, Fig. 3.4b). Titanium oxide grains adjacent to uraninite appear corroded and are partly replaced by chlorite-like phyllosilicates containing patches of Y-bearing mineral aggregates (analyses 12, 13, 14, 15, Table 21.2). The Y-bearing phase contains heavy REE and is amorphous to X-rays. It has also crystallized adjacent to galena- and phyllosilicate-bearing rims of uraninite. At the contact, altered Ti and U oxides and the unidentified yttrian phase reacted with one another and formed an unidentified Ti-U-Y-Si-Th mineral phase which has a high U/Th ratio of 7.2 (analysis 13, Table 21.2).

The rutile-anatase has been ultimately replaced by Al-rich chlorite which apparently derived its Al from the muscoite groundmass (Fig. 21.4). Part of the titanium leached from rutile reacted with U, Si, Y and other ions and thus remained at the site of crystallization, whereas about 30% Ti has been removed. The alteration of Ti oxides took place during an advanced hydrothermal phase associated with replacement of micas by chlorite. The Ti minerals contain some Nb. The Nb/Ti ratio increases in the complex (hydrothermal?) Ti-bearing mineral aggregates (analyses 12, 13, Table 21.2).

Associations of uraninite, uranothorite, pyrochlore, chlorite, titanite and carbonates

Uraninite, pyrochlore and titanite occur in prominent chlorite-serpentine rims in microcline-rich granite pegmatites affected by postmagmatic hydrothermal alteration (Fig. 21.2, 21.7C, analyses 16, 17, 18, 19, Table 21.2). The pyrochlore from the Baie-Johan-Beetz area contains higher concentrations of titanium than that of niobium and thus differs from the pyrochlore from the Bancroft area which contains more Nb (Fig. 21.7C-5, analysis 16, Table 21.2; Rimsaite 1982a, analyses 3, 3a, 15, 16, 17, Table 3.2; 1983b, Fig. 11.8). The Nb and Ti minerals apparently crystallized during hydrothermal phase of crystallization. The pyrochlore contains marked quantities of U and Y (9.7%-21.7%), less abundant Th (the U/Th ratio being between 4.3 and 5), and possibly a trace of Pb (or Pb quantity below limits of detection). The radioactive Ti-Nb minerals contain Y in their structure and in disseminated secondary yttrian inclusions and specks (Fig. 7; Rimsaite, 1981a, Figs. 17.5A, 17.6B). Pyrochlore group minerals were

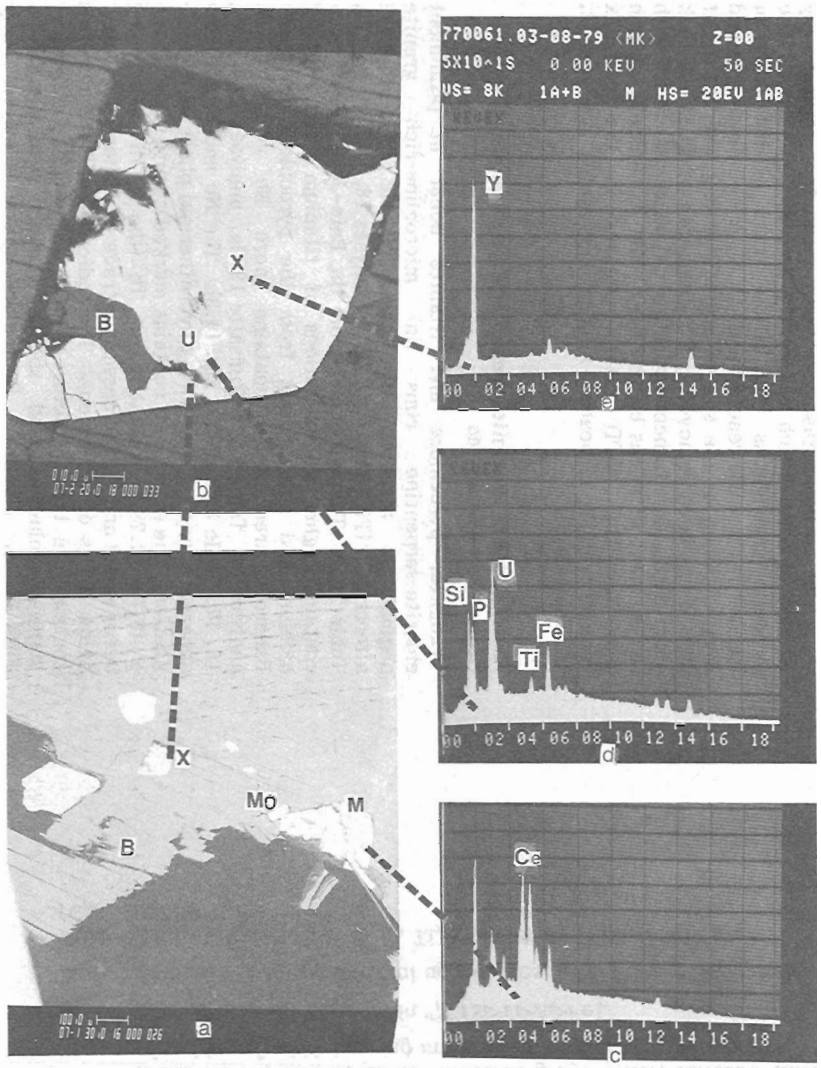

Figure 21.5. *Association of xenotime, monazite, molybdenite and radioactive minerals in biotite (GSC 203532-Q). Table 21.3 presents semiquantitative analyses of the minerals.*

a – BEI of biotite with disseminated crystals of xenotime (X), monazite (M) and molybdenite (Mo, XRD = 60162: molybdenite 2H).

b – BEI of xenotime (X) which has inclusions of biotite and U mineral, (U), xenotime crystal enlarged from "a".

c – EDS of monazite in "a" (P>Ce>La>Th>Ca); analysis 2 in Table 21.3.

d – EDS of uraniferous inclusion in xenotime in "b" (U>Si>P>Fe>Ti).

e – EDS of xenotime in "b" (Y overlaps with P).

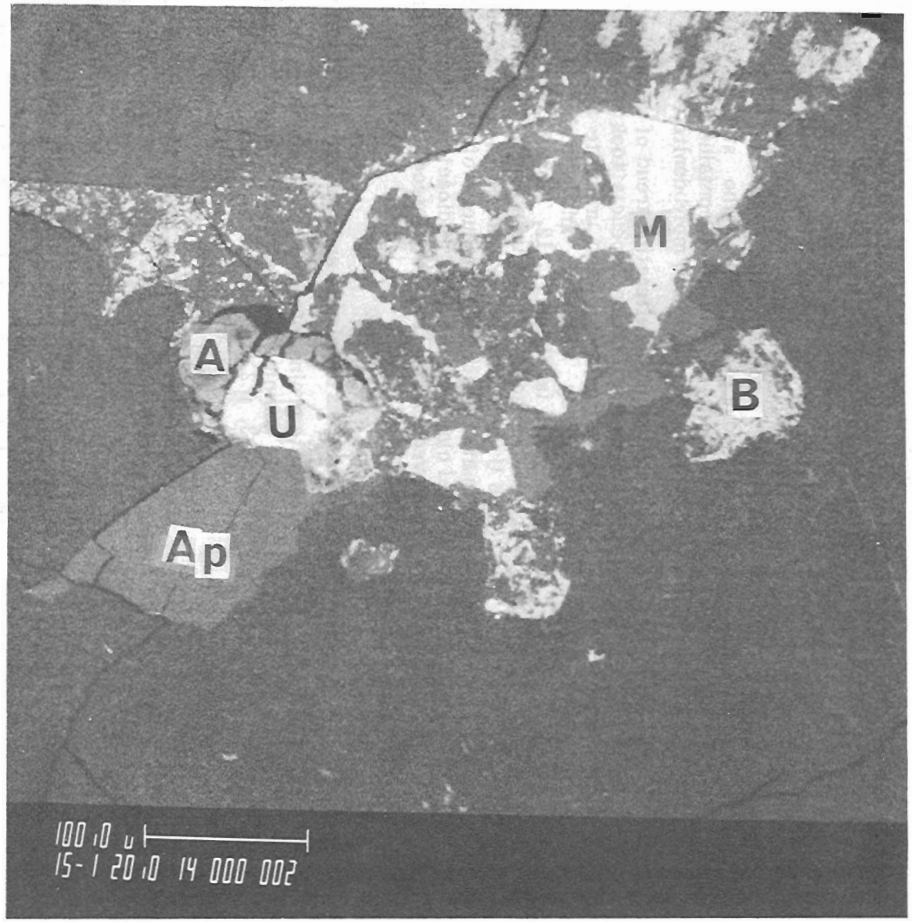

Figure 21.6. *Association of primary and secondary REE and radioactive minerals. Alteration of monazite (M) to bastnaesite (B) and to phyllosilicates. Monazite is associated with apatite (Ap), altered uraninite (U) and galena altered to anglesite (A). Grandroy Deposit (GSC 203414-Q). Additional examples of REE phosphates partly replaced by bastnaesite-like aggregates are documented by Rimsaite (1981a, Fig. 17.5C; 1981b, Fig. 4.3B).*

metamict and showed a great diversity in chemical composition within a single crystal. Similar chemical variations and substitutions in the pyrochlore structure, such as of Na(Ta) by Ti; OH, F by O; ClO_2 and CaF_2 by oxonium, and causes for the metamict state of pyrochlore have been postulated by Pyatenko (1966). In occurrence "D" in the Baie-Johan-Beetz area, Ti-U-Th-(Nb)-Y minerals have been altered. Titanite was replaced by anatase and brookite aggregates embedded in calcite. Ti and U released from adjacent altered Ti and U minerals reacted to form brannerite-like U-Ti mineral aggregates having variable U/Ti ratios and variable Si content, similar to that in the Bancroft area (Rimsaite, 1982c, Fig. 31.7b,c,e,f; 1983a, analyses 7, 8, Table 3.1). Chlorite-serpentine rims enclosing uraninite, pyrochlore and U-Ti-bearing minerals are rich in iron and contain Ti inclusions. Similar Fe-rich rims on uraninite have been found in the leucocratic ore in the Bancroft area (Rimsaite, 1980, Fig. 38.3).

SYENITE PEGMATITE CONTAINING BIOTITE, URANINITE, URANOTHORITE, ZIRCON, APATITE, ALLANITE, XENOTIME, MONAZITE, HYDROXYL-BASTNAESITE AND SECONDARY AMORPHOUS PHYLLOSILICATES AND U, Zr, AND REE MINERAL AGGREGATES

Syenite pegmatites are made up mainly of paleosome remnants rich in oligoclase crystals and contain local segregations of recrystallized biotite and complex associations of ore and accessory minerals (analyses 16, 17, 18, 19, Table 21.1, Fig. 21.1, 21.5, 21.6). Although many primary and secondary accessory minerals cluster together, several groups, such as phosphates, titanium-uranium-yttrium-zircon minerals and secondary mineral associations in fractures will be discussed separately.

Association of apatite, REE phosphates and carbonates, allanite and secondary amorphous silicates

A common complex mineral association consists of apatite, allanite, galena, monazite which is partly replaced by bastnaesite, uraninite, uranothorite, xenotime zircon and secondary phyllosilicates (Fig. 21.1, 21.6). Apatite, monazite and xenotime crystallize in biotite or in oligoclase adjacent to biotite. Xenotime commonly contains inclusions of uraninite and uranothorite which may react with the host to form yttrian envelopes around radioactive inclusions (analyses 1 and 2, Table 21.3). Xenotime hosts heavy REE, whereas monazite contain thorium (4.3%) and light REE listed in the following order of decreasing abundance: Ce, La, Nd, Pr, and Sm. Although REE phosphates are considered to be among the most stable minerals resistant to alteration and commonly form detrital deposits of REE and Th, mineralogical studies of radioactive and REE occurrences in the Grenville structural province showed that in an uraniferous environment, apatite, monazite and xenotime alter. They liberate phosphoric acid which can react with uranium to form secondary uraniferous phosphates (Rimsaite, 1982b, 1982c, Fig. 31.3). Monazite is overgrown by, and locally has altered to REE carbonates of the hydroxyl-bastnaesite group and to poorly crystallized and amorphous REE mineral aggregates and phyllosilicates (Fig. 21.6; Rimsaite, 1979, 1982c, Fig. 31.4a,c,d). The bastnaesite-like overgrowths on monazite contain higher proportion of La than does the host monazite, whereas hydroxyl-bastnaesite which replaces monazite contains similar proportions of REE to those in the monazite (analyses 3 and 4, Table 21.3). The monazite and associated bastnaesite have been altered and ultimately replaced by fine grained amorphous or poorly crystalline REE mineral aggregates and phyllosilicates, including chlorité, glauconite-celadonite, sericite and disordered goethite. Poorly crystallized bastnaesite which forms in an amorphous REE-bearing groundmass has also been described by Sverdrup et al. (1959). Several modes of occurrence and diverse relationships between allanite, monazite and bastnaesite have been postulated in the literature. Those include: (1) bastnaesite crystallizing after allanite and monazite (this study and Sverdrup et al., 1959); (2) bastnaesite replacing parisite and altering to rhabdophanite, a hydrous REE phosphate (Semenov et al., 1961); (3) anhydrous REE carbonates replaced by F-bearing bastnaesite, which in turn was replaced by hydroxyl-bastnaesite (in turn altered to allanite and partly replaced by monazite) i.e.: anhydrous REE carbonates, followed by F-bastnaesite, by OH-bastnaesite, by allanite and by monazite (Zdorik, 1966); (4) monazite, lanthanoan bastnaesite and Nd-synchisite are all secondary and have crystallized in karstic bauxite (Maksimovic and Pantó, 1978).

Because Ce oxidizes and by changing its valency from 3 to 4 becomes soluble and can easily be removed, and because ^{144}Ce is one of the fission products, natural behaviour of Ce is of scientific and practical importance, particularly in connection with fixation of ^{144}Ce in proposed nuclear waste disposal sites (Rimsaite, 1982d). Thus the stability and separation of Ce from the other REE has been studied by several investigators, including Ronov et al. (1967), Balashov and Kudinov (1966), and Maksimovic and Pantó (1978). The last reference discussed redistribution of REE during latheritic weathering among secondary alteration products. Neodymium and lanthanum have been fixed in bastnaesite group minerals: bastnaesite-La and synchisite-Nd and Ce, Nd and La in secondary monazite. These and the studies referred to previously indicate that carbonates can temporarily capture Ce and thus delay contamination of the environment. However, Balashov and Kudinov (1966) and Ronov et al. (1967) who studied the stability of REE in laboratory and in nature, showed that Ce oxidizes in slightly alkaline environment at Eh = + 0.3 and becomes soluble. Furthermore, Ce can be removed from Ce-bearing minerals by leaching with bicarbonate-bearing ($NaHCO_3$, $KHCO_3$) solutions. All REE carbonates and calcite are soluble in acid solutions of 3.5 pH. Before being destroyed and ultimately replaced by phyllosilicates, allanite, monazite and F-bearing bastnaesite can be replaced by metastable OH-bastnaesite (Fig. 21.6; Gerasimovsky, 1964; Zdorik, 1966). Supergene REE carbonates commonly contain more La and Nd than the associated secondary monazite (analyses of La-bastnaesite, Nd-synchisite and of secondary monazite in Maksimovic and Pantó, 1978). Mineralogical and crystallographic data on hydroxyl-bastnaesite (kischtymite) and on F(OH)-bastnaesite can be found in Struntz (1944).

The example provided here in Figure 21.6 shows that about one third of the monazite has been replaced by bastnaesite which has similar proportions of REE to that in monazite, and about one third of monazite and bastnaesite has been replaced by phyllosilicates. This suggests that about one third of the original REE has been removed from the site of crystallization.

In the Grandroy Deposit, allanite is less abundant than associated coffinite, bastnaesite, monazite and biotite. Allanite in intergrowths with coffinite (XRD = 65117) crystallizes late in the sequence of crystallization as overgrowths on biotite and associated accessory minerals. The chemical composition of allanite apparently depends on the mineralogical-petrographic environment of crystallization. Thus, according to Zdorik and Kupriyanova (1964), allanite from carbonatite is rich in Al and ferrous iron, whereas allanite from alkalic rocks is poor in Al, rich in ferric iron, has high Si/Al ratio of more than 4 and Fe/Al ratio of more than 1. Allanite crystals from radioactive occurrences in the Grenville structural province are generally poor in alumina

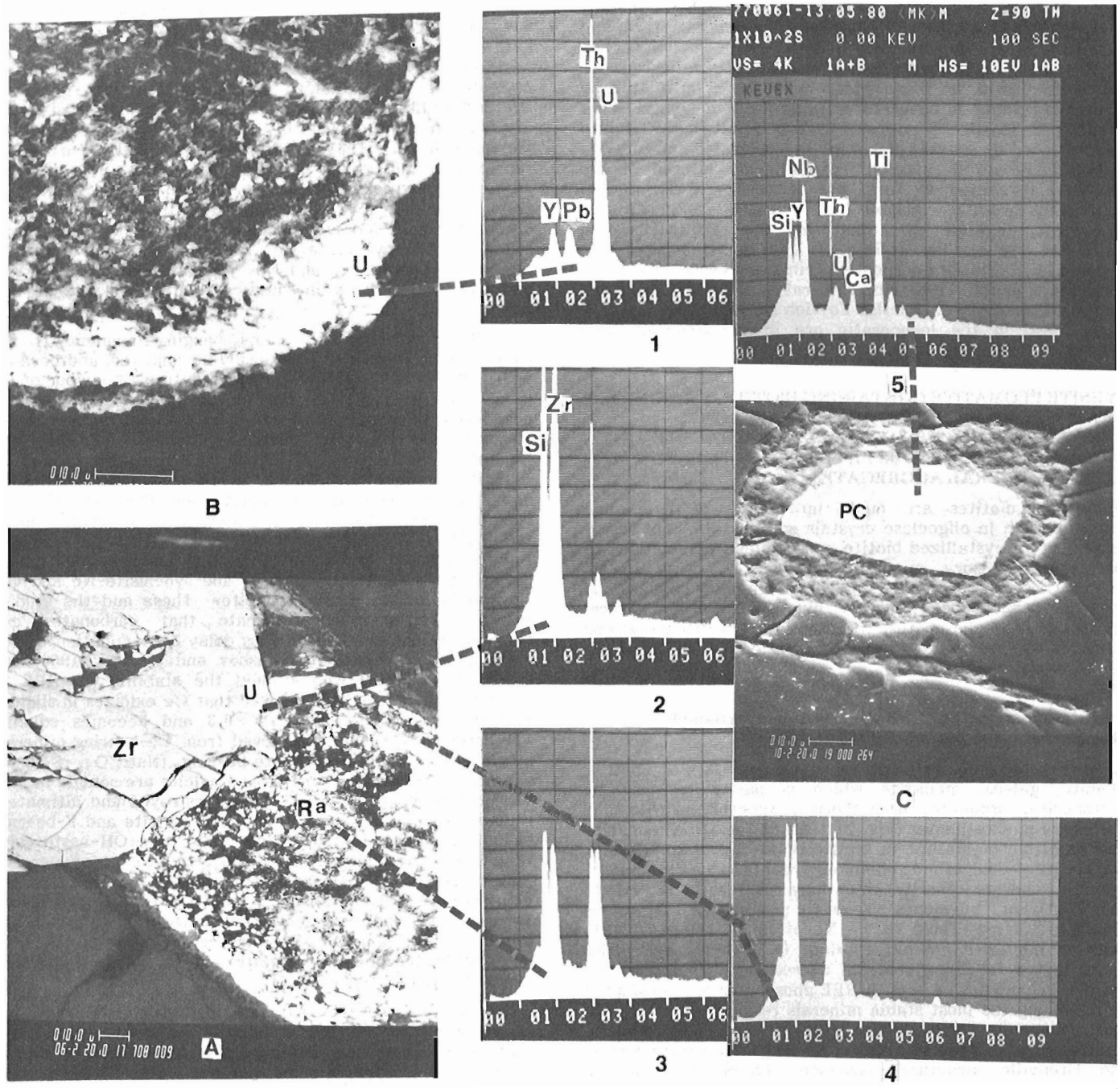

A – BEI of zircon (Zr) intergrown with metamict, altered Si-Y-U-Th grain (Ra). Fractured zircon has an uraniferous edge (U).

B – Enlarged edge of Si-Y-U-Th grain in "A". The edge consists of coffinite and uraninite (XRD = 65213: coffinite structure and uraninite).

1. *EDS of white rods in uraninite-coffinite edge in "B" (U>Th>Y = Pb).*
2. *EDS of radioactive edge (U) in zircon in "A" (Zr = Si>U = Th>Ca>Fe).*
3. *ED spectrum of metamict Si-Y-U-Th grain in "A" (Si≥Y≥U = Th).*
4. *EDS of another spot in the metamict Si-Y-U-Th grain in "A" (Si = Y≥U>Th, low Fe, Ti, Ca). Note lower intensity of Th peak of spectrum 4 compared to that in spectrum 3.*

C – Metamict pyrochlore (PC, XRD = 65203: metamict) in Fe-rich rim of phyllosilicates (XRD = 65021: chlorite and/or serpentine).

5. *EDS of pyrochlore in "C" (Ti≥Nb>Y≥Si>U>Ca> Th>Fe>Ce).*

Figure 21.7. *Association of U, Th, Y, Si minerals and zircon. Pyrochlore grains enclosed in rims of Fe-rich chlorite-serpentine aggregates. Similar Y-bearing grains occur also in anatase aggregates (Rimsaite, 1981a, Fig. 17.5A). GSC 203577-Q,V*

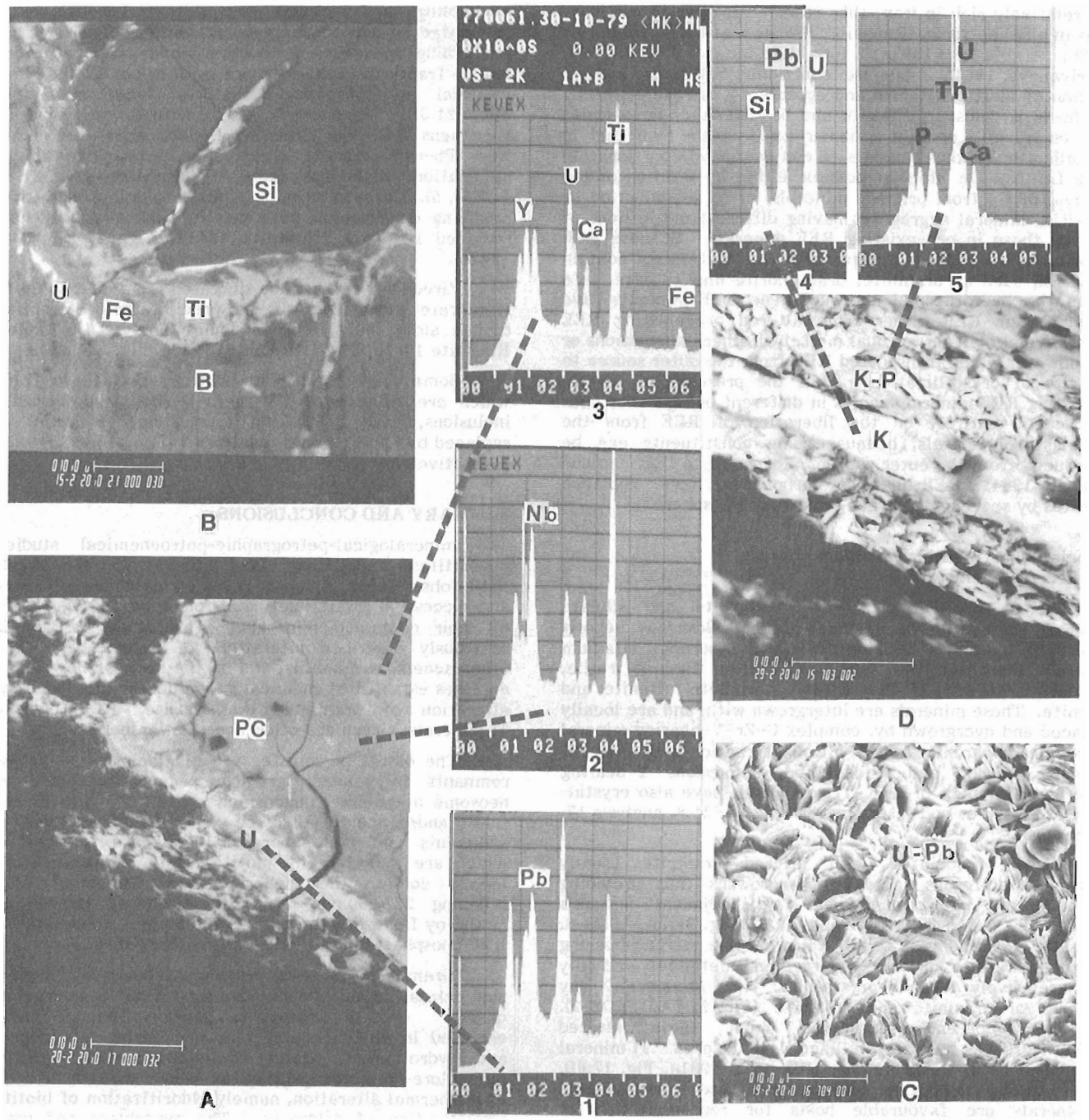

A – BEI of mottled pyrochlore with lacey U-rich rims (U) which extend into fractures of adjacent rock-forming minerals.

B – BEI of three types of mineral aggregates filling interstices and fractures in biotite (B) and quartz (Si): Fe-rich (Fe, dark grey); Ti-Si-Ca-U-Pb (Ti, light grey) and U-Si-Fe-Pb-Ti (U, white).

1. *ED spectrum of U-rich rim on pyrochlore in "A" (U>Pb = Ti≥Si>Nb>Ca>Th = Ce>Fe.*
2. *ED spectrum of grey Ti-Nb-rich phase in pyrochlore in "A" (Ti>Nb>Si = U = Ca>Y>Ce>Fe>Nd).*
3. *ED spectrum of light grey U-Y-rich phase in pyrochlore in "A" (Ti>U>Y = Nb Si≥Ca>Fe).*

C – BEI of crenulated, U-Pb-rich flakes (U-Pb) filling fractures and vugs in Grandroy Deposit (compare Fig. 21.1, U^{II}).

D – BEI of secondary U mineral aggregates, maily kasolite, uranophane, boltwoodite and phosphuranylite (K, P) filling fractures and interstices between altered uraninite and monazite and Grandroy Deposit.

4. *ED spectrum of dense white band in "D" (U>Pb>Si; XRD = 61182: kasolite).*
5. *EDS of flaky mineral aggregates in "D" (U>Pb = Si≥P = Ca>Ce), probably intergrowths of kasolite and phosphuranylite (XRD = 60159).*

Figure 21.8. *Heterogeneous, mottled pyrochlore. Radioactive and REE mineral aggregates in fractures and interstices (GSC 203577-Z)*

and relatively rich in iron, thus resembling allanite compositions in alkaline rocks (Rimsaite, 1983a, analysis 5, Table 3.2; 1982b, Table 1; 1982c, Fig. 31.6a,b,c,d; Zdorik and Kupriyanova, 1964). Allanite commonly postdates crystallization of biotite, titanite and epidote. It is overgrown by and hosts K-feldspar, chlorite and bastnaesite. Bastnaesite rims on allanite contain a higher La/Ce ratio than that in host allanite and thus bastnaesite can capture proportionately more La than Ce which is possible either by addition of La, removal of Ce from primary minerals, or by introduction of new REE mineral aggregates having different proportions of REE to those in pre-existing REE minerals. Because REE carbonates have also overgrown minerals that do not contain any REE, such as uraninite, uranothorite and titanite, late magmatic, hydrothermal and supergene REE minerals have derived their REE either from altered pre-existing REE minerals and/or from residual melt, hydrothermal solutions or groundwater which transported REE from the outer source to the site of crystallization. Thus the presence of several coexisting REE mineral species in different parageneses does not depend entirely on the liberation of REE from the pre-existing minerals, because some constituents can be introduced from the outer source. According to Dorfman and Varshall (1964) REE-bearing carbonates have replaced silicates by scavenging carbon from the atmosphere.

Associations of titanium, uranium, yttrium and zirconium minerals

In addition to REE phosphate, carbonate and silicate minerals, radioactive occurrences "D" and Grandroy Deposit contain Ti, Zr and Y-bearing accessory minerals. Titanium minerals identified by X-ray diffraction include rutile, pseudorutile ($Fe^{+3}{}_2\,Ti_3O_9$), anatase, brookite, titanite and ilmenite. These minerals are intergrown with, and are locally replaced and overgrown by, complex U-Zr-Y-bearing mineral aggregates apparently as a result of interaction with adjacent uraninite, zircon and unidentified, amorphous Y-bearing minerals. Complex U-Zr-Y-Ti compounds have also crystallized in fractures and interstices (Fig. 21.7, 21.8, analysis 17, Table 21.3).

Zircon associated with altered uraninite usually contains uraniferous spots or overgrowths thus providing evidence of reactions between two adjacent minerals (analyses 6, 7, 8, 9, 10, Table 21.3, Fig. 21.7A, EDS-2; Rimsaite, 1981b, Fig. 4.3, 4.4). Radioactive yttrium-bearing grains adjacent to zircon are altered and metamict, and only their relatively fresh recrystallized rims produced X-ray patterns of uraninite and coffinite (Fig. 21.7A,B, EDS-1). Yttrium, apparently liberated from these altered Y-U-Th-grains has crystallized in altered Ti mineral aggregates as irregular patches (Rimsaite, 1981a, Fig. 17.6B, EDS-1), thus indicating that altered and recrystallized Ti minerals are favourable hosts for reprecipitation of liberated heavy REE.

Associations of secondary U, Ti, Zr, REE mineral aggregates in fractures and interstices

In the Baie-Johan-Beetz area, about one third of radioactive, REE and other ions leached from altered minerals recrystallized in fractures and interstices and were thus retained in the host rock. The study of material-filling fractures has provided information and evidence on the mobility and fixation of radionuclides and on their geochemical relationships with REE and with host minerals (Fig. 21.8). Pyrochlore, biotite, muscovite, Ti minerals and zircon are favourable hosts for precipitation of chemically complex mineral aggregates and multi-minerallic crusts which have fixed mobilized U, Si, Ti, Zr, Th, Pb and other ions (analyses 18 and 19, Table 21.3: Fig. 4.3A,D,E, Rimsaite, 1982b; Table 2-III, IV, V, Fig. 3D,E, 1983a, Fig. 3.4, 1981b). Radioactive crusts in biotite contain abundant U and Pb, resembling in chemical composition kasolite, whereas associated muscovite in fractures contains U-Ti-rich crusts, resembling brannerite in chemical composition. Material in biotite fractures contains much lead, in contrast to Pb-poor material in muscovite fractures (analyses 18 and 19, Table 21.3). Interstices and fractures in minerals in specimens from the Grandroy Deposit are filled commonly with Pb-rich kasolite which locally has crystallized in association with secondary U phosphates (Fig. 21.8C, D, EDS-4, 5). Kasolite ultimately alters to uranophane and in an oxidizing environment both kasolite and uranophane can be replaced by clays (Rimsaite, 1981a, Fig. 17.7E,F,G; 1979; 1982d).

Zirconium can also be liberated from altered cyrtolite. It migrates along fractures and precipitates preferentially in biotite along (001) cleavage planes (analysis 10, Table 21.3; Rimsaite 1981b, Fig. 4.4B,D,E,F; 1983a, Fig. 3.7f,g).

Some heavy and light REE precipitate in fractures which are filled with Ca-Th-Zr-P-(U)-bearing crusts and inclusions, with Fe-Ti-rich crusts, and in grains partly replaced by hydrocarbons (analyses 7, 8, 9, 10, 17, 19, 15, 16 respectively).

SUMMARY AND CONCLUSIONS

The mineralogical-petrographic-petrochemical studies of pegmatites and their host rocks in the east of Baie-Johan-Beetz, Quebec revealed evidence of evolution and successive crystallization of four types of pegmatites and of their contained minerals. This study has confirmed previously described alterations of radioactive, REE and other accessory minerals, and on the basis of new SEM-EDS analyses established chemical and mineralogical trends during alteration of uraninite, uranothorite, REE phosphates, Ti minerals, zircon and other accessory minerals.

The oldest pegmatites are plagioclase-rich paleosome remnants in younger granitic pegmatites, made up of neosome microcline, quartz and albite. Pegmatites contain fresh and/or partly digested xenoliths of adjacent metasediments and metagabbro. Plagioclase-rich pegmatites which are underlain by biotite schist and biotite granite locally contain the highest concentrations of uranium, reaching 277 000 ppm U in the Grandroy Deposit. The Grandroy Deposit also contains the highest concentrations of REE phosphates in the Baie-Johan-Beetz area.

Granite pegmatites contain remnants of plagioclase-rich paleosome and variable concentrations of microcline and quartz. Granite pegmatites contain Th-poor uraninite, enclosed in phyllosilicate rims, and during late pegmatitic and hydrothermal phases of crystallization, grade into pyrochlore-uraninite pegmatites which exhibit evidence of hydrothermal alteration, namely chloritization of biotite and sericitization of feldspars. The pyrochlore and uraninite grains occur in thick chlorite-serpentine rims.

The succeeding pegmatitic phase comprises dry peristerite-rich pegmatites which locally contain inclusions of U-poor metagabbro, radiating crystals of tourmaline and allanite, garnet and biotite flakes containing radioactive inclusions and coatings. The peristerite pegmatite occupies a vast area east of Baie-Johan-Beetz and seldom contains more than 50 ppm U.

The youngest pegmatitic phase is made up of cleavelandite in intergrowths with quartz and K-feldspar, and abundant white mica which replaces all pre-existing minerals and represents a hydrothermal stage of crystallization. These late cleavelandite pegmatites occur north of Baie Quétachou and contain local segregations of biotite, fergusonite-samarskite and spessartite.

All ore and accessory minerals show evidences of slight to complete alteration and various types of replacements. Uraninite has been affected by two main types of alteration: (1) replacement by Pb-rich mineral aggregates and (2) alteration to lead-depleted oxides, phosphates and silicates. Relatively stable REE phosphates and silicates also alter under the effect of radioactive solutions. These and previously published studies provide evidence that leached radioactive and REE can temporarily be fixed in secondary minerals, such as REE carbonates and uraniferous phosphates, hydrous silicates or in crust-filling fractures and interstices and coating altered minerals. However, these secondary mineral aggregates are metastable and in the Baie-Johan-Beetz area ultimately are being replaced by poorly-crystalline or amorphous phyllosilicates, goethite and carbonaceous grains. Because Ce^{+3} oxidizes to soluble Ce^{+4} at Eh = + 0.3, in an oxidizing environment Ce separates from the other light REE and becomes preferentially depleted from the site of crystallization.

In the Baie-Johan-Beetz area about one third of radioactive and REE have been retained in the original minerals, about one third was captured and fixed in secondary mineral aggregates in fractures and as crusts, and one third has been removed from the site of crystallization.

REFERENCES

Balashov, Y.A. and Kudinov, Y.A.
1966: On separation of Ce from REE during weathering of calcite and parisite in carbonatites; Academy of Sciences of U.S.S.R., Mineralogical Museum, Transactions no. 17, p. 176-180 (In Russian).

Blais, R.
1956: Rapport préliminaire sur la région de Pashashibou Comté de Saguenay; Province de Québec, Ministère des mines, R.P. 316, 8 p.

Broegger, W.C.
1890: Die Mineralien der Syenitpegmatitgänge der Südnorwegischen Augit- und Nephelinsyeniten; Groth Zeitschrift für Mineralogie, v. 16, 661 p.

Cameron-Schimann, M.
1978: Electron microprobe study of uranium minerals and its application to some Canadian deposits; unpublished Ph.D. thesis, University of Alberta, Edmonton, Canada, 337 p.

Cooper, G.E.
1957: Région de Johan Beetz district electoral de Saguenay; Rapport Géologique 74; Province de Québec, Ministère des Mines, 57 p.

Dorfman, M.D. and Senderova, V.M.
1964: Galenite and its oxidation products in a pegmatite in Khibinsky alkaline massif; Academy of Sciences of U.S.S.R., Mineralogical Museum, Transactions no. 15, p. 203-207 (In Russian).

Dorfman, M.D. and Varshal, G.M.
1964: On the question of weathering of rincolite; Academy of Sciences of U.S.S.R., Mineralogical Museum, Transactions no. 15, p. 115-122 (In Russian).

Gerasimovsky, V.V.
1964: Bastnaesite and parisite from northern Pribaikal; Academy of Sciences of U.S.S.R., Mineralogical Museum, Transactions no. 15, p. 194-202 (In Russian).

Gerasimovsky, V.I., Volkov, V.P., Kogarko, N.L.,
Polyakov, A.I., Sapyikina, T.V., and Balashov, Y.A.
1966: Geochemistry of Lovozero alkaline massif; Nauka, Moscow, 400 p. (In Russian).

Kupriyanova, I.I., Volkova, M.I., and Goroshchenko, Z.I.
1964: REE minerals in a molybdenum deposit in European U.S.S.R.; Academy of Sciences of U.S.S.R., Mineralogical Museum, Transactions no. 15, p. 123-133 (In Russian).

Maksimovic, Z. and Pantó, G.
1978: Minerals of the rare earth elements (REE) in karstic bauxites: synchisite-(Nd), a new mineral from Grebnik deposit; in Bauxites: Alumina and Aluminum, Proceedings, 4th International Congress in Athens, p. 540-552.

Nordenskiöld, A.E.
1868: Om hydrofluoceritens rätta sammausättining; Öfversigt af (Svenska) Konglica Vetenskaps-Akademiens Förhandlingar no. 6, 25 Ärgang, p. 339-402.

Oftedal, I.
1929: Über die Kristalstruktur von Bastnaesit; Groth Zeitschrift für Kristallographie, v. 72, no. 3, p. 239-248.

Pyatenko, Y.A.
1966: Second Pauling's Rule and pyrochlore group minerals; Academy of Sciences of U.S.S.R., Mineralogical Museum, Transactions no. 17, p. 119-123 (In Russian).

Rimsaite, J.Y.H.
1967: Optical heterogeneity of feldspars observed in diverse Canadian rocks; Schweizerische Mineralogische und Petrographische Mitteilungen, v. 47/1, p. 61-74.

Rimsaite, J.
1979: Natural amorphous materials, their origin and identification procedures; in Developments in Sedimentology 27, ed. M.M. Mortland and V.C. Farmer; International Clay Conference (Oxford), 1978, p. 567-576.

1980a: Mineralogy of radioactive occurrences in the Grenville structural province, Bancroft area, Ontario: a progress report; in Current Research, Part A, Geological Survey of Canada, Paper 80-1A, p. 253-264, 1980.

1980b: Selected mineral suites and evolution of radioactive pegmatites in the Grenville structural province, Canada; 26e Congrès Géologique International (Paris), Résumés III, p. 999.

1981a: Petrochemical and mineralogical evolution of radioactive rocks in the Baie-Johan-Beetz area, Quebec: a preliminary report; in Current Research, Part A, Geological Survey of Canada, Paper 81-1A, p. 115-131, 1981.

1981b: Isotope, scanning electron microscope and energy dispersive spectrometer studies of heterogeneous zircon from radioactive granite in the Grenville structural province, Quebec and Ontario; in Current Research, Part B, Geological Survey of Canada, Paper 81-1B, p. 25-35, 1981.

1982a: Mineralogical and petrochemical properties of heterogeneous granitoid rocks from radioactive occurrences in the Grenville structural province, Ontario and Quebec; in Uranium in Granite, ed. Y.T. Maurice; Geological Survey of Canada, Paper 81-23, p. 19-30, 1982.

1982b: Alteration of radioactive minerals in granite and related secondary uranium mineralizations; in Ore Genesis – The State of the Art, ed. G.C. Amstutz, et al.; Springer-Verlag, Berlin, Heidelberg, New York, p. 269-280.

Rimsaite, J. (cont.)
1982c: The leaching of radionuclides and other ions during alteration and replacement of accessory minerals in radioactive rocks; in Current Research, Part B, Geological Survey of Canada, Paper 82-1B, p. 253-266.

1982d: Mode of occurrence of secondary radionuclide-bearing minerals in natural argillized rocks: a preliminary report related to a barrier clay in nuclear waste disposal; in Current Research, Part A, Geological Survey of Canada, Paper 82-1A, p. 247-259, 1982.

1983a: Selected mineral associations in radioactive occurrences in the Grenville structural province: a progress report; in Current Research, Part B, Geological Survey of Canada, Paper 83-1B, p. 23-37, 1983.

1983b: Mineralogical, petrochemical and petrographic-textural studies of ore grade and lower grade radioactive rocks from the Bancroft area, Ontario; in Current Research, Part B, Geological Survey of Canada, Paper 83-1B, p. 93-108, 1983.

Ronov, A.B., Balashov, Y.A., and Migdisov, A.A.
1967: Geochemistry of REE in the sedimentary cycle; Geokhimiya, no. 1, p. 3-17 (1967). Geochemia International v. 4, no. 1, p. 1-17.

Rose, E.R.
1979: Rare-earth prospects in Canada; Canadian Mining Metallurgical Bulletin, v. 72, no. 805, p. 110-116.

Semenov, E.I., Chkomiyakov, A.P., and Bykova, A.V.
1961: Hypergene bastnaesite in weathering crust of an alkaline massif; Academy of Sciences of U.S.S.R., Mineralogical Museum, Transactions no. 11, p. 202-204.

Sharma, K.N.M. and Franconi, A.
1970: Grenville 1970. Region des rivieres Magpie, Saint-Jean, Romaine; Ministere des Richesses Naturelles, Rapport Geologique 163, 73 p.

Strunz, H.
1944: Mineralogische Tabellen; Akademische Verlaggsgeselschaft Becker, Erler, Kom.-Geselschaft, Leipzig, 1941. Lithoprinted by Edwards Brothers, Inc., Ann Arbor, Michigan, 1944, 287 p.

Sverdrup, T.L., Bryn, K.Ø, and Saebo, P.C.
1959: Contributions to the mineralogy of Norway: No. 2 bastnaesite, a new mineral for Norway; Norsk Geologisk Tidsskrift v. 39, p. 237-247.

Zdorik, T.B.
1966: Burbankite and its alteration products; Academy of Sciences of U.S.S.R., Mineralogical Museum, Transactions no. 17, p. 60-75 (In Russian).

Zdorik, T.B., Kuprijanova, I.I., and Kumskova, N.M.
1964: Crystalline allanite from several metasomatic occurrences in Siberia; Academy of Sciences of U.S.S.R., Mineralogical Museum, Transactions v. 15, p. 208-214 (In Russian).

APPENDIX 21.1

Description of samples in Table 21.1

1. Pegmatitic segregations in metasediments. Albite, quartz and poikilitic spessartite crystals embedded in, and partly replaced by muscovite. Spessartite accounts for 2.7% MnO.
2. Blue-grey to pink peristerite pegmatite. Lamellar oligoclase (Rimsaite, 1967, Fig. II-4) partly replaced by patches of microcline and muscovite. A few grains of biotite, apatite, allanite and xenotime coated with radioactive crusts.
3. Mafic bands in peristerite pegmatite. Ferromagnesian minerals (45%) consist mainly of blue, recrystallized hornblende and less abundant biotite and magnetite. Clear patches surrounded by dark minerals consist of plagioclase and quartz. Accessory minerals are apatite, epidote, titanium oxide and zircon.
4. Blue-grey peristerite pegmatite. Coarse grained plagioclase with deformed twinning lamellae, quartz and microcline in intergrowths with coarse biotite laths which are chloritized and fringed by sericite. Radioactive inclusions of titanite in biotite are surrounded by large pleochroic haloes. Prominent pleochroic haloes along edges in biotite infer presence of secondary radioactive coatings. Tourmaline is an accessory mineral.
5. Concentrate of chloritized biotite from peristerite pegmatite "4". Uranium and thorium occur in coatings on biotite flakes.
6. Mafic bands adjacent to pegmatite. Mainly euhedral hornblende crystals, interstitial plagioclase with sericitized centres (Rimsaite, 1967, Fig. I-2), a few flakes of chloritized biotite and disseminated grains of K-feldspar and apatite.
7. Hornblende-biotite gneiss underlying radioactive pegmatite. Hornblende and/or biotite bands containing titanite, anatase, apatite, zircon and monazite grains in a matrix of granular plagioclase and quartz.
8. Hornblende concentrated from gneiss "7".
9. Biotite concentrated from gneiss "7". Biotite contains more Al, Ti, K, Rb, H_2O and F than the associated hornblende "8".
10. Fine grained fraction (-170 mesh, particle size less than 100 μm) of pegmatite in gneiss "7". Fine grained secondary radioactive mineral aggregates account for 18 ppm U and 4 ppm Th.
11. Pink stained portions of radioactive pegmatite "10".
12. White pegmatite containing yellow patches stained by uranyl-bearing minerals which account for 538 ppm U. The pegmatite is made up of quartz, microcline with enclosed oligoclase grains rimmed by albite (Rimsaite, 1967, Fig. IV-10). Biotite streaks grade into titanite which is replaced by allanite.
13. Cleavelandite pegmatite hosting fergusonite-samarskite and garnet. Quartz, deformed antiperthitic cleavelandite with sericite and muscovite replacing K-feldspar in antiperthitic blebs, and microcline. Muscovite associated with calcite replace feldspars.
14. Muscovite concentrated from pegmatite "13". Muscovite contains less fluorine than biotite "9" from pegmatite "7".
15. Cleavelandite-microcline intergrowths from pegmatite "13".
16. Gneissic portion of syenite pegmatite from Grandroy Deposit. Mainly plagioclase, streaks of biotite, accessory minerals: xenotime, monazite overgrown and partly replaced by La-rich bastnaesite (Rimsaite, 1982c, Fig. 31.4a-g), allanite, zircon, uraninite, uranothorite, galena and alteration products. Analyses of minerals and of alteration products are provided in Tables 21.2 and 21.3. In this radioactive pegmatite, oligoclase accounts for higher Ca/Na ratio of 0.3 than that in cleavelandite pegmatite "13" which is U-poor and has low ratio Ca/Na of 0.1.
17. Biotote-poor aplitic portion of pegmatite "16" (Rimsaite, 1981a, Fig. A,B).
18. Biotite concentrated from pegmatite "16".
19. Fine grained fraction (-170 mesh, particle size less than 100 μm) of pegmatite "16" containing uranyl-bearing mineral aggregates which account for relatively high concentration of uranium and for the high U/Th ratio of 13.2.

APPENDIX 21.2

Notes on samples in Table 21.2

1. Uranothorite associated with uraninite, zircon and altered monazite and xenotime, Fig. 21.1, Grandroy Deposit (Rimsaite, 1981a, sample location map in Fig. 17.1).
2. Uraninite, Th-rich from radioactive pegmatite, northeast of Turgeon Lake, occurrence "A" (see sample location map in Rimsaite, 1981a, Fig. 17.1).
3. Uraninite from radioactive pegmatite, southeast of Turgeon Lake, occurrence D (Rimsaite, 1981a).
4. Thorian phase in uraninite "3".
5. Uranium-rich phase in the phyllosilicate rim on uraninite "3".
6. Thorium-poor uraninite associated with pyrochlore (Fig. 21.2). Microcline pegmatite from radioactive occurrence D-1, host rock analysis 28 in Rimsaite, 1981a, Table 17.2.
7. Uraninite partly replaced by Fe-rich mineral aggregates, associated with uraninite "2".
8. Pb-Th-bearing rim on uraninite "7".
9. Pseudomorphous replacements of uraninite by anglesite and amorphous hydrocarbon-like material (Rimsaite, 1981a, Fig. 17.4C).
10. Uraninite pseudomorphously replaced by galena (XRD = 65253: galena and uraninite). Galena has oxidized to anglesite (XRD = 65246: anglesite structure) at a biotite-muscovite contact (Rimsaite, 1981a, Fig. 17.3). Radioactive occurrence "E".
11. Grey amorphous phase, associated with "10" (probably hydrocarbon-like material).
12. Altered Ti oxide from the same polished thin section as the altered uraninite "10" and "11" (Fig. 21.3).
13. Titaniferous U-REE-bearing aggregates adjacent to "12" (Fig. 21.4).
14. Chlorite-like phyllosilicates replacing Ti minerals "12" (Fig. 21.4).
15. Unidentified metamict Y-Si-U-Th phase associated with uraninite, uranothorite and brannerite-like phases in rutile-anatase aggregates (XRD = 65205, 65208: anatase, pseudorutile; XRD = 65144: dolomite, kasolite, brookite; Rimsaite, 1981a, Fig. 17.5A, 1982a, Fig. 3.4f).
16. Pyrochlore in chlorite-serpentine-like rims "19" associated with uraninite "6", Fig. 21.2 (XRD = 65203: metamict).
17. Titanium-rich phase in uraninite "6" (Fig. 21.2).
18. Ti-U-bearing rim on uraninite "6" (Fig. 21.2).
19. Iron-rich chlorite-serpentine-like groundmass and thick rims enclosing Ti and U minerals in altered microcline pegmatite, Fig. 21.2 (XRD = 65201: chlorite-serpentine).

APPENDIX 21.3

Notes on analyzed spots in Table 21.3

1. Xenotime with radioactive inclusions, Fig. 21.1 (XRD = 65204: xenotime). Grandroy Deposit (Rimsaite, 1981a).
2. Uranium-rich inclusion in xenotime (Fig. 21.5, 21.6).
3. Monazite associated with uraninite, partly replaced by bastnaesite and phyllosilicates, (XRD = 65187, 65191, 65178: monazite; 65148: bastnaesite; 65162: chlorite group).
4. Hydroxyl-bastnaesite group minerals (XRD = 65148) replace monazite "3" (Fig. 21.6).
5. Chlorite-like phyllosilicates associated with sericite (XRD = 65414) and amorphous phases replace monazite "3" and bastnaesite "4", Fig. 21.6 (XRD = 65175: glauconite-celadonite; 65176 = chlorite group; 65164: disordered geothite; 65157: amorphous).
6. Fresh zircon from Grandroy deposit.
7. Radioactive inclusion in zircon (Fig. 21.7).
8. Fe-U-rich edge of zircon.
9. Uraniferous phase near the edge of a complex radioactive zircon (Rimsaite, 1981b, Fig. 4.3E).
10. Radioactive Zr-bearing crusts filling fractures.
11. Oxidized uraninite partly altered to uranophane, associated with uraninite "2" in Table 21.2. Note losses of Pb and Th.
12. Uranophane (XRD = 65250) from Grandroy Deposit (Rimsaite, 1981a).
13. Kasolite from Grandroy Deposit, Fig. 21.6, 8-4 (XRD = 65183, 65247, 65248, 65251: kasolite).
14. Lead-rich pseudomorphs after uraninite (XRD = 65225, 65226: uraninite and possibly $PbUO_4$).
15. Unidentified, amorphous, probably carbonaceous material pseudomorphously replacing uraninite.
16. Uraninite remnant in amorphous material "15".
17. Uranium-Pb-Fe-Y-bearing crusts in fractures.
18. Radioactive Pb-rich crusts in biotite fractures. Grandroy Deposit.
19. Radioactive Ti-Th-Y-bearing crusts in fractures of muscovite in two mica pegmatite, radioactive occurrence "E" (Rimsaite, 1981a).

22. GOLDENVILLE FORMATION, EASTERN SHORE, NOVA SCOTIA: STRATIGRAPHIC CORRELATION AND PRELIMINARY SEDIMENTOLOGICAL RESULTS[1]

Contract 22ST.23233-3-0351

John W.F. Waldron[2] and Lyndon R. Jensen[2]

Waldron, J.W.F. and Jensen, L.R., Goldenville Formation, Eastern Shore, Nova Scotia: stratigraphic correlation and preliminary sedimentological results; in Current Research, Part A, Geological Survey of Canada, Paper 84-1A, p. 147-155, 1984.

Also in Mines and Minerals Branch, Report of Activities, 1983, Nova Scotia Department of Mines and Energy, Report 84-1, 1984.

Abstract

The Cambro-Ordovician Goldenville Formation consists of repetitively interbedded slates and metamorphosed poorly sorted sandstones which have been previously interpreted as turbidites. Measurements of vertical magnetic gradient over well-exposed coastal sections allow recognition of marker horizons which can be traced laterally. We have subdivided a package 2.5 to 3 km thick into about 15 units, some of which have been traced 15 km along strike and across the Sober Island syncline.

Measured sections in the correlated units show major lateral facies changes, including crosscutting erosional contacts at the base of sandstone-dominated packets. Vertical sequences show both thinning- and thickening-upwards trends. A preliminary classification of sediments into seven facies has been adopted. These indicate a variety of depositional mechanisms. Further work on the distribution of facies should lead to an improved understanding of the depositional system.

Résumé

La formation cambrienne-ordovicienne de Goldenville se compose de couches interstratifiées répétitives de schistes ardoisiers et de grès métamorphisés mal triés qui ont déjà été identifiés comme étant des turbidites. Le calcul du gradient magnétique vertical dans des sections littorales bien découvertes permet de reconnaître des horizons repères qu'il est possible de suivre latéralement. Les auteurs ont subdivisé une section de 2,5 à 3 km d'épaisseur en environ 15 unités, dont certaines ont été suivies sur une distance de 15 km dans la direction des couches et en travers du synclinal de Sober Island.

Les sections mesurées dans les unités mises en corrélation présentent des changements latéraux majeurs de faciès, notamment des contacts d'érosion transversaux à la base des sections dominées par du grès. Les séquences verticales s'amincissent ou s'épaississent en montant. Les sédiments sont classés provisoirement en sept faciès qui indiquent une gamme de processus de sédimentation. Des travaux plus poussés sur la répartition des faciès fourniront une meilleure connaissance du système de sédimentation.

INTRODUCTION

The Goldenville Formation forms the lower part of the Cambro-Ordovician Meguma Group, which underlies most of southern mainland Nova Scotia. The Goldenville Formation, together with the overlying Halifax Formation, is folded in upright, open to tight subhorizontal folds trending in an arcuate pattern from almost north-south in western Nova Scotia to east-west in the east. The Goldenville Formation is at least 5600 m thick, and consists of grey metamorphosed sandstones with subordinate interbedded greenish slates. Its base is nowhere exposed. The formation has resisted all attempts at regional stratigraphic subdivision because of its lithological uniformity and the lack of fossils.

The Goldenville Formation is particularly well exposed in the area shown in Figure 22.1, where Harris (1971) was able to trace certain beds along strike between Phoenix Island and Taylor Head. We have been able to extend this correlation both laterally and vertically, using a vertical gradient magnetometer to identify marker horizons, and have carried out a sedimentological field investigation based on these results. Interpretation of the data in this investigation is still in progress; in this report we discuss the geophysical correlation techniques and briefly describe the principal sedimentary facies present. We do not here propose any comprehensive model for the depositional system, since a large volume of data collected in the 1983 field season remains to be analyzed.

GENERAL GEOLOGY

The Goldenville Formation in the area of Figure 22.1 consists predominantly of grey to greenish-grey poorly sorted fine- to medium-grained sandstones in which an originally clay-rich matrix is altered to metamorphic chlorite. There are occasional coarser sandstones and granule conglomerates. The sandstones occur in beds from 1 cm to several metres thick, although amalgamated packages may be over 50 m thick. The sandstones show a variety of sedimentary structures including sole-marks, abundant parallel lamination, various types of cross stratification, bioturbation, and water-escape structures. Interbedded greenish slates make up less than 30% of the sequence. They show parallel and cross laminations, though some appear devoid of primary structures. A major syncline (the Sober Island syncline) runs through the northern part of the area (Fig. 22.1). Slaty cleavage in the finer grained sediments and a sporadic spaced pressure-solution cleavage (Henderson, 1983; O'Brien, 1983) in the sandstones appear axial planar to this fold; they increase in intensity towards its axial trace.

The shapes of deformed sand volcanoes suggest a strain ratio in the plane of bedding of around 2:1 on the limbs of the fold, with the long axis of the strain ellipse parallel to the bedding-cleavage intersection lineation. The volcanoes may underestimate the true strain, however, if they deform inhomogeneously with their generally finer grained matrix. The sediments are cut by several generations of quartz veins, some of which are parallel to the beds. Haynes (1983)

[1] Contribution to the Canada-Nova Scotia Co-operative Mineral Program 1981-84. Project carried by Geological Survey of Canada.

[2] Geology Department, Saint Mary's University, Halifax, Nova Scotia B3H 3C3

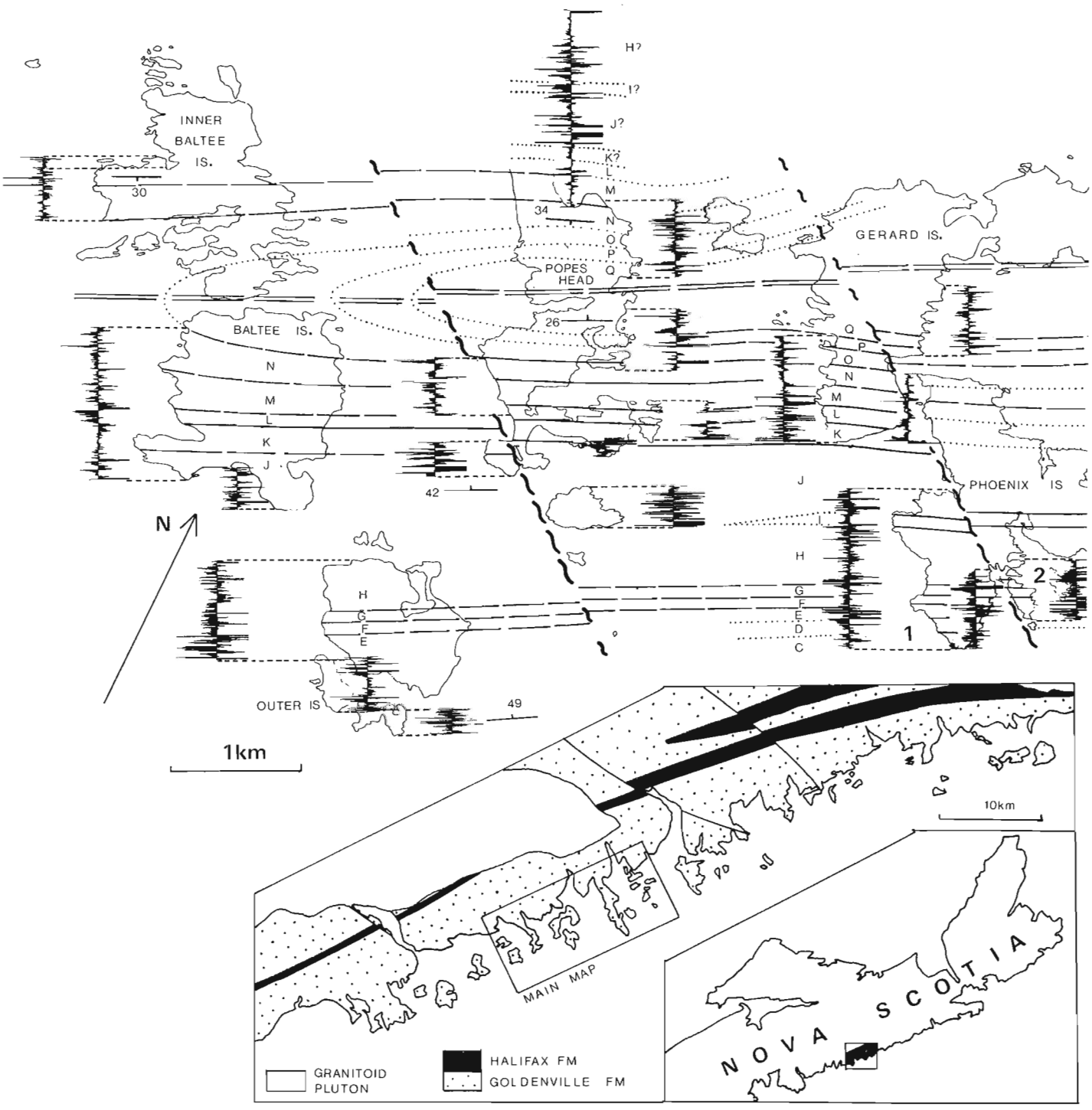

Figure 22.1. *Map of area densely covered by vertical gradient magnetometer traverses, showing proposed correlations and inferred extent of magnetically characterized subdivisions C to Q. Strike of boundaries taken from airphotographs, field measurements, and locally in the core of Sober Island syncline from Harris (1971). Many minor faults not shown. Numbers indicate location of measured sections shown in Figure 22.3.*

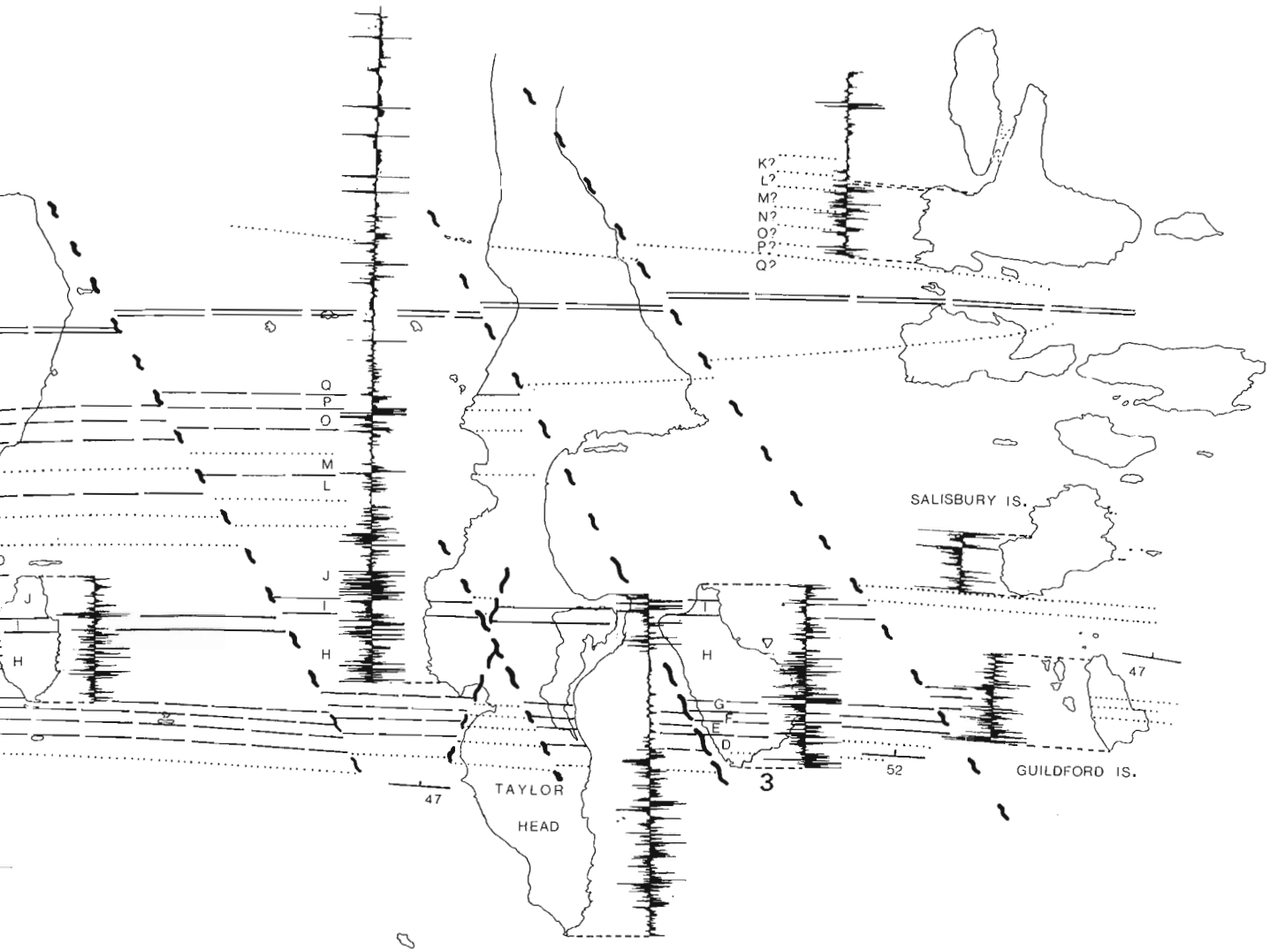

43 Strike and dip of bedding

Vertical magnetic gradient measured on coastline traverses

−20 0 20 Scale (gammas/metre)

J / I Correlation of magnetically identified units

Approximate correlation

Extrapolation along strike

Approximate axial trace of Sober Island syncline

Major faults - approximate

- inferred

suggested a sedimentary origin for some bed-parallel veins farther east; however, the veins observed by us were sharply bounded and showed no mixing with argillaceous sediment or other evidence for a seafloor origin. A set of NW trending faults is present in the area (Fig. 22.1). Many of these can be seen on airphotographs. They consistently appear to have a major sinistral strike-slip component of movement.

PREVIOUS SEDIMENTOLOGICAL WORK

The Goldenville Formation was named by Woodman (1904a), who interpreted the formation as a product of a turbulent shallow-marine depositional environment, and remarked (1904b) upon the lateral discontinuity of the sandstone layers. Phinney (1961) was the first to propose a deep-marine, turbidite origin for the sandstones. Subsequently Campbell (1966) identified a predominant northeastward paleocurrent direction in the formation, and postulated deposition in a deep-sea trough. Schenk (1970) systematically studied the entire Meguma Group using a grid sampling system, and proposed that turbidity-current deposits had been extensively reworked by contour-following bottom currents. Harris (1971), in a study of the Taylor Head area (Fig. 22.1) described the various sedimentary structures in detail and postulated deposition mainly by turbidity currents. Schenk (1973) compared the Meguma sediments with recent abyssal plain deposits of the western North Atlantic, whereas Harris and Schenk (1975) equated the facies of the Goldenville Formation with mid-fan deposition in the submarine fan model of Walker and Mutti (1973), and suggested grain-flow and fluidized-flow as possible depositional mechanisms in addition to turbidity currents.

GEOPHYSICAL WORK

Previous sedimentary studies in the Goldenville Formation have been hampered by the lack of marker horizons in the thick sequence of monotonous sandstones and slates. Stern and Henderson (1983) carried out a magnetic survey at ground level of a part of the formation, and showed that measurements of the vertical gradient of the total field could define stratigraphically controlled anomalies with sufficient resolution to permit tracing of individual sand packages along strike. We have used this method to subdivide and correlate within a package about 3 km thick on the south limb of the Sober Island syncline. The correlation has so far been extended about 15 km along strike between Salisbury and Baltee islands (Fig. 22.1). We have also correlated this package with outcrops to the north of the Sober Island syncline.

Methods

Lines for magnetic surveying were laid out using a Brunton compass and survey tape. Lines were selected along well exposed coastlines and where possible were oriented perpendicular to the local strike of bedding. Strike-parallel offsets were used to accommodate irregularities in the coastline wherever practical; elsewhere, lines oblique to strike were used. No elevations were surveyed, since survey lines were predominantly in coastal areas with a vertical relief of generally less than 5 m. To facilitate correlation of magnetic anomalies with individual beds, tie-in points were marked at 20 m intervals along the survey lines.

An EDA-instruments PPM-500 vertical gradient magnetometer was used to measure total field and vertical gradient at 2 m intervals along the survey lines. The results were plotted during the field operation, using an HP85 desk-top computer at the field camp.

The vertical gradient magnetometer consists essentially of two total-field proton magnetometers mounted 1 m apart in a single vertical pole. The value recorded is the difference (in gammas) between the two total field values. Compared with a conventional magnetometer the instrument emphasizes the magnetic effects of near-surface bodies and steeply dipping layers, and is thus particularly suited to differentiating exposed units which differ in their magnetization but are outwardly lithologically uniform. Under such circumstances the instrument can resolve anomalies separated horizontally by as little as 5 m. The amplitude of the anomalies falls rapidly with distance from source, so that traverses across overburden produce relatively flat profiles, as for example along the barrier beach on the east coast of Taylor Head (Fig. 22.1). Even in such intervals, however, the resolution provided by the vertical gradient is found to be superior to that of the total field data, although the reduced amplitude makes correlation more difficult.

It was found that adequate correlation in the area of Figure 22.1 could be achieved with fairly closely spaced (1-3 km) traverse lines, but that it was first necessary to use airphotographs to determine strike and locate major faults. In less well exposed areas a much denser spacing of survey lines would be needed for unambiguous correlation. No correction could be made for the effect of topography, which undoubtedly influenced some readings. When positive features coincided with steep topographic slopes, a large adjacent negative anomaly was frequently recorded, whereas large negative gradients were rare on level ground. The results thus contain effects of local topographic features, which modify the shapes and amplitude of some anomalies. No attempt has been made, therefore, to model the magnetic properties of individual layers, which would require precise topographic surveying along and adjacent to the traverse lines.

Results

Figure 22.1 shows the variation in vertical magnetic gradient on across-strike profiles in the region between Salisbury and Baltee islands, where a package of the Goldenville Formation about 2.5 km thick is particularly well exposed. The top of this package lies about 1.5 km below the top of the Goldenville Formation according to the cross-section of Harris (1971). A number of conspicuous features on the magnetic profiles can be correlated between profiles, allowing subdivision of the package on the south limb of the Sober Island syncline into about 15 stratigraphic units, as shown in Figure 22.1. Correlation with the north limb of the syncline is more tentative; the profile on Taylor Head has low amplitude due to overburden, and is interrupted by spurious peaks due to metal stream culverts. Probable correlation is therefore shown only for two traverses to the east and west of Taylor Head. Outcrops were found to be relatively poor on south-dipping fold limbs throughout the area studied, possibly owing to the plucking effects of south-flowing ice during glaciation.

Figure 22.2 shows a vertical gradient profile from the east coast of Phoenix Island (Fig. 22.1) plotted against height in the stratigraphic section. A graphic log of the corresponding interval is shown alongside for comparison. Large positive gradients are clearly associated with packages of thickly bedded sandstone. This supports Stern and Henderson's (1983) attribution of the magnetic anomalies to a detrital component (magnetite) in the sandstone. Nevertheless, some thick sandstones do not correspond to major peaks; the magnetic profiles cannot therefore be used to map lithologies or facies directly.

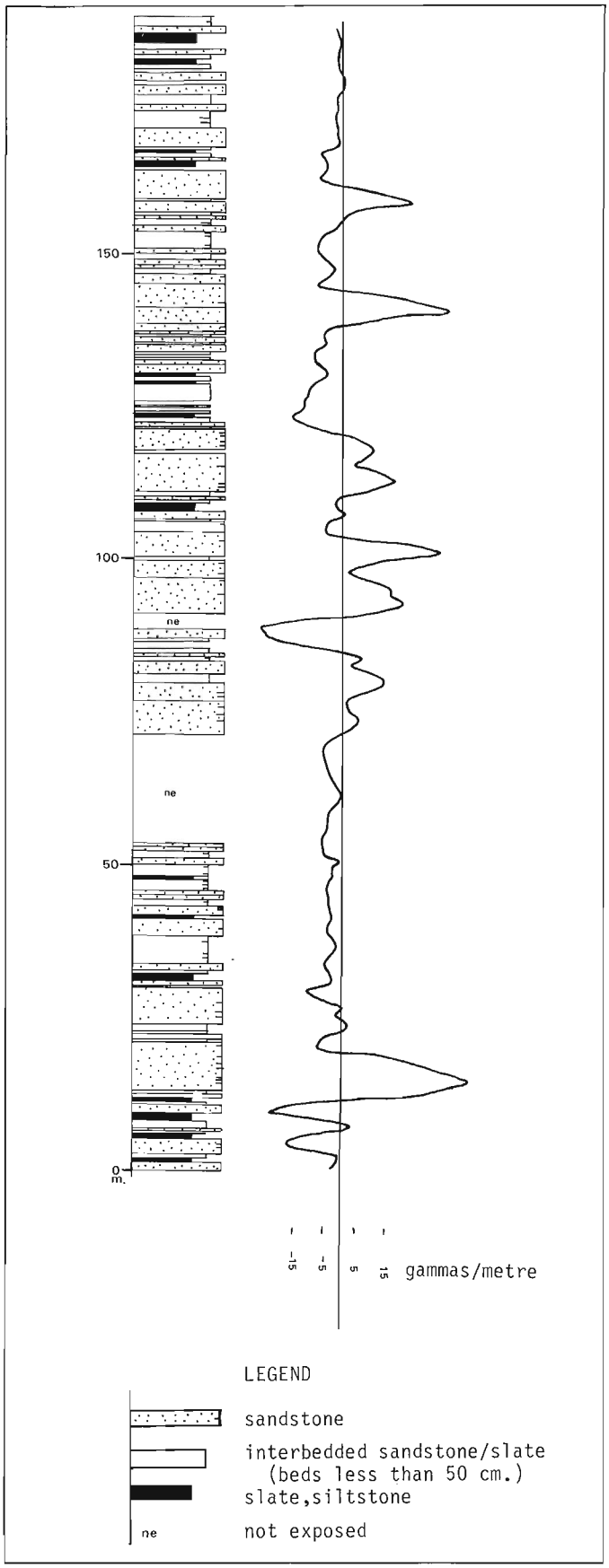

Figure 22.2. *Comparison of a portion of the stratigraphic log and vertical gradient profiles, east coast of Phoenix Island.*

The correlation of vertical gradient profiles provides good control of the apparent offset of a number of faults, most of which can be accurately located on airphotographs. Note also that small thickness changes can be seen in some units as they are traced along strike; in general, it is not possible to determine whether these variations are primary or tectonic in origin, but the disappearance of a conspicuous interval of negative gradients west of Phoenix Island is almost certainly the result of localized erosion prior to the deposition of a large lenticular sand body.

SEDIMENTOLOGY

Methods

Stratigraphic sections were measured layer-by-layer along all gradiometer survey lines (Fig. 22.1) that crossed continuous or near-continuous coastal outcrop. These sections totalled about 8 km in aggregate stratigraphic thickness.

For each layer the following features were recorded on specially devised recording forms: thickness, whether thickness varied significantly, lithology (sandstone, slate, intermixed, quartz vein), nature of basal surface (sharp or gradational), and a list of sedimentary structures present. A program for the HP85 computer was written to accept these data typed in at the keyboard and to plot graphic logs of the sections measured, initially at the scale of 1:500.

Following lateral correlation using plots of vertical magnetic gradient, certain segments of the stratigraphic sequence were selected for detailed study. Computer-drawn graphic logs at a scale of 1:50 were annotated in the field with the following additional information: estimated average and maximum grain size, description of all sedimentary structures in their vertical sequence, sorting and roundness of grains where visible, direction of paleocurrents indicated by flutes, grooves and other sedimentary structures.

Sedimentary facies

We have adopted a preliminary classification of the sediments into seven main types. Typical examples of most of these are identified in Figure 22.3 and are shown in field photographs (Figs. 22.4 to 22.8).

1. Intraclast conglomerate (Fig. 22.4). This type of sediment is restricted to a few horizons within the sequence investigated. It consists of predominantly angular argillaceous clasts ranging from a few centimetres to 2 m in length, within a matrix which varies from medium sandstone to granule conglomerate (Fig. 22.4). Tectonic deformation has caused the clasts to flatten considerably and the matrix in some instances to be folded. The beds range from 3 to 10 m in thickness and are associated with thick massive and crosslaminated sandstones. Internal sedimentary structures are rare, with the clasts being scattered homogeneously throughout the bed. Some "rafts" of laminated coarse to very coarse sandstone (up to 0.2 m thick) are found on Taylor Head within the lower portion of one such bed.

   The argillaceous clasts appear lithologically similar to slate beds occurring elsewhere in the sequence, and are thought to be products of intrabasinal erosion.

2. Internally scoured sandstones (Fig. 22.3, 22.5, 22.6). These sandstones commonly occur in amalgamated packages, within which recognizable depositional units range from 2 to 10 m in thickness, averaging around 3.5 m. The most characteristic sedimentary structures are large flute-like scour structures typically around 0.15 m deep, 0.35 m wide and 0.8 m long. These are filled with crosslaminated sandstone as shown in Figure 22.5; the crosslaminations typically "feather-out" down-current

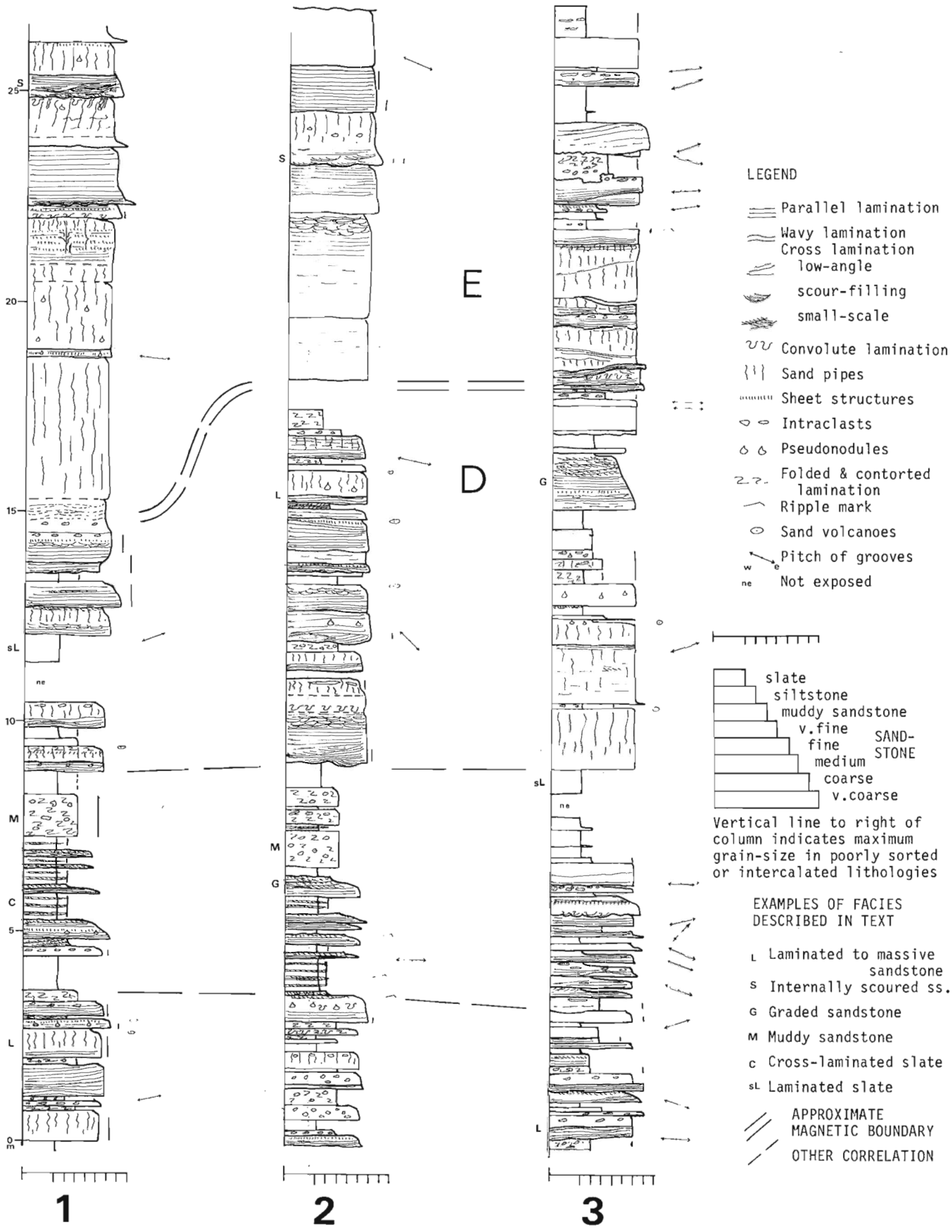

Figure 22.3. *Three laterally equivalent sections across the boundary between magnetic units "D" and "E", illustrating lateral variations in bed thickness and sedimentary structures. Examples of sediment types mentioned in the text are indicated by small letters to the left of the columns. Locations of sections 1, 2 and 3 are marked in Figure 22.1.*

Figure 22.4. *Flattened intraformational conglomerate: angular slate clasts (dark) surrounded by a matrix of very coarse sand and granule-size material, Outer Island. Scale is 1 metre.*

(generally towards the east). Locally a single scoured surface is seen to climb within a sandstone layer from west to east; elsewhere numerous localized scours are present at different levels. The crosslaminated sands are invariably coarser grained than sediments above and below, often containing very coarse sand or granule laminae immediately above the scour surface.

Scours are not usually developed throughout a sand layer. Frequently the scoured portion overlies generally finer, parallel- or wavy-laminated sandstone (Fig. 22.5) which may show inverse grading near the base of the layer. Above the scoured interval crosslamination usually gives way in turn to wavy lamination, parallel lamination, and/or massive sandstone with abundant dewatering pipes and sheets, and occasional vertical burrows. Grading is confined to the top few centimetres. Sand volcanoes or ripple marks may be developed at the top surface.

The internally scoured sandstones were clearly rapidly deposited by fast-flowing currents. Multiple scours imply repeated eroson and deposition, suggesting that major fluctuations in current velocity occurred within each episode. Pipe and sheet structures, and sand volcanoes were produced after deposition as a result of water-escape from loosely packed sand.

3. Laminated to massive sandstone (Fig. 22.3, 22.7). This is the most common type of sandstone found in the area. The beds range from 0.4 to 3.0 m thick with a typical thickness around 0.8 m. They consist mainly of fine to medium sandstone with grading confined to the top few centimetres. The lower contacts are sharp, with frequent tool marks and rarer flutes indicating eastward paleocurrents. Rarely, a thin layer of very coarse sand to granule size sediment is present within the tool marks. Typically such beds may be divided into two portions. The lower portion, about one third of the total thickness, is characterized by parallel to wavy laminations, low-angle crosslaminations, or rarely by massive sandstone. The laminations sometimes show curving, convex-upward shapes. Conspicuous parting surfaces may be present. The upper portion (usually about two thirds of the bed) is usually massive, but contains vertical or steeply inclined pipes or sheets of slightly coarser, better sorted sand. More rarely this interval shows convolute lamination or pseudonodules, parallel lamination and/or dish-structures, and mudstone intraclasts. Sand volcanoes are common on the top surface.

Figure 22.5. *Internally scoured sandstone: parallel lamination passing upward into crosslaminated scour depressions. Gerard Island. (Scale 0.30 m).*

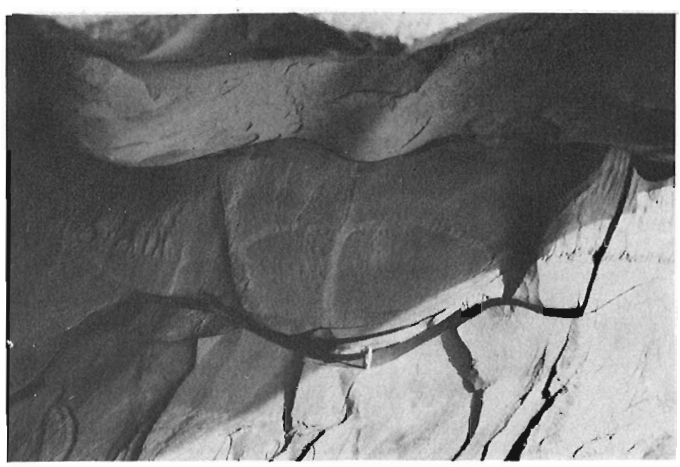

Figure 22.6. *"Nested" flute marks showing internal cross-lamination, occurring within internally scoured sandstones. Gerard Island. Matchbook (lower centre) for scale.*

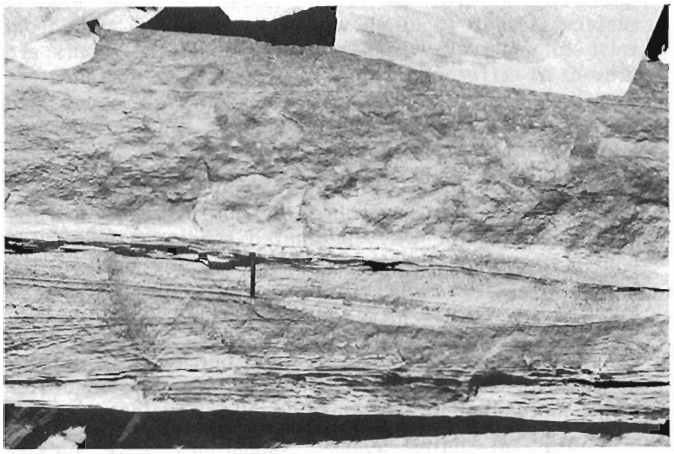

Figure 22.7a. *Laminated to massive sandstone with wavy lamination in basal portion succeeded by a vaguely parallel-laminated to massive unit with inclined sand pipes. Phoenix Island. Pencil (centre) is 14 cm long.*

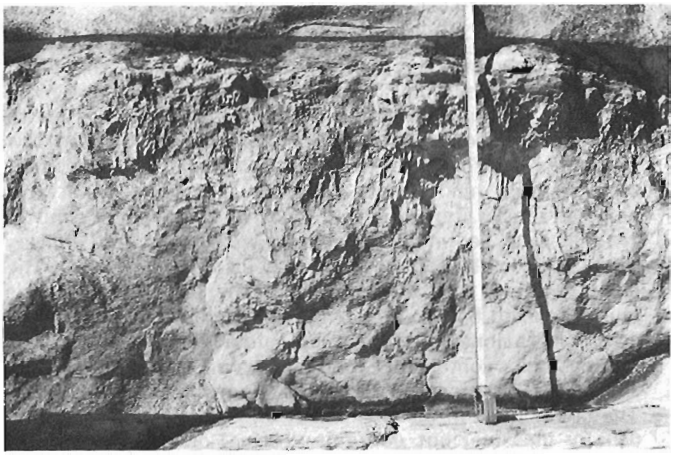

Figure 22.7b. *Laminated to massive sandstone. The lower portion of the bed is parallel-laminated. Abundant sand pipes occupy the upper portion. Pale lumps at top of bed are sand volcanoes seen in cross-section. Gerard Island. Scale is 1 m long.*

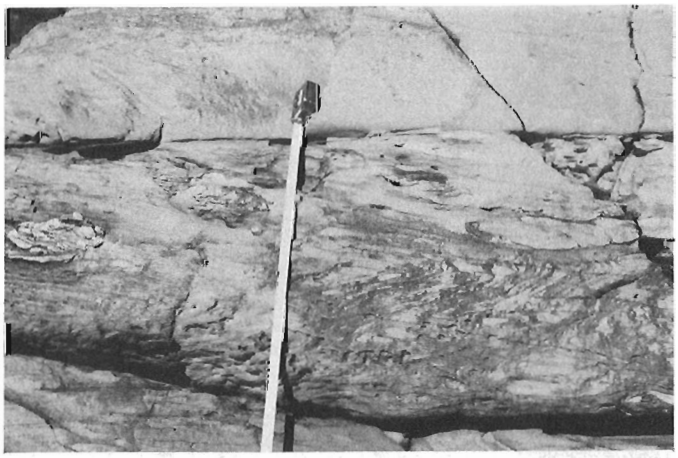

Figure 22.8. *Thin folded laminae of sandstone (lower right) and sandstone pseudonodules (paler) within slate. Gerard Island. Scale tape 70 cm long.*

Laminated to massive sandstones again indicate rapid deposition under high energy conditions. Homogenization of the upper parts of the beds was primarily due to water escape.

4. Graded sandstones (Fig. 22.3). Sandstone beds showing continuous grading from base to top are less common in the sections studied than the above two types, being frequent only in muddy intervals between large sand packets. Bed thicknesses range from 0.05 to 1.0 m, but are typically 0.2 m. The sandstones are usually parallel laminated and pass up into ripple-drift crosslaminated silts. Their sequences of sedimentary structures can be accommodated within the Bouma (1962) sequence, characteristic of "classical" turbidites.

5. Muddy sandstones (Fig. 22.8). This category includes a range of sediment types characterized by the presence of very poorly sorted, highly cleaved muddy sandstone. Within this sediment, fine sandy and shaly laminae are often highly contorted, probably as a result of slump folding (Fig. 22.8). Elsewhere, traces of argillaceous intraclasts are visible within the poorly sorted sediment. These sandstones are invariably associated with the finer grained sediment types, often occurring at the base of a slate interval. They are interpreted as products of sediment remobilization by local down-slope movements.

6. Crosslaminated slate (Fig. 22.3). This material consists of crosslaminated silt beds from 0.005 to 0.2 m thick, intercalated with finer slate. Parallel laminated or crosslaminated sand appears rarely at the base of the crosslaminated silt beds. Often the size and frequency of silt bands decreases upwards through a fine grained interval until only starved silt ripples or wisps occur.

7. Laminated slate. Fine grained slates occur between sandstones of all types and intercalated between crosslaminated silts. Most slate intervals show occasional parallel laminations or isolated slightly coarser laminae, but some are apparently homogeneous. Internal features are often indistinguishable because of the strong slaty cleavage. These slates are believed to represent "steady-state" deposition under low energy conditions between sand depositing events.

LATERAL CONTINUITY AND VERTICAL SEQUENCES

Figure 22.3 shows graphic logs of three short, laterally equivalent sections containing most of the above listed sediment types, and illustrating the considerable lateral variability of the sands beds. The following features should be noted: (1) Basal surfaces of major amalgamated sand packages frequently crosscut underlying units, suggesting major channelization of the sandstone packets. (2) Short (5-20 m) sequences may show either thinning- and fining-upward cycles or thickening- and coarsening-upwards cycles. Thinning-upwards cycles are usually equated with channel fills in submarine fan models (e.g. Walker and Mutti, 1973), but are also known to occur in other environments. Further work on the data collected in the 1983 field season will be concentrated on analysis of these vertical and lateral facies relationships in order to arrive at a better understanding of the depositional system.

REFERENCES

Bouma, A.H.
1962: Sedimentology of some Flysch Deposits. A Graphic Approach to Facies Interpretation; Amsterdam, Elsevier Publishing Co., 168 p.

Campbell, C.F.
1966: Paleocurrents and sedimentation of part of the Meguma Group (Lower Paleozoic) of Nova Scotia, Canada; unpublished M.Sc. thesis, Dalhousie University.

Harris, I.M.
1971: Geology of the Goldenville Formation, Taylor Head, Nova Scotia; unpublished Ph.D. thesis, Edinburgh University, 224 p.

Harris, I.M. and Schenk, P.E.
1975: The Meguma Group; in Ancient Sediments of Nova Scotia, ed. I.M. Harris; Society of Economic Paleontologists and Mineralogists, Eastern Section Guidebook, p. 17-38.

Haynes, S.J.
1983: Typomorphism of turbidite-hosted auriferous quartz veins, southern Guysborough County; in Nova Scotia Mines and Minerals Branch, Report of Activities 83-1, p. 183-224.

Henderson, J.R.
1983: Analysis of structure as a factor controlling gold mineralization in Nova Scotia; in Current Research, Part B, Geological Survey of Canada, Paper 83-1B, p. 13-21.

O'Brien, B.H.
1983: The structure of the Meguma Group between Gegogan Harbour and Country Harbour, Guysborough County; in Nova Scotia Mines and Mineral Branch, Report of Activities 83-1, p. 145-181.

Phinney, W.C.
1961: Possible turbidity-current deposit in Nova Scotia; Geological Society of America, Bulletin, v. 72, p. 1453-1454.

Schenk, P.E.
1970: Regional variation of the flysch-like Meguma Group (Lower Paleozoic) of Nova Scotia compared to Recent sedimentation off the Scotian Shelf; in Geological Association of Canada, Special Paper 7, p. 127-153.

1973: Nova Scotia, Morooco and continental drift; in Earth Sciences Symposium on Offshore Eastern Canada; Geological Survey of Canada Paper 71-23, p. 219-222.

Stern, R.A. and Henderson, J.R.
1983: Observations on the nature and origin of magnetic total field and vertical gradient anomalies over the Goldenville Formation in Nova Scotia; in Current Research, Part B, Geological Survey of Canada, Paper 83-1B, p. 57-65.

Walker, R.G. and Mutti, E.
1973: Turbidite facies and facies associations; in Turbidites and deep-water sedimentation; Society of Economic Paleontologists and Mineralogists, Pacific Section, Short Course Notes, p. 119-157.

Woodman, J.E.
1904a: Nomenclature of the gold-bearing metamorphic series of Nova Scotia; American Geologist, v. 33, p. 363-370.

1904b: The sediments of the Meguma Series of Nova Scotia; American Geologist, v. 34, p. 13-34.

23. GEOLOGY OF LOMOND MAP AREA, NEWFOUNDLAND

EMR Research Agreement 152-4-82

M. Nyman[1], L. Quinn[1], D.N. Reusch[1], and H. Williams[1]
Precambrian Geology Division

Nyman, M., Quinn, L., Reusch, D.N., and Williams, H., Geology of Lomond map area, Newfoundland; in Current Research, Part A, Geological Survey of Canada, Paper 84-1A, p. 157-164, 1984.

Abstract

The Lomond map area displays a complete section of the major tectonic elements of western Newfoundland from Precambrian crystalline basement through a Cambrian-Ordovician cover sequence to the highest structural slices of the Humber Arm Allochthon.

Granitic rocks of the Grenvillian Long Range Inlier are unconformably overlain by a thin clastic unit, a shale-limestone unit, and a prominent white quartzite unit, all of Early Cambrian age. These are followed by a thick carbonate section of late Cambrian to Middle Ordovician age.

Transported sedimentary rocks in lower structural slices of the Humber Arm Allochthon are separated into four units. These are traceable across the area and all are truncated by a thin mélange at the base of the allochthon. Higher structural elements of the allochthon occur to the west and include huge discrete volcanic blocks and ophiolite slices.

Intensity of deformation increases across the area from northwest to southeast. Tight folds in the cover sequence imply detachment from the underlying basement. Neither structural studies nor stratigraphic analysis support the idea of a transported Long Range basement inlier.

Résumé

La région cartographique de Lomond présente une section complète des éléments tectoniques principaux de la partie ouest de Terre-Neuve, du socle cristallin précambrien en passant par une séquence couverture cambrienne-ordovicienne jusqu'aux lambeaux structuraux les plus élevés de l'allochtone de Humber Arm.

Les roches granitiques de la fenêtre grenvillienne de Long Range sont couvertes en discordance par une mince unité clastique, une unité de schiste argileur et de calcaire et une unité proéminente de quartzite blanc; toutes ces roches datent du Cambrien ancien et sont suivies par une section épaisse de carbonate datant du Cambrien récent à l'Ordovicien moyen.

Les roches sédimentaires transportées dans les lambeaux structuraux inférieurs de l'allochtone de Humber Arm sont classées en quatre unités qui peuvent être suivies en travers de la région et qui sont toutes coupées par un mélange peu épais à la base de l'allochtone. Des éléments structuraux plus élevés de l'allochtone sont présents à l'ouest et comprennent d'énormes blocs volcaniques discrets et des lambeaux d'ophiolite.

L'intensité de la déformation augmente du nord-ouest vers le sud-est. La présence de plis serrés dans la séquence de couverture indique que celle-ci s'est détachée du socle sous-jacent. Ni les études structurales, ni l'analyse stratigraphique n'appuient l'hypothèse voulant que la fenêtre de socle de Long Range ait été transportée.

INTRODUCTION

The main geological elements of western Newfoundland are a crystalline Precambrian basement, a Cambrian-Ordovician sedimentary cover sequence and a variety of rocks in structural slices that make up the Humber Arm Allochthon. Mapping of the Lomond area (12 H/5), begun in 1982, is now complete at 1:50 000 scale. This work continues a field investigation that will ultimately cover the entire Humber Arm Allochthon and nearby parts of the basement and its cover sequence (Williams, 1973; Schillereff and Williams, 1979; Williams and Godfrey, 1980; Williams, 1981; Williams et al., 1982, 1983; Quinn and Williams, 1983). The Lomond area provides an opportunity to study basement-cover relationships and structural styles along the southern margin of the Precambrian Long Range Inlier, and to compare the stratigraphy of the Cambrian cover sequence there with that of the type area in the Strait of Belle Isle (Schuchert and Dunbar, 1934). Road cuts along the highway leading to Gros Morne National Park display key new exposures. Relationships here bear on the now fashionable question of whether or not the Long Range Inlier is autochthonous or allochthonous. The area also provides an opportunity to study a wide zone of sedimentary rocks of the Humber Arm Allochthon and relationships along the complicated trailing edge of the Bay of Islands Complex. From northeast to southwest the area exhibits a complete section from crystalline Precambrian basement to the highest structural slices of the Humber Arm Allochthon.

During the present study, Nyman mapped the northeast part of the area in connection with studies of the crystalline basement and its cover sequence, Quinn mapped the South Arm area and other parts of the Humber Arm Allochthon during sedimentary and structural studies, Reusch mapped parts of the cover sequence between East Arm and Bonne Bay Big Pond, and Williams carried out reconnaissance mapping and tectonic studies throughout the area. Geology of North Arm Mountain is partly after Smith (1958) and Rosencrantz (1983).

The area has rugged terrain that for the most part is heavily wooded. The tops of hills underlain by ophiolite complexes and crystalline basement are more barren, as are some high central areas. Much of the exposure is along streams. Woods roads are useful in reaching many parts of the area, and more isolated spots were reached by helicopter. Some coastal sections are accessible by foot, but other require a boat.

The area is connected to Deer Lake by a paved highway and gravel roads connect Wiltondale to the South Arm of Bonne Bay.

[1] Department of Earth Sciences, Memorial University of Newfoundland, St. John's, Newfoundland A1B 3X5

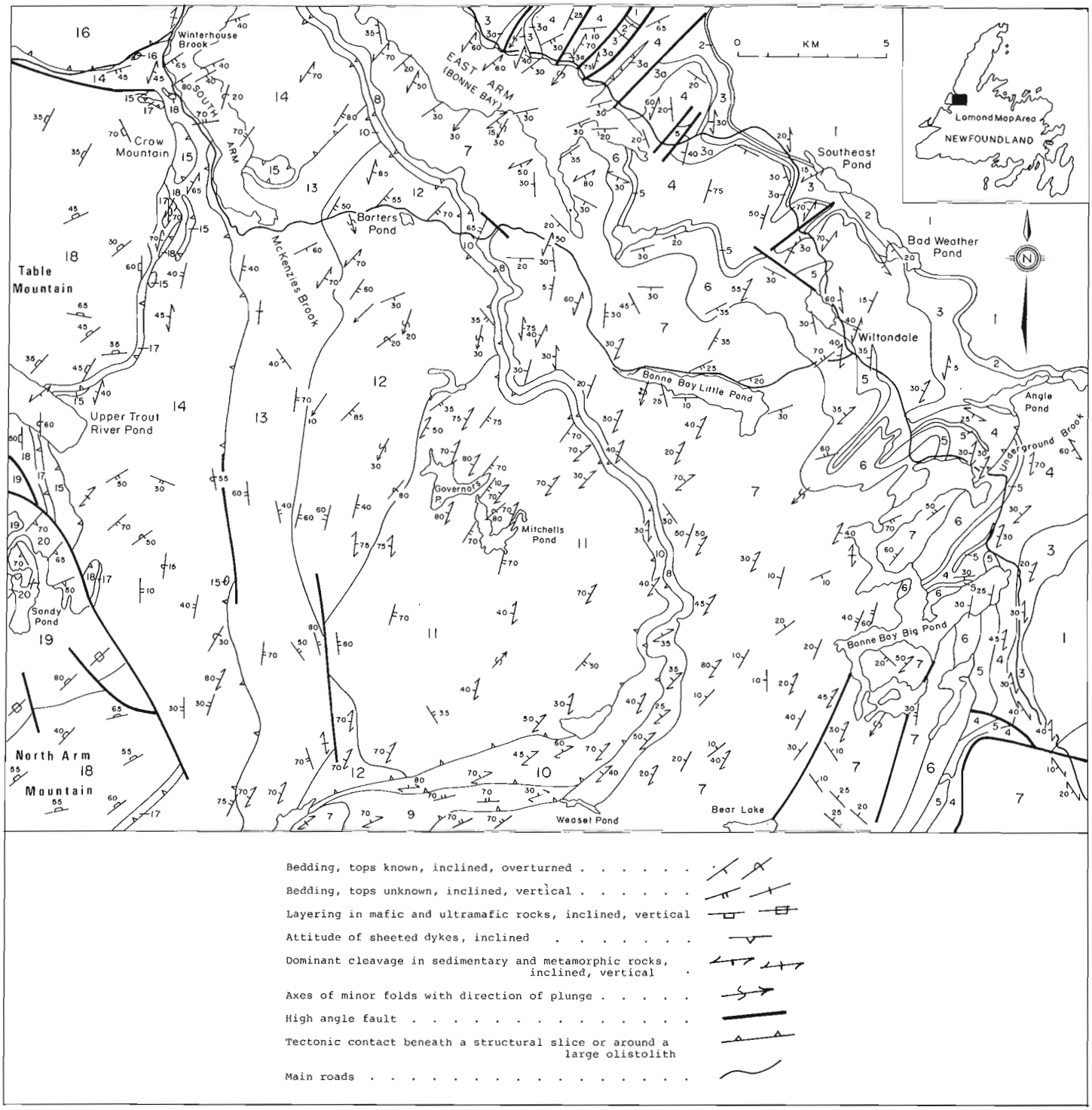

Figure 23.1. *Geological map of the Lomond area, 12 H/5, Newfoundland. All geological contacts are approximate.*

LEGEND

HUMBER ARM ALLOCHTHON

UPPER CAMBRIAN TO LOWER ORDOVICIAN

BAY OF ISLANDS COMPLEX

20 Sheeted diabase dykes

19 Medium-to coarse-grained layered to massive gabbroic rocks, minor amphibolite

18 Harzburgite, dunite and related serpentinized ultramafic rocks

17 Greenschist, black amphibolite and garnetiferous amphibolite, local quartz-feldspar gneiss

LITTLE PORT COMPLEX

16 Massive to foliated gabbro and amphibolite, tonalite, diabase dykes, mafic pillow lavas and pillow breccia

CROW MOUNTAIN FORMATION

15 Green and red pillow lava, pillow breccia and fragmental volcanic rocks, massive lava, minor mafic dykes, red and grey shale and limestone

CAMBRIAN TO LOWER ORDOVICIAN

BONNE BAY GROUP

WINTERHOUSE FORMATION

14 Thick-bedded grey to pink weathering coarse feldspathic sandstone, graded beds with pebbly bases, minor red and green shale; chaotic near contacts with higher structural slices

McKENZIES FORMATION

13 Thin-to medium-bedded grey limestone, buff weathering limestone, crosslaminated limy siltstone and dark grey shale; locally chaotic with blocks of buff weathering limy siltstone and grey sandstone in shale matrix

BARTERS FORMATION

12 Thin bedded dark grey shale with thin-bedded brown weathering quartzite, thick white quartzite units, local coarse conglomerate

MITCHELLS FORMATION

11 Thick bedded grey to white quartzite, quartz greywacke, green and purple slate

10 Chaotic grey shale with sandstone blocks, black and green scaly shale with limestone and limestone breccia blocks.

WEASEL GROUP

9 Thin bedded grey limestone and buff shale, dark grey shale and limestone with local limestone breccia, limestone conglomerate with sandy limestone matrix.

AUTOCHTHONOUS ROCKS

MIDDLE ORDOVICIAN

8 Medium-to thin-bedded grey shale, grey sandstone, buff weathering sandstone, local limy shale and limestone

UPPER CAMBRIAN TO MIDDLE ORDOVICIAN

ST. GEORGE AND TABLE HEAD GROUPS

7 Medium-to thick-bedded grey limestone, dense fine grained white limestone, grey to buff dolomite, minor shale; recrystallized limestone and marble (east)

MIDDLE TO UPPER CAMBRIAN

WILTONDALE FORMATION

6 Thin-to medium-bedded buff to white dolomite and dolomitic marble, green dolomitic shale, minor black limestone; grey shaly limestone and chlorite schist (east)

UNDERGROUND FORMATION

5 Medium-to thick-bedded grey limestone with thick oolitic or pseudo-oolitic units, conspicuous grey limestone with button algae at base, minor shale

LOWER CAMBRIAN

HAWKE BAY FORMATION

4 Thick, massive to crossbedded white and pink quartzite; thin-to medium-bedded white, green and brown sandstone with minor conglomerate, shale and limestone; green to brown quartz phyllite and schistose quartzite with minor calcareous chlorite-magnetite schist (east)

FORTEAU FORMATION

3 Medium-to thin bedded alternating grey-green shale and grey to buff weathering limy siltstone and limestone; limestone with archeocyathids at base; grey calcareous phyllite and schist (east); 3a, black calcareous shale and buff weathering grey-green calcareous sandstone and quartzite

BAD WEATHER FORMATION

2 Medium to coarse grey-green arkosic sandstone, quartz-pebble conglomerate, minor shale

PRECAMBRIAN (HELIKIAN)

LONG RANGE COMPLEX

1 Pink to grey foliated granite, coarse grained massive granite, pink gneisses, minor metadiabase

The western and northern parts of the Lomond area were mapped in reconnaissance style by Troelson (1947), and the area is part of the Sandy Lake map area that was mapped by Baird (1960). The ophiolitic rocks of North Arm and Table Mountains were mapped by Smith (1958), and parts of the Bonne Bay area were mapped by Brinex in the 1950s. Some of the carbonate rocks along East Arm of Bonne Bay have been studied more recently by Levesque (1977).

Acknowledgments

Our work in western Newfoundland is supported by operating grants from Natural Sciences and Engineering Research Council of Canada, the Department of Energy, Mines and Resources, and fellowships from Memorial University of Newfoundland. We thank all of these institutions. We also wish to acknowledge the field assistance and canoe hauling expertise of Alex Pittman, and the hospitality of Lise Sorenson and Ella Manuel of Woody Point and the Mitchells of Pasadena. Thanks are extended to Viking Helicopters for field support and for providing a scholarship of 5 hours free flying time to one of us (M.N.), to Bill Bonnell and the Forest Research Centre at Midland for the use of their facilities, to J.F. Casey and E. Rosencrantz for the use of an unpublished compliation of the geology of North Arm Mountain, and to Winston Howell for drafting Figure 23.1.

GENERAL GEOLOGY

Rocks of the Lomond area range in age from Precambrian to Middle Ordovician (Fig. 23.1). The oldest rocks are foliated granites and gneisses of the Long Range Complex and these are overlain with profound unconformity by an autochthonous sedimentary cover sequence. Lower units of the cover sequence are of Cambrian age and they are continuous along the margin of the basement complex. The lowest unit is a thin arkosic sandstone (Bad Weather)[1] that rests directly on basement rocks. It is overlain by a limestone-shale unit (Forteau), a quartzite unit (Hawke Bay) and two carbonate units (Underground and Wiltondale) in order of decreasing age. Ordovician parts of the autochthonous cover sequence are much thicker and dominanted by carbonate rocks of the St. George and Table Head groups. A thin unit of grey shale and sandstone occurs at the top of the cover sequence and is best exposed at Gadds Harbour just to the north of the map area in Bonne Bay.

The autochthonous sequence is structurally overlain to the southwest by a variety of transported rocks that make up the Humber Arm Allochthon. The base of the allochthon is marked by a thin continuous chaotic unit of sandstone, quartzite and limestone blocks in a shaly matrix. Lower slices of the allochthon are composed of sedimentary rocks of the Bonne Bay Group (Mitchells, Barters, McKenzies, and Winterhouse formations). Upper slices consist of volcanic rocks (Crow Mountain) and ophiolite suites (Little Port and Bay of Islands complexes). Sedimentary rocks of a recently discovered structural slice at the base of the allochthon toward the southwest are assigned to the Weasel Group.

The transported rocks exhibit a variety of structures in different attitudes that are not recognized in the autochthonous sedimentary sequence. These vary from intense foliations and tectonic banding in ophiolitic rocks, folded schistosities in the metamorphic sole of the Bay of Islands Complex to scaly cleavages, rootless folds and overturned beds in sedimentary rocks. These structures relate to the geneses of certain of the ophiolitic rocks and to the assembly and transport of the allochthon.

Later structures trend northeast and affect the allochthonous and autochthonous rocks alike. These increase in intensity from northwest to southeast across the area and

[1] New names are informal

are most evident in cover rocks above the Long Range Complex as traced from East Arm to Wiltondale. Toward the northwest, the rocks are affected by a single steep cleavage and they are disposed in open folds about gently southwest plunging axes. Toward the southeast, the rocks display recumbent folds, and an early cleavage is folded with the bedding about southwest plunging axes. The prominent northeast-trending cleavage recognized across the area has opposing dips on opposite sides of a steep zone at East Arm. Toward the west, cleavage dips eastward. Toward the east, cleavage dips westward.

AUTOCHTHONOUS ROCKS

Basement complex

Precambrian rocks of the Long Range Complex (Baird, 1960) form the high hills in the northeast portion of the ara near Bad Weather Pond and east of Bonne Bay Big Pond. These rocks represent the southern extremity of the Long Range Grenvillian Inlier, which forms most of the Great Northern Peninsula of western Newfoundland. The dominant lithology is pink K-feldspar porphyritic to equigranular phaneritic granite, with minor granitoid gneisses. Local northeast-trending, dark green metadiabase dykes cut the granitic rocks.

In the northwest near Southeast Pond, a thin zone of retrogression and chloritization is recognized at the basement-cover contact and local schistosity in the basement rocks is roughly parallel to the dominant cleavage in the cover rocks. In the southeast at Bonne Bay Big Pond, the basement rocks are more deformed. There, a roadcut exposure has a schistosity which crosses a metadiabase dyke and granitic host alike, and the schistosity has an orientation similar to that in surrounding metasedimentary rocks. An isolated outcrop of basement rocks farther north displays a complex structural style similar to that in nearby phyllites. These features confirm that the basement rocks were affected by localized and inhomogeneous Paleozoic deformation.

Sedimentary cover rocks

The Cambrian-Ordovician cover sequence is divided into seven units of formational rank. Established nomenclature is used where appropriate. The new formational names, i.e. Bad Weather, Underground and Wiltondale, are all informal.

Bad Weather formation

A thin clastic unit that unconformably overlies the Long Range Complex is named the Bad Weather formation. It is well exposed near Angle Pond and Bad Weather Pond, and in a highway roadcut near Southeast Pond.

At the highway roadcut, the unit consists of medium- to coarse-grained, dark green to black arkosic sandstones, with minor conglomerates and shales. The basement contact is diffuse with fragmented angular boulders of underlying granite within the sandstones. Conglomerates occur as isolated pockets and may represent channel lag deposits. Near its top, the sandstones are interbedded with thin shales. Total thickness at this locality is 9 m.

Other exposures found along the edge of the high hills consist predominantly of clast-supported, quartz granule to pebble conglomerate with scattered feldspar grains. Grading is preserved in places, but in general, depositional structures are absent. The Bad Weather formation occupies the same stratigraphic position as the Bradore Formation (Schuchert and Dunbar, 1934) to the north, but it is thinner and in places coarser.

Forteau Formation

About 90 to 100 m of locally fossiliferous shales, siltstones and limestones that conformably overlie the Bad Weather formation are assigned to the Forteau Formation (Schuchert and Dunbar, 1934). Correlation with the Lower Cambrian Forteau Formation is based on lithic similarity and stratigraphic position. Best exposures are near East Arm and at the highway roadcut near Southeast Pond. More deformed and metamorphosed varieties outcrop along the south shore of Angle Pond and along the highway east of Bonne Bay Big Pond.

In the East Arm area the base of the unit is marked by a 2 m buff to light pink limestone, overlain by thin-bedded blue-grey limestones interbedded with green shales. The limestones contain **Salterella** fragments. At its top, the Forteau has 20 m of thin-bedded alternating black calcareous shales and bright rusty weathering green-grey limy sandstones and quartzites, which outcrop between East Arm and Bad Weather Pond (Unit 3a, Figure 23.1). The thin sandstones display crosslamination and scattered trilobite fragments occur in the shales.

Southeast of Bad Weather Pond, the Forteau Formation is variably deformed and metamorphosed, consisting of blue-grey calcareous phyllite and schist, with thin (2 cm) buff weathering sandy limestones. The sandy limestones commonly show tight asymmetric folds with an axial plane foliation parallel to the slaty cleavage in shaly zones.

Hawke Bay Formation

A thick sequence of quartzites that conformably overlie the Forteau Formation are assigned to the Hawke Bay Formation (Schuchert and Dunbar, 1934). Outcrops along the north shore of East Arm are relatively undisturbed and consist of 150 m of medium- to thick-bedded white to pink vitreous quartzites. Green to brown quartz sandstones, with scattered trilobite fragments, and thin green and black shale horizons are interbedded with the quartzites. As well, there are local thin rusty weathering, dark blue to black limestone and oolitic limestone beds. Since the lower and upper contacts are not exposed in East Arm, the measured thickness is minimal.

The lithological and structural character of the formation changes southeast of Bad Weather Pond. An arcuate ridge west of Angle Pond consists predominantly of thin-laminated (1-5 mm) dull brown weathering green quartzite with thin beds (12-15 mm) of buff to white vitreous quartzite. Where the thin-laminated variety has sufficient finer grained material separating individual laminae, isoclinal folds are apparent, with extremely attenuated limbs. Around more competent beds, the deformation is much more variable and a variety of fold shapes are developed.

Quartzites and quartz phyllites along the highway north of Bonne Bay Big Pond display east-verging, asymmetric minor folds that in most cases affect an earlier fabric. Outcrops along the brook draining Angle Pond and along Underground Brook are complexly deformed schistose quartzites with sericite or chlorite forming thin smears on cleavage surfaces. In a number of outcrops, rusty weathering dark green calcareous chlorite-magnetite schists occur within the deformed quartzites. Magnetite forms euhedral porphyroblasts, commonly surrounded by carbonate material. This particular lithology is found in various locations along a prominent quartzite ridge which begins near Angle Pond and trends east and then southwest to form the core of a major southwest-plunging anticline near Bonne Bay Big Pond.

Quartzites in the Lomond area are lithologically and stratigraphically similar to quartzites at Hawke Bay to the north. Lower Cambrian fossils occur in this formation elsewhere (Palmer and James, 1980).

Undergound formation

A distinct unit at the base of the thick carbonate section developed in the autochthon is informally referred to as the Underground formation, after exposures along Underground Brook. Other examples occur near Bonne Bay Big Pond and in a fault bounded block just east of East Arm. These rocks are conformable with the underlying quartzites and consist of approximately 100 m of medium- to thick-bedded dark grey to black limestone with distinct rusty brown weathering dolomitized oolites and spectacular "button algae" (Schuchert and Dunbar, 1934). In outcrops near Bonne Bay Big Pond, both oolites and button algae are locally deformed and in one place the beds are isoclinally folded. Troelsen (1947) assigned these rocks to the lower part of his East Arm Formation, while Levesque (1977) included them in the South Head Formation. The Underground formation as used here is restricted to the dark limestones described above. Following the recently proposed subdivisions of James et al. (1983) this unit is correlated with the late Middle Cambrian March Point Formation.

Wiltondale formation

The Wiltondale formation is best exposed along the highway near Wiltondale and at the southeast end of East Arm. It conformably overlies the Underground formation and is composed of thin- to medium-bedded, orange weathering buff to white microcrystalline dolomite and dolomitic marble, with minor green dolomitic shales, grey shaly limestones and minor stromatolitic limestone.

Effects of deformation are apparent in a few places. Strained oolites occur in outcrops just northwest of Bonne Bay Big Pond and a complexly deformed chlorite schist outcrops with dolomitic marbles in a quarry between Angle Pond and Bonne Bay Big Pond. The contact with overlying Ordovician carbonates of the St. George Group is delineated by the first occurrence of monotonous thick-bedded massive dark grey dolomite.

Rocks of the Wiltondale formation were previously assigned to the East Arm Formation by Troelsen (1947), which was later redefined by Levesque (1977). Comparisons between the Wiltondale and similar rocks in the Highlands of St. John to the north (D. Boyce, personal communication, 1983) and on Port au Port Peninsula to the south suggest that it is a correlative of the Upper Cambrian Petit Jardin Formation.

St. George and Table Head groups

A thick carbonate sequence, which underlies much of the Lomond area, is correlated with the Lower Ordovician St. George Group and the Middle Ordovician Table Head Group. Levesque (1977) reported a minimum thickness of 560 m for the St. George Group, but felt it might be considerably thicker. Overall, the carbonate section is probably in excess of 1000 m. No attempt was made to separate these groups during the present study.

The carbonates are mainly medium- to thick-bedded grey limestones and buff dolomites with cherty nodular limestones and minor shales. For detailed descriptions the reader is referred to Levesque (1977). Thin white shaly beds among thick-bedded limestones in a quarry at the east end of Bonne Bay Little Pond are possible bentonites.

The thick-bedded carbonates are less deformed than clastic units in lower parts of the cover sequence. Along East Arm, the rocks are folded about gently southwest-plunging axes and an associated steep cleavage dips eastward. At Bonne Bay Little Pond, cleavage dips west, and near the west end of the pond the rocks are cut by an east-directed thrust, and folds are locally overturned eastward. In contrast, large areas near Bear Lake exhibit gently dipping homoclinal sections. At Bonne Bay Big Pond and southeastward the rocks are everywhere tightly folded.

Map unit 8

A thin unit of dark grey shales with associated grey sandstones conformably overlies the top of the carbonate sequence wherever continuous stratigraphic sections are exposed. Poorly preserved graptolites of Middle Ordovician age have been reported from this unit at the Wiltondale-South Arm road (Troelson, 1947; J. Botsford, personal communication, 1983). The unit represents the top of the autochthonous cover sequence.

HUMBER ARM ALLOCHTHON

Rocks of the Humber Arm Allochthon underlie the western half of the area. The base of the allochthon is marked by a shaly chaotic unit (unit 10) with blocks of grey sandstone, white quartzite, limestone and limestone breccia. The chaotic unit overlies the autochthonous shale (unit 8), except at Weasel Pond and westward. There, the autochthonous shale is missing and the carbonate sequence (unit 7) is separated from chaotic rocks (unit 10) by a sequence of thin-bedded shales and limestones, dark grey shale and limestone breccia, and limestone conglomerate with a sandy matrix. These rocks are atypical of the top of the autochthon; some resemble the Cambrian Reluctant Head Formation to the south (Williams et al., 1982) and others resemble the Cooks Brook and Middle Arm Point formations (Stevens, 1970) of the Humber Arm Allochthon. The rocks are therefore assigned to the Weasel group and they are interpreted to occupy a separate structural slice, the Weasel slice.

Sedimentary rocks above the basal chaotic unit of the Humber Arm Allochthon are separated into four units. These rocks are, in most respects, similar to those of the Curling Group (Stevens, 1970) of the Humber Arm Supergroup. However, there are significant differences and the stratigraphic relationships of some units are in doubt. The sedimentary rocks are therefore assigned to the Bonne Bay group and its subdivisions are given informal names.

Higher structural slices of the Humber Arm Allochthon overlie sedimentary rocks of the Bonne Bay group. Huge volcanic blocks between Upper Trout River Pond and South Arm are assigned to the Crow Mountain formation. Farther west, the sedimentary rocks are structurally overlain by the Little Port and Bay of Islands complexes (Williams, 1973).

Bonne Bay group

The Bonne Bay group consists of four formations, which from southeast to northwest are the Mitchells, Barters, McKenzies and Winterhouse. These units trend north to northeastward across the area and each is truncated by the chaotic shale unit (unit 10) that defines the structural base of the allochthon.

Mitchells formation

The Mitchells formation is best exposed at Mitchells Pond and consists mainly of thick-bedded massive white quartzite, with minor quartz greywacke and purple and green slate.

Graded bedding is observed in places. The contact with the Barters formation is not exposed but relationships at Governors Pond suggest an overturned stratigraphic contact with the Barters above the Mitchells.

Barters formation

This formation takes its name from its best exposures in the vicinity of Barters Pond. It is characterized by dark grey shales with buff weathering sandy laminae. These are interbedded with thin brown weathering quartzites. In several places the shales show distinctive bedding plane features, some of which are related to loading. Thick-bedded quartzites occur in places, and distinctive quartzite conglomerates (Quinn and Williams, 1983) outcrop on the South Arm-Wiltondale road.

The contact with the McKenzies formation to the west is enigmatic. In the Bonne Bay area it is tectonic. At Middle Trout River in the central part of the area, the contact may be stratigraphic. There, it is marked by folded beds of sandy oolite that resembles a lithology describd by Stevens (1965) at the base of the Cooks Brook Formation.

McKenzies formation

The McKenzies formation is best exposed on the south shore of South Arm and in McKenzies Brook. It is characterized by three main lithologies: buff-brown weathering, locally crosslaminated, thin- to medium-bedded dolomitic siltstone; yellow or grey weathering thin- to medium-bedded platy limestone; and dark grey-black shale. Proportions of these components vary considerably throughout the region. In the Bonne Bay area, limestone is relatively minor. In central parts of the area it is the most common component.

Contacts with the Winterhouse formation are tectonic and marked by chaotic zones. At two places, Foul Point and Trout River, volcanic blocks occur at the contact.

Winterhouse formation

The Winterhouse formation is traceable across the entire area and it is named for exposures at Winterhouse Brook. It consists of a sequence of thick-bedded, massive, grey-green feldspathic greywackes. The beds are commonly graded with many having pebbly bases. Detritus includes cloudy quartz, pink feldspar (of varying abundance), micas, shale chips, and local chert and granite fragments. Associated with the greywackes are red and green shales and minor siltstones.

The Winterhouse formation is chaotic or semichaotic throughout much of its western exposure, particularly near tectonic contacts with overlying structural slices. Sedimentary rocks of the Winterhouse formation are cut by gabbroic dykes on the north side of Upper Trout River Pond.

Correlation

No sharp stratigraphic contacts were observed between any two formations in the Bonne Bay group, nor have fossils been found in situ. The following correlations with the Curling Group at Humber Arm are made therefore on lithology alone.

The Mitchells formation is correlated with the late Precambrian-Cambrian Summerside Formation. The Barters formation is correlated with the Irishtown Formation, with conglomerates at Barters Pond resembling those at McIvers (Stevens, 1965; Williams, 1973; Quinn and Williams, 1983). the McKenzies formation is a probable equivalent of the combined Cooks Brook and Middle Arm Point formations, although it contains neither limestone breccias nor black and green shales as reported for the Cooks Brook and Middle Arm Point, respectively. The Winterhouse formation is correlated with the Blow Me Down Brook.

In a previous communication (Quinn and Williams, 1983), sandstones on the east side of South Arm were correlated with the Summerside Formation of the Curling Group. We now feel that a misinterpretation was made and that rocks on both sides of South Arm are the same.

These correlations suggest that oldest rocks of the Bonne Bay group occur to the southeast and youngest to the northwest, yet the predominant dipping and facing directions are to the southeast. This, combined with the occurrence of internal chaotic zones, e.g. in McKenzies Brook, suggest that the Bonne Bay group may be thrust imbricated. There is no assurance therefore that the present position of some units, such as the Winterhouse formation, has any stratigraphic significance.

Crow Mountain formation

Volcanic rocks that form several discrete huge flocks along the eastern margin of the Bay of Islands Complex are assigned to the Crow Mountain formation. The rocks are mainly red and green pillow lavas, volcanic breccias, dykes, massive flows, and minor shales and limestones.

Contacts with higher structural units are not exposed, but the Crow Mountain volcanics are separated from sandstones of the Winterhouse formation by thin mélange zones.

Little Port Complex

The Little Port Complex (Williams, 1973) occurs in the northwest corner of the area, structurally above the Winterhouse formation. Its rocks are gabbros, amphibolites, mafic dykes, pillow lavas, volcanic breccias and plagiogranite. The contact with the Winterhouse formation is marked by a mélange zone, exposed on the Trout River road near Winterhouse Brook. Here, red and black graphitic shales are in tectonic contact with volcanics of the Little Port Complex. This zone extends south into Winterhouse Brook where two large blocks of gabbro and volcanic breccia are found in a matrix of black and green shale and argillite.

Bay of Islands Complex

The Bay of Islands Complex (Williams, 1973) forms Table Mountain and North Arm Mountain. It is the highest structural element of the Humber Arm Allochthon. Table Mountain consists almost entirely of ultramafic rocks. North Arm Mountain contains ultramafic rocks, gabbros and mafic dykes.

A narrow metamorphic sole occurs along the southeast margin of North Arm Mountain and along the east margin of Table Mountain. The metamorphic rocks are mainly greenschist, black amphibolite and garnetiferous amphibolite. Where the sole is overthickended south of Crow Mountain, it contains lenses of quartz-feldspar gneiss and ultramafic rocks. Offset of the metamorphic sole between North Arm Mountain and Table Mountain, and a local occurrence of ultramafic and metamorphic rocks east of Sandy Pond, provide some measure of the structural displacement between the North Arm and Table Mountain massifs.

CONCLUSIONS

Rocks of the map area fit well with a model of an evolving continental margin that was destroyed by the obduction of oceanic crust and the tectonic transport of slope/rise sediments westward across the continental shelf. According to this model, the Long Range Complex represents Grenvillian basement near the rifted continental edge, the overlying mainly carbonate sequence represents an ancient carbonate bank and continental shelf, sedimentary rocks of

the Bonne Bay group are transported slope/rise deposits, and volcanic rocks and ophiolitic complexes are a sampling of oceanic islands and oceanic crust, respectively.

A growing awareness of thin-skinned tectonics along the west flank of the Appalachian Orogen (Ando et al., 1983; Ratcliffe and Harwood, 1975; St. Julien et al., 1983) and conceptual models for the Anticosti Basin (G.M. Quinlan and C. Beaumont, personal communication, 1983) combine to suggest major westward transport of basement and cover rocks in western Newfoundland. The present study sheds little new evidence to support the notion of an allochthonous Long Range Inlier and the major thrusts demanded by the model remain undetected.

Local thrusting of basement rocks above a thin arkosic cover occurs along the eastern margin of the Long Range Inlier at its northern end at Canada Bay (Williams and Smyth, 1983). Thrusting of Grenvillian basement also occurs at Hughes Lake to the south of the Long Range (Williams et al., 1982) and much farther south at Grand Lake (Kennedy, 1980). These examples occur either at the east side of the Long Range Inlier or along the trend of its eastern side. In the Hughes Lake and Grand Lake examples, the cover sequences are thick monotonous meta-arkoses, metagreywackes and psammitic schists in excess of several kilometres and the basement and cover are affected by Paleozoic greenschist to amphibolite facies regional metamorphism.

The overall setting of the Long Range Inlier with southwest dipping strata above the basement at its south end, and northeast dipping strata above the basement at its north end, suggests a major dome that is affected by high angle faults along its western side and local thrusts along its eastern side. Deformation within the cover, especially in eastern exposures, implies detachment from the underlying basement. These surfaces of detachment must lie within the cover as the basement-cover contact is a preserved unconformity.

The stratigraphy of the cover sequence in the Lomond area matches that of undeformed autochthonous rocks in the Strait of Belle Isle. This fact, coupled with an entirely different stratigraphy above transported basement occurrences at Hughes Lake and Grand Lake contradict the suggestion of an allochthonous Long Range Inlier.

RERERENCES

Ando, C.J., Cook, F.A., Oliver, J.E., Brown, L.D., and Kaufman, S.
1983: Crustal geometry of the Appalachian orogen from seismic reflection studies; in Contributions to the Tectonics and Geophysics of Mountain Chains, ed. R.D. Hatcher, H. Williams, and I. Zietz; Geological Society of America, Memoir 158, p. 83-101.

Baird, D.M.
1960: Sandy Lake (west half), Newfoundland; Geological Survey of Canada, Map 47-1959.

James, N.P., Knight, I.G., and Chow, N.
1983: Middle and Upper Cambrian platform carbonates, western Newfoundland, anatomy of a high-energy shelf; in Program with Abstracts, Newfoundland Section G.A.C., Evolution of the ancient continental margin of western Newfoundland, Memorial University of Newfoundland.

Kennedy, D.P.
1980: Geology of the Corner Brook Lake area, western Newfoundland; in Current Research, Part A, Geological Survey of Canada, Paper 80-1A, p. 235-240.

Levesque, R.J.
1977: Stratigraphy and sedimentology of the Middle Cambrian to Lower Ordovician shallow water carbonate rocks, western Newfoundland; unpublished M.Sc. thesis, Memorial University of Newfoundland, 276 p.

Palmer, A.R. and James, N.P.
1980: The Hawke Bay Event: a circum-Iapetus regression near the Lower-Middle Cambrian boundary; in Proceedings, The Caledonides in the U.S.A., ed. D.R. Wones; Virginia Polytechnic Institute and State University, Memoir 2, p. A3.

Quinn, L. and Williams, H.
1983: Humber Arm Allochthon at South Arm, Bonne Bay, west Newfoundland; in Current Research, Part A, Geological Survey of Canada, Paper 83-1A, p. 179-182.

Ratcliffe, N.M. and Harwood, D.S.
1975: Blastomylonites associated with recumbent folds and overthrusts at the western edge of the Berkshire massif, Connecticut and Massachusetts, a preliminary report; in Tectonic studies of the Berkshire Massif, western Massachusetts, Connecticut and Vermont; United States Geological Survey, Professional Paper 888.

Rosencrantz, E.
1983: The structure of sheeted dikes and associated rocks in North Arm massif, Bay of Islands ophiolite complex, and the intrusive process at oceanic spreading centers; Canadian Journal of Earth Sciences, v. 20, p. 787-801.

Schillereff, S. and Williams, H.
1979: Geology of Stephenville map area, Newfoundland; in Current Research, Part A, Geological Survey of Canada, Paper 79-1A, p. 327-332.

Schuchert, C. and Dunbar, C.O.
1934: Stratigraphy of western Newfoundland; Geological Society of America, Memoir 1, 123 p.

Smith, C.H.
1958: Bay of Islands igneous complex, western Newfoundland; Geological Survey of Canada, Memoir 290, 132 p.

St. Julien, P., Slivitsky, A., and Feininger, T.
1983: A deep structural profile across the Appalachians of southern Quebec; in Contributions to the Tectonics and Geophysics of Mountain Chains, ed. R.D. Hatcher, H. Williams, and I. Zietz; Geological Society of America, Memoir 158, p. 103-111.

Stevens, R.K.
1965: Geology of the Humber Arm area, west Newfoundland; unpublished M.Sc. thesis, Memorial University of Newfoundland.

1970: Cambro-Ordovician flysch sedimentation and tectonics in west Newfoundland and their possible bearing on a proto-Atlantic ocean; in Flysch Sedimentology in North America, ed. J. Lajoie; Geological Association of Canada, Special Paper no. 7, p. 165-177.

Troelson, J.C.
1947: Stratigraphy and structure of the Bonne Bay – Trout River area; unpublished Ph.D. thesis, Yale University.

Williams, H.
1973: Bay of Islands map area, Newfoundland; Geological Survey of Canada, Paper 72-34, 7 p.

1981: Geological map of Stephenville map area, north half, southwestern Newfoundland; Geological Survey of Canada, Open File 726.

Williams, H. and Godfrey, S.C.
1980: Geology of the Stephenville map area, Newfoundland; in Current Research, Part A, Geological Survey of Canada, Paper 80-1A, p. 217-221.

Williams, H. and Smyth, W.R.
1983: Geology of the Hare Bay Allochthon; in Geology of the Strait of Belle Isle area, northwestern insular Newfoundland, southern Labrador, and adjacent Quebec; Geological Survey of Canada, Memoir 400, p. 109-141.

Williams, H., Gillespie, R.T., and Knapp, D.A.
1982: Geology of Pasadena map area, Newfoundland; in Current Research, Part A, Geological Survey of Canada, Paper 82-1A, p. 281-288.

1983: Geology of the Pasadena map area, western Newfoundland (1:50 000 scale map and marginal notes); Geological Survey of Canada, Open File 928.

24. PRELIMINARY GEOLOGICAL RECONNAISSANCE OF THE HILL ISLAND LAKE AND TALTSON LAKE AREAS, DISTRICT OF MACKENZIE

Project 820011

H.H. Bostock
Precambrian Geology Division

Bostock, H.H., Preliminary geological reconnaissance of the Hill Island Lake and Taltson Lake areas, District of Mackenzie; in Current Research, Part A, Geological Survey of Canada, Paper 84-1A, p. 165-170, 1984.

Abstract

Precambrian rocks in the vicinity of Hill Island Lake occupy a north-south oriented central belt comprising greywacke-mudstones intruded by muscovite granite and pegmatite, and two flanking granitic gneiss terranes. On the west flank the gneisses include a zone within which remnants of Archean paragneiss are preserved. On the east flank the gneisses have been intruded by syntectonic or pretectonic gabbro bodies, and surround a large lens of augen gneiss. Diabase dykes of probable Helikian age are most common in the eastern gneisses. The central belt is separated from gneisses to the east by a complex zone of gneissic tectonites. This zone bifurcates about a northern wedge of gneisses resembling those of the eastern belt, but which have been brecciated and altered, and upon which Nonacho conglomerates are locally preserved.

Graded beds and minor folds indicate that the greywacke-mudstones underwent early, gently plunging, isoclinal folding. Later intersecting cleavage in both sediments and tectonites displays a complex pattern suggesting shearing with primarily sinistral displacement along the tectonite zone. This zone is part of an extensive fault system extending northward from Lake Athabasca to the Slave-Chantrey mylonite belt south of Great Slave Lake.

Résumé

Les roches précambriennes aux environs du lac Hill Island se trouvent dans une zone centrale orientée nord-sud qui se compose de grauwackes et de mudstones traversés par un granite à muscovite et une pegmatite et de deux terrains de gneiss granitique contigüs. Les gneiss du flanc ouest contiennent une zone au sein de laquelle sont conservés des restes d'un paragneiss archéen. Sur le flanc est, des gabbros syntectoniques ou post-tectoniques traversent les gneiss qui entourent une grosse lentille de gneiss oeillé. Des filons de diabase datant probablement de l'Hélykien sont communs dans les gneiss du côté est. Une zone complexe de tectonites gneissiques sépare la zone centrale des gneiss à l'est. Cette zone de tectonites bifurque autour d'une lame de gneiss semblables aux gneiss de la zone est mais qui sont bréchifiés et altérés et sur lesquels les conglomérats de Nonacho sont conservés par endroits.

Le granuloclassement et la présence de plis mineurs indiquent que les grauwackes-mudstones ont subi un plissement précoce, isoclinal, à inclinaison douce. Le clivage entrecroisé plus récent dans les sédiments et les tectonites présente une configuration complexe qui laisse croire qu'il y a eu cisaillement avec déplacement surtout vers la gauche le long de la zone de tectonites. Cette zone fait partie d'un vaste réseau de failles qui s'étend vers le nord à partir du lac Athabasca jusqu'à la zone de mylonite de Slave-Chantrey au sud du Grand lac des Esclaves.

INTRODUCTION

Field investigations preliminary to systematic geological mapping of the Hill Island Lake (NTS 75 C) and Taltson Lake (NTS 75 E) areas at 1:250 000 scale were undertaken in the summer of 1983. Two months were devoted to mapping in the vicinity of Hill Island Lake to investigate relations between greywacke-mudstones previously correlated with the Tazin Group (Mulligan and Taylor, 1969) and conglomerates of the Nanacho Group both of which were known to occur at subgreenschist facies metamorphic grade in this area. Information was also sought which might indicate whether the Tazin-like rocks can be correlated with the Tsu Lake gneisses which comprise rocks of similar sedimentary facies but are typically of much higher metamorphic grade, Bostock (1982). Two weeks were spent on a preliminary examination of part of the Slave-Chantrey mylonite belt with S. Hanmer of the Geological Survey, in order to facilitate co-ordination of subsequent detailed and reconnaissance mapping in this belt, and two weeks were spent in examination of other local areas of interest within the Taltson Lake sheet. Support was provided for N. Culshaw in detailed mapping at Rutledge Lake (central to NTS area 75E), and for R. Stevenson in examination of a lead-bearing feldspar (amazonite) occurrence near Portman Lake (southeast of Hill Island Lake) as part of a M.Sc. theses study.

THE HILL ISLAND LAKE AREA

Precambrian rocks in the vicinity of Hill Island Lake comprise two regions of predominantly granitic gneisses (Fig. 24.1, units 2, 2a and 2b) separated by a central, north-south oriented belt of greywacke-mudstones (unit 3a) that has been intruded along its western margin by muscovite granite and pegmatite. A zone of gneissic tectonites (unit 7) follows the east margin of the central belt and has included within it large remnants of schist (unit 3b) and of gneiss (unit 2).

Gneisses west of Hill Island lake and south of Natael Bay (units 1 and 2a) are mostly medium grained, and steeply east-dipping, with variable proportions of biotite- to hornblende-rich bands and xenoliths that are at least partly derived from mafic dykes. At the western limit of mapping these gneisses (1) include prominent remnants of paragneiss comprising pelites, semipelites, some quartzite and minor calc-silicate gneiss like the Tsu Lake gneiss of the Fort Smith area (Bostock, 1982). Rb-Sr whole-rock isochrons for pegmatites intruded into similar rocks in Alberta (Baadsgaard et al., 1972) suggest that these gneisses have ages greater than about 2500 Ma. To the east the gneisses (unit 2a) are free of recognizable paragneiss remnants, and commonly contain zones of potassium feldspar-megacrystic gneiss. The valley separating these two lithological units locally contains exposures of gneissic tectonite.

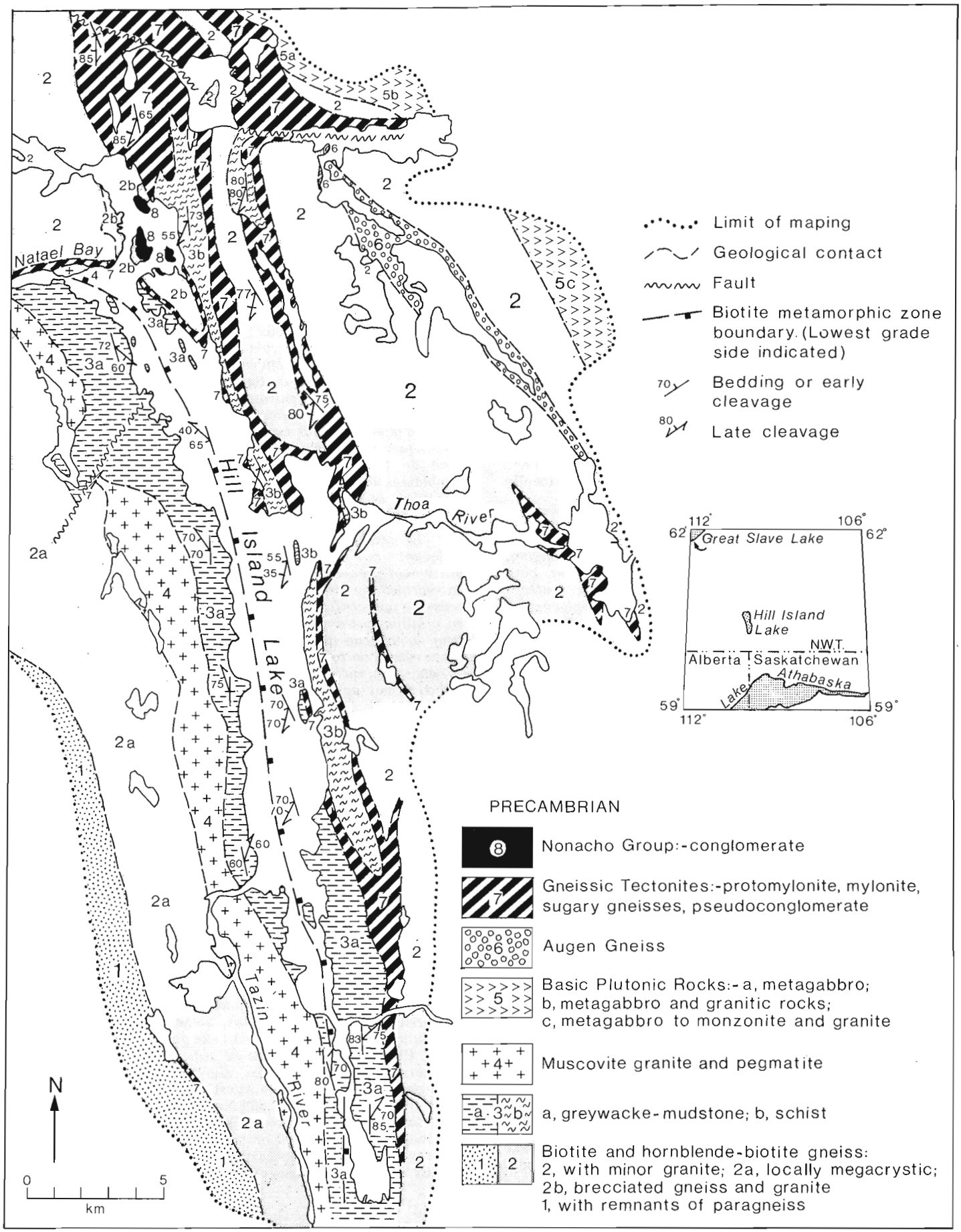

Figure 24.1. *Geological map of the vicinity about Hill Island Lake.*

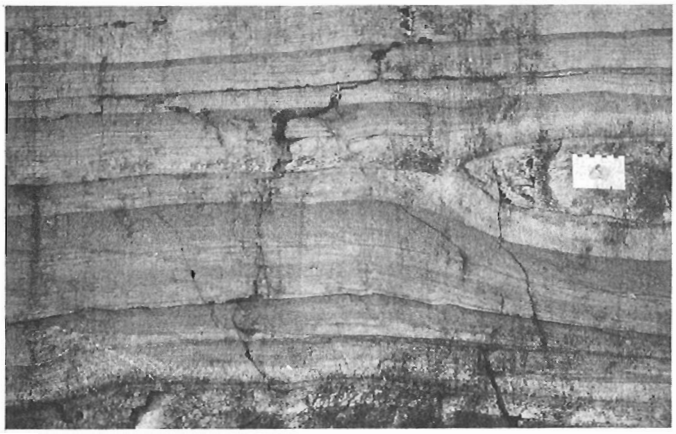

Figure 24.2. *Looking west at graded beds in the greywacke-mudstones near Tazin River. A lens of calc-silicate gneiss underlies the scale. Cleavage strikes southwesterly and is visible as fine streaking in the darker mudstone layers (black rectangles on the border of the scale are each 1 cm long).*

Greywacke-mudstones in the eastern part of the central belt are well bedded from laminated mudstone to massive siliceous siltstone units up to several metres thick. Most prominent are siltstone-mudstone units 10 to 20 cm thick that are commonly graded. Bands of calcareous siltstone in boudin-like lenses are widespread but not abundant (Fig. 24.2). Less common are thin beds of coarse sand (5 to 7 mm grain size), and sulphide-bearing mudstones. In the western part of the belt these rocks are intruded by foliated muscovite granite and pegmatite (unit 4). Inclusions of the greywacke-mudstone are widespread and locally abundant within the granitic rocks. Metamorphic grade rises from sub-biotite zone in the eastern part of the belt to cordierite zone rocks nearer the granite contact. The distribution of cordierite is sporadic, none having been found in the southern part of the lake basin, and a poorly defined zone of cordierite-free pelitic gneiss having been found adjacent to the granite contact south of Natael Bay. In this zone mudstone laminae forming the tops of graded beds are commonly followed by conformable quartz-feldspar veins, and the rocks are coarser grained than those of the same unit to the east. No alumino-silicate minerals have been recognized in the field within this zone despite the fact that cordierite suggests that the rocks have reached amphibolite facies. Their absence may reflect potash metasomatism related to emplacement of the muscovite granite. The east contact of the greywacke-mudstones comprises a complex zone of gneissic tectonite (unit 7).

The muscovite granite is medium grained, and grey to white or pink with up to about 10% muscovite flakes which typically show a foliation and are crinkled. Pegmatite, which is most abundant in the southern part of the granite body, is locally intruded into the granite, but also shows a discontinuous foliation parallel to the elongation of the intrusion. Black tourmaline is evident at scattered points within it. The west contact of the granite is not exposed, but at the one place where the greywacke-mudstones approach the west edge of the central belt they are schistose.

The granitic gneisses east of Hill Island Lake are mostly variable, fine grained, and steeply dipping. Biotite- and biotite-hornblende-bearing schlieren and inclusions are common. Pre- or syntectonic gabbro to monzonite is intrusive into the gneisses along the northeast margin of the area mapped. Zones of protomylonite and mylonite are present locally. A long narrow lens of augen gneiss lies near the northeast edge of the area mapped. It is strongly foliated and comprises pink to white granular feldspar in elongate lenses commonly up to 3 cm in a grey matrix of quartz, feldspar and biotite-chlorite that is mostly fine grained. The augen gneiss is variably interbanded with amphibolitic layers and, unlike the gneissic tectonites to the west, is cut sharply by granitic dykes. Remnants of recognizable paragneiss are relatively rare, and no zones of paragneiss remnants like those of the western belt were found. Late north- to northwest- trending diabase dykes, probably part of the Sparrow dyke swarm (McGlynn et al., 1974), are common in the eastern gneisses and in the northern wedge (dykes not shown on the map, Fig. 24.1) but are scarce in the central belt and western gneisses.

The tectonite zone which separates the central belt from the eastern gneisses is divisible into three main parallel bands and a number of outlying bodies that vary in width and lithology. In the north a splay from the western band curves westward along the north shore of Natael Bay. South of the estuary of Thoa River the three bands appear to draw together. A long lens or belt of chlorite-sericite, and some chlorite-sericite-garnet and biotite-muscovite-andalusite schists separate the western and central tectonite bands. Locally, in the northern part of the schist belt, where the schists are least deformed, they are lithologically similar to the greywacke-mudstones to the west. The local presence of andalusite may reflect the absence of potash metasomatism associated with emplacement of muscovite granite rather than an original difference in composition between the two sequences. The central and eastern bands of the tectonite zone are separated by a ridge of granitic gneiss that extends northward from Thoa River estuary, and is only slightly less sheared than are the rocks of the tectonite zone itself.

Lithologies within the tectonite bands are variable. The western band, which is mostly covered by the lake, consists largely of protomylonites in which the porphyroclasts are typically less than a few millimetres in diameter. The central zone is predominantly protomylonite commonly containing coarse potassium feldspar porphyroclasts (Fig. 24.3). The eastern zone comprises protomylonite, fine grained massive, banded, or intricately folded sugary gneiss, and pseudoconglomerate. The latter consists of small bodies of abundant angular to ovoid, unsorted clasts of fine grained sugary gneiss, scattered fragments of vein quartz and rare amphibolite in a fine gritty matrix, and can commonly be found in contact with fractured to undisrupted fine grained sugary gneiss. Unlike the Nonacho conglomerates it is free of granite clasts and is typically composed of fragments of the immediately adjacent country rocks. Similar gneisses extend along the east margin of the tectonite zone south of

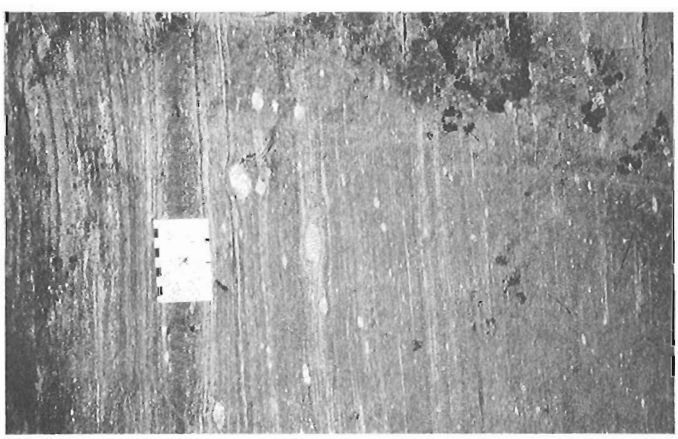

Figure 24.3. *Looking north at protomylonite containing coarse potassium feldspar phenoclasts.*

Thoa estuary. At two places along the east margin of the eastern tectonite zone, narrow bands containing blocks of gneissic to massive pyroxene-hornblende-plagioclase gneiss (Fig. 24.4) and plagioclase-hornblende-biotite metagabbro like some rocks in unit 5 were found. These rocks occur either in a matrix of gneissic tectonite or in migmatitic mafic gneiss with a plagioclase-rich neosome. The expanded northern part of the mylonite zone northeast of Hill Island Lake consists of gneissic tectonites which include protomylonite and a large proportion of fine grained to sugary gneisses that are finer grained than the country rocks to the east and west.

The gneissic tectonites which splay westward from the main tectonite zone east of Natael Bay, define the south margin of a wedge of granitic gneisses that resemble those that occur east of Hill Island Lake. Unlike the latter, however, structural trends within these gneisses trend mostly east. Near the lake they are brecciated and show severe alteration, pseudotachylyte veins are present locally, and in places tiny patches of fluorite have been observed. In the northern bay of Hill Island Lake these gneisses are unconformably overlain by beds of the Nonacho Group. These beds consist mostly of coarse polymictic conglomerate with rounded to angular clasts primarily of fine- to coarse-grained equigranular granitic rocks up to 2 m diameter in an unfoliated matrix of quartz-feldspar-chlorite grit with small local patches of weakly bedded, better sorted sands. Other lithologies that occur as clasts in the conglomerate include granitic gneiss, amphibolite, megacrystic granite, vein quartz, gabbro, and some massive immature sandstone-siltstone. At scattered localities, poorly sorted beds up to several metres thick can be recognized, indicating that the Nonacho conglomerates dip moderately to steeply north at their southern margin, and eastward elsewhere. The eastern and southwestern sides of the wedge are fringed by protomylonite and mylonite that appear to have been derived in part form shearing out of small bodies of muscovite granite, and of country rocks including granitic gneiss, schist and greywacke-mudstone, but not conglomerates of the Nonacho Group.

Structural investigation of the Hill Island Lake area was concentrated on the greywacke-mudstones, Nonacho conglomerates, and adjacent gneissic tectonites. The earliest structures recognized in the greywacke-mudstones are isoclinal, gently plunging folds (Fig. 24.5) with wavelengths mostly less than about 70 m suggested by common reversals in facing direction of graded beds. Although there appears to be a predominance of west-facing beds, rapid reversals have precluded mapping of any of these folds at the present scale of investigation. Cleavage associated with these folds does not appear to be as strong as that related to later deformation, despite the fact that the folds are isoclinal.

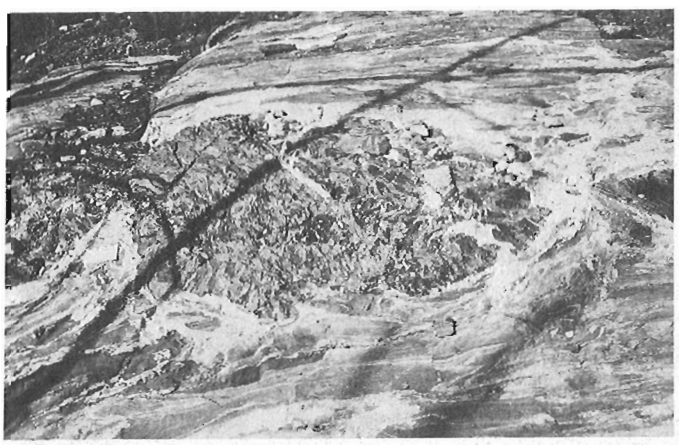

Figure 24.4. *Looking west at a pyroxene-hornblende-rich gneiss inclusion within mafic migmatite at the east margin of the eastern tectonite zone. Black layers are hornblende-rich and grey layers are pyroxene-rich.*

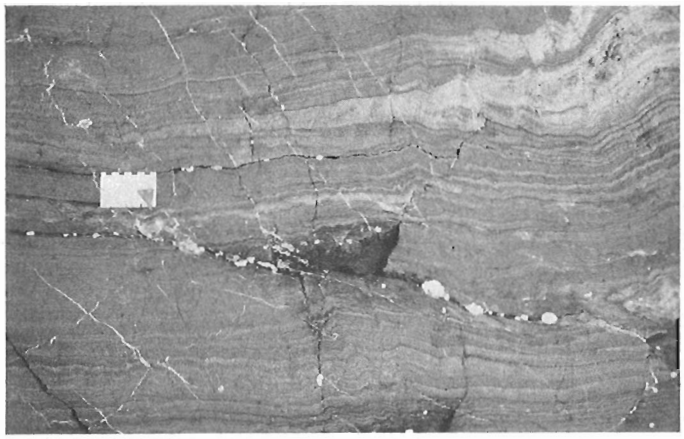

Figure 24.5. *Looking west at a gently plunging F1 isoclinal fold keel in laminated mudstone. The keel is transected by southwest-trending cleavage axial planar to minor "s" folds on either limb of the isocline.*

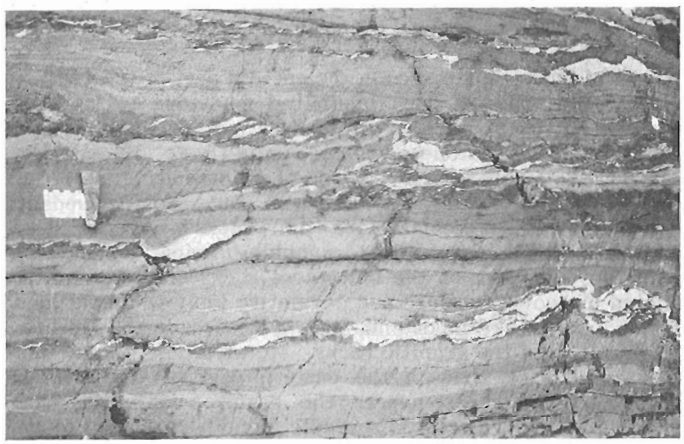

Figure 24.6. *Looking west-southwest at graded beds in schistose greywacke east of Natael Bay. Quartz-rich veins are concentrated along mudstone tops of graded beds. Veins and beds show minor folding roughly axial planar to northeasterly trending cleavage, and together with minor fault imbrication in the centre of the figure suggest dextral shear.*

Later deformation is indicated predominantly by one, or locally two, crosscutting cleavages that vary in trend in different parts of the area mapped. Minor folds are common but no major folds associated with these later cleavages have been recognized.

In the region south of Natael Bay, and on the west side of the peninsula opposite Natael Bay to the east, the southerly trending, isoclinally folded beds are cut by a prominent more southeasterly trending, moderately to steeply southwest dipping cleavage (Fig. 24.6). Scattered minor folds associated with the cleavage are mostly gently plunging and of "z" type. This structural pattern continues in the rocks west of Hill Island Lake as far south as the inflexion in the coast opposite the estuary of Thoa River, beyond which it appears to die out. The rocks showing this pattern are cut by a prominent steeply dipping, mylonite-bearing fault zone which extends in a southwesterly direction from the southern tip of the northern wedge into the gneisses of the western fault belt. To the north of this fault a third

cleavage giving rise to prominent kink bands is locally evident. The fault offsets the contact between rocks of the western and central belts in such a manner as to suggest sinstral transcurrent movement or reverse movement south-side-up, or a combination of the two.

Schists within the tectonite zone which fringe the east shore of Hill Island Lake, and are thought to be correlative with the greywacke-mudstones to the west, are characterized by remnant bedding, early cleavage, or schistosity that is north-south oriented. This structure is intersected by prominent southwesterly directed cleavage which is moderately to steeply northwestward dipping, and is axial planar to minor folds that are mostly of "s" type. A similar structural pattern persists the full length of Hill Island Lake in the east, and in the southern part of the lake basin, south of Tazin River mouth, it crosses from schists on the east side into greywacke-mudstones of lowest metamorphic grade on the west. The same pattern can be found in isolated schist remnants within the eastern tectonites and locally can be recognized within the tectonites themselves (Fig. 24.7).

The structural data obtained from the greywacke-mudstones and related schists suggest that they were deformed initially by gently plunging isoclinal folds roughly parallel to the present lake basin. Subsequent deformation varies from place to place and does not appear to have related major folds. For example, on either side of Hill Island Lake south of Natael Bay, minor folds are disposed in a pattern that superficially suggests the presence of a northward-plunging antiform or southward-plunging synform with axis down the central part of the basin. However, there is no evident symmetrical repetition of lithologies on either side of the lake, and the large angle of intersection of cleavage on either side of the lake does not suggest the existence of such a structure. It is likely therefore that the late cleavage patterns reflect shear related to deformation evident in the zone of tectonites that follows the east margin of Hill Island Lake. The predominant pattern, which is expressed throughout the tectonite zone and crosses westward into greywacke-mudstones in the southern part of the Hill Island Lake basin, suggests sinistral shear. This is supported by local imbrication structures in the mylonitic rocks (Fig. 24.8). The opposing cleavage pattern, which is exposed only on the west side of the lake from Natael Bay south to a few kilometres south of the estuary of Thoa River, suggests dextral shear. It is supported by a few observations of shear-modified boudins (Fig. 24.9). This local opposing pattern implies some structural inhomogeniety in the rocks on the west side of the shear zone. One possibility is that the northern fault wedge has been forcibly emplaced along the west side of the shear zone. Possible sinistral offset along the subsidiary fault that projects southwest across the lake from the apex of the wedge (Fig. 24.1) may reflect outward stress in the adjacent rocks during such forceful emplacement.

Although the structures described above suggest that there has been extensive sinistral shear along the Hill Island Lake tectonite zone, there are two aspects of the zone which suggest that this movement may have occurred during a late phase of tectonism. The most compelling of these is the fact that cleavage is developed not only in the schists and greywacke-mudstone, but also cuts some of the gneissic tectonites. Continued deformation of the latter should result in rotation of cleavage into the plane of shear so that only a late cleavage can persist. The more conjectural aspect consists of the asymmetry of lithologies within the tectonite zone itself with sugary gneisses primarily on the eastern side. Development of sugary texture, likely due to recrystallization of tectonites, may reflect somewhat earlier, perhaps vertical, displacements along this zone, or it is possible that continuing sinistral shear was accompanied by a vertical component sufficient to accomplish this effect.

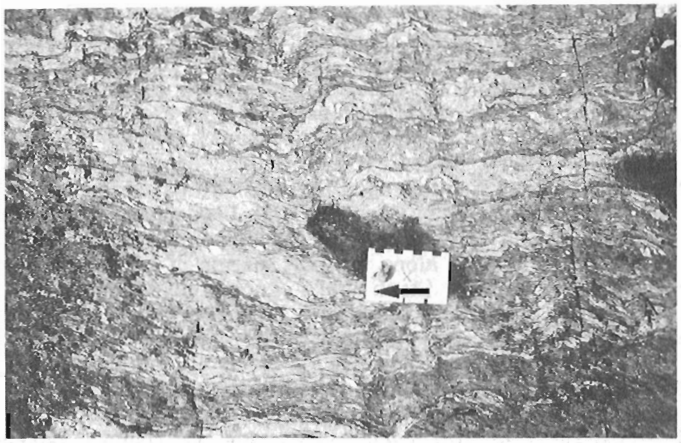

Figure 24.7. *Looking west at banded schistose protomylonite within the eastern tectonite zone. White phenoclasts up to 1.5 cm are rounded feldspars elongate parallel to cleavage which is axial planar to minor "s" folds. Possible imbrication sigmoids resembling those in the less deformed greywacke west of Hill Island Lake are present. In this case, however, folds, cleavage and imbrication suggest sinistral shear.*

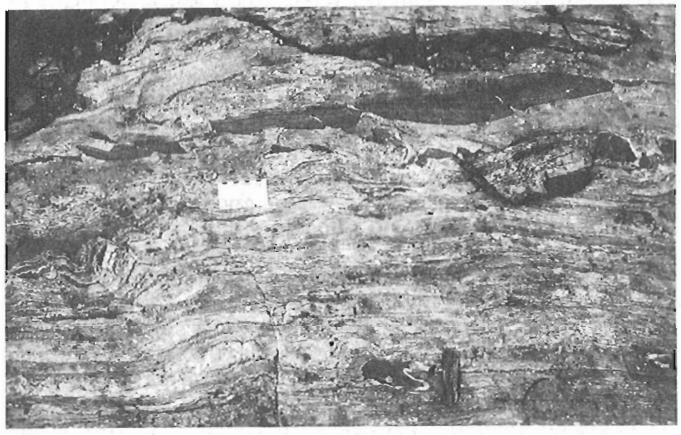

Figure 24.8. *Looking west at protomylonite showing amphibolite boudins and minor "s" folds in the tectonite zone south of Thoa River estuary. Imbrication of boudins and minor folds suggest sinistral shear.*

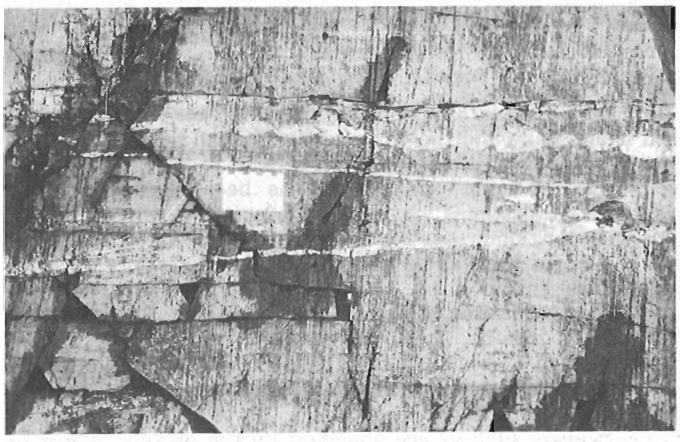

Figure 24.9. *Looking west at a thin boudined siltstone layer in greywacke south of Natael Bay. Boudins show apparent shear band modification indicating dextral shear (black rectangles at the upper margin of the scale are each 1 cm long).*

The Hill Island Lake mylonite zone projects southward and parallels Tazin River to the Saskatchewan border, where it meets a prominent fault zone shown by Koster and Baadsgaard (1970) that extends south and east to Lake Athabasca. To the north, if westward offset along the north shore of Natael Bay is included, it continues through Yatsore and Lady Grey lakes (Fort Smith area, NTS 75 D, Bostock, 1982) to impinge upon the northern extension of the Allen Fault (defined by Godfrey and Langenberg, 1978, in Alberta). It thus forms an important element in the regional fault system that lies along the east margin of the Hudsonian megacrystic granite (Arch Lake gneiss of Godfrey and Langenberg, 1978) from near Lake Athabasca north as far as the Slave-Chantrey mylonite belt south of Great Slave Lake. Unlike the Allen Fault, however, it forms a locus throughout its length for preservation of discontinuous remnants of low grade metasedimentary rocks (at Yatsore Lake, Bostock, 1982; at Hill Island Lake, and at Thainka Lake, Saskatchewan, Koster, 1961). This, and the decreasing retrogression of high grade gneisses which takes place westward toward and across the Allen Fault (Bostock, 1982) imply that the crustal level of exposure is progressively higher toward the east, and that significant vertical as well as horizontal movements likely occurred along these faults.

The greywacke-mudstones at Hill Island Lake were classified with the Tazin Group by Mulligan and Taylor (1969) who also included the high grade gneisses bearing remnants of pelitic rocks (east half of western lithological belt). The present mapping shows that most lithological variations in the Tsu Lake gneiss in the Fort Smith area (Bostock, 1982) find counterparts in the Hill Island Lake rocks, if allowance is made for large differences in metamorphic grade. Thus most of both sequences were derived from greywacke-mudstone units and show graded beds where least deformed. Local quartzite units of the Tsu Lake gneiss find potential counterparts in thick-bedded siliceous siltstones at Hill Island Lake. Calc-silicate beds in the Tsu Lake gneiss may be compared with fine grained multicoloured boudined layers characterized locally by recessive weathering within some siltstone units (Fig. 24.2). Graphite- and sulphide-bearing units like those in the Tsu Lake gneisses have also been found in the Hill Island Lake section. Lithological data therefore lend some support to the implication of Mulligan and Taylor (1969) that the greywacke-mudstones at Hill Island Lake may be correlative to the Tsu Lake gneiss in spite of the vast difference in metamorphic grade. Similar comparisons may be possible with parts of the Tazin Group exposed in Saskatchewan south of the present map area. Unlike the Hill Island Lake sediments, other low grade metasedimentary sequences in adjacent parts of Alberta, Saskatchewan and the Northwest Territories are characterized by conglomerate, distinct shale-quartzite units, or volcanic rocks.

The age relations between the greywacke-mudstones at Hill Island Lake and the Nonacho Group can only be inferred because bridging lithologies or structures to which both might be related are not known. It has been shown that the greywacke-mudstones are polydeformed, whereas the Nonacho conglomerates show only fracturing and tilting, but are devoid of cleavage. The greywacke-mudstones furthermore, are intruded by subsequently deformed muscovite granite whereas the Nonacho proper is not known to be intruded by granite. Potential correlation of the greywacke-mudstones with the Tsu Lake gneisses adds further strength to the inference that the greywacke-mudstones are distinctly older than the Nonacho Group. On the other hand, no clasts of greywacke, such as are abundant on the present shores of Hill Island Lake, are present in the Nonacho conglomerates, and it is evident that the two units occupy separate fault blocks brought together by shearing. It remains possible therefore, though probably unlikely, that the two were deposited at the same time or in reversed order, but in widely separated basins that had very different tectonic environments. The absolute ages of both the Nonacho Group and the greywacke-mudstones are constrained by the age of the Sparrow dyke swarm (1700 Ma, McGlynn et al., 1974), but dykes of this swarm within the northern wedge are locally severely brecciated indicating that deformation associated with brecciation of the wedge took place at least partly after that date.

THE TALTSON LAKE AREA

Preliminary reconnaissance along the Slave-Chantrey mylonite belt at Laloche River (northwest part of NTS 75E), and at Little Deskenetlata Lake (southwest corner of NTS 75 E) included examination of high grade paragneisses comprising pelitic and calc-silicate gneiss (originally mapped by Reinhardt, 1969). Among the latter are massive layers of plagioclase-rich gneiss and some associated banded amphibolites likely derived from impure calcareous sediments. Local bands of marble up to 20 m wide were seen north of Laloche River and thin-bedded carbonate-bearing units up to some 4 m thick were found along northern Deskenetlata Lake. If these rocks are correlative with the Tsu Lake gneiss (Bostock, 1982), this suggests a northwestward facies change in a widespread supracrustal unit from predominantly arenaceous and pelitic in the southeast toward increasing carbonate content in the northwest.

Local reconnaissance in the southeastern part of the Taltson Lake sheet shows that high grade pelitic to semi-pelitic gneisses are substantially more common within the granitic rocks of this area than was previously thought. They appear to form discontinuous remnants of a single belt of high grade paragneisses extending from Alberta (NTS 74 M) through Pilot Lake (NTS 75) to Rutledge Lake (NTS north 75 E). Small bodies of severely deformed high grade mafic igneous rocks were found in association with metasediments near the east margin of this belt 12 km west of King Lake.

REFERENCES

Baadsgaard, H. and Godfrey, J.D.
1972: Geochronology of the Canadian Shield in northeastern Alberta II. Charles-Andrew-Collin Lakes Area; Canadian Journal of Earth Sciences, v. 9, p. 863-881.

Bostock, H.H.
1982: Geology of the Fort Smith Map-Area, District of Mackenzie, Northwest Territories (NTS 75D); Geological Survey of Canada, Open File 859, map and 53 p.

Godfrey, J.D. and Langenberg, C.W.
1978: Metamorphism in the Canadian Shield of Northeastern Alberta; in Metamorphism in the Canadian Shield, ed. J.A. Fraser and W.W. Heywood; Geological Survey of Canada, Paper 78-10, p. 129-138.

Koster, F.
1961: Geology of the Thainka Lake Area (West Half) Saskatchewan; Saskatchewan Department of Mineral Resources, Report 61, p. 1-28.

Koster, F. and Baadsgaard, H.
1970: On the geology and geochronology of northwestern Saskatchewan, I. Tazin Lake Region; Canadian Journal of Earth Sciences, v. 7, p. 919-927.

McGlynn, J.C., Hanson, G.N., Irvine, E., and Park, J.K.
1974: Paleomagnetism and age of Nonacho Group sandstones and associated Sparrow dykes, District of Mackenzie; Canadian Journal of Earth Sciences, v. 11, p. 30-42.

Mulligan, R. and Taylor, F.C.
1969: Geology, Hill Island Lake; Geological Survey of Canada, Map 1203A (with marginal notes).

Reinhardt, E.W.
1969: Geology of the Precambrian rocks of Thubun Lakes map-area in relationship to the McDonald Fault System, District of Mackenzie (75E/12 and parts of 75E/13 and 85H/9); Geological Survey of Canada, Paper 69-21, p. 1-29.

25. DEFORMATION AND METAMORPHISM OF THE CORONATION SUPERGROUP AND ITS BASEMENT IN THE HEPBURN METAMORPHIC-PLUTONIC ZONE OF WOPMAY OROGEN: REDROCK LAKE AND THE EASTERN PORTION OF CALDER RIVER MAP AREAS, DISTRICT OF MACKENZIE

Project 810020

M.R. St-Onge, J.E. King[1] and A.E. Lalonde[2]
Precambrian Geology Division

St-Onge, M.R., King, J.E., and Lalonde, A.E., Deformation and metamorphism of the Coronation Supergroup and its basement in the Hepburn Metamorphic-Plutonic Zone of Wopmay Orogen: Redrock Lake and the eastern portion of Calder River map areas, District of Mackenzie; in Current Research, Part A, Geological Survey of Canada, Paper 84-1A, p. 171-180, 1984.

Abstract

In the Hepburn Metamorphic-Plutonic Zone of Wopmay Orogen, basement to the early Proterozoic Coronation Supergroup is exposed continuously by a major northeast-southwest cross fold to within 25 km of the Wopmay Fault Zone. The extent of a Proterozoic overprint on the basement units is limited to a retrograde chlorite schistosity parallel to, and within 100 m of the unconformity. Overlying the basement are between 300 and 600 m of autochthonous early Proterozoic sediments and mafic volcanics which show relatively little strain. Structurally above the low strain domain is a high strain ductile domain characterized by several sets of east-verging recumbent folds. The high strain domain is interpreted to be the ductile equivalent of the brittle basal décollement in the Asiak Foreland Thrust and Fold Belt. The Calderian thermal culmination, exposed in oblique section by the late cross fold, has the profile of an east-verging thermal lobe, rooted west of the basement-cored folds. The underside of the thermal culmination is outlined by inverted mineral isograds and is underlain by basement that remained, in part, relatively cold during metamorphism. Emplacement of the Hepburn Intrusive Suite is coincident with upper structural levels within the Calderian thermal culmination and no Hepburn plutons are found in the basement units. Mesoscopic geometry of structures in the Wopmay Fault Zone documents a history of predominantly dextral simple shear with a large component of resolved pure shear.

Résumé

Dans la zone métamorphique-plutonique Hepburn de l'orogène Wopmay, le socle du supergroupe Coronation datant du Protérozoïque inférieur, est mis à jour par un pli majeur d'orientation nord-est à sud-ouest. Cet affleurement du socle se trace de façon continue jusqu'à 25 km du complexe de la faille Wopmay. Les traces d'activité tectonique protérozoïque sur les unités du socle se limitent à une schistosité de chlorite rétrograde qui est parallèle à la discordance sise moins de 100 m plus loin. De 300 à 600 m de roche sédimentaire et de roche volcanique relativement peu déformée et dont la mise en place date du début du Protérozoïque, reposent sur le socle granitique. Au-dessus du domaine de faible distortion, se situe un domaine de forte distorsion caractérisé par plusieurs générations de plis couchés à vergence est. Le domaine de forte distorsion est considéré comme étant l'équivalent plastique du décollement de base que l'on retrouve dans la zone de chevauchement et de plissement des avant-pays Asiak. Le paroxysme thermique Calderian, mis à jour en coupe oblique par les plis tardifs, a un profil de lobe thermique fermé vers l'est et ancré à l'ouest des massifs de roche de socle. La base du paroxysme thermique est marquée par une série d'isogades inversés et repose sur le socle dont certaines parties sont demeurées relativement froides au cours de la phase de métamorphisme. La mise en place de la suite intrusive Hepburn s'est faite dans les niveaux structuraux supérieurs du paroxysme thermique Calderian et on ne retrouve aucun pluton Hepburn dans les unités du socle. La géométrie des structures mésoscopiques dans le complexe de la faille Wopmay indique une historie de cisaillement dextre avec une forte composante de compression.

INTRODUCTION

In the metamorphic-plutonic zone of the early Proterozoic Wopmay Orogen (McGlynn, 1970; Fraser et al., 1972; Hoffman, 1980b) late, postmetamorphic cross folds expose structures and units of both the easterly transported and thickened marginal prism (Hoffman and Bowring, 1983; St-Onge et al., 1983a) and the underlying Archean(?) basement (St-Onge et al., 1983b). In the southern Redrock Lake map area (NTS 86 G), Proterozoic and Archean(?) units deformed during the Calderian Orogeny (Hoffman and Bowring, 1983; St-Onge et al., 1983b) are exposed by a major northeast-southwest cross fold (Fig. 25.1) which provides, on both limbs, a complete section of the metamorphic-plutonic complex.

Work during the 1983 field season has completed 1:100 000 scale mapping of the early Proterozoic units east of the Wopmay Fault in both the Redrock Lake (86 G) and the Calder River (86 F) map areas. All of the exposed Archean(?) basement in both map areas was traversed except for the extreme SE corner of the Redrock Lake sheet. The results of the fieldwork can be outlined as follows.

1. Archean(?) basement is exposed continuously from Redrock Lake westward to within 25 km of the Wopmay Fault Zone. The basement units, which in the Redrock Lake area consist of foliated syenogranites and monzogranites intrusive into a basic volcanic section (St-Onge et al., 1983b), are dominated to the west by biotite- and hornblende-bearing quartzofeldspathic gneisses.
2. Proterozoic structures involving basement in the metamorphic-plutonic zone west of Carousel Massif, consist of two, large-scale antiforms, both cored by gneissic units of probable Archean age (St-Onge et al., 1983b). The easternmost fold structure, the Scotstoun Massif, shows no evidence of a Proterozoic fabric in the

[1] Department of Geological Sciences, Queen's University, Kingston, Ontario K7L 3N6
[2] Department of Geological Sciences, McGill University, Montreal, Quebec H3A 2A7

basement units. Twenty kilometres west, the Exmouth Massif is characterized by a local, probably Proterozoic fabric in the basement gneisses.

3. The Archean(?) basement, from the Carousel massif to the Exmouth Massif, is consistently overlain by 300-600 m of autochthonous early Proterozoic sediments and mafic volcanics which are relatively unstrained. Within the autochthonous strata the transition from the Epworth Group passive margin sequence to the initial rift deposits of the Akaitcho Group occurs on the west limb of the Scotstoun Massif.
4. Structurally above the low-strain domain and spectacularly well developed in the south hinge zone of the Exmouth Massif is a high ductile strain domain characterized by several sets of east-verging, recumbent folds of bedding and of tectonic fabric. This polydeformed domain is interpreted to be the ductile equivalent to the brittle decollement which, to the east, is folded around both the Scotstoun Massif and the Carousel Massif (St-Onge et al., 1983b; Tirrul, 1983).

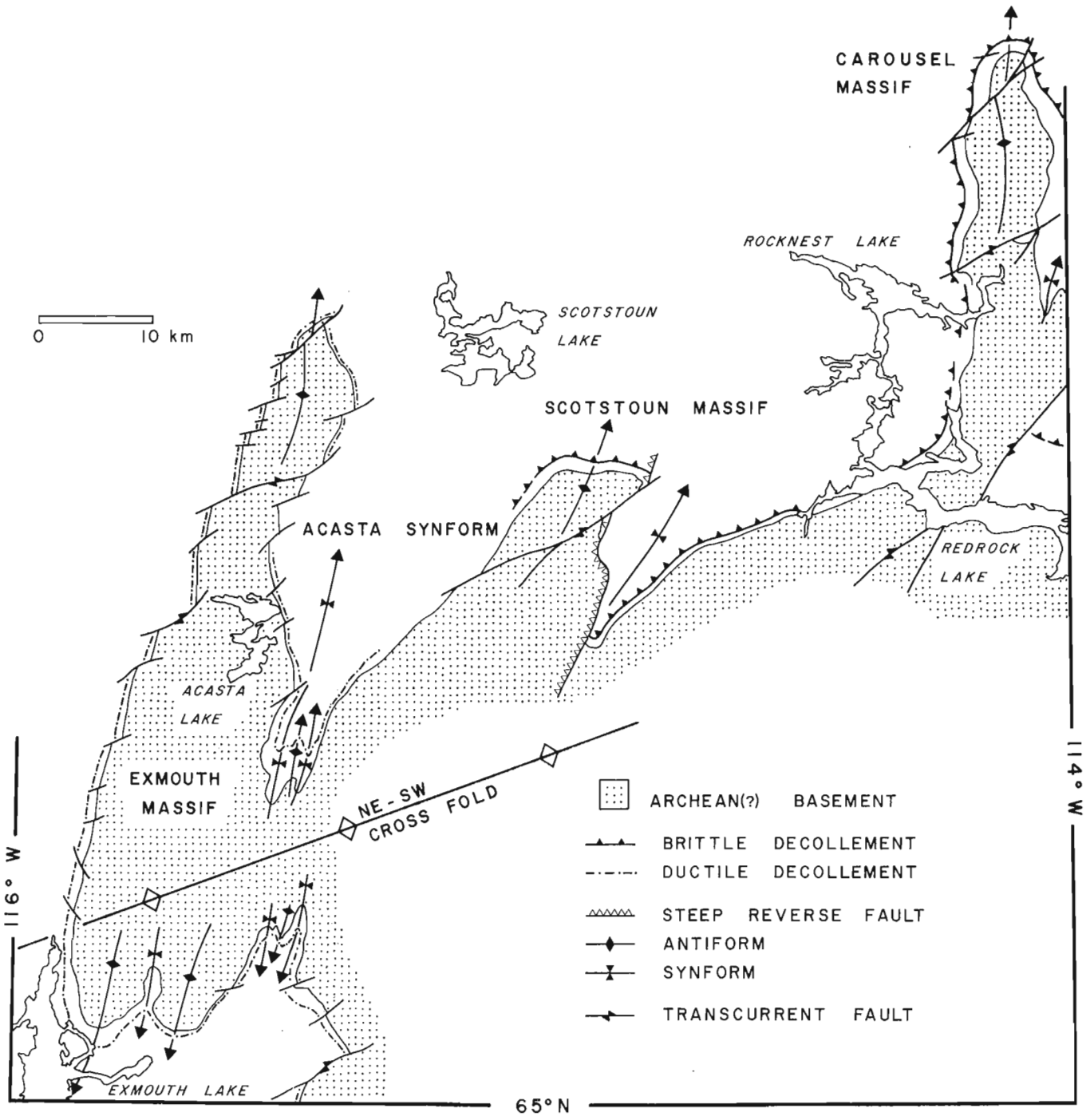

Figure 25.1. *Location of the three basement massifs and the regional décollement as exposed by a major northeast-southwest cross fold.*

5. Movement on the ductile decollement, and therefore easterly directed transport of the deforming marginal prism over the basement, is pretectonic to syntectonic with respect to development of the Calderian thermal culmination and emplacement of the associated granitic batholith. Movement predates the formation of the basement cored folds which deform all of the recumbent fold structures.

6. The Calderian thermal culmination in the metamorphic-plutonic zone is documented both in the deep structural sections exposed west of the Exmouth Massif, and in the higher structural levels exposed in the north- and south-plunging keel between the Scotstoun and Exmouth massifs (Acasta synform). The cross-sectional profile of the thermal culmination is that of an east-verging thermal lobe with lower grade rocks above, beside (on the east side), and beneath the high grade core containing the Hepburn Batholith. The underside of the Calderian thermal culmination is outlined by the trace of four "hot-side-up" mineral isograds (St-Onge, 1981), which progressively mark the first occurrence of muscovite + staurolite, muscovite + andalusite, mucovite + sillimanite and sillimanite + K-feldspar in pelitic schists and gneisses.

7. Emplacement of the Hepburn Intrusive Suite plutons is mostly coincident with the Calderian thermal culmination and restricted to the thickened and easterly transported Proterozoic marginal prism. No plutons of the Hepburn Intrusive Suite have been found within the basement to the Coronation Supergroup.

8. The mylonites and anastomosing brittle faults of the Wopmay Fault Zone (St-Onge et al., 1983) are continuous southward. The mylonites are characterized in places by well developed "c" and "s" fabrics (Berthé et al., 1979), associated shear bands, and a pervasive horizontal lineation. Mesoscopic geometry suggests an overall dextral sense of shear during mylonitization.

9. The Acasta River Intrusive Suite comprises two circular plutons of black alkali-feldspar syenite which have been emplaced into the Proterozoic sediments of the south-plunging Acasta synform. The plutons have remarkably well preserved mineralogical features. These plutons precede the late transcurrent faulting event (Hoffman, 1980a).

BASEMENT TO THE CORONATION SUPERGROUP

The Exmouth Massif is the westernmost of three large-scale, basement-cored fold structures that are present in the Redrock Lake map area (Fig. 25.1). Basement to the

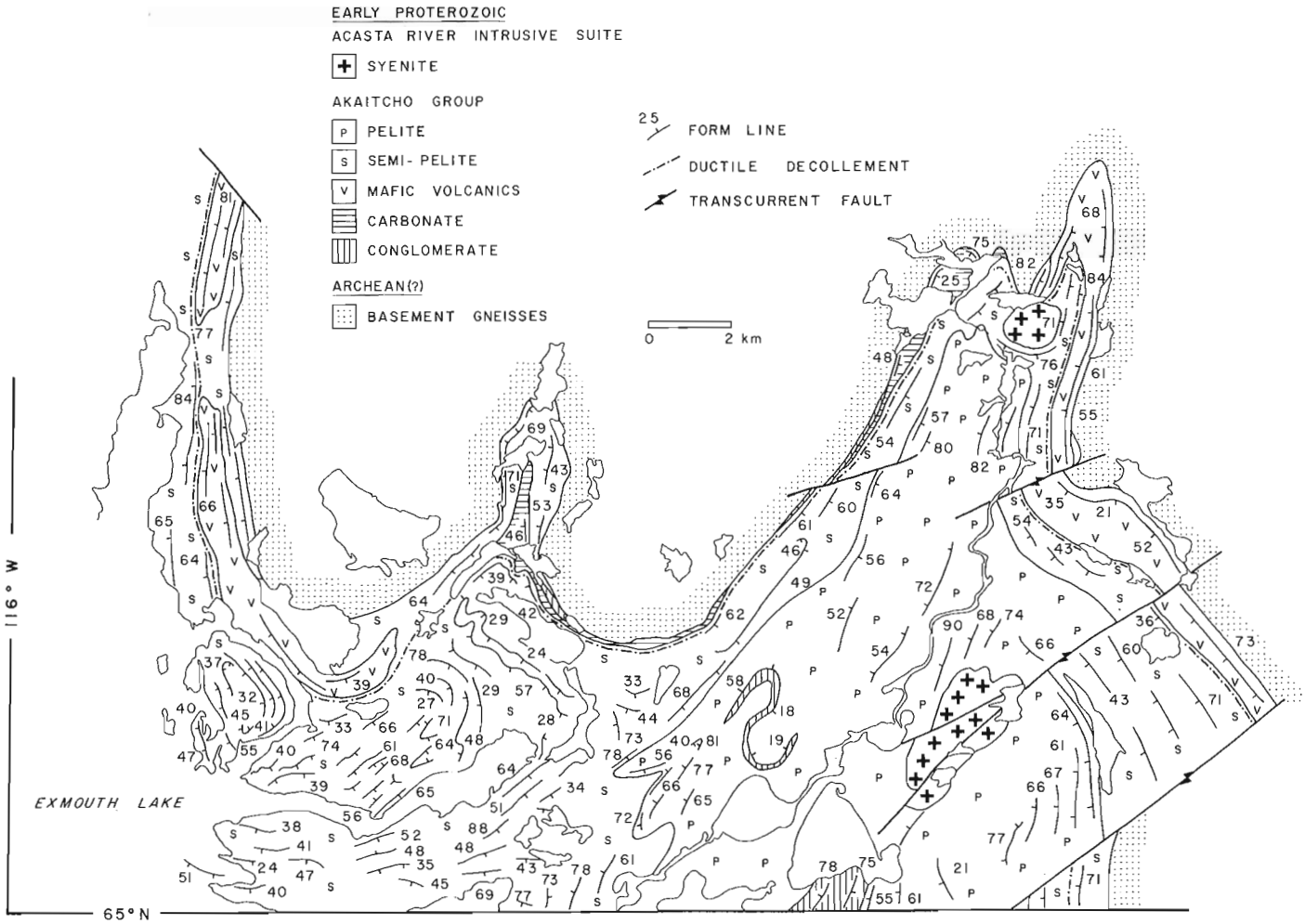

Figure 25.2. Major stratigraphic units of the Akaitcho Group with the ductile décollement, and form lines in both high and low strain domains east of Exmouth Lake.

Coronation Supergroup (Hoffman, 1981) was mapped previously to the east in the Carousel Massif and in the area south and southwest of Redrock Lake (Fraser, 1960, 1974; St-Onge et al., 1982, 1983b). Work during the summer of 1983 shows that exposed basement is continuous across the Carousel, Scotstoun and Exmouth massifs (Fig. 25.1) with a distinct variation in lithology from east to west. Coring the Carousel Massif is a foliated to gneissic biotite-monzogranite intrusive into the north margin of the Archean(?) Redrock Lake volcanic belt (St-Onge et al., 1983b). Basement to the Scotstoun Massif is a pink gneissic biotite syenogranite which also intrudes the metavolcanic rocks. The granite grades abruptly westward into a monotonous sequence of north striking, steeply dipping, biotite- and hornblende-bearing quartzofeldspathic gneisses. Amphibolite layers and boudins are locally abundant in the core of the Exmouth Massif.

The Exmouth Massif is the only structure in which a possible Proterozoic fabric is recognizable in the basement units. The fabric, a schistosity defined by an alignment of (retrograde) chlorite grains, appears to both parallel and be confined to within 100 m of the Akaitcho basal unconformity. The basement of both the Scotstoun Massif and the Carousel Massif, although obviously folded at a regional scale (Fig. 25.1), shows no recognizable macroscopic evidence of Proterozoic deformation.

AUTOCHTHONOUS PROTEROZOIC STRATA

As previously discussed (St-Onge et al., 1983b), a basal decollement which acts as a sole fault to the east-verging Calderian structures (Tirrul, 1983), is located about 300 m above the basement-cover interface, thereby preserving a significant thickness of autochthonous, early Proterozoic, stratigraphy (Fig. 25.1). To the east, around Carousel and Scotstoun massifs, the lower sequence comprises Odjick Formation quartzite, siltstone, some dolomite and a distinctive volcanic member (St-Onge et al., 1982, 1983b; Tirrul, 1983). To the west, in the Acasta synform, the lower autochthonous strata comprise discontinuous dirty quartzites, stromatolitic dolomites (now marble) and mafic metavolcanics. On the west limb of the synform (Fig. 25.2), extensive coarse, clastic-filled channels composed of polymict (quartz, gneiss, and granite) conglomerates associated with quartz-feldspar grits, lie directly on basement. These are overlain by the continuation of the stromatolitic marble unit, in turn conformably blanketed by a section of siltstones, pelites and metavolcanics. Around the Exmouth Massif (Fig. 25.2), the lower strata become a complex mix of conglomerates, feldspathic quartzites, siltstones, magnetite-bearing siltstones, dolomite and mafic metavolcanics, typical of the rift-environment Akaitcho Group (Easton, 1980, 1981b).

The lower autochthonous strata, resting directly on basement, thus contain the stratigraphic transition from the passive margin facies of the Epworth Group to the initial rift facies of the Akaitcho Group, with the transition situated on the west limb of the Scotstoun Massif (Fig. 25.1).

DUCTILE DÉCOLLEMENT

The brittle décollement and associated eastern transport of the deformed Coronation prism, typical of the Asiak Fold-Thrust Belt (St-Onge et al., 1982; Tirrul, 1982, 1983) can be traced westward (Fig. 25.1) to the hinge zone of the

a) Interlayered marble and siltstone showing three sets of folds. GSC 203780-P

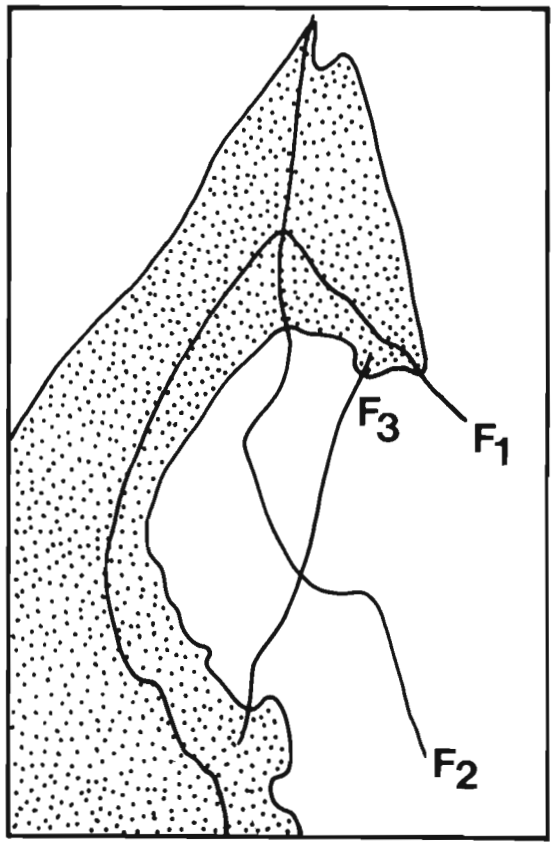

b) Axial traces of folds in Figure 25.3a; F_3 is coaxial with the folds of basement.

Figure 25.3

Scotstoun Massif (St-Onge et al., 1983b). West of this longitude, and structurally above the main zone of translation, early recumbent folds of bedding become increasingly more prominent until, in the southern hinge zone of the Exmouth Massif, at least two sets of recumbent folds (of bedding and of bedding plus cleavage) are well developed (Fig. 25.3). Fold closures and west-dipping axial planes suggest an overall east-vergence. Elongated sillimanite pods are coaxial with the early recumbent fold sets, indicating the folds formed during the high-T conditions associated with the Calderian thermal culmination. All early recumbent structures are folded about upright northeast-trending axial planes, coaxial and apparently coeval with the open folds of basement. Only biotite-chlorite-muscovite growth appears to be associated with the later structures, suggesting relatively retrograde thermal conditions during their development.

The main zone of translation, clearly recognized to the east as a brittle decollement, consists in the Exmouth Massif-Acasta synform area (Fig. 25.2) of a more diffuse zone of ductile translation which separates a structurally lower, relatively low strain domain from the overlying complexly folded recumbent domain. The low strain domain is characterized by forsterite-bearing marbles in which primary features such as stromatolites are perfectly preserved (Fig. 25.4), by conglomerates in which only the fine matrix records strain, and by the absence of recognizable recumbent folding. The high strain domain is characterized by multiple recumbent fold generations (Fig. 25.3), as described above, and by intensely deformed conglomerates. The strain gradient between the two domains is narrowly confined (Figs. 25.1, 25.2), occupying approximately the same structural position with respect to the basement as the brittle décollement to the east, and thus may be considered its ductile equivalent – a "ductile décollement". Total shortening on the ductile decollement and within the highly strained recumbently folded allochthonous Akaitcho Group must be at least equivalent to the 47 km of east-west shortening documented in the Asiak Fold-Thrust Belt (Tirrul, 1983) and is probably greater.

Figure 25.4. Stromatolitic marble, 25 m from basement. The metamorphic assemblage is forsterite-dolomite. GSC 203780-N

Documentation of the early sets of recumbent fold structures as being premetamorphic and synmetamorphic, places a clear constraint on the timing of movement for the ductile décollement in the metamorphic-plutonic zone. Easterly translation with respect to basement and the mantling autochthonous cover, must have preceded and accompanied the development of the Calderian thermal culmination. This was followed, during the waning stages of metamorphism, by continued east-west compression which folded the basement, the low strain domain, both the ductile and brittle décollement, and the mineral isograds.

CALDERIAN THERMAL CULMINATION

Structural relief generated by the major postmetamorphic northeast-southwest cross fold in the Redrock Lake area allows a full, down-plunge cross-section of the Calderian thermal culmination to be constructed. West and northwest of Exmouth Lake (Fig. 25.5), at the deeper structural levels corresponding to the axis of the cross fold, cover rocks consist of biotite-K-feldspar-plagioclase gneisses and amphibolites. These units can be traced across a series of mineral isograds, and up structural section into lower grade mafic flows, pelitic schists and arkosic sediments of the Akaitcho Group west of the Hepburn Intrusive Suite (Fig. 25.5).

In both the south-plunging and north-plunging hinge zones of the Acasta synform, pelitic mineral isograds (Fig. 25.5) can be mapped above the basement unconformity in the previously described lower Akaitcho Group units (Fig. 25.2). In both hinge zones, metamorphic grade increases going up structural section, away from the basement gneisses. The mapped mineral isograds are therefore "hot-side-up" (St-Onge, 1981) and the mineral zones are thermally inverted above a "colder" basement. The map pattern of the mineral isograds (Fig. 25.5) shows that some basement areas, notably the northern end of the Exmouth Massif, were heated to the higher temperatures associated with the metamorphosed units of the Akaitcho Group. Of significance, however, is the presence of areas of basement and cover that remained relatively "cold".

The mineral isograds in the north hinge of the Acasta synform can be projected across a covered area and match the isograd suite found on the east side of that part of the Calderian thermal culmination associated with the Hepburn Batholith at higher structural levels (Hoffman et al., 1980, 1981; St-Onge, 1981, in press). The portion of Figure 25.5 north of the cross fold can therefore be viewed as an oblique cross-section of the thermal culmination, with the mineral isograds outlining a thermally hot zone grading into lower grades – north, up structural section; east, at more or less constant structural level; and south, down structural section to basement.

HEPBURN PLUTONIC SUITE

Systematic mapping of basement gneisses in the Exmouth Massif and the Scotstoun Massif failed to recognize any intrusive rocks of the Hepburn Plutonic Suite (Hoffman et al., 1980; St-Onge et al., 1982) although small plutons of grey biotite granodiorite, similar to the rocks of the granodiorite and tonalite suite of the Hepburn Batholith, are intruded into the autochthonous Akaitcho Group sediments below the structural decollement. These small plutons are intrusive

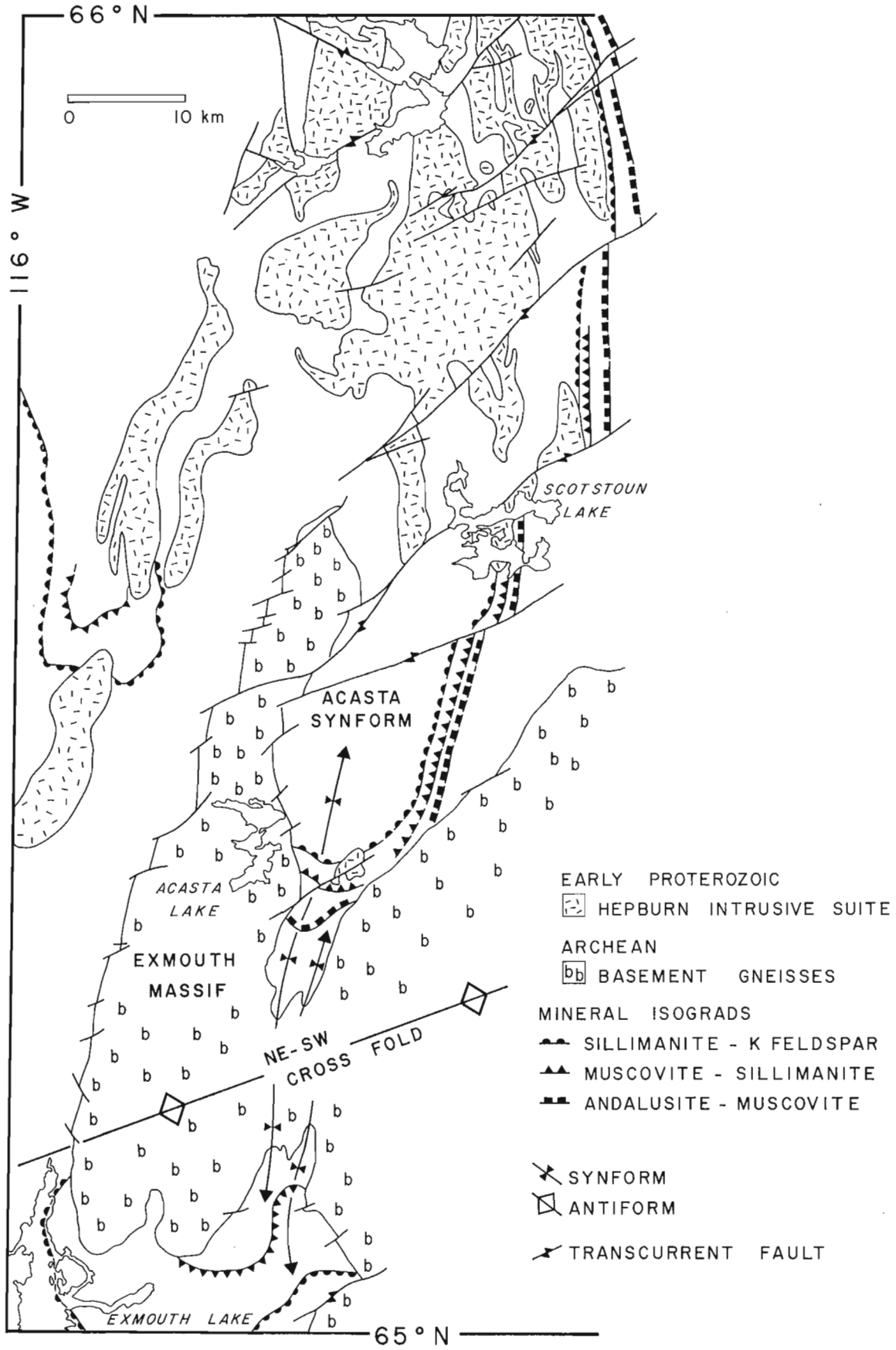

Figure 25.5. *Underside of the Calderian thermal culmination as outlined by the sequence of inverted isograds. Note that on both limbs of the cross fold metamorphic grade increases away from the basement gneisses, up structural section to culminate, on the north side, with the Hepburn Batholith.*

into metamorphic mineral zones of lower grade than the sillimanite-K-feldspar migmatites (Fig. 25.5) generally associated with the Hepburn Plutonic Suite (St-Onge, 1981, in press), an association also noted in the Hepburn Lake (86 J) map area to the north (Hoffman et al., 1981).

The bulk of the Hepburn Plutonic Suite, then, is coincident with the Calderian thermal culmination, and is emplaced structurally well above the basement unconformity and the ductile decollement. More specifically, the Hepburn plutons appear clustered where the higher structural levels within the thermal culmination are coincident with the transition from the Akaitcho Group mafic volcanics, semi-pelites and arkosic sediments to the thick Epworth Group and Asiak Group pelite section (Hoffman et al., 1981; St-Onge et al., 1983b).

WOPMAY FAULT ZONE

Introduction

The Wopmay Fault Zone (Easton, 1981a) is a 5 to 10 km wide north-south belt of protomylonites to ultramylonites and sheared, tectonostratigraphically independent blocks which have been structurally interleaved along late, anastomosing brittle faults. The belt truncates the western part of the Hepburn Metamorphic-Plutonic Zone.

As previously reported (St-Onge et al., 1983b; King et al., 1983) high grade gneissic equivalents of Akaitcho Group rocks are heterogeneously but progressively overprinted by a mylonitic fabric which increases in intensity with proximity to the fault zone. Adjacent to the fault zone, the regional foliation is typically drawn into macroscopic (5 km half-wavelength) en echelon folds, plunging moderately to either the northwest or southeast, which appear to be coaxial and possibly coeval with the mylonitic overprint, suggesting a dextral drag along the fault zone. These folds are typically truncated by the easternmost of the late brittle faults, but at Eyston Lake (65°10'N) the western limb of one of these folds is continuous into the mylonites of the Wopmay Fault Zone and a complete strain gradient into the fault zone can be documented.

The mylonites

Ultramylonites are restricted to narrow belts in the eastern part of the Wopmay Fault Zone, apparently recording the locus of the greatest ductile strain. The mylonite foliation is typically steep and contains a poorly to moderately developed, near-horizontal mineral (quartz-feldspar) elongation lineation. Local isoclinal folds of mylonite foliation may be coaxial or ambiguous (rotated?) with respect to the lineation. In one extremely coaxially folded area, one sheath fold was identified.

West of the ultramylonite belts are fault-bounded blocks of heterogeneously sheared migmatitic paragneisses and granites. The sheared granitic units have proved to be the most useful for the study of mesoscopic strain patterns in the fault zone, due to their originally isotropic nature. Structures which can be used for kinematic interpretations, such as "c" and "s" planes (Berthé et al., 1979) and shear bands (White et al., 1980) are clearly preserved. Two outcrop areas representative of the regional structural setting were carefully examined. In both, the mylonitic to schistose foliation is steeply dipping and the mineral elongation is near horizontal. In one, "c" and "s" planes are the predominant feature and when observed on a horizontal surface, consistently indicate a dextral sense of shear (Fig. 25.6). In the other, the predominance of shear bands and narrow, mylonitized zones, suggests higher strains. The outcrop is characterized by a schistose to mylonitic foliation cut by statistically dominant, centimetre-scale, dextral shear bands or by metre-scale dextral or sinistral shear bands. Consistent time relationships between these two scales cannot be established and they are likely coeval. K-feldspar megacrysts, aligned along the foliation, may be boudinaged or obliquely split in either a dextral or sinistral sense (Fig. 25.7a,b) but are always associated with the dextral shear bands. The geometry in both outcrops indicates a history of predominantly dextral simple shear with a large component of resolved pure shear. This substantiates the overall dextral sense of shear in the Wopmay Fault Zone as interpreted from less well developed structures elsewhere and from the geometry of the synkinematic en echelon folds.

Timing

The bulk of recorded ductile shearing within the fault zone is interpreted to have occurred late in the Calderian thermal event, as evidenced by the sheared Akaitcho Group gneisses and the presence of synkinematic biotite in thin section. Plutons of the Bishop Intrusive Suite (St-Onge et al., 1983b) which are dated at 1850 Ma by U-Pb on zircon (S. Bowring, personal communication) intrude the mylonitized gneisses but are sheared in proximity to the fault zone, thus providing a time pin for some of the ductile displacement in the fault zone. The late brittle faults, which displace the early

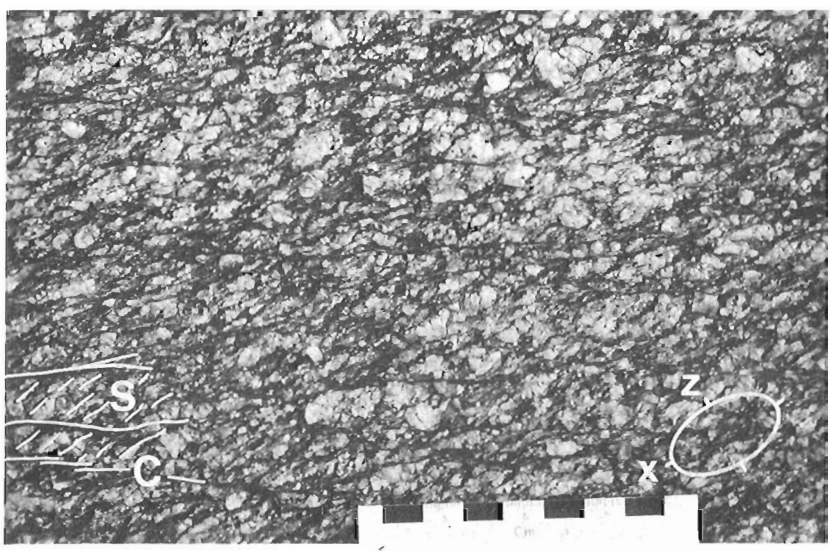

Figure 25.6

Sheared granitic unit in Wopmay Fault Zone, showing developed "c" and "s" planes indicative of a dextral sense of shear. GSC 203780-V

a) Sheared granitic unit in Wopmay Fault Zone showing obliquely split feldspar (sinistral), main schistose to mylonitic foliation and dextral shear bands. GSC 203780-T

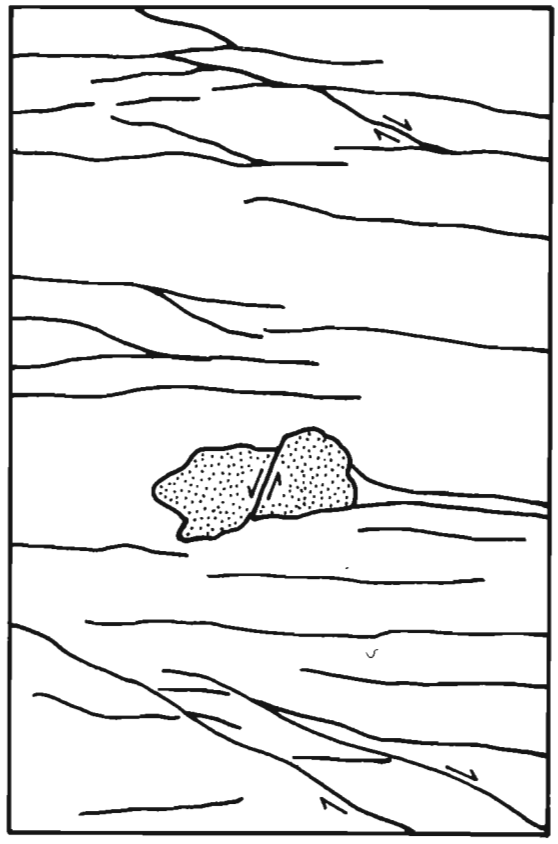

b) Line drawing of Figure 25.7a indicating sense of displacement.

Figure 25.7

mylonites, are in turn pinned by two suites of granitic plutons which intrude the fault traces. One of these is petrographically and texturally very similar to plutons of the Great Bear Batholith and comprises small plutons of quartz syenite. The second suite includes massive medium- to fine-grained biotite granodiorite to tonalite plutons which typically occur as long narrow bodies (St-Onge et al., 1983b). Dating of these units will provide an upper age bracket to the main displacements recorded in the Wopmay Fault Zone.

ACASTA RIVER SUITE

The Acasta River Suite comprises two small syenitic plutons emplaced in the south-plunging Acasta synform (Fig. 25.2). The plutons are 1 and 2 km in diameter, display sharp intrusive contacts, and have associated narrow thermal aureoles. The northern, smaller pluton consists of alkali-feldspar syenite with subordinate amounts of alkali-feldspar quartz syenite. Feldspars are pink and the ferromagnesian phases include amphibolite and biotite. The southern, larger intrusion (Fig. 25.2) is characterized by alkali-feldspar syenite with a locally well developed trachytic flow-foliation (Fig. 25.8). Large perthite phenocrysts in this pluton are a striking dark grey to black. The ferromagnesian phases include bright green (sodic?) pyroxene, amphibole and late biotite. Two late transcurrent faults (Hoffman, 1980a) cut the intrusion.

The Acasta River Suite is petrographically distinct from both the Hepburn Intrusive Suite (Hoffman et al., 1980; St-Onge et al., 1982, 1983b) and the Bishop Intrusive Suite (St-Onge et al., 1983b). The syenites are possibly the youngest in the metamorphic-plutonic zone and an age determination would yield a valuable "maximum" for the second collision event (Hoffman, 1980a; Hoffman and Bowring, 1983) in Wopmay Orogen.

DISCUSSION

Significant progress was made during the summer of 1983 in understanding the geometry and the tectonic evolution of the Hepburn Metamorphic-Plutonic Zone of Wopmay Orogen. Key relationships established in the course of the systematic mapping include the recognition of the Archean(?) basement and the extent of its involvement in the early Preoterozoic Calderian Orogeny. The mapping of the low strain zone above the basement unconformity, and its transition into the structurally higher, polydeformed, high strain domain of recumbent folds involving both bedding and tectonic fabric, provides an unprecedented opportunity to study the behaviour of a major regional basal decollement in a ductile regime.

The attitude of the mapped mineral isograds and the documentation of their regional inversion on the underside of the Calderian thermal culmination above the granitic basement, places important constraints on the shape of the

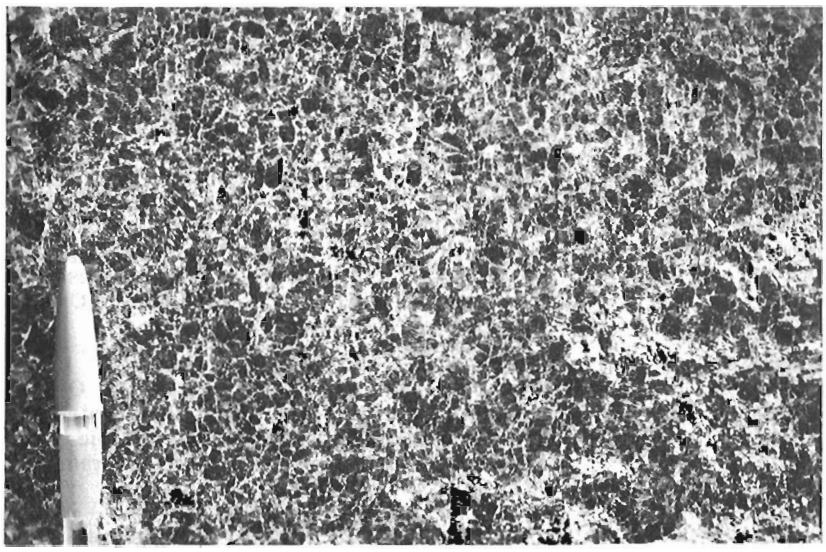

Figure 25.8

Black K-feldspar of the Acasta River Intrusive Suite showing vertical flow foliation. GSC 203780-J

metamorphic culmination. The development of the thermal high above relatively "colder" basement requires that the metamorphic complex be the result of heat carried with and/or into the easterly transported and deforming Coronation Supergroup prism.

The complete absence of Hepburn Intrusive Suite plutons within the basement, and the emplacement of most plutons at the higher structural levels within the Calderian thermal culmination that is floored by the sequence of inverted isograds, are certainly indications that the majority of plutons did not simply rise from the basement units through the lower Proterozoic strata to their final level of emplacement. Rather, it would seem that pluton generation within the easterly transported and thickened marginal prism is required, and in this regard it is interesting to note that the principal cluster of Hepburn Intrusive Suite plutons always sits on the Akaitcho Group-Epworth and Recluse groups transition.

Finally, studies of kinematic indicators in sheared units of the Wopmay Fault Zone illustrate how subtle (Fig. 25.6) the evidence can be for the dextral simple shear motion that characterized the belt.

ACKNOWLEDGMENTS

Julie Jackson, Steve Jackson, Dave Scott and Lesia Zalusky are sincerely thanked for their assistance, independent mapping and enthusiasm during an exciting summer that started in winter. We appreciated the discussions with Herb Helmstaedt (Queen's University) during his visit in his capacity as J. King's thesis advisor. We would like to thank Win Bowler and Martin Irving for their skillful expediting from the DIAND Geology Office in Yellowknife. And, finally, we are grateful to Larry Zurloff of Latham Island Airways for all his good humoured assistance in extending our range of traversing.

REFERENCES

Berthé, D., Choukroune, P., and Jegouze, P.
1979: Orthogneiss, mylonite and non coaxial deformation of granites: the example of the South Armorican Shear Zone; Journal of Structural Geology, v. 1, p. 31-42.

Easton, R.M.
1980: Stratigraphy and geochemistry of the Akaitcho Group, Hepburn Lake map area, District of Mackenzie: An initial rift succession in Wopmay orogen (early Proterozoic); in Current Research, Part B, Geological Survey of Canada, Paper 80-1B, p. 47-57.

1981a: Geology of Grant Lake and Four Corners Lake map area, Wopmay Orogen, District of Mackenzie; in Current Research, Part B, Geological Survey of Canada, Paper 81-1B, p. 83-94.

1981b: Stratigraphy of the Akaitcho Group and the development of an early Proterozoic continental margin, Wopmay Orogen, Northwest Territories; in Proterozoic Basins of Canada, ed. F.H.A. Campbell, Geological Survey of Canada, Paper 81-10, p. 79-95.

Fraser, J.A.
1960: North-central District of Mackenzie, N.W.T.; Geological Survey of Canada, Map 18-1960.

1974: The Epworth Group, Rocknest Lake area, District of Mackenzie; Geological Survey of Canada, Paper 73-39, 23 p.

Fraser, J.A., Hoffman, P.F., Irvine, T.N., and Mursky, G.
1972: Bear Structural Province; in Variations in Tectonic Styles in Canada, ed. R.A. Price and R.J.W. Douglas; Geological Association of Canada, Special Paper 11, p. 183-185.

Hoffman, P.F.
1980a: Conjugate transcurrent faults in north-central Wopmay Orogen (early Proterozoic) and their dip-slip reactivation during post-orogenic extension, Hepburn Lake map area, District of Mackenzie; in Current Research, Part A, Geological Survey of Canada, Paper 80-1A, p. 183-185.

1980b: Wopmay Orogen: A Wilson Cycle of early Proterozoic age in the northwest of the Canadian Shield; in The Continental Crust and its Mineral Deposits, ed. D.W. Strangway; Geological Association of Canada, Special Paper 20, p. 523-549.

Hoffman, P.F. (cont.)
1981: Revision of stratigraphic nomenclature, foreland thrust-fold belt of Wopmay Orogen, District of Mackenzie; in Current Research, Part A, Geological Survey of Canada, Paper 81-1A, p. 247-250.

Hoffman, P.F. and Bowring, S.A.
1983: Extensive effects of three different collisions on the foreland of Wopmay Orogen, northwest Canadian Shield; Geological Association of Canada, Program with Abstracts, v. 8, p. A33.

Hoffman, P.F., St-Onge, M.R., Easton, R.M., Grotzinger, J., and Schulze, D.W.
1980: Syntectonic plutonism in north-central Wopmay Orogen (early Proterozoic), Hepburn Lake map area (86J), District of Mackenzie; in Current Research, Part A, Geological Survey of Canada, Paper 80-1A, p. 171-177.

Hoffman, P.F., St-Onge, D.A., Easton, R.M., and St-Onge, M.R.
1981: Preliminary geological map of Hepburn Lake, District of Mackenzie; Geological Survey of Canada, Open File 784.

King, J.E., St-Onge, M.R., and Lalonde, A.E.
1983: Wopmay Fault Zone – a major mylonite and brittle fault belt, Internal Zone, Wopmay Orogen; Geological Association of Canada, Program with Abstracts, v. 8, p. A37.

McGlynn, J.C.
1970: Bear Province; in Geology and Economic Minerals of Canada, ed. R.J.W. Douglas; Geological Survey of Canada, Economic Geology Report 1, p. 77-84.

St-Onge, M.R.
1981: "Normal" and "inverted" metamorphic isograds and their relations to syntectonic Proterozoic batholiths in the Wopmay Orogen, Northwest Territories, Canada; Tectonophysics, v. 76, p. 295-316.

St-Onge, M.R. (cont.)
– Geothermometry and geobarometry in pelitic rocks of north-central Wopmay Orogen (early Proterozoic), Northwest Territories, Canada; Geological Society of America, Bulletin. (in press)

St-Onge, M.R., King, J.E., and Lalonde, A.E.
1982: Geology of the central Wopmay Orogen (Early Proterozoic), Bear Province, District of Mackenzie: Redrock Lake and the eastern portion of Calder River map areas; in Current Research, Part A, Geological Survey of Canada, Paper 82-1A, p. 99-108.

St-Onge, M.R., King, J.E., and Lalonde, A.E.
1983a: The Calderian Orogeny of Wopmay Orogen, N.W.T.: Evolution of an early Proterozoic collision-generated metamorphic-plutonic zone; Geological Association of Canada, Program with Abstracts, v. 8, p. A66.

St-Onge, M.R., Lalonde, A.E., and King, J.E.
1983b: Geology, Redrock Lake and eastern Calder River map areas, District of Mackenzie: The central Wopmay Orogen (early Proterozoic), Bear Province; in Current Research, Part A, Geological Survey of Canada, Paper 83-1A, p. 147-152.

Tirrul, R.
1982: Frontal thrust zone of Wopmay Orogeny, Takijuq Lake map area, District of Mackenzie; in Current Research, Part A, Geological Survey of Canada, Paper 82-1A, p. 119-122.

1983: Structure cross-sections across Asiak Foreland Thrust and Fold Belt, Wopmay Orogen, District of Mackenzie; in Current Research, Part B, Geological Survey of Canada, Paper 83-1B, p. 253-260.

White, S.H., Burrows, S.E., Carreras, J., Shaw, N.D., and Humphreys, F.J.
1980: On mylonites in ductile shear zones; Journal of Structural Geology, v. 2, p. 175-187.

26. PERALKALINE GRANITE NEAR HARE HILL, SOUTH OF GRAND LAKE, NEWFOUNDLAND

Project 730044

J.B. Whalen and K.L. Currie
Precambrian Geology Division

Whalen, J.B. and Currie, K.L., Peralkaline granite near Hare Hill, south of Grand Lake, Newfoundland; in Current Research, Part A, Geological Survey of Canada, Paper 84-1A, p. 181-184, 1984.

Abstract

In previous work, quartzofeldspathic gneisses and granites in the Hare Hill area were interpreted to be Grenvillian. The granites vary from massive to strongly sheared and metamorphosed and, in places, grade into granitic gneisses. Lithologically and petrologically, granites in the Hare Hill area strikingly resemble the massive, undeformed, unmetamorphosed, alkaline to peralkaline granites of the Topsails igneous terrane.

If the Hare Hill terrane represents a deformed equivalent of the Topsails terrane, the implications for the tectonics of western Newfoundland are quite profound. The locations of the Cabot Fault and Baie Verte-Brompton line must be reconsidered and all Newfoundland ophiolites cannot be made to lie near the same zone of generation. Clarification of the nature and timing of the post-Silurian tectonothermal event which affected the Hare Hill terrane may require reinterpretation of the tectonics of this region. The existence of basement in the form of anorthosite and granulites in the Hare Hill terrane suggests that continuous Grenville basement may form the substrate of the Humber zone and the Topsails terrane.

Résumé

Dans les travaux antérieurs, les gneiss et les granites quartzofeldspathiques de la région de Hare Hill sont considérés comme appartenant au Grenvillien. Les granites varient de massifs à fortement cisaillés et métamorphisés et, par endroits, se transforment en gneiss granitiques. Du point de vue de la lithologie et de la pétrologie, les granites de la région de Hare Hill ressemblent énormément aux granites alcalins et hyperalcalins massifs, non déformés et non métamorphisés du terrain igné de Topsails.

Si le terrain de Hare Hill représente l'équivalent déformé du terrain de Topsails, l'étude de la tectonique de la partie ouest de Terre-Neuve en sera grandement influencée. Il faudra réexaminer les positions de la faille de Cabot et de la limite Baie-Verte-Brompton. Toutes les ophiolites de Terre-Neuve ne pourront être situées près de la même zone de génération. Il faudra peut-être réinterpréter l'histoire tectonique de cette région afin d'éclaircir la nature et la chronologie de l'événement tectonothermique post-silurien qui a touché le terrain de Haire Hill. L'existence d'un soubassement d'anorthosite et de granulites dans le terrain de Hare Hill laisse croire qu'un soubassement grenvillien continu pourrait former le substrat de la zone de Humber et du terrain de Topsails.

INTRODUCTION

In previous communications (Whalen and Currie, 1982, 1983) we pointed out the distinctive character of the Topsails igneous terrane of western Newfoundland, notably the unusually leucocratic and undeformed nature of the igneous rocks, and the very widespread occurrence of alkaline to peralkaline granites. We noted that there seemed to be a possible continuation of the highly potassic leucocratic granite 50 km to the southwest of the Topsails terrane, on the opposite side of a major lithologic and tectonic boundary (Cabot Fault), around Hare Hill (Fig. 26.1). Further laboratory and field investigations have confirmed the presence of substantial amounts of alkaline to peralkaline granite around Hare Hill. The occurrence and structural state of these rocks pose difficult problems for tectonic models of western Newfoundland.

GEOLOGICAL SETTING

Knapp et al. (1979) described the geology around the south end of Grand Lake. Figure 26.2 is a slightly modified version of their geological map, and the following summary essentially presents their interpretation.

The region can be divided into two domains, a Lower Paleozoic carbonate platform sequence to the west, and crystalline rocks to the east. The crystalline rocks consist of quartzofeldspathic gneisses, granite and anorthosite alternating with zones of semipelitic to psammitic schists. The granitic and plagioclase hornblende gneisses (unit 1a) together with an isolated occurrence of calc-silicates and quartzite (unit 1b) were interpreted as basement and correlated with the Grenvillian Long Range and Indian Head complexes (Riley, 1962). The metasedimentary schists (unit 5) were interpreted to form an Hadrynian and/or Lower Paleozoic cover sequence to this basement, while two large bodies of massive to locally sheared pink, coarse grained granite to syenite were thought to be Precambrian intrusions locally affected by Paleozoic deformation. South of Grand Lake, the southward continuation of the Corner Brook Lake or Grand Lake Thrust juxtaposes the Precambrian gneisses (unit 1a) and the Paleozoic carbonate cover (unit 3), while along Grand Lake a Paleozoic cover sequence (unit 5) is separated from Ordovician pillow lavas of the Glover Formation (unit 8) by the Cabot Fault, interpreted to be a fundamental fault marked by the presence of highly deformed granite or mylonite (unit 13).

DESCRIPTION OF OCCURRENCES

Hare Hill exhibits a considerable variety of granitic rocks. The southeast side of the hill exposes coarse grained, red amphibole-biotite quartz syenite containing large anhedral arfvedsonite aggregates, or more rarely aggregates of aegirine, which are poikilitic with numerous zircon and opaque mineral inclusions. Ragged pale to very dark chocolate-brown biotite aggregates partly replace amphibole. Quartz and K-feldspar have been mainly recrystallized to mosaics of smaller grains. Sphene rims and replaces opaque minerals (ilmenite?). Very similar, variously deformed, quartz syenites occur along the west side of Tulk's Pond. The main part of Hare Hill reveals apparently gradational changes from

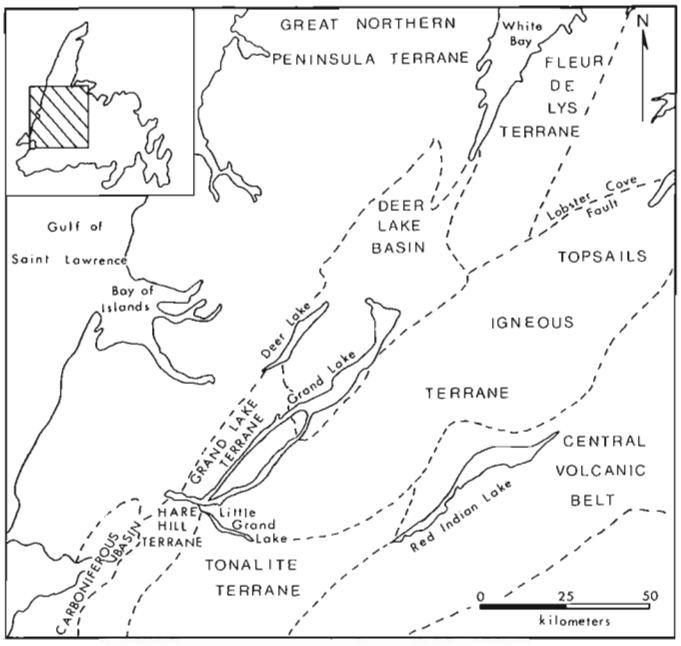

Figure 26.1. *Locations of the Topsails and Hare Hill terranes and other geological terranes of Western Newfoundland.*

red, coarse grained, amphibole quartz syenite and granite to pink, medium grained amphibole-biotite granite and aplite with abundant quartz veins. In all of these granitic phases the mafic minerals are partly to completely pseudomorphed by opaque minerals and ragged biotite, and quartz and feldspar have been recrystallized. Areas of shearing and mylonitization occur ubiquitously but irregularly, so that gradations exist over a few metres from massive to intensely sheared granite.

Northeast of Tulk's Pond, coarse grained, red, slightly foliated aegirine granite outcrops, characterized by large "clotty" quartz grains with a sugary appearance. Large anhedral aegirine grains and aggregations have been partly altered to a striking red-brown biotite and minor riebeckite. The coarse grained quartz, K-feldspar and clinopyroxene have been recrystallized to aggregates of smaller, anhedral grains. To the northeast of this occurrence, an extensive area of medium grained biotite granite and fine grained aegirine aplite contains irregular vein or pod-like masses of quartz up to 2 m wide by 5 m long. The cuspate, irregular boundaries of these segregations suggest that they are, in part at least, pegmatitic segregations. A mafic dyke cutting the granite has been partly broken up and altered to biotite schist.

All of these variants were included within unit 12a by Knapp et al. (1979). They also included within this unit coarse grained foliated amphibole-biotite diorite and medium grained biotite-amphibole granite gneiss on Goose Hill. The latter lithology grades to coarse muscovite schist containing 1-5 cm rounded quartz and granite inclusions. This in turn grades to relatively massive, red, one-feldspar, amphibole-biotite granite of Topsails type.

Along a main logging road south of Tulk's Pond, extensive exposure of highly fractured, sheared, red biotite-amphibole quartz syenite lies within unit 1a of Knapp et al. (1979). The rock varies from slightly to strongly foliated, and the prominence of fine to medium grained biotite aligned parallel to foliation varies directly with strength of foliation. The least deformed parts strikingly resemble the moderately deformed quartz syenites west of Tulk's Pond and south of Hare Hill. As in those rocks, large anhedral arfvedsonite aggregates have been extensively replaced by chocolate brown biotite, and quartz and potash feldspar have been recrystallized to fine grained anhedral aggregates. Abundant aggregates of anhedral sphene possibly represent a replacement of original ilmenite. These rocks appear to represent more highly deformed and metamorphosed equivalents of the quartz syenites of Hare Hill and Tulk's Pond.

DISCUSSION

Lithologically the granites in the Hare Hill region strikingly resemble the Topsails amphibole granite and its various marginal phases. The amphibole quartz syenite exhibits a more mafic and quartz-poor composition than any noted in the Topsails, but mineralogically and texturally there are close resemblances in the mode of occurrence and composition of the mafic minerals, and in the presence of abundant zircon+opaque inclusions in amphibole. The mineralogy demonstrates that these granites, like those of the Topsails, vary from alkaline to peralkaline in composition, and strongly suggests that they resemble the Topsails granites in high Zr content, and probably in contents of other elements accommodated in zircon (for example Nb and REE). In contrast to the massive, undeformed and unmetamorphosed nature of the Topsails graintes the alkaline to peralkaline granites southwest of Grand Lake vary from massive to strongly sheared, and have been variably metamorphosed. All gradations exist from massive peralkaline granite, mapped by Knapp et al. (1979) as belonging to unit 12a, to peralkaline granite gneiss mapped as unit 1a. Apparently the distinction between these units is essentially structural, and by no means clear-cut. A significant proportion of the granitic gneiss of unit 1a may represent highly deformed equivalents of Topsails-type granites (unit 12a).

On the grounds of juxtaposition of two occurrences of an unusual rock type, we believe the Hare Hill occurrences to be related to the Topsails terrane. However, there are two other possibilities which we discuss briefly before considering the consequences of such a correlation. (1) The alkali granites might, as interpreted by Knapp et al. (1979), be Precambrian and unrelated to the Topsails. We believe this to be unlikely because (a) the probability of juxtaposition of unrelated occurrences of lithologically identical and mineralogically unusual rocks is very low, and (b) neither the magmatic nor tectonic history leading to peralkaline granite generation (long continued magmatic activity in a complexly faulted region) has been observed or suggested in the Precambrian of western Newfoundland. (2) The alkali granites might be Phanerozoic but unrelated to the Topsails. We believe this possibility to be even less probable than the first. In the case of a Precambrian origin it could reasonably be argued that the Precambrian history is poorly known, and that occurrence of peralkaline magmatism cannot be ruled out. The Phanerozoic history is believed better understood (Williams, 1979), and the only possibility in this case would be to argue for an exotic terrane of unknown provenance to be fortuitously juxtaposed with the Topsails.

If the Hare Hill occurrences represent rocks equivalent to the Topsails terrane, the implications for the tectonics of western Newfoundland are quite profound. One of the basic assumptions of all current tectonic models supposes the Cabot Fault to be a fundamental feature separating rocks of very different affinities, continental basement from oceanic and island arc material according to the model of Williams (1978). A corollary of this view is that all ophiolite complexes in western Newfoundland originated in a single zone, which can be identified, in part at least with the Cabot

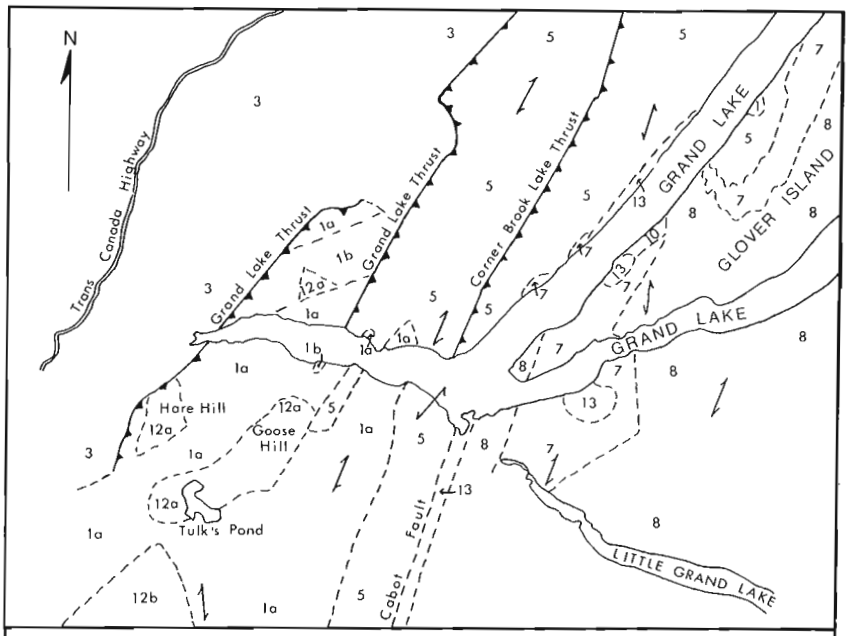

LEGEND

INTRUSIVE ROCKS

13 Carboniferous and older granites

12 Precambrian: 12a, granites; 12b, anorthositic rocks

DEVONIAN AND OLDER

10 Clastic sedimentary rocks

MIDDLE ORDOVICIAN TO LOWER CAMBRIAN

8 Glover Formation: pillow lavas and volcanoclastic sediments

7 Glover Island Complex: mafic rocks of ophiolitic affinity

5 Fleur De Lys Supergroup: semipelitic schists and psammitic gneisses

3 Platformal sedimentary rocks: carbonates and shales

PRECAMBRIAN

1 1a, granitic gneiss and amphibolite; 1b, schists and gneisses with minor quartzite and calc-silicate gneiss

Geology after Knapp et al. (1979)

Geologic contact

Foliation

Thrust fault

Road

Figure 26.2. *Geology of the south end of Grand Lake, Newfoundland modified from Knapp et al. (1979).*

Fault (Baie Verte-Brompton line of Williams and St. Julien, 1978). Correlation of the Topsails and Hare Hill occurrences strongly attacks both these views. The Topsails granites are post-Silurian, and accordingly were offset 50 km in a right-hand sense in post-Silurian time, according to our correlation. No chain of ophiolites, or zone of production of ophiolites can be assumed to cross this very leucocratic and continentally derived belt of rocks, hence the only possibility is to offset the Cabot Fault 50 km to the west at the foot of Grand Lake, so as to pass through a region of very little outcrop in the vicinity of the Trans Canada Highway. In such a case the Baie Verte-Brompton line cannot pass eastward from the foot of Grand Lake to the Annieopsquotch complex (Herd and Dunning, 1979), and all Newfoundland ophiolites cannot be made to lie near the same zone. Rather there must be two or more zones of generation. The widespread and erratic distribution of ophiolitic fragments has been pointing toward this conclusion for some time (Whalen and Currie, 1983). Fragmentary but suggestive evidence against very large scale separation of terranes around Grand Lake has likewise been accumulating for some time. The Ordovician Glover Formation of basalt and associated sedimentary rocks crosses Little Grand Lake (Knapp et al., 1979) and disappears in the "tonalite terrane". As pointed out by Whalen and Currie (1983), the Hungry Mountain complex of the Topsails terrane appears to be equivalent to the tonalite terrane to the south. Knapp et al. (1979) considered the Fleur de Lys Group to be exposed on the west shore of Grand Lake, on Glover Island, and to the south of the lake, that is on both sides of the Cabot Fault and also on both sides of the cross-fault which we consider to offset the Cabot Fault. The southwest part of the Topsails terrane exhibits a strong positive Bouguer gravity anomaly, readily visible on the recent 1:2 000 000 compilation (Haworth et al., 1980); the cause is uncertain but is not the result of the bedrock exposed, that is, diorite and leucocratic alkali granite. A similar anomaly occurs over the Steel Mountain anorthosite complex south of Hare Hill, suggesting that the two anomalies once formed a single anomaly over a large anorthosite complex. Massif-type anorthosite, long thought typical of the Grenville province must occur east of the Cabot Fault according to the present interpretation. Granulite grade metamorphic rocks occur in the tonalite terrane (Herd and Dunning, 1979) and in the Topsails terrane south of Sheffield Lake. Both the anorthosite and the granulites can reasonably be correlated with undoubtedly Grenville rocks in the Long Range. Further, recent work by Chorlton (1981) and Wilton (1983) suggested that most, or all, of southwestern Newfoundland belongs to the same terrane, rather than to two very different terranes as previously supposed (Brown, 1976; McKerrow and Cocks, 1977). These considerations raise fundamental questions about the whereabouts of relicts of the Iapetus Ocean. The present data would be more compatible with the opening and closing of a number of much smaller basins floored by oceanic material, but separating fragments of the same terrane. Clearly the problems of the relations of various parts of Newfoundland cannot be considered solved without a much better understanding of the plutonic rocks. To the extent that western Newfoundland has been used as a model for ancient orogenic belts since the pioneering work of Bird and Dewey (1970), this model must be considered somewhat compromised.

The structure of the Hare Hill occurrences likewise casts an interesting light on the later tectonic history of western Newfoundland. If they are Topsails equivalents, they have undergone a tectonothermal event to which the rest of the Topsails was not subjected. After emplacement of the Topsails granites, the southern part of the Topsails terrane

including the Hare Hill region, was displaced westward, presumably along a northwest-southeast trending fault running through Little Grand Lake and the southern end of Grand Lake. The Hare Hill segment was subsequently strongly deformed and metamorphosed, probably in amphibolite facies. The nature and timing of this event cannot be fixed precisely, but it seems reasonable to identify it with the event producing isoclinal overturned folding in the Carboniferous section on the west shore of Grand Lake, on strike with the structure in the Hare Hill region. A young event of this magnitude would require reinterpretation of the tectonics of this region. We suggest that K-Ar dating of secondary biotite in the Hare Hill alkali granites could date this event. We also point out that many tectonic interpretations of southwest Newfoundland assume implicitly that major deformation (a) is Devonian or older and (b) extends over the whole of the area considered. The Hare Hill region casts strong doubt on both assumptions.

Although many of the deformed host rocks of the Hare Hill alkali granites may be deformed equivalents of slightly older granites in the Topsails terrane, the presence of the Steel Mountain anorthosite and the granulite complex substantiates the existence of basement, presumably Grenvillian. Although these units have not been observed in situ in the Topsails, granulites occur as screens and inclusions in the granites, and indirect evidence suggests that anorthosite may be present at depth. Continuous Grenville basement may form the substrate of the Humber zone (Williams, 1978) and the Topsails terrane. We previously stated that the occurrence of huge volumes of highly potassic felsic igneous rocks in the Topsails terrane requires the presence of continental crust. The Hare Hill segment of the Topsails terrane may expose part of this continental basement.

Finally, we wish to call attention to the overall progress in Western Newfoundland geology that has been made by detailed work on the plutonic terranes (Whalen and Currie, 1982, 1983; Dunning, 1981; Chorlton, 1981; Wilton, 1983). We believe that fundamental geological advances in this region will henceforth rest heavily on advances in the understanding of the plutonic rocks.

REFERENCES

Bird, J.M. and Dewey, J.F.
1970: Lithosphere plate-continental margin tectonics and the evolution of the Appalachian orogen; Geological Society of America Bulletin, v. 81, p. 1031-1060.

Brown, P.A.
1976: Ophiolites in southwest Newfoundland; Nature, p. 712-715.

Chorlton, L.
1981: Geology of the La Poile River area (110/16) Newfoundland; Newfoundland Department of Mines and Energy, Mineral Development Division, Report 80-3.

Dunning, G.R.
1981: The Annieopsquotch ophiolite complex, southwestern Newfoundland, and its regional relationships; in Current Research, Part B, Geological Survey of Canada, Paper 81-1B, p. 11-15.

Haworth, R.T., Daniels, D.L., Williams, H., and Zietz, I.
1980: Bouger gravity anomaly map of the Appalachian orogen; Memorial University of Newfoundland, Map 3a.

Herd, R.K. and Dunning, G.R.
1979: Geology of the Puddle Pond map area, southwestern Newfoundland; in Current Research, Part A, Geological Survey of Canada, Paper 79-1A, p. 305-310.

Knapp, D., Kennedy, D., and Martineau, Y.
1979: Stratigraphy, structure and regional correlation of rocks at Grand Lake, western Newfoundland; in Current Research, Part A, Geological Survey of Canada, Paper 79-1A, p. 317-325.

McKerrow, W.S. and Cocks, L.R.M.
1977: The location of Iapetus Ocean suture in Newfoundland; Canadian Journal of Earth Sciences, v. 14, p. 488-499.

Riley, G.C.
1962: Stephenville map-area, Newfoundland; Geological Survey of Canada, Memoir 323.

Whalen, J.B. and Currie, K.L.
1982: Volcanic and plutonic rocks in the Rainy Lake area, Newfoundland; in Current Research, Part A, Geological Survey of Canada, Paper 82-1A, p. 17-22.

1983: The Topsails igneous terrane of western Newfoundland; in Current Research, Part A, Geological Survey of Canada, Paper 83-1A, p. 15-23.

Williams, H.
1978: Tectonic-lithofacies map of the Appalachian orogen; Memorial University of Newfoundland, Map 1.

1979: Appalachian Orogen in Canada; Canadian Journal of Earth Sciences, v. 16, p. 792-807.

Williams, H. and St. Julien, P.
1978: The Baie Verte-Brompton Line in Newfoundland and regional correlations in the Canadian Appalachians; in Current Research, Part A, Geological Survey of Canada, Paper 78-1A, p. 225-229.

Wilton, D.H.C.
1983: The geology and structural history of the Cape Ray Fault Zone in southwestern Newfoundland; Canadian Journal of Earth Sciences, v. 20, p. 1119-1133.

27. SEDIMENTARY SETTING OF AN EARLY PROTEROZOIC COPPER OCCURRENCE IN THE COBALT GROUP, ONTARIO: A PRELIMINARY ASSESSMENT

Project 760027

F.W. Chandler
Precambrian Geology Division

Chandler, F.W., Sedimentary setting of an Early Proterozoic copper occurrence in the Cobalt Group, Ontario: a preliminary assessment; in Current Research, Part A, Geological Survey of Canada, Paper 84-1A, p. 185-192, 1984.

Abstract

Copper sulphide mineralization, apparently of sedimentary origin, occurs in the Early Proterozoic Cobalt Group at the contact between a quartz arenite at the top of the Lorrain Formation and the siltstone-rich Gordon Lake Formation.

To date, assessment of the context of the mineralization has rested on mutually contradictory interpretations of the depositional environments of the formations of the group.

Preliminary study of sedimentary structures and of textures of framework grains and of zircon heavy mineral grains supports the view that the quartz arenite of the Lorrain Formation is fluvial and that the Gordon Lake Formation records marine transgression through supratidal to shallow subtidal environments. The overlying Bar River Formation quartz arenite is probably shallow marine with emergence.

Thus the mineralization seems to occur in a transgressive marine sequence at the contact between a fluvial and a tidal unit.

Résumé

La minéralisation en sulfure de cuivre, vraisemblablement d'origine sédimentaire, se présente dans le groupe de Cobalt du Protérozoïque ancien au contact d'une quartzite sédimentaire au sommet de la formation de Lorrain et de la formation de Gordon Lake, riche en silstones.

A ce jour, l'évaluation du contexte de la minéralisation dépend d'interprétations mutuellement contradictoires des milieux de sédimentation des formations du groupe.

L'étude préliminaire des structures sédimentaires et des textures des grains du réseau et des grains de zircon et de minéraux lourds confirment l'hypothèse voulant que la formation de Lorrain soit d'origine fluviale et que la formation de Gordon Lake enregistre une transgression marine passant d'un milieu supratidal à un milieu subtidal peu profond. La quartzite sédimentaire sus-jacente de la formation de Bar River proviendrait d'un milieu marin peu profond émergeant.

La minéralisation semble donc se présenter dans une séquence marine transgressive, au contact d'une unité fluviale et d'une unité intertidale.

INTRODUCTION

Apparently stratabound disseminated copper sulphide mineralization (Pearson, 1980) occurs in the Cobalt Group of the Early Aphebian Huronian Supergroup (Card et al., 1972) along the north shore of Lake Huron. The group consists in ascending order of the Gowganda Formation (up to 5100 m thick), famous as the earliest well-documented glacial deposit, the Lorrain Formation (2500 m thick), an upward-maturing arenite, the Gordon Lake Formation (1100 m thick, Card, 1976), a thinly bedded sequence of varicoloured mudstone to sandstone with sulphate nodules near its base and last, the Bar River Formation (900 m thick), a quartz arenite. The stratabound mineralization occurs at two stratigraphic levels. One occurs near Sault Ste Marie in the lower part of the Lorrain Formation where green argillite overlies pink and red feldspathic sandstone (Pearson, 1979); the other occurs at the contact of the Lorrain Formation and the overlying Gordon Lake Formation at Stag Lake and possibly Cobre Lake (Fig. 27.1) and is best known from drill core (Pearson, 1979). The geology of the host rocks of the second horizon is the subject of this preliminary note.

According to Pearson (1979, p. 297) low grade copper mineralization is most abundant at Stag Lake within 2 m of the contact of the Lorrain and Gordon Lake formations and occurs over a strike length of 3.2 km. Anhydrite nodules (also Wood, 1970) in the lower part of the Gordon Lake Formation suggested to Pearson (op. cit.) a sabkha mode of deposition. He felt that the mineralization is of redbed type, the copper-bearing solutions having risen through the upper part of the Lorrain Formation to be deposited by reductants at the base of the Gordon Lake Formation.

Although no significant discoveries have been made, he noted the limited exploration of the recessive mineralized horizon, pointing to a similar situation in Michigan where in spite of a long history of exploration, extensive sedimentary copper at the recessive base of the possibly correlative (Young, 1966) Early Proterozoic Kona Dolomite was recognized only in the 1960s. Perhaps significantly, a second occurrence of disseminated copper mineralization was reported on the south shore of Cobre Lake (Fig. 27.1) in grey sandstone float, probably from the Gordon Lake Formation, 10 km west of the Stag Lake occurrence (Brian Wilson, personal communication, 1983).

The sedimentary environments of the formations of the Cobalt Group hosting the copper mineralization are disputed. Although aware of this uncertainty, Pearson (1980) accepted that the Lorrain Formation is fluvial in origin and that the Gordon Lake Formation may be tidal to supratidal or deep water in origin.

Because this possible new occurrence at Cobre Lake suggests that copper mineralization might be more widespread at the poorly exposed Lorrain-Gordon Lake contact and because of the uncertainty of the depositional environments of the host rocks, a study of the sedimentology of the Lorrain, Gordon Lake, and Bar River formations was commenced near Cobre Lake (Fig. 27.1) by the writer in the summer of 1983.

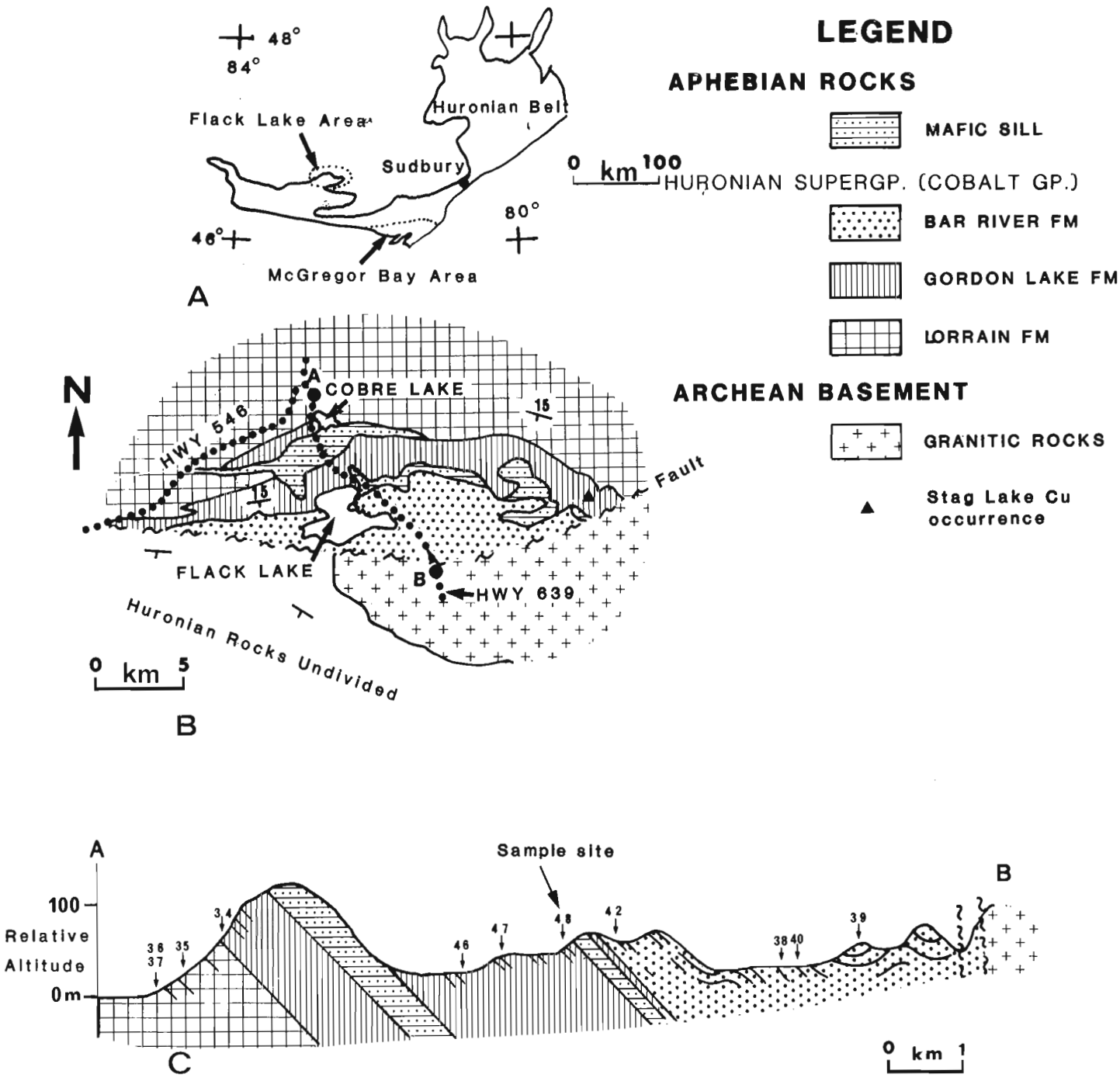

Figure 27.1. A. Location map. B. Geological map of Flack Lake area (after Ont. Geol. Surv. map 2419). C. Geological section A-B from Figure 27.1B.

PREVIOUS WORK

From paleocurrent patterns and textural and mineralogical maturity nearly all previous workers agreed that the quartz arenite member at the top of the Lorrain formation was deposited in a beach-shallow marine environment, with some bimodal textures indicating eolian action (Card, 1976; Casshyap, 1971; Hadley, 1968; Siemiatkowska, 1977, 1978; Pettijohn, 1970; Young, 1973). But Wood (1970), Frarey and Roscoe (1970, p. 153) and Roscoe and Frarey (1970, p. 257) felt that the paleocurrent pattern indicated a fluvial mode of deposition and suggested that weathering might have influenced the unit's mineralogical maturity.

The Gordon Lake Formation consists of a middle, mainly siltstone, portion up to 900 m thick and mainly sandstone upper and lower parts about 90 m thick (Card, 1976, 1978). Siemiatkowska (1978, p. 40) reported a similar division. A marine origin is agreed by all. In the McGregor Bay area Card (1976) suggested a tidal flat origin. In the Flack Lake area Wood (1970, p. 166) concurred, citing mudracks. Likewise Frarey (1977, p. 56) regarded the mudcracks as evidence of a "probably nearshore marine, to-littoral, possibly lagoonal environment". Wood (1970) pointed to nodular sulphate in the lower part of the formation as possibly of supratidal or lagoonal origin and suggested that the silt of the formation might be glacial loess.

Card (1978, p. 126) later reinterpreted the mudcrack-like structures that characterise the middle four fifths of the formation as syneresis cracks. Using sedimentary structures such as laminated bedding, graded bedding, convolute bedding, ripple marks and ripple- drift bedding as evidence of Bouma sequences Card (1978, p. 124, 126) moved to a turbidite origin below wave base for "parts of the formation". Collinson and Thompson (1982) regarded syneresis cracks as subaqueous in origin and arising by reorganization of porous clay due to flocculation or because of volume changes in some clay minerals induced by salinity variation. Such structures occur in a variety of marine and non marine environments, but the marginal marine setting is especially favourable because of the likelihood of changes in salinity.

Pettijohn (1970, p. 247) and Card (1970, p. 157) observed that the Bar River Formation is texturally and mineralogically too mature to be fluvial and is likely to be marine. Wood (1970) commented that good sorting and roundness, bimodal texture, polymodal crossbed directions and mudcracks signified a hybrid beach-eolian environment. But Frarey and Roscoe (1970, p. 153) discounted textural data, feeling that the mineralogical maturity was imposed on a fluvial unit by its weathering history.

Clearly then, there is marked contradiction in the interpretations of all three units.

PRESENT STUDY

Sedimentary structures

No observations of significance were made on the Lorrain Formation. In the silty upper half of the Gordon Lake Formation no mudcracks, but many syneresis cracks and many of the structures used by Card (1978) to suggest turbidite origin were seen. All these structures tend to be arranged in upward-fining cycles thinner than about 50 cm (Fig. 27.2a).

The contradictions among the various explanations of the sedimentology of the Gordon Lake Formation can be resolved if these cycles, i.e. Card's (1976) evidence of deep-water turbidite deposition, are reinterpreted as follows.

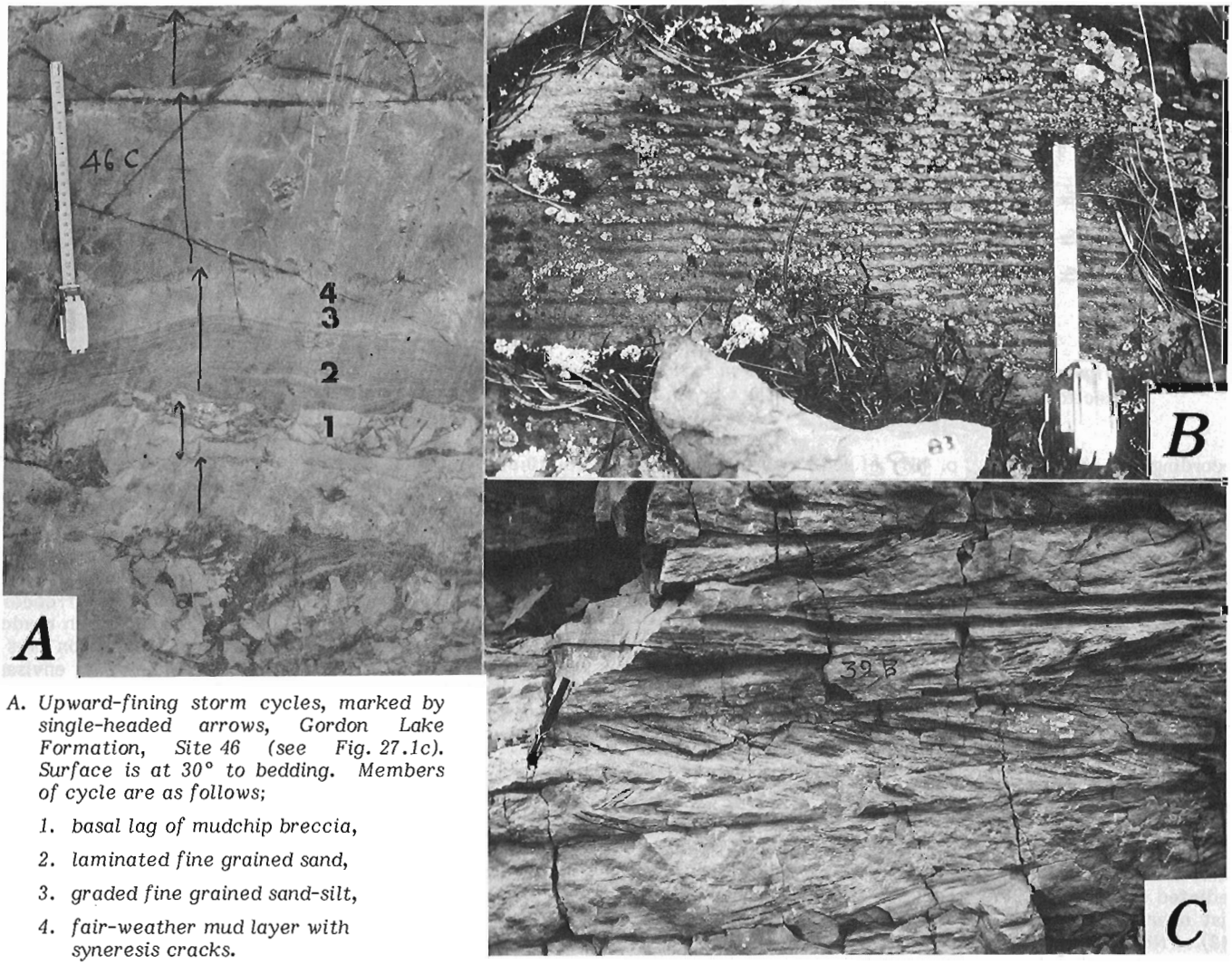

A. *Upward-fining storm cycles, marked by single-headed arrows, Gordon Lake Formation, Site 46 (see Fig. 27.1c). Surface is at 30° to bedding. Members of cycle are as follows;*

1. *basal lag of mudchip breccia,*
2. *laminated fine grained sand,*
3. *graded fine grained sand-silt,*
4. *fair-weather mud layer with syneresis cracks.*

B. *Small-scale, λ=1.5 cm, linear wave ripples, Bar River Formation, Site 38, indicative of water only several centimetres deep.*

C. *Apparently multidirectional small-scale crossbeds Bar River Formation. Vertical section, site 39, suggestive of tidal action. Felt pen gives scale.*

Figure 27.2

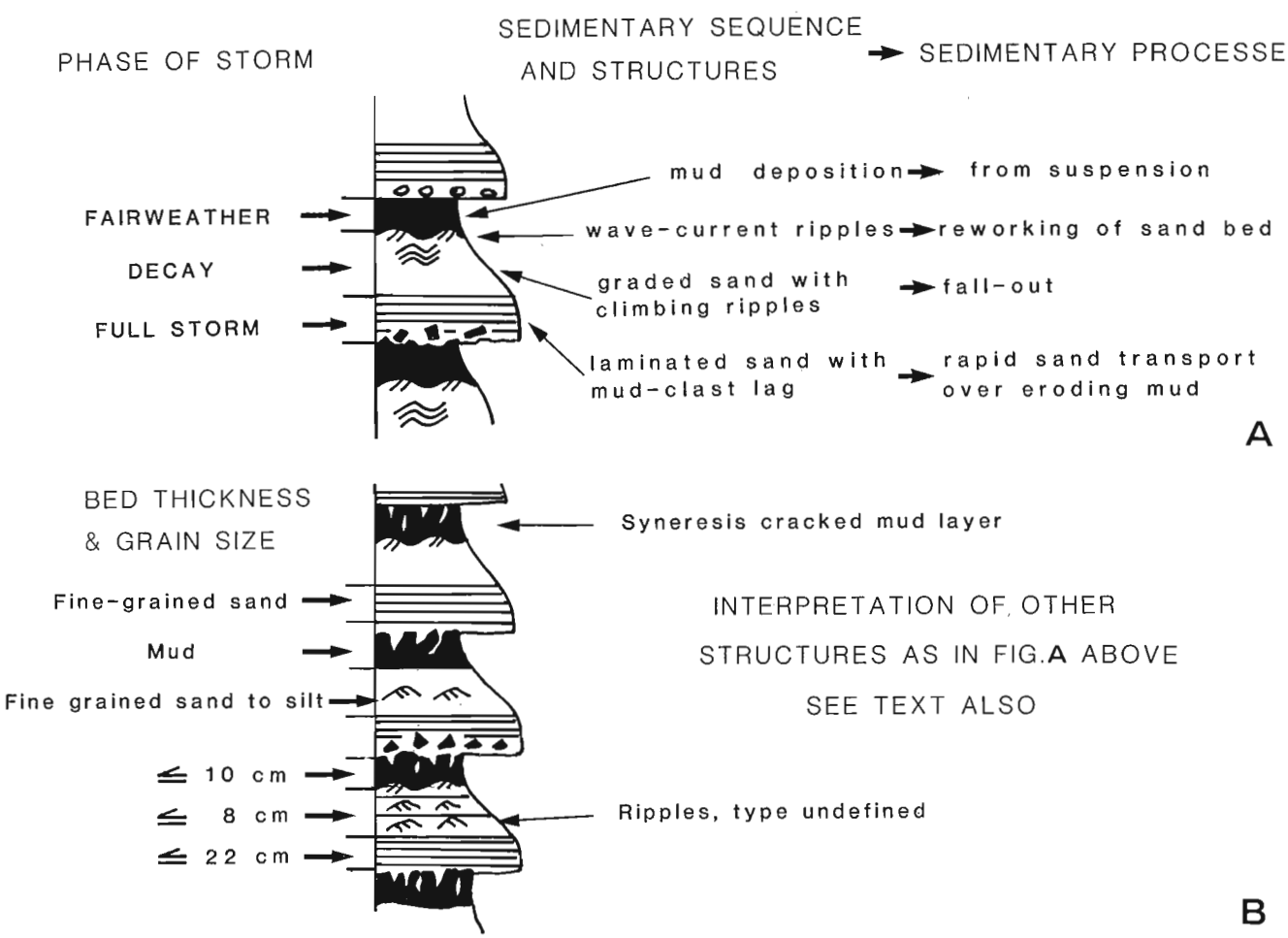

Figure 27.3. *A. A model for storm sand layers, simplified from Allen (1982). B. Composite section of upward-fining cycles in the Gordon Lake Formation, Flack Lake area.*

According to Allen (1982, p. 487 et seq.) storms moving toward a coast generate, in shallow water, currents which transport offshore large amounts of coarse grained coastal sediment into deeper regions in which mud normally accumulates during fair weather. The displaced sediment is laid down in sharp-based graded sand layers resembling Bouma sequences but distinguished from them by the presence of wave ripples.

By this model the thickness and internal structure of the storm bed varies according to its position on the shelf. But in general (Fig. 27.3a) the base of the layer is sharp and may be erosional and lie upon a lag deposit. The lower part of the bed can be parallel-laminated due to rapid transport of fine grained sand. The upper part may be graded and contain climbing ripples from fall-out during storm decay and the top of the bed may be reworked into current-wave ripple forms.

In general sand beds in the Gordon Lake Formation near Flack Lake (e.g. sites 46, 47) are (Fig. 27.3b) similar to those predicted by Allen's (1982) model and similar cycles probably exist near Endikai Lake, 20 km west (Siemiatkowska, 1978, p 42). Near Flack Lake the basal member of the bed is laminated (Fig 27.2a), is usually about 5-8 cm thick but can range up to 22 cm. It may overlie a breccia derived from the mudstone at the top of the underlying bed. The middle part of the bed is composed of units, 6-15 cm thick of graded fine grained sand, in some cases with ripples. Climbing ripples were not recognized but have been seen by Card (1976, p. 22, "ripple-drift cross-lamination"). The top part of the bed, up to 10 cm thick, is an apple green to maroon aphanitic quartz-muscovite siltstone, in some cases brecciated, in others with syneresis cracks best developed at its upper contact. According to this explanation the mudstone layers, already broken by formation of syneresis cracks give rise to the "chert breccia" layers noted by many earlier writers (e.g. Frarey, 1977, p. 56). Presence of many occurrences of linear wave-ripples (eg. site 48) in the formation in roadcuts northeast of Flack Lake indicates that deposition was at many times above wave base rather than below as envisaged by Card (1978). The presence of many such ripples is evidence (Allen, 1982) for a storm origin as opposed to a deep turbidite genesis.

Figure 27.4. *(facing)*

A, B. Zircons from quartz arenite of the Lorrain Formation, sites 36 and 37 (30 m stratigraphically below 36) respectively. Note euhedral ends of some grains indicating that the sediment has had a limited abrasion history. Use scale in D.

C, D. Zircons from quartz arenite of the Bar River Formation, sites 38 and 39 respectively. Grains with euhedral ends are absent and the zircon suite especially in D, is more rounded, both indicating a more rigorous abrasion history.

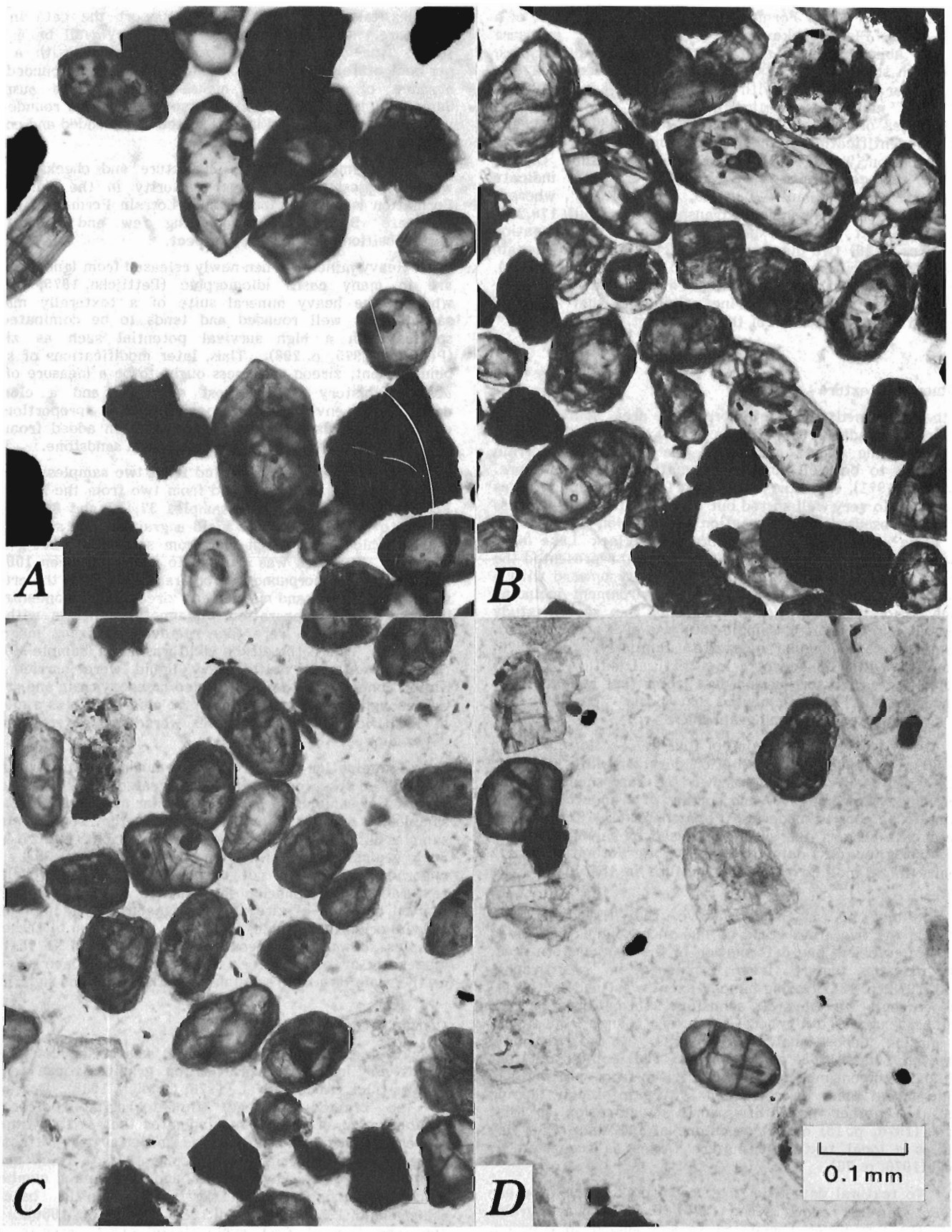
A
B
C
D
0.1 mm

In the Bar River Formation, (site 38), at the outlet of a creek into Flack Lake good bedding-surface exposure contains abundant wavy and straight-crested wave ripples, some with subsidiary crests, mudcracks and mudchip layers. Some linear wave ripples with wavelengths of 1.5 (Fig. 27.2b) and 2 cm, indicate formation in a depth of only several centimetres of water (Reineck and Singh, 1980, p. 32), and support identification of mudcracks from the lower part of the formation (Wood, 1970) as evidence of exposure. On one bedding surface at site 38 four trough crossbeds indicate transport toward azimuth 030,080, 045, and 078°, whereas three planar crossbeds indicate transport to azimuth 170,257, and 280°. At several exposures higher in the formation (e.g. sites 39,40) two-dimensional roadcut exposures contain quartz arenite with apparently opposed crossbeds (Fig. 27.2c). These data support Wood's (1970, p. 167) suggestion that the formation is of shallow marine origin and that exposure occurred during deposition of the lower part.

Sedimentary texture

In the deformed and metamorphosed area southwest of Sudbury (Chandler, 1969, Plates 24-26), Card (1976, 1978) considered the quartz arenite at the top of the Lorrain Formation to be well sorted and mature to supermature. Casshyap (1971), from the same area, found the unit to be as a rule well to very well sorted but that the original roundness had been obscured by deformation and solution pressure. In the little deformed or metamorphosed Flack Lake area (Chandler, 1969), Siemiatkowska (1977, 1978) represented the Lorrain Formation as increasing in maturity upward with a maturity indicative of a high energy environment including beach reworking. Surprisingly her only thin section study reported (1977, Table 6, sample 260) was of a poorly sorted, subrounded to subangular quartzite. Similarly, Wood (1970) seemed unwilling to accept a low textural maturity for the unit, noting varied sorting and dust trains that indicated low roundness (p. 71) but commented that "perhaps dust trains do not always indicate original grain shape".

Petrographic examination of four thin sections from the top 80 m of the Lorrain Formation quartz arenite at Cobre Lake (sites 34-37, Fig. 27.1) showed all four samples to be subrounded (Powers, 1953) and sorting of framework quartz grains to be poor to moderate (Pettijohn et al., 1972, p. 585). These data support the suspicion raised by Siemiatkowska's and Wood's (op. cit.) data that the Lorrain Formation quartz arenite might not be texturally mature in the Flack Lake area.

It may be, as implied above, that the differences between the two areas could be due to problems introduced by metamorphism and deformation in the southeastern area. For example, apart from problems in petrography, Card (1978, p. 122) finding bimodal (southwest and southeast) paleocurrents in several sandstone formations in the southeast suggested a general southward change from fluvial to marine depositional environments in the Huronian. However Young (1968) and Chandler (1969) pointed out that such paleocurrent modes could have arisen from splitting of a single modal class by collection failure in steeply dipping rocks. Another possibility worth examination is that Card's (1976, p. 18) cherty sandstone of the MacGregor Bay area is a local texturally mature facies as suggested by Wood (1970, p. 76).

No textural data from the Gordon Lake Formation are presented in this report. Wood (1970) described quartz grains from the Bar River Formation as subrounded to rounded, equigranular and inequigranular or bimodal with good sorting. Card (1978) described them as rounded and well sorted and Siemiatkowska (1978) as rounded to subrounded and bimodal. Samples taken near Flack Lake support the data in the literature. One from site 38, might very well be a well sorted fine- to very fine-grained sandstone with a few per cent of feldspar grains. Grains are now subrounded but absence of dust trains makes this estimate suspect. Sample 39 is poorly sorted, coarse grained and rounded to well rounded; sample 42 is well sorted and rounded and coarse grained.

In summary, both the literature and checks by the writer suggest that textural maturity in the Bar River Formation is greater than in the Lorrain Formation quartz arenite. But these data, being few and subject to postdepositional effects, are suspect.

Heavy minerals when newly released from igneous rocks are in many cases idiomorphic (Pettijohn, 1975, p. 205) whereas the heavy mineral suite of a texturally mature sandstone is well rounded and tends to be dominated by species with a high survival potential such as zircon (Pettijohn 1975, p. 206). Thus, later modifications of shape being absent, zircon roundness ought to be a measure of the abrasion history of the host quartzite and a clue to depositional environment especially if a proportion of euhedral crystals is assumed to have been added from the Archean basement to any Huronian fluvial sandstone.

Zircons were concentrated from two samples from the Lorrain Formation (36, 37) and from two from the Bar River Formation (38, 39). From samples 37, 37 and 38 600 g of quartzite were required to yield a grain mount suitable for petrographic examination and from sample 39 1800 g were required. The rock was crushed to a size between 100 and 200 mesh and superpanned. Iron fragments from the crusher were removed by hand magnet and zircons were concentrated by heavy liquid separation. Magnetic minerals with the zircon concentrate were then removed by Franz magnetic separator. Where the zircon yield was small (sample 39) two further treatments with heavy liquid were carried out. Zircon concentrates were sprinkled on epoxy resin and ground thin enough for internal zoning to be clearly seen as a method of identification. The samples were then covered with a cover slip.

Examination of the four grain mounts by the writer and an unbiased observer (K. Currie) suggested that the degree of abrasion of samples 36 and 37 is similar and less than that of samples 38 and 39. More important is that some grains in samples 36 and 37 have euhedral terminations (Fig. 27.4a, b). Such grains are absent from samples 38 and 39. Such unabraded grains are not to be expected in polycyclic or texturally mature marine shelf quartz arenites, but reflect limited abrasion of zircons from igneous rocks, implying an alluvial origin for samples 36 and 37. Inspection of these two samples shows that zircon rounding is varied so that any diagenetic overgrowth formation would have been selective on the scale of a hand specimen and therefore not significant.

CONCLUSIONS

It is well established that tropical weathering can develop quartz-clay-iron oxide profiles on granitic rocks tens of metres thick (Abbott et al., 1976; Goldich, 1938). Dominance of the braided (bedload) fluvial regime before the establishment of land plants indicates that at that time the suspension load of fine grained material was effectively separated from fluvial sands (Long, 1978). Thick quartz-kaolinite regoliths have been found between a number of thick Proterozoic quartzites and granitic basement (MacDonald, 1980; Patterson, 1981; Donaldson, 1966). Thus the formation of first cycle fluvial quartz arenites from weathering of granites is not now in doubt.

As a class, fluvial sandstones are texturally immature (Kuenen, 1959; Russel and Taylor, 1937) whereas shallow marine sands, including shallow marine quartz arenites are commonly texturally mature (Klein, 1977). In the last few years a number of quartz arenites of both pre- and post-land-vegetation age have been identified to be fluvial on grounds other than textural (Ramaekers, 1979; Klitzsch et al., 1979; Bartow, 1982) and immature textures have been recorded from some of these quartz arenites (Ramaekers, 1979; Trevena, 1979). So it is reasonable to expect textural immaturity in first-cycle fluvial quartz arenites derived from granitic terranes.

These textural data (samples 36, 37) suggest deposition of the Lorrain Formation quartz arenite as a first cycle fluvial sand formed by weathering of granitic rocks.

Interpretation of the Gordon Lake Formation as a tidal flat deposit has in part stemmed from misinterpretation of syneresis cracks as desiccation cracks indicative of exposure. Correct reinterpretation of these structures, with identification of Bouma sequences led Card (1978) to advocate a deep-water turbidite origin for much of the formation. Reinterpretation of the Bouma-like sequences as shallow water storm beds with wave ripples implies that most of the formation is of shallow subtidal origin. Presence of sabkha-type sulphate nodules at the base of the formation suggests that the formation records a marine transgression through the supratidal to the subtidal zone. The storm bed model, with its implication of proximity to the coast would explain the syneresis cracks if they formed by salinity changes, more easily than would Card's (1978) deep water turbidite model.

Textural data and polymodal crossbed paleocurrent data and presence of mudcracks indicate that the Bar River Formation formed under a tidal marine regime with emergence of sand shoals.

In conclusion, the sequence from the quartz arenite of the Lorrain Formation to the Bar River Formation represents one of marine transgression. Evidence of emergence in the Bar River Formation suggests that the unit should be more closely studied. The copper sulphide mineralization lying at the contact of the Lorrain and Gordon Lake formations occurs at a transition from fluvial to tidal marine conditions.

ACKNOWLEDGMENTS

Jennifer Graves cheerfully performed the tedious labour of preparation of zircon concentrates; A. Greer mounted the concentrates. I. Jonasson critically read the manuscript and provided perceptive comments.

REFERENCES

Abbott, P.L., Minch, J.A., and Peterson, G.L.
1976: Pre-Eocene paleosol south of Tijuana, Baja California; Journal of Sedimentary Petrology, v. 46, p. 355-361.

Allen, J.R.L.
1982: Sedimentary structures their character and physical basis; Developments in Sedimentology, v. 30b, Elsevier, 663 p.

Bates, R.L.
1981: Pure rocks the height of refinement; Open Earth, No. 15, 1981-D, p. 24-27.

Bartow, J.A.
1982: Anauxite-bearing kaolinitic quartzose sandstone – A climatically controlled petrofacies; in 11th International Congress on Sedimentology, McMaster University, Ontario, Canada, Abstracts of Programs, p. 84.

Blatt, Harvey
1982: Sedimentary Petrology; Freeman, (Pub.), 564 p.

Butler, G.P., Harriss, P.M., and Kendall, C.G. St. C.
1982: Recent evaporites from the Abu Dhabi coastal flats; in Depositional and Diagenetic Spectra of Evaporites – A Core Workshop, ed. C. Robertson Handford, R.G. Loucks, and G.R. Davies; Society Economic Paleontologists and Mineralogists, Core Workshop, No. 3, Calgary Canada, p. 33-64.

Card, K.D.
1970: Comment; in Symposium on Basins and Geosynclines of the Canadian Shield, ed. A.J. Baer; Geological Survey of Canada, Paper 70-40, p. 157.

1976: Geology of the McGregor Bay – Bay of Islands Area, Districts of Sudbury and Manitoulin; Ontario Division of Mines, Geoscience Report 138, 63 p.

1978: Geology of the Sudbury – Manitoulin area, Districts of Sudbury and Manitoulin; Ontario Geological Survey, Report 166, 238 p.

Card, K.D., Church, W.R., Franklin, J.M., Frarey, M.J., Robertson, J.A., West, G.F., and Young, G.M.
1972: The Southern Province; in Variations in Tectonic Styles in Canada, ed. R.J.W. Douglas; Geological Association of Canada, Special Paper 11, 25th Ann. Volume, p. 335-380.

Casshyap, S.M.
1971: Petrology and sedimentation of Huronian Arenites, South of Espanola, Ontario; Canadian Journal of Earth Sciences, v. 8, p. 20-49.

Chandler, F.W.
1969: Geology of the Huronian rocks of Harrow Township area, Ont., and surrounding areas, north shore of Lake Huron, Ont.; unpublished Ph.D. thesis, University of Western Ontario, 327 p.

Collinson, J.D. and Thompson, D.B.
1982: Sedimentary structures, George Allen and Unwin, 194 p.

Donaldson, J.A.
1966: Study of the Dubawnt Group; in Report of Activities, May to October, 1965, Geological Survey of Canada, Paper 66-1, p. 22.

Frarey, M.J.
1977: Geology of the Huronian Belt between Sault Ste. Marie and Blind River, Ontario; Geological Survey of Canada, Memoir 383, 87 p.

Frarey, M.J. and Roscoe, S.M.
1970: The Huronian Supergroup north of Lake Huron; in Symposium on Basins and Geosynclines of the Canadian Shield, ed. A.J. Baer; Geological Survey of Canada, Paper 70-40, p. 143-158.

Goldich, S.S.
1938: A study in rock-weathering; Journal of Geology, v. 46, p. 17-58.

Hadley, D.G.
1968: Sedimentology of the Huronian Lorrain Formation, Ontario and Quebec, Canada; unpublished Ph.D. thesis, University of Baltimore, Md., 301 p.

Klein, George de Vries
1977: Clastic Tidal Facies, CEPCO (Pub.), Champaign Illinois (Pub.) 149 p.

Klitzsch, E., Harms, J.C., Lejan-Nicol, A., and List, F.K.
1979: Major subdivision and depositional environments of Nubia Strata, Southwestern Egypt; American Association of Petroleum Geologists Bulletin, v. 63, p. 967-974.

Kuenen, Ph. H.
1959: Experimental abraison 3, Fluviatile action on sand; American Journal of Earth Sciences, v. 127, p. 172-190.

Long, D.G.F.
1978: Proterozoic stream deposits; some problems of recognition and interpretation of ancient sandy fluvial systems, in Fluvial Sedimentology, Canadian Society of Petroleum Geologists, Memoir 5, p. 313-341.

MacDonald, C.C.
1980: Mineralogy and geochemistry of a Precambrian regolith in the Athabasca Basin; unpublished M.Sc. thesis, University of Saskatchewan, Saskatoon, 151 p.

Patterson, J.G.
1981: Amer Lake: An Aphebian fold and thrust complex; unpublished M.Sc. thesis, University of Calgary, 106 p.

Pearson, W.N.
1979: Copper metallogeny, north shore region of Lake Huron, Ontario; in Current Research, Part A, Geological Survey of Canada, Paper 79-1A, p. 289-304.

1980: Copper metallogeny, north shore of Lake Huron, Ontario; unpublished Ph.D. thesis, Queen's University, 403 p.

Pettijohn, F.J.
1970: The Canadian Shield, a Status Report; in Basins and Geosynclines of the Canadian Shield, ed. A.J. Baer; Geological Survey of Canada, Paper 70-40, p. 239-264.

1975: Sedimentary Rocks; Third edition, Harper and Row, 628 p.

Pettijohn, F.J., Potter, P.E., and Siever, R.
1972: Sand and Sandstone; Springer, 618 p.

Powers, M.C.
1953: A new roundness scale for sedimentary particles; Journal of Sedimentary Petrology, v. 23, p. 117-119.

Ramaekers, P.
1979: Stratigraphy of the Athabasca Basin; in Summary of Investigations 1979, Saskatchewan Geological Survey, Miscellaneous Report 79-10, p. 154-160.

Reineck, H.-E. and Singh, I.B.
1980: Depositional sedimentary environments, with reference to terrigenous clastics; 2nd, revised and updated edition, Springer, 549 p.

Roscoe, S.M. and Frarey, M.J.
1970: Comments; in Symposium on Basins and Geosynclines of the Canadian Shield, ed. A.J. Baer; Geological Survey of Canada, Paper 70-40, p. 255-262.

Russell, R.D. and Taylor, R.E.
1937: Roundness and shape of Mississippi River Sands; Journal of Geology, v. 45, p. 225-267.

Siemiatkowska, K.M.
1977: Geology of the Wakomata Lake area, District of Algoma; Ontario Division of Mines, Geoscience Report 151, 57 p.

1978: Geology of the Endikai Lake Area, District of Algoma; Ontario Geological Survey, Report 178, 79 p.

Trevena, A.S.
1979: Studies in sandstone petrology; Origin of the Precambrian Mazatzal Quartzite and provenance of detrital feldspar; unpublished Ph.D. thesis, University of Utah, 390 p.

Wood, J.
1970: The stratigraphy and sedimentation of the upper Huronian rocks in the Rawhide Lake-Flack Lake area, Ontario; unpublished M.Sc. thesis, University of Western Ontario, 235 p.

Young, G.M.
1966: Huronian stratigraphy of the McGregor Bay area, Ontario: relevance to the paleogeography of the Lake Superior Region; Canadian Journal of Earth Sciences v. 3, p. 203-210.

1968: Sedimentary Structures in the Huronian Rocks of Ontario; Paleogeography, Paleoclimatology, Paleoecology, v. 4, p. 125-153.

1969: Inorganic origin of corrugated vermiform structures in the Huronian Gordon Lake Formation near Flack Lake Ontario; Canadian Journal of Earth Sciences, v. 6, p. 795-799.

1973: Tillites and aluminous quartzites as possible time markers for middle Precambrian (Aphebian) rocks of North America; in Geological Association of Canada, Special Paper 12, p. 97-127.

28. A RECONSIDERATION OF SOME GEOLOGICAL RELATIONS NEAR SAINT JOHN, NEW BRUNSWICK

Project 730044

K.L. Currie
Precambrian Geology Division

Currie, K.L., A reconsideration of some geological relations near Saint John, New Brunswick; in Current Research, Part A, Geological Survey of Canada, Paper 84-1A, p. 193-201, 1984.

Abstract

The Saint John region comprises two contrasting terranes. Northwest of the Long Reach, sills of biotite granite and a younger pluton of peralkaline granite intrude a thick Silurian sedimentary section. No Cambrian or Precambrian rocks outcrop. Across the major Belleisle Fault, rocks consist mainly of Late Precambrian plutonic, hypabyssal and volcanic units intruding an older Precambrian terrane, all overlain by scattered occurrences of Eocambrian to Ordovician sedimentary rocks. Silurian sedimentary rocks and Devonian plutons were not observed southeast of the Belleisle Fault. Carboniferous cover on opposite sides of the fault may not be correlative, since latest movement on the fault postdates at least part of the cover. The southeastern part of the Saint John region exhibits intense Late Carboniferous or younger thrusting from the southeast. Many small thrusts cut the rocks, repeating known units. A major cataclastic zone with exotic slices (schuppen zone) roughly follows the shore of the Bay of Fundy. This zone probably marks the boundary of two terranes, but the nature of the terrane to the southeast (Meguma terrane?) is obscured by a Triassic basin underlying the Bay of Fundy.

Résumé

La région de Saint-Jean se compose de deux terrains contrastant. Au nord-ouest de Long Reach, des filons-couches de granite à biotite et un pluton plus récent de granite hyperalcalin traversent une épaisse section sédimentaire silurienne. Aucune roche cambrienne ou précambrienne n'y affleure. De l'autre côté de la grande faille de Belleisle, les roches se composent surtout d'unités plutoniques, hypabyssales et volcaniques du Précambrien récent, qui traversent un terrain précambrien plus ancien; le tout est recouvert par des venues éparses de roches sédimentaires éocambriennes à ordoviciennes. Les roches sédimentaires siluriennes et les plutons dévoniens n'ont pas été observés au sud-est de la faille de Belleisle. Il est possible qu'aucune corrélation de la couverture carbonifère ne puisse être établie des deux côtés de la faille puisque le dernier mouvement de la faille est survenu après l'accumulation d'au moins une partie de la couverture. La partie sud-est de la région de Saint-Jean montre des signes d'un chevauchement intense à partir du sud-est survenu dans le carbonifère récent ou plus récemment. Un grand nombre de petites failles chevauchantes coupent les roches, faisant se répéter les unités connues. Une grande zone cataclastique contenant des lambeaux exotiques (zone imbriquée) longe plus ou moins le rivage de la baie de Fundy. Cette zone marque vraisemblablement la limite de deux terrains, mais la nature du terrain sud-est (terrain de Meguma?) est cachée par un bassin triassique qui est sous-jacent à la baie de Fundy.

INTRODUCTION

After one hundred and fifty years of investigation the geology of the Saint John region, New Brunswick, remains poorly understood. Although the major lithological divisions were established many years ago (Hayes and Howell, 1937; Alcock, 1938), and reasonably complete, modern compilations of the exposures exist (Ruitenberg et al., 1979; McCutcheon and Ruitenberg, 1974), reliable lithostratigraphic columns have not been established for any of the major rock units. Therefore the details, and even the style of the sedimentology and structure remain imperfectly known. The ages and natures of igneous and metamorphic activity have hardly been seriously considered. Previous publications reported progress in stratigraphic and structural studies, and in igneous and metamorphic petrology (Currie et al., 1981; Nance, 1982; Currie and Nance, 1983). The present report applies these results, derived from investigations in Saint John city, to a much larger tract of ground extending from the Silurian sedimentary cover on the northwest to the Carboniferous overthrust belt on the southeast. The present work benefitted greatly from advice and criticism by I. Patel and S. Tanoli on Cambrian stratigraphy, and by N. Rast and R.A. Grant on Carboniferous stratigraphy and structure.

TABLE OF FORMATIONS

In the classic scheme of Hayes and Howell (1937) and Alcock (1938), the rocks of the Saint John region fell into five major divisions, namely the Green Head Group, a platformal carbonate-quartzite-shale assemblage of probable Helikian age; the Golden Grove suite of igneous and metamorphic plutonic rocks; the Coldbrook Group, an Hadrynian volcanogenic assemblage; the Saint John Group, a Cambro-Ordovician sedimentary succession; and an extensive, mainly clastic Carboniferous succession. The present work demonstrates that further subdivision must be made for 1:50 000 scale mapping. The Table of Formations selected for the present purpose is given in the legend to Figure 28.1, and its rationale discussed below.

Brookville gneiss (map unit A_b)

The Brookville gneiss, a mesocratic quartz-plagioclase-hornblende ± biotite gneiss locally containing schlieren, patches and nebulous enclaves of biotite granite gneiss and muscovite-tourmaline pegmatite, as well as relicts of mafic dykes, forms a reactivated basement to the Saint John area.

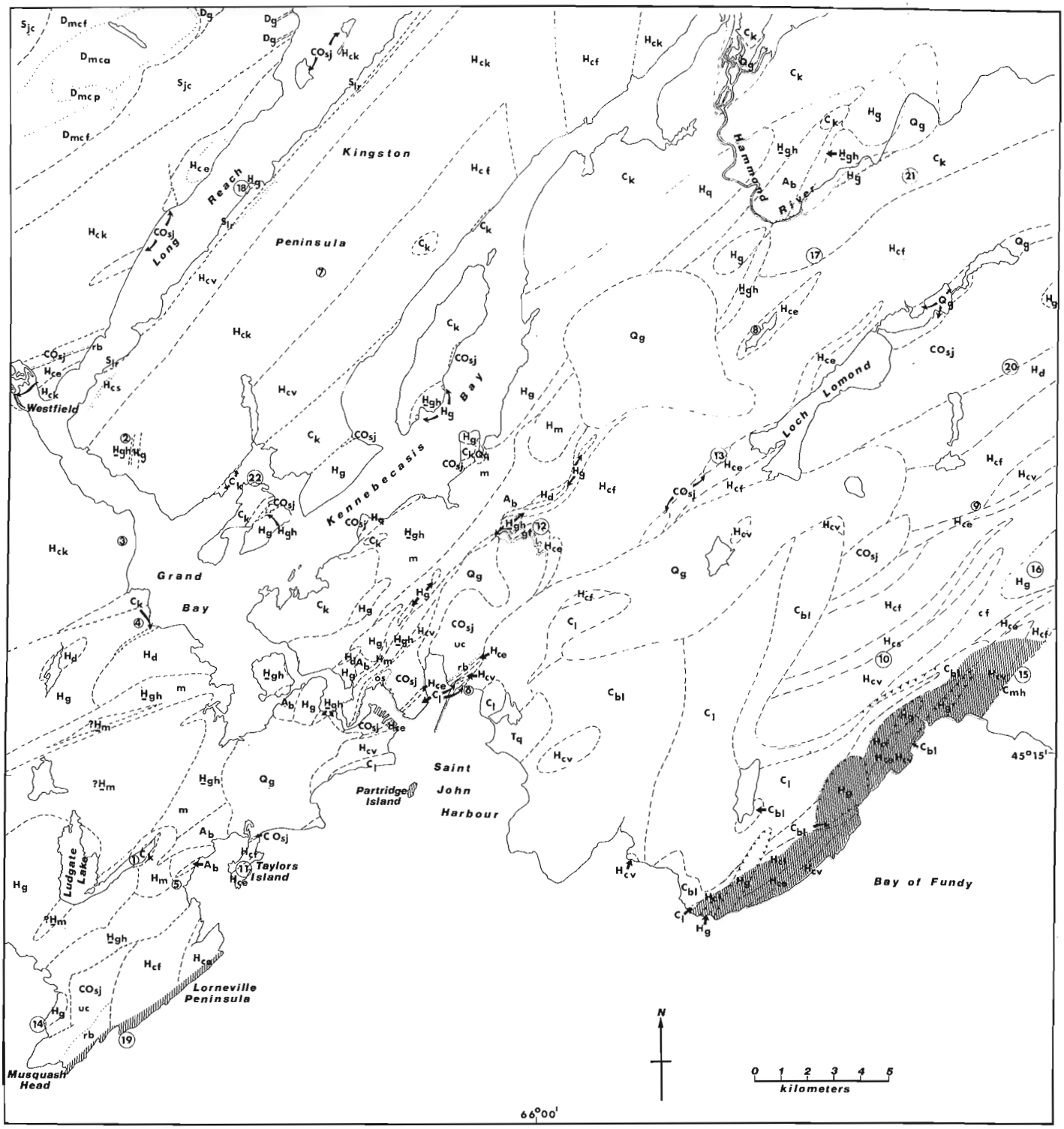

Figure 28.1. *Revised geological map of the Saint John region, New Brunswick.*

QUATERNARY

Q_g Glacial drift, boulder till, stratified fluviolacustrine sand and gravel

– unconformity –

TRIASSIC

T_q QUACO FORMATION: crumbly red to brown conglomerate, minor sandstone

– unconformity –

CARBONIFEROUS

C_{mh} McCOY HEAD FORMATION: Grey to reddish conglomerate, sandstone, minor shale

– relations uncertain, perhaps gradational –

C_l LANCASTER FORMATION: grey lithic arenite with rusty siltstone, minor pebbly beds, rare tuffaceous beds

– gradational interfingering contact –

C_{bl} BALLS LAKE FORMATION: Red shale and siltstone with conglomerate and sandstone lenses

– relations uncertain –

C_k KENNEBECASIS FORMATION: red to brown conglomerate, interbedded red sandstone and siltstone, flaggy grey lithic arenite, black siltstone

– unconformity –

DEVONIAN

D_{mc} MOUNT CHAMPLAIN PLUTON: (a) grey alkali granite, (f) red microgranite and felsite, (p) porphyritic granite

– intrusive contact –

D_g medium grained biotite granite and granodiorite, hornblende syenodiorite, all slightly epidotized

– intrusive contact (to S_{jc}) –

SILURIAN OR YOUNGER

SD_d gabbro, diabase and augite porphyrite dykes

– intrusive contact (to CO_{sj}) –

SILURIAN

S_{jc} JONES CREEK FORMATION: grey-green to black thin-bedded shale and siltstone, commonly hornfelsed

– relations uncertain, probably faulted –

S_{lr} LONG REACH FORMATION: basalt flows and dykes commonly feldsparphyric, minor interbedded siltstone and limy shale

– intrusive contact (to H_c) –

CAMBRIAN AND ORDOVICIAN

CO_{sj} SAINT JOHN GROUP: (rb) Ratcliffe Brook Formation, red sandstone, pebble conglomerate, white to grey arenite, (gf) Glen Falls Formation, white quartz pebble conglomerate, (uc) Hanford Brook, Hastings Cove, Agnostus Cove and related formations, grey to grey-green siltstone, sandstone, minor shale, (os) black shale and siltstone, mainly of Ordovician age

– unconformity or disconformity –

EOCAMBRIAN

H_{ce} Pink to purple feldspathic sandstone, volcanogenic conglomerate, bright red tuff

– gradational contact –

H_c COLDBROOK GROUP: (f) mainly tuff, agglomerate, lahars, (v) mainly salic and mafic flows, (s) mainly siltstone and chert

– relations uncertain, possibly gradational –

H_{ck} KINGSTON COMPLEX: dyke complex of rhyolitic, dioritic and rare altered basaltic dykes, with rare fault slices of H_g and H_{gh}

– gradational contact –

GOLDEN GROVE SUITE (H_g, H_d, H_m)

H_g hornblende granodiorite, hornblende-biotite granite, epidote alaskite. All phases locally megacrystic

– intrusive to gradational contact –

H_d diorite, minor granodiorite and gabbro, abundant basalt dykes and dyke fragments

– intrusive to gradational contact –

H_m gabbro, hornblendite, perknite, strongly altered and metasomatized

– intrusive contact –

HELIKIAN

$?H_m$ MARTINON FORMATION: purplish black graded siltstone, sandstone, carbonate conglomerate or breccia

– relations uncertain, possibly unconformable –

H_{gh} GREEN HEAD GROUP: (m) grey-blue to buff marble, (q) white to lilac quartzite (p) olive to black siltstone and pelitic schist

– intrusive to unconformable contact –

APHEBIAN

A_b BROOKVILLE GNEISS: Fine-banded quartz-plagioclase-hornblende-biotite gneiss, chloritized gneiss with K-feldspar porphyroblasts, biotite granite gneiss.

Geological contact, approximate (may be faulted locally)

Fault, apparently high angle

Fault, apparently low angle

Zone of severely brecciated rock, mylonite, flaser gneiss and other cataclastic rocks.

Geology by K.L. Currie, 1980, 1982, 1983, R.D. Nance, 1980, 1982, G.E. Pajari Jr. 1980, and R.K. Pickerill 1980. Geological compilation and interpretation by K.L. Currie.

Map localities mentioned in text

1. Spruce Lake
2. Bayswater
3. Grand Bay village
4. Martinon
5. Hybrid igneous rocks on Lorneville highway
6. Saint John Dry Dock
7. Whites Mills
8. Hunter Lake
9. St. Martins road, bridge over Black River
10. Black River, Garnett Settlement area
11. Taylors Island
12. Mystery Lake
13. Sproul Road
14. Musquash Harbour granite
15. Emerson Creek
16. Granite west of Emerson Creek
17. Langstreth Brook
18. Holder Point
19. Tiner Point
20. Baxter Mountain
21. Damascus
22. Kennebecasis Island fossil locality

The gneiss forms an intricate, mutually intrusive assemblage with the Green Head Group along the southeastern side of a central core of plutonic rocks (Fig. 28.1), and occurs elsewhere as contorted, altered and metasomatized screens between plutons. Currie et al. (1981) illustrated and discussed evidence indicating that the Brookville gneiss represents reactivated basement.

Green Head Group (map unit H_{gh})

The Green Head Group comprises major grey to buff marble, white to lilac quartzite, and minor black siltstone and pelitic schist. Marble and occasionally siltstone occur as dyke-like masses throughout the Golden Grove suite and Brookville gneiss, which they intrude and include. In large areas of Green Head Group the marble commonly shows intricate flow patterns, and quartzite, siltstone and mafic dykes appear as boudins. Because of the ubiquitous flowage, an internal stratigraphy to the Green Head Group could not be successfully defined (Currie et al., 1981). However, the readily recognizable lithologies of the group form a valuable stratigraphic marker. New discoveries of these lithologies near Bayswater (locality 2*), Tiner Point (locality 19) and Black River (locality 10) suggest a considerably wider initial distribution of the Green Head Group than suspected from previous studies. Evidence for a Helikian age of the Green Head Group has been presented by Wardle (1977).

Martinon Formation (map unit ?H_m)

The Martinon Formation consists of grey to purplish-brown siltstone, sandstone and minor pebbly sandstone, with a distinctive basal marble conglomerate or breccia. The formation occupies a single syncline west of Saint John. The basal unit contains small fragments of chert as well as siltstone and marble cobbles. Many of the latter are strongly flattened and folded, and display striking multicoloured rinds suggesting an intricate metasomatic history. The matrix of the fragmental unit appears very rich in chlorite, suggesting a possible volcanogenic component, and the unit locally contains thin basaltic sills. The typical Martinon siltstone and sandstone commonly show grading, and locally small channels. Basalt sills are abundant, so that much of the unit is hornfelsed. On the west side of the syncline the distinctive fragmental unit appears twice, apparently repeated by faulting, whereas on the east side it is missing, presumably faulted off. The Martinon Formation clearly differs from the Green Head Group in lithology, sedimentology and structural style. The statement of Leavitt (1963) that it lies unconformably above the Green Head Group appears correct, but its age remains uncertain. It must be older than the Golden Grove suite by which it is unequivocally intruded south of Ludgate lake.

Golden Grove suite (map units H_g, H_d and H_m)

The Golden Grove suite includes many small plutons which together form a central crystalline core to the map area. Following Hayes and Howell (1937) I have divided the suite into three units, namely generally granitoid plutons (H_g), dioritic rocks (H_d), and gabbroic to ultramafic rocks (H_m). These divisions tend to be rather arbitrary and some plutons cross compositional boundaries.

The mafic to ultramafic plutons (unit H_m) range from hornblende gabbro to hornblendite, perknite and pyroxenite, now all much altered and hybridized by younger intrusive material (Currie et al., 1981). Dykes of this material are abundant in the other plutons, but always appear as much broken, altered and assimilated material.

The dioritic plutons (unit H_d) contain substantial amounts of quite massive tonalite to hornblende diorite, locally grading toward the hornblende gabbro of unit H_m, but potassium feldspar consistently occurs along fractures, or in nebulous schlieren-like zones, and toward the edges the rocks tend to pass gradationally toward granodiorite. The margins of these bodies are infested by swarms of variably altered, boudinaged and assimilated mafic dykes, which locally have mechanically disintegrated to produce spectacular hydrid rocks (for example at map locality 5).

Granitoid plutons (unit H_g) range from granodiorite to epidote alaskite. Typically they exhibit complex gradational and hybridized boundaries against the Brookville gneiss and other plutons, and sharp, hornfelsed contacts against the Green Head Group and Martinon Formation. Megacrystic potassium feldspar occurs sporadically throughout the plutons and their contact aureoles, and quartz tends to occur in large, roughly equant, bluish grains. Hornblende forms the sole, or dominant dark mineral, except for some minor late phases.

An upper limit for the age of the Golden Grove suite is fixed by the unequivocal presence of its debris in the basal Cambrian Ratcliffe Brook Formation (for example at Baxter Mountain, locality 20). Radiometric ages have consistently given younger but erratic results. In part this may be due to the complex nature of the petrogenesis, and resulting difficulties in unequivocally defining age of formation (Currie et al., 1981). In part it may also be due to unfortunate sample selection. The age of 392 ± 55 Ma obtained by Olszewski and Gaudette (1982) north of Musquash Head (locality 14), was obtained on material which had not only been moderately to severely altered to chlorite and epidote, but lay in a major fault zone, and underwent metasomatic reaction with neighbouring marble producing characteristic bleached feldspars.

Coldbrook Group and related rocks (map units H_{ck}, H_{cv}, H_{cf}, H_{cs} and H_{ce})

The Coldbrook Group, according to the conventions which have grown up during the past half century, comprises not only the Late Precambrian volcanogenic sequence in the region of Saint John but also presumed equivalent hypabyssal rocks. The Coldbrook Group exhibits such a variety of lithologies and styles of occurrence that subdivision appears necessary. I have adopted a three-fold division, namely (i) the dyke complex of the Kingston Peninsula and adjacent areas, first distinguished by O'Brien (1976), here termed the Kingston complex, (ii) volcanogenic rocks including flows, fragmentals (tuffs, lahars, volcanic breccia), and minor sedimentary rocks (fine banded siltstone and chert), and (iii) red sedimentary rocks with a volcanogenic component (rose to purple feldspathic sandstone, conglomerate with feldspathic matrix, red tuff).

The Kingston complex (unit H_{ck}) forms a belt roughly 10 km in width crossing the mapped area from northeast to southeast. This belt may be continuous with the zone recognized to the southwest by Rast and Currie (1976). A new highway west of the Saint John River provides a virtually continuous exposure across the belt, which consists of essentially vertical salic and mafic dykes 5 to 50 m in width alternating in fairly regular fashion. Salic dykes range from almost aphanitic grey rhyolite with pink feldspar phenocrysts, through red or grey felsite, to microgranite, locally graphic. Mafic dykes include minor chloritized basalt and fine grained amphibolite, similar to dykes in the Green Head complex, and the altered dykes of the Golden Grove suite, and major fine grained, commonly porphyritic hornblende diorite. Typically, contacts of dykes are welded but not chilled, so that relative

* Localities mentioned in the text are numbered in Figure 28.1 and listed in the legend to that figure.

ages cannot be determined. Rarely dyke margins may show slickensides, or open mesoscopic folding, right hand along the northwest part of the belt, and left-hand on the opposite side. A few basaltic dykes exhibit weak cleavage parallel to trend, but most dykes appear massive. The dyke complex contains rare slices of other lithologies which must be transported, namely volcanic fragmental rocks at Grand Bay and Whites Mills (localities 3 and 7), purplish quartzite and plutonic granite west of Bayswater (locality 2), and siltstones of the Saint John Group just northwest of the map. The foliation in these slices invariably parallels the local dyke direction, which is commonly north-northwest, although considerable regions on the Kingston Peninsula trend north-northeast. Slices of supracrustal rocks do not appear west of a major north-northwest-trending mylonite and gouge zone exposed west of Westfield.

Volcanogenic rocks of the Coldbrook Group (units H_{cv}, H_{cf} and H_{cs}) consist of mafic to salic flows (unit H_{cv}), extensive tuff and fragmental rocks (unit H_{cf}) and a significant amount of intercalated sedimentary rocks (unit H_{cs}), outcropping along both edges of the Kingston Peninsula, and in a wedge-shaped area extending northeast from downtown Saint John. The best preserved and exposed sections occur east of Hunter Lake (locality 8) and along the highway to Saint Martins (locality 9). These sections exhibit a sequence, from the bottom up, of (a) mafic and salic flows, (b) fragmental volcanogenic rocks (tuff, crystal tuff, lapilli tuff, mudflows, agglomerates), (c) volcanogenic sedimentary rocks (tuff, graded siltstone, chert), (d) mafic tuffs with minor flows, (e) red feldspathic sandstone, tuff and conglomerate, commonly capped by basalt flows. Subdivision (e) has been separately mapped as unit H_{ce}.

The lower flow rocks (H_{cv}) tend to be relatively massive, and completely recrystallized to granoblastic fabrics (amphibolites and felsites). Pillows were recognized in two localities. Epidote and chlorite veins, patches and porphyroblasts appear ubiquitously. Fragmental volcanic rocks (H_{cf}) vary greatly in composition and degree of preservation. Almost massive grey-green to maroon tuffs occur commonly, recognizable by a characteristic hackly, "chipped" weathered surface. Red crystal tuffs, agglomerate, and greenish lapilli tuffs with lapilli up to 5 cm diameter occur commonly, but cannot be successfully separately mapped. However, the dominant rock type contains a purplish to greenish muddy matrix with disseminated cobbles and clasts of volcanic rocks in varying degrees of stretching and disintegration. Recognizable sedimentary rocks (H_{cs}) occur toward the top of the fragmental section as interbeds of grey to pale green siltstone, banded on a centimetre scale and commonly grading upward from silty bases to cherty tops. This material varies in thickness from lenses a metre or less wide, to a section nearly 400 m thick which was traced more than 10 km northeast from Black River (locality 10). Essentially identical rocks occur on the northwest side of the Kingston Peninsula, around Hunter Lake (locality 8), and at Taylors Island (locality 11). In all these locations the sedimentary rocks are overlain by relatively fresh, vesicular mafic flow rocks, or by grey-green tuffs.

Although both basic and acid materials occur within the Coldbrook Group, the bulk of the rocks appear to be of intermediate composition. This field observation may be true of the group in general, since of the 24 chemical analyses reported by McCutcheon (in Ruitenberg et al., 1979) which contained less than 3% normative corundum, 5 were broadly basaltic (less than 52% SiO_2), 4 were rhyolitic (greater than 65% SiO_2), and the remainder andesitic.

Rocks placed in map unit H_{ce} have been variously mapped in the past, with the volcanic rocks of the Coldbrook Group, with the Saint John Group, or with the Carboniferous "Mispec Group". They can be readily distinguished from the Ratcliffe Brook Formation of the Saint John Group by (a) the highly feldspathic nature of the sediments (The Ratcliffe Brook Formation is feldspathic only in rare and thin tuffaceous beds.), (b) the occurrence of conglomerates entirely composed of large rounded volcanic debris, (c) the common presence of mafic tuffs and/or flows. A Precambrian age for at least some localities can be unequivocally demonstrated since they conformably to disconformably underlie the basal Cambrian Ratcliffe Brook Formation south of Mystery Lake (locality 12) and on Sproul Road (locality 13). The Eocambrian section consists of rose to brown highly feldspathic, crossbedded coarse sandstone, intensely red, virtually massive tuff horizons up to 5 m thick, and pebble to cobble conglomerates, occasionally containing vein quartz fragments, but predominantly containing volcanic clasts. Some of the sandstones contain small amounts of detrital muscovite. Basalt flows occur near the top of the section along Saint Martins Road and at Hunter Lake, Black River, Taylors Island, and northwest of Long Reach. This Eocambrian sedimentary section, for which a type section could be defined along the hydro line south of Mystery Lake, forms a previously unrecognized element in the geology of the Saint John district.

Saint John Group (map unit CO_{sj})

Hayes and Howell (1937) subdivided the Saint John Group into eleven formations on the basis of paleontology. Since the group is sparsely fossiliferous, a simplified lithostratigraphy is required for mapping purpose. I adopted the same system used by Hayes and Howell, namely basal Ratcliffe Brook Formation (rusty to grey sandstone and pebble conglomerate), Glen Falls Formation (white quartzite and quartz-pebble sandstone), Middle to Upper Cambrian (grey to greenish-black siltstone and sandstone, mainly of the Hanford Brook, Hastings Cove and Agnostus Cove formations), and Ordovician (black shale and siltstone). The details of the lithostratigraphy are currently under investigation by S. Tanoli (University of New Brunswick). The present mapping discovered two new localities of Saint John Group, one on Musquash Head, the other on Taylors Island, and discredited another on Langstreth Brook (locality 17) which yielded Carboniferous plant fossils. New outcrop exposed in gravel pits and road cuts shows the structure of the Saint John Group to be more complex than envisaged by Hayes and Howell (1937), which had been largely accepted by subsequent workers. The group occurs in a series of en echelon basins, which south of the Kingston complex trend north-northeast, and to the north trend east-northeast. Internally the basins appear intricately folded, as can be seen around Mystery Lake, where the Glen Falls Formation can be used to unravel an intricate series of folds and faults. All of the southern group of basins appear to be fault-bounded on the northwest side, in all cases with loss of much of the northwestern limb of the basins. As a result of the improved lithostratigraphy of the Saint John Group introduced by Tanoli and Patel (personal communication, 1983), it can now be seen that the lithostratigraphic units are remarkably uniform over the whole of the mapped area, suggesting the group formed in a relatively large basin.

Long Reach Formation (map unit S_{lr})

The Long Reach Formation forms a narrow belt on the eastern side of the Long Reach, consisting mainly of feldsparphyric basaltic lavas, locally amygdaloidal. Minor interbedded grey-green feldspathic arenite and limestone contain fossils indicating a Llandovery to Wenlock age (Boucot et al., 1966). The eastern contact of the Long Reach Formation against the Coldbrook Group is nowhere exposed, but a roadcut near the supposed site of the contact contains

spectacularly feldsparphyric basaltic dykes, possibly belonging to the Long Reach Formation, cutting more altered and metamorphosed andesitic rocks assigned to the Coldbrook Group. The western margin of the Long Reach Formation can be observed on Holder Point (locality 18) where basalts are faulted against a granite of Golden Grove type (unit H_g). This exposure suggests that the Long Reach Formation may lie entirely on the east side of the Long Reach, forming a large fault sliver within the Kingston complex similar to those previously noted.

Jones Creek Formation (map unit S_{jc})

West of the Belleisle Fault the Jone Creek Formation of siltstone and pelitic siltstone yields an abundant fauna of Pridolian age (Berry and Boucot, 1970). Much of the formation within the mapped area consists of hornfels, and completely exposed sills of granite occur commonly. The lithologically similar Saint John Group totally lacks acid intrusions, and hornfelsing occurs only in narrow zones around mafic dykes.

The contact of the Jones Creek Formation against the Kingston dyke complex can be observed in numerous places. The Jones Creek Formation has been intensely brecciated and mylonitized over a zone several tens of metres wide. These relations, together with the striking difference in intrusive style just mentioned, suggest this contact must be a major transcurrent fault.

Silurian or Devonian granitoid rocks (map unit D_g)

Demonstrably post-Silurian granitic rocks occur only northwest of the fault mentioned above. The older granitic rocks consist of medium grained hornblende-biotite granite, granodiorite and syenodiorite, all mildly epidotized. These rocks form sills in the Jones Creek Formation, and occur along the eastern end of the younger Mount Champlain pluton. The syenodiorite, which has a colour index higher than 50 and abundant pink feldspar, forms the most unusual and striking member of this suite.

Mount Champlain pluton (map unit D_{mc})

The Mount Champlain pluton forms a mass of batholithic dimensions stretching off the mapped area to the west. The central parts of the pluton, as on Mount Champlain itself, consist of pale grey-green leucocratic granite with distinctive blue alkaline amphibole. Marginal portions tend to be pinker and distinctly porphyritic, while the contacts of the pluton display a carapace of red felsite and rhyolite up to 300 m thick. The central parts consist of one feldspar granite, but many of the porphyritic portions are two feldspar rocks. Evidence of high level intrusion abounds (miarolitic cavities up to 2 cm across, porphyritic patches, rhyolite-felsite margin, extensive hornfels collar), but the hornfels exhibits few dykes. In petrographic character and tectonic setting the Mount Champlain pluton resembles alkali granites of the Topsails terrane of Newfoundland (Whalen and Currie, 1983).

Basaltic dykes (map unit SD_d)

The Saint John Group and older rocks contain a distinctive suite of fine- to medium-grained, relatively fresh basaltic dykes. Such dykes generally trend north-northeast, parallel to the tectonic grain, range from 30 to 200 cm in width, and weather to a smooth brown surface. They occur most commonly in the Hanford Brook and Agnostus Cove formations, but also cut the Ratcliffe Brook Formation, the Eocambrian sequence, Golden Grove suite and Brookville gneiss. The dykes appear to form a swarm about 2 km in width. Their age has not been definitely established, but they do not cut the Carboniferous section.

Kennebecasis Formation (map unit C_k)

Traditionally, the Carboniferous section fell into two major parts, the Kennebecasis Formation to the northwest, and the "Mispec Group" to the southeast. Mapping in 1982 showed that the "Mispec Group" contained very diverse lithologies of several ages (Currie and Nance, 1983). This years work revealed problems with the Kennebecasis Formation. Over much of the mapped area the basal unit of the formation is a flaggy grey to buff sandstone with darker siltstone layers, which lithologically rather resembles the younger Lancaster Formation. Diagnostic fossils from Kennebecasis Island (locality 22) and the Hammond River just east of the mapped area suggest a latest Devonian or Early Mississippian age (Hayes and Howell, 1937, p. 107), which by extension has been attached to the formation as a whole. Where the flaggy sandstone is absent, the basal unit of the formation consists of coarse, locally derived conglomerate. The higher parts of the formation consist of two or more upward-coarsening cycles from buff or red siltstones through sandstones to conglomerate, with the thickness of the cycles varying from 20 to 100 m. Near Damascus (locality 21) a coarse conglomerate layer immediately overlying the basal flaggy sandstone contains very abundant float of red fossiliferous limestone, shale and gypsum derived from the nearby Upham Formation of Windsor age.

This conglomerate clearly must be of post-Windsor age, and is in fact lithologically indistinguishable from the Pennsylvanian McCoy Head Formation. This exposure requires that either (a) the Kennebecasis Formation spans a considerable part of Carboniferous time, upper boundary undefined, or (b) the Kennebecasis Formation should be divided into several units of differing age, for which the present stratigraphic and paleontological evidence are quite insufficient. In either case the reasons previously offered for the sharp distinction between the Kennebecasis Formation and the Lancaster and Balls Lake formations break down.

Lancaster, Balls Lake and McCoy Head formations (map units C_l, C_{bl} and C_{mh})

The Carboniferous section along the Bay of Fundy falls into a grey, fossiliferous lithic arenite division (Lancaster Formation) and a red siltstone-shale division with conglomerate lenses (Balls Lake Formation). The Lancaster Formation unconformably overlies older rocks, and grades and interfingers southeast with the Balls Lake Formation (Currie and Nance, 1983). As with the Kennebecasis Formation, the Lancaster Formation gives diverse fossil dates, despite an apparent geographical continuity (Currie and Nance, 1983). Alternative explanations are an interfingering time-transgressive character for the Lancaster (Currie and Nance, 1983), or tectonic stacking of lithologically similar but temporally diverse slices, (Rast et al., 1978). The McCoy Head Formation, separated from outcrop of the Lancaster and Balls Lake formations by a fault along Emerson Creek (locality 15), appears to rest on Lancaster-like lithic arenite, and consists of upward-fining cycles 5-10 m thick grading from brownish cobble conglomerate (with some red limestone cobbles bearing a Windsor fauna), through crossbedded sandstone to red siltstone. The lithologies appear to fit reasonably well into the subaerial debris fan model with distal fluvial reworking proposed last year for this part of the Carboniferous section (Currie and Nance, 1983), and the formation may be equivalent to, or slightly younger than, the Lancaster/Balls Lake section.

Quaco Formation (map unit T_q)

Following Alcock (1938) I consider an area of coarse, poorly indurated uncleaved conglomerate and sandstone on the east side of Saint John Harbour to be correlative to the Triassic

Quaco Formation. These conglomerates contain northwesterly derived boulders (Green Head Group marble as well as granites and volcanic cobbles). Although no fossils have been recovered from this occurrence, oil drilling operations in the Bay of Fundy have shown that the region offshore from Saint John is underlain by a Triassic basin. In contrast to the rocks along the shore, which are extremely cataclastically deformed, the Triassic section is very slightly deformed, suggesting that a major fault may roughly follow the shore.

Structure of the Saint John region

The mapped area falls into three structural zones. The northwestern zone exhibits a thick Silurian sedimentary section and extensive Devonian magmatism. No Precambrian or Cambrian rocks outcrop in this terrane. The central zone exposes mainly Precambrian rocks, including a Late Precambrian volcanic and hypabyssal section. Significant Cambrian and Carboniferous sections occur, but Silurian sedimentary rocks do not, and Devonian magmatism is absent or insignificant. The southeastern zone lithologically resembles the central zone, but possesses a distinctive Carboniferous section and exhibits characteristic low angle thrusting and recumbent folding.

The Belleisle Fault, separating the northwestern and central zones, can be mapped by intense brecciation and truncation of the Jones Creek Formation. The fault trends southwest, oblique to the Long Reach which it intersects near Greenwich. The fault cannot lie in the Long Reach, as proved by new road cuts across the southwestern end of the reach. The juxtaposition of unmetamorphosed Cambrian against hornfelsed Silurian across the fault suggests that movement can be neither high angle reverse (Brown and Helmstaedt, 1970), nor thrust (McCutcheon, 1981), since the south side exposes lower metamorphic grades than the north side. Rather the fault demonstrates major transcurrent movement juxtaposing two regions with quite different Silurian and Devonian histories.

Presence of a major transcurrent fault zone offers a plausible explanation for a number of smaller scale features of the central zone. Narrow north-trending slivers of Cambrian and Carboniferous sedimentary rocks around Grand Bay could be contained in small grabens formed at right angles to the direction of motion on the fault, while northeast-trending slivers along the Long Reach could form if the direction of motion of the southeastern block momentarily diverged from the trend of the main fault, producing tension oblique to the fault plane. This situation appears likely along the Long Reach, since the local trend of the Belleisle Fault appears distinctly more westerly than its regional trend. If this explanation is valid, latest motion on the fault was predominantly left-lateral, since the block southeast of the Long Reach must move relatively eastward to produce tension.

If the transcurrent movement was long lived, and extended over a zone some kilometres in width, a similar mechanism could explain several long-standing puzzles. Formation of tensional troughs followed by closing during continued transcurrent movement could explain the presence of slivers of intensely deformed Saint John Group along Kennebecasis Bay, as well as the narrow belts of Carboniferous sandstone at Spruce Lake (locality 1), Martinon (locality 4) and Grand Bay, and the exotic slivers found within the Kingston complex. On a somewhat larger scale a similar mechanism might explain the main belt of Kennebecasis Formation which appears to have accumulated in fault troughs, but is now strongly folded, and locally overturned and thrust along the edges. The stratigraphy and structure of the formation appear to conform to the criteria suggested by Reading (1980) for sedimentation in transcurrent fault zones.

Wardle and O'Brien (1975), Currie et al. (1981) and Nance (1982) discussed structure of the central zone around Saint John city. Structures of Precambrian age have been generally obscured by subsequent deformation, and the readily mapped upright to overturned folds appear to result from deformation in Paleozoic time, possibly the Taconic and Acadian orogenies. Current mapping extends the number of folds of similar attitude and geometry. Several observations suggest that the region had been block faulted prior to folding. Boulders of diorite of the Golden Grove occur in the Ratcliffe Brook Formation at Baxter Mountain (locality 20), a granite ridge west of Emerson Creek appears to be the source of granite pebbles in the Garnett Settlement area (locality 16), and a spine of Coldbrook Group apparently was the source of pebbles in conglomerates of the Eocambrian section west of Loch Lomond. Precambrian units were probably juxtaposed along faults prior to deposition of the Saint John Group.

Currie and Nance (1983) proposed that the southeastern overthrust zone consisted of an essentially autochthonous terrane, consisting of the Lancaster and Balls Lake formations and parts of the Coldbrook Group, which had been over-ridden, cleaved and locally "wrinkled" in recumbent style by an unidentified allochthonous terrane. They identified the contact of the two parts with a zone of extreme deformation containing numerous imbricate slices which approximately follows the Bay of Fundy shore. Work this year shows that this zone continues along the southeastern shore of Lorneville Peninsula and Partridge Island. Within this zone the rocks are commonly mylonites or cataclasites not attributable to any particular unit, although numerous small, recognizable slivers occur, including a totally exotic slice of black and white carbonaceous sediments containing a rhyolite dyke on Tiner Point (locality 19). If the northeastern and southwestern sections of similar deformational style belong to the same zone, a substantial right-hand offset must occur in Saint John harbour. This could be due to a modest east side down displacement on a north-northwest-trending fault, such as that observed in road cuts west of Grand Bay.

The above model places stratigraphic units in appropriate order, and assumes that displacements between them are relatively small, except for the bounding schuppen zone. The alternative view, championed by Rast and coworkers (Rast and Grant, 1973; Rast et al., 1978) supposes all of the Lancaster and Balls Lake formations to be allochthonous, the volcanic rocks to be Carboniferous (rather than Precambrian), and all of the geology east of the Lancaster-Saint John contact to be dominated by stacks of thrust slices. The Rast model raises theoretical problems. Superposed thrust slices emplaced from the east might be expected to produce a largely west-facing, inverted section, in which structurally higher slices expose deeper parts of the stratigraphic pile. However, with some minor and local exceptions the Balls Lake and Lancaster formations form an upright southeast-facing sequence, and according to the stratigraphy of Rast et al. (1978) the slices become younger from northwest to southeast.

A critical observational test of the competing models can be applied on a recently made series of road cuts around the Saint John Dry Dock (locality 6 of Fig. 28.1) and Willetts Food Warehouse. A sketch and interpretation of this area is given in Figure 28.2. On the Currie and Nance (1983) model this exposure contains a complete stratigraphic section through the lower Saint John Group, except for a small part of the Hanford Brook Formation which has been cut out by minor faults, a section through the underlying Eocambrian red beds, complete with transition to mafic volcanics, and the unconformable contact of the (fossiliferous) Lancaster Formation on the basalt. The inverted, west-facing

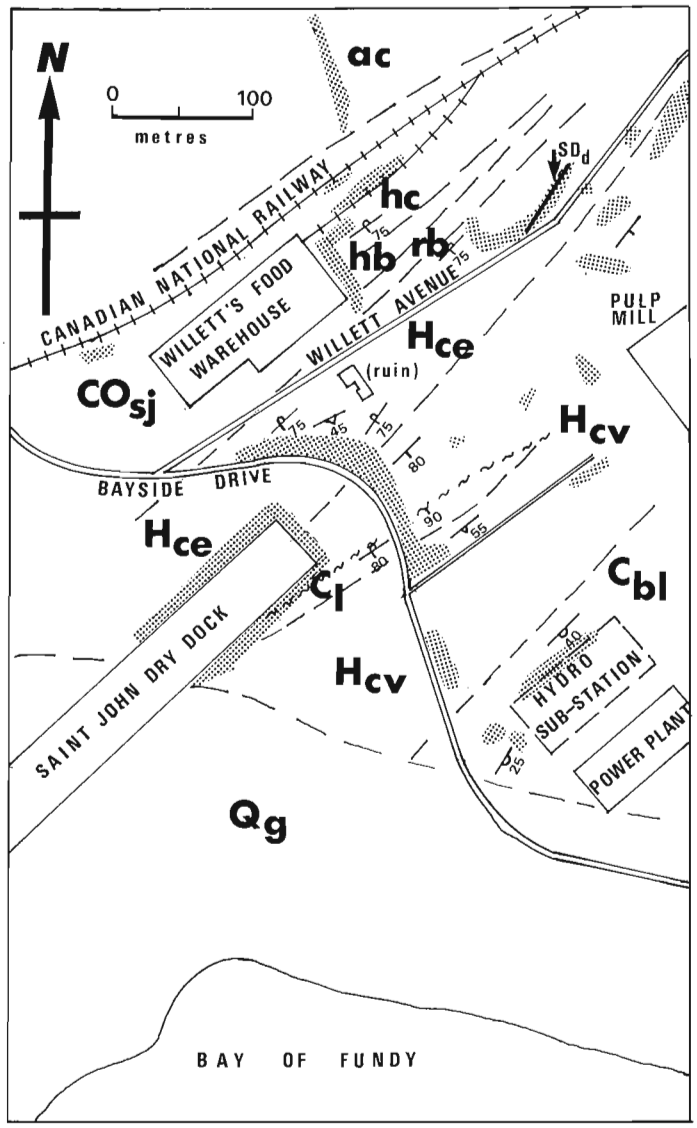

Figure 28.2. *Geological sketch of the area around the Saint John Dry Dock. Outcrop shaded. Lithological unit symbols as in Figure 28.1, with the following additions; stipple-rock outcrop, hb-Hanford Brook Formation, hc-Hastings Cove Formation, ac-Agnostus Cove Formation. Bedding, tops known, inclined, overturned, cleavage, inclined.*

character of the Lancaster can be explained by a small fold, such as is exposed a few hundred metres to the east at the mouth of Little River. The Rast (1980) model requires a major thrust somewhere in this section to separate Cambrian (or Eocambrian) and Carboniferous strata. None of the possibilities look appealing. A fault between the Saint John Group proper and the red beds seems ruled out because of the presence of a typical Saint John dyke in the upper part of the red beds. A fault within the red beds requires the trace to separate lithologically similar material, none of which is particularly strongly deformed, and to exhibit quite a sinuous trace in order to avoid awkward outcrops. A fault between the basalt and the Lancaster Formation would identify the "Variscan front" with an apparently minor normal fault, and separate lithologically identical basalts into two different ages.

DISCUSSION

New information obtained in this years work, as well as previous information not yet integrated into tectonic models, appear to require some significant changes to large scale models of this region. Recognition of the Belleisle Fault as a major transcurrent structure shows that the Precambrian and Lower Paleozoic geology of the Saint John region cannot be directly compared to that of central New Brunswick, since the two regions were in differing, non-adjacent locations when the Paleozoic and older rocks developed. Although this fact has been used in various forms for some time, even models that assume a separate Avalonian plate may encounter difficulties with other aspects of the geology. Thus Rast (1980) assumes the Kingston complex and correlative dykes to be a swarm associated with continental breakup and the formation of the Iapetus Ocean. In such a case, however, the dykes should be predominantly basalt, which is not the case. An andesite-rhyolite dyke swarm on the scale observed appears to be unusual, but could perhaps be explained by the ideas of Condie (1975), according to which initial rise of a plume, followed by abortive rifting and collapse of the plume would lead to subsidence of the crust into hot mantle, and consequent melting of the crust with generation of andesitic and more acid rocks. Such a sequence would appear more plausible in a long-continued strike-slip environment with cycles of 'transpression' and 'transtension' (Reading, 1980) than in an ordinary oceanic rifting environment. The available age information (Olszewski and Gaudette, 1982; Olszewski et al., 1980) suggest a long-lived, or repetitive cycle of activity extending from 800 Ma to virtually the base of the Cambrian. This also suggests an environment other than continental breakup. Very tentatively, it may be suggested that the Bellisle Fault zone, which may encompass a significant portion of the mapped region, has a very long episodic history extending back into Precambrian time.

The post-Devonian history of this zone likewise poses a number of unsolved problems. In passing, note that the folding of the Cambrian rocks, whether or not it precedes the deposition of the Carboniferous section, cannot be confidently assigned to standard divisions such as 'Taconic' or 'Acadian' since it cannot be demonstrated that this region was ever in a suitable position to be involved in these events. The latest minor movement on the Bellisle Fault certainly postdates the Mount Champlain pluton, supposed by McCutcheon (1981) to be of Carboniferous age.

It cannot be assumed without further demonstration that the post-Westphalian deformation affecting the Lancaster/Balls Lake section is definitely younger than latest movement on the Belleisle Fault. Indeed if the latter marks the northwestern edge of "Avalonia", and if the latest deformation marks the arrival of the Meguma terrane, presumably along the transcurrent Cobequid Fault, it would seem reasonable to expect some simultaneous adjustments along the Belleisle Fault. Note that the arrival of "Avalonia" followed by arrival of the Meguma block also suggests a process of accretion of blocks to North America. This pattern of tesselate terranes separated by major transcurrent faults has now been recognized in both Newfoundland (Whalen and Currie, 1983) and Cape Breton Island (Currie, 1983). Major transcurrent movements appear in some cases to both precede and follow the now classical subduction cycles, but the correct correlation of these diverse processes is as yet unknown.

REFERENCES

Alcock, F.J.
1938: Geology of Saint John region, New Brunswick. Geological Survey of Canada, Memoir 216, 65 p.

Berry, W.B.N. and Boucot, A.J.
1970: Correlation of the North American Silurian rocks. Geological Society of America, Special Paper 102, 289 p.

Boucot, A.J., Johnson, J.G., Harper, C., and Walmsley, V.G.
1966: Silurian brachiopods and gastropods of southern New Brunswick. Geological Survey of Canada, Bulletin 140, 45 p.

Brown, R.L. and Helmstaedt, H.
1970: Deformation history in part of the Lubec-Belleisle zone of southern New Brunswick; Canadian Journal of Earth Sciences, v. 7, p. 748-767.

Condie, K.C.
1975: Mantle-plume model for the origin of Archaean greenstone belts based on trace-elements distributions; Nature, v. 258, p. 413-414.

Currie, K.L.
1983: Geochronological evidence for basement-cover relations in the Canadian Appalachians; Geological Society of America, Abstracts with Program.

Currie, K.L. and Nance, R.D.
1983: A reconsideration of the Carboniferous rocks of Saint John, New Brunswick; in Current Research, Part A, Geological Survey of Canada, Paper 83-1A, p. 29-36.

Currie, K.L., Nance, R.D., Pajari, G.E., and Pickerill, R.K.
1981: Some aspects of the pre-Carboniferous geology of Saint John, New Brunswick; in Current Research, Part A, Geological Survey of Canada, Paper 81-1A, p. 23-30.

Hayes, A.O. and Howell, B.F.
1937: Geology of Saint John, New Brunswick; Geological Society of America, Special Paper 5, 146 p.

Leavitt, E.M.
1963: Geology of the Precambrian Greenhead Group in the Saint John area; unpublished M.Sc. thesis, University of New Brunswick, Fredericton, New Brunswick.

McCutcheon, S.R.
1981: Revised stratigraphy of the Long Reach area, southern New Brunswick; evidence for major, northwestward-directed Acadian thrusting; Canadian Journal of Earth Sciences, v. 18, p. 646-656.

McCutcheon, S.R. and Ruitenberg, A.A.
1974: Preliminary Geological Map, Annidale-Nerepis Project, sheets N28, N29, N30, 028; New Brunswick Department of Natural Resources, Mineral Resources Branch, Plates 74-76, 74-84.

Nance, R.D.
1982: Structural reconnaissance of the Green Head Group, Saint John, New Brunswick; in Current Research, Part A, Geological Survey of Canada, Paper 82-1A, p. 37-43.

O'Brien, B.H.
1976: The geology of parts of the Coldbrook Group, southern New Brunswick; unpublished M.Sc. thesis, University of New Brunswick, Fredericton, New Brunswick.

Olszewski, W.J. and Gaudette, H.E.
1982: Age of the Brookville Gneiss and associated rocks, southeastern New Brunswick; Canadian Journal of Earth Sciences, v. 19, p. 2158-2166.

Olszewski, W.J., Gaudette, H.E., and Poole, W.H.
1980: Rb-Sr whole rock and U-Pb zircon ages from the Greenhead Group, New Brunswick; Geological Society of America, Abstracts with Program, v. 12, p. 76.

Rast, N.
1980: The Avalonian plate in the northern Appalachians and Caledonides; in The Caledonides in the U.S.A., ed. D.R. Wones; Virginia Polytechnic Institute, Department of Geology, Memoir 2.

Rast, N. and Currie, K.L.
1976: On the position of the Variscan front in southern New Brunswick and its relation to Precambrian basement; Canadian Journal of Earth Sciences, v. 13, p. 194-196.

Rast, N. and Grant, R.H.
1973: Transatlantic correlation of the Variscan-Appalachian orogeny; American Journal of Science, v. 273, p. 572-579.

Rast, N., Grant, R.H., Parker, J.S.D., and Teng, T.C.
1978: The Carboniferous deformed rocks west of Saint John, New Brunswick; in Guidebook for Field Trips in Southeastern Maine and Southwestern New Brunswick, ed. A. Ludman; New England Intercollegiate Geological Conference, 70th Annual Meeting, Queens College Press, Flushing, New York.

Reading, H.G.
1980: Characteristics and recognition of strike-slip fault systems; International Association of Sedimentology, Special Publications, v. 4, p. 7-26.

Ruitenberg, A.A., Giles, R.S., Venugopal, D.V.,
Buttimer, S.M., McCutcheon, S.R., and Chandra, J.
1979: Geology and mineral deposits, Caledonia area; New Brunswick Department of Natural Resources, Mineral Development Branch Memoir 1.

Wardle, R.J.
1977: The stratigraphy and tectonics of the Green Head Group; its relation to Hadrynian and Paleozoic rocks, southern New Brunswick; unpublished Ph.D. thesis, University of New Brunswick, Fredericton, New Brunswick.

Wardle, R.J. and O'Brien, B.H.
1975: The Precambrian of the Saint John area and Kingston peninsula and its relationship to the Paleozoic; in Geology of Southwestern New Brunswick-Field Guide; Geological Society of America, Penrose Conference Field Guide.

Whalen, J.B. and Currie, K.L.
1983: The Topsails igneous terrane of western Newfoundland; in Current Research, Part A, Geological Survey of Canada, Paper 83-1A, p. 15-23.

29. PETROLOGY OF EARLY CAMBRIAN AND DEVONO-CARBONIFEROUS INTRUSIONS IN THE LOCH LOMOND COMPLEX, SOUTHEASTERN CAPE BRETON ISLAND, NOVA SCOTIA

Project 650056

Sandra M. Barr[1], D.F. Sangster, and R.F. Cormier[2]
Economic Geology Division

Barr, S.M., Sangster, D.F., and Cormier, R.F., Petrology of early Cambrian and Devono-Carboniferous intrusions in the Loch Lomond complex, southeastern Cape Breton Island, Nova Scotia; in Current Research, Part A, Geological Survey of Canada, Paper 84-1A, p. 203-211, 1984.

Abstract

Rhyolite porphyry and granodiorite of the Loch Lomond complex, southeastern Cape Breton Island, were previously interpreted to be comagmatic and late Hadrynian – early Cambrian in age. Rb-Sr isotopic data reported here confirm the early Cambrian age of the granodiorite and related dykes (544 ± 21 Ma) but indicate that the rhyolite porphyry may be much younger (368 ± 30 Ma). Both intrusions have petrological features in common with other granitoid rocks of similar ages in the area, but the rhyolite porphyry is more evolved than most, with very high Rb/Ba and Rb/Sr.

Résumé

Le porphyre rhyolitique et la granodiorite du complexe de Loch Lomond, dans le sud-est de l'Île du Cap-Breton, ont déjà été interprétés comme étant comagmatique et d'âge hadrynien récent-cambrien ancien. Les données isotopiques Rb-Sr présentées dans ce rapport confirment que la granodiorite et les filkons associés datent du Cambrien ancien (544 ± 21 Ma), mais indiquent que le porphyre rhyolitique pourrait être beaucoup plus récent (368 ± 30 Ma). Les deux intrusions ont des éléments pétrologiques en commun avec d'autres roches granitoïdes d'âges similaires dans la région, mais le porphyre rhyolitique est plus évolué que la plupart des roches et contient des rapports très élevés de Rb/Ba et de Rb/Sr.

INTRODUCTION

The Loch Lomond complex (O'Reilly, 1977) is the largest of several granitoid intrusions in southeastern Cape Breton Island (Fig. 29.1). Mapping by Weeks (1954) indicated that the complex consists of rhyolite in the northeast, granite in the southwest, and dioritic rocks in the southeast. Weeks assumed that at least the two felsic lithologies were contemporaneous on the basis of mineralogical similarity, and assigned them a Devonian age as for other granitoid plutons in the region. However, radiometric age dating subsequently showed that the southwestern part of the Loch Lomond complex and other major plutons in southeastern Cape Breton Island are actually late Hadrynian to early Cambrian in age, although smaller intrusions to the northeast are Devonian (Cormier, 1972, 1979, 1980; Stevens et al., 1982).

During the summer of 1981, a suite of samples was collected from the felsic northern and southwestern parts of the Loch Lomond compelx (Fig. 29.2). This work was done in conjunction with studies of the Yava lead deposit (Vaillancourt and Sangster, 1984), located in Pennsylvanian clastic rocks near the northwestern margin of the Loch Lomond rhyolite, in order to assess the possibility that the granitoid rocks may have been a source for the lead. This report is a description of the petrology and an interpretation of the age of the Loch Lomond complex based on these samples.

REGIONAL GEOLOGY

As mapped by Weeks (1954), the late Hadrynian Fourchu Group occurs in two belts in southeastern Cape Breton Island: a northern belt extending along the southeastern shores of the Bras D'Or Lakes and East Bay, and a larger southern belt extending along the southeastern coast of the Island, in a broad band widening to the northeast (Fig. 29.1). The Fourchu Group consists of varied metavolcanic (predominantly pyroclastic), meta-intrusive, and metasedimentary rocks, interpreted to have formed in an ensialic volcanic arc (Keppie et al., 1979).

The widespread volcanic and sedimentary rocks which flank the Loch Lomond pluton to the southeast were interpreted by Weeks (1954) to be largely of Cambrian age, overlying the Fourchu Group. However, Smith (1978) placed much of this terrane into the "Giant Lake Complex" which he considered to be Fourchu-equivalent, and also revised the stratigraphy of overlying Cambrian rocks in the area. This re-interpretation was followed by Keppie (1979) and is shown in Figure 29.2.

These rocks as well as the granitoid intrusions are in faulted or unconformable contact with Carboniferous clastic sedimentary rocks (Fig. 29.1, 29.2). Occurrences of manganese minerals, barite, celestite, and galena in these sedimentary rocks along the western margin of the Loch Lomond complex have made this area a focus for exploration in Cape Breton Island (O'Reilly, 1977; Felderhof, 1978).

FIELD OBSERVATIONS

The field work of this study concentrated on the rhyolite (actually rhyolite porphyry) and granite (actually granodiorite) of the northern and southwestern areas of the Loch Lomond complex, as mapped by Weeks (1954). The main contact zone between these units was not observed and, except for clearly nonconformable contacts with clastic sedimentary rocks to the west, no contacts were observed between the granitoid rocks and other rock units. Intrusive relationships indicated in Figures 29.1 and 29.2 are taken from Weeks (1954), Smith (1978), and Keppie (1979). The dioritic and other granitoid rocks of the southeastern part of the Loch Lomond complex were not sampled during the present study.

[1] Dept. of Geology, Acadia University, Wolfville, N.S., Canada B0P 1X0
[2] Dept. of Geology, St. Francis Xavier University, Antigonish, N.S., Canada B2G 1C0

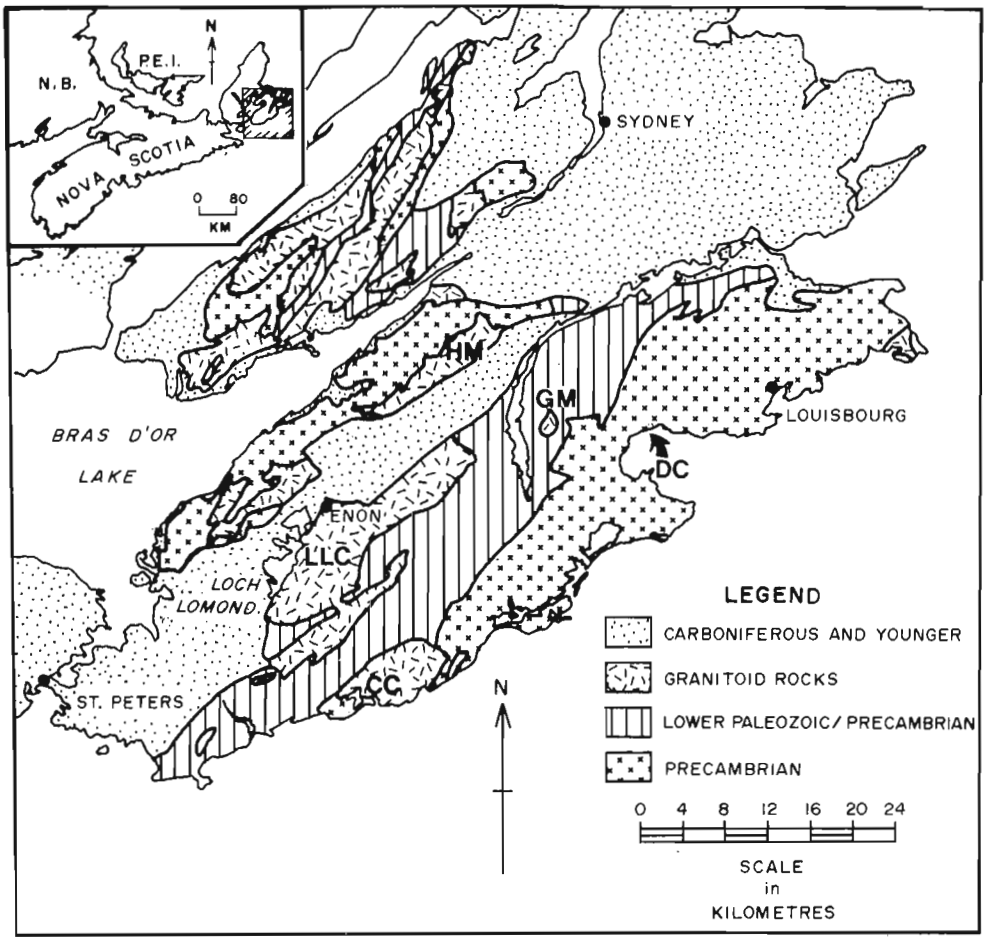

Figure 29.1

Simplified geological map of southeastern Cape Breton Island (after O'Reilly, 1977) showing the location of the Loch Lomond complex (LLC). Other plutons referred to in the text are Huntington Mountain (HM), Gillis Mountain (GM), Deep Cove (DC), and Capelin Cove (CC).

The medium grained pink to greenish grey granodiorite of the southwestern part of the complex varies in texture and mafic mineral content. Finer grained, more mafic areas and pegmatoid patches with large hornblende needles may represent largely digested xenolithic material. Also present are abundant rounded mafic (metavolcanic?) xenoliths ranging in size from 1 cm to 1 m or more. The granodiorite is cut by abundant felsic dykes up to several metres in width and generally trending about 100°. Mafic dykes are also abundant; these generally trend approximately north-south, and are highly fractured. At sample locality 3 (Fig. 29.2) a mafic dyke in the granodiorite appears to have been intruded by a sparsely porphyritic felsic dyke.

The rhyolite porphyry of the northern part of the complex is a dense, typically pink, aphanitic rock with variable proportions of feldspar and quartz phenocrysts. No felsic or mafic dykes were observed in the rhyolite. However, a small area of fine grained equigranular monzodiorite in the northeastern corner of the rhyolite body (Fig. 29.2) may be a dyke or plug. It was considered by Smith (1978) to be Devonian.

PETROGRAPHY

The granodiorite of the Loch Lomond complex is medium grained and inequigranular (subporphyritic). Subhedral to euhedral plagioclase crystals are set in a finer grained, typically granophyric matrix of quartz and potassium feldspar. The plagioclase is zoned, but generally of oligoclase composition, and intensely sericitized. The mafic minerals, which form 12 to 20 per cent of most samples, are

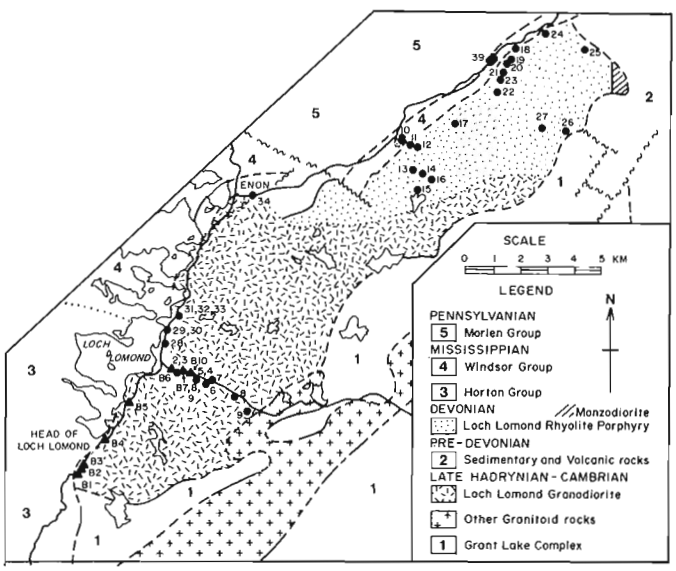

Figure 29.2. Sample locations in the Loch Lomond complex. Numbered dots are from this study; triangles with B numbers are age-dated samples from Cormier (1972).

chloritized biotite and amphibole, and replacement is complete in most samples. Epidote is also abundant, as scattered crystalline masses and replacing amphibole. The modal compositions generally plot in the low quartz/high K-feldspar part of the granodiorite field of Streckeisen (1976).

The felsic dykes in the granodiorite vary in texture but are typically aplitic or fine grained allotriomorphic granular. The dyke, which cuts the mafic dyke at sample locality 3 (Fig. 29.2), is sparsely porphyritic with quartz, plagioclase, and K-feldspar phenocrysts in an equigranular quartz-feldspar groundmass. The dyke at sample locality 5 (Fig. 29.2) is wholly granophyric in texture. Samples from these two dykes were selected for chemical analyses (see next section).

The rhyolite porphyry of the northern part of the Loch Lomond complex consists of potassium feldspar, quartz, and plagioclase phenocrysts in a fine grained groundmass. The relative proportions of phenocrysts and groundmass vary from about 50:50 to 25:75. Typically the most abundant phenocrysts are euhedral to subhedral zoned crystals of sanidine displaying partial sericitization. Of nearly equal abundance are clear, anhedral quartz phenocrysts which exhibit evidence of minor resorption at their margins. Plagioclase phenocrysts are somewhat less abundant, and occur in clusters of relatively small grains or as isolated larger grains. They are generally subhedral and highly altered to sericite. Rare muscovite phenocrysts are present in some samples. The groundmass consists of granular potassium feldspar and quartz, with minor plagioclase and biotite/chlorite. Sericite and iron oxides are abundant. In at least one area in the north-central region (sample 27; Fig. 29.2), the rock is particularly fine grained and displays flow alignment in the groundmass, as compared to the granular texture of other samples. This sample is highly altered and contains abundant carbonate.

GEOCHEMISTRY

Methods

Thirty-four samples from locations in Figure 29.2 were selected for chemical analyses. Major element and Cu, Pb and Zn analyses were done by the Analytical Chemistry Laboratory of the Geological Survey of Canada, using X-ray fluorescence and atomic absorption methods. FeO and volatiles were obtained by standard rapid chemical techniques. Analyses for B, Ba, Cu, F, Li, Mo, Rb, Sn, Sr and W were done by CLIM Laboratories, Technical University of Nova Scotia, using methods described in Barr et al. (1982). Uranium and thorium were determined by neutron activation at Atomic Energy of Canada, Ottawa.

Major elements

The rhyolite porphyry is generally a highly felsic rock (Table 29.1), with SiO_2 contents ranging from 73 to 76 per cent and differentiation indices (Thornton and Tuttle, 1960) of 90 to 96. The granodiorite contains lower SiO_2 (Table 29.1), ranging from 67 to 73 per cent, and lower Thornton-Tuttle differentiation indices of 74 to 85.

Differences in major element geochemistry between these two main rock types are generally consistent with the difference in SiO_2 content, with TiO_2, Al_2O_3, Fe_2O_3T, MnO, MgO, CaO, and P_2O_5 showing a negative correlation with SiO_2 and a positive correlation with K_2O (Fig. 29.3). Na_2O shows little correlation with SiO_2. The granodiorite is unusually low in K_2O and high in MnO, and the rhyolite porphyry seems relatively high in K_2O and low in CaO. Both the rhyolite porphyry and the granodiorite contain significant amounts of normative corundum and are hence classified as peraluminous (Fig. 29.4). This is a distinctive feature, as peraluminous intrusions are apparently not common in Cape Breton Island (Barr et al., 1982). It suggests that the two rock types may be genetically related; on the basis of major element geochemistry (Fig. 29.3), the rhyolite could represent a more evolved product of the same differentiating magma as the granodiorite.

Two of the analyzed samples were not included in the calculation of the means in Table 29.2. Sample 17 is a very altered rhyolite porphyry with high carbonate content (2.5% CO_2) which contains only 66.3 per cent SiO_2 (Fig. 29.3). Sample 34 is from one of the more mafic areas in the granodiorite and contains only 60.3 per cent SiO_2 (Fig. 29.3). Other major elements in these samples are generally consistent with these intermediate SiO_2 contents (Fig. 29.3).

The two felsic dyke samples are similar in major element composition to the rhyolite porphyry, although on the more felsic side (Table 29.1, Fig. 29.3).

Trace elements

The Loch Lomond rhyolite porphyry is characterized by generally low Ba and Sr, although a few samples range up to 700 and, in one case, 1200 ppm Ba (Fig. 29.5). The granodiorite, in contrast, contains lower Rb and higher Ba and Sr. The contrasting abundances of these elements are clearly illustrated by a Ba-Rb-Sr ternary diagram (Fig. 29.6). High Rb/Sr and Ba/Sr ratios such as demonstrated by many of the rhyolite porphyry samples are generally typical of "specialized" granites (e.g. Smith and Turek, 1976). However, the wide range in these samples suggests mobilization during alteration, although the high Ba and Sr values in the highly altered sample (17) suggests that low Ba and Sr may in fact be a primary feature of the rhyolite porphyry. Variations of

Table 29.1. Means and standard deviations of major and trace element analyses from the Loch Lomond complex

	Granodiorite n = 12	Felsic Dykes n = 2	Rhyolite Porphyry n = 18
SiO_2	70.8 ± 1.3	76.1 ± 1.4	74.3 ± 0.6
TiO_2	0.41 ± 0.06	0.13 ± 0.01	0.06 ± 0.01
Al_2O_3	14.7 ± 0.5	13.4 ± 1.2	14.0 ± 0.4
Fe_2O_3	1.4 ± 0.4	0.8 ± 0.1	0.7 ± 0.3
FeO	1.4 ± 0.1	0.3 ± 0.04	0.6 ± 0.2
MnO	0.12 ± 0.04	0.03 ± 0.01	0.02 ± 0.02
MgO	0.86 ± 0.15	0.33 ± 0.19	0.12 ± 0.08
CaO	1.87 ± 0.12	0.41 ± 0.27	0.36 ± 0.12
Na_2O	3.76 ± 0.30	2.95 ± 0.64	3.49 ± 0.39
K_2O	3.11 ± 0.34	4.69 ± 1.60	4.80 ± 0.51
P_2O_5	0.12 ± 0.03	0.03 ± 0.01	0.01 ± 0.01
B	6 ± 2	8 ± 4	9 ± 3
Ba	770 ± 80	385 ± 35	176 ± 282
Cu	10 ± 3	47 ± 47	13 ± 5
F	390 ± 30	235 ± 78	300 ± 140
Li	9 ± 5	1 ± 0	15 ± 12
Mo	0.9 ± 0.2	0.8 ± 0.1	0.8 ± 0.2
Pb	8 ± 8	6 ± 8	30 ± 9
Rb	76 ± 21	143 ± 1	200 ± 42
Sn	1.8 ± 0.6	1.3 ± 0.1	2.3 ± 0.9
Sr	241 ± 58	60 ± 9	53 ± 19
Th	12 ± 2	16 ± 11	25 ± 6
U	2.7 ± 0.3	5.4 ± 1.6	4.5 ± 2.7
Zn	62 ± 9	24 ± 9	31 ± 10

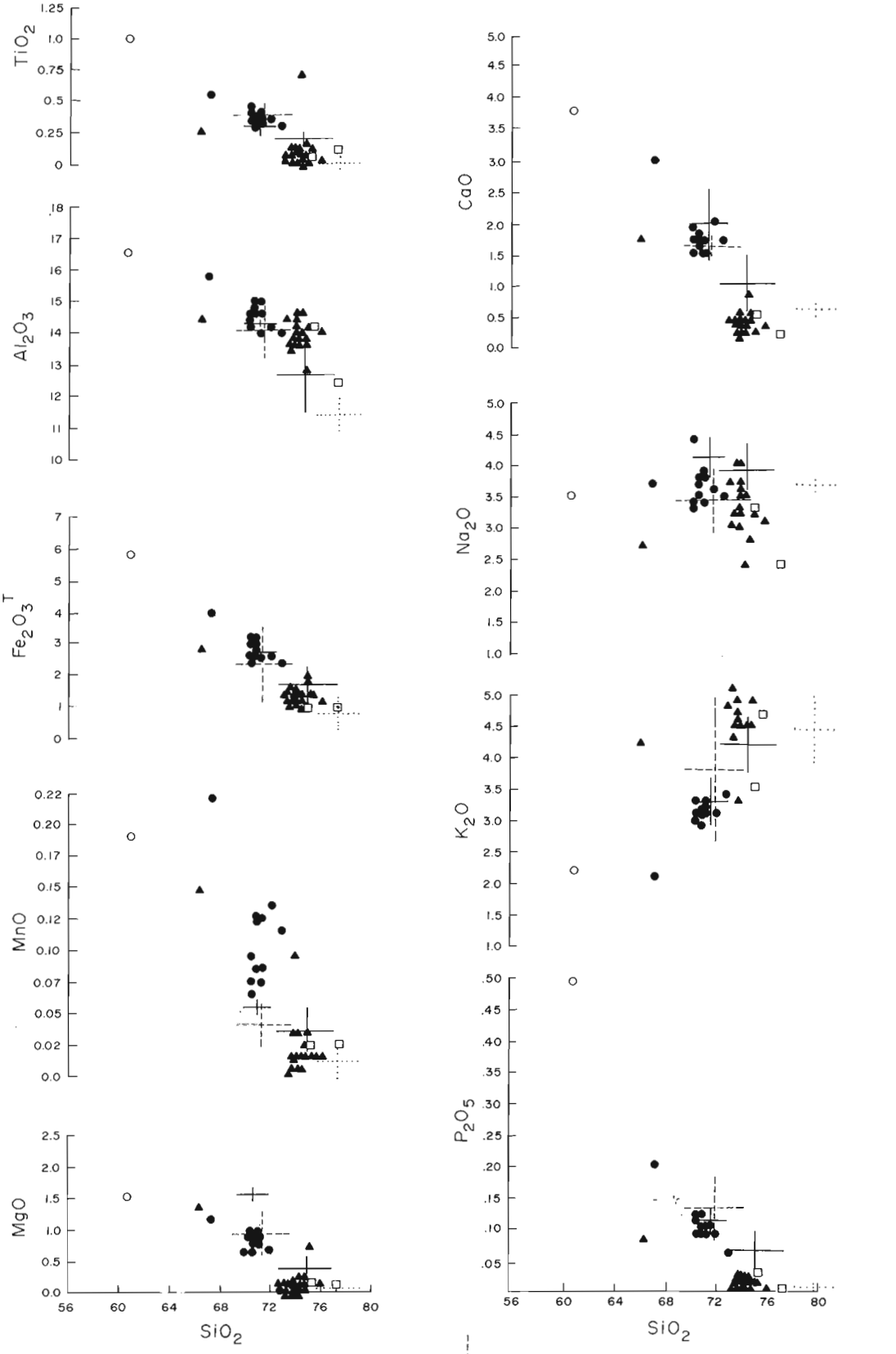

Figure 29.3. *Silica variation diagrams for major element oxides (from Barr et al., 1982).*

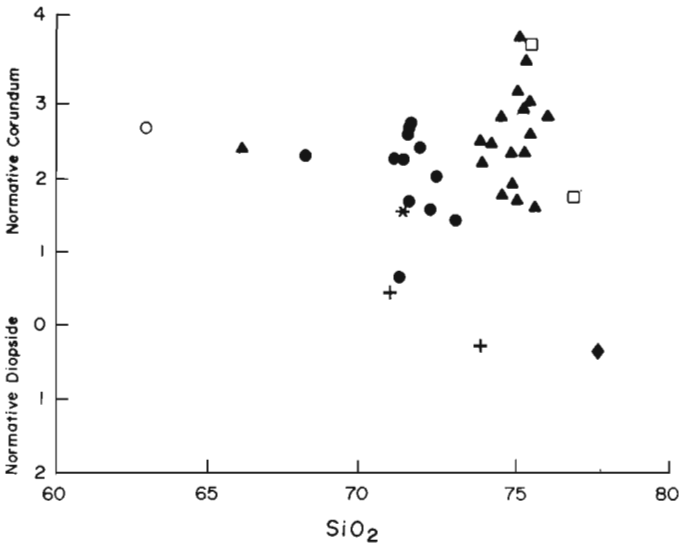

Figure 29.4. *Plot of CIPW normative corundum or diopside against SiO_2. Symbols are as in Figure 29.3, except mean values are indicated by asterisk (Deep Cove granite), diamond (Petit de Grat leucogranite), and crosses (Huntington Mountain quartz monzonite and leucogranite).*

Table 29.2. Rb-Sr isotopic data, Loch Lomond complex

Sample #	Rb(ppm)	Sr(ppm)	$^{87}Rb/^{86}Sr$	$^{87}Sr/^{86}Sr$*
Granodiorite				
2	80.3	178	1.31	0.7173
7	99.6	210	1.37	0.7154
33	93.4	242	1.12	0.7167
36	97.5	230	1.23	0.7172
B1	52.7	568	0.272	0.7114
B2	49.4	348	0.416	0.7128
B3	39.4	310	0.373	0.7125
B4	53.8	329	0.479	0.7075
B9	88.1	197	1.30	0.7176
B10	79.6	172	1.34	0.7132
Felsic Dyke				
3	151	63.7	6.91	0.7607
B5	182	37.4	14.2	0.8164
B6	119	92.2	3.76	0.7372
B7	163	55.2	8.58	0.7697
Rhyolite Porphyry				
12	158	48.0	9.55	0.7541
16	187	34.3	15.9	0.7926
20	283	54.0	15.3	0.7956
22	233	43.4	15.6	0.7867
24	234	20.1	34.2	0.8863
39	280	29.7	27.7	0.8518

*Normalized to a value of 0.1194 for the ratio $^{87}Sr/^{88}Sr$

these elements are particularly interesting because of barite and celestite occurrences in the Loch Lomond area (see Discussion).

The two felsic dykes overlap in Ba, Rb and Sr with the rhyolite porphyry, but comparatively low Rb and moderate Ba and Sr place these samples in a more normal position for felsic rocks on the Ba-Rb-Sr plot (Fig. 29.6), close to altered rhyolite porphyry sample 17.

Cu and especially Pb show a wider range in the rhyolite porphyry than in the granodiorite (Fig. 29.7), with an isolated high value of 2580 ppm Pb in rhyolite porphyry sample 19. Other high values up to several thousand ppm have also been reported during earlier reconnaissance surveys in the area (G. O'Reilly, personal communication, 1982).

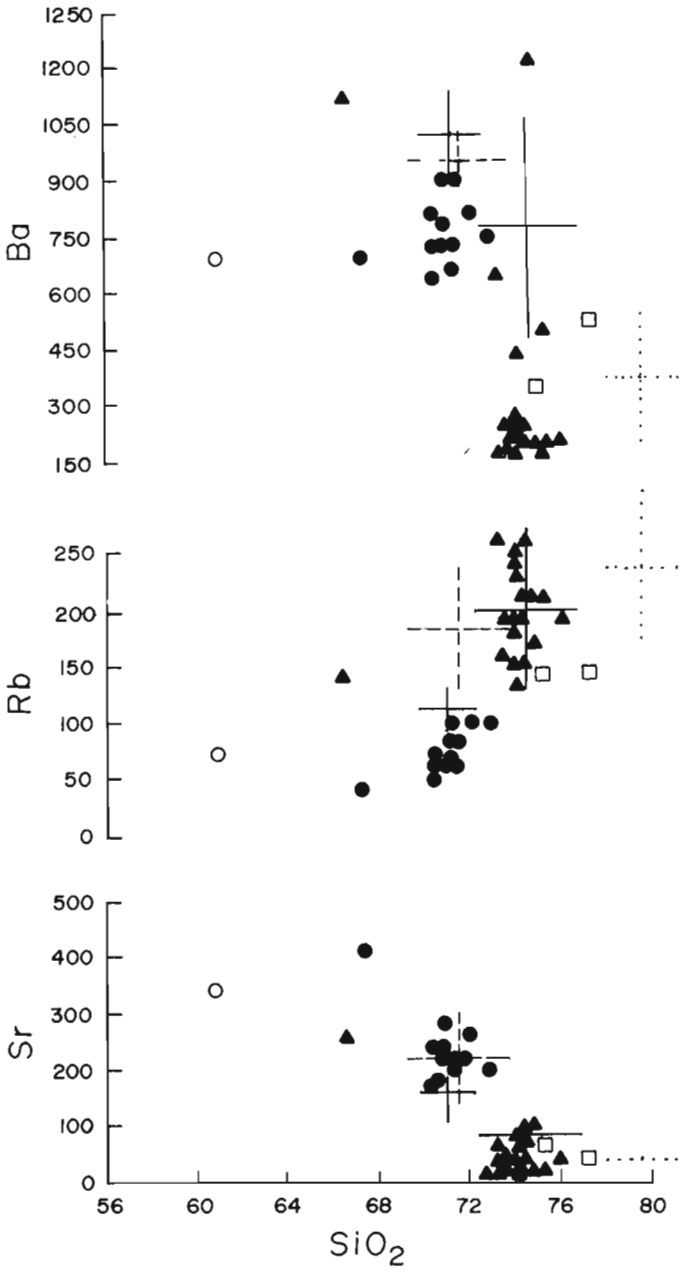

Figure 29.5. *Silica variation diagrams for Ba, Rb and Sr, with symbols and lines as in Figure 29.3.*

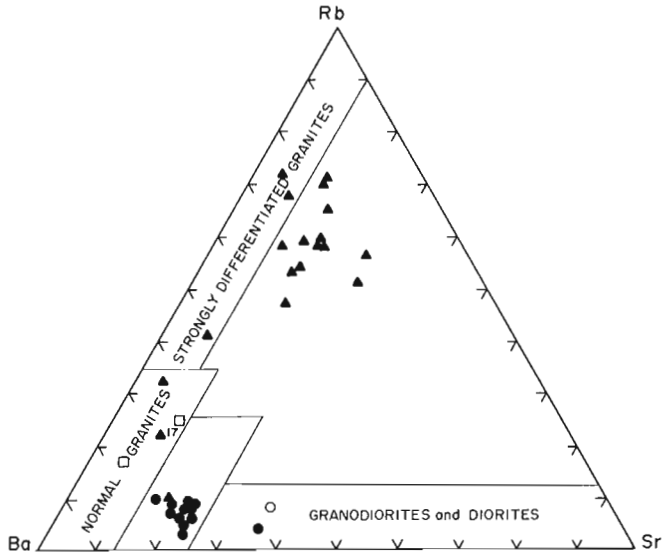

Figure 29.6. *Ternary plot for Ba-Rb-Sr, with symbols as in Figure 29.3. Fields are from El Bouseily and El Sokkary (1975).*

The felsic dykes, like the granodiorite, are low in Pb, but one has an anomalous Cu content (80 ppm).

Molybdenum and Zn values do not display any unusual patterns (Fig. 29.7) and W is below the detection limit of 4 ppm in all samples.

Both U and Th show as widespread in the rhyolite porphyry, but the granodiorite data are more clustered (Fig. 29.8). Sn also shows some spread (Fig. 29.8), as do Li, B and F (Fig. 29.9). Relatively high Li, B and F in the altered, CO_2-rich sample (17) suggest that these elements may have been redistributed by alteration.

The felsic dykes do not appear to be distinctly different from the rhyolite porphyry in trace element characteristics.

AGE

The southwestern part of the Loch Lomond complex was previously dated by Cormier (1972) who reported a Rb-Sr isochron age of 548 ± 18 Ma (as recalculated by Keppie and Smith, 1978) from a suite of samples collected along the roads between Head of Loch Lomond, and Frambois (B numbers in Figure 29.2). As part of the present study, these 9 samples were re-analyzed together with an additional 11 samples from the present study. Analyses were done by R.F. Cormier using routine isotope dilution methods and mass spectrometry. Relevant data are presented in Table 29.2. The samples include 6 from the rhyolite porphyry, 10 from the granodiorite, and 4 from felsic dykes in the granodiorite.

The six rhyolite porphyry samples define a good isochron at 368 ± 30 Ma and initial $^{87}Sr/^{86}Sr$ of 0.7076 ± 0.0095 (Fig. 29.10). The 10 granodiorite samples cluster near or slightly above this isochron, with very low $^{87}Rb/^{86}Sr$ ratios reflecting the exceptionally low Rb content of the granodiorite previously discussed. However, when combined with the 4 felsic dyke samples, a fourteen-point whole-rock isochron is obtained which gives an age of 544 ± 21 Ma (Fig. 29.10). Although the granodiorite samples (because of very low $^{87}Rb/^{86}Sr$ values) could lie on either the rhyolite porphyry isochron or the felsic dyke isochron, it seems impossible for them to plot on the younger rhyolite porphyry isochron because the granodiorite was intruded by

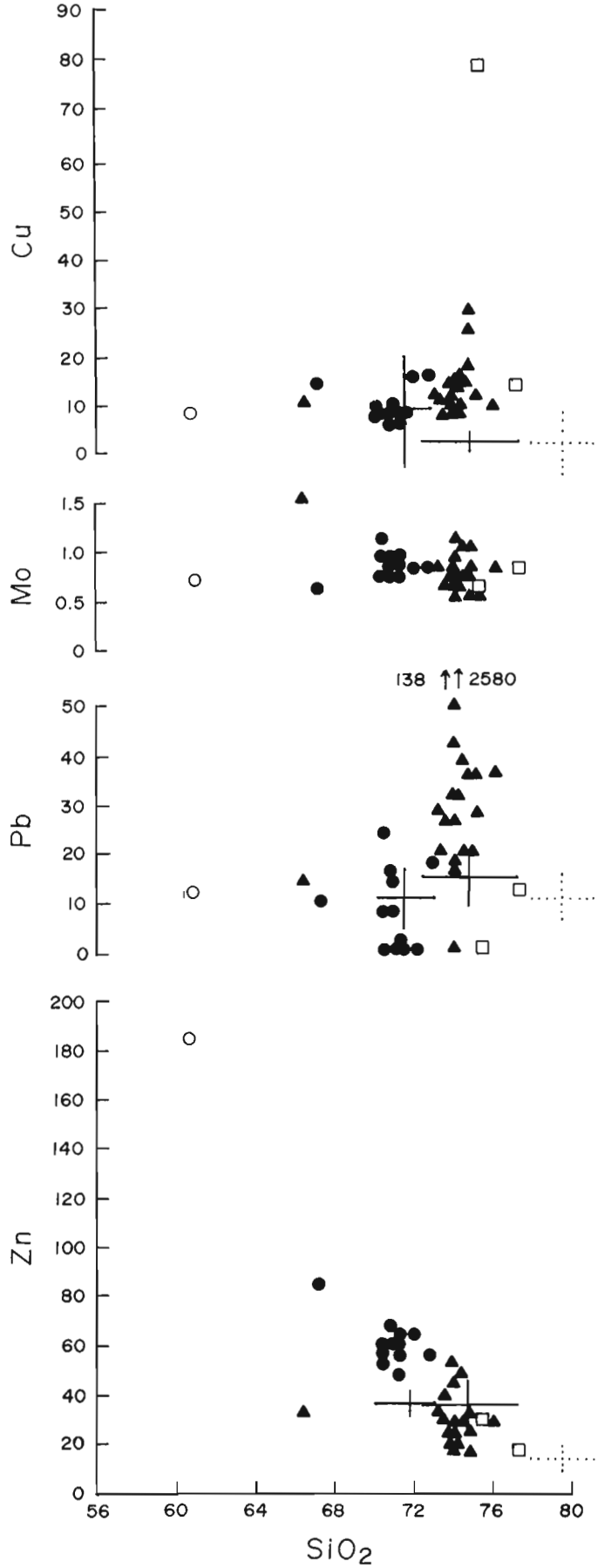

Figure 29.7 *(right). Silica variation diagrams for Cu, Mo, Pb and Zn, with symbols and lines as in Figure 29.3.*

the felsic dykes. Alternatively the entire suite of rhyolite porphyry samples has been re-set by a younger thermal event, or the felsic dyke samples are giving erroneous yet consistent data. Neither explanation seems likely.

Hence the data suggest that the two parts of the Loch Lomond complex, although appearing to form a single pluton, are in fact quite different in age. The rhyolite porphyry is late Devonian or early Carboniferous, and thus similar in age to two small plutons to the northeast (Fig. 29.1): Gillis Mountain which has given ages of 384 ± 10 Ma (Cormier, 1979) and 400 ± 13 Ma (Stevens et al., 1982), and Deep Cove which has given ages of 342 ± 25 Ma (Cormier, 1972; Keppie and Smith, 1978) and 387 Ma (M. Zentilli, personal communication, 1982). The highly

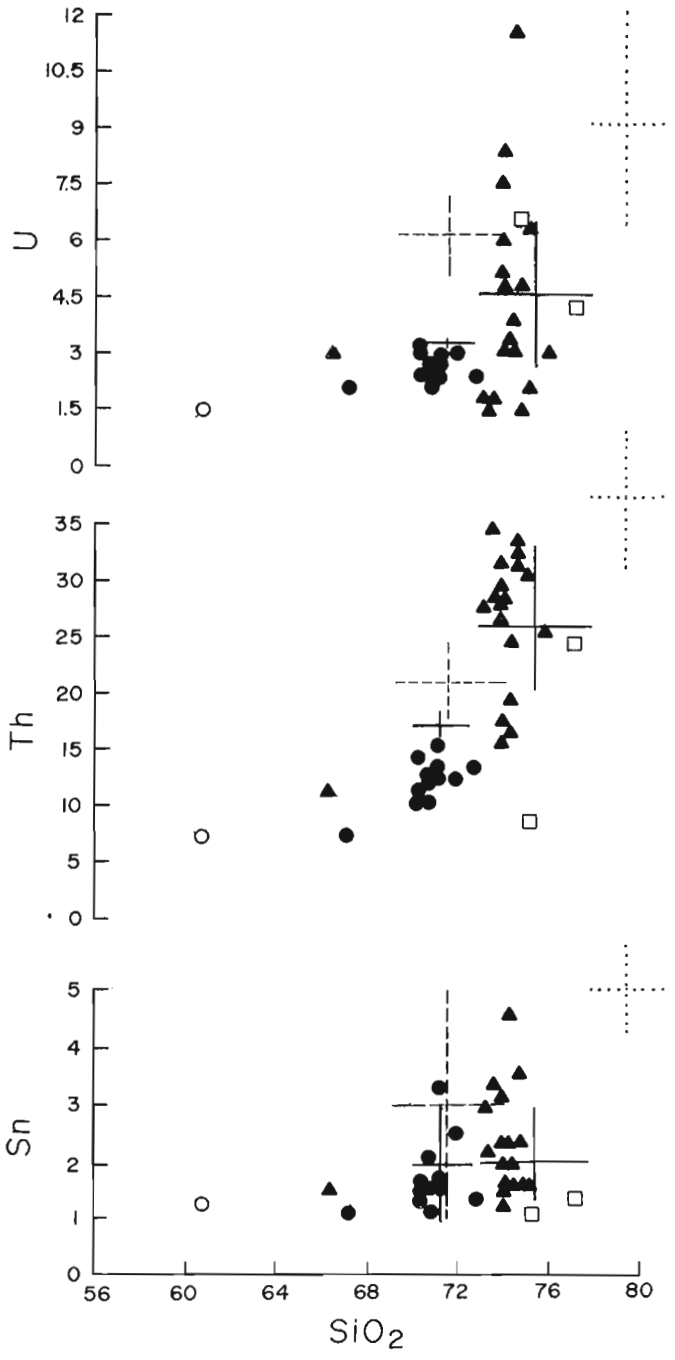

Figure 29.8. Silica variation diagrams for U, Th and Sn, with symbols and lines as in Figure 29.3.

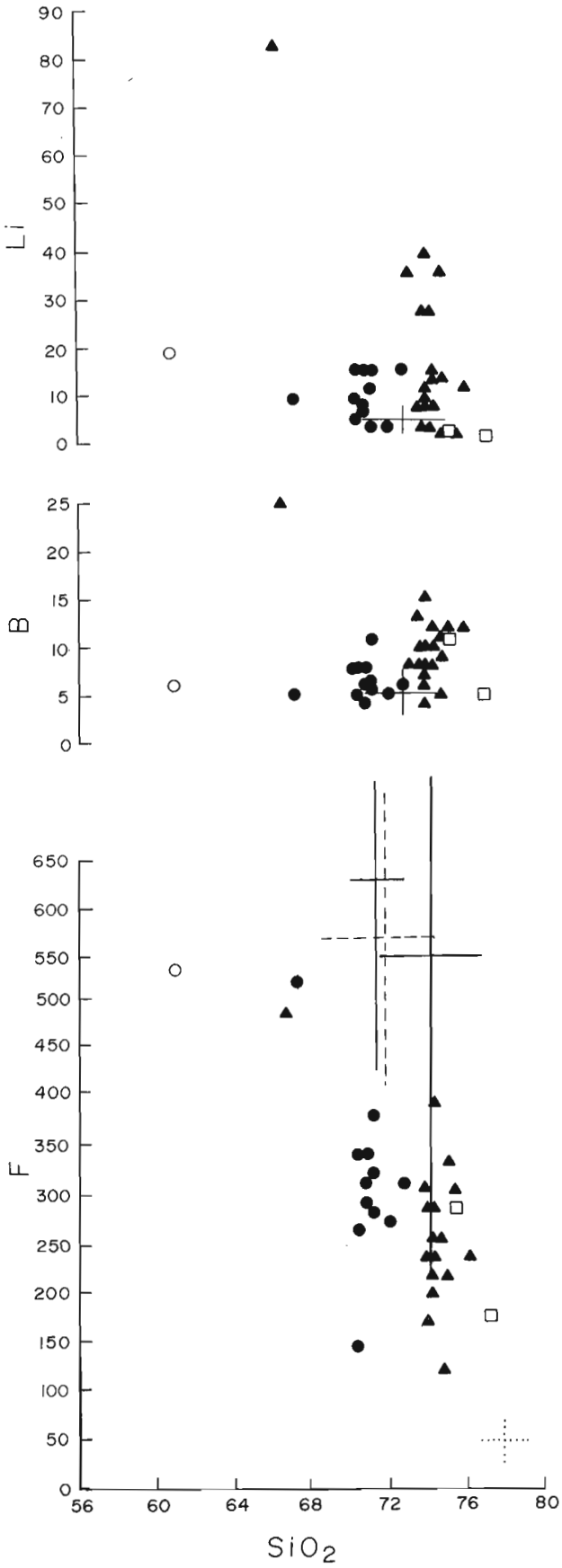

Figure 29.9. Silica variation diagrams for Li, B and F, with symbols and lines as in Figure 29.3.

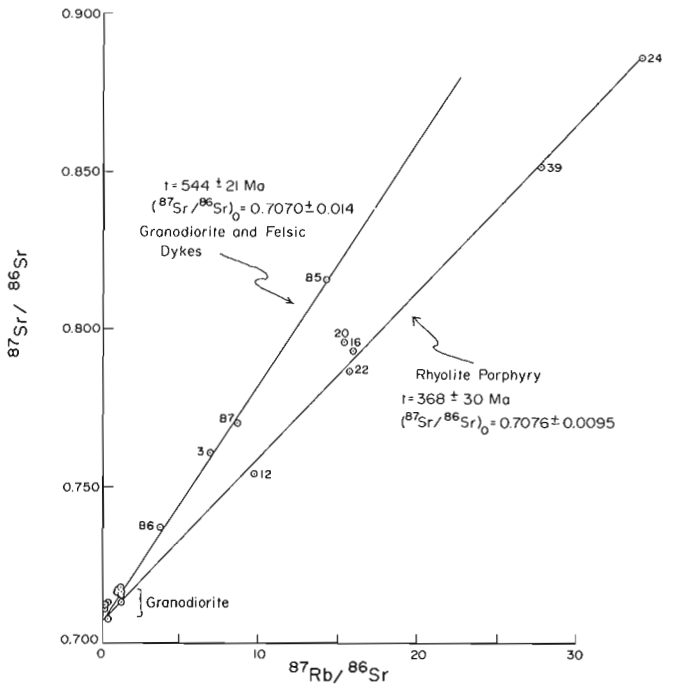

Figure 29.10. *Rb-Sr isochrons for samples from the Loch Lomond complex. Sample locations are shown in Figure 29.2. Analytical data are given in Table 29.2. Ages are calculated using a value of 1.42 x 10^{-11} $year^{-1}$ for the decay constant of ^{87}Rb. Error estimates are at the 95% confidence level (two standard deviations).*

felsic Petit de Grat pluton 40 km to the southwest in the southeastern corner of Cape Breton Island has also given young radiometric ages (357 ± 11 Ma; Cormier, 1980).

In contrast, the granodiorite of the Loch Lomond complex may be early Cambrian (as previously suggested by Cormier, 1972), similar to the Capelin Cove pluton to the south (545 ± 28 Ma; Cormier, 1972; Keppie and Smith, 1978) and the Huntington Mountain pluton to the north (573 ± 30 Ma; Cormier, 1980). Because the dated samples include felsic dykes, one of which is cut by a mafic dyke, an episode of mafic dyke emplacement apparently occurred during cooling of the pluton, before emplacement of late-stage felsic dykes.

DISCUSSION

The apparent age difference between the granodiorite and rhyolite porphyry of the Loch Lomond complex was an unexpected result of this study because outcrop distribution suggests that the two lithologies are part of the same pluton, as do general petrographic similarities noted by Weeks (1954). The rhyolite porphyry is a high-level or subvolcanic intrusion (although of an unusually large size) and the granodiorite also appears to have been emplaced at relatively shallow depths, on the basis of its subporphyritic texture and abundant interstitial granophyre.

However both the Devonian Gillis Mountain-Deep Cove plutons and late Hadrynian-early Cambrian Huntington Mountain pluton also have been interpreted to be relatively high-level intrusions (Barr and O'Beirne, 1981; Barr et al., 1982), especially the Gillis Mountain pluton which may have been as shallow as 2 km. The Gillis Mountain pluton consists of a much less felsic suite of rocks than the rhyolite porphyry and hence petrological comparisons are inappropriate. The Deep Cove granite (interpreted to have been comagmatic with Gillis Mountain by Barr et al., 1982) is more evolved and hence more readily compared to the Loch Lomond rhyolite porphyry. It contains somewhat lower average SiO_2 than the rhyolite porphyry and hence differs slightly in major element composition (Fig. 29.3) but like the rhyolite porphyry, it contains normative corundum (Fig. 29.4). The Deep Cove granite is generally higher in Ba and Sr but similar in Rb (Fig. 29.5). It has similar levels of U, Th, and Sn (Fig. 29.8), but higher F (Fig. 29.9). Cu, Pb, Zn and Mo values are much higher (exceeding the scales in Fig. 29.7) but this is because Deep Cove pluton contains abundant sulphide mineralization (Barr et al., 1982). Hence, although the petrological data cannot confirm a relationship between these late Devonian high-level intrusions, they are not inconsistent with that interpretation. If so, then this intrusive episode was much more widespread than previously recognized.

Comparison of the rhyolite porphyry with the small Petit de Grat pluton is also of interest. Petit de Grat pluton consists of leucogranite which is highly felsic, and shows some striking similarities to the rhyolite porphyry (Fig. 29.3, 5, 7, 8, 9), including low F, Ba and Sr and high U and Th. However it is very low in Al_2O_3. The cataclastic texture of the Petit de Grat leucogranite suggests that it is located in a major fault zone where hydrothermal alteration may have been extensive, further evidence that the abundance of the trace elements may be strongly affected by alteration. Hence chemical similarity between the rhyolite porphyry and the Petit de Grat leucogranite need not indicate any direct or indirect genetic relationship.

Comparison of the Loch Lomond granodiorite with rocks of the Huntington Mountain pluton of similar age also does not lead to clear indications of genetic relationships. The Huntington Mountain pluton includes minor amounts of quartz monzonite with content of SiO_2 similar to that in the Loch Lomond granodiorite (Fig. 29.3). However the Huntington Mountain rocks are generally lower in Al_2O_3 and higher in CaO, Na_2O and MgO (Fig. 29.3), with only minor normative corundum. They also have lower Zn and higher Th, F, and Mo (Fig. 29.7-29.9). A major part of the Huntington Mountain pluton consists of granite which is similar in SiO_2 content to the much younger Loch Lomond rhyolite porphyry (Fig. 29.3). However the two are very different in contents of Al_2O_3 (Fig. 29.3), Ba (Fig. 29.5), Cu and Pb (Fig. 29.7), and F (Fig. 29.9) and the granite does not contain any normative corundum (Fig. 29.4).

The significance of the normative corundum, especially in the Loch Lomond granodiorite (as well as Gillis Mountain and Deep Cove plutons) is not clear. The general features of these rocks (for example, abundance of amphibole and relatively low initial $^{87}Sr/^{86}Sr$ ratios) are not usual features of peraluminous granitoid rocks (e.g. Chappel and White, 1974). Hence the origin of their peraluminous chemistry remains problematical.

Mineralization has been reported at two localities within the Loch Lomond granodiorite: pyrite-chalcopyrite-bornite in altered rocks 0.8 km east of Enon (O'Reilly, 1977) and sulphide mineralization in quartz veins near Loch Lomond village (A. Hudgins, personal communication, 1982). Galena has been observed in minor amounts in the rhyolite porphyry near its western margin. However, the most significant mineralization in the area appears to be located in clastic sedimentary rocks to the west of the intrusion. As these rocks postdate the intrusion, the mineralizing effect of the granitoid rocks is not directly magmatic. But it is intriguing that the elements in which the intrusive rocks show most distinct anomalies are those which occur in these deposits.

More detailed investigation of the petrology and petrogenesis of the Loch Lomond complex, including the dioritic rocks, based on detailed field mapping is continuing.

ACKNOWLEDGMENTS

This work was partially funded by Natural Sciences and Engineering Research Council Grant A-4230 to S.M. Barr.

REFERENCES

Barr, S.M. and O'Beirne, A.M.
1981: Petrology of the Gillis Mountain pluton, Cape Breton Island, Nova Scotia; Canadian Journal of Earth Sciences, v. 18, p. 395-404.

Barr, S.M., O'Reilly, G.A., and O'Beirne, A.M.
1982: Geology and geochemistry of selected granitoid plutons of Cape Breton Island; in Nova Scotia Department of Mines and Energy, Paper 82-1, 177 p.

Chappell, B.W. and White, A.J.R.
1974: Two contrasting granite types; Pacific Geology, v. 8, p. 173-174.

Cormier, R.F.
1972: Radiometric ages of granitic rocks, Cape Breton Island, Nova Scotia; Canadian Journal of Earth Sciences, v. 9, p. 1074-1086.

1979: Rubidium/strontium isochron ages of Nova Scotian granitoid plutons; in Nova Scotia Department of Mines and Energy, Report 79-1, p. 143-147.

1980: New rubidium/strontium ages in Nova Scotia; in Nova Scotia Department of Mines and Energy, Report 80-1, p. 223-233.

El Bouseily, A.M. and El Sokkary, A.A.
1975: The relation between Rb, Ba, and Sr in granitic rocks; Chemical Geology, v. 16, p. 207-219.

Felderhof, G.W.
1978: Barite, celestite, and fluorite in Nova Scotia; in Nova Scotia Department of Mines Bulletin 4, 463 p.

Keppie, J.D.
1979: Geological map of the Province of Nova Scotia, scale 1:500,000; Nova Scotia Department of Mines and Energy.

Keppie, J.D. and Smith, P.K.
1978: Compilation of isotopic age data of Nova Scotia; in Nova Scotia Department of Mines, Report 78-4.

Keppie, J.D., Dostal, J., and Murphy, J.B.
1979: Petrology of the late Precambrian Fourchu Group in the Louisbourg area, Cape Breton Island, Nova Scotia; in Nova Scotia Department of Mines and Energy, Paper 79-1, 18 p.

O'Reilly, G.A.
1977: Field relations and mineral potential of the granitoid rocks of southeast Cape Breton Island; in Nova Scotia Department of Mines, Report 77-1, p. 81-87.

Smith, P.K.
1978: Geology of the Giant Lake area, southeastern Cape Breton Island, Nova Scotia; in Nova Scotia Department of Mines and Energy, Paper 78-3.

Smith, T.E. and Turek, A.
1976: Tin-bearing potential of some Devonian granitic rocks in southwestern Nova Scotia; Mineralium Deposita, v. 11, p. 234-245.

Stevens, R.D., Delabio, R.N., and Lachance, G.R.
1982: Age determinations and geological studies; Geological Survey of Canada, Paper 81-2, p. 46.

Streckeisen, A.
1976: To each plutonic rock its proper name; Earth Science Review, v. 12, p. 1-33.

Thornton, C.P. and Tuttle, O.F.
1960: Chemistry of igneous rocks, 1. Differentiation index; American Journal of Science, v. 258, p. 664-684.

Vaillancourt, P.D. and Sangster, D.F.
1984: Petrography of mineralization at the Yava Sandstone lead deposit, Nova Scotia; in Current Research, Part A, Geological Survey of Canada, Paper 84-1A, report 47.

Weeks, L.J.
1954: Southeast Cape Breton Island, Nova Scotia; Geological Survey of Canada, Memoir 277, 112 p.

30. SEDIMENTOLOGY AND BASIN ANALYSIS OF THE PRECAMBRIAN CONCEPTION GROUP, AVALON ZONE, NEWFOUNDLAND

EMR Research Agreement 64-04-83

Scott Gardiner[1] and Rick N. Hiscott[1]
Precambrian Geology Division

Gardiner, S. and Hiscott, R.N., Sedimentology and basin analysis of the Precambrian Conception Group, Avalon Zone, Newfoundland; in Current Research, Part A, Geological Survey of Canada, Paper 84-1A, p. 213-216, 1984.

Abstract

The Mall Bay and Drook Formations of the Hadrynian Conception Group were studied in the area of St. Mary's Bay, Avalon Peninsula, Newfoundland.

These predominantly fine grained siliciclastic sediments contain thinly-bedded (5-15 cm) classical turbidites which form coarsening upward cycles. A few minor channels are present. This evidence suggests that deposition occurred basinward of the inner fan within a turbidite fan depositional environment. Specifically, the sequences of the facies observed are interpreted to be the products of lobe, interlobe, lobe fringe, fan fringe and basin plain sedimentation. Minor deposition and reworking of sediment by contour currents is also possible.

Paleocurrent analysis, using solemarks, ripples, and sandstone fabric in thin sections, indicates dominant flow toward the northeast, with some south, southeast and south-westerly paleoflow directions. This indicates that the volcanic (and/or granitic) source terrane was nearby, probably to the southwest.

Résumé

Six sections stratigraphiques bien découvertes qui représentent les formations de Mall Bay et de Drook du groupe précambrien (hadrynien) de Conception ont été étudiées dans la région de la baie Sainte-Marie dans la presqu'île Avalon, à Terre-Neuve.

Ces sédiments siliceux-clastiques à grains surtout fins contiennent des couches peu épaisses (5 à 15 cm) de turbidites classiques qui forment des cycles au sein desquels la granulométrie devient plus grossière vers le haut. On y trouve quelques chenaux peu importants. Ces indications laissent croire que la sédimentation s'est produite en direction du bassin sur la surface intérieure du cône dans un milieu de sédimentation formé par un cône de turbidité. Plus particulièrement, les séquences de faciès observées correspondraient à la sédimentation dans un lobe, dans une région interlobaire, en marge d'un lobe, en marge d'un cône et dans une plaine de bassin. Il se peut également que des courants de densité aient mis en place et remanié une partie des sédiments.

L'analyse des paléocourants, déterminés suite à l'étude des structures de remplissages, les rides, de la texture et de la structure des grès dans les sections minces, indique que l'écoulement principal se faisait vers le nord-est, bien que certains paléocourants se déplaçaient vers le sud, le sud-est et le sud-ouest. Le terrain volcanique, granitique ou les deux, source des sédiments, se situait donc à peu de distance, vraisemblablement au sud-ouest.

INTRODUCTION

This paper discusses detailed sedimentology, including paleocurrent and basin analysis, of the Hadrynian Mall Bay and Drook formations (as defined by Williams and King, 1979) within the lowermost Conception Group, Avalon Zone, Newfoundland. Five well exposed, coastal stratigraphic sections in the western part of the Trepassey map area (Fig. 30.1) were measured. Despite inaccessibility, which precluded detailed measurement, thickness estimates and interpretation were still attempted for a sixth outcrop at Frapeau Point. Previous study of the Conception Group sediments of the southern Avalon Peninsula (Fig. 30.2) has been limited to regional field mapping (Koh, 1969; Misra, 1969a; Williams and King, 1979). The till-like (mixtite) Gaskiers Formation (Gravenor, 1980) and Precambrian fossils of the Mistaken Point Formation (Anderson and Misra, 1968) within the Conception Group have received further attention for the purposes of regional and intercontinental correlation (King, 1982).

Some reconnaissance study of the Conception Group has been done on the northern Avalon Peninsula (Rose, 1952; Hutchinson, 1953; McCartney, 1967). Evidence from the present study, however, indicates that there are lithological sedimentological and stratigraphical differences between sediments of the Conception Group in the south compared to northern equivalents.

General geology

The Conception Group consists of Hadrynian siliciclastics of predominantly volcanic provenance, which have been folded into broad, northeast-southwest-trending, gently plunging anticlinoria and synclinoria. North of the study area these sediments conformably overlie volcanics of the Harbour Main Group with some local disconformity (e.g. basal conglomerate at Turks Gut near Marysvale, Conception Bay) (Williams and King, 1979). In the southern Avalon Peninsula, however, the base of the group is not exposed; in addition, the Mall Bay Formation, which has no recognized equivalent strata to the north or east, is present. The till-like (mixtite) Gaskiers Formation has tentatively been correlated (King, 1982, p. 58) with similar lithologies in the northern Avalon Peninsula (e.g. at Portugal Cove, Bacon Cove and east of Pouch Cove). However, this correlation is uncertain because the mixtite outcrops in the northern Avalon Peninsula cannot be traced directly into those in the south within the study area. The 3 to 5 km thickness of the Conception Group is conformably

[1] Department of Earth Sciences, Memorial University of Newfoundland, St. John's, Newfoundland A1B 3X5

overlain by the St. John's (about 2000 m) and Signal Hill (about 1500 m) groups. The preliminary depositional setting for these two overlying groups involves upward transition from deltaic sedimentation into alluvial facies (Williams and King, 1979).

SEDIMENTOLOGY

Mall Bay Formation

This name was proposed by Williams and King (1979) for all strata (about 800 m) underlying the Gaskiers Formation mixtites. The lowermost parts of the formation are best exposed at the lighthouse at Pt. La Haye, with continuous exposure upward to the contact with the base of the Gaskiers Formation.

Facies MB-1: thin-bedded sandstone/argillite

This facies consists of grey to buff coloured, medium- to fine-grained volcanic litharenites and quartzose sandstones interbedded with argillite. It is predominantly thin-bedded (1-10 cm), displaying subtle graded bedding and parallel lamination with abundant solemarks (toolmarks) and asymmetrical current ripples. This facies is dominated by Bouma BCE sequences in beds which thicken and typically coarsen upward in cycles up to 3 m thick. Bouma ABCE sequences are present in the thicker beds. Beds are laterally continuous over distances of 0.8 km.

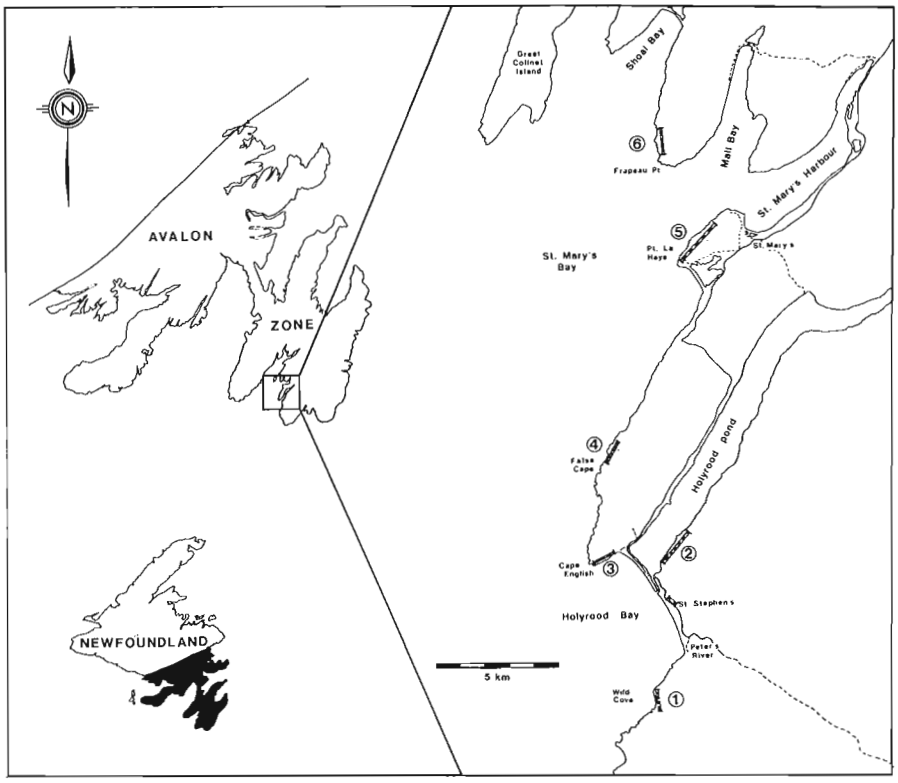

Figure 30.1. *Location map of the six outcrops studied. A seventh outcrop at St. Stevens was examined but not measured.*

Solemarks and ripples indicate flow in a southwesterly direction. In addition, oriented samples were collected in the relatively coarser (fine- to medium-grained) sandstone beds for grain fabric measurement. Stewart (1982) concluded that fabric analysis in the Conception Group is a valuable tool in determining paleoflow directions.

Facies MB-2: argillite

Parallel laminated, green to brown silty argillites with abundant current ripples and rare climbing ripples comprise this facies. Flow directions are dominantly toward the south and southeast. Unique to this facies at Pt. La Haye, are thin (1-15 cm), quartzose, very fine grained sandstones with lateral pinchouts into the adjacent argillites. These winnowed, well sorted beds exhibit scoured bases with 1 to 4 cm argillite clasts, parallel lamination and rare climbing ripples.

Facies MB-3: rippled siltstone-argillite

This facies is composed of lenticular and wavy bedded argillites exhibiting linguoid and straight-crested asymmetrical current ripples on bedding surfaces. Rare climbing ripples are also present. All ripples indicate a prevalent easterly direction of flow. No sole marks were evident. Some small (1-3 cm wide) clastic dykes were also observed. This facies gradually coarsens upward into facies MB-4 (thick-bedded massive sandstone), fine- to medium-grained, thick-bedded (0.5 to 2.0 m), massive,

ERA	GROUP	THICKNESS(m)	FORMATIONS
Precambrian (Hadrynian)	Signal Hill	~1500	Cape Ballard Ferryland Head Gibbett Hill Cappahayden
	St. John's	~2000	Renews Head Fermeuse Trepassey
	Conception	~4000	Mistaken Pt. Briscal Drook Gaskiers Mall Bay
	Harbour Main	~1500	

Figure 30.2. *Precambrian stratigraphy of the Avalon Peninsula in and around the study area.*

quartzose, sandstones with minor local channelling. Rare multiple grading, and solemarks are present within the thicker beds of facies MB-4. Facies MB-1 and MB-2 comprise the lowermost part of the Mall Bay Formation. The middle and uppermost parts of the formation (facies MB-3 and MB-4) are best exposed at False Cape (Fig. 30.1) although they are also found northeast of Pt. La Haye along the coast toward St. Mary's.

With the absence of major channels, the thin-bedded, laterally continuous nature of facies MB-1 and MB-2, combined with the fine grain size, Bouma sequences and small coarsening upward cycles, suggests a fan fringe or basin plain setting within a turbidite fan depositional environment. The minor coarsening upward cycles are the products of progradation of the distal portion of fans. Based on the criteria of Stow and Lovell (1979), the winnowed, well sorted, scoured, discontinuous sand beds found within the argillites of facies MB-2 may be the products of reworking and redeposition by contour currents. Further petrography and paleocurrent analysis using fabric in thin sections will help to determine if these deposits are indeed contourites.

The thick-bedded, massive, and multiple graded sandstones of facies MB-4 are interpreted to represent deposition on the smooth and partially channelled portion of suprafan lobes in the mid fan depositional setting. The lenticular and wavy bedded argillites of facies MB-3 may represent interlobe muds which are periodically influenced by weak currents relict from the main turbidity flows. Further evidence of this process is the presence of the climbing ripples, which suggest a sediment supply rather than exclusively sediment reworking. Stow and Lovell (1979) suggested that a continuum exists between dilute turbidity currents, bottom currents and hemipelagic settling. Therefore, these fine grained sediments may also be affected by contour currents.

Drook Formation

Williams and King (1979) modified the earlier stratigraphic nomenclature and Misra (1969a) to define this, the thickest (approximately 1500 m) and most extensive formation within the Conception Group. The cherty, siliceous siltstones and argillites of the Drook Formation are characteristic of much of the Conception Group throughout the Avalon Peninsula (Williams and King, 1979, p. 4).

Within the study area the Drook Formation is best exposed and accessible at Holyrood Pond, Frapeau Point, Wild Cove, and, to a lesser degree at Cape English (Fig. 30.1). Excellent exposures also occur in cliffs at Peter's River and north of Cape English toward False Cape, but rugged shorelines and rough seas precluded detailed study.

Facies D-1: medium-bedded graded sandstone

This facies consists largely of grey to olive green, medium bedded (10-50 cm), fine- to medium-grained sandstones with abundant solemarks including toolmarks, groove casts and flutes. Consistent northeasterly flow directions predominate at Holyrood Pond. At Cape English, paleocurrent indicators show flow to the west and southwest with some easterly flow directions. Convolute laminae horizons up to 15 cm, parallel lamination and grading are common. Rare dish structures and loaded ripples are present. Some local channelling (Holyrood Pond) and multi-layer slide folds (Cape English) are present. Excellent development of ball and pillow structures is unique to the section at Cape English.

Facies D-2: argillite

This facies is similar to argillites of facies MB-2 within the Mall Bay Formation. Green, brown, and purple colour, parallel lamination, grading and asymmetrical ripples characterize this facies. The base of individual beds is rarely exposed. However, when exposed, grooves indicate flow in a northeast-southwest trend.

Facies D-3: thick-bedded graded sandstone

Thick (1-4 m), massive, coarse grained sandstones exhibiting Bouma AE sequences, multiple grading, scouring and large (long axes up to 0.5 m) shale clasts comprise this facies. Spectacular large scale (0.1-1.0 m) convolute laminated horizons are common. No channelling is present. Complex multiple slides and fine grained conglomerate characterize a small outcrop at St. Stephen's.

We tentatively interpret the Drook Formation as lobe (facies D-3) and lobe fringe (facies D-1) deposits with periods of interlobe sedimentation recorded by the argillites of facies D-2. The coarsening upward cycles may represent gradual lobe progradation with abrupt fan switching leading to abandonment and subsequent deposition of fines by dilute turbidity currents.

DISCUSSION

The interpretation of the Mall Bay and Drook formations as turbidite fan deposits must be consistent with depositional environment of the intervening Gaskiers Formation. Gravenor (1980) determined that the mixtites of the Gaskiers Formation were deposited by debris flows involving sediments of glacial origin which were initially deposited on the shelf before downslope transport. The presence of the tillite at the top of the overall coarsening-upward cycle within the Mall Bay Formation implies a gradual progradation of shelf and slope glacial debris over turbidites at the base of a slope. This regressive sequence is indicative of a gradual sea level lowering in the late Proterozoic as suggested by Anderson (1972) and Anderson and Bruckner (1971). The abrupt change to deeper water sedimentation of the Drook Formation suggests a rapid rise in sea level due to deglaciation, followed by progradation of lobes in a fan environment. This interpretation is also in agreement with that of Hiscott (1981) for the deep water sediments of the late Proterozoic Rock Harbour Group which is thought to be, in part, correlative with the lower Conception Group.

Only the Mall Bay Formation at Pt. La Haye and False Cape yielded sufficient paleocurrent data to allow evaluation of stratigraphic variations in paleoflow within the Conception Group. Correlation between separate outcrop locations of the Drook Formation is not possible. However, the flow directions of certain facies, beds or outcrops in both the Mall Bay and Drook formations remain useful for regional interpretation in this part of the Avalon Zone, particularly in light of the consistency of the directions obtained.

Petrologic study of Conception Group sandstones will undoubtedly enhance our understanding of provenance, depositional mechanism (through fabric study), and perhaps depositional environment (i.e. with respect to sorting, roundness and maturity of sediment).

The tectonic setting during sedimentation of the Conception Group and for the entire Avalon Zone in Newfoundland is uncertain. Present tectonic models range from island arc (Hughes and Bruckner, 1971, 1972; Hatcher, 1972; Rast et al., 1976) to subduction and Basin and Range type rifting (Papezik, 1970; Nixon and Papezik, 1979; Schenk, 1971; Strong et al., 1974) to continental extension and rifting (Rankin, 1975). The age dates of 600 to 700 Ma for these rocks (Anderson, 1972) and others in the Avalon Zone are difficult to reconcile in terms of an island arc or subduction model related to the Appalachian Orogen, because Iapetus did not close until Late Ordovician-Silurian time (Williams and King, 1979). It appears that the late Precambrian rocks of the Avalon Zone were derived from a Precambrian cycle that preceded, and was unrelated to, the

opening and evolution of the Early Paleozoic proto-Atlantic (Williams and King, 1979). At this stage, this much can be said; based on preliminary paleocurrent analysis, petrology, and thickness of the sedimentary pile, it seems that these sediments were deposited in a relatively small arc-related basin associated with volcanic terranes which were proximal to the fan depocenters. Detailed paleogeography of the basin will be determined following a synthesis of data which is not yet available.

ACKNOWLEDGMENTS

This study constitutes a M.Sc. project of the first author under supervision of the second. Partial funding of this project by Texaco Canada Resources Ltd., an EMR Research Agreement and an NSERC operating grant to the second author are gratefully acknowledged. An NSERC postgraduate scholarship to the first author defrayed personal expenses. The authors also acknowledge Ewan Cumming for his able field assistance and Mrs. Elizabeth Power and family for their hospitality. Transportation to coastal outcrops provided by Mike St. Croix and Wayne Dobbin is appreciated.

REFERENCES

Anderson, M.M.
1972: A possible time span for the Late Precambrian of the Avalon Peninsula, southeast Newfoundland in light of fossils, tillites and rock units within the succession; Canadian Journal of Earth Sciences, v. 9, p. 1710-1726.

Anderson, M.M. and Bruckner, W.D.
1971: Late Precambrian glacial deposits in southeastern Newfoundland – a preliminary note; Geological Association of Canada Proceedings, A Newfoundland Decade, v. 24, no. 1, p. 95-102.

Anderson, M.M. and Misra, S.B.
1968: Fossils found in the Precambrian Conception Group of southeastern Newfoundland; Nature, v. 220, p. 680-681.

Gravenor, C.P.
1980: Heavy minerals and sedimentological studies on the glaciogenic Late Precambrian Gaskiers Formation of Newfoundland; Canadian Journal of Earth Sciences, v. 17, p. 1331-1341.

Hatcher, R.D.
1972: Developmental model for the Southern Appalachians; Geological Society of America Bulletin, v. 83, p. 2735-2760.

Hiscott, R.N.
1981: Stratigraphy and sedimentology of the Late Proterozoic Rock Harbour Group, Flat Islands, Placentia Bay, Newfoundland Avalon Zone; Canadian Journal of Earth Sciences, v. 18, p. 495-508.

Hughes, C.J. and Bruckner, W.D.
1971: Late Precambrian rocks of eastern Avalon Peninsula, Newfoundland – a volcanic island complex; Canadian Journal of Earth Sciences, v. 8, p. 899-915.

1972: Late Precambrian rocks of eastern Avalon Peninsula, Newfoundland – a volcanic island complex: Reply; Canadian Journal of Earth Sciences, v. 9, p. 1059-1060.

Hutchinson, R.D.
1953: Geology of the Harbour Grace map area, Newfoundland; Geological Survey of Canada, Memoir 275, 43 p.

King, A.F.
1982: Guidebook for Avalon and Meguma Zones, The Caledonide Orogen; International Geological Correlation Project 27, NATO Advanced Study Institute, 308 p.

Koh, S.
1969: Geology of the Trepassey Area, Avalon Peninsula, Newfoundland; M.Sc. thesis, Memorial University of Newfoundland, Geology Department, 143 p.

McCartney, W.D.
1967: Whitbourne Map Area, Newfoundland; Geological Survey of Canada, Memoir 341, 135 p.

Misra, S.B.
1969a: Geology of the Biscay Bay – Cape Race Area, Avalon Peninsula, Newfoundland; M.Sc. thesis, Memorial University of Newfoundland, Geology Department, 139 p.

1969b: Late Precambrian (?) fossils from southeastern Newfoundland; Geological Society of America Bulletin, v. 82, p. 979-988.

Nixon, G.T. and Papezik, V.S.
1979: Late Precambrian ash-flow tuffs and associated rocks of the Harbour Main Group near Colliers, eastern Newfoundland: chemistry and magmatic affinities; Canadian Journal of Earth Sciences, v. 16, p. 167-181.

Papezik, V.S.
1970: Petrochemistry of volcanic rocks of the Harbour Main Group, Avalon Peninsula, Newfoundland; Canadian Journal of Earth Sciences, v. 7, p. 1485-1498.

Rankin, D.W.
1975: The continental margin of eastern North America in the Southern Appalachians: the opening and closing of the proto-Atlantic Ocean; American Journal of Sciences, v. 275, p. 298-336.

Rast, N., O'Brian, B.H., and Wardle, R.J.
1976: Relationships between Precambrian and Lower Paleozoic rocks of the "Avalon Platform" in New Brunswick, the Northeast Appalachians and the British Isles; Tectonophysics, v. 30, p. 315-338.

Rose, E.R.
1952: Torbay Map Area, Newfoundland; Geological Survey of Canada, Memoir 265, 64 p.

Schenk, P.E.
1971: Southeastern Atlantic Canada, northwestern Africa and continental drift; Canadian Journal of Earth Sciences, v. 8, p. 1218-1251.

Stewart, J.
1982: Evaluation of sandstone fabric as a paleocurrent indicator, Late Precambrian Conception Group, Avalon Peninsula, southeastern Newfoundland; Honours B.Sc. thesis, Memorial University of Newfoundland, Geology Department, 74 p.

Stow, D.A.V. and Lowell, J.P.B.
1979: Contourities: their recognition in modern and ancient sediments; Earth Science Reviews, v. 14, p. 251-291.

Strong, D.F., Dickson, W.L., O'Driscoll, C.F., Kean, B.F., and Stevens, R.K.
1974: Geochemical evidence for eastward Appalachian subduction in Newfoundland; Nature, v. 248, p. 37-39.

Williams, H. and King, A.F.
1979: Trepassey Map Area, Newfoundland; Geological Survey of Canada, Memoir 389, 24 p.

31. GEOLOGY OF THE EARLY PROTEROZOIC ROCKS IN PARTS OF THE LEITH PENINSULA MAP AREA, DISTRICT OF MACKENZIE

Project 820009

R.S. Hildebrand, I.R. Annesley[1], M.V. Bardoux[2], W.J. Davis[3], D. Heon[3], I.G. Reichenbach[4], and T. Van Nostrand[5]
Precambrian Geology Division

Hildebrand, R.S., Annesley, I.R., Bardoux, M.V., Davis, W.J., Heon, D., Reichenbach, I.G., and Van Nostrand, T., Geology of the early Proterozoic rocks in parts of the Leith Peninsula map area, District of Mackenzie; in Current Research, Part A, Geological Survey of Canada, Paper 84-1A, p. 217-221, 1984.

Abstract

On southern Leith Ridge a variety of deformed and undeformed granitoid intrusions cut deformed sillimanite-melt-bearing paragneisses. In the Hottah Lake-Fishtrap Lake area rocks of the Hottah Terrane are mostly cordierite-bearing paragneisses intruded by foliated plutons. The plutons are unconformably overlain by sedimentary and volcanic rocks of the MacTavish Supergroup and the supracrustal section was intruded by plutons of the Great Bear Batholith.

Résumé

Dans la partie sud de la créte Leith, une gamme d'instrusions granitoides déformées et non déformées traversent des paragneiss à sillimanite déformés. Dans la région des lac Hottah et Fishtrap, les roches du terrain de Hottah comprennent surtout des paragneiss à cordiérite coupés par des plutons feuilletés. Ces plutons reposent en discordance sous des roches sédimentaires et volcaniques du supergroupe de MacTavish; les plutons du batholite de Great Bear ont fait intrusion dans la section supérieure de la croûte.

INTRODUCTION

This paper reports the results of the second field season of a three-year project to map the early Proterozoic rocks of the Leith Peninsula (86 D) and Rivière Grandin (86 E) map areas in order to identify and characterize rocks of the Hottah Terrane, the poorest known of the tectonic zones of Wopmay Orogen. During the 1983 field season mapping of the Leith Peninsula map sheet was completed at 1:50 000 scale and 1:16 000 scale in selected areas. Earlier work in the area includes that of Kidd (1936), McGlynn (1976), Hildebrand (1983), and Hildebrand et al. (1983).

Acknowledgments

We thank Winifred Bowler (DIAND) and Martin Irving (GSC) for their expediting; Larry Zurloff (Latham Island Airways Ltd.) and Simon Hanmer for stimulating discussions.

GEOLOGY OF SOUTHERN LEITH RIDGE

The oldest rocks of the southern Leith Ridge area (Fig. 31.1) are metasediments of the Holly Lake metamorphic suite. They are intimately intruded by numerous small deformed and undeformed igneous bodies ranging in composition from alkali feldspar granite to gabbro. Larger plutons of deformed biotite syenogranite, little deformed to undeformed porphyritic biotite granite, and undeformed muscovite-biotite granite also occur in the mapped area.

Metasedimentary rocks of the Holly Lake metamorphic suite (Hildebrand et al., 1983) are mostly sillimanite migmatites which have a well developed foliation, and locally, a moderately developed lineation. The migmatites are typically well-banded rocks comprising layers rich in quartz-sillimanite and others containing dominantly quartz, feldspars, and micas. Most layers have an average thickness of about one centimetre. In many places, especially near younger fault zones, the rocks contain abundant chlorite, but elsewhere relatively fresh biotite and muscovite are the dominant micaceous minerals. Small (1-5 cm long) melt pods, some of which contain tiny garnets, occur throughout the northern half of the area but are absent in outcrops to the south. Locally, there are fist to football size spherical to lozenge-shaped bodies, probably boudins, of muscovite and/or sillimanite-garnet rocks included within the gneisses. Foliation within the gneisses trends near north or slightly north of west, but on a small scale is tightly to isoclinally folded about steeply plunging axes. A steeply dipping mineral lineation is locally well developed.

Myriads of pre-, syn-, and post-tectonic igneous bodies of too small a size to show on the map intrude the gneisses. They include gabbro, quartz diorite, diorite, granodiorite, quartz-feldspar porphyries, medium grained granite, pegmatite, aplite, and alkali feldspar granite. Age relationships between many of the small intrusions are complicated by multiple intrusive events and superimposed shearing and boudinage.

The oldest are probably gabbros which occur as boudins within the metasedimentary gneisses. The gabbros are fine- to medium-grained homogeneous rocks of variable strain states. Generally, the finer grained varieties have the strongest penetrative fabric, typically a foliation and weakly developed lineation. Many of the coarser grained gabbros have deformed marginal zones and minerals within a few centimetres of the contacts define a weak foliation.

Fine- to medium-grained equigranular alkali feldspar granite occurs mostly as irregular bodies up to 15 m across. Biotite is the dominant mafic mineral and makes up to 10% of the rock. Most bodies appear undeformed but some have a weak planar alignment of biotite flakes.

Dykes, sills, and podiform bodies of pegmatite up to a metre across are very common. Most are parallel to, or slightly oblique to, the fabric of the metasedimentary rocks. Many are sheared.

[1] Department of Geology, Ottawa University, Ottawa, Ontario
[2] Department of Geological Sciences, Queen's University, Kingston, Ontario K7L 3N6
[3] Department of Geological Sciences, McGill University, Montreal, Quebec
[4] Department of Geology and Geophysics, University of Connecticut, Storrs, Connecticut 06268, U.S.A.
[5] Department of Earth Sciences, Memorial University of Newfoundland, St. John's, Newfoundland A1B 3X5

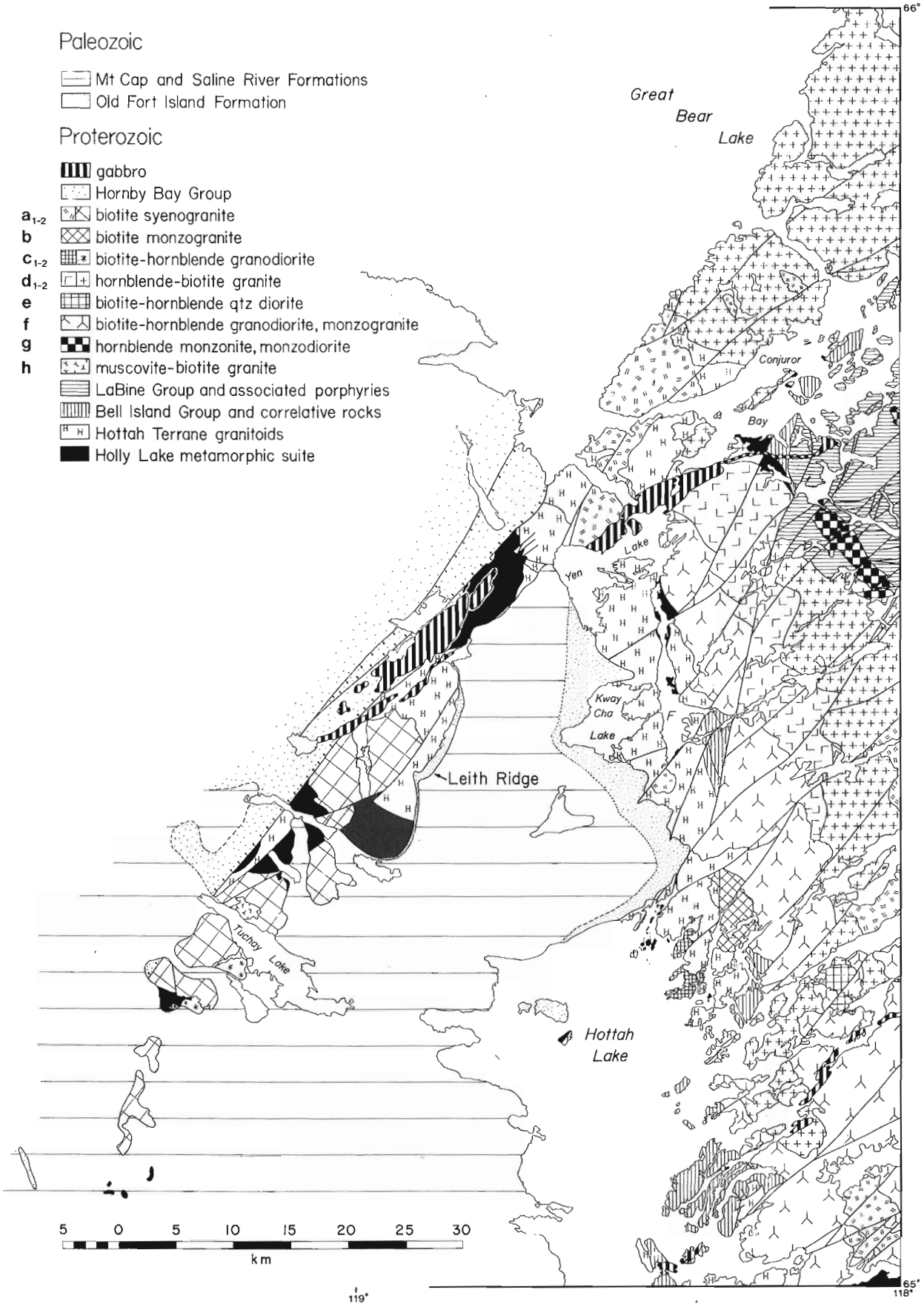

Figure 31.1. *Generalized geological map of the Leith Peninsula map area. F = Fishtrap Lake.*

Irregular intrusions of fine grained quartz diorite and diorite typically have a strong penetrative fabric defined by flattened quartz and aligned mafic minerals. Enclaves of metasedimentary rocks are especially abundant and in many places the country rocks are cut by numerous veins of quartz diorite.

Fine- to medium-grained biotite granodiorite intrusions range from small dykes or sills to larger bodies several hundred metres across. They exhibit a wide range of strain states: the larger intrusions generally do not have a penetrative fabric, while the smaller bodies are commonly foliated. Biotite and flattened quartz define the foliation which is more intense near the margins of many deformed intrusions.

Quartz-plagioclase porphyries too small to show on the map are not common but do occur throughout the area. They form semiconcordant bodies, or sheets, that have a well developed lineation defined by stretched phenocrysts.

Deformed coarse grained porphyritic biotite syenogranite identical to that mapped on the northern part of Leith Ridge in 1982 (Hildebrand et al., 1983), occurs southwest of Holly Lake and in a few scattered outcrops at the southern end of the ridge. The granite is typically an L/S tectonite with a planar element defined by biotite and a lineation defined by stretched potassium feldspar megacrysts.

The most common rock type on Leith Ridge is potassium feldspar porphyritic biotite granite (unit a_2). Its age relations with respect to rocks of the Great Bear Magmatic Zone are unknown. The granite contains 10-30% potassium feldspar phenocrysts up to 5 cm long enclosed in a fine- to medium-grained groundmass of quartz, plagioclase, alkali feldspar, and biotite. The more porphyritic phases are syenogranite, while the less porphyritic phases are monzogranite. Biotite, commonly forming clots to 1 cm, constitutes up to 10% of the rock. A few local zones contain a per cent or two of muscovite. In many places around Tuchay Lake the potassium feldspar phenocrysts define a weak lineation. The orientation is variable but trends from 090 to 150 predominate.

Sheets up to 10 m thick of fine grained biotite granite intrude the porphyritic granites north of Tuchay Lake. Local pegmatites contain books of muscovite 2-3 cm across.

South of Tuchay Lake, porphyritic granite is intruded by a medium grained muscovite-biotite granite (unit h) containing sparse tabular potassium feldspar phenocrysts to 3 cm. The sharp irregular contact abruptly truncates the lineation of phenocrysts in the older porphyritic granite, and dips shallowly toward the porphyritic granite. Numerous dykes and sills of the muscovite-bearing granite cut the porphyritic granite adjacent to the contact.

The muscovite-bearing intrusion is itself cut by a fine grained equigranular biotite granodiorite (unit c_2). The contact is razor sharp, very irregular in detail, and dips variably from 45° northward to nearly vertical. Locally the granodiorite contains potassium feldspar phenocrysts adjacent to the contact, probably plucked from the muscovite-bearing intrusions. A large number of angular to rounded enclaves of the muscovite-biotite granite also occur within 10 m of the contact.

On the north side of Tuchay Lake a biotite-muscovite to muscovite-biotite syenogranite (unit h) intrudes porphyritic biotite granite and cuts abruptly across the trend of lineated potassium feldspar phenocrysts. The contact is sharp. This intrusion contains sparse tabular phenocrysts of potassium feldspar.

All of the above rocks are cut by numerous faults of variable orientations. Faults showing the largest separation are usually northeast-trending. The fault zones contain brecciated, crushed, and altered fragments of the country rocks engulfed in quartz stockworks. The fault zones are cut by east-trending diabase dykes that are probably part of the Cleaver Diabase swarm (Hoffman, 1982; Hildebrand, 1982, 1983).

HOTTAH AND FISHTRAP LAKES AREA

The oldest rocks of this area are probably paragneisses of the Holly Lake metamorphic suite. They occur intermittently in a north-trending band from northern Fishtrap Lake southward to islands in the northern part of Hottah Lake. The metamorphic rocks are intruded by a suite of plutons, all of which are deformed to some degree. Rocks of the MacTavish Supergroup unconformably overlie the deformed plutons and are in turn cut by undeformed plutons of the Great Bear Batholith. Northeast-trending gabbro sheets intrude all of the above rocks.

Holly Lake metamorphic suite

Rocks of the Holly Lake metamorphic suite in the Fishtrap-Hottah Lakes area are generally well layered and almost everywhere strike about north and dip close to vertical. Layers are mostly quartzofeldspathic alternating with layers rich in cordierite porphyroblasts (~2 cm). The layers range in thickness up to 0.3 m but locally minor amphibolite bands are up to 1 m thick. The southeasternmost exposures of metasedimentary rocks in the northern Hottah Lake area are stretched pebble conglomerates containing quartz, mafic volcanic, and siliceous porphyritic pebbles in a medium grained sandy matrix. As the conglomerate occurs on islands surrounded by islands of granitic rocks, their relationship to the layered paragneisses is unknown.

The paragneisses have three well developed foliations. The oldest is a steeply-dipping, northeast-trending cleavage that appears to predate the growth of cordierite porphyroblasts. The second, and by far the most dominant, is a north-south, layer parallel fabric that is also steeply dipping. The third fabric defined by flattened porphyroblasts of cordierite trends northwest, also dips steeply, and is only locally well developed. This fabric may be an axial plane cleavage related to small scale folds of layering.

In some areas the metamorphic rocks are intruded by granitoid bodies up to 2 m thick that are generally concordant with the layering. They range up to 2 m thick and intrusions have a north-south penetrative fabric defined by flattened quartz and aligned biotites. Locally, near contacts of Hottah Terrane granitoid plutons, thin veins of granitic material are intruded along the traces of the first and second fabrics.

Hottah Terrane granitoid rocks

The oldest granitoid rock of the area is medium- to coarse-grained porphyritic biotite granite. It occurs on islands in northern Hottah Lake and its relationship to the paragneisses was never seen. The granite is generally an L/S tectonite with potassium feldspar megacrysts up to 4 cm long defining the lineation and about 10% aligned biotite flakes. Xenoliths of this rock occur in most of the younger Hottah Terrane plutons. On a few islands in northern Hottah Lake the deformed porphyritic granite occurs as xenoliths within a fine grained hornblende diorite which itself occurs as xenoliths within slightly foliated granodiorite. Outcrops of the diorite other than as xenoliths were not found.

The remainder of the granitoid rocks of the Hottah Terrane in the Hottah Lake area are mostly plutons of biotite-hornblende granodiorite, quartz diorite and tonalite that occur on islands too small to show on Figure 31.1. They generally have a north-south foliation.

In the Fishtrap Lake area a composite pluton of biotite monzogranite-granodiorite cuts rocks of the Holly Lake metamorphic suite and is probably a Hottah Terrane pluton. The pluton is medium- to coarse-grained, with the monzo granite being potassium feldspar porphyritic. Biotite, occurring in clots up to 1 cm across, is the sole ferromagnesiam mineral seen in hand specimen. The contact between monzogranite and granodiorite is gradational over several metres. The pluton is generally only weakly deformed except where cut by ductile shear zones up to 1 m wide. The relationship of this pluton to others of the Hottah Terrane at Hottah Lake is unknown due to transcurrent faults and Paleozoic cover.

MacTavish Supergroup (Bell Island Group)

Coarse grained to granular arkose that unconformably overlies rocks of the Hottah Terrane is the oldest stratigraphic unit of the Great Bear Magmatic Zone. Locally, a breccia containing angular blocks of quartz to 15 cm in a sandy matrix occurs just above the unconformity. The arkose is generally well-bedded, with common trough laminations defined by heavy mineral bands. Paleocurrents are mostly toward the west-southwest. The unit fines upward to medium grained arkosic sandstone. In places there are 2 m thick beds of volcanogenic sandstone. Only one complete section of the arkose (30 m thick) occurs in the area.

A 25 m thick siliceous lava flow occurs locally above the arkose. It is red weathering, aphyric, and has zones of autoclastic breccia at its top. Two amygdaloidal basalt flows overlie the siliceous lava. They have well developed flow top breccias and are intercalated with minor basaltic breccias of probable pyroclastic origin.

The lava flows are overlain by 20-40 m of ashstone, siltstone and sandstone. Beds range in thickness from 1-10 cm. The lower part of the section contains calcareous lenticles, concretions and beds which weather recessively, giving the rock a ribbed appearance on the outcrop. Most sedimentary rocks above the lava flows are metamorphosed, probably to albite-epidote assemblages, adjacent to a gabbro sill that intrudes the middle of the section.

At least 1 km of pillow basalts, pillow breccias, and silicified sedimentary rocks cut by gabbro sills overlies the sedimentary-volcanic section. The top of the pillow basalt pile is truncated by younger plutons of the Great Bear Batholith and therefore its original thickness in this area is unknown.

The entire sedimentary-volcanic sequence is similar to that found to the south and described by Hildebrand et al. (1983). The sections mapped during the past season are all northeast-facing monoclines that are part of the west limb of a large syncline, located to the southwest on Bell Island, and separated from it along right-lateral transcurrent faults. Total separation across the faults is about 30 km.

Great Bear Batholith

A pluton of massive, fine- to medium-grained, biotite-hornblende granodiorite (unit c_1) intrudes granitoid rocks of the Hottah Terrane on islands in Hottah Lake. Its age relationships with respect to other plutons of the Great Bear Batholith are unknown because the pluton only intrudes rocks of the Hottah Terrane. Since it is completely undeformed and very fresh in appearance it is considered to be of Great Bear age. The rock is distinctive in that it contains up to 10% prisms of hornblende up to 0.5 cm long and approximately 1% euhedral crystals of brown sphene. Biotite makes up to 5% of the rock. In many places near the contact well developed intrusion breccias containing foliated country rocks are surrounded by thin veins of granodiorite. Most blocks of country rock, which range up to 5 m across, are angular and show evidence of rotation. The granodiorite typically weathers white, but adjacent to joints is altered to pale red. Muscovite-bearing monzogranodiorite-granodiorite occurs on a few islands in the central parts of the pluton. The contacts are not exposed.

The largest pluton of the Great Bear Batholith is a medium grained biotite-hornblende granodiorite (unit f) that extends southward from Yen Lake to just beyond the southern boundary of the map area, a distance of 45 km. The pluton is characterized by euhedral prisms of hornblende up to 1.5 cm long and clots of quartz up to 1 cm across. It is fairly homogeneous in composition but locally there are up to 10% potassium feldspar phenocrysts that shift the modal mineralogy into the monzogranite field.

Other large granitoid plutons (units d_{1-2}) of biotite and hornblende-biotite granites are younger than the granodiorite. They are massive, medium grained rocks that vary from potassium feldspar porphyritic syenogranite to nonporphyritic monzogranite. Contacts between individual plutons are sharp and internal contacts between porphyritic and nonporphyritic phases are gradational. Mafic content varies from about 10 to 15%.

A small pluton of biotite-hornblende quartz diorite (unit e) intrudes both the large granodiorite and a syenogranite east of the north end of Hottah Lake. It cuts across the contact of the two larger plutons. The body is fine grained, slightly plagioclase porphyritic, and contains abundant enclaves of the two older granitoid plutons. The contact is very irregular in detail.

Another small pluton of medium grained, biotite monzogranite (unit b) intrudes granitoid rocks of the Hottah Terrane and the granodiorite at the northeast end of Hottah Lake. The pluton is medium grained and potassium feldspar porphyritic. The phenocrysts range up to 2 cm long and make up from about 3 to 15% of the rock. The contact is sharp and a fine grained border phase occurs adjacent to it.

TRANSCURRENT FAULTS

The eastern half of the map area is cut by numerous northeast-trending transcurrent faults typical of the rest of the Great Bear Magmatic Zone. They are part of a regional conjugate set that is found throughout Wopmay Orogen (Hoffman, 1982). In the externides of the orogen, slip along the faults can, for the most part, be accounted for purely by rotation of the faults (Hoffman and St-Onge, 1981). That is, the deformation is one of regional pure shear in which each element within the system rotates about a vertical axis away from the direction of principal shortening.

The system of transcurrent faults occurring along the eastern side of Hottah Lake (Fig. 31.1) provides some constraints on the large scale boundary conditions of faulting in the Great Bear Magmatic Zone. Figure 31.2 shows the faults, the unconformity between rocks of the Hottah Terrane and Great Bear Magmatic Zone exposed on the west side of a syncline, and the synclinal axis. Separation of a from b is about 30 km. If the fold axis, which can be used as a piercing point to solve for true displacement continues to plunge northwestward in the more northerly blocks, then the displacement must be even greater than the separation of a from b, for as shown on Figure 31.2b the distance x^1 is even greater than x. There could be a component of dip-slip movement on the faults but consider the relationships along the southernmost fault shown on the diagram. There, the distance from the unconformity to the trace of the fold axis is slightly greater along the north side of the fault than on the south side. This suggests a component of dip-slip movement, north side down, which makes the strike-slip component even larger than that suggested above.

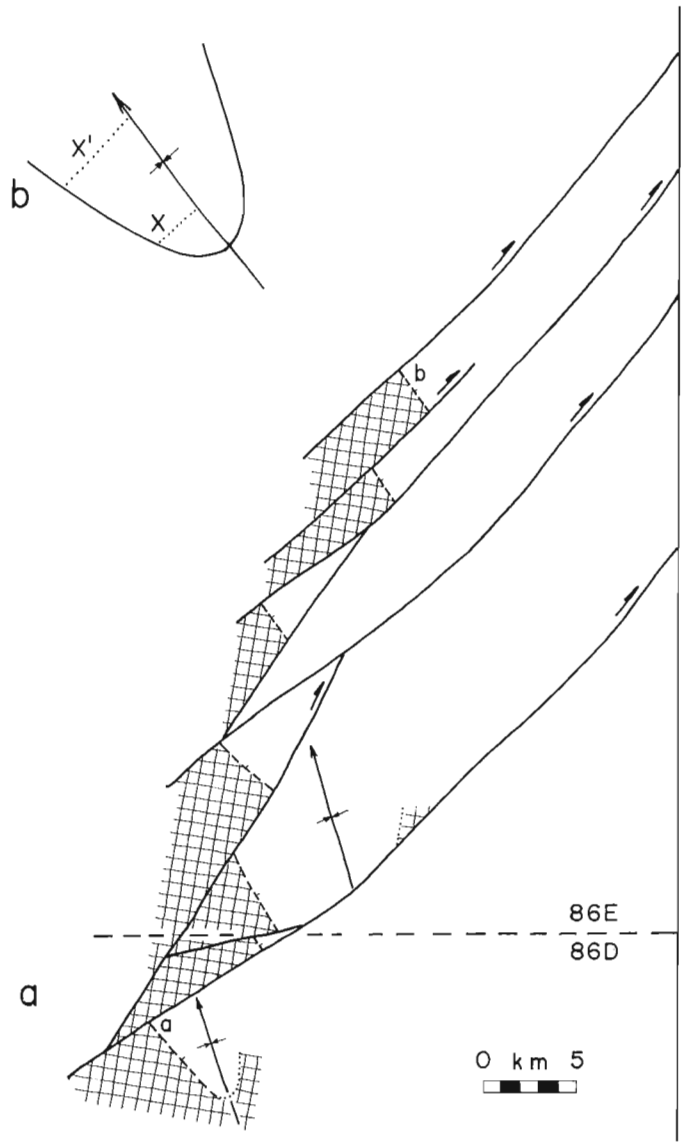

Figure 31.2. *a) Diagram showing transcurrent faults, northeast-dipping unconformity (dashed line) between Hottah Terrane (hatched pattern) and Great Bear Magmatic Zone, and synclinal axis along the east side of Hottah Lake. Separation of the unconformity from a to b is about 30 km. b) Sketch of an unfaulted syncline illustrating that true displacement must be even longer than separation of the fold limb because the distance x^1 is larger than x.*

In order to account for the fault activity within large scale pure shear boundary conditions, a counterclockwise rotation of the faults of about 90° is required. Since the regional direction of maximum shortening was roughly east-west (Hoffman and St-Onge, 1981) this would entail rotation through a principal plane of the finite strain ellipsoid. This being kinematicaly unacceptable, the boundary conditions must have included a component of simple shear and probably the operation of deformation mechanisms other than fault-slip alone.

REFERENCES

Hildebrand, R.S.
1982: Geology of the Echo Bay-MacAlpine Channel area, District of Mackenzie; Geological Survey of Canada, Map 1546A.

1983: Geology of the Camsell River-Conjuror Bay area, early Proterozoic cauldrons, stratovolcanoes, and subvolcanic plutons; Geological Survey of Canada, Paper 83-20.

Hildebrand, R.S., Bowring, S.A., Steer, M.E., and Van Schmus, W.R.
1983: Geology and U-Pb geochronology of parts of the Leith Peninsula and Rivière Grandin map areas, District of Mackenzie; in Current Research, Part A, Geological Survey of Canada, Paper 83-1A, p. 328-341.

Hoffman, P.F.
1982: The northern internides of Wopmay Orogen; Geological Survey of Canada, Open File 882.

Hoffman, P.F. and St-Onge, M.R.
1981: Contemporaneous thrusting and conjugate transcurrent faulting during the second collision in Wopmay Orogen: implications for the subsurface structure of post-orogenic outliers; in Current Research, Part A, Geological Survey of Canada, Paper 81-1A, p. 251-257.

Kidd, D.F.
1936: Rae to Great Bear Lake, Mackenzie District, N.W.T.; Geological Survey of Canada, Memoir 187.

McGlynn, J.C.
1976: Geology of the Calder River (86F) and Leith Peninsula (86E) map areas, District of Mackenzie; in Report of Activities, Part A, Geological Survey of Canada, Paper 76-1A, p. 359-361.

32. AN ESTIMATE, BASED ON MAGNETIC INTERPRETATION, OF THE MINIMUM THICKNESS OF THE HORNBY BAY GROUP, LEITH PENINSULA, DISTRICT OF MACKENZIE

Project 820009

P.H. McGrath[1] and R.S. Hildebrand
Precambrian Geology Division

McGrath, P.H. and Hildebrand, R.S., An estimate, based on magnetic interpretation, of the minimum thickness of the Hornby Bay Group, Leith Peninsula, District of Mackenzie; in Current Research, Part A, Geological Survey of Canada, Paper 84-1A, p. 223-228, 1984.

Abstract

A minimum thickness of 2 km of Hornby Bay Group northwest of Leith Ridge is deduced on the basis of magnetic modelling and upward continuation analyses of aeromagnetic profile data. The analyses are predicated on the assumption that Cleaver Diabase, which produces aeromagnetic anomalies over Great Bear Magmatic Zone and Hottah Terrane, also occurs within the basement beneath the Hornby Bay Group but with a magnetic expression masked by this group. The two analyses confirm the basic similarity of the modelling and upward continuation interpretation techniques.

Résumé

D'après l'établissement de modèles et les analyses de type ascendant de données aéromagnétiques, le groupe de Hornby Bay au nord-ouest de la créte de Leith aurait une épaisseur minimale de 2 km. Les analyses se fondent sur la supposition que la diabase de Cleaver, qui produit des anomalies aéromagnétiques au-dessus de la zone magmatique de Great Bear et du terrain de Hottah, se présente également dans le socle sous le groupe de Hornby Bay, mais que la présence de ce groupe masque son expression magnétique. Les deux analyses confirment la similarité fondamentale des méthodes d'établissement de modèles et d'interprétation de type ascendant.

INTRODUCTION

The aeromagnetic technique has been applied extensively in a reconnaissance role in petroleum exploration to determine distances below survey altitude to the upper surface of anomaly-causing magnetic sources. These distances, minus the survey elevation, often coincide with depths to crystalline basement, and as a result aeromagnetic data are employed to map variations in thickness of the overlying sedimentary section – thickness is used to mean vertical thickness above basement as opposed to stratigraphic thickness. This application of aeromagnetic technology, which is well documented by Nettleton (1976), is possible because the intensity of magnetization of sedimentary rocks is generally much less than that of crystalline rocks.

Aeromagnetic technology was utilized in a Precambrian environment by Steenland and Brod (1960) to map a portion of the Blind River Basin which contains early Proterozoic sediments deposited on an Archean basement. As with Phanerozoic sediments, no magnetic effects were detected related to the early Proterozoic sediments, which are predominantly quartzites and argillites with minor amounts of conglomerate. There are, however, extensive magnetic sources within the sedimentary section caused by basic and diabasic intrusives (Roscoe, 1956). In order to perform the analysis it was necessary to identify and eliminate this type of anomaly before the thickness of the sedimentary sequence could be determined.

In the present case, aeromagnetic anomalies produced by a dyke swarm, called Cleaver Diabase by Hoffman (1982), are used to provide an estimate of the minimum thickness of the Proterozoic Hornby Bay Group in the vicinity of Leith Peninsula at the east end of Great Bear Lake, N.W.T. Unlike the situation in the Blind River Basin where depths of the basin floor were interpreted, only a minimum estimate of thickness is possible, in that no magnetic anomalies attributable to basement are detected over the Hornby Bay Group to the northwest of Leith Ridge, and hence only the minimum thickness required to mask the dyke anomalies can be inferred, greater thicknesses being allowed by the geophysical model. The estimate was obtained using two mathematically similar interpretational procedures applied to aeromagnetic data obtained over the Great Bear Magmatic Zone, and which were digitized along a line perpendicular to the strike of the dyke swarm. One procedure involved modelling the dyke anomalies followed by the calculation of model anomaly curves at increasing altitudes above the model until the modelled dyke anomalies disappeared. In the other procedure the aeromagnetic data were incrementally continued upward until the magnetic anomalies produced by the Cleaver Diabase were lost.

The aeromagnetic data employed for the interpretation were published by the Geological Survey of Canada as Aeromagnetic Maps 8246G, 9090G, 9093G and 9106G. The survey was drape flown with a total-field magnetometer at a mean terrain clearance of 300 m by Geoterrex Limited and Northway Survey Corporation during 1976 and 1977, and the resultant data were published in map form at scales of one inch to one mile and one inch to four miles.

REGIONAL GEOLOGY

Leith Peninsula lies at the southwest corner of Great Bear Lake (Fig. 32.1). The so-called "Leith Ridge" (Balkwill, 1971) is a northeast-trending ridge of early Proterozoic rocks up to 300 m in altitude above the rest of Leith Peninsula, which is underlain mostly by flat-lying Paleozoic sedimentary rocks. The geology of the Leith Ridge has been described by Hildebrand et al. (1983, 1984), and only a brief synopsis is presented here.

The ridge is composed, for the most part, of metasedimentary and intrusive rocks of the Hottah Terrane, one of five tectonic zones of Wopmay Orogen. To the northwest, and east, Hottah Terrane is unconformably underlain by rocks of the Great Bear Magmatic Zone which comprises volcanic and plutonic rocks. Both Hottah Terrane and Great Bear Magmatic Zone were cut by northeast-trending transcurrent faults. Intrusions of Cleaver Diabase postdate the transcurrent faulting and trend about 295°.

[1] Resource Geophysics and Geochemistry Division

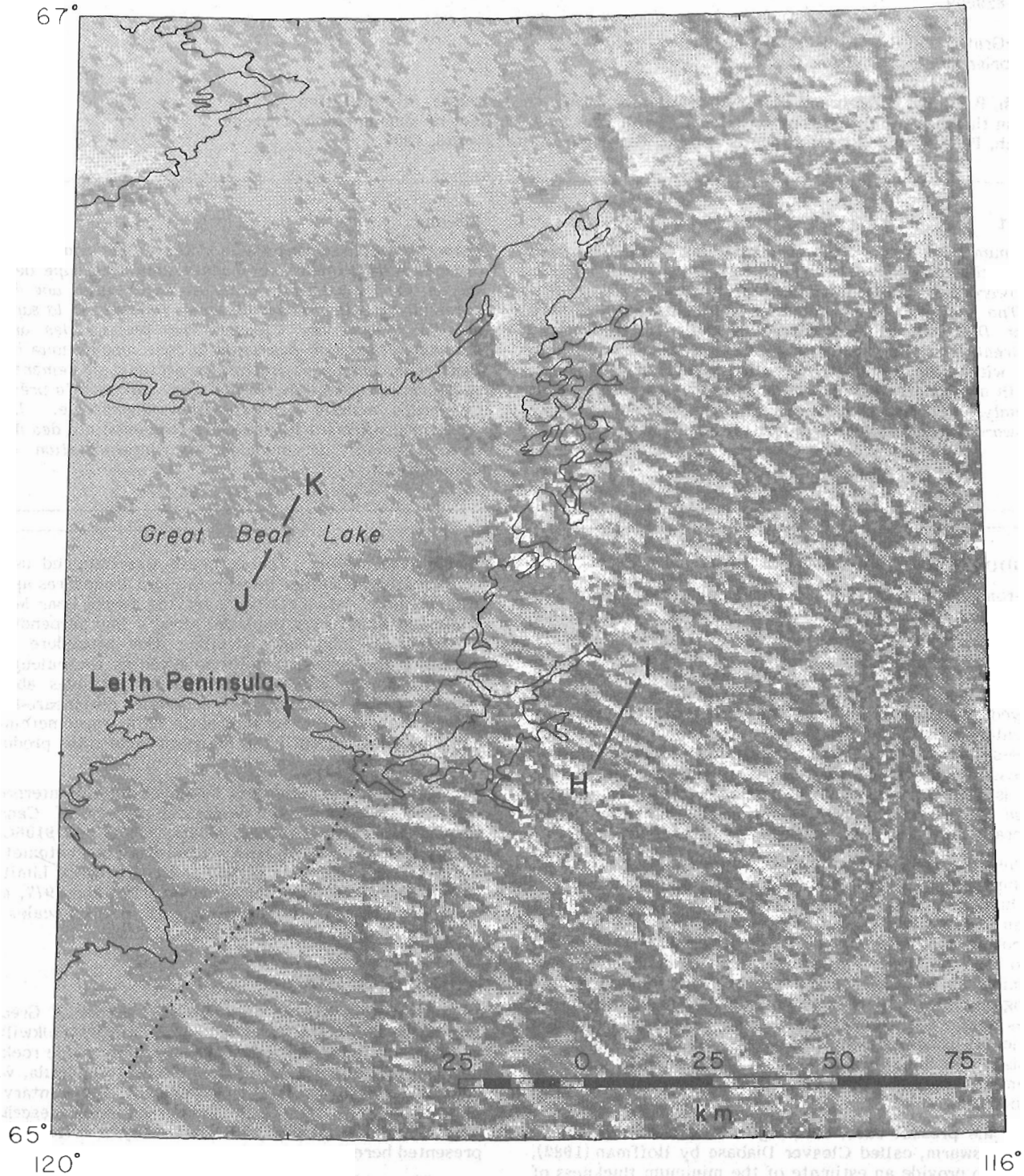

Figure 32.1. *Computer-generated shaded-relief magnetic map of the Leith Peninsula area, District of Mackenzie. The original aeromagnetic data were drape flown at a 300 m terrain clearance along E-W flight lines spaced 800 m apart, and the resultant aeromagnetic maps were digitized at an 812.8 m interval. To enhance the Cleaver Diabase magnetic anomalies, the digitized aeromagnetic data were illuminated using a sun azimuth of 025° and an inclination of 40° above the horizontal. The Cleaver Diabase is represented by the strong linear features which strike 295° and are transected, in part, by line HI. Line HI is situated over Great Bear Magmatic Zone and line JK is along strike of the Cleaver Diabase but over the Hornby Bay Group. The dotted line represents the trace of northeast-trending normal faults bounding the northwest side of Leith Ridge.*

On Leith Ridge (see Fig. 31.1 of Hildebrand et al., 1984) rocks of the Hottah Terrane, cut by Cleaver Diabase, are unconformably overlain by about 30 m of nearly flat-lying Hornby Bay Group. The Hornby Bay Group is capped by thin gabbro sheets that cause no, or only slight, magnetic anomalies. The northwestern side of Leith Ridge is bounded by northeast-trending, northwest-side-down normal faults of post-Hornby Bay Group age which place rocks of the Hornby Bay Group against rocks of the Hottah Terrane. In sections northwest of the faults the sub-Hornby unconformity is never seen. Thus a complete section of Hornby Bay Group is not exposed and its thickness is unknown. Because the unconformity at the base of the Hornby Bay Group has been a target for uranium exploration, and may be so again in the future, it is important to know the thickness of the sedimentary sequence. For example, how deep will exploratory drilling have to go in order to encounter the unconformity and any associated mineralization? The normal faults along the east side of the ridge are part of a much larger set of post-Hornby Bay Group extensional features found along the western and northern margins of Wopmay Orogen (Kerans et al., 1981).

On the aeromagnetic maps Cleaver Diabase dykes have conspicuous magnetic anomalies (Fig. 32.1) trending 295°. The dykes and their associated anomalies are for the most part abruptly truncated by the northeast-trending normal faults bounding the northwest side of Leith Ridge (dotted line, Fig. 32.1).

We do not see the basement to the Hornby Bay Group west of the normal faults. Thus, we have no way of knowing whether or not rocks of the Hottah Terrane or Cleaver Diabase continue west of the fault. For example, a major change in basement type across the faults might be responsible for the disappearance, or change in width, of the dykes. Therefore, this analysis is predicated on the assumption that dykes of Cleaver Diabase cut basement beneath the Hornby Bay Group west of the normal faults. If the dykes do in fact exist beneath the Hornby Bay Group west of the faults, then it could be possible that Hornby Bay weathering has affected their magnetic signature. However, this is not likely to be the cause of the disappearance of the magnetic anomalies because the depth of weathering beneath the Hornby Bay is limited to within 10 or 15 m of the unconformity (Hildebrand et al., 1983), and because Cleaver Diabase dykes found unconformably beneath Hornby Bay Group on Leith Ridge, immediately adjacent to the faults, have associated anomalies. Thus, we consider that the magnetic anomalies disappear because they are cut by the normal faults and now lie beneath sufficient Hornby Bay Group to mask the magnetic signature of the dykes.

THE GEOPHYSICAL PROBLEM

Dykes of Cleaver Diabase produce magnetic anomalies with amplitudes of <10 to 300 nanoteslas (1 gamma = 1 nT). The dyke anomalies, which strike approximately 295°, appear as linear magnetic highs on total-field magnetic anomaly maps. Their presence is obscured somewhat by magnetic anomalies caused by larger geological bodies; hence, in order to enhance the dyke anomalies, a shaded-relief map was generated from a derived set of aeromagnetic data which were digitized at an interval of 812.8 m for the 1 to 1 million Coloured Magnetic Map Series (Teskey et al., 1982). The aeromagnetic data were illuminated artificially with a sun azimuth of 025° and a sum inclination of 40° above the horizon. The shaded-relief method is described by Horn and Bachman (1978), and the appropriate software was provided by D.J. Teskey of the GSC (Dods et al., in press). The resultant data were plotted by an Applicon Colour Plotter and are reproduced in Figure 32.1 in grey tones. In this presentation the Cleaver dyke swarm is represented by the strong linear features which trend 295°.

The line HI in Figure 32.1 is situated over the Great Bear Magmatic Zone, whereas line JK is over rocks of the Hornby Bay Group now buried beneath Great Bear Lake. Aeromagnetic map data along these two lines were digitized at 190 and 380 m intervals respectively, and the regional graident defined by the International Geomagnetic Reference Field, DGRF 1976.5 (IAGA Division 1 Working Group 1, 1981), was subtracted from each profile. The resultant data, minus the mean value of each profile, are illustrated in Figure 32.2. Note the complete lack of identifiable dyke anomalies on line JK as contrasted with line HI. By modelling, and by upward continuation of the data on line HI, the minimum thickness of Hornby Bay strata required to produce a profile similar to JK was calculated.

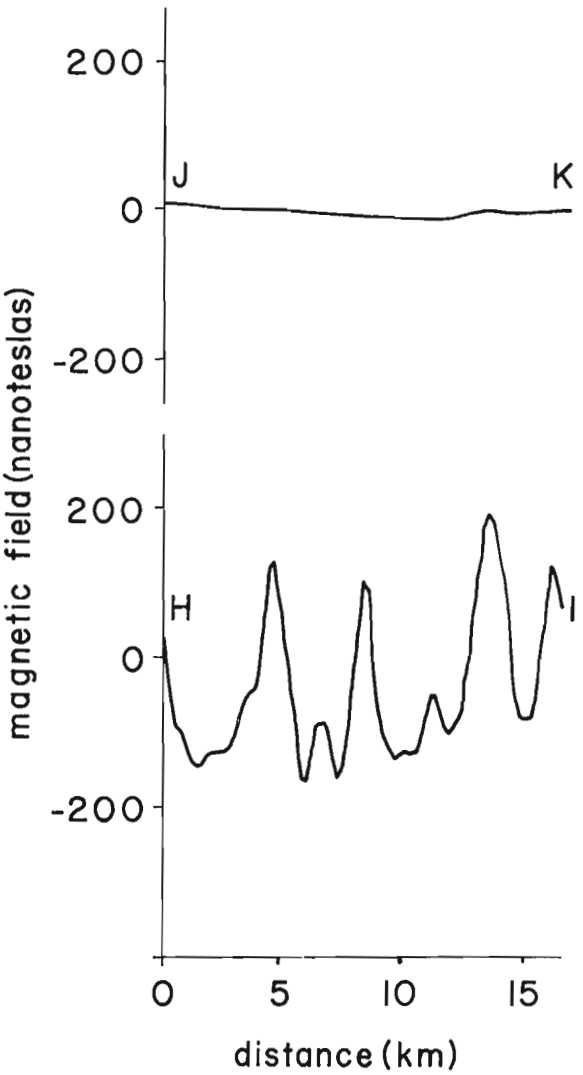

Figure 32.2. Aeromagnetic data along lines HI and JK, which were digitized at 190 and 380 m intervals respectively on one inch to one mile aeromagnetic maps published by the GSC. A regional magnetic field represented by the Definitive Geomagnetic Reference Field for 1976.5 was subtracted from the digitized data, as was the mean value of the resultant data. The spike-like magnetic anomalies along profile HI have amplitudes from 50 to 300 nT, and are related to Cleaver Diabase which cut the Great Bear Magmatic Zone. To the northwest, profile JK is orthogonal to the 295° strike of Cleaver Diabase, and shows the lack of magnetic anomalies over the Hornby Bay Group.

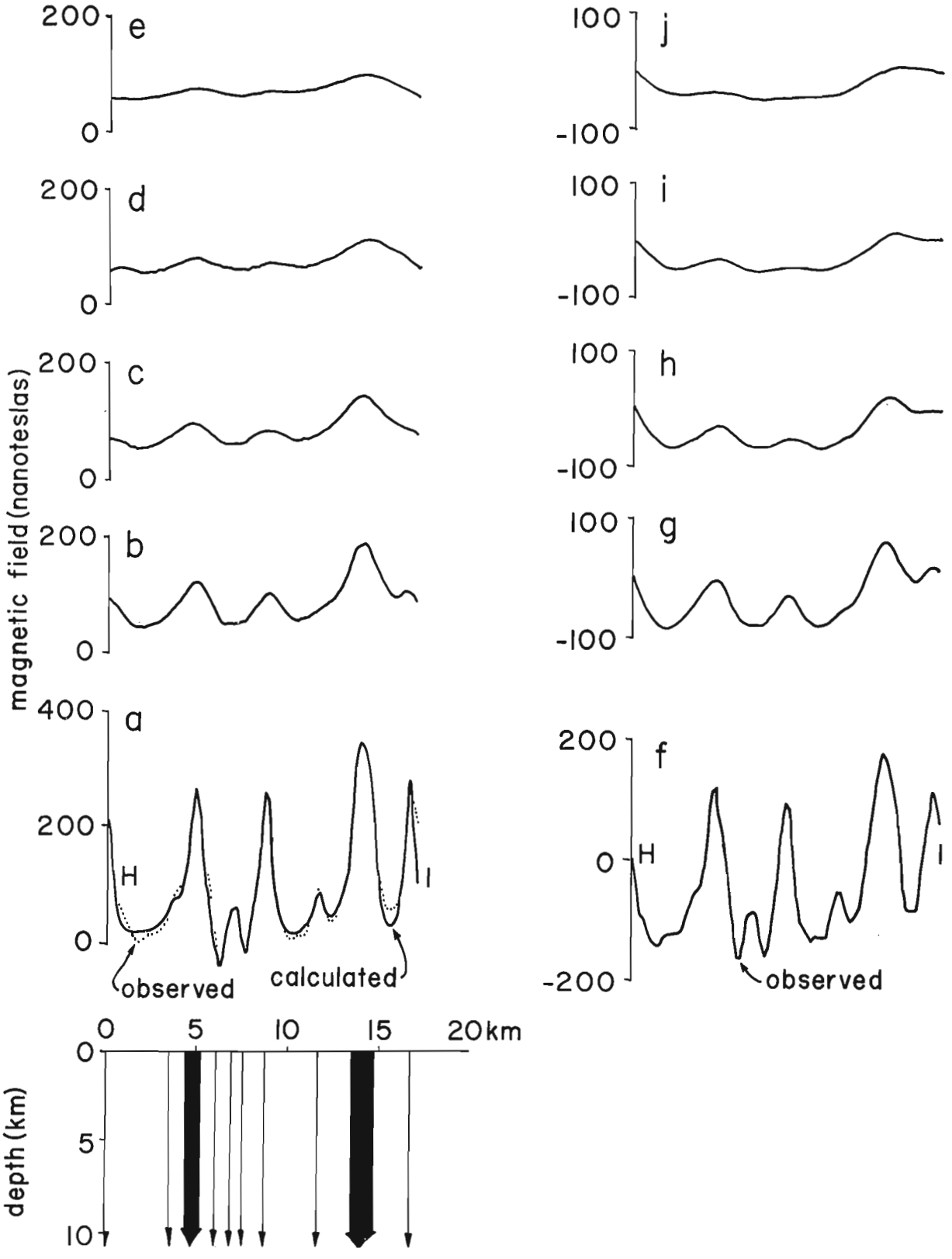

Figure 32.3. *Illustration of the results of modelling on the left, and of upward continuation on the right.*

The digitized observed magnetic profile along line HI is shown as a dotted line in Figure 32.3a and solid line in Figure 32.3f.

The calculated model profile (solid line, Figure 32.3a) was generated for a 300 m elevation from the interpreted model dykes illustrated immediately below Figure 32.3a.

Figures 32.3b-e show the magnetic field at elevations of 1.0, 1.5, 2.0 and 2.5 km above, and generated by, the same model dykes.

Figure 32.3g-j show the upward continued versions of profile 32.3f at elevations of 1.0, 1.5, 2.0, and 2.5 km respectively.

MAGNETIC MODELLING METHOD

The digitized aeromagnetic map data along profile HI (Fig. 32.1, 32.2) were modelled using a procedure described by McGrath et al. (1983). To perform the analysis, it was assumed that the Cleaver Diabase dykes were magnetized uniformly, and that it was necessary to consider only magnetization contrasts between the dykes and the surrounding country rock.

Main geomagnetic field parameters in the Great Bear Lake area were obtained from I, D and F maps of Canada for 1970 published by the Earth Physics Branch. A field declination of 039°, an inclination of 82.5°, and a field intensity of 59700 nT were used in the interpretation.

Ten two-dimensional tabular bodies were used to represent Cleaver Diabase dykes (Fig. 32.3a). No ground control for the dykes along profile HI was available for the interpretation. Hence, the causative bodies were assumed to be vertical, and except for two models, were arbitrarily assigned a thickness of 30 m, which is typical of Cleaver Diabase. Thicknesses of 800 and 1200 m were necessary to model the anomalies situated at 5 and 14 km along profile HI. The greater thicknesses of these two bodies probably reflects zones of two or more closely spaced (< flight elevation) dykes. All of the dykes were assumed to be magnetized by induction, except the two bodies at 6 and 7.5 km, which were assumed to be reversely magnetized because of associated negative anomalies. The intensity of magnetization of the dykes was assumed to be variable. This is not a critical assumption since, neglecting the two thick dyke models, it is only the product of dyke thickness with intensity of magnetization which can be resolved. Excluding the 800 and 1200 m thick bodies, it would be equally valid to assume a constant intensity of magnetization with variable dyke thickness, while using the same thickness-magnetization products of the various models.

A model anomaly profile was calcualted at the flight elevation of 300 m, and is shown in Figure 32.3a by the solid line. A base level adjustment of 180 nanoteslas was added to the aeromagnetic data (dotted line, Fig. 3a) in order to bring the original observed data along profile HI (Fig. 2) into agreement with the calculated profile in a least squares sense.

Figures 32.3b, c, d and e illustrate derived anomaly profiles at elevations of 1.0, 1.5, 2.0, and 2.5 km above ground level respectively, which were generated from the same model data used to calculate the model data shown in Figure 32.3a. In comparing these profiles with the observed profile JK (Fig. 32.2), it would appear that at least 2 km of Hornby Bay Group would be required to mask the Cleaver Diabase aeromagnetic anomalies. In this analysis we have assumed that the dykes are of large vertical extent (>1.5 km from a mathematical viewpoint). Given dykes of limited depth extent would result in a more rapid decay in the amplitudes of the calculated anomaly profile with increasing elevation than is shown in Figure 32.3b-e. However, this would seem to be an unlikely scenario.

In applying the modelling technique the possible contribution of remanent magnetization has been ignored. Measurements of remanent intensities by Strangway (1965) for Archean dykes in Ontario and Quebec indicate that remanent magnetization can make a significant contribution to the shape of the resultant magnetic anomaly. However Gay (1963) showed that the depth of a thin dyke may be determined independently from its direction of magnetization, and hence also independently of anomaly shape changes resulting from remanence effects. It is unlikely therefore that remanent magnetization would play a significant role in the present analysis other than for the two reversely magnetized models.

UPWARD CONTINUATION METHOD

The transformation of the magnetic field into what the field would be at another elevation is rather easily achieved in the spectral frequency domain (Gunn, 1975). By taking the Fourier transform of the magnetic field, the frequency domain representation of the field is obtained. Multiplying the various Fourier coefficients by $e^{2\pi h (u^2 + v^2)^{\frac{1}{2}}}$ and performing an inverse Fourier transform on the modified coefficients yields the magnetic field which would exist at level h above or below the original observed field – h is negative for upward continuation and u and v are spatial frequencies.

In the present application it is assumed that the field was produced by two-dimensional sources which strike perpendicular to the profile HI (Fig. 32.1, 32.2, 32.3a, f). In order to obtain a better estimate of the spectral content of profile HI, the profile was arbitrarily extended by twelve points at each end of the profile using the Burg prediction operator (Anderson, 1974), and further extended to a total length of 2000 points with zeros (Henry and Graefe, 1971). The Fourier transform of the extended profile and the subsequent inverse Fourier transform of the modified Fourier coefficients were obtained using the discrete fast Fourier transform computer software provided by Grenner (1968) which is based on the method of Cooley and Tukey (1965). The Fourier coefficients were multiplied by $e^{2\pi hu}$, since v = 0 in this case. The resultant profiles at elevations of 1.0, 1.5, 2.0, and 2.5 km above ground level are illustrated in Figure 32.3g, h, i, and j respectively. Again in comparing these results with profile JK (Fig. 32.2), it would appear that at least 2 km of Hornby Bay Group are required to mask the magnetic anomalies generated by the Cleaver Diabase.

DISCUSSION OF RESULTS

The two estimates of a minimum thickness of 2 km of Hornby Bay Group required to mask the magnetic expression of Cleaver Diabase yielded by the modelling and by the upward continuation techniques are mutually consistent, and confirm the basic similarity of the two interpretation techniques. Conceptually, the modelling method is easier to understand, however, many more assumptions are required in its application. The upward continuation method as applied here only requires that the sources be two-dimensional, and thus it must be considered a more objective method. The central portion of the profiles obtained at a given elevation, using both the modelling and upward continuation techniques, are very similar although significant differences occur within 3 km of either end of the profiles. This end effect probably results from the fact that in applying the discrete fast Fourier transform, frequency components which are longer than the data profile are poorly resolved, hence some problem with the upward continuation method could be anticipated. In all other respects the two methods yield very similar results.

ACKNOWLEDGMENTS

We thank S.D. Dods for his assistance with the gridded aeromagnetic data, D.J. Teskey for providing the computer software used to generate the shaded-relief magnetic map, and P.F. Hoffman and E.J. Schwarz for their constructive comments on the manuscript.

REFERENCES

Anderson, N.O.
1974: On the calculation of filter coefficients for maximum entropy spectral analysis; Geophysics, v. 39, no. 1, p. 69-72.

Balkwill, H.R.
1971: Reconnaissance geology, southern Great Bear Plain, District of Mackenzie; Geological Survey of Canada, Paper 71-11, 47 p.

Brenner, N.
1968: Cooley-Tukey fast Fourier transform – FOURT, IBM Contributed Program Library, 360D-13.4.001.

Cooley, J.W. and Tukey, J.W.
1965: An algorithm for the machine calculation of complex Fourier series; Mathematics of Computation, v. 19, p. 297-301.

Dods, S.D., Teskey, D.J., and Hood, P.J.
– The new 1:1 000 000 magnetic anomaly map series of the Geological Survey of Canada; compilation techniques and interpretation; in Society of Exploration Geophysicists volume "The utilitiy of regional gravity and magnetic anomaly maps". (in press)

Gay, S.P., Jr.
1963: Standard curves for interpretation of magnetic anomalies over long tabular bodies; Geophysics, v. 28, no. 2, p. 161-200.

Gunn, P.J.
1975: Linear transformations of gravity and magnetic fields; Geophysical Prospecting, v. 23, p. 300-312.

Henry, R.F. and Graefe, P.W.U.
1971: Zero padding as a means of improving definition of computed spectra; Manuscript Report Series no. 20, Marine Scinces Branch, published for Environment Canada by Dept. of Energy, Mines and Resources, Ottawa, 10 p.

Hildebrand, R.S., Bowring, S.A., Steer, M.E., and Van Schmus, W.R.
1983: Geology and U-Pb geochronology of parts of the Leith Peninsula and Riviere Grandin map areas, District of Mackenzie; in Current Research, Part A, Geological Survey of Canada, Paper 83-1A, p. 329-342.

Hildebrand, R.S., Annesley, I.R., Bardoux, M.V., Davis, W.J., Heon, D., Reichenbach, I.G., and Van Nostrand, T.
1984: Geology of the early Proterozoic rocks of parts of the Leith Peninsula map area, District of Mackenzie; in Current Research, Part A, Geological Survey of Canada, Paper 84-1A, report 31.

Hoffman, P.F.
1982: The Northern Internides of Wopmay Orogen; Geological Survey of Canda, Open File 882.

Horn, B.K.P. and Bachman, B.L.
1978: Using synthetic images to register real images with surface models; Communications of the association for Computing Machinery, v. 21, no. 11, p. 914-924.

IAGA Divison 1 Working Group 1
1981: International Geomagnetic Reference Fields: DGRF 1965, DGRF 1970, DGRF 1975, IGRF 1980; Eos, American Geophysical Union, Transactions, v. 62, no. 49, p. 1169-1170.

Kerans, C., Ross, G.M., Donaldson, J.A., and Geldsetzer, H.J.
1981: Tectonism and depositional history of the Helikian Hornby Bay and Dismal Lakes groups, District of Mackenzie; in Proterozoic Basins of Canada, ed. F.H.A. Campbell; Geological Survey of Canda, Paper 81-10, p. 157-182.

McGrath, P.H., Henderson, J.B., and Lindia, F.M.
1983: Interpretation of a gravity profile over a contact zone between an Archean granodiorite and the Yellowknife Supergroup using an interactive computer program with partial automatic optimization; in Current Research, Part B, Geological Survey of Canada, Paper 83-1B, p. 189-194.

Nettleton, L.L.
1976: Gravity and Magnetics in Oil Prospecting; McGraw-Hill, Inc., 464 p.

Roscoe, S.M.
1956: Geology and Uranium deposits, Quirke Lake-Elliot Lake, Blind Rvier area, Ontario; Geological Survey of Canada, Paper 56-7.

Steenland, N.C. and Brod, R.J.
1960: Basement mapping with aeromagnetic data – Blind River Basin; Geophysics; v. 25, no. 3, p. 586-601.

Strangway, D.W.
1965: Interpretation of the magnetic anomalies over some Precambrian dykes; Geophysics, v. 30, no. 5, p. 783-796.

Teskey, D.J., Dods, S.D., and Hood, P.J.
1982: Compilation techniques for the 1:1 million magnetic map series; in Current Research, Part A, Geological Survey of Canada, Paper 82-1A, p. 351-358.

33. GOLD, TIN, URANIUM AND OTHER ELEMENTS IN THE PROTEROZOIC NONACHO SEDIMENTS AND ADJACENT BASEMENT ROCKS NEAR MACINNIS LAKE, DISTRICT OF MACKENZIE

Project 760047

Y.T. Maurice
Resource Geophysics and Geochemistry Division

Maurice, Y.T., Gold, tin, uranium and other elements in the Proterozoic Nonacho sediments and adjacent basement rocks near MacInnis Lake, District of Mackenzie; in Current Research, Part A, Geological Survey of Canada, Paper 84-1A, p. 229-238, 1984.

Abstract

Heavy mineral layers in a pink arkose-quartz-rich conglomerate unit of the Nonacho Group contain notable amounts of U, Th, Sn, Nb, Ta and Au. Enrichment in Th, Sn, Nb, Ta and to a lesser extent in U is related to the detrital dispersal and accumulation of thorite-uranothorite, cassiterite and a suspected but undetected Nb-Ta mineral. These minerals probably originated from sources to the west of the Nonacho basin, in the Fort Smith belt. The clastic minerals are consistently enriched in the heavy mineral layers throughout the arkose-conglomerate unit although Sn appears to be more concentrated towards the base of the sedimentary pile. A decline in the concentrations of the various clastic minerals from south to north is also apparent and reflects increasing distance from source.

Hydrothermal enrichment in U and Au is superimposed upon the detrital pattern in the arkose-conglomerate unit. This activity appears to have been confined to the area adjacent to the southeastern shore of MacInnis Lake and is probably related to hydrothermal activity that led to the formation of nearby U-Cu-Au-Ag veins in basement rocks as well as in Nonacho Group sediments. Uranium is believed to have precipitated in the intergranular spaces of heavy mineral layers in the arkose-conglomerate unit as a result of interaction with Ti compounds and/or in response to reducing conditions associated with the presence of magnetite. Gold is more erratically distributed and is not confined to the heavy mineral layers.

Résumé

Des couches de minéraux lourds dans une unité d'arkose rose et de conglomérat quartzifère faisant partie du groupe de Nonacho contiennent des quantités appréciables de U, Th, Sn, Nb, Ta et Au. L'enrichissement en Th, Sn, Nb, Ta et, dans une certaine mesure, en U est relié à une dispersion détritique suivie d'une accumulation de thorite-uranothorite, de cassitérite et d'un minéral de Nb-Ta présumé mais non-identifié. Ces minéraux proviennent probablement de sources à l'ouest du basin de Nonacho, dans la zone de Fort Smith. Les minéraux clastiques sont distribués assez uniformément dans les couches de minéraux lourds à travers l'unité d'arkose et de conglomérat quoique le Sn ait tendance à être plus concentré vers la base de la séquence sédimentaire. On remarque aussi une baisse de la concentration des divers minéraux clastiques du sud vers le nord ce qui reflète une augmentation de la distance les séparant de la source.

Un enrichissement hydrothermal en U et en Au est superposé au patron détritique dans l'unité d'arkose et de conglomérat. Il semblerait que cette activité ait été limitée à une zone adjacente à la rive sud-est du lac MacInnis et elle est probablement reliée à une activité hydrothermale qui est à l'origine de veines d'U-Cu-Au-Ag que l'on retrouve dans les roches du socle ainsi que dans les sédiments du groupe de Nonacho de cette région. On croit que l'U a précipité dans les espaces intergranulaires des couches de minéraux lourds de l'unité d'arkose et de conglomérat à la suite d'une réaction avec des composés de Ti et/ou en réponse aux conditions réductrices reliées à la présence de magnétite. L'Au est distribué moins régulièrement et n'est pas restreint aux couches de minéraux lourds.

INTRODUCTION

The MacInnis Lake area, situated some 240 km southwest of Yellowknife in the Lower Proterozoic Nonacho Basin contains a variety of radioactive and sulphide occurrences. The mineralogy, geochemistry, and geological setting of some of them have been described by Maurice and Plant (1979) and Gandhi and Prassad (1980).

One type of radioactive occurrence was thought to be worthy of further attention because of its high content of Sn (0.2%), Au (2 ppm), and Nb and Ta (300 and 150 ppm respectively), a rather unusual assemblage in the Canadian Shield. These metals are found in paleoplacer-type concentrations in arkosic sandstones and quartz-rich conglomeratic beds at the base of the Nonacho Group. A lithogeochemical study was initiated to: (1) examine the distribution of these elements in the host rocks; (2) investigate the mineralizing processes including a search for possible source rocks; and (3) assess the importance and geological significance of this type of mineralizaion. Concurrently with this work, a sampling program of surficial material was carried out in the region in an attempt to develop a suitable exploration method for this type of deposit. This report, however, presents only the results of the lithogeochemical study.

GEOLOGY

The Nonacho basin has been described by Henderson (1937) as an intermontane basin filled with fresh water clastic sediments. Its total thickness is probably about 12 000 m (L. Aspler, personal communication, 1982). Deposition of the sediments apparently began about 1950 Ma with uplifting of the Fort Smith belt, a north-south oriented expanse, west of the Nonacho basin, dominated by a massive megacrystic granite batholith (Bostock, 1981, 1982).

Gandhi and Prassad (1980) published a geological map of the MacInnis lake area which is reproduced with some modifications (after McGlynn, 1978 and S.S. Gandhi, personal communications, 1981) in Figure 33.1. The oldest rocks in the study area are a variety of gneisses which together with granites and minor amounts of gabbroic rocks

form the basement. These are unconformably overlain by an oligomictic granite boulder conglomerate which represents the basal unit of the Nonacho Group. This unit forms a north-south band east of MacInnis Lake and is approximately 500 m thick. The lower portion is composed of angular fragments, some as large as 50 cm, similar to the granitic basement on which it rests, cemented by an arkosic matrix, largely chloritized. Henderson (1937) observed that the angularity of the fragments and the close packing is such that this conglomerate resembles a crushed or brecciated granite and called it a talus conglomerate. Away from the basement, the clasts gradually become subangular to rounded and there is more variety in the type of clasts although granite remains by far the most abundant.

The granite boulder conglomerate passes upwards (eastwards) into a thick sequence of grey to greenish grey arkose which is the most abundant rock type in the Nonacho basin. Where seen, the contact appears conformable with a 50 m transition zone of interlensed conglomerate and arkose. In the southern part of the Nonacho basin, the grey arkose is separated from the granite boulder conglomerate by a thick unit of polymictic conglomerate not seen in the MacInnis Lake area. The grey arkose and underlying polymictic conglomerate are regarded as predominantly fluvial sediments.

To the west of the granite boulder conglomerate, and in fault contact with it, is a narrow zone of finer grained sediments that extends almost continously from MacInnis Lake to the northeastern tip of the Nonacho basin, a distance

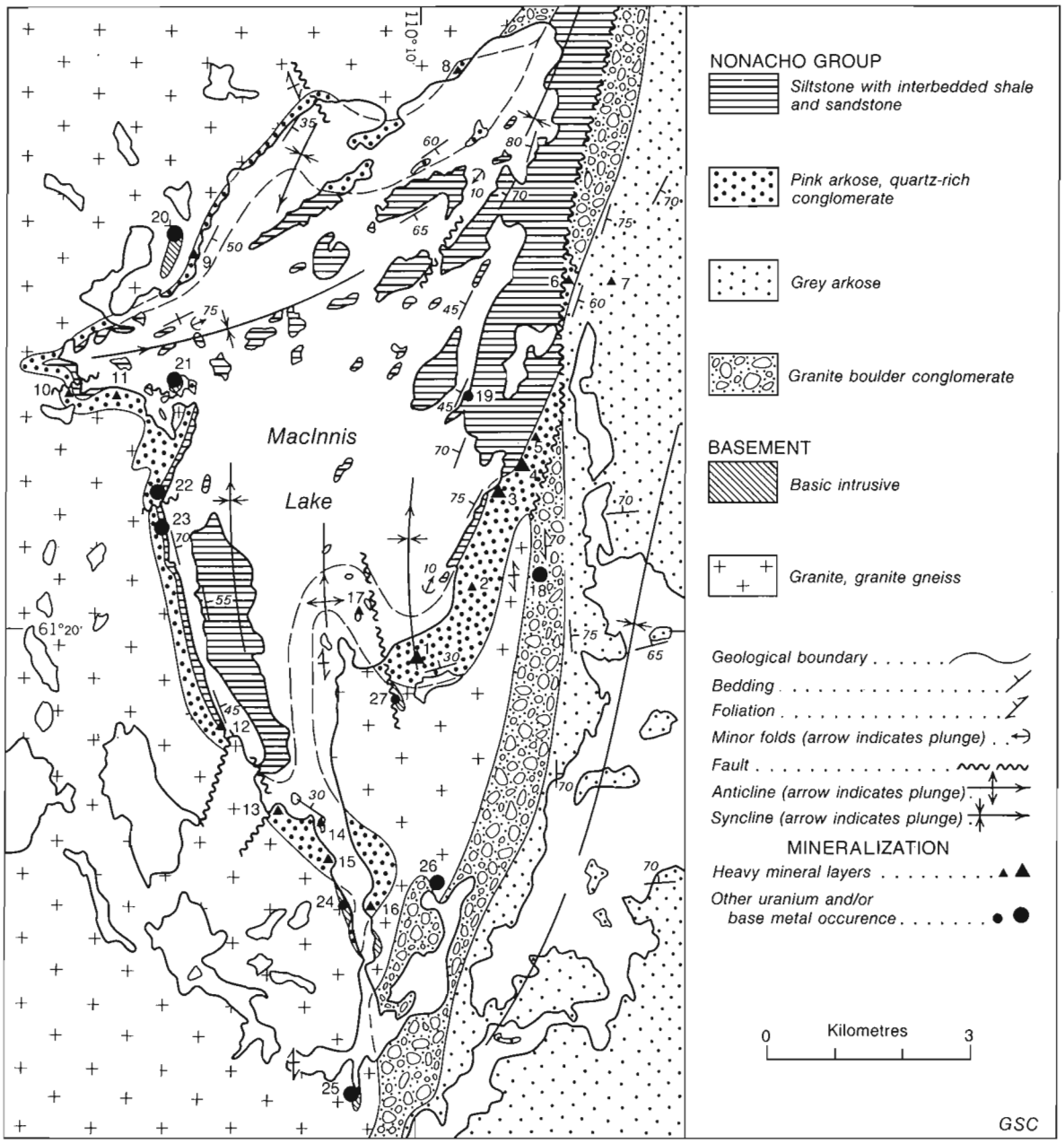

Figure 33.1. *Geology and location of mineral occurrences, MacInnis Lake area (modified from Gandhi and Prassad, 1980 after McGlynn, 1978, and S.S. Gandhi, pers. comm., 1981).*

of over 100 km. L. Aspler (personal communication, 1982) found turbidite facies in these sediments near Nonacho Lake some 50 km north of MacInnis Lake suggesting a relatively deep water depositional environment. In the MacInnis Lake area, he interpreted the fine sediments, mostly thinly bedded dark grey to green and pink siltstones with interbedded fine sandstones and shales as having been deposited by sheet floods flowing into ephemeral ponds. These fine sediments are underlain by interbedded pink arkoses and conglomerates that have an abundance of subrounded to well rounded quartz pebbles cemented by an arkosic matrix. This quartz-rich conglomerate and interbedded pink arkose occur along the rim of MacInnis Lake and together with the overlying fine sediments occupy a synclinal structure that underlies most of the lake basin. The conglomerate-arkose facies has a maximum thickness of 300-400 m near the southeastern shore of the lake but is much thinner (40-50 m) along the western shore. Individual lenses and beds may reach 50 m in thickness and show abundant crossbedding. This unit is not known to occur elsewhere in the Nonacho Basin and could represent a deltaic deposit containing sediments of distinctive provenance. It unconformably overlies basement rocks.

MINERALIZATION

Radioactivity in the quartz-rich conglomerate and interbedded pink arkose near the eastern shore of MacInnis Lake has been known since the late 1950s. Several occurrences were trenched and drilled, but mineralization was found to be discontinuous and tonnage was far too low to be of economic interest. Moffat (1974) reported concentrations of up to 0.24% U_3O_8 and 0.8% Sn in hematite-rich layers that range from 2 to 5 cm in thickness. He did not report the presence of gold nor did he mention elevated Nb and Ta in these layers.

Figure 33.1 shows the location of hematite-rich layers that were sampled in the course of the present study (localities 1 to 17). They all occur within pink arkose except occurrence 7 which is found in the grey arkose that overlies the granite boulder conglomerate. The layers are stratabound, dark grey to black, composed largely of detrital heavy minerals, generally within the buff to pink arkosic sandstone facies but also occasionally in the conglomeratic beds where they become part of the matrix. They range from thin, single grain layers, traceable for a few centimetres, to massive bands, 10 to 15 cm thick, that are continuous over several metres. Generally, individual bands are composed of alternating thin heavy mineral and quartzofeldspathic layers that show delicate sedimentary structures.

The heavy mineral assemblage as seen in thin sections consists of well rounded to subrounded, sand size (0.2-0.5 mm) grains of hematite, cassiterite, zircon, tourmaline, thorite-uranothorite, thorian monazite, and xenotime set in a matrix composed predominantly of sericite and hematite. Native gold was not seen in the thin sections but several flakes of the metal were found in a -100 + 75 µm heavy mineral fraction of a sample from locality 1 (Gandhi and Prassad, 1980).

The detrital hematite grains show relict textures suggesting that they formed by oxidation of original ilmenite and magnetite-chromite grains (Fig. 33.2a, b). Figure 33.2a shows a core of magnetite-chromite at the centre of a rounded hematite grain. Figure 33.2b shows subparallel exsolution of rutile in hematite that probably resulted from oxidation of an original grain of ilmenite.

The hematite in the matrix forms lath-like crystals that tend to mantle the detrital grains. They invariably contain detectable amounts of titanium. The mantling hematite and the micaceous matrix are intergrown and have a poorly developed subparallel lineation at an angle to the bedding (Fig. 33.2c). These characteristics point to a mild metamorphism of the rock.

The earlier study by Maurice and Plant (1979) revealed the presence of an interstitial uranium phase believed to represent over 85% of the total uranium content of the rock. Figure 33.3 shows a section across a specimen of heavy mineral-rich arkose with the corresponding autoradiograph. The detrital U- and Th-bearing minerals appear on the autoradiograph as discrete sources. The interstitial uranium phase produces a poorly defined haze. Note that both the discrete sources and the haze tend to be confined to the hematite-rich layers.

In a backscatter image obtained with a scanning electron microscope (Fig. 33.2b), a uranium mineral appears as tiny bright spots along the periphery of the rounded grains and filling a small fissure in the hematite-rutile grain. This phase was not positively identified but it has a uraninite-pitchblende composition intermixed with Pb. There seems to be a tendency for this uranium mineral to mantle the rutile-hematite grains in preference to the magnetite-chromite-hematite grains. Uranium was not detected by microprobe in the lath-like hematite or the micaceous material in the matrix. However, a fission track image made from a thermal neutron irradiated sample (Fig. 33.4) shows clearly that uranium is dispersed throughout the matrix and fills hairline cracks. Maximum track activity is reached in the vicinity of the opaque iron oxide grains, but activity continues at a lesser intensity into the quartzofeldspathic zone.

No phases containing Nb or Ta were found despite their high content in some samples. These elements could be present in relatively low concentrations in the clastic iron oxide grains. Under the microscope, sulphides were rarely seen in the heavy mineral layers. Small amounts of pyrite, however, were occasionally seen in the matrix near thorite-uranothorite grains and sometimes within the grains themselves (Fig. 33.2d). In outcrop, small amounts of chalcopyrite were found to impregnate the conglomerate in the trenches at locality 3 and pyrite occurs in joints at locality 4. These were the only occurrences of sulphides in the arkosic beds observed by the writer and they do not appear to be related to the concentrations of heavy minerals. Moffat (1974) also reported finely disseminated pyrite in drill core at localities 14 and 17.

The other mineral occurrences in the area, numbered 18 to 27 in Figure 33.1, contain base metals and/or radioactive minerals. Those containing radioactive minerals (all except 19, 24 and 27) have been described by Maurice and Plant (1979) and Gandhi and Prassad (1980). The mineralization occurs in fractures, shear zones, or quartz veins within granitic (26) or basic (20, 21, 25) basement rocks, or Nonacho Group sediments (18, 22, 23). The host rock is generally heavily chloritized and the main radioactive phase is pitchblende. Chalcopyrite, pyrite, calcite, hematite, and in places galena and bornite, are also present in the veins along with a variety of secondary uranium and copper minerals. Gandhi and Prassad (1980) reported up to 2.16 ppm Au and 0.5 ppm Au at localities 18 and 22 respectively.

Occurrences 19, 24, 27 are small, non-radioactive, and were discovered while conducting field work described in this paper. Occurrence 19 consists of small pods of galena in a quartz vein that cuts siltstones with interbedded shales and fine sandstones. Occurrences 24 and 27 both contain disseminated chalcopyrite in a gabbroic sill or flow at or near the contact between the granitic rocks of the basement and the quartz-rich conglomerate of the Nonacho Group.

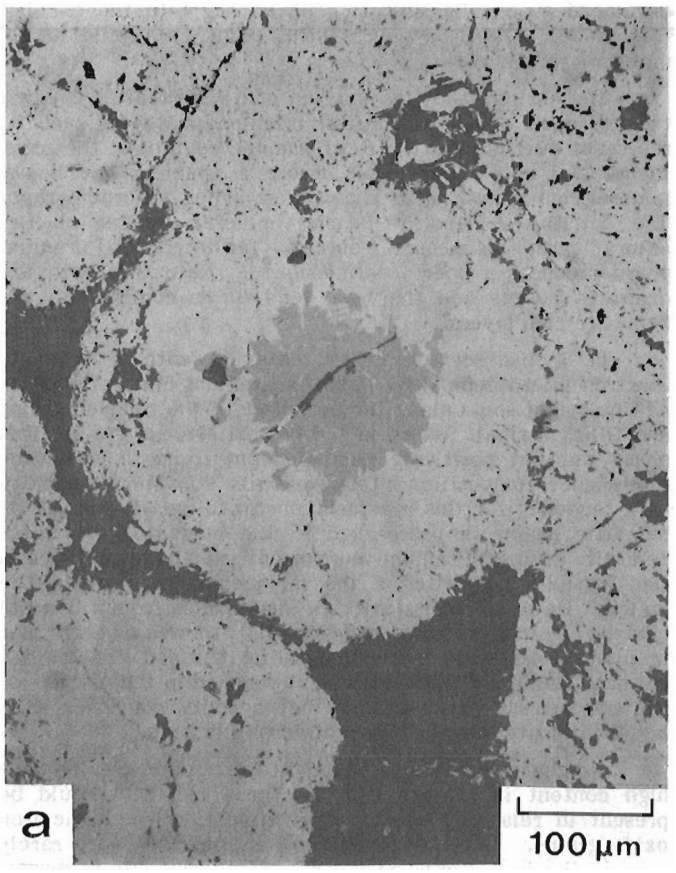
a
100 µm

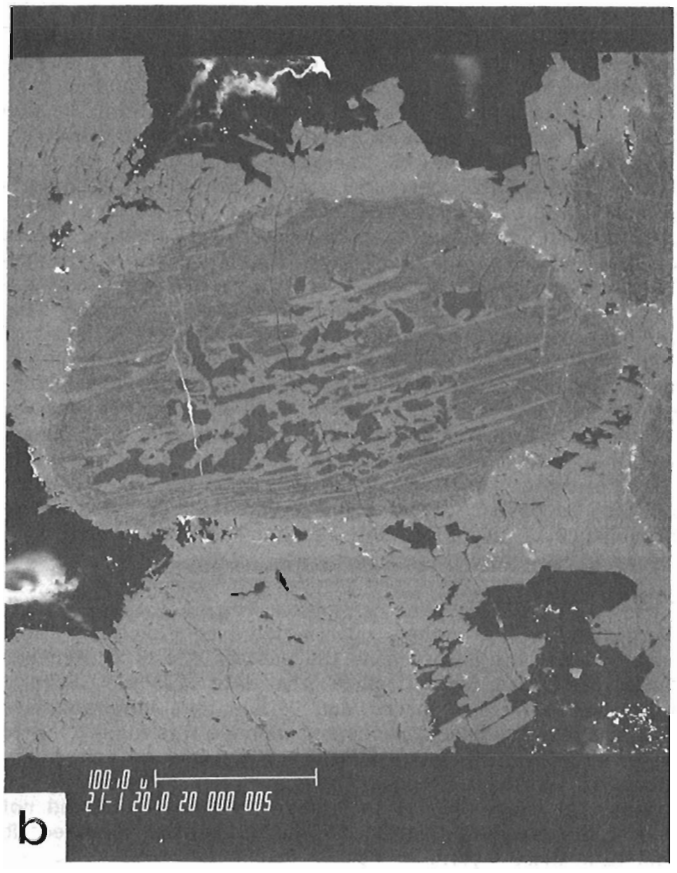
b

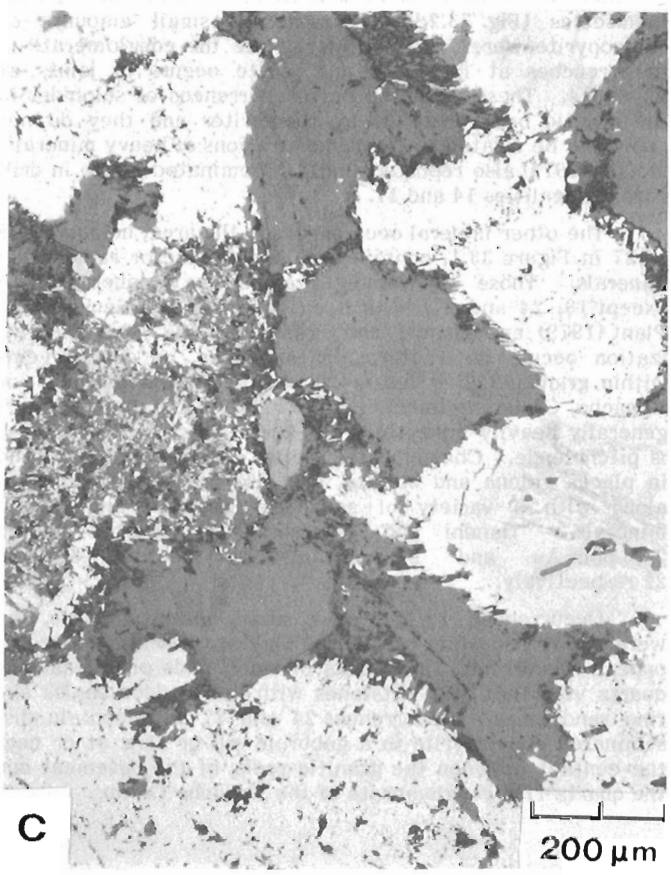
c
200 µm

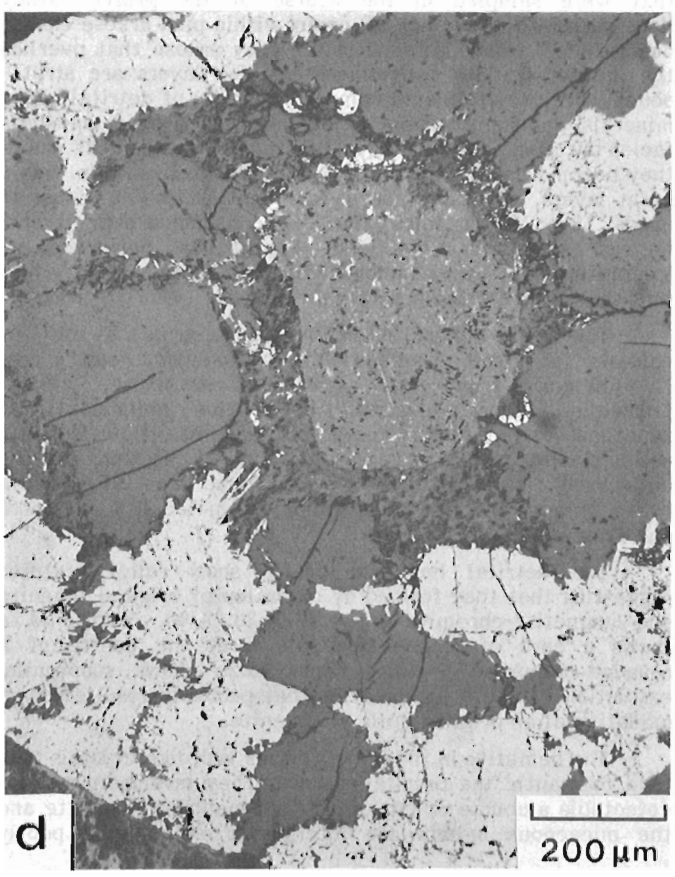
d
200 µm

SAMPLING AND ANALYTICAL PROCEDURES

One or several representative grab samples were collected at each of localities 1 to 27 (Fig. 33.1). Several of these showings had been trenched (large symbols in Fig. 33.1) which greatly facilitated sampling. In addition to sampling the mineralization, several representative samples of the country rock and quartz veins were collected throughout the study area.

The samples were crushed, ball milled and anlayzed for the elements listed in Table 33.1. This table also gives the analytical method, the effective detection limit, the precision at the 95% confidence level, and the concentration levels at which this precision applies. The precision was calculated from replicate analyses of a control sample prepared from a heavy mineral-rich bulk sample taken at locality 1 (Fig. 33.1). This sample contains relatively low concentrations of W and Cu resulting in rather poor precisions for these elements in Table 33.1. At higher concentrations, these precisions would be expected to improve considerably. The gold analyses are considered adequate despite the apparently low precision which is probably due to the difficulty of mixing native gold in samples by conventional grinding and blending techniques.

RESULTS

The concentration of the various elements in the samples containing the heavy mineral layers depends to a large extent upon the actual abundance of heavy minerals in the samples. Because the samples collected contained heavy minerals in variable proportions, a direct comparison of element concentrations in the samples would be rather meaningless. To overcome this problem, comparison will be made, not only between the absolute concentrations of the elements, but also between their ratio to iron. Iron is a good common denominator because it is the principal constituent of the heavy mineral layers and its concentration in the arkose reflects, better than any other element, the abundance of heavy minerals in the rock. Iron concentrations in the arkose vary from about 1% in samples containing no visible heavy mineral concentrations to 40% in samples composed almost exclusively of heavy minerals.

Table 33.1. Analytical methods, detection limits and precision.

Element	U	Th	Nb	Ta	Sn	W	Au	Ag	Cu	Fe
Method	NAA	NAA	XRF	NAA	XRF	Col	NAA*	AA	AA	AA
D. Limit	0.1	1	1	5	1	2	10	0.1	1	0.1
% Precision**	±2	±8	±9	±11	±6	±136	±86	n.a.	±47	±16
at (concentration)	750	400	75	100	1300	7	550	n.a.	5	15

- All concentrations in ppm except Au (ppb) and Fe (%); n.a. = not available
- NAA: neutron activation analyses by X-Ray Assays Laboratories, Thornhill, Ontario; *preconcentration by fire assay (10 gr).
- AA: atomic absorption using air-acetylene flame and HF sample decomposition by Geochemistry Subdivision, Geological Survey of Canada.
- XRF: X-ray fluorescence using compressed disc by Bondar-Clegg & Co. Limited, Ottawa, Ontario.
- Col: Colorimetric using carbonate fusion and zinc dithiol reagent by Geochemistry Subdivision, Geological Survey of Canada.

**precision at 95% confidence level.

Local distribution of metals in heavy mineral layers (Loc. 1, 3, and 4)

Localities 1, 3, and 4 (Fig. 33.1) were selected for a detailed study of metal distribution in heavy mineral-bearing arkose because the trenches provided for easy access to sample material. Table 33.2 gives the concentration of several elements and the corresponding element/Fe ratio in heavy mineral-bearing samples from four trenches at locality 1 and several samples from single trenches at localities 3 and 4. For each of trenches 1, 3, and 4 at locality 1, results are also given for one sample of arkose containing no visible heavy minerals (hereinafter called "pure arkose").

Figure 33.5 represents a north-south cross section through locality 1. Trenches 1 to 3 are shown in the figure; trench 2 is located approximately 60 m west of the section and is stratigraphically between trenches 1 and 3. Trench 4 is located about 60 m east of the section and is stratigraphically below trench 3.

At locality 1, Th, Nb and Ta show element/Fe ratios that are similar from one trench to another (Table 33.2). These ratios also tend to be similar or slightly lower in the heavy mineral-bearing rocks compared to the pure arkose. The Sn/Fe ratio, on the other hand, shows a progressive increase from trench 1 to trench 4 (downwards stratigraphically). It is interesting to note that the Sn/Fe ratio in the pure arkose samples from trenches 3 and 4 tends to reflect the ratio in the heavy mineral-bearing samples from those trenches. In trench 1 however, the Sn/Fe ratio of the pure arkose is significantly higher than the ratio of the heavy mineral-bearing samples from that trench.

The gold content of most samples from locality 1 is low except for one sample from trench 4 which contains 730 ppb Au. Uranium behaves more erratically than the other elements both in its absolute concentration and in its ratio to Fe. Unlike the other elements, the proportion of U to Fe is considerably lower in the pure arkose compared to the heavy mineral-bearing samples in trenches 1, 3, and 4 at locality 1. At localities 3 and 4, U and U/Fe ratio are lower than at locality 1 except for two samples that are unusually rich in U (0.43% and 1.3%). Most of the other elements tend to be more erratic at localities 3 and 4 compared to locality 1 and Au is considerably richer. The samples containing unusually high levels of U are relatively low in Th, Nb, Ta, and Sn in relation to their Fe content but contain near average or above average Au, Ag, and Cu. One sample from locality 3 containing disseminated chalcopyrite (SU, see Table 33.2) also has elevated Au but relatively low U.

***Figure 33.2** (opposite)*

Photomicrographs of heavy mineral layers.

a) Recrystallized round hematite grain, with a core of euhedral chromite (Cr, Fe (Zn)) grading out to magnetite (Fe (Ti, Cr)).

b) Backscatter scanning electron microscope image showing subparallel lamellae of rutile (light grey) in hematite. Tiny white specks of an unidentified U phase are distributed along the detrital grain margins and in a hairline crack in hematite-ilmenite grain.

c) Quartz and orthoclase (dark), small zircon (light grey) and hematite (white) grains in a sericite-hematite matrix. Subparallel latch-like hematite crystals growing into the matrix mantle clastic hematite grains. Grain with intergrowth (centre right) is hematite with patches of rutile and three inclusions of apatite.

d) Large grain of thorite (pitted) containing and surrounded by spotty pyrite. Latch-like hematite is growing from recrystallized hematite grain (light grey). Note radial cracks originating from thorite grain.

Table 33.2. Selected elements and their ratio to iron in heavy mineral layers, localities 1, 3 and 4.

	U ppm	U/Fe$^{x10^4}$	Th ppm	Th/Fe$^{x10^4}$	Nb ppm	Nb/Fe$^{x10^4}$	Ta ppm	Ta/Fe$^{x10^4}$	Sn ppm	Sn/Fe$^{x10^4}$	W ppm	W/Fe$^{x10^4}$	Au ppb	Au/Fe$^{x10^7}$	Ag ppm	Ag/Fe$^{x10^4}$	Cu ppm	Cu/Fe$^{x10^4}$	Fe%
LOC. 1																			
Trench no. 1																			
Pure arkose	25	23	37	34	11	10	5	5	21	19	16	14.5	<10	-	0.1	0.09	2	1.8	1.1
Arkose + HM	31	6	230	45	53	10	22	4	57	11	<2	-	<10	-	0.2	0.04	2	0.4	5.1
Arkose + HM	440	51	280	33	39	5	29	3	111	13	<2	-	<10	-	0.1	0.01	3	0.3	8.6
Arkose + HM	630	68	210	23	50	5	32	3	104	11	<2	-	12	1.3	0.4	0.04	4	0.4	9.2
Arkose + HM	520	39	410	30	68	5	53	4	129	10	2	0.1	13	1.0	0.2	0.01	3	0.2	13.5
Trench no. 2																			
Arkose + HM	41	14	150	52	40	14	14	5	37	13	10	3.4	<10	-	0.2	0.07	2	0.7	2.9
Trench no. 3																			
Pure arkose	7	5	54	39	13	9	6	4	28	20	<2	-	<10	-	<0.1	-	1	0.7	1.4
Arkose + HM	34	10	120	36	37	11	18	5	110	33	<2	-	<10	-	0.1	0.03	2	0.6	3.3
Arkose + HM	280	32	200	23	48	5	34	4	170	19	<2	-	<10	-	0.2	0.02	2	0.2	8.8
Arkose + HM	470	49	260	27	37	4	37	4	179	19	6	0.6	12	1.3	0.1	0.01	3	0.3	9.5
Arkose + HM	400	28	300	21	53	4	46	3	305	21	4	0.3	<10	-	0.2	0.01	2	0.1	14.5
Trench no. 4																			
Pure arkose	7	5	43	33	10	8	9	7	65	50	<2	-	<10	-	0.1	0.08	1	0.8	1.3
Arkose + HM	650	57	300	26	75	7	65	6	546	47	20	1.7	17	1.5	<0.1	-	4	0.3	11.5
Arkose + HM	1400	78	540	30	78	4	130	7	1111	62	4	0.2	12	0.7	0.2	0.01	4	0.2	18.0
Arkose + HM	1400	64	660	30	119	5	190	9	2251	102	6	0.3	730	33	0.2	0.01	5	0.2	22.0
LOC. 3																			
Arkose + SU	16	7	66	29	13	6	9	4	59	26	8	3.5	180	78	0.4	0.17	4100	1783	2.3
Arkose + HM	35	6	40	7	<1	-	6	1	55	10	6	1.1	130	24	0.1	0.02	9	1.7	5.4
Arkose + HM	65	11	540	89	160	26	140	23	967	159	4	0.7	380	62	0.5	0.08	17	2.8	6.1
Arkose + HM	13000	1182	34	3	10	1	10	1	55	5	4	0.4	130	12	1.4	0.13	235	21	11.0
LOC. 4																			
Arkose + HM	9	6	15	11	3	2	5	4	31	22	4	2.9	810	578	0.1	0.07	3	2.1	1.4
Arkose + HM	7	5	62	41	20	13	15	10	120	80	2	1.3	10	7	0.2	0.13	1	0.7	1.5
Arkose + HM	65	36	91	51	17	9	5	3	57	32	2	1.1	56	31	0.2	0.11	2	1.1	1.8
Arkose + HM	13	6	66	30	24	11	8	4	19	9	6	2.7	10	5	0.1	0.05	2	0.9	2.2
Arkose + HM	23	7	160	47	156	46	81	24	744	218	2	0.6	170	50	0.1	0.03	2	0.6	3.4
Arkose + HM	4300	782	12	2	<1	-	<5	-	22	4	2	0.4	280	51	3.3	0.60	13	2.4	5.5
Arkose + HM	66	5	560	47	400	33	230	19	1701	142	12	1.0	340	28	0.4	0.03	5	0.4	12.0

HM = Heavy mineral concentrations SU = Sulphides

Table 33.3. Average element contents and their ratio to iron in heavy mineral layers, localities 2, 5 to 17.

Localities	N	U ppm	U/Fe$^{x10^4}$	Th ppm	Th/Fe$^{x10^4}$	Nb ppm	Nb/Fe$^{x10^4}$	Ta ppm	Ta/Fe$^{x10^4}$	Sn ppm	Sn/Fe$^{x10^4}$	W ppm	W/Fe$^{x10^4}$	Au ppb	Au/Fe$^{x10^7}$	Ag ppm	Ag/Fe$^{x10^4}$	Cu ppm	Cu/Fe$^{x10^4}$	Fe%
2	1	420	13	850	26	200	6	150	5	1285	40	28	0.9	130	4.0	0.1	0.003	6	0.2	32.5
5	1	14	2	270	36	97	13	58	8	517	70	6	0.8	<10	-	<0.1	-	3	0.4	7.4
6	3	51	2	500	22	150	7	76	3	177	8	5	0.2	12	0.5	0.2	0.007	7	0.3	22.6
7	5	17	1	101	8	39	3	8	<1	6	<1	5	0.4	<10	-	0.2	0.013	12	1.0	12.3
8	3	4	1	29	7	7	2	5	1	10	2	2	0.4	<10	-	<0.1	-	5	1.1	4.3
9	1	5	4	44	34	15	12	6	5	20	15	<1	-	49	38	0.1	0.077	3	2.3	1.3
10	1	20	5	210	54	56	14	14	4	11	3	8	2.1	<10	-	<0.1	-	5	1.3	3.9
11	1	5	3	66	35	33	17	18	9	81	43	6	3.2	<10	-	<0.1	-	3	1.6	1.9
12	1	9	4	100	45	28	13	31	14	350	159	<1	-	23	10	0.1	0.045	4	1.8	2.2
13	1	2	1	13	9	<1	-	<5	-	3	2	<1	-	<10	-	<0.1	-	3	2.1	1.4
14	2	33	7	148	30	96	19	46	9	128	26	5	1.0	<10	-	1.3	0.265	2	0.4	5.0
15	1	9	4	110	50	30	14	14	6	85	39	4	1.8	11	5	<0.1	-	6	2.7	2.2
16	1	4	2	45	26	15	9	6	4	27	4	6	3.5	<10	-	<0.1	-	2	1.2	1.7
17	1	33	7	110	24	32	7	14	3	56	12	<1	-	<10	-	0.1	0.022	2	0.4	4.6

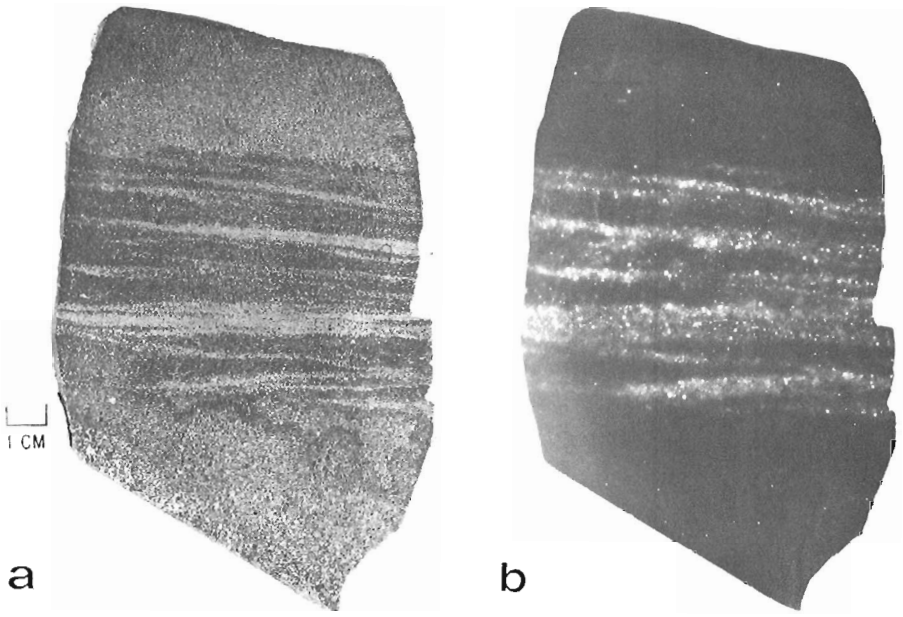

Figure 33.3

Heavy mineral layer in arkose.

a) Polished surface

b) Autoradiograph of (a)

Regional distribution of metals in heavy mineral layers (Loc. 2, 5 to 17)

Table 33.3 gives the average concentrations of the elements and their ratios to Fe in heavy mineral-bearing samples from the other occurrences in the region. All the samples included in Table 33.3 show at least some heavy mineral layering, but judging from the low amount of Fe at some localities, the heavy minerals may not contribute significantly to the overall composition of the rock. The low concentration of Fe in those samples does not necessarily reflect a scarcity of heavy minerals at those localities but is due rather to difficulties experienced in sampling the heavy mineral layers from the massive and glacially rounded outcrops. Nonetheless, some trends are noteworthy.

Except for the sample collected at locality 2, U is low, with concentrations and U/Fe ratios considerably lower than those found at locality 1. Th, Nb, Ta, and Sn on the other hand, produce ratios to Fe that, in a general way, are comparable with those obtained in heavy mineral-bearing samples from localities 1, 3 and 4 (Table 33.2). Note, however, that samples from localities 7 (grey arkoses) and 8 (near the northern end of the lake) contain less Th, Nb, Ta and Sn in relation to their content of Fe than the samples from most of the other occurrences listed in Table 33.3.

With few exceptions (e.g., localities 2 and 9), the Au content at the localities listed in Table 33.3 is close to or below the detection limit of 10 ppb. Also, Ag and Cu were not found to be significantly enriched at any of those localities.

Distribution of metals in vein-type sulphide and/or radioactive occurrences (Loc. 18 to 27)

The results of the analyses for U, Th, Au, Ag, and Cu of radioactive and/or sulphide-bearing samples from localities 18 to 27 (Fig. 33.1) are presented in Table 33.4. The values for Nb, Ta, Sn, and W were close to or below the analytical limit of detection in those samples and are not shown in Table 33.4.

The U/Th ratios from the U-rich samples in Table 33.4 are very high and are compatible with U/Th ratios found in vein-type U deposits generally. In comparison, the heavy mineral layers contain abundant detrital Th-bearing minerals that produce much lower U/Th ratios (see Tables 33.2, 33.3). Note, however, that the very high U samples at localities 3 and 4 (Table 33.2) have U/Th ratios that are comparable with the high ratios in Table 33.4.

Gold and silver were detected in most of the samples included in Table 33.4. The Au content seems to be considerably higher in the occurrences on the east side of MacInnis Lake (Loc. 18, 19, 26). Note also that Au and Ag are present in similar concentrations in the high U samples at localities 3 and 4 and in the chalcopyrite-bearing sample at locality 3 (Table 33.2). The similarities between the geochemistry of some samples from occurrences 3 and 4 and samples from the vein-type occurrences on the east side of MacInnis Lake and their relative proximity to one another suggest that these occurrences were affected by the same mineralizing event. Hydrothermal mineralizing fluids, enriched in Cu, U, Au and Ag, infiltrated the rocks, filling fractures in the granite pebble conglomerates (Loc. 18), the siltstones (Loc. 19) and the basement granites (Loc. 26), and filled intergranular spaces in the pink arkose (Loc. 3, 4). In

Table 33.4. Selected elements in sulphide-bearing occurrences, localities 18 to 27

Loc.	U ppm	Th ppm	Au ppb	Ag ppm	Cu ppm
18	2	9	110	1.6	13000
	760	28	13	0.6	6
	21	25	2000	0.5	2
	4200	18	770	0.8	12
	1700	9	210	1.0	36
19	2	6	330	0.6	230
20	680	5	<10	1.0	56
21	110	3	<10	0.1	74
	270	3	130	3.3	4000
	430	8	<10	0.8	185
	4200	48	<10	0.3	54
22	7300	16	11	9.0	168
23	47	39	41	1.6	12000
24	6	2	69	0.6	6000
25	830	11	11	3.0	32
	5600	6	31	1.4	57
	890	3	16	0.8	650
26	230	10	<10	2.0	1700
	1900	<1	130	11.6	35000
	200	<1	160	3.8	15000
27	1	1	<10	<0.1	2000

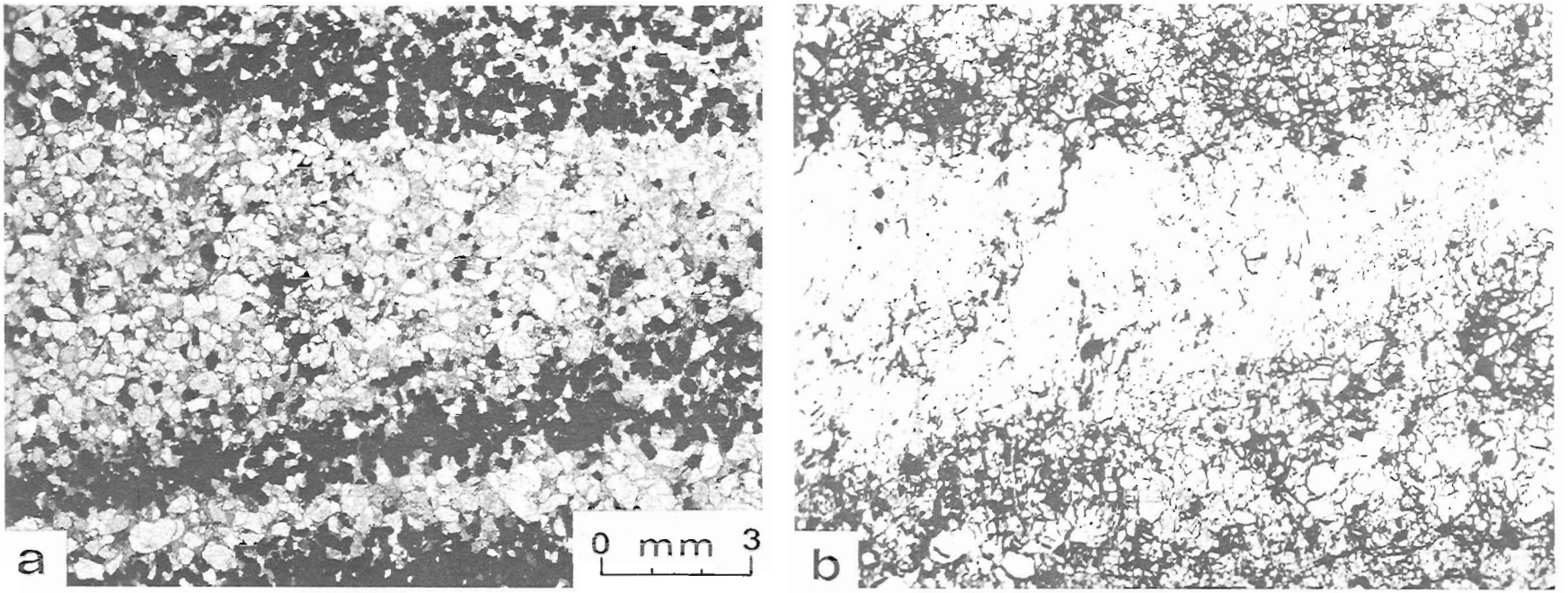

a) *Photomicrograph in transmitted light*

b) *Uranium distribution (fission tracks) of same area*

Figure 33.4 *Heavy mineral layer in arkose*

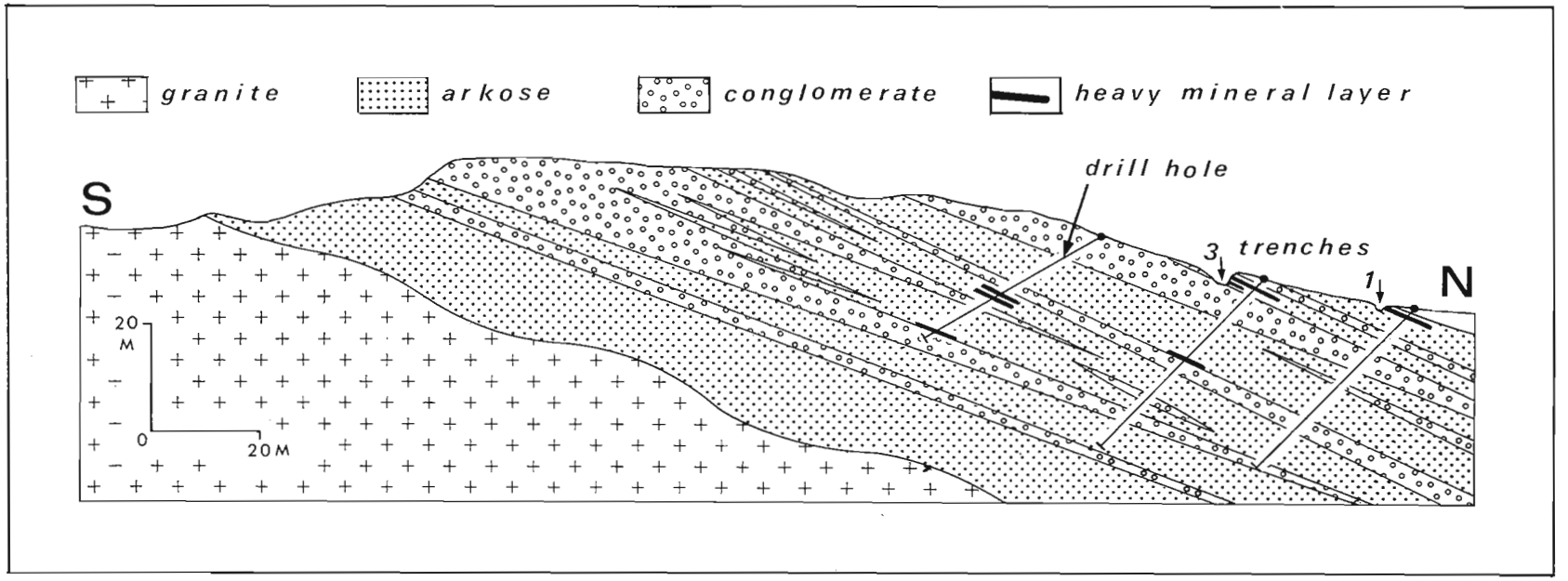

Figure 33.5. *North-south section across locality 1 (Fig. 33.1), from Gandhi and Prassad (1980).*

Table 33.5. Range of element concentrations in different rock types in MacInnis Lake area.

Rock unit (see Fig. 33.1)	N	U ppm	Th ppm	Nb ppm	Ta ppm	Sn ppm	W ppm	Au ppb	Ag ppm	Cu ppm	Fe%
Nonacho Group											
Siltstone, shale	3	5- 9	21-24	9-20	<5	6- 7	2- 8	<10-11	<0.1	2-28	2.8- 5.7
Pink arkose, conglomerate	6*	1- 5	15-41	1- 9	<5-8	5-37	<1- 4	<10-17	<0.1-0.1	1- 4	0.8- 1.2
Grey arkose	1	3	16	2	<5	6	4	39	0.1	4	2.1
Granite boulder congl.	2	2- 9	8-26	2- 3	<5	5- 6	2- 6	<10-15	0.2	2-16	2.1- 4.8
Basement											
Gabbro	3	<1- 1	<1- 2	<1- 6	<5	<1- 2	2- 6	<10	<0.1-0.1	68-96	9.3-11.0
Granite	3	1- 5	17-28	<1- 1	<5	<1- 8	2- 8	<10	0.1-0.2	9-10	0.5- 1.9
Granite gneiss	3	1- 2	17-54	<1- 1	<5	<1- 3	2- 8	<10	<0.1	4-24	0.9- 1.9
Quartz veins	10	<1-11	<1- 9	<1	<5	<1- 6	<1-16	<10	<0.1-0.4	1-38	0.1- 1.7

*Excludes data for "pure arkoses" from locality 1 (Table 33.2)

the pink arkose, this process was superimposed on an earlier syngenetic detrital mineralizing event that had led to enrichment in Th, Sn, Nb and Ta with minor U. The hydrothermal activity in the pink arkose probably resulted in some redistribution of Fe to account for the relatively high Fe content (and low Th, Sn, Nb, Ta ratios to Fe) of the high-U samples from localities 3 and 4.

Metal content of unmineralized rocks

Table 33.5 gives element ranges for representative unmineralized bedrock samples from scattered locations throughout the study area. This survey was far from exhaustive but a few interesting observations are made.

For example, the siltstones and shales are generally richer in U than the underlying pink arkose despite the fact that U mineralization occurs in the arkose. This reflects the higher chemical absorbance capacity of the finer grained sediments. Note that Nb, W, Cu and Fe are also richer in the siltstones and shales. According to Rankama and Sahama (1950), both Nb and W become enriched in the hydrolyzates during the sedimentary cycle; the higher Cu concentrations may be due to the increased scavenging ability of these rocks caused by their higher Fe content. Sn, however, is significantly higher in the arkose than in the siltstone-shale unit.

Gold has been detected in all of the major units of the Nonacho Group but none of the basement rocks seem to contain detectable gold including a number of quartz veins that intersect these rocks. U, Nb and Sn are also generally more concentrated in the Nonacho Group sediments than in the basement.

DISCUSSION

The MacInnis Lake area has been subjected to at least two different mineralizing events. The earliest involves the synsedimentary accumulation of detrital cassiterite, thorite-uranothorite, thorian monazite and a suspected but undetected Nb-Ta mineral along with magnetite, ilmenite, tourmaline, zircon and xenotime. These minerals are concentrated in mechanically controlled layers within the arkosic phase of a deltaic sandstone-conglomerate formation on the southwestern edge of the Nonacho basin. Although the Sn, Th-U, Nb-Ta mineral content of the heavy mineral layers is not constant (Tables 33.2, 33.3) these minerals are consistently present in the heavy mineral layers throughout the pink arkose-conglomerate unit. Somewhat higher concentrations of Th, Sn, Nb and Ta in the southeast (Loc. 1 to 4) and lower concentrations in the north (Loc. 8) seem to reflect distance of travel and are compatible with a postulated south to north paleocurrent direction in the MacInnis Lake area (Gandhi and Prassad, 1980). In the southeast, where the host formation is the thickest, it appears that Sn decreases from the bottom to the top of the sedimentary pile.

With regard to the source of the detrital minerals, Maurice and Plant (1979) pointed out that the assemblage in the MacInnis Lake area resembles one that characterizes the southern part of the Slave Province. However, the megacrystic granite in the Fort Smith belt and its peripheral zone, which contain an abundance of thorian monazite, were later recognized to be favourable for the occurrence of Sn and W mineralization (Charbonneau, 1980). Recently, Bostock and Thompson (1983) reported two scheelite occurrences in veins near the margin of the Fort Smith granite; one of these is located only 40 km south of MacInnis Lake. Although W is not significantly enriched at MacInnis Lake (see Tables 33.2, 33.3, 33.5), the frequent association of Sn with W in granitic rocks supports the concept that the detrital minerals in the pink arkose at MacInnis Lake originated from the Fort Smith belt. Tungsten minerals are much less resistant to mechanical and chemical disintegration than cassiterite, which could explain their absence from the heavy mineral layers. These minerals may still be abundant in the Fort Smith belt and should be pursued. Charbonneau (personal communication, 1983) indicated that part of the megacrystic granite may still be covered by metasedimentary cap rock and that these areas should constitute good exploration ground for Sn and W.

The second mineralizing event consisted of hydrothermal activity leading to U-Cu-Au-Ag mineralization. Where fractures and shear zones were the main conduits, this activity led to the formation of veins in basement rocks or Nonacho Group sediments. In the case of the pink arkose, high porosity allowed the mineralizing fluids to percolate through and to deposit the metals at favourable sites. It appears that this activity, as far as the arkose is concerned, was restricted to the area close to the southeastern shore of MacInnis Lake where high U concentrations and some sulphides are found. This hydrothermal activity is probably responsible for the interstitial uranium phase that characterizes heavy mineral-bearing samples with elevated U/Fe ratios ($U/Fe \times 10^4 > 10$). These high ratios are only found on the southeastern side of MacInnis Lake (Loc. 1-4), which suggests that the hydrothermal activity did not affect the arkose elsewhere.

Gold is also more concentrated on the southeast side of MacInnis Lake. Furthermore, Au is not only enriched in samples containing heavy minerals but is also found with chalcopyrite at locality 3, in low-Fe samples at locality 4 and in the high-U samples at localities 3 and 4 (Table 33.2). These observations suggest that the gold in the arkose is at least in part hydrothermal and was introduced at the same time as Cu and most of the U.

Unlike Cu and Au, U is more or less confined to the heavy mineral layers. This initially led to the belief that the U that constitutes the interstitial uraniferous phase in those layers originated from the heavy mineral layers themselves,

possibly from the alteration of a clastic U-bearing mineral such as uranothorite with subsequent remobilization of the U, perhaps during diagenesis. However, uranothorite was not found to be highly altered in the rocks, and besides, this mineral is not generally very abundant in the heavy mineral layers. The U content of samples from localities 5 to 17 (Table 33.3) probably reflects the content of detrital uranothorite in the heavy mineral layers throughout the pink arkose.

Uranium is believed instead to have precipitated in the intergranular spaces of the heavy mineral layers from the percolating hydrothermal Cu-Au-U-bearing solutions in response to favourable chemical conditions. Reducing conditions associated with the presence of ferrous iron (magnetite) could have favoured precipitation of U compounds but the presence of Ti-bearing minerals such as ilmenite or sphene may have had a greater influence on the retention of U. Nash et al. (1981) stated that Ti hydroxide is a very effective concentrator of uranyl ion at low temperatures and pointed out that elevated temperatures are needed to reduce uranyl ions by ferrous iron. Although the temperature of the fluid phase as it percolated through the arkose is not known, the apparent preferential distribution of interstitial U in the vicinity of Ti-bearing grains in samples from MacInnis Lake (see Mineralization) may be indicative of the importance of the Ti minerals in retaining U.

The precipitation of U in heavy mineral layers as a result of redox reactions or reaction with Ti compounds may be a common U-enrichment mechanism in clastic sediments deposited after oxygenation of the atmosphere. At MacInnis Lake, the U source was linked to hydrothermal activity in the region because of its Cu-Au association, but it is reasonable to assume that similar build up of U could occur simply as a result of groundwater circulation.

There may yet have been other mineralizing events in the MacInnis Lake area. In all likelihood, the U-bearing vein type occurrences on the west side of MacInnis Lake are genetically related to those on the east side despite some differences in their chemical and mineralogical constituents; those on the west side are lower in Au but higher in Ag and generally contain more galena and less chalcopyrite than those on the east side. The non-radioactive Cu occurrences (Loc. 24 and 27), however, are probably syngenetic and unrelated to the main hydrothermal phase. An independent event may also be postulated for the galena-bearing quartz vein at locality 19 although enrichment in Cu and Au may suggest a genetic link with the main hydrothermal event.

ACKNOWLEDGMENTS

The writer benefited from discussions with B.W. Charbonneau, H.H. Bostock, S.S. Gandhi, S.B. Ballantyne, and L. Aspler. G.M. Lecheminant is thanked for her meticulous work on the microprobe, and the scanning electron and optical microscopes.

REFERENCES

Bostock, H.H.
1981: A granitic diapir of batholithic dimensions at the west margin of the Churchill Province; in Current Research, Part B, Geological Survey of Canada, Paper 81-1B, p. 73-82.

1982: Geology of the Fort Smith map area, District of Mackenzie, Northwest Territories (NTS 75D); Geological Survey of Canada, Open File 859, 53 p.

Bostock, H.H. and Thompson, D.L.
1983: Fluorescent minerals from the Fort Smith area, District of Mackenzie, N.W.T.; in Current Research, Part B, Geological Survey of Canada, Paper 83-1B, p. 401-402.

Charbonneau, B.W.
1980: The Fort Smith radioactive belt, Northwest Territories; in Current Research, Part C, Geological Survey of Canada, Paper 80-1C, p. 45-57.

Gandhi, S.S. and Prassad, N.
1980: Geology and uranium occurrences of the MacInnis Lake area, District of Mackenzie; in Current Research, Part B, Geological Survey of Canada, Paper 80-1B, p. 107-127.

Henderson, J.F.
1937: Nonacho Lake area, Northwest Territories; Geological Survey of Canada, Paper 73-2, 22 p.

Maurice, Y.T. and Plant, A.G.
1979: Some mineralogical and geochemical characteristics of uranium occurrences in the Nonacho Lake area, District of Mackenzie; in Current Research, Part B, Geological Survey of Canada, Paper 79-1B, p. 179-188.

McGlynn, J.C.
1978: Geology of the Nonacho Basin, District of Mackenzie; Geological Survey of Canada, Open File 543.

Moffat, G.W.
1974: An investigation of the radioactive mineral occurrences of the Great Slave Lake – Athabasca Lake region of the District of Mackenzie in the Northwest Territories; unpublished B.Sc. thesis, University of Toronto, 115 p.

Nash, J.T., Granger, H.C., and Adams, S.S.
1981: Geology and concepts of genesis of important types of uranium deposits; Economic Geology, 75th Anniversary Volume, p. 63-116.

Rankama, K. and Sahama, T.G.
1950: Geochemistry; Chicago University Press, Chicago, 912 p.

34. PRELIMINARY GRAVITY, MAGNETIC AND REFRACTION SEISMIC RESULTS FROM THE ABITIBI BELT, QUEBEC

Project 830026

E.J. Schwarz, L. Laverdure[1], L. Losier[2], and E. Poterlot[2]
Resource Geophysics and Geochemistry Division

Schwarz, E.J., Laverdure, L., Losier, L., and Poterlot, E., Preliminary gravity, magnetic and refraction seismic results from the Abitibi belt, Quebec; in Current Research, Part A, Geological Survey of Canada, Paper 84-1A, p. 239-246, 1984.

Abstract

Gravity, aeromagnetic and seismic data are presented for the Abitibi greenstone belt and interpreted in a preliminary way. The Bouguer gravity shows a regional negative of about -45 mgal on which are superposed local negative anomalies. The latter are generally due to granite intrusions which individually model downwards to about 5 km. Modelling complete profiles yields nearly 10 km. The regional anomaly may be explained in many ways but may indicate Moho depth variations up to about 6 km with a slight dip east. The seismic records for the two fanshots also suggest a small easterly dip of the Moho and the in-line profile indicates a Moho depth of 37.6 km on the Val d'Or – Matagami recorder line. The 1:1 000 000 magnetic anomaly coloured and shaded relief maps indicate a higher residual field background over the somewhat more metamorphosed eastern part of the belt. The preliminary results indicate qualitative correlations between the different groups of data and it is hoped eventually to arrive at a best fitting geophysical model which could then be reconciled with geological hypotheses on the origin and evolution of this mineralized belt.

Résumé

Les auteurs présentent et interprètent de façon provisoire des données gravimétriques, aéromagnétiques et sismiques pour la zone de roches vertes de l'Abitibi. La gravité de Bouguer donne une anomalie négative régionale d'environ -45 mgal sur laquelle sont superposées des anomalies négatives locales. Ces dernières sont généralement produites par des intrusions de granite qui s'étendent à une profondeur d'environ 5 km. L'établissement des profils complets donne une profondeur d'environ 10 km. L'anomalie régionale s'explique de nombreuses façons mais pourrait indiquer des variations de la profondeur du Moho allant jusqu'à 6 km, avec une légère inclinaison vers l'est. Les deux tirs en éventail ont donné des enregistrements sismiques qui laissent également croire que le Moho serait légèrement inclinée vers l'est, tandis que le profil en ligne indique que le Moho se situe à une profondeur de 37,6 km le long du tracé Val d'Or-Matagami. Les cartes topographiques des anomalies magnétiques en couleurs et estompées à 1/1 000 000 indiquent que le champ résiduel de fond est plus intense au-dessus de la partie est de la zone où le degré de métamorphisme atteint un niveau légèrement plus élevé. Les résultats préliminaires indiquent l'existence de corrélations qualitatives entre les divers groupes de données; les auteurs espèrent mettre au point éventuellement le meilleur modèle géophysique qui puisse alors s'accorder avec les hypothèses géologiques sur l'origine et l'évolution de cette zone minéralisée.

INTRODUCTION

The Abitibi greenstone belt is a large structure consisting of metavolcanic and metasedimentary rocks pierced by granite intrusions. It contains important base metal and gold deposits. The surface geology has been investigated in detail but the deep crustal structure of the belt is essentially unknown. For this reason an integrated geophysical study of the area was begun in 1981 by a group of Quebec Universities (École Polytechnique, McGill, Université de Montréal, and Université du Québec à Chicoutimi). The data base for this study consists of the gravity data from the Earth Physics Branch, the aeromagnetic data from the Geological Survey of Canada, and refraction seismic data obtained in 1982 under a joint program of the COCRUST and Quebec Universities groups. A magnetotelluric survey was initiated by the Earth Physics Branch followed up by the École Polytechnique and the Ministère de l'Energie et des Ressources du Québec. This report deals briefly with the preliminary interpretation of the gravity, aeromagnetic, and seismic refraction data.

GEOLOGICAL SETTING AND DATA BASE

The Abitibi greenstone belt forms part of the Archean Superior Geological Province. The belt is formed by mildly metamorphosed volcanics and sediments, and granite batholiths. The volcanics range from ultramafic (old) to intermediary (young) in composition. Recent geological compilations and interpretations have been given by Goodwin and Ridler (1970), Baragar and McGlynn (1976), and Dimroth et al. (1982, 1983a,b). Figure 34.1 represents an overview of the geology from Card and Sanford (1983) and the Ministère de l'Energie et des Ressources (1969).

The density of the gravity stations varied between 16 and 48 per 50 km square allowing the preparation of a fairly detailed contour map (Laverdure, 1983). This 1:1 000 000 map shows only minor differences from a computer interpolated map using a "kriging" method (Taylor, 1980) based on the same data. Density measurements were performed on 163 surface samples. The results compare well with the results obtained by Gibb et al. (1969) for 347 samples.

The aeromagnetic data utilized are digitized total field data obtained from the 1:63 360 contour maps produced by the Geological Survey of Canada and the Ministère de l'Energie et des Ressources du Québec. The data were compiled to 1:1 000 000 magnetic anomaly maps.

The seismic refraction data is from 31 recorders lined up along the road from Val d'Or to north of Matagami. A reversed profile was obtained from shot points near Val d'Or and Matagami and fans were obtained from shots near Timmins and Chibougamau.

[1] Earth Physics Branch, 1 Observatory Crescent, Ottawa
[2] École Polytechnique, Montréal, Québec

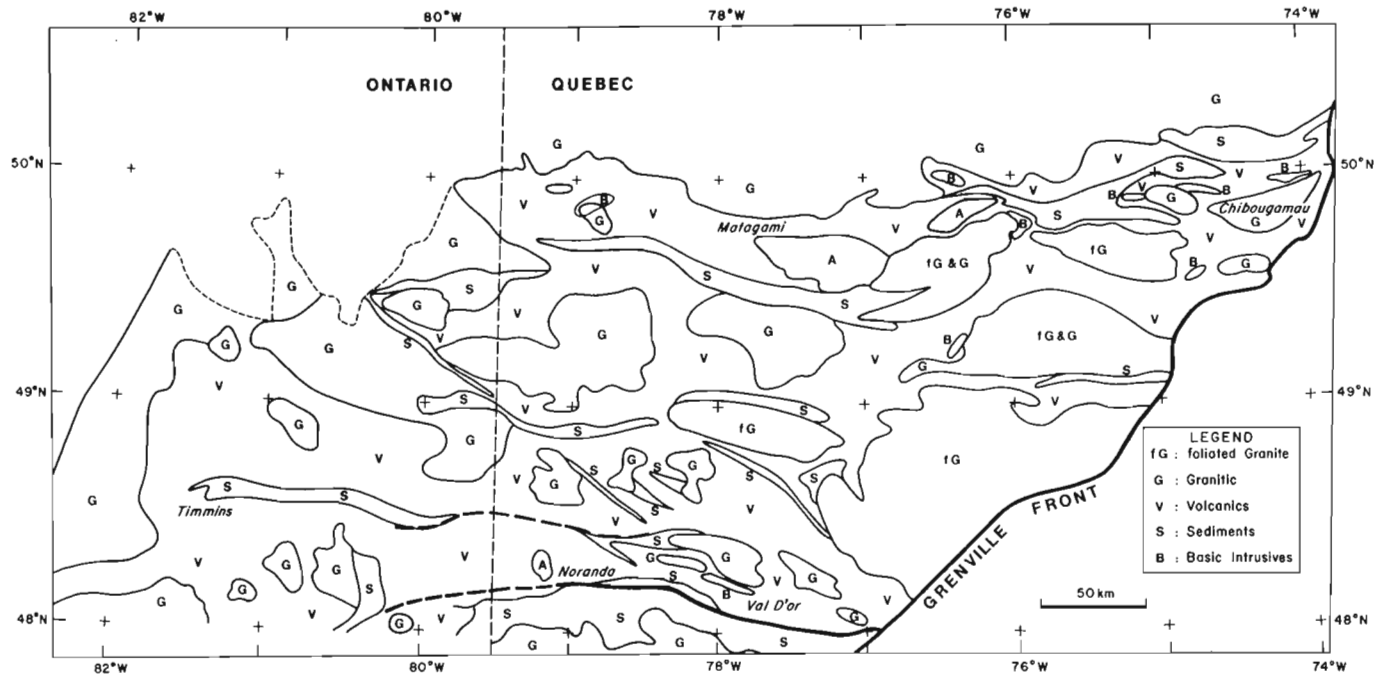

Figure 34.1. *Geological sketch map of the Abitibi belt.*

GRAVITY RESULTS

A comparison between the geological and Bouguer gravity maps (Fig. 34.1, 34.2) allows the following qualitative observations:

1. The Abitibi belt is a regional negative (-40 to -50 mgal) with superposed local negatives and a few small relative highs. Most of the local negatives can be correlated with granite batholiths (see also Gibb et al., 1969).
2. The belt is bounded to the northwest by the Kapuskasing gravity high and to the southeast by the Grenville Front which shows values of less than -100 mgal farther east (see also Thomas, 1974).
3. The Bouguer gravity field over the area surrounding the Abitibi belt shows less variation than that over the belt itself. This is probably due to the more varied lithology of the belt.
4. The general trend in the belt and surrounding areas except Kapuskasing and the Grenville Front is east-west. However, Figure 34.2 shows a north-south band containing relative highs near 80°W. The magnetic colour and shaded relief maps, which are discussed in a later section of this paper, indicate a high density of Matachewan diabase dykes at this longitude. Thus, the gravity may well indicate the presence of buried basic intrusions other than the outcropping dykes. Another band runs west-northwest from about 76°W, 46°N.
5. The northern half of the belt contains the lowest values (-90 mgal). These are more pronounced local lows rather than an indication of a lower regional negative in the northern part.

Separation of the local lows and the regional have been done graphically and by upward continuation using a grid size of 22 km. Correspondence between both is good at elevations of 44 to 66 km. The local lows have been modelled using methods proposed by Jacoby (1970) and Nagy (1966). The results of these studies on 7 anomalies (Table 34.1) are coherent and show that the local negatives can be produced by extrapolating the outcropping granite plutons individually down to a depth of up to 5 km. Modelling complete profiles yields nearly 10 km.

The regional low was modelled either by varying the depth of the interface between an upper layer containing the batholiths, volcanics, sediments and possibly acidic, highly metamorphosed, rocks at depth and a lower granulitic layer or by varying the depth to the Moho. The results indicate (Laverdure, 1983) that the thickness of the upper layer could vary by about 1 km and the depth to the Moho by about 5 km as shown in the three dimensional diagram of Figure 34.3.

AEROMAGNETIC SURVEY RESULTS

Coloured magnetic anomaly and shaded magnetic relief maps on a scale of 1:1 000 000 were prepared after compilation of the original aeromagnetic data had been done following Teskey et al. (1982) and Dods et al. (in press).

Figure 34.4 shows the black and white reproduction of the coloured magnetic anomaly map. It is based on a digitized square grid of about 800 m centred on the flight lines of the original 1:63 360 contoured maps. These data were obtained at a flight altitude of 305 m. After levelling and other corrections, the "core field" (IGRF) was subtracted from the total field to yield the residual field which is due essentially to the magnetic sources within the crust. Figure 34.5 represents the shaded magnetic relief map based on the same data illuminated from the southeast at an angle of 40° from the horizontal. A comparison between these figures and Figure 34.1 shows:

1. In contrast to gravity, there is no clear difference in signature between the Abitibi belt and the surrounding Precambrian terrane (Fig. 34.4) at least for wavelengths larger than a few kilometres.

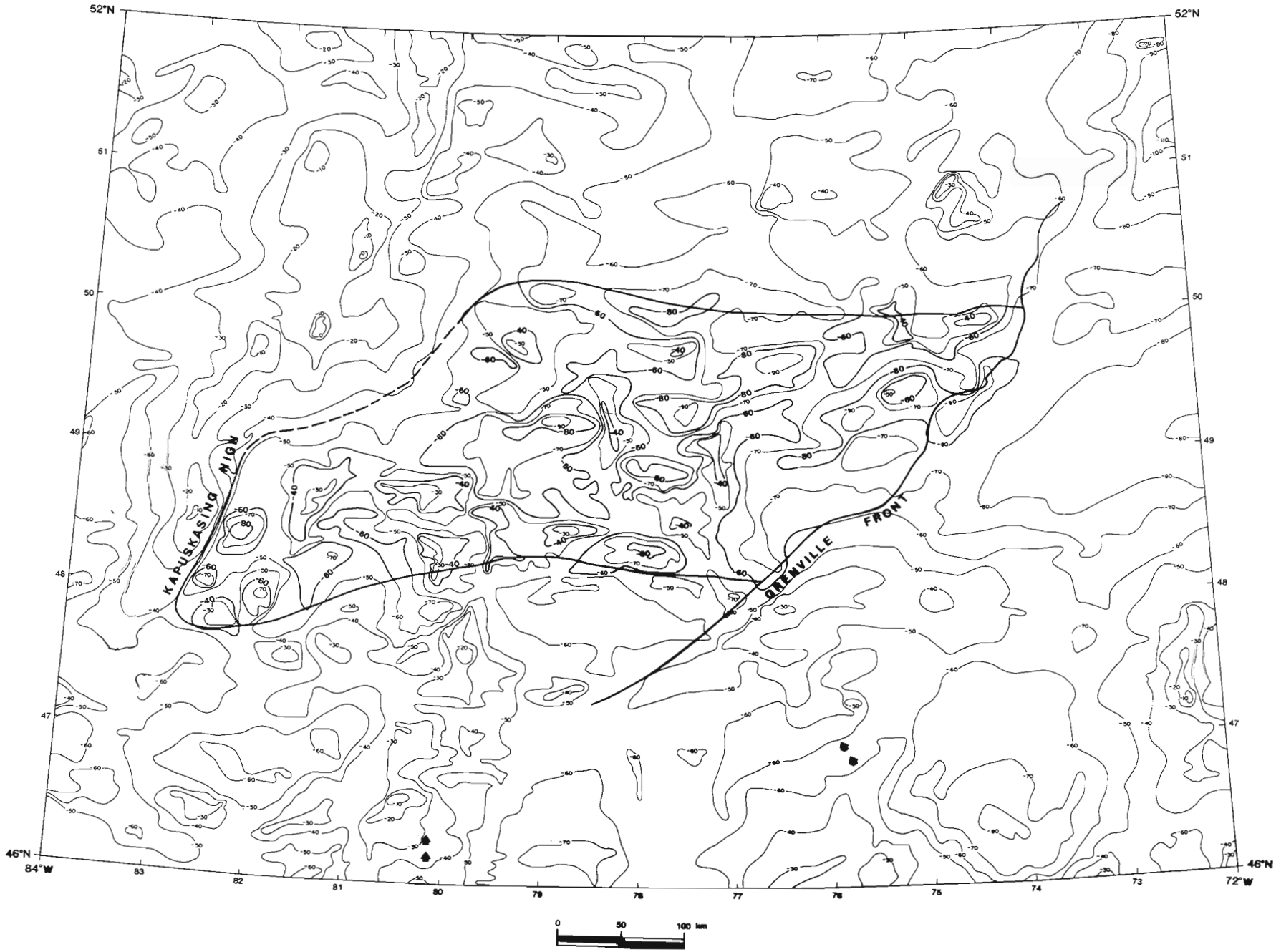

Figure 34.2. *Bouguer gravity map of the Abitibi belt contoured at 10 mgal intervals.*

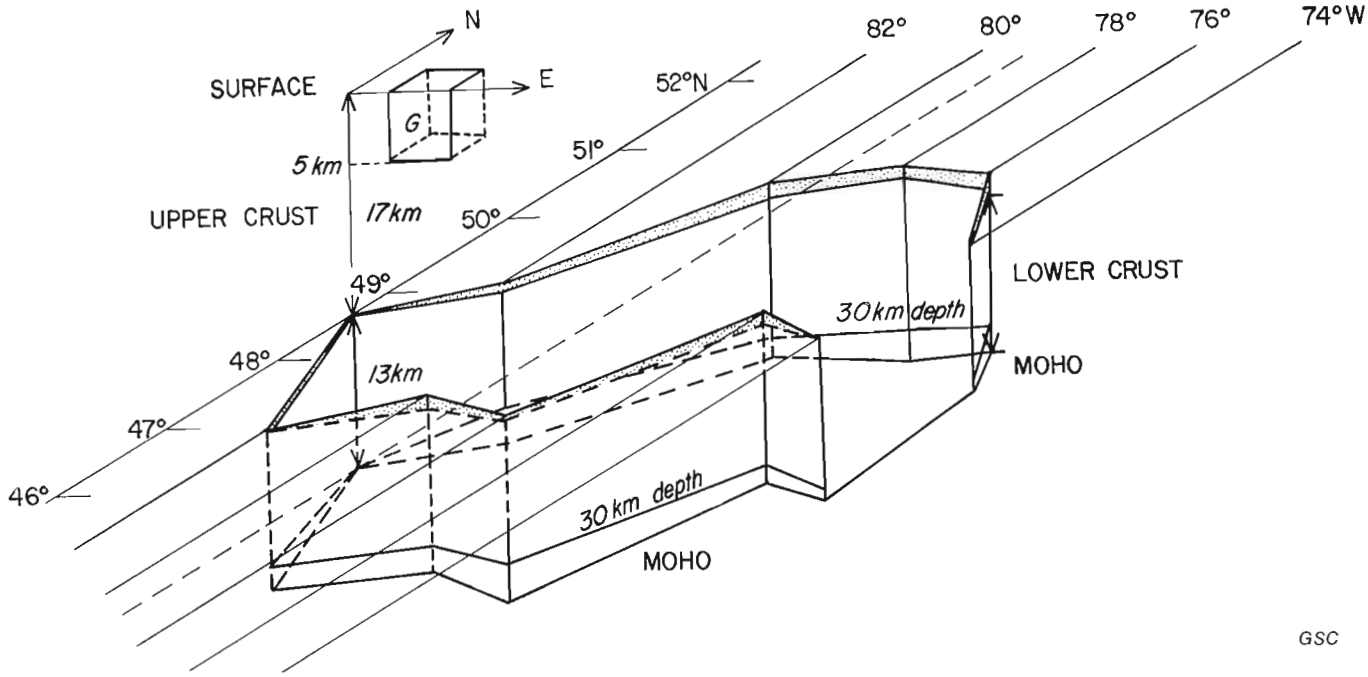

Figure 34.3. *Three dimensional block diagrams showing depth to a lower granulite layer and the Moho based on the observed negative regional gravity anomaly. A thinner low-density upper crust would enhance the topography of the Moho and/or of the interface between the upper and a lower crustal layer. G: granite plutons.*

2. There is a substantial change in field intensity within the belt. The background intensity in the eastern part is $\geq$ +200 nT which decreases gradually to about -200 nT in the western part (Fig. 34.4). Figure 34.1 shows that the eastern part is predominantly formed by foliated granite-gneiss plutons (orthogneiss), while west of about 78°W the plutons are composed of granite, monzonite, granodiorite and syenite (e.g. Ministère de l'Energie et des Ressources, 1969). On the metamorphic map of the Shield (Geological Survey of Canada, 1978), the eastern plutons are classified under amphibolite facies while those in the west are considered to represent lower amphibolite facies. The background intensity may thus be related to metamorphic grade of the plutons but this is not clear for the metavolcanic and metasedimentary rocks. Furthermore, the large northeast trending Abitibi diabase dyke maintains its magnetization contrast with the country rock (Fig. 34.5). The foliated granites north of the belt also show relatively high field intensities but the apparently nonfoliated pluton at about 49.3°N, 79°W shows also a high intensity. Another possible explanation is that a relatively strong magnetic lower layer (granulite?) occurs closer to the surface in the eastern part.
3. Very high residual field intensities and strong horizontal gradients throughout the belt and also in the surrounding terrane are correlatable with diorite-gabbro to peridotite-serpentinite intrusions.
4. Magnetic structure is best examined using Figure 34.5. Northeast-trending diabase dykes (Abitibi) are clearly visible. North-south trending lines in the western part of the belt probably indicate Matachewan dyke swarms. Figure 34.4 shows that the large Abitibi dyke shows a decrease in intensity towards the southwest but Figure 34.5 shows that it maintains its contrast with the

Table 34.1. Depth extent of granite batholiths using Jacoby's (1970) method and a 3-dimensional prism model proposed by Nagy (1966)

Batholith number	east-west Dimension (°W)	(km)	north-south Dimension (°N)	(km)	radius (km)	Jacoby (km)	Nagy (km)
1	78.45-77.97	9	48.33-48.53	19.5	7.5	3.7	4.5
3	78.51-77.93	9	48.64-48.85	27	9.0	4.8	4.3
5	77.21-77.02	11	47.90-48.10	16	6.6	4.3	3.3
7	79.41-78.82	29	48.49-48.87	29	12.5	3.0	3.2
9	77.14-75.80	34	49.31-49.942	46	18.75	3.0	3.0
10	78.89-75.80	11	48.58-48.74	12	5.5	3.4	3.6
12	79.52-79.24	8	48.67-48.842	10	4.5	3.9	4.1

Longitude and latitude indicate limits of each pluton

country rock. Granitic plutons, foliated or not, display a rather homogeneous magnetic expression. In general, their boundaries show high magnetic relief which has been ascribed by Letros et al. (1983) to magnetite enrichment in the Kirkland Lake area. Large faults such as the Cadillac Break show magnetic relief along most of their course.

Magnetic property studies of surface samples to be used in modelling of major sources in the area are in progress. Power spectrum analysis and field continuation are also being carried out in an attempt to further interpret the data. A vertical derivative map may also show a better correlation with the surface geology than the total field data used in this preliminary study.

SEISMIC REFRACTION RESULTS

The seismic refraction data are expected to provide quantitative measurements of the depth to the Moho thus constraining the various models available for the interpretation of the regional gravity low over the

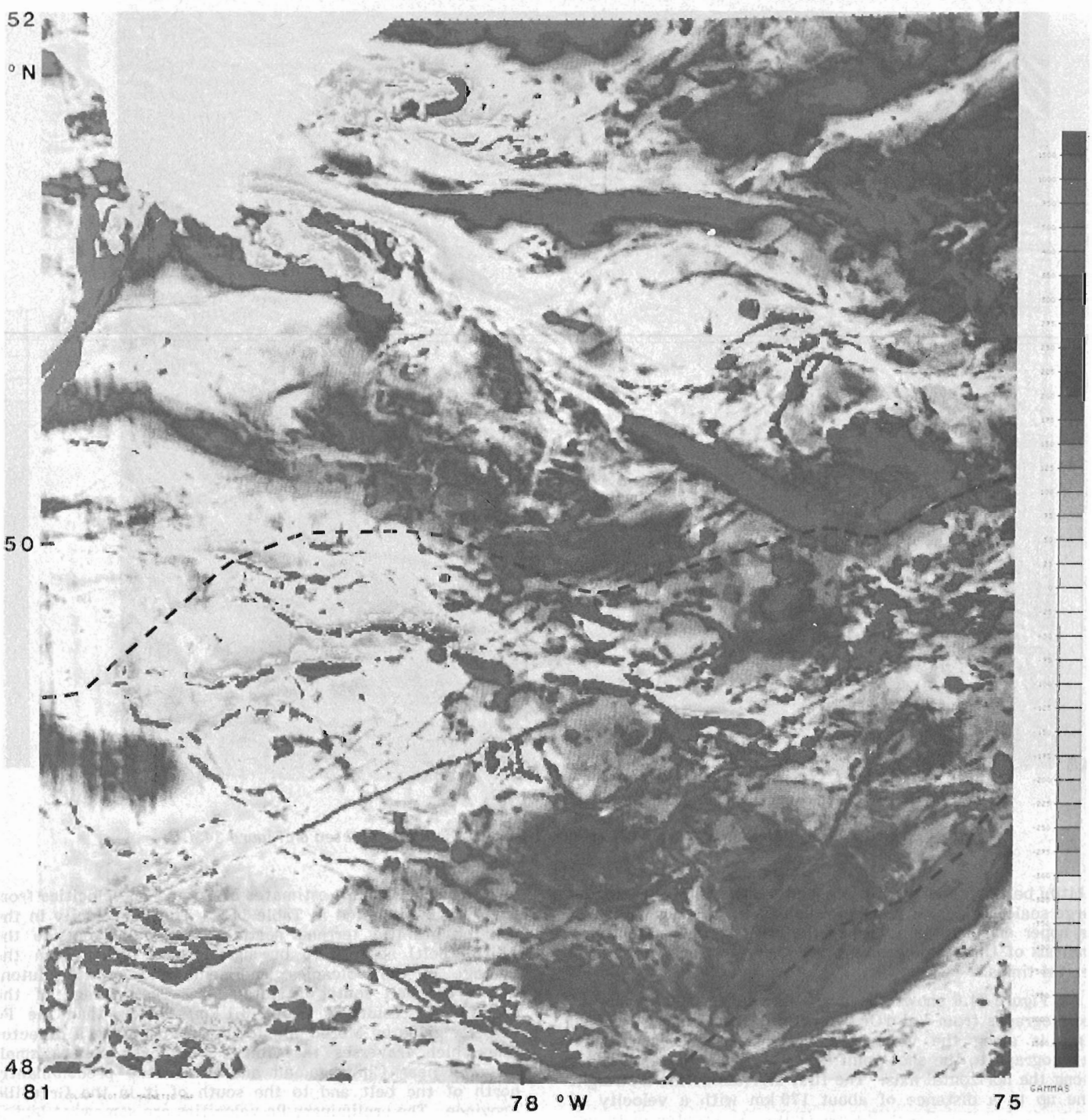

Figure 34.4. Black and white reproduction of colour plotted residual aeromagnetic field map over the Abitibi belt (altitude 305 m) between 75 and 81° West. The dashed line outlines the belt.

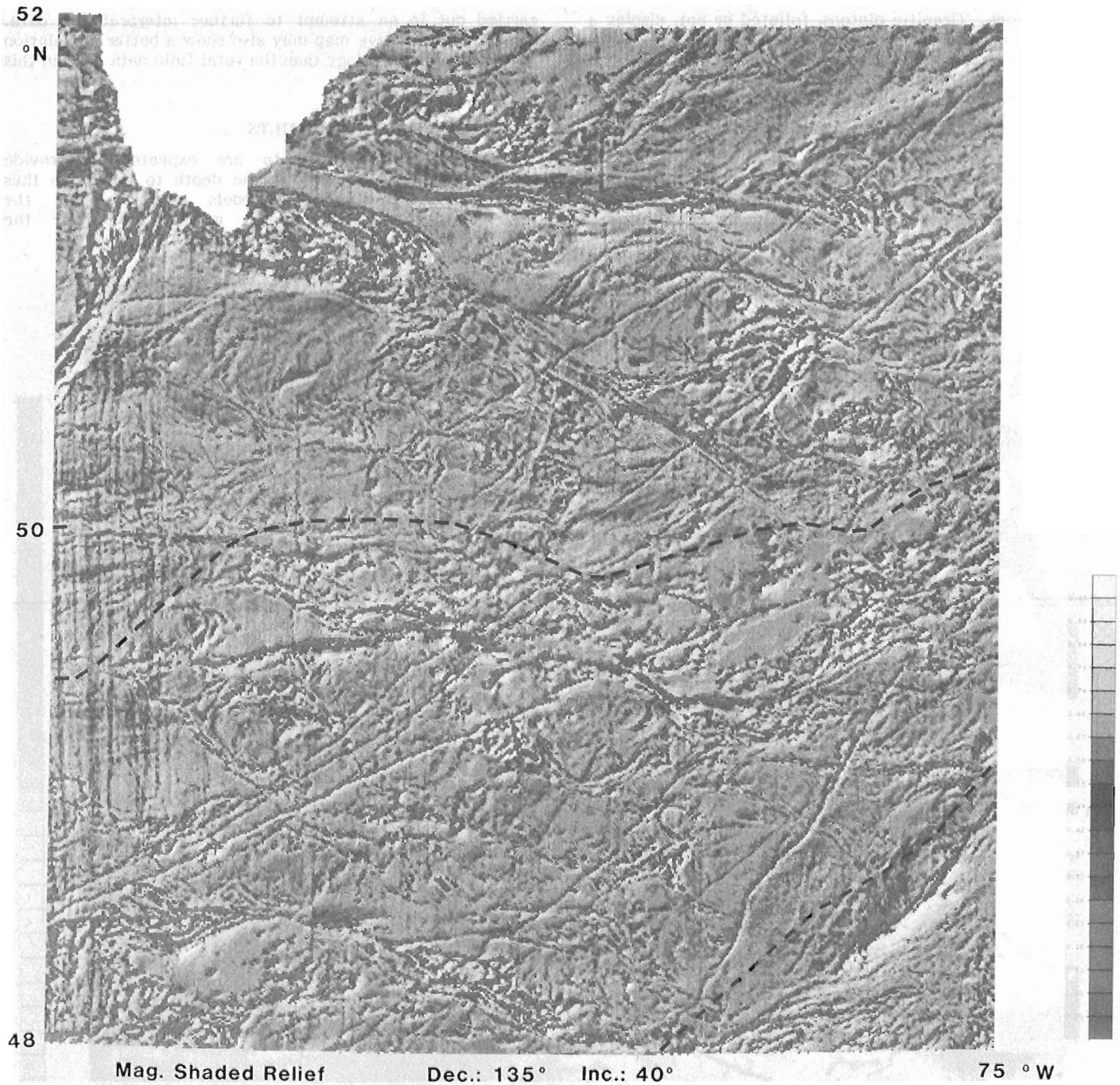

Figure 34.5. *Magnetic shaded relief map based on the data depicted on Figure 34.4.*

Abitibi belt. In addition, it is hoped to obtain information on large scale horizontal features (such as an interface between an upper and a lower layer) of the crust by a more detailed analysis of the seismograms other than the analysis of first arrival times.

Figure 34.6 shows the available records for the line of seismographs from Val d'Or to north of Matagami. Reduced time is along the vertical axis and distance from each seismograph to the shot point (A: Matagami; B: Val d'Or) is along the horizontal axis. The first arrivals define a straight line up to a distance of about 170 km with a velocity of 6.3 km/s for the direct P wave (Pd). At greater distances (≥170 km, Fig. 34.6B) a velocity of 8.45 km/s is indicated for the head wave. The first arrivals in this segment of the diagram are due to the P wave refracted on the Moho (Pn). The crossover distance of the two lines from the shot point yields a Moho depth of 37.6 km.

The preliminary estimates of Pd and Pn velocities from the 4 shots are listed in Table 34.2. The Pd velocity in the foliated granitic terrane north of Matagami (outside the Abitibi belt) appears to be significantly higher than the average in the volcanics, sediments and granite plutons within the belt south of Matagami. The average of the preliminary results is about 0.1 km/s lower than the Pd velocity given by Mereu and Jobidon (1971) along a detector line which traverses the Abitibi belt over only a small distance near Chibougamau and is located predominantly north of the belt and to the south of it in the Grenville Province. The preliminary Pn velocities are somewhat higher (about 8.5 km/s) than those of Mereu and Jobidon (mean of 8.15 km/s and a range of 7.56 to 8.85 km/s).

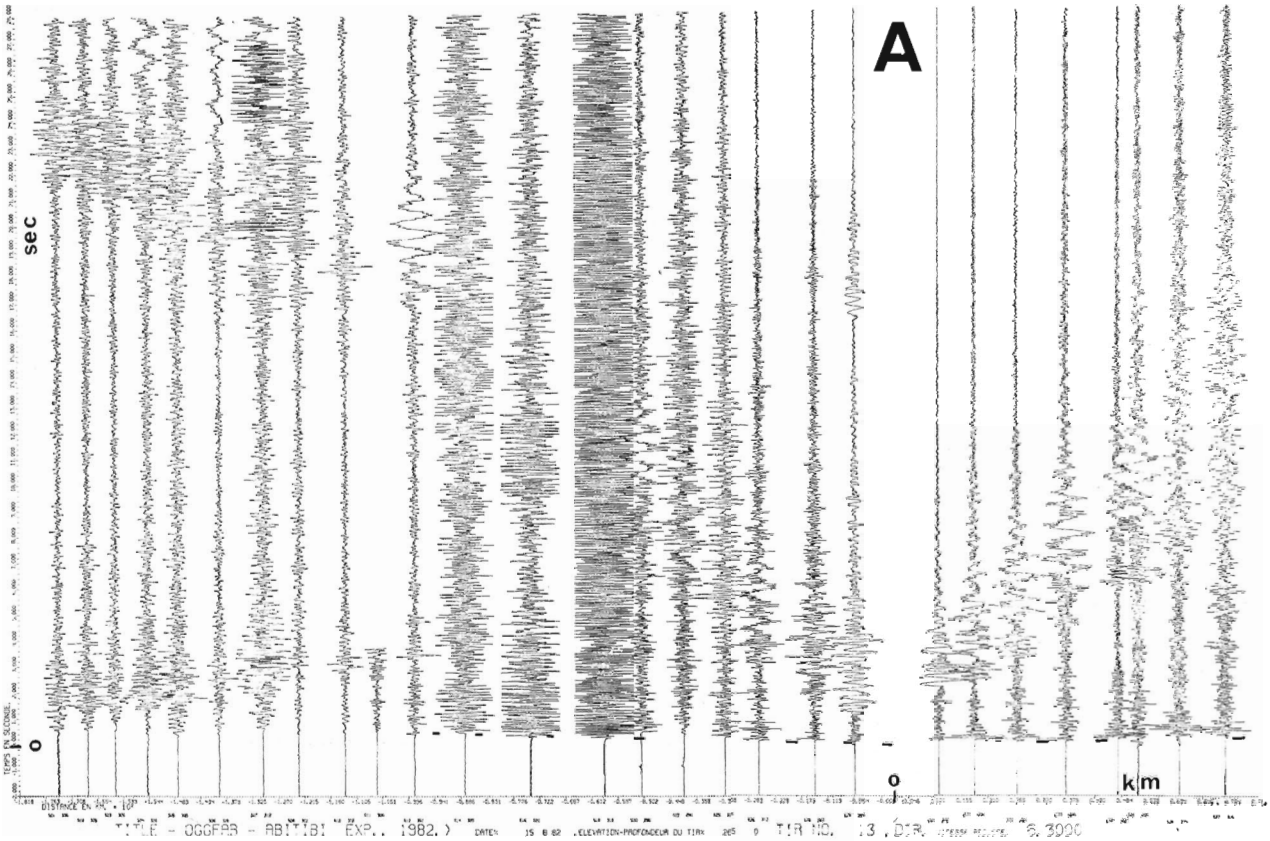

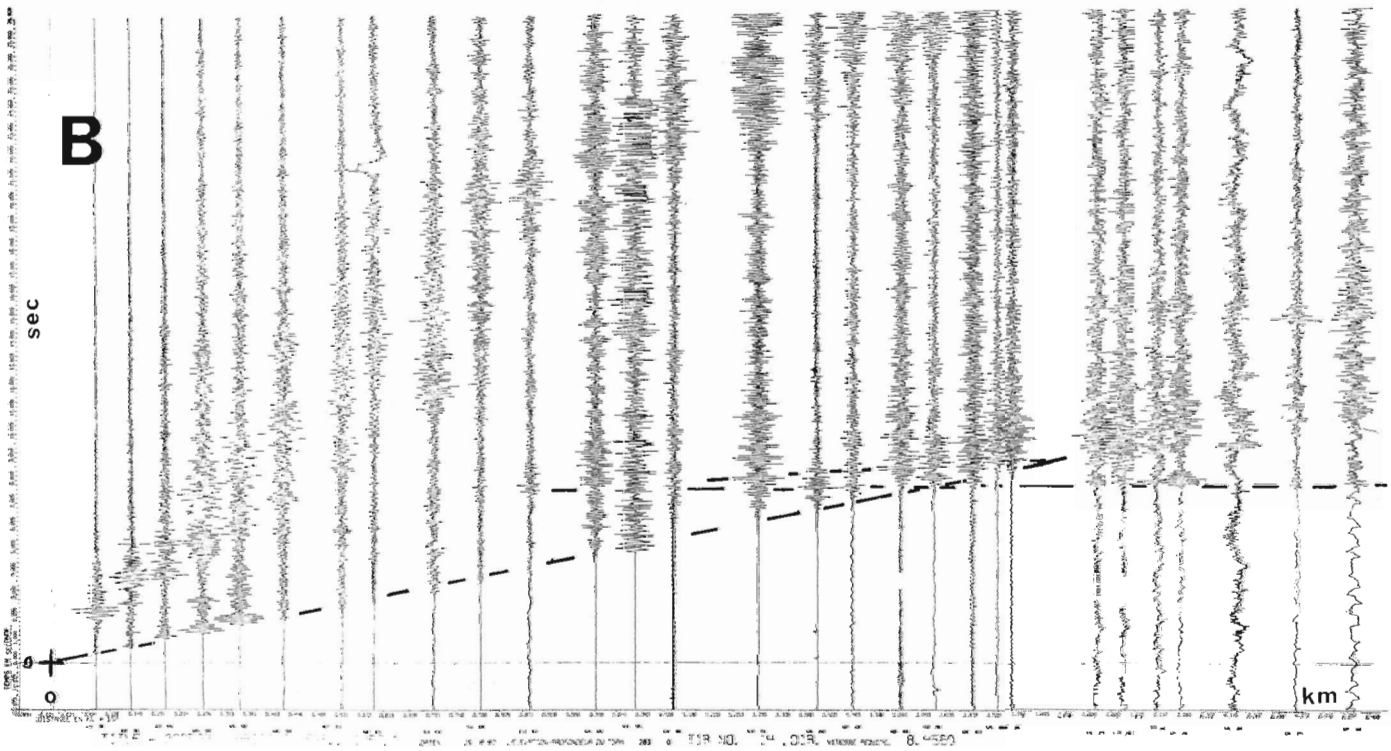

Figure 34.6. *Seismic wavetrains plotted as a function of reduced time (shottime = o) and distance from shotpoints Matagami (A) and Val d'Or (B). Reduced time (= arrival time – distance (shot point to each recorder)/velocity (6.3 in A and 8.4 in B)) is used to better show travel time anomalies due to in-homogeneities and variation in Moho depth.*

Table 34.2. Preliminary P wave velocities in crust (Pd) and upper mantle (Pn) from the 4 shots in km/s

Shot	Matagami	Val d'Or	Timmins	Chibougamau
Crust	North:6.36 South:6.26	6.27		
Upper Mantle		8.46	8.24	8.84
Detector line runs from Val d'Or to north of Matagami				

The fan shot from Timmins yields a Pn velocity of 8.24 km/s while that from Chibougamau yields 8.84 km/s. This difference may be due to a tilt of the Moho of about 2° east. Taking the east-west width of the belt as 500 km, this would indicate that the Moho would be about 17.5 km deeper in the east than in the west. This appears to be rather excessive but it is interesting that the regional gravity negative also indicates a deepening of the Moho towards the east although only by a maximum of about 6 km. A coherent picture would emerge if the Kapuskasing gravity high is to be explained by a shallow Moho. On the other hand, Mereu and Jobidon (1971) suggest the Moho near Chibougamau is about 35 km deep increasing rapidly to over 40 km under the nearby Grenville Front. Recognition and identification of later arrivals in the seismograms is being attempted and eventually modelling using ray tracing will be done.

CONCLUDING REMARKS

This is the first stage of an integrated geophysical study in which the models arrived at by the use of several geophysical methods and the surface geology must constrain each other so that the best geophysical model to explain the observations can be selected. This model then has to be reconciled with geological hypotheses on the origin and evolution of the Abitibi belt. This and direct geophysical information on the within-belt structure should be useful in mineral exploration within the Atibiti belt.

ACKNOWLEDGMENTS

We thank Drs. M.D. Thomas and A.K. Goodacre of the Earth Physics Branch for the use of the gravity data. Dr. D.J. Teskey and Mr. S.D. Dods of the Geological Survey of Canada provided programs and advice in obtaining the aeromagnetic maps. Dr. G.F. West of the University of Toronto helped with the seismic recorders and other equipment used in the processing of the records. Student support was provided by a Natural Science and Engineering Research Council Group Strategic Grant. The help of COCRUST in the seismic experiment is acknowledged. Dr. A.G. Green of the Earth Physics Branch provided us with seismic interpretation programs.

REFERENCES

Baragar, W.R.A. and McGlynn, J.C.
1976: Early Archean basement of the Canadian Shield: a review of the evidence; Geological Survey of Canada, Paper 76-14, 21 p.

Card, K.P. and Sanford, B.V.
1983: Geological map, 1:1.000 000, Timmins, NM-17; Open File 956.

Dimroth, E., Imreh, L., Rocheleau, M., and Goulet, N.
1982: Evolution of the south-central part of the Archean Abitibi belt, Quebec, Part 1; Canadian Journal of Earth Sciences, v. 19, no. 9, p. 1729-1758.

Dimroth, E., Imreh, L., Goulet, N., and Rocheleau, M.
1983a: Evolution of the South-Central segment of the Archean Abitibi belt, Quebec, Part II; Canadian Journal of Earth Sciences, v. 20, no. 9, p. 1355-1373.

1983b: Evolution of the South-Central segment of the Archean Abitibi belt, Quebec, Part III; Canadian Journal of Earth Sciences, v. 20, no. 9, p. 1374-1388.

Dods, S.D., Teskey, D.J., and Hood, P.J.
– The new 1:1 000 000 magnetic anomaly map series of the Geological Survey of Canada; in Utility of Regional Gravity and Magnetic Maps; Society of Exploration Geophysics, Special Volume. (in press)

Geological Survey of Canada
1978: Metamorphic map of the Canadian Shield, Map 1475A.

Gibb, R.A., van Boeckel, J.J.G.M., and Hornal, R.W.
1969: A preliminary analysis of the gravity anomaly field in the Timmins-Seneterre mining areas; Publication Dominion Observatory, Ottawa, no. 58, 25 p.

Goodwin, A.M. and Ridler, R.H.
1970: The Abitibi orogenic belt; in Precambrian Basins and Geosynclines of the Canadian Shield, ed. A.J. Baer; Geological Survey of Canada, Paper 70-40, p. 1-30.

Jacoby, W.R.
1970: Gravity diagrams for thickness determination of exposed rock bodies; Geophysics, v. 35, no. 3, p. 471-475.

Laverdure, L.
1983: Gravimetrie de la Ceinture volcanique de l'Abitibi; mémoire M.Sc.A., École Polytechnique, Montreal, 106 p.

Letros, S., Strangway, D.W., Tasillo-Hirt, A.M., Geissman, J.W., and Jansen, L.S.
1983: Aeromagnetic interpretation of the Kirkland Lake-Larder Lake portion of the Abitibi greenstone belt, Ontario; Canadian Journal of Earth Sciences, v. 20, no. 4, p. 548-560.

Mereu, R.F. and Jobidon, G.
1971: A seismic investigation of the Crust on a line perpendicular to the Grenville Front; Canadian Journal of Earth Sciences, v. 8, p. 1553-1583.

Ministère de l'Energie et des Resources
1969: Carte géologique du Québec, A.F. Laurin, coordonnateur.

Nagy, D.
1966: The gravitational attraction of a right rectangular prism; Geophysics, v. 31, no. 2, p. 372-397.

Taylor, J.
1980: A computer program for contouring oceanographic data using optimum interpolation; Canada Department of Fisheries and Oceans, Marine Environmental Data Service, Ottawa, Technical note No. 33, 131 p.

Teskey, D.J., Dods, S.D., and Hood, P.J.
1982: Compilation techniques for the 1:1 million magnetic map series; in Current Research, Part A, Geological Survey of Canada, Paper 82-1A, p. 351-358.

Thomas, M.D.
1974: The correlation of gravity and geology in south-eastern Quebec and southern Labrador; Earth Physics Branch, Ottawa, Gravity map series, No. 64-67, 96-98, 49 p.

35. A PRELIMINARY REPORT ON DRIFT PROSPECTING STUDIES IN LABRADOR: PART II

Project 820039

R.A. Klassen
Terrain Sciences Division

Klassen, R.A., A preliminary report on drift prospecting studies in Labrador: part II; in Current Research, Part A, Geological Survey of Canada, Paper 84-1A, p. 247-254, 1984.

Abstract

A study of glacial history and till geochemistry in east-central Labrador was continued during 1983. The last directions of regional ice flow were northeastward in the northern part of the area, and eastward to southeastward in the southern part. An earlier northward to north-northeastward phase of flow is recognized. Trace element geochemistry of clay-size and of pebble-size fractions of till is influenced by weathering (soil development). Trace metals are most abundant within the C soil horizon and decrease upward through the B and A horizons. Variations in the regional geochemistry of copper, nickel, and uranium in till generally match changes in regional bedrock type.

Résumé

L'étude de l'histoire glaciaire et de la géochimie des tills dans le centre-est du Labrador s'est poursuivie en 1983. L'écoulement régional le plus récent de la glace s'est fait en direction du nord-est dans la partie nord de la région et vers l'est et le sud-est dans la partie sud. Une phase d'écoulement plus ancienne vers le nord au nord-nord-est y est identifiée. La géochimie des oligo-éléments dans les fractions de till de la taille des argiles et des galets dépend du degré d'altération (évolution des sols). Les métaux à l'état de traces sont plus abondants dans l'horizon C et leur quantité diminue vers le haut dans les horizons B et A. Les variations dans la géochimie régionale du cuivre, du nickel et de l'uranium dans le till suivent généralement les changements dans le type de socle régional.

INTRODUCTION

The history of regional ice movement and the composition of drift in central and eastern Labrador have been studied by the Geological Survey to assist the development of drift prospecting techniques. Areas of fieldwork during 1982 and 1983 included the eastern part of Snegamook Lake (13K) and western part of Rigolet (13J) map areas (Melody Lake area), and during 1983, the eastern part of Ossokmanuan Lake (23H) and western part of Winokapau Lake (13E) map areas, (Churchill Falls area). This report refers only to results of field and laboratory work from the Melody Lake area; it expands on earlier comments by Klassen (1983) concerning ice flow directions and presents geochemical data based on analysis of samples collected during 1982.

Acknowledgments

Field assistance was capably and cheerfully provided by Mr. E. Ochs. Dr. C.F. Gower, Department of Mines and Energy, Newfoundland, provided camp logistical support and geological information concerning bedrock units and the origins of erratics, and he is thanked for his help. Mr. R. Bartlett, pilot, is thanked for his help and flying skills.

BEDROCK GEOLOGY

The study area occupies parts of the Nain and Grenville structural geological provinces and parts of the Makkovik Sub-Province. Bedrock includes a crystalline complex of gneiss, granite, and granitoid rocks of Archean to Helikian ages, and a sequence of sedimentary and volcanic supracrustal rocks of Aphebian and Helikian ages (Fig. 35.1). The supracrustal rocks include the Aphebian Moran Lake and Aillik groups, and the Paleohelikian Bruce River and Seal Lake groups. In the southern part, sedimentary rocks of the Hadrynian Double Mer Formation outcrop. The Proterozoic supracrustal rocks form part of the Central Mineral Belt of Labrador and are known to contain uranium and copper mineralization (Ryan, 1981, 1982a, b).

PREVIOUS WORK

Surficial materials of the study area have been mapped at 1:250 000 scale by Fulton et al. (1980a, b). Brief descriptions of ice flow directions in the Melody Lake area have been given by Vanderveer (1982) and Klassen (1983), who estimated that the last directions of regional ice flow were towards the east and southeast in the southern part of the study area and towards the northeast in the northern part. Both authors also found indications of ice flow oriented at about north to north-northeast. Klassen (1983) described erratics of sedimentary rock within the Melody Lake area derived from bedrock sources located more than 50 km to the west.

METHODS

The program of field sampling was conducted with helicopter (Bell 206) support. Sampling during 1983 was extended to the south and east of areas visited during 1982 to provide more complete coverage of the region. During reconnaissance mapping flights, landings were made to examine surficial deposits, landforms, and the evidence of ice flow directions, and till was sampled routinely for examination of clast lithology and for geochemical analysis. Throughout the study area till samples were collected at a density of about 1 per 10 000 ha for the purpose of characterizing regional variation in till composition. Samples were spaced more closely, at about 1 per 100 to 1 per 10 ha, near areas of known mineralization (eg. Michelin deposit) and areas of known mineralized erratics. Pits were dug to depths of 40-100 cm, depending on the depth to bedrock and the presence of coarse clasts, and samples were collected from the least oxidized soil horizon encountered near the base of the pit. To investigate the influence of weathering (e.g., soil development) on geochemistry, soil horizons were sampled sequentially in 15 test pits located throughout the area.

[1] Contribution to Canada-Newfoundland co-operative mineral program 1982-84. Project carried by Geological Survey of Canada

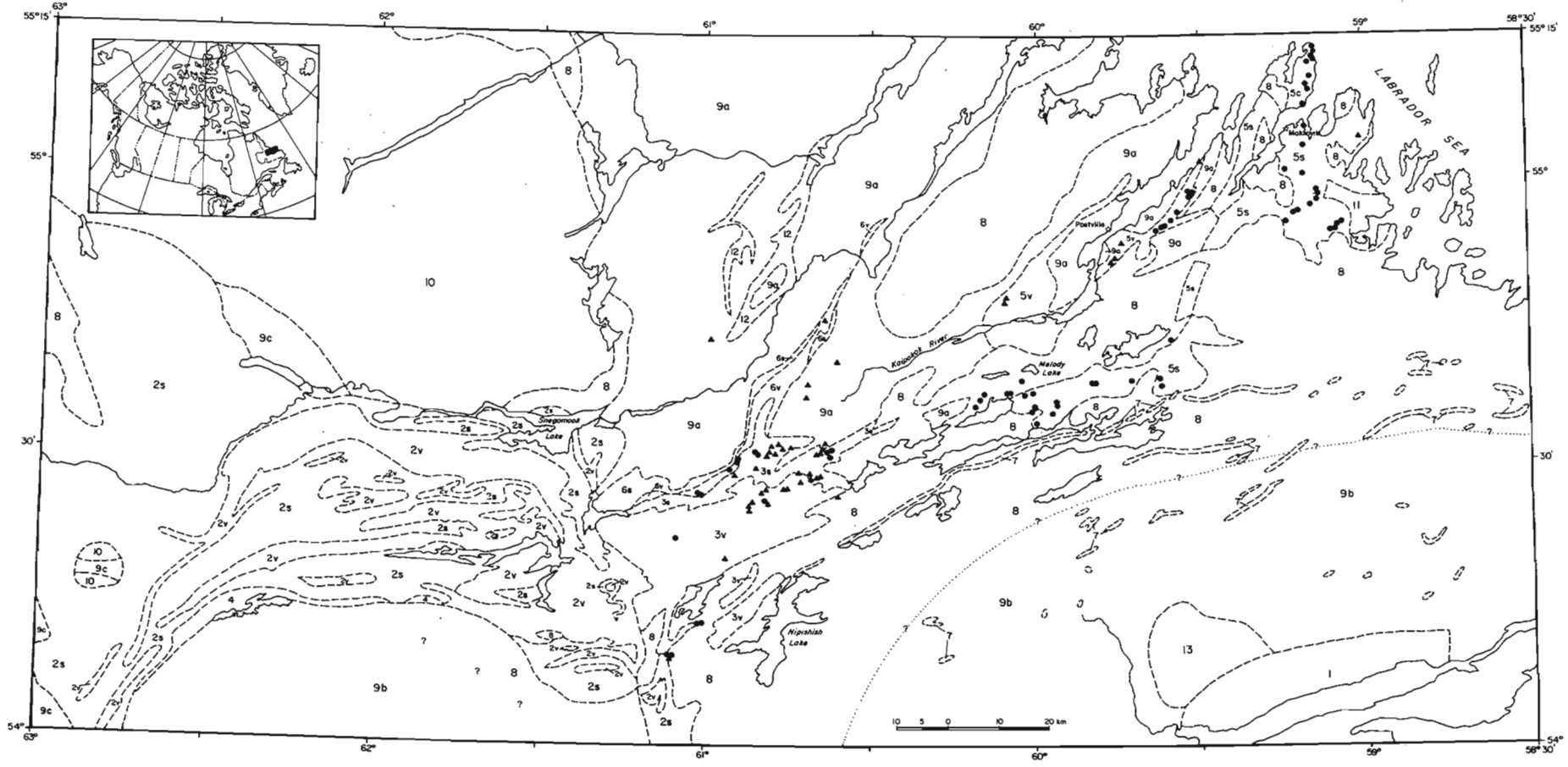

1 Double Mer Formation (Hadrynian)
conglomerate, arkose, sandstone

☼ 2 Seal Lake Group (Paleohelikian)
2s quartzite, conglomerate, arkose, sandstone, shale
2v mafic sills and flows

☼ 3 Bruce River Group (Paleohelikian)
3s conglomerate and sandstone
3v mafic and felsic volcanic rocks

☼ 4 Letitia Lake Group (Paleohelikian)
felsic volcanic rocks, sedimentary rocks

☼ 5 Aillik Group (Aphebian)
5s rhyolite, acid volcanogenic sediments, conglomerate
5v metabasalts, metasiltstones and sandstones

☼ 6 Moran Lake Group (Aphebian)
6s mudstone, slate, quartzite, siltstone, sandstone, dolostone
6v mafic volcanic and metavolcanic rocks

★ Intrusive and Metamorphic Rocks

7 Gabbro (Michael Gabbro)

8 Granitoid Intrusive Rocks

9 Gneiss
9a Hopedale Metamorphic Complex
9b Grenville Province
9c Churchill Province

10 Anorthosite Suite

11 Gabbro (Adlavik Intrusive Complex)

12 Metavolcanic rock and volcanogenic sediments

13 Mafic Intrusive (granulite facies)

Mineralization
▲ Copper
● Uranium

☼ Supracrustal rocks of the Central Mineral Belt
★ no stratigraphic order implied

Figure 35.1. *Generalized geological map of the Melody Lake study area and adjacent regions, east-central Labrador. Geology after Greene (1970), Gandhi (1978), Wardle and Bailey (1981), Gower et al. (1982), and Ryan (1981, 1982a, b).*

Figure 35.2

Bouldery ribbed moraine, shown forming a ridge oriented across the central part of the photograph between the lakes, is common within the study area. The boulders, which are large (>2 m) and form a nearly continuous cover, are most common in areas of granitoid bedrock south of Kaipokok River. Tree cover provides ground scale. (GSC 203803-I).

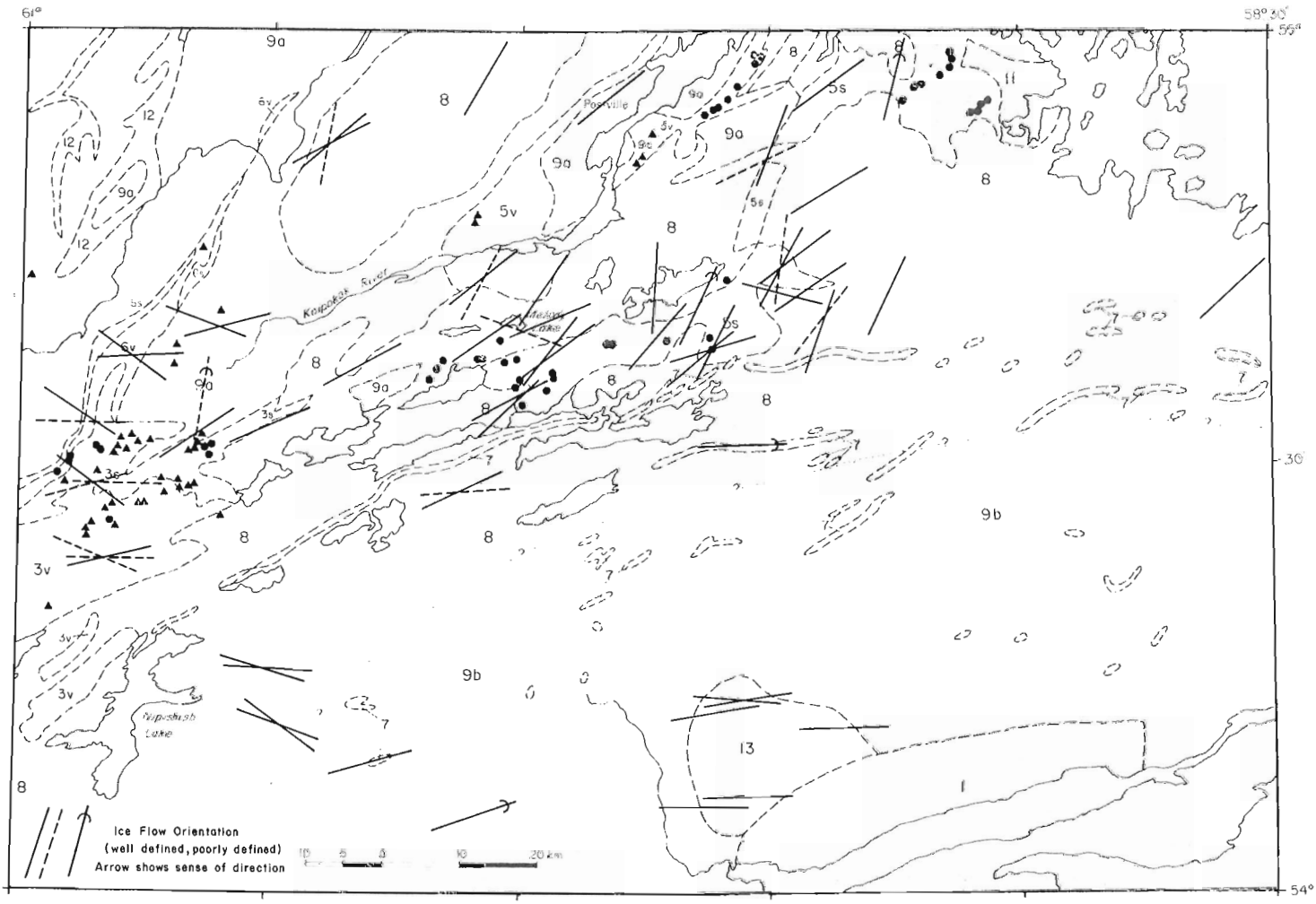

Figure 35.3. *Ice flow trends, based chiefly on glacial striae. Regional ice movement was generally eastward, based on streamlined bedrock landforms. Striae trending nearly north, found at four locations, are considered to predate the last phase of regional ice flow. A magnetic declination of N32°W has been assumed for all measurements. Bedrock geology is explained in Figure 35.1.*

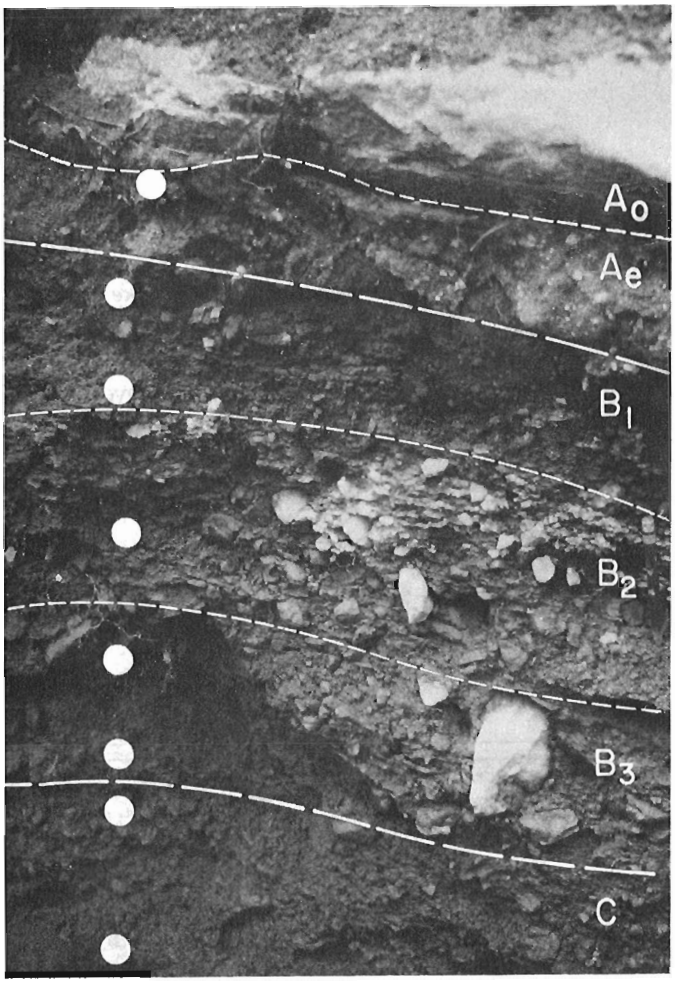

Figure 35.4. Podzol-like soil profile showing the different soil horizons commonly encountered during excavation of sample pits. Samples were collected at the points marked, and their trace metal contents are given in Figure 35.5. (GSC 203803-P).

The geochemical properties of till reported here are based on analysis of the clay-size (<0.002 mm) and of the pebble-size (2-4 mm) fractions. The two size fractions were chosen to compare the trace metal contents of two components of till that are considered likely to be distinct in their mineralogical and lithological makeup, and to further examine the influence of near-surface weathering. Clay is considered likely to retain elements released during weathering due to its higher content of phyllosilicate minerals and, consequently, its relatively high cation exchange capacity. Analysis for copper, lead, zinc, nickel, chromium, molybdenum, manganese, and iron was done, using atomic absorption methods, by Bondar-Clegg and Company Ltd. (Ottawa). Analysis for uranium was done using fluorimetric and delayed neutron activation methods.

RESULTS AND DISCUSSION

Surficial geology

Within the Melody Lake area till is extensive at the surface and is characteristically sandy and bouldery. In the northern part, till is thin (<2 m) to discontinuous over hilltops, and is much thicker across valley floors where it forms extensive areas of ribbed moraine (Rogen moraine) (Fig. 35.2). In areas of granitoid rocks, south of Kaipokok River, till is dominated by large (>2 m) boulders that form a nearly continuous surface cover. Sampling of till in such areas can be extremely difficult due to the boulder cover.

In the southern part of the area, which is underlain by gneisses of the Grenville Province, till appears generally to be sandier and thicker, forming extensive areas of hummocky drift and streamlined landforms in the lee of bedrock hills. Some till deposits were found to be partially stratified, containing sand lenses and minor bedding, and are considered to have been deposited during deglaciation.

Directions of ice movement

Glacial striae vary in orientation from north-northeast to southeast within the Melody Lake study area (Fig. 35.3). Across the northern part of the area nearly all striae are oriented generally northeast, and across the southern part they are generally southeast to east. Because many were measured on hilltops and, in some cases, are oriented across topographic trends, the striae are thought to be the product of the last major phase of regional ice movement. Streamlined crag-and-tail landforms in the southern part (Fulton et al., 1980a) are similar in orientation to the striae reported here and indicate that ice flow was eastward towards the Labrador Sea; no evidence of flow having a westward component has been recognized.

At four separate locations striae and small grooves trending north to north-northeast, across the regional trends reported above, were observed (Fig. 35.3). At three of the sites the glacial markings were poorly defined and were not found within glacial polish. The fourth site was located near the coast, at the summit of Monkey Hill (elevation 700 m a.s.l.), overlooking the town of Makkovik, where all recorded striae in glacial polish trended N13°E; the streamlined form of bedrock at the summit indicated northward ice flow.

The nearly northward-oriented striae are interpreted to have been formed prior to the last regional phase of ice flow because they are not found generally within glacial polish and are poorly preserved. They indicate that a dispersal centre could have been located south to southwest of the study area during their formation. Alternatively, the ice moving eastward towards the Labrador Sea could have been turned northward within the Melody Lake area by flow from a separate dispersal centre located to the east or southeast.

With regard to the marked variations in directions of ice flow within the study area, reported above, the orientations of glacial dispersal trains could be expected to vary accordingly. Prospecting for the bedrock sources of dispersal trains requires that the regional history of ice flow be known to establish how local flow directions could have changed during the course of glaciation.

Distributions of indicator lithologies

Erratics of sedimentary rock, including red arkosic sandstone, conglomerate, and red quartzite derived from Proterozoic units west of Nipishish Lake (Fig. 35.1), were found as far east as the area of Postville and the western flanks of Mount Benedict. Their distribution is extended eastward of that reported by Klassen (1983) and demonstrates glacial transport distances of more than 100 km. Source areas are considered to most likely include the Seal River and Bruce River groups (Fig. 35.1).

Compositional evidence of early northward ice flow has not been recognized.

Till geochemistry

Soil profiles appear commonly to be Podzol-like, having a surface organic-rich Ao horizon, a bleached eluviated Ae horizon and iron-stained B_1 and B_2 horizons all of which overlie sediment without obvious weathering – the C horizon (Fig. 35.4). At wet, poorly drained sites, soils generally lack an eluviated horizon, the zone of iron stain is wider, and iron oxides can form a cemented (ortstein) layer.

Trace element geochemistry of till varies with the position of the sample within the near-surface zone of weathering. Among samples collected from individual soil profiles, the content of trace metals within clay is consistently greatest within the least weathered part of the profile exposed at the base of sample pits and decreases upwards to the eluviated horizon (Fig. 35.5). Metal concentrations within the clay-size fraction can change by an order of magnitude between the bottom and top of metre-deep pits for some of the elements analyzed. Although relative change in metal content is much greater within clay, profiles of the trace metal variation in the pebble-size fraction appear similar to those based on analysis of clay and metal concentrations decrease upward within test pits.

The geochemical differences observed within the sample pits are associated here with weathering processes and are not the result of compositional change associated with a bipartite sequence of 'basal' till and overlying 'ablation' till. Neither lithological nor gross textural change was noted within the test pits to indicate the presence of two compositionally distinct sediment types. In addition, the patterns of change in trace elements match closely those of iron and manganese which are easily mobilized and are associated with soil development.

The abundance of trace metals is not greatest within the iron-stained B horizon, contrary to the generalized profile shown by Levinson (1974, p. 98). The profiles (Fig. 35.5) indicate that in both size fractions, trace elements are depleted in the A and B horizons relative to their levels within sediment of the underlying C horizon. Similar trends

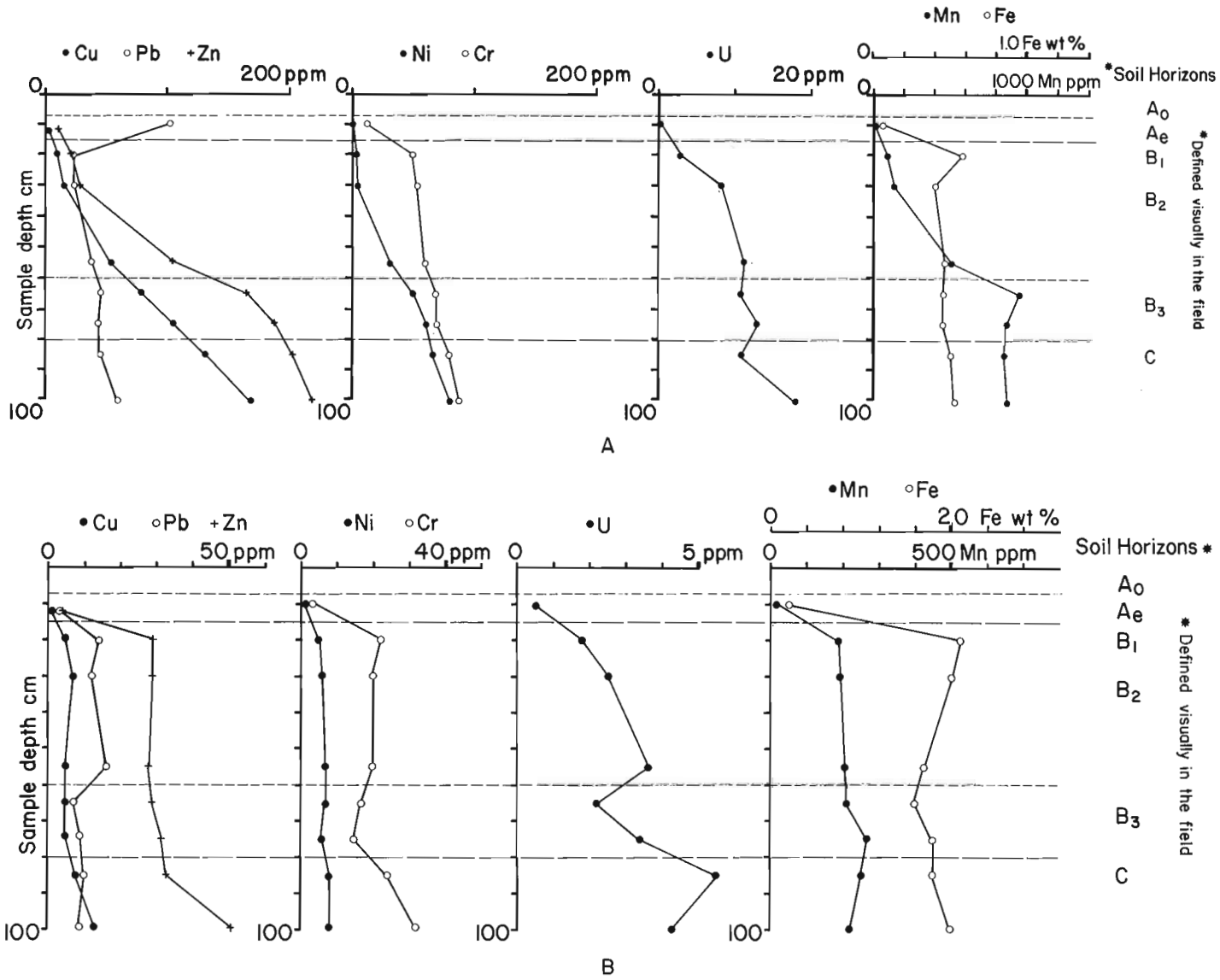

Figure 35.5. *Trace element variation in (A) clay-size (<0.002 mm) and (B) pebble-size (2-4 mm) fractions within the soil profile shown in Figure 35.4. The pit was dug within a dispersal train of uraniferous erratics, and metal contents are generally greater than found elsewhere in the study area. The shapes of the trace element profiles are, however, typical.*

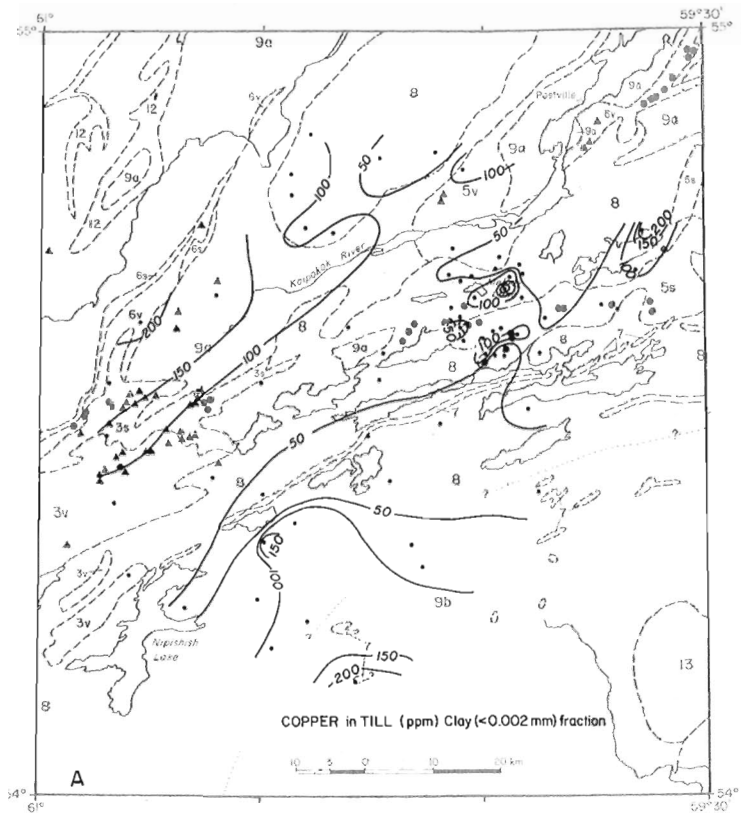

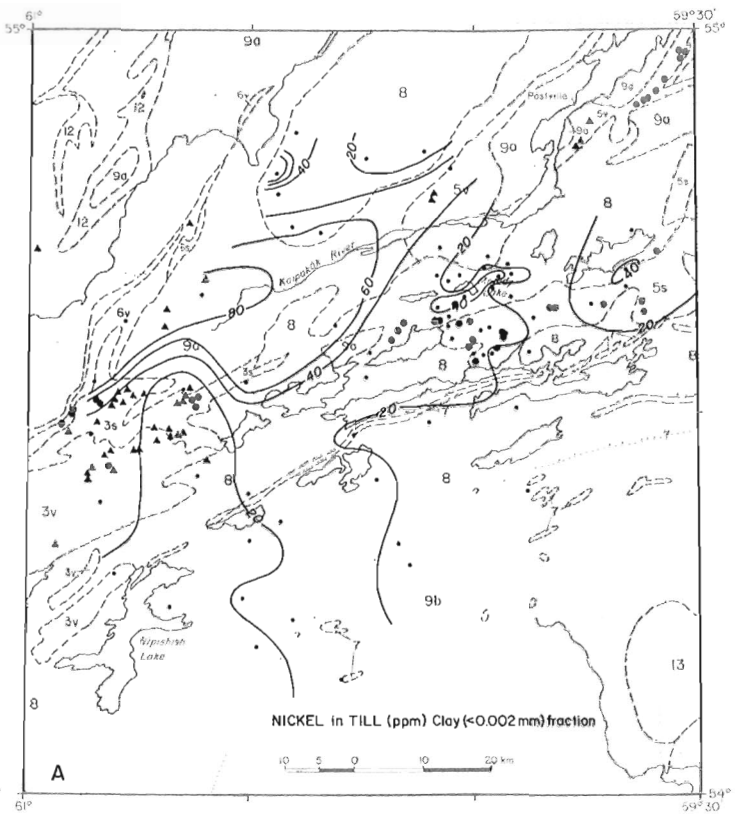

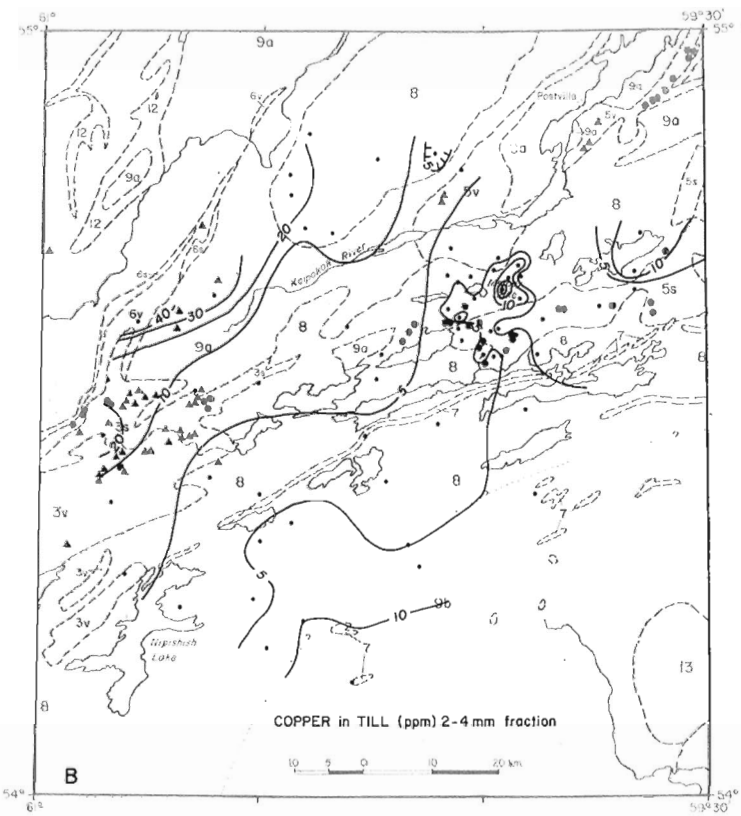

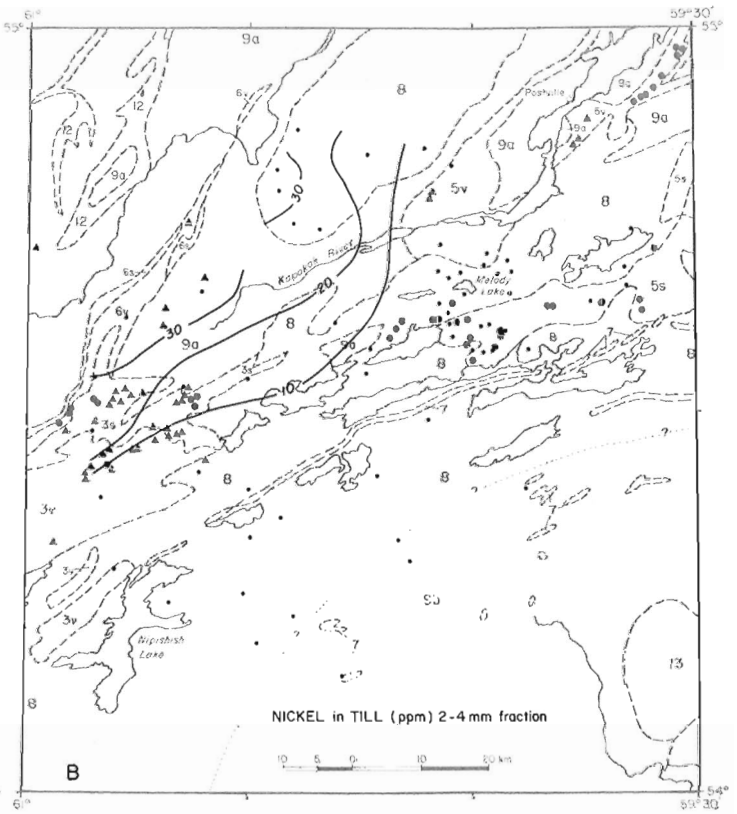

Figure 35.6. *Regional variation in the copper content in the (A) clay-size (<0.002 mm) and (B) pebble-size (2-4 mm) fractions of till. Bedrock geology is explained in Figure 35.1.*

Figure 35.7. *Regional variation in the nickel content in the (A) clay-size (<0.002 mm) and (B) pebble-size (2-4 mm) fractions of till. Bedrock geology is explained in Figure 35.1.*

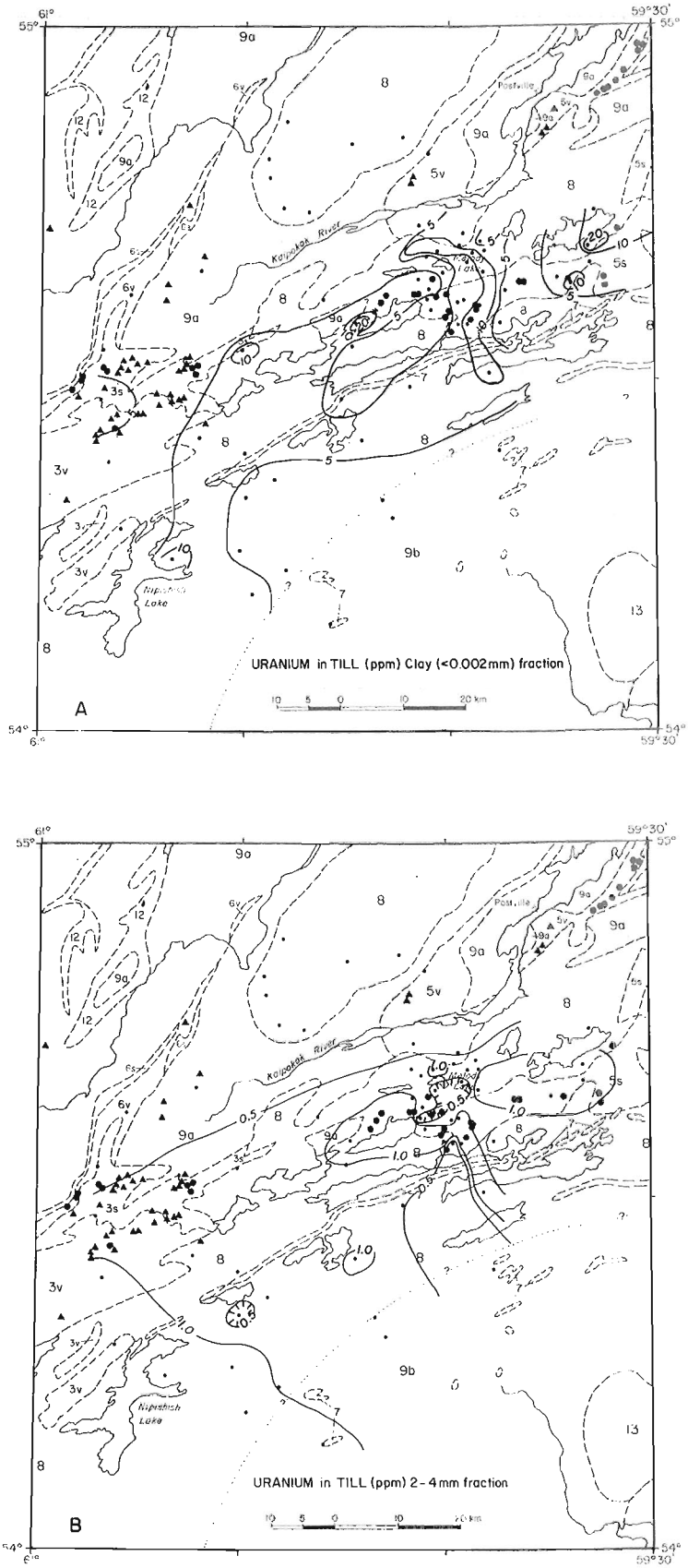

Figure 35.8. Regional variation in the uranium content in the (A) clay-size (<0.002 mm) and (B) pebble-size (2-4 mm) fractions of till. Bedrock geology is explained in Figure 35.1.

were found in pits dug in areas of 'background' and 'anomalous' metal levels. Because there is less relative change in metal concentration among samples collected near the base of the B or upper C soil horizons, the least oxidized sediment provides a better basis for geochemical comparison among samples from different sites.

Despite the geochemical variation related to weathering, broad trends in the geochemistry of till appear to reflect differences in regional bedrock geology (Fig. 35.6 to 35.8). The general distribution of trace elements in till is similar for the clay and pebble fractions, although contour patterns are slightly more complex for the clay fraction. Contoured patterns follow the regional northeast to east strike of the principal bedrock units, and trace element levels can vary significantly across the study area.

Copper and nickel levels are greatest in the northwest part of the study area, in areas of gneiss of the Nain Province, and are least in the southeastern part in areas of gneiss and granitoid rocks of the Grenville Province. Areas of Bruce River volcanic rock in the west-central part, which are characterized by numerous reported sites of copper mineralization (Ryan, 1982a, b), are not associated with regionally higher levels of copper in till (Fig. 35.1).

High copper and nickel concentrations at the western edge of the granite complex north of Kaipokok River could be due either to the composition of local bedrock or to northeastward glacial transport of metal-enriched till. Although the correct interpretation is not known, it is noted that elsewhere over the granite, metal concentrations are low. Till to the southwest (up ice) of the granite, however, is characterized by regionally elevated metal levels.

Regional geochemical patterns associated with uranium differ from those of copper and nickel and outline a central zone of enrichment that is more or less coincident with supracrustal rocks of the Central Mineral Belt and, in particular, the Aillik Group. Within the central zone, single samples characterized by anomalously high uranium levels occur. The significance of the anomalous samples is unclear, although they would appear to be related to local bedrock sources. Sites of known uranium mineralization (Fig. 35.1) are reported by Ryan (1982a, b).

CONCLUSIONS

The principal directions of ice flow within the study area during the last regional phase of glaciation are northeastward in the northern part of the area and eastward to southeastward in the southern part. There is indication of an earlier, nearly northward to north-northeastward phase of flow. Erratics of sedimentary rock derived from supracrustal bedrock suites have been found to the eastern limits of the area, demonstrating glacial transport distances of more than 100 km.

The geochemistry of till is influenced by weathering (soil formation), and trace metal levels are greatest within sediment of the least weathered (C horizon) zone for the clay-size (<0.002 mm) and pebble-size (2-4 mm) fractions. Consequently, analysis of the till collected from the C horizon is considered to provide the best basis for geochemical comparison of samples collected from different sites.

Patterns of regional geochemical variation in till generally outline the major geological units, although elevated metal levels do not necessarily indicate areas of greatest mineral potential, as indicated by the distribution of mineralized showings in bedrock. The trace element levels in till reported here provide a background for the recognition of anomalous samples encountered at a more detailed scale of sampling within the Melody Lake area.

REFERENCES

Fulton, R.J., Hodgson, D.A., Mining, G.V., and Thomas, R.D.
1980a: Surficial materials, Rigolet, Labrador; Geological Survey of Canada, Map 26-1979, scale 1:250 000.

Fulton, R.J., Hodgson, D.A., and Mining, G.V.
1980b: Surficial materials, Snegamook Lake, Labrador; Geological Survey of Canada, Map 29-1979, scale 1:250 000.

Gandhi, S.S.
1978: Geological setting and genetic aspects of uranium occurrences in the Kaipokok Bay – Big River area, Labrador; Economic Geology, v. 73, no. 8, p. 1492-1522.

Gower, C.F., Flanagan, M.J., Kerr, A., and Bailey, D.G.
1982: Geology of the Kaipokok Bay – Big River area, Central Mineral Belt, Labrador; Department of Mines and Energy, Newfoundland and Labrador, Report 82-7, 77 p.

Greene, B.A.
1970: Geological map of Labrador; Department of Mines, Agriculture and Resources, Province of Newfoundland and Labrador, scale 1:1 000 000.

Klassen, R.A.
1983: A preliminary report on drift prospecting studies in Labrador; in Current Research, Part A, Geological Survey of Canada, Paper 83-1A, p. 353-355.

Levinson, A.A.
1974: Introduction to Exploration Geochemistry; Applied Publishing, Calgary, 612 p.

Ryan, B.
1981: Volcanism, sedimentation, plutonism and Grenvillian deformation in the Helikian basins of Central Labrador; in Proterozoic Basins of Canada, ed. F.H.A. Campbell; Geological Survey of Canada, Paper 81-10, p. 361-378.

1982a: Geology of the Central Mineral Belt (central part – sheet 1); Mineral Development Division, Department of Mines and Energy, Government of Newfoundland and Labrador, Map 82-3.

1982b: Geology of the Central Mineral Belt (central part – sheet 2); Mineral Development Division, Department of Mines and Energy, Government of Newfoundland and Labrador, Map 82-4.

Vanderveer, D.G.
1982: Reconnaissance glacial mapping in the Melody Lake – Anna Lake area, Labrador; in Current Research, Report 82-1, ed. C.F. O'Driscoll and R.V. Gibbons; Department of Mines and Energy, Newfoundland and Labrador, p. 235-236.

Wardle, R.J. and Bailey, D.G.
1981: Early Proterozoic sequences in Labrador; in Proterozoic Basins of Canada, ed. F.H.A. Campbell; Geological Survey of Canada, Paper 81-10, p. 331-359.

36. ICE FLOW DIRECTIONS AND DRIFT COMPOSITION, CHURCHILL FALLS, LABRADOR[1]

Project 820039

R.A. Klassen and A. Bolduc[2]
Terrain Sciences Division

Klassen, R.A. and Bolduc, A., Ice flow directions and drift composition, Churchill Falls, Labrador; in Current Research, Part A, Geological Survey of Canada, Paper 84-1A, p. 255-258, 1984.

Abstract

Two principal phases of regional ice flow are identified in the area of Churchill Falls, Labrador: an early phase of northeastward flow and a later phase of eastward to southeastward flow. Evidence of northeastward flow indicates that a dispersal centre of the Laurentide Ice Sheet may have been located south of Churchill River prior to Late Wisconsinan time. Most striae and glacially streamlined landforms are associated with the later phase. Drift composition appears to be the product of eastward to southeastward ice flow; erratics derived from the Labrador Trough are widespread.

Résumé

Deux phases principales d'écoulement glaciaire régional sont identifiées dans la région de Churchill Falls, au Labrador: une phase ancienne d'écoulement en direction nord-est et une phase plus récente vers l'est et le sud-est. Les traces d'écoulement vers le nord-est indiquent qu'il existait peut-être un centre de dispersion de l'inlandsis des Laurentides au sud du fleuve Churchill avant la fin du Wisconsinien. La plupart des stries et des formes de relief profilées par la glace sont associées à la phase plus récente. La composition des sédiments glaciaires semble être le résultat d'un écoulement vers l'est et le sud-est; des blocs erratiques provenant du fossé du Labrador sont très répandus.

INTRODUCTION

The history of ice movement and the composition and geochemical properties of till in the area of Churchill Falls, Labrador, were investigated by the Geological Survey during the summer of 1983. The project is part of a study initiated during 1982 in the area of east-central Labrador (Klassen, 1983, 1984) to assist mineral exploration in the region. This is a preliminary account of the results of 1983 fieldwork; no laboratory analyses of samples are currently available. The study area includes the western part of Winokapau Lake (13 E) and eastern part of Ossokmanuan Lake (23 H) map areas; Churchill Falls lies in the centre of the study area (Fig. 36.1). The area is crossed by roads built to service dikes of the Smallwood Reservoir, the Twin Falls power development, and to connect Esker, on the Quebec North Shore and Labrador Railway, with Churchill Falls and Goose Bay.

Acknowledgments

Ms. H. Earnshaw and Mr. E. Ochs are thanked for their assistance in the field. The Churchill Falls (Labrador) Corporation allowed use of its facilities, and both the Corporation and people of the town of Churchill Falls provided much helpful assistance during the course of field operations. Dr. A. Thomas, Newfoundland Department of Mines and Energy, helped greatly in the identification of erratics and their source areas. This work forms part of an M.Sc. thesis study in progress by A. Bolduc.

BEDROCK GEOLOGY

The Churchill Falls study area occupies parts of the Churchill and Grenville structural geological provinces. The southern part of the area is underlain mainly by quartzofeldspathic gneisses. The northern part is characterized by quartzofeldspathic gneisses and granulites; by intrusive rocks, including anorthosites, gabbros, and acidic intrusives; and by sedimentary and volcanic supracrustal rocks of the Aphebian Petscapiskau Group, which outcrop along the southern part of the Smallwood Reservoir (Greene, 1970). Rocks of the Labrador Trough, including sedimentary and volcanic rocks, lie within the westernmost part.

PREVIOUS WORK

The first descriptions of surficial deposits within the study area were given by Low (1896) based on observations made during his travels through the region. Later Quaternary geological work was assisted by roads and supply services associated with hydroelectric development at Twin Falls and at Churchill Falls. Kirby (1961) described esker systems along the road between Twin Falls and Esker, and Morrison (1963, 1966) described glacial striae, till fabric, and aspects of till composition in the study area. Morrison first identified an early phase of ice flow from the southwest and a later phase of flow from the northwest. Fulton et al. (1975), Fulton and Hodgson (1979), and Fulton et al. (1981a,b) conducted an inventory survey of the Quaternary geology of the area which resulted in a report on glacial retreat in the area and surficial materials maps at 1:250 000 scale.

METHODS

A four-wheel-drive vehicle was used to examine the surficial geology along roads, and helicopter (Bell 206) was used to extend field sampling and observations into areas without roads. Surficial deposits were sampled at intervals of 1 to 10 km along roads, generally from borrow pits made during road construction. Large (>20 m) stratigraphic sections encountered along Churchill, Metchin, and Unknown rivers were also sampled. In all, about 450 samples were collected. Striae orientations were measured and recorded at most sample sites; magnetic declination was taken as N30°W throughout the study area.

DIRECTIONS OF ICE MOVEMENT

Two sets of glacial striae are recorded that are distinct in age and orientation (Fig. 36.1). The most widespread and best developed set is displayed prominently on the stoss and upper surfaces of streamlined bedrock and is aligned

[1] Contribution to Canada-Newfoundland Co-operative mineral program 1982-84. Project carried by Geological Survey of Canada.

[2] Carleton University, Ottawa, Ontario K1S 5B6

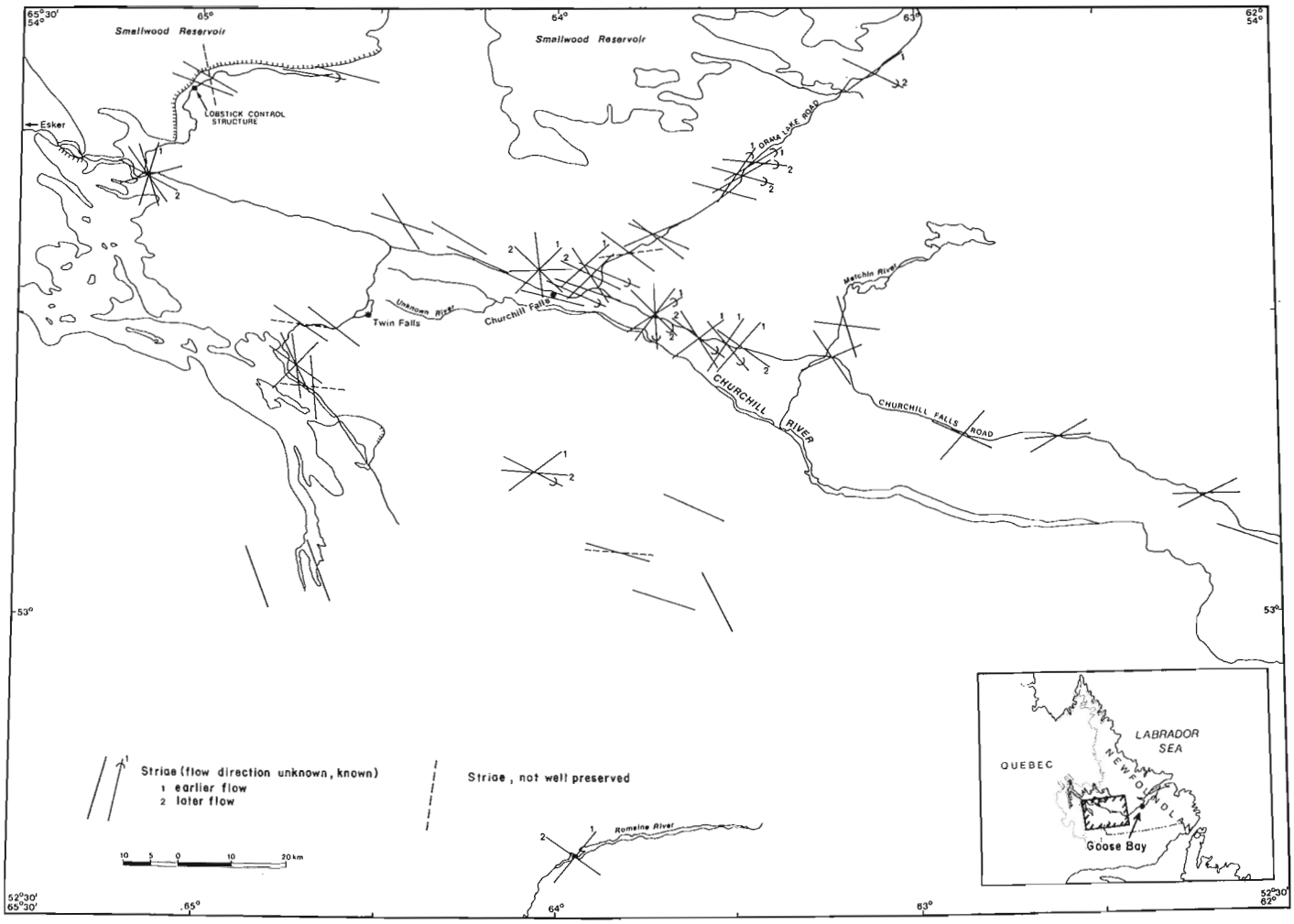

Figure 36.1. *Striae trends within the Churchill Falls study area. The most common striae set is aligned generally southeast; these striae were formed during the last phase of regional ice flow. A widespread, earlier-formed set of striae trends northeast. Magnetic delineation is assumed to be N30°W.*

generally with the streamlined form of the outcrops (Fig. 36.2a). Striae are oriented east to southeast and are consistent with regional patterns of ice flow given by Prest et al. (1968). The striae are considered to have been formed during the last regional phase of ice flow by ice flowing from north-central Quebec.

The second set of striae is oriented northeast, directly across trends of the last regional phase of ice flow (Fig. 36.2b). These striae are developed commonly on the lee surfaces of streamlined bedrock and were found along the Churchill Falls road between the road to Lobstick dykes and Metchin River, a distance of more than 170 km. They have also been reported in the area of Romaine River, 100 km south of Churchill Falls (A. Thomas, personal communication, 1983). Streamlined glacial landforms that are oriented southwest-northeast are shown north of the Churchill Falls road between the Orma Lake road and Metchin River on the regional surficial geology map of Fulton et al. (1981b). The northeast-oriented striae are considered to predate the last phase of regional ice flow because they are preserved only on the lee side of bedrock and are not found across the upper surfaces. Ice flow was towards the northeast during their formation, based on small-scale stoss-and-lee features on surfaces bearing the striae.

DISTRIBUTION OF ERRATICS

Erratics derived from supracrustal rocks of the Labrador Trough and Petscapiskau Formation occur throughout the study area. The erratics include iron formation, quartzite, slate, carbonate rocks, and arkosic sandstones. For purposes of field identification, only erratics of iron formation and carbonate rocks are considered to have been derived from the Trough, and their known distribution is consistent with eastward to southeastward ice flow of the last regional phase of glaciation. A single erratic of iron formation, which is also thought to have been derived from the Labrador Trough, was found in till near Goose Bay (east of the study area) and represents glacial transport of more than 300 km to the southeast. The bulk of coarse clasts within till, however, is composed of erratics of crystalline and metamorphic rocks that are not considered to be far travelled.

An erratic of augen gneiss that appears to be derived from bedrock south of Churchill River (A. Thomas, personal communication, 1983) was found 40 km northeast of the river. The rock was strongly deformed and recrystallized, and no similar bedrock is known, on a regional basis, north of Churchill River. It is considered to be compositional evidence of the earlier, northeastward phase of ice flow.

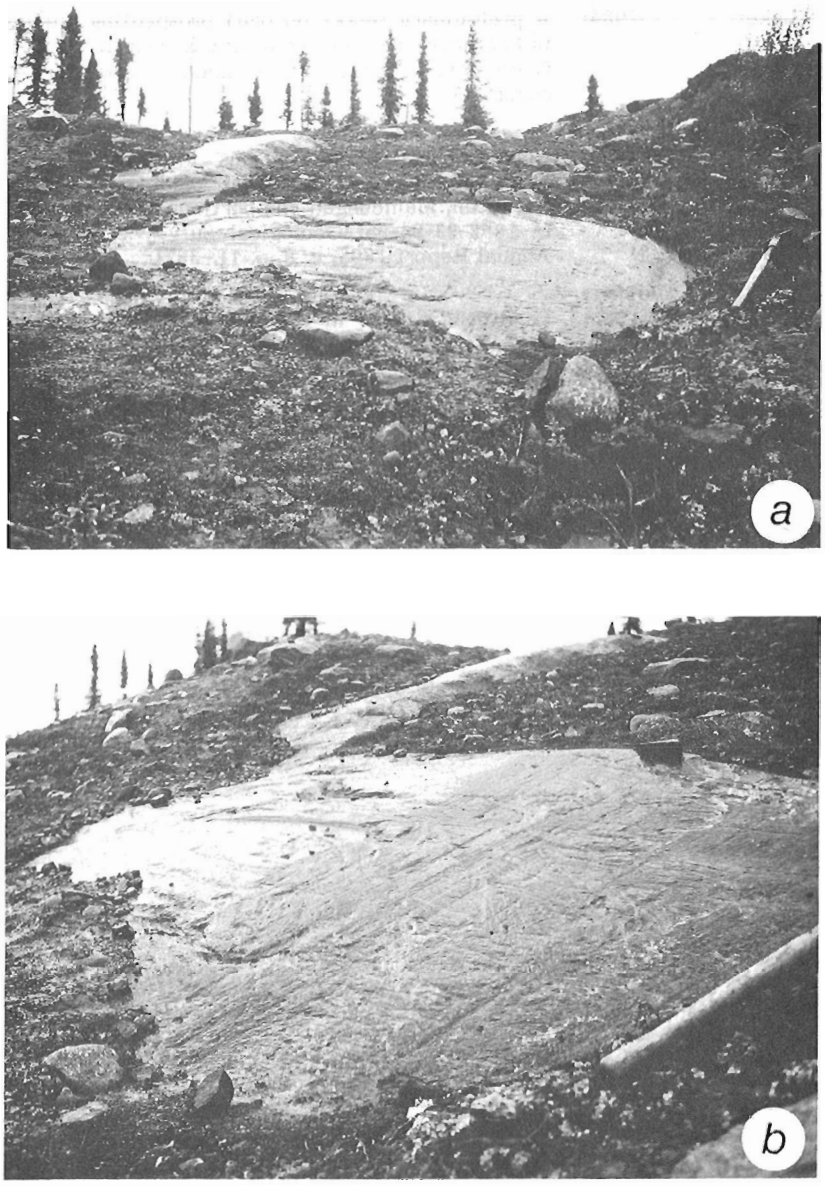

Figure 36.2. Glacially polished bedrock bearing two distinct sets of striae. The youngest striae trend southeast and occur on the upper surface of the bedrock (A); the older striae, trending northeast, are commonly preserved on the southeastern face of outcrops (B).

No similar evidence has been recognized in the area of streamlined landforms having a northeast orientation west of Metchin River.

Red till was found along the Lobstick road, north of the Lobstick control structure, and along the Orma Lake road, beyond a point about 50 km northeast of the town of Churchill Falls (Fig. 36.1). Red till also extends eastward along the Churchill Falls road from a point about 40 km east of Esker. It was not found, however, at the junction with the Lobstick road.

The red colouring is interpreted to have been produced by erosion of rocks from the Petscapiskau Group southeast of Lake Michikamau in the case of the till found on the Orma Lake road, and from erosion of the Sims Formation west of Sandgirt Lake in the case of the till on the Churchill Falls road. The source of the red till on the Lobstick road has not been resolved yet, but is tentatively linked with rocks of the Petscapiskau Group, north of Lobstick Lake.

DISCUSSION

Implications for glacial history

The widespread distribution of northeast-oriented striae and the compositional evidence of northeast transport by ice indicate that the northeast phase of ice flow was of large scale and likely represents an important phase of glaciation. Evidence of northeast flow, predating the last regional flow, found in the Schefferville area (Kirby, 1961) to the northwest may be related and contemporaneous. The northeast-oriented striae of the Churchill Falls area predate the last, presumably Late Wisconsinan, glaciation and could relate to early or mid-Wisconsinan stages in the development and growth of the Laurentide Ice Sheet. Their orientation indicates that ice flow was northeastward from a dispersal centre southwest of the study area that may have been situated on the broad height-of-land located south of Churchill Falls and north of St. Lawrence River. The dispersal centre may have later shifted westward and northward to northern Quebec.

Implications for drift prospecting

Based on the widespread distribution of erratics derived from the Labrador Trough, preliminary interpretations of field observations are that drift composition is largely the product of eastward to southeastward glacial flow. However, the orientation of large streamlined landforms west of Metchin River and the single erratic of augen gneiss derived from bedrock south of Churchill River indicate that drift may also contain a component that underwent initially northeastward glacial transport. Search for the bedrock source of mineralized erratics within the study area could be made more complex by such an earlier phase of transport.

CONCLUSIONS

Within the Churchill Falls area the last direction of regional ice flow was eastward to southeastward. This ice flow is predated by a northeastward phase of flow that may be associated with a major dispersal centre of the Laurentide Ice Sheet located south of Churchill River.

The drift contains erratics derived from the Labrador Trough, and drift composition appears generally to be controlled by the last phase of regional ice flow.

REFERENCES

Fulton, R.J. and Hodgson, D.A.
1979: Wisconsin glacial retreat, southern Labrador; in Current Research, Part C, Geological Survey of Canada, Paper 79-1C, p. 17-21.

Fulton, R.J., Hodgson, D.A., and Mining, G.V.
1975: Inventory of Quaternary geology, southern Labrador; An example of Quaternary geology – terrain studies in undeveloped areas; Geological Survey of Canada, Paper 74-46, 14 p.

Fulton, R.J., Hodgson, D.A., and Mining, G.V.
1981a: Surficial Materials, Ossokmanuan Lake; Geological Survey of Canada, Map 29-1979.

Fulton, R.J., Hodgson, D.A., Thomas, R.D., and Mining, G.V.
1981b: Surficial Materials, Winokapau Lake; Geological Survey of Canada, Map 21-1979.

Greene, B.A.
1970: Geological map of Labrador; Department of Mines, Agriculture and Resources, Province of Newfoundland and Labrador, scale 1:1 000 000.

Kirby, R.P.
1961: Movements of ice in central Labrador-Ungava; Cahiers de Géographie de Quebec, no. 10, p. 205-218.

Klassen, R.A.
1983: A preliminary report on drift prospecting studies in Labrador; in Current Research, Part A, Geological Survey of Canada, Paper 83-1A, p. 353-355.

Klassen, R.A. (cont.)
1984: A preliminary report on drift prospecting studies in Labrador: Part II; in Current Research, Part A, Geological Survey of Canada, Paper 84-1A, report 35.

Low, A.P.
1896: Report on the explorations in the Labrador Peninsula along the East Main, Koksoak, Hamilton, Manicuagan and portions of other rivers in 1892-93-94-95; Geological Survey of Canada, Annual Report 1895, v. 8, p. 1L-387L.

Morrison, A.
1963: Landform studies in the middle Hamilton River area, Labrador; Arctic, v. 6, p. 273-275.

1966: Glacial geomorphology of the Churchill Falls area, Labrador; unpublished Ph.D. thesis, Department of Geography, McGill University.

Prest, V.K., Grant, D.R., and Rampton, V.N.
1968: Glacial map of Canada; Geological Survey of Canada, Map 1253A, 1:5 000 000.

37. LATE WISCONSINAN GLACIATION AND DEGLACIATION OF WOLLASTON PENINSULA, VICTORIA ISLAND, NORTHWEST TERRITORIES

Project 830018

David R. Sharpe
Terrain Sciences Division

Sharpe, D.R., Late Wisconsinan glaciation and deglaciation of Wollaston Peninsula, Victoria Island, Northwest Territories; in Current Research, Part A, Geological Survey of Canada, Paper 84-1A, p. 259-269, 1984.

Abstract

Detailed study of glacial landforms has allowed a sequence of ice retreat maps to be produced for Wollaston Peninsula showing frontal and/or areal stagnation of full ice cover. Frontal retreat consists of a sequence of end moraine fragments and ice marginal outwash terraces and fans that can be traced across central Wollaston Peninsula. These features indicate that free drainage occurred to the west coast during this frontal retreat. Little evidence exists for damming of glacial meltwater.

Areal stagnation produced large tracts of hummocky moraine when active ice became detached from extensive thin, cold-based, upland ice. This areal stagnation can be related to a large continuous moraine system – Colville moraine – and a zonation of landforms adjacent to it. The glacial landforms are arranged as a regular sequence representing an energy profile across a former ice stream. This arrangement of landforms supports the concept of complete ice cover for Wollaston Peninsula as do landform arrangements on the adjacent landmass south of Dolphin and Union Strait (Melville Hills).

The till deposited by this latest glacial advance can be traced continuously across the upland on Wollaston Peninsula. Stratigraphic sections show only one transgressive regressive marine sequence that relates to this glacial advance. The 300 m end moraine ice limit previously proposed for Wollaston Peninsula represents an ice position ending in the sea well short of the full glacier cover. If this moraine represents the Late Wisconsinan limit, a second marine limit should be evident – a prediction that is not borne out by field studies.

Résumé

L'étude détaillée des reliefs glaciaires a permis de produire une série de cartes du recul glaciaire dans la péninsule Wollaston; ces cartes montrent la stagnation frontale, aréolaire ou les deux de toute la couverture de glace. Le recul frontal est marqué par une série de fragments de moraines frontales et de terrasses et de cônes fluvio-glaciaires marginaux qu'il est possible de suivre en travers de la partie centrale de la péninsule Wollaston. Ces éléments indiquent qu'il y a eu drainage libre vers la côte ouest au cours du recul frontal. Il y a peu d'indications de l'endigage des eaux de fonte glaciaires.

La stagnation aréolaire a produit de vastes étendues de moraines bosselées lorsque la glace active s'est détachée de la glace étendue, peu épaisse et à base froide des hautes-terres. Il est possible d'établir un lien entre la stagnation aréolaire et un vaste réseau morainique continu, les moraines Colville, et une zonation des formes de terrain qui y sont contigues. Les formes de terrain glaciaires sont réparties en une séquence régulière qui représente un profil énergétique en travers d'un ancien torrent glaciaire. Cette répartition topographique, ainsi que celle de la masse continentale au sud du détroit de Dolphin et Union (collines Melville), appuie la notion que la couverture de glace était complète dans la péninsule Wollaston.

Le till déposé au cours de cette dernière avancée glaciaire peut être suivi continuellement de part de d'autre des hautes-terres dans la péninsule Wollaston. Les sections stratigraphiques montrent qu'il n'existe qu'une seule séquence marine transgressive-régressive liée à cette avancée glaciaire. La limite glaciaire de la moraine frontale de 300 m, antérieurement proposée pour la péninsule Wollaston, représente une position de la glace qui se termine dans la mer, bien avant la limite de la couverture glaciaire complète. Si la moraine en question représente une limite datant du Wisconsinien supérieur, une deuxième limite marine devrait également être manifeste; à date, les études sur le terrain n'ont pas réussi à confirmer cette prédiction.

INTRODUCTION

The extent and timing of the northwest limit of the Laurentide Ice Sheet during Wisconsinan time have recently been elucidated for Banks Island (Vincent, 1978, 1980, 1982, 1983). This work is continuing on adjacent Victoria Island and similarities between the Banks Island and Victoria Island data have been pointed out (J-S. Vincent, personal communication, 1982). Vincent (1982) suggested full glacial cover during Early Wisconsinan time and partial glacial cover during Late Wisconsinan time for Wollaston Peninsula (Fig. 37.1), Victoria Island.

This report presents field evidence that leads to an alternate hypothesis for glacial cover on Wollaston Penninsula.

Methods

The glacial landforms of Wollaston Peninsula have been mapped in detail based on aerial photograph interpretation (1:60 000) and four weeks of fieldwork. These results are presented in two ways. First, a zoned assemblage of landforms has been identified and illustrated for southern Wollaston Peninsula. Second, a series of ice position diagrams is presented to illustrate a deglaciation pattern for western Wollaston Peninsula. These two data sets form the basis for comparing the relative ice extent on Wollaston Peninsula.

Melville Hills on the adjacent mainland were studied by airphoto interpretation only. This allowed a comparison with landform assemblages and the glacial limits on southern Wollaston Peninsula.

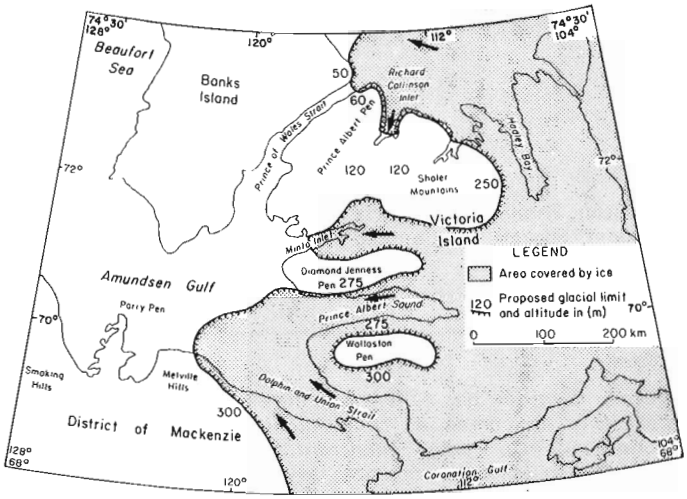

Figure 37.1. *Location map (from Vincent, 1982) showing the glacial limit proposed by Vincent.*

General morphological relationships

The general glacial features of Victoria Island – ground moraine, morainal ridges, drumlins, flutings, striae, and eskers – were mapped by Fyles (1963).

The present work identified morphostratigraphic units comprising various types of hummocky moraine and ground moraine, end moraine, drainage systems, lake and marine features. This has allowed identification of various ice marginal positions and landform relationships. For example, a continuous suite of landforms from hummocky moraine, large well defined end (or lateral) moraines, shear moraine, fluted till, drumlinoid till, to a full drumlin field can be traced from former ice marginal stagnation areas to former areas of strong active ice flow (Fig. 37.2). An understanding of the former areas of ice marginal retreat, ice streaming, and ice stagnation has an important bearing on the chronology and extent of glacial events.

It is clear from Figure 37.2 and from Fyles (1963, map, Plate IV) that a horseshoe-shaped major moraine system around Wollaston Peninsula marks a dramatic change in glacial form; this break has been taken as the Late Wisconsinan/Early Wisconsinan boundary by Vincent (1982; Fig. 1). The nature and implications of this moraine system will be discussed first by examining the zonation of landforms along the southern flank of Wollaston Peninsula in particular.

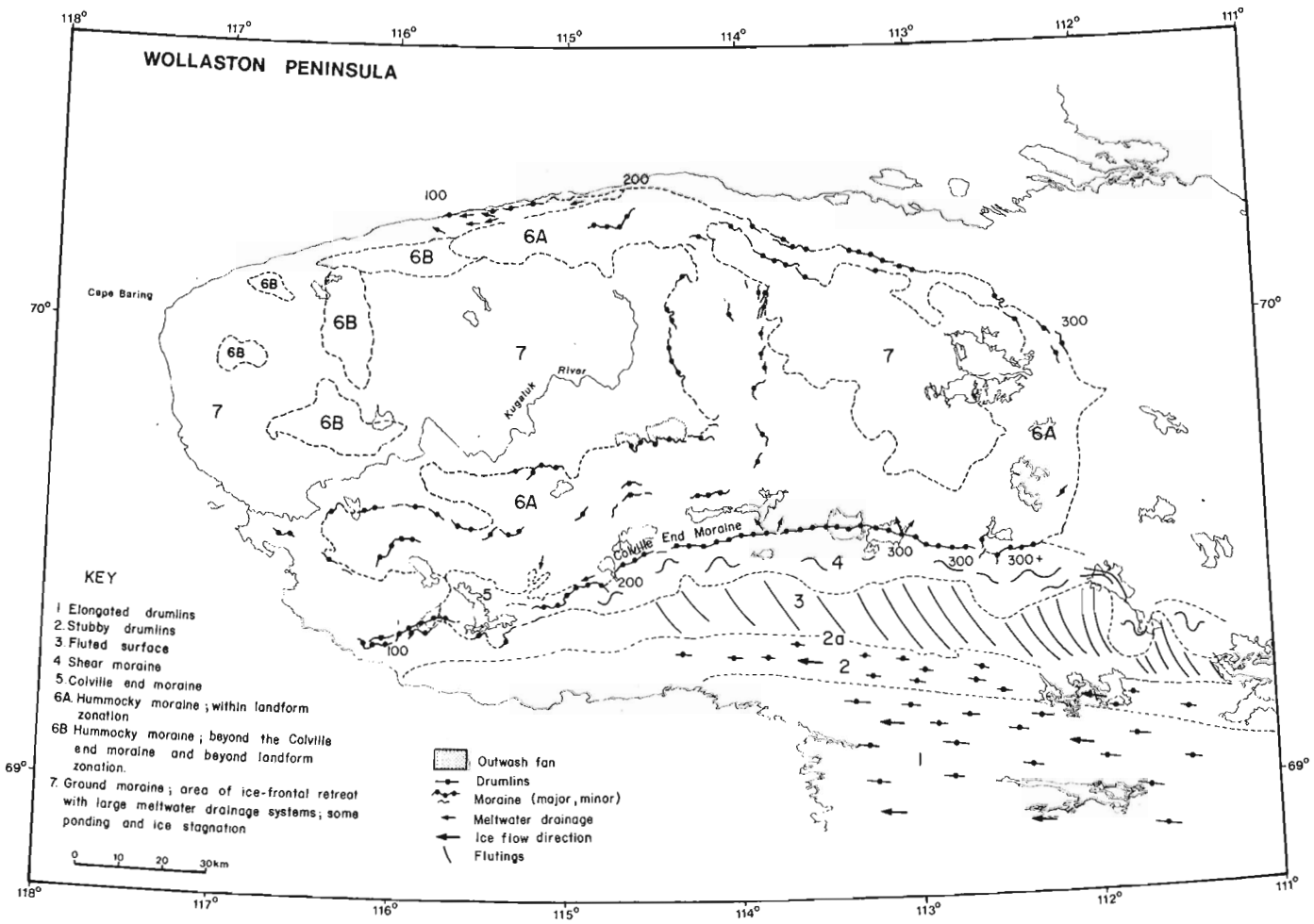

Figure 37.2. *Landform zonation on southern Wollaston Peninsula, Victoria Island, ranging from drumlin forms to hummocky moraine.*

LANDFORM ZONATION

Wollaston Peninsula

To help establish the glacial limit for the latest glacial event on Wollaston Peninsula it is useful to look at the landform suite associated with the last ice withdrawl on the south side of Wollaston Peninsula (Fig. 37.2, 37.3). The pattern is orderly and continuous such that the landform suite appears to represent deposition from a single ice stream which moved from east to west along Coronation Gulf and Dolphin and Union Strait. It seems possible to relate the landforms to the velocity gradient across this ice stream. The sequence of landforms comprises the following, in order (outwards) from the active centre of the ice stream to stagnant forms at the margin (cf. Fig. 37.2):

1. Drumlins: elongated, thin, well formed (flow direction, east to west).
2. Drumlins: short, stubby, well formed (flow direction, east to west).

2a. No drumlins: a clear line beyond which no well formed drumlins occur (occasional drumlinoid form).

3. Fluting: a broad zone of subtle, variable length fluting, tangential to main ice flow direction (flow to the northwest).
4. Shear moraine: wide zone of sheared, deformed, possibly stacked lateral moraine ridges (final compressive flow from south to north).
5. End moraine: continuous large end moraine system (Colville).
6. Hummocky moraine: wide zone of ice stagnation topography – hummocky moraine, plateau moraine, and ridge moraine.

– Late Wisconsinan/Early Wisconsinan boundary of Vincent (1982) –

7. Ground moraine: area of ice marginal retreat with small end moraines, minor hummocky moraine, meltwater drainage, and ponding.

1. Elongated drumlins

The elongated drumlins form a field 15-20 km wide and more than 50 km long. Individual drumlins are symmetrical, 3 km long, 100 m wide, and 10-30 m high. The elongated drumlin landform can also be considered as a larger field up to 40 km wide including larger (to 7 or 8 km), wider (to 200 m), slightly older forms (subtle fluting crosscutting) that impart a herringbone pattern to the field (Fig. 37.4). This pattern (not shown in detail in Fig. 37.2) consists of the large drumlins forming an oblique pattern (to main flow) that is related to expanding glacial flow. These herringbone patterns occur as dominant elements of other large, formerly active ice streams north of Prince Albert Sound. These streamlined forms indicate strong ice flow up to 120 m a.s.l. (at 113°W).

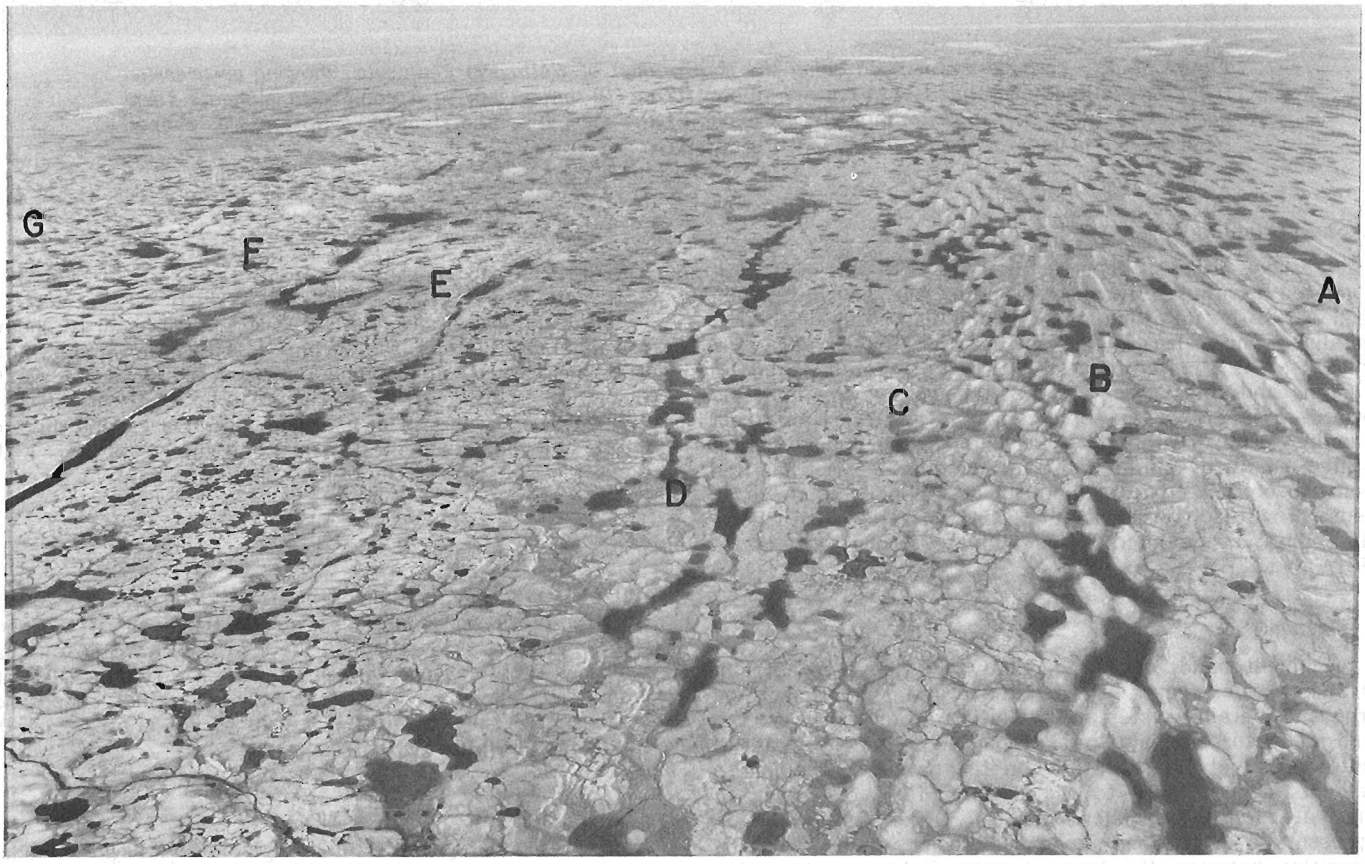

Figure 37.3. *Landform zonation on southern Wollaston Peninsula; view to the east: A, streamlined drumlins; B, stubby (curved) drumlins; C, drumlinoid form; D, fluting (not visible from this angle); E, shear moraine; F, end moraines; and G, hummocky moraine. NAPL T328L-204*

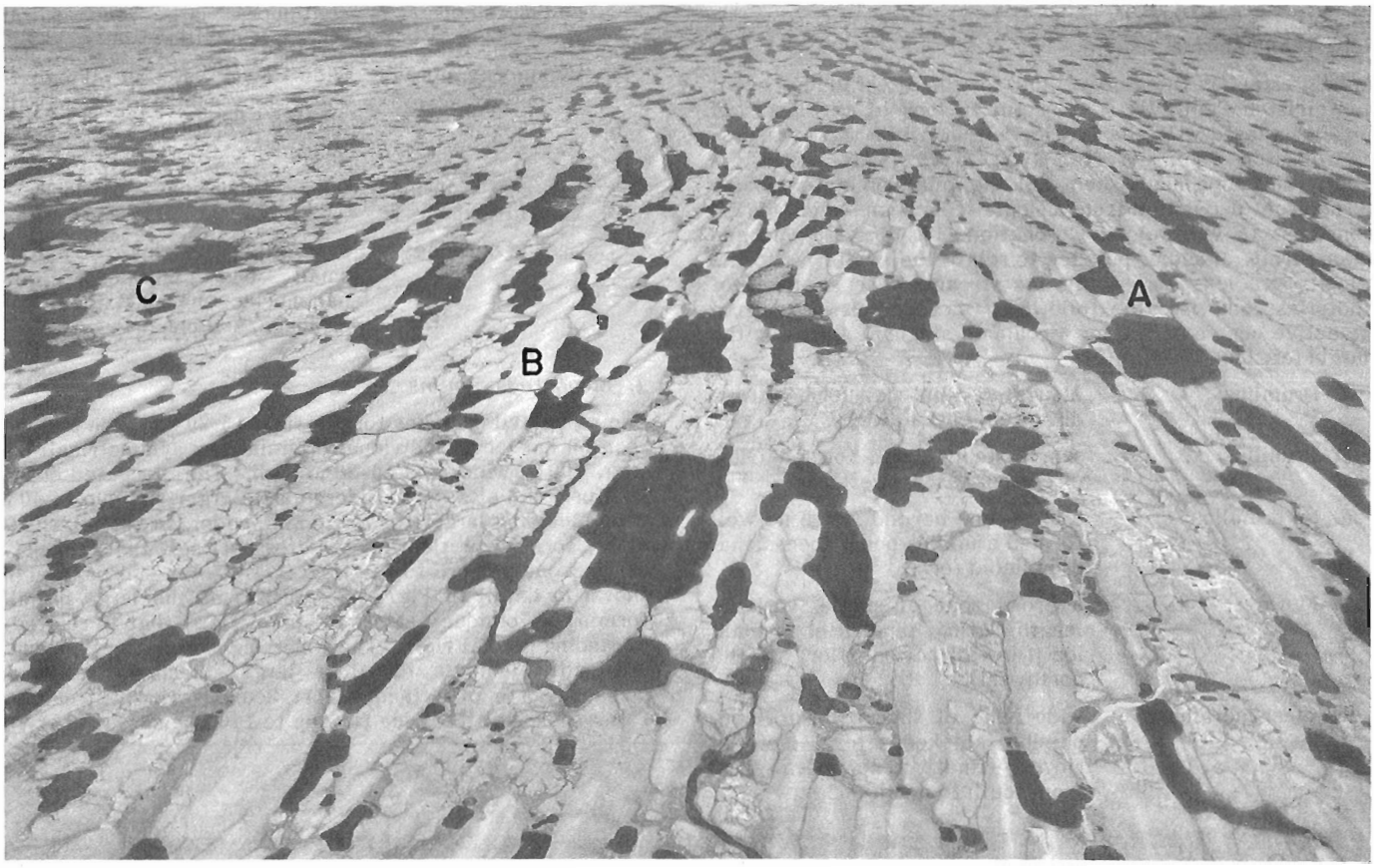

Figure 37.4. *Large drumlin field along the south coast of Wollaston Peninsula showing progression from streamlined drumlins (A) to curved stubby forms (B) that comprise a composite elongate form parallel to those at A. Drumlinoid forms occur at the margin of the field (C). Notice drop-shaped form within elongate drumlin at B. NAPL T321L-178*

2. Short drumlins

Short, stubby drumlins occur at the edge of the major field of elongated drumlins. The short drumlins are generally 100 m long, tens of metres wide, and 10-20 m high. This subfield of drumlins is more densely packed than the field of elongated drumlins; it is oriented parallel with the elongated (Fig. 37.4) drumlins and forms the edge of the larger drumlin field towards less active ice streaming. The transition from drumlins to no drumlins is gradational and in places poorly formed, small, oval drumlinoid forms occur. This transition seems to be related to availability of sediment as the next landform suite involves glacial fluting on terrain with little till. These streamlined forms indicate strong flow up to 160 m a.s.l..

3. Fluting

A prominent band, of fluted, thinly drift-covered terrain, 10-20 km wide, occurs between the drumlin fields and the large end moraine system. The fluting, which forms curved bands of features from 1 to 5 km long, is prominent on aerial photographs yet imperceptible on the ground. The longer elements occur closer to the drumlin field or closer to relatively fast-flowing ice streams. The fluted terrain represents a transitional zone of erosion contrasting the deposition between the large drumlin fields and thick ice marginal accumulations. Fluting has been recognized to 185 m a.s.l.

4. Shear moraines

The broad end moraine system (zones 4, 5, Fig. 37.2) comprises a belt that can be subdivided into a zone of sheared, deformed moraine ridges and possible thrust sheets, forming 10-12 km of the 25 km-wide end moraine system. The zone consists of individual end moraine loops that can be traced out separately. A large kettle-lake network forms a divide between the shear moraine and a large end moraine ridge and an adjacent fluvial meltwater system. The elevation of these moraines indicates active ice to 225 m a.s.l.

5. End moraine

An end moraine complex (informally herein named the Colville moraine) comprises two or three sharp morainal ridges with a large adjacent ice marginal terrace and fan system. These features are continuous for 200 km eastward from sea level. They denote marginal deposition (compressive flow) by active ice up to 366 m a.s.l. on the south side of Wollaston Peninsula.

5a. Glaciofluvial outwash

A prominent continuous (>100 km) glaciofluvial system occurs on the distal side of the Colville moraine (not mappable on Fig. 37.2). The deposits occur as fans or deltas built from the active ice margins situated to the south; stream flow was to

the west. In addition, smaller (10 per cent of sediment) fans and deltas originated from adjacent stagnating ice to the north. Water and sediment beyond this margin remained in closed depressions in the hummocky terrain. Elevations near the upstream end of the outwash system occur to 325 m a.s.l.

6. Hummocky moraine

Adjacent to the large end moraine formed by active ice is a broad area (up to 45 km wide) of hummocky moraine. This stagnant ice area, in part, provided sediment and drainage into the large glaciofluvial system adjacent to the active glacial ice but for the most part sediment accumulated as kames, kettle fills, and hummocks comprising till, and stratified current-bedded sands (Fig. 37.5). As much as 40 per cent of this area consists of kettle depressions forming thaw lakes. Thaw-slump processes have been active in this terrain from the time of deposition until the present. The hummocky terrain can be traced continuously as a large belt (that rises to 300 m+ elevation) to the east and north along the former ice margin in northern Wollaston Peninsula (Fig. 37.2). The margin of this hummocky terrain has been interpreted as representing the Late Wisconsinan limit by Vincent (1982) because of its similarity to another drift sheet that marks the Late Wisconsinan limit on Banks Island.

7. Ground moraine and meltwater channels

Large areas of low relief ground moraine (Fig. 37.5) occur along the perimeter of the hummocky moraine together with a series of outwash fans relating to drainage and sedimentation from the stagnant ice mass (Fig. 37.2). This drainage system (discussed below) forms the last stage in the deglaciation pattern traced from western to central Wollaston Peninsula and is marked by end moraine fragments representing mainly ice frontal retreat rather than ice stagnation. This area (Fig. 37.5, zone 7) is considered to be older (Early Wisconsinan) by Vincent (1982) and the evidence for and against this major time boundary will be considered in the discussion.

Melville Hills

The landform assemblage on Melville Hills (Fig. 37.1) was assessed by airphoto interpretation. These landforms do not occur in the same regular sequence as outlined for Wollaston Peninsula (Fulton, 1981). A drumlin landscape, however, can be traced from sea level to approximately 400 m a.s.l., indicating active ice to this elevation. A large outwash system occurs at elevations higher than 500 m. Although fresh glacial topography occurs above this elevation (500 m), it would be speculative to extend ice limits beyond approximately 500 m a.s.l. without corroborating field data. The landform couple of streamlined flow (to 400 m) and ice marginal drainage (to 500 m), however, appears to be analogous to the Wollaston Peninsula landform suite to allow projection of glacial ice across to Wollaston Peninsula. While the possibility arises that the drumlin field on the Melville Hills is an older land system, the drumlin fields on both sides of Dolphin and Union Strait range from near sea level to their respective elevations and they also have the same orientation; thus were probably produced by the same or contemporaneous converging ice streams.

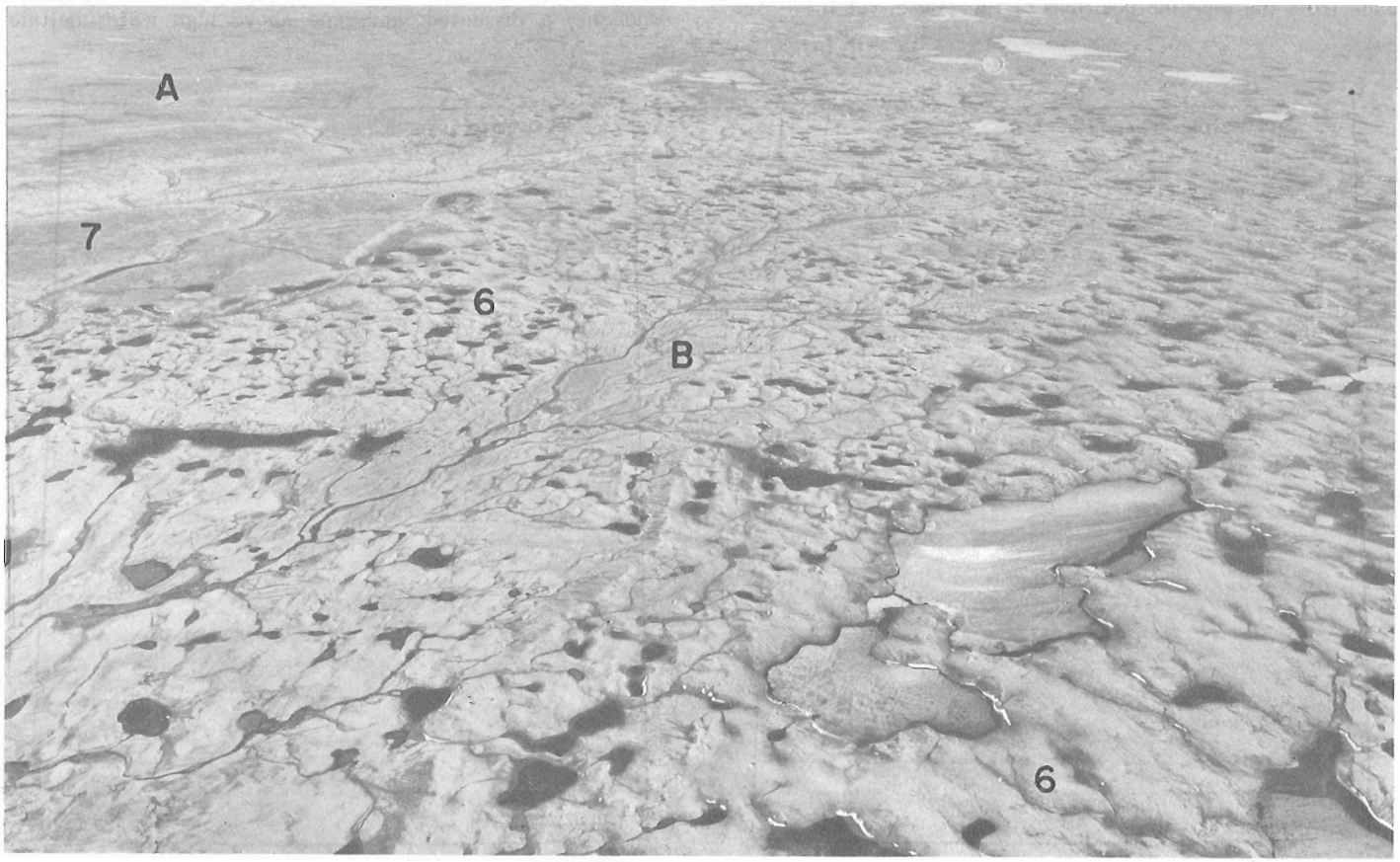

Figure 37.5. *View to northwest over ground moraine of low relief (zone 7, Fig. 37.2). Note subtle fluting (A) of the surface and the large drainage system (B) that dominates the foreground together with hummocky moraine (zone 6) that is fresh beyond the Colville moraine. NAPL T347R-20*

Ice margin positions

A series of sequential ice position diagrams, presented in five phases, illustrate ice marginal retreat across central Wollaston Peninsula. The boundary between the landscape characterized by ice marginal retreat and the landscape characterized by in situ stagnation and melting is discussed.

A second major land system occurring beyond the landform zones of Figure 37.2 consists of a broad till plain interrupted by various end moraine fragments and meltwater systems that outline a pattern of ice frontal retreat. There are areas of ice stagnation within the till plain that are similar in form to zone 6 (Fig. 37.5), but these do not affect the following summary.

Phase 1 (Ponding)

The first ice-free areas on Wollaston Peninsula are recorded as glaciolacustrine basin fills; later drainage events formed erosional channels or built terrace systems. The first lacustrine basin (at 240 m) appeared in an upland area (Fig. 37.6) in response to ice thinning and ice drawdown as the glacier flowed off the central arm of the peninsula. Ice bounded all sides of the triangular proglacial lake herein called glacial Lake Wollaston. While meltwater ponded in glacial Lake Wollaston, drainage (probably subglacial) occurred to the south as shown by stepped erosional terraces. This drainage enhanced glacial thinning and drawdown along the Kugaluk River basin as rapid ice streaming created a detailed converging fluting network along the basin. End moraines on the north and east sides of glacial Lake Wollaston dammed the lake while hummocky moraine was being formed to the west. Glacial ice thinned and melted back from the moraine positions of this phase, yet there was enough activity to produce ice movement to the northwest as indicated by fluted till plains west and southeast of glacial Lake Wollaston (Fig. 37.6). At the same time topographically induced ice flow occurred to the southwest and westward.

Phase 2 (ponds to streams)

Shortly after this time land was uncovered near Cape Baring (Fig. 37.7, 37.8) as ice thinned on the uplands while ice streams remained in Prince Albert Sound and Amundsen Gulf. Evidence for this is inland drainage (to the southeast, Fig. 37.7, 37.8), which formed southeastward-sloping outwash terraces at 140 m; these were built into a small proglacial lake in which kame-delta features occur to 170 m a.s.l. (Fig. 37.8). This compares with younger, high-river terraces, graded to sea level, that occur at 110-115 m and lower; these terraces slope with the present drainage to the northwest (Fig. 37.8). The extent of stagnant ice is indicated by a large area of generally hummocky terrain (Fig. 37.2, zone 6B).

Phase 3 (ice marginal streams)

The earliest evidence of marginal retreat of the major ice streams paralleling Wollaston Peninsula is 30 km northeast of Cape Larsen where outwash systems (A, Fig. 37.9) drained to the west indicated by terraces just above marine limit (at 140 m). As ice retreated from Cape Baring (Fig. 37.9) marine limit was established at about 110-115 m a.s.l. about 11 000 years ago as dated by marine shells (10 700 ± 100 BP, GSC-3566) found in and on marine silt overlying till at 91 m.

As the ice melted back east of central Kugaluk River valley, drainage to the west increased dramatically, producing a dissected landscape above high water deltaic

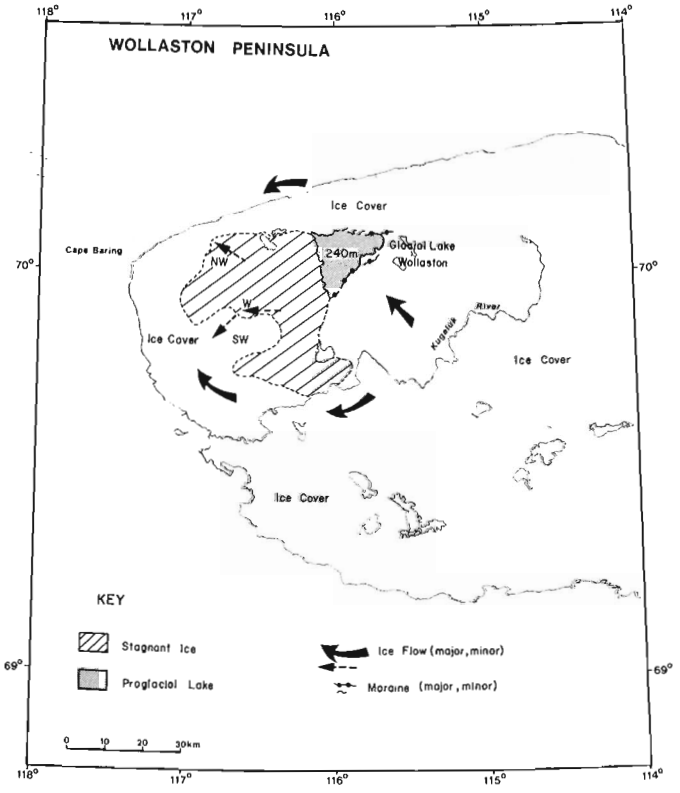

Figure 37.6. *Phase 1: (ponding). Ice margins and conditions during formation of glacial Lake Wollaston.*

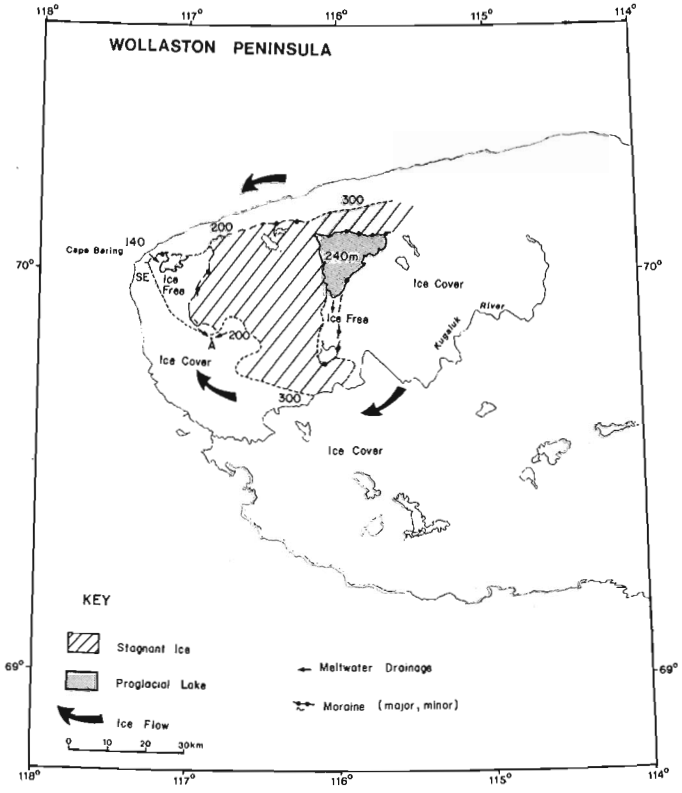

Figure 37.7. *Phase 2: (ponds to streams). Ice margin and conditions during southeast-forming glaciofluvial terrace sequence at Cape Baring.*

Figure 37.8. *View to northwest to Cape Baring indicating area of southwest-flowing glacial meltwater (A) establishing ice limits at Phase 1. Terraces (B) indicate flow to the northwest after kame-deltas (C) were formed. NAPL T345R-73*

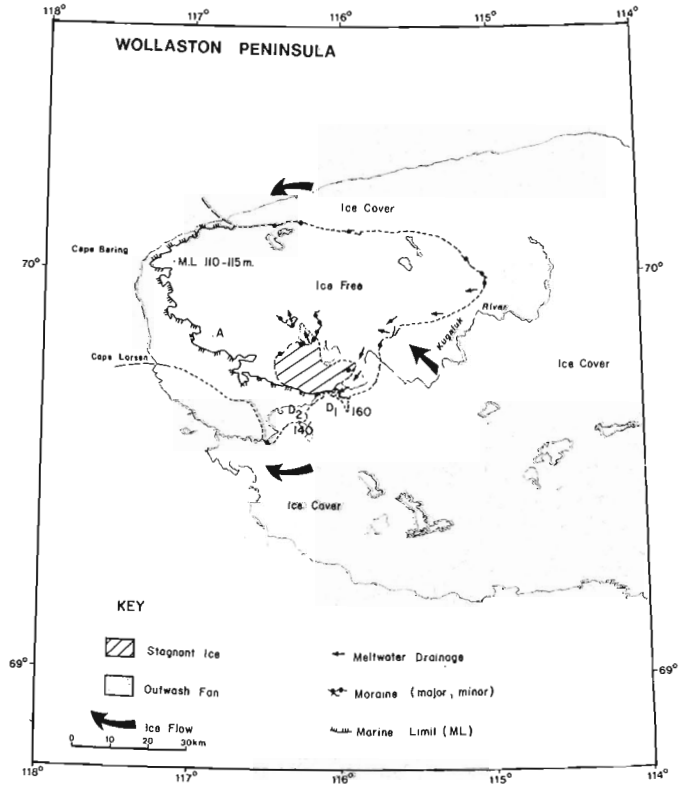

Figure 37.9. *Phase 3: (ice marginal streams). Development of large meltwater drainage systems when ice margin is positioned east of central Kugaluk River valley.*

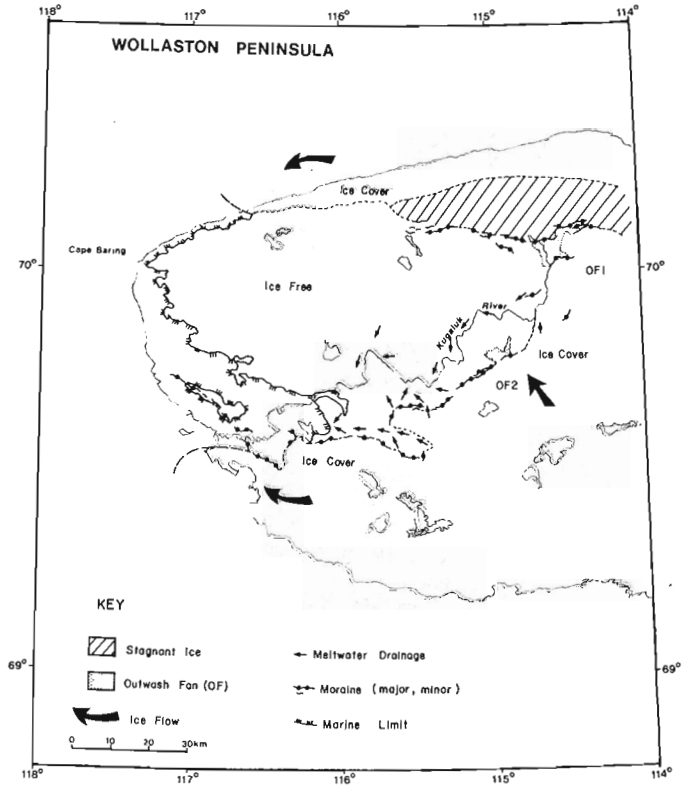

Figure 37.10. *Phase 4: (outwash fans). Development of large subaerial outwash fans along with extensive meltwater drainage system.*

deposits at 160 and 140 m a.s.l. (D_1, D_2, Fig. 37.9) and a marine washed surface below these deposits. At this position (Fig. 37.9) major drainage occurred from melting ice in the east that drained westward down the Kugaluk River system at D_1 (160 m, lacustrine) and later at D_2 (140 m, marine). End moraine fragments, which can be followed from near Cape Larsen eastward adjacent to Kugaluk River and back to the northwest, aid in tracing the drainage systems. The area of stagnant ice (Fig. 37.9) formed hummocky moraine similar in character to that in zone 6 (Fig. 37.2).

Phase 4 (outwash fans)

The best continuous ice marginal drainage system crosses the central plateau of Wollaston Peninsula where it is highlighted by subaerial outwash fans (indicated by intricate braided pattern) located at OF_1 and OF_2 (Fig. 37.10). The alluvial fans lead to an elaborate drainage system downslope, characterized by drainage along discrete channels that entrenched existing ice-filled valleys along Kugaluk River. The fact that alluvial fans developed rather than lacustrine deltas is significant in terms of the glacial history of Wollaston Peninsula. Alluvial fan formation associated with ice marginal positions (moraines) indicates that central Wollaston Peninsula had ice cover in the east, north, and south, yet meltwaters were able to drain freely to the west (Fig. 37.10, 37.11). Ice encircling Wollaston Peninsula, but not overtopping it, would block drainage down Kugaluk River to create lakes in the interior because of the flat topography (see the area below the 300 m contour, Fig. 37.12). Minor ice marginal lakes, however, are responsible for the delta at 160 m on the lower Kugaluk River (discussed in Phase 3).

Phase 5 (Colville moraine)

The best example of concentrated ice marginal drainage is associated with the large moraine system (Colville moraine) that extends continuously for more than 150 km along the southern flank of Wollaston Peninsula (Fig. 37.12, 37.13). The drainage system carried meltwater westward from the ice front at the Colville moraine on the south and also from stagnating ice that blocked drainage to the north (shown as hummocky moraine in Fig. 37.12). The Colville moraine system comprises some of the largest and most continuous moraines mapped in Canada.

Alluvial fans and deltas occur in the east half of the moraine complex whereas the larger channels formed a large ice-marginal glaciomarine delta (Fig. 37.12) at 120-130 m a.s.l.

DISCUSSION

The presence of landform zonation, including areal stagnation of large ice masses, controls certain details of late glacial history as does the sequence of ice marginal retreat positions.

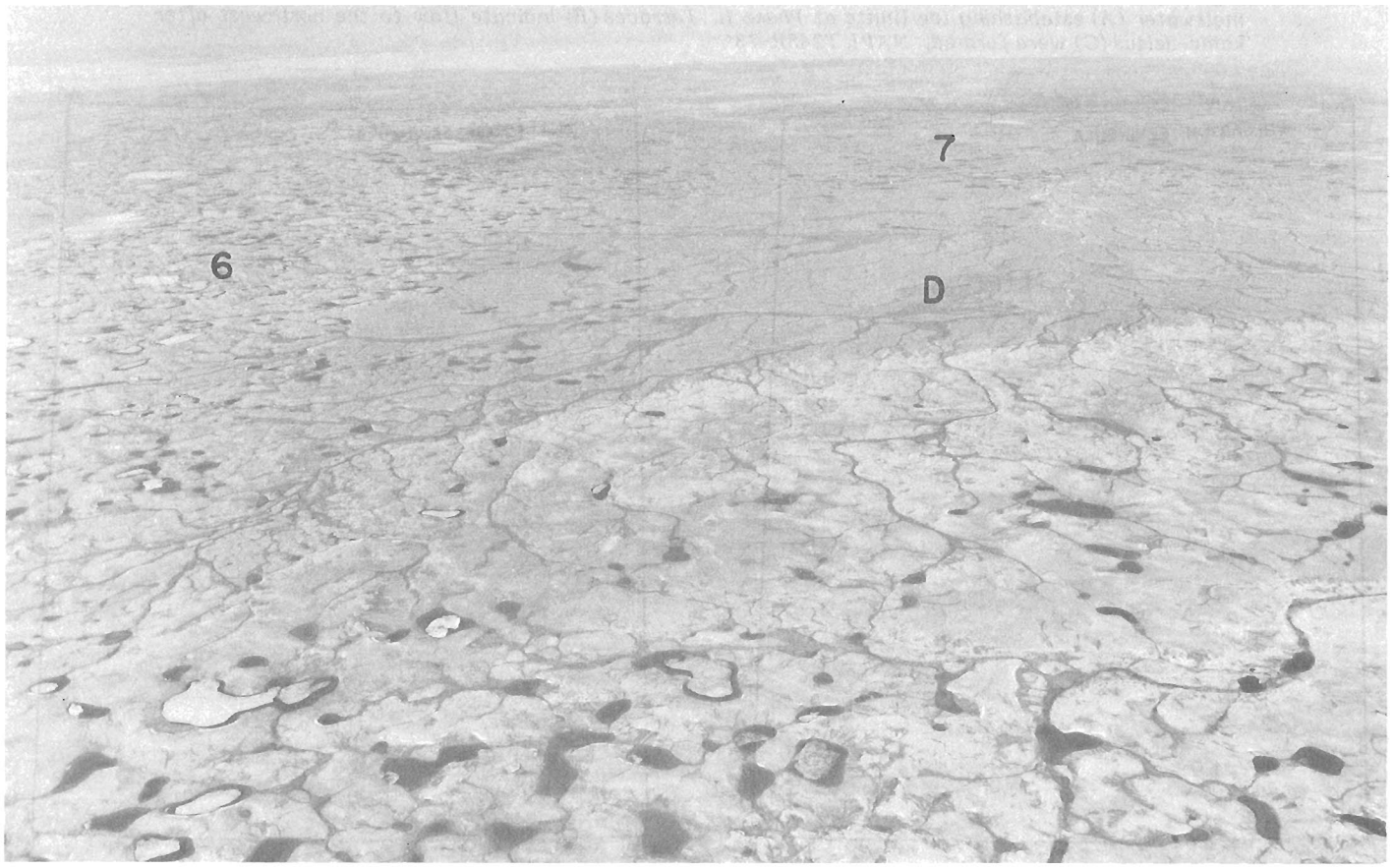

Figure 37.11. *View to west across zone 7 terrain (Fig. 37.2, ground moraine) showing well developed outwash system (D) indicating open drainage to the west during formation of large areas of hummocky moraine as landform zone 6. NAPL T330L-108*

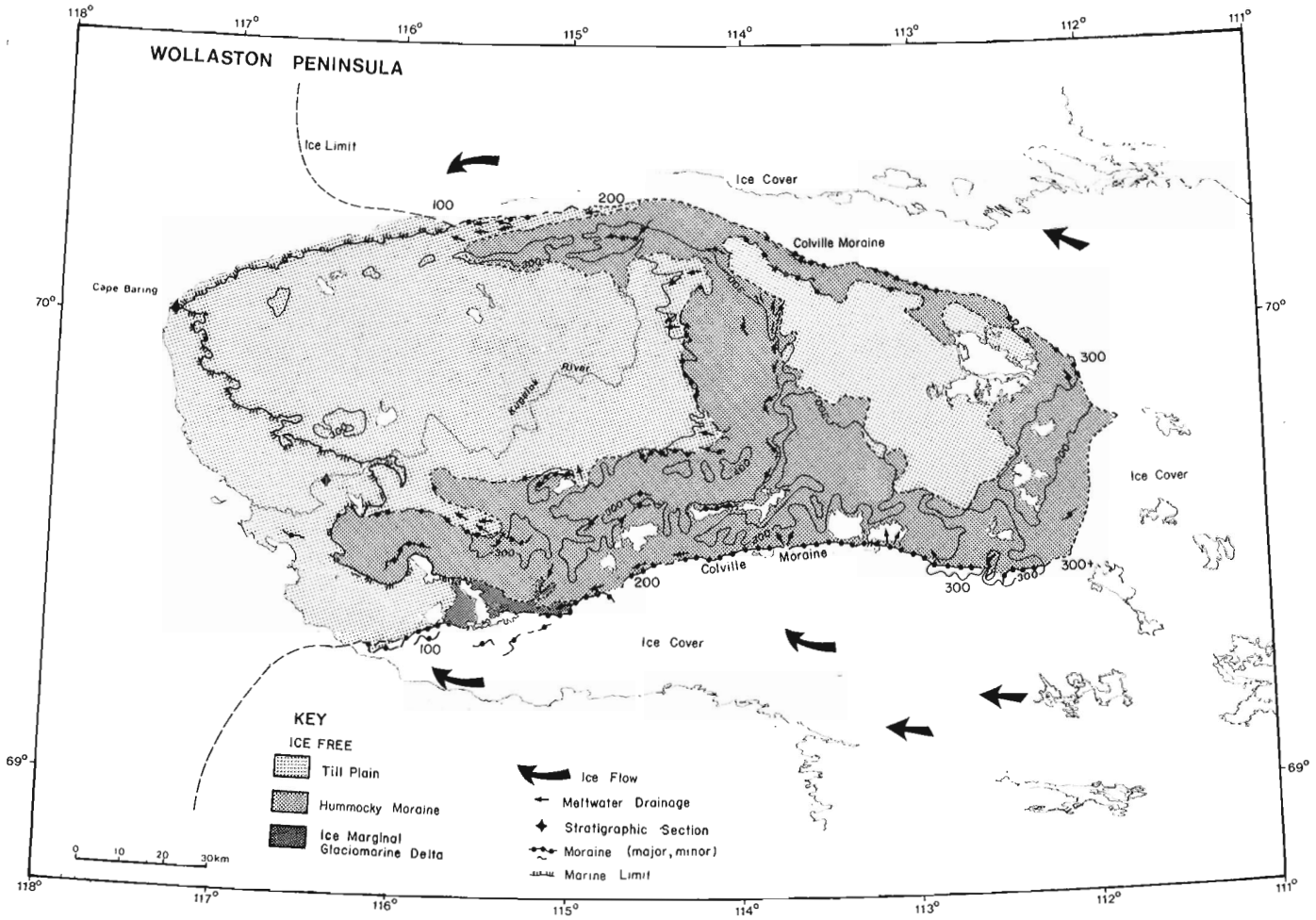

Figure 37. 12. *Phase 5: (Colville moraine). Ice margins during formation of the major moraines (Colville) encircling Wollaston Peninsula, Victoria Island.*

Implications of landform zonation and the Colville moraine system

What does the zoned set of landforms and the Colville moraine tell us about late glacial history and ice cover on Wollaston Peninsula?

First, hummocky moraine outside the Colville moraine system has the same fresh, rugged glacial character as that within the moraine system (Fig. 37.5). The contrast of fresh versus subdued glacial form on aerial photographs led Vincent (1983, Fig. 37.1) to suggest that a significant age difference exists between the hummocky moraine and the low ground moraine beyond it. By mapping hummocky moraine based on fresh glacial form, however, one can extend the last glacial limit far beyond zone 6 and into zone 7. This extension could be considered a Late Wisconsinan position.

Secondly, the examination of hummocky moraine (with fresh form) also establishes ice limits greater than the 300 m of Vincent (1982) because the elevation of this hummocky moraine on Wollaston Peninsula exceeds 400 m at a number of localities (Fig. 37.12). These elevations (of ice stagnation topography) by themselves imply that the last ice completely covered Wollaston Peninsula. This is more evident if we consider that the profile of an active ice margin would have been higher than the elevation at which hummocky moraine occurs.

Thirdly, if we consider the active ice margin (major end moraine, zone 5, Fig. 37.2) represented by the Colville moraine as the Late Wisconsinan limit, we can see a continuous end moraine system ranging from 300 m(+) elevation in the east to 100 m in the west. If this 3:1 ice gradient were applied to Vincent's (1982, Fig. 1) glacial limit at 300 m in the western end of Wollaston, then any reasonable active ice profile up-ice, to the east, would cover Wollaston Peninsula and possibly rise to 500 or 600 m a.s.l. The landforms on the higher Melville Hills to the southwest indicate ice limits of at least 500 m a.s.l.

Fourthly, if the Colville (end) moraine represents the Late Wisconsinan limit, then a sea level relating to Late Wisconsinan time and to an Early Wisconsinan marine limit should be exposed in the ice-free area beyond the Colville moraine (Fig. 37.12). No field evidence has been found to support this hypothesis of two marine transgressions on northwest Wollaston Peninsula. In fact marine limit measurements on a large glaciomarine delta in contact with the Colville Moraine are approximately 120-130 m (Fig. 37.12); this elevation is compatible with marine limit down-ice of about 115 m at Cape Baring.

Finally, the Colville moraine system basically represents a line of separation between dead-ice topography (beyond), down-ice of the moraine system, and streamlined

Figure 37.13. *View west along the Colville moraine system (A-A'-A") showing the prominent outwash-fan system marking the outer margin of active ice. NAPL T328R-185*

landforms up-ice from the moraine system. The line between stagnant and active ice features is topographically controlled as it occurs at a break-in-slope, representing the transition from flat upland carbonate terrain in the centre of Wollaston Peninsula to scarp-front erosional slopes adjacent to the sea basins (Prince Albert Sound, Dolphin and Union Strait, and Coronation Gulf) bordering southwestern Victoria Island. This seems to be an adequate explanation of the morphological break rather than age. The age explanation is a plausible hypothesis but it seems to have no corrobarating data.

Implications of ice retreat sequence

The major significance of the ice frontal retreat sequence (Phases 1 to 5) is that ice configurations produced only local ponding of meltwater (Fig. 37.6). In fact ice configurations clearly illustrate continuous meltwater drainage during deglaciation of ice cover east of glacial Lake Wollaston (Fig. 37.9, 37.10). It could be argued that this drainage system simply represents the final events in a previously blocked drainage system. If we consider an ice configuration similar to that proposed by Vincent (1982; Fig. 1), however, one would except a lacustrine basin to develop because of the level topography below (west of) his glacial limit of 300 m (Fig. 37.12, for elevations). To confirm this possibility one would expect to find raised deltas at the margin of this basin and a covering of lacustrine sediment, through which any subsequent stream activity would have eroded. What is present in that area are outwash fans (Fig. 37.10) at various ice marginal positions that trace ice withdrawl (not all can be shown here). Only thin patchy lacustrine sediments exist.

The till plain in central Wollaston Peninsula could be argued to represent an older surface with an ice configuration that allowed drainage from the younger ice margin at the topographic break (Fig. 37.2).

First, the outline of fresh hummocky moraine extends beyond (similar to the outline of Vincent, 1982) those areas that can be tied directly to landform zonation that more clearly represent the latest ice movement (Late Wisconsinan) affecting Wollaston Peninsula (Fig. 37.10). This implies that intermediate landforms and ice positions are approximately contemporaneous.

Secondly, if the hummocky moraine adjacent to the Colville moraine (Fig. 37.12) is the Late Wisconsinan limit, one would expect crosscutting relationships with older landforms found to the northwest. In general, however, the end moraine segments beyond this hummocky moraine are consistent and conformable with the Colville moraine positions (especially the network of outwash fans that mark these ice marginal positions). In addition, ice-controlled glaciofluvial landforms are transitional between the hummocky and till plain landscapes.

A fundamental question being raised here concerns whether the type of landform and more subtle morphology of a till plain are significantly different in age (a glacial stadial or greater) than larger, fresher landforms such as hummocky moraine. The answer seems to be that freshness and "older looking" can, and often do, imply age but not absolutely so. Consider that these two areas are simply areas of different glacial form – till plain and hummocky moraine. The fact is that the dynamics of the ice sheet, controlled by topography,

sheared and deformed (compressive flow) thick glacial deposits around the perimeter of Wollaston Peninsula. This led to a different depositional record. On the level central uplands, thinner, smaller landforms developed from what was a thin ice sheet that may well have been cold based (probably only a few hundred metres thick) during its early (erosional?) period and was only warm based and depositional under extending flow in a late retreating sequence. The common occurrence of transverse morainal forms supports this concept of late stage deposition.

Finally, the hypothesis of two ages of sediments (Early and Late Wisconsinan) suggested by Vincent (1982) requires such stratigraphic evidence as two marine transgression-regression sequences.

However, stratigraphic exposures in the Cape Baring and Kugaluk River (Fig. 37.12) areas of Wollaston Peninsula provide supporting evidence for full glacial cover of Wollaston Peninsula during the latest ice advance. Briefly, the stratigraphy at each locality consists of one advance-retreat sequence (glaciomarine mud, till, glaciomarine mud) overlying a lower till unit. The upper till unit consists of basal till (lodgment or melt-out) as indicated by the high percentage of striated clasts. This till has uniform lithological characteristics that have been used to trace it to the upper reaches of Kugaluk River in central Wollaston Peninsula at elevations to 300 m. The till is associated with several landforms (fluted till plain, till plain, transverse moraine, and end moraine) in the areas featuring streamlined landforms and featureless till plain. It is one lithostratigraphic unit despite the variety of morphological settings.

SUMMARY

Based on the record of glacial landforms, ice marginal positions, landform sequences, and stratigraphy, it appears that glacial ice covered all of Wollaston Peninsula during Late Wisconsinan time. This record shows large glaciofluvial meltwater systems draining meltwater from successive ice marginal positions rather than those ice marginal positions producing deltaic-lacustrine sediments in enclosed basins, as would be expected by the configuration of Vincent (1982). Further, the concept of a zoned landform system is useful in defining glacial limits. The hummocky moraine associated with the Colville moraine defines an ice limit above 300 m in northwestern Wollaston Peninsula, sufficient to suggest active ice cover over the whole peninsula in Late Wisconsinan time. If, on the other hand, the Colville end moraine system represents the Late Wisconsinan glacial maximum, then one would expect to find evidence for two distinct marine limits beyond the moraine because the Colville end moraine intercepts present day sea level well short of the maximum extent of glacial cover on Wollaston Peninsula. This dual marine limit has not been found beyond the Colville moraine. It appears that one continuous marine limit can be mapped from Cape Baring as well as east along the coast of Wollaston Peninsula. Stratigraphic information to date shows only one marine transgressive-regressive sequence.

The implications of these findings of a more extensive Late Wisconsinan limit on Wollaston Peninsula indicate (1) that differences of glacial form and landform size do not necessarily imply age difference and (2) that the position of the Late Wisconsinan ice margin is beyond Wollaston Peninsula. While it is proposed that ice overlapped Wollaston Peninsula, it may only have been a few hundred metres thick as indicated by the small-scale landforms on the central upland. I believe critical evidence can be found by ground studies along the Melville Hills with respect to landform relations and elevation. A well dated uplift curve for southwestern Victoria Island or dates on marine deposits of Phases 3, 4, and 5 would also help confirm or alter the pattern of Late Wisconsinan ice retreat proposed in this report.

REFERENCES

Fulton, R.J.
1981: Dolphin and Union Strait; in Landsat Images of Canada – A Geological Appraisal, ed. V.R. Slaney; Geological Survey of Canada, Paper 80-15, 102 p.

Fyles, J.G.
1963: Surficial geology of Victoria and Stefansson islands, District of Franklin; Geological Survey of Canada, Bulletin 101, 38 p.

Vincent, J-S.
1978: Limits of ice advance, glacial lobes, and marine transgressions on Banks Island, District of Franklin: a preliminary interpretation; in Current Research, Part C, Geological Survey of Canada, Paper 78-1C, p. 53-62.

1980: Les glaciations quaternaires de l'île de Banks, Arctique canadien; thèse de D.Sc. non-publiée, Université de Bruxelles, 248 p.

1982: The Quaternary history of Banks Island, N.W.T., Canada; Géographie physique et Quaternaire, vol. XXXVI, nº 1-2, p. 209-232.

1983: La géologie du Quaternaire et la géomorphologie de l'île Banks, Arctique canadien; Commission géologique du Canada, Mémoire 405.

38. SURFICIAL DEPOSITS OF THE REDROCK LAKE AREA, DISTRICT OF MACKENZIE

Project 830017

D.A. St-Onge
Terrain Sciences Division

St-Onge, D.A., Surficial deposits of the Redrock Lake area, District of Mackenzie; in Current Research, Part A, Geological Survey of Canada, Paper 84-1A, p. 271-278, 1984.

Abstract

Extensive areas of the Redrock Lake region are covered by surficial sediments, which have been grouped into these categories: till, outwash, glaciolacustrine silt, deltaic gravel, and sandy alluvium. Except for recent alluvium, the deposition of the sediments is related to the overriding of the Redrock Lake area by two ice streams originating to the east, and to the subsequent downwasting of this ice mass. The regular spacing of "glaciofluvial corridors" every 10 to 12 km testifies to the enormous amount of water that resulted from ice melting. The abundance of outwash, minor diamicton ridges, stony ice contact glaciolacustrine rhythmites, and the absence of major moraine ridges strongly suggest the gradual downwasting of an ice mass with no significant readvance pulses.

Résumé

De larges superficies de la région du lac Redrock sont recouvertes de dépôts meubles, qui pour fin de description, sont groupés en six catégories: le till glaciaire épais ou discontinu, le fluvioglaciaire, les silts glaciolacustres, les graviers deltaïques et les alluvions sableux. A l'exception des alluvions récents ces sédiments ont été mis en place lorsque deux courants de glace venus d'un centre de dispersion à l'est traversaient la région et lors de la fonte de cet appareil glaciaire. L'espacement régulier de "corridors fluvioglaciaires" à tous les 10-12 km témoigne de l'énorme quantité d'eau produite par la fonte de la glace. L'abondance de sédiments fluvioglaciaires, les crêtes mineures de diamicton, les rythmites lacustres de contact glaciaire et l'absence de crêtes morainiques importantes sont des arguments importants en faveur de l'hypothèse d'une décrépitude glaciaire régionale sans ré-avancée discernable.

INTRODUCTION

Parts of the Redrock Lake area are extensively covered by unconsolidated deposits. This is particularly the case of a 5 to 20 km-wide belt extending from Coppermine River in the northeast to Acasta Lake in the southwest. Figure 38.1 identifies the major lithological units and associated landforms. Systematic mapping at 1:100 000 during the summers of 1981, 1982, and 1983 has yielded the following results.

1. Two ice streams originating from a dispersal centre to the east were responsible for the abundant ice flow features in the region.
2. During deglaciation powerful meltwater streams deposited large quantities of outwash sediment along glaciofluvial corridors which occur every 12-15 km. There is evidence to suggest that esker ridges were built in relatively short segments.
3. Coarse gravel deltas at approximately 365 m a.s.l. were constructed in a high-level phase of glacial Lake Coppermine (St-Onge and Guay, 1982).
4. Deformed rhythmites demonstrate that the headwaters of the Kamut outlet phase of glacial Lake Coppermine (St-Onge et al., 1981) were in stagnant glacier ice occupying low-lying areas along the Rocknest-Redrock-Point lake basins.
5. The evidence suggests that deglaciation proceeded by the gradual downwasting of an ice mass with no discernible readvance pulses.

SURFICIAL MATERIALS

Glacial till

Glacial till is the most abundant unconsolidated sediment in the Redrock Lake map area (NTS 86 G; Fig. 38.1). Although it can be generally described as a diamicton composed of blocks and boulders in a silty sand matrix, its grain size varies from pebbles distributed in a silty sand matrix to accumulations of openwork boulders. For mapping purposes, two classes of till are recognized: (1) a till blanket, with average thickness in excess of 2 m, which effectively masks all traces of underlying bedrock and (2) a till veneer, generally less than 2 m thick, which is composed of bouldery material distributed as irregular patches, mostly in the western and northern part of the area (Fig. 38.1).

Two ice streams originating from a dispersal centre to the east were responsible for the deposition of the thick till. Drumlins moulded of this sandy till identify these two ice flows: (1) the fan-shaped Scotstoun Lake flow in the north and (2) the east-west Irritation Lake flow in the south. The drumlins are commonly 1500 to 2000 m long, 500 to 600 m wide, and 30 to 50 m high. The drumlins in the Scotstoun field have the shape of "the inverted bowl of a spoon" (Flint, 1971, p. 101). Bedrock in this region is dominated by pelites which are easily fragmented because of the pronounced schistosity; till derived from this bedrock has a characteristic silt-sand matrix.

In the Irritation Lake area the drumlins are narrower and considerably more stony. This reflects the underlying bedrock, dominated by granites and by quartzo-feldspathic gneiss, which yields a stony till with a sparse sand gravel matrix.

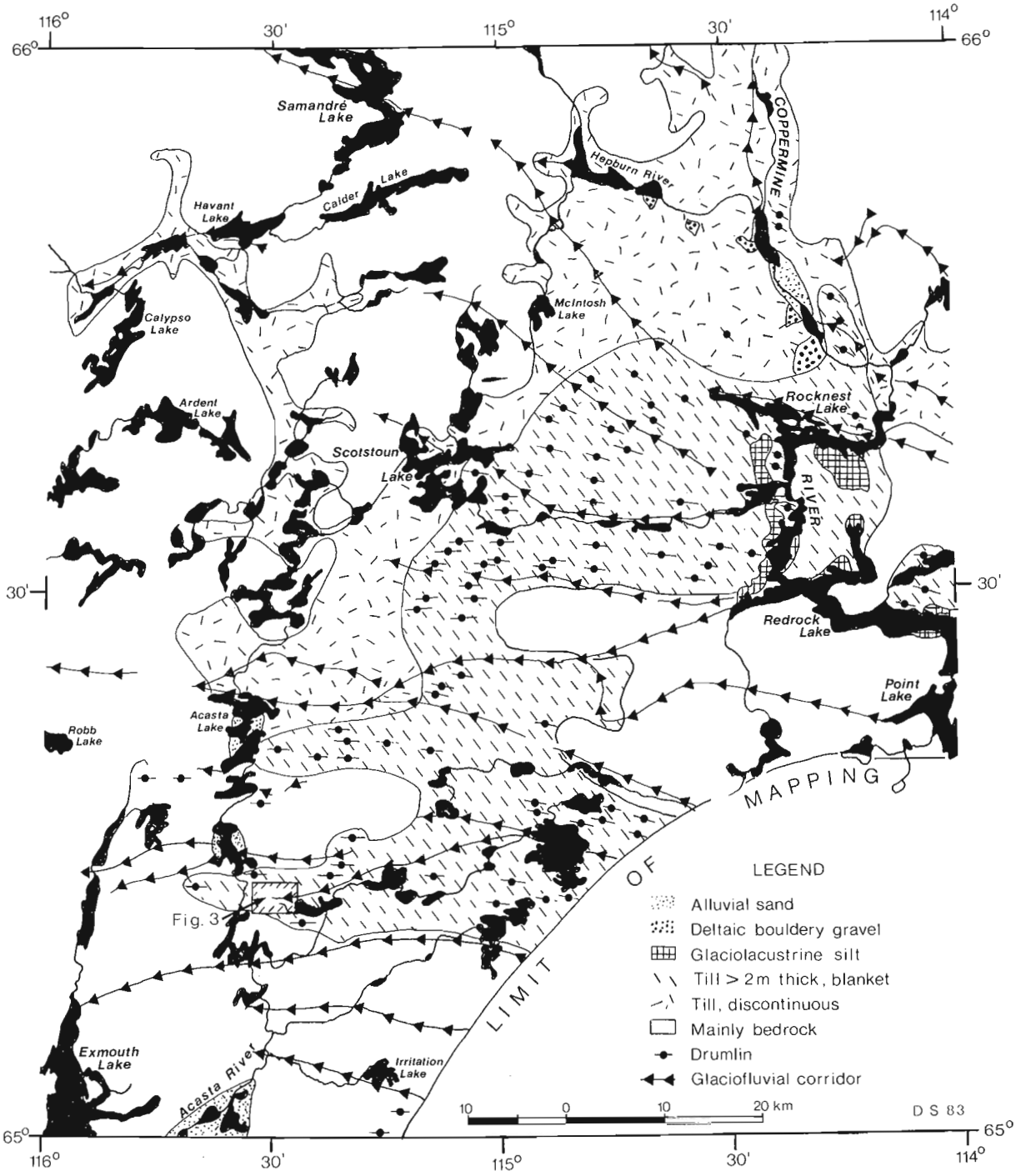

Figure 38.1. *Generalized surficial geology of Redrock Lake area (86 G).*

The two drumlin fields are separated by a major glaciofluvial corridor extending from Redrock Lake to the north end of Acasta Lake (Fig. 38.1). An esker, which occupies major segments of this corridor, shows no evidence of glacial overriding. Its irregular crest profile indicates that it was built within an ice mass and not as an interlobate feature. This suggests that the two ice streams were part of a single ice mass.

To the west and north of the drumlin fields, irregular patches of stony till partly mantle the underlying bedrock. This stony till, which includes large erratics and patternless ablation debris, was left behind by downwasting ice.

Glaciofluvial corridors

The melting of glacial ice produced enormous amounts of water that entrained sediments which were redeposited as gravel and sand. These powerful meltwater streams not only deposited sediments, in places they removed all but the largest boulders in their path. Thus corridors were created in which stretches of bare bedrock alternate with ice contact features which include esker ridges, transverse and circular ridges, and minor morainic ridges.

Glaciofluvial corridors occur at regular intervals (Fig. 38.1): along a north-northeast to south-southwest transect, spacing averages 12-15 km. They represent the former beds of major meltwater streams which have lost all their tributary streams as a result of the melting of the ice. The frequency of corridors indicates a high drainage density, and the size of the transported material, commonly 60-80 cm diameter, implies powerful streams.

Eskers are the most prominent components of glaciofluvial corridors. These sinuous, steep-sided, sharp-crested ridges with an irregular crest profile are up to 30 m high but more commonly are 10-20 m high. Although the eskers may be continuous for 20 km or more, they are far from being homogeneous in composition.

Esker material ranges from coarse sand to boulders 60-80 cm in diameter. Boulders are not distributed randomly through the esker material but form the principal component of short esker segments, averaging 10-30 m in length. These segments of extremely coarse openwork structure or diakene sediments (Lundqvist, 1979, p. 10) commonly occur at intervals of every 1.5-2 km. It is likely that boulders did not travel far along the esker tunnel; carried by fast moving water flowing down steeply dipping ice tunnels, they were deposited as soon as the gradient flattened, i.e. when the water reached the main tunnel at the base of the ice. Gravel and coarse sand were deposited downstream. This interpretation of grain size distribution implies that, although

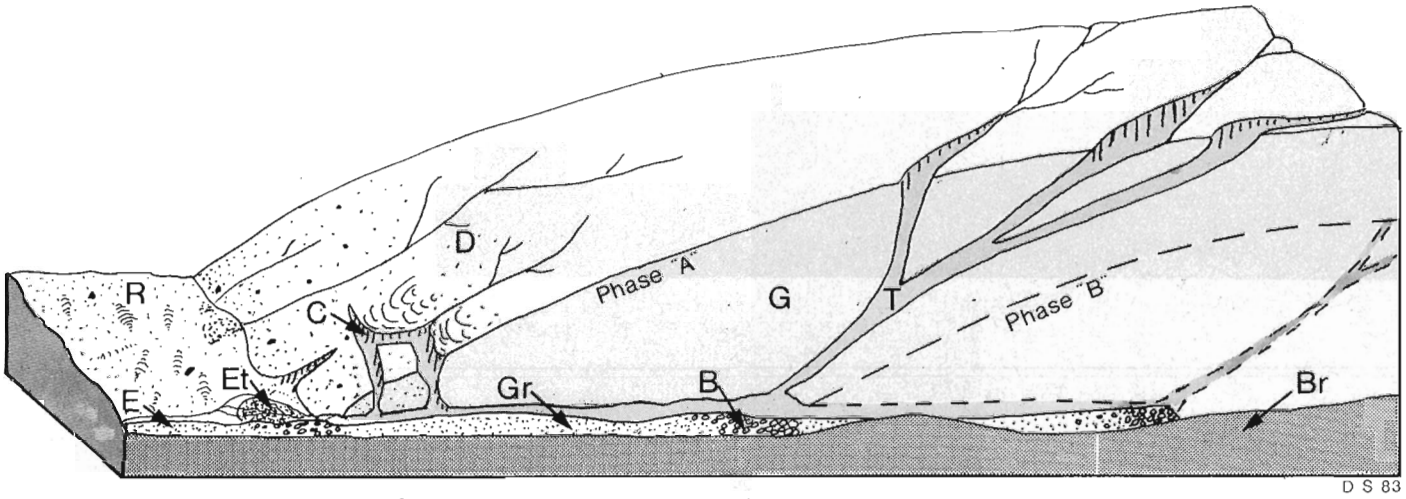

Figure 38.2. *Origin of sediments and associated landforms along a glaciofluvial corridor. Note that during phase B the constricted flow above a bedrock knob prevents sedimentation; this will result in a "washed surface". E, esker; Et, esker terrace; Gr, gravel and sand; B, boulders; R, ridges; C, crevasses; D, debris; G, glacier ice; T, tunnel; Br, bedrock.*

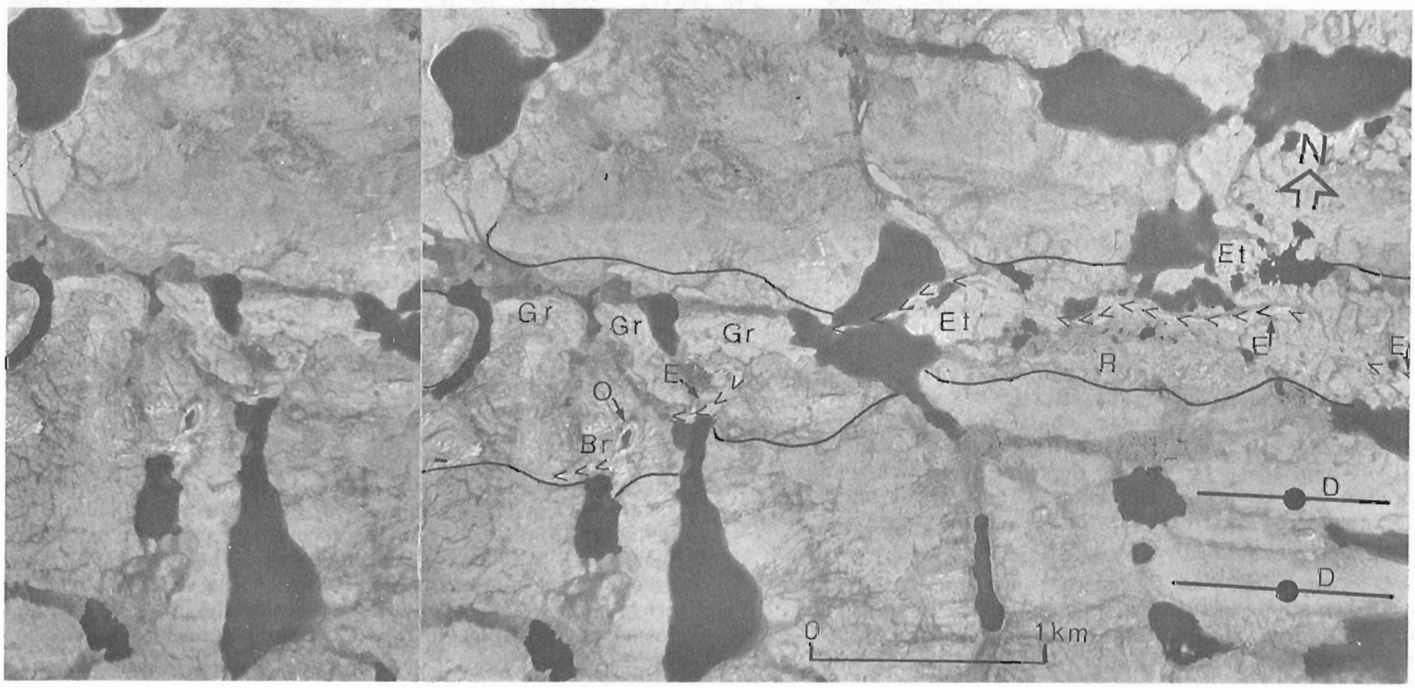

Figure 38.3. *Stereogram of glaciofluvial corridor and associated landforms. E, esker; Et, esker terrace; Gr, gravel and sand; O, oval ridge (Fig. 38.4, 38.5); Br, bedrock; R, minor Ridges. Note well developed drumlins (D) typical of Irritation Lake drumlin field. NAPL A11532-135, 136.*

Figure 38.4

Low level oblique airphoto of an oval ridge of outwash cobbles, gravel and sand; view is southeast. Notice bedrock outcrop in the east and west and the small esker to the south-southeast of the ridge (downstream).

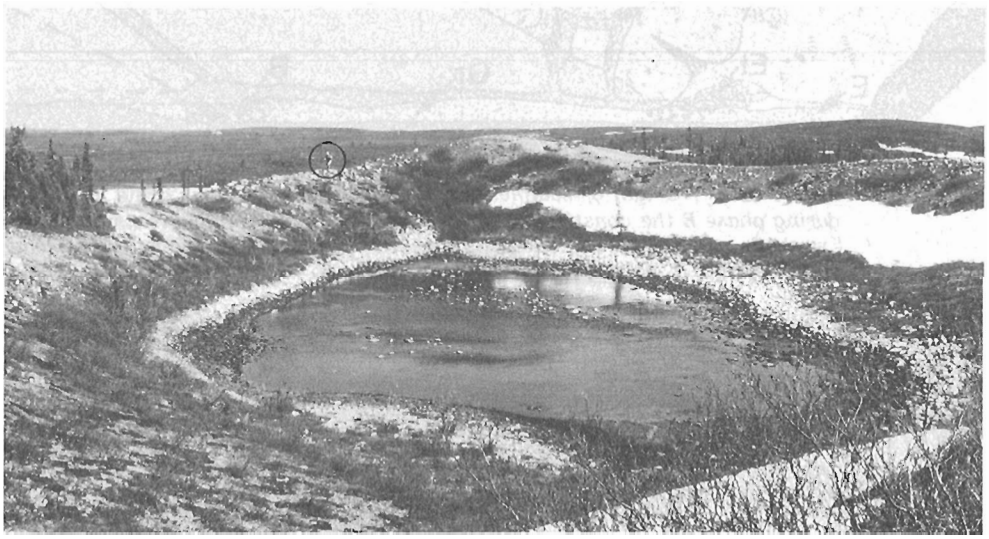

Figure 38.5

Ground view of the oval ridge shown in Figure 38.4; view is north. Figure in the circle gives scale. Note the uneven crest line and the varied material ranging from cobbles to sand.

esker ridges may be continuous for several tens of kilometres, they are in fact constructed of successive, comparatively small segments (Fig. 38.2).

Flat-topped terraces, commonly fan shaped, occur along the eskers. These outwash terraces were formed when meltwater was no longer confined to an ice tunnel (St-Onge et al., 1981, p. 329). Along the esker shown in Figure 38.3 these fan-shaped deposits occur upstream (east) of the coarse esker segments. They are interpreted as sedimentation where meltwater flowed into the open at the margin of the ice.

Two minor landforms that are associated with the eskers in the glaciofluvial corridors are an oval ridge of bouldery gravel and ridges of boulders, gravel, and sand transverse to corridor alignment (Fig. 38.3).

Figures 38.4 and 38.5 show an oval ridge of outwash cobbles and coarse gravel, approximately 140 m long and 70 m wide. It occurs at the western end of a glaciofluvial corridor just east of Acasta River (Fig. 38.3). The long axis of the ridge has an azimuth of 10°. The ridge is between 7 and 11 m above the central depression; interior and exterior slopes are in the 25 to 30° range. The northern crest rises 17 m above the surrounding bedock, which is partly covered by a thin veneer of till and sandy gravel. A small esker of bouldery gravel extends southwest from the oval ridge and climbs partly up the east-facing side of a bedrock hill (Fig. 38.3, 38.4). To the east (upstream) is another small esker, 4-5 m high, composed of boulders 30-50 cm in diameter (Fig. 38.6). Similar forms have been described by Lundqvist (1979, p. 27) who speculated that these "circular eskers" were formed by the "filling of subglacial channels or crevasses". Because he did not describe the material of these forms, however, it is difficult to make any direct comparison.

The oval ridge is part of an outwash complex deposited by a high velocity stream. This is demonstrated by the coarseness of the material of both the esker and the ridge as well as by the occurrence of washed bedrock to the

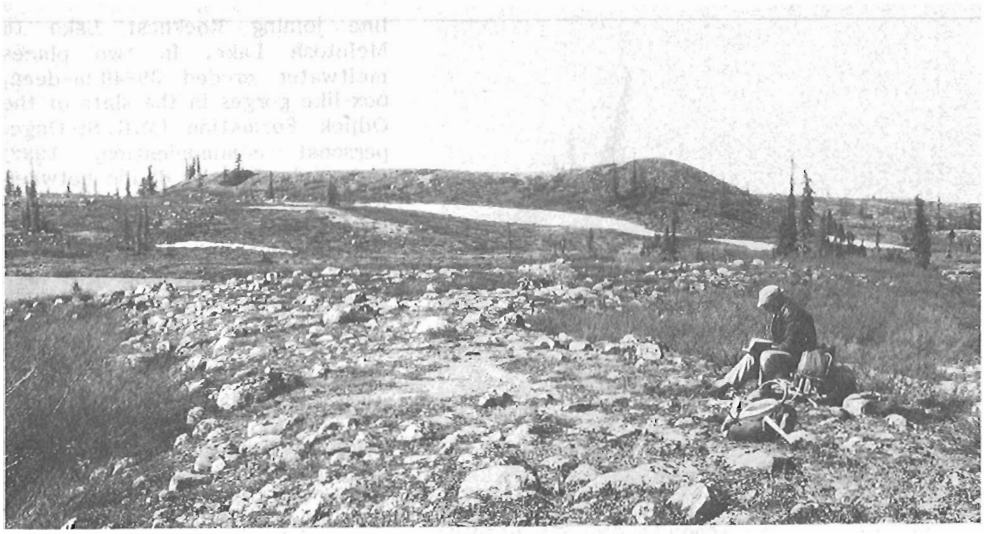

Figure 38.6

Profile view of an oval ridge (cf. Fig. 38.4, 38.5) from a small bouldery esker to the east (upstream).

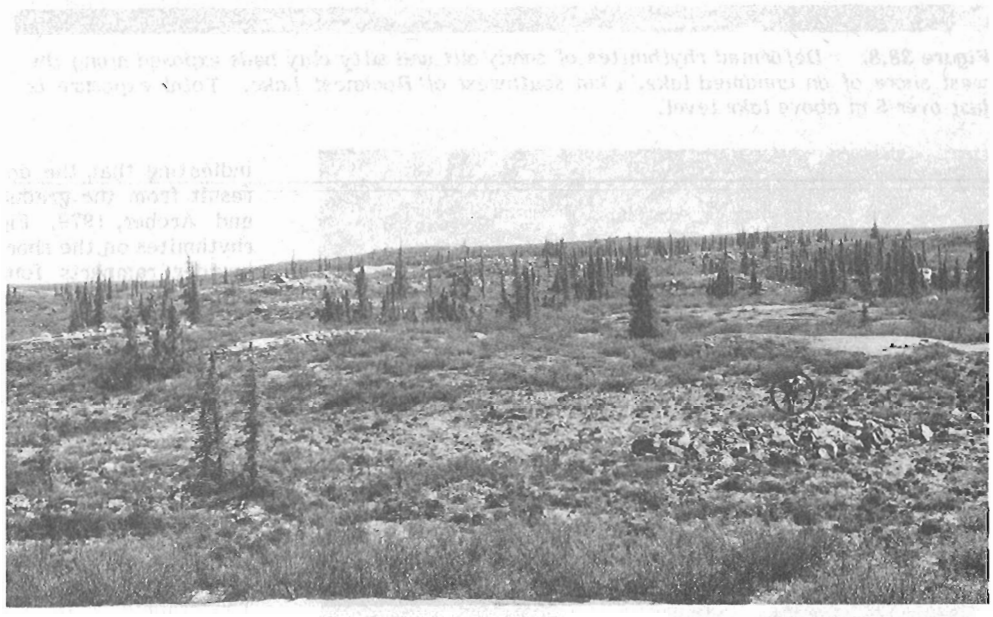

Figure 38.7

Small ridges in a glaciofluvial corridor. Meltwater flow was generally from left (east) to right (west). Note figure for scale. Bouldery ridges, 1 to 5 m high, are aligned transverse to meltwater flow. Tails of well sorted sand are parallel meltwater flow and commonly occur on the downslope side of a bouldery tranverse ridge.

west (downstream). The ridge likely formed by rapid sedimentation around an ice block which had collapsed from the ice tunnel roof. Although this local widening reduced stream velocity sufficiently to allow sedimentation of cobbles and of coarse gravel, downstream flow was still sufficiently constricted to nearly completely preclude sedimentation – hence the bare bedrock of the surrounding area which is typical of glaciofluvial corridors.

Minor ridges of bouldery gravel or diamicton occur within the glaciofluvial corridors and are generally aligned at right angles to them. The ridges occur in swarms 0.5-1 km wide and up to 10 km long, but more commonly 3-5 km (Fig. 38.3, 38.7). Individual ridges are generally 1-5 m high, height, 10-80 m long, and 10-30 m wide; a typical ridge would be 3 m high, 30 m long, and 20 m wide, with slopes of 10-15°. They are always associated with glaciofluvial corridors although eskers are not always present. The material, which is always coarse, varies from openwork boulder structure to blocks in a sandy gravel matrix. In places "tails" of well sorted sand are found on the downstream (westerly) side of the small ridges.

The upland surface on which the ridges are located precludes the possibility of formation in contact with glacial lake water, thus they are not genetically related to cross-valley moraines which they resemble (Andrews, 1963). More likely they result from the filling of crevasses and other depressions near the front of a downwasting ice mass (Fig. 38.2). They are associated with eskers because both result from the accumulation of material in local topographic lows. Sediment flows on the ice surface would transport material towards crevasses which opened largely as the result of the collapse of the ice tunnel near the glacier front. As pointed out by Lawson (1981), the nature of sediment flows on a glacier is varied and depends on the amount of water involved. The material of the transverse ridges, ranging from diamicton to gravel, is a result of this complex sedimentation process.

Deltas

North of Rocknest Lake, west of Coppermine River, and south of Hepburn River several large perched deltas occur. They are composed of coarse bouldery gravel, indicating deposition by high energy meltwater flow which originated on

Figure 38.8. Deformed rhythmites of sandy silt and silty clay beds exposed along the west shore of an unnamed lake, 1 km southwest of Rocknest Lake. Total exposure is just over 5 m above lake level.

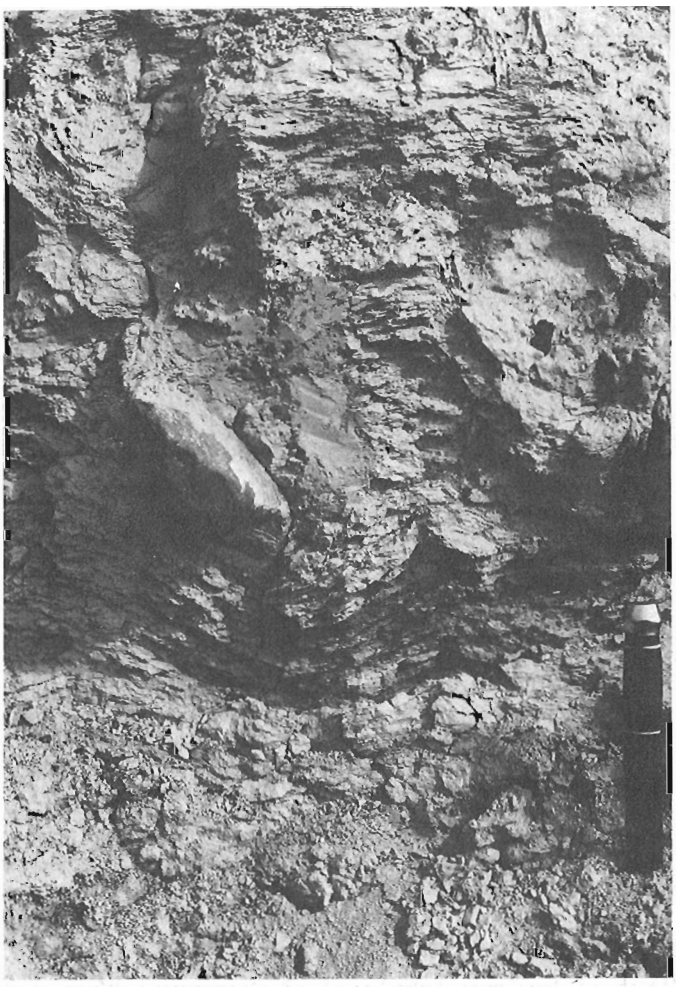

Figure 38.9. Detailed view of rhythmites from the left centre of Figure 38.8. Note poorly defined rhythmite beds and bedding deformed by dropstones.

an ice mass lying to the south of a line joining Rocknest Lake to McIntosh Lake. In two places meltwater eroded 30-40 m-deep, box-like gorges in the slate of the Odjick Formation (M.R. St-Onge, personal communication, 1982) that underlies the divide between Rocknest Lake and Hepburn and Coppermine rivers. The deltas, which lie at approximately 365 m a.s.l., were constructed in a high level phase of glacial Lake Coppermine (St-Onge and Guay, 1982).

Glaciolacustrine silt

South of Rocknest Lake numerous lakes and streams are fringed by a silty clay rhythmite deposit (Fig. 38.1, 38.8).

The rhythmites, which contain numerous stones and small (<50 cm) boulders, generally are intensely deformed (Fig. 38.9). In some cases fresh exposures show that the lower units are more deformed than the upper, indicating that the deformations are, in part syngenetic and result from the gradual melting of buried glacier ice (Shaw and Archer, 1979, Fig. 3, p. 354). Also, typically, these rhythmites on the shores of modern lakes are associated with boulder ramparts found up to 30 m offshore and 0.5-1 m below the water surface. Together these observations indicate that the rhythmites were deposited between hillsides of bedrock or till while large blocks of dead ice still occupied low areas; the boulders melted out from the margins of the ice blocks and dropped onto the rhythmites (Fig. 38.10). Final melting of the glacier ice caused the deformations by triggering extensive collapse within these sediments. The boulder ramparts owe their origin to subsequent stream or wave erosion, which washed out part of the fine material and concentrated the boulders just below the present water line.

The upper surface of most of these deposits is less than 10 m above the level of Redrock and Rocknest lakes. Topographic maps give an elevation of 375 m a.s.l. for Redrock Lake; Rocknest Lake, which is farther downstream and below an important set of rapids, must be 5 to 10 m lower. Based on these elevations, the rhythmites of the Rocknest-Redrock-Point lakes area could have been deposited in proglacial lakes whose level was controlled by the 365 m a.s.l. Kamut Lake outlet of glacial Lake Coppermine (St-Onge et al., 1981). In other words, present evidence indicates that the headwaters of the Kamut outlet phase of glacial Lake Coppermine were in stagnant ice from the disintegrating Scotstoun-Irritation lakes ice mass. Seasonal sedimentation in these water bodies formed the rhythmites now exposed along lakes and rivers.

Alluvial sand

Along Coppermine and Acasta rivers are extensive sand terraces, 1 to 10 m above present river level, which mark stages in the downcutting by modern rivers since deglaciation (St-Onge et al., 1981).

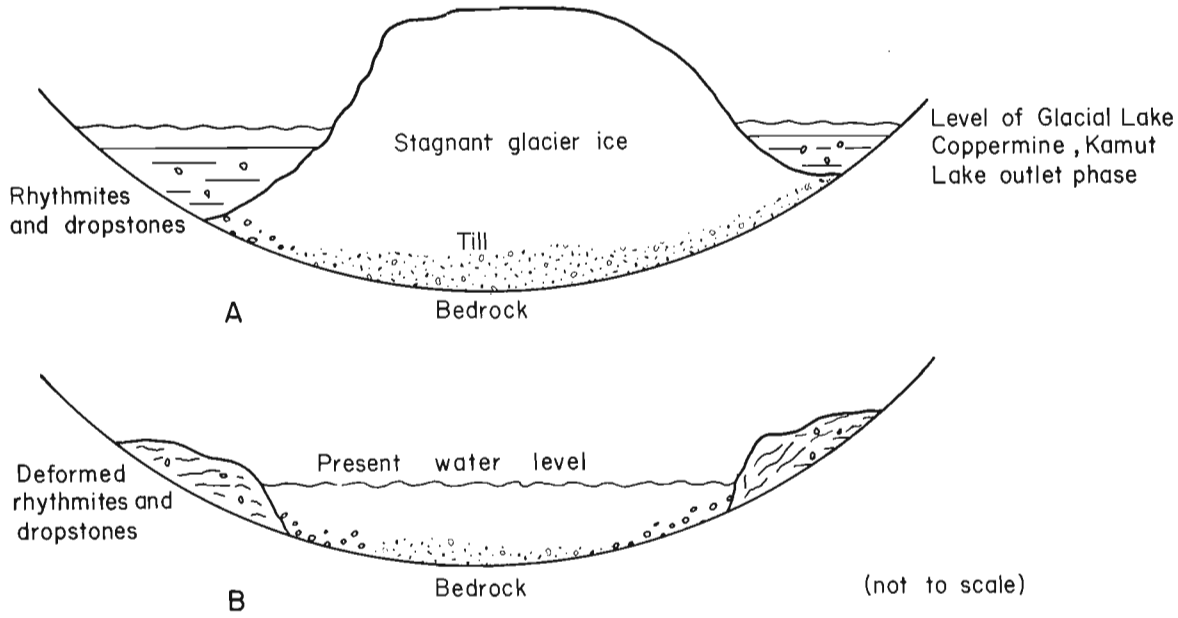

Figure 38.10. Proposed origin of deformed bouldery rhythmites on the shores of present lakes.

Exposed bedrock

Extensive areas, particularly in the west and northwest of the Redrock Lake area are not mantled by overburden. There, the resistant granitic and metamorphic rocks have rugged relief with nearly continuous outcrops interrupted only by scattered erratics and frost heaved rocks.

INTERPRETATION

Strongly drumlinized till was deposited by two ice streams moving west to northwesterly across the Redrock Lake area. No extensive morainic ridges mark phases in ice retreat. Rather, regularly spaced glaciofluvial corridors occupied by eskers and minor transverse ridges, together with strongly deformed glaciolacustrine rhythmites, suggest a downwasting ice mass with no discernible readvance pulses. Eskers, which in places are continuous for tens of kilometres, were built up in short segments of 1-2 km length. That none of these eskers shows any sign of glacial overriding is a strong argument in favour of the downwasting model proposed here.

Time of deglaciation is not known beyond the fact that glacial Lake Coppermine existed at least 11 000 radiocarbon years ago.

ACKNOWLEDGMENTS

The systematic mapping of the surficial geology of the Redrock area was supported by the Geological Survey of Canada. Dr. M.R. St-Onge, Precambrian Geology, is especially thanked for all the help he provided to the author and his assistants during the 1981-82-83 summers. The numerous observations made by bedrock geologists are gratefully acknowledged. The Department of Indian and Northern Affairs (DINA) provided financial and logistical assistance to graduate students. I am particularly grateful to Dr. W. Padgham, Resident Geologist (DINA), Yellowknife, for his help and advice. W. Bowler and M. Irving provided expert ratio expediting service.

REFERENCES

Andrews, J.T.
1963: Cross-valley moraines of the Rimrock and Isortok River Valley, Baffin Island, N.W.T.; Geographical Bulletin, no. 19, p. 49-77.

Flint, R.F.
1971: Glacial and Quaternary Geology; John Wiley and Sons, Inc., 892 p.

Lawson, D.E.
1981: Distinguishing characteristics of diamicton at the margin of the Matanuska glacier, Alaska; Annals of Glaciology, v. 2, p. 78-84.

Lundqvist, J.
1979: Morphogenetic classification of glaciofluvial deposits; Sveriges Geologiska Undersokning, serie C, nr 767, 72 p.

St-Onge, D.A., Geurts, M.A., Guay, F., Dewez, V., Landriault, F., and Lévéille, P.
1981: Aspects of the deglaciation of the Coppermine River region, District of Mackenzie; in Current Research, Part A, Geological Survey of Canada, Paper 81-1A, p. 327-331.

St-Onge, D.A. and Guay, F.
1982: Quaternary geology of upper Coppermine River valley, District of Mackenzie; in Current Research, Part A, Geological Survey of Canada, Paper 82-1A, p. 127-129.

Shaw, J. and Archer, J.
1979: Deglaciation and glaciolacustrine sedimentation conditions, Okanagan Valley, British Columbia, Canada; in Moraines and Varves, ed. Ch. Schluchter, A.A. Balkena, Rotterdam, p. 347-356.

39. MORPHOLOGY AND DESCRIPTION OF AN OUTLIER POPULATION OF TREE-SIZED WILLOWS ON WESTERN VICTORIA ISLAND, DISTRICT OF FRANKLIN

Project 760058

S.A. Edlund and P.A. Egginton
Terrain Sciences Division

Edlund, S.A. and Egginton, P.A., Morphology and description of an outlier population of tree-sized willows on western Victoria Island, District of Franklin; in Current Research, Part A, Geological Survey of Canada, Paper 84-1A, p. 279-285, 1984.

Abstract

Near the head of Minto Inlet, on western Victoria Island, discontinuous thickets of ***Salix alaxensis*** *(feltleaf willow), ranging in age from less than 5 years to at least 81 years, reach heights of up to 8 m. They thrive in half a dozen deep valleys and sheltered ravines along the north shore of the inlet, where the microclimate is favourable. These outliers represent disjunct populations more typical of floodplains near treeline, several hundred kilometres to the south and west.*

Résumé

Près du fond de l'inlet Minto, dans la partie ouest de l'île Victoria, des halliers discontinus de ***Salix alaxensis*** *(saule feutré), dont l'âge varie de moins de 5 ans à au moins 81 ans, atteignent une hauteur maximale de 8 m. Ces arbres croissent très bien dans une demi-douzaine de vallées profondes et de ravins abrités le long de la rive nord de l'inlet, là où le microclimat leur est favorable. Les halliers isolés représentent des peuplements distincts qui sont plus typiques des plaines d'inondation près de la limite des arbres, située à plusieurs centaines de kilomètres vers le sud et l'ouest.*

Introduction

Feltleaf willow, **Salix alaxensis**, is a common colonizer of modern floodplains at or near treeline. It has been reported along rivers in central and northern Alaska (Hanson, 1951; Bliss and Cantlon, 1957; Spetzman, 1959; Viereck and Little, 1972); northern Yukon Territory (Drew and Shanks, 1965); and Mackenzie Delta (Gill, 1973). In addition, isolated thickets have been reported from locations well north of treeline, particularly Bathurst Inlet (Bird and Bird, 1961), southern District of Keewatin (Edlund, 1983), and northern Quebec (Maycock and Matthews, 1966), as well as western Victoria Island (Porsild, 1955; Peterson et al., 1981; Edlund, 1983). Willow thickets along the north shore of Minto Inlet, Victoria Island, are the northernmost members of a disjunct population of tree-sized willows found north of treeline in North America (Fig. 39.1) and are therefore of considerable interest. Indeed, the area has been proposed as an ecological reserve (Nettleship and Smith, 1975). This report describes one outlier population of feltleaf willow in the Minto Inlet area.

STUDY AREA

The study area is an unnamed, broad river valley, 5 km long and 1 km wide, near the head of Minto Inlet, western Victoria Island (71°34'N, 115°21'W). Although not unique, it contains the most extensive and tallest (8 m) thickets of erect willow in this region. The valley is located in rugged terrain on the north side of Minto Inlet, in the Shaler Mountain physiographic region (Fyles, 1962; Fig. 39.1). It is part of a series of cuestas formed on tilted Precambrian sedimentary and volcanic bedrock (Thorsteinsson and Tozer, 1962). Ravines and deep valleys have developed in the more easily eroded calcareous sedimentary rocks; dark gabbro dykes and sills form the prominent topographic features.

On one side of the valley, a steep scarp, which faces northwest, rises abruptly to an elevation of 180-200 m. The hills of the more gently southeastward-dipping slopes on the opposite side reach only 100 to 150 m. The entire area was glaciated during the Wisconsinan and most of the surrounding countryside is masked by till, ice contact, and glaciofluvial deposits. Bedrock outcrops only on the steep scarp faces and in small knobs. The modern floodplain consists of a series of bars and cross-over channels. The flood channels are used for only a limited period during the spring freshet.

The vegetation of the surrounding area is typically Low Arctic (Polunin, 1951) with a rich **Dryas** (mountain avens) – dwarf shrub tundra with abundant and diverse legumes. This is the most common type of community on the extensive areas of moderately to well drained materials. Local patches that are poorly drained support wet sedge meadows, which may include a semi-erect willow (**S. lanata** ssp. **Richardsonii**) component reaching 30 to 50 cm in height. The feltleaf willow thickets are almost entirely restricted to the modern floodplain.

The sheltered valleys in the Minto Inlet area are distinctly warmer than the nearby plateau and hilltops. A difference of 20°C from plateau top to an adjacent valley floor, on which grew tall willow thickets, was observed on 31 July, 1982. The study site was consistently 1 to 9°C warmer than two other camps (Fig. 39.1) on Wollaston Peninsula to the south, during the week of 7 to 15 July, 1983. The temperature at the study site never dropped below 9°C that week and reached a high of 21°C. The advanced state of anthesis and copious seed dispersal of feltleaf willow during this week, as compared with those at Holman on the western tip of Diamond Jenness Peninsula to the southwest, indicate that the growing season in this valley started at least two to three weeks earlier.

FELTLEAF WILLOW FORM AND OCCURRENCE

Salix alaxensis, the only tall, thicket-forming willow in this valley, has a growth form typical of many erect shrubs in that it produces numerous (5-20) stems. These mature together and form clumps with trunks, usually the same age and size, that radiate from a central core. This species readily reproduces vegetatively; in addition to the main trunks, suckers sprout from the base of most tree-sized clumps, where the canopy permits light penetration to the base. In some places solitary trunks of feltleaf willow may occur, but these are atypical and are most likely the result of severe browsing.

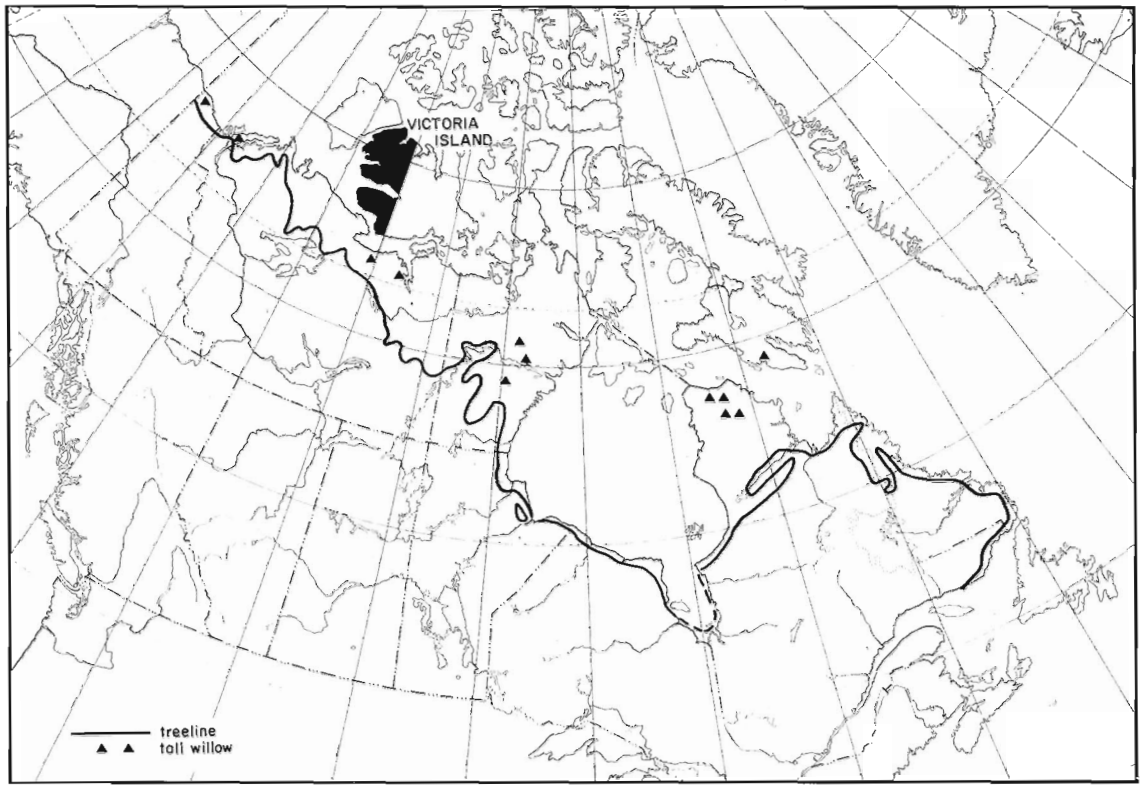

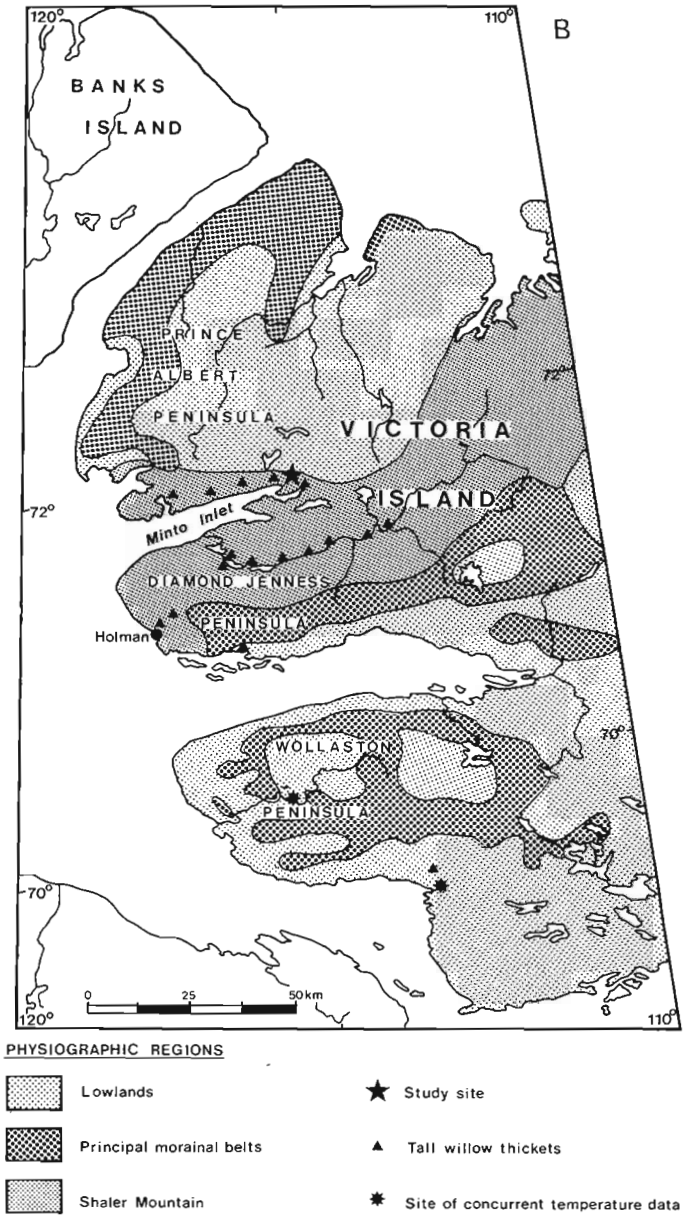

Figure 39.1. *(A) Known locations of tall willows in northern Canada above treeline. (B) Western Victoria Island and the study site on the north shore of Minto Inlet. Also shown are the physiographic regions (from Fyles, 1962), locations of other tree-sized willows on western Victoria Island, and locations where concurrent weather data were recorded during the second week of July 1983.*

Throughout its range, the feltleaf willow is found almost exclusively on modern floodplains. This species requires well drained, aerated, nurient-rich materials, and an adequate moisture supply throughout its entire growing season. It rarely occurs on materials that are imperfectly to poorly drained.

At the Minto Inlet study site dense thickets and scattered clumps of feltleaf willow reach heights of 0.2 to 8 m on the modern floodplain; thickets occur on stable floodplain bars. The willow also occurs locally at 100 to 150 m elevation along a ravine in the scarp face. Discontinuous thickets stretch from the mouth of the river for 5 km upstream, where the river leaves a deep, narrow canyon. Where the willow occurs in low scattered clumps, either colonizing herbaceous species or continuous **Dryas**-legume tundra is the predominant ground cover. In denser, taller thickets there is little if any understory, only a few etiolated forbs and a few shade-tolerant herbs and bryophytic species occur.

To study the growth and distribution of feltleaf willow in this valley, a series of bars half way along the river were selected; these included those bars with the tallest willow (Fig. 39.2). Two line transects were laid out across a well vegetated portion of the floodplain: A-B perpendicular to the river and C-D parallel to it (Fig. 39.2, 39.3A, B). Cross-sections of feltleaf willow trunks were taken at 10 m intervals along the transects, to study age and growth rates. The heights of the thickets, zones of dense canopy, and a variety of other data were also collected at each site.

RESULTS AND DISCUSSION

The river in the study area has a main channel which may possibly flow year round. The cross-channels and some, if not all, bars crossed by the transect are flooded annually. Flood-stage debris was found deposited in thickets near the main channel at heights of 0.3 to 1.2 m above the ground. At the leading edge of thickets on these bars, willow trunks are commonly scarred on the upstream side, probably due to ice scour at the time of break-up. Willow thickets on bars farther away from the main channel show little signs of flood debris or ice scour, although minor cross-over channels may contain clods of debris.

Soils

Soils in the study area consist primarily of coarse gravels with variable amounts of sand. Beneath dense thickets, litter has accumulated to depths of 4 to 10 cm and a mixture of humus and eolian or fluvial sand under the litter in places is 20 to 30 cm deep. No buried wood was discovered anywhere in the valley. Organic matter appears to come from the decomposition of leaf litter. The active layer may reach more than 1 m, but because of coarse gravels, no pits greater than 60 cm deep were excavated.

Growth rates

Examination of the growth data shows that there is no relationship between the average annual growth increment for the years 1978-82 and tree age or tree size (diameter or height) (Table 39.1; Fig. 39.3A, B). Growth increments varied from 0.1 to 1.2 mm per year. The oldest willows (50 to 81 years) had annual growth increments that varied widely and were generally equal to or greater than the much younger trunks.

The tallest willows along the transects occurred in the zone adjacent to the major channel (Fig. 39.4). Although the tallest willows (6-8 m) commonly were among the oldest trees, height does not vary directly with age. The oldest trunk (81 years) was only 60 cm high, whereas the tallest trunk was only 51 years old. Trunks of 1 to 2 m height varied in age from 21 to 56 years.

Figures 39.3 and 39.5 show that on a bar midway along A-B (sites 11, 12, 13), a localized group of willows are currently much shorter than the clumps were in the past. Some event killed the older willow trunks, which were from 1.5 to 2 m high, and which were at least 45 years old. Regrowth from the same root stock is only about 21 years old and reaches a maximum height of only 0.5 m but has average growth increments similar to other thickets (Table 39.1). This bar had the most extensive zone of dieback in the valley. Other bars at similar distances from the main channel show 10 to 20% dead branches, usually in the top 20 to 30 cm, but rarely down to ground level. The cause of this dieback is unknown. Possibly there may have been a shift in the distribution of snow (insultation) in this area; drifts which once accumulated to depths of 1.5 to 2 m may now only reach 0.5 m.

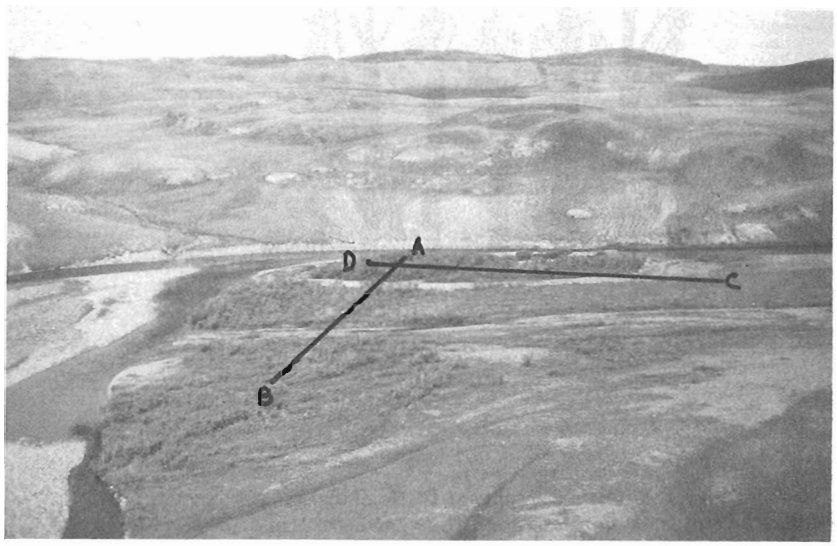

Figure 39.2

Location of two line transects on the modern floodplain. Note the proximity of this bar to the scarp face behind.

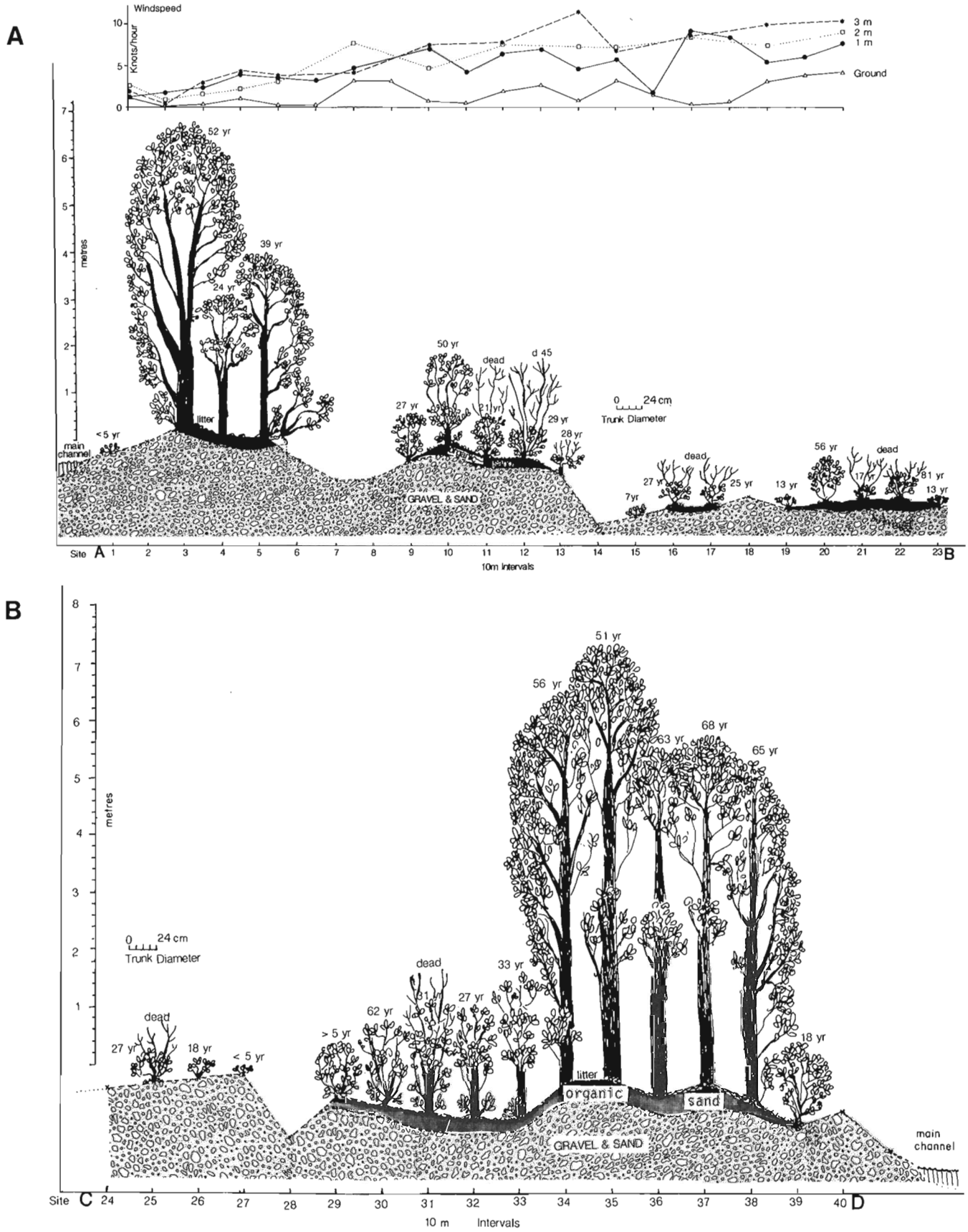

Figure 39.3. *Schematic diagram of (A) transect A-B and (B) transect C-D, showing the ground profile; presence of willow; height, age, and approximate diameter of willows; and organic accumulation. Wind speed along A-B at ground level, 1 m, 2 m, 3 m, is shown above the profile.*

Table 39.1. Growth data for feltleaf Willow, based on analysis of tree rings, along transects A-B and C-D

Transect	Site no.	Age (years)	Diameter including bark (cm)	Width of last 5 years growth mm	Average growth increment 1978-82 (mm)
A	1	<5	2.0	-	-
|	3	52	16.2	5.7	1.1
|	4	24	7.3	5.3	1.1
|	5	39	6.9	2.8	0.6
|	9	27	1.8	1.6	0.3
|	10	50	6.5	0.7	0.1
|	11	21	1.7	0.8	0.2
|	12a	45	3.0	2.5	0.4
|	12d	29	3.2	2.1	0.4
|	13	28	2.1	0.6	0.1
|	15	7	0.6	1.1	0.2
|	16	27	1.8	1.2	0.2
|	17	35	1.7	1.3	0.3
|	19	13	0.9	1.1	0.2
|	20	56	5.7	1.4	0.3
|	21	17	1.6	1.0	0.2
|	22	81	5.8	1.4	0.3
B	23	13	2.0	1.5	0.3
C	25	27	3.4	2.1	0.4
|	26	18	1.7	1.6	0.3
|	27	<5	0.5	-	-
|	29	<5	2.0	-	-
|	30	62	3.1	0.5	0.1
|	31	31	4.9	2.2	0.4
|	32	27	8.2	3.0	0.6
|	33	33	6.2	5.0	1.0
|	34	56	9.8	6.0	1.2
|	35	63	13.2	4.5	0.9
|	36	69	10.3	6.9	1.4
|	37	68	10.7	3.0	0.6
|	38	65	9.6	2.8	0.6
D	39	18	3.2	2.5	0.5

The only parameter to which growth increments can be related directly appears to be the distance from the major channel (Fig. 39.6) and, coincidentally, from the north valley wall. Willows on stabilized bars (willows older than 5 years) showed greatest growth rates (0.9 to 1.2 mm) and greatest height (6-8 m) when 30 to 50 m from the major channel. On the other hand, the lowest annual growth increments (0.1 to 0.3 mm) occurred farthest from the active channels.

Erect shrub-tree growth form

Several factors may affect the development and survival of the tree growth form: growing season temperatures, snow cover, moisture availability, exposure to desiccation, ice crystal abrasion, and browsing.

Summer temperatures

The limit of trees has long been correlated with summer temperatures. Both the latitudinal and the elevational limits of trees have long been shown to approximate the 10°C mean isotherm for July.

Our limited data suggest that for this valley, the mean isotherm for July is above 10°C; the mean daily temperature for the second week of July 1983 was of 15.2°C. Minimum temperatures never dropped below 9°C during that week, and reached a maximum of 21°C. This was several (1 to 9°C) degrees warmer than areas to the south. High temperatures were also recorded in July 1982 where an afternoon temperature of 28°C occurred in a similar valley. If these limited temperature data are representative of the long term record, it is not surprising that the tree form occurs in some of the willows in this valley.

Snow cover

Severe winter temperatures seem to have little effect on the growth of trees and shrubs, as long as they are covered by snow. Shrub height in the Low Arctic is also correlated with snow depth. Indeed, survival of all arctic shrubs seems to depend on the protection of lower stems and branches by deep drifts of snow, which prevent desiccation as well as

Figure 39.4. Tall feltleaf willow thickets near the edge of the main channel. Figure is standing at station 2 on transect A-B.

Figure 39.5. Local dieback of 1.5-2 m-high feltleaf willow thickets. This event, which occurred about 30 years ago did not kill the root stock. Regowth has levelled off at about 0.5 m height.

abrasion by ice crystals, and which moderate temperatures (Bliss, 1962; Savile, 1972). The depth of snow during winter and spring is probably a major factor in the survival of these tree-sized willow thickets.

The tallest (6-8 m) willows in the Minto Inlet study area are located on bars near a 20 to 30 m-high river-cut scarp. These thickets lie in the lee of the scarp protected from north and northeasterly prevailing winds in winter. Drifting snow, which accumulates more deeply in areas of thickets, may accumulate to even greater thicknesses in this place. Willows on other river bars, not in the lee of the scarp face, rarely are above 3 m high. These shorter thickets, however, also show a similar pattern when profiled at right angles to the main channel: the tallest thickets are closest to the main channel. It appears that conditions for optimal growth of feltleaf willow occur on channel bars nearest the main channel.

It is not likely that the entire valley fills with snow, even locally, to depths of 6 to 8 m; depths of 1-2 m are more probable. Figure 39.7. shows the severe pruning that occurs on erect willows at the edge of an inactive terrace. Matthews (1983) reported that similar willow thickets (greater than 5 m high) in northern Quebec are not entirely covered by snow in winter; drifts reach no more than 1.5 m depths.

Moisture availability and exposure

How tall willows survive the severely cold winters, when their tops are exposed to desiccating winds and ice crystal abrasion, is not known; however, some possibilities deserve further research. Polunin (1940) suggested that tall (2-5.5 m) birch forests in Greenland are associated with an unfrozen subsoil layer that persists through winter. The death of branches of tall shrubs extending above snow drifts is thought to be due to severe desiccation during winter when plants are unable to maintain transpiration since their groundwater supply is frozen. In areas such as along main river channels, where water may run nearly year round, there may be zones near the channel where the ground does not completely freeze or freezes for only short periods during winter. Dense thickets promote the early accumulation of snow, which in turn insulates the soil from more severe temperatures. Thus the water supply may be available nearly year round to willows in this area near the main channel.

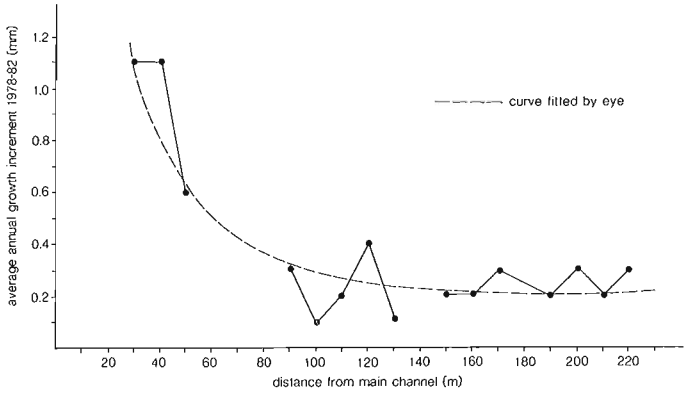

Figure 39.6. *Average growth increment (1978-82) versus distance from main channel along transect A-B. The fastest growing trunks are on the stable bars closest to the main channel.*

Browsing

The shape, extent, and degree of pruning cannot be solely attributed to wind abrasion, desiccation, or freezing. Local extensive bark and bud stripping and the production of solitary trunks appear to be caused by hares (Petersen et al., 1981). Such damage occurs along edges of dense thickets and throughout more open thickets. The absence of terminal and lateral buds on some parts of branches at the edge of thickets, commonly the zone between 1 and 2 m above the ground, and the abundance of ptarmigan scat directly beneath, suggest that these thickets also provide shelter and winter forage for ptarmigan. Grazing by large herbivores, particularly muskoxen, may also modify shrubs and branches up to several metres.

Comparisons with northern Quebec

Maycock and Matthews (1966) reported the presence of fallen and decaying trunks of willow and extensive peat deposits under thickets in areas of willow thickets in northern Quebec. They also suggested that these willow thickets may be relicts of a willow forest that grew during a more extensive warming, perhaps dating back to the Hypsithermal Interval. Their largest willows (ca. 60 years old) showed extensive deterioration of heartwood.

No evidence for this degree of antiquity was found at the Minto Inlet site. With the exception of the zone where some event killed local clumps right to ground level, no evidence was found of major periods of death and regeneration of this population. Perhaps willow thickets at Minto Inlet responded to a warming period in the north during the 1930s and 40s when there was also an increase in the growth of tree-sized willows in tundra areas of Labrador and northern Quebec (Maycock and Matthews, 1966). It was surprising that no deterioration of heartwood occurred in any of the specimens at Minto Inlet; this suggests that these thickets are healthy, relatively young, and in phase with the present climate.

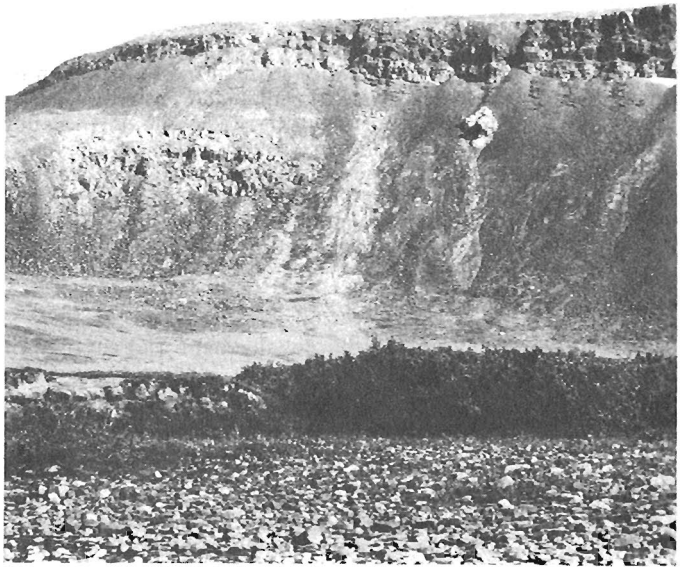

Figure 39.7. *Natural pruning of metre-high willows along the edge of an inactive terrace. The canopy barely extends above the 1 m height of the terrace. Shrubs (**S. lanata**) on the higher terace rarely reach heights of more than 30 cm (photo by V. Thomas).*

SUMMARY

The growth of extensive but discontinuous tree-sized willow thickets in a valley in the Minto Inlet area seems to be a response to several climatic and edaphic factors. Feltleaf willow thickets, 2 to 8 m high, require warmth, snow cover, and well drained, aerated, nutrient-rich soils, such as those found on gravels on the modern floodplain. This valley is considerably warmer than the surrounding hills and coastal areas. It appears that the requirement of a mean July temperature of 10°C for the tree growth form to survive is met in the valley, and may even be exceeded.

Variation in the height and density of the willow thickets on the modern floodplain can be attributed to variation of microhabitat conditions. Variation in height and annual growth increment correlates with the distance from the main channel: the tallest (6-8 m), fastest growing (0.9 to 1.2 mm per year) erect willows occur on the stable bars nearest the main channel. This may be a function of availability of moisture during both summer and winter, the degree of aeration, and drainage of the soil. Once established, the thickets promote accumulation of snow by trapping windblown snow; this insulation may also help with winter survival. Local topography also influences the depth of snow and thus tree height.

Willow thickets in the Minto Inlet area appear to be healthy and in phase with the present day climate rather than a relict of an earlier, warmer period. The heartwood of all willows sampled was solid. Feltleaf willow clumps of at least 81 years old occur on the stable bars of the floodplain, with the youngest trees (less than 5 years old) most commonly found on the partially stabilized bars undergoing primary colonization.

No sign of decadence occurs in most of these thickets, although a locally catastrophic event 30 years ago killed the above-ground shoots of one group of willow thickets. Regeneration from these has occurred and modern annual growth increments are equal to undamaged trunks of clumps on similar bars.

ACKNOWLEDGMENTS

Excellent field logistics support was provided by Polar Continental Shelf Project. Appreciation is also extended to D.R. Sharpe for co-ordinating the field logistics and to Sharpe and F.M. Nixon, who made available their weather data from their Wollaston Peninsula camps. Comments by J.A. Heginbottom, who critically read this manuscript, were incorporated in the text.

REFERENCES

Bird, J.B. and Bird, M.B.
1961: Bathurst Inlet, Northwest Territories, Canada; Geographical Branch, Memoir 7, 66 p.

Bliss, L.C.
1962: Adaptations of arctic and alpine plants to environmental conditions; Arctic, v. 15, no. 2, p. 117-144.

Bliss, L.C. and Cantlon, J.E.
1957: Succession on river alluvium in northern Alaska; American Midland Naturalist, v. 58, p. 452-469.

Drew, J.F. and Shanks, R.E.
1965: Landscape relationships of soils and vegetation in the forest-tundra ecotone, Upper Firth River valley Alaska-Canada; Ecological Monographs, v. 35, no. 3, p. 285-306.

Edlund, S.A.
1983: Reconnaissance vegetation studies on western Victoria Island, Canadian Arctic Archipelago; in Current Research, Part B, Geological Survey of Canada, Paper 83-1B, p. 75-81.

Fyles, J.G.
1962: Physiography; in Banks, Victoria and Stefansson islands, Arctic Archipelago, by R. Thorsteinsson and E.T. Tozer; Geological Survey of Canada, Memoir 330, p. 8-17.

Gill, D.
1973: Ecological modifications caused by removal of tree and shrub canopies in the Mackenzie Delta; Arctic, v. 26, no. 2, p. 95-111.

Hanson, H.C.
1951: Characteristics of some grassland, marsh and other plant communities in western Alaska; Ecological Monographs, v. 21, no. 4, p. 317-378.

Maycock, P.F. and Matthews, B.
1966: An arctic forest in the tundra of northern Ungava, Quebec; Arctic, v. 19, p. 317-378.

Matthews, B.
1983: Letter to the editor; Arctic, v. 36, no. 3, p. 291.

Nettleship, D.N. and Smith, P.A. (ed.)
1975: Ecological Sites in Northern Canada; Canadian Committee for the International Biological Programme, Conservation Terrestrial, 330 p.

Peterson, E.G., Kabzems, R.D., and Levson, V.M.
1981: Terrain and vegetation along the Victoria Island portion of a Polar Gas combined pipeline system; Prepared by Western Ecological Services (B.C.) Ltd. for Polar Gas Environmental Program (Toronto), 136 p.

Polunin, N.
1940: The birch 'forests' of Greenland; Nature, v. 140, p. 939-940.

1951: The real Arctic: suggestions for its delimitation, subdivision, and characterization; Journal of Ecology, v. 7, no. 3, p. 308-315.

Porsild, A.E.
1955: The vascular plants of the western Canadian Arctic Archipelago; National Museum of Canada, Bulletin 135, 226 p.

Savile, D.B.O.
1972: Arctic adaptations in plants; Department of Agriculture, Monograph 6, 81 p.

Spetzman, L.A.
1959: Vegetation of the arctic slope of Alaska; United States Geological Survey, Professional Paper 302-B, 58 p.

Thorsteinsson, R. and Tozer, E.T.
1962: Banks, Victoria and Stefansson islands, Arctic Archipelago; Geological Survey of Canada, Memoir 330, 83 p.

Viereck, L.A. and Little, E.L.
1972: Alaska Trees and Shrubs; United States Department of Agriculture and Forestry Service, Washington, D.C., Agriculture Handbook no. 410, 265 p.

40. INVESTIGATION OF DIATOMS FOUND IN SURFACE SNOW FROM THE SYDKAP ICE CAP, ELLESMERE ISLAND, NORTHWEST TERRITORIES

Project 720078

Sigrid Lichti-Federovich
Terrain Sciences Division

Lichti-Federovich, S., Investigation of diatoms found in surface snow from the Sydkap Ice Cap, Ellesmere Island, Northwest Territories; in Current Research, Part A, Geological Survey of Canada, Paper 84-1A, p. 287-301, 1984.

Abstract

Qualitative diatom analysis of surficial snow from a polar ice cap resulted in the delineation of two principal floristic components: an allochthonous marine element and an autochthonous freshwater constituent comprising 105 identified taxa. Predominance of aerophilous diatoms affirms positive correlation with other extreme, nonaquatic biotopes.

Résumé

L'analyse qualitative de diatomées provenant de la neige à la surface d'une calotte glaciaire polaire a permis de reconnaître deux composantes florales principales, soit un groupe allochtone marin et un groupe autochtone d'eau douce composé de 105 taxons identifiés. La prédominance des diatomées aérophiles confirme la corrélation positive avec d'autres biotopes non aquatiques extrêmes.

INTRODUCTION

This preliminary report is based on the cursory examination of surface snow from the Sydkap Ice Cap (Fig. 40.1). Although priority was given to glaciological and palynological investigations, the diatom analytical study of surficial snow from arctic ice caps had originally been perceived as a hopeful adjunct to palynological investigations, with the special aim of aiding elucidation of dispersal phenomena and with the intent of augmenting earlier records of diatoms found in ice and snow.

Diatoms inhabiting glacial and nival biotopes have received little attention. Although the literature is replete with reports focussing on other algal groups, such as Chlorophyceae, Xanthophyceae, and Cyanophyceae, systematic research of nival biotopes with regard to Bacillariophyceae has been scant (c.f. Kol, 1968; see also Lichti-Federovich (1980) for citations of earlier references to diatom enumerations from red snow). This dearth of diatom analytical investigations may in part be due to a lack of impetus to conduct intensive studies caused by the reported scarcity of diatoms in nival habitats, doubtless, a consequence of small sample size. Since the collection of surface snow from the polar ice caps was undertaken without prescience of either presence or abundance of diatoms, it was with great pleasure to realize their relative plenitude.

This report represents the first diatom analytical investigation of a nival biotope from a polar ice cap. Its main purpose is to establish the presence of diatoms in such highly specialized habitat and to attempt their taxonomic and autecologic delineation. Implications of dispersal phenomena and sources of dissemination will constitute the focal point of a sequel to the present report. This follow up will incorporate additional diatom analytical data from surficial snow of the 'Central Ellesmere' ice cap and the Agassiz Ice Cap (Fig. 40.1).

MATERIAL AND METHODS

The Sydkap Ice Cap is located in the southern part of Ellesmere Island; the various investigations were carried out in May 1982, at 76°53.4'N, 86°02.3'W and at an elevation of 1400 m (Fig. 40.1). Collection of approximately one year's accumulation of surface snow, representing the previous summer's melt layer and winter deposition, required excavation of a pit to below melt layer level to accurately determine one year's snow accumulation depth. Using a straight-sided wall of the pit as guide line, a 50 cm^2 surface area was roped off. With handsaw and shovel all snow within this area down to melt layer depth was removed into 26 x 30 inch 'heavy duty' plastic bags. The melt layer, representing last summer's thaw and freeze interval, was collected separately. All bags were weighed in the field, then transported to Resolute, Cornwallis Island, for melting and filtering.

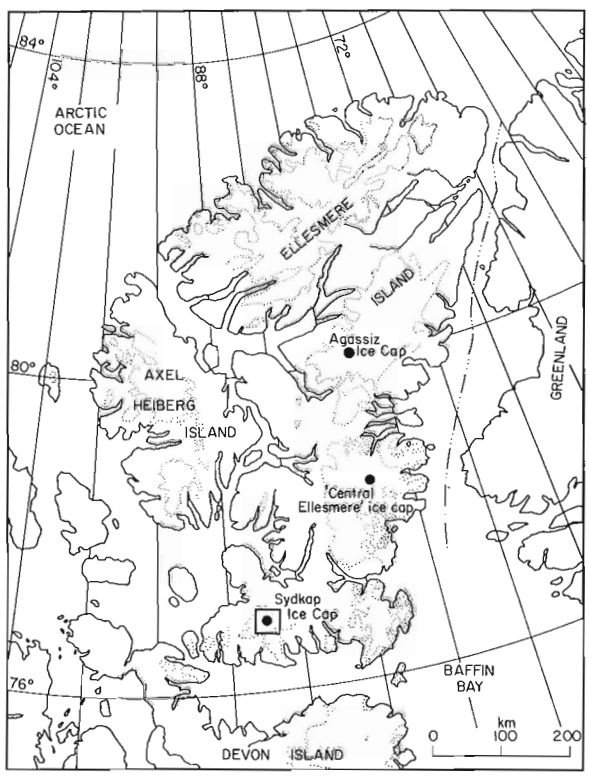

Figure 40.1. Location of the Sydkap Ice Cap.

Table 40.1. List of freshwater diatoms and their respective ecologies from surface snow of the Sydkap Ice Cap

	Halobien rate	pH	Oxygen requirements	Current rate	Aerophilous	Aerial	Subaerial	Eu-aerial	Pseudoaerial	Terrestrial	Hydroterrestrial	Eu-terrestrial	Subterranean	Soil: General	Soil: Surficial soil (litter)	Soil: Thin layer on rock	Rock: General	Rock: Moist	Rock: Bare	Mosses: General	Mosses: Hydric	Mosses: Mesic	Mosses: Xeric	Dry lakes	Thermal waters	Climatic Geographic affinity	Elevation (m)
ACHNANTHES Bory																											
*?**A. broenlundensis** Fog.																											
A. flexella (Kütz.) Brun	hphob. F2	acf. J,F2	high C1											F1												cosmo.? F1 nord. mont. W3	
A. hungaria Grun.	ind. F2	alkf. J,F2	high C1																							cosmo. F2	
A. kryophila Pet.		ind. Z	high C1															H6		F1	K2,H6					nord. mont. K2,K3	
A. lapponica Hust.	hphob. F	acf. J,F			W3,K2													H7			K2,H7					nord. alp. K2,K3,W3	
A. levanderi Hust.		ind.? Z															P2	H7								nord. alp. K3	
A. marginulata Grun.	ind. F2	alkf. F1 acf. C1		rheof. P2	K2									P2			P2			P2 H6						nord. alp. K2,K3,H7 temp. mont. K1 alp. boreal P4	
A. minutissima Kütz.	ind. F	ind. J,F	high C1		W3				S					T						F1,K2 P2						cosmo. H2 nord. mont. W3	2930, H4
A. pygmaea (Schum.) Cleve																		H7									
A. rupestris Krasske					K2				H6																	nord. alp. K3 north. mont. K2 mont. H6	
A. spp.																											
AMPHORA Ehrenberg																											
A. ovalis (Kütz.) Kütz. var. **pediculus** (Kütz.) V.H.	ind. F2	alkf. J,F2																								cosmo. F2,W3	
ANOMOEONEIS Pfitzer																											
A. serians (Bréb.) Cleve var. **brachysira** (Bréb.) Cleve	hphob. F2	acf. J,F2																			K3	K3	K3			cosmo. K4,F2	2930, H4
A. zellensis (Grun.) Cleve	hphob. F	acf. F																								nord. mont. K1 nord. alp. K3 cosmo.? F2	
CALONEIS Cleve																											
*__C. aerophila__ Bock					B											B				B	B						
C. bacillum (Grun.) Cleve	ind. F2	alkf. F2,J			Vo	P2	U2		S						L2					S,S1 U2,W5				V		cosmo. F1,W3	
C. clevei (Lagerst.) Cleve		alkf. Z1																									
C. silicula (Ehr.) Cleve var. **alpina** Cleve		alkf. J																								cosmo. W3	

Table 40.1 (cont.)

	Halobian rate	pH	Oxygen requirements	Current rate	Aerophilous	Aerial	Subaerial	Eu-aerial	Pseudoaerial	Terrestrial	Hydroterrestrial	Eu-terrestrial	Subterranean	Soil: General	Soil: Surficial soil (litter)	Soil: Thin layer on rock	Rock: General	Rock: Moist	Rock: Bare	Masses: General	Masses: Hydric	Masses: Mesic	Masses: Xeric	Dry lakes	Thermal waters	Climatic Geographic affinity	Elevation (m)
CERATONEIS Ehrenberg																											
C. arcus (Ehr.) Kütz.	ind. F	ind. F	high C1	rheob. W3 rheof. P2 W1,W5,H7										F1												cosmo. W3	
C. arcus var. **linearis** Holmb.	ind. F	ind. F	high C1																J1								2450-2650, J1
CYCLOTELLA Kützing																											
C. bodanica Eul. var. **intermedia** Mang.																											
C. comta (Ehr.) Kütz. (fragment)	ind. F	alkf. J ind. F												Fo													2750, H4
CYMBELLA Agardh																											
?**C. cesati** (Rabh.) Grun. var. **capitata** Krieg.	ind. F	ind. F	high C1																								
C. cuspidata Ehr.	ind. F2	ind. F2,J																		F1	K2					cosmo. F2,W3	
C. latens Krasske	hphob. F	acf. F												F1													2750, H4
C. laevis Naeg.		alkf. W4												F1						F1		K1					
C. obtusa Greg.	ind. F	alkf. F												F1												cosmo. W3	
C. similis Krasske	ind. F2	ind? F2																			K1					Europe F2	2750, H4
C. stauroneiformis Lag.																					K1					nord. alp. H4,K3	2750, H4
C. ventricosa Kütz.	ind. F2	ind. J,F2	high C1		Vo									L2					J1	F1 L2				Vo		cosmo. F2,K4,W5	2650, J1 2930, H4
C. spp.																											
DENTICULA Kützing																											
D. rainierensis Sov.																								P4			630, P4
D. spp.																											
DIATOMA De Candolle																											
D. elongatum Ag.	hphil. F	alkf. F	high C1																	F1						N.A. & S.A. W3	
EUNOTIA Ehrenberg																											
E. monodon Ehr. var. **major** (W. Smith) Hust.	hphob. F2	acf. J,F2		rheof. H7																						S.A. K4	
E. praerupta Ehr. var. **inflata** Grun.	hphob. F	acf. F																								north. Europe H7 cosmo.? F2	
E. praerupta var. **musicola** Pet.	hphob. F	acf. J,F																		H6,P2						mount. & lowl. H7	
FRAGILARIA Lyngbye																											
F. brevistriata Grun.	ind. F2	alkf. F2,J	high C1		Vo									L2,N										Vo		cosmo. F2,W3	
F. construens (Ehr.) Grun.	ind. F2	alkf. F2,J	high C1	lim. H7																						cosmo. F2,K4	
F. elliptica (Schum.) Haw.																											

Table 40.1 (cont.)

	Halobien	pH	Oxygen requirements	Current rate	Aerophilous	Aerial	Subaerial	Eu-aerial	Pseudoaerial	Terrestrial	Hydroterrestrial	Eu-terrestrial	Subterranean	Soil: General	Soil: Surficial soil (litter)	Soil: Thin layer on rock	Rock: General	Rock: Moist	Rock: Bare	Mosses: General	Mosses: Hydric	Mosses: Mesic	Mosses: Xeric	Dry lakes	Thermal waters	Climatic Geographic affinity	Elevation (m)
F. intermedia Grun.	ind. F2	alkf. F2	high C1											N,N1				H7								cosmo. F2	
F. pinnata Ehr.	ind. F2	alkf. F2,J	high C1		Vo									N										Vo		cosmo. F2,W3	
F. vaucheriae (Kütz.) Pet.	ind. F2	alkf. F2,J		rheof. W5											L2											cosmo.? F2	
HANTZSCHIA Grunow																											
H. amphioxys (Ehr.) Grun.	ind. F2	ind. F2,J alkf. F			V,P2		U2	P1				P3	M M1					D,R1, U2		L2,S1, W5,U2	K1		F3	V		cosmo. F2,W3,K3	2930, H4
H. amphioxys fo. **capitata** O. Müll.	ind. F	alkf. F												L2									F3				
MELOSIRA Agardh																											
M. roeseana Rab.	ind. F2	ind. F2			K4	P2	U2o U3		H5 P2 S									P2 R1	J1	K2,S1, U2,U3						alp. H5,U3 cosmo. F2,K4	2930, H4 2400-2650, J1
MERIDION Agardh																											
M. circulare (Grev.) Ag.	ind. F2	alkf. F2,J	high C1	rheob. H4 rheof. H6, W5										L2	L2				J1	L2						cosmo. F1,W3	
NAVICULA Bory																											
N. begeri Krasske					H6 K2																H6				K2	north. Europe H6 nord. alp. K2 arctic alp. W4	
N. cari Ehr. var. **angusta** Grun. (fragment)		acf. C1									P3	P3															
N. cincta Kütz. var. **heufleri** (Grun.) V.H.	hphil. F	alkf. Z			P1					P1				L1,P2		P1											
N. cocconeiformis Greg.	hphob. F2	ind. F2	high C1											P1				P2			K2	P2				nord. mont. W3 north. Europe K2 cosmo.? F2	
N. cohnii (Hilse) Grun.	hphil. F	ind. Z				P2											P1,P2 P5	H1,P1								alp. H5 mont. Q3	
N. contenta Grun.	ind. F2	alkf. F1 acf. C1 ind. F			V	P2	U2,U3		H5 P3			P3					P2	P2		K2,P2 U2			F3 K1			cosmo. F2	
N. contenta fo. **biceps** (Arn.) Grun.	ind. F2	ind. F alkf. F2				P2	U2,U3		S					P5				R1		S1,S2 U2,U3			F3			mont. H6,Q3 cosmo. F2,H6	
N. contenta fo. **parallela** Pet.	ind. F2	ind. F alkf. F2				P2	U3											K1				K1 P5	F3			mont. H6, Q3 cosmo. F2, H6	
N. cryptocephala Kütz.	ind. F2	alkf. F2			H6									F1,N					J1				F1			cosmo. F2,W3	2650, J1 2930, H4
N. cryptocephala var. **veneta** (Kütz.) Grun. **N. gebhardi** Krasske	hphob. K2 ind. F2	alkf. F2			K2																					cosmo. F2,W3	
N. gibbula Cleve	hphob. F	acf. F			H6		U3			H6			P3	P3						F1,K2 S1,U3			F3			nord. alp. K3 cosmo.? H6	2930, H4
N. hungarica Grun. var. **arctica** Petr. & Freese	hphil. P7	ind.? P7 alkf. P7																									
N. minima Grun.	ind. F	ind. F							H6					L1,N Q2,T								K1				cosmo. W3	

Table 40.1 (cont.)

	Halobien rate	pH	Oxygen requirements	Current rate	Aerophilous	Aerial	Subaerial	Eu-aerial	Pseudoaerial	Terrestrial	Hydroterrestrial	Eu-terrestrial	Subterranean	Soil: General	Soil: Surficial soil (litter)	Soil: Thin layer on rock	Rock: General	Rock: Moist	Rock: Bare	Mosses: General	Mosses: Hydric	Mosses: Mesic	Mosses: Xeric	Dry lakes	Thermal waters	Climatic Geographic affinity	Elevation (m)
N. mutica Kütz.	ind. F2 hphil. F	ind. F	high C1		H4,U2 V		U3							R,P6 L,L2 E,P1 P3	L2			R1		K1,K4 X1,S K2,L2 U3			F3	V		cosmo. F1,K4,W3 alp. U1,U3	730, U1
N. mutica Kütz. fo.																											
N. mutica var. **nivalis** (Ehr.) Hust. (fragment)	ind. F	ind. F			Vo	H6														H6,S1			F3	Vo		cosmo. H6	
N. mutica var. **ventricosa** (Kütz.) Cleve et Grun.		ind. Z			P1,V															P2							
?**N. paramutica** Bock					H6	B																					
N. rotaeana (Rabh.) Grun.	ind. F2 H6	ind. F2 H6	high C1	rheob. H4	H6									F1				H6	J1							cosmo. F2,W3	2650, J1
N. seminulum Grun.	ind. H6, F	ind. H6, F												L1,Q2 T								K1					
N. sohrensis Krasske var. **musicola** (Pet.) Krasske		alkf.?Z1	high C1	lim. H6	H6													H6			H6						
N. tenelloides Hust.	ind. F2	alkf. F2	high C1		H6,K4 P4				S					L1,L2						K4						cosmo. K4,W3 cosmo.? F2	
N. viridula Kütz.	ind. F2	alkf. F2																								cosmo. F2,W3	
N. viridula Kütz. fo.																											
N. spp.																											
NEDIUM Pfitzer																											
N. affine (Ehr.) Pfitz. (fragment)	ind. F2	alkf. F2								P1				L2												cosmo. F2,W3	
?**N. rosenkrantzii** Fog.																											
NITZSCHIA Hassal																											
N. debilis (Arn.) Grun.	ind. F2	alkf. F2			P1						P3			P1,P2						K3						cosmo. F2	
?**N. ignorata** Krasske	ind. F2	ind. F2 alkf. F																								cosmo.? F2	
?**N. ovalis** Arn.	meshal. K2																										
N. thermalis Kütz. var. **minor** Hilse		alkf. F																									
N. spp.																											
PINNULARIA Ehrenberg																											
?**P. appendiculata** (Ag.) Cleve var. **irrorata** (Grun.) Hust.														P2						P2					P2		
P. balfouriana Grun. ex. Cleve	ind. F	acf. F			K2		U3							P5						F1,U3		K1				temp. mont. K1 nord. mont. K2 nord. alp. K3,H4	
P. borealis Ehr.	ind. F2	ind. F1 acf. J			F2,P1 P2		U2,U3	P1,X			P1	P3		E,F2, J2,L2 P1,R	L2		E	P5	J1	K1,K2 L2,U3 X			K1 F3			cosmo. F1,W3 alp. U3	2930, H4

Table 40.1 (cont.)

	Halobien rate	pH	Oxygen requirements	Current rate	Aerophilous	Aerial	Subaerial	Eu-aerial	Pseudoaerial	Terrestrial	Hydroterrestrial	Eu-terrestrial	Subterranean	Soil: General	Soil: Surficial soil (litter)	Soil: Thin layer on rock	Rock: General	Rock: Moist	Rock: Bare	Mosses: General	Mosses: Hydric	Mosses: Mesic	Mosses: Xeric	Dry lakes	Thermal waters	Climatic Geographic affinity	Elevation (m)
P. borealis fo. **lanceolata** Pet.						P2																					
P. brebissonii (Kütz.) Rabh.											P3			L2,P2 P3,P5 W5,R				P1		W5							
P. brebissonii var. **diminuta** (Grun.) Cleve														L2,P6						L2							
P. divergens W. Smith var. **bacillaris** (M. Perag.) Mills																											
P. fasciata (Lagerst.) Hust.							U3													K2,U2	K2						
***P. intermedia** (Lagerst.) Cleve	ind. F	ind. F			F1					P1,P3				P1,J2 J3,P2 L1							K2					nord. K2 north. alp. H3 arctic C	
P. krookii (Grun.) Cleve	hphil. Z1	ind. F2																								cosmo? F2	
P. microstauron (Ehr.) Cleve	ind. F2	acf. J ind. F2								P1	P1,P3		S	L1,T							K2					cosmo. F1,K4	
P. obscura Krasske	ind. F2	ind. F2			K3							P3	P3	F3	L2					K2	K4	K1				cosmo. F2	
P. parva (Ehr.) Greg. var. **lagerstedtii** Cleve fo. **interrupta** Pet.		acf. Z												J2,J3, W5						W5							
P. subcapitata Greg. var. **sublanceolata** Pet.	ind. F	ind. F												P2						P2							
?**P. sublinearis** (Grun.) Cleve																											
P. substomatophora Hust.																											
P. spp.																											
STAURONEIS Ehrenberg																											
S. agrestis Pet.	ind. F2	ind. F2			Plo									P1												cosmo.? F2	
S. anceps Ehr.	ind. F2	ind. F2, J							?P3		P2			F1,L2 P3,P6 T				H6		F1,P2	K2				H6	cosmo. F2,W3	2930, H4
S. borrichii (Pet.) Lund	ind. F2	ind. F2	high C1											L2,Q1	L2												
S. borrichii var. **subcapitata** (Pet.) Lund					H7									L2													
?**S. nugsuaqensis** Foged																										cosmo.? F1 cosmo. H7	
S. obtusa Lag. (fragment)	ind. F2 P4	ind. F2 alkf. P4			H7		U3							F1			H6	U3		F1,U3		H6	K1			alp. U3, K1 temp. mont. K1	
S. phoenicenteron (Nitzsch) Ehr. (fragment)	ind. F2	ind. J F2												L2,Q2						K2,Q3							
S. thermicola (Pet.) Lund fo. **lanceolata** Hust.			high C1		H7																						
S. spp.																										cosmo. H7	

Table 40.1 (cont.)

	Halobien rate	pH	Oxygen requirements	Current rate	Aerophilous	Aerial	Subaerial	Eu-aerial	Pseudoaerial	Terrestrial	Hydroterrestrial	Eu-terrestrial	Subterranean	Soil: General	Soil: Surficial soil (litter)	Soil: Thin layer on rock	Rock: General	Rock: Moist	Rock: Bare	Mosses: General	Mosses: Hydric	Mosses: Mesic	Mosses: Xeric	Dry lakes	Thermal waters	Climatic Geographic affinity	Elevation (m)
STEPHANODISCUS Ehrenberg																											
S. astraea (Ehr.) Grun. var. **minutula** (Kütz.) Grun.	ind. F2	alkf. J alkf. F2			Vo																			V		cosmo. F2	
SYNEDRA Ehrenberg																											
S. tabulata (Ag.) Kütz. (fragments)	meshal. F2	alkf. J, F																								cosmo. F2	
TABELLARIA Ehrenberg																											
T. fenestrata (Lyngb.) Kütz. (fragment)	hphob. F2 ind. F	acf.J ind. P4, Z																	J1							cosmo. F2	
T. flocculosa (Roth.) Kütz.	hphob. F2	acf. J1, F2	high C1																		K2					cosmo. F2	2936, H4 1850-2800, J1

acf. – acidophilous; alkf. – alkaliphilous; alp. – alpine; cosmo. – cosmopolitan; hphil. – halophilous; hphob. – halophobous; ind. – indifferent; limno – limnobiontic; meshal. – meshalobous; mont. – montane; N.A. – North America; nord. – nordic; north. – northern; rheob. – rheobiontic; rheof. – rheophilous; o – rare.

* denotes most abundant representation of particular taxon within genus

Key to references listed in Table 40.1

B – Bock 1963
C – Cleve-Euler 1955
C1 – Cholnoky 1968
D – Deflandre 1926
E – Johansen, Rushforth and Brotherson 1981
F – Foged 1953
F1 – Foged 1955
F2 – Foged 1979
F3 – Florin 1970
H1 – Hustedt 1922
H2 – Hustedt 1924
H3 – Hustedt 1942
H4 – Hustedt 1943
H5 – Hustedt 1950
H6 – Hustedt 1961-66
H7 – Hustedt 1959
H8 – Hustedt 1930
J – Jörgensen 1948
J1 – Jaag 1945
J2 – John 1942
J3 – Fritsch and John 1942
K1 – Krasske 1932
K2 – Krasske 1938
K3 – Krasske 1943
K4 – Krasske 1948
L – Lund 1945, 1946
L1 – Lund 1945
L2 – Loescher 1981
M – Moore and Karrer 1919
M1 – Moore and Carter 1926
N – Feher 1936
N1 – Feher and Frank 1936
O – Ostrup 1918
P1 – Petersen 1915
P2 – Petersen 1928
P3 – Petersen 1935
P4 – Patrick and Reimer 1966, 1975
P5 – Patrick 1977
P6 – Reimer 1970
P7 – Patrick and Freese 1961
Q1 – Sauer 1955
Q2 – Schelhorn von 1936
Q3 – Simonsen 1953
R – Anderson and Rushforth 1976
R1 – St. Clair and Rushforth 1976
S – Stoermer 1962
S1 – Dodd and Stoermer 1962
T – Hayeck and Hulbary 1956
U1 – Skvortzow 1930
U2 – Skvortzow 1937
U3 – Skvortzow 1938
V – Van Landingham 1966
W1 – Messikommer 1946
W2 – Messikommer 1949
W3 – Messikommer 1949-50
W4 – Messikommer 1953
W5 – Messikommer 1953-54
X – Beger 1927
X1 – Beger 1928
Z – Foged 1958
Z1 – Foged 1964

The essential treatment of the surface snow at Resolute was one of concentration and volume reduction. The snow-filled plastic bags were reweighed and the snow was melted in large cooking pots on a 4-burner propane stove. Meltwater filtration, primarily designed for palynological studies, consisted of a pressure tank connected to a filter holder and to a mattress foot pump which during breakdown was replaced by a bicycle hand pump. For diatom analytical work a 0.8 µm pore size nuclepore filter was selected to ensure optimal retention of the diatomaceous faction.

Continuation of sample preparation in Ottawa included processing and simultaneous removal of the diatom-bearing material from the filter membrane by treatment with hydrogen peroxide and potassium dichromate. After repeated washings with distilled water, the residue was mounted in Hyrax. Routine microscopic examination of 8 randomly selected slides to record location of specimens, using coordinates, preceded critical identification with a Leitz x 90 oil immersion objective. To supplement the species list, an additional low magnification (x 125) scan of 12 slides was made. Species enumeration (Table 40.1), therefore, is based on the examination of 20 slides, selected at random. The following represents the summary data of the Sydkap surface snow collection:

Depth of surface snow	58 cm
Depth of melt layer	16 cm
Total weight of snow	76.48 kg
Total volume of snow	76.32 L
Number of filters	16
Number of slides	121

Although less critical for the present study, since it is only exploratory and primarily designed to determine the presence of diatoms, certain methodological weaknesses should nevertheless be mentioned. Aside from the absence of suitable laboratory facilities, it was essentially the lack of time that determined the choice of concentration method, favouring the nonregulatory pressure filtration procedure over a more gradual mode of concentration by normal settling and decantation methods. Whether the fairly high incidence of fragmented diatoms, mostly of the genus **Synedra**, is attributable to the pressure filtration method cannot be determined with any certainty. But taking into account the rigidity of the siliceous diatom frustule, in contrast to the comparative pliability of a pollen wall, the possibility of fracture of diatom cells (especially the elongate, thin valves and frustuls of **Synedra** spp.) during filtration cannot be dismissed entirely. Furthermore, the fact that fragmentation affected both the allochthonous and the autochthonous diatom component seems to substantiate the likelihood that breakage resulted from use of the pressure filtration method.

SYSTEMATICS

Alphabetical enumeration of the freshwater diatom taxa from the Sydkap Ice Cap, based on the examination of 20 randomly selected slides, is presented in Table 40.1. This species list includes all taxa that could be identified and collectively the unidentified forms that could be assigned to genus only. To facilitate comparison with other diatom lists, any changes in diatom synonymy due to recent revisions or amendments were not incorporated, but are tabulated separately (Table 40.2).

Morphological determination was primarily supported by the following "classical" monographs: Hustedt (1930, 1959, 1961-66); Cleve-Euler (1952, 1953, 1955); Foged (1953, 1955, 1958, 1964, 1972, 1973); Patrick and Reimer (1966); Mölder and Tynni (1970, 1972); and Tynni (1975, 1976, 1978, 1980). Taxonomic delineation was also greatly aided by: Lund (1946); Petersen (1950); Bock (1963); Schimanski (1973); Lange-Bertalot (1977, 1978, 1980a,b,c); Lange-Bertalot and Bonik (1978); Lange-Bertalot and Simonsen (1978); Lange-Bertalot and Ruppel (1980); and Krammer (1980).

Table 40.2. Revised Synonymy

Synedra tabulata (Agardh) Kützing	**Fragilaria tabulata** (Agardh) Lange-Bertalot
Fragilaria intermedia Grunow	**Fragilaria capucina** var. **vaucheriae** (Kützing) Lange-Bertalot
Fragilaria vaucheriae (Kützing) Petersen	
Nitzschia thermalis var. **minor** Hilse	**Nitzschia homburgiensis** Lange-Bertalot

For preparation of the ecological section of Table 40.1, 81 scientific papers were scrutinized. Citing of these literature references, however, is limited to those yielding the greatest amount of information. No attempt was made to condense the various ecological groupings in Table 40.1, but rather the original terminology cited by the various authorities was retained, even if some of the nomenclature appears and, in fact, is synonymous.

The fact that the species list represents a cursory investigation, based on a limited number of slides and plagued by certain taxonomic uncertainties, will no doubt ensure its future extension. Furthermore, augmentation of several new taxa, whose systematic treatment lies beyond the scope of this report, will greatly enhance its floristic-ecologic falue.

TAXONOMIC LIMITATIONS

Before delving into a detailed discussion of the diatom floristic results, it is essential to examine the taxonomic limitations that affect the diatom enumeration from the Sydkap Ice Cap and impel me to echo Jaag's statement (1945, p. 19) in which he relates the difficulties encountered in the attempt to describe the micro-vegetation of bare rocks: "Die Aufnahme der Artenliste..... bot uns anfanglich kaum geahnte und fast unbezwingbare Schwierigkeiten, und diese wurden wahrend der ersten Jahre, die der Untersuchung gewidmet waren, nicht geringer sondern immer grosser, je mehr Material uns durch die Hande ging"[1].

Aside from fragmentation, obstruction by detrital matter, and the girdle view orientation of many Pinnularias, it is the minuteness of diatoms, especially those representing the genera **Navicula** and **Achnanthes**, which imposes taxing difficulties on identification. This reduction in size, commonly accompanied by a concomitant increase in striation density, is not only a salient feature characterizing the Sydkap diatom flora, but it has been readily observed and documented by diatomists investigating other extreme, non-aquatic biotopes (Petersen, 1915, 1935; Bristol, 1920; Beger, 1927; Hustedt, 1930, 1942; Gistl, 1933; von Schelhorn, 1936; Lund, 1945, 1946; Bock, 1963; Reimer, 1970). Taxonomic delineation is further hampered by the faintness of striae of many small diatoms. As Lund (1946) pointed out, this impediment is especially critical since the number of striae in a given linear dimension (10 µm) represents one of the main criteria in taxonomic delimitation. Whether this structural phenomenon is induced by the lack of nutrients, especially silica, resulting in "Kummerformen", necessitates further investigation.

[1] The compilation of the species list..... presented us at the beginning with scarcely imagined and almost insurmountable difficulties, and these did not decrease during the first years of investigation, on the contrary, they became steadily greater the more material we examined.

As early as 1876, Schumann investigating diatomaceous gatherings collected from different elevations in the High Tatra, a mountain range bordering Poland and Czechoslovakia, observed this increase in density and faintness of striation and proposed temperature/elevation as the main casual factor of these structural changes.

More recently, Lange-Bertalot and Simonsen (1978), comparing type material from various localities for their systematic revision of **Nitzschia romana**, noticed that this species in alpine regions or oligotrophic waters produces populations which are delicately structured, whereas populations of **N. romana** from rivers of plains or mesotrophic waters are more coarsely formed. This evidence, no doubt, lent support to and aided formulation of Lange-Bertalot's concept that these morphological modifications are based on ecological conditions.

In addition to valve size reduction, increase in striation density, and faintness of structural elements, Lund (1945, 1946) recorded a change in the direction of striae in some soil diatoms. Drawing upon this evidence, alteration in the orientation of striae as a diagnostic feature, routinely used in diatom identification, has become invalidated or at least should be applied with caution when determining the taxonomic position of small, nonaquatic forms. Once again it should be stressed that these morphological variations are not random phenomena, but they are observed in diatoms inhabiting all extreme, nonaquatic environments.

While it is beyond the scope of this report to discuss the various theories put forth to elucidate the underlying cause of these structural phenomena and to evaluate their soundness (several interpretations of these modifications have already been repudiated), nevertheless, mention should be made of Lund's (1945) proposal that the morphological differences between aquatic and terrestrial forms are genetically induced.

Aside from acknowledging taxonomic restrictions imposed by the structural modifications of diatoms, this discussion need also consider limitations based on the current state of diatom systematics, which is fraught with confusion and uncertainty. In this context I acknowledge and laud the invaluable contribution by Lange-Bertalot to the clarification of taxonomic problems, especially concerning such systematically enigmatic groups as **Nitzschia** and **Navicula.**

From Lange-Bertalot's (1977, 1978, 1980a,b,c) excellent but as yet rather limited revision (i.e. in view of the enormous scope and multiplicity of diatom systematics), two generalizations are emerging. Firstly, there is an apparent general tendency towards species reduction. This supposition does not rest on purely speculative grounds but is supported by Lange-Bertalot's results of his systematic evaluation of the genus **Nitzschia.** More specific examples include the substantiated taxonomic identity of **Navicula imbricata** with **N. mutica** (Lange-Bertalot and Bonik, 1978); the established synonymy of **Navicula perpusilla, N. exilissima,** and **N. fragilarioides** with **N. gallica** (Lange-Bertalot, 1980b); and the documented conspecifity of **Achnanthes minutissima, A. microcephala, A. linearis,** and **A. affinis** (Lange-Bertalot and Ruppel, 1980). Secondly, by contrast, in Lange-Bertalot's systematic overview there is manifested a marked inclination towards increased valve structure variability based on difference in ecological conditions and geographic origin and evidenced by ecological and geographic variants. Such "phenotypic plasticity" is expressed by the extensive variability of many **Nitzschia** species (see previous reference to variations in striation density of **N. romana**), and it is also affirmed by the **Navicula mutica** form cycle.

Not only are restrictive measures imposed on a valid taxonomic determination by the use of descriptions and drawings of earlier publications, but taxonomic ambiguities are also closely linked to the light optical limits of ordinary microscopic observation. In his comprehensive review of the highly problematic group **Nitzschia lanceolatae,** Lange-Bertalot (1977) stressed the absolute necessity for submicroscopic examination of diatom valves with scanning electron and transmission electron optical techniques. For example, he contends that diagnosis of **Nitzschia palea** and differentiation from morphologically similar taxa such as **N. intermedia** are light optically impossible (1977, p. 272). He concludes: "The section of the **Nitzschiae lanceolatae** can no longer be differentiated without the aid of submicroscopical characteristics" (1977, p. 284). Reference to taxonomic limitations with specific application to the nival diatom association from the Sydkap Ice Cap is provided in the section entitled Notes on Some Species.

FLORISTIC RESULTS

Floristic assessment of the nival diatom collection from the Sydkap Ice Cap permits differentiation of two main constituents: a readily perceived allochthonous marine element, obviously its most salient feature, and an autochthonous freshwater constituent. The euhalobous component represented by **Biddulphia aurita, Conscinodiscus subtilis, C. radiatus, Diploneis interrupta, Fragilariopsis cylindrus, Navicula directa** var. **subtilis, Amphora** sp. (Oxyamphora), **Cocconeis scutellum** var. **stauroneiformis, C. costata, Rhaphoneis amphiceros,** and fragments of **Coscinodiscus centralis, Thalassiosira** spp., **Melosira sulcata, Navicula cancellata, Chaetoceros** sp., **Trachyneis aspera, Thalassionema nitzschioides,** as well as other unidentified centric fragments, is associated with long-distance dispersal. Allochthony and implied long-distance dispersal are further evidenced by a minor siliceous biogenic constituent of marine origin comprising the silicoflagellate **Distephanus, Actiniscus,** a pyrrophytic alga, radiolaria fragments, and various sponge spicules.

The authochthonous freshwater component of this nival diatom assemblage, differentiated on the basis of species abundance and distributional aspects, is documented in Table 40.1.

A possible third, yet minor floristic element, much less easily discerned, may be formulated as a freshwater constituent of allochthonous origin. Demarcation between the authochthonous and allochthonous freshwater component, although somewhat arbitrary, is based on the presence of rheophilous diatoms in the allochthonous constituent and on the limited occurrence of hydrophytic taxa of predominantly aquatic habitat.

NOTES ON SOME SPECIES

Of particular interest, especially in view of its complete absence from Foged's (1953, 1955, 1958, 1972, 1973) Greenland diatom enumerations, is the repeated occurrence of **Navicula gebhardi** in the permanent snow collections from the Sydkap Ice Cap. To date this species has been recorded from only one locality: Krasske (1938) cited the scattered occurrence of **N. gebhardi** in moss from Adventsbay, Spitsbergen. In this context, mention should perhaps be made of Hustedt's (1961-66, p. 185) intended placement of **N. gebhardi** into the genus **Pinnularia.** Recent scanning electron analytical examination of some cryoconite containing **N. gebhardi** (DT-82-127; Stub 1099, 131-133) provided conclusive evidence and morphological justification for Hustedt's proposed generic change.

Equally intriguing is the presence in this diatom assemblage of **Denticula** aff. **rainierensis. D. rainierensis** has been found in hot springs (100°C) at an elevation of 640 m (Patrick and Reimer, 1975). Bock's (1970) discovery of a

Table 40.3. Freshwater diatoms from the Sydkap Ice Cap (1400 m a.s.l.) recorded previously from nival and glacial biotopes

Diatom species	Type of snow/ice	Country	Elevation m a.s.l.	Lat./Long.	Reference
ACHNANTHES Bory					
A. broenlundensis Fog.	red snow	Canada			Lichti-Federovich, GSC Diatom Report 78-15
A. minutissima Kütz.	snow	Hungary	lowland		Istvanffi 1898
AMPHORA Ehrenberg					
A. ovalis (Kütz.) Kütz. var. pediculus Kütz.	red snow	Greenland		76°44'N, 73°03'W	Lichti-Federovich 1980
CALONEIS Cleve					
C. bacillum (Grun.) Cleve	red snow	Greenland		76°44'N, 73°03'W	Lichti-Federovich 1980
C. clevei (Lagerst.) Cleve	red snow	Greenland		76°44'N, 73°03'W	Lichti-Federovich 1980
CERATONEIS Ehrenberg					
C. arcus (Ehr.) Kütz.	red snow	Canada			Lichti-Federovich GSC Diatom Report 78-15
CYCLOTELLA Kützing					
C. comta (Ehr.) Cleve	red snow	U.S.S.R.	3350		Philippov 1934
	snow	Hungary	lowland		Istvanffi 1898
EUNOTIA Ehrenberg					
E. praerupta var. musicola Pet.	red snow	Greenland		76°44'N, 73°03'W	Lichti-Federovich 1980
FRAGILARIA Lyngbye					
F. pinnata Ehr.	red snow	Greenland		76°44'N, 73°03'W	Lichti-Federovich 1980
HANTZSCHIA Grunow					
H. amphioxys (Ehr.) Grun.	red snow	Canada (Baffin Bay)			Ehrenberg 1851
	red ice	U.S.S.R.	3100-3400		Philippov 1934
	coloured snow	Japan			Kobayashi & Fukushima 1952
	green snow	Japan			Kobayashi & Fukushima 1952
	snow	Greenland	365	73°10'N	Ehrenberg 1875
	red snow	Greenland		76°44'N, 73°03'W	Lichti-Federovich 1980
MELOSIRA Agardh					
M. roeseana Rabh.	red snow	Greenland		76°44'N, 73°03'W	Lichti-Federovich 1980
	ice cave	Hungary	250		Kol 1957
NAVICULA Bory					
N. cocconeiformis Greg.	red snow	Greenland		76°44'N, 73°03'W	Lichti-Federovich 1980
N. contenta Grun.	brown snow	Japan			Fukushima 1954
	green-brown snow	Japan			Fukushima 1954
N. gibbula Cleve	red snow	Canada			Lichti-Federovich GSC Diatom Report 78-15
N. mutica Kütz.	dirty snow	U.S.S.R.	3100-3400		Philippov 1934
	red snow	U.S.S.R.	3100-3400		Philippov 1934
	red snow	U.S.S.R.	2300-2700		Philippov 1934
	red snow	Greenland		76°44'N, 73°03'W	Lichti-Federovich 1980
N. mutica var nivalis (Ehr.) Hust.	red snow	U.S.S.R.	3100-3400		Philippov 1934
N. mutica var. ventricosa (Kütz.) Cleve et Grun.	red snow	Greenland		76°44'N, 73°03'W	Lichti-Federovich 1980
N. rotaeana (Rabh.) Grun.	dirty snow	Ecuador			Lagerheim 1892
	snow	Spitsbergen			Roy 1885-86
N. seminulum Grun.	red ice	Antarctica		78°S	Fritsch 1912
	snow	Spitsbergen			Roy 1885-86
	dirty snow	Ecuador			Lagerheim 1892

Table 40.3 (cont.)

Diatom species	Type of snow/ice	Country	Elevation m a.s.l.	Lat./Long.	Reference
NEIDIUM Pfitzer					
N. affine (Ehr.) Pfitz.	snow	Greenland	365	73°10'N	Ehrenberg 1875
NITZSCHIA Hassal					
N. thermalis Kütz. var. minor Hilse	red snow	Greenland		76°44'N, 73°03'W	Lichti-Federovich 1980
PINNULARIA Ehrenberg					
P. borealis Ehr.	red snow	Baffin Bay			Ehrenberg 1851
	red snow	South Orkneys		61°S	Fritsch 1912
	red snow	U.S.S.R.	3100-3400		Philippov 1934
	green snow	Japan			Fukushima 1954
	snow	Hungary	lowlands		Istvanffi 1898
	snow	Greenland	365	73°10'N	Ehrenberg 1875
P. brébissonii (Kütz.) Rabh.	red snow	U.S.S.R.	3350		Philippov 1934
	green-brown snow	Japan			Fukushima 1954
	red snow	Greenland		76°44'N, 73°03'W	Lichti-Federovich 1980
P. brébissonii var. diminuta (Grun.) Cleve	red snow	Greenland		76°44'N, 73°03'W	Lichti-Federovich 1980
P. intermedia (Lagerst.) Cleve	red snow	Greenland		76°44'N, 73°03'W	Lichti-Federovich 1980
P. krookii (Grun.) Cleve	red snow	Greenland		76°44'N, 73°03'W	Lichti-Federovich 1980
P. microstauron (Ehr.) Cleve	red snow	Greenland		76°44'N, 73°03'W	Lichti-Federovich 1980
P. parva (Ehr.) Greg. var. lagerstedtii Cleve fo. interrupta Pet.	red snow	Greenland		76°44'N, 73°03'W	Lichti-Federovich 1980
STAURONEIS Ehrenberg					
Stauroneis anceps Ehr.	red snow	Greenland		76°44'N, 73°03'W	Lichti-Federovich 1980
SYNEDRA Ehrenberg					
Synedra tabulata (Ag.) Kütz.	red snow	Greenland		76°44'N, 73°03'W	Lichti-Federovich 1980

Denticula aff. **rainierensis** in a soil layer from a cliff in England may permit this taxon's aerophilous characterization. Such autecological delineation is further substantiated by distributional studies of aerophilous diatoms in and near Icelandic thermal waters (Petersen, 1924; Krasske, 1938).

A matter of special concern relates to the systematic assessment of the most common **Achnanthes** species in the nival diatom assemblage which, after some deliberation, has been tentatively aligned with **Achnanthes broenlundensis** as described by Foged (1955, p. 39). **A. broenlundensis** is of common occurrence in Pearyland, North Greenland, and of rare occurrence in Spitsbergen. More specific distributional data of this taxon include a plant mat in a brook located in a fell field (450 m a.s.l.); scrapings from a stone in a river; green algae with coatings on gravel; wet, mossy meadow soil; swamp mud on the bottom of a mossy, water-covered meadow; and mosses from the shore of a lake (Foged, 1955, 1958, 1964). Conspecifity, however, of **A. broenlundensis** with **A. saxonica** recorded from wet moss and irrorated rocks in montane areas (Hustedt, 1959) appears more than likely, even more so since striation density as sole distinguishing species specific criterion has lost its diagnostic value especially in view of ecologically and geographically determined variants. Consideration also of the autecological characterization of **A. saxonica** as indicator of high oxygen concentration (Cholnoky, 1968) strongly suggests synonymy.

Furthermore, the attempt at taxonomic determination of the floristic elements of this arctic diatom association brought to attention the necessity for systematic revision of the smaller **Pinnularia** forms, as well as the need for clarification of the systematic relationship of **Navicula cincta** var. **heufleri** with morphologically closely aligned species such as **N. umida, N. certa**, and **N. libonensis.** The latter taxon has been reported from the walls of a huge cave in South Africa (Schoeman, 1970).

As pertains to all taxonomic ambiguities, clarification of systematic relationships between morphologically similar taxa and determination of range of structural variability within a specific taxon can only be attained by submicroscopic examination of additional material from different habitats and geographical areas. It is evident that systematic inadequacies and taxonomic disorder impose limitations on interpretations in diatom analytical studies. Resolution, therefore, of these taxonomic problems not only represents the most fertile area for diatom research at present, but also the most essential so as to ensure a sound unified systematic basis and to impart a measure of validity to the application of diatom analysis as a scientific tool.

DISCUSSION

Consideration of this diatom flora immediately brings to the fore several interesting features: Aside from the presence of an allochthonous marine constituent, the most striking aspect is the presence of a clearly defined autochthonous diatom component, based on relative abundance and autecological characterization of its structural elements. Thus it is regretable that substantiation of the distinctive character of this nival diatom flora is impeded by a lack of comparative floristic studies from similar cryo-biotopes, since verification of the fundamental structure of this highly specialized diatom association can only be affirmed by floristic concomitants from other permanent snow habitats in polar regions.

As Table 40.3 indicates, some of the diatom taxa found in the surface snow from the Sydkap Ice Cap have been previously recorded from various nival and glacial biotopes, most of which, with regard to diatoms, served as a source for incidental collections rather than systematic investigations.

Some floristic similarity, however slight because of the limited number of diatoms, is afforded by chance collections from two marginal inland ice locations and one from a cryoconite hole on the northeast coast of Greenland (Petersen, 1924). Floristic semblance to diatom enumerations based on more systematic investigations of marginal inland ice collections in Norway and Iceland (Mölder, 1949) is understandably less recognizable since these collections originate from aquatic habitats and any similarity, therefore, rests mainly on the concomitant occurrence of hydrophytic taxa. Of interest, however, is Mölder's observation of the smallness of diatoms from locations close to the ice margin and from supraglacial meltwater-filled depressions on the ice. He related this size reduction to temperature in terms of shortened growing season and to possible nutrient deficiencies.

Considering the absence of a well defined floristic analogue, it is more intriguing to not only ascertain broad patterns of similarity, but to confirm close compositional parallels with various aerial or xerotic biotopes such as litho-biotopes, moss, and soil habitats.

Studies by Bock (1963) provide a critical appraisal of the environmental factors controlling the diatom distribution in extreme biotopes. Within the limits of observation, supported by the distinctive element in the Sydkap diatom flora of aerophilous and halophilous forms indicative of osmoregulatory processes due to desiccation gradients and high oxygen concentration, I concur with his proposal that lack of moisture is the prime casual factor determining floristic composition of diatom coenoses in extreme biotopes. Floristic comparison studies, however, of melt layer (summer interval) and surface snow (winter interval) are required to test the validity of this assumption.

Another aspect of significance relates to the marked presence of species of cosmopolitan distribution in an environment of such high latitude and elevation. Although the arcto-nordic-alpine element, though rather limited, cannot be completely denied, there is a marked tendency towards cosmopolitan affinity. Evidence for this pronounced ubiquity is likely to increase with continued research into geographically and altitudinally widely differing biotopes. An excellent example is provided by the distribution record of **Pinnularia intermedia**, designated as an arctic (Cleve-Euler, 1955) and nordic (Krasske, 1943) freshwater form. Recent records of **Pinnularia intermedia** not only extend its range in aquatic habitats to the temperate region, with recorded occurrences in South Dakota and Wyoming (Patrick and Reimer, 1966), but they also extend its range in nonaquatic environments. Lund (1945) described it as a common terrestrial diatom found in British soils, and recently it was discovered in scrapings from a wall in the Timpanagos Cave National Monument, Utah (St. Clair and Rushforth, 1976).

The distinct cosmopolitan nature of the diatom association from the Sydkap Ice Cap lends support to the now widely accepted concept that temperature plays a rather insignificant role, its effects superseded by those of other environmental factors.

In summary, it may be stated that consideration of the identifiable correlation between the diatom flora characterizing various xeric biotopes and that of the surface snow from the Sydkap Ice Cap as reflected by the predominance of aerophilous taxa and the presence of halophilous species, predicates a similar range of environmental conditions. Thus in a habitat where the available moisture in the form of meltwater is frozen during winter months, the main environmental factor controlling the distributional and compositional aspects of the diatom flora relates to the desiccation tolerance or xero-tolerance of its species.

CONCLUSION

Although merely an exploratory study, this diatom analytical enquiry is the first systematic attempt to qualitatively assess the diatom flora of a polar 'desert' biotope. Apart from providing a substantial number of diatom taxa for inclusion into a general check list of diatoms from cryo-biotopes, this study conclusively demonstrates the close interrelation between environmental parameters and diatom flora, reflected in its floristic composition; it also validates the use of diatom analytical methods for the assessment and delineation of environmental conditions. These results, though preliminary, also illustrate scope and potential and present justification for continuing research of nival biotopes.

Future diatom analytical investigations of the snow and ice of polar ice caps are aimed at augmenting the present species list, at clarifying taxonomic ambiguities, and at describing new taxa with the aid of electron optical analyses. In helping to resolve the issue of long distance dispersal phenomena, implicitly verified by the allochthonous marine component, future research will utilize epifluroescence or Cumar R-9, combined with phase contrast microscopy, to readily determine the live to dead diatom ratio, thus facilitating the assessment of the autochthonous versus allochthonous diatom faction. If feasible, these findings will be integrated with data derived from palynological investigations. In addition to diatom floristic comparison studies of melt layer and surface snow, representing summer and winter interval respectively, an examination of the micro stratification of diatoms in the surface layers will provide information on distributional aspects. Such proposed studies, aside from the relative abundance of diatoms, should also be aided by the unparalleled uniformity of this arctic biotope, subject to interaction of fewer chemical variables than those of most aquatic habitats and where the interrelation of biological factors is limited to the lower forms of life.

ACKNOWLEDGMENTS

I wish to acknowledge my appreciation for financial backing furnished by G.D. Hobson, Director, Polar Continental Shelf Project (PCSP). I would particularly like to thank R.M. Koerner (PCSP) who was instrumental in providing both opportunity and much needed support. I also want to thank Jocelyn Bourgeois PCSP for her assistance in the field and laboratory, and for her delightful companionship. To J. Smol, Queen's University, Kingston, I extend my sincere thanks for his review of the manuscript.

REFERENCES

Anderson, D.C. and Rushforth, S.R.
1976: The cryptogam flora of desert soil crusts in southern Utah, U.S.A.; Nova Hedwigia, v. 28, p. 691-729.

Beger, H.
1927: Beiträge zur Ökologie und Soziologie der luftlebigen (atmophytischen) Kieselalgen; Berichte der Deutschen Botanischen Gesellschaft, v. 45, p. 385-407.

1928: Atmophytische Moosdiatomeen in den Alpen; Zürich, Naturforschende Gesellschaft Zürich, Festschrift, Hans Schinz, Beilage zur Vierteljahrsschrift, no. 15, p. 382-404.

Bock, W.
1963: Diatomeen extrem trockener Standorte; Nova Hedwigia, v. 5, p. 199-254.

1970: Felsen und Mauern als Diatomeenstandorte; Diatomaceae II; Beihefte zur Nova Hedwigia, Heft 31, p. 395-441.

Bristol, M.
1920: On the Alga-Flora of some desiccated English soils: an important factor in soil biology; Annals of Botany, v. 34, p. 35-79.

Cholnoky, B.J.
1968: Die Ökologie der Diatomeen in Binnengewässern; Verlag von J. Cramer, 699 p.

Cleve-Euler, A.
1952: Die Diatomeen von Schweden und Finnland; Kungliga Svenska Vetenskapsakademiens Handlingar, Fjarde Serien, v. 3, no. 3, p. 1-153.

1953: Die Diatomeen von Schweden und Finnland; Kungliga Svenska Vetenskapsakademiens Handlingar, Fjarde Serien, v. 4, no. 5, p. 1-225.

1955: Die Diatomeen von Schweden und Finnland; Kungliga Svenska Vetenskapsakademiens Handlingar, Fjarde Serien, v. 5, no. 4, p. 1-232.

Deflandre, G.
1926: Contribution à la flore algologique de la Basse-Normandie; Bulletin de la Societé Botanique de France v. 73.

Dodd, J.D. and Stoermer, E.F.
1962: Notes on Iowa diatoms I. An interesting collection from a moss-lichen habitat; Iowa Academy of Science, v. 69, p. 83-87.

Ehrenberg, C.G.
1851: Über eine frische Probe der die Crimson Cliffs scharlachroth färbenden Substanz aus der Baffins-Bai und das sie begleitende kleinste Leben; Monatsberichte der Akademie der Wissenschaften in Berlin, p. 741-744.

1875: Das unsichtbar wirkende Leben der Nordpolarzone am Lande und in den Meerestiefgründen bei 300 mal verstärkter Sehkraft, nach Materialien der Germania erläutert; in Geographische Geseilschaft in Bermen. Die zweite deutsche Nordpolarfahrt in den Jahren 1869 and 1870. Bd. 2, p. 437-467.

Feher, D.
1936: Untersuchungen über die regionale Verbreitung der Bodenalgen; Archiv fur Microbiologie, Bd. 7, p. 439-476.

Feher, D. and Frank, M.
1936: Untersuchungen über die Lichtökologie der Bodenalgen; Archiv für Mikrobiologie, Bd. 7, p. 1-31, 490.

Florin, M.B.
1970: Late glacial diatoms of Kirchner Marsh, southeastern Minnesota; Nova Hedwigia, v. 31, p. 667-756.

Foged, N.
1953: Diatoms from West Greenland; Meddelelser om Grønland, v. 4, no. 6, p. 1-86.

1955: Diatoms from Peary Land, North Greenland; Meddelelser om Grønland, v. 128, no. 7, p. 1-90.

1958: The diatoms in the basalt area and adjoining areas of Archean rock in West Greenland; Meddelelser om Grønland, v. 156, no. 4, p. 1-146.

1964: Freshwater diatoms from Spitsbergen; Tromso Museums Skrifter, v. 11, 204 p.

1972: The diatoms in four postglacial deposits in Greenland; Meddelelser om Grønland, v. 194, no. 4, p. 1-66.

Foged, N. (cont.)
1973: Diatoms from Southwest Greenland; Meddelelser om Grønland, v. 194, no. 5, p. 1-84.

1979: Diatoms in New Zealand, the North Island; Bibliotheca Phycologica, v. 47, p. 1-225.

Fritsch, F.E.
1912: Freshwater Algae; in National Antarctic Expedition 1901-1904; National History (Zoology and Botany, London), v. 6, p. 1-60.

Fritsch, F.E. and John, R.P.
1942: An ecological and taxonomic study of the algae of British soils. II. Consideration of the species observed; Annals of Botany, N.S. v. 6, no. 23, p. 371-395.

Fukushima, H.
1954: Studies on the cryoalgae of Japan. II. Cryoxenous algae from Japan; Nagao, v. 4, p. 31-35.

Gistl, R.
1933: Zur Kenntnis der Erdalgen; Archiv für Mikrobiologie, v. 3, p. 634-649.

Hayek, M.W. and Hulbary, R.L.
1956: A survey of soil diatoms; Proceedings of the Iowa Academy of Science, v. 63, p. 327-338.

Hustedt, F.
1922: Bacillariales aus Schlesien I; Berichte der Deutschen Botanischen Gesellschaft, Bd. 40, p. 98.

1924: Die Bacillariaceen – Vegetation des Sarekgebirges; Naturwissenschaftliche Untersuchungen des Sarekgebirges, Bd. 3, Botanik (Bd. 6), p. 525-626.

1930: Die Kieselalgen. I. Teil; in Kryptogamen-Flora von Deutschland, Österreich und der Schweiz, Bd. VII, ed. L. Rabenhorst; Akademische Verlagsgesellschaft Geest und Portig K.-G., Leipzig, 920 p.

1942: Aerophile Diatomeen in der nordwestdeutschen Flora; Berichte der Deutschen Botanischen Gesellschaft, v. 60, p. 55-73.

1943: Die Diatomeen einiger Hochgebirgsseen der Landsschaft Davos in den Schweizer Alpen; Internationale Revue der gesamten Hydrobiologie und Hydrographie, v. 43, p. 124-197, 225-280.

1950: Die Diatomeenflora norddeutscher Seen mit besonderer Berücksichtigung des holsteinischen Seengebietes. V-VII. Seen in Mecklenburg, Lauenburg und Nordostdeutschland; Archiv für Hydrobiologie, v. 43, p. 329-458.

1959: Die Kieselalgen. 2. Teil; in Kryptogamen-Flora von Deutschland, Österreich und der Schweiz, Bd. VII, ed. L. Rabenhorst; Akademische Verlagsgesellschaft Geest und Portig K.-G., Leipzig, 845 p.

1961: Die Kieselalgen. 3. Teil; in Kryptogamen-Flora von Deutschland, Österreich und der Schweiz, Bd. VII, ed. L. Rabenhorst; Akademische Verlagsgesellschaft Geest und Portig K.-G., Leipzig, 816 p.

Istvanffi, J.
1898: Die Kryptogamen-Flora des Balatonsees und seiner Nebengewässer; in Resultate der Wissenschaftlichen Erforschung des Balatonsees, herausgegeben von der Balatonsee-Commission der Ungarischen Geographischen Gesellschaft, Bd. 2, Theil 2, Sect. 1, 148 S, Commissionsverlag von Ed. Holzel, Wien.

Jaag, O.
1945: Untersuchungen über die Vegetation und Biologie der Algen des nackten Gesteins in den Alpen, im Jura und im Schweizerischen Mittelland; Beiträge zur Kryptogamenflora der Schweiz, v. 9, no. 3, p. 1-560.

Johansen, J.R., Rushforth, S.R., and Brotherson, J.D.
1981: Subaerial algae of Navajo National Monument, Arizona; Great Basin Naturalist, v. 4, p. 433-439.

John, R.P.
1942: An ecological and taxonomic study of British soils. "The distribution of the surface-growing algae; Annals of Botany, N.S. v. 6, p. 323-349.

Jørgensen, E.G.
1948: Diatom communities in some Danish lakes and ponds; Biologiske Skrifter, v. 5, no. 2, p. 5-140.

Kobayashi, Y. and Fukushima, H.
1952: On the red and green snow in Japan III; Nagaoa, v. 2, p. 65-75.

Kol, E.
1957: Algologiai vizsgalatok a satorhegyseg jeges Barlangjaban. Bot. Kozlemenyek (Budapest), v. 47, p. 43-50.

1968: Biologie und Limnologie des Schnees und Eises I. Kryovegetation; in Die Binnengewässer, A. Thieneman, E. Schweizerbart'sche Verlagsbuchhandlung, Stuttgart.

Krammer, K.
1980: Morphologic and taxonomic investigations of some freshwater species of the diatom genus **Amphora** Ehrenberg; Bacillaria, v. 3, p. 197-225.

Krasske, G.
1932: Beiträge zur Kenntnis der Diatomeenflora der Alpen; Hedwigia, p. 92-134.

1938: Beitrage zur Kenntnis der Diatomeenflora von Island und Spitzbergen; Archiv fur Hydrobiologie, Bd. 33, p. 503-533.

1943: Zur Diatomeenflora Lapplands; Berichte der Deutschen Botanischen Gesellschaft, Bd. 61, p. 81-88.

1948: Diatomeen tropischer Moosrasen; Svensk Botanisk Tidskrift, v. 42, no. 4, p. 405-443.

Lagerheim, G.
1892: Die Schneeflora des Pichincha. Ein Beitrag zur Kenntnis der nivalen Algen und Pilze; Berichte der Deutschen Botanischen Gesellschaft, v. 10, p. 517-534.

Lange-Bertalot, H.
1977: Eine Revision zur Taxanomie der **Nitzschiae lanceolatae** Grunow; Nova Hedwigia, Bd. 28, Heft 2-3, p. 253-307.

1978: Zur Systematik, Taxonomie und Ökologie des abwasserspezifisch wichtigen Formenkreises um **"Nitzschia thermalis"**; Nova Hedwigia, Bd. 30, p. 635-652.

1980a: New species, combinations and synonyms in the genus **Nitzschia**; Bacillaria, v. 3, p. 41-77.

1980b: Zur systematischen Bewertung der bandförmigen Kolonien bei **Navicula** and **Fragilaria**; Nova Hedwigia, Bd. 33, p. 723-787.

1980c: Zur taxonomischen Revision einiger ökologisch wichtiger **"Naviculae lineolatae"** Cleve; Cryptogamie : Algologie, v. 1, no. 1, p. 29-50.

Lange-Bertalot, H. and Bonik, K.
1978: Zur systematisch-taxonomischen Revision des ökologisch interessanten Formenkreises um **Navicula mutica** Kützing; Botanica Marina, v. 21, p. 31-37.

Lange-Bertalot, H. and Ruppel, M.
1980: Zur Revision taxonomisch problematischer, ökologisch jedoch wichtiger Sippen der Gattung **Achnanthes** Bory; Archiv für Hydrobiologie, Supplement 60, p. 1-31.

Lange-Bertalot, H. and Simonsen, R.
1978: A taxonomic revision of the **Nitzschiae lanceolatae** Grunow; Bacillaria, v. 1, p. 11-111.

Lichti-Federovich, S.
1980: Diatom flora of red snow from Isbjørneø, Carey Øer, Greenland; Nova Hedwigia, Bd. 33, p. 395-431.

Loescher, J.H.
1981: Diatoms (Bacillariophyceae) from Sheeder Prairie, Guthrie County, Iowa; Proceedings of the Iowa Academy of Science, v. 88, no. 2, p. 63-69.

Lund, J.W.G.
1945: Observations on soil algae. I. The ecology, size and taxonomy of British soil diatoms; Cambridge, New Phytologist, v. 45, pt. 1, p. 196-219.

1946: Observations on soil algae. I. The ecology, size and taxonomy of British soil diatoms; Cambridge, New Phytologist, v. 45, pt. 2, p. 56-110.

Messikommer, E.
1946: Beitrag zur Kenntnis der Algenflora der Gewässer im Gebiete der Grauen Hörner; Vierteljahrsschrift der Naturforschenden Gesellschaft in Zürich, Jahrgang 91, no. 3,4, p. 237-253.

1949: Algologische Erhebungen im St. Gallischen Abschnitt der NW-Sardonagruppe; Vierteljahrsschrift der Naturforschenden Gesellschaft in Zürich, v. 94, p. 231-251.

1949: Weiterer (Zweiter) Beitrag zur Algenkunde des Kantons Schaffhausen; Mitteilungen der Naturforschenden Gesellschaft Schaffhausen, v. 23, p. 45-174.

1953: Beitrag zur Kenntnis der Algenflora des Urner Reusstales (Zentralschweiz); Hydrobiologia, v. 6, p. 1-43.

1953: Beitrag zur Kenntnis der Algenflora des Kantons Unterwalden; Mitteilungen der Naturforschenden Gesellschaft Schaffhausen, v. 25, p. 48-132.

Mölder, K.
1949: Die Diatomeenflora einiger Eisrandstandorte in Norwegen und Island; Archivum Societatis Zoologicae Botanicae Fennicae 'Vanamo', v. 4, no. 1, p. 126-137.

Mölder, K. and Tynni, R.
1970: Über Finnlands rezente und subfossile Diatomeen IV; Geological Society of Finland Bulletin, v. 42, p. 129-144.

1972: Über Finnlands rezente und subfossile Diatomeen VI; Geological Society of Finland Bulletin, v. 44, p. 141-149.

Moore, G.T. and Carter, N.
1926: Further studies on the subterranean algal flora of the Missouri Botanical Garden; Annals of the Missouri Botanical Garden, v. 13, no. 2, p. 101-140.

Moore, G.T. and Karrer, J.L.
1919: A subterranean algal flora; Annals of the Missouri Botanical Garden, v. 6, p. 281-307.

Östrup, E.
1918: Freshwater diatoms from Iceland; in Rosenvinge et Warming. "Botany of Iceland", v. 2, pt. 1, no. 5, p. 1-96.

Patrick, R.
1977: Ecology of freshwater diatoms and diatom communities (Chapter 10); in Academy of Natural Sciences, Philadelphia, Botanical Monograph, v. 13, 498 p.

Patrick, R. and Freese, L.R.
1961: Diatoms (Bacillariophyceae) from northern Alaska; Proceedings of the Academy of Natural Sciences of Philadelphia, v. 12, no. 6, p. 129-301.

Patrick, R. and Reimer, C.W.
1966: The diatoms of the United States; Academy of Natural Sciences, Philadelphia, v. 1, Monograph no. 13, 688 p.

1975: The diatoms of the United States, Academy of Natural Sciences, Philadelphia, v. 2, Monograph no. 13, 213 p.

Petersen, J.B.
1915: Studier over Danske aerofile alger; Danske videnskabernes selskab Skrifter, 7. Raekke, Naturvidenskabelig, og matematisk Afdeling 12, Raekke 7, p. 271-380.

1924: Freshwater-algae from the north coast of Greenland collected by the late Dr. Th. Wulff; Meddelelser om Grønland, v. 44, p. 307-319.

1928: The aerial algae of Iceland; The Botany of Iceland, v. 2, p. 328-447.

1935: Studies on the biology and taxonomy of soil algae; Dansk Botanisk Arkiv, v. 8, no. 9, p. 1-180.

1950: Observations on some small species of **Eunotia**; Dansk Botanisk Arkiv, v. 14, no. 1, p. 1-19.

Philippov, G.S.
1934: Die Mikroflora des roten Schnees im Kaukasusgebirge; Bulletin de l'Academie des Sciences de l'URSS, no. 7, p. 1031-1037.

Reimer, C.
1970: Some diatoms (**Bacillariophyceae**) from Cayler Prairie; Diatomaceae II, p. 235-249.

Roy, J.
1885: The flora and fauna of snow and ice; The Scottish Naturalist, v. 2, new series, p. 122-127.

St. Clair, L.L. and Rushforth, S.R.
1976: The diatoms of Timpanogos Cave National Monument, Utah; American Journal of Botany, v. 63, no. 1, p. 49-59.

Sauer, L.M.
1955: Im Gebiet der Sowjetunion erstmalig beobachtete terrestrische Diatomeen; Botanicheskie Materialy, otdel sporovykh rastenii, Bd. 10, p. 106-111.

Schelhorn, von M.
1936: Zur Ökologie und Biologie der Erdalgen; Naturwissenschaft und Landwirtschaft, Heft 18, p. 1-54.

Schimanski, H.
1973: Beitrag zur Diatomeenflora von Erlangen; Nova Hedwigia, Bd. 24, Heft 2-4, p. 237-336.

1978: Beitrag zur Diatomeenflora des Frankenwaldes; Nova Hedwigia, Bd. 30, p. 557-633.

Schoeman, F.R.
1970: Diatoms from the Orange Free State, South Africa and Lesotho 1; Diatomaceae II, Nova Hedwigia, Heft 31, p. 331-353.

Schumann, J.
1867: Die Diatomeen der Hohen Tatra; Verhandlungen der kaiserlich-königlichen zoologisch-botanischen Gesellschaft in Wien, v. 17, p. 1-102.

Simonsen, R.
1953: Diatomeen aus holsteinischen Kleingewässern; Schriften des Naturwissenschaftlichen Vereins, v. 26, no. 2, p. 109-123.

Skvortzow, B.W.
1930: Alpine diatoms from Fukien Province, South China; The Philippine Journal of Science, v. 41, p. 39-52.

1937: Subaerial diatoms from Hangchow, Chekiang Province, China; Bulletin of the Fan Memorial Institute of Biology (Botany), v. 7, no. 6, p. 219-230.

1938: Subaerial diatoms from Pin-Chiang-Sheng Province, Manchoukou; Philippine Journal of Science, v. 65, no. 3, p. 263-281.

Stoermer, E.F.
1962: Notes on Iowa diatoms II. Species distribution in a subaerial habitat; Proceedings of the Iowa Academy of Science, v. 69, p. 87-96.

Tynni, R.
1975: Über Finnlands rezente und subfossile Diatomeen VIII; Geological Survey of Finland, Bulletin 274, p. 1-55.

1976: Über Finnlands rezente und subfossile Diatomeen IX; Geological Survey of Finland, Bulletin 284, p. 1-37.

1978: Über Finnlands rezente und subfossile Diatomeen X; Geological Survey of Finland, Bulletin 296, p. 1-55.

1980: Über Finnlands rezente und subfossile Diatomeen XI; Geological Survey of Finland, Bulletin 312, p. 1-93.

Van Landingham, S.L.
1966: Diatoms from dry lakes in Nye and Esmeralda counties, Nevada, U.S.A.; Nova Hedwigia, Bd. 11, p. 221-241.

41. ACCOUNT OF FIELD OBSERVATIONS ON ROCK UNITS AND STRUCTURAL FEATURES OF THE SYENITIC COMPLEXES OF THE MONT-LAURIER AREA, CENTRAL METASEDIMENTARY BELT OF THE GRENVILLE PROVINCE

Project 760061

L. Corriveau [1]
Precambrian Geology Division

Corriveau, L., Account of field observations on rock units and structural features of the syenitic complexes of the Mont-Laurier area, Central Metasedimentary Belt of the Grenville Province; in Current Research, Part A, Geological Survey of Canada, Paper 84-1A, p. 303-306, 1984.

Abstract

The late tectonic syenitic complexes of the Mont-Laurier area within the Central Metasedimentary Belt of the Grenville Province were examined during the 1983 field season. They consist predominantly of syenite, but quartz-syenite, monzonite, diorite, melasyenite and pyroxenite also occur. Nepheline syenite is a peripheral unit in some plutons. Most units show well preserved primary igneous textures although some rocks are recrystallized to a certain extent. Foliation in the country rock deflects around these intrusions and is locally crosscut by undeformed syenite dykes associated with the intrusions.

Résumé

Les complexes tectoniques récents de syénite de la région de Mont-Laurier au sein de la zone métasédimentaire centrale de la province de Grenville ont été étudiés en 1983, au cours de la saison sur le terrain. Ces complexes se composent principalement de syénite, mais contiennent également de la syénite quartzifère, de la monzonite, de la diorite, de la syénite mélanocrate et de la pyroxénite. La syénite néphélinique forme une unité périphérique dans certains plutons. La plupart des unités manifestent des textures ignées primaires bien conservées, bien que certaines roches aient été plus ou moins recristallisées. La foliation dans la roche encaissante est déviée autour de ces intrusions et par endroits, des filons de syénite non déformés associés aux intrusions la traversent.

INTRODUCTION

Circular to elliptical syenitic complexes with evident igneous textures have been regarded as a characteristic of late or possibly post-tectonic igneous activity within the Central Metasedimentary Belt of the Grenville Province. These plutons intrude the Grenville Supergroup which comprises abundant marble and calc-silicate rocks, and subordinate quartzofeldspathic and pelitic gneiss, quartzite, and amphibolite. The intrusive complexes consist predominantly of syenite, but nepheline syenite, melasyenite, granite, monzonite, diorite and pyroxenite, have been reported (Davidson et al., 1979).

Mapping of the syenitic complexes in the Mont-Laurier area has been in general restricted to reconnaissance scales of 1:250 000 and 1:63 360 (Wynne-Edwards et al., 1966; Osborne, 1935; Aubert de la Rue, 1948, 1953, 1956); there is a limited amount of more detailed mapping at a scale of 1:20 000 (Rive, 1976). Studies at an M.Sc. level have been undertaken by Durocher (1977), and a "these de 3ieme cycle" has been submitted by Tabet, Abdul-Malak (1978).

Mapping at a 1:20 000 scale was undertaken during the 1983 field season in order to examine systematically all of the syenitic complexes in the Mont-Laurier area, as well as to establish their relationship to the Grenvillian Orogeny. The rocks in this region are, on the whole, poorly exposed in detail, and contacts between units are rarely seen. Locations are shown in Figure 41.1.

This report provides a preliminary description of the rock types and structural features observed in the Kensington, Satellite, Cameron, and Lac-Rouge complexes, and their relationship to the granulite facies metamorphism of the Grenville Supergroup, previously described by Indares (1982). The mapping of the complexes at Ste-Véronique (Rive, 1976), in Loranger County, and at Gracefield (Durocher, 1977) has been found to be generally reliable, although there is little field evidence to support Durocher's proposal of a well-developed mineralogical (modal) zoning in the Gracefield complex.

This project is being conducted in conjunction with a study of the Grenville Province of Ontario and western Québec by A. Davidson, and will form the basis of a Ph.D. thesis at McGill University under the supervision of R.F. Martin, R. Doig, and D. Francis. Field assistance was ably provided by Yves-Denis Gagnon.

GEOLOGY OF THE SYENITIC COMPLEXES

Kensington complex

The Kensington complex is a northeasterly elongate pluton which underlies an area of some 40 km^2 and is situated east of the town of Maniwaki. The complex may be crudely subdivided into three moderately heterogeneous units: a crescent-shaped body of pink syenite lacking biotite, which occupies the western margin; a crescent-shaped body of biotite-bearing syenite which, in part, is enveloped by the biotite-absent syenite; and a dominantly mafic body, oval in plan, occupying the eastern part of the complex, and consisting of monzodiorite, pyroxene meladiorite and pyroxenite. The proportion of alkali feldspar to plagioclase in the syenite and monzodiorite has not yet been evaluated on account of extensive alteration of the feldspars. Albite twins are rarely observed.

The pink syenite contains centimetric laths of alkali feldspar with less than 10 per cent interstitial medium- to fine-grained clinopyroxene, typically rimmed by amphibole, minor titanite, apatite and magnetite, and rare quartz and biotite. Biotite is observed to form thin decimetre-long sheets in the syenite at one locality. Feldspar laths are more or less internally recrystallized to finer grain. This unit is typically massive, but steeply plunging lineations and subvertical foliations defined by alkali feldspar laths are locally observed. Decimetric cauliflower-shaped aggregates of clinopyroxene accompanied by abundant titanite, scapolite, and calcite are found next to some calc-silicate xenoliths.

[1] Department of Geologicial Sciences, McGill University, Montreal, Quebec H3A 2A7

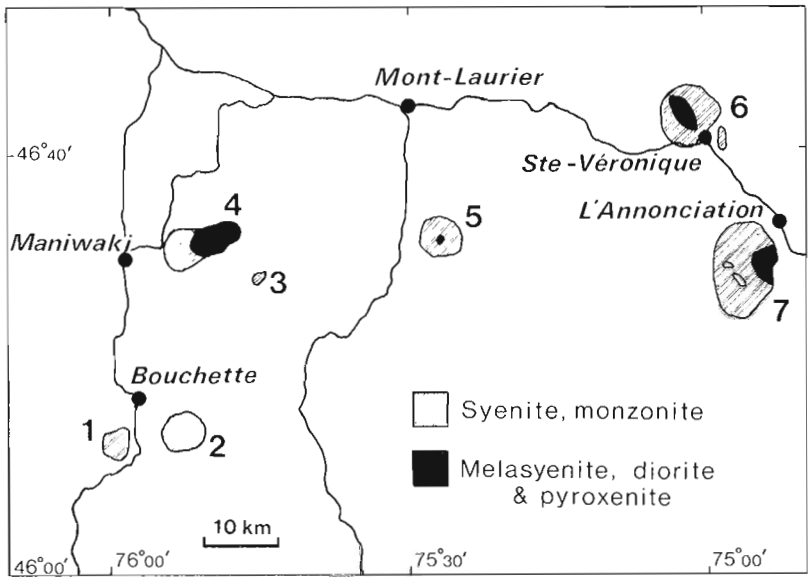

1. *Gracefield,*
2. *Cameron,*
3. *Satellite,*
4. *Kensington,*
5. *Lac-Rouge,*
6. *Ste-Véronique,*
7. *Loranger.*

Figure 41.1

Location of syenitic plutons in the Mont-Laurier area, Québec.

The biotite-bearing syenite is characteristically grey; colour index is variable. Mafic minerals form clusters and fill interstices in those rocks with abundant well-developed feldspar laths, and are more evenly distributed in more mafic rocks with hypidiomorphic granular texture in which the feldspar laths are poorly developed to nonexistent. Feldspar grains commonly have a grey core surrounded by a white, fine grained rim, and fracturing and alteration of the cores are commonly observed. Mafic minerals are clinopyroxene, amphibole, biotite, magnetite and minor apatite. Amphibole typically rims clinopyroxene. Mineral proportions vary widely from outcrop to outcrop, but few discrete contacts were observed. Biotite crystals and feldspar laths locally define foliation and lineation. Only a few country rock inclusions were observed in this unit.

The eastern part of the complex consists of moderately heterogeneous grey monzodiorite that is texturally and mineralogically similar to the grey biotite-bearing syenite. The proportion of plagioclase to alkali feldspar is not known, and the term monzodiorite should thus be considered a field term. Meladiorite and pyroxenite zones are typically massive, medium grained and homogeneous. Clinopyroxene is the main mafic constituent and its subrounded grains are typically bordered by subhedral biotite. These rocks contain fine grained interstitial feldspar with minor magnetite, pyrrhotite, and apatite.

Dykes of pyroxenite, monzodiorite, syenite, and porphyritic syenite were observed to have cut all phases of the Kensington complex, and thus do not aid in interpreting the timing of the various intrusive events in the complex. No exposures of the contact between the Kensington complex and paragneisses of the Grenville Supergroup have been observed.

Satellite complex

Wynne-Edwards et al. (1966) observed syenite just east of the Kensington complex; although their map shows a pluton approximately 30 km^2 in area, this syenite is now known to underlie less than 2 km^2. The discrepancy is likely due to former emphasis on interpretation of aeromagnetic patterns. The syenite is pink, massive, medium grained, moderately homogeneous, and consists of random laths of alkali feldspar (<20%) in a finer grained feldspathic matrix. The rocks also contain minor amounts of quartz (5%), biotite (<10%), clinopyroxene (<5%), amphibole (<5%) and magnetite (1%). Despite its proximity to the Kensington complex, the Satellite syenite differs from the Kensington syenite phase on account of its quartz content.

Cameron pluton

The Cameron pluton is a circular body of moderately heterogeneous syenite underlying a 30 km^2 area situated south of Bouchette (Fig. 41.1). It is characterized by a marked positive aeromagnetic anomaly reflecting its magnetite content (4%).

Syenitic rocks along the margin and in the northwest quadrant are typically massive, pink, medium grained syenite with an hypidiomorphic granular texture. They contain abundant alkali feldspar (>85%) with lesser biotite (<10%), amphibole (<10%), clinopyroxene (<2%), magnetite (<2%) and apatite (<1%). Biotite occurs in small clusters, or as rims around amphibole crystals.

The syenitic rocks in the central parts of the intrusion are usually grey with a slightly higher clinopyroxene (<10%) and magnetite (<5%) content. Some of the pink and grey syenites contain non-oriented decimetric sheets of biotite a few millimetres thick, producing a distinctive texture.

A third phase of the intrusion is medium grained, grey, and most of its alkali feldspars occur as coarse, blocky crystals displaying blue or golden irridescence. Colour index varies from 10-25 per cent, and bulk composition grades from syenite to melasyenite rich in clinopyroxene, amphibole and biotite.

In contact with country rocks, the syenite is massive, heterogeneous, rich in clinopyroxene, and locally contains country rock xenoliths. A major quartz syenite dyke trends north for 1 km within the southern part of the pluton, but syenite dykes have not been observed in the country rocks.

Gracefield complex

The Gracefield complex, located west of the Cameron intrusion, is composed of two distinct syenite intrusions, termed syenite I and II by Durocher (1977). The syenite I intrusion is a small 7.5 km^2 crescent-shaped body of syenite,

with minor nepheline syenite and melasyenite. The crescent arms enclose an oval (4 km^2) body of pink syenite (syenite II) characterized by random decimetric sheets of biotite. Dykes of syenite II crosscut syenite I.

Syenite I is moderately heterogeneous pink to grey, massive and medium to coarse grained. Mafic mineral content and proportion vary from outcrop to outcrop, but there does not appear to be a concentric distribution within the pluton, as was suggested by Durocher (1977). A variety of textures were observed: nonoriented grey laths of alkali feldspar with less than 20 per cent interstitial clinopyroxene, amphibole, biotite, bright orange calcite, needles or rounded crystals of apatite, magnetite, and ilmenite; pink to grey laths of alkali feldspar in a finer grained pink feldspathic matrix; and an hypidiomorphic texture with centimetric biotite clusters.

Nepheline syenite is restricted to the margin of the pluton but melasyenite occurrences are scattered throughout. Pockets of melasyenite within the leucocratic syenite and irregular, gradational mixtures of these two phases were observed near the contact between the main leucocratic syenite and melasyenite bodies. The melasyenite is characterized by medium grained hypidiomorphic clinopyroxene and amphibole enclosed by interstitial of poikilitic alkali feldspars. These rocks may contain up to 10 per cent calcite or apatite.

Syenite II appears to be more homogeneous than syenite I and consists of hypidiomorphic medium grained alkali feldspar with minor clinopyroxene, magnetite and apatite. Biotite forms less than 20 per cent of this syenite and occurs as non-oriented thin sheets up to 15 cm long and 10 cm wide. Melasyenite is also reported within the syenite II phase (Durocher, 1977).

The syenite may display vertical foliation or horizontal lineation near the contact with country rocks.

Lac-Rouge pluton

The Lac-Rouge pluton is a circular body of nondeformed megacrystic syenite and apatite-rich pyroxenite underlying a 25 km^2 area situated southeast of Mont-Laurier. The syenite weathers readily along crystal interfaces, resulting in extensive erosion of the pluton that has led to a circular depression bounded by hills of country rock. This depression corresponds to a positive aeromagnetic anomaly. Only fifteen outcrops of the syenitic intrusion have been found.

Megacrystic syenite appears to be the most extensive rock type and consists predominantly of coarse grained (1-4 cm) euhedral to subhedral alkali feldspar which may be weakly oriented to give a variably inward dipping foliation that strikes parallel to the contact of the intrusion. Clinopyroxene, amphibole, biotite, and minor calcite and apatite are interstitial to feldspar laths. Clinopyroxene segregations and rounded inclusions of medium grained syenite are present.

The megacrystic syenite is crosscut by numerous porphyritic syenite dykes with various orientations. These dykes also cut the Grenville Supergroup gneiss within one hundred metres of the intrusion.

The country rock is locally fenitized. Fenitization is expressed by heterogeneous syenitic material between amphibolite layers concordant to the foliation in the country rock. In the vicinity of this zone, quartzite is rich in clinopyroxene and is crosscut by veinlets of feldspar. Veins with mafic minerals rich in apatite were also observed.

Ste-Véronique complex

The Ste-Véronique ring complex underlies a 50 km^2 area northwest of l'Annonciation (Fig. 41.1). It consists of an oval-shaped pyroxenite and melasyenite central stock, rimmed by syenite which grades outward to peripheral nepheline syenite (Rive, 1976). The central stock is characterized by igneous layering defined by different types of pyroxenite and melasyenite. Layers of melasyenite with feldspar clusters (spotted shonkinite of Rive, 1976) have been observed at the southwest margin of the central stock. The surrounding syenitic rocks are homogeneous and consist of medium grained grey laths of alkali feldspar with 20 per cent interstitial biotite, amphibole, clinopyroxene, apatite, and titanite. The syenite is usually well foliated, forming an inward dipping concentric pattern around the intrusion core.

A single dyke of spotted melasyenite was observed to have crosscut the main syenite. The syenite is also crosscut by a decimetric dyke of medium to coarse grained syenite that contains numerous segregations of clinopyroxene, titanite, and apatite. Clinopyroxene inclusions within alkali feldspar are common. Thin pyroxenite dykes crosscut the syenite, and melasyenite is crosscut by irregular syenite dykes.

Loranger complex

The Loranger complex is a large (105 km^2), oval-shaped, composite pluton. Its eastern part consists of a circular diorite stock, rimmed on the western side by four different crescent-shaped leucocratic monzonite intrusions.

The outermost crescent is composed of pink, strongly recrystallized quartz-and biotite-bearing monzonite. The second crescent consists of pink syenite with minor centimetric grains of alkali feldspar in a thoroughly recrystallized fine grained matrix. Foliation is displayed by oriented clusters of biotite. Quartz, apatite, and magnetite may also be present. The third crescent is the most extensive monzonite phase and is composed of grey, coarse, blocky alkali feldspars, commonly zoned and set within a finer matrix of recrystallized feldspar. Biotite, apatite, and magnetite are also present. Inclusions of fine grained, massive feldspathic rocks, calc-silicates, quartzofeldspathic and pelitic gneiss, and quartzite are common.

The innermost crescent consists of a grey monzonite with coarse- to medium-grained equant euhedra of alkali feldspar, with interstitial biotite, magnetite, amphibolite, and apatite. No evidence was found for recrystallization of this phase, although the intrusion contains inclusions of recrystallized and foliated monzonite. Porphyritic monzonite dykes crosscut this monzonite and the country rocks in places. The dioritic rocks in the eccentric core of the intrusion are heterogeneous and consist of plagioclase laths with interstitial clinopyroxene rimmed by amphibole, biotite and magnetite. They are crosscut by fine- to medium-grained diorite dykes.

Late dykes

Composite dykes composed of fine grained grey rock mixed with syenite, quartz syenite, or, more commonly, aplite, crosscut all plutons as well as the country rocks. These dykes are in turn crosscut by aplitic and pegmatitic dykes that are locally granophyric and contain fluorite and/or molybdenite. Grey feldspars in the syenites become pink next to these felsic dykes.

In the Kensington complex, epidote veins crosscut the plutonic rocks, and feldspar grains are pink within a few centimetres of these veins. Epidote is also locally scattered throughout the rock, and clinopyroxene crystals are rimmed by blue amphibole.

DEFORMATION, RECRYSTALLIZATION, AND RELATIONSHIP OF THE INTRUSIONS TO THE COUNTRY ROCK

Most of the syenitic intrusions of the Mont-Laurier area show little evidence of penetrative deformation, even at their contacts. Nevertheless, there is field evidence to suggest that intense recrystallization has locally obliterated primary igneous textures such as that given by lath-shaped feldspars. A major shear zone bounds the west margin of the Gracefield pluton; minor shear zones and mylonites are observed throughout the region. Contact relationships of these intrusions have yet to be investigated in detail. Rive (1976) reported hybridization and recrystallization of the country rock around the Ste-Véronique complex. Gauthier described the paragneiss sequence as deviating around and being conformable to the margins of the Cameron and Gracefield complexes (except the north-south shear zone on the west side of the Gracefield complex).

The age of these intrusions is not well constrained. Biotite K-Ar isotopic ages are about 850 Ma, but recrystallization may have caused Ar loss from the biotite grains investigated by Doig and Barton (1968). Older ages of 1005 and 1226 Ma (biotite, K-Ar) were determined by Doig and Barton (1968) and Vivier (Tabet Abdul-Malak, 1978) on the pyroxenite stock of the Ste-Véronique complex. These older ages are not in accord with rare evidence of crosscutting relationships between melasyenite similar to those of the central stock and syenite rim. The Loranger monzonite gives an Rb-Sr isochron age of 1120 ± 60 Ma, with an initial ratio of 0.7030 ± 0.0005 (Bell and Blenkinsop, 1980).

ECONOMIC ASPECTS

Apatite-rich pyroxenite is present in the Ste-Véronique, Gracefield and Lac Rouge complexes. Its extent is usually small but its apatite content may be as high as 30 per cent. Molybdenite has been mined in a pegmatite dyke crosscutting the Kensington complex. No carbonatites have been recognized. Well jointed, fresh, pink syenite may be found on the eastern margin of the Cameron complex, and might be of some use as ornamental stone.

CONCLUSIONS

The seven principal syenitic plutons of the Mont-Laurier area mapped during 1983 consist of round to oval-shaped bodies varying in area from <5 to 105 km^2. Foliation and layering in the country rocks deflects around these intrusions and typically conforms to the contacts of the plutons. Rocks of syenitic composition predominate, but individual complexes may contain rocks with a wide variety of mafic mineral content. Both the Kensington and Ste-Véronique complexes are associated with abundant monzodiorite or melasyenite and pyroxenite phases. The Gracefield and Lac Rouge complexes are characterized by the presence of calcite and apatite in the syenite, and by the presence of a minor amount of apatite-rich melasyenite and pyroxenite. Nepheline syenite occurs at the periphery of some of these complexes, and quartz syenite is present in the Satellite, Cameron and Loranger plutons. Recrystallization has to some extent affected all intrusions except the Lac Rouge syenite. Local fenitization is observed immediately adjacent to some intrusions. Non-deformed syenite dykes crosscut the Grenville Supergroup and its pre-existing structure around many of the complexes.

REFERENCES

Aubert de la Rue, E.
1948: Nomingue and Sicotte map-areas, Labelle and Gatineau counties; Québec Department of Mines, Geological Report 23, 74 p.

1953: Kensington area, Gatineau and Labelle counties; Québec Department of Mines, Geological Report 50.

1956: Trente-et-un Milles Lake area, Electoral Districts of Papineau, Labelle, and Gatineau; Québec Department of Mines, Geological Report 67.

Bell, K. and Blenkinsop, J.
1980: Whole rock Rb-Sr studies in the Grenville Province of southeastern Ontario and western Québec – a summary report; in Current Research, Part C, Geological Survey of Canada, Paper 80-1C, p. 152-154.

Davidson, A., Britton, J.M., Bell, K., and Blenkinsop, J.
1979: Regional synthesis of the Grenville Province of Ontario and Western Québec; in Current Research, Part B, Geological Survey of Canada, Paper 79-1B, p. 153-172.

Doig, R. and Barton, J.R.
1968: Ages of carbonatites and other alkaline rocks in Québec; Canadian Journal of Earth Sciences, v. 5, p. 1401-1408.

Durocher, M.E.
1977: Petrology of the Gracefield Pluton; unpublished M.Sc. thesis, Ecole Polytechnique de Montreal, 210 p.

Indares, A.
1982: L'évolution des conditions de temperature et de pression pendant le metamorphisme catazonal dans la region de Maniwaki, province de Grenville, bouclier canadien, M.Sc. thesis, Université de Montréal, 255 p.

Osborne, F.F.
1935: Labelle-L'Annonciation map-area; Quebec Bureau of Mines, Annual Report, Part E, 52 p.

Rive, M.
1976: Region de Ste-Véronique; Ministère des Richesses Naturelles, Québec, Rapport Geologique 182.

Tabet, Abdul-Malak, V.
1978: Le complexe alcalin de Sainte-Véronique (Québec, Canada): petrologie et geochimie; thèse de 3ième cycle, Université Claude Bernard-Lyon.

Wynne-Edwards, H.R., Gregory, A.F., Hay, P.W., Giovanella, C.A., and Reinhardt, E.W.
1980: Whole rock Rb-Sr studies in the Grenville Province of southeastern Ontario and western Québec – a summary report; in Current Research, Part C, Geological Survey of Canada, Paper 80-1C, p. 152-154.

42. METAMORPHIC PROCESSES IN THE KISSEYNEW SEDIMENTARY GNEISS BELT. 1. INITIAL STAGES OF MIGMATITE FORMATION IN THE NOBLE LAKE AREA, MANITOBA

Project 830014

Terence M. Gordon
Precambrian Geology Division

Gordon, T.M., Metamorphic processes in the Kisseynew sedimentary gneiss belt. 1. Initial stages of migmatite formation in the Noble Lake area, Manitoba; in Current Research, Part A, Geological Survey of Canada, Paper 84-1A, p. 307-312, 1984.

Abstract

Fieldwork in the Noble Lake area (NTS 63 O/16) has indicated that several phases of deformation overlapped a single metamorphic pulse. Four types of quartzofeldspathic segregation have been recognized and placed in a tentative time sequence.

Résumé

Les travaux sur le terrain dans la région du lac Noble (NTS 63 O/16) permettent de croire que plusieurs phases de déformation ont chevauché une seule impulsion métamorphique. Quatre types de ségrégation quartzofeldspathique ont été identifiés et placés en ordre chronologique provisoire.

INTRODUCTION

The Kisseynew sedimentary gneiss belt lies between the Lynn Lake greenstone belt and the Flin Flon-Snow Lake greenstone belt at the southwest margin of the Churchill Structural Province. Much of the belt is underlain by aluminous paragneiss metamorphosed at upper amphibolite facies conditions. Rock types range from metatexite to tonalite, granodiorite, and granite.

Detailed studies in the belt include the work of Elphick (1972), Schledewitz (1972), Bailes (1975), Baldwin et al. (1979) and Lenton (1981). Reviews of the general geology and metamorphism are contained in Bailes and McRitchie (1978) and McRitchie et al. (1979). The latter paper contains an extensive list of references to previous geological work.

The belt has been interpreted as originating as a sedimentary trough filled with volcanogenic turbidites derived from the adjacent greenstone belts. Although four metamorphic and five structural events have been postulated, the dominant structures and mineralogy have been attributed to two major episodes of deformation overlapping one or two prograde metamorphic events.

The aim of this study is to estimate the physical conditions of metamorphism and migmatite formation during the evolution of the Kisseynew belt in order to constrain quantitative modelling of the tectonic history of this terrane. Work during the 1983 field season was concentrated on the particularly lichen-free outcrops of paragneiss 10 to 35 km northwest of Thompson, Manitoba, in the eastern part of the Noble Lake area (NTS 63 O/16). This area has been previously mapped by Baldwin et al. (1979). Figure 42.1 shows the distribution of outcrop and selected structural observations.

LITHOLOGY

The area studied is underlain almost entirely by paragneiss of the Burntwood River Metamorphic Suite (nomenclature of Lenton, 1981). These rocks retain 2 to 50 cm compositional layers attributable to original sedimentary bedding (Fig. 42.2, 42.3).

Psammitic gneiss layers are light grey weathering, medium grained, with rare 1 to 6 mm garnet porphyroblasts in a quartz-feldspar-biotite matrix. Pelitic gneiss layers are light brown weathering, coarse grained, and contain conspicuous 5 to 40 mm porphyroblasts of garnet, cordierite and potassium feldspar. Graphite is a common accessory. Some beds show compositional grading, but in general metamorphic recrystallization has obliterated primary sedimentary structures.

Quartzofeldspathic bodies comprise from 0 to 20 per cent of the rock. The majority of these may be classified by mineralogical and morphological criteria into four groups although some segregations have ambiguous or transitional characteristics.

Very coarse grained quartz-rich segregations occur in lenses and pods in zones within and parallel to individual layers of pelitic gneiss (Fig. 42.4). Such zones are from 1 to 15 cm in width and up to 5 m in length. Feldspar, if present, is usually concentrated at margins of individual segregations. A discontinuous selvage of various mixtures of biotite, garnet, cordierite, and, rarely, sillimanite is commonly found adjacent to individual pods. Although the original geometry of these segregations is unknown, they commonly have shapes suggestive of boudins, augen, and rootless fold hinges. Only very rarely do quartz-rich segregations cut across layering.

Potassium feldspar-rich pegmatitic pods, 1 to 50 cm in diameter form a second segregation type. These occur in pelitic to semipelitic layers, have relatively sharp contacts with the enclosing rock, but have no selvages. In the absence of minor folds these segregations are often confined to single layers and exhibit a remarkably regular spacing (Fig. 42.5). In some rocks such pods cut across quartz-rich lenses. Where small scale folding has occurred the pods are commonly located on fold limbs (Fig. 42.6) and may show evidence of deformation. In other localities the quartzofeldspathic material cuts across adjacent layers and appears unaffected by folding (Fig. 42.7).

A third type of segregation occurs in garnetiferous semipelitic layers. Medium grained quartzofeldspathic material occurs as haloes around garnet porphyroblasts (Fig. 42.8), nebulitic garnetiferous zones (Fig. 42.9), and 10 to 100 cm granitic veins and schlieren (Fig. 42.10). No mafic

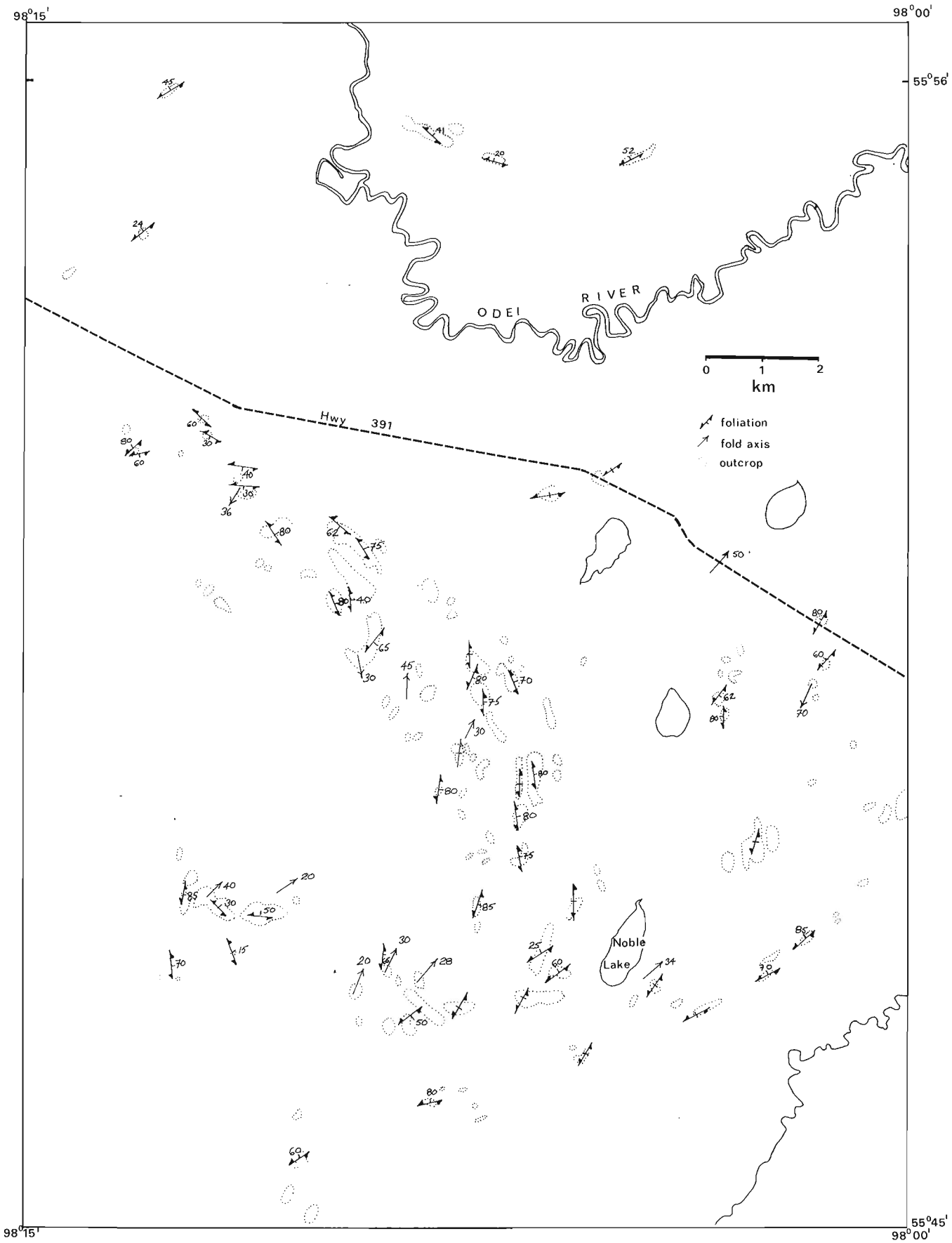

Figure 42.1. *Outcrop distribution and selected structural observations in the Noble Lake area.*

selvage were observed. Larger segregations have a lower garnet content. The irregular nature of the veins prevents a clear interpretation of their age relative to formation of minor folds. In general they appear less deformed than their host rock.

Parallel sided granitic dykes 10 to 50 cm in width, and pegmatite dykes and pods up to 5 m in width constitute the fourth type of quartzofeldspathic body. In the western part of the area they have a northeast trend and crosscut most structures. Ptygmatic folding, boudinage, and disrupted dykes are common, however, in the east.

STRUCTURAL GEOLOGY

The earliest secondary structure observed in the Noble Lake area is a mineral foliation parallel to bedding. It is defined by the subparallel alignment of mineral aggregates and tabular minerals, including biotite, garnet, and cordierite. This foliation was not observed to cut any fold hinges, although some reorientation of minerals was observed in the axial zones of particularly tight minor folds.

Bedding and foliation are deformed by open to tight mesoscopic folds with 5 to 50 cm wavelengths. These folds are disharmonic and often polyclinal (Fig. 42.11, 42.12). Fold style is partially controlled by local bedding thickness and proportion of psammite to pelite layers, thus vitiating correlations based on style. In particular, complex fold patterns suggestive of polyphase deformation (Fig. 42.13) occur mainly in areas in which 1 to 3 cm thick psammite beds alternate with thinner pelitic layers. Although many fold orientations were observed, most smaller minor folds have northeasterly trending axial traces and moderate northeast plunges.

Mineral lineations are only locally developed. In general they also plunge northeast.

Larger open to tight mesoscopic folds with wavelengths of at least 10 m were observed in a few places in the western part of the area. These folds often have rounded hinge zones and in places appear to deform axial surfaces of smaller disharmonic folds (Fig. 42.14). Folds of this size and style usually plunge moderately to the northeast but are also locally involved in complex shallow basin and dome structures.

In the eastern part of the area mesoscopic folds are tight to isoclinal and foliation is subparallel to axial planes. The presence of feldspar augen (Fig. 42.15) and disrupted granitic dykes (Fig. 42.16) suggest that this is a late foliation that has affected pre-existing quartzofeldspathic segregations.

Late stage joints, forming a northeast- and northwest-trending conjugate set, are the youngest structures observed in the area.

Figure 42.2. *Interlayered pelitic, semipelitic and psammitic gneiss. Dark spots are garnet. 83GV1359-1. GSC 204067-C*

Figure 42.3. *Compositionally graded semipelitic and pelitic layers. Dark spots are garnet. 83GV1349-1. GSC 204067-D*

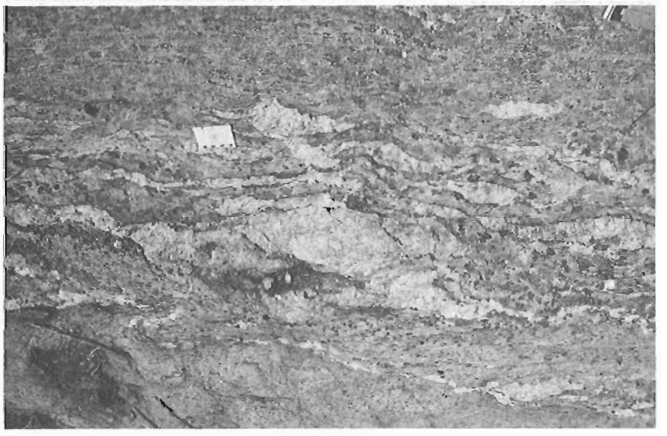

Figure 42.4. *Quartz-rich segregations in pelite layer. Dark selvages are garnet and biotite. 83GV1250. GSC 204068*

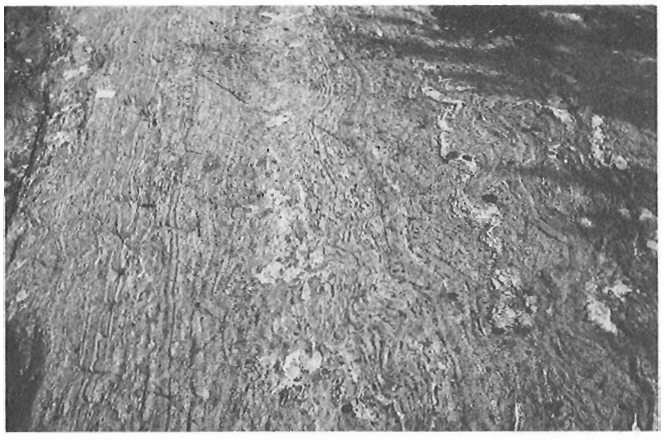

Figure 42.5. *Pegmatitic segregations confined to single bed at photo centre. 83GV1356-2. GSC 204067-B*

Figure 42.6. *Pegmatitic segregations on fold limbs in garnetiferous pelitic gneiss. 83GV1356-3. GSC 204068-B*

Figure 42.7. *Pegmatitic segregations crosscutting semipelitic and pelitic gneiss layers. 83GV1352-1. GSC 204067-T*

Figure 42.8. *Granitic haloes around garnet porphyroblasts in semipelite. 83GV1347-1. GSC 204067-Y*

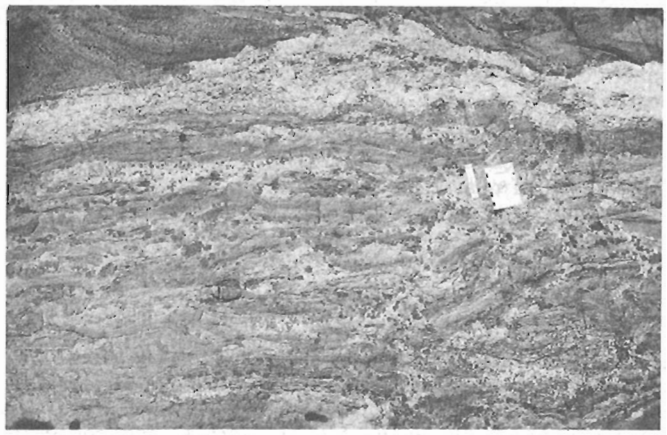

Figure 42.9. *Nebulitic garnetiferous granitic veins. 83GV1348-2. GSC 204067-X*

Figure 42.10. *Garnetiferous granitic schlieren and veins. 83GV1357-1. GSC 204067-Z*

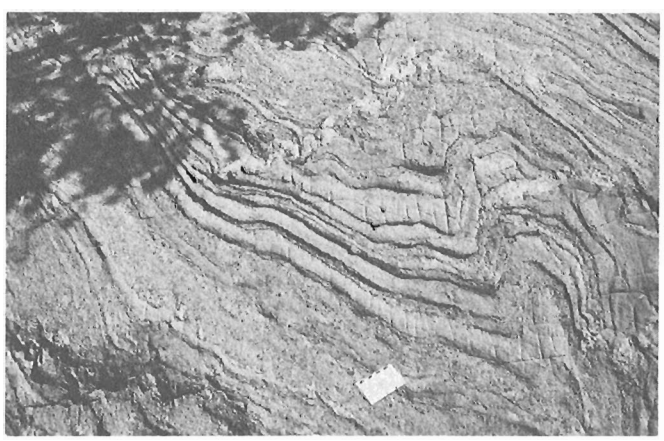

Figure 42.11. *Disharmonic polyclinal folds in interlayered psammitic and pelitic gneiss. 83GV1076-3. GSC 204067-V*

Figure 42.12. *Tight folds in pelitic gneiss in foreground are not reflected in 10 cm psammitic gneiss layer above. 83GV1144-2. GSC 204067-I*

Figure 42.13. *Complex fold pattern in interlayered psammitic and pelitic gneiss. 83GV1076-2. GSC 204067-W*

Figure 42.14. *Northeast-plunging open fold with smaller scale complex folds on limbs. 83GV1404. GSC 204067-Q*

METAMORPHISM

Only preliminary petrographic work has been done. The maximum mineral assemblage observed in pelitic gneiss is quartz-oligoclase(An_{28})-perthitic microcline-biotite-garnet-cordierite-graphite-opaque-sillimanite-fibrolite-spinel-zircon. Garnet and microcline are often poikiloblastic, enclosing quartz, plagioclase, and biotite. Fibrolite and sillimanite are commonly restricted to cores of cordierite porphyroblasts, although some sillimanite occurs between biotite, garnet, quartz, and plagioclase. Spinel is always enclosed in cordierite. Zircon occurs as both euhedral crystals and rounded grains. A comparison with similar assemblages studied in detail by others (e.g. Lee and Holdaway, 1977; Newton and Haselton, 1981) suggests metamorphic temperatures near 700°C and pressures between 0.4 and 0.6 GPa.

All quartzofeldspathic segregations contain quartz, plagioclase, and potassium feldspar. Although the coarse grain size precludes accurate modal estimates, compositions appear to include granite and granodiorite. Garnet, sillimanite, and minor biotite and cordierite occur in small, varying amounts in segregations.

Yardley (1978) summarized several criteria that may be used to distinguish mechanisms of migmatization. Based on these, a tentative interpretation of processes operating on the Noble Lake area rocks is possible. The early formed quartz-rich segregations and pegmatitic pods probably result

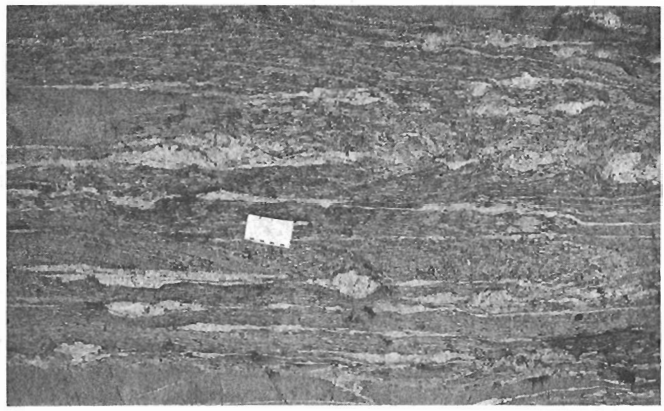

Figure 42.15. *Feldspar augen in strongly foliated gneiss in eastern part of map area. 83GV1368-2. GSC 204067-R*

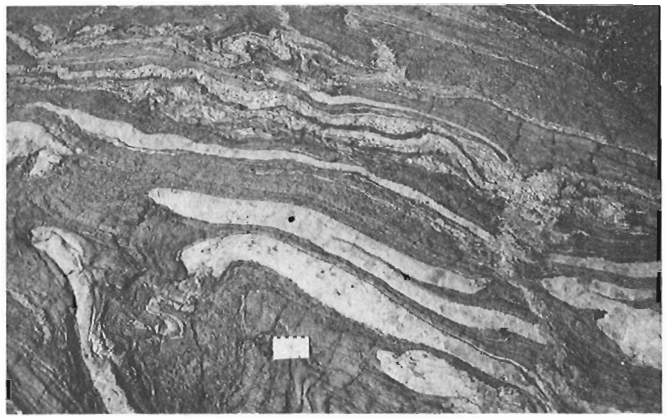

Figure 42.16. *Folded and disrupted granitic veins in eastern part of map area. 83GV1378-2. GSC 204067-S*

from metamorphic segregation enhanced by the presence of a water-rich fluid and localized by planes of weakness. The later formed garnetiferous schlieren and granitic veins probably represent silicate melts resulting from anatexis. Further mineralogical work will test and refine this model.

PRELIMINARY INTERPRETATION

Observations to date are consistent with the following continuum of overlapping events:

1. Development of quartz-rich segregations and mafic selvages in pelitic layers.
2. Growth of tabular garnet and cordierite as a foliation imposed parallel to bedding.
3. Potassium feldspar blastesis and growth of pegmatitic pods during development of northeast-trending folds.
4. Continued deformation resulting in complex folds simultaneously with anatexis and production of garnetiferous granitic veins and schlieren.
5. Emplacement of crosscutting granitic and pegmatitic dykes.
6. Local imposition of a strong northeast-trending foliation with disruption of pre-existing dykes.
7. Development of brittle fractures.

Although structures indicate several deformational episodes, there is no compelling evidence for more than one prograde metamorphic event. Analysis of structural data and mineralogical studies will be used to test these interpretations.

REFERENCES

Bailes, A.H.
1975: Geology of the Guay-Wimapedi Lakes area; Manitoba Mineral Resources Division, Geological Services Branch, Publication 75-2, 104 p.

Bailes, A.H. and McRitchie, W.D.
1978: The transition from low to high grade metamorphism in the Kisseynew sedimentary gneiss belt, Manitoba; in Metamorphism in the Canadian Shield, ed. J.A. Fraser and W.W. Heywood; Geological Survey of Canada, Paper 78-10, p. 155-177.

Baldwin, D.A., Frohlinger, T.G., Kendrick, G., McRitchie, W.D., and Zwanzig, H.V.
1979: Geological maps 78-3-1 to 78-3-22. Geology of the Nelson House-Pukatawagan region (Burntwood Project); Manitoba Mineral Resources Division.

Elphick, S.C.
1972: Geology of the Mynarski-Notigi Lakes area; Manitoba Mines Branch, Publication 71-2C, 48 p.

Lee, S.M. and Holdaway, M.J.
1977: Significance of Fe-Mg cordierite stability relations on temperature, pressure, and water pressure in cordierite granulites; American Geophysical Union, Geophysical Monograph 20, p. 79-94.

Lenton, P.G.
1981: Geology of the McKnight-McCallum Lakes area; Manitoba Mineral Resources Division, Geological Survey, Geological Report GR79-1, 39 p.

McRitchie, W.D., Peters, J., and Frohlinger, T.G.
1979: History of exploration and geological work in the Nelson House-Pukatawagan region (Burntwood Project); Manitoba Mineral Resources Division, Geological Report 78-3 (Part II).

Newton, R.C. and Haselton, H.T.
1981: Thermodynamics of the garnet-plagioclase-Al_2SiO_5-quartz geobarometer; in Thermodynamics of Minerals and Melts, ed. R.C. Newton, A. Navrotsky, and B.J. Wood; Springer-Verlag, New York, p. 131-147.

Schledewitz, D.C.P.
1972: Geology of the Rat Lake area; Manitoba Mines Branch, Publication 71-2B, 57 p.

Yardley, B.W.D.
1978: Genesis of the Skagit Gneiss migmatites, Washington, and the distinction between possible mechanisms of migmatization; Geological Society of America, Bulletin, v. 89, p. 941-951.

43. GEOLOGY OF PARTS OF THE DEEP ROSE LAKE AND PELLY LAKE MAP AREAS, DISTRICT OF KEEWATIN

Project 820007

Subhas Tella, D.L. Thompson[1], and D.T. James[2]
Precambrian Geology Division

Tella, S., Thompson, D.L., and James, D.T., Geology of parts of the Deep Rose Lake and Pelly Lake map areas, District of Keewatin; in Current Research, Part A, Geological Survey of Canada, Paper 84-1A, p. 313-322, 1984.

Abstract

Intensely deformed and metamorphosed layered orthogneisses, well foliated granitoid rocks, and massive to weakly foliated quartz diorite to granite collectively constitute an Archean and/or Aphebian basement to the supracrustal rocks of the Aphebian Amer group, and the Helikian Thelon Formation. Deformed supracrustal belts of uncertain age, in part consisting of stromatolite(?) bearing carbonate units, occur in the area.

The Amer group strata are made up of two clastic sequences – a lower conglomerate and orthoquartzite, and an upper feldspathic sandstone. The two are separated by mudstone, slate, and phyllite. Field data suggest an increase in intensity of deformation and metamorphism from southwest to northeast.

Faults and shear zones transect the area on all scales. Structural and metamorphic data from the northeast trending Chantrey Mylonite Zone suggest that the latest displacement on the zone was one of low angle oblique-slip with an apparent dextral sense of shear.

Résumé

Des orthogneiss stratifiés fortement déformés et métamorphisés, des roches granitoïdes bien feuilletées et une diorite quartzique massive à faiblement feuilletée qui se transforme en granite forment le socle archéen, aphébien ou les deux sous les roches supracorticales du groupe aphébien d'Amer et de la formation hélikienne de Thelon. Des zones supracorticales déformées, d'âge incertain, composées en partie d'unités carbonatées à stromatolites(?), se trouvent également dans la région.

Les couches du groupe d'Amer comprennent deux séquences clastiques, soit une unité basale composée d'un conglomérat et d'une orthoquartzite ainsi qu'un grès feldspathique supérieur. Ces deux unités sont séparées par de la pélite, du schiste argileux et de la phyllite. Les données recueillies sur le terrain semblent indiquer que l'intensité de la déformation et du métamorphisme s'accroît du sud-ouest vers le nord-est.

Des failles et des zones de cisaillement traversent la région à toutes les échelles. Les données structurales et métamorphiques sur la zone mylonitique de Chantrey orientée vers le nord-est semblent indiquer que le déplacement le plus récent le long de la zone comprenait un mouvement oblique à angle faible avec cisaillement dextral apparent.

INTRODUCTION

Bedrock mapping in the northwest half of the Deep Rose Lake (NTS 66G) and in eastern parts of the Pelly Lake (NTS 66F) map areas, at a scale of 1:250 000, was completed during the 1983 field season. Preliminary results of mapping in the southeast half of the Deep Rose Lake map area were reported previously (Tella et al., 1983). The map area (Fig. 43.1) is part of a region previously mapped by Wright (1955, 1967) at a scale of one inch to eight miles. M.J. Jackson, visiting scientist, Australian Bureau of Mineral Resources, spent one week in the area examining selected stratigraphic sections within the Aphebian Amer group.

Acknowledgments

We thank R.I. Macfie, A.C. Dobson, R.S. Kat, S. Smith, our field assistants, and M. Fahrig, cook, for their excellent support during the summer. Boris and Liz Kotelewetz, Baker Lake, provided expediting services. W. Martin, R. Hafen, and D. McNab of PanAir Helicopters provided the rotary wing support. We also thank A.N. LeCheminant for his co-operation and assistance.

GENERAL GEOLOGY

The distribution of rock units, and the orientation of selected fabric elements in the Deep Rose Lake and Pelly Lake map areas are shown in Figure 43.1, 43.2. The northern portion of the region is underlain by deformed and metamorphosed Archean and Aphebian gneissic, granitic, and schistose rocks. To the south, they are unconformably overlain by deformed and weakly metamorphosed supracrustal rocks of the Aphebian Amer group and by undeformed Helikian clastic rocks of the Thelon Formation. Deformed supracrustal rocks of uncertain age, and consisting of stromatolitic(?) dolomite, chert, siltstone, slate-phyllite, mafic schist and metagreywacke, occur in the northern and northeastern parts of the map area. Several other metasedimentary outliers consisting of deformed polymictic conglomerate, orthoquartzite, pelite, and mafic rocks have been found northeast of Sand Lake. They define a narrow (1-2 km wide) northeast trending, discontinuous belt that extends for over 60 km along strike. The rocks within the belt are tentatively correlated with the Amer group. Faults and shear zones, characterized by both ductile and brittle deformation textures, affect both the basement and the cover rocks. The Chantrey Mylonite Zone (Fig. 43.1) represents the northeastern segment of the Slave-Chantrey Mylonite Zone (Heywood and Schau, 1978).

Bedrock exposures are generally good in the region north and southwest of Lower Garry lake, and along a narrow strip that extends from Sand Lake to northwest of Deep Rose Lake (Fig. 43.1). Except for small, scattered outcrops, bedrock is rare in the rest of the map area due to heavy glacial drift-cover.

[1] Department of Earth Sciences, Princeton University, Princeton, NJ, U.S.A.
[2] Department of Geological Sciences, Queen's University, Kingston, Ontario

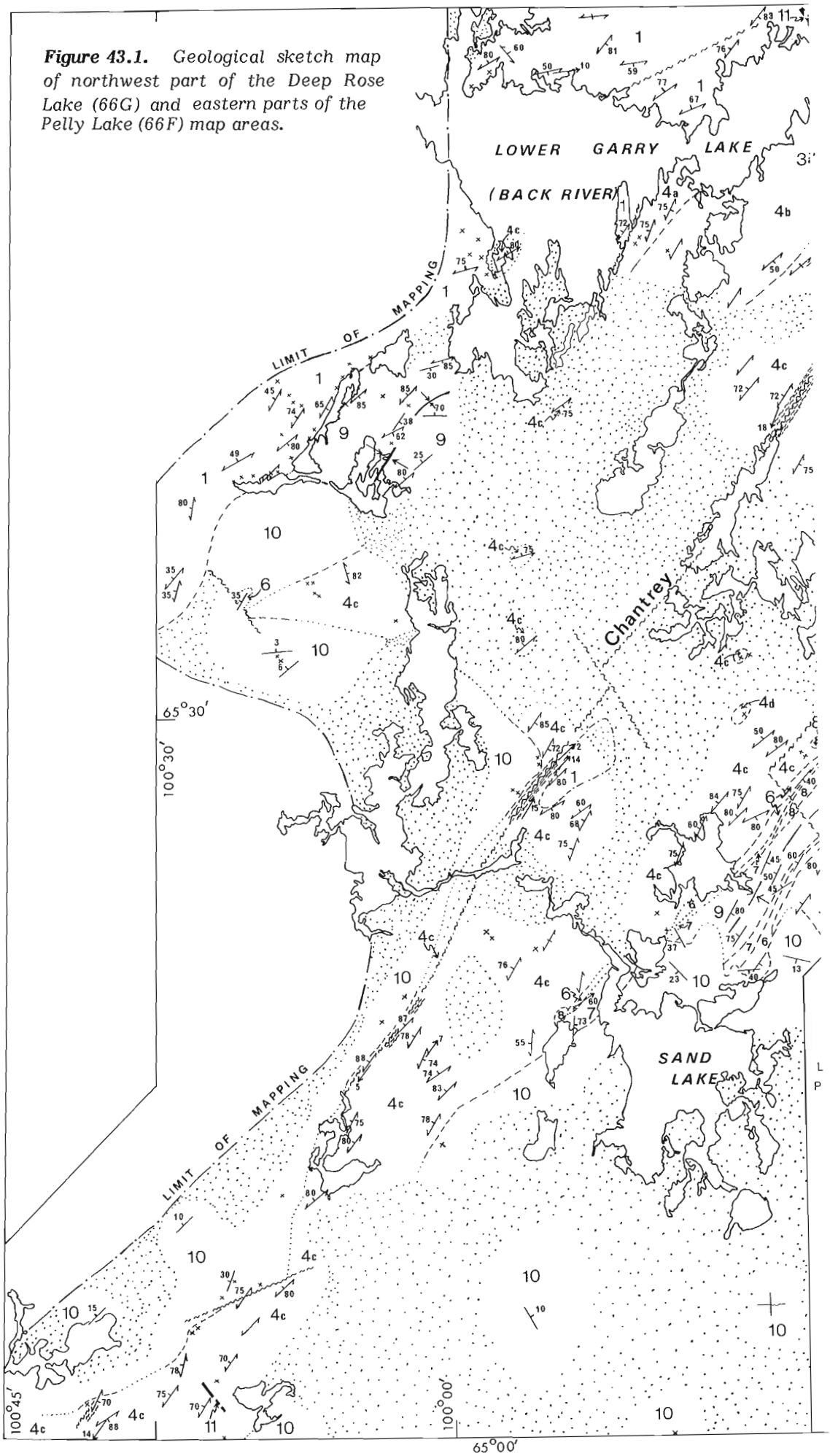

Figure 43.1. *Geological sketch map of northwest part of the Deep Rose Lake (66G) and eastern parts of the Pelly Lake (66F) map areas.*

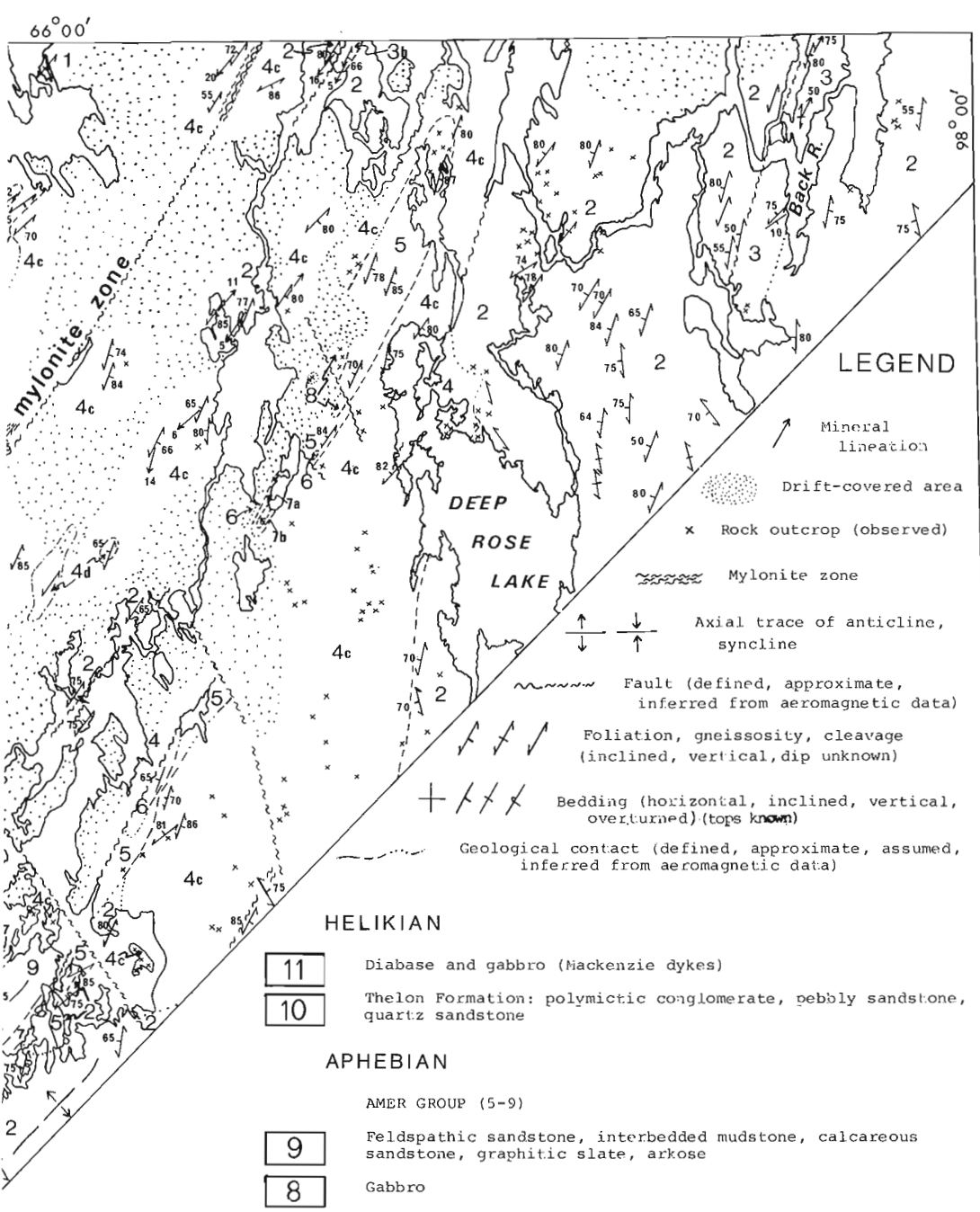

LEGEND

- Mineral lineation
- Drift-covered area
- Rock outcrop (observed)
- Mylonite zone
- Axial trace of anticline, syncline
- Fault (defined, approximate, inferred from aeromagnetic data)
- Foliation, gneissosity, cleavage (inclined, vertical, dip unknown)
- Bedding (horizontal, inclined, vertical, overturned) (tops known)
- Geological contact (defined, approximate, assumed, inferred from aeromagnetic data)

HELIKIAN

11 Diabase and gabbro (Mackenzie dykes)

10 Thelon Formation: polymictic conglomerate, pebbly sandstone, quartz sandstone

APHEBIAN

AMER GROUP (5-9)

9 Feldspathic sandstone, interbedded mudstone, calcareous sandstone, graphitic slate, arkose

8 Gabbro

7 Mudstone, siltstone, minor quartz wacke; mafic volcanic rocks and chlorite schist (7a), slate-phyllite (7b)

6 Orthoquartzite: white, grey, and green quartzite; quartz-mica schist; minor pebbly quartzite and conglomerate

5 Polymictic pebble- to cobble conglomerate

ARCHEAN AND/OR APHEBIAN

4 Granitoid rocks: Potash feldspar augen gneiss (4a) with abundant inclusions of older mafic rocks;
Hornblende-biotite granite (4b): well foliated and mafic-rich, in part mylonitic
Granite (4c): massive to weakly foliated, mafic-poor. Includes minor mafic schist and amphibolite (4d)

3 Metasedimentary rocks: Stromatolitic dolomite, interbedded chert, siltstone; slate-phyllite (3a); actinolite-chlorite schist, metagreywacke, and intercalated slate and dolomite (3b)

2 Hornblende-biotite granite, granodiorite: well foliated; in part megacrystic (K-feldspar), and massive. Contains inclusions of older gneiss, migmatite, amphibolite and gabbro;

1 Garry Lake Complex: Layered gneiss complex consisting of quartz-feldspar-biotite gneiss, porphyroblastic (K-feldspar) augen gneiss, granodiorite, tonalite, and granite gneiss; minor amphibolite and metagabbro. Intruded by younger plutonic rocks

5 10 15

KILOMETRES

OLOGICAL MAPPING

S.TELLA
D.L.THOMPSON
D.T.JAMES

1983

ARCHEAN AND/OR APHEBIAN BASEMENT (UNITS 1-4)

Basement rocks have been subdivided into four broad categories based on lithology, structure, and metamorphism: a) Garry Lake Complex, b) foliated granitoid rocks, c) metasedimentary and metamafic rocks, and d) massive to foliated granitoid rocks.

Garry Lake Complex (unit 1)

The northeast trending orthogneiss complex consists of interlayered grey to pink, quartz-feldspar-biotite gneiss, porphyroblastic (K-feldspar) augen gneiss, grey to black, mafic-rich, hornblende-biotite gneiss, tonalite, and granite gneiss. The complex is exposed to the north and southwest of Lower Garry Lake. Northwest of Sand Lake a sliver of similar gneisses is preserved adjacent to the Chantrey Mylonite Zone (Fig. 43.1). Minor amounts of amphibolite, metagabbro, and biotite paragneiss are locally present within the complex. Layering in the gneisses is in the order of centimetre to metre scale and quartzofeldspathic layers predominate over mafic layers. Sheets, dykes, and veins of deformed granite, pegmatite, and quartz monzonite, possibly representing several periods of igneous activity, cut the gneisses.

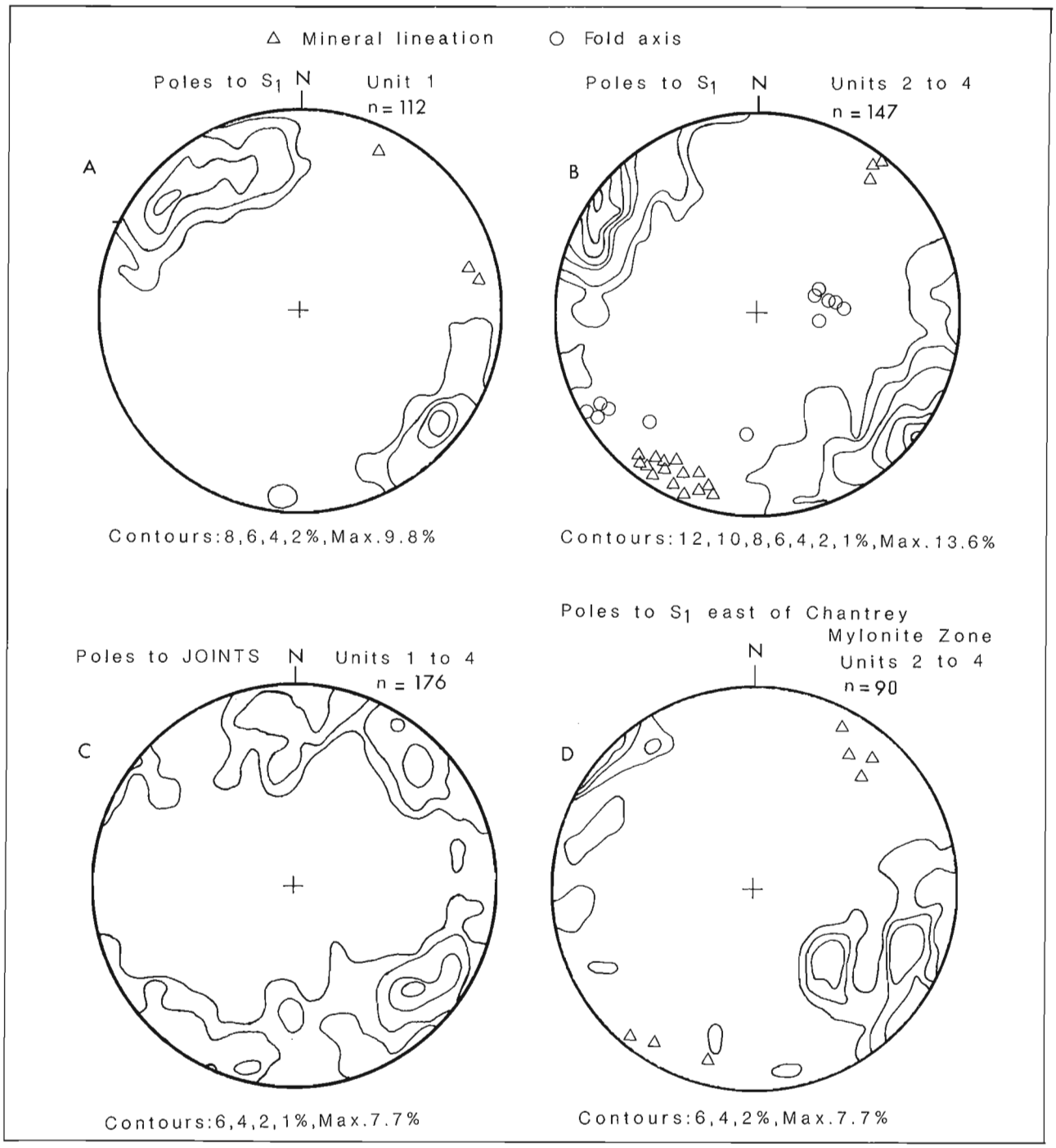

Figure 43.2. *Equal area lower-hemisphere projections of selected fabric elements in the region.*

Field relations and structural data indicate that the Garry Lake Complex has undergone at least two events of deformation and metamorphism. Northeast trending regional foliation (Fig. 43.2A) is the most common penetrative fabric element (S_1), and represents a syntectonic metamorphic fabric developed during the first event (D_1). The fabric is defined by an alignment of hornblende and biotite. First generation mesoscopic folds are relatively rare. They are tight isoclinal structures that plunge steeply to the northeast. A mineral (hornblende) lineation (L_1), recognized at a few localities, plunges shallowly (5-10°) to the east-northeast. Regional metamorphic grade is within the middle to upper amphibolite facies. The second event is marked by a penetrative, but locally developed, second cleavage (S_2). The cleavage (not shown in Fig. 43.2), which represents a syntectonic (D_2) metamorphic (greenschist grade) fabric, trends north- to north-northeast and dips steeply (70-90°W). Several mylonite and breccia zones are locally developed on a scale of few centimetres to tens of centimetres. They record later deformational events that affected the Garry Lake Complex.

Foliated granitoid rocks (unit 2)

Well foliated, granitoid metaplutonic rocks are widely exposed northeast and north of Deep Rose Lake, and to a lesser extent, northeast of Sand Lake. The constituent mineralogy includes quartz, K-feldspar, plagioclase, amphibole, biotite, and opaques. Relative proportions of K-feldspar and plagioclase are variable, and mafic constituents (mostly biotite, 10-20%) are altered to chlorite. North- to northeast-trending foliation, defined by alignment of amphibole, biotite, and feldspars, is present throughout the unit. A penetrative mineral lineation (quartz and feldspar rodding) is well developed adjacent to the Chantrey Mylonite Zone. The lineation commonly plunges (5-20°) to the southwest, with local reversals to the northeast. Rocks within the unit show local compositional and structural heterogeneities. Highly deformed parts of the unit grade into massive to megacrystic (K-feldspar) portions, suggesting an igneous protolith for the rocks. The rocks within the unit contain abundant inclusions of older paragneiss, migmatite, amphibolite and gabbro.

Metasedimentary and metamafic rocks (unit 3)

Rocks of supracrustal origin occur in the northeastern part of the map area (Fig. 43.1) north and south of the Back River. They include grey to buff weathering, stromatolitic(?) dolomite, interbedded chert, and minor grey siltstone and slate. The unit, which has an exposed width of less than 250 m and a strike length of approximately 15 km, is well layered (Fig. 43.3) on a scale of a few centimetres to up to 1 metre. Interlayers consisting of elliptical structures (Fig. 43.4), interpreted as flattened stromatolites(?), occur at several structural levels within the unit. The layers are up to 1 m thick, and individual elliptical stromatolites(?) range from a few centimetres to tens of centimetres long. A northeast trending and steep dipping (80-90°SE) cleavage overprinted the dolomite, and deformed stromatolites(?) are aligned in the planes of the fabric. Stromatolite-free layers are composed of fine grained, grey- to buff dolomitic limestone with thin (1-10 cm) intercalations of siliceous dolomite and chert. Tight, northeast trending, upright isoclinal folds (Fig. 43.5), noted within these layers, attest to the intense deformation undergone by the rocks. Interference fold structures with distinctive 'sheath fold' geometry (Fig. 43.6) are well developed in the carbonate-chert layers. The 'sheath' axes plunge steeply (70-75°) northeast. Bedding is transposed along the cleavage planes (Fig. 43.7), and S_0/S_1 intersection lineations commonly plunge northeast at steep angles (55-75°).

Contact relationships of unit 3 with adjacent foliated rocks of unit 2 are uncertain. The western contact is in part covered by the Back River system, but the highly sheared character of rocks in unit 2, together with steep dips in rocks of unit 3, suggest that they are in fault contact. The eastern contact, which is in part drift covered, is parallel to the Back River and may be fault bounded as well. Possible correlatives of unit 3 may be the Chantrey Group metasedimentary rocks which have been described in the region to the northeast (Heywood, 1961; Frisch and Patterson, 1983).

Minor exposures of slate-phyllite (3a), and actinolite-chlorite schist, metagreywacke, intercalated grey slate, and thinly laminated, buff weathering dolomitic rocks (3b) are present east of Lower Garry Lake, and 20 km northwest of Deep Rose Lake respectively (Fig. 43.1). Tight, upright

Figure 43.3

Layering in stromatolitic(?) dolomite, with intercalations of siliceous carbonate and chert. GSC 204039-K

Figure 43.4

Deformed (elliptical) stromatolites(?) in carbonate unit 3. Alignment is parallel to a northeast trending cleavage in the unit. GSC 203944-U

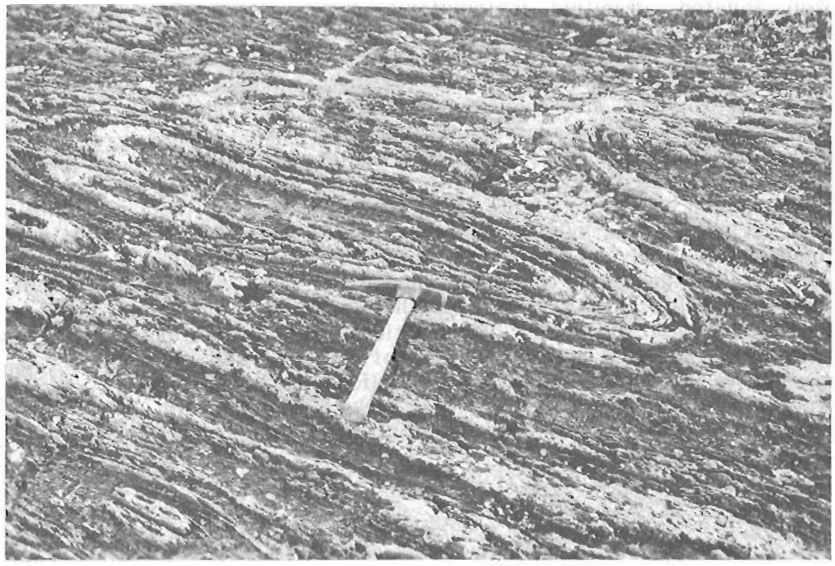

Figure 43.5

Tight isoclinal folds in carbonate-siliceous dolomite-chert layers (unit 3). GSC 203944-S

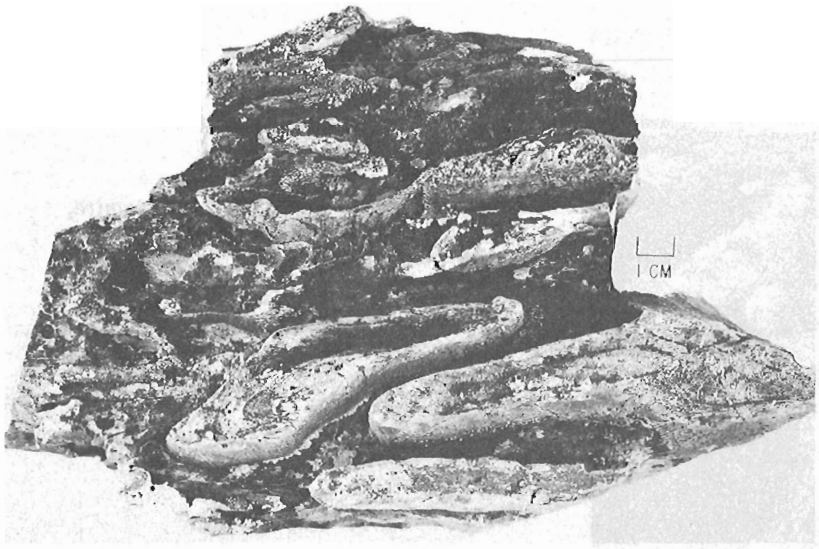

Figure 43.6

Interference fold structures ('sheath folds') in unit 3. GSC 203308-U

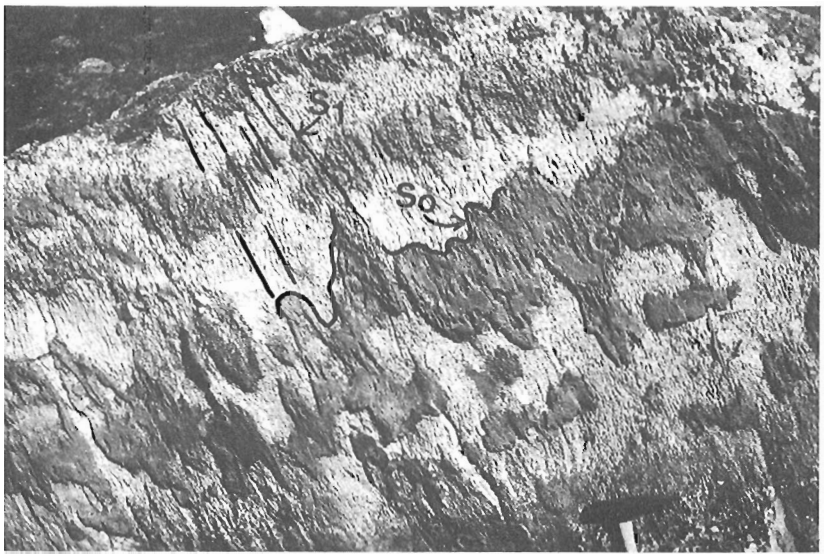

Figure 43.7

Bedding (S_0)-cleavage (S_1) relation in interbedded crystalline limestone (light) and siliceous carbonate (dark) (unit 3). Note the transposed siliceous carbonate layers along the cleavage planes. GSC 204039-C

isoclinal folds with shallow (5-15°) northeast plunge are commonly developed in dolomite layers (3b). The relative age relationships of 3a and 3b to unit 3 are uncertain, but they are included in the unit on the basis of some structural and lithological similarities.

Massive to foliated granitoid rocks (unit 4)

Several distinctly different plutonic rocks that range in composition from quartz diorite to granite are scattered throughout the region south and southeast of Lower Garry Lake (Fig. 43.1). They are subdivided into three lithological units (4a-4c) on the basis of composition, texture, and degree of deformation. All are deformed and weakly metamorphosed, with the exception of unit 4c, which is massive and relatively undeformed. A penetrative northeast trending planar fabric overprinted these rocks on a regional scale (Fig. 43.1, 43.2B,D).

Unit 4a consists of coarse grained, gneissic hornblende-biotite granite which locally contains abundant inclusions of older gneissic and mafic rocks (Garry Lake Complex?), and discontinuous layers of augenitic (K-feldspar) quartz monzonite. The unit is in fault contact with the Garry Lake Complex. Rocks within unit 4b are compositionally similar to those in 4a. They are medium- to coarse-grained, pink, and free of inclusions. Mafic minerals (hornblende, biotite) make up more than 15 per cent of the rock. Northeast trending mylonite zones are locally developed within the rocks of the unit, and extensive epidote alteration zones are common. The presence of abundant inclusions, coarser grain size, and megacrystic character of unit 4a distinguishes it from unit 4b.

Unit 4c consists of a massive, coarse grained, pink, porphyritic granite. Hornblende and biotite make up less than 5 per cent of the rock, and in some localities they are completely absent. A penetrative, northeast trending shear fabric is well developed within the unit adjacent to the Chantrey Mylonite Zone and other subsidiary shear zones. Contact relationships with units 4a and 4b are uncertain, but the massive and relatively undeformed state of many of these rocks suggests that they postdate the rocks in the other two units.

The granitoid rocks (4a-4c) are less deformed and metamorphosed than the rocks in the Garry Lake Complex, and therefore they are considered to be younger (Aphebian?) than the Garry Lake Complex.

Remnants of older mafic rocks, consisting of deformed amphibolite and mafic schist (4d), are present within the granite terrane (4c).

Metasedimentary rocks of the Aphebian Amer group unconformably overlie the granite 15 km northeast of Sand Lake (Fig. 43.1).

APHEBIAN AMER GROUP (UNITS 5-9)

Deformed and weakly metamorphosed sedimentary and igneous rocks of the Amer group occur in a tight, upright syncline northeast of Sand Lake (Fig. 43.1). Several outliers of the group west and northwest of Deep Rose Lake define a narrow (1-2 km) northeast trending belt which has a strike length of over 60 km. Rocks which are lithologically similar to upper parts of the Amer group occur southwest of Lower Garry Lake (Fig. 43.1).

The Amer group consists of two clastic sequences – a lower conglomerate, quartzite (units 5 and 6), and an upper interbedded sequence of feldspathic sandstone, calcareous sandstone, mudstone, graphitic slate, and arkose (unit 9). The two are separated by intercalated mudstone, siltstone, and slate (unit 7). Gabbroic rocks (unit 8) occur as minor stocks and sills within the group. The lithological character and stratigraphic relationships of rocks within units 6 to 9 are similar to those described from the southeast half of the Deep Rose Lake map area (Tella et al., 1983), and will not be treated further. Only pertinent new data and field relationships are presented here.

Approximately 20-25 km northeast of Sand Lake a polymictic, pebble- to boulder-conglomerate (unit 5, Fig. 43.1) unconformably overlies the basement complex and is in apparent fault contact with feldspathic sandstone (unit 9). Clasts in the conglomerate are predominantly composed of granodiorite and granite, minor lithic feldspar and vein quartz, and rarely, white quartzite. Based on the presence of white orthoquartzite clasts, Tella et al. (1983) suggested a post-Amer group age for this unit. However, this year's mapping northwest of Deep Rose Lake revealed that the conglomerate is a locally developed basal unit of the Amer group. The conglomerate is conformably overlain by white orthoquartzite. Approximately 5 km west of Deep Rose Lake the conglomerate, composed mainly of pink granite clasts, is overprinted by a penetrative, northeast trending and steeply dipping (75-90°) cleavage. A majority of the clasts are highly strained and aligned in the cleavage

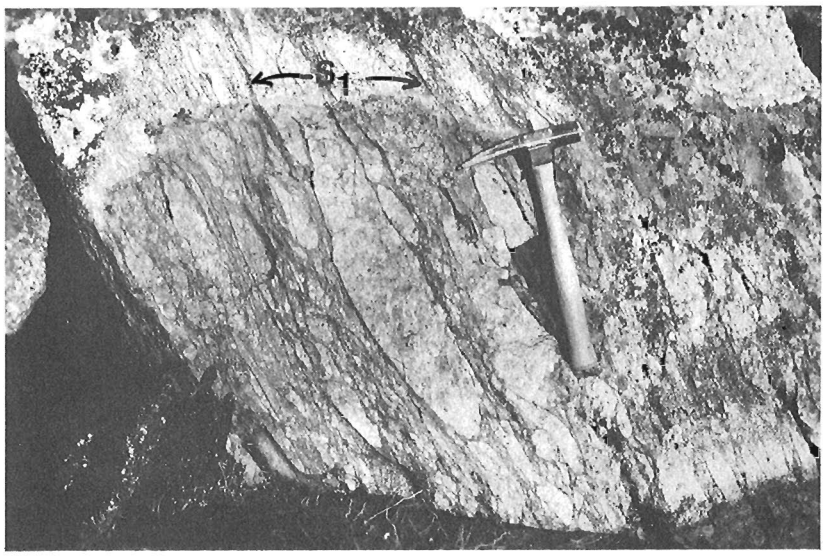

Figure 43.8

Highly strained polymictic conglomerate, Amer group (unit 5). The clasts are aligned parallel to the cleavage (S_1) planes. GSC 203944-Z

Figure 43.9

Bedding (S_0)-cleavage (S_1) relationships in the basal parts of the Amer group strata (units 5,6). Bedding is relatively flat. Intersection lineations plunge shallowly towards the observer. GSC 203944-X

planes (Fig. 43.8). Bedding (S_0), and cleavage (S_1) (Fig. 43.9) yield intersection lineations that plunge to the southwest at shallow angles (10-15°).

A layered supracrustal sequence consisting of deformed mafic volcanic rocks and chlorite schist (7a) and slate-phyllite (7b) is exposed 10 km west of the Deep Rose Lake (Fig. 43.1). The grey-green to black volcanic rocks, probably andesitic(?) flows, are fine grained, equigranular, and locally porphyritic (plagioclase and amphibole). They are in conformable contact with the slate-phyllite sequence. Northeast trending, upright, tight isoclinal folds are locally present in the slate-phyllite sequence. The fold axes plunge to the southwest at shallow angles (10-20°). Although the contact relationships of this sequence with respect to the conglomerate and quartzite (units 5 and 6) are uncertain, consistent southwest plunging intersection lineations observed in units 5 and 6 suggest that units 7a and 7b structurally, and probably stratigraphically, overlie unit 6.

The Amer group is moderately to intensely folded and faulted. Mesoscopic folds are relatively rare in the region. Mapping in 1983 delineated two major synclines in the area – one northeast of Sand Lake, and the other southwest of Lower Garry Lake. The boundary of the Amer group with basement rocks (units 1, 2, 4) is marked by northeast trending, high angle faults, shear zones, and rarely by unconformable relationships. Field observations suggest an apparent increase in the intensity of deformation and metamorphism from southwest to northeast.

HELIKIAN THELON FORMATION (UNIT 10)

The Thelon Formation, consisting of flat lying to gently dipping (3-25°), light grey to pink, grey weathering, pebble to boulder, clast supported conglomerate, pebbly sandstone, and gritty sandstone unconformably overlies the basement rocks and the Amer group. The unit is poorly exposed in the region. Scattered outcrops, separated by drift cover, are exposed south and west of Sand Lake, and west of the Chantrey Mylonite Zone (Fig. 43.1). Poor to well sorted, cobble to boulder polymictic conglomerate occurs at the base. The clast compositions are predominantly white, grey, and pink quartzite, and rarely red mudstone. Pebbly conglomerate and sandstone, and maroon to pink, feldspathic sandstone with

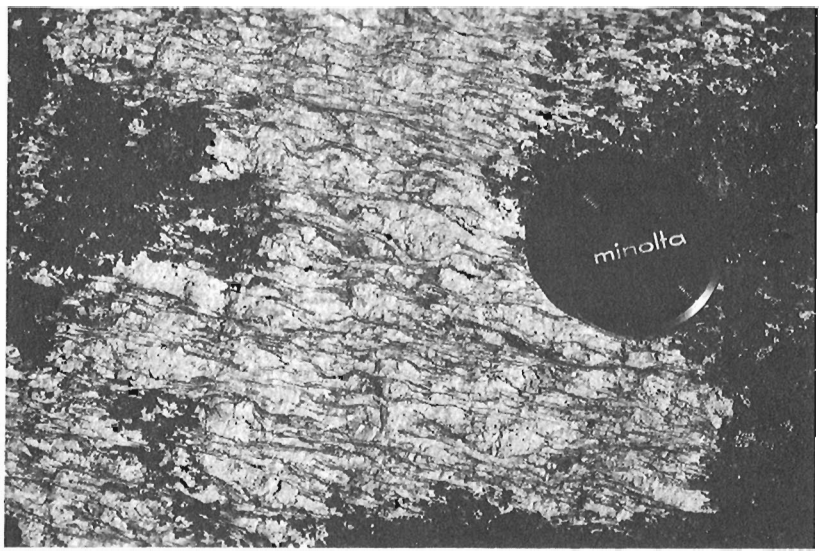

Figure 43.10

Chantrey Mylonite Zone. Elongate ribbons of quartz wrap around potash feldspar (augenitic) megacrysts. GSC 204039-I

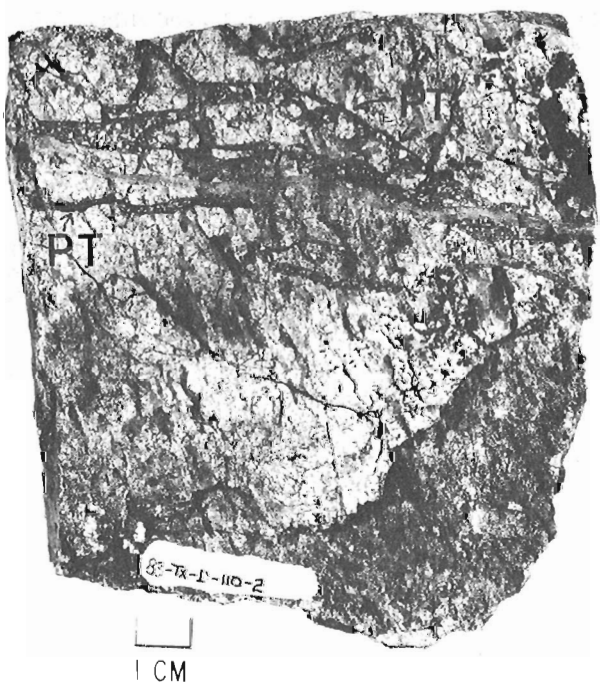

Figure 43.11. *Breccia zones with pseudotachylite fractions cutting mylonitic layering; Chantrey Mylonite Zone. GSC 203308-V*

fining upward cycles are interbedded with the conglomerate. Well developed regolith zones are locally preserved at the base of the conglomerate, adjacent to the Chantrey Mylonite Zone, west and northwest of Sand Lake. Red hematitic weathering profiles, clay- and chlorite-rich zones are common. The Thelon Formation rocks are displaced by northeast and northwest trending faults, some of which are reactivated older basement structures.

The lithological character of the Thelon Formation in the southeast half of the Deep Rose Lake area has been described by Tella et al. (1983), and elsewhere in the region by Donaldson (1965, 1969) and LeCheminant et al. (1983).

LATE INTRUSIVE ROCKS

Biotite lamprophyre and syenite dykes (not shown in Fig. 43.1) are present at several localities within the Garry Lake Complex (unit 1). Northwest-trending, medium- to coarse-grained diabase and gabbro dykes (unit 11) related to the Mackenzie swarm intrude the basement complex and the cover rocks. They show a pronounced magnetic expression on the aeromagnetic Map 7870G (Geological Survey of Canada, 1974).

FAULTS AND SHEAR ZONES

Several northeast trending cataclastic and mylonitic zones, and northwest trending brittle faults affect both the basement and the cover rocks. The Chantrey Mylonite Zone, a segment of the Slave Chantrey Mylonite Zone (Heywood and Schau, 1978), is coincident with a pronounced linear aeromagnetic anomaly (Geological Survey of Canada, 1974). Bedrock exposure is rather poor along the length of the zone, but scattered outcrops that show well defined ductile and brittle deformation textures can be linked by the linear geophysical expression of the zone. Where exposed, the zone has a minimum thickness of 100-150 m and appears to have been derived from a dominantly granitoid protolith (unit 4).

Progressive transformation of granite into mylonite can be demonstrated at two localities – one 15 km northwest of Sand Lake, and the other approximately 30 km west of Deep Rose Lake. The mylonitic foliation, which is defined by elongate quartz ribbons, wraps around K-feldspar augens (Fig. 43.10). A penetrative mineral stretching lineation (quartz and feldspar rodding) is consistently present throughout the length of the mylonite zone. The lineation plunges shallowly (2-20°) to the southwest, although local reversals to the northeast are noted in a few localities. Crosscutting breccia zones, some characterized by locally generated pseudotachylite fractions (Fig. 43.11), have also been noted. Kinematic markers (mostly rotated feldspar grains in the planes of fabric) indicate apparent dextral and sinistral senses of displacement along the zone, suggesting a complex tectonic history. Other shear zones in the region are shown to have had multiple displacement histories (Tella and Heywood, 1978; Tella et al., 1983). Although no marker horizons are present to determine the nature and cumulative displacements along the Chantrey Mylonite Zone, kinematic indicators and subhorizontal to shallow plunging lineations suggest that, at least, the latest movement on the zone was one of low angle oblique-slip.

The Slave-Chantrey Mylonite Zone was postulated to represent a fundamental crustal break that separates deeper level Queen Maud Block (granulite grade) in the northwest from intermediate to higher level Committee Bay Block (amphibolite to greenschist grade) in the southeast (Heywood and Schau, 1978). The field data from the Deep Rose Lake area are insufficient at present to substantiate such a statement. Middle to upper amphibolite grade (unit 1) rocks are exposed northwest of the Chantrey Mylonite Zone in contrast to greenschist facies rocks within and southeast of the zone. If the difference in metamorphic grade is taken to represent different levels of juxtaposed crust, then the shallow oblique-slip displacements together with consistent southwest plunging stretching lineations suggest that rocks northwest of the Mylonite Zone were uplifted relative to those in the southeast with an apparent dextral sense of displacement. Implicit in this statement is an assumption of simple-shear model. Petrofabric studies are being undertaken at selected localities in an attempt to better define the tectonic history of the zone and its regional significance.

REFERENCES

Donaldson, J.A.
1965: The Dubawnt Group, Districts of Keewatin and Mackenzie; Geological Survey of Canada, Paper 64-20.

1969: Descriptive notes (with particular reference to the Late Proterozoic Dubawnt Group) to accompany a geological map of central Thelon Plain, Districts of Keewatin and Mackenzie (65M, NW1/2, 66B,C,D, 75P, E1/2); Geological Survey of Canada, Paper 68-49, 4 p., Map 16-1968.

Frisch, T. and Patterson, J.G.
1983: Preliminary account of the geology of the Montresor River area, District of Keewatin; in Current Research, Part A, Geological Survey of Canada, Paper 83-1A.

Geological Survey of Canada
1974: Deep Rose Lake; Geophysical Series (Aeromagnetic) Map 7870G.

Heywood, W.W.
1961: Geological notes, northern District of Keewatin; Geological Survey of Canada, Paper 61-18, 9 p.

Heywood, W.W. and Schau, M.
1978: A subdivision of the northern Churchill Structural Province; in Current Research, Part A, Geological Survey of Canada, Paper 78-1A, p. 139-142.

LeCheminant, A.N., Ashton, K.E., Chiarenzelli, J., Donaldson, J.A., Best, M.A., Tella, S., and Thompson, D.L.
1983: Geology of Aberdeen Lake map area, District of Keewatin: preliminary report; in Current Research, Part A, Geological Survey of Canada, Paper 83-1A, p. 437-448.

Tella, S. and Heywood, W.W.
1978: The structural history of the Amer mylonite zone, Churchill Structural Province, District of Keewatin; in Current Research, Part C, Geological Survey of Canada, Paper 78-1C, p. 79-88.

Tella, S., Ashton, K.E., Thompson, D.L., and Miller, A.R.
1983: Geology of the Deep Rose Lake Map area, District of Keewatin; in Current Research, Part A, Geological Survey of Canada, Paper 83-1A, p. 403-409.

Wright, G.M.
1955: Geological notes on central District of Keewatin; Geological Survey of Canada, Paper 55-17.

1967: Geology of the southeastern barren grounds, parts of the Districts of Mackenzie and Keewatin (Operation Keewatin, Baker, Thelon); Geological Survey of Canada, Memoir 350.

44. SLOCAN LAKE FAULT: A LOW ANGLE FAULT ZONE BOUNDING THE VALHALLA GNEISS COMPLEX, NELSON MAP AREA, SOUTHERN BRITISH COLUMBIA

Project 830006

Randy Parrish
Precambrian Geology Division

Parrish, R., Slocan Lake fault: a low angle fault zone bounding the Valhalla gneiss complex, Nelson map area, southern British Columbia; in Current Research, Part A, Geological Survey of Canada, Paper 84-1A, p. 323-330, 1984.

Abstract

The Valhalla gneiss complex contains deformed high-grade metasedimentary rocks and granitoid units, some of which are as young as 63.5 Ma. Strain and related mylonitic foliation and east-west stretching lineation are well developed on the east side of the complex structurally beneath the moderately east-dipping, northerly trending Slocan Lake fault. This fault juxtaposes ductilely deformed and retrograded lower plate granitoid units against brecciated, fractured, and hydrothermally altered rocks of the Jurassic Nelson batholith of the upper plate. Preliminary field and geochronological data suggest that some of this ductile strain and faulting is as young as earliest Tertiary, although geochronologic investigations have yet to be completed. Some of the deformation is considerably older. The fault zone is exposed along the southeastern shore of Slocan Lake, and probably dies out to the north. It probably joins the Champion Lakes fault south of Castlegar. Fabrics in the ductile shear zone indicate that displacement is upper plate to the east.

Résumé

Le complexe de gneiss de Valhalla comprend des roches métasédimentaires et des unités granitoïdes déformées et fortement métamorphisées dont certaines datent de seulement 63,5 m.a. La foliation due à la déformation et la foliation mylonitique associée, ainsi qu'une linéation d'étirement à direction est-ouest sont bien développées sur le côté est du complexe, sous la faille de Slocan Lake à orientation nord et à faible pendage vers l'est. Cette faille juxtapose les unités granitoïdes de la plaque inférieure, qui ont subi une déformation ductile et un métamorphisme régressif, et les roches bréchifiées et fracturées du batholite jurassique de Nelson de la plaque supérieure, qui ont subi une altération hydrothermale. Les données provisoires recueillies sur le terrain et les données géochronologiques semblent indiquer qu'une partie de la déformation ductile et des failles date du Tertiaire le plus ancien, bien que les études géochronologiques ne soient pas encore achevées. Une partie de la déformation est beaucoup plus ancienne. La zone de faille affleure le long du rivage sud-est du lac Slocan et se termine peut-être vers le nord. Elle rejoint vraisemblablement la faille des lacs Champion au sud de Castlegar. La texture et la structure dans la zone de cisaillement ductile indiquent qu'il y a eu déplacement vers l'est de la plaque supérieure.

INTRODUCTION

The Vahalla gneiss complex, named by Reesor (1965) for gneissic rocks of the Valhalla Range, consists of a variety of foliated granitoid rocks similar in composition to the Nelson batholith directly to the east (Fig. 44.1). Little (1960) considered it part of the batholith but distinguished differing granite types. He and Ross and Kellerhals (1968) also noted a mylonite band extending along the east side of Slocan Lake on a distinctive topographic ledge.

The distinction between the gneisses to the west and the batholith to the east of this structural zone was emphasized by Ross and Kellerhalls (1968) who suggested a Precambrian age for the gneisses. The geochronological recognition of Precambrian basement rocks in Thor-Odin and Frenchman Cap areas (Wanless and Reesor, 1975; Duncan, 1978) and their structural interpretation as a series of large basement-cored nappes (I.J. Duncan, personal communication, 1977; Brown, 1978) suggested that these gneiss complexes were not the result of diapirism as originally suggested by Reesor (1965). Meanwhile, interpretation of "core complexes" as Tertiary plutonic diapirs and/or crustal-scale mega-boudins has become well established for many areas of similar geology in western United States (Coney, 1980). Although late metamorphic low-angle bounding faults are distinctive features of many "core complexes", their interpretation as either extensional listric normal faults or folded compressional décollements is not always clearcut.

The Valhalla complex is clearly bounded on the east by one of these faults, and this paper describes the lithologies and structure of this complex fault zone as a basis for interpreting existing and future geochronologic data on the rocks involved.

GENERALIZED STRUCTURE

The Valhalla complex comprises the lower plate of the Slocan Lake fault (Parrish, 1981), consisting of low-dipping plutonic and metasedimentary rocks disposed in sheets up to 2 km thick. These dip outward from two domal culminations, the Valhalla dome west of Slocan, and the subordinate Passmore dome near Passmore (Fig. 44.1). Along the east margin of the complex a ductile shear zone affects many, if not all, lower plate units. A brittle detachment, with related development of breccia and other altered fault rocks, overlies the ductilely deformed rocks and marks the transition to undeformed, but altered upper plate rocks of the Nelson batholith. The foliation in lower plate rocks adjacent to the brittle fault dips east 30-40° (Fig. 44.2); the brittle fault zone also dips moderately eastwards. Its precise dip is difficult to determine because of poor outcrop, although it is considered to be the same as the foliation. No rocks have been observed to cut either the fault zone or the ductile fabric in the lower plate. The age of this faulting and the age of some of the penetrative fabric in lower plate rocks most likely postdates the emplacement of the youngest granitoid rocks of the gneissic complex.

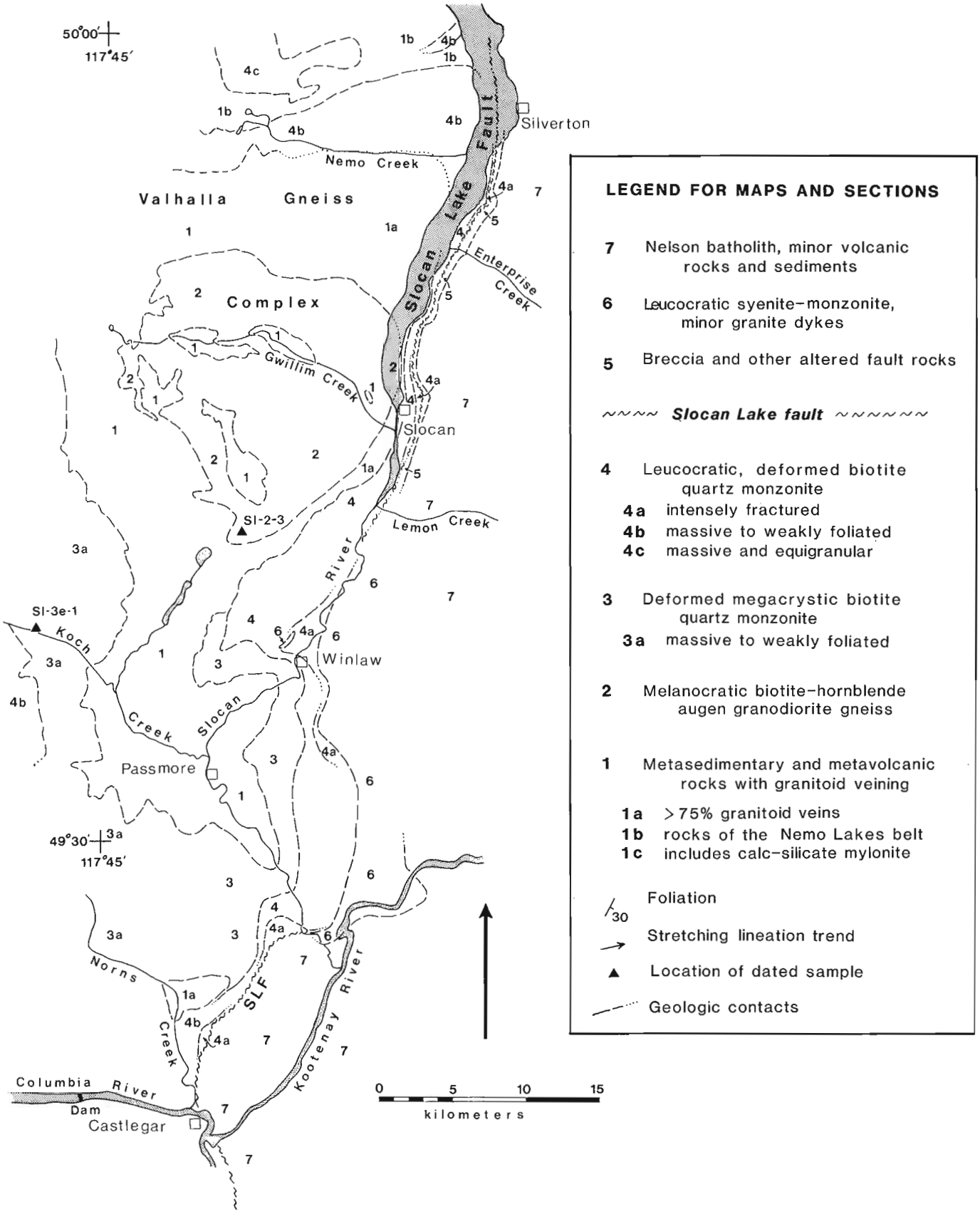

Figure 44.1. *Part of the northwestern Nelson west half map-area; legend also applies to Figure 44.2 and Figure 44.8. Locations of dated samples are shown by filled triangles. Geology of the Valhalla dome is modified from Reesor (1965).*

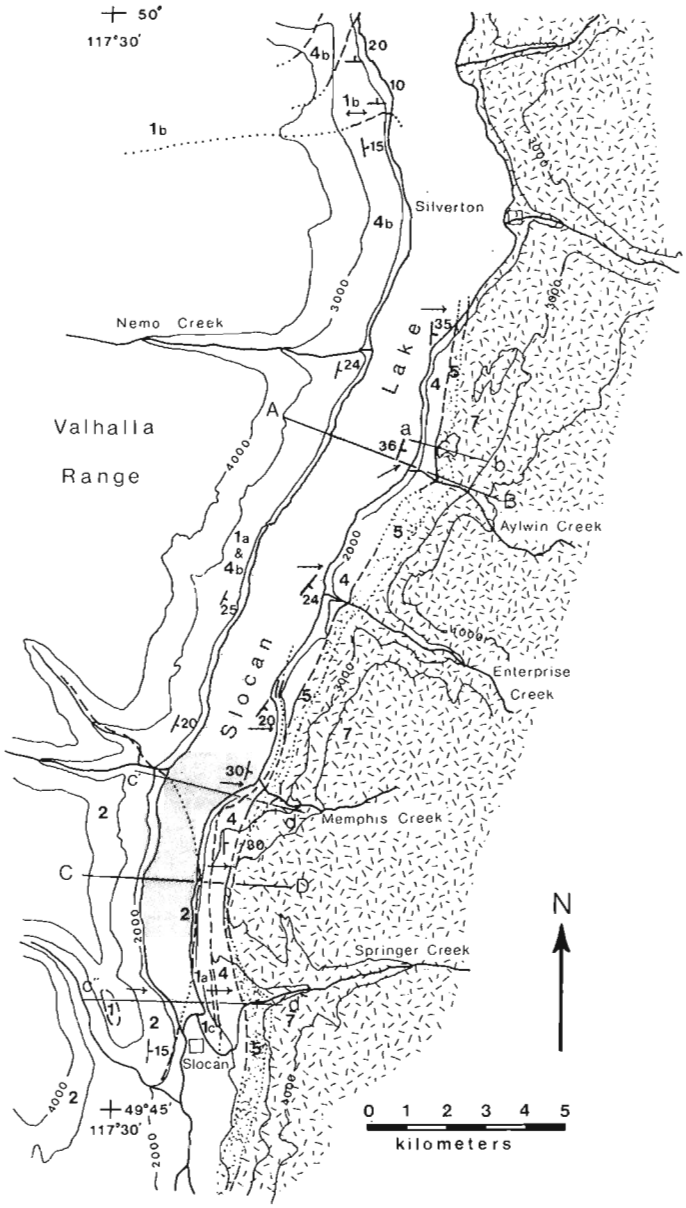

Figure 44.2. Detailed geological map of southern Slocan Lake. Subdivision of unit 4 is not shown here. The contact between units 4 and 5 is the Slocan Lake fault. Lineation symbols refer to trends of extensional lineations, and foliation symbols are those of granitoid rocks. See Figure 44.1 for legend.

Lithologic units (order does not imply relative age)

Metasedimentary and metavolcanic rocks (1)

Pelitic, calcareous, amphibolitic, and quartzo-feldspathic metasedimentary rocks are exposed in several lenses structurally low in the complex and have been described by Reesor (1965) and, on the north side of the dome, by Parrish (1981). These are extensively intruded by leucocratic granitic rocks which in places comprise more than 75 per cent of the volume (map unit 1a). Except in the Nemo Lakes belt on the north side of the dome (map unit 1b), the stratigraphic correlation or order is uncertain. Spectacular scapolite and diopside-bearing porphyroclastic calcareous mylonite (unit 1c) occurs in the ductile shear zone on the east side of the dome and truncates all rocks with which it is in contact. Disrupted sheath folds with curvilinear, predominantly east-trending axes, are common in this highly strained zone.

Veined mafic-rich granodioritic gneiss (2)

A mafic-rich biotite-hornblende K-feldspar-augen granodiorite gneiss with veins of leucocratic gneiss occurs in the core of the complex and has been described by Reesor (1965) and dated at one locality (shown on Fig. 44.1) by Parrish and Ryan (1983) at 89 ± 2 Ma. It occurs in several sheets alternating with rocks of unit 1. It is distinguished in the field from other granitoid units (described below) on the basis of its mafic rich character (see Reesor (1965) for more details).

Foliated K-feldspar-megacrystic biotite quartz monzonite (3)

A very distinctive, biotite (± hornblende) quartz monzonite with large (up to 10 cm) megacrysts of K-feldspar occurs above unit 1 on the southern and southwestern side of Valhalla dome and is particularly well developed near Passmore. On the east side of the Passmore dome, the unit has a well developed foliation with elongate megacrysts lying subparallel or slightly inclined to it (Fig. 44.3). Thin mylonite zones which are paralllel to foliation are occasionally developed within this unit on the east side (Fig. 44.4). The foliation is much less developed to the west where the fabrics are slight and probably igneous in origin (unit 3a). Only in fine grained mylonite is lineation well developed. The inclination of megacrysts to the plane of foliation indicates a top side to the east sense of shear.

Foliated leucocratic biotite quartz monzonite (4)

Unit 4 consists of a well foliated and lineated leucocratic biotite quartz monzonite (Fig. 44.5). The rock has less than 10 per cent biotite and is only slightly porphyritic. It has an extremely consistent fabric and lithology on the east side of the complex. Massive to weakly foliated lithologies of similar compositions (unit 4b) occur on the north side of the Valhalla dome near Nemo Creek, on the south west side near Koch Creek, and north of Castlegar. A strongly fractured and altered version (4a) of this unit (Fig. 44.6) generally lacks biotite and contains porphyroclastic muscovite in a mylonitic matrix. It is exclusively found just beneath or west of brittlely deformed rocks of the fault zone and is equivalent to the crush zone of Reesor (1965, p. 33). Thin (20 cm) bands of very fine grained mylonite were observed near Slocan and pseudotachylite was seen in one locality near Memphis Creek.

Massive biotite quartz monzonite of the Snowslide Creek stock (4c) occurs on the extreme north side of the complex; it intrudes rocks of the high grade Nemo Lakes belt (Parrish, 1981) and may not be related to unit 4 elsewhere.

Breccia and other altered fault zone rocks (5)

The contact between unit 4 and unit 5 is interpreted as a fault. Above the fault unit 5 includes brecciated mylonitic(?) leucogranite, fractured, and brecciated plutonic rocks of the Nelson batholith, and altered polymictic volcanic breccia. No consistent fabric is present in these rocks, and most have experienced intense fracturing and lower greenschist facies hydrothermal alteration. The massive porphyritic granitoid texture, easily discernable in most cases, is similar to undeformed, unaltered Nelson batholith rocks farther east.

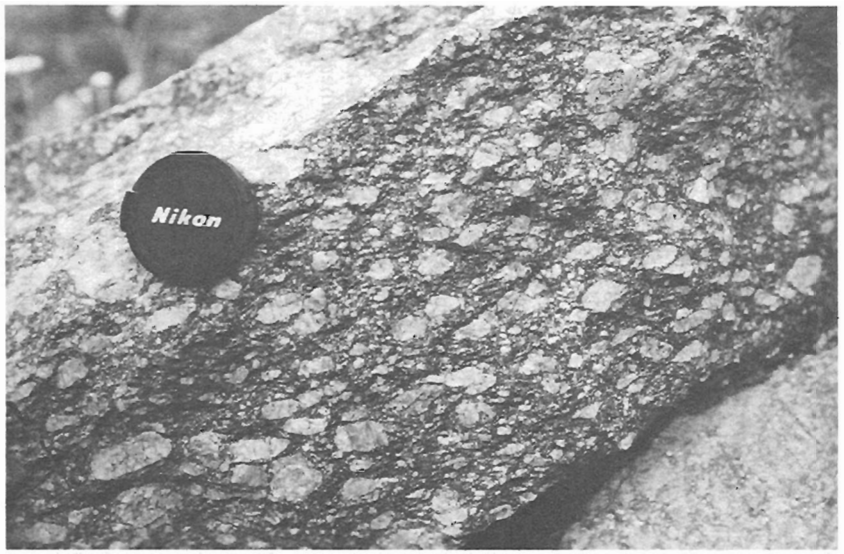

Figure 44.3. *Photograph, looking south, of megacrystic quartz monzonite of unit 3 south of Winlaw. The shear plane bounds the upper surface of the rock dips from right to left moderately. Most megacrysts dip less steeply and indicate top side down to the left (east) as the sense of shear.*

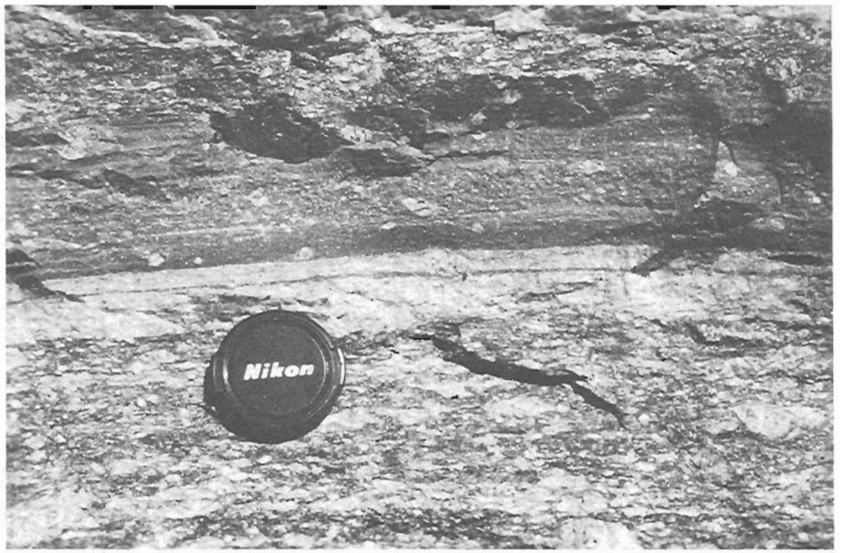

Figure 44.4. *Mylonitic band within unit 3 between Passmore and Castlegar near the mouth of Goose Creek. Lineation is much better developed within the mylonite than in adjacent layers. Note augen of former megacrysts.*

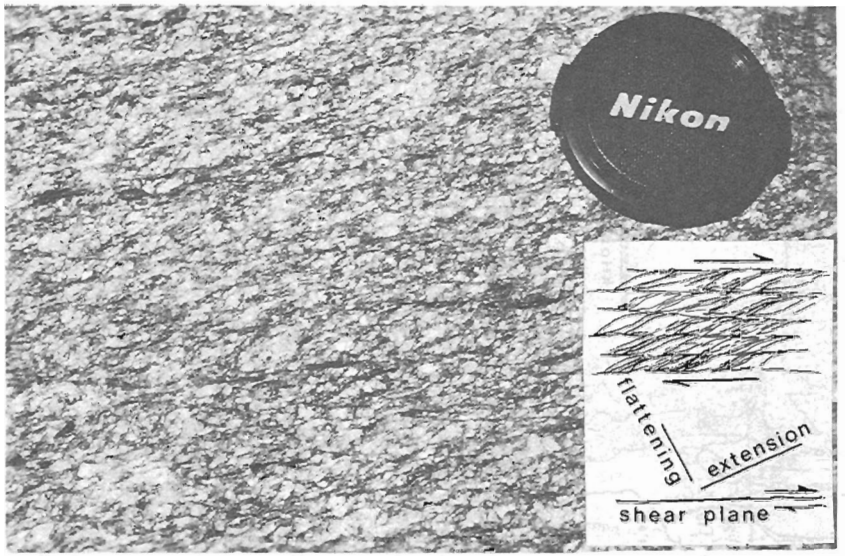

Figure 44.5. *Photograph, looking northwards, of deformed leucocratic quartz monzonite (unit 4) showing both the homogeneous lithology and fabric indicating transport as shown. Inset is based on the work of Berthe et al., 1979.*

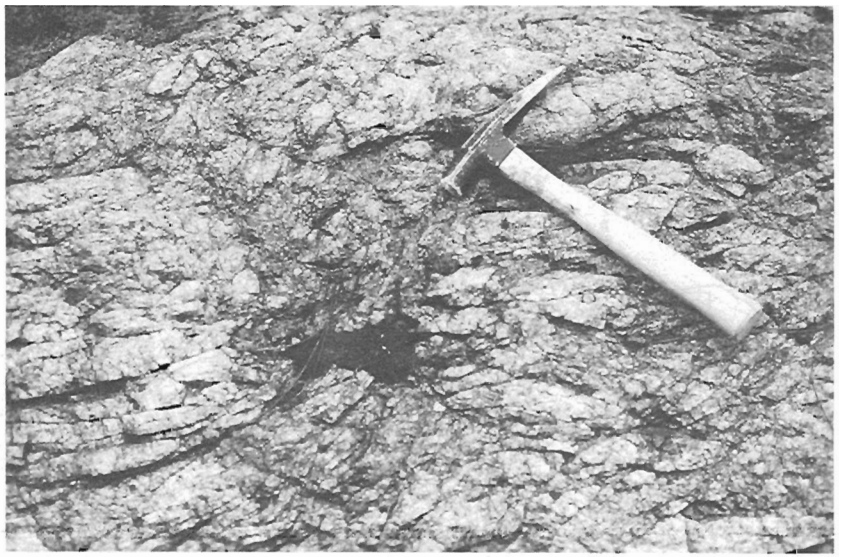

Figure 44.6. *Fractured and folded unit 4a 5 km north of Castlegar.*

Leucocratic syenite-monzonite (6)

A distinctive, foliated leucocratic pyroxene and/or hornblende-bearing syenite or monzonite occurs along the eastern side of the complex between Lemon Creek and Kootenay River (Fig. 44.1). It was recognized by Little (1960) and Reesor (1965) although their interpretations differed. Little viewed it, as well as gneissic rocks of the Valhalla Range, as part of the Nelson intrusions of Jurassic age; Reesor concluded that it was one of the latest intrusions in the Valhalla complex as it did not possess the penetrative fabric common to the gneisses. Actual contacts have not been observed, and nowhere have dykes of this material been seen to intrude other rocks. Consequently its relation to the fault is not clear. Its western boundary is along the projected extension of the fault, suggesting a fault relationship, although texturally the rock is not as altered as structurally equivalent granitic rocks of the upper plate. Crosscutting, unaltered, and undeformed granitic dykes cut the unit, although they are minor in volume. The foliation in this unit is clearly igneous in origin.

Nelson batholith and related rocks (7)

A lack of penetrative fabric distinguishes plutonic rocks of the Nelson batholith from gneisses of the lower plate. Although not studied in detail, this unit includes megacrystic and porphyritic granitoids, quartz-feldspar porphyries and hypabyssal rocks, as well as minor volcaniclastic rocks of generally low metamorphic grade, similar to metasedimentary pendants within the batholith. The Slocan Group north of Silverton and east of Slocan Lake would also be included as an upper plate lithology.

Relationships between units

The structural sequence described here can be thought of as a series of somewhat discontinuous layers. Unit 3 is either very thin, structurally or intrusively truncated, or absent northeast of Winlaw along the fault zone (Fig. 44.1, 44.2), but is very well developed to the south. Where the syenite-monzonite of unit 6 is in contact with unit 4, unit 5 was not observed. Five kilometres south of Winlaw, unit 4 contains large, apparently randomly oriented muscovite porphyroblasts near the contact with unit 6. These may be related to contact metamorphism from unit 6; however, the possibility that unit 6 is in fault contact with the gneiss complex is still open. Near Koch Creek on the west side of the dome, units 3 and 4 are massive to weakly foliated. Five kilometres north of Castlegar, metasediments are overlain by a thin unit 3 and a weakly foliated unit 4. Either unit 3 becomes non-megacrystic to the south (in which case it would closely resemble unit 4) or it thins, being replaced by unit 4. The age relationships of the two are unknown.

Dip of the fault

Based on structural and metamorphic arguments, the Slocan Lake fault was postulated for northern Slocan Lake by Parrish (1981) It was thought to be the same feature as a steep fault mapped northeast of Slocan by Reesor (1965). Detailed mapping (Fig. 44.2) has shown that the fault separates ductilely deformed gneisses from brittlely deformed plutonic rocks of the Nelson batholith. The fault zone emerges on land 3-4 km south of Silverton and winds irregularly along a distinctive topographic ledge on the east shore of Slocan Lake (Fig. 44.7). All of the creeks which cross the fault have been mapped, and deflections in the fault trace can be documented, especially near Aylwin and Enterprise creeks and on a high topographic ridge between Memphis and Springer creeks.

Regular changes of strike of gneissic foliation cause geological contacts to deflect eastward north of Memphis Creek. An eastward dip of the fault zone is required unless irregular changes of fault strike are invoked. Assuming that fault strike changes sympathetically with the strike of foliation in the gneisses, orthogonal cross-sections have been constructed (Fig. 44.8) along lines A-B and C-D with subsidiary sections a-b, c'-d', and c"-d", shown in Figure 44.2. The contacts between units 1a and 4, and between 4 and 5 are sharp and mappable at this scale, especially in transverse creeks. The boundary between units 5 and 7 is somewhat arbitrary and cannot be considered firm, at least for the purposes of dip determinations.

Both sections in Figure 44.8 require both gneissic units, their foliations, and the contact between units 4 and 5 (the Slocan Lake fault) to dip moderately east about 30-40°, given the previous assumptions. A much shallower dip is precluded by mapping constraints, but changes in the strike of the fault would allow the dip to approach 60° east for some localities. During this study no significant evidence was found to support the existence of a steep fault truncating the gently eastward dipping fabric of the gneisses, as was suggested by Reesor (1965) and Ross and Kellerhals (1968).

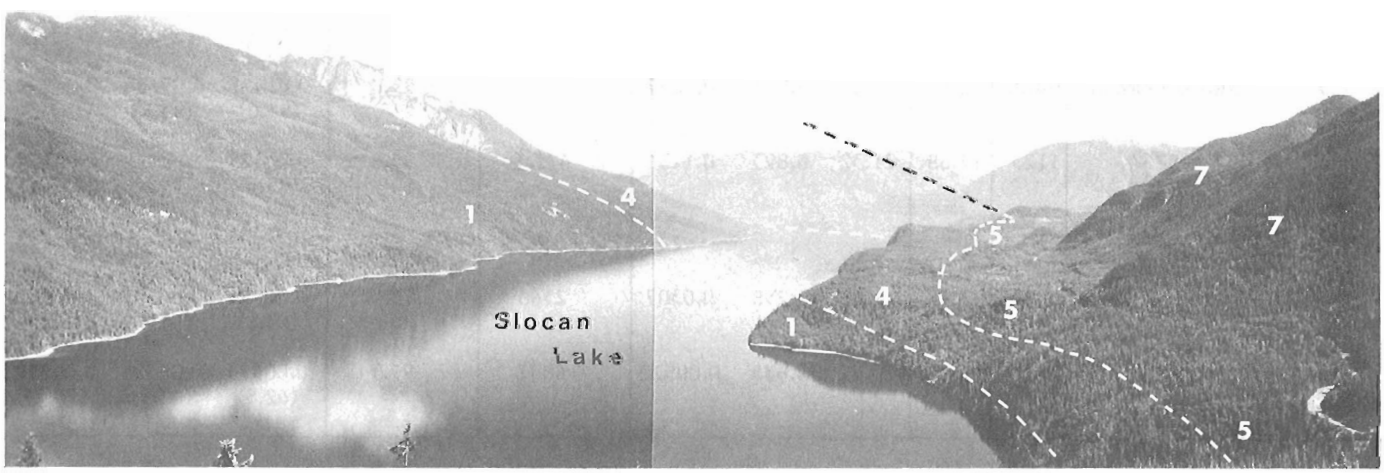

Figure 44.7. *North-looking photograph of the Slocan Lake Valley from the ridge between Memphis and Springer creeks. White dashed line is the surface trace of Slocan Lake fault; black dashed line is the fault projected into the air to the west. Steep slopes to the east are Nelson batholith unit 7. Unit 5 is largely present in the topographically recessive ledge.*

It should be emphasized that no fabric element was observed in the fault zone rocks of unit 5 or of fractured unit 4a to indicate the movement sense of the brittle fault.

Shear sense of the ductile shear zone

The fabric of units 1-4 was studied to ascertain the sense of shear in these ductilely deformed rocks. The method used was to observe the sense of asymmetry of inclined, rotated elongate feldspar crystals and quartz ribbon grains in rocks of mica-poor composition. As illustrated in Figure 44.5, progressive shear strain causes flattening and extension of quartz and feldspar at angles to the plane of shear (Berthe et al., 1979). The plane of shear in unit 4 contains a well developed lineation, and a sigmoidal mica foliation wraps around feldspars and merges with the plane of shear. This fabric is distinctive in unit 4 and very homogeneous in development. The overwhelming sense of shear observed is upper rocks down to the east, as shown in Figure 44.4 and 44.5. The lineation is an extension lineation and is accompanied by extension fractures in feldspar and related mineral elongation. Its trend is approximately 090°. This 090° direction is the direction of transport of upper relative to lower rocks in the ductile shear zone and is shown on Figure 44.8.

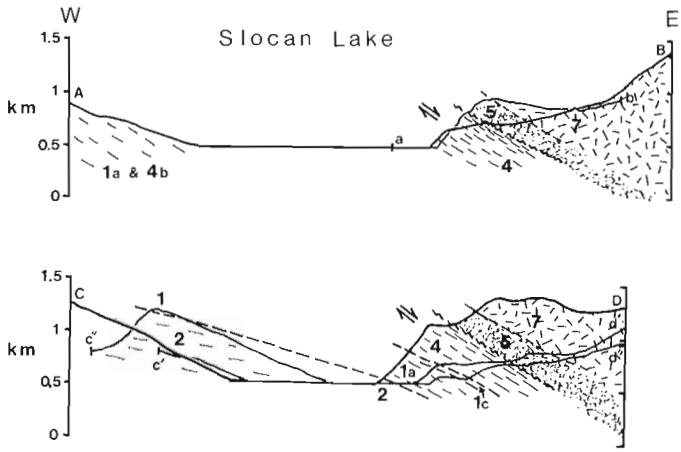

Figure 44.8. *North-looking cross-sections along lines shown in Figure 44.2. See Figure 44.1 for legend. Unit 4a is grouped into Unit 4.*

The fabric of unit 3 was occasionally useful for shear sense determination as shown in Figure 44.3, and unambiguous determinations were nearly all top down to the east, the same as determined in unit 4. The metamorphic grade during the most recent faulting and ductile deformation was probably greenschist as biotite was stable but apparently hornblende was not. Quartz (± chlorite, pyrite) is the predominant mineral occupying extension fractures in feldspar.

Because sillimanite and other high temperature minerals are well preserved in unit 1 near Passmore and elsewhere beneath unit 3, the retrogression which accompanied the ductile deformation was superimposed upon a pre-existing high grade metamorphic fabric. That there

Table 44.4. U-Pb data for zircons from Valhalla gneiss complex

Analysis*	Fraction	U (ppm)	Pb (ppm)	Isotopic Abundances** $^{206}Pb = 100$			$\frac{^{206}Pb}{^{204}Pb}$ meas.	% Radiogenic Pb	Ratios and (Ages)*** $\frac{^{206}Pb}{^{238}U}$	$\frac{^{207}Pb}{^{235}U}$	$\frac{^{207}Pb}{^{206}Pb}$
				^{208}Pb	^{207}Pb	^{204}Pb					
SL-2-3 (Unit 2), location: 49°41'18"N, 117°37'30"W											
1	+200	775.5	12.22	19.20	5.955	0.0698	1242	95.9	0.01443 (92.4)	0.09806 (95.0)	0.04927 (160.9)
2	+200 Mag	795.8	12.21	17.93	5.321	0.0306	1246	98.2	0.1439 (92.1)	0.09661 (93.6)	0.04871 (133.7)
3	200-325 NMag	840.8	12.70	15.80	5.943	0.0697	1032	95.8	0.01422 (91.0)	0.09644 (93.5)	0.04918 (156.2)
4	-325	1123	17.68	21.32	6.893	0.1156	671.1	93.0	0.01395 (89.3)	0.1000 (96.8)	0.05199 (285.1)
SL-3e-1 (Unit 3a), location: 49°37'30"N, 117°49'20"W											
5	+200 NMag	1337	13.37	11.00	5.258	0.0307	2566	98.0	0.00994 (63.8)	0.06587 (64.8)	0.04807 (102.5)
6	100-200	1325	12.86	10.92	4.835	0.00512	6837	99.7	0.00973 (62.5)	0.06388 (62.9)	0.04759 (79.1)

* Analyses performed at geochronology laboratory, University of British Columbia.
** Corrected for blank with composition = 8/4, 37.0; 7/4, 15.54; 6/4, 17.75.
*** Isotopic composition of common Pb based on 95 Ma and 65 Ma Pb age derived from the model of Stacey and Kramers (1975).
$\lambda_{238} = 0.155125 \times 10^{-9}$/yr, $\lambda_{235} = 0.98485 \times 10^{-9}$/yr, $^{238}U/^{235}U = 137.88$

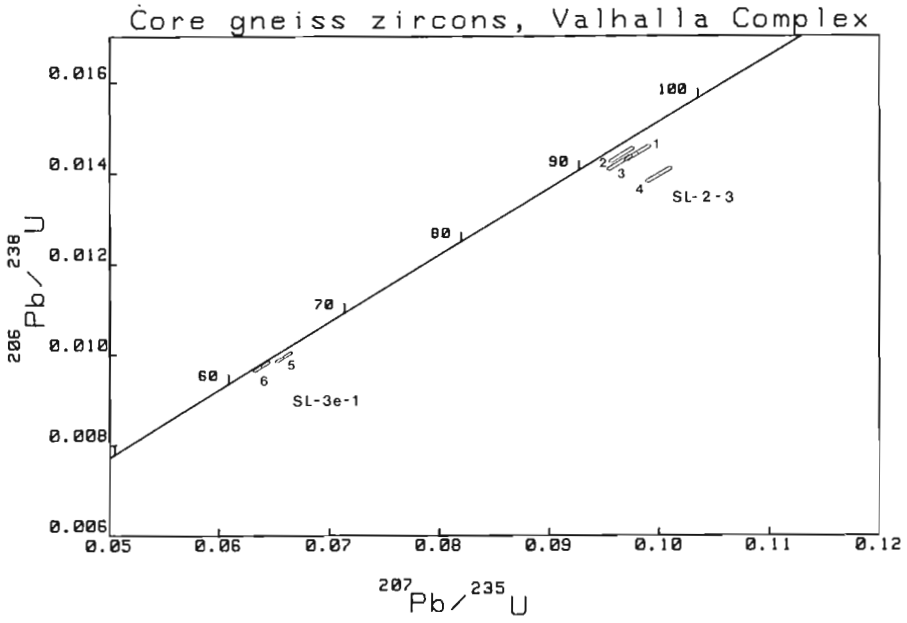

Figure 44.9

U-Pb concordia diagram for zircons from samples SL-2-3 and SL-3e-1. Analytical methods are similar to those described in Parrish and Wheeler (1983). See Table 1 for analytical data. Errors shown are at two-sigma level (95% confidence).

was a pre-existing metamorphic-deformational history prior to the emplacement and deformation of units 3 and 4 is particularly clear on the west side of the complex. There, shear fabrics in units 3 and 4 are absent, but metasediments as well as unit 2 are highly strained, recording a previously existing, probably earlier Mesozoic, deformational history. A similar argument for older metamorphism and deformation has been made for the Nemo Lakes belt on the north side of the complex (Parrish, 1981).

The relationship of brittle faulting to ductile deformation is problematic as it is difficult to prove a relationship between the two. Supportive of a relationship is the close spatial relation between well developed, down to the east ductile fabric in units 3, 4 and brecciated unit 4a and the brittle fault. Also, the lack of such ductile and brittle features to the west suggests that the fault does not conform to the shape of the dome. These fabrics (ductile and brittle) are only weakly developed to the south just north of Castlegar (Fig. 44.1), but they do remain related in both space and intensity. There seems to be a correlation between development of this fabric, strain across the fault zone, and structural relief of the domes directly to the west, all of which are apparently at their maximum in the vicinity of Slocan. Significantly, the ductile and brittle features can be strongly argued to have similar orientation.

Continuation of the fault

The continuation of the fault to the south and north bears significantly upon its tectonic significance. Parrish (1981) suggested that the fault continues out the northern end of Slocan Lake and terminates within the Slocan Group. A re-examination of exposures of rocks on the northwest shore of Slocan Lake has revealed no new information to alter the author's previous interpretation. Weakly foliated granitoid rocks near Nemo Creek pass northwards along the lakeshore into a high-grade metamorphic belt and then abruptly into the undeformed Wragge Creek pluton. On the north side of the pluton are Slocan Group slates of biotite grade or lower. The pluton imparts a contact aureole on these rocks, and andalusite is well developed in places. Continuing the fault within or directly on either side of this pluton seems unlikely.

To the south, both ductile fabric and brittely deformed fault zone rocks are considerably less developed, although fractured rocks of unit 4a confidently indicate the trace of the fault. The fault then joins the Champion Lakes fault of Simony (1979) and Little (1982) and continues as a moderately east dipping fault zone into the Trail pluton (C. Corbett and P. Simony, personal communication, Sept. 1983). It is considered a relatively high level, brittle feature south of Castlegar. There is therefore no evidence that this fault zone diverges significantly from a predominantly north-south trend; analogies to the Monashee décollement of Read and Brown (1981), an arched décollement of predominantly Mesozoic age, are therefore inappropriate on the basis of present data, despite their considerable similarity. If the fault does die out to the north (north of Slocan Lake) and south (south of Trail), then it suggests that total displacement is not large, perhaps several kilometres, but not tens of kilometres.

GEOCHRONOLOGY

Two units have been dated by U-Pb methods on zircon, the preliminary results having been previously summarized by Parrish and Ryan (1983). Sample SL-2-3, from the veined gneiss of Reesor (1965) – unit 2 of this report, is a mafic-rich hornblende-biotite K-feldspar augen granodiorite (see Fig. 44.1 for location). The zircons are from the mafic-rich part, not from the later leucocratic veins. The rock is highly strained but not mylonitic. The analytic data are listed in Table 44.1. Previous K-Ar dates from this locality, cited in Wanless et al., 1978, 1979 are 52.2 ± 2.5 for biotite (recalculated with new constants) and 55.5 ± 2.9 Ma for hornblende. U-Pb dates vary from 89-97 Ma and, when plotted on a conventional concordia diagram of Figure 44.9, show a small amount of inherited zircon Pb of presumed Precambrian age. Projected from a wide range (1 Ga-3 Ga) of upper intercept ages, the most reasonable lower intercept age through the main data is 89 ± 3 Ma, considered the age of crystallization of the mafic-rich part of unit 2 at this locale. Analytical problems related to inhomogeneities in sample aliquots have probably contributed to the scatter in the data.

Sample SL-3e-1, from unit 3 where it is only slightly foliated near Koch Creek (Fig. 44.1), is a biotite-hornblende K-feldspar megacrystic quartz monzonite. U-Pb zircon determinations are virtually concordant at 63.5 ± 1 Ma, considered to be the age of emplacement at this locality. Because this rock does not contain the fabric previously described in unit 4 and shown in both Figures 44.3 and 44.5, it cannot be proven that the ductile deformation is less than 63.5 Ma old, despite the implication of this field summary. Further geochronological work is in progress on units 2, 3, 4, 6 as well as several plutons to the north of the complex to place tighter constraints on the age of rocks and deformation. These plutons include the Snowslide Creek stock, the Ruby Range stock, the Wragge Creek stock, and the Whatshan Batholith.

TECTONIC SUMMARY

Lithologic units and structural relationships have been described indicating the presence of a ductile shear zone developed in metaplutonic rocks, some of which may be earliest Tertiary in age. A brittle fault zone was developed structurally above, and probably during at least some of the ductile deformation. The sense of shear, as determined by asymmetric fabric in mylonitic rocks of units 3 and 4, is consistently top down to the east, and the east-west lineation is a direction of extensional strain. The most recent faulting and ductile deformation was accompanied by greenschist conditions. The fault extends from the north end of Slocan Lake to at least Castlegar, a distance of over 100 km, and it maintains its predominantly north-south trend throughout its extent. Because it is considered to terminate north of Slocan Lake and south of Trail, without changing trend, it is not considered a folded décollement; as such its displacement is likely several, but not tens of kilometres. It is probably not related to the older and different Monashee décollement to the northwest described by Read and Brown (1981).

Plutonism may have been directly related to the development of the shear and/or fault zones by providing a diapiric bouyancy for the rise and east-west extension of the dome and the partial collapse of upper plate rocks. This would imply a temporal relationship between the two, as yet unproven. In this interpretation, the lower plate rocks may have been emplaced upwards and towards the west in a regional east-west extending tectonic environment. Alternatively, if the plutons are unrelated to the faulting, then the origin and mechanisms of deformation are less clear. Further geochronological studies, presently in progress, are needed to shed light on this complex and interesting problem.

ACKNOWLEDGMENTS

I thank R.L. Brown and L.B. Chorlton, both of Carleton University, for stimulating discussions of field relationships, mylonites, and regional geological comparisons during the course of field work. Barry Ryan was responsible for some of the U-Pb analyses presented.

REFERENCES

Berthe, D., Choukroune, P., and Jegouzo, P.
1979: Orthogneiss, mylonite, and non-coaxial deformation of granites: the example of the South Armorican shear zone; Journal of Structural Geology, v. 1, p. 31-42.

Brown, R.L.
1978: Structural evolution of the southeast Canadian Cordillera: A new hypothesis; Tectonophysics, v. 48, p. 133-151.

Coney, P.J.
1980: Cordilleran metamorphic core complexes: An overview; in Cordilleran metamorphic core complexes, ed. M.D. Crittenden, Jr., P.J. Coney and G.H. Davis; Geological Society of America Memoir 153, p. 7-34.

Duncan, I.J.
1978: Rb/Sr whole rock evidence for three Precambrian events in the Shuswap Complex, southeast British Columbia; Abstracts with programs, Geological Society of America, v. 10, p. 392-393.

Little, H.W.
1960: Nelson map-area, west half, British Columbia (82F W 1/2); Geological Survey of Canada, Memoir 308, 205 p.

1982: Geology of the Rossland-Trail map-area, British Columbia; Geological Survey of Canada, Paper 79-26, 38 p.

Parrish, R.R.
1981: Geology of the Nemo Lakes belt, northern Valhalla Range, southeast British Columbia; Canadian Journal of Earth Sciences, v. 18, no. 5, p. 944-958.

Parrish, R. and Ryan, B.
1983: Pb-U zircon dates reflecting late Cretaceous-early Tertiary plutonism, deformation, and isotopic resetting, Valhalla complex, southeast British Columbia; Geological Association of Canada, Program with Abstracts, v. 8, p. A53.

Parrish, R. and Wheeler, J.O.
1983: A U-Pb zircon age of the Kuskanax batholith, southeastern British Columbia; Canadian Journal of Earth Sciences v. 20, p. 1751-1756.

Read, P.B. and Brown, R.L.
1981: Columbia River fault zone: southeastern margin of the Shuswap and Monashee complexes, southern British Columbia; Canadian Journal of Earth Sciences, v. 18, p. 1127-1145.

Reesor, J.E.
1965: Structural evolution and plutonism in Valhalla gneiss complex, British Columbia; Geological Survey of Canada, Bulletin 129, 128 p.

Ross, J.V. and Kellerhals, P.
1968: Evolution of the Slocan syncline in south-central British Columbia; Canadian Journal of Earth Sciences, v. 5, p. 851-872.

Simony, P.S.
1979: Pre-Carboniferous basement near Trail, British Columbia; Canadian Journal of Earth Sciences, v. 16, p. 1-11.

Stacey, J.S. and Kramers, J.D.
1975: Approximation of terrestrial lead isotope evolution by a two-stage model; Earth and Planetary Science Letters, v. 26, p. 207-221.

Wanless, R.K. and Reesor, J.E.
1975: Precambrian zircon age of orthogneiss in the Shuswap metamorphic complex, British Columbia; Canadian Journal of Earth Sciences, v. 12, p. 326-332.

Wanless, R.K., Stevens, R.D., Lachance, G.R., and Delabio, R.N.
1978: Age determinations and geological studies, K-Ar isotopic ages, Report 13; Geological Survey of Canada, Paper 77-2.

1979: Age determination and geological studies, K-Ar isotopic ages, Report 14; Geological Survey of Canada, Paper 79-2.

45. RUTLEDGE LAKE, NORTHWEST TERRITORIES; A SECTION ACROSS A SHEAR BELT WITHIN THE CHURCHILL PROVINCE

Project 800009

N.G. Culshaw
Precambrian Geology Division

Culshaw, N.G., Rutledge Lake, Northwest Territories; a section across a shear belt within the Churchill Province; in Current Research, Part A, Geological Survey of Canada, Paper 84-1A, p. 331-338, 1984.

Abstract

Rutledge Lake affords a section across a steeply dipping gneiss belt which is coincident with part of a north-south trending tectonic zone of regional extent. Within the zone a long history of transcurrent shear and uplift was accompanied both by high grade metamorphism in the west (low to medium pressure granulite facies) and subsequent low grade mylonitization in the east. During the low grade episode extension parallel to the zone within the high grade western segment was accomplished by movement on small, discordant and steeply dipping retrograde shear zones and along large scale faults.

The gneisses themselves are composed of two compositionally distinct metasedimentary units and several granitoid components, including an S-type granite and a charnockitic gneiss. If the postulate is accepted that small mafic and ultramafic bodies are deformed dykes, then, since they are restricted in occurrence to certain units, the gneiss belt may be divided on a time basis. The oldest lithologies are therefore the units in which the ultramafic bodies occur, charnockitic gneiss and a greywacke-shale derived paragneiss. Since Cu mineralization is associated with these mafic and ultramafic bodies, exploration should be targeted at these host lithologies.

Résumé

Le lac Rutledge présente une section en travers d'une zone de gneiss à pendage abrupt qui coincide avec une partie d'une zone tectonique régionale orientée nord-sud. Au sein de la zone, une longue histoire de cisaillement transversal et de soulèvement a été accompagnée d'un degré élevé de métamorphisme dans l'ouest (faciès à granulites de pression basse à moyenne) et par la suite, d'un faible degré de mylonitisation dans l'est. Durant ce dernier épisode, il y a eu extension parallèle à la zone au sein du segment ouest fortement métamorphisé à la suite de mouvements le long de petites zones discordantes, à fort pendage, de cisaillement régressif et le long de failles importantes.

Les gneiss comportent deux unités métasédimentaires de composition distinctes et plusieurs composantes granitoïdes, notamment un granite de type S et un gneiss à charnockite. Si l'on accepte l'hypothèse voulant que les petites masses mafiques et ultramafiques sont des dykes déformés, puisque ces masses se présentent uniquement dans certaines unités, il sera donc possible de diviser la zone de gneiss en unités chronologiques. Les lithologies les plus anciennes contiennent donc les masses ultramafiques, le gneiss à charnockite et un grauwacke-schiste argileux dérivé d'un paragneiss. Puisque la minéralisation en Cu est associée à ces masses mafiques et ultramafiques, les travaux d'exploration devraient donc se concentrer sur ces lithologies minéralisées.

INTRODUCTION

Rutledge Lake lies within the Churchill structural province some 75 km south of Great Slave Lake (Fig. 45.1) within NTS area 75 E and within the area of GSC magnetic anomaly maps 1566A (1:1 000 000 scale), 1637G and 1638G (1":1 mile scale). The geology of the rocks which underlie the lake is of interest since several copper prospects are situated there. Field work was undertaken for a limited period in June and July (45 days, one mapping crew), sponsored by the Geology Division of Northern Affairs, Yellowknife (DIAND), with support from the Geological Survey of Canada, Precambrian Geology Division. Mapping of the lakeshore geology was carried out at a scale of 1:30 000, with additional foot and airborne reconnaissance traversing of the hinterland of the lake.

Rutledge Lake (Fig. 45.2) is underlain by a complex high grade (low to moderate P granulites) gneiss belt which is composed of several distinct orthogneiss and paragneiss units. The probable oldest paragneiss and a charnockitic orthogneiss are host to small ultramafic and mafic bodies which are tentatively interpreted to be deformed dykes. These ultramafic bodies accompany the copper mineralization. Thus, future exploration should be aimed at the lithologies, which are host to these ultramafic bodies. The lake also exposes a section across a major north-south trending transcurrent crustal shear or tectonic zone. Deformation within this zone took place at both high and lower grade of metamorphism and appears to have migrated eastward with time and declining metamorphic grade. Narrow, discordant zones of retrogression and shearing within the western high grade straight gneisses are interpreted as expressions of wall rock strain during shearing in the lower grade mylonites on the eastern side and may be of use in determining the kinematics of the tectonic zone.

GEOLOGICAL AND TECTONIC SETTING

Although the region surrounding Rutledge Lake has not been mapped for over 45 years (Henderson, 1939), the geology to the south (but north of 60°) is presently being investigated (Bostock, 1982) and the lithological components of paragneiss and granite appear to have much in common with the Rutledge Lake area.

Rutledge Lake is situated on the boundary between north-south trending positive and negative magnetic anomalies (Fig. 45.1). To the south this boundary is coincident with a belt of highly deformed gneisses which include mylonites (Bostock, 1982). At their northern end the anomalies curve northeastward into the wide positive magnetic anomaly marking the Slave-Chantrey Mylonite Zone

(Heywood and Schau, 1978) which lies along the southern shore of the Great Slave Lake (Fig. 45.1). A pair of northerly trending, parallel, positive and negative magnetic anomalies, similar to those at Rutledge Lake, lies to the north of the Slave-Chantrey anomaly. These are apparently offset 150-200 km to the northeast and are generally coincident with the Thelon Tectonic Zone (Thompson and Henderson, 1983). Zones of faulting and "mylonites" roughly identical with or on strike with the tectonic zone and magnetic anomalies of Rutledge Lake figure in recent geological and tectonic studies (Godfrey and Langenberg, 1978; Nielsen et al., 1981; Gibb et al., 1983).

Considering, therefore, the probable regional extent of this tectonic zone and its, as yet uncertain, relationship with both the Slave-Chantrey Mylonite Zone and the Thelon Tectonic Zone, its geological evolution is of the greatest interest.

GENERAL GEOLOGY

The gneiss belt at Rutledge Lake (Fig. 45.2) is composed of four types of granitoid gneiss, three types of supracrustal gneiss, and associated minor metabasite bodies. For the purpose of mapping, these may be combined into several units (Fig. 45.2). The Rutledge Lake complex (unit 1a, b) contains

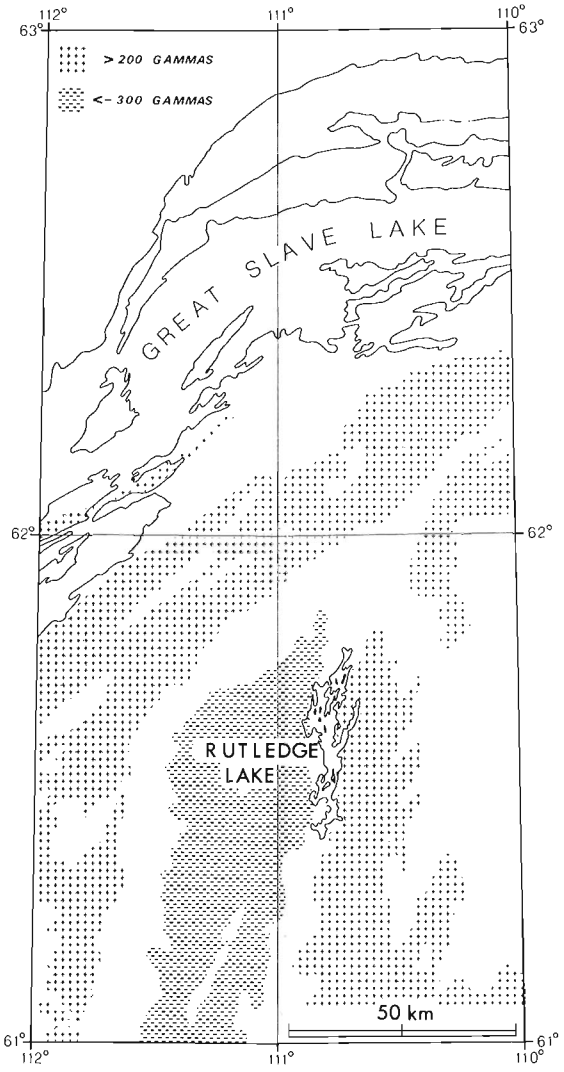

Figure 45.1. Location map, showing features of the magnetic anomaly pattern (from GSC Map 1566A).

layered metasedimentary and granitoid gneiss which underlies most of the lake. Unit 2, the Mama Moose complex, is a distinctive metasedimentary gneiss-metabasite complex which forms discontinuous enclaves along the east side of the belt. Unit 3 is a charnockitic gneiss which forms a sizeable mass in the northwest of the lake, but which forms smaller slices throughout the Rutledge Lake complex. The western boundary of the Rutledge Lake complex is gradational as its granitic component loses the innumerable paragneiss enclaves typical of the complex and becomes progressively less deformed, assuming the character of a weakly foliated, quite massive S-type granite (unit 4). The eastern side of the belt is bounded by the Eastern granite (unit 5), a composite of two granite types, which merges eastward into the granite-derived belt of mylonites (unit 6).

The Rutledge Lake complex is composed of steeply dipping layered metasedimentary gneiss and granitic gneiss which are interlayered on all scales, from decimetre to hundred metre scale. There is a general zonation to the complex, the centre being composed predominantly of paragneiss with individual units up to several hundred metres wide sandwiched between sinuous, thin granitic layers. The reverse is true at the margins, gneissic granite is predominant compared to the discontinuous paragneiss horizons.

The granite component of the complex is predominantly a pale buff, pink or white weathering leucocratic gneiss of granite to granodiorite composition. It has a strong LS fabric of blue quartz blades set in a very fine sugary feldspathic matrix. The quartz blades are highly attenuated (aspect ratios in excess of 10:1), indicating that the fabrics formed during large homogeneous strains. The feldspars comprise orthoclase, some microcline, and plagioclase with occasional relict mesoperthite grains. Small inclusions of metasedimentary material are common in the granite close to the paragneisses. These range from xenocrysts, small xenocryst aggregates to smeared-out pelitic strips. Garnet, sillimanite and spinel xenocrysts have been noted in thin section. The granite gneiss thus has some characteristics of an S-type granite (White and Chappell, 1977).

In the east, close to the largest mass of the Mama Moose complex, the granite is more heterogeneous. Here it ranges from bright pink leucogranite, through grey megacrystic granodiorites, to melanocratic garnet-bearing quartz monzonites, and granites. A leucosome is sparsely developed in these rocks.

The paragneiss component of the Rutledge Lake complex has a range of compositions characterized by three end members: a migmatitic pelitic gneiss containing garnet, sillimanite, cordierite and spinel, a quartzite with minor pelitic horizons, and a quartz-feldspar metawacke. These gneiss types are interlayered on a centi- to a decametre scale. When these first order gneiss types are interlayered on a fine scale a second order of gneiss types is produced. Thus, for example, a thick horizon of thinly interlayered migmatitic pelite and metawacke (second order) may be interlayered with a thick horizon of garnetiferous quartzite (first order). The overall impression is of a metamorphosed greywacke-shale sequence. This essentially primary layering may be additionally complicated with the addition of thin granite sheets. Many of these paragneisses appear to have undergone considerable homogeneous strains comparable to the granites with which they are interlayered. They display such features as boudinage, augen structures and tight to isoclinal folds with axes parallel to the lineation. A common aspect, related to strain, of the paragneisses is that when viewed on surfaces in zone with stretching lineation and fold axes, they appear to be extremely straight gneiss, whereas when viewed on surfaces perpendicular to the stretching direction they have a tightly folded appearance.

Several features further characterize these rocks: the ubiquitous large egg-shaped garnet porphyroblasts; the common blue colour of the quartz; and the occasional presence of rusty zones, sometimes graphitic, in pelitic members. A minor but very common member of this unit are narrow, commonly discontinuous, horizons of fine grained mesocratic hypersthene-plagioclase-quartz-biotite gneiss.

The Mama Moose complex (unit 2) is outlined on the aeromagnetic maps by prominent positive anomalies. It has paragneiss and metabasic components. The metabasite forms thick (50-200 m), steeply dipping continuous layers within the predominant paragneiss. Unlike the paragneiss of the Rutledge Lake complex, these rocks are not generally intimately interlayered with granite.

The paragneiss component of the complex is a relatively uniform pelitic migmatite free of layering, containing abundant magnetite and large crystals of sillimanite. The fine grained granite leucosome forms between one third and one half of the rock. Although cordierite is visible in hand specimen at only a few localities, in thin section it is seen to be extremely abundant. Garnet, in contrast, is subordinate and in many sections is absent. Noteworthy features of these rocks are the total lack of mica and the dark colour of the fresh surfaces of even the most quartz-rich of them.

The metabasites are massive to layered, medium- to fine-grained mafic granulites composed of orthopyroxene, clinopyroxene, plagioclase, and minor biotite. At the margins of these bodies there is a curious mélange composed of small, aligned elliptical fragments of the metabasite crowded into a medium grained granitoid matrix. There is no vestige of primary features remaining in the metabasites, which have granoblastic metamorphic textures. However, considering that they are only associated with metasediments, a metavolcanic protolith is favoured.

The charnockitic gneiss (unit 3) is a lineated granodioritic to tonalitic orthogneiss which forms discrete bodies, free of metasedimentary inclusions, and with sharp,

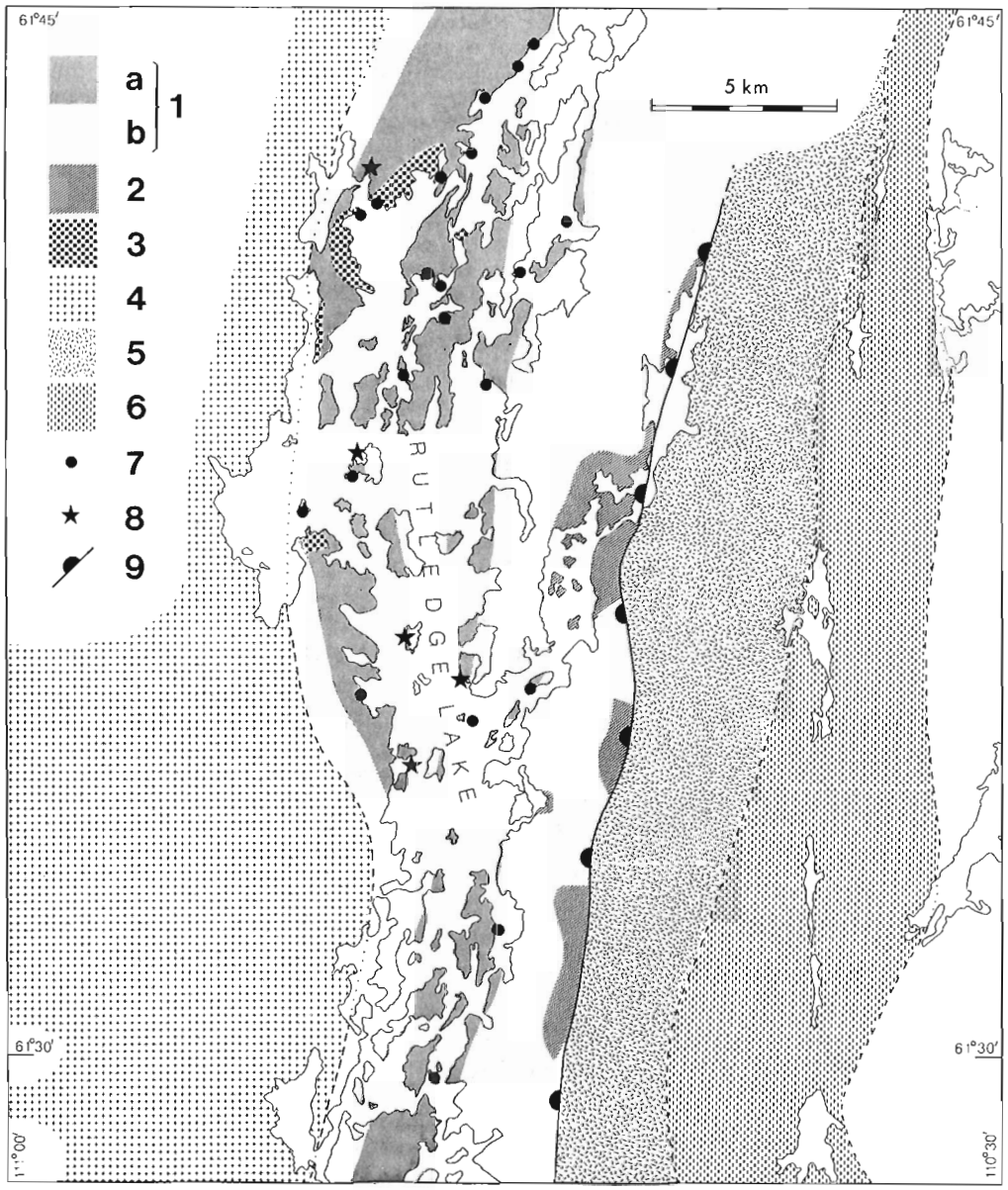

1. *Rutledge Lake complex, interlayered granite gneiss and paragneiss; 1a, dominant paragneiss; 1b, dominant granite gneiss.*
2. *Mama Moose complex, paragneiss and metabasite.*
3. *Charnockitic gneiss.*
4. *S-type granite, weakly foliated.*
5. *Eastern granite, gneissic megacrystic granite and pink leucogranite with metabasite enclaves.*
6. *Mylonites of granitoid protolith.*
7. *Small mafic and ultramafic bodies.*
8. *Cu mineralization (associated with unit 7).*
9. *Hypersthene-out, hornblende-in isograd; teeth on high grade side.*

Figure 45.2. *Geology of Rutledge Lake area. The boundary between units 1 and 4 is gradational. The boundaries of unit 6 were derived from air photo interpretation.*

strongly deformed margins with its host. Hypersthene accompanied by biotite and magnetite is set in a fine granoblastic matrix of orthoclase and plagioclase, evidently derived by recrystallization from mesoperthite, which survives as coarser grains showing strong undulatory extinction.

The terrain to the west of the lake is underlain by a medium grained, weakly foliated, pale pink granite (unit 4), probably a less deformed equivalent of the granite component of the Rutledge Lake complex. Megacrystic granite has only been recognized during reconnaissance in the extreme west. The granite, an S-type composed essentially of perthite and quartz, contains garnet, spinel and sillimanite, some of which is included as tiny grains within feldspars. Recrystallization of the the feldspars is incipient, expressed as very fine new grains at perthite boundaries. Within this less deformed granite terrane two narrow metasedimentary belts have been recognized, trending northeast and southwest, at a high angle to the Rutledge Lake belt. These belts, not shown in Figure 45.2, are located some 5 km from lake, in the northwest and southwest, respectively, of the area.

The Eastern granite (unit 5) is composed of a grey, strongly deformed and recrystallized megacrystic granodiorite and a pink leucogranite. The pink granite is in many places charged with amphibolite inclusions. These rocks become more frequently cut by epidote-filled fractures closer to the belt of mylonite (unit 6).

The (proto-) mylonites of the mylonite belt are predominantly derived from a granitic protolith. They are pink weathering, but dark and aphanitic on fresh surfaces. Many are charged with numerous feldspar porphyroclasts. Cataclasite is developed along a lineament which lies within the mylonites and which is interpreted as a late fault. A linear positive magnetic anomaly which lies along part of this belt is coextensive with banded mylonite formed of granitic mylonite and medium grained amphibolite. The banded mylonites lie along strike from large amphibolite bodies which lie within the southernmost part of the mylonite shown in Figure 45.2 – the presumed source of the amphibolite inclusions within the mylonites.

Small ultramafic and mafic bodies (units 7 and 8) are a volumetrically minor but very significant component of the gneiss belt, where they are closely associated with copper mineralization. Many are only a few decimetres wide and one or two metres long, although a few of the larger bodies occupy entire outcrops. The occasional presence of pyroxene porphyroclasts and of a strong tectonic fabric suggest they originated as somewhat longer bodies which were subsequently boudinaged.

Most commonly the ultramafic rocks are fine, dark green, granular and somewhat micaceous. Both ortho- and clinopyroxene display kinking and undulatory extinction and are variably altered to secondary amphibole. In the least altered ultramafic body, lying close to the northernmost mineralized body (Fig. 45.2), an assemblage of spinel-olivine-orthopyroxene-amphibole is preserved. Mafic bodies are less abundant than ultramafic bodies. They include two-pyroxene mafic granulites of gabbroic composition. Locally they are interlayered with the ultramafic types.

Numerous narrow diabase dykes transect the lake, trending 140 to 160°. They outcrop most frequently in the centre and at the northern end of the lake, clustering around two large dykes (ca. 20 m wide) which cross the lake at these locations. These appear to be entirely fresh and to postdate all except the latest faulting, and are correlated with the Sparrow Dykes (Bostock, 1982).

A second late magmatic addition is represented by scattered granite porphyry dykes. Like the diabase dykes, these 4-5 m wide bodies trend northwest-southeast.

RELATIONS BETWEEN LITHOLOGICAL UNITS

The gneiss belt at Rutledge Lake has a deceptively simple layered structure, which is discouraging at first sight to unravelling the age relations of the units. Certain observations, nonetheless, allow a tentative history to be postulated, which could be tested by radiometric dating.

Firstly, as far as is known, the small ultramafic and mafic bodies (units 7 and 8) only occur in certain lithologies. Thus, if the assumption is correct that they are deformed dykes, they may serve as time markers. They have only been observed in the paragneiss component of the Rutledge Lake complex, where they are crosscut by the granite gneiss, and in the charnockitic gneiss (unit 3).

The granite gneiss component of the Rutledge Lake complex appears to be younger than both the paragneiss component of the complex and the charnockitic gneiss (unit 3). Although small veins of granite crosscut in some places, the granite gneissosity and paragneiss layering are generally concordant. This age relation is supported by the abundance of small paragneiss inclusions within the granite gneiss. The relative age of the granite gneiss and the charnockite gneiss (unit 3) is shown by the inclusion of charnockite blocks in both weakly and strongly foliated granite gneiss. The granite gneiss itself is derived from the medium grained granite (unit 4), which lies to the west of the lake, by recrystallization and grain size refinement of the feldspar fraction which accompanied formation of quartz ribbons during deformation. The mesoscopic changes which accompany this transition can be observed on a large scale in traverses across the western part of the area and also on a smaller scale, in the same area, where poorly and strongly foliated granite are side by side. The S-type characteristics of this granite and the derivative gneiss serve to distinguish them from all the other granitoids.

Unlike the paragneiss of the Rutledge Lake complex, the paragneiss and metabasite of the Mama Moose complex are not intimately interlayered with granite gneiss.

Of the other granitoids, the charnockitic gneiss (unit 3) contains no inclusions of paragneiss or other granitoid. In contrast, unfoliated parts of the Eastern granite (unit 5) at the margin of the Mama Moose complex (unit 2) contain inclusions of unfoliated metabasite from the complex which have amphibolite rims surrounding granulite centres, suggesting that this granite is syntectonic.

In summary, it is tentatively postulated that the paragneiss of the Rutledge Lake complex and the charnockitic gneiss predate the granite gneiss of the complex. The charnockitic gneiss may thus either predate or postdate the paragneiss, its lack of metasedimentary inclusions may be significant in this respect. The Mama Moose complex, apparently lacking ultramafic inclusions and largely free of granite interlayering, must have a fundamentally different relationship from that of the paragneiss component of the Rutledge Lake Complex to the charnockitic gneiss and the Rutledge Lake complex. The Eastern granite, incorporating foliated parts of the Mama Moose complex before it was itself foliated, was probably syntectonic.

METAMORPHISM

Metamorphism at Rutledge Lake accompanied deformation and varies in space and time in a simple manner. A widespread high grade event is recorded primarily in the pelitic paragneisses and metabasites. In most pelitic gneisses of the Rutledge Lake complex quartz - K-feldspar - cordierite - garnet - sillimanite - spinel - magnetite ± plagioclase coexist, although locally cordierite is absent. Another common assemblage in minor supracrustal horizons is

quartz - orthopyroxene - plagioclase - biotite. In pelitic rocks of the Mama Moose complex spinel is always absent and garnet is of minor importance or absent, while magnetite is very abundant; a common assemblage is: quartz - K-feldspar - cordierite - sillimanite - magnetite ± plagioclase. The metabasites from this complex contain clinopyroxene - orthopyroxene - plagioclase - biotite, whereas in an enderbitic gneiss clinopyroxene - orthopyroxene - plagioclase - quartz - magnetite ± biotite occur. Most of the charnockitic gneisses (unit 3) lack garnet and the assemblage orthopyroxene - mesoperthite - quartz - magnetite - biotite is present. There is, however, one locality where garnet - orthopyroxene - mesoperthite - quartz - biotite was recorded.

Since hypersthene is present in appropriate compositions, these are granulite facies assemblages. Notable too is the dearth of plagioclase and lack of biotite in the migmatitic pelitic rocks. In metabasic rocks garnet is lacking, while in many pelitic rocks garnet and cordierite are present together, suggesting that peak metamorphic conditions were attained at low to moderate pressures but high temperatures (680-800°C, 4-6 kb, Lee and Holdaway, 1977). Furthermore, these same authors suggest that rocks which contain coriderite - garnet - K-feldspar - quartz, which lack either sillimanite or biotite, and which are lacking or low in plagioclase, may well be restites from partial melting in which aluminous granite melts (S-type) were produced.

East of the lake the prevailing grade is lower (Fig. 45.2). This is demonstrated by the prevalence of amphibolite inclusions in the Eastern granite and in the mylonite belt. The inclusion of amphibolized mafic granulite of the Mama Moose complex within the Eastern granite indicates that the hypersthene isograd (Fig. 45.2) is a retrograde boundary. The widespread presence of green actinolitic amphibole within the banded mylonites indicates a greenschist facies grade of metamorphism.

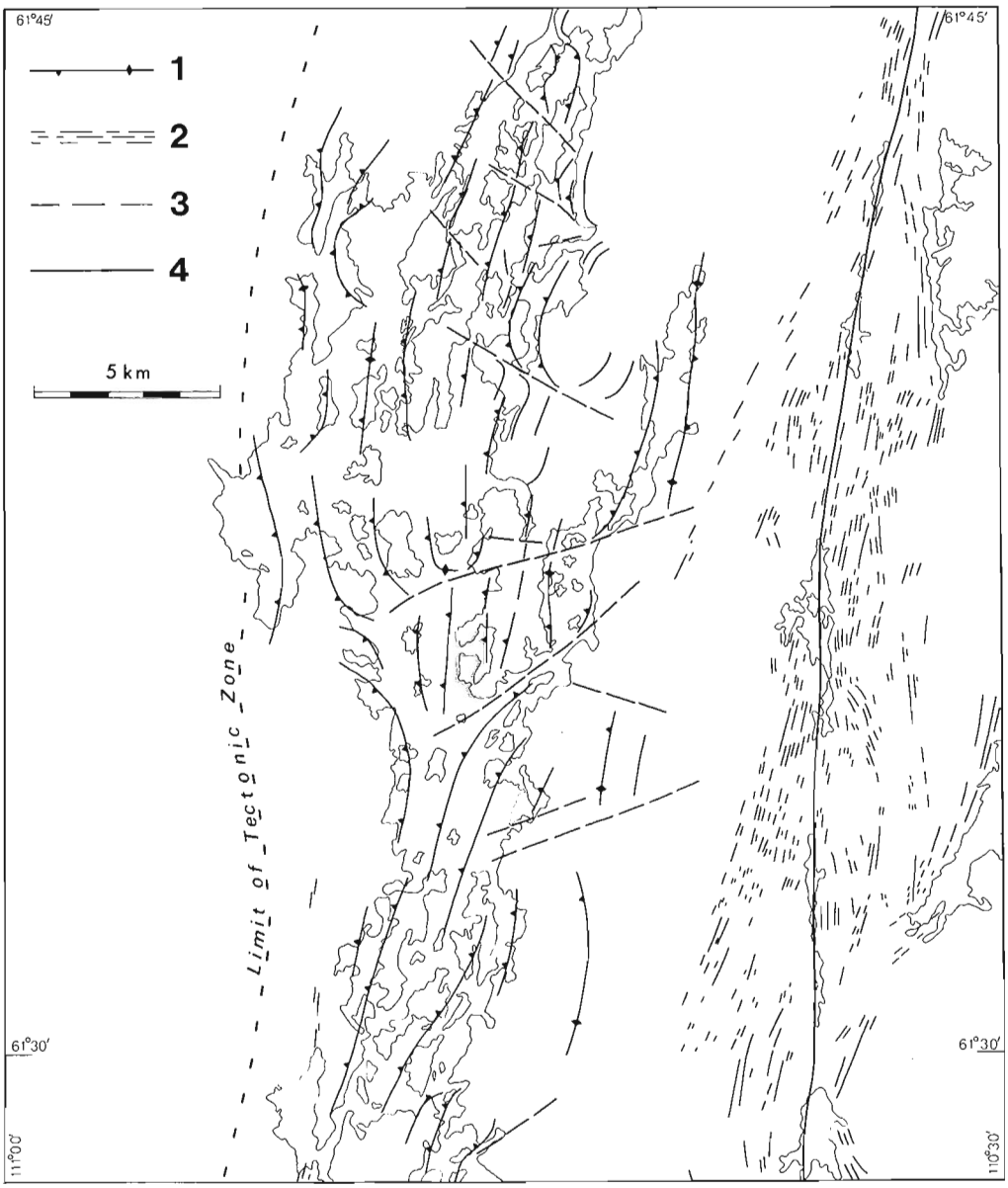

1. *Layering and foliation in zone of high grade, straight gneisses; dip 60°-80° and 81°-90° indicated.*
2. *Trace of mylonitic foliation (most interpreted from air photos).*
3. *Later faults within high grade part of zone.*
4. *Late fault within lower grade mylonite belt.*

Figure 45.3. *Structural outline of the tectonic zone at Rutledge Lake. West of the limit of the tectonic zone poorly foliated granites are predominant.*

Within the high-grade zone there are many narrow zones of greenschist facies retrogression and shearing. In these discordant zones paragneisses are converted to chloritic phyllites and the granites to aphanitic mylonites. A more pervasive incipient static lower grade overprint is seen in many of the paragneisses of the Rutledge Lake complex shown by late growth of chlorite and muscovite.

STRUCTURE

Rutledge Lake provides a section across a belt of highly strained straight gneisses and mylonites (Fig. 45.2, 45.3). The western margin of this belt, which roughly coincides with the boundaries of units 1 and 4, is marked by the appearance of highly strained granite gneiss bearing a gently plunging lineation. This stretching lineation, lying within the steeply west dipping foliation, is present both in the high grade gneisses and in the mylonites (Fig. 45.4). In contrast to the LS shape fabrics present in the granitoids, the paragneisses display tight to isoclinal folds of layering about axes lying

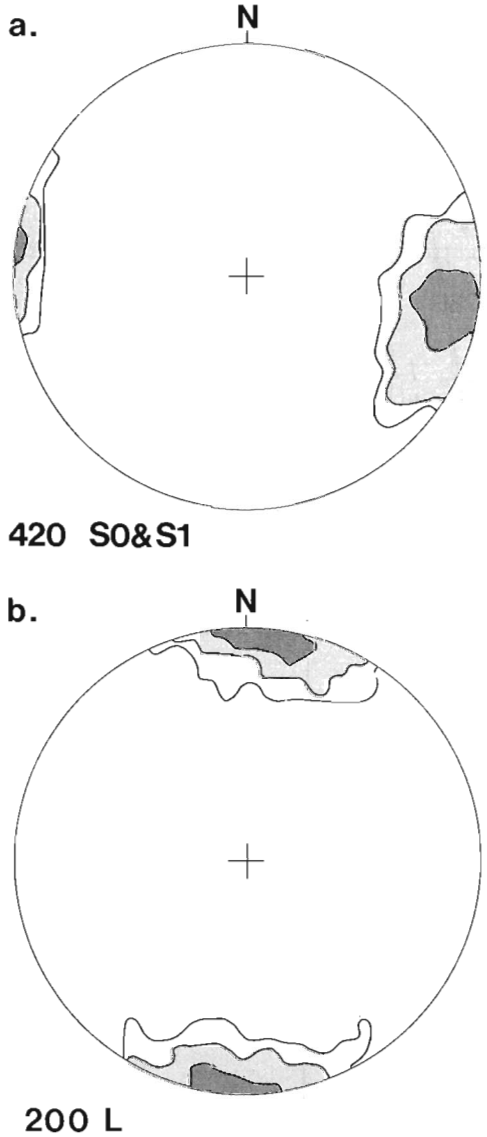

Figure 45.4. Orientation of planar and linear structures. (a) Layering in metasediments (S_0) and foliation in granite, including mylonites (S_1). (b) Stretching lineations and minor fold axes. Equal area net, lower hemisphere plots are contoured at 2, 4 and 10 per cent per 1 per cent area.

parallel to the stretching lineation. Within the mylonite belt features such as shear-bands and rotated porphyroclasts, provide abundant evidence that the regional fabric was the product of transcurrent shearing parallel to the lineation.

Since the regional lineation is present in both high and low grade zones, it is evident that with time the zone of concentrated deformation migrated eastward or contracted with falling metamorphic grade, a sequence of events which might have happened in either an episodic or progressive fashion. During shearing in the low grade eastern mylonite zone, deformation in the high grade part of the belt was concentrated along map scale faults (Fig. 45.3) and in narrow outcrop scale zones of shearing and retrogression (Fig. 45.5a).

Some of the small scale zones are concordant with the regional foliation, most notably in the south of the lake and in the rocks bordering the Mama Moose complex. Most of the zones are discordant to the regional foliation. Some of these discordant zones are developed in conjugate sets, however, the majority have northwest-southeast orientations (Fig. 45.5a). Within these zones kinematic indicators indicate subhorizontal displacement, and the wall rocks of the zones are folded about steep to vertical axes. Kinematic indicators include shear bands (White et al., 1980), rotated en echelon faults (Freund, 1974) and C and S fabrics (Berthé et al., 1979). An important aspect of these zones is their restriction to rocks in which the regional planar fabric is most strongly developed. The ubiquitous joints (Fig. 45.5b) must in part be contemporary with the formation of these zones since they are locally rotated within them.

Foliation and lineation are deformed in places close to the larger faults (Fig. 45.3). The curvature of this deformed fabric in places shows the sense of displacement along the fault, however, the curvature locally displays patterns suggestive of internal boudinage (Cobbold et al., 1971), although the angle between faults and foliation is larger than normally expected. At least in their earlier histories the large scale faults are related to the small scale shears since the smaller zones are abundantly developed near them. Moreover, both these large and small scale structures have similar orientations, although northwest-southeast and north-south orientations are equally developed in the larger structures. However, granitic rocks are locally intensely fractured and quartz veined, suggesting an important late brittle stage in their history. Whether this only accompanied faulting along the long throughgoing north-south lineament which lies within the main mylonite zone (Fig. 45.3) is not known.

The evolution of the tectonic zone may be summarized therefore as a three-step process: firstly, high-grade ductile deformation extended as far west as the boundary between units 1 and 4 (Fig. 45.2, 45.3); secondly, perhaps following uplift, shearing was concentrated in the zone of mylonites while penetrative retrograde metamorphism extended as far as the boundary between units 1 and 5; finally, perhaps as uplift continued, brittle faulting developed. During the two final stages deformation in the high-grade wall rocks of the mylonitic shear zone was restricted to small scale discordant shear zones and large scale faults. These are envisaged as analogues of extensional structures, such as shear-bands and foliation boudinage respectively, which form in strongly anisotropic materials in order to accomplish extension along the foliation (Cobbold et al., 1971; Platt and Vissers, 1980). The discordant shear zones and faults therefore facilitated subhorizontal extension within the strongly foliated high grade wall rocks during the formation of the mylonites and subsequent brittle faulting.

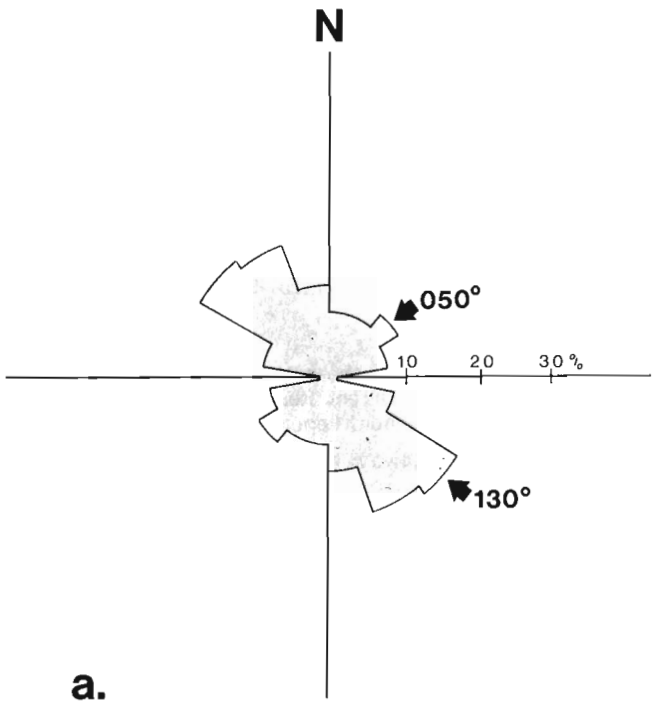

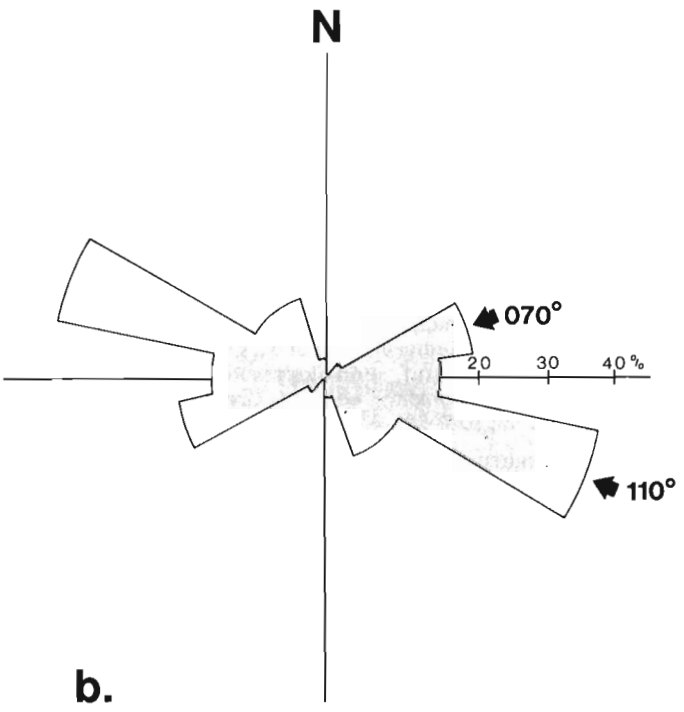

Figure 45.5. Orientation of subvertical late planar structures. (a) Trace of minor zones of shearing and retrogression within zone of high grade straight gneisses (N = 96). (b) Trace of joints (N = 47). Azimuths of maxima indicated.

If this interpretation is correct then the single dominant set of northwest-southeast trending shear zones, as well as the associated joints, may indicate a period of non-coaxial strain in the wall rocks, accompanying sinistral shear in the mylonite zone (Fig. 45.6). The large scale northwest-southeast and northeast-southwest trending faults may indicate, in part, a subsequent period of coaxial flattening across the foliation.

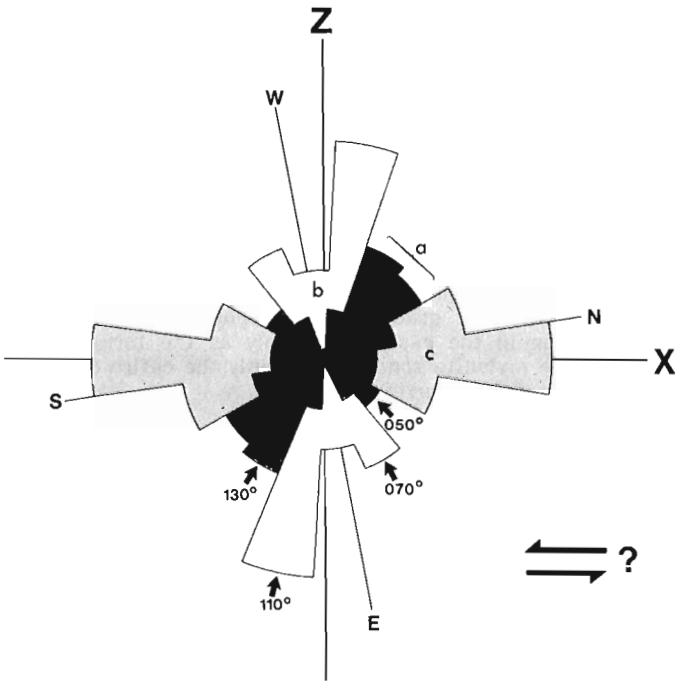

Figure 45.6. Interpretative synoptic diagram of orientation of minor structures. X-Z, structural coordinates. (a) Trace of minor zones of shearing and retrogression within zone of high grade straight gneisses. (b) Trace of joints. (c) Trace of layering and foliation (N = 420). Azimuths of maxima indicated, as in Figure 45.5. During late low grade deformation, accompanying formation of the mylonite zone, extension is accomplished along the foliation within the high grade zone (c), by movement along discordant shear zones (a), accompanied by formation of joints (b). A sinistral sense of shear is postulated.

ECONOMIC GEOLOGY

Small stratiform bodies of sulphides (dominant chalcopyrite and pyrrhotite) occur sporadically throughout the Rutledge Lake complex, the most important are shown in Figure 45.2. Cu and Ni are prominent in assays of samples from these bodies (J. Brophy, Geology Division, Northern Affairs, Yellowknife, personal communication, 1983). In all cases the mineralization is closely associated with the small ultramafic and mafic bodies (units 7 and 8) which are scattered throughout the complex (Fig. 45.2). The sulphides occur either interlayered with the ultramafic bodies, or a few metres along strike from them, or even forming the matrix of brecciated fragments of mafic granulite. In many cases sulphides are disseminated in the ultramafic or mafic host. There can be no doubt that the origin of the mafic and ultramafic bodies and of the mineralization is closely linked, their primary relationship considerably modified by prolonged tectonism. It follows from the apparent restriction of the mafic and ultramafic bodies (units 7 and 8) to the Rutledge Lake complex (unit 1) and the charnockitic gneiss (unit 3) that exploration for comparable deposits should concentrate on these lithologies.

SUMMARY AND DISCUSSION

Rutledge Lake underlies a gneiss belt comprising several granitoid gneiss units, a paragneiss-granite gneiss complex, and a predominantly paragneiss supracrustal complex. The distribution of small mafic and ultramafic bodies within these units is of great interest since, assuming that they are deformed dykes, the gneiss belt can be divided into younger

and older components. On this hypothesis the paragneiss component of the Rutledge Lake complex (unit 1) and the charnockitic gneiss (unit 3) are the oldest lithologies. The Rutledge Lake complex was derived by ductile deformation during high grade metamorphism, at low to moderate pressures, of an S-type granite charged with large paragneiss enclaves. These latter have a probable greywacke-shale protolith. The second (younger and/or allochthonous?) supracrustal complex (unit 2) is predominantly uniform and pelitic. The entire belt coincides with a steep tectonic zone of high grade straight gneisses in the west and mylonites in the east. In the west, low to moderate pressure granulite facies metamorphism accompanied deformation, while subsequent lower grade metamorphism accompanied mylonitization in the east, presumably as the terrane was uplifted. The mylonite zone and probably the entire tectonic zone is a belt of transcurrent shear.

The Rutledge Lake area, therefore, exposes a tectonic zone which has a protracted history of metamorphism and deformation, preceded by a lengthy crustal evolution. The area is, however, a microcosm of a much larger entity and more questions have been raised than answered. The following are some of the more intriguing queries are: How long is the history of transcurrent shear and uplift? What is the relation of the tectonic zone to the Slave-Chantrey Mylonite Zone which lies as close as 25 km to the north? What is its relation, if any, to the Thelon Tectonic Zone? What is the significance of the low pressure granulite facies metamorphism? What does the existence of two distinct supracrustal assemblages signify and is the deduction of sinistral shear within the belt correct?

REFERENCES

Berthé, D., Choukroune, P., and Jegouzo, P.
1979: Orthogneiss, mylonite and non-coaxial deformation of granites: the example of the South Armorican Shear Zone; Journal of Structural Geology, v. 1, no. 1, p. 31-42.

Bostock, H.H.
1982: Geology of the Fort Smith map area, District of Mackenzie, Northwest Territories (NTS 75D); Geological Survey of Canada, Open File 859.

Cobbold, P.R., Cosgrove, J.W., and Summers, J.M.
1971: The development of internal structures in deformed anisotropic rocks; Tectonophysics, v. 12, p. 23-53.

Freund, R.
1974: Kinematics of transform and transcurrent faults; Tectonophysics. v. 21, p. 93-134.

Gibb, R.A., Thomas, M.D., Lapointe, P.L., and Mukhopadhyay, M.
1983: Geophysics of proposed Proterozoic sutures in Canada; Precambrian Research, v. 19, p. 349-384.

Godfrey, J.D. and Langenberg, C.W.
1978: Metamorphism in the Canadian Shield of northeastern Alberta; in Metamorphism in the Canadian Shield, Geological Survey of Canada, Paper 78-10, p. 129-138.

Henderson, J.F.
1939: Taltson Lake; Geological Survey of Canada, Map 525A.

Heywood, W.W. and Schau, M.
1978: A subdivision of the northern Churchill Structural Province; in Current Research, Part A, Geological Survey of Canada, Paper 78-1A, p. 139-143.

Lee, Sang Man and Holdaway, M.J.
1977: Significance of Fe-Mg cordierite stability relations on temperature, pressure and water pressure in cordierite granulites; in The Earth's Crust: Its Nature and Physical Properties, ed. J.G. Heacock; American Geophysical Union Monograph 20, p. 79-94.

Nielsen, P.A., Langenberg, C.W., Baadsgaard, H., and Godfrey, J.D.
1981: Precambrian metamorphic conditions and crustal evolution, Northeastern Alberta, Canada; Precambrian Research, v. 16, p. 171-193.

Platt, J.P. and Vissers, R.L.M.
1980: Extensional structures in anisotropic rocks; Journal of Structural Geology, v. 2, no. 4, p. 397-410.

Thompson, P.H. and Henderson, J.B.
1983: Polymetamorphism in the Healey Lake map area – Implications for the Thelon Tectonic Zone; Abstract in Geological Survey of Canada Paper 83-8, p. 2.

White, A.J.R. and Chappell, B.W.
1977: Ultrametamorphism and granitoid genesis; in Experimental Petrology Related to Extreme Metamorphism, ed. D.H. Green; Tectonophysics, v. 43, p. 7-22.

White, S.H., Burrows, S.E., Carreras, J., Shaw, N.D., and Humphreys, F.J.
1980: On mylonites in ductile shear zones; Journal of Structural Geology; v. 2, no. 1/2, p. 175-187.

46. DISCRIMINATION BETWEEN GLACIGENIC AND WEATHERING RESIDUE DIAMICTONS, SOMERSET ISLAND, NORTHWEST TERRITORIES

EMR Research Agreement 58-4-79

R.G. Hélie[1] and J.A. Elson[2]
Terrain Sciences Division

Hélie, R.G. and Elson, J.A., Discrimination between glacigenic and weathering residue diamictons, Somerset Island, Northwest Territories; in Current Research, Part A, Geological Survey of Canada, Paper 84-1A, p. 339-344, 1984.

Abstract

On Somerset Island and in adjacent Arctic Canada it is difficult to distinguish between diamictons resulting from prolonged weathering of the rocks and those formed by glaciers. Grain size distribution parameters, including mean size, sorting, skewness, and kurtosis, have limited value for discriminating between these diamictons. Regression of sorting on mean grain size of about 15 samples of each type of diamicton distinguished some tills from weathering residues derived from crystalline rocks, but did not do so for sedimentary or mixed source rocks. Analyses of quartz grain surface features using scanning electron microscopy proved to be impractical. X-ray diffraction diagrams of the clay-size fractions show peaks for quartz, mica, and chlorite in tills whereas the peaks in weathering residues are poorly defined or absent. Diffraction diagrams are diagnostic for all of the five till samples analyzed and four of five weathering residues.

Résumé

Dans l'île Somerset et dans l'Arctique canadien adjacent, il est difficle de différencier les diamictons qui résultent de l'altération prolongée des roches de ceux qui sont produits par les glaciers. Les paramètres de la répartition granulométrique, notamment le calibre moyen, le triage, la dissymétrie et le kurtosis, n'ont qu'une valeur limitée pour l'identification de ces diamictons. La régression du triage par rapport au calibre moyen d'environ 15 échantillons de chaque type de diamicton a permis de différencier certains tills des débris de l'altération des roches cristallines mais non de ceux des roches sédimentaires ou mixtes. L'analyse des éléments superficiels des grains de quartz au microscope électronique à balayage n'est pas pratique. Des diagrammes établis par diffractométrie des particules de la classe granulométrique des argiles ont donné des sommets marqués pour le quartz, le mica et la chlorite dans les tills; les sommets sont mal définis ou absents pour les débris de l'altération. Les diagrammes de diffractométrie ont servi à diagnostiquer les cinq échantillons de till et quatre échantillons sur cinq de débris d'altération.

INTRODUCTION

The term "diamicton" was introduced by Flint et al. (1960a, b) to designate a nonsorted sediment, without any genetic connotation. Nonsorted and poorly sorted sediments are produced in several ways including glacial processes, both physical and chemical weathering, and slope movements that cause mixing of the regolith.

On parts of Somerset Island, Northwest Territories, as well as on other arctic islands, diamictons of glacial origin are difficult to separate on the basis of field observations from those caused by weathering (Netterville et al., 1976), although in some places they can be distinguished by their relationship to glacigenic landforms (Dyke, 1976). This report describes a series of laboratory tests performed in an attempt to find better means of determining the origins of these diamictons (Helie, 1981). Laboratory experiments on the genesis of diamictons by the freezing and thawing of rocks were also carried out, but are the subject of another report.

SOMERSET ISLAND

Somerset Island (Fig. 46.1) lies in the Canadian Arctic between approximately 72°-74°N and 96°-90°W. The physiography of Somerset Island was described by Craig (1964), who related the physiographic divisions to the underlying bedrock, and in more detail by Netterville et al. (1976). The Precambrian upland is a belt of crystalline rocks, 30 to 35 km wide, occupying the southern 80 per cent of the west side of the island. It is a plateau about 490 m above sea level, rising slightly from south to north, with a low relief of rounded hills separated by broad valleys. Most of the area to the east comprises the Paleozoic plateaus, which rise from less than 100 m above sea level in the south to as much as 450 m in the north part of the island; their relief rarely exceeds a few metres, and they have a cover of 1 to 3 m of rubble ranging from silt size to angular blocks. Some east- and north-flowing rivers are incised 100 to 150 m into the plateaus, but their headwaters are not incised, occupying only shallow valleys. South of Creswell Bay and along the eastern and northern periphery of the island are narrow Paleozoic lowlands, below marine limit. The drainage pattern of the Precambrian upland shows a response to rock structure with some rectangular and trellis components; the pattern on the Paleozoic plateaus is mainly dendritic but also has trellis components reflecting the gentle northward dip of the rocks in the north part of the island. Little apparent modification of the drainage network can be attributed to glaciation. The area is in the zone of continuous permafrost and periglacial processes are active.

The bedrock of Somerset Island was described by Blackadar (1967). The Precambrian rocks are quartz and biotite-bearing hornblende gneiss with quartzite, granitic gneiss, banded gneiss, and diopside marble layers, all of Aphebian age, having a north-south structural trend. These are truncated at the north end by a narrow belt of dolostone and associated clastic rocks (shale, chert, minor siltstone and sandstone) of Helikian age. All of these Proterozoic rocks are cut by diabase dykes, which are most abundant in the north.

Most of the area east of the Precambrian upland, more than half of Somerset Island, is underlain by flat-lying limestone, dolostone, dolomitic siltstone, and silty limestone ranging from Silurian to early Devonian in age (Dineley and

[1] 6412 Mary Jane Crescent, Orleans, Ontario K1C 3C3
[2] Department of Geological Sciences, McGill University, 3450 University Street, Montreal, Quebec H3A 2A7

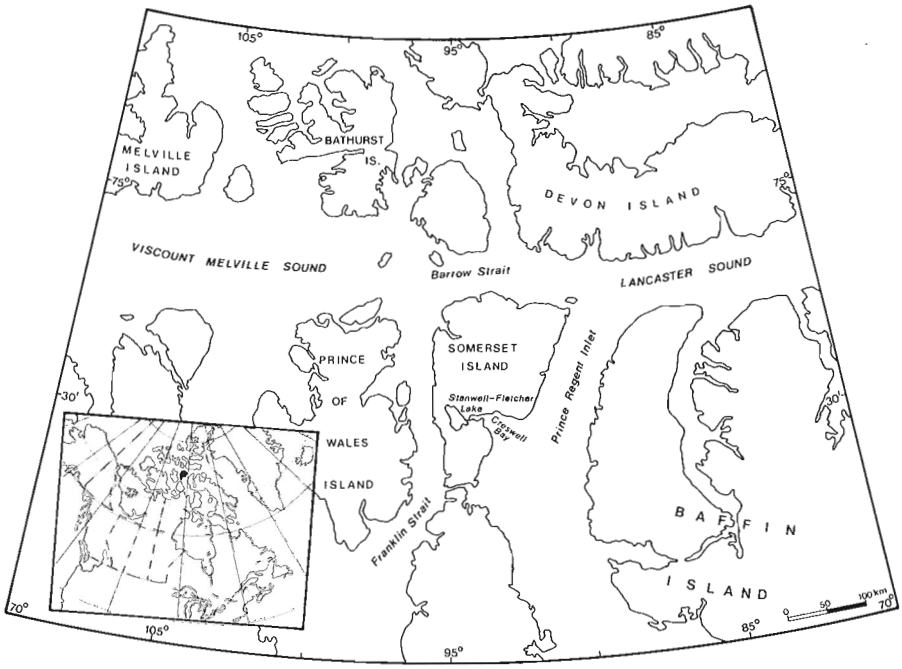

Figure 46.1

Location map showing Somerset Island.

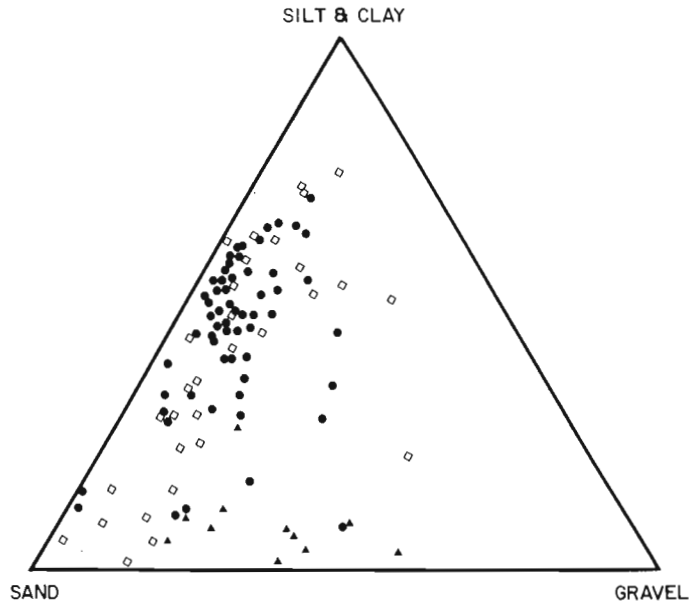

Figure 46.2. *Triangular diagram showing the general grain size distributions of diamictons on Somerset Island. Squares represent weathered rock diamictons; triangles are grus; large dots are tills.*

Rust, 1968; Jones and Dixon, 1977; Miall et al., 1978). In the northwest and central parts of the island there are outliers of early Devonian red sandstone, siltstone, and conglomerate as wide as 25 km. North of Stanwell-Fletcher Lake is an outlier of similar size of poorly lithified sandstone and shale of late Cretaceous to early Tertiary age (Dineley and Rust, 1968).

Early conceptions of the glacial history of Somerset Island have been summarized by Netterville et al. (1976). From the start it was recognized that all of the island had been glaciated at some time because of the presence of Precambrian erratics in areas of Paleozoic rocks and vice versa. It was noted that some of these erratics might have been derived from the Peel Sound Formation, a weakly cemented conglomerate. Netterville et al. (1976) and Dyke (1976, 1978a, b) deduced from the presence of tors, thick weathering residues (grus), solution features, and felsenmeer that glacier ice of middle and late Wisconsinan age was inactive in the area. Dyke (1978b, 1979) outlined parts of two areas in the Precambrian upland north and northwest of Stanwell-Fletcher Lake that were not glaciated during Wisconsinan time, although they had been glaciated previously. He also postulated that much or all of the carbonate plateaus had been covered by a thin, relatively inactive cold-based ice cap as recently as Neoglacial time (Dyke, 1978a; Dyke et al., 1982), and that active wet-based ice covered some areas underlain by gneiss, carbonate rocks, and sandstones, mainly south of Stanwell-Fletcher Lake and Creswell Bay where some glacially streamlined landforms occur. Thus Somerset Island has a variety of diamictons including till-like weathering residues in areas covered by cold-based glacier ice, till in areas covered by active wet-based glacier ice, and mixtures of till and weathering residue resulting from mass movements in the periglacial environment. Further, the characteristics of the diamictons are influenced by the source rock.

The present study is based on samples of rocks and diamictons collected by geologists of the Geological Survey of Canada between 1975 and 1979, including the late J.A. Netterville, A.S. Dyke, and R.G. Helie whose sampling in 1979 was intended to complete the suite collected by the other two. Samples were collected from depths of 5 to 15 cm in the active layer as well as in vertical sequences taken from the walls of pits dug into permafrost (Helie, 1981, p. 13). In the laboratory the samples were analyzed for grain size distribution, carbonate content, surface texture, and mineralogy of the matrix.

SOMERSET ISLAND DIAMICTONS

Grain size analyses

Most of the grain size analyses were performed in the laboratory of the Geological Survey of Canada and the size parameters (Inman, 1952) were calculated there by computer. The general nature of the diamictons is shown in Figure 46.2.

Table 46.1. Summary of all grain size parameters (Inman, 1952) for all tills and all weathered rock diamictons, with standard deviations (SD); also differences between the means of tills and weathering residues, and standard errors (SE) of the differences of the means

	Tills	Weathering residues	Differences of means
Mean grain size:			
n	58	30	
Mean (phi)	4.26	3.80	0.46
SD	± 1.36	± 1.69	SE ± 0.36
Mean sorting:			
n	59	30	
Mean So	3.43	3.12	0.31
SD	± 0.80	± 1.81	SE ± 0.35
Mean skewness:			
n	59	30	
Mean Sk	0.11	0.06	0.05
SD	± 0.25	± 0.24	SE ± 0.06
Mean kurtosis:			
n	9	8	
Mean K	1.34	1.01	0.33
SD	± 0.92	± 0.48	SE ± 0.35

Table 46.1 is a summary of the grain size parameters for all tills and weathered rock diamictons. Comparison of the mean values of the parameters shows that mean grain size, sorting coefficients, skewness, and kurtosis are similar in both types of materials. Statistical tests on the differences of the means (Table 46.1) show that larger differences than those calculated could arise by chance 95% of the time, hence the means of any of these parameters used alone will not discriminate between till and weathering residue diamictons.

A further test of the usefulness of the sedimentological parameters is shown in Table 46.2 where means and sorting coefficients of diamictons derived from crystalline rocks are separated from those derived from sedimentary rocks. No simple distinction in grain size can be made for the diamictons derived from crystalline rocks, but the difference in the means of the two types of diamicton derived from sedimentary rocks is significant at the 95% level, with the weathering residues having the smaller mean size (4.29 phi versus 3.28 phi for till). The differences between the means of the sorting coefficients are not significant.

Partial differentiation between diamictons derived from individual rock types (formations) was achieved by regression analyses of sorting on mean grain size (Table 46.2; Fig. 46.3). In the case of those formed from crystalline rocks, the regression equation for till has a very low correlation coefficient (r is -0.08); therefore in Figure 46.3A only means and two standard derivations were used for till. For the corresponding weathering residue there is a consistent increase in sorting coefficient with decreasing grain size (increase in phi value), with a correlation coefficient, r, of 0.96. In Figure 46.3A envelopes for the two types of diamictons are drawn at two standard errors (standard deviations for till) giving the 95% confidence limits.

Table 46.2. Regression equations of sorting on mean grain size for tills and weathering residues of similar lithologies. The diamictons are grouped by the rock formations upon which they occur and from which they are presumed to be wholly or mostly derived

Material	n	Regression equation	r	95% confidence limits of Y
Crystalline rocks:				
Till	19	Y = -0.03X + 4.06	-0.08	-[1]
Weathering residue	14	Y = 0.83X + 0.95	0.97	± 0.67
Clastic rocks:				
Peel Sound Formation				
Till	6	Y = 0.47X + 1.31	0.29	± 2.67
Weathering residue	6	Y = 0.65X - 0.07	0.59	± 2.11
Somerset Island Formation (undifferentiated)	5	Y = -0.48X + 6.30	-0.90	± 0.69
Carbonate rocks:				
Till[2]	11	Y = 0.32X + 2.54	0.49	± 1.01
Weathering residue	7	Y = 0.67X + 0.34	0.67	± 1.13

[1] Because of the low correlation coefficient, the 95% confidence field of mean values for tills on crystalline rocks is defined as the overall mean values ±2 standard deviations. Thus X = 5.20 ± 2.35, and Y = 3.92 ± 0.75

[2] Some of these tills are downglacier from areas of crystalline rocks and contain some material derived from them

n - number of samples; r - coefficient of correlation; the 95% confidence limits of Y are taken as 2 standard errors.

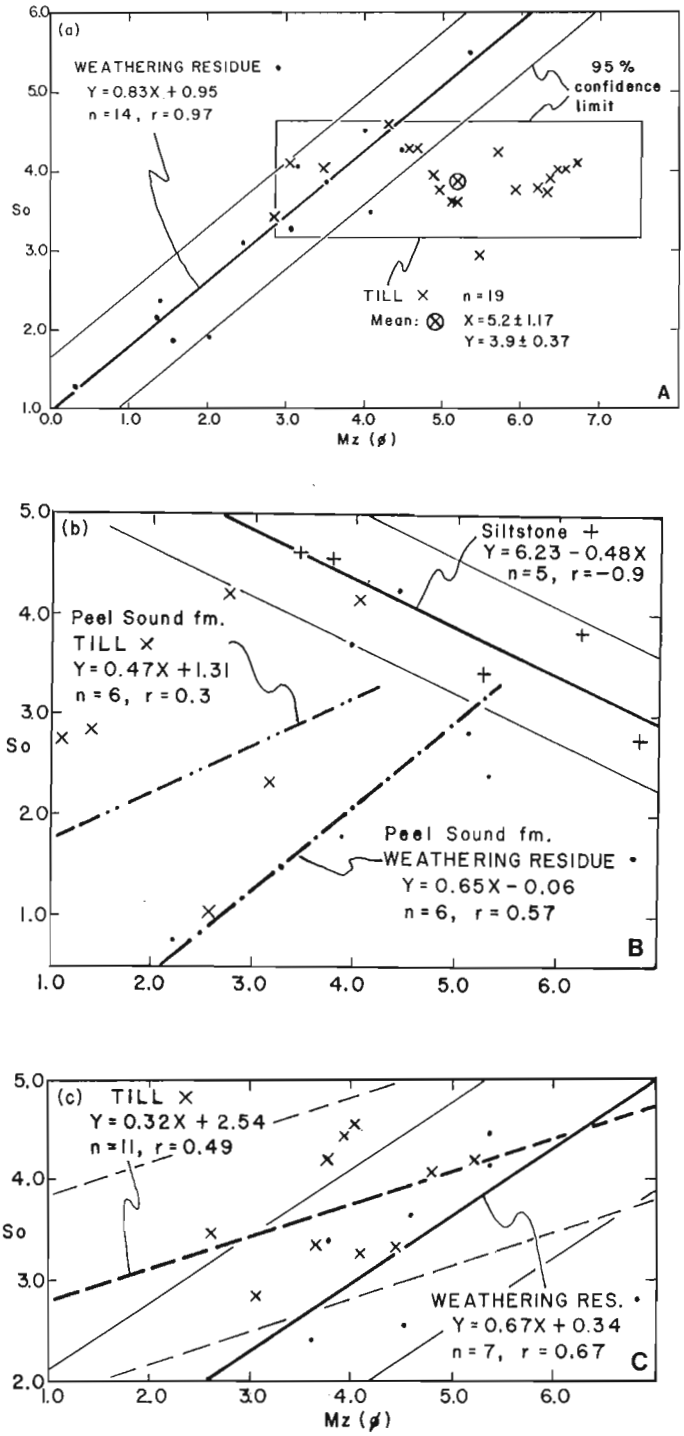

Figure 46.3. Regression curves of sorting coefficients on mean grain sizes of diamictons derived from various rocks: A. crystalline rocks; B. clastic rocks; C. carbonate rocks. The thick lines are regression curves and the corresponding parallel thin lines represent the 95% confidence limits of these curves, or two standard errors. For the till in 3A, confidence limits are taken as two standard deviations of both X and Y.

Within the overlapping zone of the two envelopes are 5 of 17 till samples (30%) and 6 of 13 weathering residue samples (46%). Thus about 70% of the tills and 55% of the weathering residues are outside of the overlap zone and might be discriminated by mean size and sorting coefficients. Regression curves for diamictons derived from clastic or dominantly clastic rocks (Peel Sound Formation, Somerset Island Formation) are shown in Figure 46.3B, but they are based on relatively few data. Diamictons on the Somerset Island Formation, siltstone, were not classified genetically and presumably include early Wisconsinan and perhaps older tills that have been exposed to a long period of arctic weathering, as well as some bedrock weathering residues, and their grain size characteristics might be expected to be similar. The regression equation, based on only five samples, has a correlation coefficient of -0.90, showing a consistent decrease in sorting coefficient with decreasing grain size. Regression curves for the Peel Sound Formation, which includes sandstone and conglomerate, are also shown in Figure 46.3B. The spread of the available data is so great that recognition of the genesis of the diamictons on the basis of grain size parameters is obviously impossible, although in general the weathering residues appear to be finer grained than the tills.

The regression curves for diamictons on carbonate rocks are shown in Figure 46.3C with their 95% confidence limits. Some samples lie outside of the area of overlap of the confidence limits and can be discriminated by these parameters. They include 40% of 10 tills and 30% of 7 weathering residues.

The amount of data presently available suggests that for recognition of the genesis of these diamictons, grain size analyses are worthwhile in areas of crystalline rocks with 55-70% chance of success, but that for diamictons on carbonate and clastic rocks the chances of success are small. A much larger body of data is needed to confirm these results.

Surface textures

The surface textures of about 15 quartz grains per sample, in the size range 0.5 to 1.0 mm, selected from a variety of samples were studied by scanning electron microscopy (SEM) using standard techniques (Helie, 1981, p. 37). Several primary surface forms are present, such as fresh conchoidal fractures and impact marks typical of tills, as well as chemical etch marks in weathering residues. These commonly occur together as a result of frost action in the specimens studied. This introduces ambiguity in the interpretation of the results, which is further compounded by mixing of the two types of diamicton in some samples. This technique may have potential use, but it was not feasible for a quick and certain identification of our diamictons. A recent study by Dowdeswell (1982) has appeared since our work was completed; he found a method of shape analysis, using Fourier techniques, that appears to be able to discriminate between cold environments that shaped grains, but it requires further research before it can be applied quickly to individual specimens.

Mineral composition (X-ray analysis)

A key to the differentiation between till and weathering residue diamicton should be in the mineralogical changes that take place during weathering. This involves both chemical and physical disintegration of the rock, although in the rigorous climate of the Arctic, the physical processes dominate. One of the first changes of a chemical nature involves the formation of clay minerals. Hence there should be readily discernible differences in the gross assemblage of minerals in the clay-size fraction of the matrix of the two diamictons; this was studied by X-ray diffraction analysis.

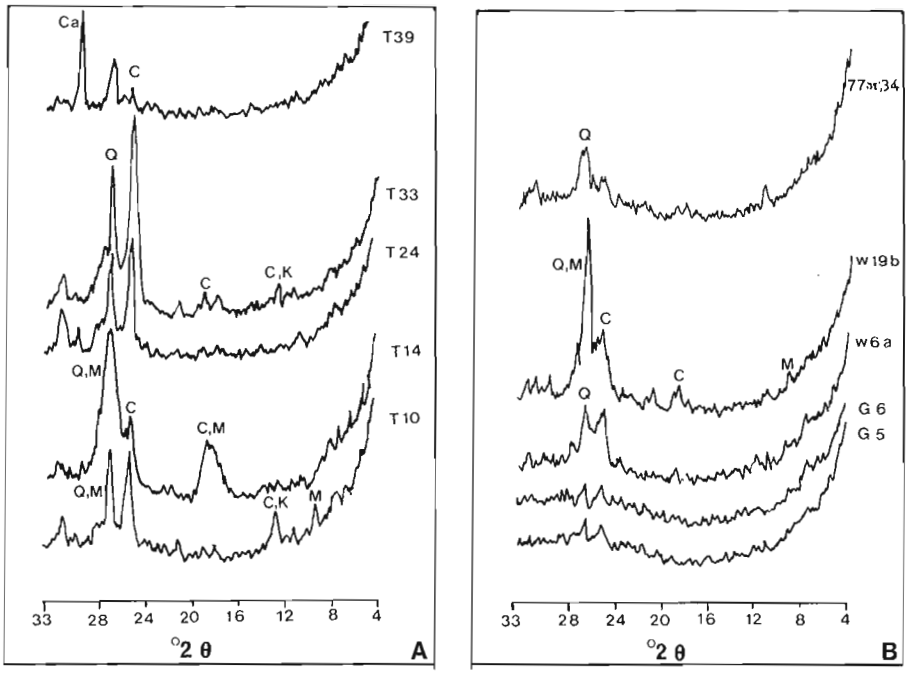

Figure 46.4

X-ray diffraction diagrams for the clay-size fraction of some diamictons using Ni-filtered CuKα radiation.

A. till samples (C = chlorite, Ca = calcite, K = kaolinite, M = mica, Q = quartz).

B. weathered bedrock (peaks as in 4A).

Oriented preparations of selected samples were made by sedimentation of the -2 μm fractions onto glass slides. General complete differences in the clay-size fractions were sought; we did not attempt to isolate and analyze quantitatively for the individual clay mineral species. A more detailed interpretation of the diffractograms was provided to us by J.D. Adshead (personal communication, 1983).

Till samples produced well defined peaks for quartz and chlorite in all the samples studied (Fig. 46.4A); the influence of mica is also noticeable. The diffractograms of bedrock weathering residues characteristically have poorly defined peaks, not far above background (Fig. 46.4B), which indicates the presence of amorphous material. One of the five weathered rock diffractograms (W19b) might be confused with that for till, although the chlorite peaks are less pronounced than in most of the tills analyzed. The diffractograms show the deterioration of chlorite and micas in the weathered rock samples rather than the expected development of clay minerals. X-ray diffraction analysis, however, is a promising method for discriminating between the two diamictons.

DISCUSSION

The simplest and most reliable way to differentiate till from weathered bedrock in the field is to find field evidence of glaciation in the case of till, and deep weathering in the case of weathering residues. Unfortunately, at many locations on Somerset Island field determination of the origin of diamictons is not possible. We have attempted to find suitable criteria based on standard laboratory analyses, some of which, such as grain size analyses, can be performed in field laboratories. The best diamicton differentiation test proved to be X-ray diffraction of the clay-size fraction which shows a deterioration of chlorite and micas, and presumably the production of amorphous material, in weathering residue diamictons. This test is simple and rapid and gave unequivocal results for 9 of the 10 specimens analyzed.

Grain size analysis parameters are useful if large enough groups of samples are available for comparison, but are ineffective for single samples. The grain size approach may work well for some specific lithologies, such as gneiss, but is not effective for diamictons derived from mixed source rocks. The number of samples that gives average skewness values that discriminate between till and weathering residue may be as great as 50 each when multiple source lithologies are grouped, because of large standard deviations. In the case of a single lithology (gneiss), regression analysis of the sorting coefficient on mean size gives characteristic curves for each type of diamicton with about 10 samples of each genetic type.

Examination of the surface features of quartz grains by SEM has potential value and is likely to be effective if the Fourier shape analysis suggested by Dowdeswell (1982) is applied, but our rapid and simple type of examination is insufficient. Several genetic types of surface forms are superimposed upon each other.

CONCLUSION

No single test performed in this study unequivocally confirms the origin of a given diamicton, for two reasons: First, mixing of the two types of diamicton occurred where actively eroding glacier ice overrode weathered bedrock, producing till having some features that are normally diagnostic of weathered rock. Second, periglacial processes active today produce features in all diamictons that can be confused with features that would otherwise have been diagnostic of the diamictons studied. For example, frost splitting of grains in weathering residue will produce microfractures similar to those found in till that has been subjected to the same process as well as primary comminution. Qualitative X-ray diffraction analysis of the clay-size fraction is the best means of distinguishing between diamictons of glacial origin and those resulting from weathering processes.

ACKNOWLEDGMENTS

We are grateful to the Geological Survey of Canada for permission to use samples collected during their field operations and grain size data produced in their laboratories. A.S. Dyke suggested this project and provided logistical support for Helie's field operations, in part through the courtesy of the Polar Continental Shelf Project. Laboratory work at McGill University was supported by a research contract to J.A. Elson from the Department of Energy Mines and Resources, Canada. Comments by J.D. Adshead on the interpretation of the X-ray diffractograms are much appreciated.

REFERENCES

Blackadar, R.G.
1967: Precambrian geology of Boothia Peninsula, Somerset Island and Prince of Wales Island, District of Franklin; Geological Survey of Canada, Bulletin 151, 61 p.

Craig, B.G.
1964: Surficial geology of Boothia Peninsula and Somerset, King William, and Prince of Wales Islands, District of Franklin; Geological Survey of Canada, Paper 63-44, 10 p.

Dineley, D.L. and Rust, B.R.
1968: Sedimentary and paleontological features of the Tertiary-Cretaceous rocks of Somerset Island, Arctic Canada; Canadian Journal of Earth Sciences, v. 5, p. 791-799.

Dowdeswell, J.A.
1982: Scanning electron micrographs of quartz sand grains from cold environments examined using Fourier shape analysis; Journal of Sedimentary Petrology, v. 52, p. 1315-1323.

Dyke, A.S.
1976: Tors and associated weathering phenomena, Somerset Island, District of Franklin; in Report of Activities, Part B, Geological Survey of Canada, Paper 76-1B, p. 209-216.

1978a: Indications of neoglacierization on Somerset Island, District of Franklin; in Current Research, Part B, Geological Survey of Canada, Paper 78-1B, p. 215-217.

1978b: Glacial history of and marine limits on southern Somerset Island, District of Franklin; in Current Research, Part B, Geological Survey of Canada, Paper 78-1B, p. 218-224.

Dyke, A.S., Dredge, L.A., and Vincent, J-S.
1982: Configuration and dynamics of the Laurentide Ice Sheet during the late Wisconsin maximum; Geographie physique et Quaternaire, v. XXXVI, p. 5-14.

Flint, R.F., Sanders, J.E., and Rodgers, J.
1960a: Symmictite: a name for nonsorted terrigenous sedimentary rocks that contain a wide range of particle sizes; Geological Society of America Bulletin, v. 71, p. 507-510.

1960b: Diamictite, a substitute term for symmictite; Geological Society of America Bulletin, v. 71, p. 1809-1810.

Helie, R.G.
1981: Differentiation and genesis of diamictons on Somerset Island, N.W.T.; unpublished M.Sc. thesis, McGill University, Montreal.

Inman, O.L.
1952: Measures for describing the size distribution of sediments; Journal of Sedimentary Petrology, v. 22, p. 125-145.

Jones, B. and Dixon, O.A.
1977: Stratigraphy and sedimentology of Upper Siberian rocks, northern Somerset Island, Arctic Canada; Canadian Journal of Earth Sciences, v. 14, p. 1427-1452.

Miall, A.D., Kerr, J.W., and Gibling, M.R.
1978: The Somerset Island Formation: an upper Silurian to lower Devonian intertidal/supratidal succession, Boothia Uplift region, Arctic Canada; Canadian Journal of Earth Sciences, v. 15, p. 181-189.

Netterville, J.A., Dyke, A.S., Thomas, R.D., and Drabinsky, K.A.
1976: Terrain inventory and Quaternary geology, Somerset Island, Prince of Wales, and adjacent Islands; in Report of Activities, Part A, Geological Survey of Canada, Paper 76-1A, p. 145-154.

47. PETROGRAPHY OF MINERALIZATION AT THE YAVA SANDSTONE-LEAD DEPOSIT, NOVA SCOTIA[1]

Projects 830012 and 650056
Contract 15SR.23233-3-0312

P.D. Vaillancourt[2] and D.F. Sangster
Economic Geology Division

Vaillancourt, P.D. and Sangster, D.F., Petrography of mineralization at the Yava sandstone-lead deposit, Nova Scotia; in Current Research, Part A, Geological Survey of Canada, Paper 84-1A, p. 345-352, 1984.

Also in Mines and Minerals Branch, Report of Activities, 1983, Nova Scotia Department of Mines and Energy, Report 84-1, 1984.

Abstract

The Yava sandstone-lead deposit in Cape Breton Island, Nova Scotia is in an Upper Carboniferous fluviatile sandstone above an unconformity over Lower Carboniferous sediments and a Devonian rhyolite basement. The lead occurs as disseminated galena filling the interstices of the sandstone grains.

Yava is on the southeast flank of the Salmon River sub-basin on the eastern platform border of the Fundy Basin. The deposit is comprised of 3 zones over a strike length of 3000 m which occur in paleovalleys, where sandstone is thickest, between intervening basement highs.

The sandstone at Yava is grey to green and massive to crossbedded. Quartz grains constitute between 70 and 85 per cent of the sandstone; the clay content varies from a strong kaolinite association with galena to a more chloritic association in the non-mineralized intervals. Galena is the dominant sulphide mineral but pyrite and minor sphalerite are present as well. The quartz grains have overgrowths of secondary silica. Pyrite occurs usually as amorphous masses forming a groundmass to isolated quartz grains. Sphalerite is mostly as inclusions in galena and in fractures of broken pyrite grains. Coal fragments, at the base of the sandstone, are also well mineralized with pyrite and galena being more abundant than in the sandstone. Sulphides occur as infillings to plant cells or along fractures in compacted coal.

Résumé

Le gisement de grès plombifère de Yava dans l'Île du Cap-Breton, en Nouvelle-Écosse, se présente dans un grès fluviatil du Carbonifère supérieur situé au-dessus d'une discordance sus-jacente à des sédiments du Carbonifère inférieur et à un socle rhyolitique dévonien. Le plomb se présente sous forme de galène disséminée dans les vides entre les grains de grès.

Le gisement de Yava se trouve sur le flanc sud-est du sous-bassin de la rivière Salmon, sur la marge est de la plate-forme de la baie de Fundy. Il comporte trois zones sur une longueur de 3 000 m qui se situent dans des paléovallées, là où le grès atteint son épaisseur maximale, entre les crêtes intermédiaires du socle.

Le grès de Yava est gris à vert, massif ou à stratifications entrecroisées. Les grains de quartz forment entre 70 et 85% du grès; la teneur en argile varie d'une association marquée de la kaolinite avec la galène à une association plus chloriteuse dans les intervalles stériles. La galène est le principal minéral sulfuré, mais on trouve également de la pyrite et de petites quantités de sphalérite. Les grains de quartz ont des accroissements de silice secondaire. La pyrite se présente généralement en masses amorphes qui forment une matrice autour des grains isolés de quartz. La sphalérite se présente normalement sous forme d'inclusions dans la galène et dans les fractures dans les grains cassés de pyrite. Les fragments de charbon à la base du grés sont également bien minéralisés; la pyrite et la galène y sont plus abondantes que dans le grès. Les sulfures se présentent sous forme de remplissages dans les cellules végétales ou le long de fractures dans le charbon comprimé.

INTRODUCTION

The Yava deposit in southeastern Cape Breton, Nova Scotia, is a former lead producer wherein galena is hosted in Upper Carboniferous fluviatile sandstone. The sandstone lies above an unconformity over Lower Carboniferous shales and a Devonian rhyolite basement. The Yava area is part of the Salmon River sub-basin. The Yava deposit is an outstanding example of a sandstone-lead occurrence of continental affiliation and presents a unique opportunity to contrast mineralization styles with other lead-zinc occurrences of similar type (Bjørlykke and Sangster, 1981). Within this framework, a petrographic study on the host sandstone as well as the coal and sulphide mineral occurrences at Yava was undertaken.

The study of the host rock will not only include petrographic descriptions but will consider results from X-ray diffraction traces on clays from the sandstone. The nature of occurrence of galena, pyrite and sphalerite in sandstone as well as coal will also be reviewed with the objective of identifying common mineral associations and environments favorable to sandstone-lead occurrences.

REGIONAL GEOLOGY AND STRATIGRAPHY

The Yava deposit is located on the southeast flank of the Salmon River sub-basin on the eastern platform border of the Fundy Basin (Fig. 47.1). The Salmon River sub-basin forms an elongate, wedge-shaped syncline which gently plunges to the southwest and is truncated by faults along the northwestern and southwestern flanks. At Yava, lead-bearing rocks of the Canso Group of Namurian age lie unconformably on Viséan Windsor Group rocks and a basement composed of Cambrian granodiorite and a Devonian rhyolite porphyry (Barr et al., 1984; this volume).

Basement in the immediate Yava area consists of a red, quartz-feldspar porphyry which has been described as a rhyolite (Fig. 47.2). The overlying Windsor Group sediments

[1] Contribution to Canada-Nova Scotia Co-operative Mineral Program 1981-84. Project carried by Geological Survey of Canada

[2] 341 Chester Avenue, Montreal, Quebec H3R 1W6

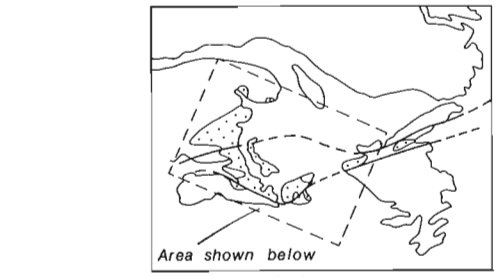

Index map

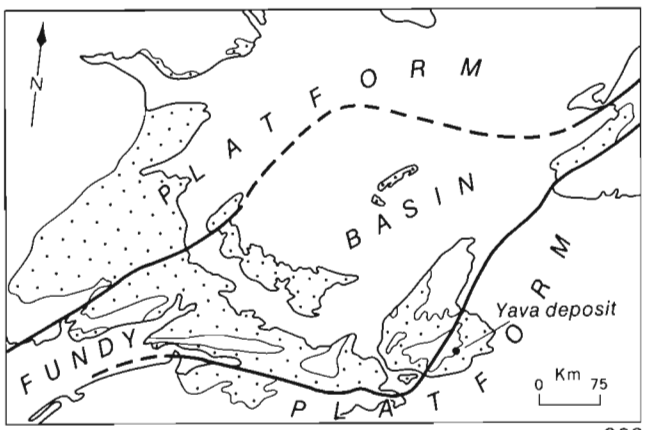

Figure 47.1. *Location map showing position of the Yava deposit relative to Carboniferous sedimentary cover (shaded), pre-Carboniferous basement (unshaded), and major tectonic elements (from Hacquebard, 1972).*

have a maximum thickness of 150 m and consist mostly of limestone overlain by gypsiferous black shale and red to green mudstones. The overlying Namurian age rocks are up to 240 m thick and are dominated by fine- to medium-grained grey to green sandstone with thin shale interbeds and random coal fragments. The sandstone sequence is generally underlain by conglomerate up to 3 m thick and, in places, a calcareous breccia. The base of the sandstone is characterized by the presence of mineralized coal fragments.

GEOLOGY OF THE YAVA DEPOSIT

The Yava deposit is a monomineralic lead occurrence with proven reserves of 1.8 million tonnes at 4.2% Pb (Bonham, 1982). Stratiform disseminated galena occurs as cement to the sandstone. The sandstone dips 15 degrees to the northwest.

Yava is comprised of three zones: the west, central and east which occur within a strike length of 3000 m and extend down dip for 600 m (Bonham, 1982). The galena at Yava is related to the topography of the basement rocks, occurring in the paleovalleys, where sandstone is thickest, between intervening basement highs (Fig. 47.3).

PETROGRAPHY OF THE SANDSTONE

Sandstone is the major host for galena and makes up more than 90% of the Namurian strata at Yava. The sandstone is very homogeneous along strike and in vertical section. It is grey to green in colour, generally grey near the base of the section, where galena occurs, and green near the top of the section in unmineralized sandstone. It is mostly massive but may also have parallel or large-scale crossbeds to small-scale ripple crossbeds.

Grains are sub- to anhedral, semi-rounded and fine to coarse grained (0.1 to 2 mm). The lower galena bearing horizons appear to be slightly more coarse grained. The quartz grains in mineralized sandstone are characterized by secondary silica overgrowths which form straight edge boundaries with galena (Fig. 47.4).

Quartz grains comprise between 70 and 85% of the sandstone, with the matrix consisting mostly of clay minerals and microcrystalline quartz. Minor feldspar in the form of isolated microcline grains is also present and is distinctive by

Table 47.1. Clay composition relative to depth of hole and Pb content

Sample	Kaolinite/Chlorite	%Pb
51-18	1.62	0.25
51-20	1.47	1.10
248-5	1.18	0.15
248-13	2.5	1.86
248-18	2.35	1.2
248-21	1.9	?
251-11	0.86	NM
251-26	1.25	<1.0
251-46	2.34	1.32
251-55	3.37	7.40
263-30	2.16	NM
263-41	2.75	1.83
263-51	2.79	7.41
268-8	1.67	NM
268-10	3.67	1.9
272-27	1.17	<2.0
272-29	3.08	13.58
283-16	4.68	1.44
283-22	5.56	6.52
283-26	2.70	1.0
303-15	1.02	NM
303-79	2.28	<1.0
303-88	3.31	5.0
352-140	1.15	NM
352-145	1.62	0.3
352-148	1.83	2.5
354-131	0.71	NM
354-146	1.24	1.8
354-152	4.62	4.52
363-53	0.95	NM
363-100	0.66	NM
363-141	1.31	<1.0
363-155	1.55	1.05
363-160	1.86	2.0

First column to the left is the hole number followed by the depth of the sample in metres. The middle column is the kaolinite/chlorite ratio measured by peaks of X-Ray diffraction patterns; the peaks for the kaolinite (002) and chlorite (004) values are at approximately 25 degrees. The column to the right is the percentage of lead; NM denotes non-mineralized or very minor mineralization.

its weathered appearance with no well defined grain boundaries (Fig. 47.5). The borders of microcline grains are commonly replaced by carbonate or clay minerals. Muscovite also occurs, forming isolated large sinuous blades up to 3 mm long which overprint the matrix (Fig. 47.6). Minor gypsum is found near the base of the sandstone sequence. Preliminary petrographic and SEM investigations on polished thin sections from the west zone indicate that barite occurs with galena in the sandstone (Fig. 47.7); however, this association appears to be erratic and further work is needed to assess the importance of barite at Yava.

The presence of carbonate is also erratic but appears to be most prominent with coal where it forms a matrix to quartz and sulphide grains. Calcite is most noticeable under cathode ray luminescence where in some sections it appears as a matrix to detrital quartz grains. It is also present as a late stage occurrence in the interstices of quartz grains with secondary overgrowths.

CLAY MINERALOGY

The petrography of sandstone at Yava suggests that the sandstone high in the stratigraphic sequence has proportionately more green clay occupying pore space, and consequently is more chlorite rich than the grey galena-bearing sandstone at the base of the sequence. Research was initiated to investigate variations in clay mineralogy in mineralized versus unmineralized sandstone to detect compositional trends which could correlate with the abundance of galena. i.e. could the clay composition in sandstone be related to galena distribution? As a result of this investigation, powders of clay material from sandstone were made and subsequently analyzed by X-ray diffractometer at the Geological Survey of Canada.

Scott (1980) determined from analyses that the clay content of the sandstones is between 75 and 90% kaolinite, with lesser amounts of illite, chlorite and montmorillonite. Scott, however, did not report any systematic compositional variations in clay compositions within the deposit. The analyses done for this study (Table 47.1) showed that, of 34 samples in 11 drill holes examined, 10 of the 11 holes demonstrated an increase in the kaolinite/chlorite ratio sympathetic with an increase in the lead content down the hole into mineralized sandstones (the eleventh hole was inconclusive due to an insufficient number of samples). Although the kaolinite/chlorite ratio changes were not quantitatively proportional to the variation in lead content, the changes generally correlated. The results suggest that kaolinite is the dominant clay mineral in the lower grey mineralized portion of the sandstone and that chlorite is associated with the unmineralized upper green sandstone.

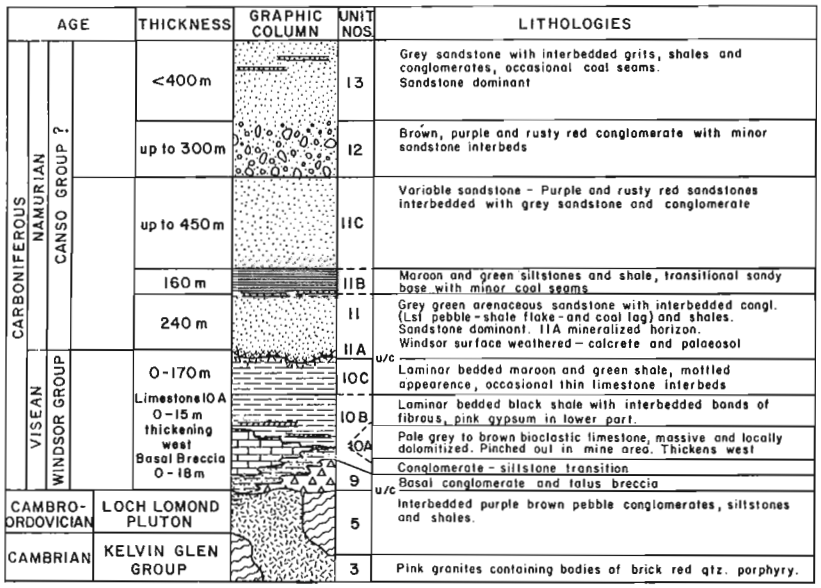

Figure 47.2

Stratigraphy in the Salmon River sub-basin (from Bonham, 1982). Note that the Loch Lomond pluton is a composite pluton consisting of both Cambrian and Devonian phases (Barr et al., this volume).

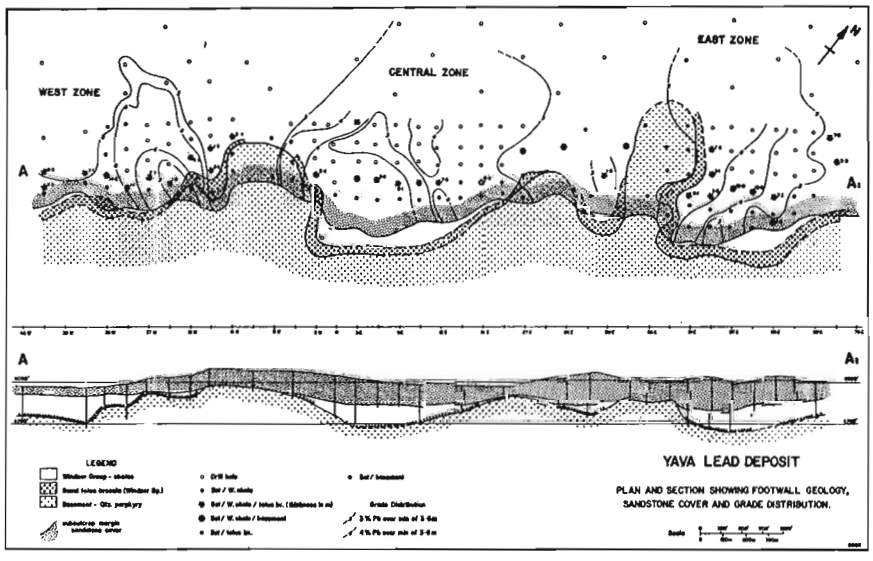

Figure 47.3

Map and longitudinal section of the Yava deposit (from Bonham, 1982).

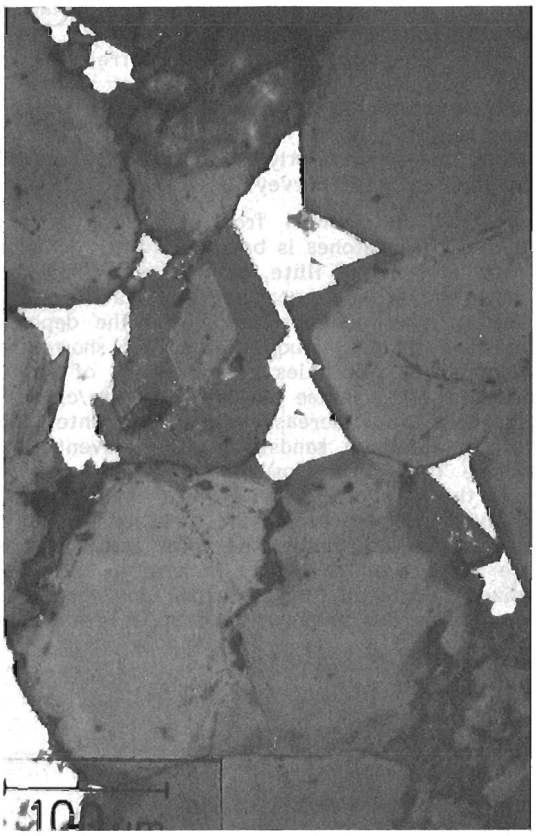

Figure 47.4. *Straight-edge contacts between galena and silica overgrowths on detrital quartz grains. Bar scale is 100 μm.*

Figure 47.6. *Large muscovite grain in host rock sandstone. Bar scale is 0.5 mm.*

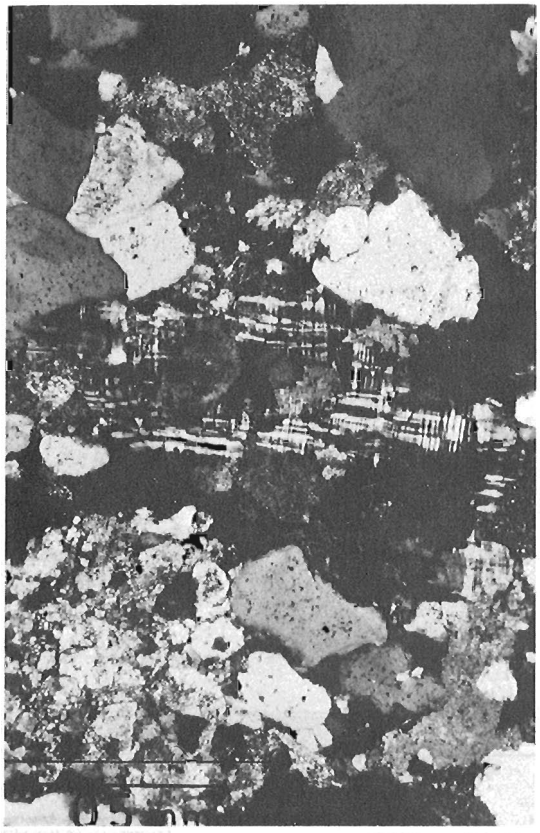

Figure 47.5. *Weathered feldspar grain with carbonate and clay minerals at grain boundaries. Bar scale is 0.5 mm.*

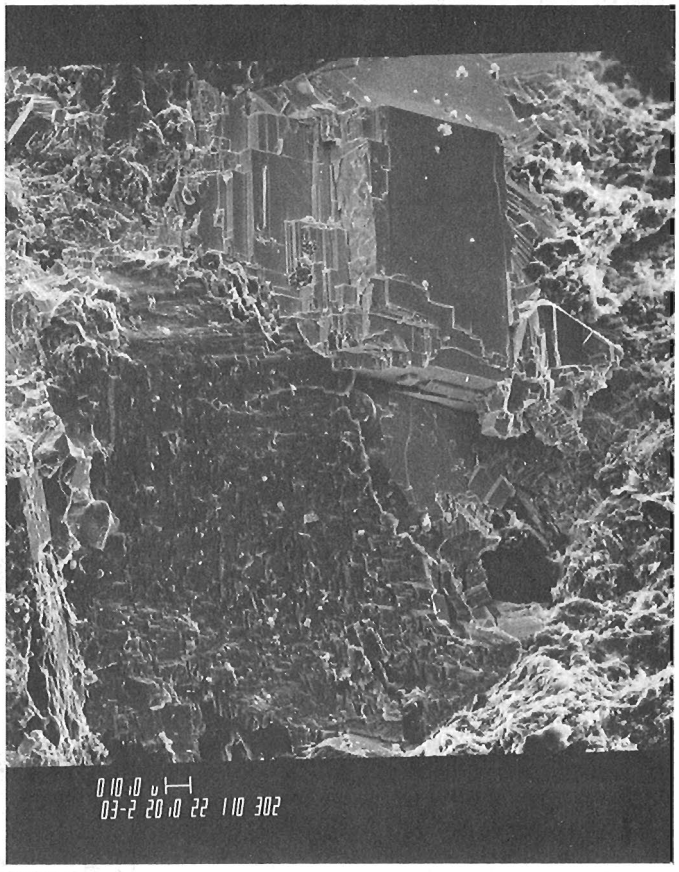

Figure 47.7. *Scanning electon photomicrograph of barite (large grain occupying lower left quadrant) in contact with galena (upper centre). Irregular-textured mineral on right is kaolinite.*

The X-ray diffraction traces also showed that illite increased proportionately to chlorite as a function of lead content; however, the results are not as consistent as the kaolinite/chlorite ratios, and further work is needed.

SULPHIDE PETROGRAPHY IN SANDSTONE

The sulphide mineral assemblage at Yava consists of galena, pyrite and spalerite, with rare chalcopyrite. Galena is the dominant sulphide mineral and occurs mostly as disseminations in granular sandstone in the form of parallel bands, crossbeds, ripple sets, roll fronts or circular clusters. Other forms such as cusps, wisps and arrowheads are reported by Bonham (1982).

In thin section, galena occurs mostly as anhedral grains up to 0.4 mm but averages 0.2 mm. The grains, which partially to wholly fill pore spaces, are interstitial between clastic quartz grains and clay silicate matrix. Generally, galena appears as isolated grains but these may also coalesce to form an interconnected pattern within the sandstone. In areas of galena mineralization, quartz grains have secondary silica overgrowth features and galena typically forms straight edge boundaries with the overgrowths. This form of mineralization is characterized by re-entrant angles between galena and the overgrowths. It is also common for galena to have irregular outlines where it is not bounded by quartz overgrowths (Fig. 47.8). Galena may contain inclusions of pyrite or sphalerite although, more commonly, the inclusions are small concentrations of clay material.

Pyrite is present in the sandstone sequence though it is much less abundant and more local than the galena. Pyrite is found most commonly as isolated patches in the sandstone and, in places, may be associated with galena. In the unmineralized sandstone above the galena bearing horizons, pyrite characteristically appears as clusters up to 2 cm in diameter in an otherwise barren green sandstone.

Petrographically, the mineralization style for pyrite is usually more intensive than galena; where present, pyrite acts as a cement supporting individual clastic grains appearing as islands (Fig. 47.9). The pyrite cement may occur as a homogeneous mass but usually has a fractured appearance with numerous disaggregated and broken grains, an occurrence most favourable for galena and sphalerite replacement.

Carbonate occurrence is also generally more abundant in sandstone near pyrite than galena; however, this occurrence is not ubiquitous. In general, calcite is more noticeable with pyrite near coal.

Sphalerite is not visible in hand specimen but, when seen microscopically, is usually associated with pyrite or galena and only rarely as individual grains. It is generally not abundant in the sandstone and does not represent more than 5 to 10% of total sulphide content. Within masses of galena, sphalerite occurs mostly as well defined anhedral inclusions from 0.05 mm to 0.2 mm (Fig. 47.10). Sphalerite is most abundant with galena where silica overgrowths on quartz grains are relatively insignificant and where galena forms irregular anhedral masses instead of straight edge contacts with quartz. Sphalerite also occurs as inclusions in pyrite but is more typical as a replacement along grain boundaries or margins of fractured pyrite grains.

Figure 47.8. *SEM photomicrograph (back scatter) of galena (light) in interstices of quartz grains (dark). Bright, square pyrite grain in upper centre.*

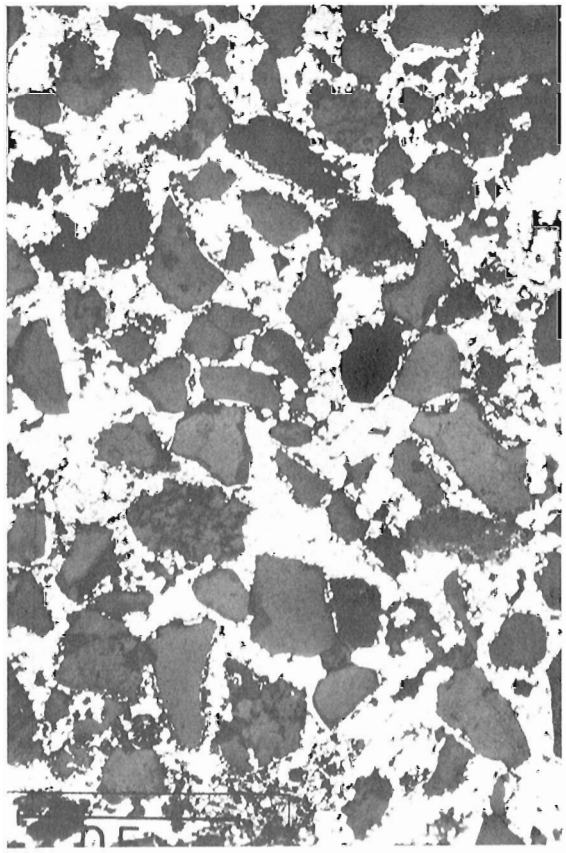

Figure 47.9. *Detrital quartz grains (dark) completely cemented with pyrite (light). Bar scale is 0.5 mm.*

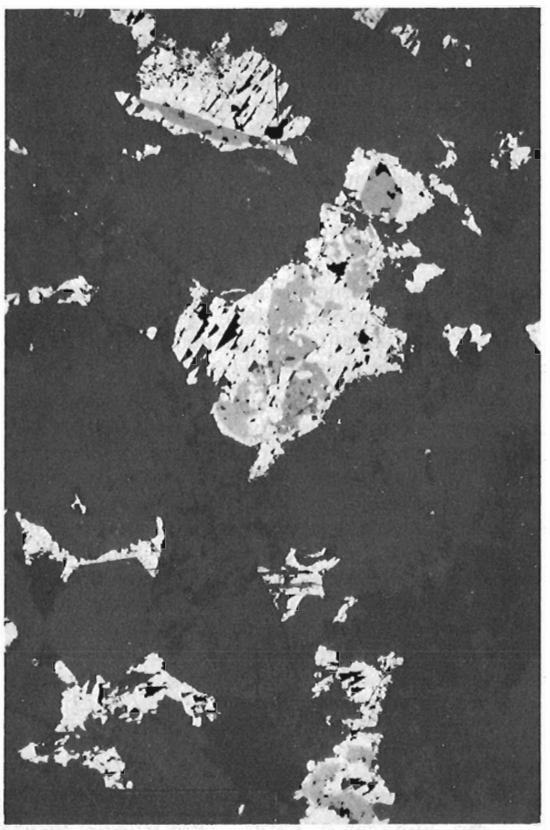

Figure 47.10. *Irregular sphalerite inclusions (light grey) in galena (light). Bar scale (lower left) is 0.5 mm.*

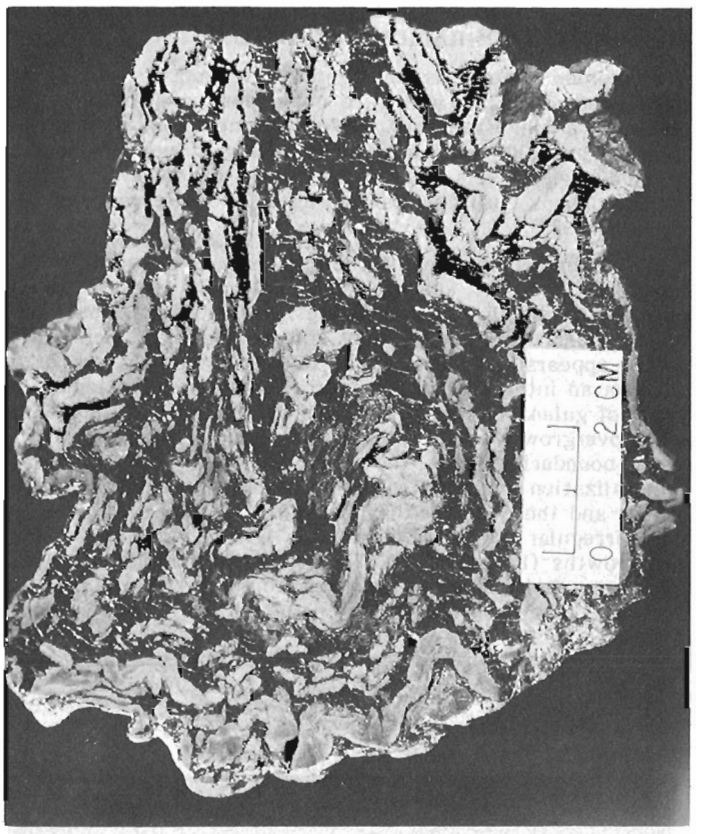

Figure 47.12. *Pyrite- "coal" aggregate. Light-coloured irregular masses consist of pyrite replacing woody material in which the cellular structure is still preserved. Black areas are masses of high-reflectance "coal". Note galena-filled cleats in "coal".*

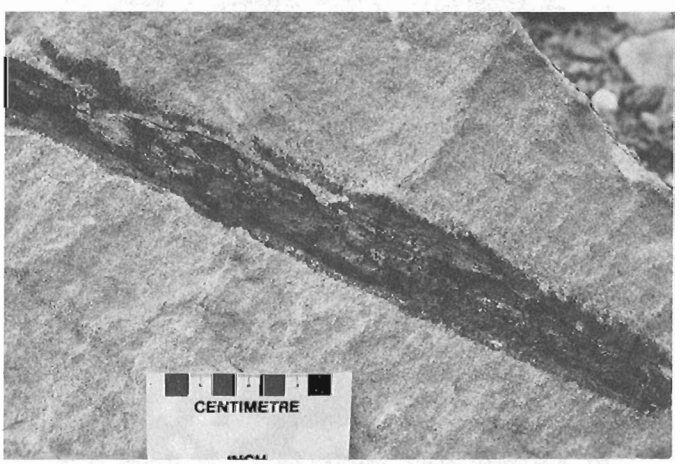

Figure 47.11. *Partly silicified branch(?) surrounded by incomplete "crust" of pyrite.*

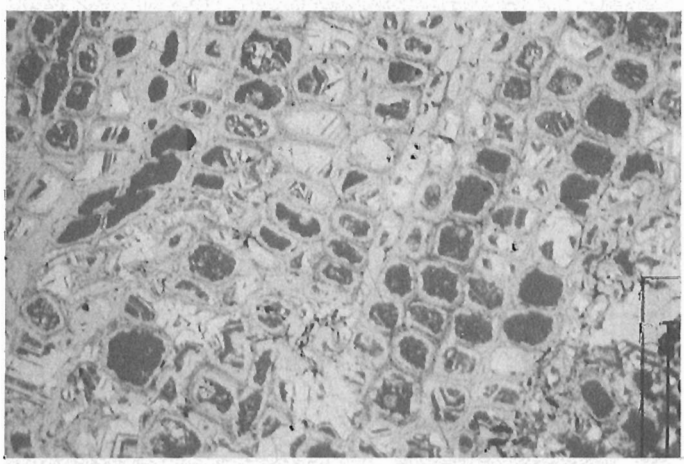

Figure 47.13. *Pyrite (light grey) and sphalerite (dark) within wood cells; galena (white) replaces cell walls. Bar scale is 100 μm.*

SULPHIDE PETROGRAPHY IN COAL

The coal at Yava has special significance because it occurs in the form of randomly oriented tree fragments or logs around, and in which, there is abundant galena and pyrite (Fig. 47.11). Although mineralization in coal represents only 15% of total sulphide content at Yava (Bonham, 1982), it is nevertheless important because it contributes to the understanding of paragenesis and shows some important mineral relationships.

Sulphide minerals usually occur as amorphous patches or lenticular to boudin forms throughout the coal fragments, a feature probably attributable to compaction (Fig. 47.12). Pyrite, the most abundant sulphide mineral, followed by galena and sphalerite, appears as an early phase after which other sulphide minerals were emplaced.

Petrographically, mineralization textures range from open cellular fill to deformed or cataclastic and fractured. In the cellular fill mineralization, a network of near-circular cells are filled with a pyrite core surrounded by galena (Fig. 47.13). Cell cavities that are not sulphide-bearing are usually filled with silica. Where galena is not surrounding each cell, it occurs as thin veins running through the cell structure. The pyrite core may be in various stages of replacement by galena or, more commonly, sphalerite. In early stages of replacement, sphalerite occurs as thin bands 0.01 mm thick forming geometric growth zones within each cell in the pyrite groundmass (Fig. 47.14). The sphalerite growth bands are oriented independently of the cavity walls or the galena surrounding the cell and appear to have grown as a separate phase. Sphalerite also serves as a groundmass for isolated pyrite framboids, spherical clusters of pyrite grains from 0.01 to 0.05 mm in diameter. When replacement is in an advanced stage, the entire pyrite core may be replaced by sphalerite.

The more deformed coal has a different mineralization style, as the replacement of pyrite is more extensive. Coal material is crushed and fractured, leaving broken fragments and contorted remnants of coal and coal cells. Galena replacement is more pervasive, it forms envelopes around pyrite patches where the coal cells may only remain as faint outlines or are nonexistent. In the most deformed areas, there are no visible cell cavities. Galena is also widespread filling fractures and cleats in coal.

Sphalerite replacement varies greatly but appears to be mostly in the heavily fractured areas along the margins of galena-filled cleats and fractures (Fig. 47.15). Sphalerite also occurs in the outer areas of galena envelopes surrounding pyrite.

Not all coal is mineralized; in the upper non-galena bearing sandstone where coal is much less abundant, it is not silicified and is characterized by an absence of sulphide minerals.

Paragenesis

On the basis of ore mineralogy and relationships between grains, a paragenetic sequence would begin with early diagenetic pyrite in coal and locally reduced areas in the sandstone. Near coal, carbonate also appears to have precipitated early. Sphalerite in coal and sandstone formed in associated with the pyrite as inclusions and, in places, as groundmass.

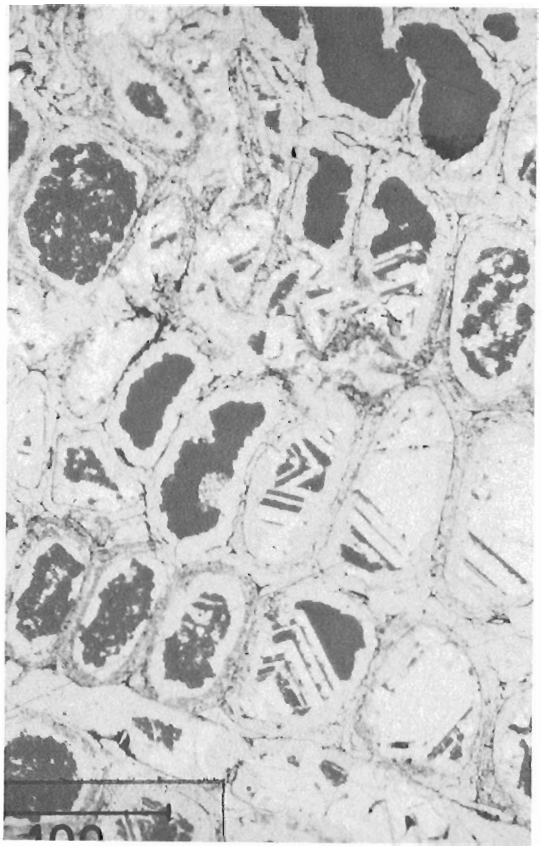

Figure 47.14. *Pyrite (light grey) and sphalerite (dark) alternating in growth zones within wood cells. Cell walls replaced by galena. Bar scale is 100 μm.*

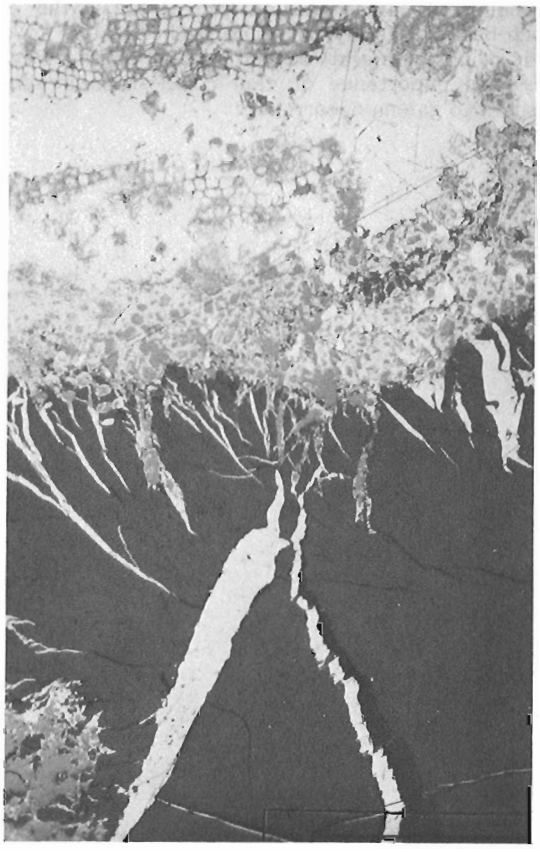

Figure 47.15. *Galena-filled cleats in coal (dark). Note main mass of cellular-textured portion of photo is filled with pyrite; sphalerite fills cells near edge of woody material and galena replaces cell walls. Sphalerite also partially extends into galena-filled cleats. Bar scale is 0.5 mm.*

Silica overgrowths on quartz grains as well as the silicification of coal fragments followed the early pyrite and sphalerite and marked the beginning of the major mineralizing event. Galena shortly postdated the secondary overgrowths, occurring in the available pore space and in reaction with earlier sulphide stages. Barite, where present, occurred contemporaneously with galena. As a final phase, carbonate cement filled in some unoccupied pore spaces and sphalerite also occurred in reaction with earlier galena.

CONCLUSIONS

The sandstone at Yava is remarkably uniform in composition, texture and mineralization style. Galena is the dominant sulphide mineral and is related to the distribution of secondary silica, the clay composition and grain size of the sandstone, as well as the occurrence of silicified coal. However, it is difficult to determine if the features related to galena occurrence are the result of diagenesis or were controls to mineralization.

For a better understanding of the mineralization process, future petrography must consider regional aspects of galena occurrence in the Salmon River sub-basin. Terra Nova, a deposit similar to Yava, has proportionately more sphalerite than Yava and is the only indication of metal zonation in the area. Beyond the deposit, the coal in unmineralized sandstone is not silicified; identifying a "silica line" between coals in mineralized and unmineralized sandstone would be helpful in delineating the extent of galena occurrence as well as determining the significance of silicification. Southwest of Yava, Windsor carbonates in contact with basement rocks contain galena and the study of its occurrence in these rocks would also contribute to the understanding of mineralization processes in the Salmon River sub-basin. Finally, it would be instructive to expand the study of clay minerals beyond the immediate Yava area to assess the importance of clay composition in sandstone with respect to galena occurrence.

REFERENCES

Barr, S.M., Sangster, D.F., and Cormier, R.F.
1984: Petrology of Early Cambrian and Devono-Carboniferous intrusions in the Loch Lomond complex, southeastern Cape Breton Island Nova Scotia; in Current Research, Part A, Geological Survey of Canada, Paper 84-1A, Report 29.

Belt, E.S.
1968: Carboniferous continental sedimentation, Atlantic Provinces, Canada; in Geological Society of America, Special Paper 106, ed. G. De V. Kelvin, p. 127-176.

Bjørlykke, A. and Sangster, D.F.
1981: An overview of sandstone-lead deposits and their relation to red-bed copper and carbonate-hosted lead-zinc deposits; Economic Geology, 75th Anniversary Volume, 1981. p. 179-213.

Blatt, H.
1982: Sedimentary Petrology; W.H. Freeman and Company, San Francisco, 564 p.

Bonham, O.
1982: Geology of the Yava sandstone-lead deposit, Cape Breton, Nova Scotia, unpublished MSc. thesis, Dalhousie University, Halifax, Nova Scotia, 181 p.

Hacquebard, P.A.
1972: The Carboniferous of eastern Canada; International Stratigraphie Géologie du Carbonifère Congress, Trefeld, Compte Rendu, v. 1, p. 69-90.

Hutcheon, I.
1983: Aspects of the diagenesis of coarse grained siliciclastic rocks; Geoscience Canada, v. 10, no. 1, p. 4-14.

Scott, P.
1980: Geochemistry and petrography of the Salmon River lead deposit, Cape Breton Island, Nova Scotia; Unpublished MSc. thesis, Acadia University, Wolfville, Nova Scotia, 111 p.

48. EARLY CRETACEOUS DEPOSITS IN THE GAYS RIVER LEAD-ZINC MINE, NOVA SCOTIA

Project 810033

E.H. Davies, S.O. Akande[1], and Marcos Zentilli[2]
Atlantic Geoscience Centre, Dartmouth

Davies, E.H., Akande, S.O., and Zentilli, M., Early Cretaceous deposits in the Gays River lead-zinc mine, Nova Scotia; in Current Research, Part A, Geological Survey of Canada, Paper 84-1A, p. 353-358, 1984.

Abstract

Pollen and spore analyses of six samples of semiconsolidated sediments from the Gays River mine suggest their age is Aptian to possibly Early Albian. These sediments, previously interpreted as Pleistocene deposits, clearly postdate lead-zinc mineralization, provide further evidence of a widespread pre-Aptian weathering (and karstification) episode in Atlantic Canada, and constitute a local record of post-mid Cretaceous deformation and coalification.

Résumé

L'analyse de pollens et de spores dans six échantillons de sédiments semi-consolidés provenant de la mine de Gays River indique que ces sédiments datent de l'Aptien ou peut-être de l'Albien inférieur. Ces sédiments, antérieurement interprétés comme étant des dépôts pléistocènes, ont été déposés après la minéralisation en plomb-zinc; ils fournissent un autre indice de l'existence d'une importante période pré-aptienne d'altération (et de karstification) dans l'Atlantique canadien, ainsi qu'un antécédent local de la déformation et de la houillification qui a eu lieu après le Crétacé moyen.

INTRODUCTION

Semiconsolidated sediments, previously believed to be Pleistocene glacial till in sinkholes (MacEachern and Hannon, 1974; Hannon, 1980), have been intersected by drilling and underground workings at the Gays River mine and have been the source of mining engineering problems. Six samples of this material have been palynologically analyzed to determine the age, and one sample has been analyzed for vitrinite reflectance.

The Gays River lead-zinc ore deposit, owned and operated until 1982 by Imperial Oil Ltd. and Cuvier Mines Ltd. (Hannon, 1980), is located 65 km NE of Halifax and 10 km SE of the village of Shubenacadie, at latitude 45°02'north, longitude 63°22'west in central mainland Nova Scotia (Fig. 48.1). The deposit lies within a sequence of carbonates and evaporites, part of the Lower Carboniferous Windsor Group (Bell, 1958; MacEachern and Hannon, 1974; Hannon, 1980). It overlies a paleotopographic high of the crystalline basement, which separates what have been called the Shubenacadie and Musquodoboit depositional basins (Fig. 48.1; Hannon, 1980; Boehner, 1981; Giles and Boehner, 1982). The mineralization consists of stratiform and discordant orebodies within a dolomitized carbonate reef complex of Early Mississippian age (MacEachern and Hannon, 1974; MacLeod, 1975a,b; Hannon, 1980; Akande, 1982; Akande and Zentilli, 1983).

Cretaceous sediments have been reported in the Musquodoboit River valley and in the vicinity of the village of Shubenacadie (Stevenson and McGregor, 1963; Lin, 1971) and have been mapped by Giles and Boehner (1982). Studies by King et al. (1970), and King (1970) indicate the presence of well-stratified Cretaceous deposits beneath the central and eastern portions of the Scotian shelf. However, the full areal extent and stratigraphy of the Cretaceous deposits of Nova Scotia is still poorly known. Ongoing palynological studies, in conjunction with a survey by the Nova Scotia Department of Mines and Energy, suggest that there are numerous isolated deposits of Cretaceous age in southern Cape Breton and mainland Nova Scotia north of St. Margarets Bay.

SAMPLE LOCATION AND SELECTION

All of the samples examined for the presence of pollen and spores were collected from accumulations of semiconsolidated sediments referred to collectively as "trench" material. The term "trench" was used by the mine geologists to describe the long, narrow, sinuous, sediment-filled karstic ditch at the carbonate/evaporite contact within the Gays River mine. This "trench" roughly follows the strike length of the northeasterly trending orebody (Fig. 48.2) and consists of gravels, sand, silt, clay, and minor coaly materials. The sediments are semiconsolidated, water-saturated and commonly occur in close proximity, or directly overlie, the high grade parts of the sulphide deposit; this has been the source of many mining difficulties during exploitation, such as unstable ground and flooding, which may have contributed to the premature closure of the mine.

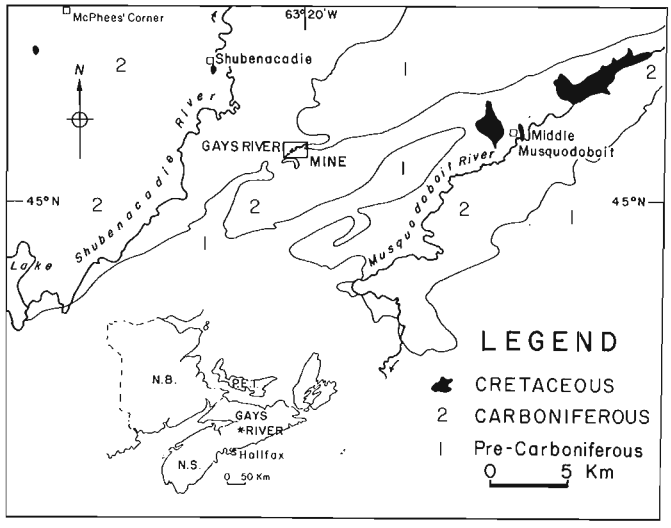

Figure 48.1. Distribution of Cretaceous sediments on central Mainland Nova Scotia (after Giles and Boehner, 1982), showing the location of the Gays River mine.

[1] Department of Geology and Mineral Sciences, University of Ilorin, Ilorin, Nigeria
[2] Department of Geology, Dalhousie University, Halifax, Nova Scotia B3H 3J5

Plate 48.1

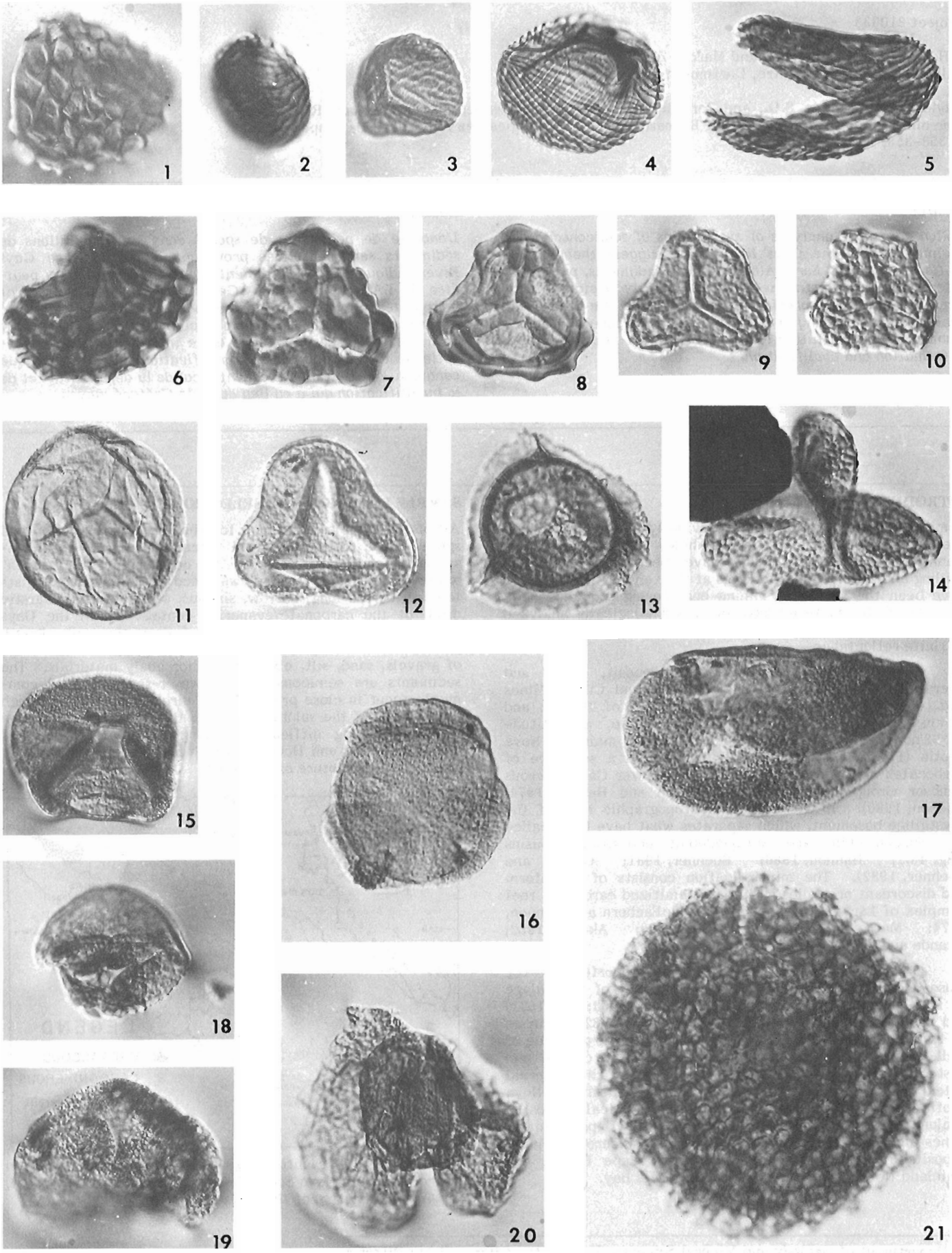

Four samples of the semiconsolidated sediments were collected from 2 drillholes at specific localities in the mine (Fig. 48.2). Three of these samples: DH2-324, DH2-372 and DH2-409 were collected from a dewatering-hole DH2 at footages 324 ft., 372 ft., and 409 ft. respectively. The fourth sample AGR 285-230 was taken from hole 285 at footage 230 ft. An additional sample of similar material was collected underground by R. Grantham of the Nova Scotia Museum, where mining had exposed the semiconsolidated sediments. Another sample (AGR 107A) of coaly material in the "trench" sediments was collected at a specific co-ordinate within the mine workings. Sample locations, and the results of palynological analyses of these semiconsolidated sediments are given in Table 48.1 and several species are illustrated in Plate 48.1.

DISCUSSION

Palynological analyses of the semiconsolidated sediments from the Gays River mine reveal the presence of abundant well preserved spore and pollen assemblages of Aptian-Early Albian age. These assemblages are closely comparable to pollen and spore assemblages found within the **Subtillisphaera perlucida** Zone and **Spinidinium vestitum** Zone of offshore Eastern Canada (Williams, 1975; Bujak and Williams, 1978) as well as Zone I of the onshore middle Atlantic States (Brenner, 1963) and the **Auritulinasporites deltaformis-Cerebropollenites mesozoicus** Assemblage Zone of the mid-Atlantic outer continental shelf of the U.S.A. (Bebout, 1981). Tertiary and Quaternary pollen were not found in these sediments. This strongly suggests that the semiconsolidated sediments are of Early Cretaceous age and not Pleistocene as

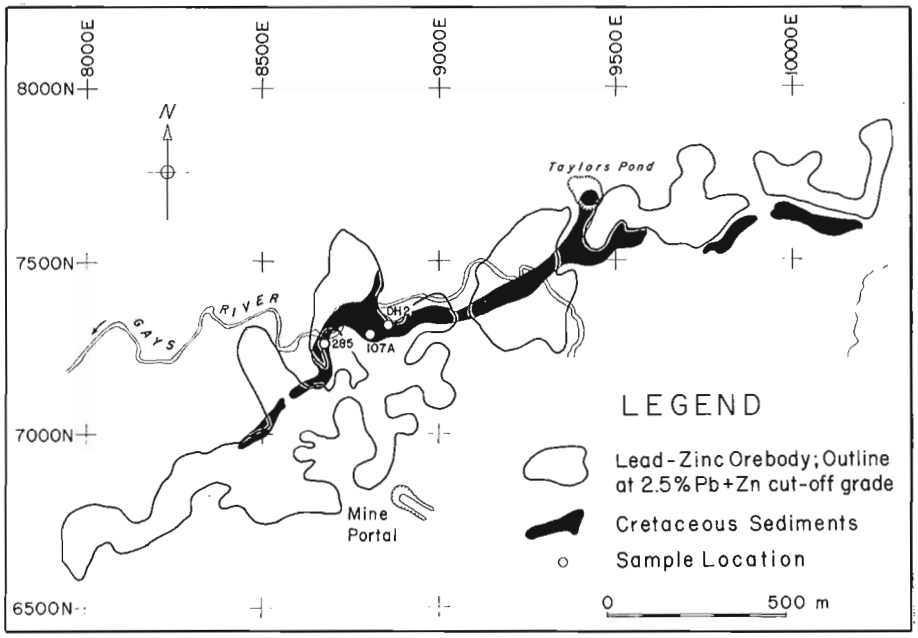

Figure 48.2

Map of the Gays River mine outlining the orebody and Cretaceous sediments in the "trench" system.

Plate 48.1

1. **Klukisporites areolatus,** P19972, GR-5, L45/2, GSC76590.
2,3. **Cicatricosisporites** sp. A, 2) P19715, J49/1, GSC76591; 3) P19974, GR-2, K36/4, GSC76592.
4. **Cicatricosisporites potamacensis,** P19715, T43/0, GSC76593.
5. **Cicatricosisporites exilioides,** P19974, GR-2, D44/4, GSC76594.
6. **Ischyosporites estherae,** P19974, GR-2, G33/3, GSC76595.
7. **Trilobosporites crassus,** P19974, GR-2, Q36/0, GSC76596.
8. **Trilobosporites trioreticulatus,** P19974, GR-2, T43/4, GSC76597.
9. **Trilobosporites purverulentus,** P19972, GR-5, E43/0, GSC76598.
10. **Impardecisporites apiverrucatus,** P19974, GR-2, U38/3, GSC76599.
11. **Calamospora** sp. A., P19970, GR-3, F36/0, GSC76600.
12. **Concavissimisporites punctatus,** P19974, GR-2, T41/0, GSC76601.
13. **Aequitriradites verrucosus,** P19974, GR-2, K41/0, GSC76602.
14. **Concavissimisporites variverrucatus,** P19974, GR-2, C47/1, GSC76603.
15. **Phyllocladidites microreticulatus,** P19974, GR-2, W36/2, GSC76604.
16. **Callialasporites trilobatus,** P19971, GR-4, E44/4, GSC76605.
17. **Parvisaccites amplus,** P19974, GR-2, K46/0, GSC76606.
18. **Parvisaccites rugulatus,** P19974, GR-2, K40/0, GSC76607.
19. **Abietineaepollenites microreticulatus,** P19972, GR-5, E40/1, GSC76608.
20. **Podocarpidites radiatus,** P19971, GR-4, K46/4, GSC76609.
21. **Schizosporis reticulatus,** P19974, GR-2, L47/0, GSC76610.

Table 48.1. Palynological analysis of the semiconsolidated "trench" samples, Gays River mine

Sample Number	Co-ordinates	Description	Pollen and Spores	Age
AGR 107A	7275.5N 8809.6E	Lignite	No palynomorph, contain resinous material	Cretaceous (P. Hacquebard, personal communication)
AGR 285-230	7245.25N 8691.98E	Semiconsolidated clay, sand and pebbles	**Abietineaepollenites microreticulatus** Brenner **Acquitriradites verrucosus** (Cookson and Dettmann) Dettmann **Cicatricosisporites potomacensis** (Brenner) **Cicatricosisporites exilioides** (Maljavkina) Bolchovitina **Cicatricosisporites venustus** **Concavissimisporites punctatus** Delcourt and Sprumont **Concavissimisporites variverrucatus** (Couper) Brenner **Impardecispora apiverrucata** (Couper) Venkatachela et al. **Ischyosporites estherae** Deak **Parvisaccites rugulatus** Brenner **Phyllocladidites microreticulatus** Brenner **Trilobosporites crassus** Brenner **Trilobosporites trioreticulatus** Cookson and Dettman	Late Aptian-Early Albian
DH2-324	7301.5N 8860.0E	Semiconsolidated clay, sand and pebbles	**Todisporites major** Couper **Calamospora** sp. A **Densoisporites microrugulatus** Brenner	I ate Jurassic-Farly Cretaceous associated with reworked Carboniferous probably Mid-Visean (M.S. Barss, personal communication)
DH2-372	7301.5N 8860.0E	Semiconsolidated clay, sand and pebbles	**Alisporites bilateralis** (Rouse) **Podocarpidites radiatus** Brenner **Callialasporites trilobatus** Balme	Late Jurassic-Early Cretaceous
DH2-409	7301.5N 8860.0E	Semiconsolidated clay, sand and pebbles	**Alisporites bilateralis** **Alisporites grandis** (Cookson) Dettmann **Cicatricosisporites delicatus** **Klukisporites areolatus** (Singh) **Parvisaccites amplus** Brenner **Parvisaccites radiatus** Brenner **Podocarpidites potomacensis** **Trilobosporites purverulentus** (Verbitskaja) Dettmann **Trilobosporites trioreticulatus**	Aptian
P 19715	-	Semiconsolidated clay, sand and pebbles	**Alisporites bilateralis** **Appendicisporites cristatus** (Markova) Pocock **Cicatricosisporites delicatus** **Cicatricosisporites** sp. A **Impardecisporites apiverrucatus** **Klukisporites areolatus** **Parvisaccites amplus** **Trilobosporites purverulentus**	Aptian

previously thought by Hannon (1980). Samples DH-324 and DH-372 contained impoverished Late Jurassic to Early Cretaceous assemblages associated with reworked Carboniferous palynomorphs, probably mid-Visean (M.S. Barss, personal communication). The reworked palynomorphs were probably derived locally from the host rock.

Vitrinite reflectance analyses were performed on the coaly materials associated with the sediments, and an average R_o value of 0.44 and a standard deviation of ± 0.03 was obtained. This suggests a lignitic rank for the coaly particles and is compatible with a Cretaceous age (P.A. Hacquebard, personal communication). This lignite is barren of palynomorphs although it contains abundant resinous material. The sample has attained a higher degree of maturation than lignite reported in the Cretaceous Shubenacadie clay pit (R_o, 0.28 ± 0.04) about 10 km north of the Gays River property (Hill, 1976); this might be related to a slightly higher geotemperature regime in proximity to the area of mineralization (P.A. Hacquebard, personal communication).

The carbonate/evaporite contact which controls the location of the "trench" displays slickensides with near-horizontal plunge (10-15°). The "trench" sediments show evidence of plastic deformation, with "boudins" expressing a north-south stretching component. Although the "trench" outline commonly follows faults controlling massive sulphide veins, the semiconsolidated sediments are not mineralized. This clearly indicates that the "trench" sediments postdate the post-Visean to pre-Aptian lead-zinc mineralization. Deformation, evidently, has been active in Mesozoic and later times, and may have contributed to the higher R_o values in the Gays River mine.

The Cretaceous sediments identified in the Gays River mine were deposited on a Cretaceous erosional surface and preserved in karst features controlled by pre-existing faulting and lithological contrasts. During the early stages of exploration at Gays River, MacLeod (1975a,b) identified in drill core zinc-rich layers directly underlying the karstic sediments. He interpreted these layers as being residual concentrations of sphalerite resulting from the selective dissolution of the host carbonates. Our work (e.g. Akande, 1982) does not rule out this interpretation, although it de-emphasizes its metallogenic importance. In fact, this pre-Aptian weathering and karstification episode nearly obliterated the mineralization at Gays River and presumably had some effect on other near-surface deposits at the time. Similarly, pre-Late Cretaceous weathering under a warm, humid climate has been held responsible for widespread bedrock decay and laterite formation in the Atlantic coastal region as far south as Long Island, New York (Blank, 1978) and as far north as Labrador (Gross, 1968), where it was responsible for residual enrichment of (otherwise uneconomic) iron formation.

For metallogenic research, exploration and development purposes, it is important to understand the timing and effects of laterization, possible supergene enrichment, karstification, infilling and subsequent deformation on similar mineral deposits in the region.

ACKNOWLEDGMENTS

The authors extend their gratitude to Imperial Oil Ltd. and Cuvier Mines Ltd. for allowing the sampling within the mine. This paper reports on part of the recently completed Ph.D. thesis at Dalhousie University by S.O. Akande, while supported by a scholarship from the Federal Government of Nigeria and NSERC operating grant (A-9036) to M. Zentilli. R. Grantham of the Nova Scotia Museum supplied one of the samples, and P. Ascoli and A.C. Grant of the Geological Survey of Canada read the manuscript and offered constructive criticism.

REFERENCES

Akande, S.O.
1982: Genesis of the lead-zinc mineralization at Gays River, Nova Scotia, Canada: a geologic, fluid inclusion and stable isotopic study; unpublished Ph.D. thesis, Dalhousie University, Halifax, Nova Scotia, 348 p.

Akande, S.O. and Zentilli, M.
1983: Genesis of the lead-zinc mineralization at Gays River, Nova Scotia, Canada; in International Conference on Mississippi Valley Type Lead-Zinc Deposits, Proceedings Volume, ed. G. Kisvarsanyi, S.K. Grant, W.P. Pratt, and J.W. Koenig; University of Missouri – Rolla, Rolla, Missouri, p. 546-557.

Bebout, J.W.
1981: An informal palynologic zonation for the Cretaceous system of the United States Mid-Atlantic (Baltimore Canyon Area) outer continental shelf; Palynology, v. 5, p. 154-194.

Bell, W.A.
1958: Possibilities for occurrence of petroleum reservoirs in Nova Scotia; Nova Scotia Department of Mines, Report, 177 p.

Blank, H.R.
1978: Fossil laterite on bedrock in Brooklyn, New York; Geology, v. 6, p. 21-24.

Boehner, R.C.
1981: Stratigraphy and depositional history of marine evaporites in the Lower Carboniferous Windsor Group, Shubenacadie and Musquodoboit structural basins, Nova Scotia, Canada; Nova Scotia Department of Mines and Energy, Open File Report 468, 28 p.

Brenner, G.J.
1963: The spores and pollen of the Potomac Group of Maryland; Maryland Department of Geology, Mines, Water Resources, Bulletin 27, 215 p.

Bujak, J.P. and Williams, G.L.
1978: Cretaceous palynostratigraphy of offshore south-eastern Canada; Geological Survey of Canada, Bulletin 297, 19 p.

Giles, P.S. and Boehner, R.C.
1982: Geological map of the Shubenacadie and Musquodoboit Basins; Nova Scotia Department of Mines and Energy, Map 82-4.

Gross, G.A.
1968: Geology of iron deposits in Canada: Volume III, Iron Ranges of the Labrador Geosyncline; Geological Survey of Canada, Economic Geology Report 22, 179 p.

Hannon, P.
1980: Gays River Lead-zinc deposit; in Trip 6: Mineral Deposits and Mineralogenic Provinces of Nova Scotia, ed. A.K. Chatterjee, S. Forgeron, P. Hannon, A. Hudgins, G. Isenor, B. McNabb, C. Miller, H.R. Oldale, J.M. Patterson, and E. Stewart; Halifax '80, Geological Association of Canada/Mineralogical Association of Canada Field Trip Guidebook, p. 74-79.

Hill, G.T.
1976: Mineralization and coal petrology of the Shubenacadie clay deposit, Nova Scotia; unpublished B.Sc. thesis, Dalhousie University, Halifax, Nova Scotia, 97 p.

King, L.H., Maclean, B., Bartlett, G.A., Jeletzky, J.A., and Hopkins, N.S. Jr.
1970: Cretaceous strata on the Scotia Shelf; Canadian Journal of Earth Sciences, v. 7, p. 145-155.

King, L.H.
1970: Surficial geology of the Halifax Sable Island map area; Marine Sciences Branch, Department of Energy, Mines and Resources, Paper 1, 16 p.

Lin, C.L.
1971: Cretaceous Deposits in the Musquodoboit River Valley, Nova Scotia; Canadian Journal of Earth Sciences, v. 8, p. 1152-1154.

MacEachern, S. and Hannon, P.
1974: Gays River lead-zinc deposit: a Mississippi Valley Deposit; Canadian Institute of Mining and Metallurgy, Bulletin, v. 63, p. 61-66.

MacLeod, J.L.
1975a: Diagenesis and sulfide mineralization at Gays River, Nova Scotia; unpublished B.Sc. thesis, Dalhousie University, Halifax, Nova Scotia, 132 p.

1975b: Diagenesis and sulphide mineralization of a section of Lower Carboniferous carbonates at Gays River, N.S.: a progress report; Geological Society of America, Abstracts with Programs, v. 7, no. 6, p. 812.

Stevenson, I.M. and McGregor, D.C.
1963: Cretaceous sediments in central Nova Scotia, Canada; Geological Society of America, Bulletin, v. 74, p. 355-356.

Williams, G.L.
1975: Dinoflagellate and spore stratigraphy of the Mesozoic-Cenozoic of offshore eastern Canada; in Offshore Geology of Eastern Canada. Volume 2 – Regional Geology, ed. W.J.M. van der Linden and J.A. Wade; Geological Survey of Canada, Paper 74-30, p. 107-162.

49. GEOLOGICAL AND GEOPHYSICAL INVESTIGATIONS IN JONES SOUND, DISTRICT OF FRANKLIN

Project 830028

B. MacLean, J.M. Woodside, and P. Girouard
Atlantic Geoscience Centre, Dartmouth

MacLean, B., Woodside, J.M., and Girouard, P., Geological and geophysical investigations in Jones Sound, District of Franklin; in Current Research, Part A, Geological Survey of Canada, Paper 84-1A, p. 359-365, 1984.

Abstract

Studies in Jones Sound from ***CSS Baffin*** *in conjunction with Canadian Hydrographic Service in 1983 included profiling with geophysical and echosounding systems, collection of surficial sediment samples in deep water areas and a few nearshore ice-front localities, as well as local aerial and onshore investigation of coast and beach.*

Much of the immediate seafloor in deeper parts of the Sound is composed of fine sediments that appear to be predominantly clay. Glacial till and other acoustically hard and texturally coarser materials, up to gravel size, also are represented.

Bedrock units of possible Precambrian to Paleozoic or younger age tentatively are inferred on the basis of adjacent onshore geology and analogies of seismic and magnetic data with those from other east coast offshore areas.

Preliminary gravity data indicate free-air anomaly values of -100 to -120 mgal in the eastern part of the Sound and less negative values in the west.

A magnetic anomaly in excess of 1000 nT occurs south of King Edward Point.

Résumé

En 1983, les études entreprises conjointement avec le Service hydrographique du Canada dans le détroit de Jones à partir du ***CSS Baffin*** *comprennaient l'établissement de profils au moyen d'appareils géophysiques et d'écho-sondeurs, le prélèvement d'échantillons de sédiments superficiels en eau profonde et aux environs de quelques falaises de glaces flottantes près du rivage, ainsi que l'étude aérienne et terrestre de certaines côtes et plages.*

Une grande partie du fond marin immédiat dans les parties plus profondes du détroit se compose de sédiments, notamment d'argiles. On y trouve également du till glaciaire et d'autres matérieux durs, de texture plus grossière, dont la taille atteint celle du gravier.

La présence d'unités rocheuses, d'âge précambrien à paléozoique ou plus récent, est déduite à partir de la géologie terrestre voisine et d'analogies établies entre les données sismiques et magnétiques et d'autres données semblables provenant d'autres régions au large de la côte est.

Les données gravimétriques préliminaires indiquent la présence d'anomalies à l'air libre variant de -100 à -120 mgal dans la partie est du détroit et d'anomalies moins négatives dans la partie ouest.

Une anomalie magnétique supérieure à 1 000 nT existe au sud de King Edward Point.

INTRODUCTION

Jones Sound lies between Devon and Ellesmere Islands at the western side of northern Baffin Bay. The geology of the Sound itself and its coastal zone are poorly known, and an opportunity was taken in 1983 to investigate this region because bathymetric charting was to be done by Canadian Hydrographic Service (Department of Fisheries and Oceans). Their interests arise from the potential of the Sound as part of a proposed tanker route from the Arctic Islands. If it is ever used as a tanker route, the possibility exists for oil spills which will affect the coastlines. Furthermore, physiographic analogy with Lancaster Sound suggests that there is at least some chance of hydrocarbon potential. As a consequence, Atlantic Geoscience Centre participated with Canadian Hydrographic Service in carrying out investigations of Jones Sound from **CSS BAFFIN** during August 2 to September 29, 1983 (Cruise 83-008). Geological and geophysical data were collected along closely spaced hydrographic charting tracks precisely positioned by onshore navigation systems installed for this survey. Sediment samples were taken and other site specific and opportunity basis investigations were undertaken.

Jones Sound is 300 km long and 55 to 75 km wide, except off King Edward Point where it narrows to 40 km. Lady Ann and Glacier straits, lying south and north of Coburg Island at the eastern entrance to the Sound (Fig. 49.1), are a minimum of 30 and 20 km wide respectively. Fram Sound, Cardigan Strait and Hell Gate form a narrow connection between Jones Sound and the Arctic Island channels to the west.

Jones Sound consists of a deep axial trough with water depths mainly between 500 and 800 m bordered by a platform shoreward on which water depths are less than 200 m. The boundary between shallow and deep water commonly is abrupt, but near its western end the Sound gradually shallows toward Fram Sound. Depths in excess of 500 m are common in Lady Ann Strait, but in Glacier Strait generally are less than 200 m.

OBJECTIVES

The main objectives of the Atlantic Geoscience Centre program were: 1) acquisition of single channel and Huntec high resolution seismic reflection profiles along north-south transects spaced at approximately 20 km intervals and on two or more east-west tie lines to provide information on both the surficial seabottom sediments and bedrock; 2) acquisition of acoustic data with 12 kHz and 3.5 kHz systems on all tracks for delineation of surficial sediment distribution; 3) collection of magnetic and gravity data for bedrock and crustal information on all tracks in Jones Sound, and to acquire gravity and magnetic tie lines through the Labrador Sea enroute north and south; 4) collection of regionally distributed surficial sediment samples in Jones Sound to provide information on textural composition, depositional environments, and age; 5) acquisition of echosounder and sediment sample profiles at two calving ice-fronts for study of variations in foraminiferal populations; 6) examination of beach and nearshore sediments in several areas selected by pre-cruise aerial reconnaissance; 7) investigation of other on- and offshore problems or site specific bedrock or Quaternary features on an opportunity basis.

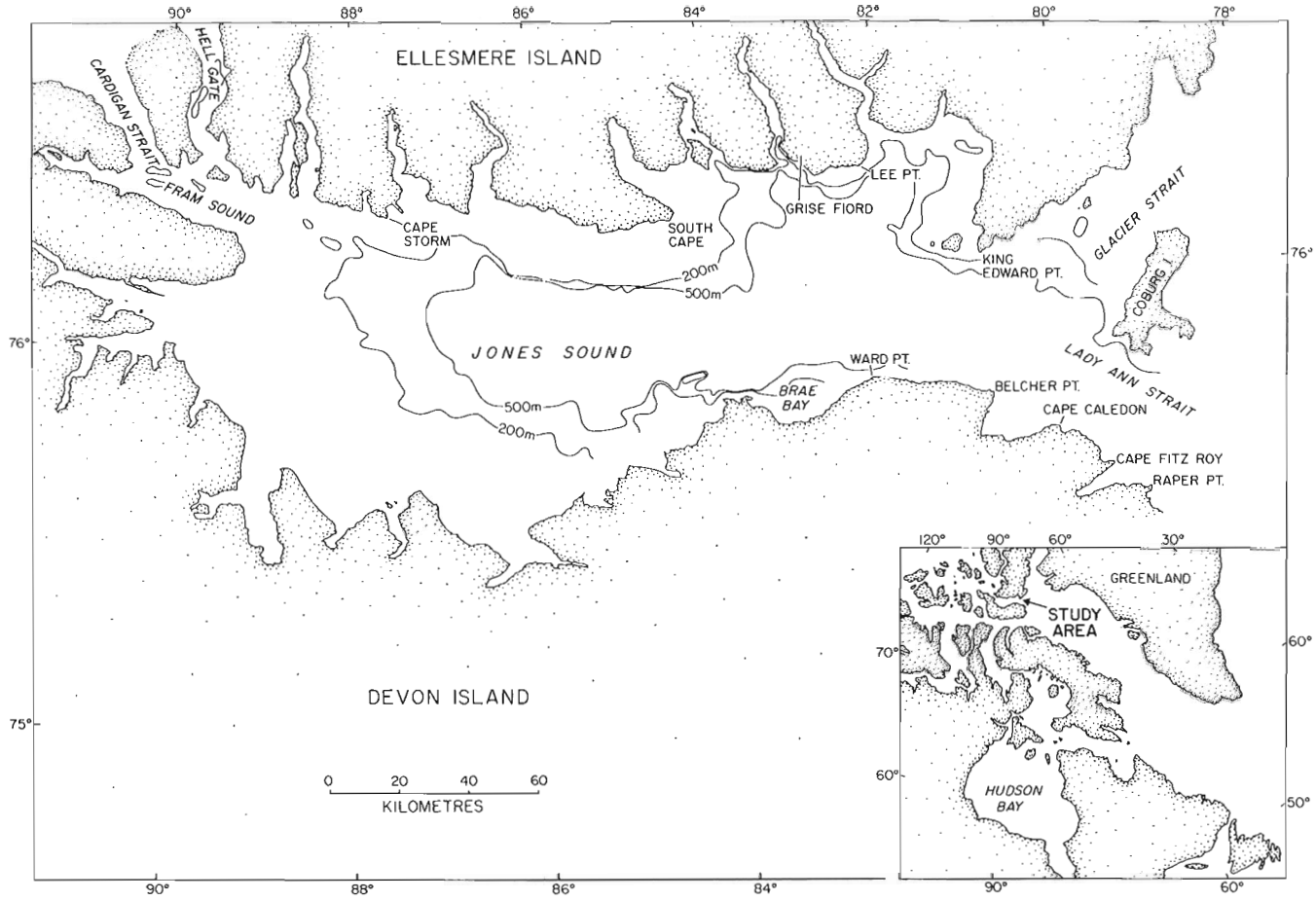

Figure 49.1. *Index map of Jones Sound study area.*

EQUIPMENT

Systems employed for the collection of geophysical and geological data from **CSS BAFFIN** included the following: a single channel seismic reflection system which utilized an EG & G sparker sound source operated at 3000 and 5000 joules in conjunction with a Nova Scotia Research Foundation CC-149 6m hydrophone; a Huntec deep tow high resolution seismic system; a Varian V75 proton precession magnetometer with a Barringer OS 1045 sensor; a Bodenseewerk KSS 30 gravity meter; and a Raytheon 12 kHz PTR echosounder. Sediment samples were collected with Shipek and Van Veen grab samplers and a 2.3 m gravity corer (two Benthos piston cores were also collected in the Jones Sound region in 1983 by **CSS HUDSON** for this program). Launch-borne systems included a Huntec hydrosonde shallow seismic profiler, Elac echosounder and small Ponar grab sampler. An E.D.A. Electronics Ltd. analogue and digitally recording 3-component fluxgate station magnetometer on loan from Earth Physics Branch (EMR) was placed at Grise Fiord to record fluctuations of the magnetic field during the survey period. Absolute measurements of magnetic inclination and declination were made at Grise Fiord for Earth Physics Branch with a fluxgate magnetometer mounted on a Jena theodolite and a portable Scintrex proton precession magnetometer.

PROBLEMS AND CONSTRAINTS

This year saw an abnormally late and bad ice season in Jones Sound and many other eastern Arctic areas. Continued presence of pack ice in high concentrations throughout most of the Sound together with extensive fog during the latter part of August and early September severely curtailed our programs. Surveying with towed instruments thus was limited by the scarcity of reasonably ice-free areas and by poor visibility in all areas due to fog. The fog also severely handicapped installation, servicing, and use of onshore Hi-Fix and Mini-Ranger navigational systems so that geophysical and geological data were acquired on only a relatively few well controlled **BAFFIN** tracks. These were in the eastern part of the Sound between King Edward Point and Coburg Island.

Mini-Ranger systems were used to provide navigational control for hydrographic tracks in the eastern part of the area. Variations in signal quality necessitated extensive post-processing of gravity data to remove spurious positional data. These problems were compounded by loss of ship speed input to BIONAV through failure of the doppler log early in the cruise, and gravity meter software problems on 0°/360° headings. Circumvention of problems arising from the KSS-30 software bug and the lack of speed log was accomplished by disabling input of speed and heading data used for fine levelling of the gravity meter platform, but at the expense of some degradation in data quality.

Hi-Fix control installed onshore in the western part of the Sound could not be used during the survey period due to ice and fog and eventual damage to the equipment resulting from a heavy buildup of ice.

Given these problems, satellite navigation and radar were the main positioning systems used for the geophysical and geological echosounding profiles acquired in the Sound.

BIONAV, the Bedford Institute integrated navigation system, experienced several involuntary shutdowns during the early part of the cruise and in general positioning data to the gravity meter from BIONAV was at a less than optimum level. This resulted in part from loss of automatic ship speed input. Most calculations of Eotvos corrections for gravity observations were made, therefore, only after careful selection of satellite and radar fixes. Considerable degradation of the gravity data due to the inability to define ship's course and velocity with sufficient accuracy and resolution results from employment of such methods.

The hull mounted 3.5 kHz acoustic system was ineffective in producing any geologically useful results additional to those obtained with much better resolution by the 12 kHz echosounder.

RESULTS

Surficial sediments

Geological data on the surficial sediments were obtained from: 12 kHz echosounder profiles on all **BAFFIN** tracks; conventional single channel seismic and Huntec high resolution profiles, where these could be run; and 33 grab samples and 3 gravity cores. Piston cores were acquired by **CSS HUDSON** at two localities to provide bio- and lithostratigraphic data at greater sediment depth than was possible with the gravity corer.

Acoustically transparent sediments composed of texturally fine material, predominantly clay, form the immediate seabed in much of the deep water area of the Sound (Fig. 49.3). These soft sediments lie on bedrock and other unconsolidated sedimentary units and commonly range from a thin layer ± 1 to 2 m up to 6 m in thickness. Thickest deposits of these sediments, up to 15 m, were observed in the eastern part of the Sound west of Coburg Island. In general they were thinner regionally in the western part of the Sound where the deep main basin begins to shallow.

A thin layer of somewhat coarser sediments consisting of silt and occasional sand sized particles locally overlies the clay at the immediate seafloor.

Acoustically harder and texturally coarser materials which commonly underlie the fine sediments occasionally outcrop at the seafloor (Fig. 49.3). Acoustic data from seismic reflection, Huntec, and 12 kHz systems together with information from samples indicate these localities include some glacial till deposits and areas of probable bedrock exposure as well as sediments containing or composed of sand or gravel.

Acoustic data suggest that the texturally coarser sediments on the south side of the Sound in the Ward Point – Belcher Point area (Fig. 49.2, 49.3) consist mainly of glacial till. Section A-B (Fig. 49.4) illustrates sediment interpreted to be glacial till overlying the bedrock throughout the length of the section. The till is variable in thickness,

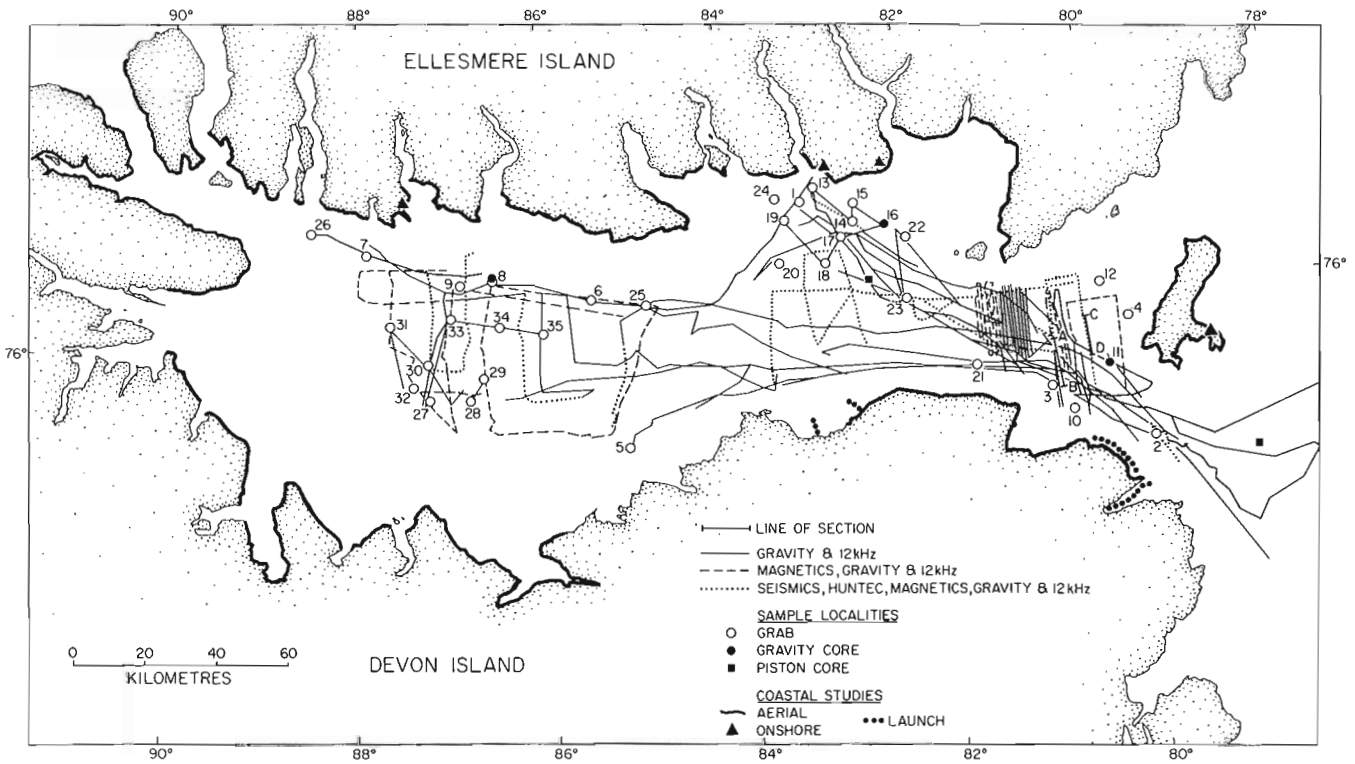

Figure 49.2. Track chart showing types of data collected and sediment sample localities. Navigational positioning was primarily by satellite navigation and radar.

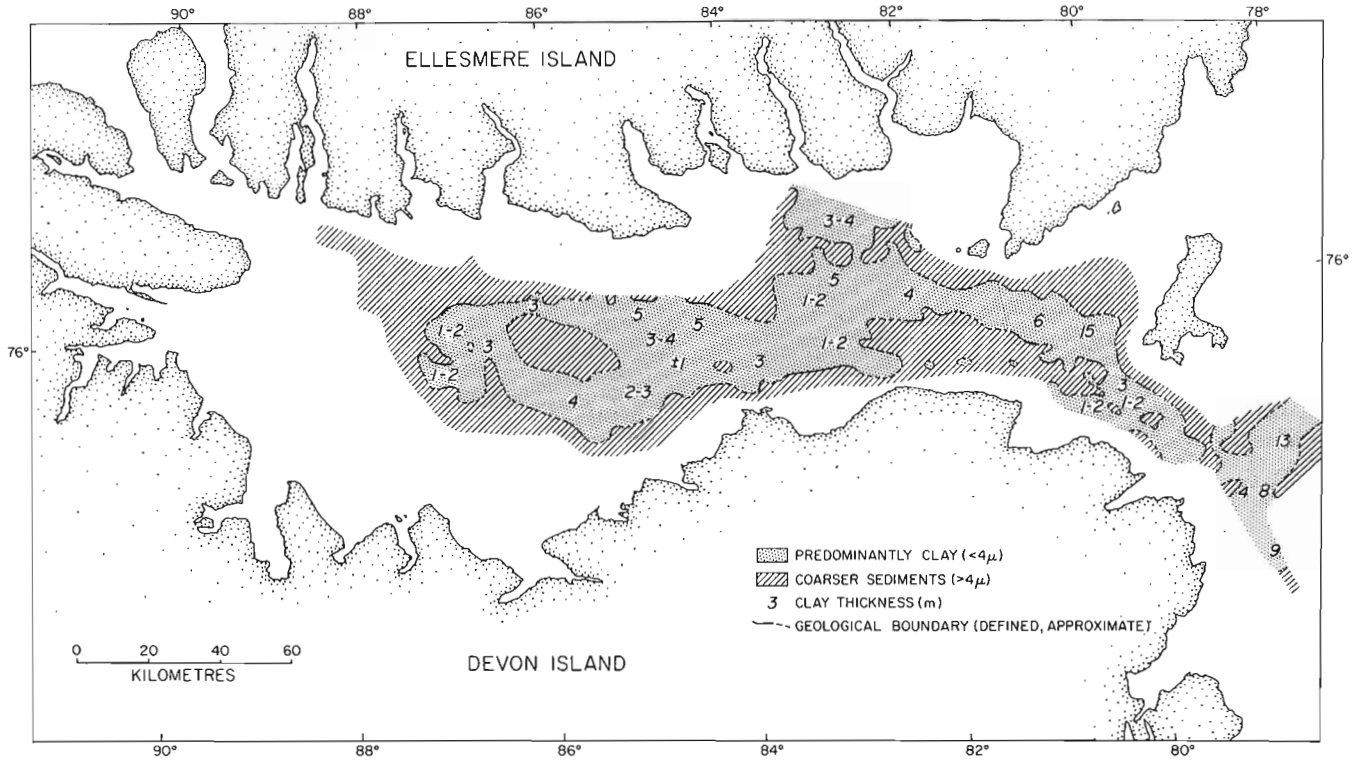

Figure 49.3. *Chart showing the distribution of unconsolidated surficial sediments at the seafloor composed primarily of: clay; and texturally coarser material, based on acoustic data and preliminary sample information. Numbers indicate clay thickness in metres.*

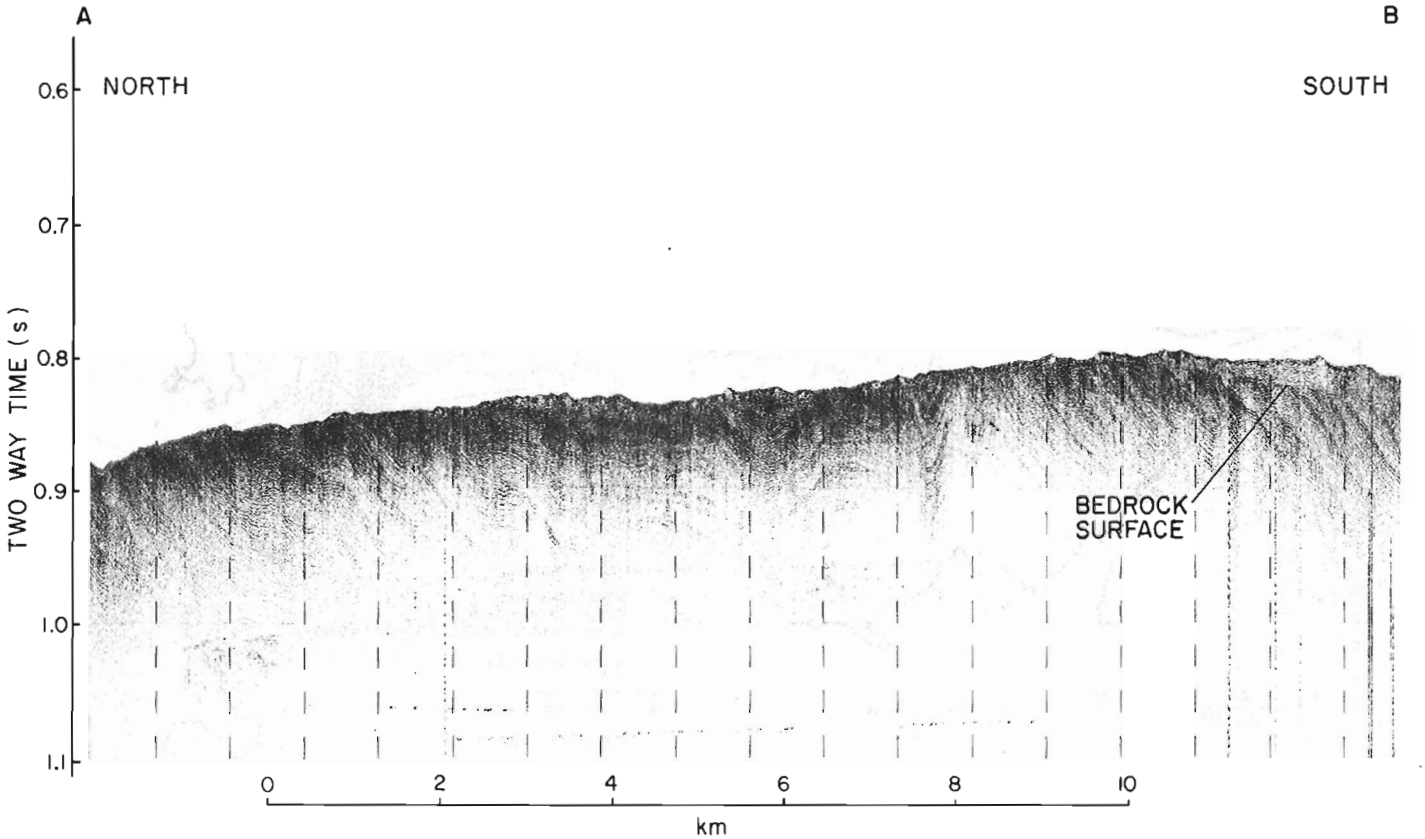

Figure 49.4. *Section A-B: (see Fig. 49.2 for location) seismic reflection profile northeast of Belcher Point illustrating folded Paleozoic or younger strata in the eastern part of the Sound. Overlying surficial sediments on the southern part of the section resemble glacial till. Huntec high resolution and 12 kHz acoustic data indicate that the latter material is exposed at the seabed in that area and that it thins and is overlain by clay to the north.*

approximately 18 m at the southern end of the section. Huntec and 12 kHz profiles indicate that the till is exposed at the seafloor along the southern half of this section and overlain by clay to the north. Section C-D (Fig. 49.5) 10.5 km to the northeast adjacent to the entrance to Glacier Strait contains a sequence of acoustically, mainly unstratified sediments up to 37 m thick that may represent glacial till along the northern two thirds of the section. Overlying sediments, composed predominantly of clay, reach 11 m in thickness and thin to both the north and the south.

Table 49.1. Sample Stations

Station	Latitude	Longitude	Depth (m)	Type of Sample
1	75°53.4'N	83°48.5'W	543	Shipek grab
2	75°38.3'N	79°46.8'W	532	Shipek grab
3	75°48.5'N	80°45.0'W	567	Shipek grab
4	75°57.4'N	79°50.1'W	582	Shipek grab
5	75°44.9'N	85°09.9'W	210	Shipek grab
6	76°08.0'N	85°30.0'W	631	Shipek grab
7	76°15.5'N	87°55.3'W	250	Shipek grab
8	76°11.5'N	86°39.9'W	652	Shipek grab
8a	76°11.5'N	86°39.9'W	652	Gravity core
9	76°10.8'N	86°53.9'W	380	Shipek grab
10	75°44.3'N	80°35.5'W	598	Shipek grab
11	75°50.5'N	80°07.0'W	560	Gravity core
12	76°03.2'N	80°06.0'W	170	Shipek grab
13	76°24.2'N	83°01.4'W	560	Shipek grab
14	76°16.8'N	82°38.9'W	690	Shipek grab
15	76°19.8'N	82°36.1'W	635	Shipek grab
16	76°15.9'N	82°18.0'W	750	Gravity core
17	76°14.5'N	82°46.6'W	706	Shipek grab
18	76°11.0'N	83°00.0'W	640	Shipek grab
19	76°18.0'N	83°08.1'W	572	Shipek grab
20	76°13.5'N	83°28.0'W	558	Shipek grab
21	75°53.0'N	81°30.0'W	570	Shipek grab
22	75°13.6'N	82°06.9'W	570	Shipek grab
23	76°04.2'N	82°10.0'W	832	Shipek grab
24	76°21.5'N	81°31.0'W	228	Shipek grab
25	76°07.0'N	85°09.0'W	777	Shipek grab
26	76°19.5'N	88°31.0'W	220	Shipek grab
27	75°53.5'N	87°15.5'W	218	Shipek grab
28	75°58.3'N	86°53.0'W	382	Shipek grab
29	75°56.2'N	86°42.5'W	572	Shipek grab
30	75°59.0'N	87°17.0'W	400	Shipek grab
31	76°04.5'N	87°40.0'W	316	Shipek grab
32	75°55.5'N	87°25.5'W	247	Shipek grab
33	76°05.8'N	87°01.0'W	581	Van Veen grab
34	76°04.4'N	86°29.9'W	543	Van Veen grab
35	76°03.0'N	86°03.0'W	520	Van Veen grab
L100	75°44.8'N	83°15.5'W	45	Ponar from launch
L101	75°45.4'N	83°16.0'W	60	Ponar from launch
L102	75°46.2'N	83°15.4'W	27	Ponar from launch
L103	75°46.3'N	83°15.4'W	16	Ponar from launch
L104	75°46.7'N	83°15.3'W	5.5	Ponar from launch
L105	75°47.4'N	83°15.4'W	17	Ponar from launch
L106	75°48.8'N	83°15.0'W	17	Ponar from launch
L107	75°44.9'N	83°12.5'W	30	Ponar from launch
L108	75°44.8'N	83°11.0'W	50	Ponar from launch
L109	75°44.7'N	83°11.0'W	68	Ponar from launch
L110	75°47.6'N	82°44.7'W	6	Ponar from launch
L111	75°47.8'N	82°44.5'W	12	Ponar from launch
L112	75°36.0'N	80°08.5'W	44	Ponar from launch
L113	75°36.0'N	80°08.5'W	41	Ponar from launch
L114	75°36.0'N	80°08.5'W	85	Ponar from launch
L115	75°32.8'N	80°05.0'W	53	Ponar from launch
L116	75°28.7'N	80°22.5'W	78	Ponar from launch

Till or modified till is a probable component of the coarser textural unit in many areas, particularly along the south side of the Sound and on the north side in the area southeast of Cape Storm. Similar sediments also occur at the seabed in the isolated coarser sediment outcrop area intersected by 76°00'N and 86°00'W. Where sampled at stations 9, 12, 27, 32 and 35 the surface of the sediments had undergone some modification, presumably through winnowing by bottom currents.

Sediments sampled in a few areas flanking or marginal to the axial trough ranged in textural composition from clayey and silty to sandy and gravelly, or mixtures of these components. Gravel was recovered at stations 7 and 26 at 250 and 220 m depth, respectively, and gravel and/or sand are likely to be prevalent at the seafloor in water depths of this range and shallower.

Bedrock

Onshore geology (Fortier et al., 1963; Frisch, 1983) and a preliminary interpretation of the bedrock geology offshore in Jones Sound are illustrated in Figure 49.6. The offshore interpretation is based on acoustic and magnetic characteristics of the rocks revealed by seismic reflection and magnetometer profiles. The broad tentative age appellations applied to the offshore units are strictly provisional, based on analogies of the above data to known rocks in other Canadian east coast offshore areas, as well as the likelihood that onshore units in this area may be represented in offshore sequences.

Seismic reflection and magnetic profiles indicate that rocks interpreted to be of Precambrian age underlie the western entrance to Glacier Strait and are present in Lady Ann Strait (Fig. 49.6). A 1000 gamma magnetic anomaly and a 15 mgal gravity anomaly locally are associated with these rocks where they form a bathymetric high southeast of King Edward Point. Seismic and magnetometer profiles south of Cape Storm indicate that the westernmost part of the Sound is underlain by rocks that apparently constitute acoustic basement and which have a higher amplitude magnetic anomaly pattern than the adjacent strata to the east. The existing data, however, are not considered sufficiently definitive to establish whether these are Precambrian rocks, or Lower Paleozoic strata which possibly form a thin cover over Precambrian rocks. These rocks are referred to as Lower Paleozoic or earlier in Figure 49.6.

The strata lying immediately north and east of those just discussed permitted somewhat greater penetration of energy from our seismic system and were characterized by a lower and relatively smoother magnetic anomaly pattern. These rocks are identified as undifferentiated Paleozoic on Figure 49.6.

Folded and faulted sedimentary rocks which permitted moderately good penetration of seismic energy occur in the easternmost part of the Sound adjacent to the western end of Lady Ann Strait and extend to the west at least as far as the longitude of Grise Fiord. These strata are distinctly softer acoustically than those found in the western part of the Sound and are likely to postdate them. These strata are identified as Paleozoic or later on Figure 49.6. Apparent dips and structural features are indicated. Seismic reflection profiles across these strata are illustrated in Figures 49.4 and 49.5. Areal extent of the rocks of this unit farther to the west, and their contact relations with the strata there, could not be established due to persistent heavy ice concentrations in that area. It may be significant that in the eastern part of the Sound where the youngest rocks of the offshore sequence apparently occur, the rocks of the immediate shore areas are of Precambrian age whereas in the western part of the Sound

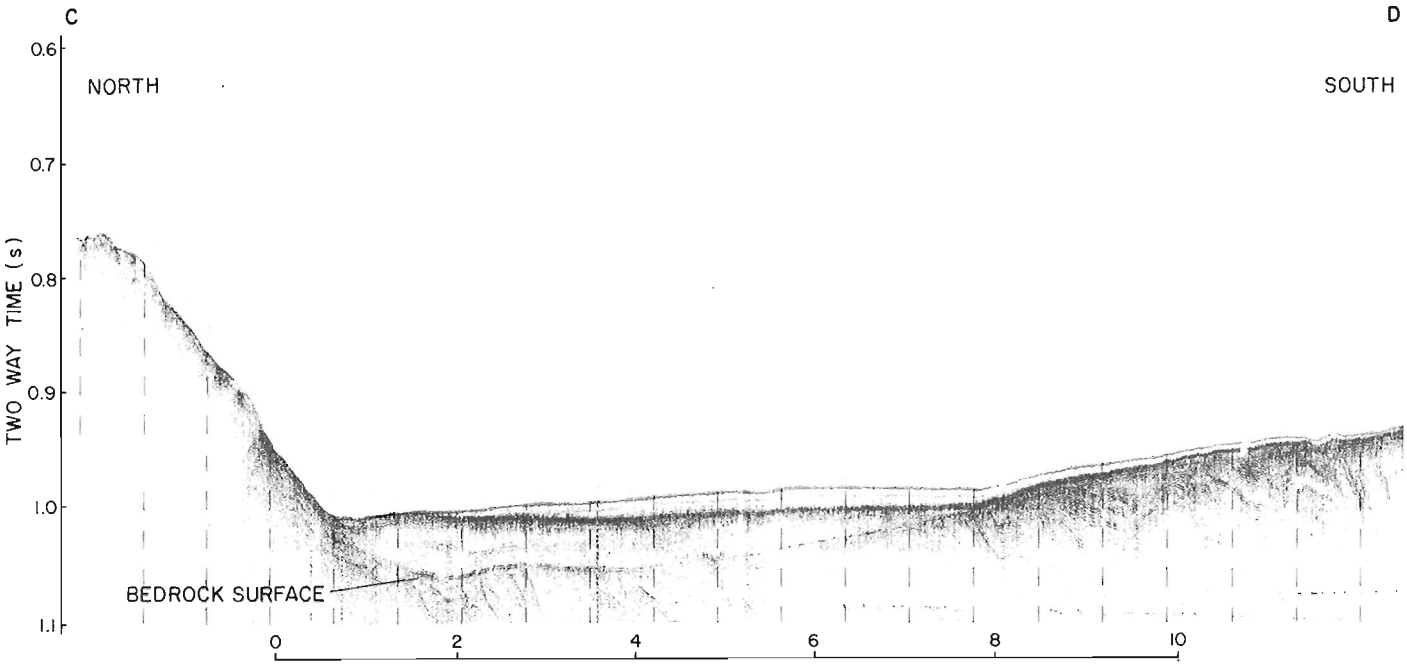

Figure 49.5. *Section C-D: (see Fig. 49.2 for location) seismic reflection profile west of Coburg Island illustrating bedrock strata and overlying surficial sediments consisting of possible till or proglacial sediments and clay.*

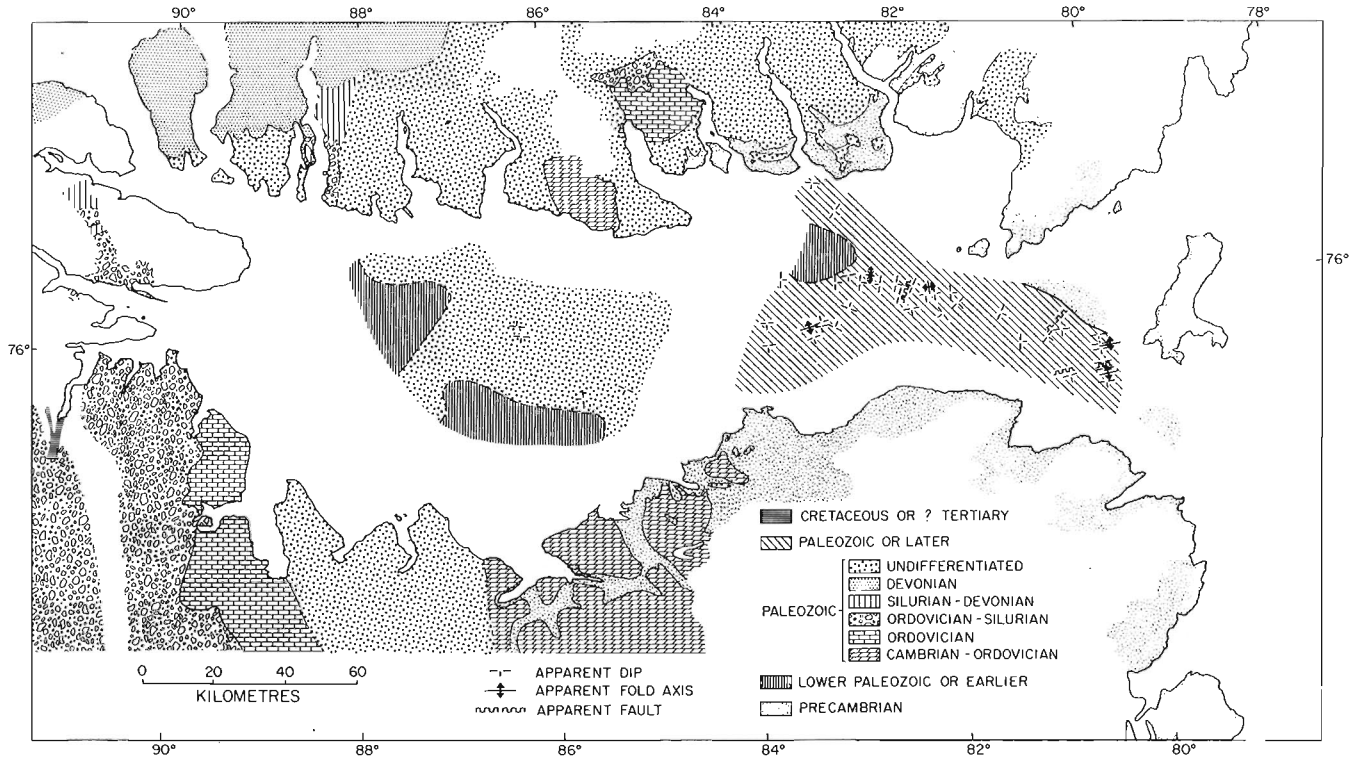

Figure 49.6. *Chart showing preliminary interpretation of bedrock geology offshore in Jones Sound based on seismic reflection and magnetometer data together with the adjacent onshore geology (after Frisch, 1983; Fortier et al., 1963).*

Paleozoic rocks outcrop along the coast and are more widespread. Cretaceous or ?Tertiary strata locally occur onshore in the latter area.

As **BAFFIN's** operations were restricted to areas greater than 200 m water depth, and many areas were inaccessible due to ice, it was not possible to establish structural relations at the steep bathymetric boundary between the deep axial trough and the fringing shallow banks.

Gravity

Because of problems mentioned previously regarding the necessity to carefully select navigational data for Eotvos corrections to be applied during postprocessing of the gravity data, preliminary results are only available for the eastern entrance to Jones Sound. Free-air anomalies are of the order of -110 to -115 mgal over the deep basin (700 m) between Cape Caledon and King Edward Point.

Between Devon and Ellesmere island, in this part of the Sound, the simple Bouguer anomaly varies from about -30 mgal on either side to about -70 mgal in the centre. A very rough calculation suggests that the -40 mgal difference might be consistent with a graben model for the Sound, in which the central block was downfaulted by about 2.5 km with the upper part containing 0.5 km of sediments. A deep (subcrustal) source for the anomaly would not produce the gravity gradient of around 1.5 mgal/km at the margins of the Sound. Obviously other models are possible and will be explored as the data are analyzed.

Data from two previous AGC cruises are available for Jones Sound (vis. HUDSON 71-032, HUDSON 77-024). The data from these cruises are consistent with those from BAFFIN 83-008 where comparisons have been possible. Free-air anomaly lows of -100 to -120 mgal are restricted to the southeast part of Jones Sound, south of 76°10'N and east of 86°W. To the north and west, the level of the free-air anomaly rises to about -60 mgal south of Lee Point and about -40 mgal near Cape Storm. Part of this variation can be attributed to shallowing of the water to the north and west but part appears to be geologic.

Magnetics

Preliminary examination of the magnetic data show them to be of good quality with no apparent degradation from magnetic storms or other variable effects. This seems to be supported by the analogue record from the station magnetometer which was placed at Grise Fiord; however, final conclusions regarding such variations await analysis of the data recorded digitally from the station magnetometer. The magnetic anomalies were computed from total field data using the new IGRF 80. Because the magnetometer does not require the same navigation standards as does the gravity meter, most of the magnetic data will be of higher quality than the gravity data.

As mentioned previously, a magnetic anomaly of over 1000 nT coincides southeast of King Edward Point with a bathymetric projection southward from the slope and the gravity high of about 15 mgal observed in both the free-air and simple Bouguer anomalies. A quick perusal of magnetic anomalies obtained on previous cruises suggests that there are similar features toward the west between King Edward Point and South Cape. Geological Survey of Canada Map 1512A, Magnetic Anomalies of Arctic Canada, indicates a northwest-southeast trend to the anomalies in Jones Sound; and the relatively high frequency of the anomalies further indicates that magnetic basement may not be deeply buried here.

Coastal Investigations

Seafloor morphology and sediments were investigated by profiling and sampling seaward of the termini of valley glaciers and calving ice fronts at localities on the south coast in the Brae Bay area and between Cape Caledon and Raper Point (Fig. 49.2). These revealed substantial till (moraine) deposits in the nearshore, seaward of the ice margins indicative of the former extent of grounded ice farther seaward. Samples and profiles were also obtained for study of variations in foraminiferal assemblages in these areas.

A wider reconnaissance was carried out by helicopter of coast and beach areas on both sides of Cardigan Strait and the south side of Farm Sound. Beach profiles and samples were obtained at Cape Storm, and onshore localities at Grise Fiord, Lee Point and on Coburg Island also were examined.

ACKNOWLEDGMENTS

Financial support of this program by the Office of Energy, Research and Development, Department of Energy, Mines and Resources is gratefully acknowledged. Grateful thanks also are extended to Captain N. Norton, M. Swim, Canadian Hydrographic Service, officers, crew, and scientific staff aboard **CSS BAFFIN** for their cooperation and assistance in carrying out the field investigations, to C. Blakeney and H. Slade for laboratory and cartographic services, respectively, and to R.F. Macnab and D.J.W. Piper for review of the manuscript.

REFERENCES

Frisch, T.
1983: Reconnaissance geology of the Precambrian Shield of Ellesmere, Devon and Coburg Islands, Arctic Archipelago: a preliminary account; Geological Survey of Canada, Paper 82-10, 11 p.

Fortier, Y.O., Blackadar, R.G., Glenister, B.F., Greiner, H.R., McLaren, D.J., McMillan, N.J., Norris, A.W., Roots, E.F., Souther, J.G., Thorsteinsson, R., and Tozer, E.T.
1963: Geology of the north-central part of the Arctic Archipelago, Northwest Territories (Operation Franklin); Geological Survey of Canada, Memoir 320, 621 p.

Taylor, R.B. and Frobel, D.H.
1984: Coastal Surveys, Jones Sound, District of Franklin; in Current Research, Part A, Geological Survey of Canada, Paper 84-1A.

50. A SYSTEM FOR VITRINITE REFLECTANCE ANALYSIS ON DISPERSED ORGANIC MATTER FOR OFFSHORE EASTERN CANADA

Project 810034

E.H. Davies and M.P. Avery
Atlantic Geoscience Centre, Dartmouth

Davies, E.H. and Avery, M.P., A system for vitrinite reflectance analysis on dispersed organic matter for offshore eastern Canada; in Current Research, Part A, Geological Survey of Canada, Paper 84-1A, p. 367-372, 1984.

Abstract

A system of vitrinite reflectance analysis of dispersed organic matter from petroleum exploratory wells has been developed to delineate thermally mature source rocks in offshore eastern Canada. The system incorporates the utilization of organic residues as byproducts for palynological sample preparation, freeze drying of the residues and mounting of three residues in one acrylic lucite stub through which holes or conduits have been drilled using a modified twist drill bit. The microscopic analysis is made with a Zeiss Photomultiplier III reflectance system attached to a Zonax microcomputer with modified software allowing automated shutter control, online readings, data manipulation and display.

Résumé

Une méthode d'analyse de la réflectance de la vitrinite dans la matière organique éparpillée provenant de puits de prospection a été mise au point afin de délimiter les roches mères ayant atteint la maturité thermique au large de la côte est du Canada. La méthode comprend l'utilisation de résidus organiques comme sous-produits pour la préparation d'échantillons palynologiques, le séchage à froid des résidus et le montage de trois résidus dans une masse de lucite acrylique à travers de laquelle des trous ou des conduits sont percés au moyen d'une mèche hélicoïdale. L'analyse microscopique se fait au moyen d'un dispositif de réflectance Zeiss Photomultiplyer III monté sur un micro-ordinateur Zonax à logiciel modifié de façon à permettre le contrôle automatisé de l'obturateur, la lecture en direct et la manipulation et l'affichage des données.

INTRODUCTION

Within the petroleum industry vitrinite reflectance has proved to be one of the key techniques in the identification of thermally mature source rocks and hence the prediction of zones of potential petroleum entrapment (Brooks, 1981; Burgess, 1977; Dow, 1977; Powell, 1982; Urban and Allen, 1977). Powell (1982) has summarized the currently available data, including some vitrinite reflectance analyses, pertaining to source rock potential of the Scotian Shelf.

In 1981 a project was initiated at the Atlantic Geoscience Centre to survey and delineate intervals of mature source rock for offshore eastern Canada through the analysis of vitrinite reflectance on dispersed organic matter (Brooks, 1981). This comprehensive study requires broad geographic and detailed stratigraphic sampling.

As a byproduct of the palynological preparations, several thousand residues of dispersed organic matter isolated from rock samples (cuttings, sidewall cores and conventional cores) of approximately 140 petroleum exploratory wells are stored at AGC. A streamlined system was required that would: 1) rapidly mount a large number of samples for reflected light examination, 2) analyze these samples expeditiously and 3) handle the large quantities of data generated by the microscopic analyses.

For the microscopic examination a Zeiss Photomultiplier III reflectance system attached to the Zeiss Zonax microcomputer was acquired. The software supplied by the Zeiss required modifications and added options for direct application to vitrinite reflectance analysis of dispersed organic matter. Also, a special method (referred to here as the conduit method) for the preparation, mounting and polishing of the samples was developed. These techniques are outlined and discussed in this paper.

THE CONDUIT METHOD FOR RESIDUE MOUNTING

Preparation of the dispersed organic residues

1. The organic fractions were isolated from the rock samples during standard palynological techniques, as outlined by Barss and Williams (1973). Unoxidized portions of these residues were stored in water in one dram glass vials.
2. With the vials properly labelled and as much water as possible removed by pipette, the samples were frozen for approximately 2 to 3 hours. They were then dried with the vials open in a VirTis freeze drier with a 305 mm (12") diameter and 305 mm (12") high stainless steel drum manifold. By stacking the boxes of vials on simple shelves up to 288 samples may be freeze dried simultaneously.
3. The partly consolidated freeze dried residues were loosened by gently tapping the vials and scraping the sides with a toothpick to obtain the maximum amount of material.

Blank stub preparation

1. Transparent cylindrical acrylic lucite stubs (also termed 'briquets', American Society for Testing and Materials, Lukens et al., 1975; or 'pellets', Gunther, 1976) with the proper dimensions, 25.4 mm diameter by 19 mm high (1" x 3/4") must be made (Fig. 50.1). These may be produced by two methods: a) by fusing acrylic lucite granules in a pneumatic press (Buehler Pneumet) or b) by cutting preformed acrylic lucite rods to the required length.
2. Through the stub three 6.4 mm ($\frac{1}{4}$") holes spaced at 120° and centred halfway along the radii are drilled to form conduit perpendicular to the flat face. The holes are started with a centre punch and drilled using a modified 6.4 mm ($\frac{1}{4}$") drill bit (see discussion) while the stub is held

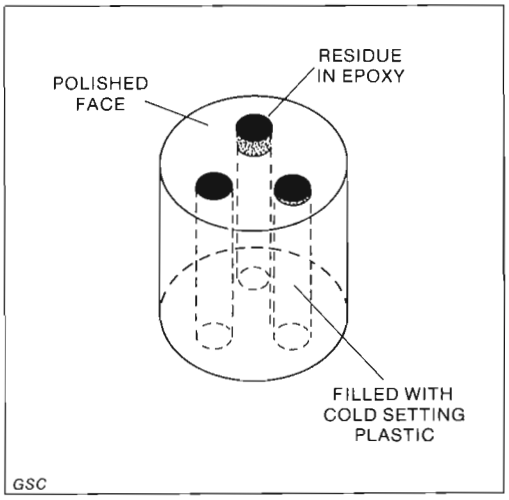

Figure 50.1. *A completed acrylic lucite cylindrical stub with three conduits drilled completely through, the residue mounted in epoxy-resin, the remainder of the conduit filled with cold-setting platic and polished.*

in the drill press by a small vice with a vertical V-groove in each jaw face. The drilling speed is set at 500 rpm. The holes are drilled to about three quarters of the depth of the stub using minimum pressure. With the holes lubricated with soap and water, the drilling is continued with decreasing pressure until the bit protrudes through the bottom completely. Subsequently, the bit is allowed to clear the partially melted plastic from the sides of the hole before the bit is raised. This prevents the stub from sticking to the bit and lifting the stub and clamp assembly.

3. Any rough edges on the bottom of the stub are removed with 240 grit paper.

Mounting the residue

1. A piece of transparent tape is placed over the holes at the smooth end of the stub.
2. The stub is labelled utilizing a glass inscribing tool.
3. The stub is inverted. Using a small powder funnel, the freeze dried organic residue is poured into the holes, one sample per hole. Care must be taken in order not to contaminate the other samples within the same stub.
4. A small amount of epoxy resin (EPO-TEK 301) is prepared following the manufacturer's instructions and poured into the holes. Just enough resin is used to wet the residue. The mixture is stirred into a paste and allowed to set. This takes 2 to 3 hours. The remainder of the hole is filled using an inexpensive cold-setting plastic, such as Ward's Bio-Plastic or Canus C-32 Resin in order to reinforce the stub. This is allowed to harden overnight. The following day, the tape is removed.

Preparation of polished surface

The procedure for polishing is similar to that for standard coal petrography mounts as outlined in the Annual Book of the American Society for Testing and Material standards (Plan No. 2, Lukens et al., 1975). The 400 grit grinding stage has been eliminated and only the final grinding stage (600 grit) is utilized on the Buehler Automet polishing equipment.

1. The stubs are positioned and levelled with the specimen holder device. The stub face is carefully ground down to the residue level on a new 600 grit paper, checking at 15 to 20 second intervals to make sure that none of the samples are destroyed.
2. The stubs are cleaned by treating in an ultrasonic bath containing distilled water, followed by rinsing with distilled water and drying with compressed air. Next, the stub face is polished on Texmet cloth using distilled water and 0.3 micron aluminum oxide powder suspension. The cleaning process is then repeated. A doubled silk cloth using 0.05 micron aluminum oxide powder suspension is used for the final polishing, followed again by cleaning. Before the final rinse, any remaining polishing suspension can be effectively removed by gentle dabbing with a cotton ball soaked in Kodak Photo-flo 200 dispersant.

DISCUSSION OF PREPARATION METHOD

The preparation of organic residue mounts, using glass slides has been outlined by Baskin (1979); however, mounting and polishing coal and organic residues on acrylic lucite stubs has become common practice in many coal petrology and palynology laboratories. The use of these stubs takes advantage of automatic polishing equipment and well known coal polishing techniques. Different methods were tested in the laboratory, such as placing a drop of epoxy resin-organic residue mixture on top of the stub. This was tried, but often it would not adhere to the stub strongly enough during grinding and polishing.

Another method where the organic residue was mixed with acrylic lucite and formed in a press (Gunther, 1976) required a large amount of organic residue, and only allowed single sample preparation.

A third method attempted to place the residues in three shallow recesses drilled or impressed in the top of the stub. This increased the number of samples mounted and polished per stub. The mixture of epoxy resin and residue adhered well. The polished surfaces of the samples were a consistent size. One major disadvantage in this recess method was found in the grinding-polishing stage. The varying amounts of residue in each hole of the stub would require 3 different grinding levels. Since the automatic polishing equipment holds 6 stubs there would be up to 18 different optimum grinding levels. As well, the vitrinite particles tended to settle to the bottom portions of the residue making it difficult to know where the optimum grinding level should be found. The difficulty of drilling holes in the stubs to a precise depth further complicates the problem. In grinding down to the smallest sample it is easy to remove some or all of the samples. This may be prevented by frequently checking the progress of grinding through the laborious task of removing the stub holder from the machine.

In order to overcome the disadvantages of the recess method, the mounted holes were drilled through the stub and the residue mounted by the conduit method outlined above. However, some initial problems in manufacturing the drilled blanks were encountered. The first attempts in drilling through the stub resulted in overheating of the drill bit causing the plastic to melt and stick to the bit. More seriously, this caused the bottom of the stub to break off when nearing completion of the conduit. The drill bit tended to thread itself into the plastic without cutting it away and thus became jammed. The key to surmounting this problem was to modify the drill bit for cutting through the brittle acrylic lucite. The machinists at the Bedford Institute of Oceanography suggested that minor changes be made to a common twist drill bit by filing the rake angle in such a manner that the cutting face would be formed to the long axis of the drill bit (Fig. 50.2), thus, increasing the

rake angle. Special low helix bits for drilling similar materials such as brass are available, but the modification of a common twist drill bit was expedient and more economical.

As well as increasing the speed of polishing, the conduit method has provided several other advantages. The settling of the vitrinite particles that caused difficulties in the recess method has become advantageous by increasing their abundance on the final polished surface and reduced grinding-polished time. Problems encountered in the recess method while stirring the epoxy resin-residue mixture were eliminated since the increased height of the hole inhibited spilling out of the holes. The amount of residue poured into the holes was not critical since the possibility of overfilling and contamination are reduced to a minimum. Samples with only minor amounts of residue could also be used with surprising success.

For the blank stubs, the following two sources were considered:

1. Individual stubs with a consistent diameter can be formed by fusing acrylic lucite granules in a Buehler Pneumet pneumatic press. A lengthy lead time is necessary to build up an inventory of blank stubs. The cycle time of heating and cooling for each blank is approximately three quarters of an hour, although only a few minutes of the operator's time at the press are required to initiate the process between cycles. It would still take, for example, one week utilizing one pneumatic press to make 50 blanks for 150 organic residue mounts.

2. Acrylic lucite rods of approximately 25.4 mm (1") diameter usually in 2.4 m (8') lengths are readily available from distributors of plastic products. These must then be cut into the required 19 mm (3/4") lengths while ensuring a very precise perpendicular cut. This may necessitate a preliminary grinding of the bottom surface on the polishing machine. The rods can be purchased precut to the required lengths or can be cut in house. The manufacturing tolerance for the diameter of the acrylic rods is stated as ±0.25 mm (0.010"), but measured as ±0.30 mm (0.012"). Most tended to be wider than smaller. The specimen holders for the Buether Automet polisher could not accommodate stubs in the wider range. A second holder was modified by machining to accommodate a range of larger stubs. The acrylic lucite rods were harder to drill than the pneumatic press stubs, causing more heat build up and requiring more lubrication during drilling. The advantage of the rods is that many blanks stubs may be obtained within a short time.

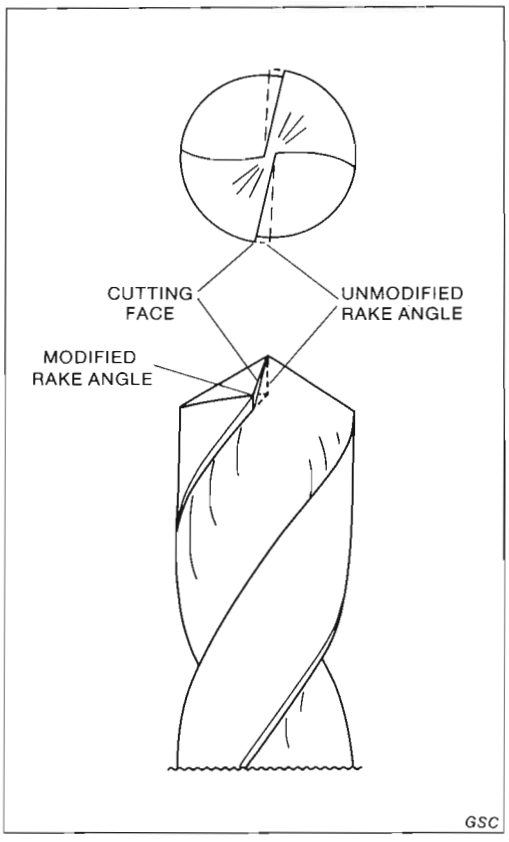

Figure 50.2. *A drill bit tip modified to prevent chipping and breakage of the acrylic lucite stubs while drilling. The rake angle is ground so that the cutting face is parallel to the long axis of the bit. The dashed lines outline the original shape of the drill bit before modifications.*

MICROSCOPIC ANALYSIS ON ZONAX SYSTEM

The advancements in sample preparation techniques, providing a relatively quick and easy system to prepare good quality polished organic residue mounts using the conduit method, have been paralleled by the acquisition of a greatly improved microscopic analysis system. Vitrinite reflectance determinations on dispersed organic material derived from cuttings of offshore petroleum exploration wells necessitate a large number of readings (up to 100) on each sample, as well as frequent sample intervals (200 m or less). The Zeiss Photomultiplier III microscope controlled by the Zonax microcomputer (a modified Intelligent Computer Systems colour 32K RAM model) brought the acquisition of the reflectance (Ro) value on a selected vitrinite particle to a single 'push button' operation. All field stop and shutter manipulations before and after taking the reading were handled automatically.

The operator is provided with a continuous display of the number of readings taken and basic statistics such as mean, minimum and maximum values, and standard deviation. The positions of the various diaphrams and shutters under computer control are shown along with the various commands available to handle the data.

The Zonax system as purchased was designed to suit a variety of microphotometric applications such as fluorometry and optical density which resulted in a system that tended to be cumbersome for routine vitrinite reflectance measurements. Many features of the software had to be stepped through and constants adjusted in order to begin the analysis. The main operating program was modified to facilitate the calibration and startup procedures and to provide more options for the user.

The hardcopy output of the system was significantly upgraded by replacing the slow thermal paper printer, supplied by Zeiss with a less expensive and versatile C-ITOH dot matrix impact printer. Some software developments were needed to write the printer drive routines to fully integrate the printer with the system. A second disc drive has been added to reduce the amount of floppy disc handling and to simplify other software routines.

Optionally, the data can either be listed (Table 50.1), plotted as a reflectogram in classes of half V-types (.05 Ro; Fig. 50.3) plotted as a histogram in variable class widths (Fig. 50.4), or saved on floppy disc. Within the same program, the list of readings can be edited to delete certain ranges of data and the edited data saved in a new file. More data may be appended by continuing to take more readings or by entering values manually. The raw data file is maintained in the case future reappraisal will be required. The final vitrinite reflectance data are used in the generation of machine-plotted thermal maturation profiles and regression lines (Fig. 50.5).

Table 50.1. Data listing and statistical parameters for readings taken on a sample from Mobil Venture B-43 well from the Scotian Basin at a depth of 4180 m

```
FILE >> K0068B DESCRIPTION FOLLOWS :
DEPTH 4180M, VENTURE B-43, MIKE AVERY, SEPTEMBER 19/83

 PT#  RO   PT#  RO   PT#  RO   PT#  RO   PT#  RO   PT#  RO   PT#  RO   PT#  RO
  1  .33    2  .4     3  .42    4  .43    5  .46    6  .47    7  .48    8  .48
  9  .49   10  .5    11  .51   12  .52   13  .59   14  .6    15  .61   16  .61
 17  .61   18  .62   19  .63   20  .63   21  .64   22  .64   23  .64   24  .64
 25  .65   26  .66   27  .66   28  .66   29  .67   30  .67   31  .68   32  .68
 33  .69   34  .69   35  .7    36  .7    37  .71   38  .71   39  .71   40  .72
 41  .72   42  .72   43  .72   44  .72   45  .73   46  .73   47  .73   48  .74
 49  .74   50  .74   51  .74   52  .74   53  .75   54  .75   55  .76   56  .77
 57  .77   58  .79   59  .8    60  .81   61  .83   62  .85   63  .9

H.V. =  418     GAIN =  1000  NUMBER OF MEASUREMENTS =  63
MINIMUM =  .33    MAXIMUM =  .9                          MEAN =  .66
STANDARD DEVIATION =  .12   COEFFICIENT OF VARIATION =  18.1818%
```

```
                                  REFLECTOGRAM
                          0         10         20         30         40  44
                          +---------+---------+---------+---------+---+
                          !
 .3   - .34  = 1   !]
 .35  - .39  = 0   !
 .4   - .44  = 3   !]]]
 .45  - .49  = 5   !]]]]]
 .5   - .54  = 3   !]]]
 .55  - .59  = 1   !]
 .6   - .64  = 11  !]]]]]]]]]]]
 .65  - .69  = 10  !]]]]]]]]]]
 .7   - .74  = 18  !]]]]]]]]]]]]]]]]]]
 .75  - .79  = 6   !]]]]]]
 .8   - .84  = 3   !]]]
 .85  - .89  = 1   !]
 .9   - .94  = 1   !]
```

Figure 50.3. *A reflectogram output arranged in preset one half V-type class widths and boundaries for the data listed in Table 50.1.*

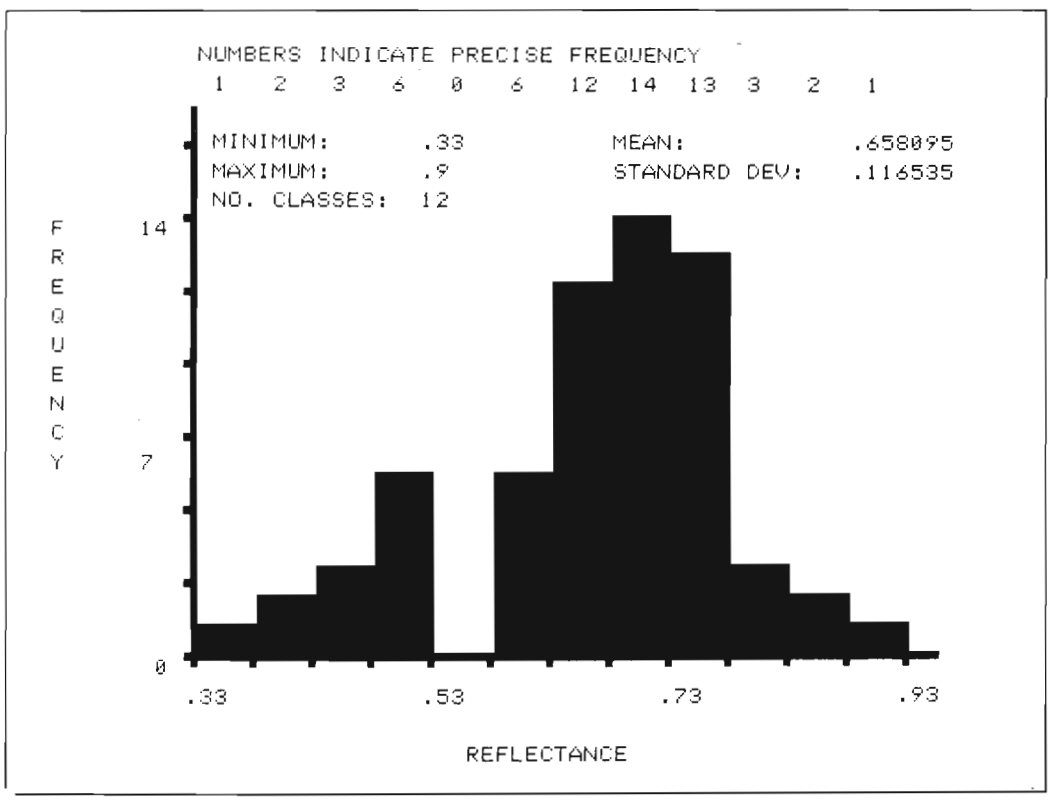

Figure 50.4. *A histogram output arranged in variable class widths and boundaries with statistical parameters for the data listed in Table 50.1.*

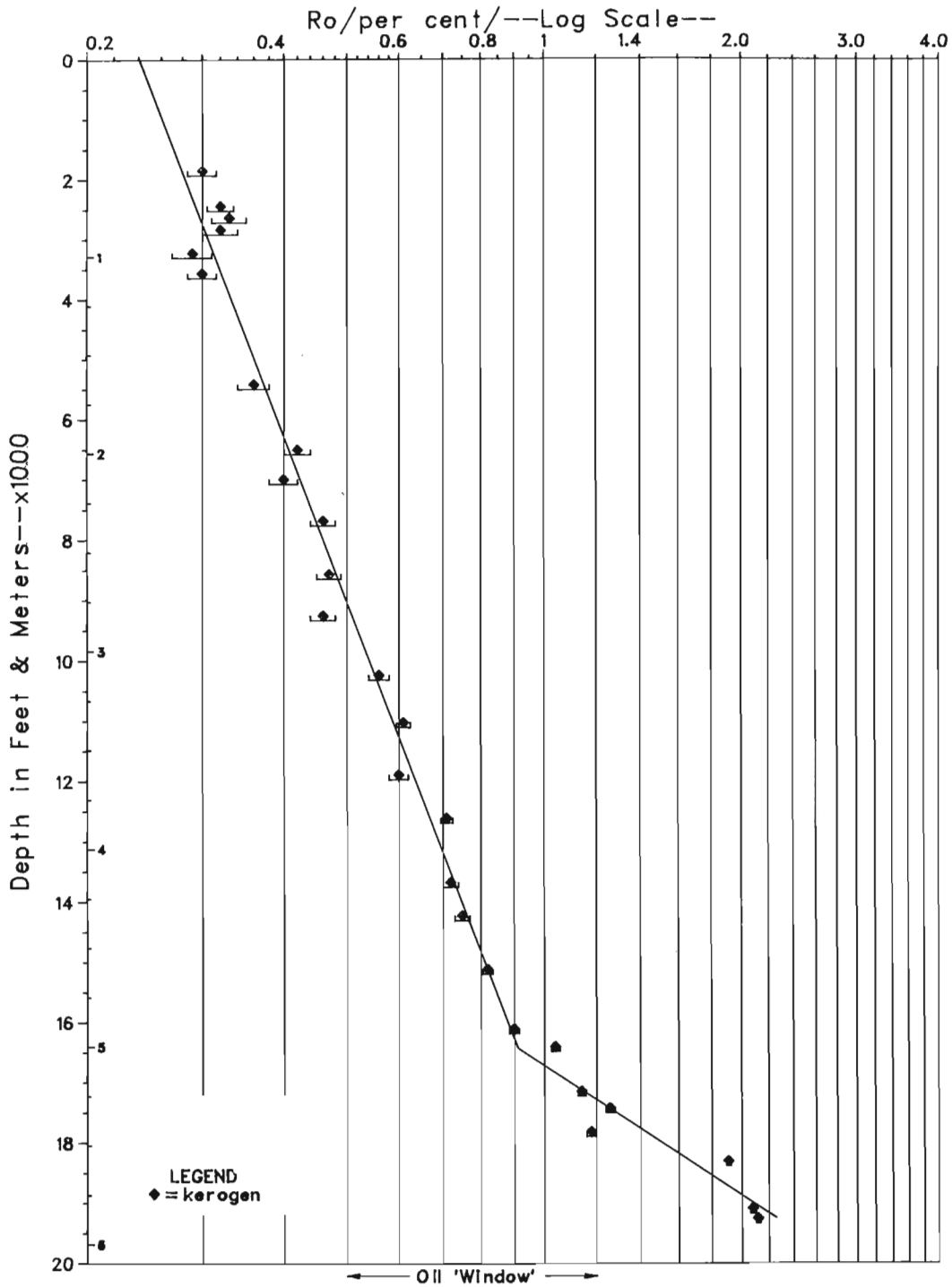

Figure 50.5. *Thermal maturation profile for the Mobil-Texaco-PEX Venture B-43 well from the Scotian Basin, showing an interval of thermal maturation (oil window) between 3000 and 5250 m. An increase in the thermal maturation gradient at 4950 m is evident from the regression lines.*

SUMMARY

The conduit method of sample preparation has reduced significantly the mounting, grinding and polishing time. The modified Zeiss Zonax reflectance microscope and microcomputer system has permitted automated microscope analysis and data manipulation. These facets have been integrated into a streamlined system for vitrinite reflectance studies of dispersed organic matter. It is anticipated that this program of analyzing the level of thermal maturation in petroleum exploration wells will lead to a more comprehensive assessment of the petroleum potential of the eastern Canadian margin and enhance its geological interpretation.

ACKNOWLEDGMENTS

The authors are grateful to J. Saunders of Plansearch Ltd. and C. Wangerski for their assistance in modifying the software, and to P. Harrison of Acadia University and W.C. MacMillan for their assistance in developing the laboratory techniques. The machine shop personnel, especially Don Knox, of the Bedford Institute of Oceanography, are thanked for providing technical assistance.

Special thanks are given to P.A. Hacquebard, J. Wade, and G.L. Williams for reading the manuscript and offering constructive criticism.

REFERENCES

Barss, M.S. and Williams, G.L.
1973: Palynology and nannofossil processing techniques; Geological Survey of Canada, Paper 73-26, 25 p.

Baskin, D.K.
1979: A method for preparing phytoclasts for vitrinite reflectance; Journal of Sedimentology Petrology, v. 49, no. 1, p. 633-635.

Brooks, J.
1981: Organic maturation of sedimentary organic matter and petroleum exploration – a review; in Organic Maturation Studies and Fossil Fuel Exploration, ed. J. Brooks; Academic Press, p. 1-37.

Burgess, J.D.
1977: Historical review and methods of determining thermal alteration of organic materials; Palynology, v. 1, p. 1-7.

Dow, W.G.
1977: Kerogen studies and geological interpretations; Journal of Geochemical Exploration, v. 7, p. 79-99.

Gunther, P.R.
1976: Palynomorph color and dispersed coal particule reflectance from three Mackenzie Delta boreholes; Geoscience and Man, v. 15, p. 36-39.

Lukens, R.P., Shenker, P.A., Cornillot, J.L., Greco, S.M., Greenhill, L.W., Haines, M.W., and Priemon, R.A. (editors)
1975: Gaseous Fuels; Coal and Coke; Atmospheric Analysis; Annual Book of American Society for Testing and Materials Standards, Part 26, Philadelphia.

Powell, T.G.
1982: Petroleum geochemistry of the Verrill Canyon Formation: a source for Scotian Shelf hydrocarbons; Canadian Petroleum Geology, Bulletin, v. 30, no. 2, p. 167-179.

Urban, L. and Allen, M.
1977: Vitrinite reflectance as an indicator of thermal alteration within Paleozoic and Mesozoic sediments from the Phillips Petroleum Company ASM-1X well, Arafura Sea; Palynology, v. 1, p. 19-26.

51. DISTRIBUTION AND STRUCTURAL SETTING OF FERTILE GRANITES AND RELATED PEGMATITES IN THE YELLOWKNIFE PEGMATITE FIELD, DISTRICT OF MACKENZIE

Contract 20SU-23233-3-0239

Robert E. Meintzer[1], Michael A. Wise[1], and Petr Černý[1]
Economic Geology Division

Meintzer, R.E., Wise, M.A., and Černý, P., Distribution and structural setting of fertile granites and related pegmatites in the Yellowknife pegmatite field, District of Mackenzie; in Current Research, Part A, Geological Survey of Canada, Paper 84-1A, p. 373-381, 1984.

Abstract

Based on field work in the 10 000 km² Yellowknife pegmatite field, the gross mineralogical, textural, and structural characteristics of the pegmatite series and granites, possibly related to the pegmatities, are described.

Field examination and limited geochemistry suggest that granites, possibly parental to the pegmatites, range in composition from alkali-feldspar granite to granodiorite, although they are predominantly syenogranite and monzogranite.

Pegmatites are divided into three geographical groups containing twenty-seven pegmatite series. The pegmatites vary from simple dykes with no rare-element minerals to those containing beryl, spodumene, cassiterite, tapiolite, ixiolite, columbite-tantalite, and microlite. In addition, zoning of the pegmatites varies from homogeneous to well-zoned. Other than locally, little relationship between structure and paragenesis of the pegmatites is observable. Though previously unrecognized, regional zonation is apparent in the pegmatites of the Northwestern group.

On the basis of mineralogical and structural data, it is not yet possible to define genetic linkage between the pegmatites and individual plutons or plutonic units.

Résumé

Le rapport décrit les caractéristiques minéralogiques, texturales et structurales grossières des séries de pegmatites et des granites vraisemblablement liés aux pegmatites de la zone de pegmatites de Yellowknife, dont la superficie est de 10 000 km²; les données sont fondées sur des travaux effectués sur le terrain. Une carte montre l'emplacement des séries de pegmatites et des plutons de granitiques.

L'étude sur le terrain et l'analyse géochimique limitée permettent de croire que la composition de ces plutons varie de celle d'un granite à feldspath alcalin à celle d'une granodiorite, bien qu'elle soit surtout équivalente à un granite syénitique et à un granite monzonitique.

Les pegmatites se divisent en trois groupes géographiques qui contiennent vingt-sept séries de pegmatites. Elles varient des filons simples, dépourvus de minéraux des terres rares, aux filons minéralisés en béryl, en spodumène, en cassitérite, en tapiolite, en ixiolite, en columbite-tantalite et en microlite. De plus, les pegmatites varient d'homogènes à bien zonées. Sauf par endroits, il semble exister peu de liens entre la structure et la paragenèse des pegmatites. Bien qu'elle n'ait pas été reconnue auparavant, la zonation régionale est évidente dans les pegmatites du groupe nord-ouest.

En se fondant sur les données minéralogiques et structurales, il n'est pas encore possible de définir de liens génétiques entre les pegmatites et les plutons ou unités plutoniques particuliers.

INTRODUCTION

A field and laboratory study of the petrology, mineralogy, petrogenesis, and structural relationships of pegmatites and intrusions in the Yellowknife pegmatite field was begun in the summer of 1980. The pegmatites of this area are known for their content of rare elements such as lithium, beryllium, tantalum, niobium, and tin.

This report is a summary of mineralogical and structural aspects of the pegmatites and fertile granites based on four summers of field work in the area. The granites are described within the overall classification of granites of the area used by Henderson (1976). A table summarizing the mineral abundances in the examined pegmatites is included and zonation of the pegmatites is discussed.

PREVIOUS STUDIES

The Slave Structural Province comprises about 190 000 km² of the northwestern Canadian Shield between Great Slave Lake on the south and Coronation Gulf on the north. McGlynn and Henderson (1972) described the general structural characteristics and Henderson (1981) reviewed the geology in regards to Archean basin evolution. Fyson (1975, 1978, 1981) described the structural characteristics of the southern part of the Slave Province and emphasized that the structural pattern in the region is not simply related to granitoid diapirism.

Ayres and Černý (1982) reviewed the geology of the pegmatite field including the granodiorities and post-tectonic two-mica granites (unit 11 below). They discussed the general characteristics of the pegmatites of the field and distinguished three distinct populations: a) Prosperous-Prelude Lakes area, b) Ross Lake area, and c) Southeastern area. Of the three groups, only the first lacks regional zonation.

GRANITES OF THE YELLOWKNIFE PEGMATITE FIELD

Pegmatitic phases are associated primarily with granites falling under units 10, 11, 12, and 13 of the Hearne Lake (851) map area of Henderson's (1976) compilation.

[1] Department of Earth Sciences, University of Manitoba, Winnipeg, Manitoba

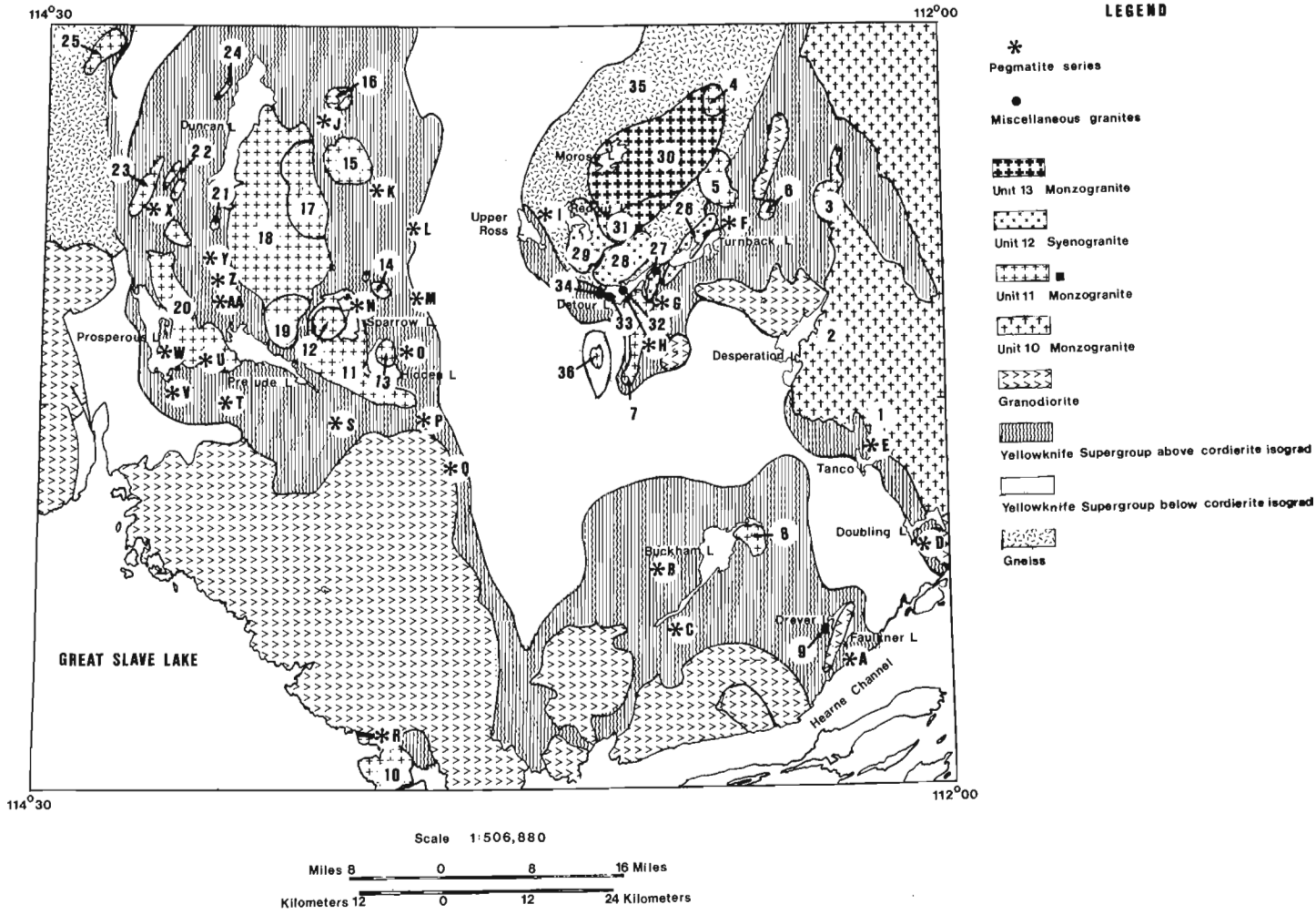

Granite Plutons

1. *Eastern*
2. *Desperation Lake*
3. *Old Grump Lake*
4. *Abediah Lake*
5. *Goon Lake*
6. *Two Bug*
7. *Tumpline Lake*
8. *Buckham Lake*
9. *McDuff*
10. *Matonabbee Point*
11. *Cameron River*
12. *Sparrow Lake*
13. *Hidden Lake*
14. *Scott Lake*
15. *Wedge Lake*
16. *Prestige Lake*
17. *Duncan Lake East*
18. *Duncan Lake West*
19. *Prelude Lake*
20. *Prosperous Lake*
21. *Staple Lake*
22. *Neck Lake*
23. *Quyta Lake*
24. *Crapaud Lake*
25. *Rocky Lake*
26. *Turnback Lake*
27. *Horse Fly*
28. *Ross River*
29. *Redout Lake*
30. *Morose Lake*
31. *Languish Lake*
32. *Island*
33. *Eagle Point*
34. *Ptarmigan*
35. *Sleepy Dragon Lake*

Pegmatite Series

A. *Faulkner Lake*
B. *Buckham Lake West*
C. *Buckham Lake East*
D. *Doubling Lake*
E. *Tanco Lake*
F. *Turnback Lake*
G. *Bug*
H. *Detour Lake*
I. *Peg*
J. *Fle*
K. *Blaisdell Lake*
L. *Sproule Lake*
M. *Thompson Lake*
N. *Sparrow Lake*
O. *Hidden Lake*
P. *Reid Lake*
Q. *Harding Lake*
R. *Slave*
S. *Upland Lake*
T. *Bighill Lake*
U. *Pontoon Lake*
V. *Tom Lake*
W. *Minipud*
X. *Murphy*
Y. *Alexie Lake*
Z. *Petey Lake*
AA. *Prelude Lake*

Figure 51.1. *The Yellowknife pegmatite field, District of Mackenzie*

Unit 10: monzogranite

Unit 10 of Henderson (1976) is a large batholith on the eastern fringe of the Hearne Lake map area (Fig. 51.1), which was sampled in three separate areas.

The granite appears to be predominantly a medium grained monzogranite in all three sample areas. Muscovite is absent to rare except in the pluton sampled at Old Grump Lake. In the vicinity of Old Grump Lake, the biotite volume is greater than that of muscovite with the exception of one muscovite granite sample. Rare tourmaline and garnet are present in the Eastern granite.

Only in the region east of Desperation Lake are pegmatitic phases commonly present. The small dykes (<20 cm wide) and pods (ca. 2 m across) are homogeneous with simple mineralogy: quartz, microcline, plagioclase, and subordinate muscovite.

Within the outcrop area east of Desperation Lake, the granite is intercalated with quartz-biotite schist and biotite-feldspar-quartz gneiss (migmatite). Crosscutting relationships indicate that the schist is the oldest unit and the granite the youngest. Contacts with the schist are largely discordant and in some areas the schist is domed over the granite. Granite apophyses pervade the schist generally parallel to the schistosity. The gneiss cuts the schist concordantly and discordantly and, in some areas, loses the gneissic texture. East of Old Grump Lake, the granite has permeated the non-porphyroblastic schist and cut across the schistosity. The granite is commonly fine grained along the margin and muscovite is absent to rare. No foliation is observable, except near Old Grump Lake where the rock was sheared as the result of movement along a north-south shear and subsequently healed.

Unit 11: monzogranite

Henderson's (1976) Unit 11 comprises two batholiths and over 18 stocks that are clustered primarily around Duncan, Prosperous, and Prelude lakes.

The Prosperous Lake stock was dated by Green et al. (1968) by Rb-Sr mineral isochron and Green and Baadsgaard (1971) by K-Ar at 2575 ± 25 Ma and 2520 ± 28 Ma, respectively. Kretz (1968) made observations on the Prestige Lake, Sparrow Lake (Cameron River), Duncan Lake, and Hidden Lake plutons and adjacent pegmatites. Furthermore, Kretz et al. (1982) discussed the Na-K-Li geochemistry of the Prestige Lake pluton.

Table 51.1 summarizes the overall textural and mineralogical variation among the plutons, although variations within the plutons are also common.

Field examination suggests that the composition of the granite ranges from syenogranite to granodiorite, but is predominantly monzogranite. Initial petrographic and chemical analyses also show the presence of microcline-albite granites. Mineralogical changes seen in hand specimen include the ratio of muscovite to biotite, including the absence of either, and the presence or absence of apatite, tourmaline, or garnet. The presence of apatite, tourmaline, or garnet in hand specimens is restricted to several plutons and is distinctive of this rock unit. Although garnet is present in the Prosperous Lake Granite, it is restricted to the western and northern portions of the pluton; the southeastern portion is non-garnetiferous. Tourmaline (schorl?) is common in the southern and southeastern portions of the Cameron River pluton.

Grain size varies from fine to pegmatitic, although it is predominantly medium or pegmatitic. Pegmatitic phases are common as dykes or pods of simple and homogeneous mineralogy: quartz, graphic and blocky (rarely) K-feldspar, plagioclase, ±muscovite, biotite, schorl, and garnet. Beryl is present in rare cases, as in the Sparrow Lake and Pontoon Lake pegmatite series. Although most of the pegmatitic phases are coeval with the granite, some probably postdate pluton emplacement. The only plutons not having pegmatitic phases are the Wedge Lake, Two Bug, Rocky Lake, and Crapaud Lake granites.

The Prestige Lake, Matonabbee Point, and McDuff granites are notable exceptions to the predominant texture of the unit. The Prestige Lake Granite is commonly coarse grained to moderately porphyritic with large K-feldspar laths (3 cm x 3 cm x 1 cm) (Kretz et al., 1982). The laths commonly define a foliation, but although Kretz et al. (1982) discerned a trend in the foliation, we find the trends to be local and seem to define swirls and eddies in the magma. Complete circles can be recognized in the space of a few metres. The Matonabbee Point granite is a massive holo-leucocratic, coarse grained rock. The K-feldspar laths range up to 3 cm long, but define little distinctive foliation as in the Prestige Lake Granite. The McDuff granite is a holo-leucocratic, fine grained phase in a dykes-like (sill?) structure possibly related to the Tan pegmatite swarm.

Foliation in the various plutons, where observed, is predominantly related to contacts or shear zones. In the southeastern Cameron River granite, the rock has an east-southeast foliation (Fortier, 1947). Just south of the

Table 51.1. Mineralogical and textural characteristics of unit 11 monzogranite plutons. The numbers refer to Figure 51.1.

MINERALOGICAL and TEXTURAL CHARACTERISTICS / PLUTONS	Biotite Absent	Msc > Bio	Bio > Msc	Muscovite Absent	Apatite	Schorl	Garnet	Pegmatitic	Coarse-grained	Medium-grained	Fine-grained
Abediah Lake (4)			x					x		x	
Buckham Lake (8)		x						x		x	
Cameron River (11)		x	x		x	x	x	x		x	
Crapaud Lake (24)				x						x	
Donor Lake (36)	x							x		x	
Duncan Lake East (17)			x		x			x		x	
Duncan Lake West (18)			x		x			x		x	
Goon Lake (5)			x					x		x	x
Hidden Lake (13)				x				x		x	
Matonabbee Point (10)			x					r	x		
McDuff (9)	x										x
Neck Lake (22)		x	x					x		x	
Prelude Lake (19)		x	x		x	x		x		x	
Prestige Lake (16)		x						x	x	x	
Prosperous Lake (20)		x	x			r	x	x		x	
Quyta Lake (23)				x				x		x	
Rocky Lake (25)		x								x	
Scott Lake (14)		x	x		x	r		x		x	
Sparrow Lake (12)			x			x	x	x		x	
Staple Lake (21)		x						x		x	
Tumpline Lake (7)		x	x		x			x		x	
Two Bug (6)			x							x	
Wedge Lake (15)		x								x	

x=present; r=rare

southeastern lobe of the Southeastern Granodiorite, shearing has produced augen granite in the margins of the Matonabbee Point granite.

Contacts with the Yellowknife Supergroup vary, but are primarily strongly discordant with the granite cutting across bedding, foliation, or flow-banding in schists or metafelsites. Apophyses of granite commonly extend into the country rock. Sill-like intrusions of the granite are also visible, notable in the west-central portion of the Duncan Lake Granite.

Contact relationships with other rocks are variable. In the northern part of the Tumpline Lake granite, the granite cuts a fine grained biotite granodiorite. The Abediah Lake pluton in the northeast has permeated contacts with the Morose Lake granite to the west and veined and permeated contacts with the gneisses to the southeast. The Two Bug granite has veined contacts with the Burwash Formation to the west. The contact of the Quyta Lake granite with schist on the southeastern margin is strongly discordant, with apophyses of granite extending randomly into the schist. Rafts and screens of schist are quite common within 400 m of the contact.

Unit 12: syenogranite

This unit includes several stocks between Upper Ross and Turnback lakes. The most westerly body was named the Redout Lake Granite by Hutchinson (1955) and considered to be the parental granite to the swarm of pegmatites on its western flank.

These rocks vary little from pluton to pluton. Modally they are predominantly syenogranites. Biotite is the common accessory mineral; muscovite is only present in the Redout Lake Granite. All plutons are pegmatitic, especially along the southern margin (Turnback Lake, Horse Fly, and Ross River plutons) and the western margin (Redout Lake Granite). A few rafts of metasediments are seen in the southern half of the Turnback Lake granite. Gneiss is found in all plutons, but is more commonly mixed with the Ross River and Redout plutons; the gneiss is not equivalent to the Ross Lake Granodiorite.

Pegmatitic phases occur as irregular pods and dykes and are simple and homogeneous, being composed of quartz, graphic (rarely blocky) K-feldspar, plagioclase ± muscovite, biotite, and tourmaline. No contacts with metasedimentary rocks are observed.

Unit 13: monzogranite

Henderson (1976) designated a porphyritic monzogranite batholith near Morose and Languish lakes as unit 13. Davidson (1972) divided the unit into two plutons based on the loss of phenocrysts in the southern portion of the unit. The larger, porphyritic pluton is here designated the Morose Lake granite and the smaller, rarely porphyritic pluton is designated the Languish Lake granite.

Most of the Morose Lake granite observed is a medium grained porphyritic muscovite-biotite monzogranite. Muscovite is not commonly observed in hand specimen. The phenocrysts of K-feldspar attain 5 cm in length and are commonly twinned according to the Carlsbad law. Plagioclase crystals reach a maximum of ca. 1.25 cm and commonly show a pinkish alteration. The granite becomes distinctively less porphyritic towards its southern, eastern, and northern margins.

On the south, the rock grades into the Languish Lake granite by loss of porphyritic texture. Gneiss bodies cut by veins of unit 12-type granite and Languish Lake granite occur within the Languish Lake pluton. To the east, the Morose Lake granite is intermingled with gneisses. Though commonly veined, the contact in this area is predominantly a permeated one. The northeastern contact with the Abediah Lake granite is mostly a permeated one, although crosscutting relationships do show the Abediah Lake granite to be younger.

Pegmatitic phases are present as small dykes and irregular pods in both the Morose Lake and Languish Lake granites. The pegmatites are simple and homogeneous and contain quartz, graphic (rarely blocky) K-feldspar, plagioclase ± rare muscovite, biotite, schorl, and garnet.

Miscellaneous granites

Besides the units described above, several other smaller plutons may be related to the larger pegmatite series.

The Island granite was observed only on the eastern half of a large island in Detour Lake where it is crosscut by unit 12 granite.

The Island granite is fine grained and appears to have a monzogranitic composition with biotite and muscovite accessory minerals. In addition, there are poikiloblasts of tourmaline which produce a slight polka-dot appearance. On the eastern side of the island, the granite cuts older gneisses and schist. This rock may be a microgranite referred to by Davidson (1972).

The Ptarmigan granite and the Eagle Point granodiorite are small bodies located southwest of Detour Lake towards Victory Lake. The Eagle Point granodiorite is a medium grained biotite granodiorite which Davidson (1972) stated may be parental to other pegmatites in the area. The Ptarmigan granite is a biotite-muscovite monzogranite with a variable ratio of biotite to muscovite. This granite is more likely related to the pegmatities of the area, as it is pegmatitic and cut by pegmatite dykes.

The Sleepy Dragon Lake granite is a fine- to medium-grained biotite syenogranite, rarely with muscovite, which is commonly gneissoid. It occurs about 0.7 km east of Sleepy Dragon Lake where it contains short pegmatite dykes up to one metre across and pods of simple, homogeneous mineralogy: quartz, graphic K-feldspar, plagioclase, and ± muscovite. Yellow beryl was noted in one dyke. Cutting gneiss and tonalite, the granite appears to be the youngest rock in the area with the exception of a microgranite near Sleepy Dragon Lake.

PEGMATITES

In the following description of pegmatite series, swarms, and bodies, emphasis is placed on features relevant to the structure and mineralogy, and the terminology of Černý (1982) is used.

Mineral abundances in pegmatite series are indicated in Table 51.2. Estimates of mineral abundances are based on field observations and are aimed mainly at comparison of abundances of individual species in different pegmatite series rather than at abundances of different species within a single pegmatite body. Unless otherwise noted, the host rock for the pegmatites is nodular quartz-biotite schist of the Burwash Formation. All of the pegmatites are situated within the mapped cordierite-isograd.

Meintzer and Černý (1983) described the Faulkner Lake, Buckham Lake East, Buckham Lake West, Tanco Lake, and Doubling Lake series.

Faulkner Lake series

This series surrounds the Faulkner Lake leucotonalite intrusion. The McDuff granite is situated between the Bet body and the Tan swarm. The pegmatites occur as dykes and

Table 51.2. Parageneses of pegmatite series of the Yellowknife pegmatite field

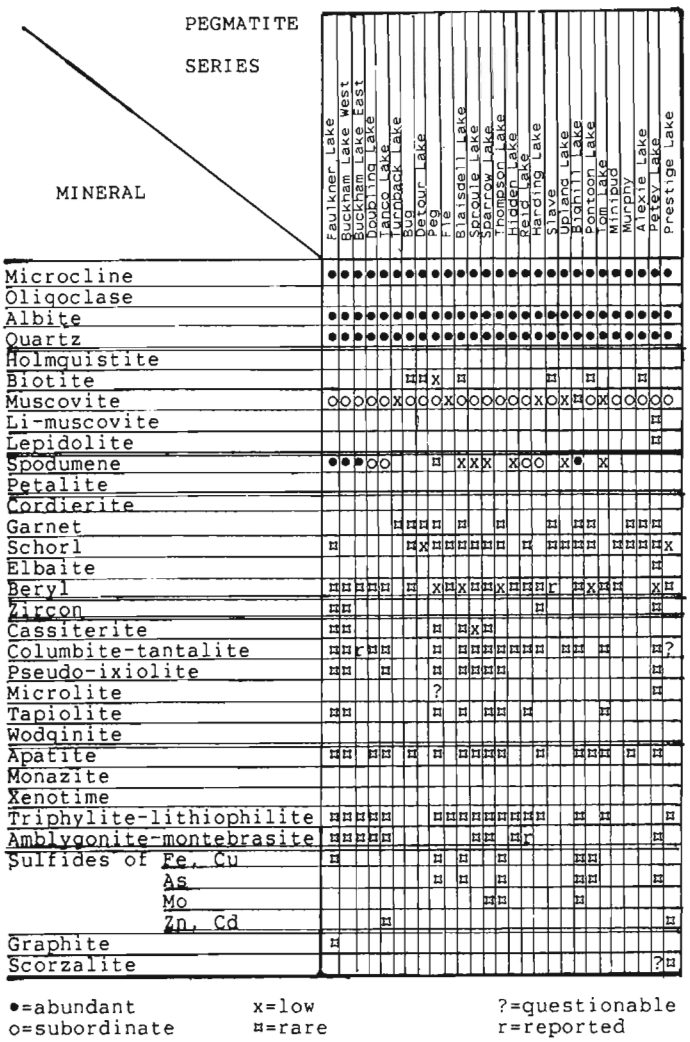

•=abundant o=subordinate x=low ¤=rare ?=questionable r=reported

sills and are concordant to slightly discordant. The Moose pegmatite is emplaced along a fracture system. With the exception of Tan-3, all the pegmatites strike generally north-northeast with steep dips. Zonation of the pegmatites varies from patchy to well-developed with the best development of zoning occurring in Bet and Moose. In both of these pegmatites, spodume crystals and amblygonite blocks reach 2 and 1 m in size respectively. Mineralogically this series contains some of the more fractionated pegmatites of the field and includes secondary metasomatic ab + msc assemblages. Sn, Nb, and Ta mineralization is present as cassiterite, tapiolite, disordered ferrocolumbite, and disordered ferrotantalite.

Buckham Lake West series

This series is scattered west of the northern part of Buckham Lake, 4-13 km from the margins of the Buckham Lake biotite-muscovite leucogranite. The pegmatites occur as concordant to slightly discordant, generally lenticular bodies. The Lit swarm and Hid strike to the northeast and Mac strikes west-northwest. Zonation is well-developed in the Mac dyke where 3 m long spodumene and 1 m long microcline crystals are found, but is poorly developed elsewhere. Albitization is generally extensive and mineralization is almost on par with the Faulkner Lake series. Cassiterite, manoganoan-tantalian ixiolite, ferroan-tantalian ixiolite, tapiolite, and disordered ferrocolumbite and ferrotantalite are present.

Buckham Lake East series

The pegmatites lie east of the southwestern arm of Buckham Lake, about 8 km southwest of the Buckham Lake leucogranite. The Bin swarm and Mut strike northeast and appear to be slightly discordant to concordant to the country rock. Lens is concordant, but strikes north-northwest. Zonation is poor in these pegmatites, especially in the Bin swarm. Spodumene mineralization is very uniformly distributed in all. Metasomatic albitization is present in all bodies, but is patchy in Mut where no Be, Nb-Ta, or Sn mineralization has been noted. Although columbite-tantalite series minerals have been reported in Bin and Lens, we found none.

Tanco Lake series

The Tanco Lake series is the most diversified and contains the most individual pegmatities of any of the series in the southeastern part of the field. The bodies are located within 1 km of the northern and eastern shores of Tanco Lake and within 300-2500 m of the western margin of the Eastern granite. The Jo swarm consists of two dykes which are primarily concordant. The Thor Eco swarm consists of many concordant and discordant pegmatites. One set of dykes has a predominant strike to the northwest (between Tanco and Echo lakes) and another strikes to the north-northeast (southeast of Tanco Lake).

Despite local similarities, broad generalizations about mineralogy versus structural emplacement are not possible. Within the Central bodies, the northwest-trending set comprises mostly homogeneous or poorly-zoned dykes that display the effects of tectonism that took place before, during, and after crystallization. Deformation of the schist wallrock to the point of shearing and brecciation is common. A ladder-type structure (Fig. 52.2) with elongate K-feldspar and lath-shaped spodumene in uniform subparallel orientation across the dykes is typical of most of the Central bodies.

In contrast, the northeast-trending set displays random orientation of the crystals in roughly zoned bodies which bridge, and interconnect with, the northwest-trending dykes. Post-crystallization tectonic disturbance is minimal, as is albitization, and primary structures indicate solidification in a static regime. Rare-element mineralization is virtually absent.

Zonation varies from absent to moderate. Albitization, too, is variable, but is most extensive in the Arachide bodies south of Tanco Lake. Disordered ferrocolumbite and disordered ferrotantalite have been identified.

Doubling Lake series

This series consists of two pegmatites, Usk and Was, less than 1 km from the western margin of the Doubling Lake leucogranodiorite. Was strikes north-northwest and is roughly concordant, while Usk strikes west-northwest and cuts across the schistosity. The Was pegmatite is homogeneous and fine grained over almost its entire exposed extent. Usk displays poor zoning with spodumene present in randon orientation throughout its width. Albitization is fairly extensive in Usk producing saccharoidal albite and fine-grained muscovite and hosts the predominant portion of the Nb-Ta mineralization. Thin blades of columbite-tantalite are present in both pegmatites, however, tapiolite and beryl have been identified in Usk only.

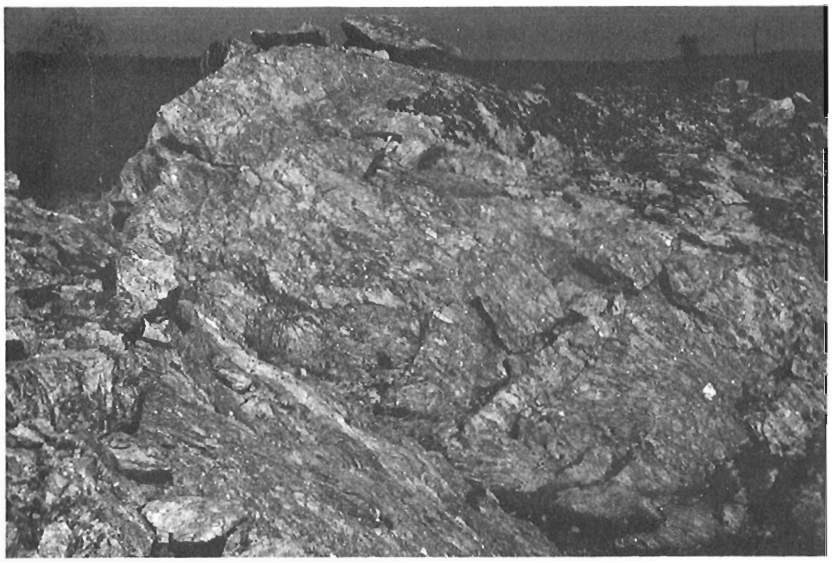

Figure 51.2

Alignment of spodumene and microcline crystals perpendicular to the walls (ladder-type structure) of Central pegmatite, Thor Echo swarm, Tanco Lake series.

Turnback Lake series

This series includes a group of simple pegmatites situated on a peninsula extending southwards into Turnback Lake; all are located within 200 m of the Turnback Lake granite. The pegmatites occur as generally concordant northeast-striking bodies in schist adjacent to a contact with Cameron River metafelsites. The Eaglet swarm consists of ellipsoidal bodies in comparison to the lenticular forms of Eyrie and Talon. All pegmatites in this series are homogeneous with rare, poor zoning (Eaglet swarm). No albitization or rare-element minerals are present.

Bug series

The Bug series occurs over a 3 km expanse south-southwest of the Turnback Lake granite and within 2 km east of the Horse Fly granite and the Tumpline Lake biotite-muscovite granite. The bodies occur generally concordantly in metafelsites (Ant, Tick, Beetle) and schist (Skeeter swarm). Metavolcanic rafts are commonly found in the pegmatites. All of the dykes are homogeneous with weak zoning observable only in the larger bodies (Beetle). No rare-element mineals are present except for rare beryl in Ant and Tick.

Detour Lake series

This series includes the Demon and Ptarmigan swarms located within 1 km of bodies of units 11 and 12 granites and the Ptarmigan and Island granites. The Demon bodies are for the most part less than one metre wide and cut Island granite, gneiss, quartz-biotite schist, and skarn. The largest dyke is 6 by 88 m cutting gneiss and schist across the foliation. Varying in size from 0.3-6 m across, the Ptarmigan bodies have generally concordant boundaries. No rare-element minerals or secondary albitization was observed in any of these homogeneous to poorly zoned bodies.

Peg series

Hutchinson (1955) described this extensive series which is situated between Upper Ross and Redout lakes extending westwards from the western margin of the Redout Lake Granite. The dykes penetrate the Ross Lake Granodiorite. These pegmatites vary from concordant, unzoned, simple northwest-striking pegmatites in the east to highly discordant, zoned, rare-element bearing, northeast-trending dykes in the west. Sn-Nb-Ta mineralization includes cassiterite, tapiolite, disordered ferrotantalite, disordered manganotantalite, and disordered ferrocolumbite.

Fle series

This series is situated northwest of Wedge Lake and east and west of Lamoureux Lake and was partly described by Kretz (1968). The pegmatites occur in schist southwest and east of the Prestige Lake Granite and rarely in the granite itself. The pegmatites east and southwest of the pluton are all discordant to the enclosing schist which commonly has andalusite porphyroblasts. Strike of the dykes is variable and zonation is moderately developed. Within the granite, one 125 m by 0.5 m northeast-trending dyke was observed. The dyke is poorly zoned, but the mineralogy is nearly the same as that of the other dykes. Other than yellow beryl, no rare-element minerals were identified.

Blaisdell Lake series

The Blaisdell Lake series lies east and southeast and within 3 km of the Wedge Lake granite. With variable trends, some dykes are concordant, others cut across the schistosity. Bending of the schistose layers is observable as are xenoliths of schist. Zonation varies from homogeneous to good across the series and within swarms. Spodumene, commonly altered to fine grained muscovite, is present only in the Vo dykes which have a ladder-type structure. Albitization is patchy and only observed in the Vo and Melody swarms. Cassiterite, tapiolite, and disordered ferrocolumbite has been identified.

Sproule Lake series

The Fly pegmatite and the Cata swarm outcrop immediately west and south of Sproule Lake in schist approximately equidistant (5.5 km) from the Wedge and Scott Lake granites. The cordierite isograd is situated less than 1 km to the east of the Cata swarm. The dykes strike northwesterly and are strongly discordant. Zonation of the bodies varies from poor to moderate and the bodies are commonly albitized. Spodumene is oriented perpendicularly to the walls in the Fly and is severely altered to muscovite in bodies of the Cata swarm. Cassiterite and disordered manganocolumbite have been identified.

Thompson Lake series

This series extends 5 km north and south of Thompson Lake near the Scott Lake, Cameron River, and Hidden Lake plutons. All of the pegmatites penetrate schist both parallel and obliquely to the schistosity. North of Thompson Lake, the pegmatites trend to the northwest, south of the lake the trend is more variable, ranging from northwest in the east (Ki) to north-northeast in the west (Fi). Zonation ranges from homogeneous to well developed. Spodumene is generally perpendiular to the walls of bodies of the Fi and Ki swarms, but is more variably oriented in members of the Waco swarm where minor amounts of spodumene-quartz intergrowths occur. Albitization is restricted to the pegmatities north of Thompson Lake and is patchy. Sn-Nb-Ta mineralization includes cassiterite, tapiolite, disordered ferrocolumbite, and disordered manganocolumbite.

Sparrow Lake series

These pegmatites intrude the margins of the Cameron River granite (Casper) and the surrounding schist (Casper and Heidi). The Casper dykes predominantly strike north-northeast to northwest and vary from highly discordant to concordant. The Heidi dykes trend east-west predominantly, but also strike northwest to northeast along probable fractures. The east-west dykes are generally concordant to slightly discordant. The zonation is generally poor, but is moderate in rare cases. Albitization is present in both swarms, but is rare. Although beryl is present in some pegmatites within the margins of the granite and up to 200 m out from the granite, it is absent in pegmatites between 200 and 1000 m from the granite, and is present again beyond the barren zone. Disordered columbite-tantalite and tapiolite have been identified in these swarms.

Hidden Lake series

Extending eastwards 3.5 km from the Hidden Lake granite, the series penetrates schist at varying angles to the schistosity. The predominant trend changes from north-northeast in the west to northeast in the east. Pegmatites of this series are poorly zoned. Spodumene orientation varies from perpendiular to the walls in the easternmost dykes to slightly random in the Qi swarm. Albitization is patchy throughout. Columbite-tantalite minerals have been found in all swarms.

Reid Lake series

All bodies are within 2 km of the southeastern margin of the Cameron River granite. Ann and Boa are also within a few hundred metres of the northeastern margin of the Southeastern Granodiorite. All of the pegmatites are roughly concordant to the enclosing schist. Zonation is poor in all bodies and albitization is present in most bodies as patches. Spodumene is nearly perpendicular to the walls of the pegmatites; in Ann it commonly occurs in bands alternating with pink alpite. The Sn-Ta-Nb minerals are represented by columbite-tantalite series minerals are rare tapiolite (in Pancho Villa).

Harding Lake series

Paint and Jake-Da pegmatites penetrate the northeastern margin of the Southeastern Granodiorite along the northern and northwestern shores of Harding Lake respectively. The nearest granite pluton is the Cameron River, 10.5 km northwest. The dykes trend northerly and are mineralogically unzoned. A textural zonation is present as a coarsening of grain size towards the cores. Muscovite abundance is low. Spodumene occurs perpendicular to the walls and is commonly a translucent green colour. Disordered columbite-tantalite is present.

Slave series

This relatively isolated series of pegmatites occurs along the southeastern margin of the Southeastern Granodiorite and adjacent to the Matonabbee Point granite. Some of the dykes crisscross the margins of the granodiorite, others lies within the sheared schist. The pegmatites within the schist trend predominantly east-northeast and are predominantly concordant. Apophyses of the dykes cut the schist discordantly and are commonly ptygmatically folded. The quartz in all pegmatites is milky and the feldspars in the schist-hosted dykes appear to have been broken and healed. Zoning is generally poor, but is moderate in rare cases. Although beryl has been reported, none was observed by the authors. No other rare-element minerals were observed.

Upland Lake series

The Pancho Pete and Jenne swarms are situated west of Upland Lake and east of Jennejohn Lake respectively. The Cameron River granite lies about 6 km northeast. These dykes trend northeast and are discordant to the enclosing schist; xenoliths of the schist are present within the Jenne dykes. The Pancho Pete dykes are relatively narrow (3-62 cm wide), while the Jenne dykes are 60 to 120 cm wide. Zonation is absent from both swarms. Spodumene is present in the Jenne dykes and is perpendiular to the walls. Rare grains of columbite-tantalite are present in the Jenne dykes, but no rare-element minerals are visible in Pancho Pete.

Bighill Lake series

Situated on the northern and southeastern shores of Bighill Lake, respectively, are the Limo and Big swarms. The Prosperous Lake Granite lies about 4 km north. All of the bodies trend northeasterly and are discordant to the foliation of the country rock. Rafts of country rock within the pegmatites are common. Zonation is poor throughout. Muscovite is rare and albitization is present in isolated pods. Spodumene and K-feldspar are oriented perpendicularly to the walls (ladder-type structure). Columbite-tantalite series minerals are present.

Pontoon Lake series

Penetrating both schist and the southern part of the Prosperous Lake Granite, these pegmatites lie within an area bordered by Prelude, Pontoon, and Madeline lakes. The Fern swarm is spread across the southern part of the granite and an incursion of schist. The Anne Marie swarm lies within the extreme southern margin of the granite and the Bubo swarm lies about 1.5 km from the granite. Though variable in strike, the predominant trend is easterly for the northern Fern dykes, northeast for the southern Fern dykes, northwest for Anne Marie and north-northeast for Bubo. The Bubo dykes are discordant. Zonation is poor in general, although moderate zoning is attained in the eastern Fern dykes. Mineralogy of the southern bodies is simple except for isolated pods of sulphides (arsenopyrite, pyrite) in the Anne Marie bodies. Several of the Fern dykes are rich in beryl, but no other rare-element minerals were noted.

Tom Lake series

This series is the southwesternmost series of the field. It extends southwards from the Prosperous Lake Granite about 3 km. The dykes trend northeast and are discordant to the foliation of the host schist. Zonation is absent to poor. Spodumene crystals are oriented perpendicularly to the walls in the Mint and Nite swarms, but are randomly oriented in the Odin dykes. Tapiolite and disordered columbite-tantalite have been identified in this series (Mint).

Minipud series

The only pegmatite visited occurs on the eastern shore of Prosperous Lake about 1300 m west of the Prosperous Lake Granite. The dyke cuts the surrounding schist discordantly and strikes northerly. It is a well-zoned pegmatite. The only rare-element mineral observed was green to yellow beryl.

Murphy series

This swarm of pegmatites outcrops between Short Point and Neck Lakes where the swarm penetrates schist concordantly. The closest granite is the Neck Lake granite, a few hundred metres to the northeast. The bodies trend predominantly northeast. Zonation is absent to poor and the mineralogy is simple. No rare-element mineralization is present.

Alexie Lake series

This series of pegmatites represents a cross-section of pegmatites across the schist (rarely garnetiferous) terrane between the Prosperous Lake and Duncan Lake granites, just south of the Staple Lake pluton. Trends and crosscutting relationships are highly variable, but most of the broader dykes are discordant. The contacts around the Alex pegmatite of the Alexie Lake West swarm are highly deformed. Zonation is absent to slight and the mineralogy is simple. No rare-element minerals were noted.

Petey Lake series

The Petey Lake series is also a cross-section of pegmatites across the Burwash Formation schist south of the Alexie Lake series. Penetration of the schist in relation to schistosity is variable, even within individual swarms. The Lil' Rascals swarm in the west trends predominately northwesterly and is homogeneous to moderately zoned. The mineralogy of the swarm is variable and is most diverse in the Buckwheat pegmatite which, in addition to a higher than average beryl content, contains zones of albitization. The Geo swarm trends more northerly than the Lil' Rascals swarm and ranges from homogeneous to moderately zoned. Rare albitized zones are present (Dr. Bob pegmatite) along with rare columbite-tantalite. The Riber pegmatite in the east is the most fractionated body in the series and occurs as a well-zoned, northwest-trending tabular body. Riber is the only pegmatite containing elbaite, a pink Li-poor muscovite, and mixed lithian muscovite – lepidolite. Uranmicrolite, disordered columbite-tantalite and zircon have also been identified.

Prelude Lake series

The southermost partial cross-section of pegmatites across the schist terrane between the Prosperous Lake and Duncan Lake granites includes two swarms. The dykes intrude the schist at varying degrees of discordancy. The River Lake swarm strikes predominantly west-northwest and the Dike swarm trends north-northwest. The pegmatites of the River Lake swarm vary from primitive unzoned bodies (Whiskey) to poorly to moderately zoned ones (Splash). The mineralogy of the River Lake swarm is quite simple with no rare-element minerals other than beryl. The two bodies of the Dike swarm visited are Lily, which is moderately zoned, and Rose, which is homogeneous. Fine grained columbite-tantalite (?) has been found in both dykes.

DISCUSSION

Overall, a division of pegmatites into three large geographical groups can be made. These are the Southeastern, Northeastern, and Northwestern groups which correspond roughly to those delineated by Ayres and Černý (1982). However, contrary to the findings of Ayres and Černý (1982), recent sampling has indicated regional zonation in the northwestern group east and south of the Duncan Lake, Duncan Lake East, Wedge Lake, Sparrow Lake, Cameron Lake, Hidden Lake, and Prelude Lake granites, with pegmatite fractionation increasing away from the plutons. The zonation west of the Duncan Lake granite is reversed with fractionation increasing from west to east.

On the basis of gross mineralogy and textural charcteristics, any of the granite units described could be parental to pegmatites. Many of the plutons contain internal pegmatitic facies and veins, and those plutons could, indeed, be parental to a series or several series of pegmatites. However, there is great variation from pluton to pluton, even among members of the same unit, in contrast to gross uniformity of pegmatites within specific areas.

The Yellowknife pegmatite field is structurally diverse and there seems to be little relation between structure and any paragenetic features of the pegmatites, except locally. It is not yet possible on the basis of mineralogical and structural data to define a genetic linkage between the pegmatites and specific plutons or plutonic units. The paths of granite and pegmatite generation may vary widely even within a limited area (Černý et al., 1981). More definite conclusions in this respect and in regards to consanguinuity of pegmatities and granites may be reached when geochemical data are available from ongoing studies. At present, the data only suggest probable genetic relationships (Kretz, 1968; Hutchinson, 1955) or possibly a sizeable hidden pluton (Ayres and Černý, 1982).

REFERENCES

Ayres, L.D. and Černý, P.
1982: Metallogeny of granitoid rocks in the Canadian Shield; Canadian Mineralogist, v. 20, p. 439-536.

Černý, P.
1982: Anatomy and classification of granitic pegmatites; in Granitic Pegmatites in Science and Industry, ed. P. Černý; Mineralogical Association of Canada Short Course Handbook, v. 8, p. 1-39.

Černý, P., Trueman, D.L., Ziehlke, D.V., Goad, B.E., and Paul, B.J.
1981: The Cat Lake – Winnipeg River and the Wekusko Lake Pegmatite Fields, Manitoba; Manitoba Department of Energy and Mines, Economic Geology Report ER80-1, 216 p.

Davidson, A.
1972: Granite studies in the Slave Province, in Report of Activities, Part A; Geological Survey of Canada Paper 72-1A, p. 109-115.

Fortier, Y.O.
1947: Preliminary Map, Ross Lake, Northwest Territories (map and descriptive notes); Geological Survey of Canada Paper 47-16, 4 p.

Fyson, W.K.
1975: Fabrics and deformation of Archean metasedimentary rocks, Ross Lake – Gordon Lake area, Slave Province, Northwest Territories; Canadian Journal of Earth Sciences, v. 12, p. 765-776.

1978: Structures induced by granite diapirs in the Archean Greenstone Belt at Yellowknife, Canada: Implications for Archean geotectonics: A Discussion; Journal of Geology, v. 86, p. 767-769.

Fyson, W.K. (cont.)
1981: Divergent fold overturning and regional tectonics, southern Slave Province, Northwest Territories; Precambrian Research, v. 14, p. 107-118.

Green, D.C. and Baadsgaard, H.
1971: Temporal evolution and petrogenesis of an Archean crustal segment at Yellowknife, N.W.T., Canada; Journal of Petrology, v. 12, p. 177-217.

Green, D.C., Baadsgaard, H., and Cumming, G.L.
1968: Geochronology of the Yellowknife area, Northwest Territories, Canada; Canadian Journal of Earth Sciences, v. 5, p. 725-735.

Henderson, J.B. (Compiler)
1976: Geology of Yellowknife (85J) and Hearne Lake (85I), District of Mackenzie map areas; Geological Survey of Canada Open File Report 353, Scale 1:125 000, 2 sheets.

1981: Archean basin evolution in the Slave Province, Canada; in Precambrian Plate Tectonics, ed. A. Kroner; Amsterdam, Elsevier, p. 213-235.

Hutchinson, R.W.
1955: Regional zonation of pegmatites near Ross Lake, District of Mackenzie, Northwest Territories; Geological Survey of Canada Bulletin 34, 50 p.

Kretz, R.
1968: Study of pegmatite bodies and enclosing rocks, Yellowknife – Beaulieu Region, District of Mackenzie; Geological Survey of Canada Bulletin 159, 105 p.

Kretz, R., Garrett, D., and Garrett, R.G.
1982: Na-K-Li geochemistry of the Prestige Pluton in the Slave Province of the Canadian Shield; Canadian Journal of Earth Sciences, v. 19, p. 540-554.

McGlynn, J.C. and Henderson, J.B.
1972: The Slave Province; in Variations in Tectonic Styles in Canada, ed. R.A. Price and R.J.W. Douglas; Geological Association of Canada, Special Paper no. 11, p. 505-526.

Meintzer, R.E. and Černý, P.
1983: Geological studies of rare-element pegmatites in the Yellowknife Basin of the N.W.T.; in Mineral Industry Report, 1978, Northwest Territories; Canada Department of Indian Affairs and Northern Development, EGS 1983-2, p. 189-202.

52. THE EXTERNIDES OF WOPMAY OROGEN, TAKIJUQ LAKE AND KIKERK LAKE MAP AREAS, DISTRICT OF MACKENZIE

Project 810021

P.F. Hoffman, Rein Tirrul, J.P. Grotzinger[1], S.B. Lucas[2], and K.A. Eriksson[1]
Precambrian Geology Division

Hoffman, P.F., Tirrul, R., Grotzinger, J.P., Lucas, S.B., and Eriksson, K.A., The externides of Wopmay Orogen, Takijuq Lake and Kikerk Lake map areas, District of Mackenzie; in Current Research, Part A, Geological Survey of Canada, Paper 84-1A, p. 383-395, 1984.

Abstract

Some results of the final summer's fieldwork on this project are outlined as they pertain to the following topics: (1) sedimentary structures and paleoenvironment of the Odjick clastic shelf; (2) paleogeographic zonation of the Rocknest shelf-edge reef complex; (3) nature and origin of Rocknest shelf cycles; (4) correlation of the Rocknest dolomite eastward across Rockinghorse Arch into Kilohigok Basin and implications of a revised correlation of formations in the Epworth and Goulburn groups; (5) regional variation in low grade metamorphism and its relation to deformation events; (6) basement-involved folding without thrusting in the Tree River belt; and (7) development of "shingle" structures (crudely hexagonal crustal blocks) by progressive conjugate transcurrent faulting.

Résumé

Le rapport présente certains résultats des derniers travaux sur le terrain effectués dans le cadre du présent projet, dans les domaines suivants: 1) structures sédimentaires et paléoenvironnement de la plate-forme clastique d'Odjick; 2) zonation paléogéographique du complexe récifal en bordure de la plate-forme de Rocknest; 3) nature et origine des cycles de la plate-forme de Rocknest; 4) corrélation de la dolomie de Rocknest vers l'est en travers de l'arche de Rockinghorse, jusque dans le bassin de Kilohigok, et répercussions d'une corrélation révisée des formations dans les groupes d'Epworth et de Gouldburn; 5) variation régionale du métamorphisme faible et lien avec les événements à l'origine de déformations; 6) plissement sans chevauchement touchant au socle rocheux dans la zone de Tree River; et, 7) évolution des structures imbriquées (blocs grossièrement hexagonaux de la croûte) par la formation progressive de décrochements perpendiculaires.

INTRODUCTION

The externides of Wopmay Orogen (Fig. 52.1) include the foreland thrust-fold belt and contiguous autochthonous cover fringing the exposed Archean basement of Slave Craton to the east. The area preserves the landward part of a 1.9 Ga continental margin sedimentary prism, the Coronation Supergroup, which is being studied to improve our understanding of mechanisms of formation and destruction of a continental margin in Precambrian time. This project is closely allied with another studying the seaward part of the marginal prism, which ultimately became the rear part of a deformational wedge continuous with the foreland thrust-fold belt (St-Onge et al., 1984).

In the externides, the prism consists of a lower pre-orogenic sequence (Odjick and Rocknest formations) built on the subsided margin of the craton, and an upper syn-orogenic sequence (Recluse Group) deposited diachronously in a foredeep that migrated eastward in front of the tectonically prograding thrust-fold belt (Fig. 52.2). The principal deformation of the prism, the 1.89 Ga Calderian Orogeny (Hoffman and Bowring, in press), resulted in eastward-directed thrusting and folding above a basal décollement located 300 m or more above the basement, followed by low-amplitude basement-involved folding of the décollement (Tirrul, 1983; St-Onge et al., 1984).

Following hard on the heels of the Calderian Orogeny are two unrelated episodes of regional shortening (Hoffman and Bowring, in press). The earlier (D2) produced sporadic basement-involved folds and related cleavages of variable northeast trend, strongly developed especially in the Tree River Fold Belt in the northeast corner of the externides (Fig. 52.1). Transverse D2 arches of regional scale provide critical oblique sections through the entire Calderian deformational wedge (Tirrul, 1983; St-Onge et al., 1984). The younger event (D3) produced a throughgoing system of conjugate brittle transcurrent faults (Fig. 52.1) indicating east-west shortening and north-south extension.

This report, which follows the final summer of fieldwork for this project, focuses on the following observations not discussed in previous reports (Tirrul, 1982, 1983; Grotzinger, 1982; Hoffman et al., 1983; Grotzinger and Hoffman, 1983; Grotzinger and Read, in press):

1. Sedimentary structures in the Odjick Formation (Fig. 52.2) indicate clastic deposition on a prograding, storm-dominated, open marine shelf. Storm-surge ebb currents are likely responsible for paleocurrents directed uniformly offshore. An extremely rapid and extensive initial transgression of the craton is indicated.
2. In the Rocknest Formation (Fig. 52.2), a detailed paleogeographic zonation of the outer reefal rim and associated facies has been established. The discovery of abundant "neptunian" dykes and sills (synsedimentary fissures filled by submarine cements) in the reef and vadose pisolites in a persistent back-reef shoal complex add to the list of features shared with some famous Phanerozoic reef complexes. Systematic changes in correlatable cycles across the externides document repeated eastward progradation (enlargement) of the back-reef shoal complex at the expense of a persistent inner-shelf lagoon as the immediate cause of prominent Rocknest cyclicity. Incomplete shoaling of cycles in the east prove that shoaling of the entire lagoon was not required to initiate new cycles. This makes a eustatic control on cyclicity more likely and its periodicity, given the geochronological constraints (Hoffman and Bowring, in press), cannot have exceeded 50 000 years (200 cycles in 10 million years) for each 1-10 m thick cycle.

[1] Department of Geological Sciences, Virginia Tech, Blacksburg, VA 24061
[2] Department of Geological Sciences, Queen's University, Kingston, Ontario K7L 3N6

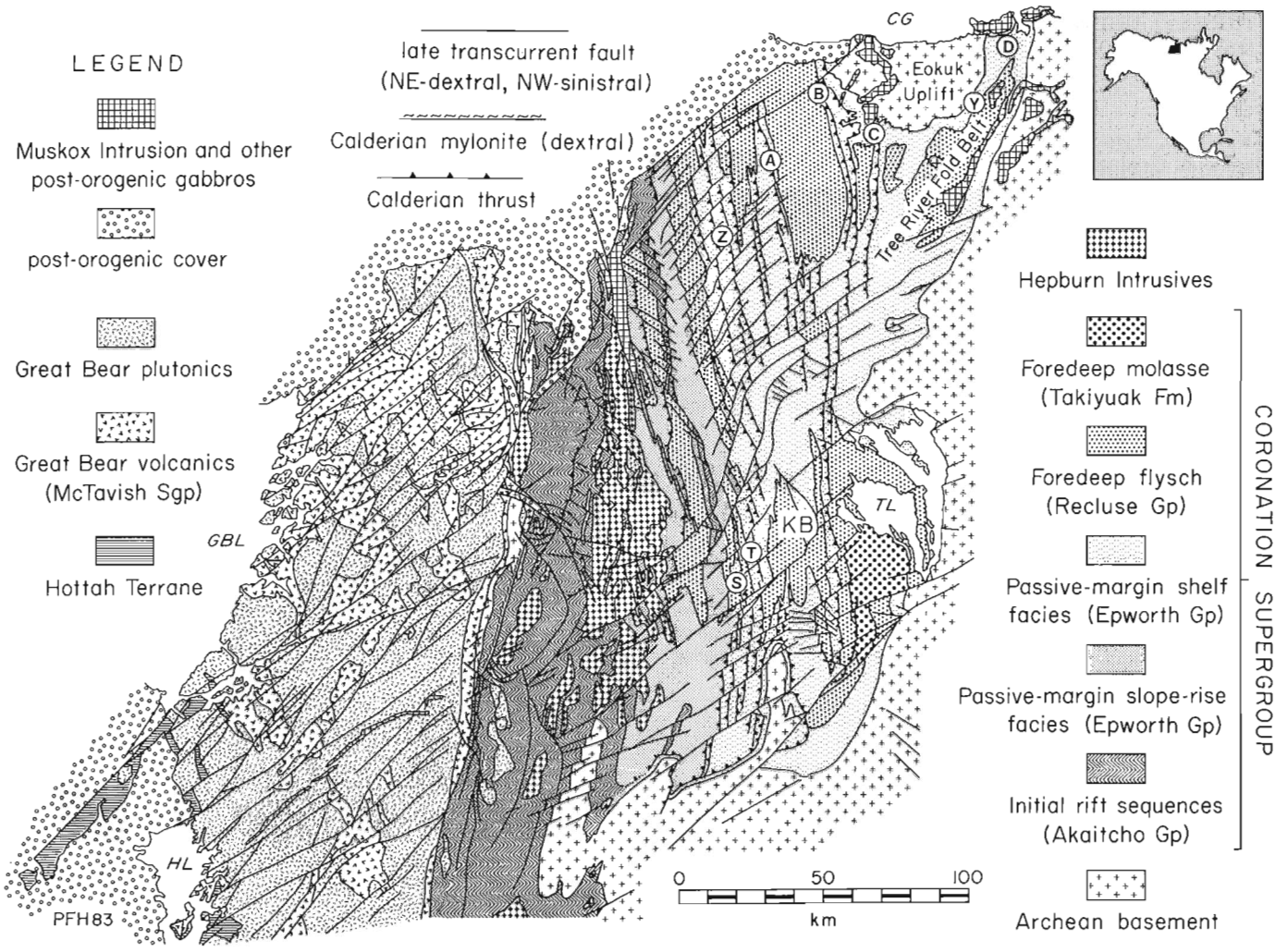

Figure 52.1. *Simplified geological map of the northern two-thirds of Wopmay Orogen, showing the locations of measured sections (A,B,C,D,S,T) of Figures 52.3-52.5, and location of areas "Y" and "Z" discussed in the text. "KB" indicates the position of the Kangaroo Block. Prominent water bodies are: CG, Coronation Gulf; GBL, Great Bear Lake; TL, Takijuq Lake; HL, Hottah Lake.*

3. The eastward extension of the Rocknest Formation has, for the first time, been traced across Rockinghorse Arch into Kilohigok Basin (Goulburn Group), where it correlates with a 21 m thick mixed dolomite and clastic unit within the Burnside River Formation. This revised correlation has important regional tectonic implications. It shows that a major source of clastic sediment, possibly the Thelon Front, was being unroofed southeast of Kilohigok Basin concurrent with the rapid opening and closing of the Coronation margin.

4. In an attempt to document variation in low grade metamorphism in the externides, colour change in a specific shale member of the Rocknest Formation was systematically recorded, hopefully to be calibrated in the laboratory by determination of illite crystallinity and/or vitrinite reflectance. The observed colour changes reflect vertical and lateral variation in metamorphic grade during both Calderian and D2 deformations. In both deformations there is a clear correlation of higher metamorphic grade with development of cleavage, penetrative strain, and degree of basement involvement in folding.

5. Mapping of the Tree River Fold Belt has reaffirmed the existence of recumbent folds of the basal unconformity without associated thrusts marginal to the basement uplifts bounding the belt. Metamorphic biotite occurs in pelite around Eokuk Uplift (Fig. 52.1), perhaps the highest grade metamorphism in the externides, but the cause of this deep-seated thermal anomaly remains problematic. Some aspects of D2 deformational mechanisms have been clarified.

6. Crudley hexagonal crustal blocks ("shingles"), bounded by D3 faults, were previously observed in north-central Wopmay Orogen and interpreted as east-vergent thrusts linked by coeval transcurrent faults (Hoffman and St-Onge, 1981). Discovery of a similar but smaller scale structure in the externides, well exposed and with excellent stratigraphic control, led to development of an alternative model in which thrusting plays at most a minor role.

DEPOSITIONAL HISTORY OF THE ODJICK CLASTIC SHELF – A PRELIMINARY ANALYSIS

The Odjick Formation (Fig. 52.2) has been subdivided into three informal Lower (Eol), Middle (Eo2) and Upper (Eo3) members (Hoffman et al., 1983). A general alluvial/coastal marine depositional model was proposed for continental shelf sediments of the Odjick Formation which were interpreted to pass laterally into submarine-fan deposits beyond a shelf-edge (Hoffman, 1973). Unlike the Rocknest Formation, the Odjick is difficult to study in detail because of inadequate outcrop, lichen cover, and poor structural control due to lack of mappable stratigraphic markers in the thick Middle Member. Nevertheless, reconnaissance observations were made by one of us (K.A.E.) on the Lower and Middle members in area "Y" of Tree River Fold Belt (Fig. 52.1), and in area "Z" which lies within the foreland thrust-fold belt (Fig. 52.1), approximately 100 km (palinspastically) from area "Y" and approximately 20 km from the shelf-edge. The specific objective was to better constrain the depositional history of the Odjick Formation.

The Lower Member in area "Y" comprises three facies arranged in vertical sequence through 55 m of section: (1) planar-laminated siltstones and mudstones in couplets less than 1 cm thick, which resemble the graded rhythmites of Piper (1972); (2) normally graded and coarse-tail graded sandstones and siltstones with interlaminated mudstones in 1 to 5 cm thick couplets; and (3) planar-laminated sandstones and siltstones in 1 to 5 cm thick units. Upper surfaces of units are scoured and draped with either mudstone or sandstone-siltstone redeposited from suspension. The latter average 10 cm in width and are analogous to small-scale hummocky cross-stratification (cf. Allen, 1981).

The sandstones and siltstones of the Lower Member in area "Y" coarsen and thicken upward into the Middle Member through a stromatolitic dolomite unit which is laterally discontinuous. The Middle Member is mainly arenaceous but contains frequent 5 to 10 cm thick mudstone drapes in the lowermost one-third of the member. Hummocky cross-stratification is the predominant sedimentary structure producing a characteristic outcrop pattern of overlapping flat-bottomed lenses. Individual hummocks average 2 m in width and 15 cm in height and where not amalgamated, individual sandstone lenses have wave-rippled tops overlain by mudstone drapes. Unlike the small-scale hummocks in the Lower Member, those in the Middle Member did not form by scour and drape but rather appear to have grown as three-dimensional bedforms.

The sequence of lithologies and sedimentary structures in the Lower and Middle members are best accommodated in a progradational, storm-dominated shelf model (cf. Brenchley and Newall, 1982; Hamblin and Walker, 1979) in which the Lower Member is assigned to an outer-shelf setting and the Middle Member to an inner-shelf setting. The boundary between the two subenvironments is arbitrarily taken at storm wave base. Sediment is supplied to the shelf from the shore zone by storm surge ebb or gradient currents (Allen, 1981). These currents are produced by the seaward return of water amassed along coastlines by onshore-directed storm winds, with the entrained sediment deposited at or below wave base. Reworking of sediment at storm wave base produces hummocky cross-stratification (e.g. Middle Member) the scale of which is a function of wave period and maximum orbital velocities of storm waves. If sufficient time exists between successive storm events, wave ripples are

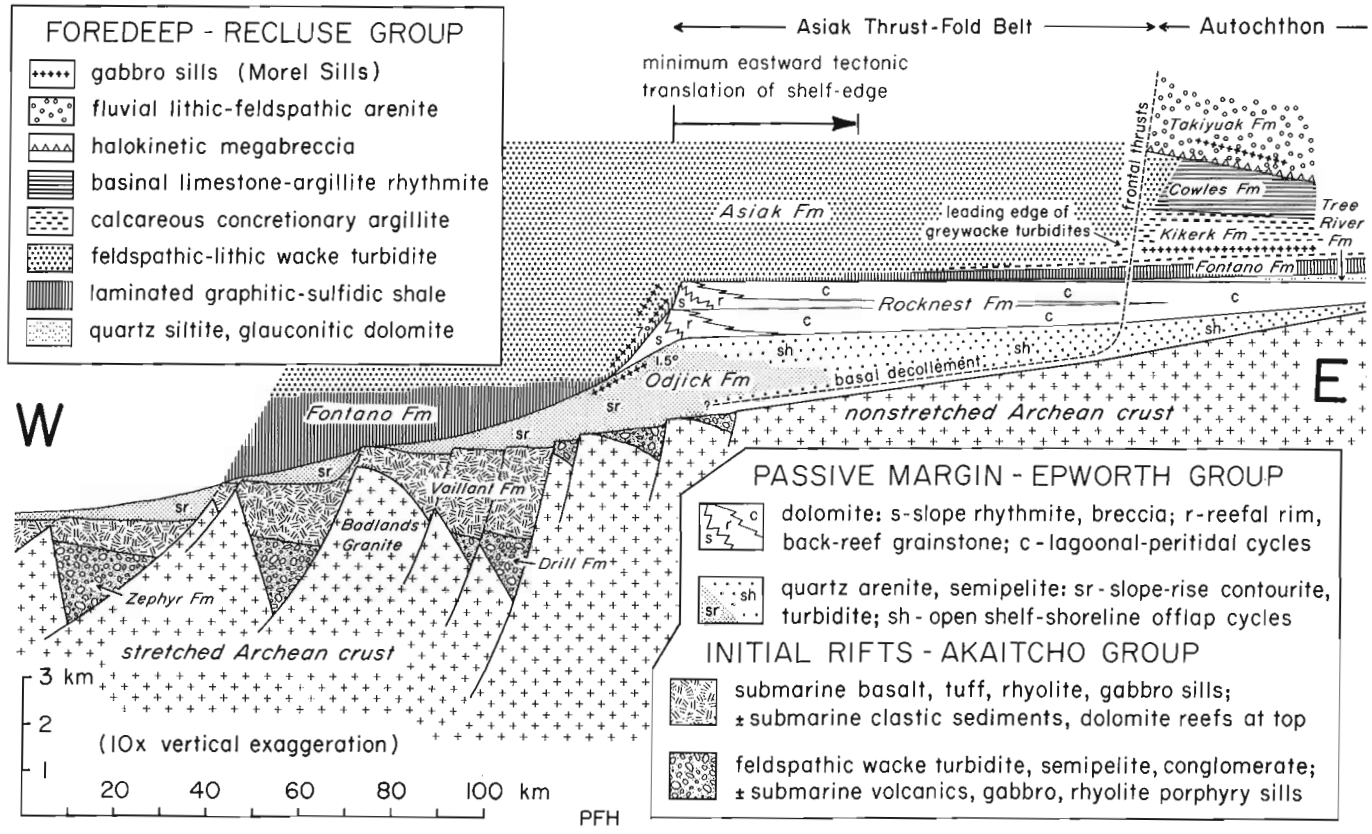

Figure 52.2. *Stratigraphic reconstruction of the Coronation Supergroup, assuming 40% tectonic shortening west of the frontal thrusts and above the basal décollement. Stratigraphic thicknesses, facies relations and estimated shortening are well controlled by down-plunge projections east of the Rocknest slope (Tirrul, 1983). To the west, the same shortening (40%) is assumed but stratigraphic thicknesses are poorly constrained. The overall construction is artificial for the Recluse Group, which was deposited as deformation progressed from west to east.*

superimposed on the upper surface of hummocks during the return to fair-weather conditions followed by settling of suspended muds during fair-weather sedimentation (e.g. lower part of Middle Member). Below storm wave base, suspended sediment is deposited from unidirectional, offshore-directed currents to produce graded and/or planar-laminated sandstones and siltstones. The thickness of these individual storm-generated units decreases outwards on the shelf (e.g. Lower Member facies 1 and 2). The planar-laminated sandstones and siltstones may be locally scoured and draped at storm wave base (e.g. Lower Member facies 3). The enclosing terrigenous sediments indicate that the stromatolitic dolomite at the top of the Lower Member is of sublittoral origin and probably developed during a prolonged period of time when the shelf was starved of terrigenous sediment.

The facies in the Lower and Middle members at area "Z" can be readily interpreted as distal time equivalents of the deposits at area "Y". The Lower Member consists mainly of laminated marlstone, mudstone and carbonate representing suspension deposits of a distal shelf environment starved of terrigenous influx. The distal shelf was not necessarily deeper than at area "Y" as evidenced by occasional edgewise carbonate breccias enclosed within the laminated sediments. The breccias are confined to the uppermost one-third of the Lower Member and are considered to reflect oscillatory reworking of lithified carbonate muds during periodic lowering of wave base. The Middle Member at area "Z" is devoid of hummocky cross-stratification and instead comprises several upward-thickening and upward-coarsening sequences of tabular sandstone beds structured by planar lamination with rare wave ripples developed at the tops of beds. Similar sequences in the 1.7 Ga Ortega Group in New Mexico are interpreted as progradational outer-shelf lobes which accumulated mainly below storm wave base (Eriksson and Soegaard, 1983).

The sequences of facies through the Lower and Middle Members of the Odjick Formation at areas "Y" and "Z" indicate a slow progradation following initial rapid transgressive drowning of the craton. A granite-pebble conglomerate and overlying stromatolitic dolomite, both of which are laterally discontinuous and total less than 1.5 m in thickness, represent the only transgressive deposits. Around Carousel Massif, the initial transgression is represented by up to 6 m of white supermature quartz arenite (St-Onge et al., 1982).

PALEOGEOGRAPHY, FACIES DISTRIBUTION, AND CYCLIC SEDIMENTATION ON THE ROCKNEST CARBONATE SHELF

During the 1983 field season, investigations of the Rocknest Formation by J.P.G. concentrated on detailed mapping and stratigraphic studies of the shelf-edge reef complex and flanking facies belts, and on changes across depositional strike within shoaling-upward cycles at the north end of the externides. Paleogeographic reconstruction of the shelf-edge complex reveals a sharply defined, narrow reefal rim composed of strongly elongate stromatolite mounds that interfinger vertically and laterally along strike with subordinate amounts of ooid/intraclast grainstone (Fig. 52.3a). The reefal rim underwent early cementation and fracturing as shown by pervasive networks of neptunian dykes and sills, filled with silica and dolomite pseudomorphs after botryoidal aragonite and other isopachous-fibrous marine cements (Fig. 52.3b, d). Early fracture porosity in the reefal rim was further enhanced by periods of submarine(?) dissolution which corroded, enlarged, and truncated fractures, and corroded parts of stromatolite mounds (Fig. 52.3c). To the east (landward), stromatolite mounds of the reefal rim pass laterally into outer-shelf deposits consisting of equally interbedded stromatolite mounds and ooid/intraclast grainstone. The outer shelf was subjected to open-marine conditions involving constant wave and tidal(?) activity as shown by the extreme elongation of stromatolites and crossbedding in grainstones. Farther to the east, outer shelf deposits pass laterally into a narrow zone of stromatolite-deficient, crossbedded and planar-laminated ooid/intraclast grainstones (Fig. 52.4) that represent shoreface deposits. These facies pass abruptly eastward into a sharply defined, laterally continuous, peritidal shoal complex (Fig. 52.4). This facies belt is dominated by precipitated cryptalgal tufa, locally thrust into tepee antiform structures, and associated with vadose pisolites and void-filling silica and dolomite pseudomorphs after botryoidal aragonite that precipitated beneath tepees and in related subhorizontal fissures (see Grotzinger and Read, in press).

With respect to the diversity and similarity of facies, and their paleogeographic position immediately behind a reefal rim, there is a striking resemblance between the peritidal shoal complex of the Rocknest Formation, the Permian Carlsbad Group of west Texas, and the Triassic Latemar Group of the Italian Alps (Assereto and Kendall, 1977). In the Rocknest Formation, the width of the

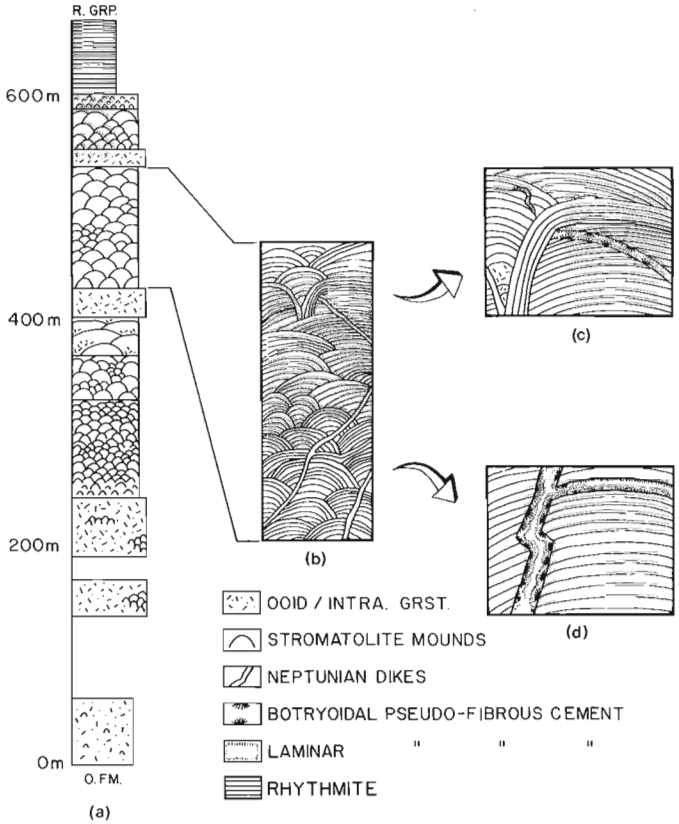

Figure 52.3. *(a) Stratigraphic section of Rocknest Formation shelf-edge facies; (b) Crosscutting neptunian dykes; (c) Details showing truncation of neptunian dyke followed by deposition of more stromatolitic laminae; (d) Details showing "fitted" relations of neptunian dyke walls, and internal cement stratigraphy. Location of section is "S" in Figure 52.1.*

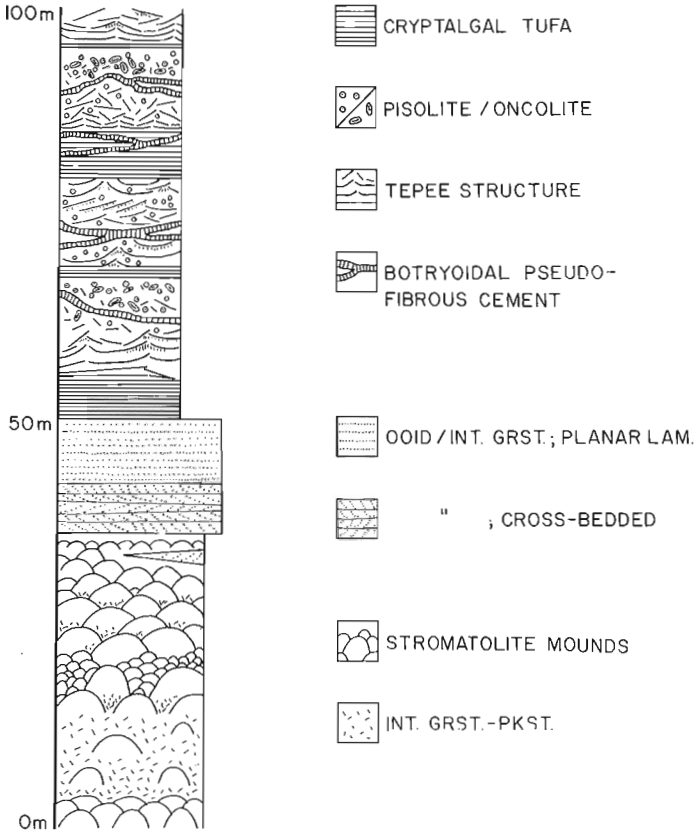

Figure 52.4. *Stratigraphic section through part of Basal Member of Rocknest Formation, 10 km (palinspastic) east of the shelf edge. The section shows a long-term progradational ramp sequence of peritidal shoal-complex facies overlying ooid/intraclast grainstones and stromatolitic boundstones. Location of section is "T" in Figure 52.1.*

peritidal shoal complex varied, but at all times (except during local drowning and backstepping of the reefal rim midway through the evolution of the platform) acted as the starting line for numerous short-term progradational cycles (1-10 m thick) of the shoal complex over a very broad (at least 150 km) inner-shelf lagoon to the east. In contrast to the outer-shelf, which was wave- and tide(?)-dominated, the inner-shelf lagoon was storm-dominated. Storm deposits include abundant rip-up breccias overlain by planar-laminated and hummocky cross-stratified siliciclastic and carbonate sands. These sequences are commonly capped by wave-rippled sands and silts, and graded silt-to-mud couplets. The inner-shelf lagoon was the site of intermixing of carbonate sediment derived from the peritidal shoal complex to the west, and siliciclastic sediment derived from a shoreline to the east. Accordingly, the ratio of carbonate to terrigenous sediment decreases from west to east.

The shoaling-upward cycles in the Rocknest Formation dominate its stratigraphy in the autochthon and all but the westernmost thrust sheets of the foreland thrust-fold belt. They can be correlated for over 200 km parallel to depositional strike (Grotzinger and Hoffman, 1983) and for over 100 km across depositional strike at the north end of the externides (Fig. 52.5). Figure 52.5 shows across-strike correlation of cycles in the lower part of the Lower Shale Member (for descriptions of members see Grotzinger and Hoffman, 1983) and the lateral facies changes that occur within them. In any given cycle, the asymmetric vertical arrangement of facies records gradual shoaling of the shelf followed by rapid submergence represented by the cycle boundary. Note that the eastern part of the shelf was consistently less aggraded than the western part. During each cycle, the extent to which the shelf aggraded at any location was directly controlled by the proximity of that location to the back-reef shoal complex; progressive west-to-east decrease in the degree of aggradation on the shelf immediately before each submergence increment is indicated by the west-to-east transgression of facies boundaries by cycle boundaries. Furthermore, correlation of the Rocknest Formation with parts of the Burnside River Formation (see below) far to the east indicates that the entire Rocknest Formation passes laterally into terrigenous sediments deposited in a shallow-shelf lagoon. These relationships show that progradation was incomplete during each cycle and that the lagoon was a permanent paleogeographic feature during evolution of the Rocknest shelf. This leads to the inescapable conclusion that complete shoaling of the shelf was not required to induce successive submergence events, and suggests a eustatic control of cyclicity on the shelf.

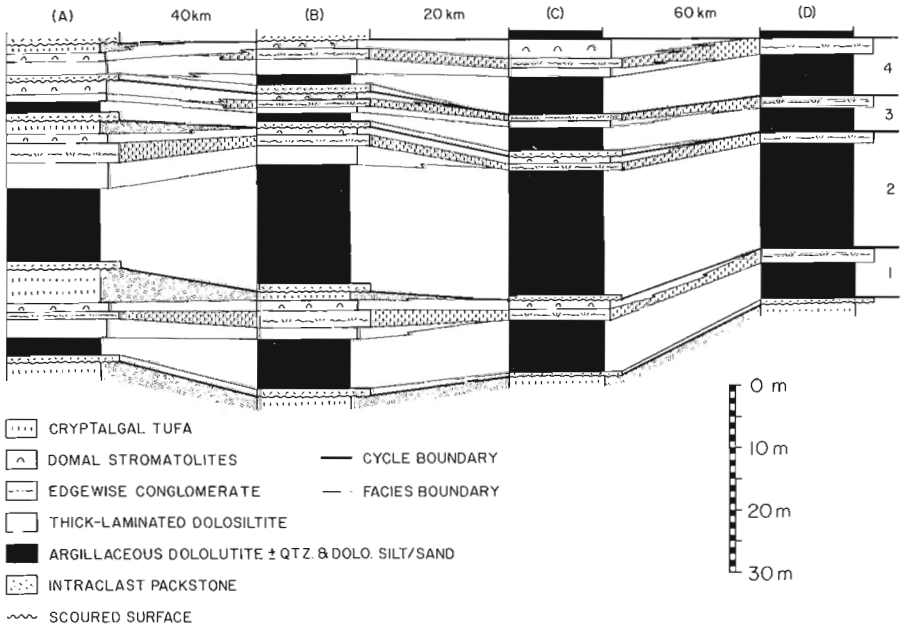

Figure 52.5. *Correlation of four shoaling-upward cycles, lower part of Lower Shale Member, Rocknest Formation, at the north end of the externides. Note eastward transgression of facies boundaries by cycle boundaries, including pinch-out of cryptalgal tufas (supratidal) and domal stromatolites (intertidal) to the east, and westward thinning of argillaceous dololutite (sublittoral). Also note lack of intraclast packstone (reworked soil) and scoured surface at base of 2, 3 and 4 at section "D", and cycle 4 at section "C", suggesting lack of exposure before resubmergence. Cycle boundaries are interpreted to be chronostratigraphic. Location of sections is shown in Figure 52.1.*

EASTWARD EXTENT OF THE ROCKNEST FORMATION

The apparent eastward disappearance of the Rocknest Formation across Rockinghorse Arch between the externides and Kilohigok Basin (Goulburn Group) has always presented a problem for regional stratigraphic correlation (e.g. Fraser and Tremblay, 1969; Hoffman et al., 1970; Hoffman, 1981; Campbell and Cecile, 1981). The problem is important because, for example, a disconformity cutting down from the top of the Rocknest Formation could indicate flexural arching during the Calderian Orogeny.

With a view to resolving this problem, a reconnaissance was made by two of us (P.F.H. and J.P.G.) to Rockinghorse Outlier, the Contwoyto Lake-Peacock Hills area, and the area south of Kuuvik Lakes (Fig. 52.6). The Western River and Burnside River formations as mapped by Campbell and Cecile (1976) in the well-exposed sections at Rockinghorse Lake are readily recognized as correlatives of the Lower (Eo1) and Middle (Eo2) members of the Odjick Formation respectively, just slightly coarser grained than in the autochthonous externides (e.g. sections 3 and Y of Fig. 52.6). At section 6, the top of the arenaceous Burnside River Formation as previously mapped (Campbell and Cecile, 1976) is overlain by an interval of dominantly fine grained clastics with minor intraclastic dolomite transitional upwards into five typical shale-dominated Rocknest cycles each capped by a thin shoal-water stromatolitic dolomite bed. This interval, 157 m thick with its top not exposed, we believe to be correlative with the transitional Upper Member (Eo3) of the Odjick Formation and the Rocknest Formation. At section 7, the same dolomitic interval, poorly exposed, is overlain in the core of a relatively tight syncline by an intrusive gabbro sill above which is a fine grained,

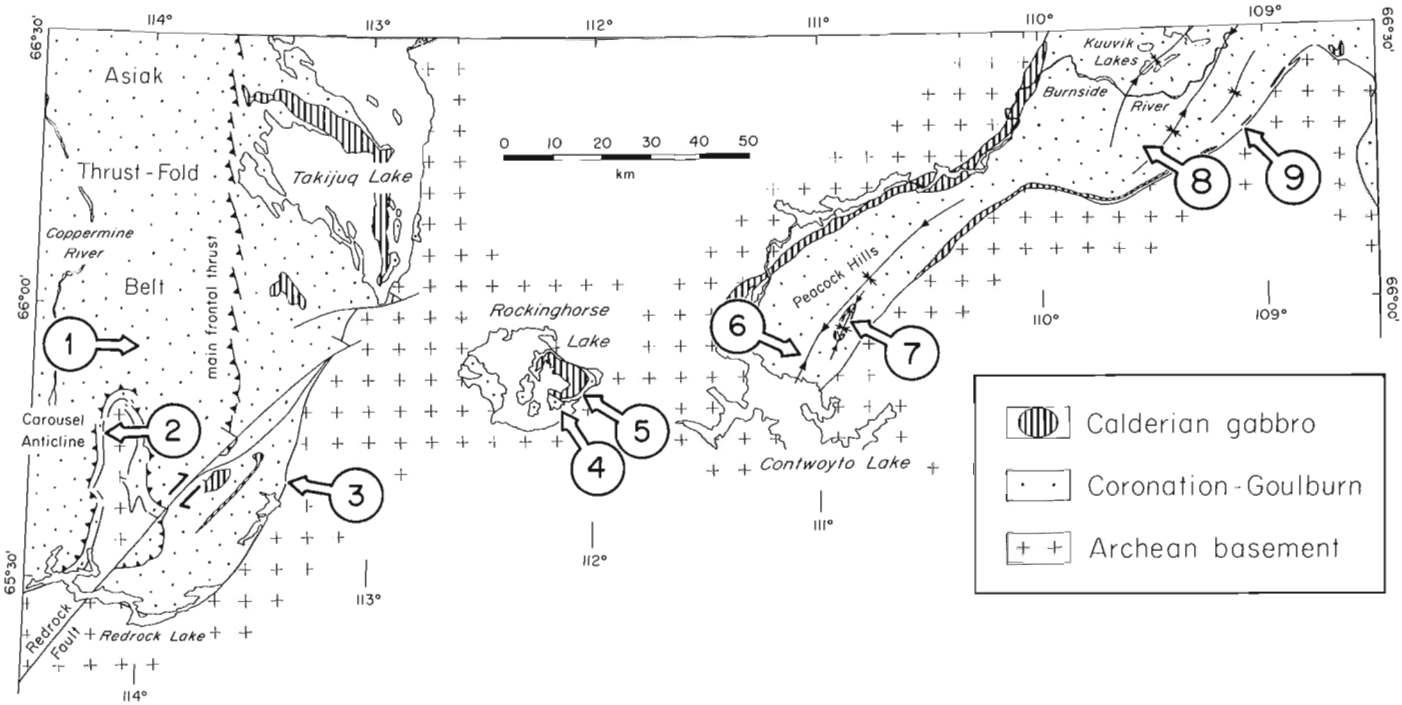

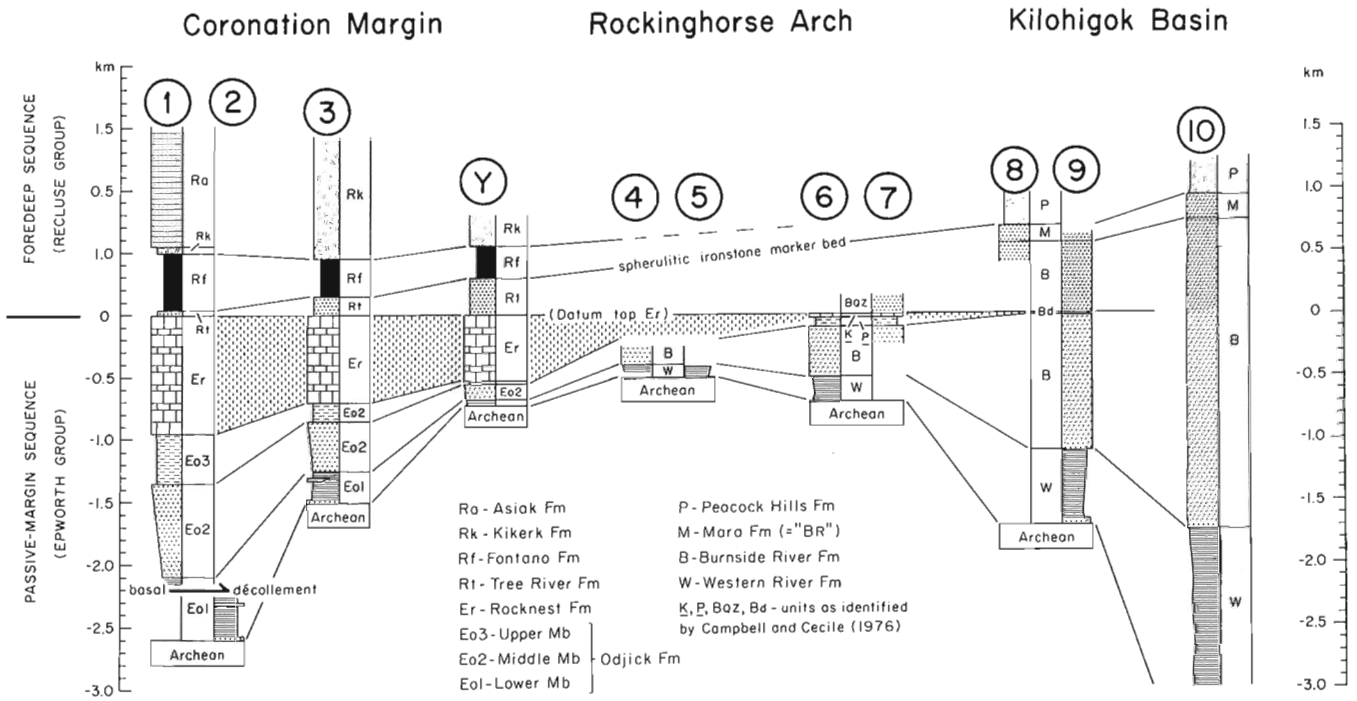

Figure 52.6. Location of sections and proposed correlation of the Rocknest Formation across Rockinghorse Arch into Kilohigok Basin. Section "Y" is located in the Tree River Fold Belt (see Fig. 52.1) and section 10 is a composite from around Bathurst Inlet.

well-indurated, white quartz arenite ("BQZ"). This quartzite is slightly coarser grained than, but otherwise very similar to, the Tree River Formation (Hoffman, 1981), which overlies the Rocknest Formation. At section 9, an exceptionally well exposed river gorge, a 21 m thick interval of mixed clastics and dolomite ("BD") occurs within the Burnside River Formation and has been traced over a wide area (Campbell and Cecile, 1976). Although we cannot be certain, based on a limited reconnaissance, we suggest that this unit is the feather-edge extension of the Rocknest Formation. No evidence of a significant disconformity occurs in this or any of the other sections and it is tentatively concluded that the Burnside River Formation represents, in part, the landward side of the Rocknest inner-shelf lagoon.

This correlation, if correct, has important regional tectonic implications, principal among which are: (1) that there was no emergent flexural arch associated with subduction of the Rocknest shelf, and (2) the Coronation margin opened and closed concurrently with unroofing of a major clastic source area, possibly the Thelon Front(?), southeast of Kilohigok Basin.

METAMORPHISM IN THE EXTERNIDES

During the course of mapping in previous field seasons it was observed that the colour of Coronation Supergroup shale shows an areal variation that apparently correlates with metamorphic grade, as indicated by mineral assemblages in mafic rocks in the Odjick Formation, by the development of slaty cleavage, and by the appearance of metamorphic biotite in Tree River Fold Belt. Systematic sampling of the Red Shale Member (Grotzinger and Hoffman, 1983) of the Rocknest Formation was completed in 1983 for a study of metamorphism in the externides.

Red Shale Member samples were graded in the field on a scale of 1 to 5 based on colour and fabric. The lowest apparent grade is represented by level 1 samples, which are moderate red (5R 4/4, Goddard et al., 1951), and generally display no tectonic fabric. A complete gradation was observed through greyish red (5R 4/2) of level 3 to samples which are medium grey (N5, level 5) with a strong slaty cleavage. Illite crystallinity and muscovite polymorph determinations of the samples are being undertaken in an effort to calibrate the qualitative grade scale.

The apparent metamorphic grade of pelite within the Red Shale Member, as reflected by colour and textural variation, is illustrated in Figure 52.7. If valid, several trends, reflecting different factors that control grade, are apparent.

To some degree, grade is controlled by structural level. This is shown by the progressive decrease in apparent grade down-plunge along the west flank of Atanigi Syncline ("A" in Fig. 52.7), and by a similar decrease down-plunge from both the north and the south into the structural depression of White Sandy Syncline. This suggests that syn-Calderian isotherms have been warped by the broad transverse D2 folds.

In the area north of Carousel Massif, a westward increase in apparent Calderian grade is also present. This is thought to be unrelated to structural depth because the thrust-fold belt has evidently not experienced major post-Calderian eastward tilting (Tirrul, 1983).

Perhaps the most surprising result is that metamorphic grade increases eastward from the thrust-fold belt toward Eokuk Uplift. This is not an effect of erosional level because the grade in the Tree River Fold Belt is higher than that around Takijuq Lake. The reason for localization of deformation and metamorphism in this region is unclear.

There appears to be a relationship between basement involvement in structures and higher metamorphic grade. This is observed in both the Tree River Fold Felt and in the area around Carousel Massif, where shallow dips on the basal unconformity characterize low grade regions, while steep to overturned attitudes are present in higher grade areas (levels 4 and 5). These observations probably reflect temperature control on basement deformation mechanisms.

NEW DATA ON TRANSVERSE (D2) FOLDING

During 1983, mapping of the Tree River Fold Belt was completed. Axial surface traces of megascopic Coronation Supergroup folds in the belt are shown in Figure 52.8. There are three conspicuous fold trends. North-trending folds (F1) restricted to the region west of 113°W are associated with thrust faults and are of Calderian age. They indicate that a decollement below the Rocknest Formation locally extends 5 km east of the frontal thrust zone. As previously reported, the Calderian structures are refolded by Tree River folds (F3) of northeast trend which dominate the region shown in Figure 52.8. They are typically open, upright to steeply inclined, and polyharmonic, with characteristic wavelengths of 600-700 m and 60-100 m. The longer wavelength folds usually involve the entire thickness of the Rocknest Formation; the higher order folds are common at the level of the Domal Stromatolite Member (Grotzinger and Hoffman, 1983), and diminish in amplitude both upward and downward in adjacent members. A less developed Tree River Fold set is parallel to the trend of the synclinorium between Eokuk and Uyarak uplifts (N30°E). The relative age of these folds is not known.

The most prominent fabric in the area is penetrative cleavage (S2) developed at a low angle (about 20°) to bedding in pelitic beds of the Rocknest and Odjick formations. The cleavage refracts strongly into dolomite and quartzite beds where it is spaced or difficult to detect. The cleavage is folded by the dominant Tree River Fold set. When bedding is restored, the cleavage dip is exclusively to the north. Its development involved a large component of bedding-parallel shear, as indicated by folded extension veins within pelite that have been rotated through vertical to their present northerly inclination, analogous to those described by Henderson (1983).

Poles to bedding and to S2 are shown for one domain (I) in Figure 52.8; for the others only bedding/cleavage intersections are shown. The intersection lineations are either indistinguishable from the orientation of younger fold hinges, or they show relative clockwise rotation. Similarly, lineations on cleavage surfaces defined by long axes of reduction spots, mineral alignment and fine corrugations have a mean northerly trend, forming an acute angle with later fold hinges.

In accord with previous observations (Hoffman, 1973; Hoffman et al., 1983), Archean basement is folded but not involved in thrusting. Most of the exposed basement/cover contact has been carefully mapped, and with a very few minor exceptions, the contact is intact. The basement has been deformed into structures that resemble large-scale mullions, with convex-upward lobes from a few metres to hundreds of metres wide, separated by pinched cusps. The margins of the lobes are commonly overturned, as shown in Figure 52.9. The basement deforms primarily by acquiring an inhomogeneously developed retrograde foliation which is particularly well developed in some cusp zones. It also deforms by way of discontinuous small-scale conjugate shear zones which accomplish northwest shortening with subvertical extension.

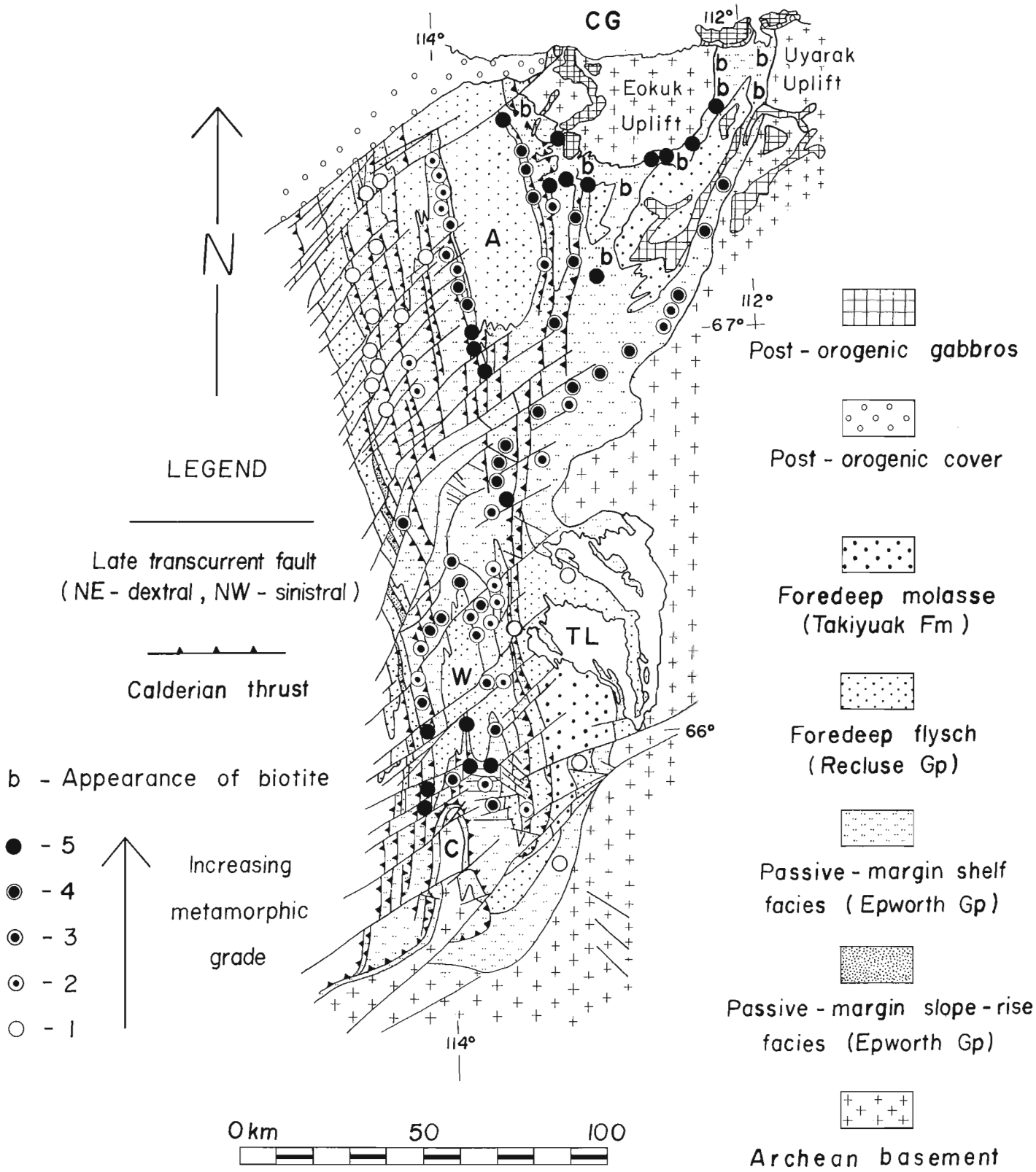

Figure 52.7. *Simplified geological map of the externides of Wopmay Orogen showing apparent metamorphic grade as indicated by the colour and fabric of shale in the Red Shale Member of the Rocknest Formation. A, Atanigi Syncline; C, Carousel Massif; CG, Coronation Gulf; W, White Sandy Syncline.*

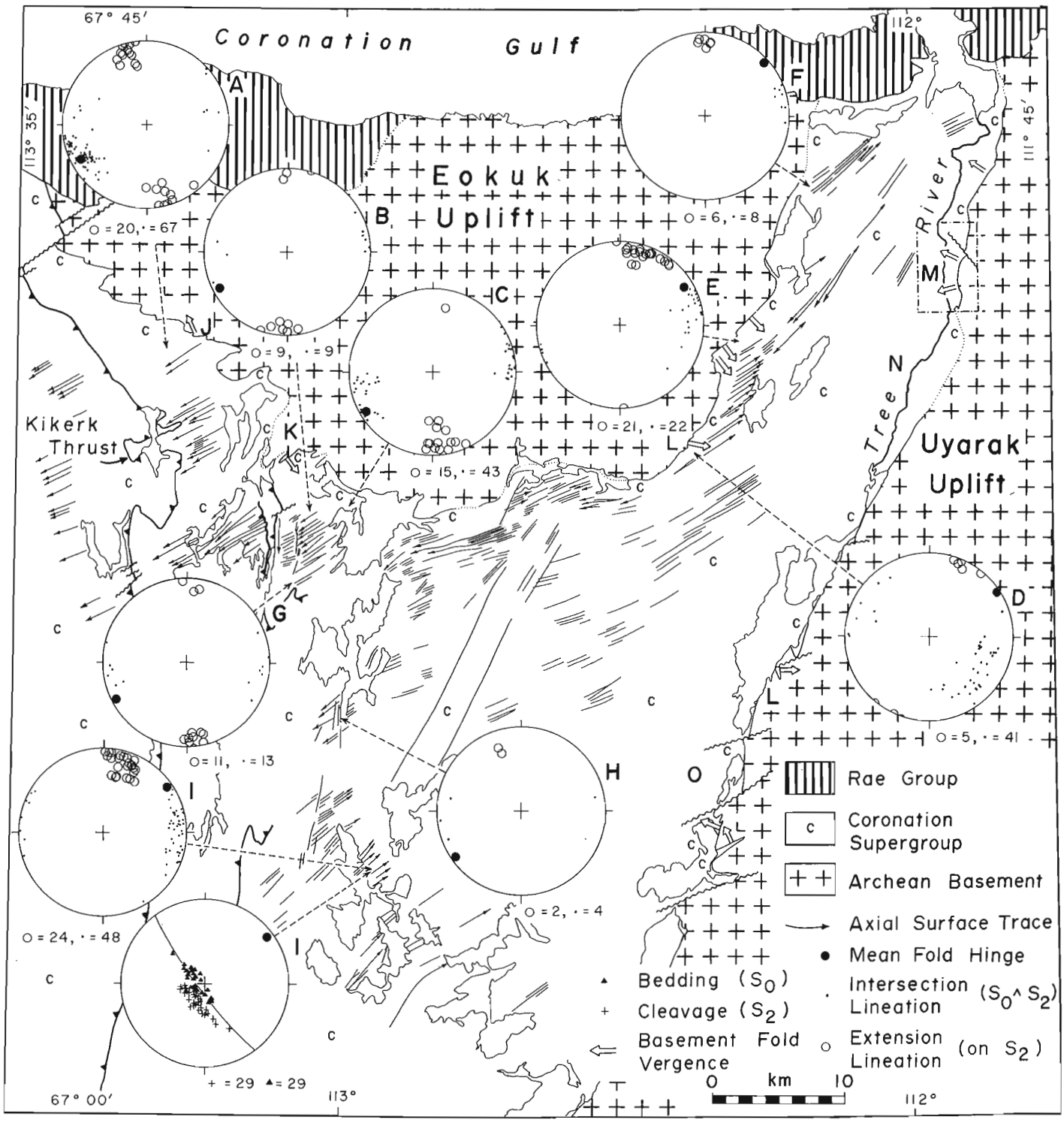

Figure 52.8. *Fold trajectory map of the Tree River Fold Belt showing basement/cover contact and selected structural data. Inset along Tree River shows the location of Figure 52.9.*

Compared with the fold pattern observed in the Rocknest and younger units, the basement surface geometry is complex. Although the dominant trend is northeast, the lobes and cusps show a wide variation in orientation and vergence, as shown in Figure 52.8. For exmaple, folds at "J" are overturned to the northwest, at "K" to the southeast, at "L" to the east, and at "M" to the west. Each is associated with one to three generations of cozonal cleavages in the adjacent cover, different in orientation from neighbouring cusps of different trend. From field relations alone the relative ages of these structures is not clear. Their development may have been broadly coeval.

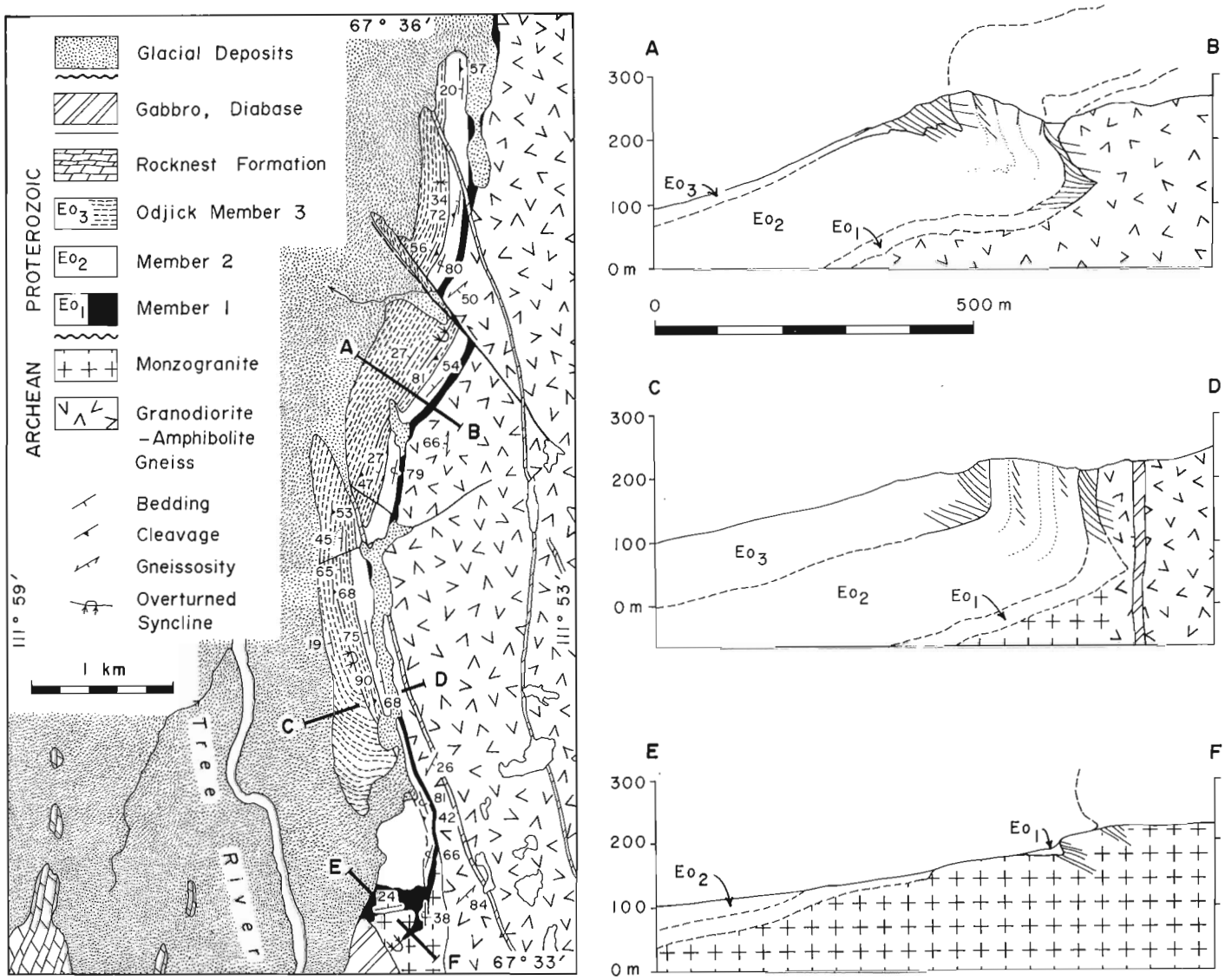

Figure 52.9. Geological map and cross-sections of a part of the western margin of Uyarak Uplift (see Fig. 52.8 for location) showing the cuspate-lobate geometry typical of the basement/cover contact in the Tree River Fold Belt. Topographic relief here is great enough for excellent structural control.

Both the shortening of the cover rocks and basement are interpreted to be due to northwest-oriented compression throughout the thickness of the lithosphere. The reason for the wide variation in orientation of basement structures may be due to the inability of an infinite half-space (analogous to the basement/cover contact) to buckle. Instead, relief is produced by penetrative strain and shape modification of perturbations into lobate-cuspate form (Smith, 1979; Ramberg, 1981, p. 151-156). No doubt, variably oriented weak zones both enhance amplification and refract regional stress trajectories.

A tectonic interpretation of the north-dipping folded cleavage (S2) is difficult. Despite the fact that subsequent fold hinges do not everywhere lie within S2, they are thought to be related to a single progressive tectonic event. Both the cleavage and Tree River folds are well developed adjacent to Eokuk Uplift, and poorly developed away from it (e.g. localities "N" and "O", Fig. 52.1). Also, a localities "C" and "E" (Fig. 52.1), the cleavage is subhorizontal and axial planar to recumbent minor folds on steeply dipping panels flanking the uplift. The simplest interpretation here is that the cleavage is axial planar to overturned folds which involve the basement. If gravitationally induced bedding-parallel shear was an important factor in the development of the cleavage, a linear uplift is required, north of the localities discussed, and presumably due to tectonic thickening. Southward migration of deformation is required to fold and overprint the north-dipping cleavage at any given locality. The cleavage was not produced by gravitational sliding of cover off the flanks of a domal uplift since the cleavage and related lineations are not concentrically and radially disposed about the uplift, respectively.

STRUCTURE OF KANGAROO BLOCK

Hoffman and St-Onge (1981) proposed that the north-central part of Wopmay Orogen is segmented into crudely hexagonal crustal blocks, each bounded by transcurrent faults linking an east-vergent thrust. These overlapping "shingles" were inferred to have developed late during a third major

compressional event (D3) affecting the orogen and which is responsible for a transcurrent fault system of regional extent. Since important support for this interpretation was based on regional variation in metamorphic pressure, now inferred to outline broad D2 structures that predate transcurrent faulting (Hoffman et al., 1983; St-Onge, in press), the question of net vertical displacement along the block boundaries remains outstanding. In this regard, the recognition in 1983 of a smaller-scale "shingle", well exposed, and offsetting Calderian structures which serve as piercing points is significant. Aspects of the development of the Kangaroo Block may apply to the larger-scale "shingles" to the west.

A simplified map of the Kangaroo Block is shown in Figure 52.10a. Except for size, its geometrical similarity to the blocks of Hoffman and St-Onge (1981) is striking. It is bounded to the northeast by Kangaroo Fault, with more than 4 km of left-slip. Its curvilinear trace merges with a major boundary fault to the southeast, with approximately 10 km of

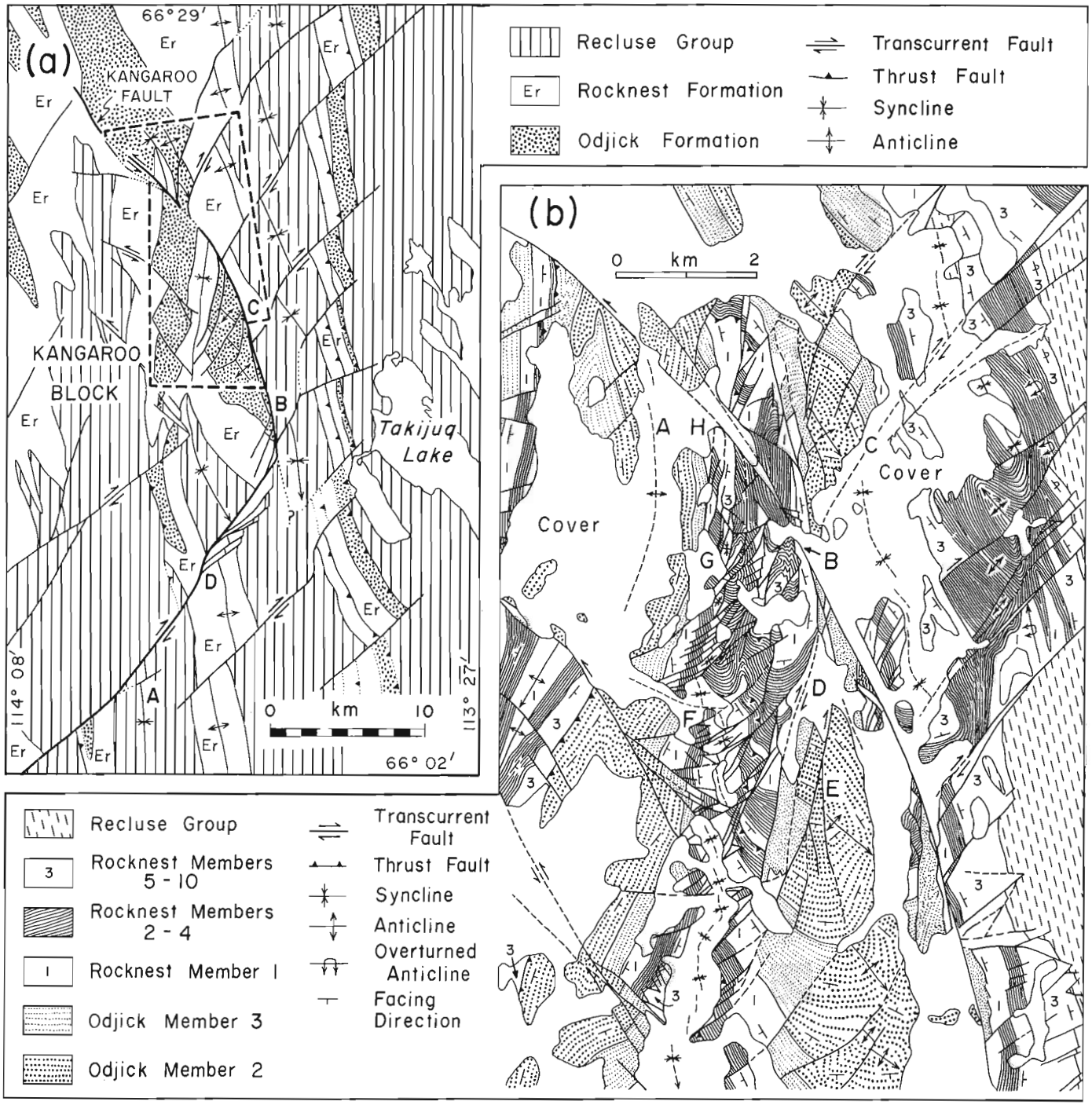

Figure 52.10. *(a) Simplified geological map of Kangaroo Block and surrounding area. (b) Geological map of the northeast margin of Kangaroo Block with 4.4 km of restored left-slip on Kangaroo Fault. The area is located within the dashed inset of Figure 52.10a and the general location of the block is shown in Figure 52.1.*

right-slip. Both within and adjacent to the block, regional structural plunge is to the south. There is no differential uplift of the block as a whole. The synclinorium at "A" (Fig. 52.10a), for example, can be traced across both boundary faults with no significant change in structural level.

Movement on Kangaroo Fault postdates the development of most adjacent structures. Its trace is marked by a prominent uninterrupted topographic lineament along which right-lateral faults are truncated. In Figure 52.10b, the geology along part of Kangaroo Fault is shown in more detail, after restoration for 4.4 km of left-slip. With this reconstruction, the anticline at "A" is partially restored, and structural panels at "B" have compatible counterparts on the north side of the fault.

With the partial reconstruction of Figure 52.10b, the right-lateral fault at "C" correlates with a braided system of north-trending faults at "D" with right separation and which splay westward. The Odjick anticline west of "C" has apparently been offset from "E" along the fault. Other north-trending faults in Kangaroo Block are also right-lateral faults that have undergone large counterclockwise rotations about vertical axes prior to offset by Kangaroo Fault. Northward from "F" to "H", a Calderian syncline cut by a swarm of right-lateral faults shows a progressive increase in apparent rotation as Kangaroo Fault is approached. Adjacent to "G", the fold and its cleavage fan have been rotated from an original northerly trend to an azimuth of 100°E.

In addition to large rotations, fault blocks within Kangaroo Block exhibit some compressive strain. North to northeasterly trending minor folds with strict chevron profiles and no associated cleavage are common along the eastern margin of the block. They fold Calderian cleavage.

Evidence for reverse slip along the eastern margin of the block is present but not overwhelming. Where exposed, the faults along the southeast margin of the block have steep dips. The fault at "B" (Fig. 52.10a) is not exposed, but Odjick Middle Member on the west side does not have a match either at "C" or "D". A minimum of a few hundred metres of west-side-up displacement is required along this margin.

In summary, Kangaroo Block was an asymmetric, late-stage development of D3 deformation. It was established after considerable slip and rotation of both right- and left-lateral transcurrent faults, when a left-lateral fault propagated into and offset major right-slip faults. Reverse slip and uplift of the block is relatively minor (less than 10% of strike-slip) and restricted to the leading edge of the block unless post-orogenic backsliding (Hoffman and St-Onge, 1981) has been important.

FUTURE WORK

A 1:250 000 scale geological map of the externides has been prepared by P.F.H. and is available for inspection in Ottawa. It is intended for final publication in colour and will probably not, because of its extreme complexity, be issued in uncoloured form as an Open File map. Geological maps at 1:50 000 scale are being prepared by R.T. to cover critical parts of the externides, namely the northwest corner, the area around Carousel Massif, the area of Kangaroo Block, and the area of intersection of frontal Calderian thrusts and the Tree River Fold Belt. R.T. will also be preparing journal articles on the three deformations. J.P.G. will likewise be preparing articles on the Rocknest Formation, its outer reef complex, shelf cycles, and precipitated carbonate cements. Metamorphism of the externides will be the subject of a B.Sc. thesis by S.B.L. at Queen's University.

ACKNOWLEDGMENTS

We were fortunate in having an outstandingly able and dedicated group of student assistants, who regularly undertook independent geological mapping. It included M.E. Grier (Queen's), C.A. Gittins (Toronto), M.D. Dayneka (Memorial), Bradford Johnson (Santa Barbara) and Mark Cunnane (Missoula). The last two are particularly commended for their unstinting efforts without remuneration. For 300 hours of helicopter service without a hitch we thank Edgeworth Helicopters of Fort Nelson, B.C., and pilot-engineer Keith Westfall. Janien Schwarz reaffirmed Napoleon's dictum that an army marches on its stomach, while Win Bowler and Martin Irving provided logistic support at Yellowknife. We were delighted to host M.J. Jackson (BMR, Canberrra, Australia) for half the summer, and briefer visits by D.R. Gray (Virginia Tech) and R.A. Price (GSC) provided valuable insights. J.P.G. is supported by National Science Foundation grant #EAR-8218618. The manuscript was critically reviewed by F.H.A. Campbell, and Simon Hanmer.

REFERENCES

Allen, P.A.
1981: Wave-generated structures in the Devonian lacustrine sediments of south-east Shetland and ancient wave conditions; Sedimentology, v. 28, p. 369-379.

Assereto, R.L.A.M. and Kendall, C.G.St.C.
1977: Nature, origin and classification of peritidal tepee structures and related breccias; Sedimentology, v. 24, p. 153-210.

Brenchley, P.J. and Newall, G.
1982: Storm-influenced inner-shelf sand lobes in the Caradoc (Ordovician) of Shropshire, England; Journal of Sedimentary Petrology, v. 52, p. 1257-1269.

Campbell, F.H.A. and Cecile, M.P.
1976: Geology of the Kilohigok Basin, Bathurst Inlet, N.W.T.; Geological Survey of Canada Open File 332, map at 1:500 000 scale.

1981: Evolution of the early Proterozoic Kilohigok Basin, Bathurst Inlet – Victoria Island, Northwest Territories; in Proterozoic Basins of Canada, ed. F.H.A. Campbell; Geological Survey of Canada, Paper 81-10, p. 103-132.

Eriksson, K.A. and Soegaard, K.
1983: Storm-deposited outer-shelf facies from Precambrian Ortega Group, New Mexico; American Association of Petroleum Geologists, Bulletin, v. 67, p. 456.

Fraser, J.A. and Tremblay, L.-P.
1969: Correlation of Proterozoic strata in the northwestern Canadian Shield; Canadian Journal of Earth Sciences, v. 6, p. 1-9.

Goddard, E.N., Trask, P.D., DeFord, R.K., Rove, O.N., Singewald, J.T. Jr., and Overdeck, R.M.
1951: Munsell rock colour chart; Geological Society of America, New York.

Grotzinger, J.P.
1982: A preliminary account of the internal stratigraphy of the Rocknest Formation, foreland thrust-fold belt of Wopmay Orogen, District of Mackenzie; in Current Research, Part A, Geological Survey of Canada, Paper 82-1A, p. 117-118.

Grotzinger, J.P. and Hoffman, P.F.
1983: Aspects of the Rocknest Formation, Asiak Thrust-Fold Belt, Wopmay Orogen, District of Mackenzie; in Current Research, Part B, Geological Survey of Canada, Paper 83-1B, p. 83-92.

Grotzinger, J.P. and Read, J.F.
– Evidence for primary aragonite precipitation, early Proterozoic (1.9 Ga) Rocknest Dolomite, Wopmay Orogen, northwest Canada; Geology. (in press)

Hamblin, A.P. and Walker, R.G.
1979: Storm-dominated shallow marine deposits: The Fernie-Kootenay (Jurassic) transition, southern Rocky Mountains; Canadian Journal of Earth Sciences, v. 16, p. 1673-1690.

Henderson, J.R.
1983: Analysis of structure as a factor controlling gold mineralization in Nova Scotia; in Current Research, Part B, Geological Survey of Canada, Paper 83-1B, p. 13-21.

Hoffman, P.F.
1973: Evolution of an early Proterozoic continental margin: the Coronation geosyncline and associated aulacogens of the northwestern Canadian Shield; Royal Society of London, Philosophical Transactions, Series A, v. 273, p. 547-581.

1981: Revision of stratigraphic nomenclature, foreland thrust-fold belt of Wopmay Orogen, District of Mackenzie; in Current Research, Part A, Geological Survey of Canada, Paper 81-1A, p. 247-250.

Hoffman, P.F. and Bowring, S.A.
– A short-lived 1.9 Ga continental margin and its destruction, Wopmay Orogen, northwest Canada; Geology. (in press)

Hoffman, P.F. and St-Onge, M.R.
1981: Contemporaneous thrusting and conjugate transcurrent faulting during the second collision in Wopmay Orogen; in Current Research, Part A, Geological Survey of Canada, Paper 81-1A, p. 251-257.

Hoffman, P.F., Fraser, J.A., and McGlynn, J.C.
1970: The Coronation Geosyncline of Aphebian age; in Symposium on Basins and Geosynclines of the Canadian Shield, ed. A.J. Baer; Geological Survey of Canada, Paper 70-40, p. 200-212.

Hoffman, P.F., Tirrul, R., and Grotzinger, J.P.
1983: The externides of Wopmay Orogen, Point Lake and Kikerk Lake map areas, District of Mackenzie; in Current Research, Part A, Geologial Survey of Canada, Paper 83-1A, p. 429-435.

Piper, D.J.W.
1972: Turbidite origin of some laminated mudstones; Geological Magazine, v. 109, p. 115-126.

Ramberg, H.
1981: Gravity, Deformation and the Earth's Crust; Academic Press, London, 452 p.

Smith, R.B.
1979: The folding of a strongly non-Newtonian layer; American Journal of Science, v. 279, p. 272-287.

St-Onge, M.R.
– Geothermometry and geobarometry in pelitic rocks of north-central Wopmay Orogen (early Proterozoic), Northwest Territories, Canada; Geological Society of America, Bulletin. (in press)

St-Onge, M.R., King, J.E., and Lalonde, A.E.
1982: Geology of the central Wopmay Orogen (Early Proterozoic), Bear Province, District of Mackenzie: Redrock Lake and the eastern portion of Calder River map areas; in Current Research, Part A, Geological Survey of Canada, Paper 82-1A, p. 99-108.

1984: Deformation and metamorphism of the Coronation Supergroup and its basement in the Hepburn Metamorphic-Plutonic Zone of Wopmay Orogen: Redrock Lake and the eastern portion of Calder River map areas, District of Mackenzie; in Current Research, Part A, Geological Survey of Canada, Paper 84-1A, report 25.

Tirrul, R.
1982: Frontal thrust zone of Wopmay Orogen, Takijuq Lake map area, District of Mackenzie; in Current Research, Part A; Geological Survey of Canada, Paper 82-1A, p. 119-122.

1983: Structure cross-sections across Asiak Foreland Thrust and Fold Belt, Wopmay Orogen, District of Mackenzie; in Current Research, Part B, Geological Survey of Canada, Paper 83-1B, p. 253-260.

53. GEOLOGICAL SYNTHESIS IN THE WESTERN SUPERIOR PROVINCE, ONTARIO

Project 820006

J.A. Percival and R.A. Stern[1]
Precambrian Geology Division

Percival, J.A. and Stern, R.A., Geological synthesis in the western Superior Province, Ontario; in Current Research, Part A, Geological Survey of Canada, Paper 84-1A, p. 397-408, 1984.

Abstract

Results are reported of reconnaissance investigations in two areas of the Superior Province of northwestern Ontario, and of a detailed study of plutonic rocks. 1) The Berens belt north of Red Lake consists mainly of foliated to massive hornblende-biotite granodiorite and minor tonalite, with inclusions of amphibolite, diorite and tonalitic gneiss, all cut by leucogranite dykes and plutons. Late biotite granodiorite and hornblende-porphyritic diorite to gabbro dykes cut leucogranite. 2) The core of the Quetico belt in Quetico Park consists of a variety of granitic rocks and metasedimentary migmatite remnants. The oldest intrusive rocks are diorite-syenite and ultramafic inclusions in tonalite and granite. Tonalite, also with paragneiss and mafic granulite enclaves, occurs as inclusions in pink biotite leucogranite. The youngest, most voluminous intrusive phase is white muscovite-bearing granite, with some biotite, garnet, sillimanite or cordierite. 3) The Perching Gull Lakes pluton of the Wawa subprovince intruded mafic and tonalitic gneiss and is cut by foliated and massive granite. The Perching Gull Lakes igneous suite includes quartz monzonite, leucodiorite, mafic syenite and monzonite, and late hornblende-granite dykes.

Résumé

Les auteurs présentent les résultats d'études de reconnaissance effectuées dans deux régions de la province du lac Supérieur dans le nord-ouest de l'Ontario et d'une étude détaillée de roches plutoniques. 1) La zone de Berens au nord du lac Red se compose surtout de granodiorite à hornblende et à biotite de nature feuilletée à massive et de petites quantités de tonalite, avec des inclusions d'amphibolite, de diorite et de gneiss à tonalite, tous recoupés par des filons et des plutons de leucogranite. Des filons récents de granodiorite à biotite et de diorite à hornblende porphyrique se transformant en gabbro traversent le leucogranite. 2) Le noyau de la zone de Quetico dans le parc du même nom comporte une gamme de roches granitiques et de restes de migmatites métasédimentaires. Les roches intrusives les plus anciennes sont de la diorite on de la syénite, et des inclusions ultramafiques dans de la tonalite et du granite. La tonalite, caractérisée par des inclusions de paragneiss et de granulites mafiques, se présente elle-même sous forme d'inclusions dans un leucogranite rose à biotite. La phase intrusive la plus récente et la plus volumineuse se compose de granite blanc à muscovite contenant un peu de biotite, de grenat, de sillimanite ou de cordiérite. Le pluton des lacs Perching Gull de la sous-province de Wawa a fait intrusion dans du gneiss mafique et tonalitique et est recoupé par du granite feuilleté et massif. La série ignée des lacs Perching Gull comprend de la monzonite quartzifère, de la diorite leucocrate, de la syénite et de la monzonite mafiques et des filons récents de granite à hornblende.

INTRODUCTION

This report summarizes the results of field investigations undertaken in the Superior Province of northwestern Ontario during 1983. In the first part, the geology of the granitoid rocks of the Berens belt is described and a compilation map presented for an area north of Red Lake, Ontario. The second part outlines the results of reconnaissance investigations of the Quetico belt in part of Quetico Provincial Park. The third part of the report deals with the detailed geology of the Perching Gull Lakes area and will form the basis of an honours B.Sc. thesis by the junior author.

Individuals who contributed to the program through discussions, field guidance and logistical support include A.H. Bailes, G.J. Boradaile, D. Elder, G.M. Stott and W. Weber. I.L. Gibson and R.W. MacQueen made helpful comments on Part III. S. Young provided capable field assistance.

PART I: THE BERENS BELT IN THE TROUT LAKE – CARROLL LAKE AREA

J.A. Percival

The Berens plutonic belt is an eastward-tapering region of mainly massive and foliated plutonic rocks extending from Lake Winnipeg in Manitoba to Pickle Lake in Ontario. It is bounded to the south by metavolcanic, metasedimentary and plutonic rocks of the Uchi belt (Thurston and Bartlett, 1981a,b) and to the north by plutonic, metavolcanic and metasedimentary rocks of the Sachigo subprovince. Helicopter-supported reconnaissance was carried out in 1983 in the south-central part of the Berens belt in areas previously mapped by Chown (1959), Donaldson (1969) and Ermanovics (1970). Recent reviews of adjacent regions to the west and east are available in Ermanovics et al. (1979) and Sage and Breaks (1982).

Most of the Berens belt is made up of medium- to coarse-grained to porphyritic rocks of granodiorite to granite composition. The most abundant rock type is foliated to massive, medium grained hornblende (10-20%), biotite (5-10%), granodiorite with up to 3% titanite and minor epidote after hornblende. Biotite is always present and hornblende, commonly more abundant than biotite, is absent in some rocks. A megacrystic variety, with up to 30% K-feldspar megacrysts or augen up to 4 cm, also constitutes a mappable unit (Fig. 53.1). Tonalite and granodiorite are similar in texture and mineralogy except for K-feldspar content. Near Aikens Lake, a body of quartz diorite with 40% combined hornblende and biotite, less than 10% quartz and relict igneous layering may constitute a discrete intrusion.

[1]Department of Earth Sciences, University of Waterloo, Waterloo, Ontario N2L 3G1

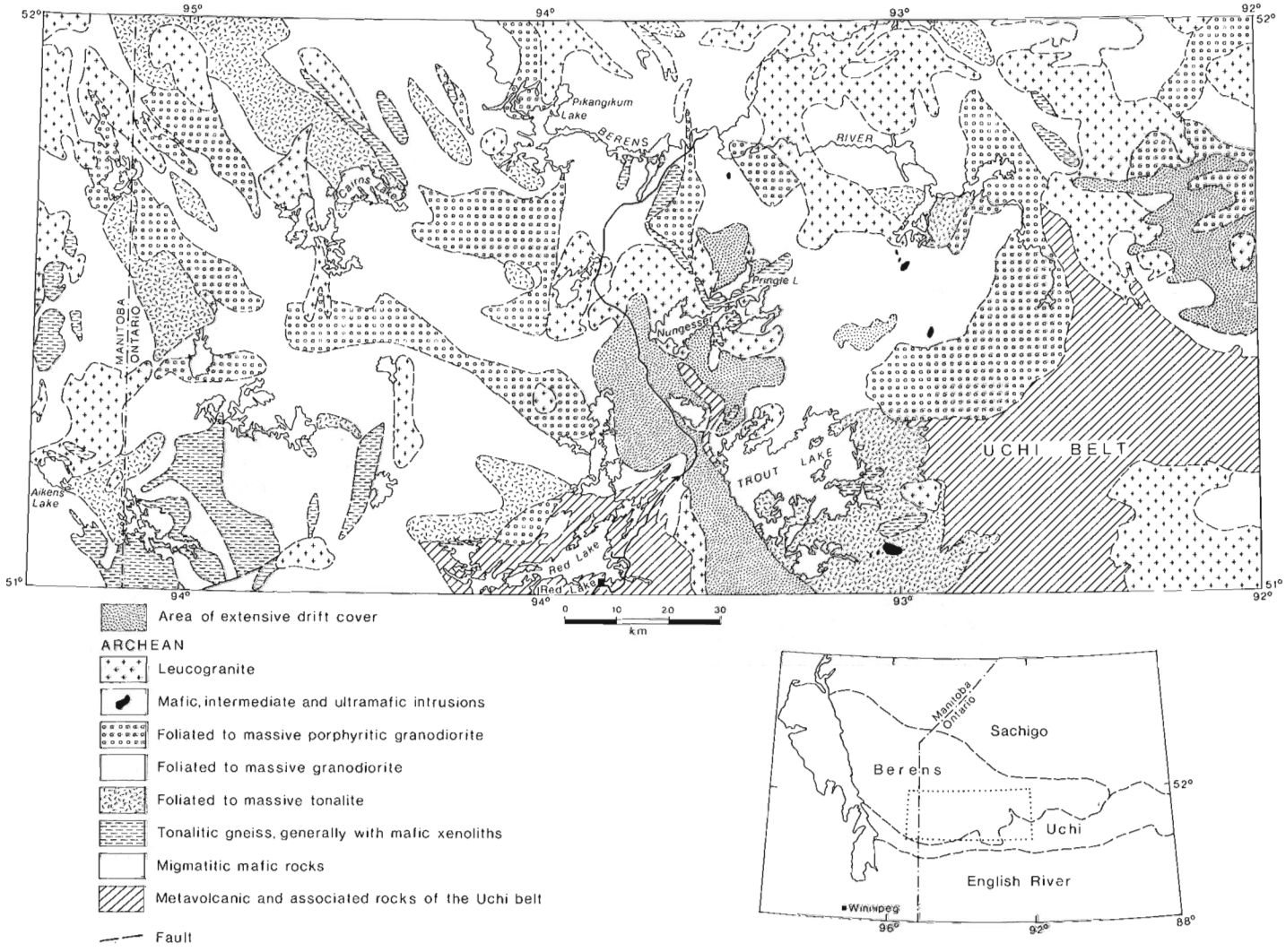

Figure 53.1. *Geological compilation map of the south-central Berens belt – modified after Ermanovics (1970), Chown (1959) and Donaldson (1969).*

Development of foliation ranges from nonexistent to strong in the granodiorite-tonalite suite. Foliated rocks commonly have sparse, wispy biotite-rich layers aligned in the plane of the foliation. Locally, where biotite-rich schlieren are abundant, the rock is gneissic.

Several small bodies of tonalitic gneiss are present within homogeneous granodiorite. They consist of thinly layered biotite or hornblende - biotite ± magnetite tonalite with hornblende - plagioclase ± clinopyroxene amphibolite and rare hornblendite xenoliths up to 4 m in long dimension. Inclusions of quartz - magnetite - pyrite meta-iron formation occur in tonalitic rocks at Pringle Lake in association with amphibolite xenoliths. Gneissosity is commonly contorted, in contrast to the simple uniform foliation in granodiorite, suggesting that the gneiss predates homogeneous granodiorite.

Where present, up to 5% xenoliths of fine- to medium-grained diorite to quartz diorite occur in granodiorite. These round to elliptical inclusions range in size from a few centimetres to 25 x 100 cm and commonly have diffuse wispy terminations. The xenoliths consist of sugary-textured hornblende and plagioclase, with some biotite and quartz, and commonly have hornblende and plagioclase porphyroblasts up to 8 mm. Biotite granodiorite 30 km northeast of Aikens Lake contains hornblende quartz diorite inclusions.

Several small bodies of massive medium- to coarse-grained gabbro to diorite are apparently mafic phases of granodiorite, whereas others cut granodiorite (Donaldson, 1969). Large angular inclusions of medium grained, massive to weakly foliated gabbro, biotite-melagabbro and hornblendite occur in granodiorite on the northwestern corner of Pikangikum Lake. The inclusions may be parts of a dismembered layered mafic body.

The granodiorite-tonalite suite is cut by bodies of massive leucogranite ranging from small aplite dykes to amoeboid plutons up to 40 km in diameter. The leucogranite is generally pink to purplish-pink and contains less than 5% biotite. Grain size varies from fine, in aplites, to pegmatitic, in dykes and patches. In plutons, the leucogranite is generally medium grained but contains pegmatitic and aplitic dykes or segregation layers. In a few outcrops, dykes of foliated leucogranite in granodiorite are cut by later dykes of massive aplite.

Rare dykes, less than 1 m thick, of medium grained, homogeneous, massive to weakly foliated biotite granodiorite to tonalite cut the leucogranite. Similarly, late dykes, up to 10 m thick, of medium grained hornblende-porphyritic diorite or gabbro cut leucogranite and are characterized by marginal flow lamination. A swarm of these dykes was observed north of Berens River, near the area mapped as migmatitic metavolcanics by Donaldson (1969). In as much as this area is underlain by mixed mafic rocks and granodiorite, the unit appears on Figure 53.1 as migmatitic mafic rocks.

A moderate to weak foliation, defined by alignment of biotite, hornblende and feldspar augen, characterizes much of the granodiorite-tonalite suite. Elongate and lenticular xenoliths and wispy layers are parallel to even the faintest mineral foliation, suggesting that the planar structures were imposed by flow during emplacement rather than by reorientation during regional deformation. Rodding lineations are much less common than foliation. Gneissosity, produced by thin amphibolite or biotite-rich layers, is rare in granodiorite.

From north to south, foliation attitude changes from dominantly northwesterly, with southwesterly dips, to more variable orientations. In the south foliation generally is parallel to contacts with rocks of the Uchi belt. Dips are generally moderate (45-70°) but vary from vertical to locally as shallow as 25°. Gneissosity in tonalitic gneiss bodies generally has no consistent orientation. For the most part, leucogranite is foliated only adjacent to late shear zones, which themselves are locally cut by small dykes of massive aplite.

Numerous small shear zones cut both foliated granodiorite and leucogranite. They consist of 1-3 mm wide strongly foliated zones of very fine grained rock associated with epidote and quartz veins. Shear zones have two main orientations, 110°-140° and 030°-040°, both with variable dip directions. These coincide with major shear zone orientations that may have accommodated significant post-pluton movement (Park, 1981).

Two rock types in the Berens belt have been isotopically dated (U-Pb on zircon). Massive leucogranite from Horseshoe Lake, some 30 km northwest of Figure 53.1, has an age of 2715 Ma (Krogh et al., 1974; Ermanovics and Wanless, 1983), only slightly younger than a late quartz monzonite pluton in the Uchi belt (2730 Ma; Nunes and Thurston, 1980). Foliated quartz diorite from McDowell Lake, immediately south of the North Spirit Lake belt of the Sachigo subprovince, is dated at 2768 Ma (Nunes and Wood, 1980).

PART II: THE QUETICO BELT IN THE QUETICO PARK AREA

J.A. Percival

The Quetico belt is a 10-100 km wide region of metasedimentary and granitic rocks that extends some 1200 km from northern Minnesota in the west to the Kapuskasing Structural Zone of Ontario in the east. Metasedimentary and associated granitic rocks extend for several hundred kilometres east of the Kapuskasing zone in what is known as the Opatica belt. The Quetico belt is bounded to the north and south by regions in which metavolcanic rocks dominate the supracrustal component, respectively the Wabigoon and Wawa subprovinces. The Quetico belt generally consists of marginal metasedimentary rocks with a metamorphic transition from chlorite-muscovite grade at the outside to migmatites adjacent to the core, which is dominantly granite and migmatite. The non-migmatitic metasedimentary rocks are viewed as parts of the Wabigoon and Wawa subprovinces by Kehlenbeck (1976) based on structural-metamorphic considerations. In this report, the belts are defined on a lithological basis so that the Quetico belt includes the marginal metasedimentary rocks. Two major batholithic regions occupy the core of the western Quetico belt, the Vermilion granitic complex of northern Minnesota (Southwick, 1972) and the Quetico Park complex in Ontario (Tanton, 1940).

The supracrustal component of the Quetico belt is sedimentary in origin. In their best-preserved state, the metasedimentary rocks are interbedded greywacke and pelite with sedimentary structures including bedding, grain size gradation, scour marks and rip-up clasts, and are interpreted as a turbidite sequence.

The rocks are variably metamorphosed and recrystallized to greenschist and amphibolite facies. Metasedimentary rocks above the migmatite "isograd" are medium- to fine-grained biotite - plagioclase - quartz ± garnet ± muscovite schists with 0-20 per cent white granite leucosome at a scale of 1-10 cm. At least two sets of folds are responsible for complex structural patterns (Kehlenbeck, 1983; Boradaile 1983). In general, however, bedding and cleavage strike easterly and dip to the north (Pirie and Mackasey, 1978).

The northern boundary of the Quetico belt is the Quetico fault west of Lac de Mille Lacs (Mackasey et al., 1974). At the southern margin, metasediments apparently overlie conformably the metavolcanic rocks of the Wawa subprovince (Giblin, 1964; Hodgkinson, 1968; Harris, 1970). The southern marginal zone of the Quetico belt in Quetico Park is characterized by a mixture of paragneiss and amphibolite xenoliths in granite.

A variety of intrusive rocks is present in Quetico Park, both in the northern Wawa subprovince and throughout the Quetico belt. The main distinguishing feature between intrusive rocks of the Wawa subprovince and those of the Quetico belt is that inclusions in the former contain hornblende whereas those in the latter are mainly biotite-rich paragneiss. Intrusive rocks of the Wawa subprovince to the east were discussed previously (Percival, 1983).

Intrusive rocks of the Saganagons volcanic belt of the Wawa subprovince include granite, granodiorite, and small bodies of gabbro, hornblendite and pyroxenite (Fig. 53.2). The most abundant rock type is homogeneous, massive to weakly foliated hornblende-biotite granodiorite to tonalite, with up to 15 per cent megacrysts of K-feldspar. The rock contains inclusions of hornblende diorite, metagabbro and phlogopite, hornblende-bearing pyroxenite and is cut by dykes of massive leucogranite.

A body of massive pink leucogranite (<5 per cent biotite) borders the Saganagons belt. The pluton contains xenoliths of amphibolite, hornblende-clinopyroxene diorite and included bodies of coarse grained pyroxenite up to 2 km in diameter. Nepheline syenite reported from this pluton by Tanton (1940) is possibly also an inclusion.

Intrusive rocks of the Quetico Park complex of the Quetico belt include, in approximate chronological order, hornblende syenite to diorite, tonalite, magnetite-bearing granite, K-feldspar porphyritic granite, biotite leucogranite and muscovite ± biotite ± garnet ± sillimanite granite (Fig. 53.2). Other intrusions, associated with metasedimentary rocks, but not part of the granitic complex, include bodies of intermediate composition such as the Blalock pluton (Pirie, 1978; Williams, 1978) and Obinidaw River pluton (Harris, 1970).

Tonalite occurs as medium- to coarse-grained homogeneous hornblende and hornblende-biotite-bearing units in the Pickerel-French Lakes area. Tonalite is present present as inclusions in magnetite-biotite granite and as discrete larger bodies containing a variety of xenoliths of

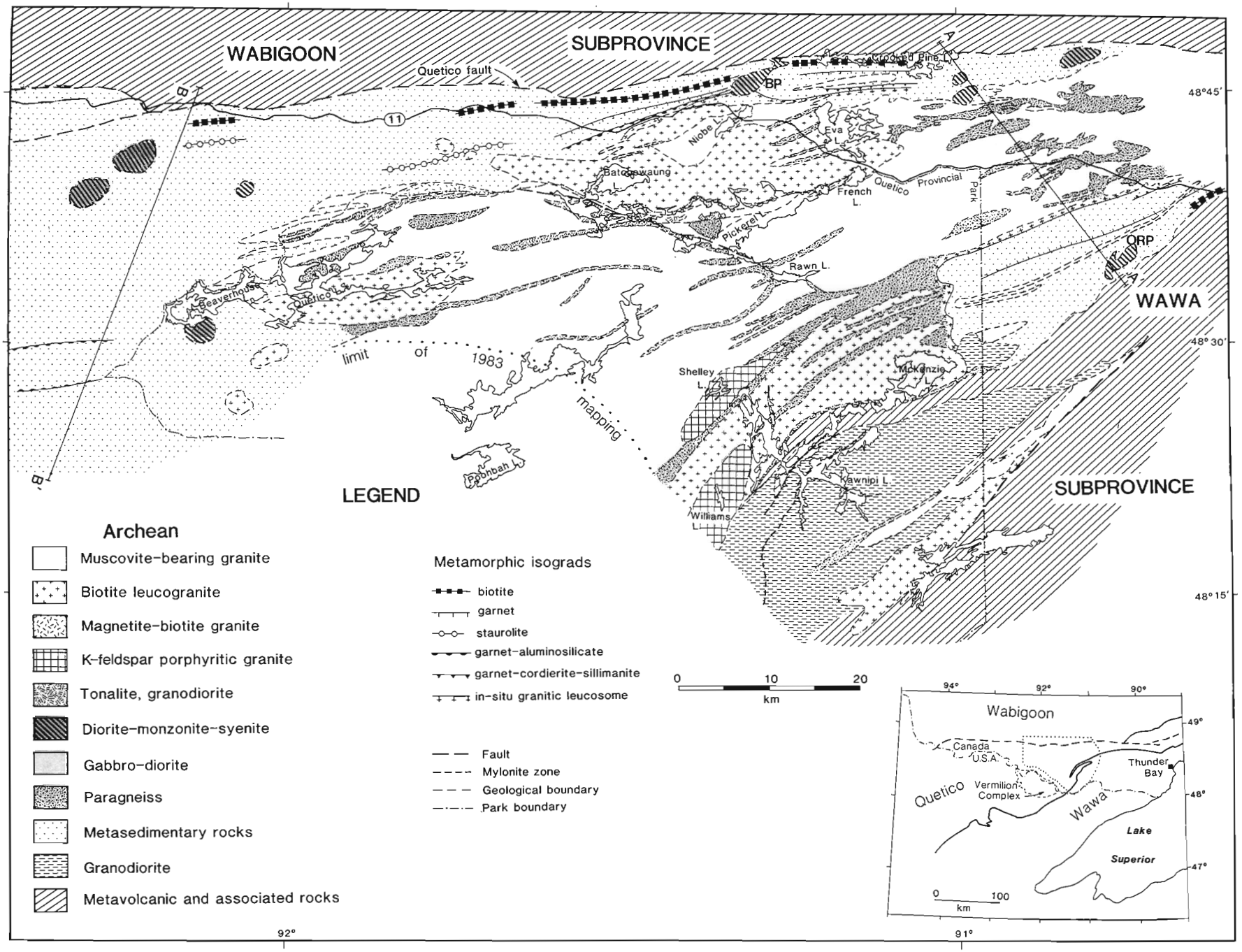

Figure 53.2. *Geological compilation map of the Quetico belt in the Quetico Park area – modified after Tanton (1940), Pirie (1978), Pirie and Mackasey (1978) and Williams (1978). BP: Blalock pluton; ORP: Obinidaw River pluton.*

paragneiss, two-pyroxene mafic granulite, metagabbro and hornblende syenite and diorite. It is cut by leucogranite and has also been noted as inclusions in granite within the northern 5-10 km of the granitic complex by Williams (1978). Tonalites and quartz diorites were described from a similar location in the Vermilion complex (Southwick, 1972).

Magnetite-biotite granite is generally associated with tonalite enclaves and is volumetrically insignificant. The rock is massive to foliated, medium grained to pegmatitic, and contains 5-10 per cent magnetite and less than 5 per cent biotite.

Porphyritic granite with 25-30 per cent K-feldspar phenocrysts up to 1 cm occurs in the Shelley Lake and Williams Lake plutons. The equant to augen megacrysts are set in a medium grained foliated matrix of biotite, chlorite, quartz, plagioclase and microcline. This rock type was described by Berger and York (1979) as quartz syenite and its biotite yielded a $^{40}Ar/^{39}Ar$ date of 2595 Ma. The plutons contain paragnesiss inclusions near the margins and are cut by dykes of muscovite-garnet-bearing pegmatite adjacent to muscovite granite plutons.

Biotite leucogranite occurs in three main bodies: McKenzie-Kawnipi lakes, Eva-Batchewaung lakes and Quetico Lake (Fig. 53.2). The rock is a pink, massive to weakly foliated, homogeneous medium grained granite with subequal proportions of plagioclase, K-feldspar and quartz and less than 5 per cent biotite. It contains 5-10 per cent generally discrete, but locally wispy paragneiss inclusions. Where interlayered with granite at the centimetre scale, the inclusions give the granite a gneissic appearance. K-feldspar megacrysts are present locally in amounts up to 15 per cent. Biotite leucogranite is cut locally by muscovite-bearing pegmatite dykes. Analyses of locally muscovite-bearing Eva Lake leucogranite are available in Williams (1978) and Smith and Williams (1980).

The most abundant rock type in the Quetico Park complex is white muscovite-bearing granite (Fig. 53.2). This body, which generally occupies the core of the belt, has an irregular outline due to interfingering contacts with paragneiss, biotite leucogranite and metasedimentary schists. The massive to foliated granite consists of subequal amounts of quartz, plagioclase and K-feldspar, with 5-10 per cent muscovite, 0-5 per cent biotite, and variable amounts of garnet, sillimanite and cordierite. Inclusions, ranging in size from centimetre-sized clots to units 500 m thick, and constituting 0-30 per cent of this unit, are biotite - plagioclase - quartz ± muscovite paragneiss. Where present as wispy biotite or muscovite-rich layers, the xenoliths give the rock a gneissic character. One 10 m coarse grained pyroxenite inclusion was noted at southern Pickerel Lake. Muscovite granite dykes cut all other rock types, suggesting that it is the youngest intrusive phase of the Quetico Park complex. Several chemical analyses of muscovite-garnet granite from the Niobe Lake area were reported by Williams (1978), who noted very low trace elements contents, including REE.

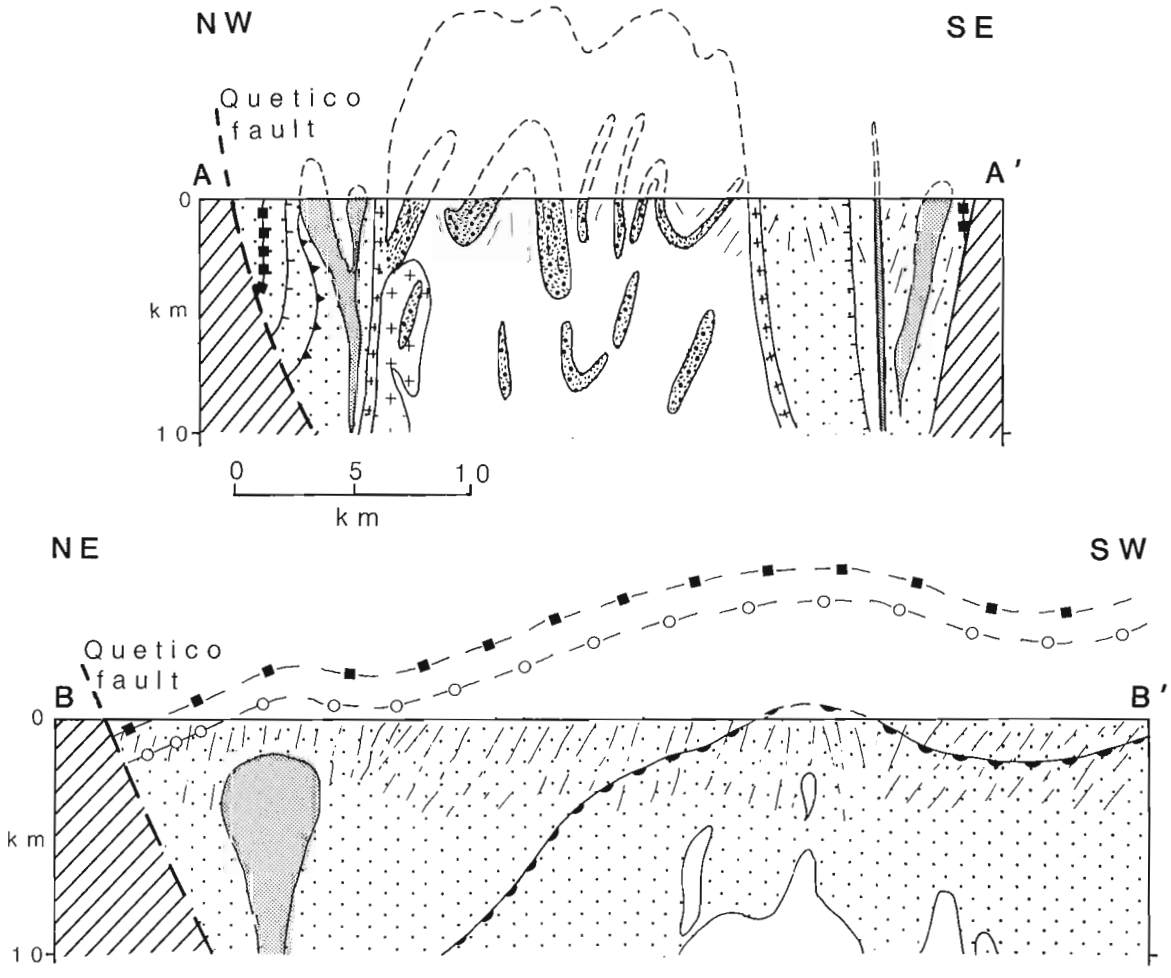

Figure 53.3. *Cross-sections A-A' and B-B' showing the relationship of metamorphic isograds in metasedimentary schists to intrusion granitoid bodies. Symbols as in Figure 53.2.*

Intrusions in the marginal non-migmatitic metasedimentary rocks of the Quetico belt are generally less siliceous than those in the core. These include the Blalock pluton of ultramafic to monzonite to diorite to granodiorite composition (Hillary, 1974; Williams, 1978; Pirie, 1978), the Obinidaw River stock of hornblende and biotite syenite (Harris, 1970) and the Poohbah Lake alkalic rock complex (Tanton, 1940; Sage et al., 1979).

Structural trends, defined by lithological contacts, xenolith alignment, foliation and gneissosity, are generally east-west in the northern Quetico belt and northeast-southwest in the south. The margins of the belt have at least two sets of folds (Sawyer and Robin, 1982a; Boradaile, 1983; Kehlenbeck, 1983) and the core has an additional set of structures (Sawyer and Robin, 1982b). Northerly dips of 20-60° are common throughout the belt, including the Quetico Park complex, where several open antiform-synform pairs were noted (Fig. 53.2). Both rodding and augen lineations plunging 0-45° southwest or northeast are rare and are generally associated with fold axes or shear zones. The cross-section in Figure 53.3 shows the general northerly dips across the belt, including northerly dipping and facing marginal low grade metasedimentary rocks (Pirie and Mackasey, 1978). The peak of metamorphism apparently coincides with the third set of structures (Sawyer and Robin, 1982a), caused by prolonged horizontal northwest-southeast shortening (Sawyer and Robin, 1982b).

Several zones of mylonite were noted in central Kawnipi Lake within the northern 5 km of the Wawa subprovince. The most southerly zone, in diorite or amphibolite, dips 5-10° north and is characterized by strong millimetre-scale layering and grain size of 0.1-0.5 mm. The mylonite is cut by massive pink leucogranite sills and dykes that are gently warped with the mylonitic foliation. To the north, a 500 m thick mylonite zone at Kawa Bay-McVicar Bay dips 20° north and has a strong positive aeromagnetic signature which has allowed extrapolation of the zone to the southwest (Fig. 53.2). The sheared rocks are fine grained, streaky foliated hornblende-biotite granodiorite with concordant mylonitic granite with ribbon quartz and K-feldspar augen. The most northerly mylonite zone occurs at the contact between granodiorite and amphibolites, where fine grained, thinly layered schists and gneisses dip northerly at 60-80°. A strong rodding lineation plunges north-northeast at 45-65°. Pegmatitic dykes in granodiorite are boudinaged in the plane of the foliation.

A pronounced northwest trending topographic lineament in the Rawn Lake-Pickerel Lake area corresponds to a zone of hematite alteration associated with fault breccia and cataclasite. Judging by the offset of units across this fault, the movement was dextral and probably not large.

Metamorphic isograds (Fig. 53.2) have been documented in several areas of the Quetico belt, summarized by Pirie and Mackasey (1978). The general sequence of isograds, based on the appearance of diagnostic assemblages in pelites (Pirie and Mackasey, 1978) is biotite, staurolite, garnet-aluminosilicate (andalusite and/or sillimanite), garnet-cordierite-sillimanite, and in situ granitic leucosome. A characteristic feature of the first granitic leucosome in some areas is the presence of accessory phases including apatite, tourmaline and pyrite. Although volatile impurities such as P_2O_5 and SO_4 do not affect the temperature of the granite solidus, boron can depress it considerably (Chorlton and Martin, 1978). Thus, to reduce uncertainty in interpretation, tourmaline-bearing leucosome should not be used to define the in situ leucosome isograd.

The spacing of isograds appears to be proportional to the width of the belt. In the Crooked Pine Lake area, the metasedimentary margin is some 5 km wide; the distance between the biotite and migmatite isograds is only 3 km (Pirie, 1978). To the west, the Quetico belt widens to about 100 km and the northern metasedimentary margin in the Beaverhouse Lake area is 50 km wide. Here the garnet-sillimanite isograd is 30 km up-grade of the chlorite zone and the staurolite zone is 20 km wide. This relationship suggests that the isograds are probably steep where closely spaced and more gently dipping where widely spaced. The metamorphism of the marginal rocks appears to be directly related to the large granite bodies in the core of the belt (Pirie and Mackasey, 1978; Williams, 1978; Southwick, 1972). Geobarometric study is underway to determine whether the isograd spacing is a function of level of exposure or of depth of granite emplacement.

The common occurrence of garnet-andalusite in metapelites is diagnostic of bathozone 2 (Carmichael, 1978), and suggests that the metamorphism occurred within ~10 km of the surface. The most obvious high-level heat source is the abundant muscovite-bearing granite of the core zone. This granite has many characteristics of "S-type" magmas (Chappell and White, 1974), implying probable derivation by partial melting of a metasedimentary source region. Thus, although shallow-level metamorphism of the margins of the Quetico belt can be attributed to magmatic heat associated with granite emplacement, the deep heat source that melted metasedimentary rocks to produce muscovite granite is cryptic.

A model for the origin of the Quetico belt must account first for the linear trough in which the sediments accumulated, and then for a period of compression, metamorphism and widespread partial melting. The processes responsible for creation of the >1200 km long sedimentary trough could also have given rise to high heat flow and/or deep-seated mafic magmatism. The initiation of sedimentary basin development has been attributed to lithospheric thinning with attendant upwelling of asthenosphere by McKenzie (1978). Modern back-arc basins such as the Sea of Japan basin are linear features bordered by volcanic arcs (e.g. Uyeda, 1982) and are characterized by high heat flow and clastic sediment accumulation. Back-arc basins are subject to abrupt changes in stress regime from tensional to compressional as a result of distant collisions. A tentative back-arc model for the Quetico belt, showing the change from a tensional stress regime during sediment deposition to compressional at the time of deformation and metamorphism, is illustrated in Figure 53.4.

The back-arc model can be tested by zircon geochronology in the Quetico belt. The sediments are predicted to be the erosion products of adjacent volcanic arcs; a comparison of the ages of detrital zircon suites from low grade metasedimentary rocks and adjacent metavolcanic rocks is needed to confirm or deny this relationship. Ages of metamorphism and plutonism in the Quetico belt should be slightly younger than those in the adjacent, mature(?) arcs. Dating of synmetamorphic granitic leucosome and various plutons will provide a basis for comparison.

PART III: GEOLOGY OF THE PERCHING GULL LAKES AREA: PRELIMINARY RESULTS

R.A. Stern

INTRODUCTION

Plutons ranging from diorite to syenite composition are common within the Wawa, Abitibi, and Wabigoon volcanic-plutonic subprovinces of the Superior Province, where they occur between volcanic rocks and gneiss in a characteristic crescent shape. A lineation or foliation is common and has been attributed to magmatic flow (Schwerdtner et al., 1979). Schulz (1982) studied a suite of small, alkalic post-orogenic

plutons in the western Wawa subprovince and suggested that they have shoshonitic affinities (Joplin, 1968; Mackenzie and Chappell, 1972).

This study attempts to characterize the geology and chemistry of the Perching Gull Lakes pluton of intermediate composition (Percival, 1983) and to investigate its relationship to the adjacent volcanic rocks of the Shebandowan belt in which shoshonites have been recognized (Shegelski, 1980). This report summarizes the geology and preliminary petrography.

REGIONAL SETTING

The Perching Gull Lake pluton is located within the Northern Light-Perching Gull Lakes plutonic terrane of the western Wawa subprovince (Fig. 53.5). The plutonic terrane is bordered to the north by the Shebandowan belt, consisting mainly of mafic to felsic, greenschist to amphibolite-grade metavolcanic rocks (Fig. 53.5). Major lithological components of the plutonic terrane were outlined by Percival (1983) and included several intermediate intrusions, among them this pluton which was mapped in greater detail by the writer in 1983.

GEOLOGY OF THE PERCHING GULL LAKES AREA

The Perching Gull Lake pluton is a crescent-shaped quartz monzonite to diorite body, bounded on the east by a narrow unit of mafic gneiss and on the west by granite (Fig. 53.5). Tonalitic gneiss and mafic metavolcanic rocks are present in the northwestern and northeastern parts of the map area. Metavolcanic rocks and derived gneiss are deduced to be the oldest rock type, followed by tonalitic gneiss, the pluton, and finally by late granite and aplite. More detailed descriptions of each map unit follow.

Mafic metavolcanic rocks and mafic gneiss

Mafic metavolcanic rocks in amphibolite facies occur in the northern part of the map area. Primary volcanic features are destroyed where these rocks grade into mafic gneiss in the southern Shebandowan belt (Fig. 53.5). Metamorphic grade decreases to greenschist facies north of the map area. Field evidence, such as lit-par-lit injections of tonalite into amphibolite at the southern edge of the Shebandowan belt, and mafic gneiss xenoliths within gneissic tonalite and within quartz monzonite of the Perching Gull Lake pluton, indicates that the mafic rocks are older than the plutonic rocks of the map area. The mafic gneiss consists of plagioclase-hornblende-clinopyroxene-magnetite-quartz assemblages, with gneissosity defined by alternating hornblende-rich and clinopyroxene-rich layers. Mafic gneisses in the plutonic terrane are interpreted to be the amphibolite facies equivalent of mafic metavolcanic rocks of the Shebandowan belt based on their similarity in composition and mineralogy and close field association.

Gneissic tonalite

Gneissic tonalite is present in the northwestern and northeastern parts of the map area. It is a fine grained, grey, quartz-plagioclase-biotite rock, with 1-2 mm-wide quartz-plagioclase layers separated by thin biotite-rich seams. Xenoliths of mafic gneiss, amphibolite, and diorite are common. Several dykes of hornblende-diorite to monzodiorite cut the gneiss and are themselves cut everywhere by ubiquitous aplite dykes.

Foliated granodiorite

Several isolated outcrops of medium grained, homogeneous, foliated granodiorite in granite are interpreted to be large enclaves. Granodiorite consists of plagioclase-quartz-K-feldspar-biotite assemblages, with the foliation defined by biotite alignment. The granodiorite is older than the host granite, but its age relative to other map units is not known.

Quartz monzonite, monzodiorite, diorite and hornblende-granite

The Perching Gull Lakes pluton consists of quartz monzonite, monzodiorite, leucocratic diorite and, possibly, hornblende granite. Abundant mafic gneiss xenoliths in quartz

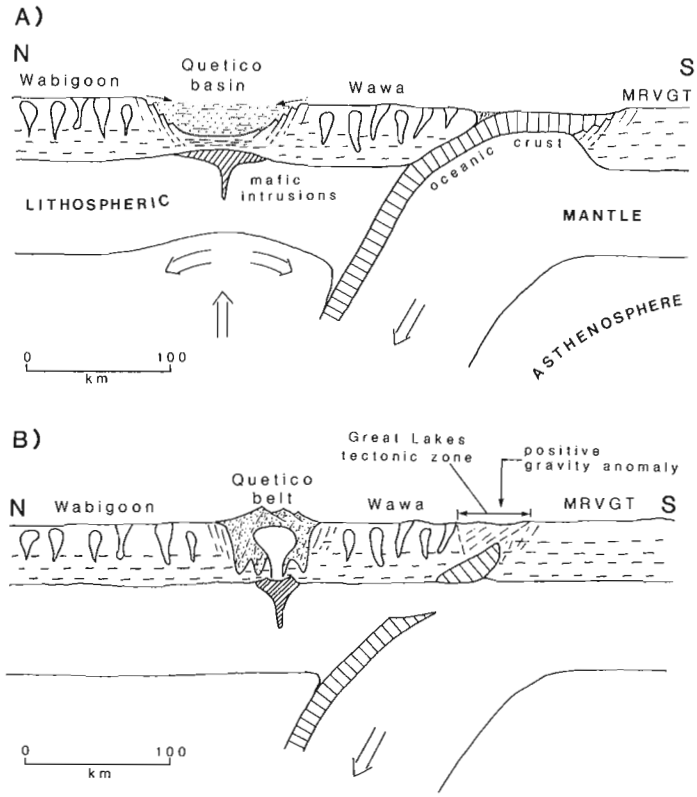

A – Sedimentary basin development (with clastic input from volcanic highlands), in response to lithospheric stretching in a tensional back-arc environment. Compensation by upwelling of asthenosphere (McKenzie, 1978) causes elevated heat flow under developing linear basin.

B – Outboard collision between Wawa subprovince and a more southerly block (Minnesota River Valley Gneiss Terrane? (MRVGT)) results in intense deformation and metamorphism associated with weakened lithosphere (Le Pichon et al., 1982) beneath the Quetico belt. Partial melting of basement and metasedimentary gneiss produces buoyant granites which rise to within 10 km of the surface. The model predicts a north-dipping contact and positive gravity anomaly for the suture, consistent with north-dipping events on a seismic reflection profile (Gibbs et al., in press) and gravity data for the Great Lakes tectonic zone (Sims et al., 1980).

Figure 53.4. *Back-arc basin analogue for the development of the Quetico belt between the Wabigoon and Wawa volcanic arcs.*

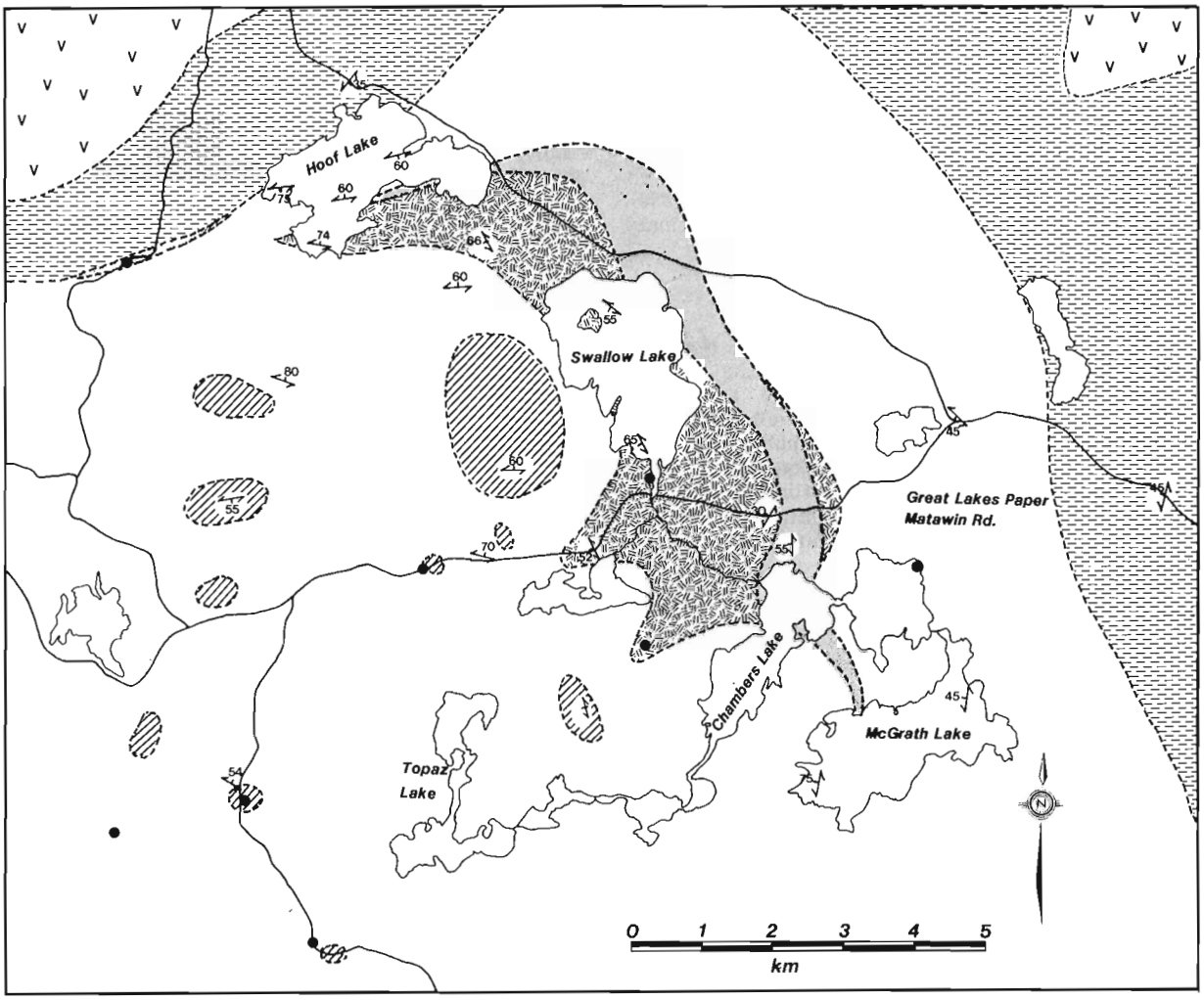

Perching Gull Lakes Suite

- massive to foliated granite
- quartz monzonite, monzodiorite, diorite, hornblende granite
- mafic monzonite, mafic syenite
- foliated granodiorite
- tonalite gneiss
- mafic gneiss
- mafic metavolcanic rocks

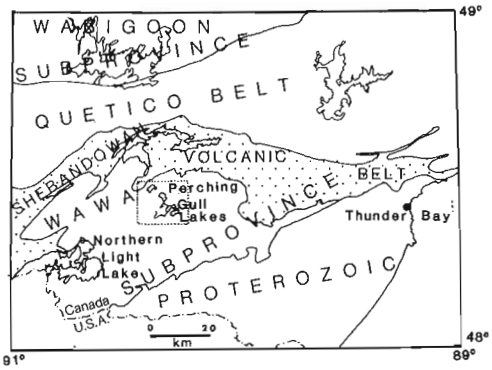

- geological contact
- strike and dip of foliation (70)

Figure 53.5. Generalized geology of the Perching Gull Lakes area. Geology by R. Stern, 1983 and J.A. Percival, 1982.

monzonite clearly indicate that the pluton is younger than mafic gneiss. Xenoliths of foliated quartz monzonite within the surrounding granite and dykes of granite in the Perching Gull Lake pluton show that granite postdates the pluton.

Most of the pluton consists of medium grained to porphyritic, foliated pink quartz monzonite, consisting of microcline, plagioclase, hornblende, biotite and quartz, with accessory magnetite, titanite, and apatite. Titanite is present in amounts up to 5 per cent, and apatite up to 3 per cent. Minor chlorite and epidote indicate some alteration. Aligned microcline megacrysts 1-2 cm in length are poikilitic and include all other phases. Partly saussuritized plagioclase crystals of oligoclase composition have well developed albite twins. Both microcline and plagioclase exhibit symplectic intergrowths with quartz. Hornblende occurs in amounts up to 20 per cent as subhedral to euhedral phenocrysts which have a sub-parallel alignment and give the rock a characteristic foliation. Another distinctive feature of the quartz monzonite is 1-3 cm clusters of minerals, including hornblende, magnetite, chlorite, titanite, and apatite.

Monzodiorite and leucocratic diorite form a small proportion of the pluton, and are characterized by greater quantities of plagioclase and biotite, with lesser amounts of quartz and microcline. Exposure is insufficient to establish any compositional zonation in the pluton, although diorite and quartz monzondiorite are apparently more abundant near the contact with mafic gneiss.

Massive, pink hornblende granite dykes intrude the quartz monzonite, and are themselves cut by late aplite dykes. The hornblende granite dykes characteristically contain mafic xenoliths, including patchy-textured mafic syenite inclusions, which have biotite-rich rims. These dykes are confined to the pluton and are viewed as possible late-stage differentiates of the Perching Gull Lake suite.

Foliation in the Perching Gull Lake pluton is concordant to the margins of the body and dips consistently to the west, except in the most northerly corner (Fig. 53.5). In general, the foliation is most strongly developed at the margins of the pluton; some central areas are massive. The foliation wraps around included mafic gneiss xenoliths whose gneissosity is mostly subparallel to the foliation.

Two types of mafic xenoliths occur throughout the pluton: (1) mafic gneiss, and (2) mafic diorite to mafic syenite. The concordant contact of the pluton with mafic gneiss on the eastern margin is characterized by a zone with numerous xenoliths of mafic gneiss. In all other places, the xenoliths are massive to foliated diorite to syenite. The xenoliths commonly form long trains, aligned parallel to the foliation in the pluton, and have weak foliations and slight elongation parallel to the foliation of the host. A xenolith of 'patchy'-textured mafic syenite has elliptical patches elongated parallel to the foliation of surrounding quartz monzonite.

Mafic syenite and mafic monzonite

Mafic syenitic to monzonitic rocks are present as centimetre to ten metre-sized xenoliths in granite and in the Perching Gull Lake pluton. The largest inclusions are shown as black dots in Figure 53.5. These rocks are medium- to coarse-grained, massive to foliated, dark grey to black, and consist of microcline-hornblende-clinopyroxene-biotite-plagioclase-quartz assemblages, with accessory titanite, apatite, fluorite, and magnetite. Some samples contain as much as 5 per cent titanite and 3-4 per cent apatite. Minor epidote, chlorite, fluorite, and saussuritized plagioclase indicate some alteration. A characteristic 'patchy' texture is produced by 2-3 cm microcline megacrysts surrounded by zones rich in hornblende (Fig. 53.6). The microcline megacrysts poikilitically enclose hornblende, clinopyroxene, biotite, plagioclase, and accessory minerals. Crystals of pyroxene are rimmed by hornblende, and hornblende is rimmed by biotite. The zones encircling the megacrysts consist of hornblende, microcline, biotite, quartz, titanite, apatite, and fluorite.

Xenoliths of mafic diorite to syenite within quartz monzonite of the Perching Gull Lake pluton indicate that the mafic rocks predate quartz monzonite. An isolated outcrop of 'patchy'-textured mafic syenite is cut by hornblende-monzonite dykes. The large isolated outcrops of mafic syenite surrounded and intruded by granite in the southwest corner of the map area (Fig. 53.5) appear to be large enclaves and have a similar relationship to enclosing granite as does the foliated granodiorite.

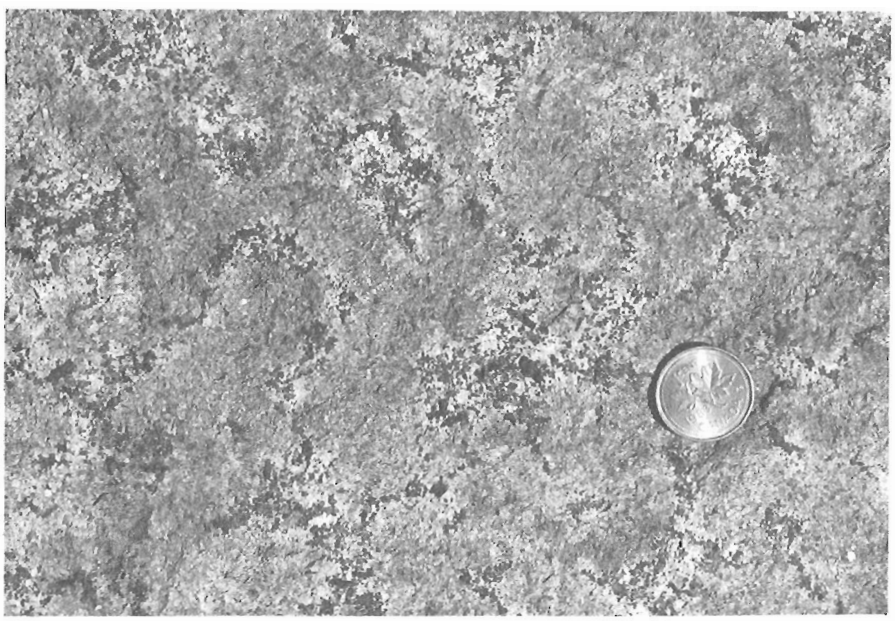

Figure 53.6

Photograph illustrating 'patchy' texture in mafic syenite, produced by 2-3 cm microcline phenocrysts surrounded by zones rich in hornblende.

Massive to foliated granite

The granites are pink, fine grained to pegmatitic rocks consisting of quartz-microcline-plagioclase assemblages with accessory biotite, in places defining a foliation. Two areas of strongly foliated granite are present, one near the magin of the Perching Gull Lake pluton, adjacent to mafic gneiss near Chambers Lake (Fig. 53.5), and the other between tonalitic gneiss and the pluton at Hoof Lake. A folded and stretched xenolith of quartz monzonite within foliated granite was observed near Chambers Lake. Dykes of granite cut all rock types of the pluton. Foliated granite is cut by massive aplite and granite pegmatite dykes, suggesting that there are two ages of granite.

DISCUSSION AND AREAS OF CURRENT RESEARCH

The close spatial relationship and similar mineral assemblages of the mafic monzonites and syenites, the quartz monzonite to diorite of the Perching Gull Lake pluton, and late hornblende-granite dykes suggests a genetic relationship between these rock types. Current studies are concerned with the chemical characteristics of the Perching Gull Lake suite, and with a comparison to volcanics of the Lower Shebandowan Lake area (Fig. 53.5). The mafic members of the Perching Gull Lake suite may be genetically related to shoshonites and trachytes of the Shebandowan belt (Shegelski, 1980) on the basis of their spatial association and potassic, relatively mafic composition. Several volcanic rock types from the Lower Shebandowan Lake area were sampled for the purpose of more detailed comparison.

Foliation in the Perching Gull Lake pluton is strongest at the margins of the pluton, and is absent in some central areas. Both the outline of the body and the internal foliation are concordant to the regional trend of gneissosity, suggesting that either the body and its surroundings were deformed together, or the body gained its foliation upon intrusion into a pre-existing structural discontinuity. The presence of igneous textures, including hornblende and microcline megacryst alignment, and the absence of significant recrystallization support the interpretation of a foliation imposed by magmatic flow. Local strong foliation adjacent to granite may have resulted from forceful intrusion by granite, as evidenced by folded quartz monzonite xenoliths in nearby granite.

The Perching Gull Lake pluton probably intruded along major lithological contacts in a terrane of mafic gneiss, tonalitic gneiss, and, perhaps, foliated granodiorite, with development of a magmatic flow foliation in a manner similar to that envisioned by Schwerdtner et al. (1979, 1983). Later granites may have used the same structural weaknesses.

CONCLUSIONS

The Perching Gull Lakes suite consists of quartz monzonite to leucodiorite, with minor mafic syenite to monzonite and late hornblende-granite dykes. The crescent-shaped Perching Gull Lakes pluton and associated rock types intruded mafic and tonalitic gneiss and possibly foliated granodiorite, and were subsequently intruded by foliated and massive granite. Foliation in the Perching Gull Lakes pluton is probably the result of magmatic flow.

REFERENCES

Berger, G.W. and York, D.
1979: $^{40}Ar/^{39}Ar$ dating of multicomponent magnetizations in the Archean Shelley Lake granite, northwestern Ontario; Canadian Journal of Earth Sciences, v. 16, p. 1933-1941.

Boradaile, G.J.
1983: Comparison of Archean structural styles in two belts of the Canadian Superior Province; Precambrian Research, v. 19, p. 179-189.

Carmichael, D.M.
1978: Metamorphic bathozones and bathograds: A measure of the depth of post-metamorphic uplift and erosion on the regional scale; American Journal of Science, v. 278, p. 767-797.

Chappell, B.W. and White, A.J.R.
1974: Two contrasting granite types; Pacific Geology, v. 8, p. 173-174.

Chorlton, L.B. and Martin, R.F.
1978: The effect of boron on the granite solidus; Canadian Mineralogist, v. 16, p. 239-244.

Chown, E.H.
1959: Geology, Carroll Lake (east half), Kenora District; Geological Survey of Canada, Map 25-1958.

Donaldson, J.A.
1969: Geology, Trout Lake; Geological Survey of Canada, Map 1200A.

Ermanovics, I.F.
1970: Precambrian geology of the Hecla-Carroll Lake map-area, Manitoba-Ontario (62P E/2, 52M W/2); Geological Survey of Canada, Paper 69-42, 33 p.

Ermanovics, I.F. and Wanless, R.K.
1983: Isotopic age studies and tectonic interpretation of Superior Province in Manitoba; Geological Survey of Canada, Paper 82-12, 22 p.

Ermanovics, I.F., McRitchie, W.D., and Houston, W.N.
1979: Petrochemistry and tectonic setting of plutonic rocks of the Superior Province in Manitoba; in Trondhjemites, Dacites and Related Rocks, ed. F. Barker, Elsevier, p. 323-362.

Gibbs, A.K., Payne, B., Setzer, T., Brown, L.D., Oliver, J.E., and Kaufman, S.
– Seismic reflection study of the Precambrian crust of central Minnesota; Geological Society of America Bulletin. (in press)

Giblin, P.E.
1964: Burchell Lake area; Ontario Department of Mines Geological Report 19, 39 p.

Harris, F.R.
1970: Geology of the Moss Lake area; Ontario Department of Mines Geological Report 85, 61 p.

Hillary, E.M.
1974: Petrology of the Sapawe stock, Rainy River District; unpublished B.Sc. thesis, Queen's University, Kingston, Ont., 67 p.

Hodgkinson, J.M.
1968: Geology of the Kashabowie Lake area; Ontario Department of Mines Geological Report 53, 35 p.

Joplin, G.A.
1968: The shoshonite association: a review; Journal of the Geological Society of Australia, v. 15, p. 275-294.

Kehlenbeck, M.M.
1976: Nature of the Quetico-Wabigoon boundary in the de Courcey-Smiley Lakes area, northwestern Ontario; Canadian Journal of Earth Sciences, v. 13, p. 737-748.

1983: Superimposed folding and its implication on the Shebandowan-Quetico subprovince boundary, Thunder Bay, Ontario (abstract); 29th Institute on Lake Superior Geology, Houghton, Michigan, p. 25.

Krogh, T.E., Ermanovics, I.F., and Davis, G.L.
1974: Two episodes of metamorphism and deformation in the Archean rocks of the Canadian Shield; Carnegie Institution of Washington, Yearbook 73, p. 573-575.

Le Pichon, X., Angelier, J., and Sibuet, J-C.
1982: Plate boundaries and extensional tectonics; Tectonophysics, v. 81, p. 239-256.

Mackasey, W.O., Blackburn, C.E., and Trowell, N.F.
1974: A regional approach to the Wabigoon-Quetico belts and its bearing on exploration in northwestern Ontario; Ontario Division of Mines Miscellaneous Paper 58, 29 p.

Mackenzie, D.E. and Chappell, B.W.
1972: Shoshonitic and calc-alkaline lavas from the highlands of Papua-New Guinea; Contributions to Mineralogy and Petrology, v. 35, p. 50-62.

McKenzie, D.P.
1978: Some remarks on the development of sedimentary basins; Earth and Planetary Science Letters, v. 40, p. 25-32.

Nunes, P.D. and Thurston, P.C.
1980: Two hundred and twenty million years of Archean evolution: a zircon U-Pb age stratigraphic study of the Uchi-Confederation Lakes greenstone belt, northwestern Ontario; Canadian Journal of Earth Sciences, v. 17, p. 710-721.

Nunes, P.D. and Wood, J.
1980: Geochronology of the North Spirit Lake area, District of Kenora – progress report; in Summary of Geochronology Studies 1977-1979, ed. E.G. Pye, Ontario Geological Survey Miscellaneous Paper 92, p. 7-14.

Park, R.G.
1981: Shear-zone deformation and bulk strain in granite-greenstone terrain of the western Superior Province, Canada; Precambrian Research, v. 14, p. 31-47.

Percival, J.A.
1983: Preliminary results of geological synthesis in the western Superior Province; in Current Research, Part A, Geological Survey of Canada, Paper 83-1A, p. 125-131.

Pirie, J.
1978: Geology of the Crooked Pine Lake area, District of Rainy River; Ontario Geological Survey Report 179, 73 p.

Pirie, J. and Mackasey, W.O.
1978: Preliminary examination of regional metamorphism in parts of Quetico metasedimentary belt, Superior Province, Ontario; in Metamorphism in the Canadian Shield, ed. J.A. Fraser and W.W. Heywood, Geological Survey of Canada, Paper 78-10, p. 37-48.

Sage, R.P., Wright, W., Chamois, P., and Higgins, C.
1979: Poohbah Lake alkalic complex, District of Rainy River; Ontario Geological Survey Preliminary Map P-2219.

Sage, R.P. and Breaks, F.W.
1982: Geology of the Cat Lake-Pickle Lake area, Districts of Kenora and Thunder Bay; Ontario Geological Survey Report 207, 238 p.

Sawyer, E.W. and Robin, P-Y.F.
1982a: Initiation, evolution and transformation of segregation veins to migmatites: effects of planar mechanical anisotropy (Abstract); in International Conference on Planar and Lunar Fabrics of Deformed Rocks, Abstracts, Zurich.

1982b: The structural history of the Quetico metasedimentary belt in the Kashabowie area, Ontario (Abstract); in Geological Association of Canada-Mineralogical Association of Canada, Program with Abstracts, v. 7, p. 79.

Schulz, K.J.
1982: The nature and significance of Archean alkalic magmatism, southern Superior Province; Geological Association of Canada-Mineralogical Association of Canada, Program with Abstracts, v. 7, p. 80.

Schwerdtner, W.M., Stone, D., Osadetz, K., Morgan, J., and Stott, G.M.
1979: Granitoid complexes and the Archean tectonic record in the southern part of northwestern Ontario; Canadian Journal of Earth Sciences, v. 16, p. 1965-1977.

Schwerdtner, W.M., Stott, G.M., and Sutliffe, R.H.
1983: Strain patterns of crescentic granitoid plutons in the Archean greenstone terrane of Ontario; Journal of Structural Geology, v. 5, p. 419-430.

Shegelski, R.J.
1980: Archean cratonization, emergence and red bed development, Lake Shebandowan area, Canada; Precambrian Research, v. 12, p. 331-347.

Sims, P.K., Card, K.D., Morey, G.B., Peterman, Z.E.
1960: The Great Lakes tectonic zone – A major crustal structure in central North America; Geological Society of America Bulletin, v. 91, p. 690-698.

Smith, I.E.M. and Williams, J.G.
1980: Geochemical variety among Archean granitoids in northwestern Ontario; in The Continental Crust and its Mineral Deposits, D.W. Strangway, ed., Geological Association of Canada, Special Paper 20, p. 181-192.

Southwick, D.L.
1972: Vermilion granite-migmatite massif; in Geology of Minnesota: A centennial volume; P.K. Sims and G.B. Morey, eds., Minnesota Geological Survey, p. 108-119.

Tanton, T.L.
1940: Quetico (west half) Rainy River District, Ontario; Geological Survey of Canada, Map 534A.

Thurston, P.C. and Bartlett, J.R.
1981a: Trout Lake-Birch Lake sheet, Kenora district; Ontario Geological Survey Map P-2386.
1981b: Red Lake sheet, Kenora district; Ontario Geological Survey Map P-2385.

Uyeda, S.
1982: Subduction zones: an introduction to comparative subductology; Tectonophysics, v. 81, p. 133-159.

Williams, J.G.
1978: Geology of the Crystal Lake area, Quetico subprovince; in Proceedings of the 1978 Archean Geochemistry Conference, ed. I.E.M. Smith and J.G. Williams, University of Toronto Press, p. 193-207.

54. ILLITE "CRYSTALLINITY" IN THE WESTERN RIVER FORMATION AND ITS SIGNIFICANCE REGARDING THE REGIONAL METAMORPHISM OF THE EARLY PROTEROZOIC GOULBURN GROUP, DISTRICT OF MACKENZIE

Project 830010

Peter H. Thompson and Martin Frey[1]
Precambrian Geology Division

Thompson, P.H. and Frey, M., Illite "crystallinity" in the Western River Formation and its significance regarding the regional metamorphism of the Early Proterozoic Goulburn Group, District of Mackenzie; in Current Research, Part A, Geological Survey of Canada, Paper 84-1A, p. 409-414, 1984.

Abstract

Illite "crystallinity" values obtained from a preliminary study of pelitic rocks of the basal Western River Formation of the Early Proterozoic Goulburn Group indicate these rocks were metamorphosed under conditions characteristic of the upper anchizone and lower greenschist facies. Published estimates of the temperatures for this transition (300-350°C) suggest that: 1) the Goulburn Group was much thicker than present estimates indicate; 2) another sedimentary sequence was on top of the Group when metamorphism occurred, or 3) tectonic stacking buried the rocks to sufficient depth for the metamorphism to occur.

Résumé

Les valeurs de la <<cristallinité>> de l'illite, calculées lors d'une étude préliminaire des roches pélitiques provenant de la formation basale de Western River dans le groupe de Goulburn du Protérozoïque ancien, indiquent que ces roches ont été métamorphisées dans des conditions caractéristiques de l'anchizone supérieure et de la partie inférieure du faciès des schistes verts. Les estimations publiées des températures de cette transition (300 à 350°C) laissent supposer que: 1) l'épaisseur du groupe de Goulburn était supérieure aux estimations actuelles; 2) une autre séquence sédimentaire recouvrait le groupe au moment du métamorphisme; ou, 3) que l'empilement tectonique a enfoui les roches à une profondeur suffisante pour permettre leur métamorphisme.

INTRODUCTION

Evidence of a Proterozoic thermal overprint in the form of the widespread occurrence of Proterozoic K-Ar mica ages (1600-2100 Ma) has been recognized for some time in the northern part of the Archean Slave Province of the Canadian Shield (Stockwell, 1969). Recent work in the Healey Lake map area (Henderson, 1979; Henderson and Thompson, 1980, 1981, 1982; Henderson et al., 1982; Thompson and Henderson, 1983) revealed a post-Archean amphibolite facies metamorphic overprint in Archean rocks and post-Archean basic dykes (Fig. 54.1). This metamorphic event has been linked to crustal overthrusting related to Proterozoic reactivation of the Thelon Tectonic Zone, a 50-100 km wide and more than 800 km long structure which is present along the eastern boundary of the Slave Province. The Goulburn Group (Fraser, 1964; Tremblay, 1971, 1976) is an early Proterozoic sequence of clastic and carbonate rocks that was deposited in the Kilohigok Basin in the northern Slave Province (Fig. 54.1) (Campbell and Cecile, 1975, 1976a, b, 1981). The scale of the event in the Healey Lake area is of such a magnitude that the thermal disturbance indicated by the K-Ar ages may be related to this event and the Goulburn Group, if deposited at this time, may also have been affected.

This preliminary study of illite crystallinity in pelitic rocks of the basal Western River Formation was done to determine if the Goulburn Group has been metamorphosed and if a more comprehensive evaluation of the extent and degree of metamorphism is justified. Although the cleavage in the Goulburn Group (Fraser, 1964; Tremblay 1971, 1976; Frith, 1982) indicates some recrystallization has occurred, the rocks are generally considered to be, at least in a relative sense, unmetamorphosed (Fraser, 1968; Tremblay, 1976; Campbell and Cecile, 1981). Extrapolation of the Healey Lake isograds northward indicates metamorphic conditions in the area of the Goulburn Group would be very low grade (<350°C). Temperatures in the range 250-350°C are sufficient to reset K-Ar mica ages (Purdy and Jager, 1976; Harrison and McDougall, 1980). Conventional petrographic methods of evaluating metamorphic grade are not adequate for clastic and carbonate rocks metamorphosed under conditions such as these. Determination of illite "crystallinity" by X-ray diffraction methods, however, is a useful tool for measuring metamorphic grade in the transitional zone between diagenesis and the greenschist facies (Kisch, 1983; Dunoyer de Segonzac, 1970). Although no attempt has been made to determine the chronology of these events, if the Goulburn Group has been metamorphosed and if the metamorphism is the one that formed the isograds in the Healey Lake area, some constraints are imposed on the timing of the proposed reactivation of the Thelon Tectonic Zone in the region and with respect to tectonic events affecting correlative rock units of the Epworth Group in Wopmay Orogen to the west and, possibly, the Amer Group in the Churchill Province to the east.

The anchizone and illite "crystallinity"

The anchizone, also referred to as the zone of incipient metamorphism (Kisch, 1983) or zone of lowest grade, represents the upper grade part of the zone between diagenesis and greenschist facies metamorphism. Dunoyer de Segonzac and Heddebaut (1971) concluded that the anchizone is developed only in orogenic and suborogenic basins and not in unfolded sedimentary basins and so it is reasonable to expect to find it in the openly folded Goulburn Group. Mineralogical characteristics of the anchizone (see Kisch, 1983) include: 1) the absence of smectite, irregular illite-smectite mixed layers, and kaolinite; 2) the predominance of illite and chlorite as layer silicates in

[1] Mineralogisches-Petrographisches, Institut de Universitat Basel, Bernoullistrasse 30, Ch4026 Basel Switzerland

clastic rocks; 3) presence of stilpnomelane, pyrophyllite and paragonitic illite/micas in appropriate compositions; 4) prehite-pumpellite facies mineral assemblages in intermediate volcanic lithic sandstones and tuffs.

Excellent reviews by Dunoyer de Segonzac (1970) and Kisch (1983) of the transition from diagenesis to greenschist facies metamorphism include sections dealing with illite crystallinity in considerable detail. Only a brief summary is presented here. Illite is a term applied to a group of clay minerals having a mica-like structure and chemistry that are transitional to phengite/muscovite, minerals characteristic of the greenschist facies. The transformation of illite to phengite/muscovite involves an increase in both the size of crystallites and in the regularity of the layers due to dehydration, fixation of potassium in the structure, and rearrangement of ions within layers. A reflection of this increasing crystallinity is the increased sharpness of the X-ray diffraction peak for the basal reflection (001) at about 10 Å (1.0 monometre). The "sharpness" or width of the peak at halfheight (measured in millimetres or in degrees $\Delta 2\theta$) is taken to be the "crystallinity" of illite. Kisch (1983) recommends that the word "crystallinity" be enclosed in quotation marks when used in this sense because the peak width is a simplication, an index of crystallinity, rather than

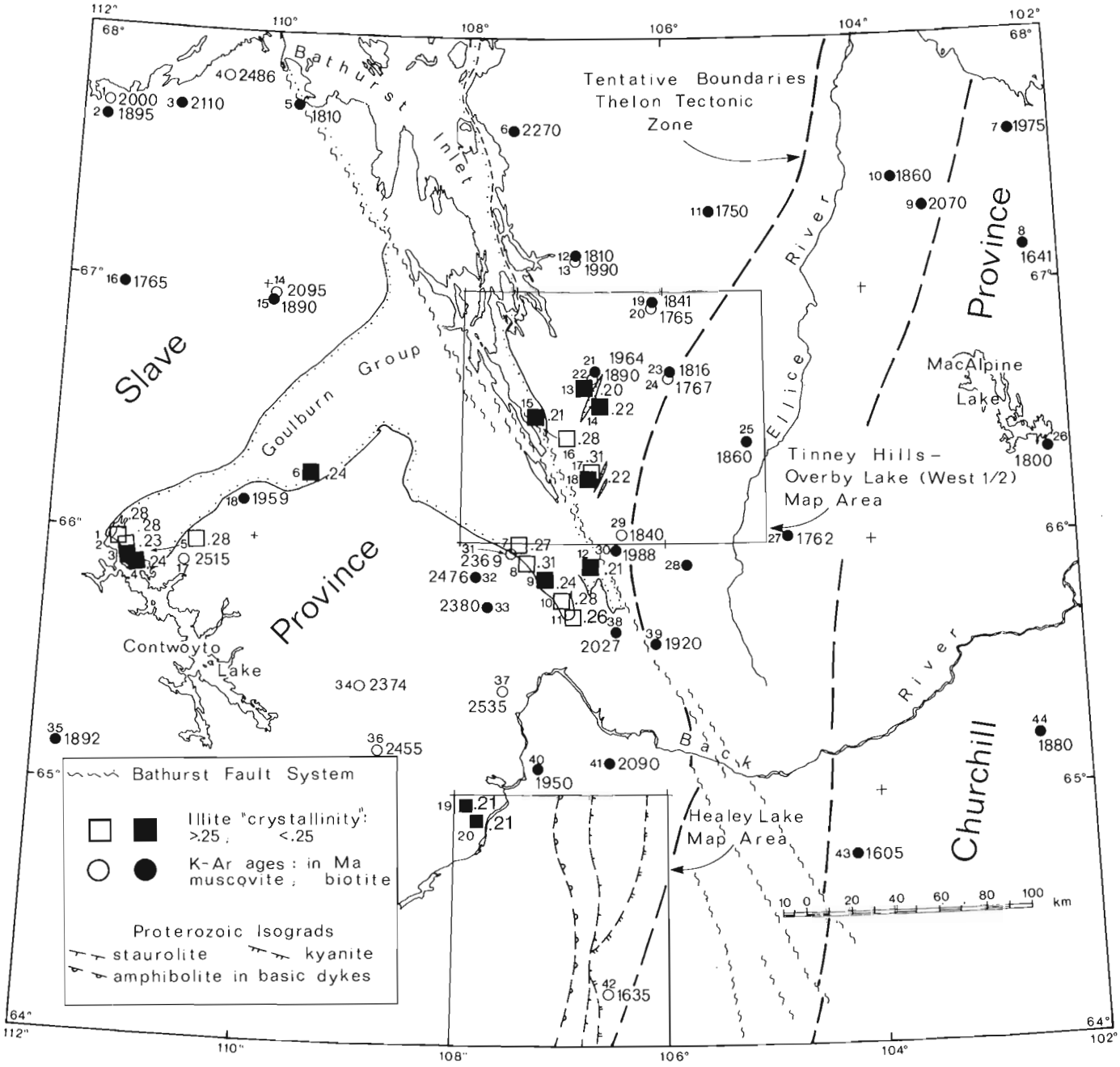

Figure 54.1. *Illite "crystallinity" in the Western River Formation of the early Proterozoic Goulburn Group and biotite and muscovite K-Ar cooling ages from the underlying Archean crystalline rocks in the northeastern District of Mackenzie. Data from two samples of low grade Archean Yellowknife Supergroup are included. Bathurst Inlet is 650 km northeast of Yellowknife, NWT. The tentative outline of the Thelon Tectonic Zone is based on the aeromagnetic anomaly map.*

a direct measurement of a complex parameter. Factors such as lithology, composition of illite and associated fluid, $P_{lithostatic}$, P_{H_2O}, time and temperature as well as the operating conditions both during the separation procedures and when the measurements are made affect the crystallinity of illite. Both Kisch and Dunoyer de Segonzac conclude that inspite of the lack of understanding of all aspects of the recrystallization of illite, regional studies of this parameter (e.g. Kisch, 1980; Frey et al., 1980; Rowsell and de Swart, 1976; Islam et al., 1982; Robinson et al., 1980) have shown that illite crystallinity is a useful index of thermal metamorphism. The anchizone is characterized by illite "crystallinities" of 0.42° to 0.25° $\Delta 2\theta$ according to Kubler (1967, 1968) with 0.25° marking the boundary with the greenschist facies.

Illite "crystallinity" in the Western River Formation

Of the 18 Western River Formation samples used in this study 14 are from the Geological Survey of Canada Collections (J.A. Fraser and L.P. Tremblay), and four were collected this past summer from localities east of Bathurst Inlet (Fig. 54.1). The two Yellowknife Supergroup rocks from the Healey Lake area are also from the GSC Collections (J.B. Henderson). The Goulburn Group samples are all from "argillite" or "siltstone" layers in the basal Western River Formation. Samples from the outliers of probable Western River Formation east of Bathurst Inlet are sufficiently recrystallized that they are, in fact, phyllites. X-ray mounts were prepared by air drying portions of the grain size fraction <2 μ obtained by sedimentation in Atterberg cylinders of samples finely ground in a tungsten-carbide Sieb mill for 30 seconds. Illite "crystallinity" standards were included in the diffractometer runs. A measure of the precision of the method was obtained by measuring the "crystallinity" of one sample (TZ-T335-83) nine times. The value obtained was 0.283 ± .011. The data for all samples including, for comparison, two samples from the lowermost greenschist facies of the Archean metamorphism in the Healey Lake map area northwest of the Back River (Fig. 54.1) are included in Table 54.1.

All samples from the Western River Formation east and west of Bathurst Inlet and from the outliers (Fig. 54.1) are within the upper grade part of the anchizone or the lower greenschist facies as defined by Kubler (1968). The highest grade illite "crystallinities" (lowest values) in the Proterozoic rocks are similar to the two values obtained from low grade Archean rocks that lack biotite but occur in an area where rocks of somewhat different compositions have biotite.

Petrographic observations confirm the implications of the illite "crystallinity" data that these rocks have been metamorphosed. Grain size is sufficient that most minerals are easily identifiable. Quartz, illite, and chlorite are the main constituents with potassium feldspar (determined by a staining technique) also important. Dolomite is present in five of the samples and plagioclase in seven. A preferred orientation of illite and chlorite is present in all samples. Half of these rocks contain small amounts of relatively coarse grained 0.1-0.5 mm plates of white mica that appear to be detrital. New very fine grained white mica with a preferred orientation has nucleated on some of these grains. Chlorite-carbonate aggregates are particularly well recrystallized. In samples 13, 14, 17 and 18 (Table 54.1) which are from the outliers, the schistosity defined by illite and chlorite has been crenulated. One specimen adjacent to sample 17 contained so much biotite that the rock was not suitable for an illite crystallinity measurement. Some of the biotite in this rock has been retrograded to chlorite indicating retrogression after the event that metamorphosed these rocks. Retrogressive chlorite and white mica younger than the peak assemblages that formed during the Proterozoic overprint also occur in the Healey Lake map-area. The occurrence of biotite in the pelitic rocks of the Goulburn Group is compatible with field observations of tremolite in the northwesternmost and tremolite and talc in southwesternmost of the outliers (Thompson and Ashton, 1984).

Sample 8 (Table 54.1, Fig. 54.1) presents an interesting test of the problem of the contribution of the detrital component in these rocks to the illite "crystallinity" obtained. Kisch (1983) points out that by using only the grain size fraction <2 μ the effect of the presence of well-crystallized detrital white mica in a clastic rock on illite "crystallinity" is reduced to acceptable levels. Sample 8 contains clastic white mica plates that Tremblay separated and found to have a K-Ar age of 2369 Ma (see Table 54.2, sample 31 for reference), which he interpreted as indicating the mica is a detrital Archean muscovite. The illite "crystallinity" of the <2 μ fraction of this rock is .313, one of the lowest grade values obtained. The detrital, presumably highly crystallized component was effectively separated from the Proterozoic illite in this case. The low proportion of identifiable clastic mica and its uniformly coarse grain size where present permit us to disregard this complication in the other samples as well.

Table 54.1. Illite "Crystallinity" (° $\Delta 2\theta$)

Map Number	Sample Number	I.C. (° $\Delta 2\theta$)
A. Contwoyto Lake		
1	B72-65 (606-11)	.28
	2T97-65 (606-12)	.28
	3T136-65 (605-23)	.23
	4T15-65 (605-20)	.24
	5T59-65 (606-23)	.28
B. West of Bathurst Inlet		
6	BK26-62b	.24
7	T52-63	.27
8	T65-63	.31
9	M150-62	.24
10	T166-63	.28
11	T199-62	.26
12	M126-62	.21
C. East of Bathurst Inlet		
13	FD12A-67	.20
14	FD46-67	.22
15	TZ-T333-83	.21
16	TZ-T335-83	.28
17	TZ-T319D-83	.31
18	TZ-T318B-83	.22
Healey Lake Map Area (Yellowknife Supergroup)		
19	HBA-T1-79	.21
20	HBA-T30-79	.21
Operating Conditions:	Goniometer 2° θ/min; Chart speed 1200 mm/hr; time constant = 1; slits 1°-2-1°	

Table 54.2

No. on Figure 54.1	G.S.C. Sample Number	Mineral	Rock Type	Age (Ma)	Reference (G.S.C. Paper No.)
1	63-67	Mu	slate	2000 ± 70	64-17
2	63-69	Bi	schist/gneiss	1895 ± 70	64-17
3	63-68	Bi	rhyolite	2110 ± 70	64-17
4	64-51	Mu	pegmatite	2486 ± 80	65-17
5	63-66	Bi	quartz diorite	1810 ± 60	64-17
6	63-61	Bi	quartz monzonite	2270 ± 70	64-17
7	64-63	Bi	granulite	1975 ± 56	65-17
8	66-90	Bi	granulite	1645 ± 55	67-2 (Part A)
9	65-69	Bi	quartz diorite	2070 ± 65	66-17
10	65-70	Bi	gneiss	1860 ± 60	66-17
11	63-79	Bi	quartz monzonite	1750 ± 70	64-17
12	63-71	Bi	granodiorite	1810 ± 70	64-17
13	63-72	Mu	granodiorite	1990 ± 70	64-17
14	61-74	Mu	quartz monzonite	2095 ± 110	62-17
15	61-75	Bi	quartz monzonite	1890 ± 100	62-17
16	63-76	Bi	quartz monzonite	1767 ± 70	64-17
17	63-64	Mu	pegmatite	2515 ± 80	64-17
18	63-63	Bi	granodiorite	1959 ± 65	64-17
19	64-49	Bi	granulite	1841 ± 60	64-17
20	64-50	Mu	granulite	1765 ± 55	65-17
21	64-52	Bi	granite	1964 ± 60	65-17
22	64-53	Mu	granite	1890 ± 60	65-17
23	63-74	Bi	schist	1816 ± 70	64-17
24	63-75	Mu	schist	1767 ± 70	64-17
25	64-62	Bi	granulite	1860 ± 55	65-17
26	63-65	Bi	diorite	1800 ± 60	64-17
27	63-62	Bi	charnockite	1762 ± 60	64-17
28	59-31	Bi	granite gneiss	1806 ± 100	60-17
29	64-48	Mu	granite gneiss	1840 ± 60	65-17
30	64-41	Bi	schist	1988 ± 52	65-17
31	64-38	Mu	argillite	2369 ± 100	65-17
32	64-37	Bi	stauro-and. gneiss	2476 ± 80	65-17
33	59-23	Bi	granite	2380 ± 120	60-17
34	78-139	Mu	pegmatite	2374 ± 54	79-2
35	63-70	Bi	quartz monzonite	1890 ± 70	64-17
36	63-73	Mu	granodiorite	2455 ± 80	64-17
37	59-24	Mu	granite (coarse)	2535 ± 130	60-17
38	63-26	Bi	granodiotite	2027 ± 60	64-17
39	63-25	Bi	gneiss	1920 ± 60	64-17
40	59-26	Bi	granite	1950 ± 105	60-17
41	59-25	Bi	schist	2090 ± 110	60-17
42	60-59	Mu	gneissic-granodiorite	1635 ± 90	61-17
43	59-30	Bi	coarse granite	1605 ± 100	60-17
44	61-86	Bi	granodiorite	1880 ± 100	62-17 (Part 1)

DISCUSSION

In summary then, the illite "crystallinity" values obtained from the Goulburn Group indicate these rocks have been subjected to a regional metamorphism of upper anchizone to lower greenschist facies. The range of values in each subarea is not excessive for this method but they highlight the need to do a relatively large number of samples in order that anomalous values can be identified. The more comprehensive sampling planned for future work will refine and extend the preliminary results discussed here. Although there is no precise temperature calibration of the illite "crystallinity" method available, qualitative estimates can be made and the implications for the Goulburn Group merit some discussion.

Estimates of the temperatures associated with the anchizone/greenschist facies boundary are in the range 300-375°C (Turner, 1981; Stalder, 1979; Cloos, 1983). In a study in the Canadian Cordillera that obtained similar values of illite "crystallinity" to those presented here McMechan and Price (1982) estimated temperatures of 375°C and depths of 17 km were involved. In the Swedish Caledonides, Kisch (1980) invoked overthrusting of a metamorphic allocthon to explain the illite "crystallinity" values typical of the upper anchizone and lower greenschist facies. In the absence of adequate stratigraphic thickness to produce observed temperatures of 100-200°C in a weakly metamorphosed sequence of clastic sedimentary rocks Hoffman and Hower (1979) also proposed overthrusting of relatively hot rocks. In view of the low estimated thickness of the Goulburn Group outside the axial zone (<1000 m), the upper anchizone/lower greenschist facies illite "crystallinity" values obtained in this study suggest that: 1) the Goulburn Group was originally much thicker than these estimates indicate; 2) another sedimentary sequence was on top of the Group when metamorphism occurred; or 3) some sort of tectonic thickening by thrusting raised the temperature to anchizone/greenschist facies conditions.

The data obtained in this preliminary study have encouraged the authors to further document the metamorphism of the Goulburn Group by sampling to the northwest and north and upward in the sequence. Zeolite facies mineral assemblages in basic flows in the Brown Sound Formation would provide an additional way of evaluating metamorphic grade in these rocks. The age of the metamorphism would be a very useful additional piece of information. The Goulburn Group may provide a means of tracing the effects of the proposed Proterozoic reactivation of the Thelon Tectonic Zone across the northern Slave Province and of relating them to tectonic events in the Wopmay Orogen to the west (Hoffman 1980; Hoffman et al., 1983).

ACKNOWLEDGMENTS

We would like to thank John B. Henderson for a very constructive critical review and John Carmichael for drafting Figure 54.1.

References

Campbell, F.H.A. and Cecile, M.P.
1975: Report on the geology of the Kilohigok Basin, Goulburn Group, Bathurst Inlet, N.W.T.; in Report of Activities, Part A, Geological Survey of Canada, Paper 75-1A, p. 297-306.

1976a: Geology of the Kilokigok Basin, Goulburn Group, Bathurst Inlet, N.W.T.; in Report of Activities, Part A, Geological Survey of Canada, Paper 76-1A, p. 369-378.

1976b: Geology of the Kilohigok Basin; Geological Survey of Canada, Open File Map 332, 1:500 000 scale.

1981: Evolution of the early Proterozoic Kilohigok Basin, Bathurst Inlet – Victoria Island, Northwest Territories; in Proterozoic Basins of Canada, ed. F.H.A. Campbell, Geological Survey of Canada, Paper 81-10, p. 103-131.

Cloos, J.
1983: Comparative study of mélange matrix and metashales from the Franciscan subduction complex with the basal Great Valley Sequence, California; Journal of Geology, v. 91, p. 291-306.

Dunoyer de Segonzac, G.
1970: The transformation of clay minerals during diagenesis and low grade metamorphisms: a review; Sedimentology, v. 15, p. 281-346.

Dunoyer de Segonzac, G. and Heddebaut, C.
1971: Paléozoique anchi-métamorphisme à illite, chlorite, pyrophyllite, allevardite, et paragonite dans les Pyrénées Barsques; Bulletin Service de Carte géologique Alsace Lorraine, v. 24, p. 277-290.

Fraser, J.A.
1964: Geological notes on northeastern District of Mackenzie, Northwest Territories (Report and Map 45-1963); Geological Survey of Canada, Paper 63-40, 16 p.

1968: Geology across Thelon Front, District of Mackenzie (76 I,J); in Report of Activities, Part A, Geological Survey of Canada, Paper 68-1A, p. 134.

Fraser, J.A. and Tremblay, L.P.
1969: Correlation of Proterozoic strata in the northwestern Canadian Shield; Canadian Journal of Earth Sciences, v. 6, p. 1-9.

Frey, M., Teichmuller, M., Teichmuller, R., Mullis, J., Kunzi, B., Breitschmid, A., Gruner, V., and Schwizer, B.
1980: Very low grade metamorphism in the external parts of the Central Alps: illite crystallinity, coal rank and fluid inclusion data; Eclogae Geologicae Helvetiae, v. 73, p. 173-203.

Frith, R.A.
1982: Second preliminary report on the geology of the Beechey Lake – Duggan Lakes map areas, District of Mackenzie; in Current Research, Part A, Geological Survey of Canada, Paper 82-1A, p. 203-211.

Harrison, T.M. and McDougall, I.
1980: Investigations of an intrusive contact, northwest Nelson, New Zealand – I Thermal, chronological and isotopic constraints; Geochimica Cosmochimica Acta, v. 44, p. 1985-2003.

Henderson, J.B.
1979: Healey Lake map area, District of Mackenzie; in Current Research, Part A, Geological Survey of Canada, Paper 79-1A, p. 400.

Henderson, J.B. and Thompson, P.H.
1980: The Healey Lake map ara (northern part) and the enigmatic Thelon Front, District of Mackenzie; in Current Research, Part A, Geological Survey of Canada, Paper 80-1A, p. 165-169.

1981: The Healey Lake map area and the enigmatic Thelon Front, District of Mackenzie; in Current Research, Part A, Geological Survey of Canada, Paper 81-1A, p. 175-180.

1982: Geology of Healey Lake map area (1:125 000 scale map and marginal notes); Geological Survey of Canada Open File 860.

Henderson, J.B., Thompson, P.H., and James, D.T.
1982: The Healey Lake map area and the Thelon Front problem, District of Mackenzie; in Current Research, Part A, Paper 82-1A, p. 191-195.

Hoffman, J. and Hower, J.
1979: Clay mineral assemblages as low grade metamorphic geothermometers: application to the thrust faulted disturbed belt of Montana, U.S.A.; Society of Economic Paleontologists and Mineralogists Special Publication 26, p. 55-79.

Hoffman, P.F., Tirrul, R., and Grotzinger, J.P.
1983: The externides of Wopmay Orogen, Point Lake and Kikerk Lake map areas, District of Mackenzie; in Current Research, Part A, Geological Survey of Canada, Paper 83-1A, p. 429-435.

Hoffman, P.F.
1980: Wopmay Orogen: A Wilson Cycle of early Proterozoic age in the northwest of the Canadian Shield; in The Continental Crust and its Mineral Deposits, ed. D.W. Strangway, Geological Association of Canada, Special Paper 20, p. 523-549.

Islam, S., Hesse, R., and Chagnon, A.
1982: Zonation of diagenesis and low grade metamorphism in Cambro-Ordovician flysch of Gaspé Peninsula, Quebec Appalachians; Canadian Mineralogist, v. 20, p. 155-167.

Kisch, H.J.
1980: Incipient metamorphism of Cambro-Silurian clastic rocks from the Jamtland Supergroup, Central Scandinavian Caledonides, Western Sweden: illite crystallinity and "vitrinite" reflectance; Journal Geological Society of London, v. 137, p. 271-288.

1983: Mineralogy and Petrology of binoial diagenesis (burial metamorphism) and incipient metamorphism in clastic rocks; in Diagenesis in sediments and sedimentary rocks, 2; ed. G. Larson and G.V. Chilingar, Developments in Sedimentology 25B, p. 289-494.

Kubler, B.
1967: La crystallinité de l'illite et les zones tout à fait supérieures du métamorphisme; dans Colloque sur les "Etages tectoniques", Neuchatel 18-21 avril 1966, Festschrift, p. 105-122.

1968: Evaluation quantitative du métamorphisme par la cristallinité de l'illite; Bulletin du Centre de Recherches de Pau-Société Nationale des Pétroles d'Aquitaine, v. 2, p. 358-397.

McMechan, M.E. and Price, R.A.
1982: Superimposed low-grade metamorhpism in the Mount Fisher area, southeastern British Columbia – implications for the East Kootenay orogeny; Canadian Journal of Earth Sciences, v. 19, p. 476-498.

Purdy, J.W. and Jager, E.
1976: K-Ar ages on rock forming minerals from the Central Alps; Memoire degli Instituti di Geologia e Mineralogia dell' Universitatà di Padova, 30, 31.

Robinson, D., Nicholls, R.A., and Thomas, L.J.
1980: Clay mineral evidence for low grade Caledonian and Variscan metamorphism in southwestern Dyfed, South Wales; Mineralogical Magazine, v. 43, p. 857-863.

Rowsell, D.M. and de Swardt, A.M.J.
1976: Diagenesis in Cape and Karoo sediments, South Africa and its bearing on their hydrocarbon potential; Transactions of the Geological Society of South Africa, v. 79, p. 81-129.

Stalder, Pierre J.
1979: Organic and inorganic metamorphism in the Taveyanne Sandstone of the Swiss Alps and equivalent sandstones in France and Italy; Journal of Sedimentary Petrology, v. 49, p. 463-488.

Stockwell, C.H.
1969: Tectonic map of Canada (1:5 000 000); Geological Survey of Canada, Map 1251A.

Thompson, P.H. and Henderson, J.B.
1983: Polymetamorhpism in the Healey Lake map area – implications for the Thelon Tecotnic Zone; in Current Activities Forum 1983 Program with Abstracts, Geological Survey of Canada, Paper 83-8, p. 2.

Thompson, P.H. and Ashton, K.
1984: Preliminary report on the geology of the Tinney Hills-Overby Lake (W½) map area – a look at the Thelon Tectonic Zone northeast of the Bathurst Fault; in Current Research, Part A, Geological Survey of Canada, Paper 84-1A, Report 55.

Tremblay, L.P.
1971: Geology of Beechey Lake map area, District of Mackenzie; Geological Survey of Canada, Memoir 365, 56 p.

1976; Geology of northern Contwoyto Lake area, District of Mackenzie; Geological Survey of Canada, Memoir 381, 56 p.

Turner, F.J.
1981: Metamorphic Petrology; McGraw-Hill Book Company, Toronto, 524 p.

55. PRELIMINARY REPORT ON THE GEOLOGY OF THE TINNEY HILLS-OVERBY LAKE (W½) MAP AREA, DISTRICT OF MACKENZIE: A LOOK AT THE THELON TECTONIC ZONE NORTHEAST OF THE BATHURST FAULT

Project 830010

Peter H. Thompson and Ken Ashton[1]
Precambrian Geology Division

Thompson, P.H. and Ashton, K., Preliminary report on the geology of the Tinney Hills-Overby Lake (W½) map area, District of Mackenzie: a look at the Thelon Tectonic Zone northeast of the Bathurst Fault; in Current Research, Part A, Geological Survey of Canada, Paper 84-1A, p. 415-423, 1984.

Abstract

The Tinney Hills-Overby Lake (W½) map area is the second in a series of problem-oriented 1:250 000 scale mapping projects directed toward obtaining a better understanding of the age, significance and origin of a major feature of the northwest Canadian Shield, the boundary between the Slave and Churchill structural provinces; 2500 km² have been completed. In the Archean rocks that make up most of the area the structural pattern outlines the transposition of complex curvilinear structures to a straight zone more than 100 km wide that forms an open arc convex to the northwest. Narrow belts of lower and middle amphibolite facies rocks are surrounded by extensive terranes of upper amphibolite facies migmatites and granulites. While variations in the metamorphic gradient are mostly continuous in the northwest, structural discontinuities may have juxtaposed relatively low and high grade rocks in the southeast half of the area. The early Proterozoic clastics and carbonate of the Goulburn Group, which unconformably overlie the Archean, have been metamorphosed and variably deformed near Bathurst Inlet and, farther east, tectonically interlayered with the basement by an event that probably predates the Bathurst Fault.

Résumé

La région cartographique de Tinney Hills-Overby Lake (moitié ouest) est la deuxième région à être portée sur carte à 1/250 000 dans la cadre d'un projet destiné à fournir une meilleure connaissance de l'âge, de l'importance et de l'origine d'un élément principal de la partie nord-ouest du Bouclier canadien, soit la limite entre les provinces tectoniques des Esclaves et de Churchill. La région portée sur carte couvre 2 500 km². Dans les roches archéennes qui forment presque toute la région, la configuration structurale trace la transposition de structures curvilignes complexes en une zone rectiligne de plus de 100 km de large ayant l'aspect d'un arc ouvert à convexité tournée vers le nord-ouest. Des zones étroites de roches des parties inférieure et moyenne du faciès des amphibolites sont entourées de vastes terrains de migmatites et de granulites de la partie supérieure du faciès des amphibolites. Bien que les variations du gradient métamorphique soient presque partout continues dans le nord-ouest, des discontinuités structurales pourraient avoir juxtaposé des roches fortement et faiblement métamorphisées dans la partie sud-est de la région. Les sédiments clastiques et la roche carbonatée du Protérozoïque ancien du groupe de Goulburn, qui reposent en discordance sur l'Archéen, ont été métamorphisés et variablement déformés près de l'inlet Bathurst; plus à l'est, ils ont été structuralement interstratifiés avec le socle lors d'un événement survenu vraisemblablement avant la formation de la faille de Bathurst.

INTRODUCTION

This preliminary report summarizes the observations made during the first of three seasons of field work proposed to map the Archean rocks and parts of the adjacent Proterozoic Goulburn Group in the Tinney Hills map area (NTS 76 J) and the west half of the Overby Lake map area (76 I) east of Bathurst Inlet (Fig. 55.1). This project is part of a continuing operation involving 1:250 000 scale bedrock mapping directed toward determining the age, origin and significance of a major feature of the northwest Precambrian Shield, the boundary between the Slave Structural Province and the Queen Maud block of the Churchill Province. On the basis of mapping of the Healey Lake area (Fig. 55.1) (Henderson, 1979; Henderson and Thompson, 1980, 1981, 1982; Henderson et al., 1982; Thompson and Henderson, 1983), 1:1 000 000 scale coloured aeromagnetic anomaly maps (Geological Survey of Canada, 1981a,b, 1982), and recent unpublished compilations of the lithology and structure of the area bounded by 62° and 68°30'N and 102° and 112°W, it is possible to tentatively outline the Thelon Tectonic Zone, a structure 50 to 100 km wide and more than 800 km long that is present along the eastern border of the Slave Province. The zone is characterized by distinctive but varied geological, geophysical and topographic features. Evidence from the Healey map area is the basis for the hypothesis that the zone is of Archean age with major tectonic events 2600 Ma ago and subsequent reactivation during the Proterozoic that may have involved major crustal thrusting toward the west. The absence north of the Bathurst Fault of the prominent paired gravity anomaly that coincides approximately with the west boundary of the zone to the south together with changes in texture and magnitude on the aeromagnetic anomaly map suggest the zone may be somewhat different in the northern segment. A major objective of this project is to test these hypotheses in the course of mapping the entire area for the first time at 1:250 000 scale and specific subareas, at 1:50 000.

GENERAL GEOLOGY

The Tinney Hills-Overby Lake (W½) area was mapped for the first time by J.A. Fraser (1964) during Operation Bathurst, a helicopter reconnaissance project that completed 153 000 km² in one season. The resulting 1:506 880 scale map outlines zones of metasedimentary rock and amphibolite correlated with the Archean Yellowknife Supergroup, an extensive terrane of heterogerous gneiss, migmatite, and granulite derived in part from the Yellowknife Supergroup,

[1] Department of Geology, Queen's University, Kingston, Ontario K7L 3N6

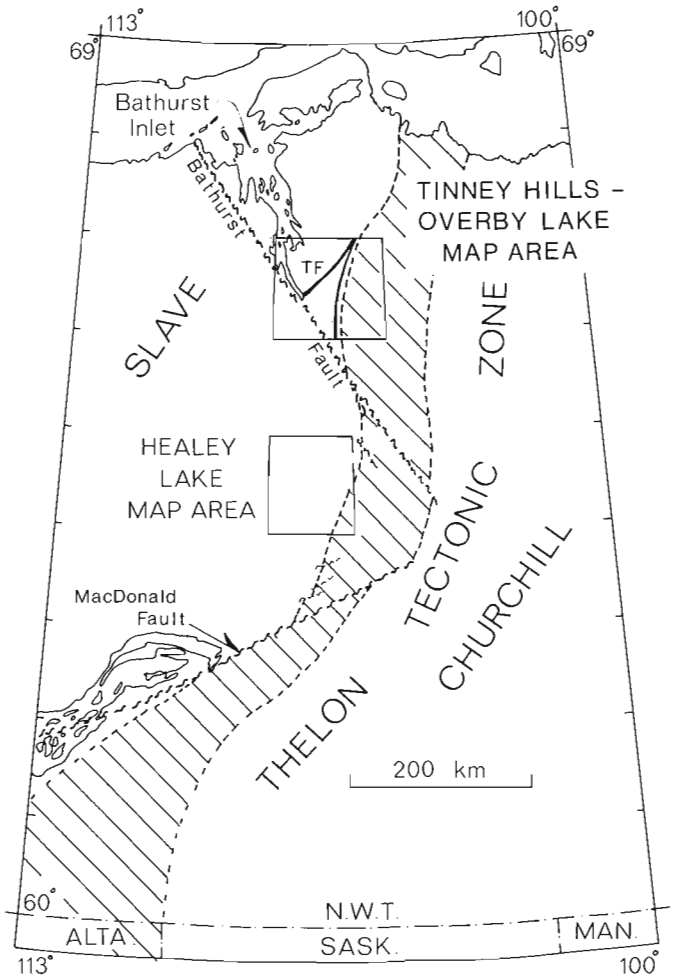

Figure 55.1. *Location map. The width of the tentative outline of the Thelon Tectonic Zone south of MacDonald Fault is an indication of the uncertainty in its position there. The heavy line inside the Tinney Hills-Overby Lake map area indicates the position of the Thelon Front according to Stockwell (1969, convex to the northwest) and Stockwell (1982, convex to the southeast).*

and a few relatively homogeneous plutonic masses. Several mylonite zones were noted east of 106°W. In the western third of the area, the early Proterozoic Goulburn Group, composed of clastic and carbonate sedimentary rocks, unconformably overlies the Archean and is cut by the major north-northwest oriented Bathurst Fault system. An outlier of closely folded quartzite and dolomite 30 km east of Bathurst Inlet was correlated with the lower part of the Goulburn Group. On the basis of this work Fraser, (1964, 1968) suggested the position of the Thelon Front, the boundary between the Slave and Churchill Provinces, should be changed from along the Bathurst Inlet (Stockwell, 1961) to form a curve convex to the southeast (Fig. 55.1) that intersected the south end of Bathurst Inlet (Stockwell, 1969). Fraser (1968) described briefly the changes across this line 50 to 60 km east of the Inlet. The tentative western boundary of the Thelon Tectonic Zone (Fig. 55.1) parallels closely the most recently revised position of the Thelon Front (Stockwell, 1982). According to regional syntheses of the western Churchill Province (Fraser, 1978) and Slave Province (Thompson, 1978) the main metamorphism in the map area is late Archean but Fraser noted evidence of Proterozoic retrogression and suggested granulite assemblages may predate the late Archean metamorphism. Campbell and Cecile (1975, 1976a,b) mapped the intracratonic Kilohigok Basin, the eastern margin of which is in the map area, and interpreted the tectonic and depositional history of the Goulburn Group within the Basin (Campbell and Cecile, 1981). A reconnaissance study of illite crystallinity in the Goulburn Group (Thompson and Frey, 1984) indicates this cover sequence has been regionally metamorphosed under conditions characteristic of the upper anchizone and lower greenschist facies.

LITHOLOGY

Goulburn Group

Mapping of Goulburn Group was limited this year to a small part of the basal Western River Formation in the main outcrop area east of Bathurst Inlet at Kenyon Lake and the narrow belt of metamorphosed dolomite, quartzite, and phyllite/metasiltstone 20 km to the northeast (Fig. 55.2) that was tentatively correlated with the Western River Formation by Fraser (1968). Fifty kilometres south of this belt, two other narrow belts with the same lithology were found (II and III, Fig. 55.2). Where the Western River Formation overlies the Archean knotted schist and leucogranitoid at Kenyon Lake, it consists of a basal quartz pebble conglomerate, overlain by quartzite, a rusty weathering clastic meta-carbonate, and meta-siltstone/slate (Campbell and Cecile, 1976b, 1981). Thick beige-weathering carbonate units occur farther west. This stratigraphy was traced continuously around several kilometre-scale folds involving basement and cover and along the unconformity to the north for more than 10 km. The pelitic rocks are well-recrystallized phyllites or slates that commonly exhibit two cleavages and, locally, more than one phase of minor folds. Biotite is absent but illite "crystallinity" measurements indicate upper anchizone/lower greenschist facies conditions have affected these rocks (Thompson and Frey, 1984). Except for the conglomerate, which is absent, the same lithologies are tightly folded and metamorphosed to a somewhat higher degree in narrow belts to the northeast and southeast (Fig. 55.2). The outliers dip moderately to steeply beneath knotted schist and/or leucogranitoid of the Archean basement. Where observed contacts are sharp and basement rocks and Goulburn Group are sheared. Quartzite, carbonate and pelite present in outliers I and III are upside down under the adjacent basement along the southeast contact. Where the southeast contact of outlier II was observed quartzite was not present. In outlier III where both contacts are exposed at one locality, the stratigraphy was not repeated and the slate/phyllite unit was on top of the leucogranitoid along the northwest contact. The similarity of the lithology and stratigraphy in outliers II and III to that in outlier I which has been correlated with the Western River Formation is the basis for correlation of outliers II and III with the basal formation of the Goulburn Group. The structural data indicates tectonic interlayering of basement and cover has occurred.

Two mica leucogranitoid

Plutonic rocks make up a relatively small part of the area mapped to date. White-weathering muscovite-biotite granodiorite occurs mainly as small bodies from several metres to several kilometres across in the sillimanite zone and in the vicinity of the migmatite isograd. They are much less common at both higher and lower grades and are absent from the pink gneiss/migmatite/granitoid unit. Small tabular bodies in the heterogeneous gneiss unit may be correlative. Most of the plutons are weakly to moderately foliated; foliations in the country rock tend to wrap around the plutons.

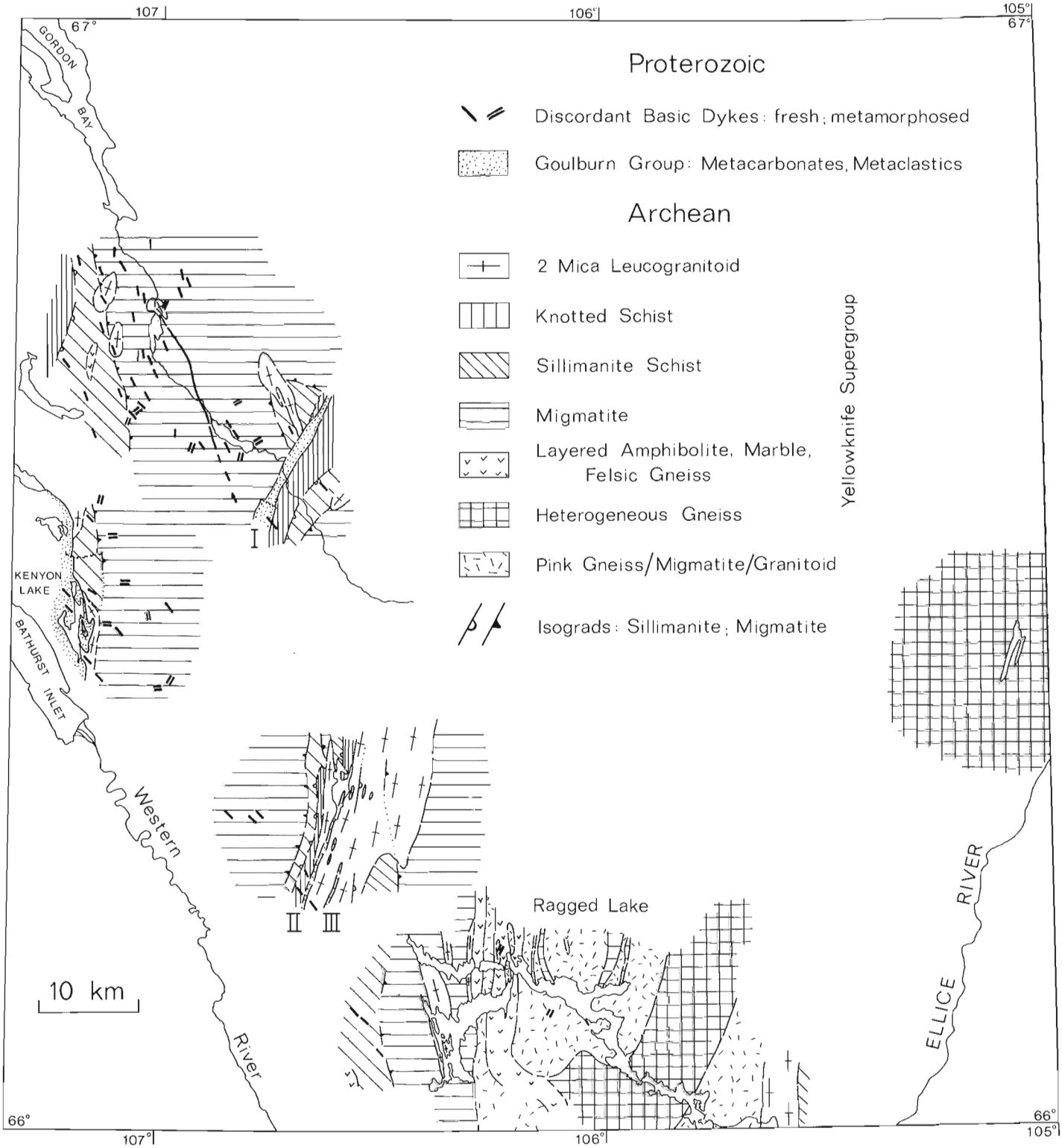

Figure 55.2. *Geology of parts of the Tinney Hills-Overby Lake map area. Roman numerals refer to outlines of Goulburn Group.*

As with the smaller bodies, the large pluton 30 km northwest of Ragged Lake contains numerous metasedimentary inclusions. This pluton is transformed to a striking reddish pink near the numerous metamorphosed gabbro/diorite sill or dykes that are present in the central part of the body. Muscovite-rich white pegmatite-leucogranitoid is more abundant in the migmatite zone west of Ragged Lake than it is in migmatites to the northwest, but individual masses are too small to show on Figure 55.2. The granodioritic body associated with the relatively low grade metasediments east of Ragged Lake contains less muscovite and is coarser grained then the plutons to the west and it has a pronounced augen texture where it is strongly deformed. Although the leucogranitoid plutons are intrusive at the present level of exposure, the abundance of muscovite and metasedimentary inclusions, the sporadic presence of garnet and the spatial relation to the sillimanite zone and migmatite isograd suggest the granitoids are derived from the Yellowknife Supergroup metasedimentary rocks at depth during the regional metamorphic event and were intruded syntectonically to their present level.

Knotted schist, sillimanite schist and migmatite

Brown to grey-brown weathering, biotite-rich, cordierite-andalusite knotted schist, with or without staurolite, typical of the Yellowknife Supergroup throughout the Slave Province are present southwest of Gordon Bay and as narrow belts near Goulburn Group outlier I and II (Fig. 55.2). Commonly bedding/schistosity relationships are preserved and graded bedding, sometimes reversed by metamorphic recrystallization, allows top determinations to be made. Retrogression of cordierite to greenish pinitic pseudomorphs and andalusite to white mica has taken place locally. With the appearance of sillimanite in knotted schist staurolite is less common and compositional layering is less readily identifiable as bedding as the rocks develop a gneissic character. Small masses (decametre to kilometre scale) of previously described leucocratic biotite-muscovite graniodiorite and pegmatite are common in the sillimanite zone.

With increasing metamorphic grade there is a transition to migmatite with schistose to gneissic rocks containing millimetre to centimetre scale lenses and layers of relatively coarse grained leucocratic quartz and feldspar with or without muscovite separated by mafic zones rich in biotite and sillimanite. Cordierite, much of it pinitized, occurs in both leucosome and melanosome/paleosome of the migmatite. Garnet is irregular in its occurrence. Where present it is often rimmed by greenish chloritic material that looks like pinitized cordierite. Potassium feldspar is also present, in many of these rocks. The terminology of Brown (1973) whereby migmatites with layering preserved, albeit contorted and discontinuous, are labelled metatexite and more homogeneous migmatite further on the way to becoming a plutonic rock is referred to as diatexite was found to be very useful in this area. Generally, immediately upgrade of the migmatite isograd, a line marking the appearance of >5-10 per cent leucosome, metatexite predominates but, within a kilometre or more, irregular zones of diatexite appear. The migmatite zone west of Ragged Lake differs from the rocks described above in that while cordierite is not present, garnet, kyanite and staurolite do occur locally, the rocks are more strongly layered, and leucogranitoid/pegmatite is prominent. The metatexite/diatexite rocks are locally strongly retrograded to chlorite white mica semi-schistose rocks. East of Kenyon Lake, an area of several hundred square kilometres has been altered in this way but the original texture and grade of the rock is evident from the weathered surfaces.

Layered amphibolite – marble – felsic gneiss

Aside from the belt near Ragged Lake, the association of fine grained layered amphibolite, marble, and felsic gneiss with subordinate fine grained metadiorite gabbro that is interpreted to be metamorphosed volcanic rocks of the Yellowknife Supergroup and associated sediments and dykes or sills is limited to three small zones, one south of Gordon Bay, one southwest of Ragged Lake and the other just north of the lake (Fig. 55.2). Zones too small to distinguish on the map are present in the metasediments east of the southwestern locality. Amphibolite, the predominant lithology, is extremely variable, occurring as fine grained massive layers, foliated masses, finely laminated amphibolite gneiss and metamorphosed breccia of amphibolite fragments in a carbonate matrix. Felsic gneiss is a fine grained to aphanitic, biotite-bearing, and tough rock. Both calcareous and dolomitic marble, locally with tremolite-actinolite occur as lenses and pods or forming the matrix of a foliated breccia. Pyritic layers with rusty weathered surfaces occur within the sequence.

Heterogeneous gneiss

The heterogeneous gneiss unit is a complex of felsic and mafic orthopyroxene granulites, mafic garnet-clinopyroxene-hornblende gneiss and migmatite, sillimanite-garnet migmatite, leucocratic garnet granodiorite, pink augen granite, and pink gneiss/migmatite/granitoid that were not subdivided. These lithologies are interlayered and interfinger at a variety of scales ranging from metres to kilometres although, in some cases, specific lithologies a few hundred metres thick may persist along strike for more than 10 km. Rusty gneiss and migmatite underlie gossans that were traced for more than 20 km along the west shore of the lake at the eastern edge of the map. Retrogression of pyroxene to amphibole and/or biotite is widespread. At the east end of Ragged Lake the heterogeneous gneiss unit is distinct from the pink gneiss/migmatite/granitoid (described below) to east and west but further mapping is required to determine if the contact with the layered amphibolite-marble-felsic gneiss unit (metavolcanic rocks of the Yellowknife Supergroup) is separating two rock units or if it is a metamorphic transformation to granulite facies. The lithologic heterogeneity of the unit together with the presence, though relatively rare, of leucogranitoid and aluminous rocks such as sillimanite-garnet migmatite suggests the unit may be in large part a supracrustal sequence but whether it is a higher grade equivalent to the Yellowknife Supergroup rocks to the west or a supracrustal component of the basement to the Yellowknife rocks remains to be seen.

Pink gneiss/migmatite/granitoid

This rock is as "homogeneous in its heterogeneity" as the rock unit considered to be basement to the Yellowknife Supergroup in the Healey Lake map area (Henderson and Thompson, 1981, 1982). The heterogeneity differs from that of the preceding unit in that the variation is mainly textural rather than mineralogical/lithological and it occurs on a smaller scale. There is a distinctive smooth, rounded, grey-pink weathered surface on outcrops that vary from granitoid to migmatite to pegmatite to gneiss within a few metres. This kind of small-scale variability is seen across distances measured in kilometres. The proportions of biotite and/or hornblende, quartz, plagioclase, and K-feldspar are never constant but the mineralogy is always the same. This unit differs from nearby supracrustal rocks in that garnet, muscovite, and aluminosilicate are absent and K-feldspar is abundant. Complex folding with axial planes parallel to the

principal foliation or layering in the rock is common. Fold hinge lines are variable. The unit is often a protomylonite with very straight, thin gneissic layering. Within the unit mapped as heterogeneous gneiss, layers or lenses of the pink gneiss/migmatite/gneiss unit occur that typically contain orthopyroxene. These are all characteristics of the basement unit in the Healey Lake area. Furthermore, a belt of metavolcanic rocks (layered amphibolite-marble-felsic gneiss) occurs between the pink gneiss/migmatite/granitoid and metasedimentary migmatites to the west (Fig. 55.2). In the Healey Lake area metavolcanic sequences commonly separate metasedimentary rocks from the basement. As the structure, mineralogy, textural variability and geological context are essentially the same as those of the probable basement unit in the Healey Lake area the pink gneiss/migmatite/granitoid is tentatively interpreted to be basement to the Yellowknife Supergroup in the Tinney Hills-Overby Lake area.

Discordant basic dykes

Northwest to north-northwest oriented diabase and gabbro dykes of the Mackenzie swarm are common in the western half of the area. Variably metamorphosed dykes or segments of dykes with attitudes ranging from north-south through 030° to 060° were observed in the northwest part of the area. Two metamorphosed dykes near Ragged Lake crosscut the fabric in the gneisses but are themselves foliated. Only these two dykes have been transformed to amphibolite, the rest are relatively low grade metadiabase.

STRUCTURAL GEOLOGY

With twenty-five per cent of the area mapped, the structural data reveal isolated segments of a long and complex tectonic history. A summary of observations is presented here along with some tentative generalizations. Detailed explanation and interpretation will follow when the mapping is further advanced. In general, the narrow belts of low grade Goulburn rocks provide a marker that separates late Archean ductile deformation that is post-Yellowknife Supergroup – pre-Goulburn Group from a post-Goulburn event. Structures in the pink gneiss/migmatite/granitoid unit unequivocally older than the Yellowknife Supergroup have not been observed. If further work confirms that folding and cleavage development in the Goulburn Group predates the Bathurst Fault system the strike slip faulting may be a later, unrelated, more brittle deformation that took place at relatively high levels in the crust.

Across the area in Archean rocks (Fig. 55.3) the principal foliation, commonly oblique to bedding at medium grade and parallel to compositional layering at high grades of metamorphism, outlines an irregular curvilinear pattern of kilometre scale folds separated by zones within which the foliations are relatively straight. The degree of "straightening" and of development of a north-northeast preferred orientation appear to increase eastward, particularly in the gneiss/granulite terrane east of Ragged Lake. The impression the map gives is one of a complexly folded, mainly high grade terrane in the process of transposition into a straight zone with the older complexities still preserved between narrow zones that parallel the new orientation. The transition across the area is complicated by the change from dominantly mica-rich metasedimentary rock west of 106°15'W to dominantly quartzofeldspathic gneisses and granulites to the east.

Over most of the area mineral lineations and fold hingelines are variable but these features define a strong preferred south-plunging orientation southwest of Ragged Lake. In the northwest part of the area most lineations plunge moderately northwest.

Mylonite zones are limited to the area dominated by quartzofeldspathic gneisses and granulites that lies east of the western contact of the pink gneiss/migmatite/granitoid (Fig. 55.2, 55.3). Ranging in thickness from several metres to tens of metres and, in one case up to two kilometres, some zones parallel prominent north-northwest or north-northeast lineaments while others are folded with the principal foliation. At the east edge of the map area, gently west-dipping granulites and migmatites with mylonitic fabrics are cut by steeply dipping north-northeast-oriented mylonites. Ten kilometres to the west of this zone, a zone of steep mylonites 2-3 km wide appears to downgrade the granulites and produce abundant biotite. Lineations in steep mylonites across the area plunge southward. The age of the folded and gently dipping mylonites is probably Archean because they are part of the fabric of the rock which has formed during the main Archean metamorphism but the steep zones may be Archean, Proterozoic or both. Within the map area the north-northeast trend is straight but on a broader scale the mylonites may be following the open curve convex to the northwest that corresponds approximately with the western boundary of the Thelon Tectonic Zone (Fig. 55.1).

Small (cm) scale sinistral ductile shear zones (Fig. 55.3) associated with pegmatoid segregations are also limited to the eastern part of the area. The migmatitic appearance of these features and the apparently low ductility of adjacent gneiss are compatible with formation under peak metamorphic conditions but they may have formed during the influx of water associated with amphibolite facies retrogression of the granulites. The orientation and mainly sinistral sense of shear of these features is not appropriate for them to be related to the steep mylonite belts nearby.

In the outliers of Goulburn Group, the northeast-southwest-oriented, moderately-to steeply-dipping principal foliation parallels approximately the same feature in underlying and overlying basement rocks. Formation of the foliation is thought to be related to an event involving tectonic stacking and interlayering of basement and cover. Minor folds of bedding and or foliation commonly do not show any symmetry with respect to contacts of the belt that would indicate a syncline was present. In the case of outlier II and III (Fig. 55.3) the minor folds point to the entire belt being on one limb of a larger structure. At this point, minor folds of the principal foliation cannot be related to a larger scale structural context but the metamorphic grade of the belts, the intensity of the deformation, and their distance from the Bathurst Fault indicate that the deformation is not related to the fault system, but, in fact, predates the strikeslip movement. The similarity in structural style, degree of involvement of the basement, intensity of deformation, in the Goulburn Group at Kenyon Lake and in the outliers, suggest much of the deformation at Kenyon Lake may also predate the fault.

METAMORPHISM

Although the main metamorphism in the Tinney Hills-Overby Lake area is considered to be Archean (Fraser, 1978) there is evidence of a Proterozoic metamorphic overprint. A number of north and northeast oriented basic dykes that intrude the Archean have been altered and recrystallized. Tremolite, talc and biotite were found in outliers of Goulburn Group and illite "crystallinities" characteristic of the upper anchizone and lower greenschist facies (Thompson and Frey, 1984) occur in the outliers and in the main sequence of Goulburn Group at Kenyon Lake. In addition, early and middle Proterozoic K-Ar cooling ages were obtained from biotite and muscovite (Fraser, 1964) in Archean rocks. This is the only clearcut evidence for Proterozoic metamorphism; the retrogression of high grade Archean rocks observed in the field could have

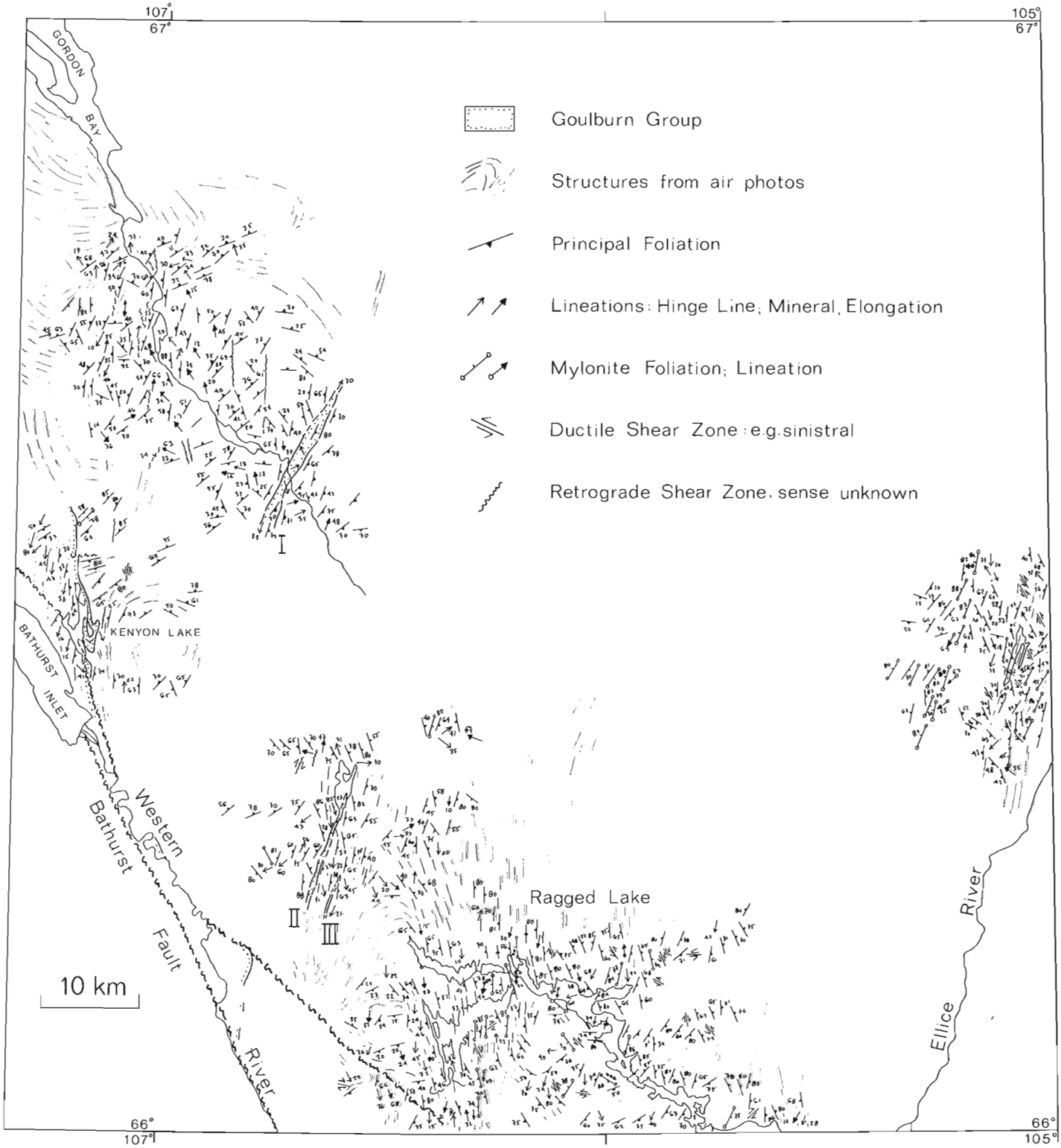

Figure 55.3. *Structural trends in parts of the Tinney Hills map area. Roman numerals refer to outliers of Goulburn Group.*

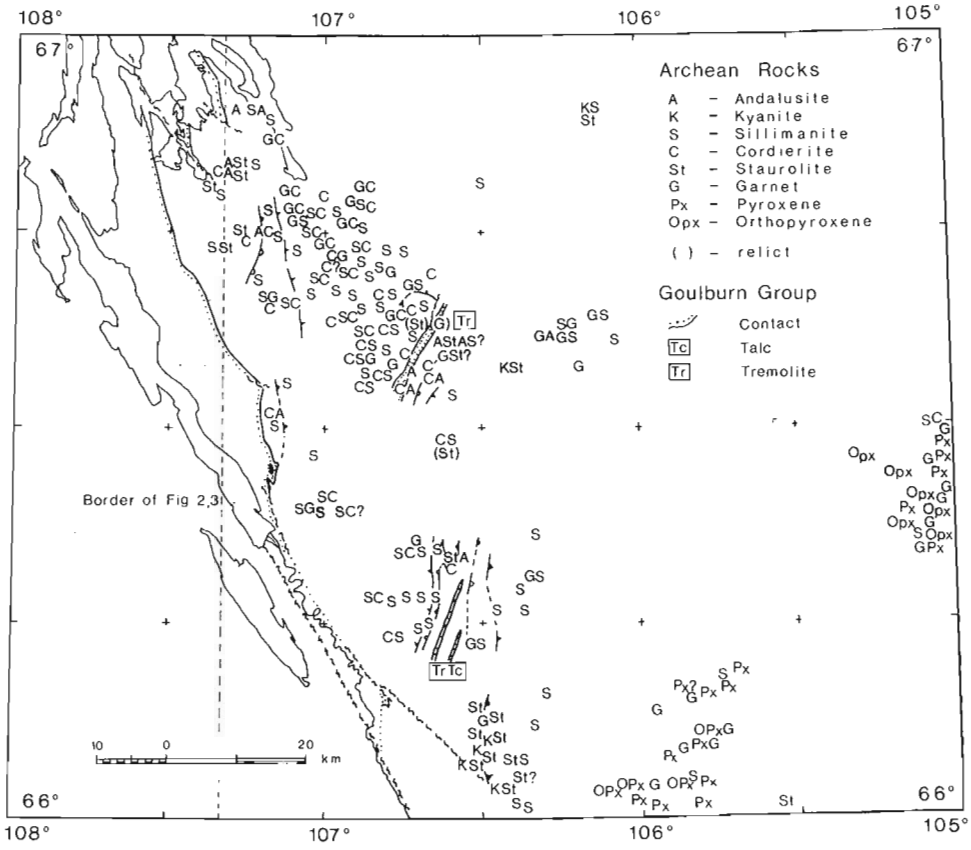

Figure 55.4

Compilation of mineral occurrences based on field observations in 1983 and petrography of samples collected by J.A. Fraser and used for regional syntheser of metamorphism (Fraser, 1978; Thompson, 1978). Although most of these minerals are considered to have formed in the late Archean, orthopyroxene may be older.

occurred during cooling after the main Archean metamorphism. In the Healey Lake area (Fig. 55.1) the grade of the Proterozoic metamorphic overprint increases eastward. As the grade of the Goulburn Group outliers is higher (tremolite-talc) than that at Kenyon Lake (Fig. 55.2), a similar gradient may be present that can be verified by detailed petrography.

A striking aspect of the Archean rocks in the area is the predominance of high grade rocks (Fig. 55.2, 55.4). Sub-sillimanite zone knotted schists are limited to narrow zones south-southwest and southeast of Gordon Bay and 40 km northwest of Ragged Lake (Fig. 55.2). The presence of cordierite and andalusite in these rocks (Fig. 55.4) indicates the metamorphism is of the low pressure type that occurs everywhere in the Slave Province (Thompson, 1978). The abundance of staurolite suggests relatively iron-rich compositions. The transition though the sillimanite zone to cordierite-sillimanite-biotite migmatites with and without K-feldspar and garnet is typical for low pressure metamorphism. The hundreds of square kilometres underlain by metatexite and diatexite of constant mineralogy is suggestive of a large volume of rock with a limited range of composition. The zone of migmatite west of Ragged Lake differs from migmatites to the northwest and west in the strongly layered and foliated character of the migmatite, the absence of cordierite, and the presence of garnet, kyanite and staurolite (to the southwest), and concordant layers and lenses of garnet amphibolite. Fraser (1968) described similar rocks 20 km east of the northern Goulburn outlier (Fig. 55.4). These rocks are similar to the kyanite-bearing migmatites in the eastern part of the Healey Lake area. Farther east, the retrograded and deformed metasediments north of Ragged Lake have been tentatively grouped with the migmatite unit. Sillimanite and garnet are present. Pelitic migmatitic rocks containing sillimanite are present in the heterogeneous gneiss unit at several localities east of Ragged Lake. An assemblage of sillimanite, garnet, cordierite, and green spinel occurrs near the east edge of the area.

Kyanite appears to occur within a narrow zone between sillimanite-bearing rocks (Fig. 55.4). If future work confirms the indication that kyanite is limited to a narrow curving zone convex to the northwest, it will define another boundary to compare with the geophysical features associated with the Thelon Tectonic Zone. In any case, although there are several possible ways of obtaining kyanite in a low pressure metamorphic terrane (Henderson and Thompson, 1980) all require that the kyanite-bearing rocks be more deeply eroded than associated contemporaneous cordierite andalusite schists. The absence of cordierite for some distance east of the kyanite localities west of Ragged Lake and the locality 60 km to the north (Fig. 55.4) may mean the appearance of Kyanite indicates a discontinuous increase in metamorphic pressure. Detailed petrography and further mapping should resolve these problems.

Retrogression of the granulites to form biotite and hornblende adds considerable complication but the presence of sillimanite locally and orthopyroxene apparently stable with plagioclase suggest the granulites are intermediate to low pressure rather than high pressure. Garnet is commonly absent from pyroxene-bearing rocks. The high grade rocks are not continuous across to the east border of the area. East of the orthopyroxene-bearing gneisses and migmatites in the heterogeneous gneiss unit, biotite- and hornblende-bearing pink gneiss/migmatite/granitoid, thin-layered gneisses and leucocratic biotite granodiorite occur (Fig. 55.2, 55.4). The chlorite-biotite-garnet schist containing relict staurolite and pseudomorphs after sillimanite that crops out east of the granitoid is the most convincing evidence of that some of these rocks never reached granulite grade.

The presence of narrow zones of relatively low grade rocks in a sea of high grade migmatite and/or granulite is characteristic of this map area. It is not known if all the variations in metamorphic grade are continuous as they are, for the most part, in the northwestern half of or if they represent structural discontinuities.

ECONOMIC MINERALS

Small gossans, 2 to 3 m by 1 m or less are scattered through the biotite-sillimanite-cordierite metatexilte and diatexite south of Gordon Bay. Commonly they are rich in amphibole, contain pyrite/pyrrhotite and rimmed by a reaction zone rich in biotite/chlorite and garnet. The same sulphides were disseminated through the gneisses and migmatites that form gossan zones 2-15 km long parallel to the west shore of the lake on the east edge of the area (Fig. 55.2) and 10 km west of the south end of the lake.

One occurrence of malachite stain was observed in the metasiltstone unit north of the granitoid/Goulburn Group contact on the east shore at the south end of the lake (UTM Zone 13W-40277701).

THELON TECTONIC ZONE

The western boundary of the Thelon Tectonic Zone corresponds with a dramatic change in the aeromagnetic anomaly map that, in the Healey Lake area (Fig. 55.1), marks approximately the western border of a straight zone of strongly mylonitized high grade Yellowknife Supergroup rocks, pink basement gneiss/migmatite, and the appearance of granulites (orthopyroxene). Kyanite-bearing migmatites occur within and immediately west of the straight zone. A similar association occurs within that part of the Tinney Hills-Overby Lake area mapped to date. The change in the aeromagnetic anomaly map from relatively low featureless topography to a prominent zone of highly variable and rugged relief occurs near of the western border of the area dominated by granulites, mylonites and quartzofeldspathic gneisses that are probably both basement to and derived from the Yellowknife Supergroup. What may be a narrow zone of kyanite-bearing rocks occurs 10 km to the west. Although the spectacular paired gravity anomaly that is associated with the western boundary of the Thelon Tectonic Zone south of the Bathurst Fault (Fig. 55.1) is not present here, the gravity anomalies in the east half of the area have a linear trend. Mapping farther eastward into the Thelon Tectonic Zone than was possible in the Healey Lake area has shown that the Archean metamorphic gradient decreases and then increases again in a way that may be due to as yet unmapped faults or ductile shear zones and that, either the granulites of the heterogeneous gneiss unit are highgrade Yellowknife Supergroup or there is a supracrustal component to the pre-Yellowknife Supergroup basement unit. Future mapping, structural studies, petrography, and geochronology will explore the extent to which these changes can be related to Archean and Proterozoic tectonic events.

ACKNOWLEDGMENTS

We would like to acknowledge the innovative, enthusiastic and hard working assistance provided by Randy Buchanan, Jim Shaver and Wanda Sheldrick. First class expediting was provided by Wynn Bowler and Martin Irving under the auspices of Bill Padgham, Chief Geologist, Department of Indian Affairs and Northern Development in Yellowknife. Ptarmigan Airways provided excellent fixed wing support. Critical reviews by John B. Henderson and John C. McGlynn were much appreciated.

REFERENCES

Brown, M.
1973: The definition of metatexis, diatexis, and migmatite; Proceedings of the Geological Association, v. 84, p. 371-382.

Campbell, F.H.A. and Cecile, M.P.
1975: Report on the geology of the Kilohigok Basin, Goulburn Group, Bathurst Inlet, N.W.T.; in Report of Activities, Part A, Geological Survey of Canada, Paper 75-1A, p. 297-306.

1976a: Geology of the Kilokigok Basin, Goulburn Group, Bathurst Inlet, N.W.T.; in Report of Activities, Part A, Geological Survey of Canada, Paper 76-1A, p. 369-378.

1976b: Geology of the Kilohigok Basin, Geological Survey of Canada, Open File Map 332, 1:500 000 scale.

1981: Evolution of the early Proterozoic Kilohigok Basin, Bathurst Inlet – Victoria Island, Northwest Territories; in Proterozoic Basins of Canada, ed. F.H.A. Campbell, Geological Survey of Canada, Paper 81-10, p. 103-131.

Fraser, J.A.
1964: Geological notes on northeastern District of Mackenzie, Northwest Territories (Report and Map 45-1963); Geological Survey of Canada, Paper 63-40, 16 p.

1968: Geology across Thelon Front, District of Mackenzie (76I, J); in Report of Activities, Part A, Geological Survey of Canada, Paper 68-1A, p. 134.

1978: Metamorphism in the Churchill Province, District of Mackenzie; in Metamorphism in the Canadian Shield, ed. J.A. Fraser and W.W. Heywood, Geological Survey of Canada, Paper 78-10, p. 195-202.

Geological Survey of Canada
1981a: Magnetic anomaly map of Lockhart River, N.W.T., NP12/13 (1:1 000 000); Geological Survey of Canada, Map 1566A.

1981b: Magnetic anomaly map of Dubawnt River, N.W.T., NP13/14 (1:1 000 000); Geological Survey of Canada, Map 1567A.

1982: Magnetic anomaly map Thelon River, NQ-12-13-14-AM (1:1 000 000); Geological Survey of Canada, Map NQ-12-13-14-AM.

Henderson, J.B.
1979: Healey Lake map area, District of Mackenzie; in Current Research, Part A, Geological Survey of Canada, Paper 79-1A, p. 400.

Henderson, J.B. and Thompson, P.H.
1980: The Healey Lake map area (northern part) and the enigmatic Thelon Front, District of Mackenzie; in Current Research, Part A, Geological Survey of Canada, Paper 80-1A, p. 165-169.

1981: The Healey Lake map area and the enigmatic Thelon Front, District of Mackenzie; in Current Research, Part A, Geological Survey of Canada, Paper 81-1A, p. 175-180.

1982: Geology of Healey Lake map area (1:125 000 scale map and marginal notes); Geological Survey of Canada Open File 860.

Henderson, J.B., Thompson, P.H., and James, D.T.
1982: The Healey Lake map area and the Thelon Front problem, District of Mackenzie; in Current Research, Part A, Paper 82-1A, p. 191-195.

Stockwell, C.H.
1961: Structural provinces, orogenies, and time classification of rocks of the Canadian Precambrian Shield; in Age determinations by the Geological Survey of Canada (compiled by J.A. Lowdon) Report 2, Isotope Ages; Geological Survey of Canada, Paper 61-17.

1969: Tectonic map of Canada (1:5 000 000); Geological Survey of Canada, Map 1251A.

1982: Proposals for time classification and correlation of Precambrian rocks and events in Canada and adjacent areas of the Canadian Shield Part I: A time classification of Precambrian rocks and events; Geological Survey of Canada, Paper 80-19, 135 p.

Thompson, P. H.
1978: Archean regional metamorphism in the Slave Province – A new perspective on some old rocks; in Metamorphism of the Canadian Shield, ed. J.A. Fraser and W.W. Heywood, Geological Survey of Canada, Paper 70-10.

Thompson, P.H. and Frey, M.
1984: Illite "crystallinity" in the Western River Formation and its significance regarding regional metamorphism of the early Proterozoic Goulburn Group, Northwestern Canadian Shield; in Current Research, Part A, Geological Survey of Canada, Paper 84-1A, Report 54.

Thompson, P.H. and Henderson, J.B.
1983: Polymetamorphism in the Healey Lake map area – implications for the Thelon Tectonic Zone; in Current Activities Forum 1983 Program with Abstracts, Geological Survey of Canada, Paper 83-8, p. 2.

56. STRUCTURE AND STRATIGRAPHY OF THE LATE PROTEROZOIC MIETTE GROUP, CUSHING CREEK AREA, ROCKY MOUNTAINS, BRITISH COLUMBIA

Project 810010
Contract 0SGB83-00034

A. Carey[1] and P.S. Simony[1]
Institute of Sedimentary and Petroleum Geology

Carey, A. and Simony, P.S., Structure and stratigraphy of the Late Proterozoic Miette Group, Cushing Creek area, Rocky Mountains, British Columbia; in Current Research, Part A, Geological Survey of Canada, Paper 84-1A, p. 425-428, 1984.

Abstract

The Late Proterozoic Miette Group comprises three units in the Rocky Mountains near McBride, British Columbia. Black slate, dark grey limestone and calcareous grits characterize the lower Miette, which is greater than 380 m thick. The 2870 m thick middle Miette is made up of interlayered sandstone to grit units and slate units. Slates dominate the upper Miette, which has an estimated thickness of 1800 m. The Miette Group is disconformably overlain by lower Cambrian quartzites. Middle and upper Miette strata form a homocline on the west limb of a major anticline which is cored by complexly deformed lower Miette strata. A penetrative slaty cleavage parallels minor folds. Two distinct crenulation cleavage sets are locally developed.

Résumé

Le groupe de Miette du Protérozoïque récent comprend trois unités dans les Rocheuses près de McBride, en Colombie-Britannique. L'unité inférieure, qui a plus de 380 m d'épaisseur, comprend du schiste ardoisier noir, du calcaire gris foncé et des grès calcaires grossiers. L'unité intermédiaire, d'une épaisseur de 2 870 m, se compose de couches interstratifiées de grès dont la texture varie de moyenne à grossière, et de schistes ardoisiers. Les schistes ardoisiers dominent dans l'unité supérieure, dont on a estimé l'épaisseur à 1 800 m. Des quartzites du Cambrien inférieur reposent en discordance sur le groupe de Miette. Les couches des unités intermédiaire et supérieure de ce dernier forment une structure monoclinale sur le flanc ouest d'un anticlinal important dont le noyau se compose de couches très déformées de l'unité inférieure du groupe de Miette. Un clivage ardoisier pénétrant longe les plis mineurs. Deux ensembles distincts de clivage crénelé ont été formés par endroits.

INTRODUCTION

During regional reconnaissance mapping in the McBride area of the Rocky Mountains, Campbell et al. (1973) recognized three units in the Late Proterozoic Miette Group. Middle and upper Miette strata are exposed over large areas of the McBride and Mount Robson map areas, but exposures of lower Miette strata are recognized only on the east flank of the Mount Robson synclinorium, adjacent to Cushing Creek. Stratigraphy of the lower Miette was poorly known, as were thicknesses for lower and middle Miette units.

The Cushing Creek area, north of McBride, British Columbia, was mapped at 1:25 000 scale during the 1983 field season (Fig. 56.1, 56.2). Unfaulted lower Miette through Cambrian strata are well exposed in this area. A complete stratigraphic section through the middle Miette was measured, and thicknesses of lower Miette (base not exposed) and upper Miette strata have been estimated. A structural cross-section (Fig. 56.3) through the study area illustrates the structural styles of the various units.

STRATIGRAPHY

The three units of the Miette Group are lithologically distinct in the Cushing Creek area (Fig. 56.4). The lower Miette is a relatively recessive, dark weathering unit consisting of a lower limestone division and an upper slate division. The lower limestone consists of: calcareous, coarse grained sandstone to granule grit; finely crystalline black limestone with layers of 'beef calcite'[2] (Tarr, 1933; Poulton, 1973); black limestone beds that contain variable amounts of silt- to coarse sand-sized quartz clasts; and rusty-to greenish-weathering, silty, black slate. The slate division consists of

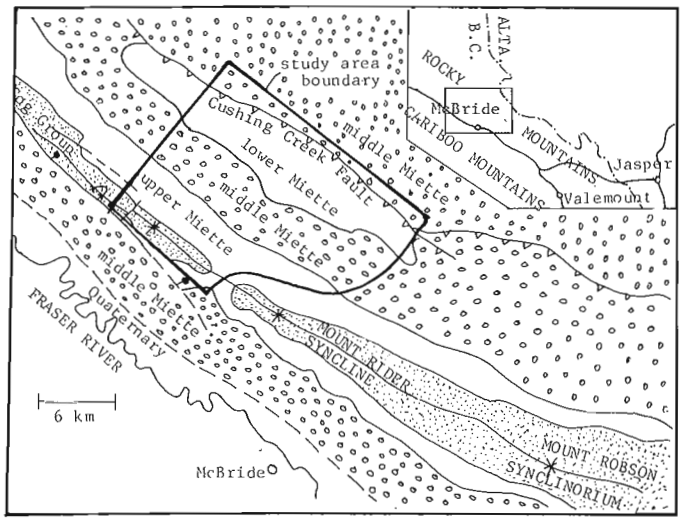

Figure 56.1. *Location map and generalized geology map (after GSC Map 1356A).*

[1] Department of Geology, University of Calgary
[2] Beef calcite is fibrous calcite with fibres (elongate parallel to c-axes) oriented perpendicular to bedding.

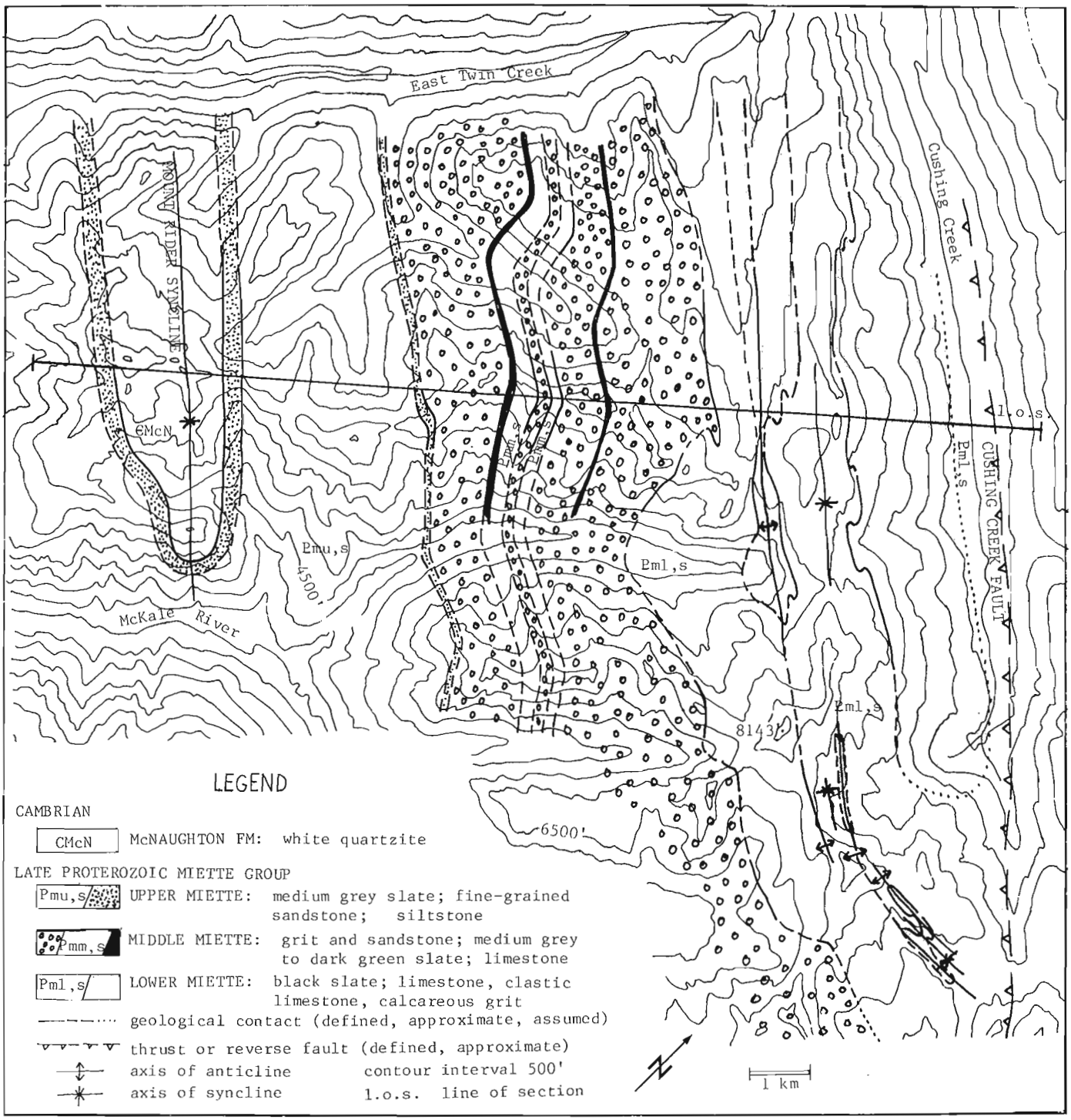

Figure 56.2. *Geological map of study area.*

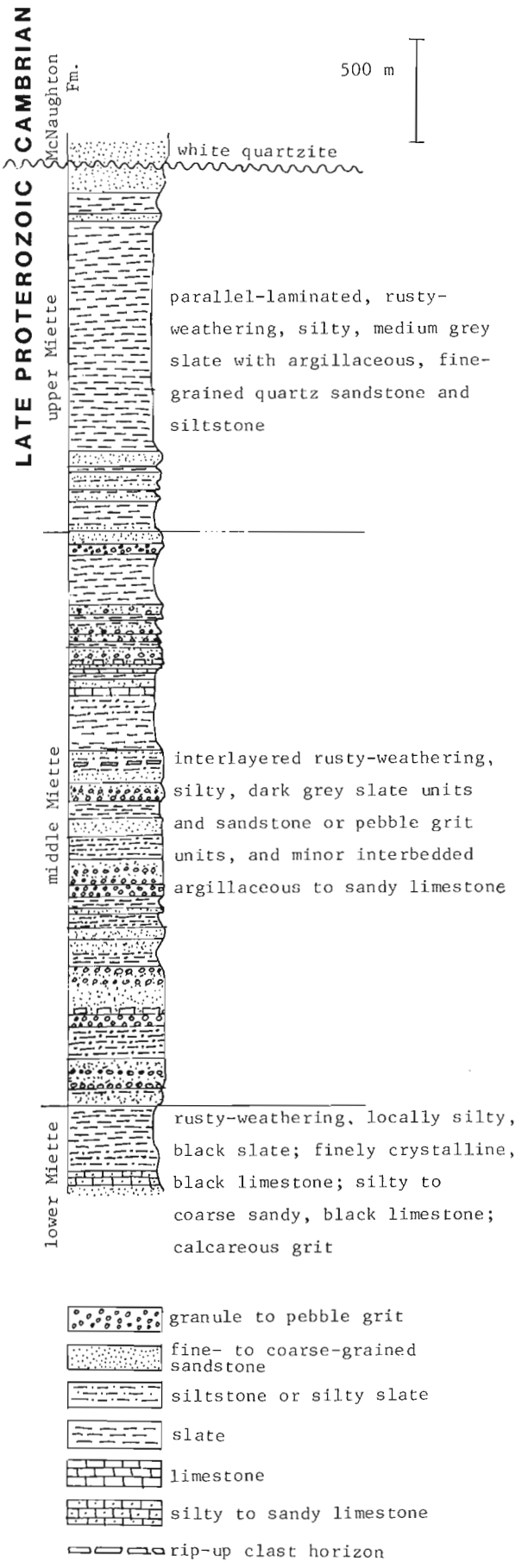

Figure 56.3 *Stratigraphic column: Cushing Creek area.*

rusty weathering, locally silty, black slate with minor fine- to medium- grained sandstone near the top. The base of the lower Miette is not exposed in the study area thus the estimated thickness of 380 m is a minimum only.

The middle Miette comprises interlayered cliff-forming stacked grit and sandstone beds (units up to 385 m thick), recessive, rusty weathering, silty, dark green to medium grey slate units (up to 210 m thick) and minor medium grey limestone. The basal contact is sharp, but the upper contact is gradational, as progressively finer grained sandstones are interbedded with silty slate. The contact has been placed above the highest unit containing granule grit. Above this horizon, sediment coarser than fine grained sandstone is rare. The measured thickness for the middle Miette is 2870 m.

Slate dominates the upper Miette, although both the base and the top of the unit contain considerable interbedded fine grained sandstone and siltstone. The greenish grey- to rusty-weathering, phyllitic, pyritic, medium grey slates often have parallel laminations of quartz silt. Rare ripple-cross-laminated, calcareous, fine grained sandstone beds occur within the unit. Thickness for the upper Miette is estimated at approximately 1800 m. This estimate is a maximum, as the minor folds and faults observed in a few localities in the upper Miette suggest that it may have a structure more complex than that depicted on Figure 56.3.

The white quartzite of the McNaughton Formation abruptly overlies the argillaceous fine grained sandstones and siltstones of the upper Miette. Contrasting lithologies across the bedding-parallel contact indicate a disconformity.

STRUCTURE

In this region, the Rocky Mountains comprise a series of large faulted synclinoria and anticlinoria, the most westerly of these being the Mount Robson Synclinorium (Fig. 56.1). The Mount Rider syncline, which forms the western portion of the study area, is a northern extension of the Mount Robson Synclinorium.

The middle and upper Miette in the study area form a continuous homoclinal succession on the east limb of the Mount Rider Syncline, but the lower Miette is more complexly folded in the core of a major anticline to the east and faulted against middle Miette strata which outcrop east of Cushing Creek (Fig. 56.3). Abundant very tight to isoclinal folds in the limestones and slates of the lower Miette are probably related to shortening and thickening of this unit in the core of the anticline. The more competent middle Miette controls the style of the major fold while the lower Miette has behaved incompetently.

A penetrative cleavage is strongly developed in Miette Group slates and is everywhere axial planar to minor folds. The cleavage dips southwest in all but the most western part of the area adjacent to the Mount Rider Syncline, where it dips northeast. It appears to outline a cleavage fan.

Crenulation cleavage is locally well developed. Two distinct sets are recognized. In the most western part of the area the crenulation cleavage has a mean orientation of approximately 035°/90°. Its orientation is consistent with strike-slip motion along the Rocky Mountain Trench (cf. McMechan, in press). To the east, the crenulation cleavage has a mean orientation of approximately 290°/60° northeast and is coaxial with structures of the main folding episode. It is possible that this crenulation cleavage developed where slaty cleavage had locally been rotated to a shallower dip during folding (cf. Gardner, 1977).

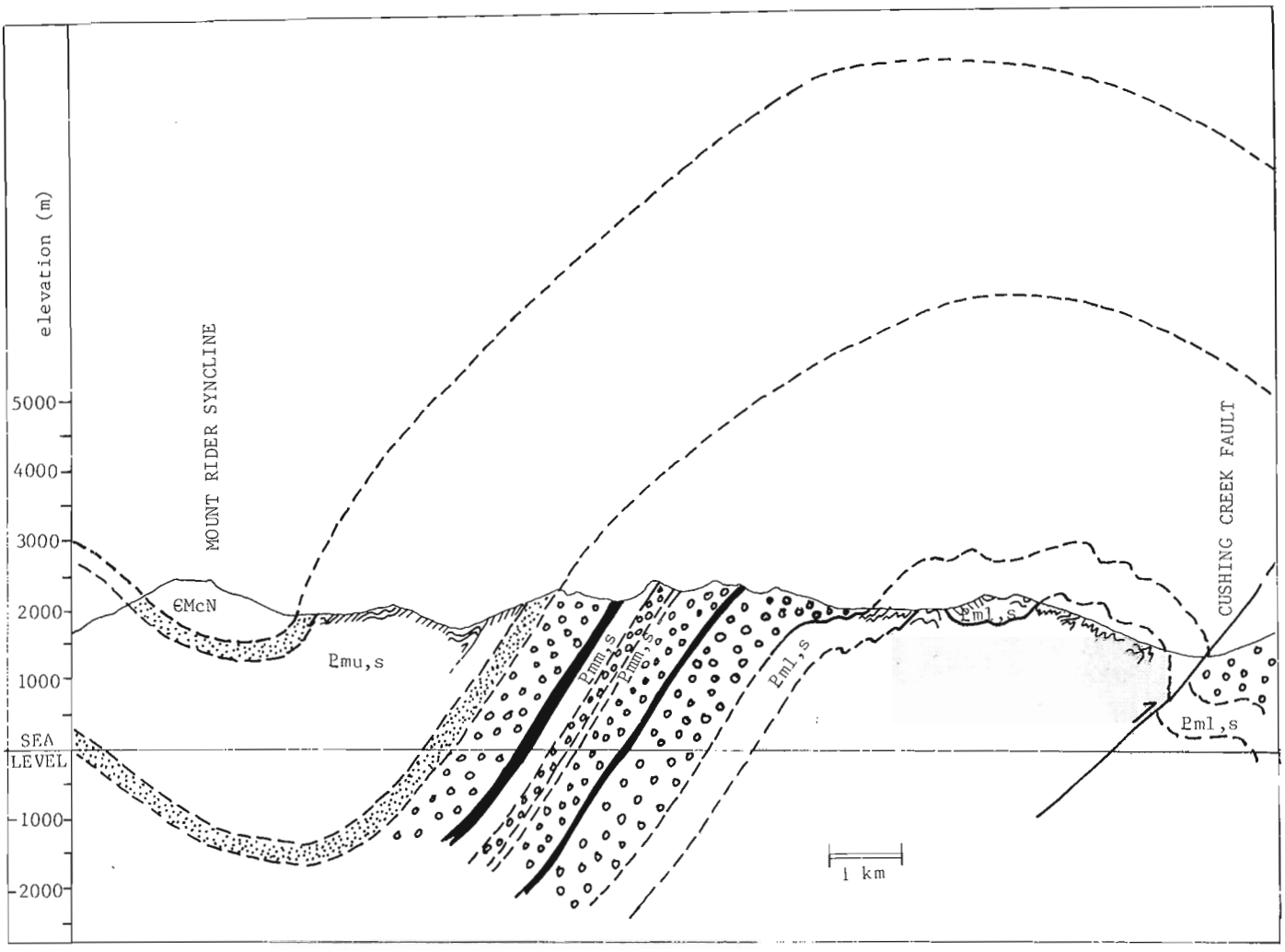

Figure 56.4. *Structural cross-section along line of section. Schematic minor folds (size exaggerated) are illustrated. No vertical exaggeration. Legend as in Figure 56.2.*

REFERENCES

Campbell, R.B., Mountjoy, E.W., and Young, F.G.
1973: Geology of McBride map-area, British Columbia; Geological Survey of Canada, Paper 72-35.

Gardner, D.A.C.
1977: Structural geology and metamorphism of calcareous lower Paleozoic slates, Blaeberry River-Redburn Creek area, near Golden, British Columbia; unpublished Ph.D. thesis, Queen's University, Kingston, Ontario, 224 p.

McMechan, M.E.
– Stratigraphy and structure, Mount Selwyn map area, Rocky Mountains, northeastern British Columbia; Geological Survey of Canada, Paper. (in press)

Poulton, T.P.
1973: Upper Proterozoic 'limestone unit', Northern Dogtooth Mountains, British Columbia; Canadian Journal of Earth Sciences, v. 10, p. 292-305.

Tarr, W.A.
1933: Origin of the 'beef' in the Lias shales of the Dorset Coast; Geological Magazine, v. 70, p. 289-294.

57. MIDDLE CAMBRIAN ACRITARCHS FROM THE CHAMBERLAINS BROOK AND MANUELS RIVER FORMATIONS AT RANDOM ISLAND, EASTERN NEWFOUNDLAND

Project 500029

F. Martin[1] and W.T. Dean[2]
Institute of Sedimentary and Petroleum Geology

Martin, F. and Dean, W.T., Middle Cambrian acritarchs from the Chamberlains Brook and Manuels River formations at Random Island, eastern Newfoundland; in Current Research, Part A, Geological Survey of Canada, Paper 84-1A, p. 429-440, 1984.

Abstract

Three Middle Cambrian acritarch microfloras from Random Island, eastern Newfoundland, are discussed: the youngest, A1, was introduced by Martin and Dean (1981); the others, A0-1 and A0 in ascending order, are new. Two species, ***Eliasum? hutchinsonii*** *Martin and* ***E. jennessii*** *Martin are new; Acritarch gen. et sp. nov. is left in open nomenclature.*

Résumé

Trois microflores à acritarches du Cambrien Moyen à Random Island, en Terre-Neuve orientale, sont examinées: la plus récente, A1, a été introduite par Martin et Dean (1981); les autres, dans l'ordre ascendant A0-1 et A0, sont nouvelles. Deux espèces, ***Eliasum? hutchinsonii*** *Martin et* ***E. jennessii*** *Martin, sont nouvelles; Acritarche gen. et sp. nov. est laissé en nomenclature ouverte.*

INTRODUCTION

W.T. Dean, F. Martin

Six acritarch microfloras from Random Island, Trinity Bay, eastern Newfoundland, reported by Martin and Dean (1981) came from the upper part of the Manuels River Formation, the Elliott Cove Formation and the Clarenville Formation. Their ages range from the middle of the Middle Cambrian (**Paradoxides hicksii** Zone in part) to the early Tremadoc (**Parabolina argentina** Zone). During the field season of 1981, palynological sampling of the same coastal section was completed by the writers as part of GSC Project 500029, and covered the lower part of the Manuels River Formation and the upper part of the underlying Chamberlains Brook Formation. The samples came from the west coast of Random Island, between 1300 m and 1500 m north-northwest of Weybridge (Fig. 57.1). Twenty-four samples are from the uppermost 53 m of the Chamberlains Brook Formation (Beds 6 to 8 of Hutchinson, 1962, p. 144) and fourteen are from the lowest 17 m of the Manuels River Formation (Beds 9 to 11 of Hutchinson, op. cit.); the highest level sampled was 14.5 m below the basal conglomerate of the overlying Elliott Cove Formation (Hutchinson, 1962, p. 143; Martin and Dean, 1981, p. 5). These thicknesses are maxima and the precision of measurements at the section is limited by the presence of several small faults and cliff slumps, particularly in the outcrop of Chamberlains Brook Formation. Our measurements agree with those given by Hutchinson (op. cit.) for the upper part of the Chamberlains Brook Formation, but not for the total of the Manuels River Formation; our estimate for the latter is 22.5 m, compared with approximately 32 m (95 ft) given by Hutchinson.

The Middle Cambrian of the Avalon and Burin peninsulas was recognized by Hutchinson (1962, p. 9, 51) as being divisible into four trilobite zones, successively, **Paradoxides bennettii** (misquoted as **bennetti**), **P. hicksii** (misquoted as **hicksi**), **P. davidis** and **P. forchhammeri**. The **P. bennettii** Zone, introduced by Howell (1925, p. 60) for the section at Manuels River, 100 km southeast of Random Island, was correlated by both Howell and Hutchinson with the whole of the Chamberlains Brook Formation. Hutchinson considered the formation to rest with probable disconformity on the Brigus Formation, upper Lower Cambrian.

No macrofossils were recorded from the Chamberlains Brook Formation of Random Island by Hutchinson (1962, p. 144) and during the present work only a single, large (median length of glabella and occipital ring = 8 to 9 cm), sheared, incomplete cranidium of **Paradoxides** (s.l.) sp. undet. was found, at a level 4.5 m below the top of the formation. The Manuels River Formation at Random Island includes the **Paradoxides hicksii** Zone in its lowest 17 m and the **Paradoxides davidis** Zone in its topmost 10.5 m. Owing to lack of faunal evidence, a satisfactory boundary cannot be drawn between these two zones which, together, were equated by Cowie et al. (1972, p. 11) with the uppermost three of four agnostid zones constituting the **Paradoxides paradoxissimus** 'Stage'. This 'Stage', is the second of three **Paradoxides** 'stages' into which Westergård (1946, p. 8) divided the Middle Cambrian of Sweden (see Fig. 57.3). Cowie et al.'s correlation is essentially similar to that of Sdzuy (1971, table 2) in which the **Paradoxides bennettii** Zone was equated with the lowest quarter (presumably **Ptychagnostus (Triplagnostus) gibbus** Zone) of the **P. paradoxissimus** 'Stage' and an undefined, upper part of the **P. oelandicus** 'Stage'. A re-assessment of the generic position of the relevant paradoxidid species is beyond the scope of this paper, but **P. hicksii** Salter, 1865 was placed in **Hydrocephalus** Barrande, 1846 by Snajdr (1958, p. 130) and, more recently, by Bergstrom and Levi-Setti (1978, Fig. 10), who also assigned **P. bennettii** Salter, 1859 questionably to the same genus.

The correlation table (Fig. 57.3) adopted here differs in minor respects from that of Cowie et al. (1972, p. 11). The changes are based on a revision of the Middle Cambrian faunas of the St. David's area, southwest Wales, by Mr. M. Lewis, University College, Cardiff, who has kindly provided relevant, unpublished data. Lewis considers **Paradoxides aurora** Salter, 1866 to be a junior subjective synonym of **P. hicksii** Salter, 1865, the vertical range of which extends from the upper part of the **Ptychagnostus gibbus** Zone to the top of the succeeding zone of **Tomagnostus fissus** and **Ptychagnostus atavus**. In addition, **Paradoxides davidis** Salter, 1863 is now known to be confined to the **Ptychagnostus punctuosus** Zone in the St. David's area.

[1] Departement de Paleontologie, Institut Royal des Sciences Naturelles de Belgique, rue Vautier, 29, B-1040 Bruxelles, Belgium
[2] Department of Geology, University College, Cardiff, CF1 1XL, United Kingdom

The above changes have some implications for the corresponding succession in eastern Newfoundland. At his detailed measured section at Manuels, Howell (1925, p. 60) drew the upper boundary of the Chamberlains Brook Formation at the top of Bed 35; succeeding Beds 36-125 were chosen by Hutchinson (1962, p. 22; Bed 26 is a misprint for Bed 36) as stratotype for the overlying Manuels River Formation. The boundary between Howell's **Paradoxides bennettii** Zone and **P. hicksii** Zone coincided with that between Beds 35 and 36. Bed 36, consisting of one and a half inches (4 cm) of white clay overlain by half an inch (1.25 cm) of soft shale (Howell, 1925, p. 50), is one of several beds (probably bentonite) that occur sporadically in the type Manuels River Formation.

The zonal agnostid **Ptychagnostus gibbus** was not recorded from eastern Newfoundland by Hutchinson (1962), though Howell (1925, p. 120) did report '**Agnostus** cf. **gibbus**' from an unspecified level in the **P. hicksii** Zone at Manuels; Howell (1925, p. 118) also listed **P. hicksii** among species from what he considered to be the **P. bennettii** Zone in Britain. Of the eponymous species of the **Tomagnostus fissus** and **Ptychagnostus atavus** Zone in Newfoundland, **T. fissus** was stated by Hutchinson (1962, p. 84) to occur only 'in the middle part' of the **P. hicksii** Zone. **P. atavus** and **Hypagnostus parvifrons** were said (Hutchison, 1962, p. 83) to occur associated in the 'upper part' of the **P. hicksii** Zone and lowest **P. davidis** Zone, a distribution difficult to accommodate within the present scheme. Published evidence for precise correlation of the topmost Chamberlains Brook Formation and lowest Manuels River Formation is thus inconclusive and none is so far available from the described section at Random Island.

LOCATION OF SAMPLES AND THEIR ACRITARCH CONTENT

W.T. Dean, F. Martin

The stratigraphic section discussed in this paper, is situated on the west coast of Random Island and is reached from the village of Weybridge. It is a southerly extension of the section described by Martin and Dean (1981) and extends from 22.5 m to 212 m south of the basal conglomerate of the Elliott Cove Formation, which forms a conspicuous, convenient reference on a coast otherwise devoid of landmarks. All the samples from the Manuels River Formation and the two stratigraphically highest ones from the Chamberlains Brook Formation are located with reference to the conglomerate.

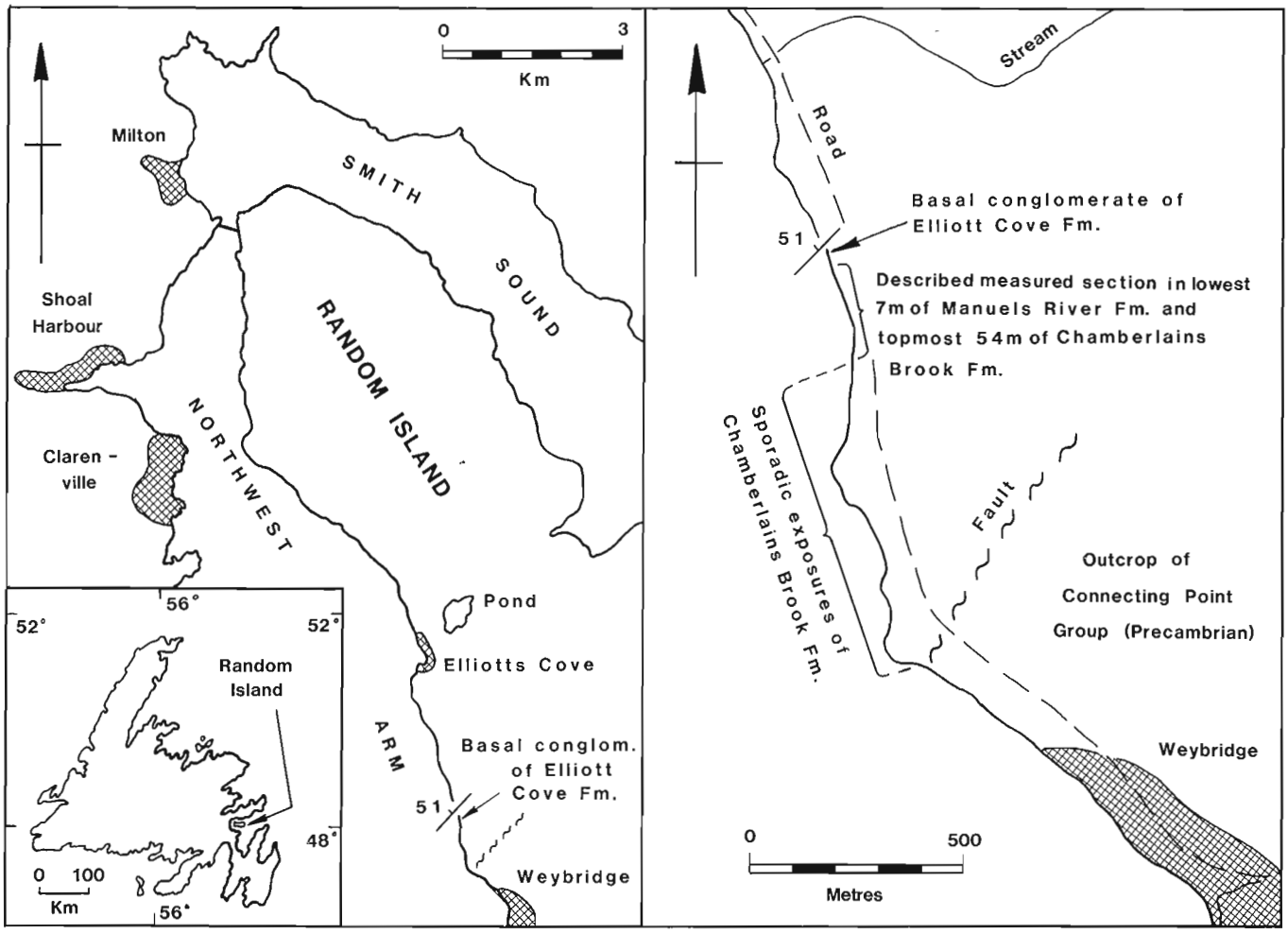

Figure 57.1. Left half: outline map of northwest half of Random Island with location of section described in text. Inset map shows position of Random Island relative to Newfoundland. Right half: locality map for described section on west coast of Random Island, northwest of Weybridge.

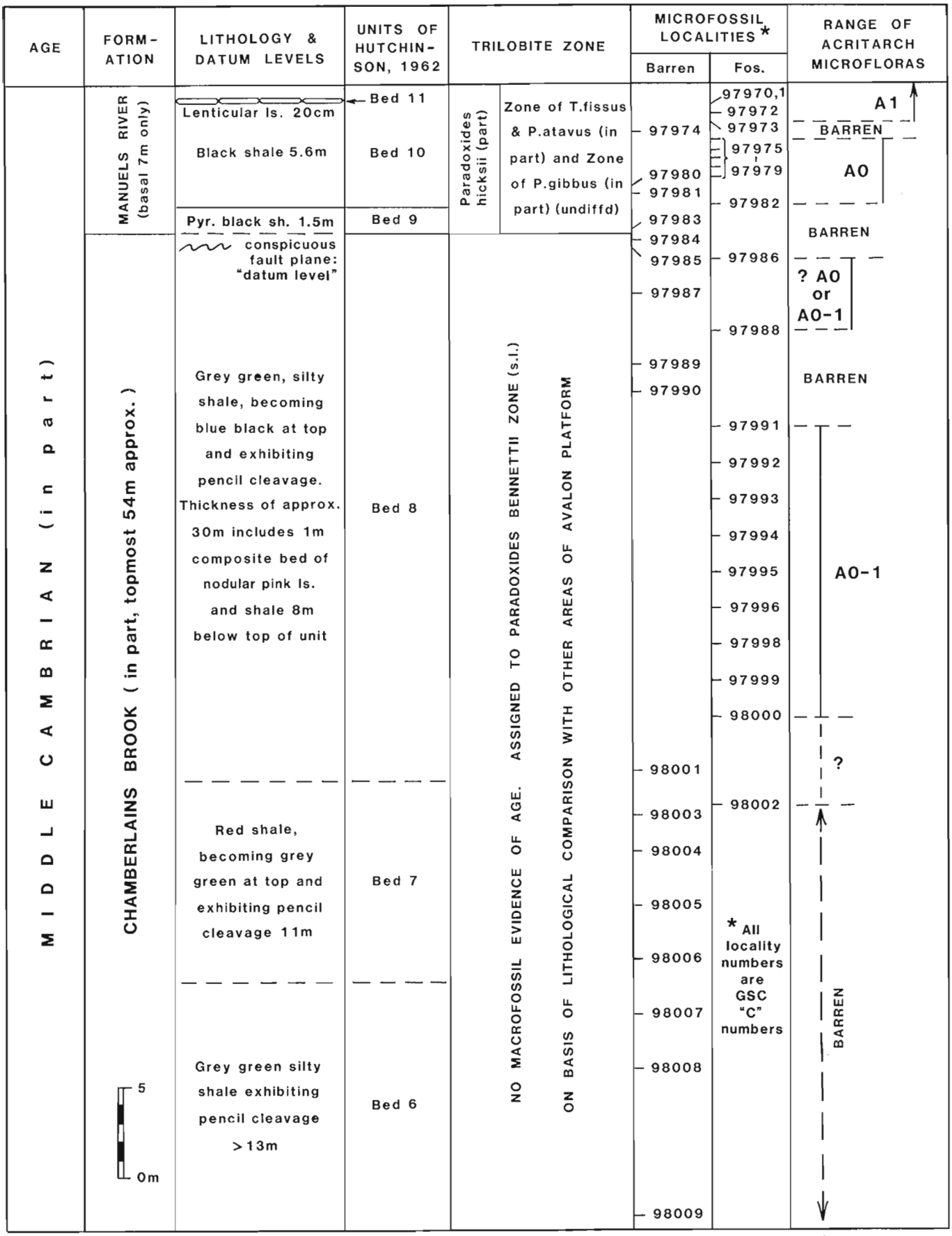

Figure 57.2. *Measured section and levels sampled in upper part of Chamberlains Brook Formation and lower part of Manuels River Formation, west coast of Random Island, approx. 1.5 km northwest of Weybridge. The fault plane used as 'datum level' appears at the top of the Chamberlains Brook Formation.*

A second datum point, used in fixing the location of the remaining samples from the Chamberlains Brook Formation, is situated on the shore 44 m south of the conglomerate and is formed by the intersection of two small faults at the foot of the cliff. GSC loc. C-97986 is immediately beneath the lower fault plane, which is indicated as 'datum level' in the accompanying list of localities and in the measured section (Fig. 57.2).

The term 'barren' in this account indicates that acritarchs are absent; no chitinozoans were found in any of the samples. When present, acritarchs are variably abundant, ranging from about ten to several thousands per gram of rock. They are very corroded and generally quite dark, though the surface of a single specimen may sometimes vary from transparent yellow to dark brown. The largest specimens often exhibit parallel cracks (for example Pl. 57.2, fig. 7) produced by compaction of the enclosing sediment. In the best preserved samples, from 10 to 20 per cent of the specimens are generically and/or specifically identifiable. The preparations containing acritarchs always show abundant, blackish sapropelic debris.

Chamberlains Brook Formation

GSC locs. C-98009, C-98008 and C-98007. Grey green, silty shale at levels respectively 52.45 m, 44.75 m and 41.75 m below datum level; all barren.

GSC locs. C-98006, C-98005, C-98004 and C-98003. Red, silty shale at levels respectively, and approximately, 38.75 m, 35.75 m, 32.75 m and 30.75 m below datum level; all barren.

GSC loc. C-98002. Grey green, silty shale approximately 30.1 m below datum level; rare acritarchs.

GSC loc. C-98001. Grey green, silty shale approximately 28.4 m below datum level; barren.

GSC loc. C-98000. Grey green, silty shale, approximately 25.4 m below datum level; rare acritarchs.

GSC locs. C-97999 and C-97998. Grey green, silty shale at levels respectively, and approximately, 23.4 m and 21.4 m below datum level; numerous acritarchs.

GSC loc. C-97996. Grey green, silty shale 19.4 m below datum level; rare acritarchs.

GSC locs. C-97995, C-97994, C-97993, C-97992 and C-97991. Grey green, silty shale at levels respectively 17.4 m, 15.4 m, 13.4 m, 11.4 m and 9.4 m below datum level; numerous acritarchs.

GSC loc. C-97990. Shale immediately above 1 m composite unit of pink and beige nodular limestones with interbedded shales; the base of the unit is formed by a 15 cm bed of semi-nodular pinkish limestone. 7.4 m below datum; barren.

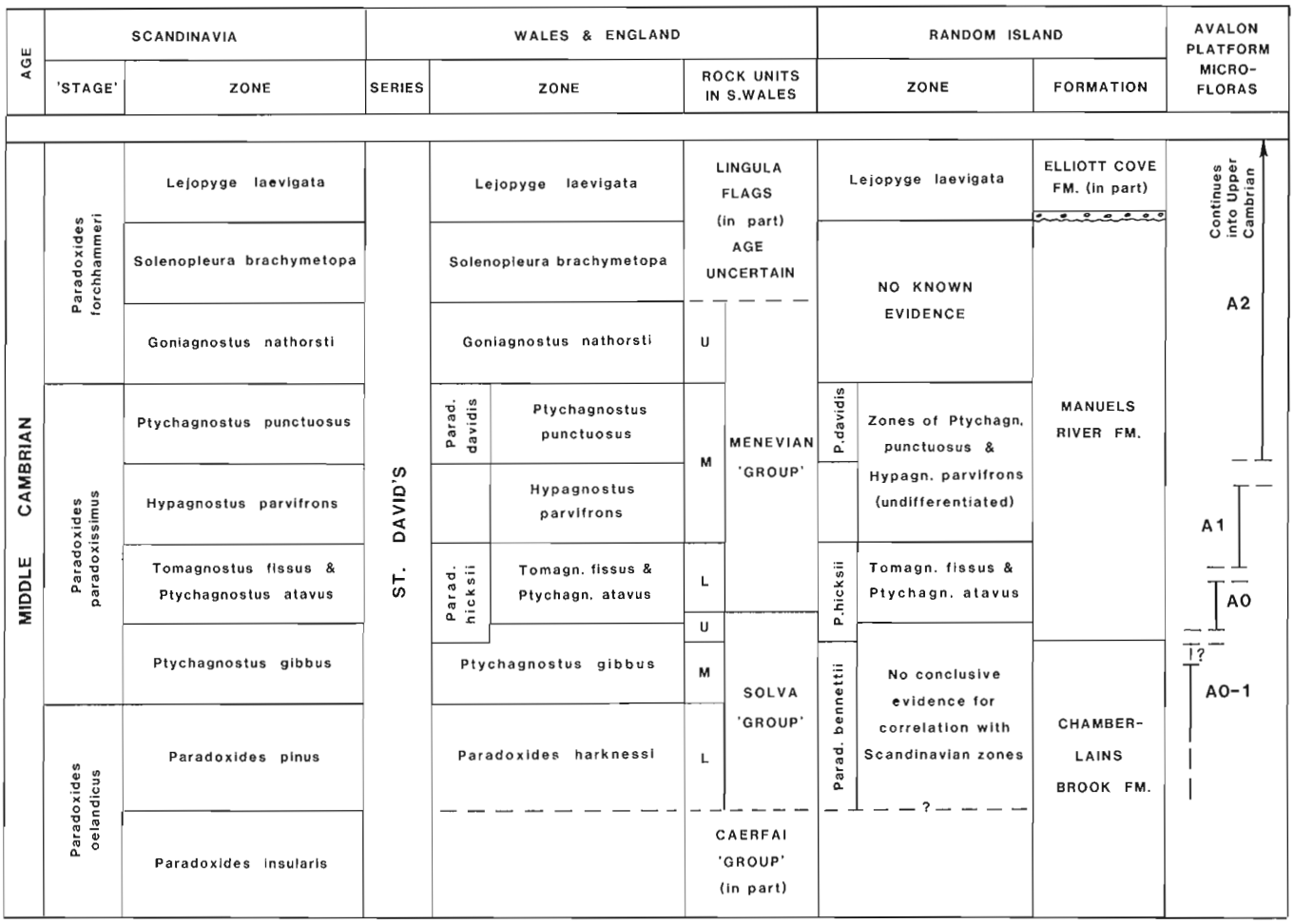

Figure 57.3. *Table showing stratigraphic ranges of Middle Cambrian microfloras in relation to corresponding trilobite zones in eastern Newfoundland, Wales and Scandinavia. The British usage follows that by Cowie, Rushton and Stubblefield (1972) but incorporates some modification of the zonal succession in South Wales based on unpublished data provided by M. Lewis.*

GSC locs. C-97989, C-97988 and C-97987. Levels in blue grey shale respectively 6 m (barren), 4 m, (rare acritarchs) and 2 m (barren) below datum level.

GSC loc. C-97986. Blue black shale immediately below datum level formed by fault plane; rare acritarchs.

GSC locs. C-97985 and C-97984. Blue black shale respectively 22.5 m (barren) and 22 m (undeterminable acritarchs) below basal conglomerate of the Elliott Cove Formation.

Manuels River Formation

Measurements are given with reference to the basal conglomerate of the overlying Elliott Cove Formation.

GSC loc. C-97983. Black, pyritic shale 21.5 m below conglomerate; barren.

GSC loc. C-97982. Black shale 20 m below conglomerate; numerous acritarchs.

GSC locs. C-97981 and C-97980. Black shale respectively 19.5 m (barren) and 19 m (undeterminable acritarchs) below the conglomerate.

GSC loc. C-97979. Black shale 18.5 m below conglomerate; numerous acritarchs.

GSC locs. C-97978, C-97977 and C-97976. Black shale respectively 18 m, 17.5 m and 17 m below conglomerate; rare acritarchs.

GSC loc. C-97975. Black shale 16.5 m below conglomerate; numerous acritarchs.

GSC loc. C-97974. Black shale 16 m below conglomerate; undeterminable acritarchs.

GSC loc. C-97973. Black shale 15.5 m below conglomerate; numerous acritarchs. The stratigraphic horizon of this sample is the same as for GSC locs. 94427 and 95174 (Martin and Dean, 1981, p. 7).

GSC loc. C-97972. Black shale 15 m below conglomerate; rare acritarchs. The horizon is the same as for GSC loc. 95173 (Martin and Dean, 1981, p. 12), the sample from which was barren.

GSC locs. C-97971 and C-97970. Black shale at levels respectively 14.65 m and 14.5 m below conglomerate; numerous acritarchs. The horizon for GSC loc. C-97970 is the same as that for GSC loc. 95172 (Martin and Dean, 1981, p. 7).

PALEONTOLOGY

F. Martin

Material and method

The microfossils were concentrated from samples of 40 grams of rock; they are neither coloured nor oxidized. All the figured specimens, including those observed by means of the scanning electron microscope, are permanently mounted in Canada balsam. Figured specimens, numbered GSC 72933 to 72973, accompanied by co-ordinates established by means of the England Finder Graticule, are in the National Type Fossil Collection, Geological Survey of Canada, Ottawa. Palynological preparations from each sample are deposited also in the Institut Royal des Sciences Naturelles de Belgique, Brussels.

In the following systematic descriptions, acritarchs described by Martin (in Martin and Dean, 1981, 1983) and for which no new information is available are omitted.

Systematic descriptions

Acritarch gen. et sp. nov.
Plate 57.1, figures 10, 17-19

Figured specimens. GSC 72935 (Pl. 57.1, fig. 10), GSC 72936 (Pl. 57.1, fig. 17), GSC 72937 (Pl. 57.1, fig. 18), GSC 72938 (Pl. 57.1, fig. 19).

Description. Based on more than five hundred clusters, each comprising about ten to fifty organisms. Specimens are never found isolated but are always agglomerated and form a sort of yellow-brown, more or less transparent cellular tissue. Each micro-organism is only slightly variable, consisting of a relatively dark central body, oval in outline and covered with a multitude of tangled, probably solid, fine filaments, many of which anastomose with each other and seem also to link the fine filaments of contiguous specimens. Scanning electron microscope photographs show little relief and do not show the form of the central body; locally, and most often at the periphery of fragmentary colonies, the photographs indicate clearly the tangle of anastomosed filaments.

Dimensions. Based on one hundred specimens. Overall diameter of clusters generally from 50 to 100 µm; length of axes of central body from 5 to 9 µm; length of filaments from 7 to 12 µm.

Discussion. The manner in which specimens are joined together not having been established, this colonial form is left in open nomenclature. The specimens differ from **Micrhystridium pallidum** Volková (1968, p. 21, Pl. 4, figs. 5-9; Pl. 11, fig. 4) from the Blue Shales, Lontova Suite, Lower Cambrian, of Estonia, known also in colonial form, in having longer, anastomosed filaments.

Occurrence. Locally abundant in the upper part of the Chamberlains Brook Formation and the lower part of the Manuels River Formation.

Genus Cristallinium Vanguestaine, 1978

Type species: **Cristallinium cambriense** (Slavíková, 1968) designated by Vanguestaine, 1978.

Cristallinium cambriense (Slavíková) Vanguestaine, 1978
Plate 57.1, figures 1-7, 9, 13

Dictyotidium cambriense sp. nov. Slavíková, 1968, p. 201, Pl. 2, figs. 1, 3.
Cristallinium cambriense (Slavíková) Vanguestaine, 1978. Martin in Martin and Dean, 1981, p. 17, Pl. 3, figs. 4, 5, 9, 11; Pl. 5, figs. 3, 5, 8, 11 (includes previous synonymy).

Figured specimens. GSC 72939 (Pl. 57.1, figs. 1, 2), GSC 72940 (Pl. 57.1, fig. 3), GSC 72941 (Pl. 57.1, figs. 4, 7), GSC 72942 (Pl. 57.1, fig. 5), GSC 72943 (Pl. 57.1, figs. 6, 9), GSC 72944 (Pl. 57.1, fig. 13).

Dimensions. Based on one hundred specimens. Diameter of central body from 25 to 54 µm; height of granules 0.7 µm or less; height of spinose or rod-like projections up to 1 µm.

Discussion. Based on five hundred specimens. The variability of size of the central body and of the ornamentation is greater than was previously described by Martin (in Martin and Dean, 1981) and links the specimens with those described by Vanguestaine (1978, p. 270), from the Cambrian of Belgium. In particular the ornamentation is not only granulate but also echinate or baculate, the lowest projections being proximally simple or divided.

Occurrence. Variably abundant in the Manuels River Formation.

Plate 57.1

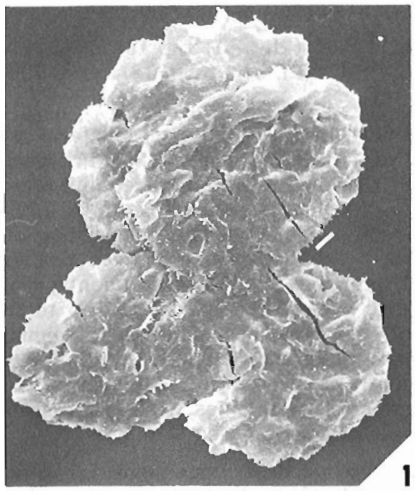
1

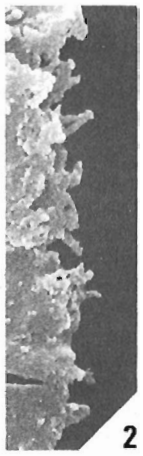
2

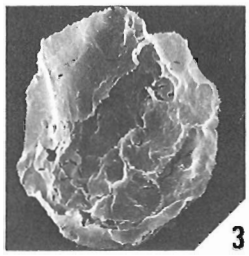
3

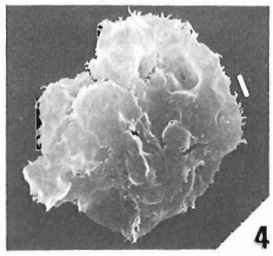
4

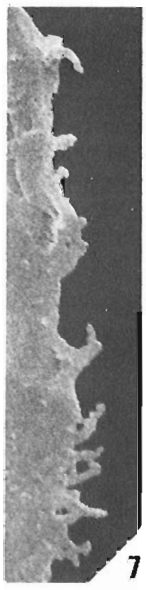
7

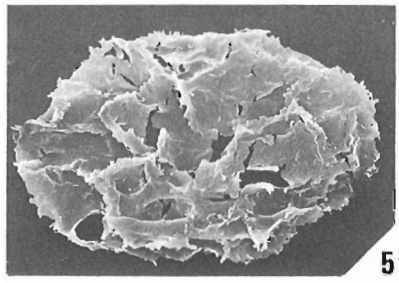
5

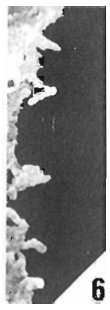
6


8

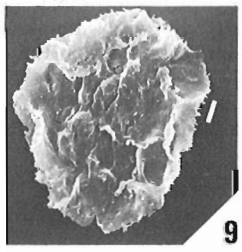
9


10


15


14

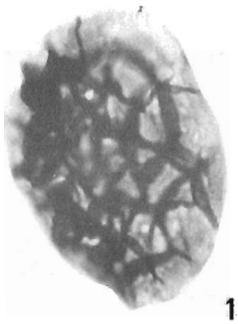
11


12


13


16

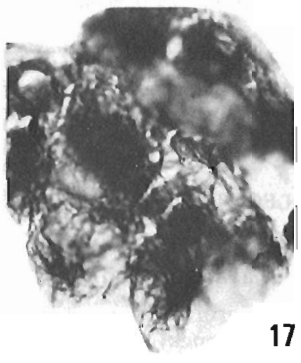
17

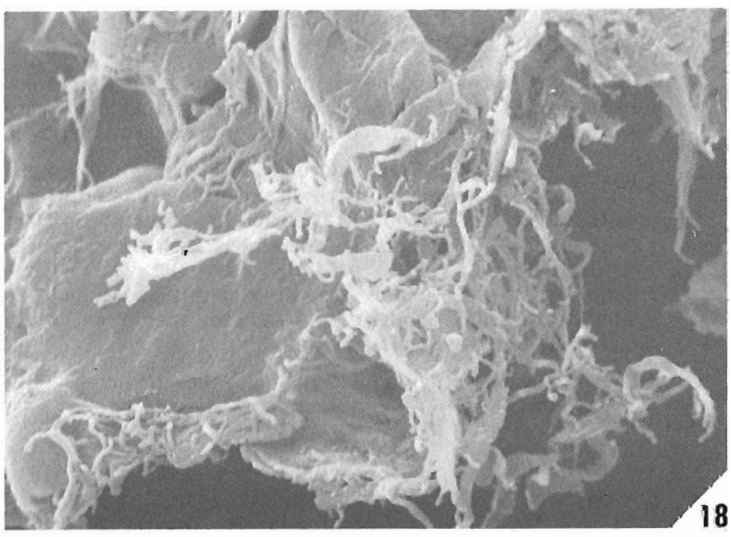
18

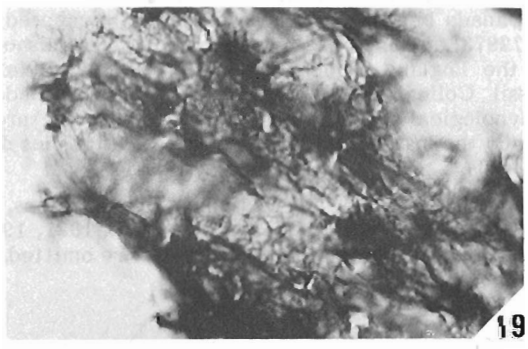
19

Genus Eliasum Fombella, 1977

Type species: **Eliasum llaniscum** Fombella, 1977 by original designation.

Eliasum? hutchinsonii Martin sp. nov.
Plate 57.2, figures 1-5, 7, 9

Holotype. GSC 72949 (Pl. 57.2, fig. 7).

Paratypes. GSC 72946 (Pl. 57.2, figs. 1, 2), GSC 72947 (Pl. 57.2, figs. 3, 9), GSC 72948 (Pl. 57.2, figs. 4, 5).

Type locality and horizon. GSC loc. C-97979, Manuels River Formation, black shale 18.5 m below basal conglomerate of Elliott Cove Formation at cliff section north of Weybridge, Random Island. The age is Middle Cambrian, **Paradoxides hicksii** Zone, equated also with the Zone of **Tomagnostus fissus** and **Ptychagnostus atavus.**

Plates

All figured specimens are in the type fossil collection of the Geological Survey of Canada, Ottawa, and have numbers with the prefix GSC. Transmitted light photographs are by F. Martin; SEM photographs are by Dr. P. Grootaert, Institut Royal des Sciences Naturelles de Belgique, Brussels.

All taxa illustrated are listed in Table 57.1; those marked with an asterisk are also described in the text.

Plate 57.1

Magnification of photographs x1000, except where otherwise stated.

Figures 1-7, 9, 13. **Cristallinium cambriense** (Slavíková) Vanguestaine, 1978.*

1, 2. GSC 72939, GSC loc. C-97982. Fig. 2 x7000.
3. GSC 72940, GSC loc. C-97979.
4, 7. GSC 72941, GSC loc. C-97982. Fig. 7 x7000.
5. GSC 72942, GSC loc. C-97979, x1500.
6, 9. GSC 72943, GSC loc. C-97982. Fig. 6 x7000.
13. GSC 72944, GSC loc. C-97979.

White lines on Figs. 1, 4 and 9 indicate portions of specimens shown enlarged in Figs. 2, 7 and 6 respectively.

Figure 8. **Cymatiosphaera crameri** Slavíková, 1968. GSC 72945, GSC loc. C-97992.

Figures 10, 17-19. Acritarch gen. et sp. nov.*

10. GSC 72935.
17. GSC 72936.
19. GSC 72938.
10, 17, 19. GSC loc. C-97993.
18. GSC 72937, GSC loc. C-97991, x10,000.

Figures 11, 12, 15. **Retisphaeridium dichamerum** Staplin, Jansonius and Pocock, 1965. GSC loc. C-97992.

11. GSC 72968.
12. GSC 72969.
15. GSC 72970.

Figures 14, 16. **Retisphaeridium howellii** Martin in Martin and Dean (1983). 14. GSC 72971, GSC loc. C-97979.
16. GSC 72972, GSC loc. C-97998.

*Described in text.

Diagnosis. Based on nine specimens. Central body elliptical in outline with two or three longitudinal folds extending from one pole to the other. Entire surface covered with generally low, apparently solid tubercles with rounded tips; some of the ornamentation is more elongated, either in the form of rods with simple or multiple bases, or in the form of tubercles which narrow at the base.

Dimensions. Based on five specimens. Length of axes of central body 46 to 55 µm and from 27 to 35 µm; maximum length of ornamentation 0.6 µm; length of tubercles from 0.1 to 0.5 µm; length of rods from 0.2 to 0.6 µm.

Discussion. The longitudinal folds of **E.? hutchinsonii** are less numerous than those of other species of the genus, and are seen more clearly in transmitted light than under the scanning electron microscope. Superficially the outline recalls that of **Leiovalia** Eisenack, 1965, in which the poles are more rounded. **E.? hutchinsonii** differs from **E. pisciforme** Fombella, 1977 in having identical ornamentation on both the folds and the areas between them.

Occurrence. Rare in the lower part of the Manuels River Formation, both at the type locality and at GSC loc. C-97982, 1.5 m below.

Eliasum jennessii Martin sp. nov.
Plate 57.3, figures 1, 2, 4-7, 12-15

Holotype. GSC 72953 (Pl. 57.3, figs. 5-7).

Paratypes. GSC 72950 (Pl. 57.3, fig. 1), GSC 72951 (Pl. 57.3, fig. 2), GSC 72952 (Pl. 57.3, fig. 4), GSC 72954 (Pl. 57.3, fig. 12), GSC 72955 (Pl. 57.3, fig. 13), GSC 72956 (Pl. 57.3, fig. 14), GSC 72957 (Pl. 57.3, fig. 15).

Type locality and horizon. GSC loc. C-97993, Chamberlains Brook Formation, 13.4 m below fault-plane that intersects foot of cliff 44 m south of basal conglomerate of Elliott Cove Formation, 1.5 km north of Weybridge, west coast of Random Island. No macrofossils found but strata assigned to early Middle Cambrian, **Paradoxides bennettii** Zone.

Diagnosis. Based on four hundred specimens. Central body elliptical in outline, two to three times longer than broad, with a few (generally four or five) longitudinal folds extending from one pole to the other. Entire surface covered with very fine ornamentation consisting of rod-like projections or spines with simple or multiple bases.

Dimensions. Based on fifty specimens. Length of axes of central body from 60 to 80 µm and 27 to 32 µm. Secondarily compressed specimens that have undergone transverse compression may measure up to 45 µm long by 32 µm wide. Maximum length and width of rods 0.6 µm and 0.1 µm.

Discussion. Secondary transverse folds, the development of which varies from one specimen to another, may modify the outline of a specimen making it appear very squat. In transmitted light the surface is variably oxidised, often partly perforated, and the ornamentation is only locally and poorly observable. Certain specimens (Pl. 57.3, figs. 2, 13) have at one of the poles a more or less circular opening with a diameter approximately one third the width of the vesicle. These openings are always deformed by crushing, as are those (Pl. 57.2, figs. 13, 15) of **E. llaniscum** Fombella, 1977 from the Chamberlains Brook Formation and Manuels River Formation at Random Island. **E. jennessii** differs from **E. pisciforme** Fombella, 1977 and **E. llaniscum** in the form and distribution of the ornamentation. It differs from **E.? hutchinsonii** in having a more massive central body, more longitudinal folds, and no rounded tubercles.

Occurrence. Variably abundant in the upper part of the Chamberlains Brook Formation.

Plate 57.2

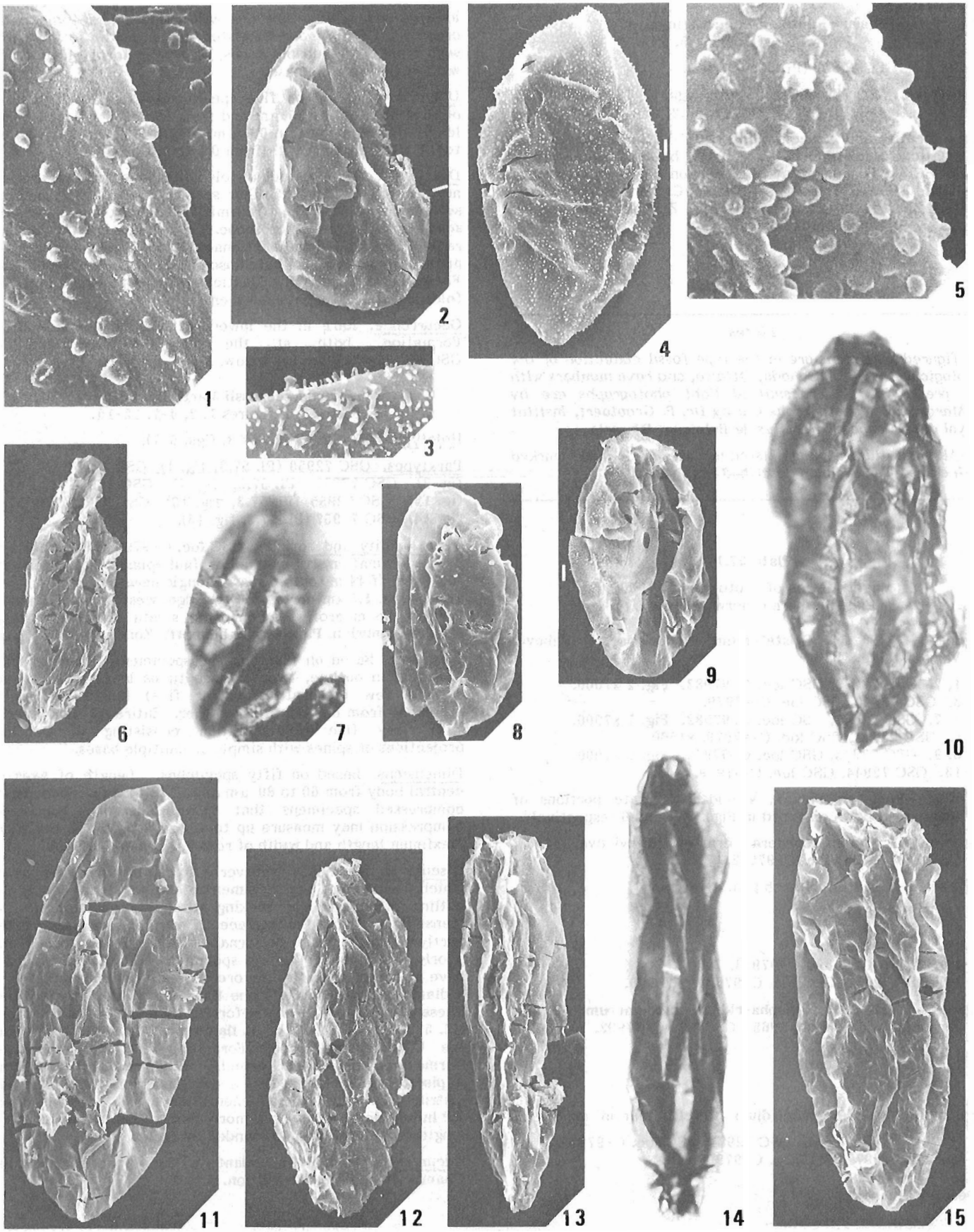

Genus Multiplicisphaeridium Staplin, 1961 emend. Staplin, Jansonius and Pocock, 1965

Type species: **Multiplicisphaeridium ramispinosum** Staplin, 1961 by original designation.

Multiplicisphaeridium sp.
Plate 57.3, figure 8

Figured specimen. GSC 72967.

Description. Based on ten specimens. Central body more or less ovoid. About thirty hollow processes present, their internal cavities communicating with that of the central body. The base of each process widens slightly and the distal extremity is simple or slightly divided.

Dimensions. Based on five specimens. Diameter of central body from 16 to 20 µm; length of appendices from 5 to 7 µm.

Discussion. The taxon is ubiquitous and no specific determination is proposed. However, the specimens are particularly comparable to those figured as **Micrhystridium obscurum** Volková, 1969 by Gardiner and Vanguestaine (1971). The last-named material came from the Ribband Group, Booley Bay Formation and the Bray Group, Thulla Formation of southeastern Ireland, the age of which, according to Gardiner and Vanguestaine, based on palynological evidence, ranges from early Cambrian to middle Middle Cambrian.

Occurrence. Rare in the upper part of the Chamberlains Brook Formation and in the lower part of the Manuels River Formation.

SEQUENCE AND CORRELATION OF THE ACRITARCH MICROFLORAS

F. Martin

The acritarch microfloras (Fig. 57.3) are defined by the first appearance of selected taxa and/or by the presence of characteristic taxa. For this reason **Leiosphaeridia** sp., **Multiplicisphaeridium** sp., **Kildinella** sp. and **Timofeevia** sp., though listed (Table 57.1) are omitted from the present discussion. The first two have an extended stratigraphic range and the last two occur only very rarely and sporadically in the described section. The vertical ranges of the microfloras are separated by intervals that either are barren or contain only undeterminable acritarchs; the oldest strata sampled proved to be completely barren. In a previous paper describing Cambrian and lower Tremadoc acritarchs from Random Island (Martin and Dean, 1981), progressively younger microfloras were numbered consecutively upwards from A1 to A6. In the present paper it has been found convenient to number older microfloras A0 and A0-1 in descending stratigraphic order.

Microflora A0-1 (Eliasum jennessii – Acritarch gen. et sp. nov. assemblage)

Stratigraphic position

Upper part of Chamberlains Brook Formation, in Bed 8 of Hutchinson (1962), from 9.4 m to 25.4 m below the conspicuous fault plane that occurs near the summit of the formation (see Fig. 57.2). Age is Middle Cambrian, tentatively correlated with **Paradoxides bennettii** Zone.

Description

The assemblage contains numerous **Eliasum jennessii** and Acritarch gen. et sp. nov. **Eliasum llaniscum** is generally present but of variable frequency. **Retisphaeridium dichamerum** Staplin, Jansonius and Pocock, 1965, **R. howellii** Martin in Martin and Dean (1983), and **Cymatiosphaera crameri** Slavikova, 1968 are present, the first of these being locally abundant.

Comparison with other parts of eastern Newfoundland

Microflora A0-1 differs from the assemblage studied by the authors (1983), from the basal Chamberlains Brook Formation, early Middle Cambrian, **Paradoxides bennettii** Zone, at Manuels River, 100 km to the southeast, in the presence of **Eliasum jennessii** and Acritarch gen. et sp. nov. and the absence of **Annulum squamaceum** (Volková) Martin in Martin and Dean (1983). At the Manuels River section **Retisphaeridium dichamerum** and **R. howellii** are abundant in the highest Lower Cambrian (**Catadoxides** Zone of Howell, 1925), 1.1 m below the summit of the Brigus Formation, and range upwards. **Eliasum llaniscum** and **Cymatiosphaera crameri** appear there at slightly higher levels, respectively 5.15 m and 7.15 m above the base of the Chamberlains Brook Formation.

Microflora A0 (Eliasum? hutchinsonii – Cristallinium cambriense assemblage)

Stratigraphic position

Microflora A0 occurs in part of Bed 10 of Hutchinson (1962, p. 144) in the Manuels River Formation, from 20 m to 16.5 m below the basal conglomerate of the overlying Elliott Cove Formation. Its lower limit is estimated as being about 10 m above the upper limit of microflora A0-1, from which it is separated by barren strata. The age is Middle Cambrian, **Paradoxides hicksii** Zone.

Description

Taxa that appear in Microflora A0 are **Eliasum? hutchinsonii** and **Cristallinium cambriense** (Slavíková) Vanguestaine, 1978. The first of these is rare and, like Acritarch gen. et sp. nov., is restricted to the lowest 1.5 m of the microflora's vertical range. **Cristallinium cambriense** and **Eliasum llaniscum** are variably abundant and sometimes common. **Retisphaeridium** is rarely present.

Plate 57.2

Magnification of photographs x1000, except where otherwise stated.

Figures 1-5, 7, 9. **Eliasum? hutchinsonii** Martin sp. nov.* All from GSC loc. C-97979.

1, 2. GSC 72946, paratype. Fig. 1 x10 000
3, 9. GSC 72947, paratype. Fig. 3 x10 000
4, 5. GSC 72948, paratype. Fig. 5 x10 000
7. GSC 72949, holotype.

White lines on Figs. 2, 4 and 9 indicate portions of specimens shown enlarged in Figs. 1, 5 and 3 respectively.

Figures 6, 8, 10-15. **Eliasum llaniscum** Fombella, 1978.

6. GSC 72958, GSC loc. C-97991.
8. GSC 72959, GSC loc. C-97982.
10. GSC 72960, GSC loc. C-97992.
11. GSC 72961, GSC loc. C-97991.
12. GSC 72962, GSC loc. C-97993.
13. GSC 72963, GSC loc. C-97993.
14. GSC 72964, GSC loc. C-97992.
15. GSC 72965, GSC loc. C-97982.

*Described in text.

Plate 57.3


1

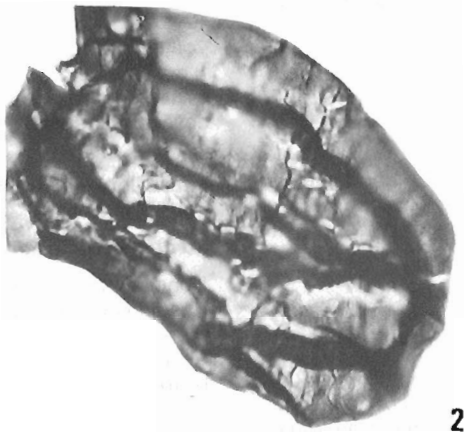
2

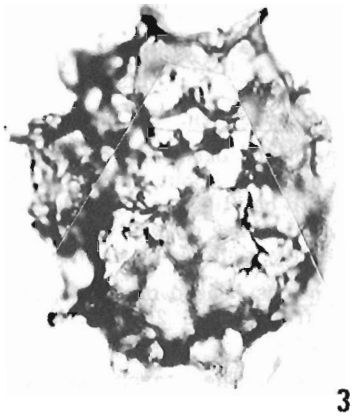
3


4

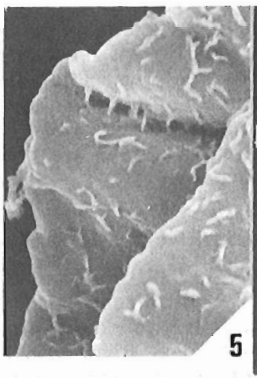
5


6

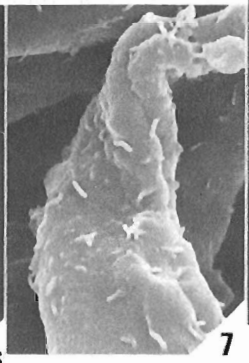
7

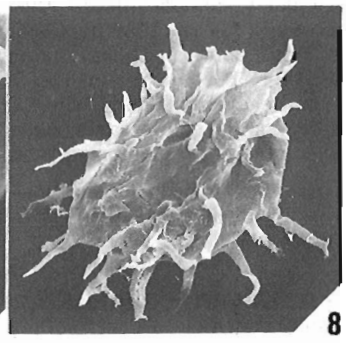
8

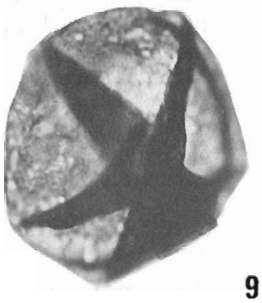
9

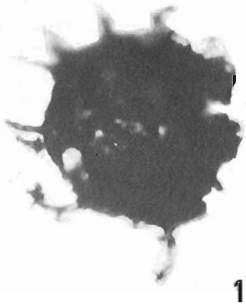
10

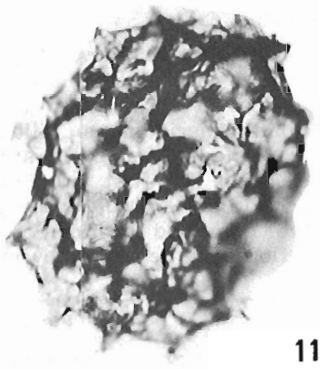
11

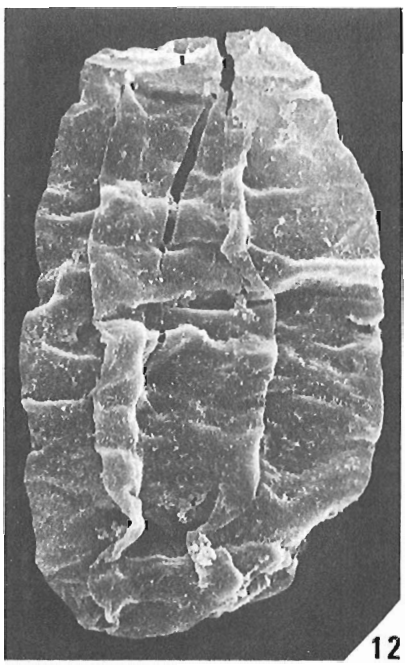
12


13

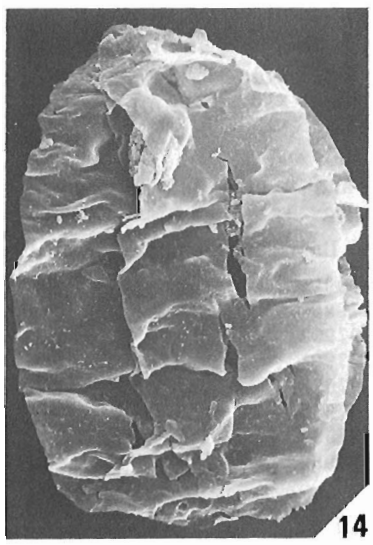
14


15

Table 57.1. Vertical distribution and abundance of acritarch genera and species in microfloras A0-1, A0 and A1 at measured section northwest of Weybridge

ACRITARCHS FROM RANDOM ISLAND	MIDDLE CAMBRIAN (in part)																					
	CHAMBERLAINS BROOK FM. (in part)												MANUELS RIVER FM. (in part)									
	GSC LOCALITIES																					
SPECIMENS PER SAMPLE: ○ = 1 (very rare) ● = 2-19 (rare) ○ = 20-100 (common) ● = > 100 (very common)	C.98002	C.98000	C.97999	C.97998	C.97996	C.97995	C.97994	C.97993	C.97992	C.97991	C.97988	C.97986	C.97982	C.97979	C.97978	C.97977	C.97976	C.97975	C.97973	C.97972	C.97971	C.97970
	MICROFLORAS																					
	?	A0-1									?		A0						A1			
LEIOSPHAERIDIA SP.	–	●	●	●	–	–	–	●	–	○	●	●	○	–	–	●	●	○	○	●	○	●
ELIASUM LLANISCUM	○	●	●	○	–	●	●	○	○	●	●	●	○	●	●	–	–	○	●	●	●	●
ACRITARCH GEN. ET SP. NOV.	–	●	–	○	●	●	○	●	●	●	–	●	○	●	–	–	–	–	–	–	–	–
RETISPHAERIDIUM HOWELLII	–	–	●	○	–	–	–	–	–	–	–	–	–	●	–	–	–	–	–	–	–	–
RETISPHAERIDIUM DICHAMERUM	–	–	●	●	–	●	–	●	○	–	–	–	–	–	–	–	–	–	–	–	–	–
ELIASUM JENNESSII	–	●	○	●	●	○	●	●	○	●	–	–	○ cf.	–	–	–	–	–	–	–	–	–
CYMATIOSPHAERA CRAMERI	–	●	–	–	–	○	○	–	●	–	–	–	–	–	–	–	–	–	–	–	–	–
MULTIPLICISPHAERIDIUM SP.	○	–	–	–	–	–	–	–	–	–	–	–	●	–	–	–	–	–	–	–	–	–
KILDINELLA SP.	–	●	–	–	–	–	–	–	–	–	–	–	●	–	–	–	–	–	–	–	–	–
TIMOFEEVIA SP.	–	–	–	–	–	–	○	–	–	–	–	–	–	–	●	–	–	–	–	–	–	–
ELIASUM? HUTCHINSONII	–	–	–	–	–	–	–	–	–	–	–	–	○	●	–	–	–	–	–	–	–	–
CRISTALLINIUM CAMBRIENSE	–	–	–	–	–	–	–	–	–	–	–	–	○	○	○	–	○	●	●	○	●	●
ADARA ALEA	–	–	–	–	–	–	–	–	–	–	–	–	–	–	–	–	–	–	○	–	○	●

Plate 57.3

Magnification of photographs x1000, except where otherwise stated.

Figures 1, 2, 4-7, 12-15. **Eliasum jennessii** Martin sp. nov.*

1. GSC loc. C-97992, GSC 72950, paratype.
2. GSC loc. C-97992, GSC 72951, paratype.
4. GSC loc. C-97993, GSC 72952, paratype.
5-7. GSC loc. C-97993, GSC 72953, holotype.

White line and arrow symbol on Fig. 6 indicate portions of specimen shown enlarged in Figs. 5 and 7 respectively. Figs. 5, 7, x10,000.

12. GSC loc. C-97993, GSC 72954, paratype, x1500.
13. GSC loc. C-97993, GSC 72955, paratype.
14. GSC loc. C-97993, GSC 72956, paratype, x1500.
15. GSC loc. C-97992, GSC 72957, paratype.

Figures 3, 11. **Adara alea** Martin in Martin and Dean, 1981.

3. GSC 72933, GSC loc. C-97971.
11. GSC 72934, GSC loc. C-97970.

Figure 8. **Multiplicisphaeridium** sp.* GSC 72967, GSC loc. C-97982, x1500.

Figure 9. **Kildinella** sp. GSC 72966, GSC loc. C-97982.

Figure 10. **Timofeevia** sp. GSC 72973, GSC loc. C-97978.

*Described in text.

Comparison

At Random Island (Martin and Dean, 1981) **Eliasum llaniscum** appears slightly higher, in microflora A1, of Middle Cambrian age (**Paradoxides hicksii** Zone in part and **Paradoxides davidis** Zone in part), but **Cristallinium cambriense** has an extended vertical range, from Middle Cambrian to Lower Tremadoc (**Parabolina argentina** Zone), in microfloras A1 to A6.

Microflora A1 (Adara alea – Eliasum llaniscum assemblage)

Stratigraphic position

The vertical range of microflora A1 has been confirmed as that indicated by Martin and Dean (1981), namely from 15.5 m to 10 m below the basal conglomerate of the Elliott Cove Formation. Its lower limit, 1 m above the upper limit of microflora A0, is located within the **Paradoxides hicksii** Zone; its upper limit lies between the **P. hicksii** Zone and the **P. davidis** Zone.

Description

Microflora A1 is characterized principally by **Adara alea, Eliasum llaniscum** and **Cristallinium cambriense.** The first of these is the only taxon whose vertical range coincides with that of microflora A1.

DISTRIBUTION OUTSIDE NEWFOUNDLAND OF SPECIES FROM MICROFLORAS A0-1, AND A1

F. Martin

Five of the eight named species present in the three microfloras are known outside Newfoundland. The holotype of **Retisphaeridium dichamerum** came from the **Albertella** Zone, lowest Middle Cambrian, in Alberta (Staplin et al., 1965). Downie (1982) recorded the species from the Gog Formation, Lower Cambrian, of Alberta and also from the Fucoid Beds in northwest Scotland and **Holmia** Shales in Norway. In the Cantabrian Cordillera, Spain, the vertical range of **R. dichamerum** and of **Eliasum llaniscum** in the Oville Formation is from lowest Middle Cambrian to the top of the Upper Cambrian – Tremadoc (undifferentiated) (Fombella, 1978, 1979); the holotype of **E. llaniscum** came from the lowest Middle Cambrian. According to Slavíková (1968) **Retisphaeridium howellii** (illustrated by her as **Retisphaeridium** sp. nov.) and **Cymatiosphaera crameri** are known from the upper part of the Middle Cambrian, **Ellipsocephalus hoffi** Subzone, in the Jince Formation of Czechoslovakia. Numerous occurrences of **Cristallinium cambriense** in Europe, the USSR and North Africa were listed by Martin (in Martin and Dean, 1981, p. 17) and its stratigraphic range is summarized below. On the basis of palynological dating of deposits containing **C. cambriense**, Jankauskas (1976) indicated that the species appears in the **Holmia** Zone, Lower Cambrian, in Estonia. Apart from this reference, the taxon is known particularly from the Middle Cambrian, the Upper Cambrian and, very rarely, the lower Tremadoc.

REFERENCES

Bergström, J. and Levi-Setti, R.
1978: Phenotypic variation in the Middle Cambrian trilobite **Paradoxides davidsi** Slater at Manuels, SE Newfoundland; Geologica et Palaeontologica, v. 72, p. 1-19.

Cowie, J.W., Rushton, A.W.A., and Stubblefield, C.J.
1972: A correlation of Cambrian rocks in the British Isles; Geological Society of London, Special Report No. 2, p. 1-40.

Downie, C.
1982: Lower Cambrian acritarchs from Scotland, Norway, Greenland and Canada; Transactions of the Royal Society of Edinburgh, Earth Sciences, v. 72, (for 1981), p. 257-285.

Eisenack, A.
1965: Die Mikrofauna der Ostseekalk 1; Chitinozoen, Hystrichosphären; Neues Jahrbuch für Geologie und Paläontologie, Abhandlungen, Stuttgart, v. 133, p. 245-266.

Fombella, M.A.
1977: Acritarchos de Edad Cambrico Medio-Inferior de la Provincia de León, España; Revista Espanola de Micropaleontologia, v. 9, p. 115-124.

1978: Acritarchos de la Formación Oville, Edada Cambrico Medio-Tremadoc, Provincia de León, España; Palinologia, Número extraordinario 1, p. 245-261.

1979: Palinologia de la Formación Oville al norte y Sur de la Cantábrica, España; Palinologia, v. 1, p. 1-16.

Gardiner, P.R.R. and Vanguestaine, M.
1971: Cambrian and Ordovician microfossils from southeast Ireland and their implications; Ireland, Geological Survey, Bulletin, v. 1, p. 163-210.

Howell, B.F.
1925: The faunas of the Cambrian **Paradoxides** Beds at Manuels, Newfoundland; Bulletin of American Paleontology, v. 11, no. 43, p. 1-140.

Hutchinson, R.D.
1962: Cambrian stratigraphy and trilobite faunas of southeastern Newfoundland; Geological Survey of Canada, Bulletin 88, 156 p.

Jankauskas, T.
1976: New acritarch species from the Lower Cambrian of the Prebaltic area; Memoir, Institute Geology, Geophysics, Academy of Sciences, USSR, Siberian Branch, v. 296, p. 187-191 (in Russian).

Martin, F. and Dean, W.T.
1981: Middle and Upper Cambrian and Lower Ordovician acritarchs from Random Island, eastern Newfoundland; Geological Survey of Canada, Bulletin 343, 43 p.

1983: Late Lower Cambrian and early Middle Cambrian acritarchs from Manuels River, eastern Newfoundland; Geological Survey of Canada, Paper 83-1B, p. 353-363.

Sdzuy, K.
1971: La subdivision bioestratigrafica y la correlacion del Cámbrico medio de España; Congreso Hispano Luso Americano de Geológia Económica, Trabajos, v. 2, sección I, p. 769-782.

Slavíková, K.
1968: New finds of acritarchs in the Middle Cambrian of the Barrandian (Czechoslovakia); Vestník Ústredního Ústavu Geologíckeho, v. 43, p. 199-205.

Snajdr, M.
1958: Trilobit Ceského Sredního Kambria; Rozpravy Ústredního Ústavu Geologíckeho, no. 24, p. 1-236 (in Czech), p. 237-280 (English summary).

Staplin, F.L., Jansonius, J., and Pocock, S.A.J.
1965: Evaluation of some acritarchous Hystrichosphère genera; Neues Jahrbuch für Geologie and Palontologie, v. 123, p. 167-201.

Vanguestaine, M.
1978: Critères palynostratigraphiques conduisant à la reconnaissance d'un pli couché Revinien dans le sondage de Grand-Halleux; Annales de la Societé Géologique de Belgique, v. 100 (1977), p. 249-276.

Volková, N.A.
1968: Acritarchs of Precambrian and Cambrian deposits of Estonia; p. 1-37 in Problematics of Riphean and Cambrian layers of the Russian Platform, Urals and Kazakhstan, Academy of Sciences of USSR, Transactions, v. 188 (in Russian).

Westergård, A.H.
1946: Agnostidea of the Middle Cambrian of Sweden; Sveriges Geologiska Undersökning, ser. C. no. 477, 140 p.

58. NEW ORDOVICIAN (TREMADOC) ACRITARCH TAXA FROM THE MIDDLE MEMBER OF THE SURVEY PEAK FORMATION AT WILCOX PASS, SOUTHERN CANADIAN ROCKY MOUNTAINS, ALBERTA

Project 500029

F. Martin[1]
Institute of Sedimentary and Petroleum Geology

Martin, F., New Ordovician (Tremadoc) acritarch taxa from the middle member of the Survey Peak Formation at Wilcox Pass, southern Canadian Rocky Mountains, Alberta; in Current Research, Part A, Geological Survey of Canada, Paper 84-1A, p. 441-448, 1984.

Abstract

The association of ***Aremoricanium? grootaertii*** *sp. nov.,* ***Athabascaella playfordii*** *gen. et sp. nov. and* ***A. rossii*** *gen. et sp. nov. characterizes the upper part of the middle member of the Survey Peak Formation at Wilcox Pass, Alberta. The rocks containing these acritarchs have not yielded macrofossils but are located between strata correlated by means of trilobites with letter zones D and E, upper Tremadoc, in Utah and Nevada.*

Résumé

*L'association d'****Aremoricanium? grootaertii*** *sp. nov.* ***Athabascaella playfordii*** *gen. et sp. nov. et* ***A. rossii*** *gen. et sp. nov. caractérise las partie supérieure du membre moyen de la Formation Survey Peak au défilé de Wilcox, Alberta. Les dépôts contenant ces acritarches sont dépourvus de macrofossils et localisés entre les zones à trilobites du Trémadoc supérieur désignées dans l'Utah et le Nevada par les lettres D et E.*

INTRODUCTION

The location (Fig. 58.1) and lithostratigraphy of the Wilcox Pass section, situated 3 km north of the Athabasca Glacier in the southern Canadian Rocky Mountains, between Banff and Jasper, has been reviewed by Dean (1978; in Dean and Martin, 1982). The relevant succession, well exposed and unfaulted, ranges in age from Upper Cambrian to Lower Ordovician and comprises, in ascending order, the Survey Peak Formation, Outram Formation and Skoki Formation in terms of the lithostratigraphy established by Aitken and Norford (1967).

The new acritarch taxa, **Aremoricanium? grootaertii** sp. nov., **Athabascaella playfordii** gen. et sp. nov. and **A. rossii** gen. et sp. nov., were obtained from three samples from the upper part of the middle member of the Survey Peak Formation. The samples were collected in summer, 1981 as part of Geological Survey of Canada Project 500029. The association is characteristic of assemblages devoid of Diacrodians in the upper, but not uppermost, Tremadoc. It is found in calcareous shales at GSC locs. C-97832, C-97833 and C-97834, the levels of which are, respectively, 134.6 m, 136.4 m and 141.8 m above the base of the middle member,

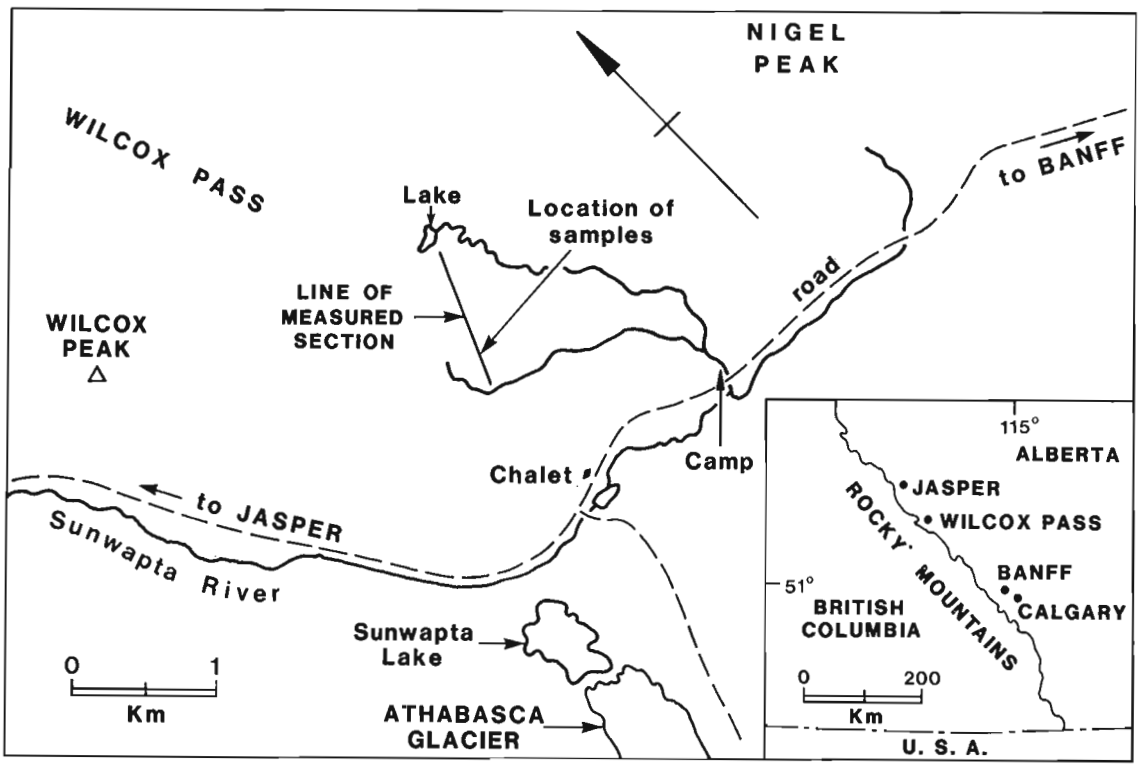

Figure 58.1. Location of described samples at Wilcox Pass.

[1] Département de Paléontologie, Institut Royal des Sciences Naturelles de Belgique, rue Vautier, 29, B- 1040 Bruxelles, Belgium

which is 199 m thick at this location. The sample sites are all within a 36 m interval of conglomerates and grey, calcareous, silty shales from which no macrofossils were obtained by Dean (1978, p. 6, Fig. 4, "no faunal evidence" interval). Strata below the 36 m interval were assigned by Dean (in Dean and Martin, 1982) to trilobite Zone D (Ross, 1949, 1951), known also as the **Leiostegium – Kainella** Zone (Hintze, 1953) in terms of the biostratigraphic units established in Utah and Nevada. Strata above the 36 m interval contain the trilobites **Paenebeltella** sp. and **Leiostegium (Evansaspis) ceratopygoides** (Raymond, 1925) and are assigned to Ross's (1949, 1951) trilobite Zone E, known also as the **Tesselacauda** Zone (Hintze, 1953).

The acritarchs, numbering some tens to about a hundred per gram of rock, are variably preserved, commonly dark with incomplete processes and observable in detail only under the scanning electron microscope. All the figured specimens, including those coated with gold for SEM examination, are permanently mounted in Canada balsam and are accompanied by coordinates established with the England Finder Graticule. They are deposited (GSC type nos. 72993-73014) in the type fossil collection of the Geological Survey of Canada, Ottawa; supplementary preparations are deposited in the Département de Paléontologie, Institut Royal des Sciences Naturelles de Belgique, Brussels.

Acknowledgments

A permit to collect samples was granted by the Director of the Western Region, Parks Canada. Dr. P. Grootaert (Institut Royal des Sciences Naturelles de Belgique) took the SEM photographs.

SYSTEMATIC DESCRIPTIONS

Genus **Aremoricanium** Deunff, 1955

Type species: **Aremoricanium rigaudae** Deunff, 1955 by original designation.

Aremoricanium? grootaertii sp. nov.
Plate 58.1, figures 1-9; Plate 58.2, figures 1-4

Acritarch gen. et sp. nov. A, Martin (in Dean and Martin, 1982, p. 138, Pl. 1, fig. 13).

Holotype. GSC 72998 (Pl. 58.1, figs. 8, 9).

Paratypes. GSC 72993 (Pl. 58.1, fig. 1), GSC 72994 (Pl. 58.1, fig. 2), GSC 72995 (Pl. 58.1, fig. 3), GSC 72996 (Pl. 58.1, figs. 4, 7), GSC 72997 (Pl. 58.1, figs. 5, 6), GSC 72999 (Pl. 58.2, fig. 1), GSC 73000 (Pl. 58.2, fig. 2), GSC 73001 (Pl. 58.2, fig. 3), GSC 73002 (Pl. 58.2, fig. 4).

Type locality and horizon. GSC loc. C-97833, Wilcox Pass. Survey Peak Formation, calcareous shale 136.4 m above base of middle member. Age is late Tremadoc.

Diagnosis. Based on one hundred specimens. Central body globular in both polar and lateral view. Orientated laterally, specimens show a prominent so-called apical tubular extension with a circular distal opening; the basal diameter of the extension is usually between one quarter and one third of the diameter of the central body. No operculum has been observed. The wall of the central body is very dark; a double membrane is observable only on damaged tubular extensions. The external surface is densely covered with small, simple spines, the tips of which are generally blunt; the surface of the tubular extension tends to exhibit fine longitudinal folds. About sixty to a hundred flexible appendices are distributed over all the surface except that of the tubular extension; they are a little more numerous on the so-called antapical pole. The appendices are usually entirely filled with an opaque substance and, if present the internal cavity never communicates with that of the central body. The base of each is cylindrical or very slightly conical, frequently ornamented with fine, longitudinal folds; the distal extremity is divided into two or four narrow straps which anastomose with those of neighbouring appendices.

Dimensions. Based on forty specimens. Diameter of central body from 35 to 56 µm; length and maximum breadth of tubular extension from 5 to 15 µm and from 15 to 18 µm respectively; length and breadth of trunk of processes from 5 to 10 µm and from 1.5 to 2 µm respectively; length of spines 0.5 µm, exceptionally 0.7 µm.

Discussion. According to observations on material in thin section from the Llanvirn (Henry, 1969, p. 78) and lower Caradoc (Deunff, 1955, p. 228, 229; 1959, p. 32; Henry, 1969, p. 89) of Brittany, France, **Aremoricanium** possesses a central body formed of two distinct layers. The internal layer, delimiting the internal cavity, shows a perforation, the position of which coincides with that of the tubular extension formed by the external layer. The external layer alone forms processes that are wide and hollow in their proximal portion and tapered and solid distally. Loeblich and MacAdam (1971) studied, by means of both the optical microscope and the SEM, Ordovician specimens of **Aremoricanium** from Oklahoma, Indiana and Ohio; they showed that the central body is composed of a single membrane which forms both the tubular extension and the processes. The processes vary considerably in form, depending on the species, but they are rarely divided. Loeblich and MacAdam suggested that the observations of Deunff and of Henry (loc. cit.) are based on

---

Plate 58.1

Figures 1-9. **Aremoricanium? grootaertii** sp. nov. Figures 1-7: paratypes. Figures 8, 9: holotypes.

Figure 1. GSC loc. C-97834, GSC 72993, lateral view, x1000.

Figures 2, 3. GSC loc. C-97832, Detail of processes.
2. GSC 72994, x1000.
3. GSC 72995, x1000.

Figures 4, 7. GSC loc. C-97834, GSC 72996.
4. Lateral view, x1500.
7. Detail of lower part, x5000.

Figures 5, 6. GSC loc. C-97834, GSC 72997.
5. Polar view, x1000.
6. Detail of lower part, x10 000.

Figures 8, 9. GSC loc. C-97833, GSC 72998.
8. Lateral view, x1500.
9. Detail of lower part, x5000.

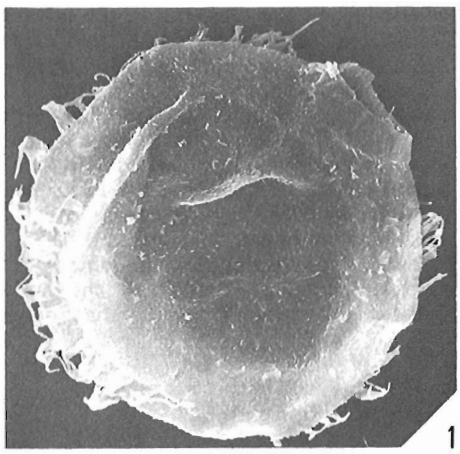
1


2


3

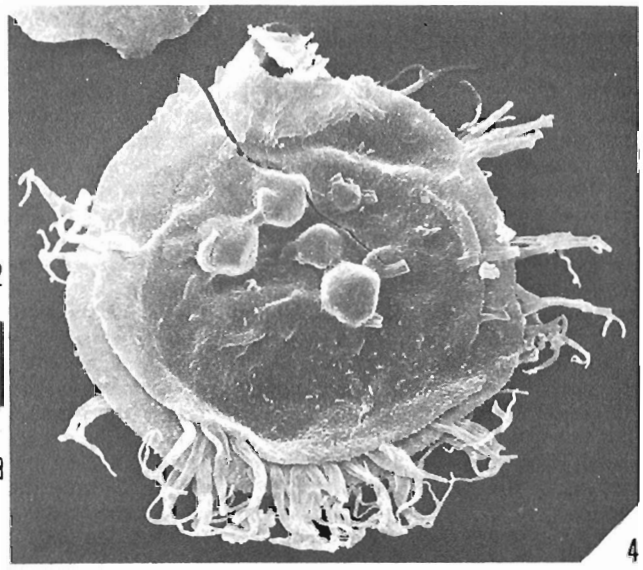
4

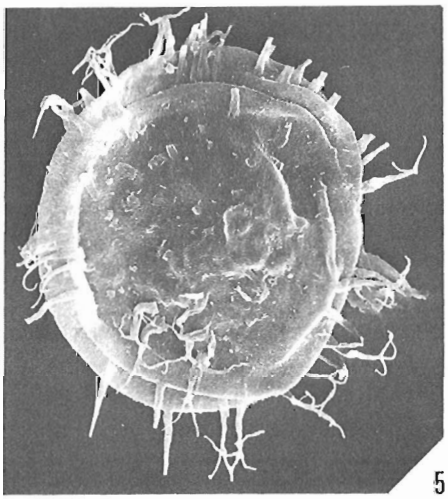
5

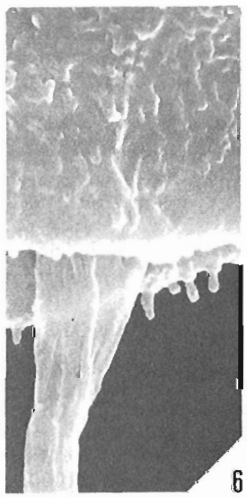
6

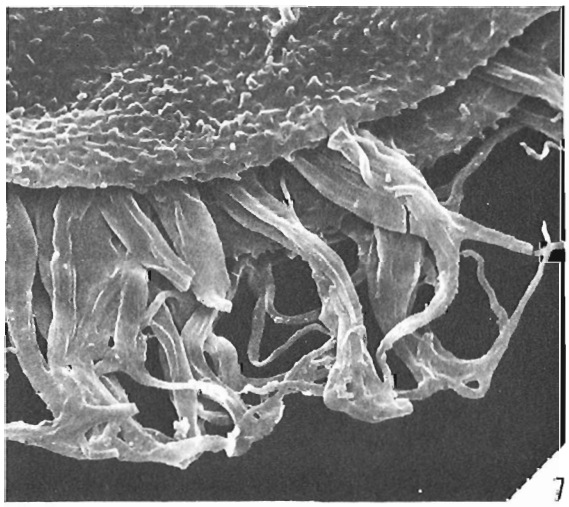
7

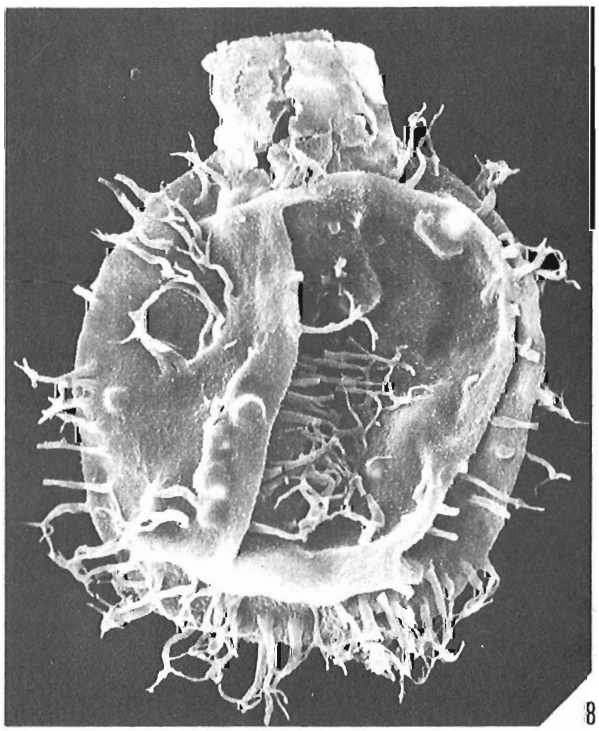
8

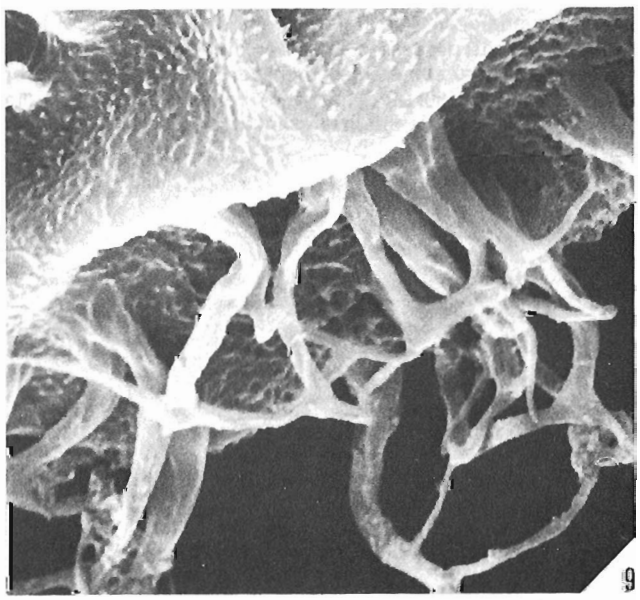
9

artifacts resulting from petrographic preparation. No internal layer was observed in transparent specimens of the genus from the upper Ordovician (Martin, 1980) and lower Silurian (Achab, 1976) of the Gaspé area, Quebec. Examination of **Aremoricanium rigaudea** from the Llanvirn and Llandeilo of Gotland (Kjellström, 1976) and the lower Caradoc of Portugal (Elaouad-Debbaj and Henry, 1980; Elaouad-Debbaj, 1981) indicates the presence of a central body composed of two distinct layers. These divergent opinions on the presence or absence of an internal central layer depend, perhaps, on the state of maturation of the microorganism or the state of preservation of the microfossil. Such is the case for **Visbysphaera** n. sp. A from the Frasnian of Belgium (Martin, 1982). In the specimens from Wilcox Pass a double membrane is locally visible on the tubular extension and not on the central body, in its strict sense. This observation and, particularly, the form of distal ramification of the generally entirely solid appendices justify the doubtful generic assignment. **Aremoricanium? grootaertii** differs from other known species of the genus in having relatively well developed ornamentation of the central body and in the form of division of the appendices. Superficially the ramification of the appendices recalls that of **Skiagia scottica** Downie, 1982, from the Lower Cambrian of Scotland, Norway and Greenland, a taxon distinguished by its hollow appendices, the tips of which, widened, funnel-shaped and often joined to one another, are only rarely subdivided further.

Occurrence. Relatively abundant at GSC locs. C-97832, C-97833 and C-97834. Present also in the middle member of the Survey Peak Formation at levels 86 m (GSC loc. 92244, in trilobite letter zone D) and 171.3 m (GSC loc. 92256, in trilobite letter zone E) above the base of the member (Martin in Dean and Martin, 1982).

Genus **Athabascaella** gen. nov.

Type species: **Athabascaella playfordii** sp. nov., here designated.

Other species of the genus: **A. rossii** sp. nov.

Diagnosis. Central body globular, with circular outline, lacking opening and with wall formed apparently of a single layer. The surface carries very numerous, well differentiated processes entirely filled with an opaque substance that clearly isolates them at the base from the internal cavity of the central body. The distal extremities of the processes are divided to form a bunch of ramifications to the third or fourth order; the tips are either slightly widened and slightly rounded, or elongated and anastomosed with those of adjacent appendices. The slightly conical or cylindrical lower parts of adjacent processes may be joined to each other by lateral expansions, sometimes incorporated in a transparent membrane. The surface of the central body and the appendices is smooth or slightly granulate.

Comparisons. **Athabascaella** gen. nov. differs from **Cymatiogalea** Deunff, 1961 emend. Deunff et al., 1974 and from **Stelliferidium** Deunff et al., 1974, both of which are known from the Tremadocian to the Llanvirn, in the mode of ramification of the always solid appendices and in the absence of a polar opening. The central body is distinguished from those of **Cymatiogalea** and **Stelliferidium** by, respectively, the absence of polygonal fields and of radiating ridges at the base of the processes. In **Tunisphaeridium** Deunff and Evitt, 1968, known from late Ordovician to late Devonian, only the distal extremities and not the lower parts of appendices are interconnected by a mesh of fine, anastomosed filaments. In **Timofeevia** Vanguestaine, 1978, of middle Cambrian to early Tremadoc age, the central body shows variably developed polygonal fields and the hollow interior of the processes communicates with that of the central body.

Athabascaella playfordii gen et sp. nov.
Plate 58.3, figures 1-9

Holotype. GSC 73007 (Pl. 58.3, fig. 7).

Paratypes. GSC 73003 (Pl. 58.3, figs. 1, 2), GSC 73004 (Pl. 58.3, fig. 3), GSC 73005 (Pl. 58.3, figs. 4, 5), GSC 73006 (Pl. 58.3, fig. 6), GSC 73008 (Pl. 58.3, fig. 8), GSC 73009 (Pl. 58.3, fig. 9).

Plate 58.2

Figures 1-4. **Aremoricanium? grootaertii** sp. nov. Paratypes.
1. GSC loc. C-97832, GSC 72999, Lateral view, x1000.
2, 3. GSC loc. C-97833.
2. GSC 73000, Polar view, x1000.
3. GSC 73001, Lateral view, x1000.
4. GSC loc. C-97834, GSC 73002, Polar view, x1000.

Figures 5-12. **Athabascaella rossii** gen. et sp. nov. Figures 5-9, 11: paratypes. Figures 10, 12: holotype.

Figures 5, 8. GSC loc. C-97834, GSC 73010.
5. Detail of upper right part, x5000.
8. x1000.

Figure 6. GSC loc. C-97832, GSC 73011, Detail of processes, x1000.

Figure 7. GSC loc. C-97832, GSC 73012, x1000.

Figure 9, 11. GSC loc. C-97834, GSC 73013.
9. x1000.
11. Detail of upper part with fragment of transparent membrane on the left, x5000.

Figures 10, 12. GSC loc. C-97834, GSC 73014.
10. x1000.
12. Detail of upper part. Lateral trabeculae and transparent membrane between the trunks of the processes, x5000.

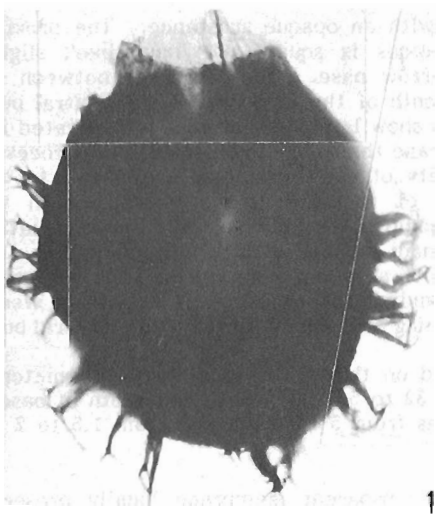
1

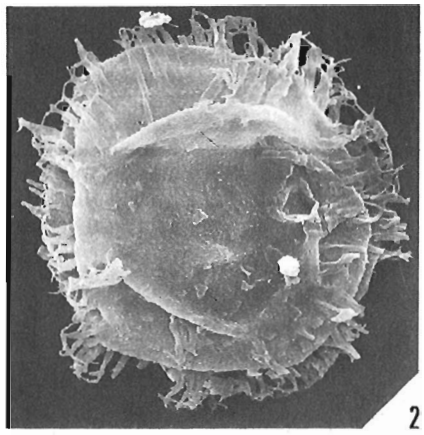
2

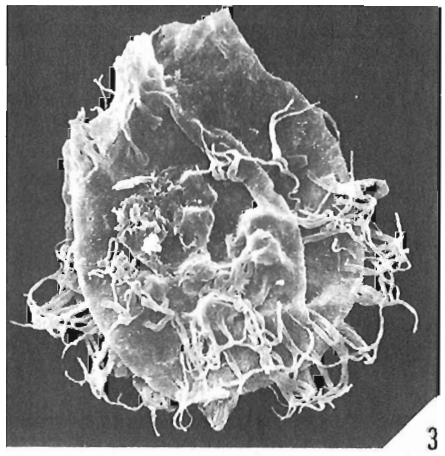
3

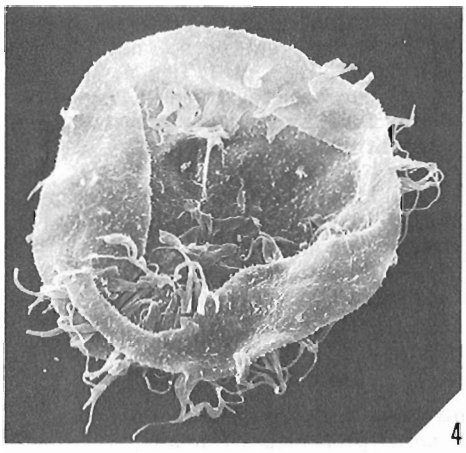
4

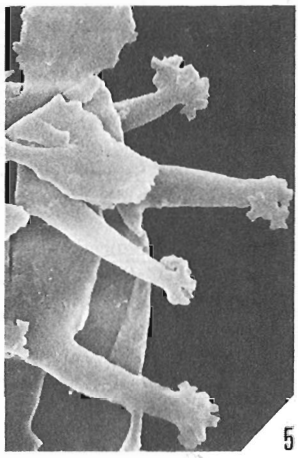
5


6

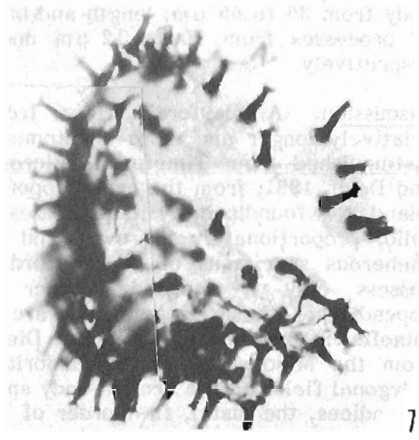
7

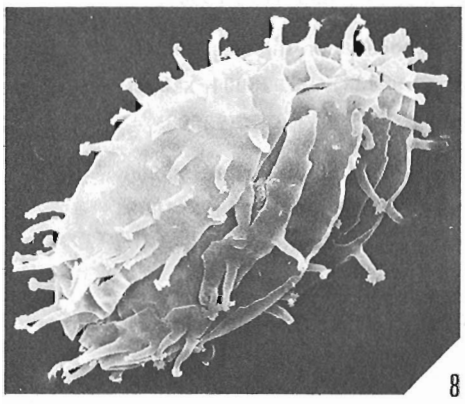
8

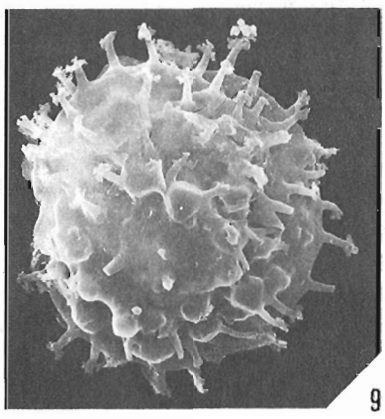
9

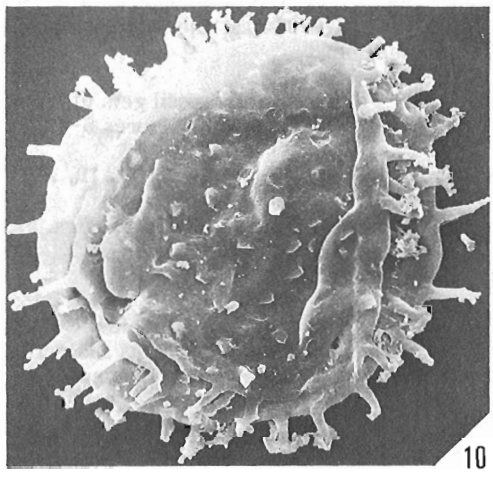
10

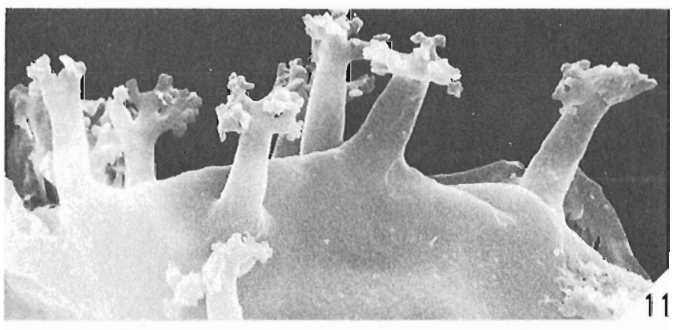
11

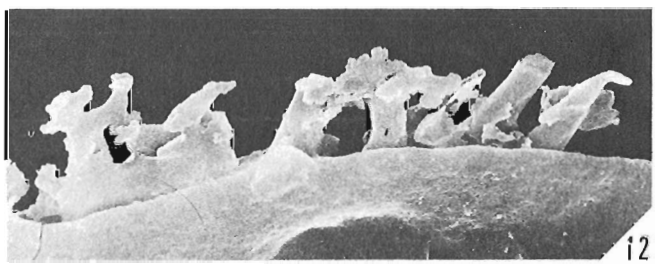
12

Type locality and horizon. GSC loc. C-97833, Wilcox Pass. Survey Peak Formation, calcareous shale 136.4 m above base of middle member. Age is late Tremadoc.

Diagnosis. Based on one hundred and twenty specimens. Central body globular with circular outline, formed apparently of a single layer. The external surface carries about eighty-five to one hundred well differentiated processes that are completely filled with an opaque substance. The lower part of the appendices, sometimes joined by lateral trabeculae, has a slightly conical, trunk-like form, with a narrow base and a length of between one sixth and one third the diameter of the central body. The distal extremity of the processes is ramified, generally from the same level, into two or, usually, three divisions of the first order which are themselves subdivided to the fourth order. The tips are slightly widened and rounded or are prolonged as fine reticulated branches that anastomose with those of adjacent appendices. The surface of the central body and of the processes is smooth or slightly granulate. No opening has been observed on the central body.

Dimensions. Based on forty specimens. Diameter of central body from 35 to 65 µm; length and breadth of base of trunk of processes from 10 to 12 µm and from 1.5 to 2 µm respectively.

Discussion. **A. playfordii** differs from **A. rossii** in having relatively longer and more anastomosed appendices. It is distinguished from **Timofeevia microretis** Martin in Martin and Dean, 1981, from the early Upper Cambrian of Random Island, Newfoundland, by its processes, which are completely solid, proportionately narrower and better differentiated. Numerous specimens of **A. playfordi** are incomplete and possess only a reduced number of non-anastomosed appendices; these specimens are distinguished from **Timofeevia lancarae** (Cramer and Diez) Vanguestaine, 1978, from the Middle and Upper Cambrian, by the absence of polygonal fields on the central body and by the entirely solid appendices, the distal, first order of which, are shorter and finer, and generally start from the same level.

Occurrence. Relatively abundant at GSC locs. C-97832, C-97833 and C-97834, in the middle member of the Survey Peak Formation.

Athabascaella rossii gen. et sp. nov.
Plate 58.2, figures 5-12

Holotype. GSC 73014 (Pl. 58.2, figs. 10, 12).

Paratypes. GSC 73010 (Pl. 58.2, figs. 5, 8), GSC 73011 (Pl. 58.2, fig. 6), GSC 73012 (Pl. 58.2, fig. 7), GSC 73013 (Pl. 58.2, figs. 9, 11).

Type locality and horizon. GSC loc. C-97834, Wilcox Pass. Survey Peak Formation, calcareous shale 141.8 m above base of middle member. Age is late Tremadoc.

Diagnosis. Based on sixty specimens. Central body globular with circular outline, formed apparently of a single layer. The surface carries about a hundred processes that are completely filled with an opaque substance. The proximal part of the processes is squat, and 'trunk-like', slightly conical with a narrow base. The length is between one seventh and one tenth of the diameter of the central body. Locally, the trunks show lateral expansions incorporated in a transparent membrane that joins together adjacent processes. The distal extremity of each appendice shows two to four short subdivisions of the first order which are in turn generally subdivided up to the fourth order. The terminations are variably widened and rounded; locally they may show expansions that unite adjoining appendices. The surface of the central body and of the processes is smooth or weakly granulate. No opening has been observed on the central body.

Dimensions. Based on thirty-five specimens. Diameter of central body from 32 to 59 µm; length and width of base of trunk of appendices from 5 to 6 µm and from 1.5 to 2 µm respectively.

Discussion. The transparent membrane locally preserved between the processes of **A. rossii** differs from that in species of **Cymatiogalea** and **Stelliferidium** by its incorporation of lateral expansions of the trunk of the processes. **A. rossii** is distinguished from Acritarch gen. et sp. nov. B (Martin in Dean and Martin, 1982, p. 138, pl. 1, figs. 4, 7), from the middle member of the Survey Peak Formation at GSC loc. 92256, Wilcox Pass, by its more robust appendices, which show expansions at the level of the trunk.

Occurrence. Relatively abundant at GSC locs. C-97832, C-97833 and C-97834. Very rare at GSC loc. 92256, 171.3 m above the base of the middle member.

Plate 58.3

Figures 1-9. **Athabascaella playfordii** gen. et sp. nov.
Figures 1-6, 8, 9: paratypes. Figure 7: holotype.

Figures 1, 2. GSC loc. C-97833, GSC 73003.
1. x1000.
2. Detail of processes on the left, x5000.

Figure 3. GSC loc. C-97833, GSC 73004, x1500.

Figures 4, 5. GSC loc. C-97833, GSC 73005.
4. x1000.
5. Detail of processes on the right, x5000.

Figure 6. GSC loc. C-97832, GSC 73006, x1000.

Figures 7, 8, 9. GSC loc. C-97833.
7. GSC 73007, x1500.
8. GSC 73008, x1000.
9. GSC 73009, x1000.

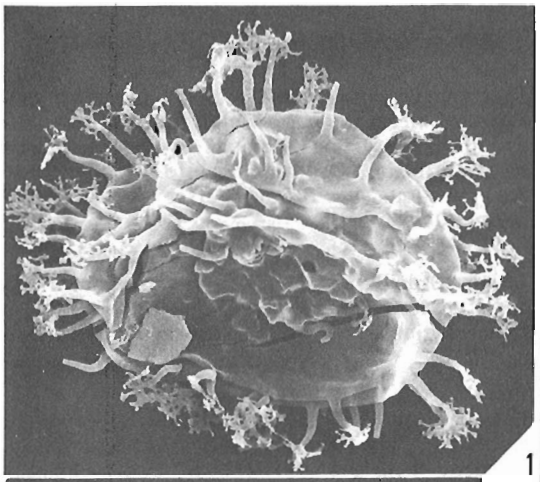
1

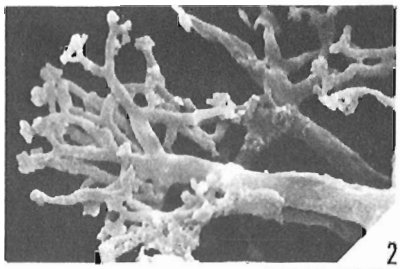
2

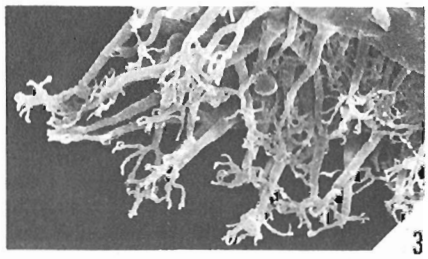
3

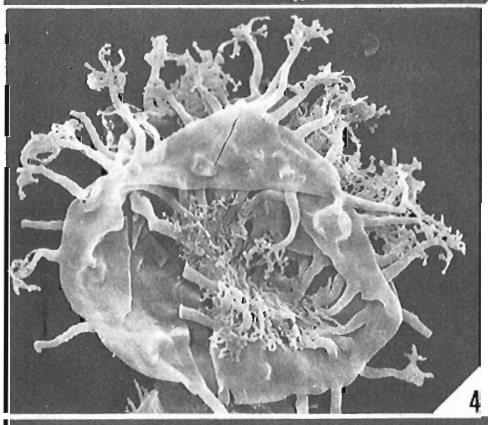
4

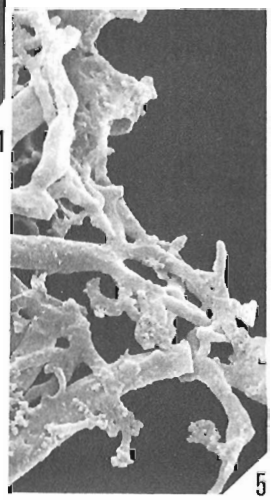
5

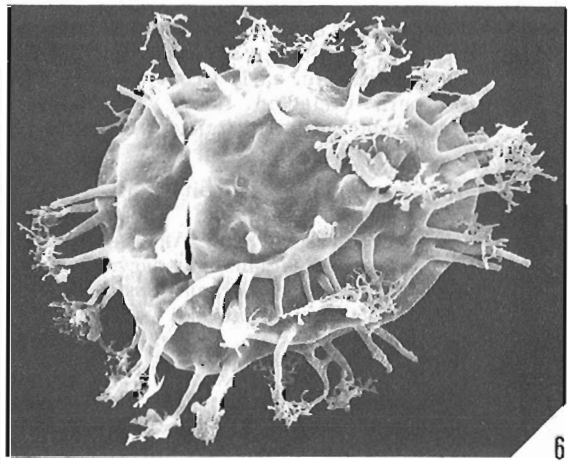
6

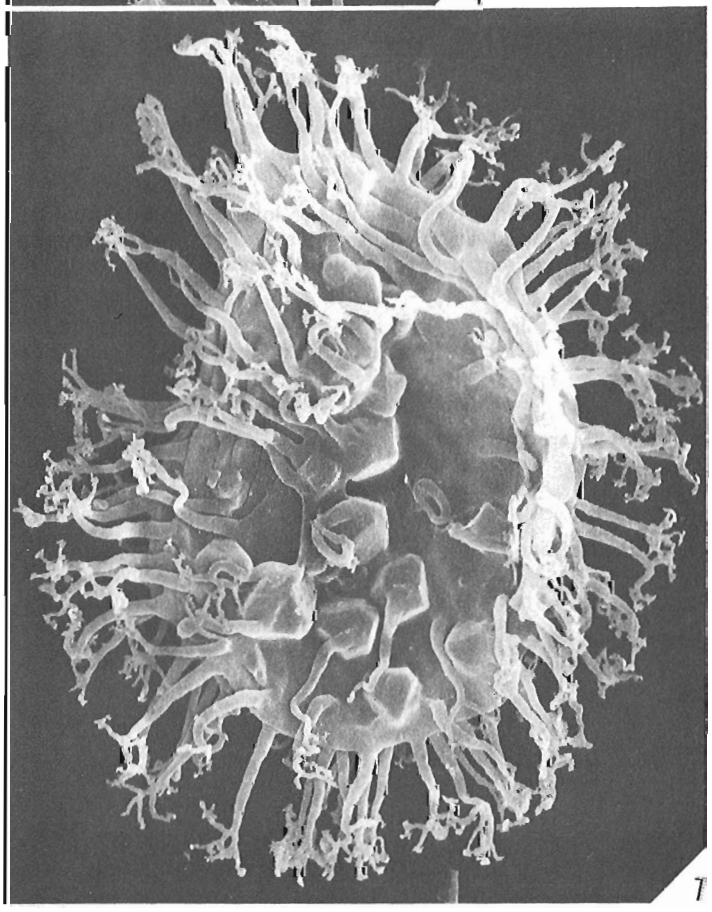
7

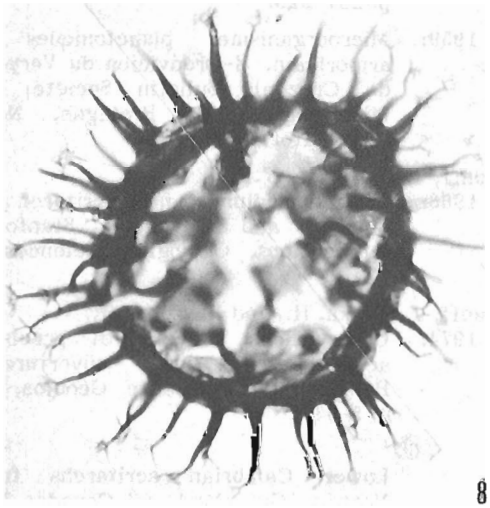
8

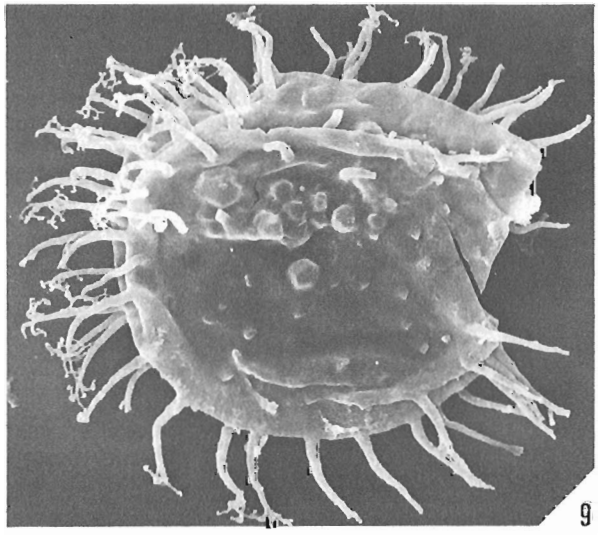
9

REFERENCES

Achab, A.
1976: Les acritarches de la Formation d'Awantjish (Llandovérien supérieur) du sondage Val Brilliant, Vallée de la Matapédia, Québec; Canadian Journal of Earth Sciences, v. 13, p. 1310-1318.

Aitken, J.D. and Norford, B.S.
1967: Lower Ordovician Survey Peak and Outram Formations, southern Rocky Mountains of Alberta; Bulletin of Canadian Petroleum Geology, v. 15, p. 150-207.

Dean, W.T.
1978: Preliminary account of the trilobite biostratigraphy of the Survey Peak and Outram Formations (late Cambrian, early Ordovician) at Wilcox Pass, southern Canadian Rocky Mountains, Alberta; Geological Survey of Canada, Paper 73-64, 10 p.

Dean, W.T. and Martin, F.
1982: The sequence of trilobite faunas and acritarch microfloras at the Cambrian-Ordovician boundary, Wilcox Pass, Alberta, Canada; in The Cambrian-Ordovician boundary: sections, fossil distributions and correlations, ed. M.G. Bassett and W.T. Dean; National Museum of Wales, Geological Series No. 3, Cardiff, p. 131-140.

Deunff, J.
1955: **Aremoricanium**, genre nouveau d'Hystrichosphères du Silurien breton; Société Géologique de France, Compte-rendu sommaire des Séances, no. 12, p. 227-229.

1959: Microorganismes planctoniques du Primaire armoricain. I-Ordovicien du Veryac'h (Presqu'île de Crozon); Bulletin Société Géologique et Minéralogique de Bretagne, Nouvelle Série, fasc. 2 (for 1958), 41 p.

Deunff, J. and Evitt, W.R.
1968: **Tunisphaeridium**, a new acritarch genus from the Silurian and Devonian; Stanford University Publications, Geological Sciences, v. 12, no. 1, 13 p.

Deunff, J., Górka, H., and Rauscher, R.
1974: Observations nouvelle et précisions sur less acritarches à large ouverture polaire du Paléozoique Inférieur; Geobios, v. 7, fasc. 1, p. 5-33.

Downie, C.
1982: Lower Cambrian acritarchs from Scotland, Norway, Greenland and Canada; Transactions of the Royal Society of Edinburgh, Earth Sciences, v. 72 (for 1981), p. 257-285.

Elaouad-Debbaj, Z.
1981: Acritarches de l'Ordovicien Supérieur du Synclinal de Buçaco (Portugal). Systématique-Biostraigraphie-Intérêt paléogéographique; Bulletin Société Géologique et Minéralogique de Bretagne, C, X (for 1978), 101 p.

Elaouad-Debbaj, Z. and Henry, J.L.
1980: Structure de la paroi de **Aremoricanium rigaudae** Deunff, 1955 (acritarches, Ordovicien); Geobios, no. 13, p. 627-632.

Henry, J.L.
1969: Micro-organismes incertae sedis (acritarches et chitinozoaires) de l'Ordovicien de la presqu'île de Crozon (Finistère): Gisement de Mort-Anglaise et de Kerglintin; Bulletin Société Géologique et Minéralogique de Bretagne (for 1968), Nouvelle Série, 100 p.

Hintze, L.F.
1953: Lower Ordovician trilobites from western Utah and eastern Nevada; Utah Geological and Mineralogical Survey, Bulletin 48 (for 1952), p. 1-249.

Kjellström, G.
1976: Lower Viruan (Middle Ordovician) microplankton from the Ekön borehole no. 1 in ÖsterGotland, Sweden; Sveriges Geologiska Undersökning, C, no. 724, 44 p.

Loeblich, A.R., Jr. and MacAdam, R.B.
1971: North American species of the Ordovician acritarch genus **Aremoricanium**; Palaeontographica, B, v. 135, p. 41-47.

Martin, F.
1980: Quelques chitinozoaires et acritarches Ordoviciens supérieurs de la Formation de White Head en Gaspésie; Canadian Journal of Earth Sciences, v. 17, p. 106-119.

1982: Acritarches et chitinozoaires de la partie supérieure du Frasnien dans un affleurement au nord immédiat de Frasnes (Belgique); Institut Royal des Sciences Naturelles de Belgique, Bulletin, Sciences de la Terre, v. 54, no. 2, 17 p.

Martin, F. and Dean, W.T.
1981: Middle and Upper Cambrian and Lower Ordovician acritarchs from Random Island, eastern Newfoundland; Geological Survey of Canada, Bulletin 343, 43 p.

Raymond, P.E.
1925: Some trilobites of the lower Middle Ordovician of eastern North America; Bulletin of the Museum of Comparative Zoology, Harvard Univerisity, v. 67, 180 p.

Ross, R.J., Jr.
1949: Stratigraphy and trilobite faunal zones of the Garden City Formation, northwestern Utah; American Journal of Science, v. 247, p. 472-491.

1951: Stratigraphy of the Garden City Formation in northeastern Utah, and its trilobite faunas; Peabody Museum of Natural History, Yale University, Bulletin 6, 161 p.

Vanguestaine, M.
1978: Critères palynostratigraphiques conduisant à la reconnaissance d'un pli couché revinien dans le sondage de Grand-Halleux; Annales Société Géologique de Belgique, v. 100 (1977), p. 249-276.

59. DEVONIAN RUGOSE CORAL BIOSTRATIGRAPHY WITH SPECIAL REFERENCE TO THE LOWER-MIDDLE DEVONIAN BOUNDARY

Project 680093

William A. Oliver, Jr.[1], and A.E.H. Pedder
Institute of Sedimentary and Petroleum Geology

Oliver, W.A., Jr. and Pedder, A.E.H., Devonian rugose coral biostratigraphy with special reference to the Lower-Middle Devonian boundary; in Current Research, Part A, Geological Survey of Canada, Paper 84-1A, p. 449-452, 1984.

Abstract

Although corals have negligible value in worldwide or intercontinental correlation, they have been successfully used for correlation within basins or biogeographic provinces. The factors responsible for their limited value in correlation make them excellent indices of environment and provinciality.

Analysis of the distribution of over 300 genera of Devonian rugose corals in 20 regions of the world and in six stages shows a maximum of endemicity and provinciality in the late Early Devonian. Because of this, corals are of least value in Devonian correlations near the Lower-Middle boundary. They are more useful in the Lochkovian, Givetian and Frasnian than in the intervening Pragian to Couvinian stages.

Résumé

Bien que les coraux soient peu utiles aux fins de la corrélation mondiale ou intercontinentale des sédiments, ils permettent d'établir des corrélations au sein de bassins ou de provinces biogéographiques. Les facteurs qui, d'une part, limitent leur valeur pour la corrélation font, d'autre part, des coraux d'excellents indices de la nature du milieu et de la provincialité.

L'analyse de la répartition de plus de 300 genres de coraux rugueux d'âge dévonien dans 20 régions mondiales et dans six étages indique que le maximum de l'endémisme et de la provincialité a lieu à la fin du Dévonien ancien. Les coraux sont donc moins utiles pour les corrélations dévoniennes établies près de la limite entre le Dévonien inférieur et le Dévonien moyen. Ils sont plus utiles pour la corrélation des étages du Lochkovien, du Givétien et du Frasnien que pour celle des étages intermédiaires du Pragien au Couvinien.

INTRODUCTION

Three great faunal realms are generally recognized in the Lower and Middle Devonian. These are: 1. Eastern Americas Realm, including eastern North America, northern South America, and, in Pragian time only, southwestern North America (Great Basin) and possibly North Africa; 2. Old World Realm, including Eurasia, Australia and western North America and North Africa, except as already noted; and 3. Malvinokaffric Realm, including central and southern South America, southern Africa, and Antarctica. The first two of these realms have large coral faunas through most of the Devonian and are the areas of concern in this paper. The third realm has very few corals and will not be discussed further.

We have compiled data on the distribution of over 300 rugose coral genera in 20 geographic areas (see key to Fig. 59.1) and six stages (Lochkovian through Frasnian) in order to measure the value of these corals for correlation and biogeographical analysis. All generic identifications were based on our own examination of specimens or published illustrations. This permitted a high level of consistency in the identification of the corals, but rendered useless a lot of published information that we could not confirm. To be objective, age assignments were based on associated or locally correlatable conodonts, tentaculites, goniatites, or graptolites wherever possible; benthic fossils such as brachiopods and trilobites were used as needed and where feasible. No age determination was based on corals; if non-coral criteria were not available, the data were not used. For our present purpose, each stage is accepted as extending in time from its base, as currently defined in its type area, to the base of the succeeding stage, as defined in its type area.

The list of coral genera by geographic area are in Oliver and Pedder (1979a, b); the first paper also includes a fuller discussion of the data compilation methods.

BIOGEOGRAPHY

Preliminary results of our biogeographic analysis are illustrated in Figures 59.1 and 59.2 and summarized in Table 59.1. The Zlichovian Stage is selected for illustration because it was apparently the time of maximum provinciality and is pertinent to a discussion of the Lower-Middle Devonian boundary.

In the Zlichovian (Fig. 59.1, 59.2), we recognize only one province in the Eastern Americas Realm, but there were at least seven Old World provinces (Mackenzie, Great Basin, North Africa-Spain, Urals, Tasman, Indigiro-Kolyma, and South China). The dashed boundary in Figure 59.1 indicates the possibility that a West and Central Europe province, possibly including the Middle East and Burma, can be separated from a Urals-Soviet Central Asia province. We emphasize that the Asian part of the map is oriented and assembled as a convenience. It seems likely that, during the Devonian, what is now Asia was several more-or-less separate continents or plates (see Oliver, 1977, p. 92-94 for discussion of base map).

Figure 59.2 illustrates diagrammatically the temporal and geographic distribution of Devonian rugose coral provinces as we tentatively recognize them. The number of provinces recognized in the two realms increases from five in the Lochkovian to eight or nine in the Zlichovian, then falls off to three or four in the Givetian. In the Frasnian, only one worldwide realm existed but it may have been divisible into two (or even more) provinces. In general, we are more confident of our Early Devonian provincial divisions than of the later ones. However, the whole study is preliminary and a degree of uncertainty is indicated in Table 59.1 by the range in number of provinces for each stage.

[1] United States Geological Survey, U.S. National Museum Building E-305, Smithsonian Institution, Washington, D.C., U.S.A. 20560

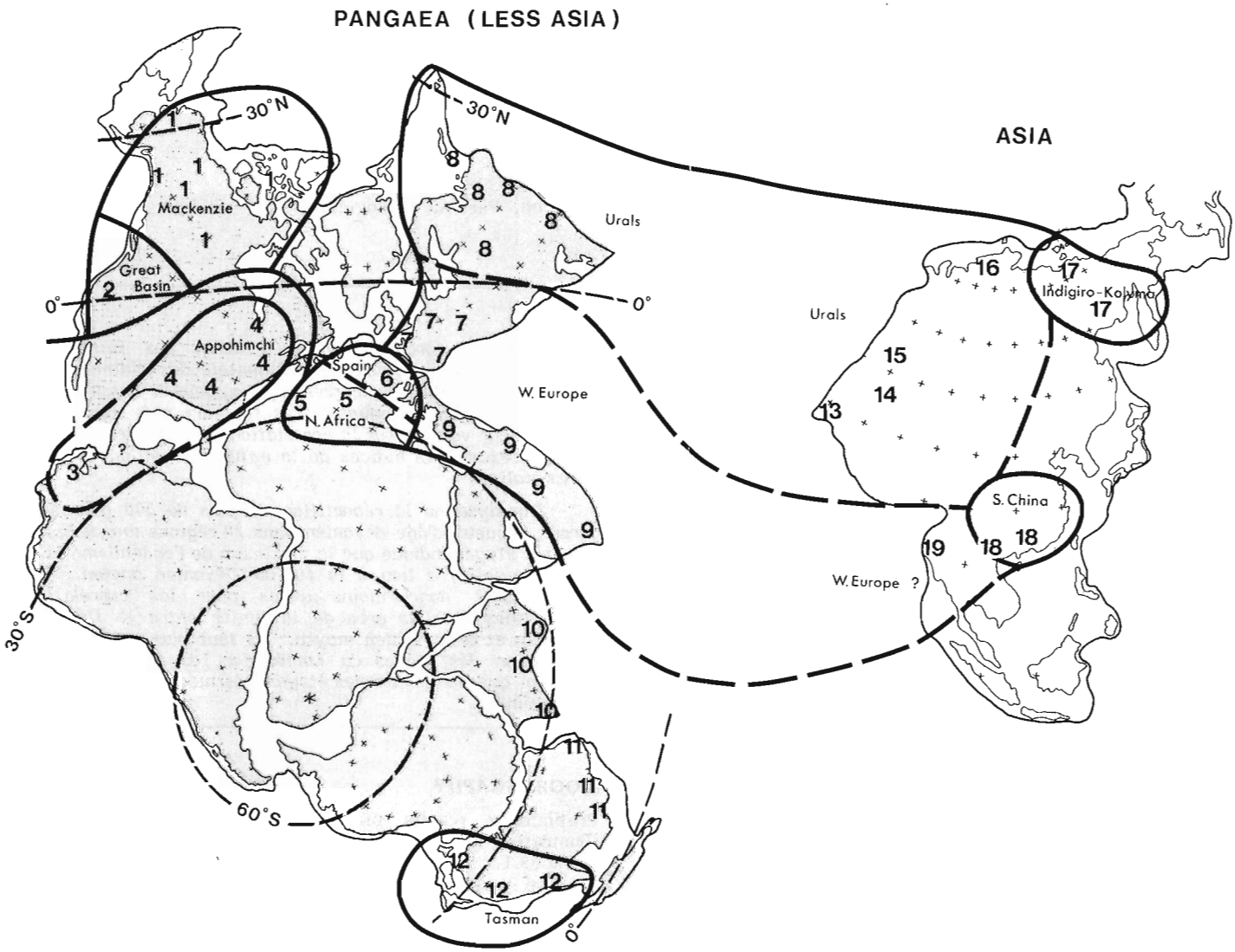

Figure 59.1. *Devonian base maps showing areas discussed in text and approximate location of Zlichovian and early Dalejan (pre-Couvinian) biogeographic provinces, based on preliminary analysis of the distribution of rugose coral genera (Oliver and Pedder, 1979a, Table 1). As Table 59.1 of the present work indicates, the Zlichovian and early Dalejan were times of maximum provinciality in the Devonian. Thick broken lines represent doubtful boundaries, and question marks (?) indicate geographic areas whose biogeographic affinities during Zlichovian and early Dalejan time are unknown because of inadequate data. Numbers refer to the areas from which lists of coral genera were prepared for analysis (see following key).*

Left side – Pangea (less Asia): reassembly of continents, equator and lines of latitude based on paleomagnetic data. Right side – Asia: this was probably divided into several continents and the modern assembly shown here is not meant as an interpretation of the Devonian configuration. See Oliver, 1977, for discussion of the construction of the maps.

Key to areas: 1. Northwestern Canada and Alaska; 2. Great Basin (Nevada and parts of surrounding states, New Mexico and western Sonora, Mexico); 3. Venezuela-Columbia; 4. Eastern North America (east of Transcontinental Arch) including southeastern Canada and Chihuahua, Mexico; 5. North Africa (Morocco, Western Sahara, Mauritania, and Algeria); 6. Spain and Pyrenees; 7. Western and central Europe (England, western and northern France, Belgium, Germany, northern Italy, Austria, Czechoslovakia, Poland, and Podolia and Volhynia, U.S.S.R.); 8. Novaya Zemlya, Urals, Timan, Russian Platform; 9. Turkey, Armenian S.S.R., Iran, Afghanistan; 10. Pakistan, India, Nepal; 11. Carnarvon and Canning Basins, Western Australia; 12. Eastern Australia and New Zealand; 13. Tyan Shan, U.S.S.R.; 14. Dzhungaro-Balkhash, U.S.S.R.; 15. Altai-Sayan, U.S.S.R.; 16. Taimyr, U.S.S.R; 17. Indingiro-Kolyma, U.S.S.R. 18. South China and Vietnam; 19. Burma. The 20th area referred to in the text is the Michigan Basin in Eastern North America which was tabulated separately by Oliver and Pedder, 1979b.

Table 59.1. The waxing and waning of endemicity in Eastern North America, and provinciality in the combined Eastern Americas and Old World Realms. Based on preliminary analysis of generic distribution data given by Oliver and Pedder (1979a). Figures differ from those in Oliver (1977, Table 1) because of a narrower definition of endemic.

	Eastern North America		World
Stage	No. of Genera	Percent Endemic	No. of Provinces
Frasnian	11	0%	2?
Givetian	36	22%	3-4
Couvinian	28	39%	3-5
Zlichovian-early Dalejan	25	76%	8-9
Pragian	9	44%	7
Lochkovian	14	57%	5

Coincident with the increase and decrease in number of provinces in the Old World Realm is the increase and decrease in the per cent of endemic genera in Eastern North America (Eastern Americas Realm; Table 59.1) which also reached a high during the Zlichovian. These two sets of data explain why inter-regional correlation by corals is easiest for Lochkovian and Givetian times and most difficult in the intervening stages, which include the Lower-Middle Devonian boundary.

CORRELATION

Only 10 per cent of the genera tabulated by Oliver and Pedder (1979a) are known from as many as half of the areas studied. Of these genera, only one occurs in as few as two stages. All other widespread genera range through three to six stages and are thus poor indices of age. Five genera are limited to one stage and occur in from four to eight of our areas; four of these are Frasnian and one is Givetian. Six genera are limited to either the Pragian, Zlichovian or Couvinian, but one of these is known to occur in more than two areas. It should be clear that inter-regional correlations based solely on generic occurrences are weak. Within North America, even stage level correlation between eastern and western provinces is not possible using present knowledge of the corals (Oliver and Pedder, 1979b).

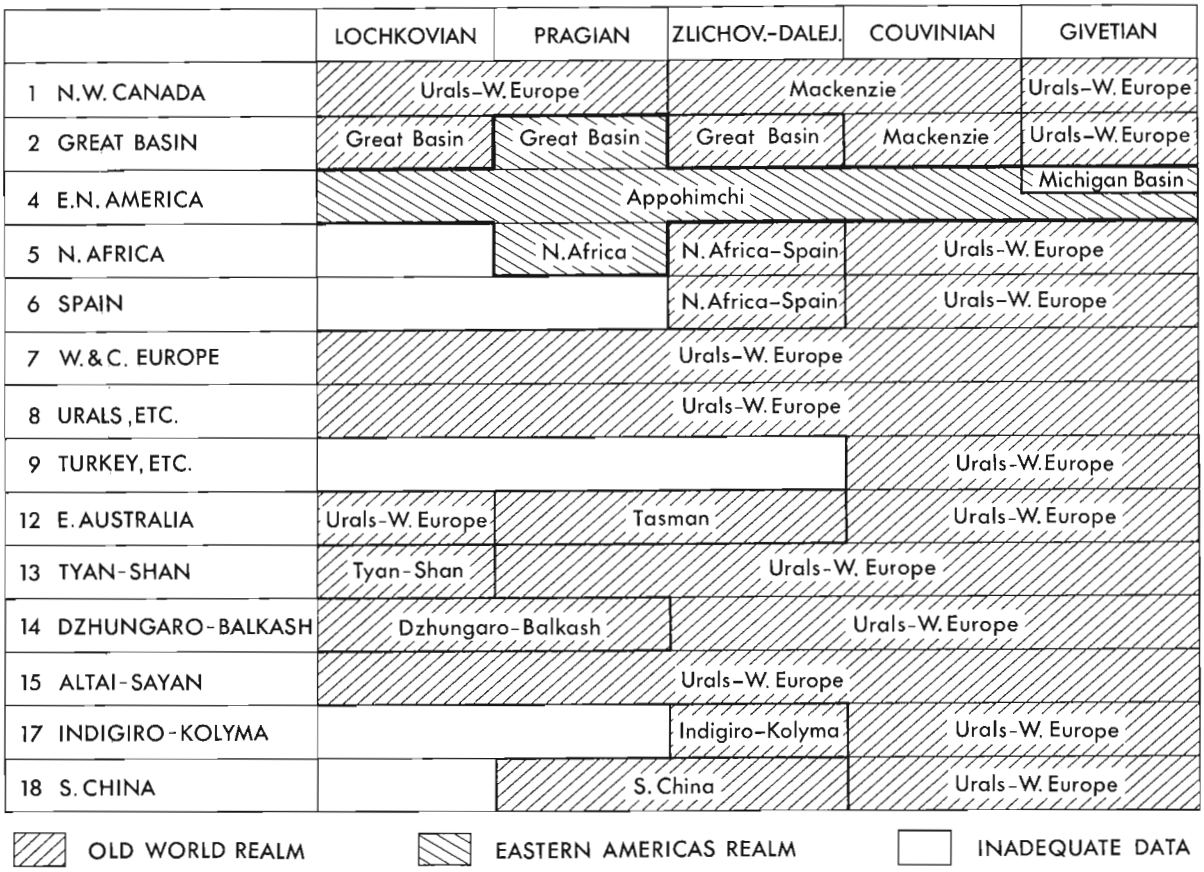

Figure 59.2. *Early and Middle Devonian coral realms and provinces based on preliminary analysis of the distribution of rugose coral genera (Oliver and Pedder, 1979a, Table 1). Numerals in left-hand column correspond to areas enumerated in Figure 59.1 (see also key in caption to Fig. 59.1). Eastern Americas Realm provinces are separated from Old World Realm provinces by thick lines and distinguishing patterns. Note that there is an Eastern Americas Realm Great Basin Province as well as Old World Realm Great Basin provinces.*

There is little agreement among coral specialists on the definition or limits of species. This reflects insufficient descriptive work and analysis, but is also due to the extremely variable morphology of most corals. Some species are known to have value in regional correlations but, as a whole, their potential is unrealized. Our experience suggests that rugose coral species tend to be geographically limited and that they have little potential correlation value beyond the province. The Old World Realm had ten times the area of the Eastern Americas and offers the best testing ground for coral-based correlations, but provincialism limits this also, as is made clear in Table 59.1. Nevertheless, within the Old World Realm, some species are relatively widespread and of value for purposes of correlation. Two examples are **Dendrostella trigemme**, which occurs in upper Couvinian and Givetian rocks in Europe, the Urals, Altai-Sayan, south China-Vietnam, eastern Australia and western Canada, and **Stringophyllum isactis**, which is known in the Givetian of Europe, the Urals, Armenia, south China, eastern Australia and western Canada. A few additional examples could be cited but would not affect our general conclusion.

Unquestionably, the real value of rugose corals in Devonian correlations is at the regional level, that is, within a single depositional basin or faunal province. Sequences of Devonian rugose coral zones have been described for Germany, parts of the USSR, eastern Australia and Nevada (see Oliver and Pedder, 1979a, for references) and sequences of coral assemblages have been described from many additional areas. However, no zonal scheme or coral sequence has yet been found to extend much beyond the region or province in which it was originally described.

SUMMARY AND CONCLUSIONS

1. Devonian corals are of negligible value for worldwide or inter-regional correlations, but have great usefulness for correlations within a depositional basin or biogeographic province.
2. Because Devonian corals are so geographically limited, they are excellent indices of biogeography.
3. The number of biogeographical provinces increased through the Early Devonian to a maximum in the Zlichovian Stage, then decreased to a minimum in the early Late Devonian, Frasnian Stage.
4. Corals are of least value in Devonian correlations during times of maximum provincialism. Consequently, their study contributes little to discussions of the Lower-Middle Devonian boundary.

REFERENCES

Oliver, W.A., Jr.
1977: Biogeography of Late Silurian and Devonian rugose corals; Palaeogeography, Palaeoclimatology, Palaeoecology, v. 22, p. 85-135.

Oliver, W.A., Jr. and Pedder, A.E.H.
1979a: Rugose corals in Devonian stratigraphical correlation; in The Devonian System, ed. M.R. House, C.T. Scrutton, and M.G. Bassett; Special Papers in Palaeontology 23, p. 233-248.

1979b: Biogeography of Late Silurian and Devonian rugose corals in North America; in Historical biogeography, plate tectonics, and the changing environment, ed. J. Gray and A.J. Boucot; Proceedings of the Thirty-seventh Annual Biology Colloquium and Selected Papers, Oregon State University Press, Corvallis, p. 131-145.

60. FIELD EVALUATION OF A MAGNETIC SUSCEPTIBILITY LOGGING TOOL

Project 810008

Q. Bristow and G. Bernius
Resource Geophysics and Geochemistry Division

Bristow, Q. and Bernius, G., Field evaluation of a magnetic susceptibility logging tool; in Current Research, Part A, Geological Survey of Canada, Paper 84-1A, p. 453-462, 1984.

Abstract

A magnetic susceptibility borehole logging tool, only recently available in North America has been evaluated in field boreholes. Repeatability of logs from the same hole is excellent, as is the agreement with drill core magnetic susceptibility measurements from three different holes.

Résumé

Un outil de diagraphie de la susceptibilité magnétique, disponible depuis peu en Amérique du Nord, est évalué dans des sondages sur le terrain. La répétition des diagraphies dans le même trou de sonde est excellente, de même que la concordance avec les mesures de la susceptibilité magnétique des carottes provenant de trois trous différents.

INTRODUCTION

Borehole logging in the mining industry is gaining ever wider acceptance as a powerful and relatively inexpensive technique for gathering data to aid in geological interpretation, or in the recognition of mineralization intersected by a drill hole. Until fairly recently however, magnetic susceptibility tools have not been generally available and the few that were have been used mostly by researchers (George and Scott, 1982).

The magnetic susceptibility of a volume of matter is a function of the amount of ferrimagnetic material contained therein thus magnetic susceptibility measurements will readily indicate the presence of minerals which contain significant concentrations of ferrimagnetic material such as magnetite, ilmenite and pyrrhotite (see e.g. Telford et al., 1976, p. 121). Anomalously low values of magnetic susceptibility can also be significant in certain geological contexts. For example the uranium "roll front" deposits of the southwestern United States are precipitated from uranium bearing, oxidizing groundwaters moving through sandstone strata, and these waters cause magnetic minerals to be altered to nonmagnetic ones, e.g. magnetite to hematite, behind the advancing roll fronts (Ellis et al., 1968; Scott and Daniels, 1976), causing anomalously low magnetic susceptibility readings.

As with any measurement technique which is specific for some parameter, (in this case ferrimagnetic material), magnetic susceptibility measurements can be used to advantage in revealing trends in related parameters e.g. lithological correlation between boreholes.

Due to the time consuming and hence expensive nature of sample-by-sample magnetic susceptibility measurements, they are not normally made on drill core unless a special requirement exists for the data. Such requirements do arise, for example, in the geological and geophysical investigations connected with radioactive waste management projects. The availability of a logging tool can reduce the measurement time from several person-weeks to a few person-hours. Furthermore a borehole log provides a more representative bulk sample than drill core, which is typically less than 60 mm diameter.

This paper presents field data from three boreholes to show the comparison between magnetic susceptibility logs made with a recently available logging tool, and the corresponding logs made by closely spaced measurements on the drill cores from the same holes. Reproducibility is demonstrated with repeat logs of the same boreholes.

BACKGROUND

The Geological Survey of Canada has a program of research aimed at improving borehole geophysical methods. In support of this a logging truck has been equipped with a computer-based data acquisition system which records parameters such as natural gamma-ray spectral data, temperature, induced polarization, resistivity and self potential in digital form together with depth.

Geo Instruments of Finland recently introduced a magnetic susceptibility logging tool which is now available in Canada through Urtec Instruments Sales Ltd. of Toronto. The tool was interfaced to the GSC logging truck in September 1983 and logs were recorded from two test holes maintained by the GSC at Bells Corners in Ottawa and from three holes at a site in the Bancroft area of Ontario. Drill core magnetic susceptibility data were available for one of the holes at Bells Corners and for two at the Bancroft location.

THE MAGNETIC SUSCEPTIBILITY TOOL

The principle of operation of the Geo Instruments model TH-3C is based on the use of a coil in an electrical bridge circuit energized at a frequency of 1400 Hz. When the tool moves through magnetically susceptible material an apparent change of the coil inductance is sensed causing the bridge to become unbalanced. Circuitary contained in the tool drives the bridge to balance automatically by changing the energizing frequency as necessary. The frequency shift is thus a measure of the magnetic susceptibility of the material through which the tool is passing and is registered as such on a continuous basis by the recording equipment.

The Maxwell-bridge circuit which is used also allows resistivity of material close to the coil to be measured simultaneously with susceptibility. This is possible by resolving the change in complex impedance seen by the bridge into its inductive and resistive vector components. (Resistive material around the coil causes the coil to behave as a transformer with the resistive material acting as a combined and distributed "secondary winding" and "load"). Resistivity measurements using this technique are limited however to a range of 10^{-1} ohm-metres to 10^{3} ohm-metres. In practice only some sedimentary formations would normally have resistivities low enough to fall within this range, while in igneous rocks only graphitic conductors or mineralized zones would be included.

Table 60.1

TECHNICAL SPECIFICATIONS: TH-3C MAGNETIC SUSCEPTIBILITY LOGGING TOOL

Susceptibility measuring ranges:

Range switch	Display	Rear panel output	Susceptibility
1	0-2 000	0-10 Vdc	0-2 000 x 10^{-5} SI
2	0-2 000	0-10 Vdc	0-20 000 x 10^{-5} SI
3	0-1 000	0-5 Vdc	0-200 000 x 10^{-5} SI

Note: The output is linear within the calibration accuracy up to 5 000 x 10^{-5} SI. On higher values a calibration curve should be consulted or a correction formula applied to the results.

Resolution: 5 x 10^{-5} SI

Temperature Drift: less than 10 x 10^{-5} SI/°C
Note: this value may be temporarily exceeded after a sudden temperature change.

Pressure effect: less than 1 x 10^{-5} SI/bar

Drift from other sources: less than 1 x 10^{-5} SI/min

Calibration accuracy: 5%

RESISTIVITY:

Resistivity measuring range:

Display	Rear panel output	Resistivity
0-2 000	0-10 Vdc	$10^{-1}\Omega m$-$10^{3}\Omega m$

MECHANICAL DATA:

Length of the electronics section of the probe: 0.6 m

Length of the coil section: 0.5 m

Minimum diameter of the probe: 42 mm

Test pressure: 150 bar (1500 m depth)

Weights: Surface module: 1.2 kg
Probe: 3.8 kg
Shipping Weight: 13 kg

TH-3C:
POWER SUPPLY:

Surface module: 4 Ah, 5 V Ni-Cd batteries, current consumption 200 mA
Probe: 4 Ah, 5 V Ni-Cd batteries, current consumption 180 mA

MECHANICAL DATA:

Length of the electronics section of the probe: 1.0 m

Length of the coil section: 0.5 m

Minimum diameter of the probe: 42 mm

Test pressure: 150 bar (1500 m depth)

Weights: Surface module: 1.8 kg
Probe: 5.0 kg
Shipping Weight: 16 kg

The tool consists of a metal tube containing the necessary circuitry and rechargeable batteries and a detachable sensing coil encapsulated in nonmetallic material. A variety of coils are available but the test runs under discussion were made with one which had the same diameter (42 mm) as the electronics portion of the tool. The metal tube is fitted with an electrical connector which is designed for use with a standard 4-pin Gearhart-Owens cable head. A surface module receives and decodes the combined magnetic susceptibility/resistivity signal which is transmitted as a frequency (susceptibility signal) superimposed on a D.C. level (resistivity). The surface module provides separate analogue outputs for the two parameters. The essential technical specifications for the TH-3C are shown in Table 60.1, taken from the manufacturers literature.

RECORDING OF MAGNETIC SUSCEPTIBILITY DATA BY THE GSC LOGGING SYSTEM

The GSC logging system has been described by Bristow (1979). One of the parameters routinely recorded with the GSC logging system is temperature. The interface for this tool is designed to measure the frequency of a monolithic voltage-to-frequency (V/F) converter housed in the temperature tool and the interface circuitry is contained on one of the circuit boards of the NOVA minicomputer, which controls the system. A very high measurement resolution is achieved by measuring the time for a fixed number of V/F converter pulses against a 10 MHz crystal controlled clock. By inserting an identical inexpensive integrated circuit V/F converter between the susceptibility output from the TH-3C surface module and the NOVA interface board, signal compatibility was readily achieved. Recording of the magnetic susceptibility logs then proceeded exactly as if temperature logs were being run, with the same software controlling the display and recording of depth and magnetic susceptibility data on standard nine-track tape.

RESULTS AND DISCUSSION

A total of five holes were logged with the TH-3C magnetic susceptibility tool. In each case the logging speed was 6.0 m/minute with a one second sampling time, giving a measurement at every 10 cm down the hole. Two logs were run in each of these holes, one down and one up. The hole diameters for Bancroft are "HQ" and for Bells Corners "NQ" (100 mm and 75 mm respectively), which are larger than the diameter for which the tool had been calibrated. A factor to correct for this was obtained from the manufacturer and applied to the data recorded. Absolute values so corrected agreed well with drill core values.

The probe incorporates compensation for quasi-static temperature changes, which is not effective when the unit is subjected to step changes in temperature. Accordingly the probe was allowed to come to thermal equilibrium by lowering it into the borehole fluid and leaving it there for 30 minutes before logging was started. The temperature variation over the total lengths of these holes is known to be of the order of 5°C or less, so that the rate of change was well within the "quasi-static" definition.

The Bells Corners test site consists of Precambrian gneiss overlain unconformably by approximately 65 m of sedimentary rocks (dolomite, sandy dolomite and sandstone). The Bancroft holes also penetrate gneiss but of a much higher degree of metamorphism and deformation than at Bells Corners, which is reflected in the greater range of susceptibility values.

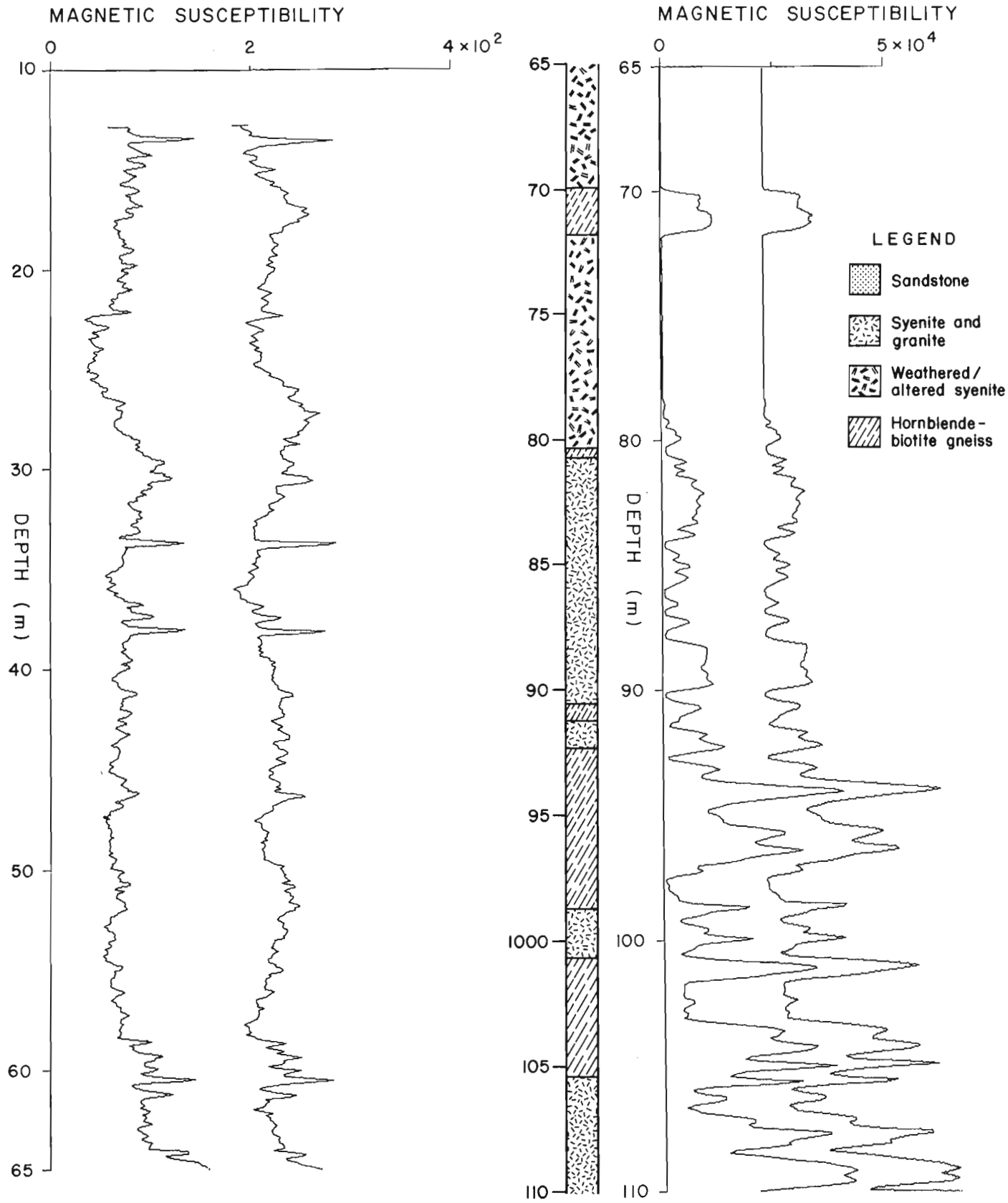

Figure 60.1. *A. Repeat logs 10-65 m in sedimentary strata of Bells Corners test hole BC-81-2. Expanded scale 0-400 x 10^{-5} SI units. B. Repeat logs 65-110 m in the Precambrian gneiss penetrated by Bells Corners test hole BC-81-2. Scale 0-50 000 x 10^{-5} SI units. (Logs offset for clarity).*

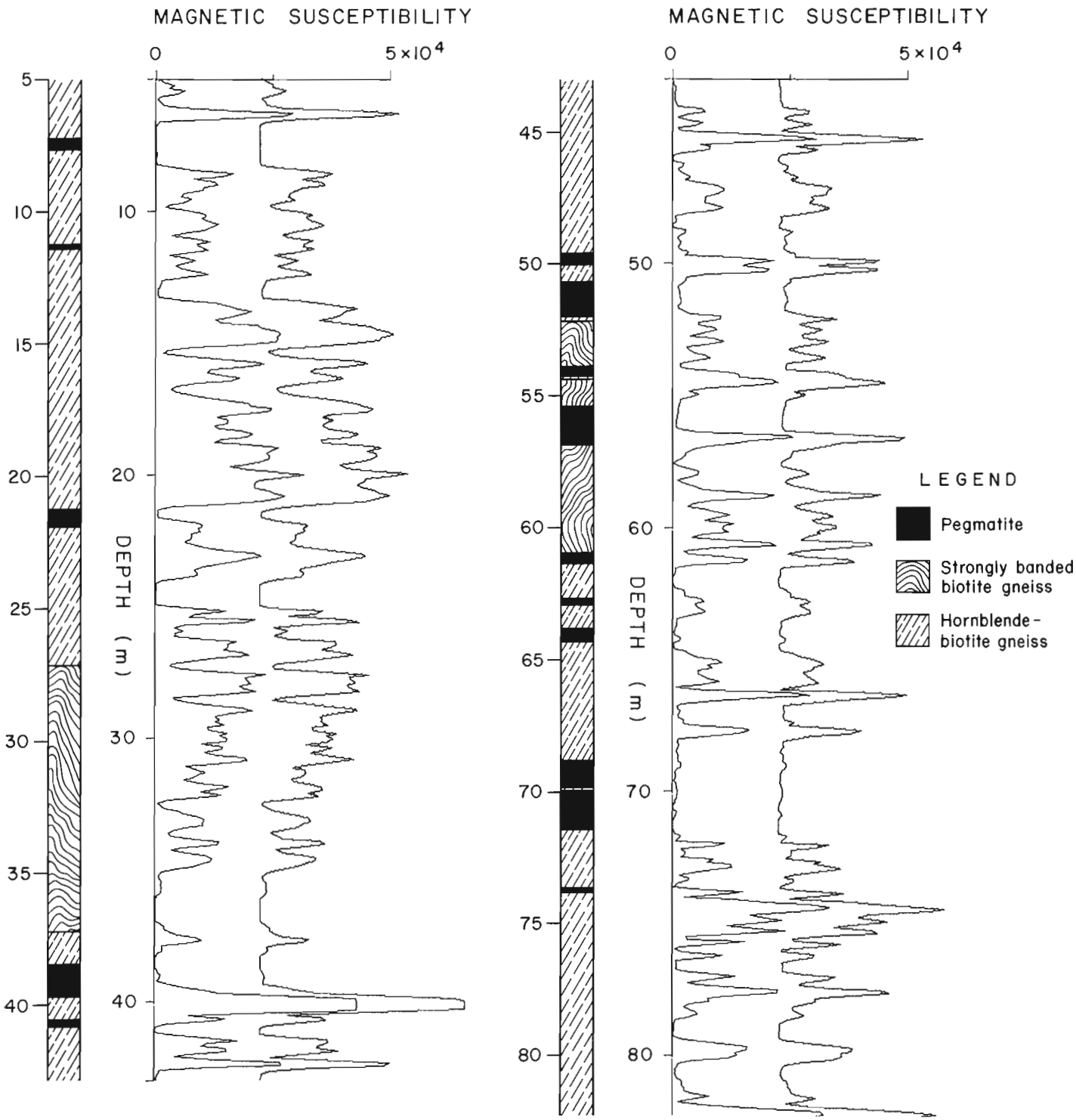

Figure 60.2. *Repeat logs in Bancroft hole No. BN-81-1. (Logs offset for clarity).*

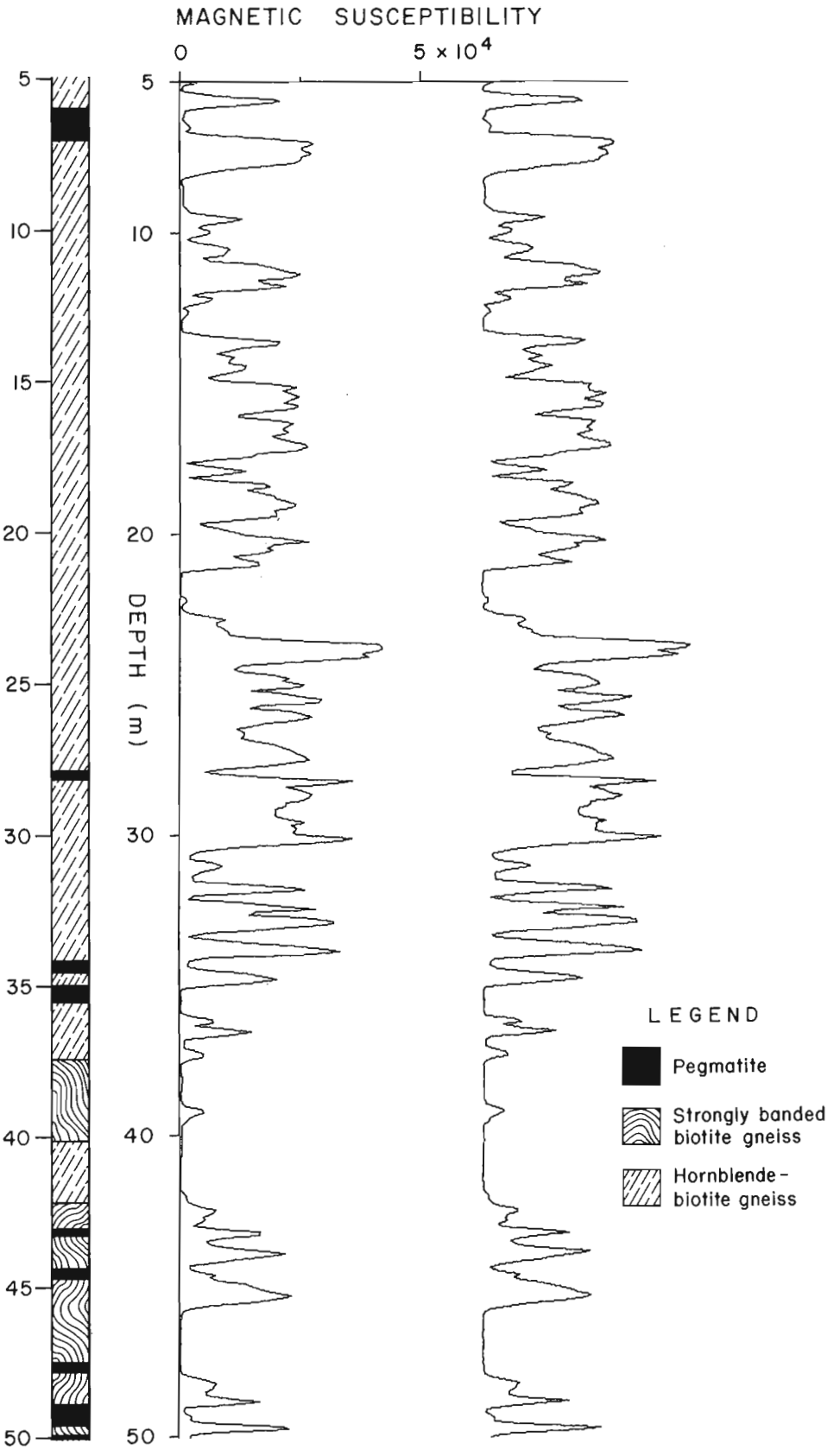

Figure 60.3. *Repeat logs in Bancroft hole No. BN-81-2. (Logs offset for clarity).*

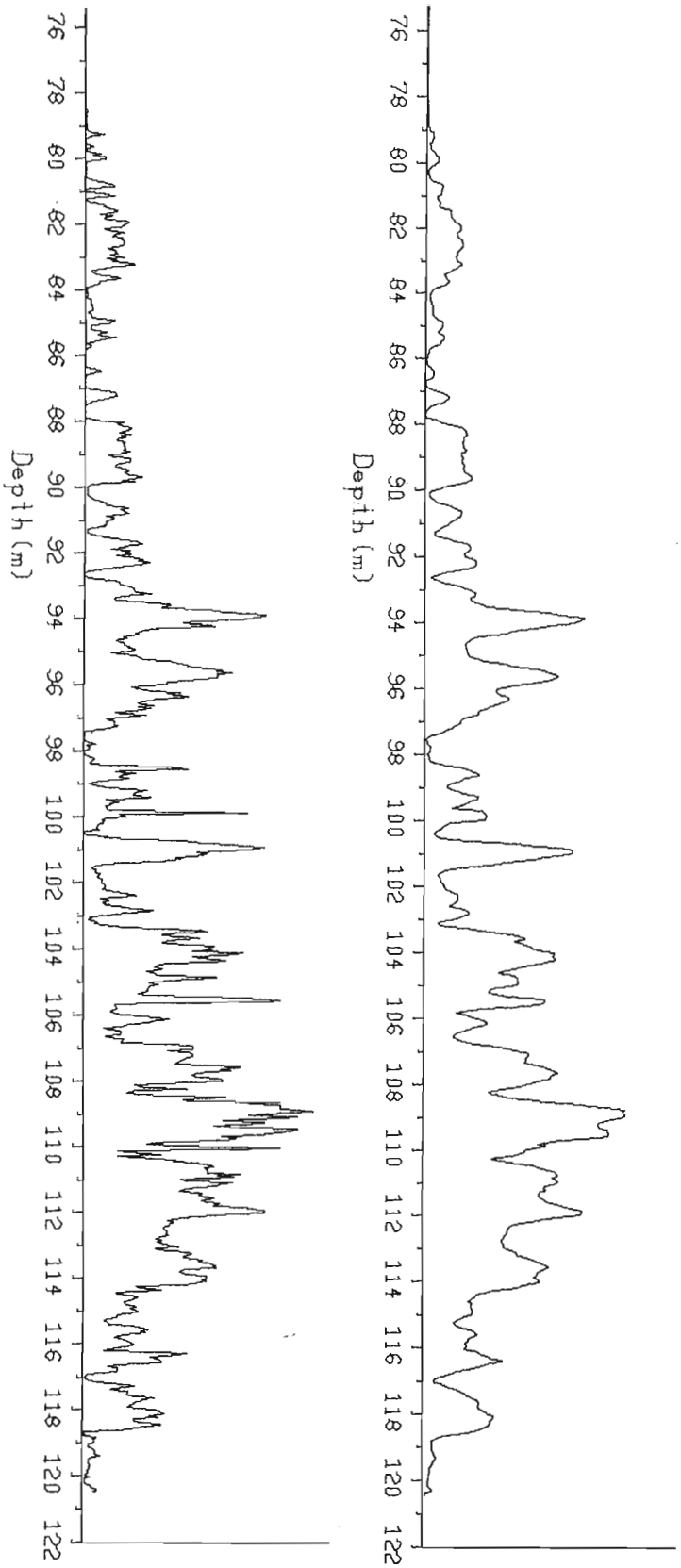

Figure 60.4. *A. Drill core magnetic susceptibility measurements on Precambrian segment of Bells Corners test hole as recorded. B. Measurements of Figure 60.4A after smoothing with 7 point running average filter.*

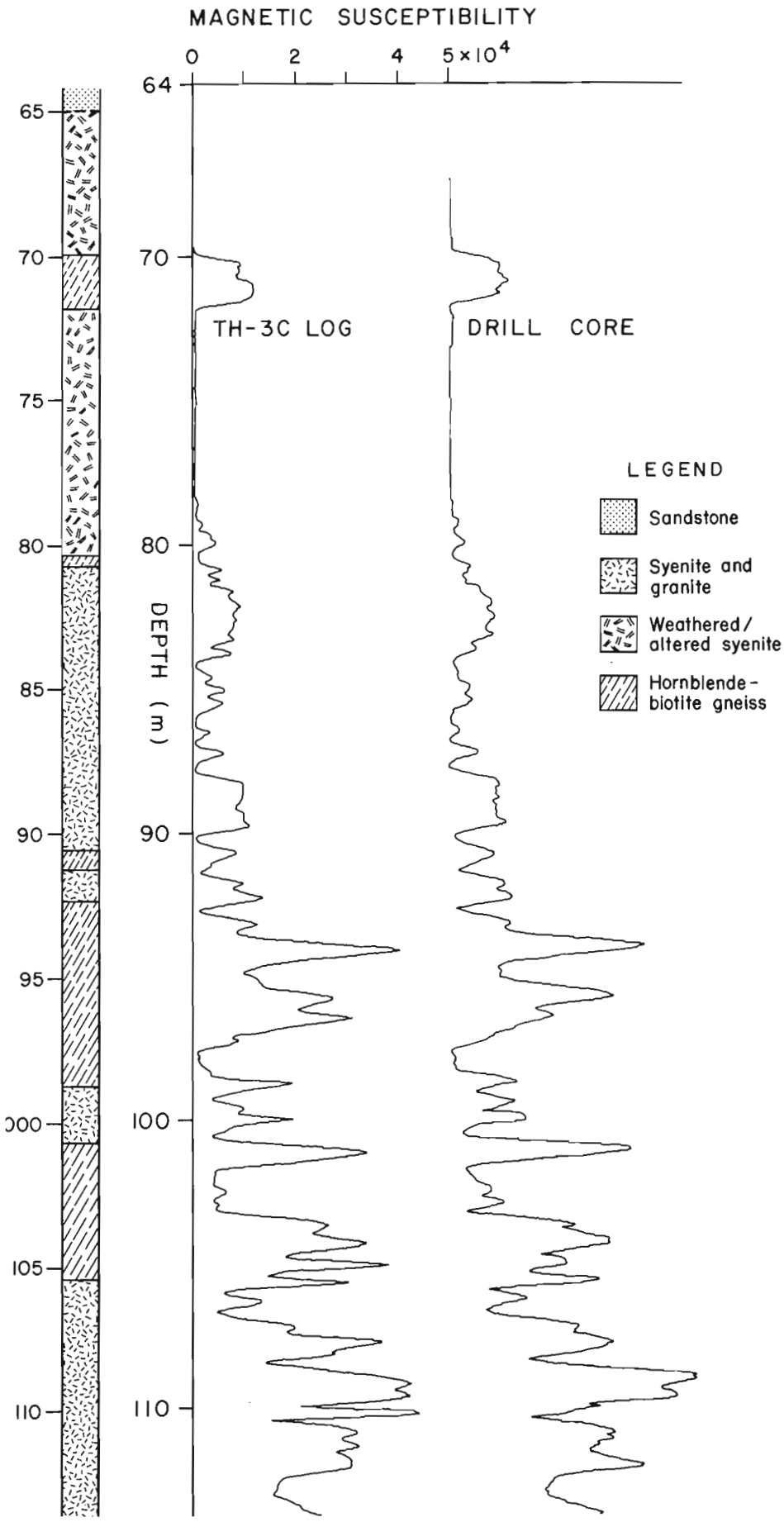

Figure 60.5. *Comparison of smoothed drill core log and TH-3C tool log for Precambrian segment of Bells Corners test hole BC-81-2 (logs offset for clarity).*

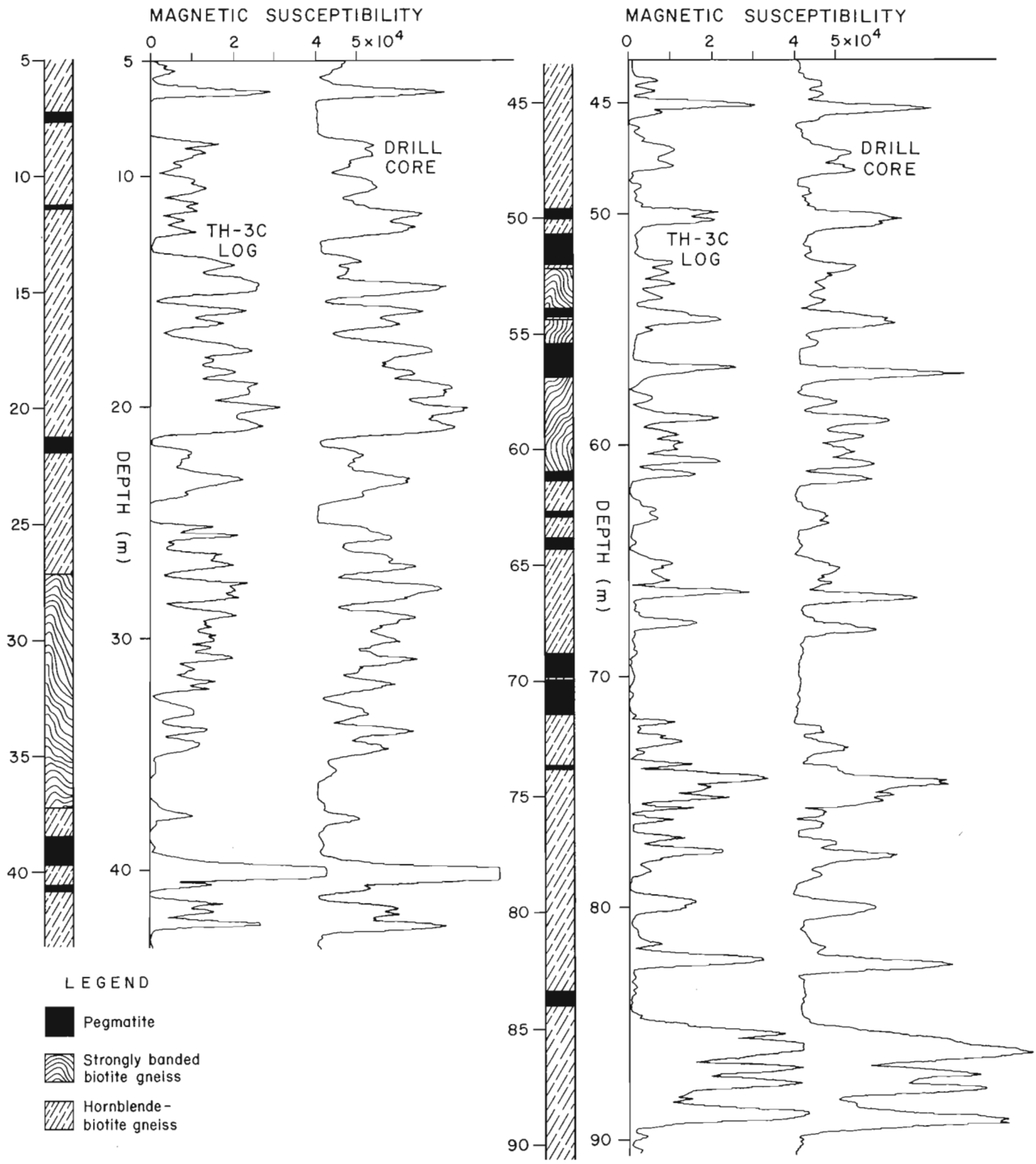

Figure 60.6. *Comparison of smoothed drill core log and TH-3C tool log for Bancroft hole No. BN-81-1.*

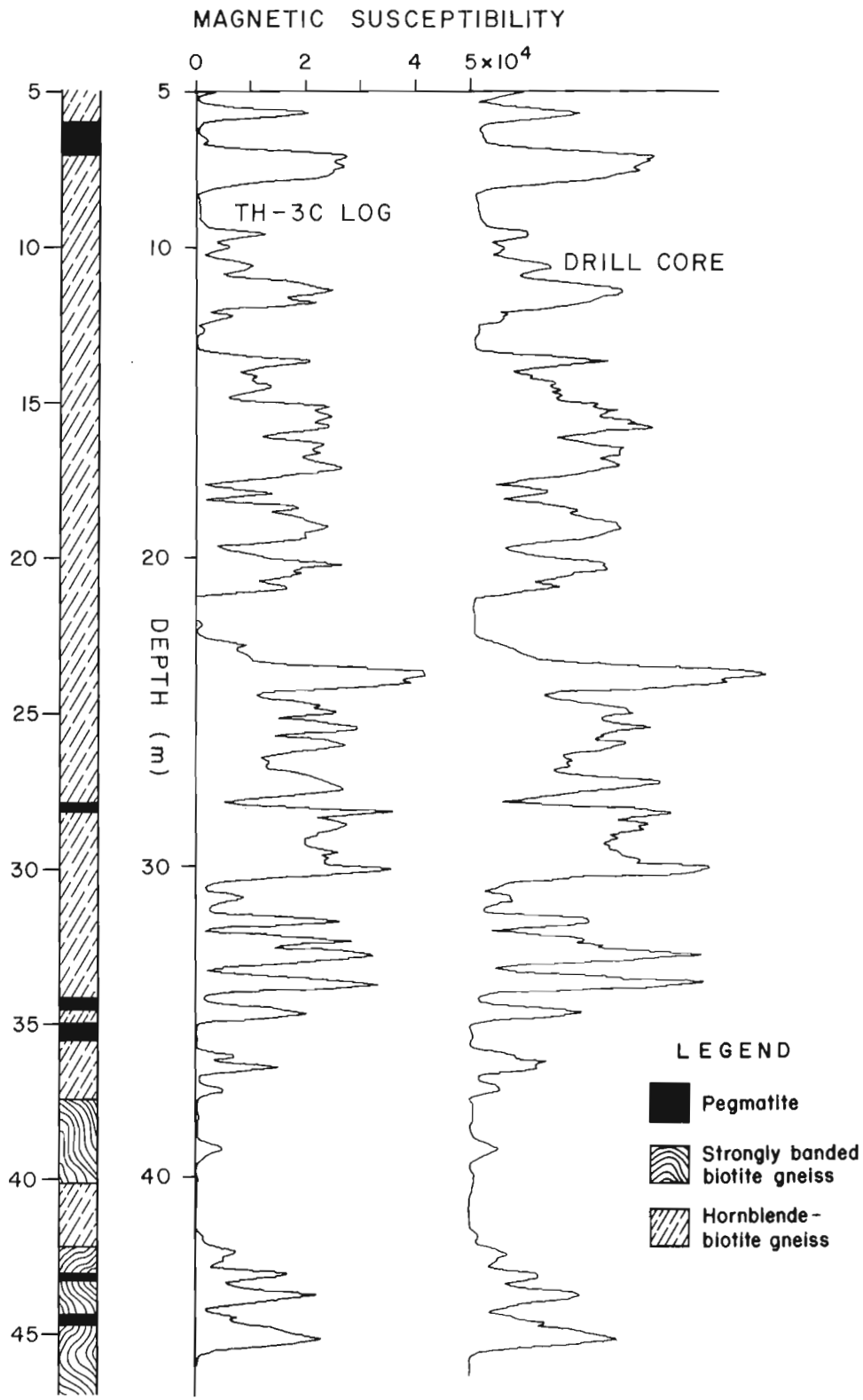

Figure 60.7. *Comparison of smoothed drill core log and TH-3C tool log for Bancroft hole No. BN-81-2.*

Figures 60.1 to 60.3 show the repeat logs obtained with the TH-3C tool in the three holes for which drill core measurements were available, (one at Bells Corners and two at Bancroft), together with the geological logs. The logs are plotted on a scale of 0-50 000 $\times 10^{-5}$SI units, with the repeat log offset by approximately 25 000 $\times 10^{-5}$SI units for clarity in every case except Figure 60.1A. The pair of logs shown in Figure 60.1A are for the sedimentary sequence of the Bells Corners hole plotted on a scale of 0-400 $\times 10^{-5}$SI units without offset. At the magnified scale which this represents it is evident that there is a displacement between the pair of approximately 100 $\times 10^{-5}$SI units. This is almost certainly due to temperature dependent base-line drift, and is not considered problematical since the lithological detail is clearly reproducible at very low signal levels, confirming the 5 $\times 10^{-5}$SI resolution capability given in the technical specifications. Excellent repeatability is apparent for all the other pairs of logs in Figures 60.1 to 60.3.

Magnetic susceptibility measurements on three drill cores had been made at 5 cm intervals. These measurements were made with a Scintrex model SM-5 magnetic susceptibility meter designed to measure on flat surfaces or drill core where geometry errors are small. Since the logging tool has a coil length of 50 cm compared with only 35 mm for the portable Scintrex instrument, it was felt that a better basis for comparison would be obtained if the core measurements were first smoothed using a seven-point running average filter, since this is in effect what the larger tool does to the real profile.

Figure 60.4 shows magnetic susceptibility measurements for the drill core from one of the holes as recorded compared with the same data after smoothing. Figures 60.5 to 60.7 show smoothed drill core measurements alongside the borehole logs for each of the three holes. The close agreement between the two in all cases provides convincing evidence that the logging tool accurately reflects the core measurements.

The relative amplitudes of the various peaks do not always correspond exactly between the pairs of logs. This is not surprising since the volume of material used for the drill core measurement represents only a small fraction of the volume sampled by the logging tool. Thus correlation of relative amplitudes at any point is an indication that the material is reasonably homogeneous in the vicinity of the borehole at that point.

CONCLUSION

The Geo Instruments TH-3C magnetic susceptibility logging tool showed excellent repeatability as evidenced by the data presented in Figures 60.1 to 60.3, and by similar data from two other holes. The validity of the measurements has been verified by the agreement between these logs and the independent measurements made on drill core from the holes.

The equipment as supplied is self contained and, interfacing to almost any logging system, either analogue or digital, is relatively simple. The principle of operation, using a Maxwell bridge circuit, calls for very close tolerances on the allowable inductance changes in the sensing coil due to changes in pressure and temperature which cause base-line drift in the signal level. These effects appear to have been minimized by careful mechanical and electrical design and allow excellent results to be achieved even in sedimentary strata where normal magnetic susceptibility levels are below the threshold of most hand held instruments. Even so, step changes in temperature of the tool should be avoided whenever possible. For example the initial step as the tool enters the borehole fluid should be avoided by allowing time for thermal equilibrium to be reached before logging is started.

Equipment of this type should find ready application in a number of fields of endeavour where borehole logging techniques are used to gather data.

ACKNOWLEDGMENTS

The authors wish to express their appreciation to Mikko Hamalainen of the Geo Instruments Company for his cooperation in making the tool available for these experiments, and to Bill Hyatt, Yves Blanchard and Jacques Parker for making modifications to the GSC logging system and conducting the logging operation.

REFERENCES

Bernius, G.R.
1981: Boreholes near Ottawa for the development and testing of borehole logging equipment – a preliminary report; in Current Research, Part C, Geological Survey of Canada, Paper 81-1C, p. 51-53.

Bristow, Q.
1979: NOVA-based airborne and vehicle mounted systems for real-time acquisition, display and recording of geophysical data; in Proceedings of Data General Corp. Users Group Conference, New Orleans, Dec. 1979.

Ellis, J.R., Austin, S.R., and Droullard, R.F.
1968: Magnetic susceptibility and geochemical relationships as uranium prospecting guides; USAEC, AEC-RI (1968) 21.

George, D.C. and Scott, J.H.
1982: Review of magnetic susceptibility logging and its application to uranium exploration; in Proceedings of Uranim Exploration Methods Symposium, OECD/IAEA, Paris, June 1982.

Scott, J.H. and Daniels, J.J.
1976: Non-radiometric borehole geophysical detection of geochemical haloes surrounding sedimentary uranium deposits; in Symposium on Exploration for Uranium Ore Deposits. IAEA/SM/208-16 Vienna 1976, p. 379-390.

Telford, W.M., Geldart, L.P., Sherriff, R.E., and Keys, D.A.
1976: Applied Geophysics; Cambridge University Press.

61. GEOLOGY OF THE IGNEOUS-METAMORPHIC COMPLEX OF SHELBURNE AND EASTERN YARMOUTH COUNTIES, NOVA SCOTIA[1]

Contract 03SU.23233-3-0442

H.D. Rogers[2] and C.E. White[2]

Rogers, H.D. and White, C.E., Geology of the igneous-metamorphic complex of Shelburne and eastern Yarmouth counties, Nova Scotia; in Current Research, Part A, Geological Survey of Canada, Paper 84-1A, p. 463-465, 1984.

Also in Mines and Minerals Branch, Report of Activities, 1983, Nova Scotia Department of Mines and Energy, Report 84-1, 1984.

Abstract

Fieldwork completed during 1983 in Shelburne County and adjacent parts of Yarmouth County indicates that the granitoid intrusions in the western part of the area are part of a single tonalite pluton (Barrington Passage pluton). Metasedimentary rocks along its margin are largely migmatized. A 2 km wide septum of metasedimentary rocks separates it from the Shelburne pluton to the east. The Shelburne pluton consists of granite and trondhjemite which is bounded on the south and east by psammites and on the north by porphyroblastic andalusite-biotite schists. Small diorite, diabase and granite intrusions are also present. East and west of the plutonic area are major synclines containing a unique assemblage of porphyroblastic andalusite-cordierite-staurolite schists and granofelses.

Résumé

Les travaux sur le terrain achevés en 1983 dans le comté de Shelburne et les parties contigües du comté de Yarmouth indiquent que les intrusions granitoïdes dans la partie ouest de la région font partie d'un seul pluton de tonalite, le pluton de Barrington Passage. Les roches métasédimentaires le long de sa marge ont été en grande partie migmatisées. Une cloison de roches métasédimentaires, large de 2 km, sépare ce pluton du pluton de Shelburne à l'est. Ce dernier se compose de granite et de trondhjémite qui sont limités au sud et à l'est par des psammites et au nord par des schistes porphyroblastiques à andalousite et à biotite. On y trouve également de petites intrusions de diorite, de diabase et de granite. À l'est et à l'ouest de la région plutonique, des synclinaux majeurs contiennent un assemblage unique de schistes porphyroblastiques à andalousite, à cordiérite et à staurotide et de granofels.

INTRODUCTION

The project area lies in southwestern Nova Scotia in Shelburne and Yarmouth counties (Fig. 61.1). Covering an area of 3200 km^2, it includes parts of NTS sheets 21A/3,4 and 20P/5,6,11,12,13,14. Although outcrop is best in coastal sections, adequate exposures occur in most inland areas. Access to these inland areas has improved considerably during the last twenty-five years, due largely to an increase in logging activity and recreational use. Combined with extensive waterways and trails these partly compensate for the large areas of stunted bush and swamp.

The geology of the project area is apparently unique within the Meguma Zone of the Appalachians because of the spectacular development of porphyroblastic andalusite, cordierite and staurolite resulting from local amphibolite facies regional metamorphism (Chu, 1978). Unusual too is the widespread development of migmatite in the area. The granitoid lithologies such as tonalite, trondhjemite and high potassium diorite (de Albuquerque, 1977, 1979) contrast with those elsewhere in the Meguma Zone. The granitoid rocks are also characterized by the pervasive development of an apparently syntectonic foliation that has gone largely unnoticed. These various features contrast strongly with those of other areas of the Meguma Zone.

The first systematic mapping of the project area was done in 1959 and 1960 on a reconnaissance scale of 1 inch = 4 miles (Taylor, 1967). The geochemistry and evolution of plutonic rocks in the area were described by de Albuquerque (1977, 1979). K-Ar and $^{40}Ar/^{39}Ar$ geochronology of these granitoid rocks was reported by Reynolds et al. (1981). These data indicated young ages of 302 and 308 Ma for the larger plutons – another distinctive feature of this area compared to elsewhere in the Meguma Zone.

The lack of detailed mapping in the area led to the development of this project and fieldwork commenced in May, 1983. A further season of fieldwork is planned for 1984. Results of the mapping, combined with petrological studies emphasizing the granitoid rocks, will form the basis of an M.Sc. thesis by the first author. Metamorphic aspects of the area will be studied by field assistants doing B.Sc. (Honours) theses at Acadia University.

METASEDIMENTARY LITHOLOGIES

The eastern and western limits of the map area are defined by the occurrence of "normal" (greenschist facies) Meguma Group lithologies. On the east this occurs to the east of Jordan Bay, and on the west to the west side of the Pubnico Peninsula (Fig. 61.1). Only Goldenville Formation (Unit 1) is present within the map area on the east side whereas both Goldenville Formation and overlying Halifax Formation (Unit 2) occur on the west side. Both formations are metamorphosed to the biotite grade of the greenschist facies (Keppie, 1979). The Goldenville Formation consists mainly of thick-bedded psammites with minor interbedded slate. The Halifax Formation consists of highly cleaved slate with minor interbedded psammite.

Along the inner margins of these units occur major synclines containing highly aluminous pelitic schists and granofelses (Unit 3), noteworthy for high concentrations of andalusite, cordierite and staurolite porphyroblasts. Within the remaining area between the synclines are a varied group of metasedimentary lithologies which have been subdivided into four groups (Fig. 61.1). Unit 4 consists primarily of thick-bedded psammites with rare interbedded porphyroblastic, biotite-rich, andalusite schist. This unit is confined to the southern part of the map area in the vicinity

[1] Contribution to Canada-Nova Scotia Co-operative Mineral Program 1981-84. Project carried by Geological Survey of Canada

[2] Department of Geology, Acadia University, Wolfville, Nova Scotia B0P 1X0

of the coastline. The rocks of Unit 5 consist primarily of biotite-rich, porphyroblastic andalusite schist, with andalusite crystals from 10 to 30 cm long being common. Minor, relatively thick (several metres) beds, of semipelite also occur in this unit, which is confined to the northern part of the map area.

A low grade, quartz-rich, garnetiferous schist (Unit 6) outcrops along the northwest shore of Great Barren Lake.

Extensive areas of migmatite (Unit 7) are superimposed on these other units, primarily on the eastern and northern margins of the Barrington Passage pluton. The type and degree of migmatization is highly variable, appearing to depend primarily on local conditions such as host rock composition.

INTRUSIVE ROCKS

The Barrington Passage Pluton (Taylor, 1967), covering an area of approximately 1300 km^2 (Fig. 61.1) is the largest pluton in the map area. The granitoid rocks described by Taylor (1967) north of Great Pubnico Lake are petrologically similar to the main body of the pluton and are included with it. The pluton consists of strongly foliated, equigranular, biotite tonalite of homogeneous composition. Its intrusion at above minimum-melt temperatures (de Albuquerque, 1977) probably explains the extensive development of migmatite along its borders. A septum of metasedimentary rocks 2 km wide separates it from the Shelburne pluton to the east.

The Shelburne pluton (Taylor, 1967) was originally described as consisting of granodiorite. However, Clarke and Muecke (1980) described it as a trondhjemite. Preliminary results from this study indicate that much of its western portion may be granite. Like the Barrington Passage pluton it possesses a strong foliation and is equigranular. Both muscovite and biotite are characteristically present. The pluton is also characterized by widespread, large scale development of simple pegmatites along its margins. Migmatite has not been found in the vicinity of the Shelburne pluton.

The presence of a large pluton in the Bald Mountain area (Fig. 6.1) has been confirmed during this study by the mapping of nine new outcrops. It is similar in outcrop to the

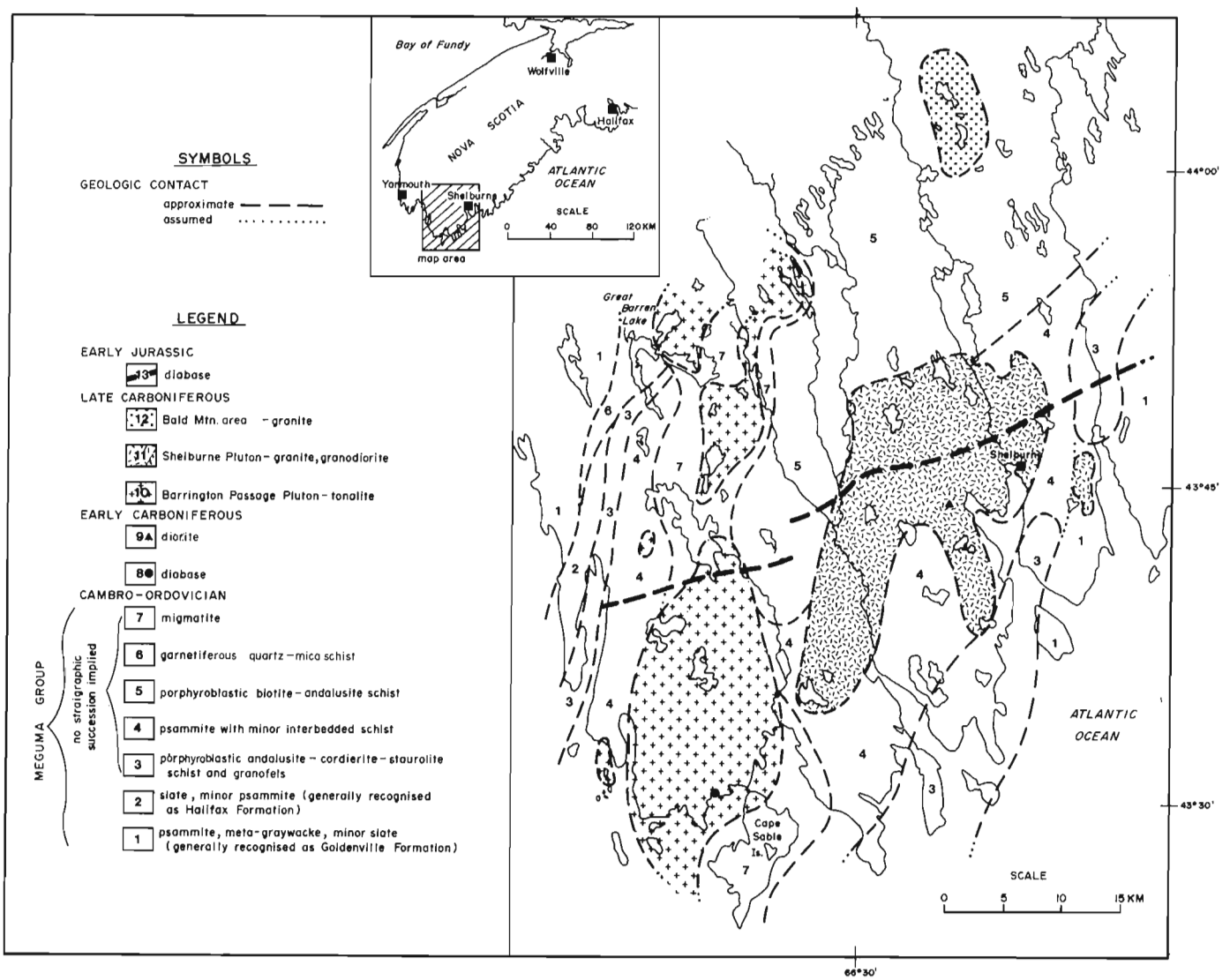

Figure 61.1. *Generalized geology of igneous and metamorphic rocks of Shelburne County and eastern Yarmouth County.*

Shelburne pluton, and preliminary geochemical results indicate a granite composition. Pegmatite development is minimal.

Other smaller bodies of intrusive rock also occur in the map area. A small mafic body (Unit 8) occurs at Murray Cove within the Barrington Passage pluton (Fig. 61.1). Taylor (1967) described it as gabbro and de Albuquerque (1979) as norite. Diabase is an adequate field term. On one of the islands in the cove this mafic rock is highly shattered and rafted by intrusive tonalite of the Barrington Passage pluton. This places an upper age limit of Late Carboniferous on its intrusion.

Unit 9 is a small (<0.5 km^2) body of massive, high-potassium diorite (de Albuquerque, 1979), within the Shelburne pluton near Birchtown, that was formerly quarried for ornamental stone. Taylor (1967) described it as a hornblende diorite. Age dating by Reynolds et al. (1981) assigned an age of 350 to 353 Ma. Taylor (1967, p. 44) referred to the fact that a number of holes drilled in the quarry in the early 1940s all passed into "grey granite" at depths as shallow as twenty-five feet. The conclusion of de Albuquerque (1979) that this pluton acquired its anomalous potassium content by contamination from granitic magmas, when combined with its age date, suggests that it was incorporated into the Shelburne pluton during intrusion. Thus, it can be explained as a large xenolith.

The Shelburne Dyke (Unit 13) is a major geological feature extending for several hundred kilometres across southwestern Nova Scotia (Papezik and Barr, 1981). Two new outcrops of this diabase dyke have been found in the map area. Their location lies along the axis of the aeromagnetic high associated with other parts of the dyke.

STRUCTURE

Folding has occurred on a regional scale producing tight, isoclinal folds, which are locally overturned. Highly erratic folding on the mesoscopic scale is common within and adjacent to the migmatites.

No evidence has yet been found of major faulting in the area. Small-scale faulting with well developed slickensides is common in the granitoid rocks, especially those of the Shelburne pluton. Friable fault zone rocks are also found in both the Shelburne and Barrington Passage plutons.

METAMORPHISM

Metamorphic grade varies from greenschist to low pressure, middle amphibolite facies. Isograds have not yet been defined, but typical maximum metamorphic assemblages include some of staurolite, cordierite, andalusite or sillimanite, muscovite, plagioclase, biotite and quartz.

DISCUSSION

Mapping has so far demonstrated that erosion has proceeded to a depth where it is just beginning to penetrate the roof of the northern part of the Barrington Passage pluton. This is evident from the distribution of tonalite in the high grade schists and migmatites in the northwestern part of the map area (Fig. 61.1). The uniform, south-dipping erosional surface has penetrated lower into the stratigraphic sequence in the coastal region, thus exposing a much greater expanse of tonalite south of Great Pubnico Lake and a greater lateral extent of migmatite on Cape Sable Island. The widespread occurrence of schists in the north and psammites in the south can also be explained by erosional bevelling of the original stratigraphic contact between the Halifax Formation (schists) and the Goldenville Formation (psammites), thus correlating Units 3 and 5 with the Halifax Formation and Unit 4 with the Goldenville Formation. Continued mapping and petrographic studies should lead to a more definitive interpretation of the stratigraphic sequence in the area.

REFERENCES

Chu, P.
1978: Metamorphism of the Meguma Group in the Shelburne area, Nova Scotia; unpublished M.Sc. thesis, Acadia University, 206 p.

Clarke, D.B. and Muecke, G.K.
1980: Field trip guidebook, trip 21: igneous and metamorphic geology of southern Nova Scotia; Geological Association of Canada Annual Meeting, Halifax, N.S.

de Albuquerque, C.A.R.
1977: Geochemistry of the tonalitic and granitic rocks of the Nova Scotia southern plutons; Geochimica et Cosmochimica, v. 41, p. 1-13.

1979: Origin of the mafic plutonic rocks of southern Nova Scotia; Geological Society of America, Bulletin, v. 90, Part 1, p. 719-731.

Keppie, J.D.
1979: Geological map of the Province of Nova Scotia; Nova Scotia Department of Mines and Energy, Halifax, N.S.

Papezik, V.S. and Barr, S.M.
1981: The Shelburne Dike, an early Mesozoic diabase dike in Nova Scotia: mineralogy, chemistry and regional significance; Canadian Journal of Earth Sciences, v. 18, p. 1346-1355.

Reynolds, P.H., Zentilli, M., and Muecke, G.K.
1981: K-Ar and $^{40}Ar/^{39}Ar$ geochemistry of granitoid rocks from southern Nova Scotia: Its bearing on the geological evolution of the Meguma Zone of the Appalachians; Canadian Journal of Earth Sciences, v. 18, p. 386-394.

Taylor, F.C.
1967: Reconnaissance geology of Shelburne map-area, Queens, Shelburne and Yarmouth counties, Nova Scotia; Geological Survey of Canada, Memoir 349, 82 p.

62. GEOCHEMISTRY OF GRANITOID CLASTS FROM MacLEAN EXTENSION OREBODY, BUCHANS, NEWFOUNDLAND, AND IMPLICATIONS ON THEIR POSSIBLE SOURCE[1]

Contract 1583327

Peter W. Stewart[2]
Economic Geology Division

Stewart, P.W., Geochemistry of granitoid clasts from MacLean Extension orebody, Buchans, Newfoundland, and implications on their possible source; in Current Research, Part A, Geological Survey of Canada, Paper 84-1A, p. 467-472, 1984.

Also in Current Research, Newfoundland Department of Mines and Energy, Mineral Development Division, Report 84-1A, 1984.

Abstract

Lithogeochemical analyses have been obtained on samples from the alkali feldspar phase of the Topsails granite, the Feeder Granodiorite and granitoid clasts from ore-horizon breccia-conglomerate beds in MacLean Extension area. The peraluminous Topsails granite is from an A-type (anorogenic) magma which is chemically distinct from the clasts and cannot be their source. The peraluminous Feeder Granodiorite and granitoid clasts are both from I-type (orogenic) magmas and have many geochemical similarities and some differences. The Feeder Granodiorite may be a late-stage differentiate of the source of the clasts. Variable alteration of the clasts complicates lithogeochemical interpretations. A revised petrographic classification of clasts is presented.

Résumé

Des analyses lithogéochimiques ont été effectuées sur la phase de feldspath alcalin du granite de Topsails, de la granodiorite Feeder et des fragments granitoïdes provenant d'un niveau minéralisé dans les couches de brèches et de conglomérats dans la région de la prolongation de MacLean. Le granite hyperalumineux de Topsails provient d'un magma de type A (anorogénique) qui diffère chimiquement des fragments et qui ne peut donc pas être leur source. La granodiorite Feeder et les fragments granitoïdes sont hyperalumineux et proviennent de magmas de type I (orogénique); ils pourraient avoir de nombreuses similarités et quelques différences géochimiques. La granodiorite Feeder pourrait être le produit de la différentiation tardive de la source des fragments. L'altération variée des fragments complique l'interprétation lithogéochmique. Une classification pétrographique révisée des fragments est présentée.

INTRODUCTION

The volcanogenic sulphide ore deposits at Buchans occur as three types: stockwork ore, in situ ore and transported ore (Thurlow, 1981a; Thurlow and Swanson, 1981). These deposits are hosted by the Buchans Group of the Newfoundland Central Volcanic Belt (Kean et al., 1981), an Ordovician-Silurian sequence of subaqueous volcanic, volcaniclastic and sedimentary rocks.

The transported ore forms a series of sulphide-bearing breccia-conglomerate beds with diverse lithic clasts, including granitoids. These beds have been interpreted as deposited by debris flows (Walker and Barbour, 1981; Binney et al., 1983).

The source of the granitoid clasts has been enigmatic. Two small intrusive bodies (Wiley's River and Little Sandy intrusions) have been interpreted to be comagmatic with the Buchans Group volcanic rocks and possible sources of the granitoid clasts. They have been collectively named the Feeder Granodiorite (Thurlow, 1981a, b).

Major and trace element analyses have been carried out for twenty-one clasts collected from 20 Level of the MacLean Extension workings. Eight samples of the Wiley's River intrusion and one sample of the Little Sandy intrusion were analyzed for the same elements. Also, seven samples of the alkali feldspar phase of the Topsails granitic complex (Taylor et al., 1980; Thurlow, 1981b) from adjacent to the Buchans Group and the Wiley's Brook intrusion were analyzed for comparison.

PETROGRAPHY

Thin sections of over 150 granitoid clasts from ore horizon boulder breccia-beds have been examined. Over 90 per cent of these were from MacLean Extension orebody, with the remainder from the Oriental orebody. A revised petrographic classification of granitoid types (Table 62.1) is considered more useful than the previous field classification (Stewart, 1983). The field clast groupings of Stewart (1983) showed no geochemical coherence or petrographic distinctivness.

Primary mineralogy of the clasts is simple and relatively consistent, i.e. quartz, plagioclase, biotite (rarely preserved, now chlorite), opaque minerals (hematite, magnetite?), apatite, zircon and sphene (rare).

Detailed petrographic examination of clasts has demonstrated that colour and mineralogical differences used in the earlier classification are primarily due to alteration. Textural differences are gradational and probably represent differences in the mode and timing of crystallization of a single magma. The clast types have been arranged to reflect these gradations, from those with the best developed crystallinity (Type 1) to the least developed (Type 5).

Type 6 clasts are texturally and mineralogically distinct. They show a weakly developed felty texture with euhedral to subhedral plagioclase laths in a groundmass of anhedral plagioclase, quartz and opaque minerals. These clasts show a higher plagioclase/quartz ratio and a higher per cent of mafic and opaque minerals than the other

[1] Contribution to Canada-Newfoundland co-operative mineral program 1982-1984. Project carried by Geological Survey of Canada.
[2] Department of Earth Sciences, Memorial University of Newfoundland, St. John's Newfoundland A1B 3X5

Table 62.1. Petrographic classification of granitoid clasts

Clast type	Grain size (average/range)	Texture	Phenocrysts	Mafic mineral content	Distinguishing features
1.	medium (1 mm/0.2-3.0 mm)	seriate porphyritic	abundant qtz + feldspar; qtz typically larger (to 5 mm)	rare biotite mostly chlorite + opaques after biotite ± epidote (<5%)	relatively coarse grained, seriate texture, i.e. gradation in grain size of groundmass to phenocrysts
2.	fine (0.5 mm/0.1-2 mm)	relatively equigranular	qtz + feldspar (to 2 mm)	rare biotite; mostly chlorite + opaques after biotite + epidote (0-5 vol. %)	relatively intermediate grain size and equigranular
3.	fine to very fine (0.3 mm/0.1-0.5 mm)	hiatal porphyritic – rare micro-granophyric areas	qtz + feldspar (1-8 mm) typically in clusters (especially feldspars)	chlorite + opaques ± epidote (<5%)	hiatal porphyritic – large difference in size between phenocrysts and groundmass; abundant phenocrysts
4.	very fine (0.2 mm/0.1-0.4 mm)	equigranular	rare qtz + feldspar (to 2 mm)	chlorite + opaques ± epidote, zoisite (<5%)	equigranular, fine grain size; lack of phenocrysts; relatively minor micro-granophyric areas
5.	very fine to fine (<0.5 mm/0.1-2 mm)	variable % of well-developed microgranophyric patches	rare, mostly qtz (to 2 mm)	chlorite + opaques ± epidote (0-5%)	abundant microgranophyre; equigranular
6.	very fine (0.2 mm/0.1-0.4 mm)	equigranular euhedral to subhedral feldspars	none	very abundant, especially opaques; biotite and chlorite (to 10%)	"lath-like" texture of feldspars; abundant mafic minerals – almost exclusively restricted to siltstone breccia, under ore horizon

clast types. This type is also chemically distinct (lower SiO_2, higher TiO_2 and CaO) and primarily restricted to the siltstone breccia unit which occurs several metres stratigraphically beneath the lower ore unit in MacLean Extension area. However rare clasts of this type have been found within the lower ore unit.

Staining with sodium cobaltinitrite for potassium feldspars suggests that all feldspars are plagioclase. The alteration and lack of twinning of feldspars has precluded petrographic determination of An content, but the geochemistry suggests that they are predominantly of albitic composition.

The dusty and pitted appearance of the feldspars and the presence of secondary minerals (sericite, calcite, epidote) in the feldspar crystals suggest that they have been saussuritized. Whether this is due to hydrothermal alteration or is a product of regional metamorphism is not known. The regional metamorphism of the Buchans Group is of the prehnite-pumpellyite facies (Henley and Thornley, 1981), and the alteration may have been a product of this metamorphism.

GEOCHEMISTRY

The study was designed to assess the relationship among three sample populations; the granitoid clasts, Feeder Granodiorite (predominantly the Wiley's River intrusion) and Topsails granite. The present geochemical results are preliminary, but do suggest several points: 1) all rock types are silica-oversaturated and peraluminous; 2) the Feeder Granodiorite and the clasts are from I-type (orogenic) magmas, whereas the Topsails granite is from an A-type (anorogenic) granite; 3) trace element abundances show significant differences between the Topsails granite and the other two populations; 4) the magmatic relationship of the Feeder Granodiorite and the granitoid clasts cannot be conclusively established, or refuted with the present evidence, and 5) the clasts have undergone varying degrees of alteration, whereas the Feeder Granodiorite and the Topsails granite are comparatively unaltered. These points are examined in more detail below.

All clast samples were found to contain greater than 70% (wt.) SiO_2 (anhydrous) with some clasts exceeding 80% SiO_2. Both the Feeder Granodiorite and the Topsails granite have a more restricted silica range of about 5% SiO_2, all above 70% SiO_2.

Because of the mobility of the alkali elements during alteration, their usefulness for classification of altered rocks is suspect. As will be discussed below, the alkali distributions in the clasts were affected by alteration. For this reason, plots of Irvine and Baragar (1971) and AFM plots are not presented, but are suggestive of a calc-alkaline affinity for all populations and Strong (1977) and Thurlow (1981a) have demonstrated that the Buchans Group is calc-alkaline.

Using the granitoid classification scheme of White and Chappell (1983), the granitoid clasts and the Feeder Granodiorite crystallized from I-type magmas and the

Topsails granite from an A-type magma (Fig. 62.1). Figure 62.1b is probably a more reliable plot than Figure 62.1a which uses alkali elements. The elements Ga and especially Al are considered to be relatively immobile during alteration. High contents of highly charged cations such as Ga, Zr and Y (see Fig. 62.1b, 62.2) are considered diagnostic of A-type magmas (White and Chappell, 1983). A-type granitoid bodies in eastern Australia are associated in space and time with volcanics rocks, as is the Topsails granite (Whalen and Currie, 1983). The presence of miarolitic and granophyric textures further substantiates the designation of the Topsails granite as an A-type intrusion (White and Chappell, 1983, p. 30).

Although I-type magmas are usually subaluminous, the Feeder Granodiorite and granitoid clasts are peraluminous. This has been considered to be indicative of a minimum-temperature melt or a highly fractionated I-type melt (White and Chappell, p. 28). This allows the possibility that the Feeder Granodiorite is the more fractionated parent of the granitoid clasts, but this has not yet been demonstrated.

Plots of paired immobile elements (Fig. 62.2) have been shown to be effective in distinguishing different magma series and their tectonic settings (Pearce and Cann, 1973; Wood et al., 1979; Palacios et al., 1983). The distinction of the Topsails granite is obvious and the correlation between the clasts and the Feeder Granodiorite is suggested. Bailey (1981) proposed that Zr and Y enrichment distinguishes anorogenic andesites from orogenic andesites, which supports the anorogenic setting of the Topsails granite. The slight enrichment of the Feeder Granodiorite in Zr and Y relative to the clasts is suggestive of a late stage differentiate (Taylor, 1965).

ALTERATION

The most common expression of hydrothermal alteration is the production of hydrous minerals from the primary anhydrous minerals. Therefore, the loss on ignition (LOI) provides a qualitative means to judge the degree of alteration. Although the LOI may be a mixture of H_2O, CO_2 and possibly sulphur-bearing gases, for evaluation of the degree of alteration, LOI is considered to be mainly H_2O and CO_2.

The variable degree of alteration of the clasts is apparent from Figure 62.3. A positive correlation between both CaO and K_2O with loss on ignition is shown in Figures 62.3b, c. The feldspars are partly altered to sericite (or muscovite) and calcite, indicating that these chemical variations are probably reflecting alteration. The very high barium content of the clasts in general, and the presence of barite as secondary veins and disseminations in the clasts is also in accord with the weakly defined positive correlation between Ba and LOI in Figure 62.3d. Magnesium shows appreciable scatter around a weak positive correlation (Fig. 62.3a). Variable amounts of chlorite and magnesium in the clasts could indicate an alteration, rather than a metamorphic origin for the chlorite. Alteration is indicated mineralogically by the saussuritization of feldspars, chloritization of biotite (no other primary mafic mineral, or relicts of other mafic minerals have been recognized) and introduction of barium and calcium as barite and calcite. The elevated Ba values in the clasts probably indicates that their alteration is related to the mineralizing event at Buchans (Thurlow, 1981a) or to migration of Ba from barite in the breccia-conglomerate beds during or after consolidation (op cit, p. 285). The presence of calcite ± barite veins in some samples analyzed could add to LOI scatter and mask chemical effects of rock alteration.

Ca and Sr are considered to behave similarly under many conditions (Taylor, 1965; Mason, 1966). This behavior and the contrasting dissimilar behavior of Rb and Sr are demonstrated in Figure 62.4. Sr content shows a corresponding increase with Ca content (Fig. 62.4b), wheras Rb (Fig. 62.4a) has a negative correlation (Fig. 62.4a). The increase of Ca and Sr contents in the clasts is believed due to the introduction of calcite and barite during alteration. Rubidium contents remain relatively constant in the clasts though Sr values increase. Unless Rb was uniformly depleted, which conflicts with the generally variable nature of the alteration, it was apparently unaffected by the alteration.

Figure 62.5 presents evidence which possible conflicts with Feeder Granodiorite being the parent of the clasts. If it were the parent, then it should have had a similar K_2O content, prior to the alteration of the clasts. If, as indicated in Figure 62.3c, K_2O has increased with degree of alteration (along with increasing Sr (Fig. 62.4)) then the clasts in

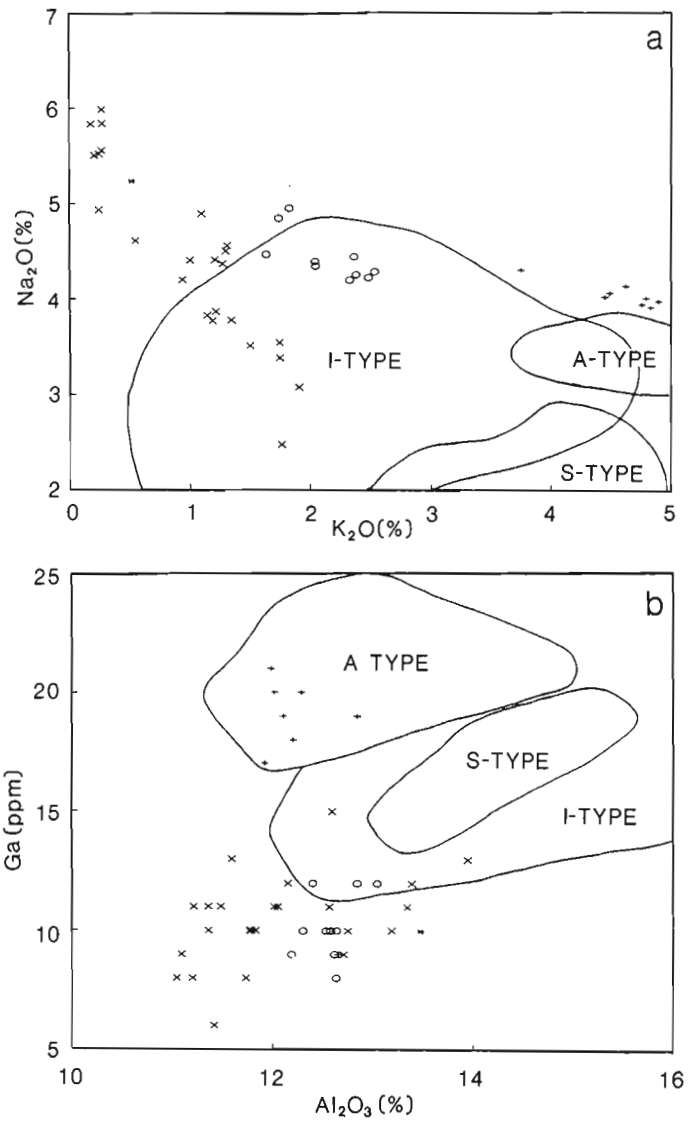

Figure 62.1. Discriminant diagram for granitoid magma series from White and Chappell (1983): a) K_2O vs Na_2O; b) Al_2O_3 vs Ga. The (x) represents a granitoid clast sample from MacLean Extension orebody, (o) represents a Feeder Granodiorite sample, the (+) represents the Topsail (alkali feldspar) granite sample, and the (*) represents the sample from the Little Sandy intrusion.

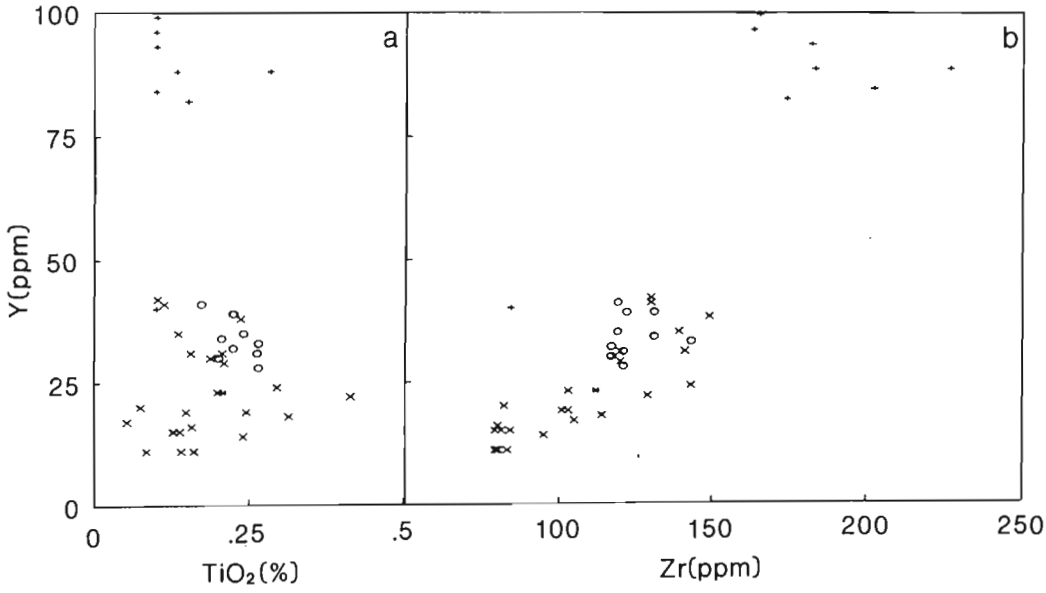

Figure 62.2

Plots of relatively immobile elements: a) TiO_2 vs Y; b) Zr vs Y, after Palacios et al., 1983. For symbols see Figure 62.1.

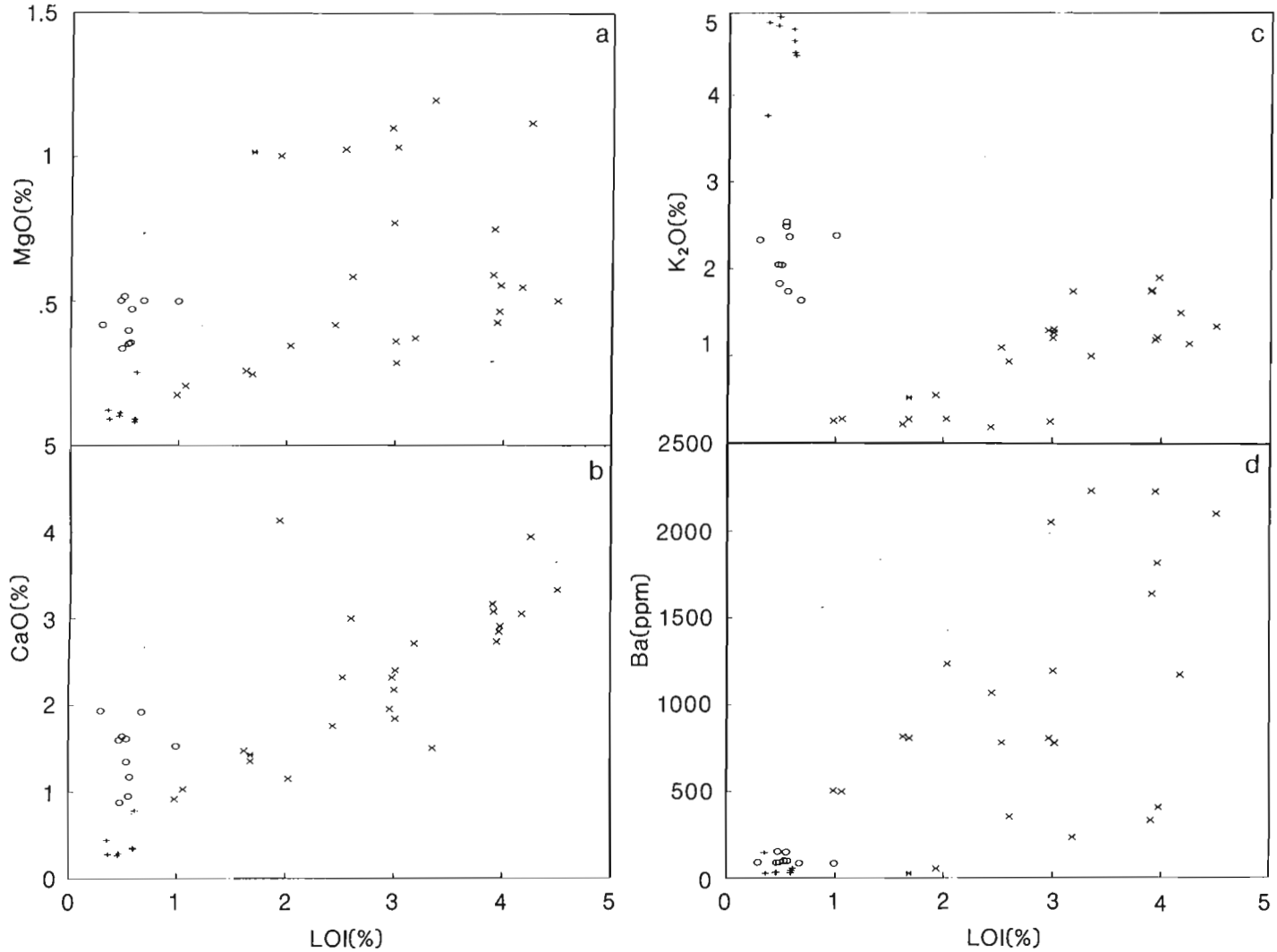

Figure 62.3. *Diagrams illustrating the effects of alteration on particular elements: a) loss on ignition (LOI) vs MgO; b) LOI vs CaO; c) LOI vs K_2O; d) LOI vs Ba. For symbols see Figure 62.1.*

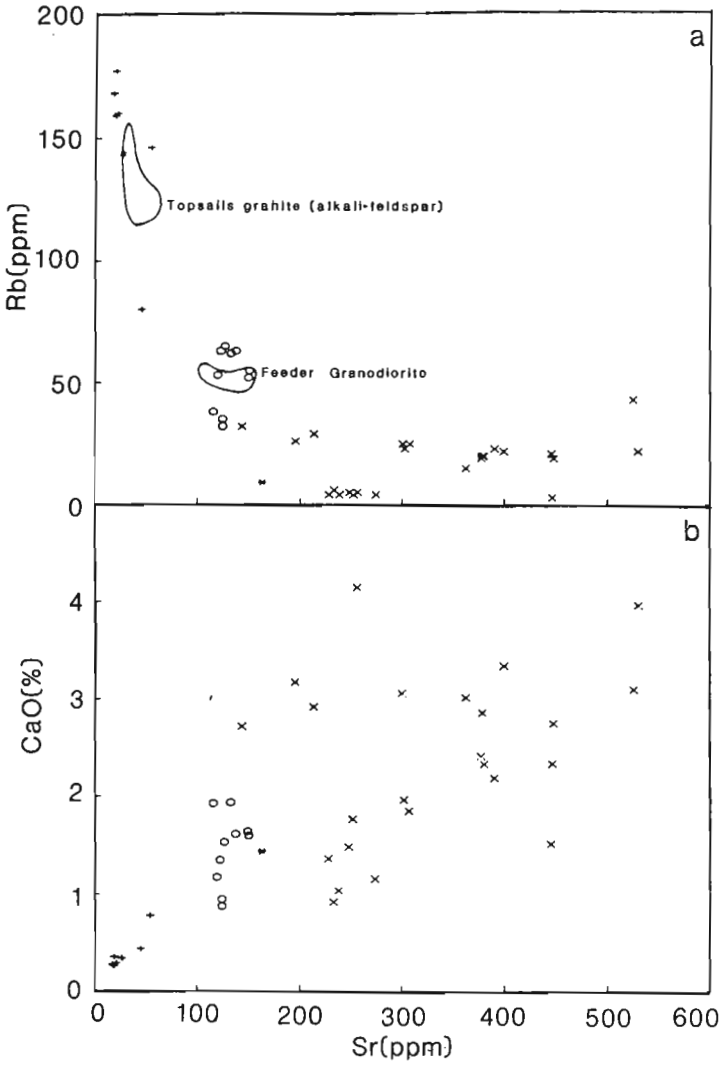

Figure 62.4. *Correlation diagrams; a) Sr vs Rb. Fields after Bell and Blenkinsop, 1981; (b) Sr vs CaO. For symbols see Figure 62.1.*

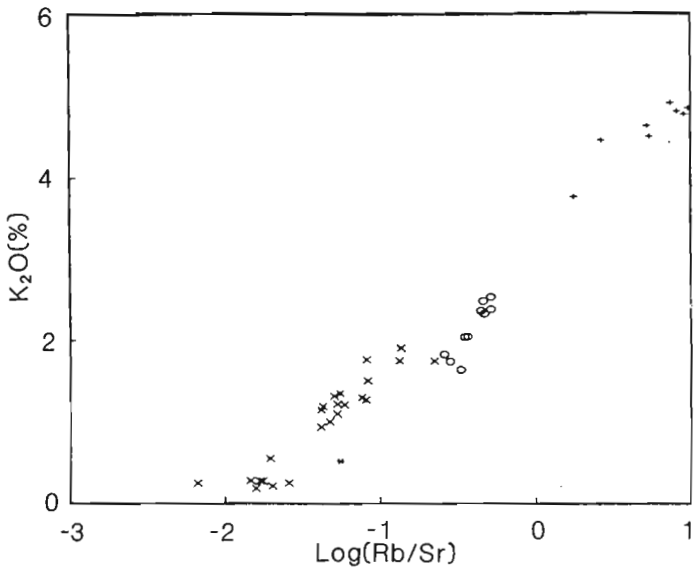

Figure 62.5. *Rb/Sr expressed logarithmically vs K_2O. For symbols see Figure 62.1.*

Figure 62.5 should plot toward the upper left part of the diagram and not the lower left part as indicated. Even if the Feeder Granodiorite is a later differentiate of the same magma and has a higher intial K_2O content, the observed trend still cannot be resolved. This underlies the difficulties in determining the changes in element contents during alteration. Work is in progress to try to resolve this problem.

The lack of apparent alteration of the Feeder Granodiorite and the Topsails granite is obvious from Figures 62.3, 62.4. The fields for the Topsails alkali feldspar phase and the Feeder Granodiorite of Bell and Blenkinsop (1981) are shown in Figure 62.4a for comparison.

One of the samples designated as a Topsails granite plots consistently outside the cluster of other Topsail samples. This is a sample of a dyke which cuts the Feeder Granodiorite and was presumed to be related to the Topsails granite, which it closely resembles megascopically. The trace element chemistry suggests that it has possibly been modified by contamination from the Feeder Granodiorite during emplacement (see Fig. 62.2a, b, especially).

The single data point for the Little Sandy intrusion is insufficient to permit any rigorous conclusions. The data do suggest however, a closer affinity to the clasts than to the Feeder Granodiorite itself. Further analyses of samples from this body are currently in progress.

CONCLUSIONS

A few preliminary conclusions can be drawn. The Topsails granite can be clearly separated petrographically and lithochemically from the Feeder Granodiorite and granitoid clasts. This is consistent with the established geological and age relationships for the Topsails granite (Thurlow, 1981b; Whalen and Currie, 1982, 1983). As first demonstrated by Thurlow (1981a), the Feeder Granodiorite has many geochemical similarities to the clasts and may have crystallized from the magma reservoir which produced the clasts. Other element combinations suggest that the Feeder Granodiorite and clasts may be separated geochemically and may not be genetically related. Further work remains to be done before this problem can be resolved.

The Feeder Granodiorite and Topsails granite are both unaltered to weakly altered, whereas, the clasts are variably altered. K_2O, CaO, MgO, Ba and Sr contents of the clasts increase erratically with increasing alteration.

ACKNOWLEDGMENTS

The author wishes to thank G. Andrew, Memorial University of Newfoundland, for the major element analyses and D. Press for assistance in the graphical presentations. The advice of J.G. Thurlow, E.A. Swanson and D.M. Barbour while in Buchans is gratefully acknowledged, and the assistance of other ASARCO and Abitibi-Price Inc. personnel in Buchans appreciated.

This study comprises a portion of the work towards a Master of Science degree at Memorial University.

Critical review of this report by R.V. Kirkham, W.H. Poole, D.F. Strong and J.G. Thurlow resulted in numerous improvements.

REFERENCES

Bailey, J.C.
1981: Geochemical criteria for a refined tectonic discrimination of orogenic andesites; Chemical Geology, v. 32, p. 139-154.

Bell, K. and Blenkinsop, J.
1981: A geochronological study of the Buchans area, Newfoundland; in The Buchans Orebodies: Fifty Years of Geology and Mining, ed. E.A. Swanson, D.F. Strong, and J.G. Thurlow; Geological Association of Canada, Special Paper 22, p. 91-111.

Binney, W.P., Thurlow, J.G., and Swanson, E.A.
1983: The MacLean Extension orebody, Buchans, Newfoundland; in Current Research, Part A, Geological Survey of Canada, Paper 83-1A, p. 313-319.

Henley, R.W. and Thornley, P.
1981: Low grade metamorphism and the geothermal environment of massive sulphide ore formation, Buchans, Newfoundland; in the Buchans Orebodies: Fifty Years of Geology and Mining, ed. E.A. Swanson, D.F. Strong and J.G. Thurlow; Geological Association of Canada, Special Paper 22, p. 205-228.

Irvine, T.N. and Baragar, W.R.A.
1971: A guide to the chemical classification of the common volcanic rocks; Canadian Journal of Earth Sciences, v. 8, p. 523-548.

Kean, B.F., Dean, P.L., and Strong, D.F.
1981: Regional geology of the central volcanic belt of Newfoundland; in The Buchans Orebodies: Fifty Years of Geology and Mining, ed. E.A. Swanson, D.F. Strong, and J.G. Thurlow; Geological Association of Canada, Special Paper 22, p. 65-78.

Mason, B.
1966: Principles of geochemistry; Wiley, New York, 3rd ed., 328 p.

Palacios, M.C., Guerra, S.N., and Campano, B.P.
1983: Difference in Ti, Zr, Y and P content in calc-alkaline andesites from island arcs and continental margin (central Andes); Geologische Rundschau, v. 72, v. 2, p. 733-738.

Pearce, J.A. and Cann, J.R.
1973: Tectonic setting of basic volcanic rocks determined using trace element analyses; Earth and Planetary Science Letters, v. 19, p. 290.

Stewart, P.W.
1983: Granitoid clasts in boulder breccias of MacLean Extension orebody, Buchans, Newfoundland; in Current Research, Part A, Geological Survey of Canada, Paper 83-1A, p. 321-324.

Strong, D.F.
1977: Volcanic regimes in the Newfoundland Appalachians; in Volcanic Regimes in Canada, ed. W.R.A. Baragar, L.C. Coleman, and J.M. Hall; Geological Association of Canada, Special Paper 16, p. 61-90.

Taylor, R.P., Strong, D.E., and Kean, B.F.
1980: The Topsails igneous complex: Silurian and Devonian peralkaline magmatism in western Newfoundland; Canadian Journal of Earth Sciences, v. 17, p. 425-439.

Taylor, S.R.
1965: The application of trace element data to problems in petrology; Physics and Chemistry of the Earth, v. 6, p. 133-213.

Thurlow, J.G.
1981a: Geology, ore deposits and applied rock geochemistry of the Buchans Group, Newfoundland; unpublished Ph.D. thesis, Memorial University of Newfoundland, 305 p.

1981b: The Buchans Group: its stratigraphic and structural setting; in The Buchans Orebodies: Fifty Years of Geology and Mining, ed. E.A. Swanson, D.F. Strong, and J.G. Thurlow; Geological Association of Canada, Special Paper 22, p. 79-90.

Thurlow, J.G. and Swanson, E.A.
1981: Geology and ore deposits of the Buchans area, central Newfoundland; in The Buchans Orebodies: Fifty Years of Geology and Mining, ed. E.A. Swanson, D.F. Strong, and J.G. Thurlow; Geological Association of Canada, Special Paper 22, p. 113-142.

Walker, P.N. and Barbour, D.M.
1981: Geology of the Buchans ore horizon breccias; in The Buchans Orebodies: Fifty Years of Geology and Mining, ed. E.A. Swanson, D.F. Strong, and J.G. Thurlow; Geological Association of Canada, Special Paper 22, p. 161-186.

Whalen, J.B. and Currie, K.L.
1982: Volcanic and plutonic rocks in the Rainy Lake area, Newfoundland; in Current Research, Part A, Geological Survey of Canada, Paper 82-1A, p. 17-22.

1983: The Topsails igneous terrane of western Newfoundland; in Current Research, Part A, Geological Survey of Canada, Paper 83-1A, p. 15-23.

White, A.J.R. and Chappell, B.W.
1983: Granitoid types and their distribution in the Lachlan Fold Belt, southeastern Australia; in Circum-Pacific Plutonic Terranes, ed. J.A. Roddick; Geological Society of America, Memoir 159, p. 21-34.

Wood, D.A., Joron, J-L., and Treuil, M.
1979: A re-appraisal of the use of trace elements to classify and discriminate between magma series erupted in different tectonic settings; Earth and Planetary Science Letters, v. 45, p. 326-336.

63. UPPER CARBONIFEROUS STRATA OF THE EAST HALF OF THE TATAMAGOUCHE SYNCLINE, CUMBERLAND BASIN, NOVA SCOTIA[1]

Contract 19SR. 23233-3-0393

R.J. Ryan[2]

Ryan, R.J., Upper Carboniferous strata of the east half of the Tatamagouche syncline, Cumberland Basin, Nova Scotia; in Current Research, Part A, Geological Survey of Canada, Paper 84-1A, p. 473-476, 1984.

Also in Mines and Minerals Branch, Report of Activities, 1983, Nova Scotia Department of Mines and Energy, Report 84-1, 1984.

Abstract

The Upper Carboniferous strata of the eastern Tatamagouche syncline area consist of fining upward cycles of conglomerates to mudstones. The strata can be divided into seven map units, in ascending order: Millsville Formation, Boss Point Formation, Cumberland Group, Pictou Group grey beds, Pictou Group lower red beds, Pictou Group middle red beds, and the Pictou Group upper red beds. Regularly interbedded lacustrine limestone marker beds facilitate definition and correlation of the upper units.

Alluvial fans developed in the south from pre-Carboniferous rocks in the present day Cobequid Highlands. Towards the north, sand and mud were deposited along low sinuosity, anastomosing rivers. Strongly unimodal paleocurrent measurements indicate flow to the north-northwest.

Copper, uranium and recently discovered lead occurrences are associated almost exclusively with carbon-rich channel lag conglomerate and sandstone.

Résumé

Les couches du Carbonifère supérieur de la partie est de la région du synclinal de Tatamagouche se composent de cycles de conglomérats se transformant en mudstones à granulométrie décrossante vers le haut. Les couches sont divisées en sept unités cartographiques, données en ordre ascendant: la formation de Millsville, la formation de Boss Point, le groupe de Cumberland, les couches grises du groupe de Pictou, les couches rouges inférieures du groupe de Pictou, les couches rouges intermédiaires du groupe de Pictou et les couches rouges supérieures du groupe de Pictou. Des lits repères de calcaire lacustre y sont interstratifiés régulièrement et facilitent la définition et la corrélation des unités supérieures.

Des cônes de déjection se sont formés au sud à partir de roches pré-carbonifères dans les hautes-terres de Cobequid actuelles. Au nord, du sable et de la boue se sont accumulés le long de rivières anatomosées à faible sinuosité. Les valeurs fortement unimodales des paléocourants indiquent que l'écoulement se faisait vers le nord-nord-ouest.

Des venues de cuivre et d'uranium et des venues récemment découvertes de plomb sont associées presque exclusivement à un conglomérat et à un grès fluviatils grossiers, riches en carbone.

INTRODUCTION

The eastern half of the Tatamagouche syncline within the Carboniferous Cumberland Basin of northern Nova Scotia was the subject of geological investigations during the 1983 field season. The rocks exposed within the study area are the Riversdale, Cumberland and the Pictou groups of continental origin (Fig. 63.1). These Upper Carboniferous rocks are folded into a gently plunging syncline trending northeast, and consist of red and grey conglomerates, sandstones and mudstones with minor limestones, totalling approximately 3400 m in thickness. The rocks form a series of fining-upward cycles, with a thickness for each cycle of approximately 200 m. The evaluation of the stratigraphy was greatly aided by the availability of approximately 80 diamind-drill hole cores totalling about 40 000 feet.

STRATIGRAPHY

The Upper Carboniferous strata of the Tatamogouche syncline can be divided into seven mappable units (Fig. 63.2, 63.3).

Riversdale Group

Millsville Formation

The term Millsville Formation was introduced by Bell (1926) to refer to exposures of reddish-brown conglomerates located in the vicinity of Millsville, Pictou County, Nova Scotia. The Millsville Formation in the eastern part of the Tatamagouche syncline is a unit comprised of dominantly red, although locally grey, boulder to pebble conglomerates and minor sandstones. The conglomerates are rarely crossbedded, but do possess poorly developed imbrication. The formation varies from 150 to 700 m in thickness. Age: Namurian.

Boss Point Formation

The Boss Point Formation was defined by Bell (1914) to include the sandstones, siltstones and shales of Westphalian A age, exposed at Boss Point Cumberland County, Nova Scotia. In the Tatamagouche area the formation consists of grey to brown, coarse- to fine-grained quartz sandstones,

[1] Contribution to Canada-Nova Scotia Co-operative Mineral Program 1981-84.
Project carried by Geological Survey of Canada and Nova Scotia Department of Mines and Energy.
[2] Department of Geology, University of New Brunswick, Fredericton, New Brunswick E3B 5A3
Present address: Department of Geology, St. Mary's University, Halifax, Nova Scotia B3H 3C3

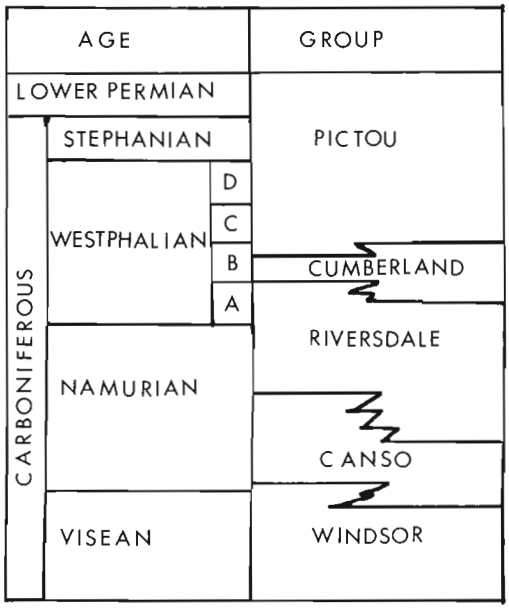

Figure 63.1. Generalized Carboniferous stratigraphy in the eastern Tatamagouche syncline, Cumberland Basin, Nova Scotia.

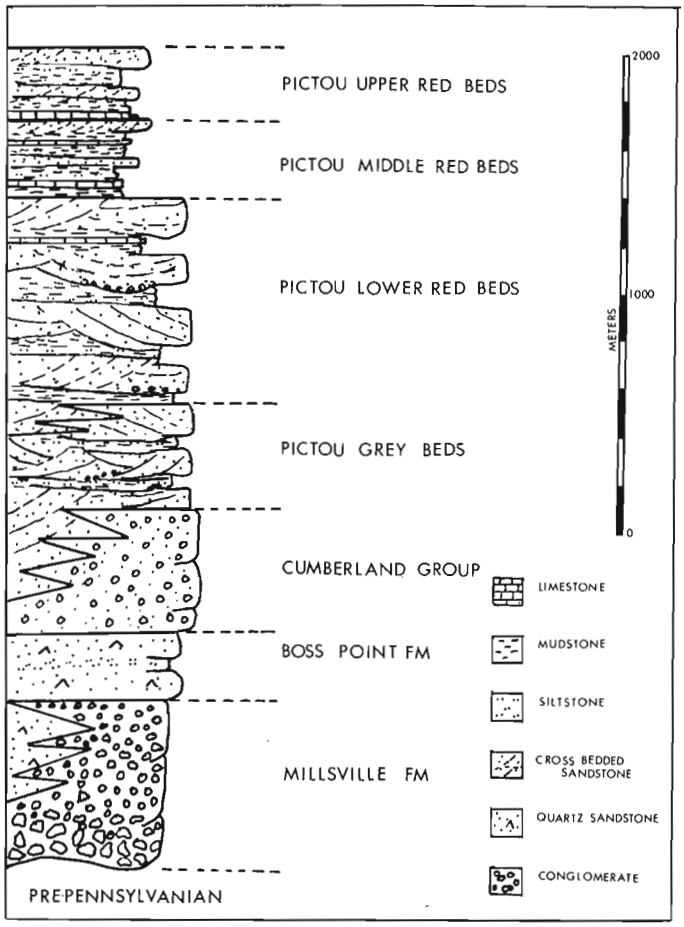

Figure 63.2. Stratigraphic column of Upper Carboniferous strata, eastern Tatamagouche syncline.

minor arkosic sandstones, and siltstones. The sandstones are usually crossbedded and are variably carbonaceous. The formation varies from 150 to 700 m in thickness within the mapped area. Age: Westphalian A.

Cumberland Group

Cumberland Coarse Facies

This unit consists of red polymictic cobble to pebble conglomerate which may contain clasts of Carboniferous sandstones. Trough crossbedding is common, and the conglomerates have moderate to good imbrication. This formation varies from being absent on the southeast limb to a thickness of 600 m on the northwest limb of the Tatamagouche syncline. Age: Westphalian B.

Pictou Group

The name Pictou Group was proposed by Bell (1926). He applied the term to the reddish-brown sandstones, mudstones, and conglomerates exposed on River John, Pictou County, Nova Scotia.

Pictou Grey Beds

These beds are made up of grey arkosic sandstones, siltstones, and mudstones. The sand to silt + mud ratio is approximately 3:1. The sandstone units are trough crossbedded and may have a calcareous mud-chip conglomerate at their base. The rocks are variably carbonaceous with some carbon-rich channel lags present. The siltstones and mudstones are ripple marked and locally are bioturbated. The thickness varies from 100 to 400 m. Age: Westphalian B-C.

Pictou Lower Red Beds

These beds are usually red, and the unit is made up of calcareous mud-chip conglomerates, arkosic sandstones, crosslaminated siltstones and bioturbated mudstones. The sand to silt + mud ratio is approximately 2:1. The sandstones and conglomerates are trough crossbedded and are variably carbonaceous. Locally calcretes are developed, which contribute the calcareous material to the mud-chip conglomerates. This unit is 800 to 900 m thick. Age: Westphalian C-D.

Pictou Middle Red Beds

This unit consists of predominantly red sandstones, conglomerates, siltstone and mudstones. The sand to silt + mud ratio is approximately 1:2. The sandstones and conglomerates are trough crossbedded and variably carbonaceous. The siltstone beds have lunate ripples with localized calcrete development. A few thin, but laterally extensive, limestone beds, probably representing deposition in large lakes which covered the central parts of the syncline, facilitate correlation. The unit is about 310 m thick. Age: Wesphalian D to Stephanian.

Pictou Upper Red Beds

This unit consists of red and locally grey conglomerates, arkoses and sandstones, siltstones and mudstones. The sand to silt + mud ratio is 1:3 to 1:4. The sandstones and conglomerates are trough crossbedded. The finer grained sedimentary rocks are lunate ripple marked and locally highly bioturbated. Mud-filled channel plugs are common.

Thin, laterally extensive lacustrine limestones and calcretes occur throughout the unit. Some carbon-rich channel lag sandstones are present within the thick channel sandstone sequences. The unit is approximately 330 m thick. Age: Stephanian to Early Permian.

SEDIMENTOLOGY AND PALEOCURRENT STUDIES

Over 300 paleocurrent measurements were recorded during the 1983 field season. Ripple marks, parting lineations, crossbed truncation ridges, preferred plant fragment orientations, flute marks, tool marks, pebble imbrications and crossbedding were all used in the paleocurrent study. The trough crossbedding yielded the most conistent of the paleocurrent determinations and therefore, it is these data that are presented in Figure 63.4 of this report.

The paleocurrent data exhibit a strongly unimodal distribution with the modal trend of north-northwest, 340°. The low variance of the paleocurrent data indicates that deposition, for the most part, occurred in a low-sinuosity flow. Only the Pictou Upper Red Bed unit exhibits significant variability in paleocurrent directions. The north-northwest paleocurrent direction persisted from the Namurian through to the Early Permian.

Field mapping, which confirmed the presence of numerous channels, together with low sand to silt ratios and unimodal paleocurrent data, suggest that during most of the Late Carboniferous the dominant depositional environment consisted of low-sinuosity streams whose configuration would have been that of anastomosing streams.

The Boss Point Formation exhibits slight variations (up to about 30 degrees) of the paleocurrent directions, which suggest a more typical meandering stream environment of deposition for the quartz sandstones of this unit.

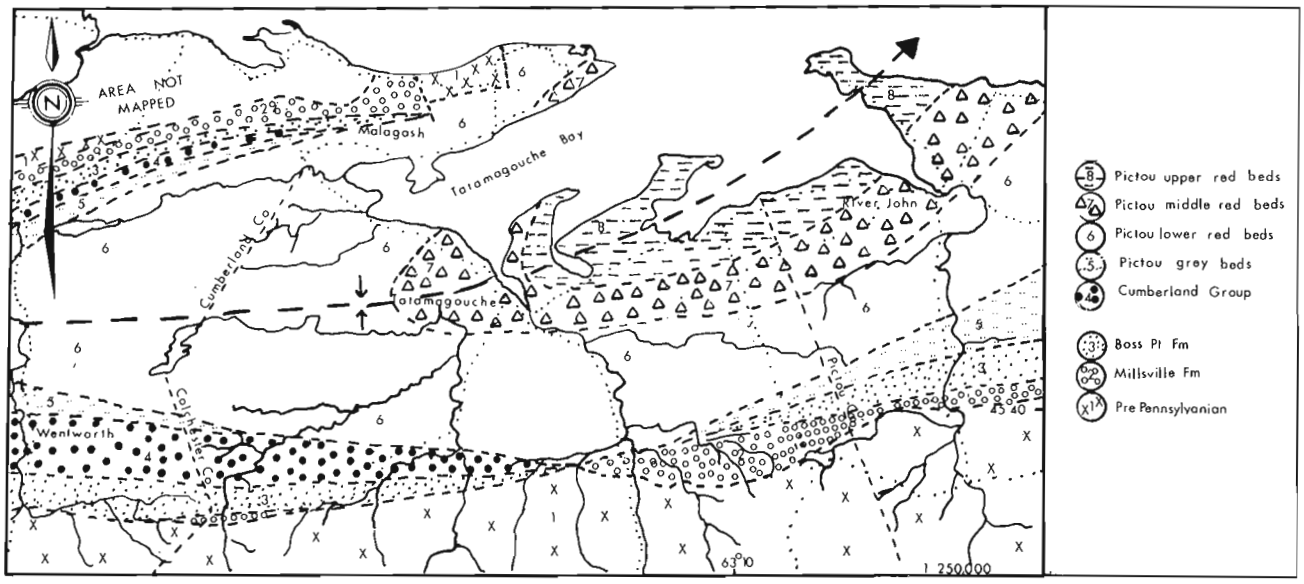

Figure 63.3. Generalized geological map of Upper Carboniferous rocks, eastern Tatamagouche syncline.

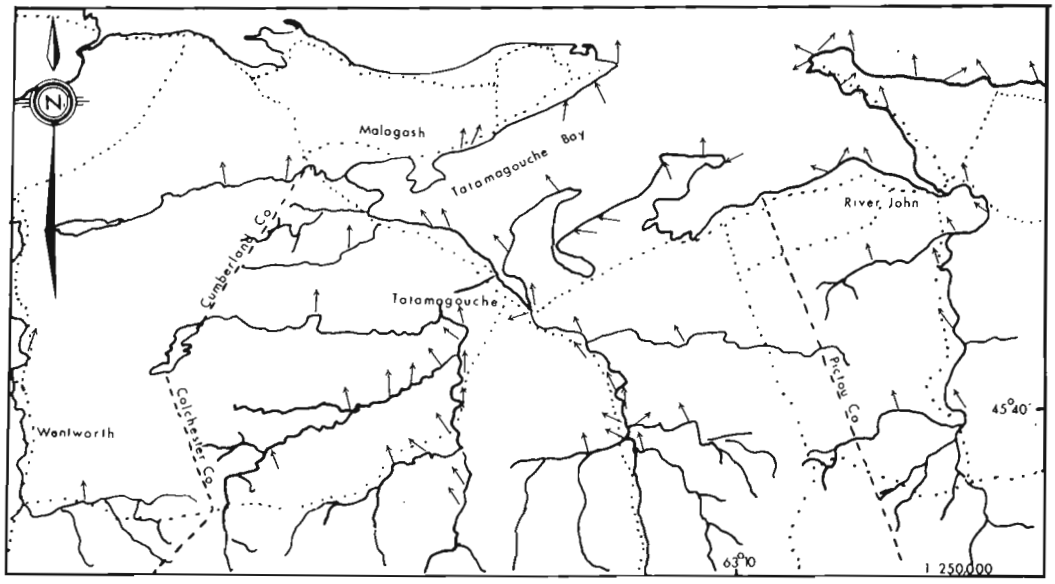

Figure 63.4. Crossbed paleocurent trends within Upper Carboniferous strata, eastern Tatamagouche syncline.

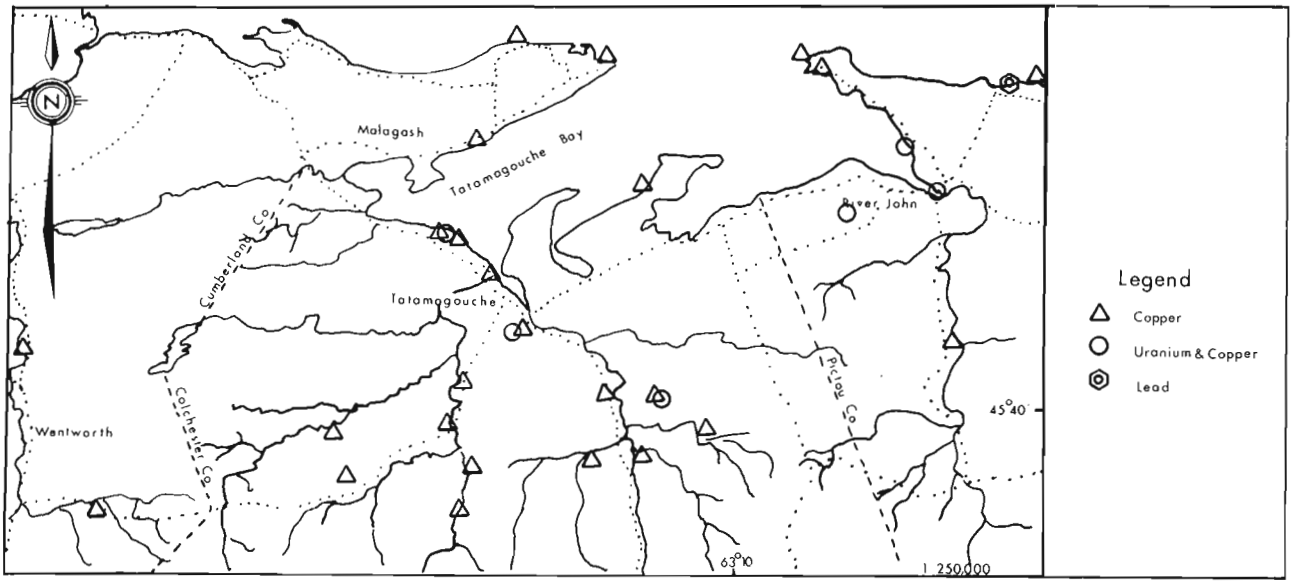

Figure 63.5. Metallic mineral occurrences in Upper Carboniferous strata, eastern Tatamagouche syncline.

The Millsville Formation and the coarse facies of the Cumberland Group represent alluvial fans, the Millsville being a proximal fan flanking the Cobequid Highlands to the south, and the Cumberland conglomerates representing a mid to distal fan produced by an uplift of the Cobequid Highlands at the end of the Westphalian A.

ECONOMIC GEOLOGY

There are 32 significant metallic mineral occurrences within the eastern half of the Tatamagouche syncline (Fig. 63.5). The copper occurrences are the most numerous, and several of these have associated uranium mineralization (McNabb, 1977; MacDonald, 1978). Several new occurrences were found during this study, most of which were copper occurrences. One lead occurrence was discovered in boulders at Skinner's Cove (Fig. 63.5). Although no geochemical results were available at the time of publication, it is strongly suspected that silver values are associated with the galena. The galena is associated with siderite and plant debris. The lithology of the boulders is consistent with that of the basal channel lag sandstones of the Pictou Middle Red Beds exposed along the cliff above the beach where the boulders were found.

Copper usually occurs as malachite, nodules of chalcocite or as chalcocite replacing carbon plant material.

Uranium occurrences can also occur with little or no associated copper mineralization (McNabb, 1977). The uranium mineralization is also very closely associated with the presence of carbon. The uranium seen as occurrences, represents the uranium bound with the carbon, left behind by the migrating uranium-bearing solutions.

Dunsmore (1977) suggested that the mineralization usually occurred near the base of fining-upward cycles in the Tatamagouche area. Almost all of the mineralization, copper, lead, and uranium, is associated with the carbon-rich channel lag sandstones which usually, although not everywhere, occur near the base of the channel sandstone units. Because the lag sandstones are part of the overall channel sequence, it is necessary to follow such beds down channel, and not down dip, in order to delineate potential mineralized zones. It is therefore vital that paleocurrent data be incorporated into any exploration model for the Tatamagouche syncline area.

ACKNOWLEDGMENTS

The author gratefully acknowledges the assistance of T. Johnson in the field and the valuable discussions with B. McNabb of Lacana and J. O'Sullivan of Esso Minerals. The author would also like to acknowledge the contributions to this paper by H.W. van de Poll.

REFERENCES

Bell, W.A.
1914: Joggins Carboniferous Section, Nova Scotia; Geological Survey of Canada, Summary Report, 1912, p. 360-371.

1926: Carboniferous Formations of the Northumberland Strait, Nova Scotia; Geological Survey of Canada, Summary Report, 1924, Part C, p. 142-180.

Dunsmore, H.E.
1977: Uranium Resources of the Permo-Carboniferous Basin, Atlantic Canada; in Report of Activities, Part B, Geological Survey of Canada, Paper 77-1B, p. 341-348.

MacDonald, C.J.D.
1978: Uranium, Tatamagouche Area, Nova Scotia; Noranda Exploration Co. Ltd., Assessment Report, Nova Scotia, 11E/11C 54-D-45(11).

McNabb, B.E.
1977: Uranium, Tatamagouche Area; Lacana Exploration, N.S. Assessment Report 11E/NW 54-D-45(01).

64. PATTERNS OF GLACIER MOVEMENT IN CUMBERLAND, COLCHESTER, HANTS AND PICTOU COUNTIES, NORTHERN NOVA SCOTIA[1]

Project 820019
Contract 19SR.23233-3-0356

R.R. Stea[2] and P.W. Finck[3]

Stea, R.R. and Finck, P.W., Patterns of glacier movement in Cumberland, Colchester, Hants and Pictou counties, northern Nova Scotia; in Current Research, Part A, Geological Survey of Canada, Paper 84-1A, p. 477-484, 1984.

Also in Mines and Minerals Branch, Report of Activities, 1983, Nova Scotia Department of Mines and Energy, Report 84-1, 1984.

Abstract

Mapping of glacial features and till sheets in Cumberland, Colchester, Hants and Pictou counties has been completed. Preliminary results indicate four major ice-flow phases. The first phase was an eastward and southeastward movement which formed a compact, reddish-brown lodgement till. After a brief recession, indicated by alteration at the top of the logdement till, a glacier moved south-southwestward across the map area. Boulder pavements separating two till sheets along the Northumberland Strait also record this change in ice-flow direction. A major flow reversal then occurred with ice flowing north and northeastward from a centre in the Southern Uplands. Erratics derived from the South Mountain batholith were transported north during this flow. Striations trending 260-290° cut across striations made by the northeastward flow and represent a final pulse of ice flow westward into the Minas Basin. The early eastward flow is speculated to be Early Wisconsinan as striations relating to it are inscribed on a wave-planed rock bench assigned a Sangamon age. The last two flow phases are assigned Late Wisconsinan ages on the basis of radiocarbon dates on surficial organic deposits.

Résumé

La cartographie des éléments glaciaires et des nappes de till dans les comtés de Cumberland, de Colchester, de Hants et de Pictou a été achevée. Les résultats préliminaires indiquent qu'il y a eu quatre principales phases d'écoulement glaciaire. La première phase a été un mouvement vers l'est et le sud-est qui a produit un till de fond compact de teinte rougeâtre. Après un retrait de courte durée, indiqué par l'altération de la surface supérieure du till de fond, le glacier s'est déplacé vers le sud-sud-ouest en travers de la région cartographiée. Des dallages de pierres séparant deux nappes de till le long du détroit de Northumberland attestent également de ce changement de la direction d'écoulement de la glace. Une importante inversion de la direction d'écoulement s'est alors produite, la glace se déplaçant vers le nord et le nord-est à partir d'un centre situé dans les hautes-terres du sud. Des blocs erratiques provenant du batholite de South Mountain ont été transportés vers le nord au cours de ce mouvement. Des stries glaciaires orientées entre 260 et 290° en recoupent d'autres produites par le mouvement vers le nord-est et représentent une avancée finale de la glace vers l'ouest, dans le bassin de Minas. Le premier mouvement vers l'est date vraisemblablement du Wisconsinien ancien puisque les stries qui lui sont associées se manifestent sur une plate-forme d'abrasion littorale datant du Sangamon. La datation au radiocarbone des dépôts organiques de surface indique que les deux derniers mouvements datent du Wisconsinien récent.

INTRODUCTION

Mapping of the surficial deposits and glacial features in northern Nova Scotia is part of a project that includes trace element analyses of till.

The area covered by this report lies between latitudes 45°15'N and 45°55'N and longitudes 62°45'W and 64°20'W.

Physiography and general geology

The study area consists of three physiographic regions: Cumberland-Pictou Lowlands, Hants-Colchester Lowlands and Cobequid Highlands (Goldthwait, 1924). The lowland areas are underlain predominantly by Early Carboniferous to Triassic sedimentary rocks. The highland region is formed by metasedimentary, volcanic and igneous rocks of Hadrynian, Silurian, Devono-Carboniferous and Early Carboniferous age that are segregated into numerous fault blocks and bounded on the south by the Minas Geofracture (Donohoe and Wallace, 1978, 1982; Keppie, 1982).

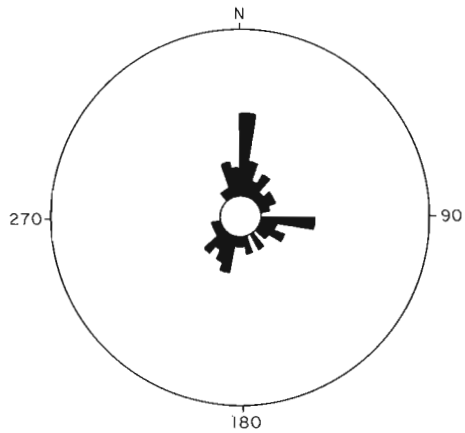

Figure 64.1. *A plot of striations measured in the map area by Chalmers (1895).*

[1] Contribution to Canada-Nova Scotia Co-operative Mineral Program 1981-84. Project carried by Geological Survey of Canada and Nova Scotia Department of Mines and Energy.

[2] Nova Scotia Department of Mines and Energy, P.O. Box. 1087, Halifax, Nova Scotia B3J 2X1
[3] 25 Vimy Avenue, Halifax, Nova Scotia B3M 1G5

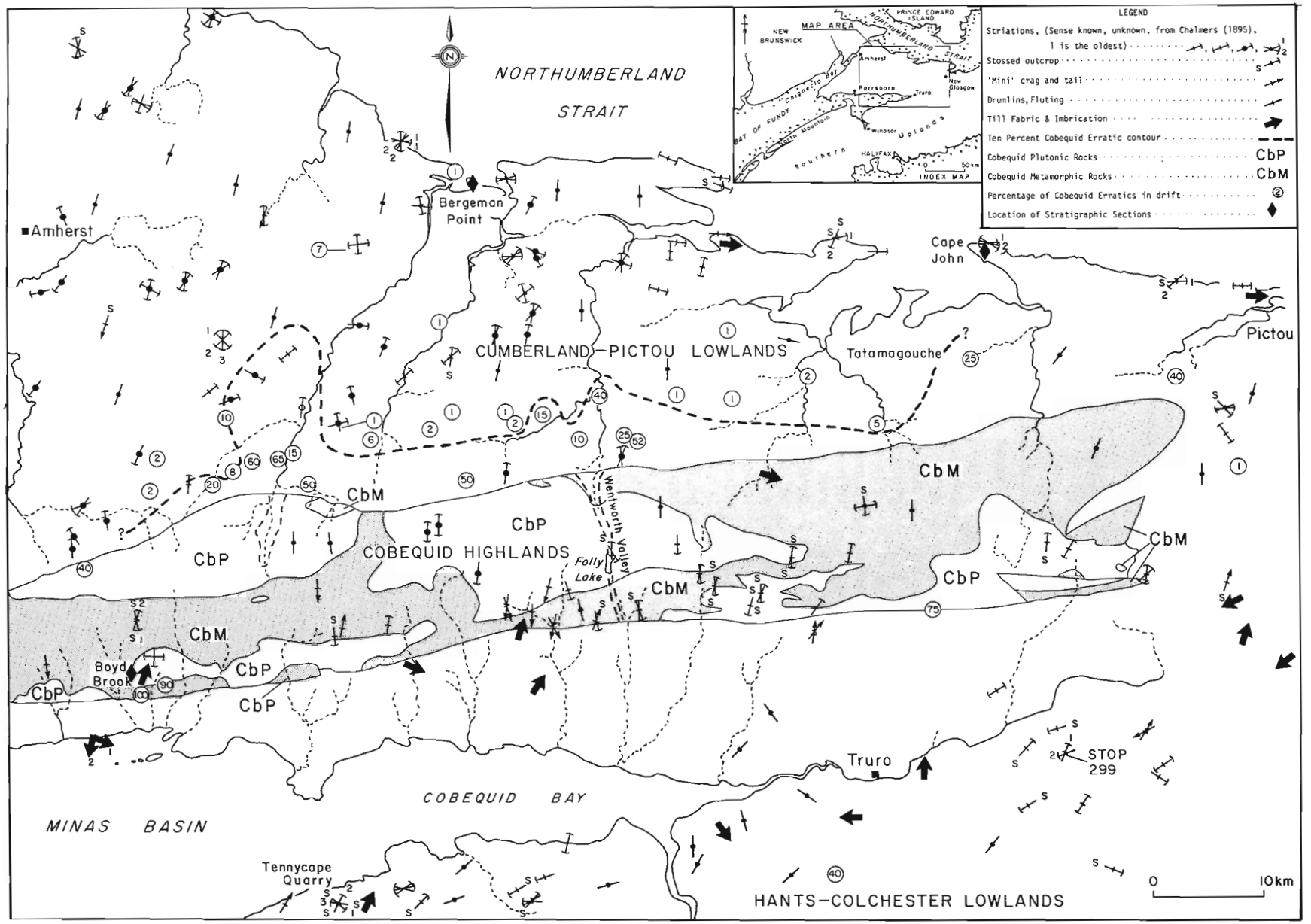

Figure 64.2. *A map of the features indicative of ice flow in parts of Hants, Pictou, Cumberland and Colchester counties.*

Summary of previous work

Chalmers (1895) developed a relative chronology of ice-flow events based on striation mapping. He recognized an early eastward movement of ice in the lowlands which he termed the Northumberland Glacier. He postulated that the centre of outflow for this glacier was the highlands of central New Brunswick. Striations indicating a south and southwestward ice flow were attributed to the 'Chignecto Glacier' centred on the isthmus of Chignecto. A plot of all his striation measurements in the map area indicates a major northward ice flow (Fig. 64.1). He attributed these striations to unnamed glaciers that had accumulated on the Cobequid Highlands and local summits in the lowlands. His interpretations are largely borne out by this study.

Prest et al. (1972) advocated a similar sequence of events, but stressed the concept of a later, northward-flowing ice cap in the eastern Cobequid Highlands based on abundant Cobequid-derived erratics in the lowlands.

Grant (1977) recognized that the last ice flow apparent in the Chignecto Bay area was opposite to the northward flow predominant in areas to the east. He suggested that these movements may have been synchronous, but not in contact.

Recent work by exploration companies in the search for uranium has provided new data on the glaciation of the Cobequid Highlands. Downey (1979) recognized two major movements in the highlands east of the Wentworth Valley. He stated that the first ice movement was toward the south-southeast and emplaced a reddish-brown till, followed by a northwestward ice flow which formed a greyish till.

Stea (1982) designated four major till-forming events in the Hants-Colchester Lowlands south of the map area. They are summarized as follows:

1. East Milford Till – formed by a regional east-southeast ice flow.
2. Hants Till – formed by southward flowing ice, later reworked by northeastward flowing ice.
3. Bennett Bay Till – formed by northward flowing ice crossing the North Mountain cuesta.
4. Rawdon Till – formed by westward flowing ice.

EROSIONAL INDICATORS OF GLACIER MOVEMENT

Cumberland-Pictou Lowlands

Stossed and striated bedrock surfaces in this region commonly record a flow towards 090-110°. Ridges with a concordant trend are also evident in the lowlands (Fig. 64.2). Large boulders embedded in till along the coast exhibit striated surfaces with bullet-nosed up-glacier terminations and abruptly truncated down-glacier terminations (cf. Boulton, 1978) that indicate an eastward flow (Fig. 64.3).

At many sites in the lowlands striations trending 204-233° clearly cut across the eastward-trending sets (Fig. 64.4). These striations are found on north-facing stoss surfaces along the coast (Fig. 64.2).

Chalmers (1895, p. 74) described striations on south-facing stoss surfaces trending 000-020°. The authors also found weakly striated, south-facing stoss surfaces, bevelling till-covered surfaces striking 230°.

Cobequid Highlands

Many striations trending 170-195° were measured on the highlands. The sense of this ice flow was verified at several localities by distinctly north-facing stoss surfaces and from pressure shadows or mini crag-and-tail features developed on quartz veins (Fig. 64.2).

South-facing stossed surfaces produced by northward flow were also seen at many sites where the southward flow was recorded. Striations developed on these surfaces ranged from 350 to 035°. The sense of this flow was verified at several localities by miniature crag-and-tail on quartz veins in the volcanic and metasedimentary rocks and on pebbles in conglomerates. At some sites the southward-trending striations are cut by the northward-trending sets, and at others the two bevelled faces meet along a line (Fig. 64.5).

At several sites in valleys on the uplands striations trending east and southeast that are preserved in deep grooves are crossed by the northward- and southward-trending sets. The occurrences of east- and southeast-trending striations on the highlands are rare.

Hants-Colchester Lowlands

Rock exposures in this region reveal evidence of two major ice flows, toward the northeast and west-southwest. The sequence of these flows is revealed at stop 299 (Fig. 64.2). Striations trending 247° crosscut wide grooves on a flat bedrock surface inscribed with black-stained striations trending 020°. At Tennycape Quarry (Fig. 64.2) striations relating to earlier southward and southeastward ice flows occur on bedrock under 6 m of till, and striations trending 028 and 281° were found near the surface (Fig. 64.6).

TILL PROVENANCE AND ERRATIC DISPERSAL

Cumberland-Pictou Lowlands

The surface till sheet throughout most of this area is a reddish-brown, jointed, sandy-silt till composed primarily of Carboniferous (Cumberland Group) sandstone clasts. It has been observed to overlie bedrock with striations trending 210° (Fig. 64.7). Igneous and metamorphic erratics are commonly found in the top 2 m of this till and on the surface. Many of these erratics are hornblende-bearing diorites of similar description to diorites making up the large plutons of the Cobequid Highlands (H.V. Donohoe, personal communication, 1983). There is a general increase in the abundances of these crystalline erratics from north to south and from west to east (Fig. 64.2). There are also areas of high erratic concentrations which are located opposite major U-shaped valley systems such as the Wentworth Valley (Fig. 64.2).

Several exposures along the coast reveal two and locally three till units. At Bergeman Point a very compact, greyish-red basal till is overlain by two less compact tills. The contact is marked by a pavement of boulders which are inscribed with striations trending 210°. Nearly the basal unit overlies bedrock with striations trending 093°.

At Cape John a 9 m section reveals three till units (Fig. 64.8). Unit I, a reddish-brown silt till, rests on bedrock with striations trending 105°. Striations on the boulder pavement between units I and II give evidence of only slight variations in the eastward flow. Boulders with striations trending 060 or 240° suggest changing flow directions, perhaps to the southwest. Unit II is a greyish-brown till with a silty matrix. Unit III is a greyish-red till with few clasts and a sandy-silt matrix. Embedded in unit III in the top 2 m are volcanic and foliated granitic boulders of probable Cobequid Highland provenance. Striations on a boulder in this unit suggested a N15°E movement. Till fabric measured below these boulders, however, reveals only modes of orientation compatible with eastward and perhaps southwestward ice flows. The pebble layer and manganese oxide coatings in the top parts of units II and III are suggestive of soil formation indicating a period of climatic amelioration.

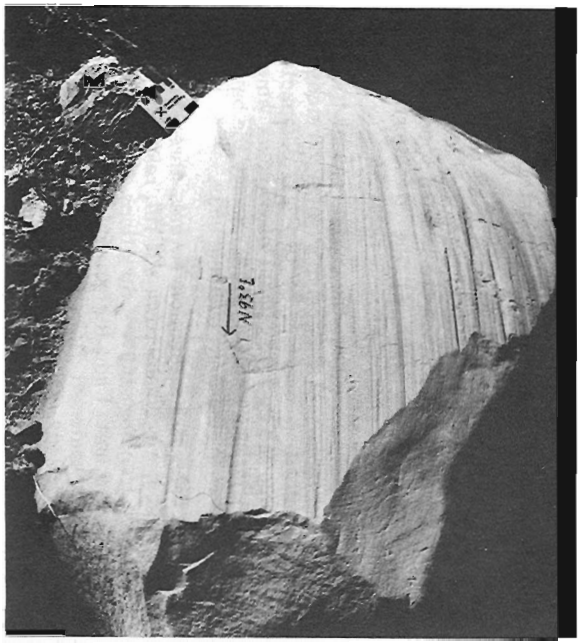

Figure 64.3. *A striated boulder with a bullet shape that indicates transport by sliding in the basal zone of traction and an eastward sense of flow (093°). Overlain by 6 m of till.*

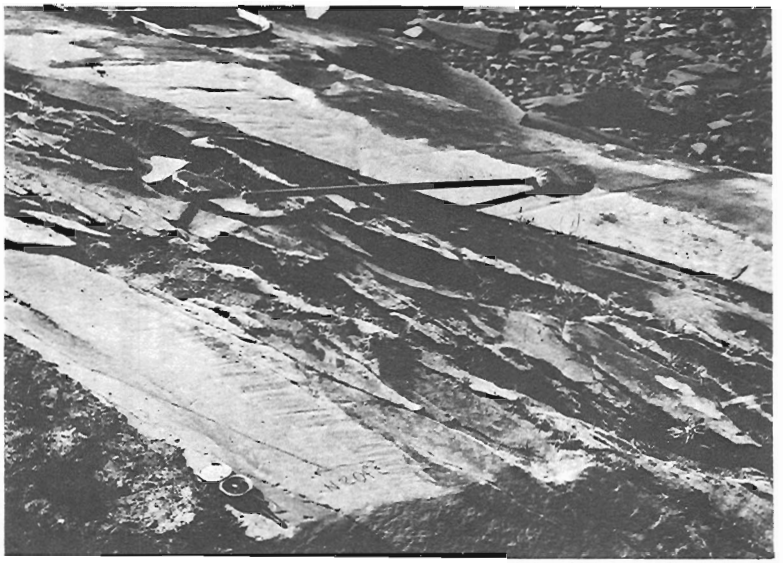

Figure 64.4. *Striations and grooves trending 204° crosscut a groove and striations trending 89°, near Pictou along the Northumberland Strait.*

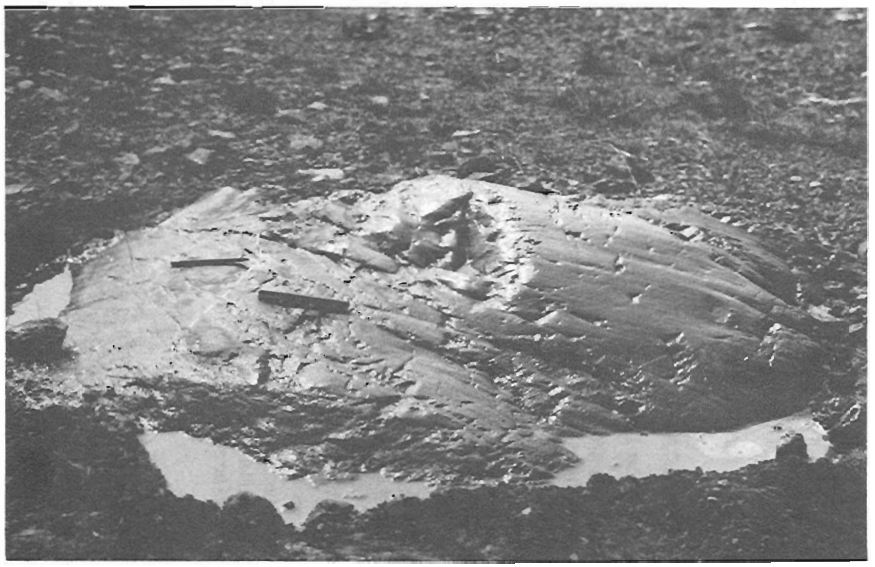

Figure 64.5. *Stoss-and-lee form and striations on Cobequid Highland granite indicate a flow towards 181°. On the south-facing part of the outcrop striations trend 011° and meet the 181° striations at a bevel contact (dashed line).*

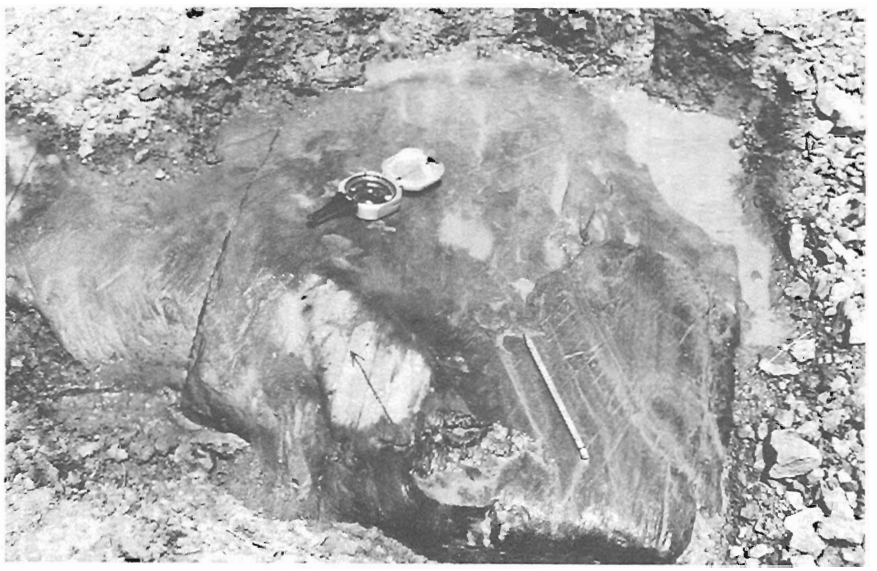

Figure 64.6. *At Tennycape Quarry an upper surface (marked by compass) bearing striations trending 281° truncates striations trending 028° (marked by pencil). The sense of flow of the 028° set was verified by miniature crag-and-tail features at a nearby locality.*

Alternatively, the manganese oxide could also represent groundwater modification of the pebble zones with no climatic significance. At Joggins, 60 km to the west, a similar alteration zone on a till produced by east-flowing ice lends some credence to the first hypothesis (Stea, 1983).

Figure 64.7. *Southwest of Amherst a reddish-brown till with Carboniferous clasts overlies a stained and striated bedrock surface. The striations trend 210°.*

Cobequid Highlands

Much of the Cobequid Highland area is veneered by a reddish-brown till with varying percentages of sandstone clasts derived from the Cumberland-Pictou Lowland region. A greyish-brown till of Cobequid Highland provenance was found to overlie the reddish-brown till at several localities and contains inclusions of the older till. The grey till was observed to overlap onto the lowland terrian to the north. At Boyd Brook this till sheet produced a fabric concordant with northwest-trending striatons and is presumed to have been formed during that flow. We concur with the conclusions of Downey (1979) that a till sheet was produced by a northward ice flow off the highlands.

Very compact, reddish-brown lodgement till with fabric striking 090-115° was discovered in valleys in the Cobequids (Fig. 64.2). In most cases it is overlain by an oxidized greyish till.

Hants-Colchester Lowlands

The surface till sheet over much of the lowlands south of the Cobequid Highlands is a reddish-brown noncalcareous, sandy-silt till made up primarily of local (Horton Group) clasts. It has been informally termed the Hants Till (Stea, 1982). This till sheet contains 1-10% Cobequid erratics, but in its upper 2 m can be found erratics derived from the South Mountain Batholith located southwest of the map area (MacNeill in Prest et al., 1972; Stea, 1982). Elsewhere the Hants Till is locally overlain by a greyish-brown till with few crystalline erratics and a strong fabric striking 260-290°. This till has informally been termed the Rawdon Till (Stea, 1982).

Under the Hants Till is a more compact greyish-red till which overlies striations trending east and southeast and contains a higher percentage of Cobequid erratics (Cornish, 1980; Stea, 1982). This lower till has been termed the East Milford Till (Stea and Hemsworth, 1979).

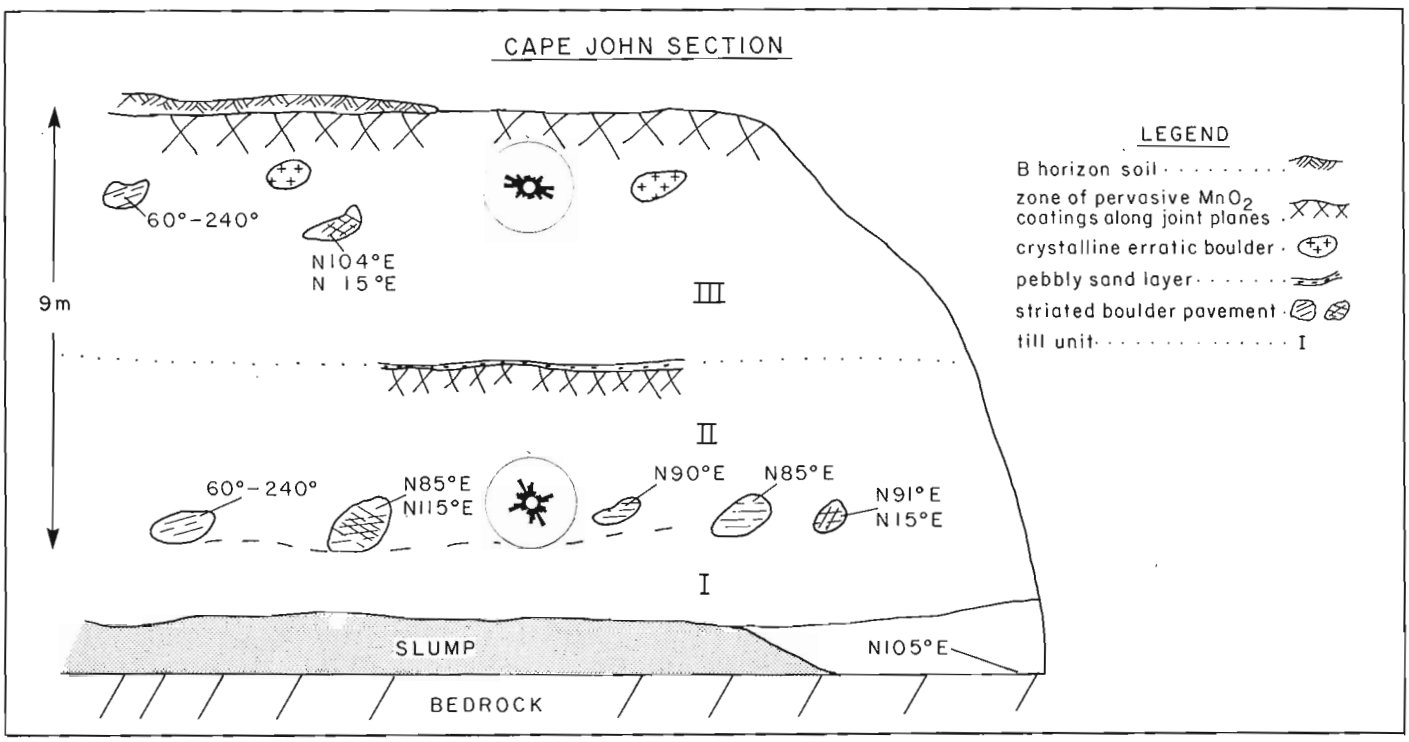

Figure 64.8. *Diagrammatic cross-section of three tills, Cape John, near Pictou, Nova Scotia.*

DISCUSSION AND CONCLUSIONS

Figure 64.9 shows a plot of all striations for which the sense of ice flow is known. Four major groupings of striation directions are apparent. The sequence of these movements can be deduced from the 'type localities' of crossing striations and superposed tills associated with these ice flows.

The oldest flow pattern, set 1 of Figure 64.9, trends 090-130° throughout the map area. North of the Cobequid Highlands the trend appears to have been due east. In the Cobequid Highlands a few striations and compact lodgement tills with an east-southeast striking fabric attest to the flow crossing the highlands. Striations under thick drift sections in the Hants-Colchester Lowlands trend southeastward. Till units I and II at Cape John described in this report, unit I at Joggins (Stea, 1983) and the East Milford Till (Stea and Hemsworth, 1979) are all considered to have been deposited by this early ice flow.

Striations trending 160-210°, represented by set 2 of Figure 64.9, cut across the early east-trending set at many localities (Fig. 64.2). These striations are most common in the Cumberland-Pictou Lowlands where they trend south and southwest and on the Cobequid Highlands where they trend generally southward. It is not known whether these striations represent a continuous ice flow conforming to topography, or if they represent a sequence of ice flows first toward the south-southeast and then toward the southwest. Unit II at Joggins (Stea, 1983) and the Hants Till (Stea, 1982) are believed to have been initially formed during this flow event.

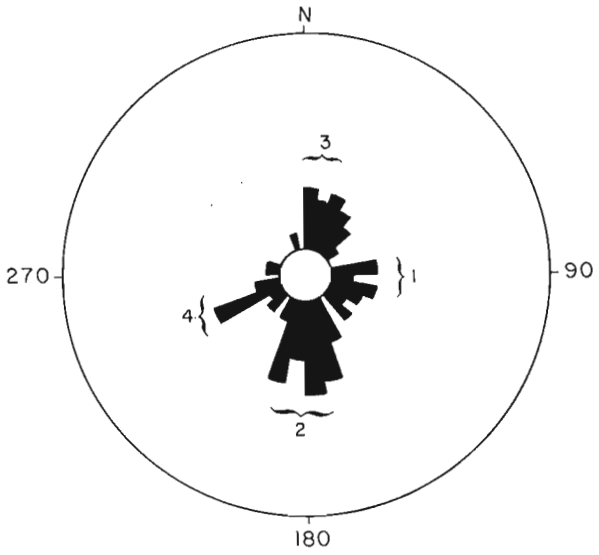

Figure 64.9. *Plot of all striations measured by the authors in the map area, for which the sense of ice flow is known. Relative ages of the four sets are noted.*

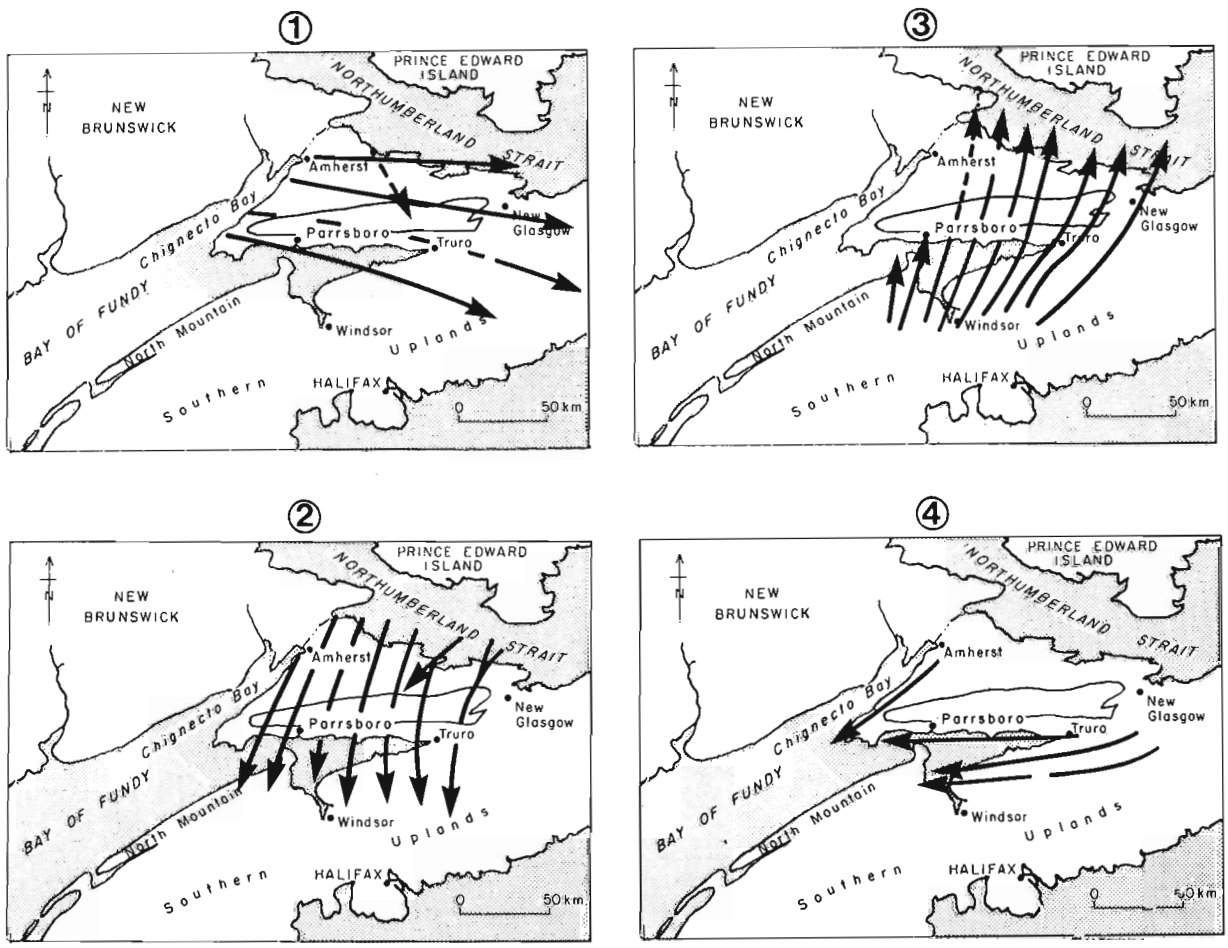

Figure 64.10. *The inferred sequence of ice flows in the map area. Flow pattern 1 is speculated to be Early Wisconsinan in age; flow patterns 3 and 4 Late Wisconsinan.*

A strong north and northeastward ice flow occurred after the period of southward ice flow in the area. The compelling evidence for this hypothesis is:

1. A till sheet and ablation boulders of Cobequid Highland provenance are overlain by a till sheet of Carboniferous provenance in the Cumberland-Pictou Lowlands and Cobequid Highlands.
2. Striations trending north and northeast are clearly cut by striations trending south at many localities in the Cobequids.

The pattern of northeastward flow in the Hant-Colchester Lowlands can be traced across the southern slope of the Cobequid Highlands (Fig. 64.2). Since there is no evidence of its limit on the southern flank of the Cobequids it is suggested that instead of a Cobequid-centred source of northward ice flow (Prest et al., 1972) the flow probably originated in the region south-southwest of the map area, i.e. on the Southern Uplands. Earlier workers considered this flow to have emplaced granite boulders on the North Mountain cuesta (Dawson, 1868; Faribault, 1920; Hickox, 1962). However, no evidence for this flow was found in the highland west of Parrsboro (Stea, 1983). The Southern Uplands ice may have been partly obstructed by the North Mountain and calving may have occurred in the deeper parts of the Minas Channel. Railton (1973) termed this ice mass the South Mountain Ice Cap.

The final pulse of ice flow appears to have been westward into Cobequid Bay and the Minas Basin. Striations relating to this flow are found throughout the Hants-Colchester Lowlands and cut the northeastward-trending set. The source of this ice may have been in the Antigonish Highlands, east of the map area. A late southwestward movement in the Chignecto Bay area (Stea, 1983) may be synchronous with the westward flow into the Minas Basin. The westward flow did not appear to affect the Cobequid Highlands, which at that time may have harboured a residual, stagnant carapace of ice.

The oldest striations, trending eastward and southeastward (set 1 of Fig. 64.9), were assigned a Wisconsinan age by Rampton and Paradis (1981) in New Brunswick. These striations were inscribed on a wave-cut rock bench which is elsewhere assigned a Sangamon age (Grant, 1980). The East Milford Till, formed by the oldest east-southeastward ice flow, overlies peat beds with wood that gave a nonfinite radiocarbon age: >52,000 BP (GSC-2684). The age of the East Milford till was speculated to be Early Wisconsinan (Stea and Hemsworth, 1979; Stea, 1982). The age of the subsequent southward and southwestward ice flow is therefore uncertain. There is some indication of soil development on the East Milford Till (Cornish, 1980; Stea, 1982) which suggests that the southward ice flow (set 2 of Fig. 64.9) may have postdated an Early-Middle Wisconsinan recessional interval. The youngest two events (sets 3 and 4 of Fig. 64.9), however, are probably Late Wisconsinan in age. The South Mountain Ice Cap, probable source of the northward and northeastward flowing ice, persisted into the Holocene (Railton, 1973). Hadden (1975) also invoked a persistent ice cover to explain a relatively young bog-bottom date (9187 ± 255 BP, I-7080) in the Hants-Colchester Lowlands. She also noted that the spruce pollen maximum zone occurred 1000 years earlier in the Folly Lake area of the Cobequid Highlands (Hadden, 1975, p. 44).

On the basis of the present study the authors would modify Grant's (1977) model of Late-Wisconsinan ice distribution to accommodate a more extensive ice flow emanating from the South Mountain Ice Cap crossing the eastern Cobequid Highlands.

Figure 64.10 summarizes the inferred sequence of ice flows in the region.

REFERENCES

Boulton, G.S.
1978: Boulder shapes and grain-size distributions of debris as indicators of transport paths through a glacier and till genesis; Sedimentology, v. 25, p. 773-799.

Chalmers, R.
1895: Report on the surface geology of eastern New Brunswick, northwestern Nova Scotia and a portion of Prince Edward Island; Geological Survey of Canada, Annual Report, v. 1, no. 7, part. M.

Cornish, R.A.
1980: Walton Shore Project, A report on a reverse-circulation reconnaissance drilling program in the Noel Lake – S. Maitland and Newcomb Corner areas; Nova Scotia Department of Mines and Energy, Assessment Report 11E/05A 07-I-29 (02).

Dawson, J.W.
1868: Acadian Geology; Oliver and Boyd, Edinburgh.

Donohoe, H.V. and Wallace, P.I.
1978: Preliminary map of the Cobequid Highlands; Nova Scotia Department of Mines, Map 78-1.

1982: Geological maps of the Cobequid Highlands – Colchester, Cumberland and Pictou Counties, Nova Scotia; Nova Scotia Department of Mines and Energy, Maps 82-6 to 82-9.

Downey, N.
1979: Cobequid Project: Uranium assessment report Cobequid IV, Nova Scotia; Nova Scotia Department of Mines and Energy, Assessment Report No. 11E/12B 54-0-64 (04).

Faribault, C.R.
1920: Kings and Annapolis Counties, Nova Scotia; Geological Survey of Canada, Summary Report, part E, p. 6-16.

Goldthwait, J.W.
1924: Physiography of Nova Scotia; Geological Survey of Canada, Memoir 140, 179 p.

Grant, D.R.
1977: Glacial style and ice limits, the Quaternary stratigraphic record, and changes of land and ocean level in the Atlantic Provinces, Canada; Geographie Physique et Quaternaire, v. 31, no. 3-4, p. 247-260.

1980: Quaternary sea-level change in Atlantic Canada as an indication of crustal delevelling; in Earth Rheology, Isostasy and Eustasy, ed. N.A. Morner; John Wiley and Sons, p. 201-214.

Hadden, K.A.
1975: A pollen diagram from a post glacial peat bog in Hants County, Nova Scotia; Canadian Journal of Botany, v. 53, p. 39-47.

Hickox, C.F. Jr.
1962: Late Pleistocene ice cap centered on Nova Scotia; Geological Society of America, Bulletin, v. 73, p. 505-510.

Keppie, J.D.
1982: The Minas Geofracture; in Major Structural Zones and Faults of the Northern Appalachians, ed. P. St-Julien and J. Béland; Geological Association of Canada, Special Paper 24, p. 264-278.

Prest, V.K., Grant, D.R., Borns, H.W., Brookes, I.A., MacNeill, R.H., and Ogden, J.G.
1972: Quaternary geology, geomorphology and hydrology of the Atlantic Provinces; 24th International Geological Congress, Guidebook A61-C61, 79 p.

Railton, J.B.
1973: Vegetational and climatic history of southwestern Nova Scotia in relation to a South Mountain Ice Cap; unpublished Ph.D. thesis, Dalhousie University, Halifax, Nova Scotia.

Rampton, V.N. and Paradis, S.
1981: Quaternary geology of the Amherst map area (21H), New Brunswick; New Brunswick Department of Natural Resources, Map Report 81-3, 36 p.

Stea, R.R.
1982: The properties, correlation and interpretation of Pleistocene sediments in central Nova Scotia; unpublished M.Sc. thesis, Dalhousie University, Halifax, Nova Scotia.

1983: Surficial geology of the western part of Cumberland County, Nova Scotia; in Current Research, Part A, Geological Survey of Canada, Paper 83-1A, p. 197-202.

Stea, R.R. and Hemsworth, D.
1979: Pleistocene stratigraphy of the Miller Creek section, Hants County, Nova Scotia; Nova Scotia Department of Mines and Energy, Paper 79-5.

65. GEOLOGY OF THE LAC GHYVELDE – LAC LONG AREA, GRENVILLE PROVINCE, LABRADOR AND QUEBEC[1]

Project 820036

A. Thomas[2], N.G. Culshaw[3], G. Mannard[4], and G. Whelan[5]

Thomas, A., Culshaw, N.G., Mannard, G., and Whelan, G., Geology of the Lac Ghyvelde – Lac Long area, Grenville Province, Labrador and Quebec; in Current Research, Part A, Geological Survey of Canada, Paper 84-1A, p. 485-493, 1984.

Also in Current Research, Newfoundland Department of Mines and Energy, Mineral Development Division, Report 84-1, 1984.

Abstract

Continuing studies of Precambrian granitoid rocks and gneiss in the Grenville Structural Province of central and south-central Labrador yield evidence of a major Paleohelikian orogenic event. A crustal block in the northern part of the map area comprises mainly polydeformed granulite facies quartzofeldspathic paragneiss which contains the mineral assemblage hypersthene, sillimanite, quartz, K-feldspar and sapphirine(?), and can be traced continuously into equivalent gneiss of known Paleohelikian age. Several gabbronorite and charnockite bodies are also present in the southwest portion of this block.

Granulite facies tonalite to quartz tonalite gneiss having the mineral assemblage pyroxene, garnet, quartz and feldspar was intruded by a body of porphyritic granodiorite-granite, parts of which were subsequently tectonized to augen gneiss and banded orthogneiss. Together these two units define a distinct crustal block covering much of the southern part of the area. Anorthosite and related gabbronoritic to charnockitic rocks of unknown age intrude both granodiorite-granite of the southern block and gabbronorite-charnockite of the northern block. The two blocks are juxtaposed along a major structure, the Lac Long lineament, which traverses the entire map area from east to west and represents a fundamental lithotectonic break of Grenvillian(?) age.

Résumé

Des études suivies des roches granitoïdes et gneissiques d'âge précambrien appartenant à la province structurale de Grenville dans les parties centrale et sud-centrale du Labrador, indiquent qu'au Paléohélikien, a eu lieu une importante phase d'orogénèse. Dans la partie nord de la région cartographique, un bloc lithosphérique se compose principalement d'un paragneiss quartzo-feldspathique à faciès des granulites déformé de façons multiples, qui contient comme assemblages minéraux de l'hypersthène, de la sillimanite, du quartz, du feldspath potassique et de la sapphirine (?), et qui se prolonge de façon continue dans des gneiss équivalents d'âge paléohélikien connu. Plusieurs corps de gabbronorite et de charnockite se manifestent également dans la partie sud-ouest de ce bloc.

Un gneiss à tonalite passant à la tonalite quartzique et à faciès des granulites, contient comme assemblage de minéraux de la pyroxène, du grenat, du quartz et du feldspath; il a été pénétré par un corps de granite et granodiorite porphyrique dont certaines parties soumises aux effets du tectonisme s'étaient transformées en gneiss œillé et en orthogneiss rubané. Ces deux unités combinées délimitent un bloc lithosphérique distinct couvrant presque toute la partie sud de la région. De l'anorthosite et des roches connexes d'âge inconnu et dont la nature varie de gabbronoritique à charnockitique, pénètrent aussi bien la granodiorite et le granite du bloc méridional que la gabbronorite et la charnockite du bloc septentrional. Les deux blocs sont juxtaposés le long de l'important linéament du Lac Long qui traverse, d'est en ouest, la région cartographique entière et qui constitue une faille géotectonique de base datant du Grenvillien (?).

INTRODUCTION

This report summarizes work carried out during the second year of a two-year project focusing on 1:100 000 scale mapping of crystalline rocks within the Grenville Structural Province of south-central Labrador. The project was initiated for three reasons: (1) to continue studies started in 1978, with particular emphasis on age and geological history of gneisses and granitoids in the Grenville Province; (2) to provide a much needed geological and geochemical data base for the sparsely mapped rocks of southern and central Labrador; and (3) to examine the bedrock mineral potential within this part of the Grenville Province.

The area covered encompasses NTS 1:50 000 sheets 13D/11, 12, 13 and 14 contained within the boundaries 63°00' to 64°00' west longitude and 52°30' to 53°00' north latitude (Fig. 65.1). It is a southward extension of the area mapped in 1982 and outlined by Thomas and Wood (1983). Part of the region north and west of Lac Long is in the province of Quebec and was mapped by N.G. Culshaw of the Geological Survey of Canada. The centre of the map area is approximately 100 km south of the town of Churchill Falls, Labrador, and access is by float-equipped fixed wing aircraft and helicopter.

[1] Contribution to Canada-Newfoundland co-operative mineral program 1982-84. Project carried by Geological Survey of Canada.

[2] Newfoundland Department of Mines and Energy, Mineral Development Division, P.O. Box 4750, St. John's, Newfoundland A1C 5T7

[3] Geological Survey of Canada, 601 Booth Street, Ottawa, Ontario K1A 0E8

[4] Department of Geological Sciences, McGill University, Montreal, Quebec H3A 2A7

[5] Department of Earth Sciences, Memorial University of Newfoundland, St. John's, Newfoundland A1B 3X5

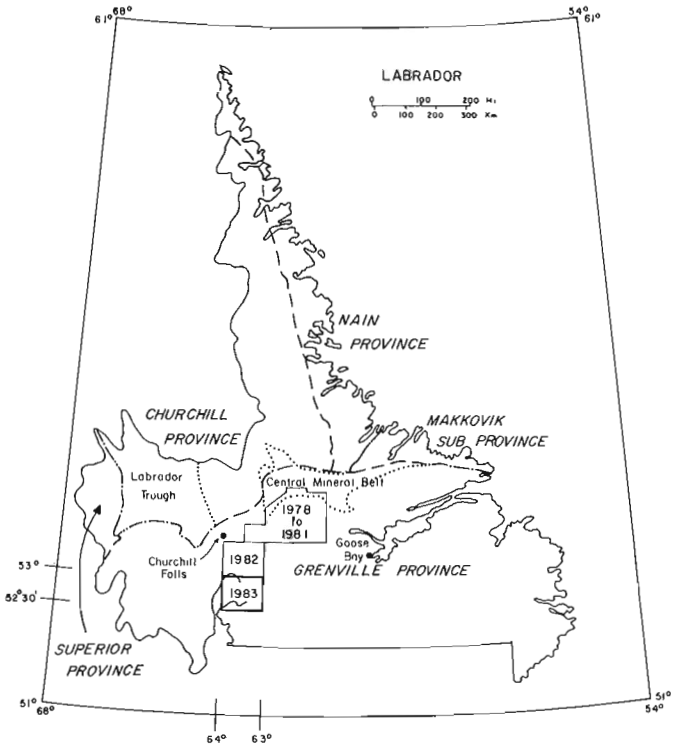

Figure 65.1. *Location of present and previous map areas in central and south-central Labrador (structural province divisions after Taylor, 1971).*

Relatively little previous work has been done in the region besides a 1:250 000 scale reconnaissance project carried out by Stevenson (1969) plus some regional and detailed mapping by BRINEX (Pyke, 1956). Thomas and Wood (1983) provided references to previous work on adjacent map areas to the north.

REGIONAL SETTING

The Lac Ghyvelde – Lac Long area comprises a granulite grade terrane of paragneiss, noritic and charnockitic igneous rocks along with their gneissose equivalents, metamorphosed granitoids and anorthosite. Beyond the map area, to the north and northwest, is a lowland terrain consisting of amphibolite grade paragneisses and orthogneisses as well as deformed granitoids. Within the northern half of the map area is a highland plateau underlain almost entirely by paragneiss which can be traced north through the southern part of the area mapped in 1982 (Thomas and Wood, 1983), and thence continuously northeastward for almost 200 km into the Red Wine Mountains granulite massif. To the west, a poorly exposed, boggy lowland terrain is underlain by a mixed assemblage of paragneiss, anorthositic to gabbroic rocks and metabasics.

To the southwest, a large body of anorthosite forms a range of high, barren hills. Part of this body becomes a narrow, northeasterly trending tongue which protrudes into the southwestern part of the map area. South and southeast of the map area, another poorly exposed lowland region contains a mixture of little metamorphosed gabbroic to granitic rocks and amphibolite grade paragneisses.

The region east of and directly adjacent to the map area can be divided into a highland plateau and extensively drift-covered lowlands. The plateau is a continuation of the one found in the northern part of the Lac Ghyvelde – Lac Long area, and is underlain by the same granulite grade paragneiss. The poorly exposed lowlands again comprise a mixed granitoid – amphibolite gneiss terrane, similar to that south of the map area.

All rocks within this part of Labrador are polydeformed and have undergone an extensive and complex geological history involving at least two distinct orogenic events at circa 1650 Ma and 1000 Ma.

GENERAL GEOLOGY

Six major and three minor lithological types have been defined (Fig. 65.2). Granulite grade tonalite to quartz tonalite gneiss (unit 1) is presently thought to be the oldest unit in the area. The gneiss is confined to a rugged highland, which makes up the southern one-third of the map area, and does not outcrop anywhere north of Lac Long. This rock type has not been observed previously in any of the other field areas examined, and may represent ancient basement remnants.

The most widespread rock type is quartzofeldspathic paragneiss (unit 2), which is well exposed in a barren upland plateau forming the entire northern half of the map area. The bulk of the gneiss has undergone granulite facies metamorphism (unit 2a), with small local patches having only reached or been retrograded to amphibolite grade (unit 2b). There are no compositional or structural differences between the two variants of gneiss; subdivision of the unit is based solely on mineralogical contrasts. Quartzofeldspathic paragneiss is correlated with Hope Lake gneiss of Emslie et al. (1978), Thomas (1981), and Thomas et al. (1981). Exposures of the gneiss can be traced continuously from the type locality at Hope Lake into the area of this study.

Strongly foliated to gneissic porphyritic granodiorite and granite (unit 5) outcrop extensively with tonalite gneiss in the southern highland, as well as in and along the southern edge of the fault-controlled glacial spillway within which Lac Long is situated. The granitoids along the spillway form a 5 to 15 km wide east-trending belt which completely transects the map area, separating tonalite gneiss in the south from quartzofeldspathic gneiss, gabbroids and charnockitic granitoids in the north. Correlation of these granitoids with those of the North Pole Brook Intrusive Suite (see Thomas, 1981; Thomas et al., 1981) and its equivalents to the north (see Thomas and Wood, 1983) is being considered at this time.

A small recrystallized body of dioritic to quartz dioritic composition (unit B) is exposed near the east-central margin of the map area. It intrudes the surrounding paragneiss, but has no apparent relationship to the other granitoids, so that its age and origin are at present unknown.

Bodies of charnockitic granite (unit 4) occur with gabbronorite, as well as anorthosite and related rocks, in a 10 km wide tongue which protrudes into the west-central part of the area, along the contact zone between quartzofeldspathic gneiss of unit 2 and granitoid gneiss of unit 5. North and northwest of Lac Long, the granite both intrudes and is intertongued with gabbronorite and paragneiss. Due to similarities in lithology and geological relationships with host rocks, charnockitic granite is correlated with the monzodiorite/quartz monzonite unit of Emslie et al. (1978) as well as unit 3 of Thomas and Wood (1983).

Gabbronorite (unit 3) is present within granulite grade paragneiss as deformed and/or boudinaged intrusive bodies. All but two of these, located northeast of Lac Ghyvelde and near the east-central edge of the area, are confined to the previously mentioned 10 km wide tongue. Due to similarities

in mineralogy, several small, deformed, lenticular ultramafic and ultramafic gneiss bodies (unit 3b) of unknown age and origin are also included within the unit. Gabbronorite is correlated with unit 2 of Thomas and Wood (1983) and the gabbro, leuconorite, anorthosite unit of Emslie et al. (1978).

Two exposures of fresh, unmetamorphosed gabbronorite (unit A) occur in sand- and bog-covered ground in the southeastern part of the area. These may belong to the circa 1380 Ma Shabogamo Intrusive Suite, but at present their origin is uncertain.

Anorthositic rocks (unit 6) in the southwest corner of the area have been subdivided into anorthosite and related gabbros (unit 6a), norites (unit 6b) and charnockitic monzonite (unit 6c). These rocks are part of a much larger anorthosite suite (presumably of Paleohelikian age) which extends from the map area southwestward to Lac Fournier in eastern Quebec. They have a close spatial relationship with gabbronorite and charnockitic granite northwest of Lac Long, and are presently thought to be Paleohelikian.

Rare, late northeasterly trending diabase dykes cut quartzofeldspathic paragneiss, gabbroids and granitoids north of Lac Long. Their absolute age is unknown, but they are not strongly tectonized and may be late syn- or post-tectonic intrusives associated with the Grenvillian Orogeny.

Rocks within the Lac Ghyvelde – Lac Long area underwent two distinct orogenies. An earlier high grade event resulted in extensive complex folding accompanied by up to granulite grade metamorphism. A later, lower grade event is responsible for further tectonism including folding, and ductile and brittle faulting.

Tonalite – quartz tonalite gneiss (unit 1)

Rocks of this unit are predominantly gneissic, although massive homogeneous zones of greater than outcrop scale were observed. Tonalite gneiss weathers grey to buff white, is grey green on fresh surface and irregularily and discontinuously banded. It consists of approximately 40% plagioclase, 30% pyroxene (augite?), less than 10% quartz and garnet ± magnetite ± minor hornblende. The rock exhibits equigranular polygonal granoblastic texture with an average grain size of 1 to 2 mm. Garnet occurs both as subhedral to anhedral porphyroblasts or crystal aggregates up to 2 cm and as fine grained polygonal groundmass crystals. The gneiss is also characterized by particularly plagioclase-garnet-rich zones, containing abundant coarse aggregates of subhedral pyroxene, possibly representative of meta-anorthositic rocks. Rounded garnet porphyroblasts and garnet aggregates of varied shapes ranging in size up to 10 or 12 cm are common to these meta-anorthositic rocks. Numerous relict mafic or ultramafic dykes and boudins, now consisting almost entirely of polygonal aggregates of hornblende and/or pyroxene, are present throughout the tonalite unit. Extensive reaction rims and bleached zones in the host tonalite occur at the rims of the dyke relicts.

These dykes have been folded, flattened and boudinaged. Even where the tonalite is massive, the selvages show complex fold interference patterns, indicating that the unit underwent pervasive deformation. In addition, cataclasis and shearing are not uncommonly found along contact zones between tonalite and gneissic granodiorite of unit 5.

The mineralogy, nature and partly massive character of the tonalite gneiss suggest an igneous or mixed igneous-sedimentary protolith. The gneiss apparently has a complicated structural-metamorphic history, and its protolith may have been as old as Archean(?).

Paragneiss (unit 2)

Granulite grade quartzofeldspathic paragneiss (unit 2a) is rusty pink to buff, with an average grain size of 1 to 4 mm, dense and extremely resistant to weathering. It is well banded, with prismatic to fibrous sillimanite, fine grained hypersthene, magnetite, rare sapphirine and minor biotite confined to melanocratic layers which pinch and swell, imparting an anastomosed appearance to the rock. Melanocratic bands vary in width up to 2 cm and commonly contain lenticular clots of densely packed aggregates of fibrolitic sillimanite, pyroxene and magnetite. Leucosome bands consist of very dense, fine- to medium-grained granoblastic polygonal aggregates of quartz, K-feldspar and plagioclase. These bands are tightly folded; they pinch and swell, and may be up to 5 cm wide. Black pseudotachylyte lenticles and discontinuous layers up to 1 cm wide are commonly parallel or subparallel to melanocratic bands; pseudotachylyte veinlets in the same size range also cut across leucosome bands. Abundant evidence of partial melting is present in the granulite paragneiss, with both layer – parallel and crosscutting quartz-feldspar sweats being common. This melting took place under dry conditions at high temperatures as evidenced by subhedral to euhedral hypersthene crystals up to 1 cm long in some sweats.

Amphibolite grade quartzofeldspathic paragneiss (unit 2b) is relatively uncommon, being confined to several small (less than 5 km), narrow lenses in granulite grade paragneiss and two narrow belts in tonalite – granitoid gneiss within the eastern part of the area. It is buff-white to pink on weathered surfaces and consists of quartz, K-feldspar, plagioclase, sillimanite, biotite, muscovite, garnet and magnetite-ilmenite. Metamorphic differentiation is well developed with mafic minerals segregated into bands up to 0.5 cm wide, separated by 2 to 3 cm wide quartz-feldspar bands. Due to the abundance of biotite and muscovite, amphibolite grade paragneiss is less dense and more fissile than its granulite grade counterpart. Granoblastic polygonal texture predominates within the quartz-feldspar bands and is in most places medium grained.

Paragneiss is extensively tectonized, with granulite facies gneiss in particular exhibiting complex minor fold patterns including mushroom, dome and basin structures plus centimetre-scale, tight, isoclinal, chevron and hook folds. The small scale fold patterns in the gneiss are identical in style to, and mimic the regional structures. As previously mentioned (Thomas and Wood, 1983), mineralogy and chemical composition of this paragneiss unit suggest derivation from a sedimentary protolith. A U-Pb age on zircon (T.E. Krogh, written communication, 1983) from a sample of granulite grade paragneiss, although discordant, has yielded a lower intercept age of 1676 Ma. This date probably represents the age of granulite grade metamorphism and therefore gives a minimum age for deposition of the protolith.

Gabbronorite (unit 3)

The bulk of the gabbronorite unit comprises norite, two-pyroxene gabbro and two-pyroxene metagabbroic gneiss to metabasite. Additional but less voluminous associated lithotypes included within this unit are noritic gneiss, pyroxene-magnetite gabbro, pyroxene-olivine gabbro, ultramafics and ultramafic gneiss.

Norite is generally massive, and ranges from a medium grained variety with well developed subophitic texture, to a rock with cumulophyric orthopyroxene. These may reach sizes of 5 cm and be spectacularly kinked. Patches of coarse

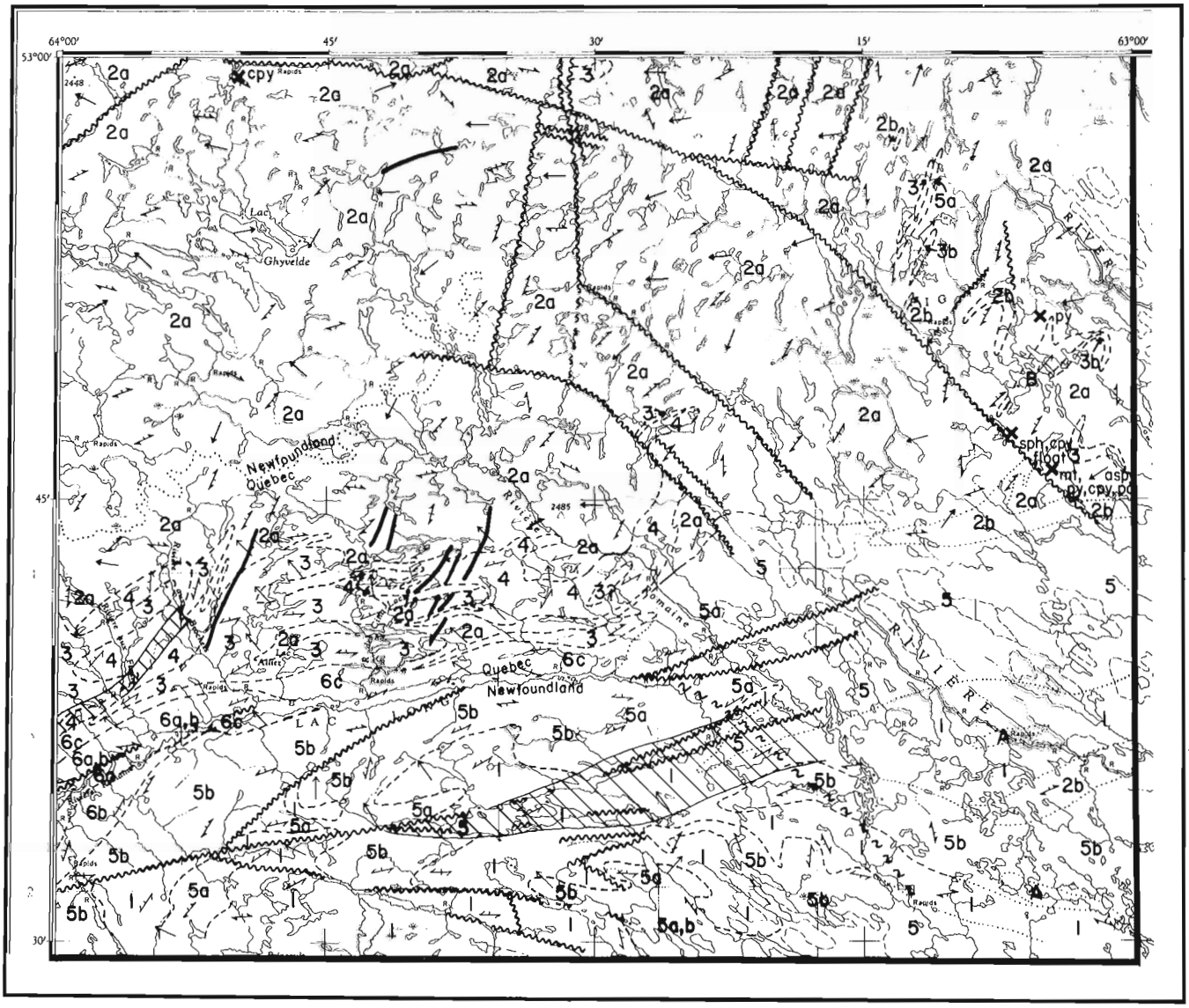

Miles Miles

Kilometres 0 5 10 15 20 Kilometres

Geological boundary *(approximate, assumed)* . . . . . .

Gneissic banding - foliation *(inclined, vertical, horizontal)* . . . . . .

Foliation *(inclined, vertical, horizontal)* . . . . . .

Plunging minor fold axes and mineral stretching lineations associated with earlier fold structures confined to the granulite grade paragneiss terrain . . .

Plunging quartz ribbon, mineral stretching and intersection lineations associated with later fault structures, shearing, mylonitization and straightened gneiss zones along the Lac Long lineament . . .

Fault *(defined, assumed)* . . . . . .

Shear zone . . . . . .

Mineral occurrence *(py - pyrite, cpy - chalcopyrite, sph - sphalerite, po - pyrrhotite, aspy - arsenopyrite, mt - magnetite)* . . . .

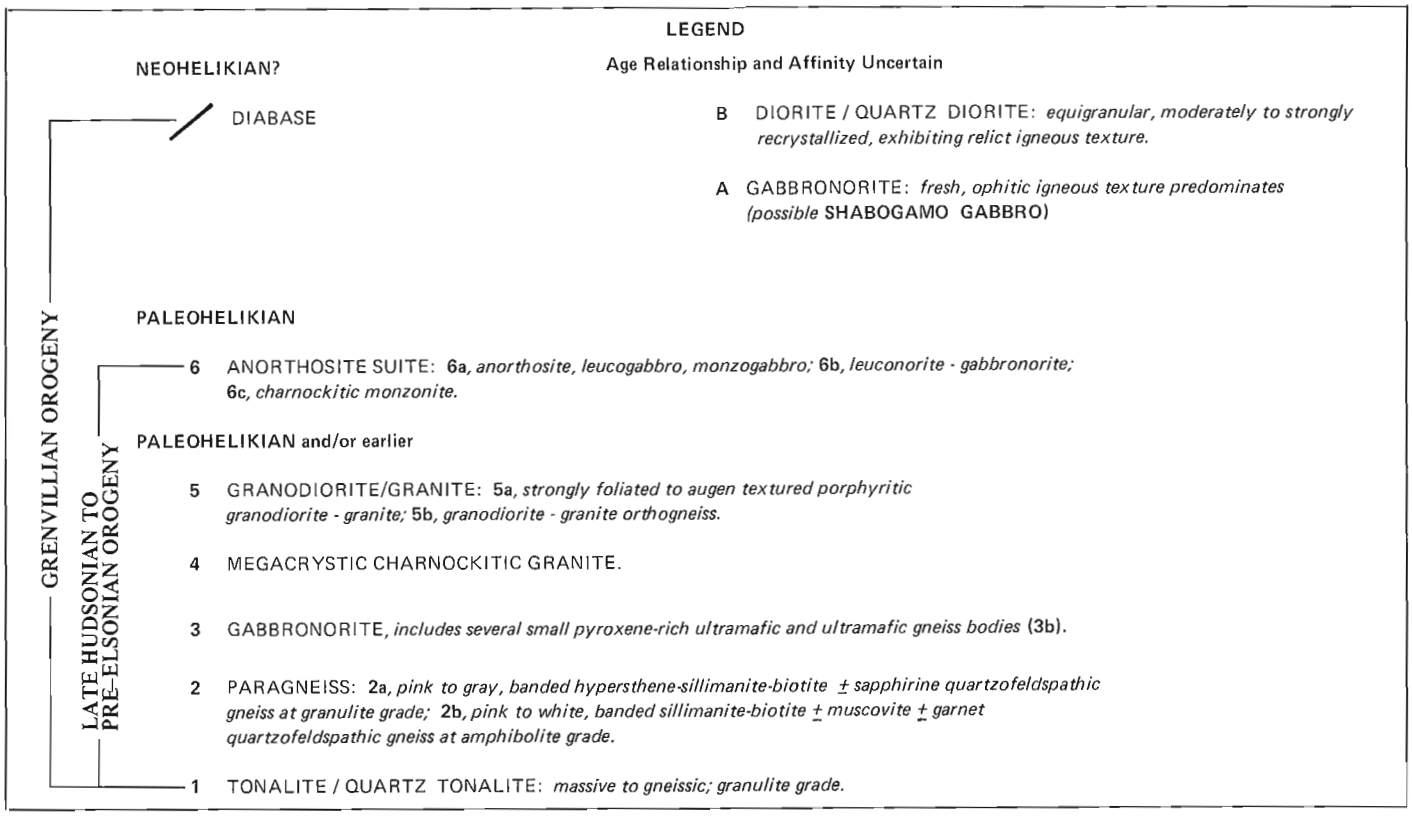

Figure 65.2. *Geology of the Lac Ghyvelde – Lac Long area, Labrador and Quebec.*

gabbroic pegmatite are also common in the norite. Plagioclase and orthopyroxene are subequal, with Fe-Ti oxides as accessories. Although primary igneous textures are discernible in this rock, plagioclase may be partly or wholly recrystallized into polygonal aggregates.

Two-pyroxene gabbro is medium grained and equigranular, with plagioclase partly recrystallized. With increased orthopyroxene content, this rock grades into norite.

Two-pyroxene metagabbroic gneiss/metabasite is the most common of the gabbroic rocks. In general it is uniform, apparently undeformed and massive, exhibiting a very fine grained, equigranular, polygonal, granoblastic metamorphic texture. However, its deformed character is shown in some localities where there is a sparsely developed granitic veining which on surfaces parallel to the stretching limitation appears to be smeared out into the regional stretching direction.

Noritic gneiss is derived from the norite and is found interspersed with gabbroic gneiss. It is equigranular, medium- to fine-grained with a polygonal metamorphic texture. Compositional heterogeneities locally form a discontinuous layering, in some places deformed into intrafolial isoclinal folds.

Pyroxene-magnetite gabbro is found only in association with norites along the northern margin of the aforementioned 10 km wide tongue, and consists of medium- to fine-grained equigranular rocks in which Fe-Ti oxides are of greater than or equal abundance to clinopyroxene.

Pyroxene-olivine gabbro underlies several small hills to the west of the lower reaches of Rivière aux Brochets. It is a uniform massive rock of high colour index, containing medium- to coarse-grained pyroxene and olivine(?).

Rocks within the ultramafic and ultramafic gneiss bodies (unit 3b) are similar to the gabbronoritic rocks, but are composed almost completely of pyroxene with little or no plagioclase.

The lithotypes in the gabbronorite unit are correlated with identical rocks found in the Red Wine Mountains, northeast of the Lac Ghyvelde – Lac Long area by Emslie et al. (1978) and Thomas et al. (1981).

Megacrystic charnockitic granite (unit 4)

Charnockitic granite is a weakly foliated megacrystic rock which weathers to a rusty-buff. Large (up to 4 cm) unrecrystallized K-feldspar megacrysts are set in a matrix of medium grained plagioclase. Quartz content averages between 15 and 20%, but may be as high as 30%. Mafic minerals, which comprise no more than 10% of the rock, include orthopyroxene, Fe-Ti oxides and a fine felted biotite which is thought to have replaced orthopyroxene. Nonmegacrystic granite, as well as pink and grey amphibolite facies metagranitoids, are found locally within charnockitic granite. The amphibolite facies granitoids exhibit a strong LS fabric associated with the development of a straight belt north and northeast of Lac Long which is discussed in more detail later.

Granodiorite – granite (unit 5)

Rocks of granodioritic to granitic composition have a much greater areal extent than the charnockitic granitoids, with two textural varieties evident. Porphyritic granodiorite to granite (unit 5a) is strongly foliated, and commonly, although not everywhere, phenocrysts are deformed into lenticular augen. Well developed porphyritic texture is preserved

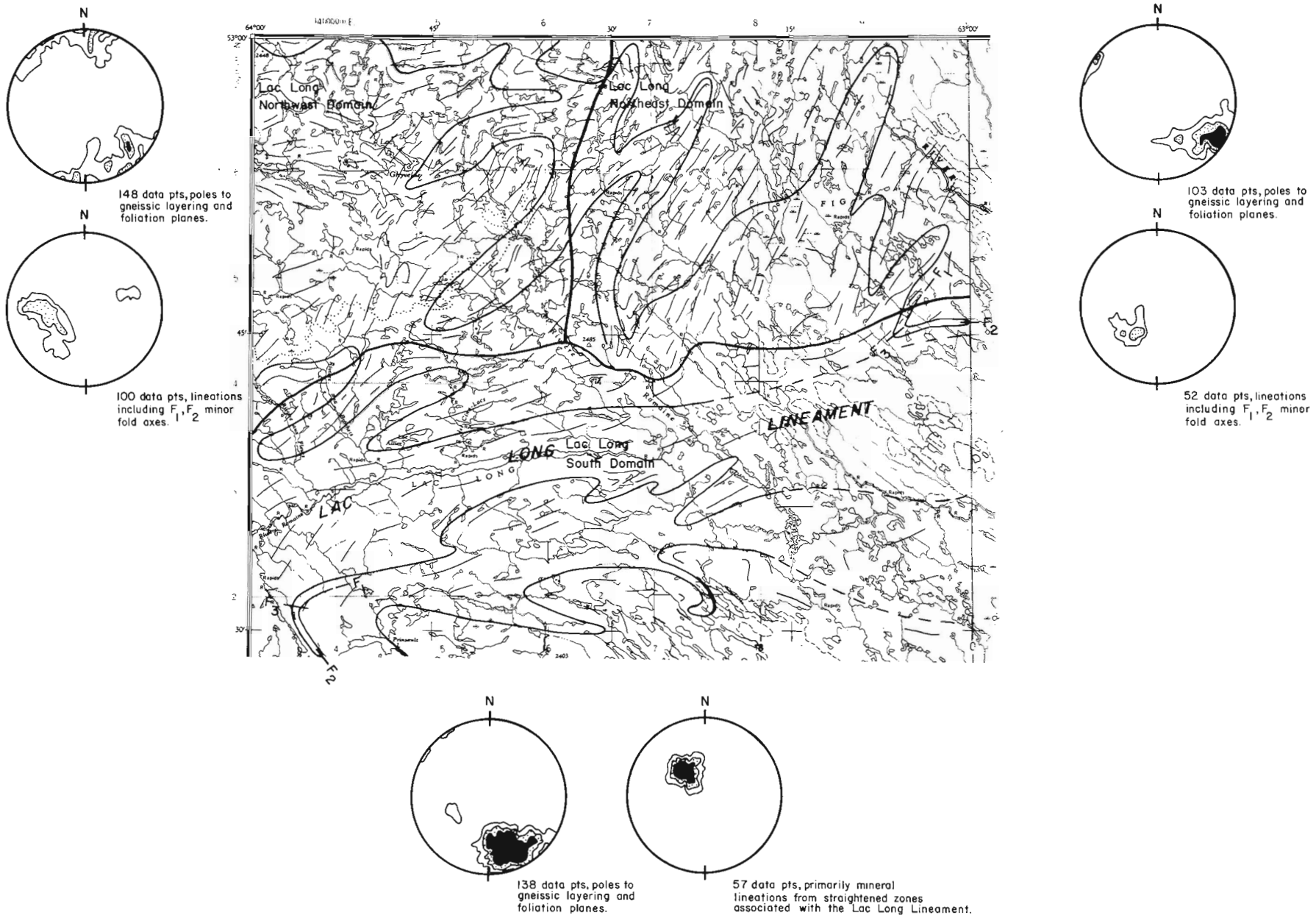

Figure 65.3. *Bedrock structural trends within the three domains of the Lac Ghyvelde – Lac Long map area; stereonet contour intervals 3, 6, 9 per cent of points per 1 per cent area of the net.*

within these rocks south of both the east and west ends of Lac Long. Unit 5a rocks consist of abundant phenocrysts of microcline ranging in size from 2 to 4 cm, set in a medium grained groundmass of quartz, plagioclase, orthoclase, biotite, hornblende and minor garnet. Extremely mafic-deficient zones may be found throughout this unit. With progressive deformation, partial groundmass recrystallization and stretching of feldspar phenocrysts into lenticular augen of preferred shape orientation occurred. In the most highly deformed rocks, total recrystallization took place, resulting in the formation of orthogneiss (unit 5b) in which feldspar phenocrysts are either obliterated or combined with groundmass quartz to form quartzofeldspathic bands. Granodiorite-granite orthogneiss consists of quartz, plagioclase, orthoclase, hornblende, ubiquitous red garnet and minor amounts of biotite. Igneous texture is completely altered to medium to coarse granoblastic polygonal texture.

The granitoid rocks of unit 5 are found as screens and dykes in unit 1 tonalite gneiss south of Lac Long. Their relationship to quartzofeldspathic paragneiss of unit 2 is unknown as no contacts were observed between the two rock types.

Anorthosite suite (unit 6)

Anorthosite, leucogabbro and monzogabbro (unit 6a) constitute approximately one-third of the mass of the anorthosite suite which protrudes into the map area. These rocks are massive to foliated, normally coarse grained but locally fine grained and flaggy. The main mineral constituent is plagioclase, usually partly or wholly recrystallized to a fine, white equigranular aggregate. Coarse (1 to 10 cm) reddish-brown phenocrysts are confined to monzogabbro and may be iron-stained plagioclase. Orthopyroxene, clinopyroxene and Fe-Ti oxides, ranging in size up to 15 cm, commonly form less than 20 % of the rock and usually exhibit subophitic texture with the pyroxene being coronitic. Rarely, deformed and kinked pyroxene and iron-titanium oxide crystals in excess of 0.5 m have been observed within some of the more leucocratic rocks.

Leuconorite and gabbronorite (unit 6b) occur along the northwest shore of Lac Long as well as west and southwest of the lake. They are igneous textured rocks that vary in weathered appearance from black to a rusty cream. Leuconorite is coarse, leucocratic and contains 20 to 30% subequal Fe-Ti oxides and orthopyroxene. Its texture is subophitic, with the two mafic minerals in places segregated into a crude layering, and locally the rock is strongly deformed and recrystallized. Gabbronorite is medium grained and consists of 30 to 50% orthopyroxene, clinopyroxene and Fe-Ti oxides in a buff-white to grey plagioclase groundmass. Plagioclase laths show varying degrees of recrystallization.

Charnockitic monzonite (unit 6c) is characterized by large K-feldspar megacrysts and an abundance of Fe-Ti oxides. As a consequence of the high oxide content, the rock is very rusty, deeply weathered, and friable. Quartz was not found in hand sample, and the freshest feldspar megacrysts have a greenish hue suggesting charnockitic mineralogy.

Gabbronorite (unit A)

This lithology is similar in mineralogy to the other gabbronoritic rocks but differs in two respects: (1) grain size is generally finer, and (2) igneous texture is extremely fresh with no recrystallization of plagioclase or mafic minerals apparent in the two small exposures examined.

Diorite – quartz diorite (unit B)

Diorite to quartz diorite is minor in occurrence and consists of medium grained recrystallized quartz, plagioclase, hornblende, biotite and rare garnet. Although it contains relicts of the "salt and pepper" igneous texture common to diorites, the rock is thoroughly overprinted with a polygonal granoblastic texture. Patchy zones appear to approach gabbroic composition. This rock may correlate with unit 6 of Thomas and Wood (1983).

STRUCTURE

Structural data support the division into two major crustal blocks, north and south of an east-west line passing through the centre of the Lac Ghyvelde – Lac Long map area (Fig. 65.3). This line is drawn along the northern edge of a locus of faults and shear zones in the vicinity of Lac Long, informally referred to as the Lac Long lineament. The northern crustal block can be further subdivided, on the basis of changes in structural trends and fold geometry, into eastern and western parts. In this way the map area is conveniently partitioned into three domains, within each of which the style and orientation of structures in internally consistent (Fig. 65.3). There is evidence on the scale of mapping for at least three major deformation events involving folding and for three fault sets.

The Lac Long northeast domain is characterized by isoclinal folds overturned to the southeast, with axial planes dipping steeply to the northwest. A lower hemisphere stereographic projection (Fig. 65.3) indicates that gneissic layering and foliation, coplanar with these axial planes, strike northeast and dip predominantly northwest. F_1, F_2, and F_3 fold axes plunge at moderate angles to the southwest, F_1 and F_2 being for the most part coaxial.

Although folds within the Lac Long northwest domain do not differ in style significantly from those in the northeast domain (i.e. three periods of deformation with refolding of earlier folds), some differences in geometry occur. F_1 and F_2 folds are isoclinal; however F_3 folds are open. F_1 and F_2 axial planes, coincident with the orientation of gneissic layering and foliation, dip steeply north-northwest and south-southeast (Fig. 65.3) on either side of vertical F_3 axial planes which strike east-northeast. There is a significant rotation of these planes with respect to their counterparts from the northeast domain, into a more westerly trend. F_1 and F_2 minor fold axes in this domain retain moderate plunges but their trends are also rotated into a predominantly westerly orientation. Note in Figure 65.3 that a small percentage of lineations including F_1 and F_2 minor fold axes plunge to the east.

The Lac Long south domain is characterized by isoclinal folds overturned to the south. Axial planes trend east-northeast to east and dip south-southeast. Lower hemisphere stereographic projection of gneissic banding and foliation planes indicates a northeasterly to east-northeasterly trend and steep northwest dips, with development of a fairly intense maximum (Fig. 65.3). F_1, F_2 and F_3 minor fold axes and associated lineations are rare, but those observed suggest a westerly plunge. Most lineations present in this domain represent mineral stretching and quartz ribbons associated with the formation of the Lac Long lineament. These have moderate northwest plunges that cluster into a strong maximum (Fig. 65.3) which contrasts sharply with that of Figure 42.7 of Thomas and Wood (1983) for rocks north of the Lac Long northern domains.

The oldest faults trend north and are in rocks belonging to the northeast and northwest Lac Long domains. These are terminated by arcuate, southeasterly trending faults which exhibit some degree of left-lateral offset movement and

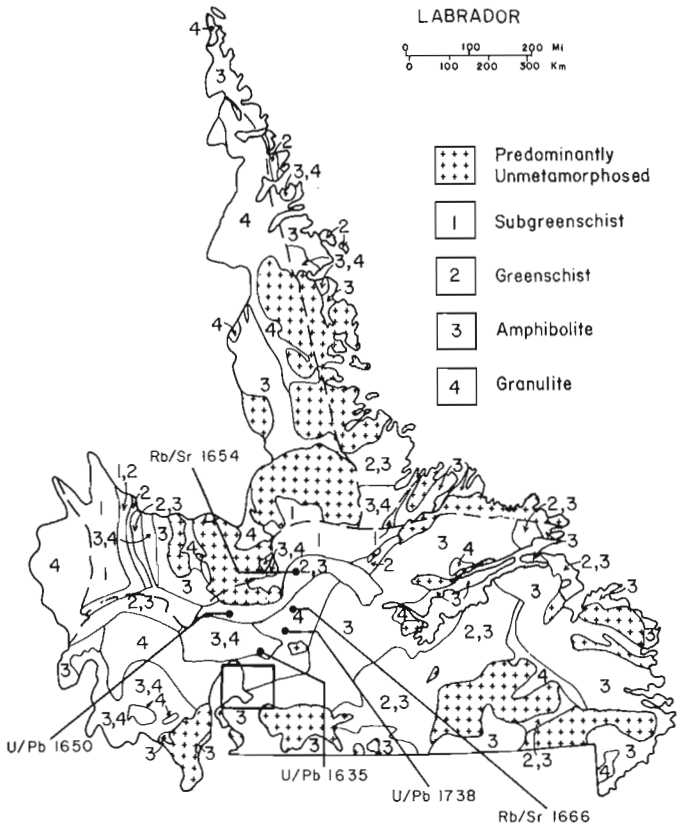

Figure 65.4. *Regional metamorphic zones in Labrador, with recent geochronological data superimposed (modified from Fraser and Heywood, 1978).*

could not be traced across the Lac Long lineament. The most recent faulting recognized occurs in association with the Lac Long lineament. This is a major structure that transects the map area from east to west, and has associated with it faults, shear zones and a strong aeromagnetic expression. Faults within the southern Lac Long domain are either parallel to, or occur as subparallel splays off the lineament.

Structures in the northern Lac Long domains are confined to quartzofeldspathic gneiss of known 1600-1700 Ma age. Structures within the Lac Long south domain occur in widely differing lithologies of unknown age. The contrasts in both lithology and structural trends between the northern and southern crustal blocks suggest that different deformational events are represented. This conclusion is supported by the presence of a straight belt within the northwest part of the Lac Long lineament, containing strongly developed LS fabrics which postdate those in the northern block, and transposed and flattened quartzofeldspathic granulite grade gneiss. It is suggested that structures within the northern crustal block are part of an old, circa 1650 Ma, orogeny and those in the southern block represent an even older orogeny, a second pulse of the 1650 Ma event, or a younger (Grenvillian?) orogenic event. Geochronological study of the tonalite gneiss should solve this problem.

METAMORPHISM

With the exception of scattered areas of the quartzofeldspathic paragneiss, local zones in charnockitic granite, diorite-quartz diorite (unit B) and granodiorite-granite (unit 5), all rocks within the Lac Ghyvelde – Lac Long region have stable metamorphic mineral assemblages characteristic of the granulite facies.

The K-feldspar, orthopyroxene, sillimanite and sapphirine assemblage in quartzofeldspathic paragneiss of unit 2 requires formation under dry conditions at high temperatures and pressures, as does the plagioclase, pyroxene, garnet, magnetite assemblage of the unit 1 tonalite gneiss.

Anorthositic, gabbronoritic and charnockitic rocks may have been emplaced in their host rocks during a regional granulite facies event as evidenced by their stable high grade mineralogy and degrees of polygonal recrystallization. The grade of the granodioritic and dioritic units is difficult to ascertain due to a lack of suitable index minerals; however, the presence of hornblende, biotite and ubiquitous garnet as well as relict igneous texture suggests that they reached a metamorphic grade no higher than amphibolite facies. It is possible that granulite facies metamorphism in the Lac Long south domain was overprinted by no greater than amphibolite facies metamorphism accompanying the younger orogenic event thought to have affected that domain. If so, this metamorphism may have caused only patchy amphibolite retrogression of the rocks north of the Lac Long lineament.

ECONOMIC GEOLOGY

Sparse sulphide mineralization is found in bedrock and float mainly in the northeast part of the area. Pyrite, magnetite with minor chalcopyrite, arsenopyrite and pyrrhotite occur in a narrow local lens of possible metamorphosed iron formation in granulite grade quartzofeldspathic paragneiss. A 20 m wide gossan within the same paragneiss unit close to a small body of gabbronorite contains pyrite mineralization.

Chalcopyrite-, sphalerite(?)- and pyrite-bearing float is also found in the general region of the bedrock mineralization, but it is emphasized that the source of this float could be distant since glaciation from the northeast was extensive. A small occurrence consisting of stringers of an unknown copper-bearing mineral is located in paragneiss 5 km north of Lac Ghyvelde, but was not examined during the course of this study.

Fe-Ti oxides are abundant in the anorthosite suite rocks examined previously by BRINEX for Ti potential. Well sorted, almost pure magnetite-ilmenite sand occurs on a small beach midway along the north shore of Lac Long suggesting that this body of rocks warrants additional study.

DISCUSSION

From the outset, in 1978, of recent studies into the nature and extent of the Grenvillian Orogeny in south-central Labrador, a number of unexpected findings have ensued. Before that time, it was concluded that amphibolite to granulite grade metamorphic events recorded in large expanses of paragneiss and orthogneiss within the region were of Grenvillian age. Similarly, it was thought that most if not all of the major structural deformation was due to the Grenvillian Orogeny.

Grenvillian structural effects have been documented in the Seal Lake Group along with subgreenschist to greenschist facies metamorphism, as far as 230 km north of the present map area. In addition there are numerous examples of circa 1000 Ma potassium-argon dates from the Seal Lake Group south into the region of this study. During the recent studies, however, a number of uranium-lead age (T.E. Krogh, written communication, 1983) and rubidium-strontium ages (Fryer, 1983) of circa 1600-1700 Ma have been obtained for high grade crystalline rocks from well within the present boundary of the Grenville Province (Fig. 65.4). These record metamorphic events in both para- and orthogneisses varying in grade from amphibolite to granulite, as well as several cooling ages of little deformed granitoids. Rb-Sr isochrons

which yield these dates are largely undisturbed. U-Pb results giving these dates are nearly concordant, with minor lead loss attributable to a circa 1000 Ma event. The dates therefore suggest that many of the presumed high grade Grenvillian gneisses in this part of Labrador belong to a much older crystalline terrane which underwent a Grenvillian metamorphic event of much less intensity than previously assumed. In summary, the geochronological, structural and metamorphic data as well as to some extent contrasting lithologies, record a previously unsuspected intense Paleohelikian orogenic event at circa 1600-1700 Ma which affected the rocks in central and south-central Labrador. This event has been informally termed the Labradorian orogeny.

ACKNOWLEDGMENTS

Lakeland Helicopters Limited and pilot J. Crawford provided air transport in the field. R. Nugent, C. O'Flaherty and G. Wong ably assisted the field survey, and cook G. Lynch is thanked for a nourishing and varied menu. The manuscript was critically reviewed by R.J. Wardle and J. Murray of the Newfoundland Department of Mines and Energy.

REFERENCES

Emslie, R.F., Hulbert, L.J., Brett, C.P., and Garson, D.F.
1978: Geology of the Red Wine Mountains, Labrador: the Ptarmigan Complex; in Current Research, Part A, Geological Survey of Canada, Paper 78-1A, p. 129-134.

Fraser, J.A. and Heywood, W.W. (editors)
1978: Metamorphism in the Canadian Shield; Geological Survey of Canada, Paper 78-10.

Fryer, B.J.
1983: Report on geochronology, Labrador mapping; unpublished summary of geochronological results obtained on samples collected from central Labrador between 1978 and 1980, 35 p.

Pyke, M.W.
1956: Report on exploration in areas G and K, Labrador; BRINEX confidential company report.

Stevenson, I.M.
1969: Lac Brûlé and Winokapau Lake map areas, Newfoundland and Quebec; Geological Survey of Canada, Paper 67-69.

Taylor, F.C.
1971: A revision of Precambrian structural provinces in northeastern Quebec and northern Labrador; Canadian Journal of Earth Sciences, v. 8, p. 579-584.

Thomas, A.
1981: Geology along the southwestern margin of the Central Mineral Belt; Newfoundland Department of Mines and Energy, Mineral Development Division, Preliminary Report 81-4, 40 p.

Thomas, A., Jackson, V., and Finn, G.
1981: Geology of the Red Wine Mountains area, central Labrador (13E/9, 10, 11, 15, 16; 13F/12, 13); Newfoundland Department of Mines and Energy, Mineral Development Division, Open File Report Lab. (573).

Thomas, A. and Wood, D.
1983: Geology of the Winokapau Lake area, Grenville Province, central Labrador; in Current Research, Part A, Geological Survey of Canada, Paper 83-1A, p. 305-312.

66. ESTIMATION OF PHYSICAL PARAMETERS OF MacLEAN CHANNEL SULPHIDE-BEARING DEBRIS FLOWS, BUCHANS, NEWFOUNDLAND[1]

Contract 08GR.23233-2-0500

W.P. Binney[2]

Binney, W.P., Estimation of physical parameters of MacLean channel sulphide-bearing debris flows, Buchans, Newfoundland; in Current Research, Part A, Geological Survey of Canada, Paper 84-1A, p. 495-498, 1984.

Also in Current Research, Newfoundland Department of Mines and Energy, Mineral Development Division, Report 84-1, 1984.

Abstract

Subaqueous sulphide-bearing debris flows were the major transport mechanism for the ore units in the MacLean channel. Measurement of the coarse blocky detritus in the flow deposits allows estimation of the yield strength of the debris flows. Yield strengths for two debris flows in the MacLean channel were estimated to be 1.0 to 1.5 x $10^3 N.m^{-2}$ and 3 to 9 x $10^3 N.m^{-2}$. Paleoslopes an be calculated using the estimated yield strength of the debris. Comparisons between calculated paleoslopes (3 and 10°) and actual bedding attitudes (0 to 15°) in the MacLean Extension orebody suggest present bedding attitudes reflect the paleoslope. Data for the sulphide-bearing debris flows are similar to literature values for non-sulphide flows. Uses of the calculations for mineral exploration include basinal analysis and prediction of locations for high grade, dense debris flow deposits at the bases of steep inclines.

Résumé

Des coulées de d'débris subaquatiques à sulfures ont été le mécanisme de transport principal des unités minéralisées dans le chenal de MacLean. Le mesurage des débris blocailleux grossiers dans les dépôts permet d'estimer la limite élastique des coulées de débris. Ces limites élastiques sont de 1,0 à 1,5 x 10^3 Nm^{-2} et de 3 à 9 x 10^3 Nm^{-2} pour deux coulées de débris dans le chenal principal. Il est possible de calculer les paléopentes à partir des limites élastiques estimatives des débris. Une comparaison des paléopentes calculées (3° et 10°) et de la disposition actuelle de la stratification (0° à 15°) dans la masse minéralisée de la prolongation de MacLean permet de croire que la disposition actuelle de la stratification reflète la paléopente. Les données sur les coulées de débris à sulfures sont semblables aux valeurs publiées pour les coulées dépourvues de sulfures. Les utilisations des calculs pour l'exploration minérale comprenment l'analyse des bassins et la prévision des emplacements des dépôts riches de coulées de débris denses accumulés au pied de pentes abruptes.

INTRODUCTION

In 1982 and 1983 the author investigated the sedimentology of the transported ore in the MacLean channel, Buchans camp. Newfoundland. Shown in plan and section in Figure 66.1, the orebodies comprise several lithologically distinct beds within a discrete stratigraphic interval. The focus of the work was the MacLean Extension orebody because it is currently being developed and mined. The adjacent MacLean orebody is mined out and most parts are inaccessible.

Individual beds containing sulphide detritus are poorly sorted with angular to subangular lithic and sulphide clasts as long as one metre or more, set in a sand-sized matrix. The base of some beds is inversely graded but most beds have a random internal fabric. The ore-bearing beds have been interpreted as debris flow deposits (Thurlow, 1977; Walker and Barbour, 1981; Calhoun and Hutchinson, 1981; Binney et al., 1983).

Binney et al. (1983) described the distinctive marginal deposits of a typical debris flow observed in the MacLean Extension workings. The contact is at a high angle between the flow centre, with its matrix of sulphides, barite and fine grained lithic detritus, and the margin of the debris flow, with its coarse (greater than 30 cm) blocks of sulphide, granitic and other lithic clasts in a detrital matrix. Such a contact indicates significant matrix strength, and is diagnostic of debris flow margins (Johnson, 1970, p. 434).

Similar debris flow marginal deposits can be observed at several locations in the MacLean Extension workings, thus confirming previous interpretations that at least some of the ore-bearing beds were deposited by debris flows. Although debris flow deposits comprise most fill in the MacLean channel, turbidity current deposits and landslide deposits have also been recognized.

Middleton and Hampton (1976) defined a debris flow as the sluggish downslope movement of mixtures of granular solids, clay minerals and water in response to gravity. Blocks are supported in the flow by the strength of the matrix and deposition occurs when the shear stress applied to the debris drops below its internal strength and the flow 'freezes' in position.

PHYSICAL PARAMETERS

Using the methods of Johnson (1970, p. 486-490) and Hiscott and Middleton (1979), some of the physical parameters of debris flows can be estimated by measurement of coarse, bouldery detritus in the flows. The debris presumably was at a point of critical equilibrium (shear stress equals yield strength) and was just supported when the flow stopped. For these conditions Johnson (1970, p. 461-487) derived an approximate relation between the yield strength (k) of the debris flow and the thickness of a block (c) supported by the flow. Other considerations are the unit weight of the debris flow (γd) and the block (γb) and the depth of penetration of

[1] Contribution to Canada-Newfoundland co-operative mineral program 1982-84. Project carried by Geological Survey of Canada.

[2] P.O. Box 1152, Truro, Nova Scotia B2N 5H1

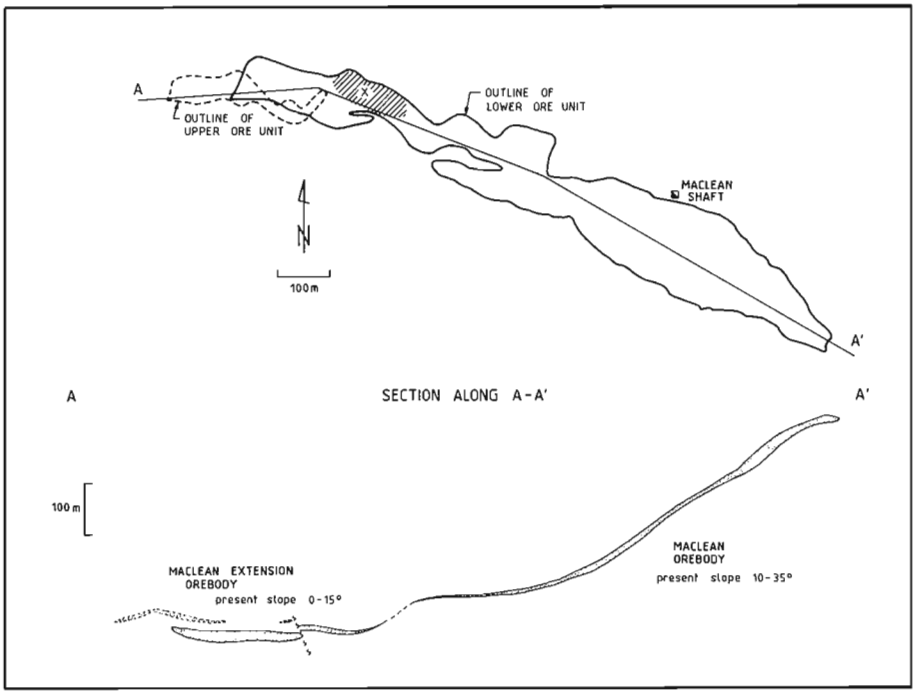

Figure 66.1

Plan and section of the orebodies of the MacLean channel.

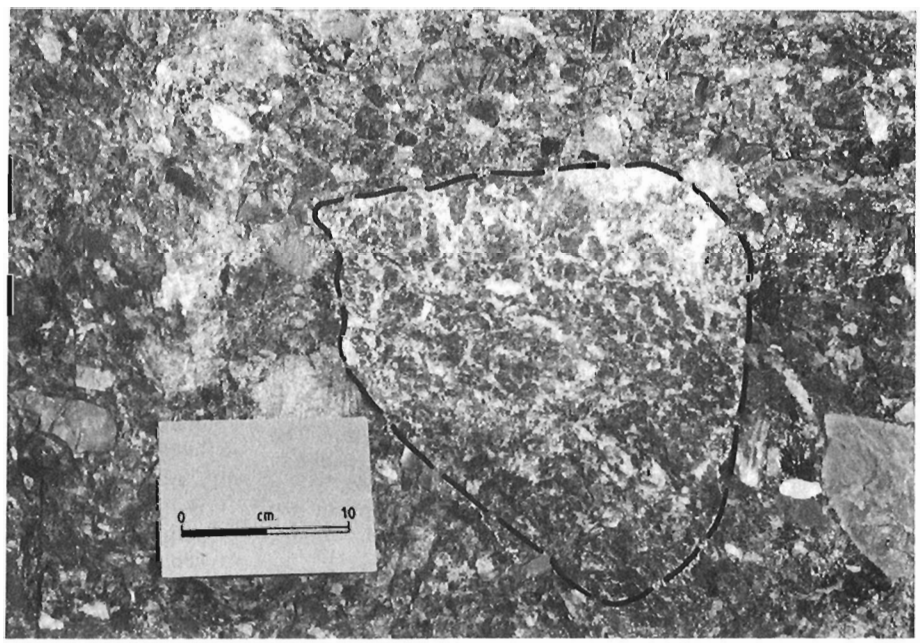

Figure 66.2

Block of barite-sphalerite-galena completely enclosed by a baritic polylithic breccia-conglomerate bed at the top of the Lower Ore unit, MacLean Extension orebody.

the block into the flow (1/n). The unit weight of a material is the product of its density ($kg.m^{-3}$) and the acceleration due to gravity (9.80 $m.sec^{-2}$). The depth of penetration (1/n) is expressed as a fraction, for example if a block is 3/4 submerged in the flow then 1/m = 3/4.

$$k \approx \frac{c}{4} \left(\gamma b - \frac{\gamma d}{n}\right)$$

The resultant value for the yield strength (k) of the debris flow is expressed in $N.m^{-2}$ where 1 N = 1 $kg.m.sec^{-2}$. This relationship is particularly amenable to underground exposures where only the thickness and length of individual clasts can be measured. Difficulty arises, however, in assessing the depth of penetration of a block into the debris flow since the upper limit of individual flows cannot everywhere be identified.

To use the relationship, estimates are needed for the unit weight (density times acceleration of gravity) of both the block and the debris flow. The sulphide blocks observed in the debris flow deposits were sufficiently lithified to break with discrete boundaries so their density is estimated from their mineralogical content. Lithic fragments were transported as clasts and their density is assumed to average 2.7 $g.cm^{-3}$. The density of the debris flow is arbitrarily assumed to be 2.4 $g.cm^{-3}$, at the dense end of the range of 2.0 to 2.5 $g.cm^{-3}$ reported for subaerial debris flow (Fisher, 1971). This is considered a reasonable assumption as the flows were transporting blocks of density 2.6 to 5.5 $g.cm^{-3}$. If the density of the flow exceeded that of the blocks there would be a buoyant effect with the lithic clasts floating to the top. This was not observed. The high percentage of sulphide and barite fragments in the deposits does support a high overall density for the debris flows.

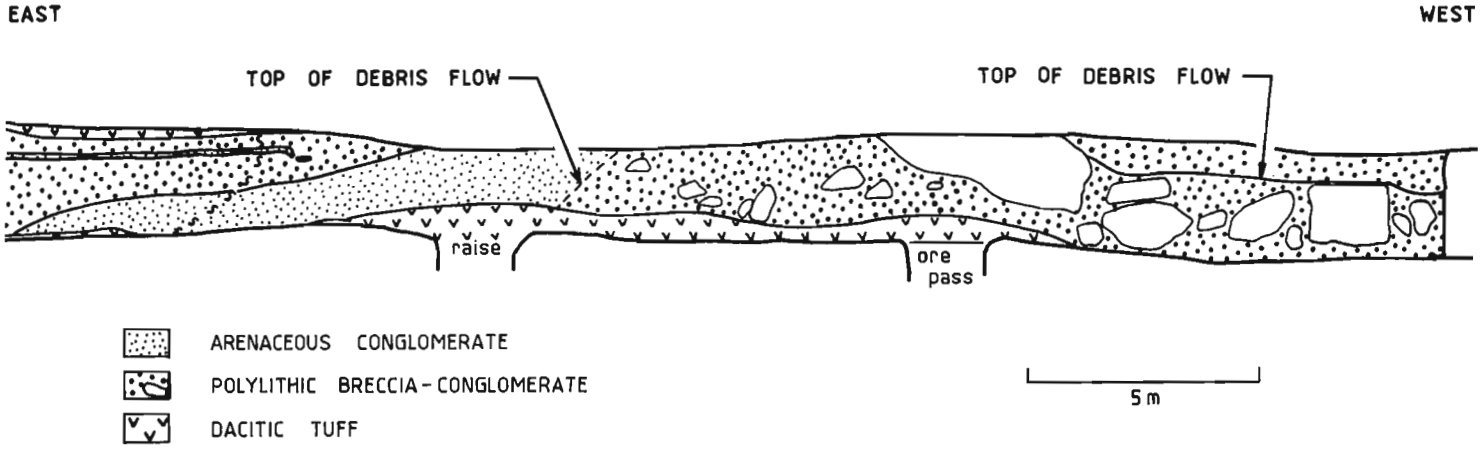

Figure 66.3. *Section of the Lower Ore unit along a sublevel wall (20-6-1), MacLean Extension orebody. Coarse detritus is observed about the snout of the northward flow. The flow is bounded to the east by arenaceous conglomerate deposited contemporaneously with it but outside of the main body of the flow.*

Individual flows would have different densities but without measurements taken during flow this cannot be quantified with respect to the deposits observed.

The use of Johnson's relationship can be illustrated with reference to a typical debris flow in the MacLean Extension workings. This flow, located at X in Figure 66.1, occurs at the top of the Lower Ore unit and is laterally extensive, covering an area in excess of 6000 m^2. Figure 66.2 illustrates one of the coarser fragments transported by this flow. The thickness of this clast of barite-sphalerite-galena is 0.23 m and it is completely enclosed by the 1.2 m baritic polylithic breccia-conglomerate bed.

$$k \approx \frac{0.23\ m}{4} \left((4.5 - \frac{2.4}{1})(10^3) kg.m^{-3}(9.80\ m.sec^{-2})\right)$$

$$\approx 1.2 \times 10^3\ N.m^{-2}$$

Other blocks of coarse detritus from this bed gave calculated yield strengths for the debris flow in the range of 1.0 to 1.5 x 10^3 $N.m^{-2}$.

Another debris flow deposit (Fig. 66.3) contains coarse blocks of sphalerite-galena and mineralized stockwork up to 4.4 m in length. The debris flow overlies dacitic tuff and forms the base of the Lower Ore unit at this location. Arenaceous conglomerate marginal to the main body of the flow forms the substrate for similar coarse debris flow deposits to the east. The yield strength for the debris flow was calculated using a sphalerite-galena boulder 1.22 m thick and a stockwork boulder 1.52 m thick, 3/4 submerged in the flow. Yield strengths needed to support these boulders are 9 x 10^3 $N.m^{-2}$ and 3 x 10^3 $N.m^{-2}$, respectively.

Johnson (1970, p. 488) also derived the relationship between the yield strength of the debris in critical equilibrium (k), the slope (δ), the thickness of the flow (Tc) and the unit weight of the debris (γd).

$$k = Tc\ \gamma d \sin \delta$$

This equation was derived using the assumption that the debris flow could be represented as an infinite sheet of plastic material, and is applicable as long as the width of the flow is greatly in excess of its thickness. Knowing the slope, thickness and unit weight of the debris, one can arrive at an independent estimate of the yield strength of the debris. In the case of the MacLean channel, where the amount of postdepositional tilting is unknown, the estimate of yield strength can be used to predict the paleoslope.

For the baritic polylithic breccia-conglomerate which had a yield strength of 1.0 to 1.5 x 10^3 $N.m^{-2}$ based on the maximum clast sizes, the calculated paleoslope is

$$\sin \delta = \frac{1.5 \times 10^3\ N.m^{-2}}{(1.2\ m)(2.4 \times 10^3 kg.m^{-3})(9.80\ m.sec^{-2})} = 0.053$$

$$\delta = 3°$$

The low slope for this bed is consistent with its position as a late debris flow in the filling of the basin. The calculated paleoslope is within the range of the present dip of the bed of 0 to 8° west.

Calculated paleoslopes for the debris flow illustrated in Figure 66.3 are approximately 10°, in very close agreement with the actual measured dip of the bed which is 12 to 15°.

These results suggest that the present slopes observed in the MacLean Extension area are a reflection of the paleoslopes that existed at the time of deposition of the sulphide-bearing beds. Due to a lack of access, this comparision of actual and predicted slopes could not be extended into the MacLean workings where the Lower Ore unit has a much steeper dip.

If the present attitudes of the rocks in the MacLean orebody are essentially those of the paleoslope, then the yield strength of the debris flows can be calculated. For the sulphide matrix ore, rich in sphalerite and galena;

$$k = (10\ m)(2.4 \times 10^3 kg.m^{-3})(9.80\ m.sec^{-2}) \sin 10°$$

$$= 4 \times 10^4\ N.m^{-2}$$

This result is high compared to the data obtained for debris flows in the MacLean Extension workings. A debris flow with this yield strength could transport boulders in excess of 6 m in diameter. The result indicates one of the limitations of these calculations since no clasts of this size have been recognized in any of the transported orebodies of the Buchans camp. Therefore, the calculated yield strength cannot be confirmed. Sources of error inherent in the calculations are the assumption that sulphide matrix ore was transported by a

simple debris flow process and the assumption that the present dip of the bed is identical to the paleoslope.

Using the Hampton number (Hiscott and Middleton, 1979) the velocity (U) that a debris flow would have to exceed for turbulent flow can be calculated. Variables include the strength of the plastic debris flow (k) and the density of the flow (ρd). For turbulent flow;

$$\frac{\rho d\, U^2}{k} \geq 1000$$

For the baritic polylithic breccia-conglomerate bed used throughout this report;

$$U^2 \geq \frac{1000\ (1.5 \times 10^3\ N.m^{-2})}{2.4 \times 10^3\ kg.m^{-3}} = 625\ m^2.sec^{-2}$$

$$U \geq 25\ m.sec^{-1}$$

Compared with velocity values for subaerial debris flows of 1 to 3 $m.sec^{-1}$ (Sharp and Nobles, 1953; Johnson, 1970, p. 512), this is an unrealistic, high velocity for a flow, especially one depositing coarse unsorted detritus. The result confirms the laminar, nonturbulent nature of flow within the debris flows of the MacLean channel.

SUMMARY AND CONCLUSIONS

The data for yield strength of the sulphide-bearing subaqueous debris flows of the MacLean channel is of the same order of magnitude as that presented by Johnson (1970, p. 490) for subaerial debris flows (1.7 to $5 \times 10^3\ N.m^{-2}$) and Hiscott and Middleton (1979) for subagueous debris flows in the Tourelle Formation ($4 \times 10^3\ N.m^{-2}$). In the MacLean channel the boulders are smaller than in the other studies, but being sulphides, are of much greater density. The variation in yield strength of the flows in the MacLean channel reflects both the diversity of the source area with high density sulphide and lithic detritus to form the flows, and the high local variability of slope in a volcanic environment which has affected the course of the debris flows.

The accuracy of the calculations is subject to the assumptions that Johnson (1970, p. 461-488) made in developing the equations and the fact that a unimodal process of clast support is assumed in applying the equations. Clasts in the MacLean channel have an apparent maximum size based on the author's studies. This may reflect the ability of the debris flows to transport coarse detritus or a limited size range of clasts in the source area.

Even with the limitations outlined, calculations of physical parameters such as debris flow yield strength and paleoslope could be important factors in exploration for sulphide-bearing debris flows such as those at Buchans. Unlike studies of subaerial debris flows, the attitude of preserved subaqueous flows is usually unknown. Even crude estimates of paleoslope may have important implications in basinal analysis and the ultimate success of a mineral exploration program. Changes in paleoslope affect the ability of debris flows with coarse detritus to continue moving downslope. A radical change in paleoslope could result in deposition of debris flows with coarse, high grade sulphide blocks at the base of a steep incline.

ACKNOWLEDGMENTS

The author would like to thank J.G. Thurlow (Abitibi-Price Inc.) and E.A. Swanson (ASARCO Inc.) for their assistance and comments based on extensive experience with the geology and ore deposits of the Buchans camp.

The paper benefited greatly from the useful comments of R.V. Kirkham and W.H. Poole who reviewed the manuscript.

REFERENCES

Binney, W.P., Thurlow, J.G., and Swanson, E.A.
1983: The MacLean Extension orebody, Buchans, Newfoundland; in Current Research, Part A, Geological Survey of Canada, Paper 83-1A, p. 313-319.

Calhoun, T.A. and Hutchinson, R.W.
1981: Determination of flow direction and source of fragmental sulphides, Clementine deposit, Buchans, Newfoundland; in The Buchans Orebodies: Fifty Years of Geology and Mining, ed. E.A. Swanson, D.F. Strong, and J.G. Thurlow; Geological Association of Canada, Special Paper 22, p. 187-204.

Fisher, R.V.
1971: Features of coarse-grained, high-concentration fluids and their deposits; Journal of Sedimentary Petrology, v. 41, no. 4, p. 916-927.

Hiscott, R.N. and Middleton, G.V.
1979: Depositional mechanics of thick-bedded sandstones at the base of a submarine slope, Tourelle Formation (Lower Ordovician), Quebec, Canada; The Society of Economic Paleontologists and Mineralogists Special Publication 27, p. 307-326.

Johnson, A.M.
1970: Physical Processes in Geology; Freeman, Cooper and Co., San Francisco, 577 p.

Middleton, G.V. and Hampton, M.A.
1976: Subaqueous sediment transport and deposition by sedimentary gravity flows; in Marine Sediment Transport and Environmental Management, ed. D.J. Stanley and D.J.P. Swift; John Wiley & Sons, p. 197-218.

Sharp, R.P. and Nobles, L.H.
1953: Mudflow of 1941 at Wrightwood, southern California; Geological Society of America, Bulletin, v. 64, p. 547-560.

Thurlow, J.G.
1977: Occurrence, origin and significance of mechanically transported sulphide ores at Buchans, Newfoundland (abstract); in Volcanic Processes in Ore Genesis, Geological Society of London, Special Publication, no. 7, p. 127.

Walker, P.N. and Barbour, D.M.
1981: Geology of the Buchans ore breccias; in The Buchans Orebodies: Fifty Years of Geology and Mining, ed. E.A. Swanson, D.F. Strong, and J.G. Thurlow; Geological Association of Canada, Special Paper 22, p. 161-185.

67. METALLOGENIC STUDIES OF GRANITE-ASSOCIATED MINERALIZATION IN THE ACKLEY GRANITE AND THE CROSS HILLS PLUTONIC COMPLEX, FORTUNE BAY AREA, NEWFOUNDLAND[1]

Project 830036
Contract 19SR.23233-3-0350

J. Tuach[2]

Tuach, J., Metallogenic studies of granite-associated mineralization in the Ackley Granite and the Cross Hills Plutonic Complex, Fortune Bay area, Newfoundland; in Current Research, Part A, Geological Survey of Canada, Paper 84-1A, p. 499-504, 1984.

Also in Current Research, Newfoundland Department of Mines and Energy, Mineral Development Division, Report 84-1, 1984.

Abstract

Cassiterite-bearing quartz-topaz greisen occurs in easterly trending veins and pods within the Ackley Granite, and as larger pods at the granite contact in the Sage Pond-Gisborne Lake area.

Minor anomalous radioactivity is associated with east-northeast-trending fractures, and with aplite veins, near the roof of a riebeckite-bearing peralkaline granite which was emplaced late in the intrusion history of the Cross Hills Plutonic Complex.

Metallogenic models for granitoid mineralization in the Fortune Bay area suggest evolution of magmatic fluids during latest pluton emplacement and crystallization, with vertical rise and ponding of these fluids at or near the granite roof.

Résumé

Un greisen à quartz et topaze, contenant de la cassitérite se présente dans des filons et des masses allongées orientés vers l'est, au sein du granite d'Ackley, et sous forme de masses plus grandes au niveau du contact avec le granite dans la région de l'étang Sage et du lac Gisborne.

Une faible radioactivité anormale est associée à des fractures orientées est-nord-est et à des filons d'aplite, près du toit d'un granite hyperalcalin à riébeckite qui a été mis en place vers la fin de l'histoire intrusive du complexe plutonique de Cross Hills.

Des modèles métallogéniques de la minéralisation granitoïde dans la région de la baie Fortune semblent indiquer qu'il y a eu évolution des magmas lors de la mise en place du pluton le plus récent, et cristallisation accompagnée de la montée verticale et de l'accumulation des fluides au niveau du toit du granite ou près de ce dernier.

INTRODUCTION

This project, started in April 1983, is designed to develop metallogenic and exploration models for granite-associated mineralization in the Ackley Granite and Cross Hills Plutonic Complex, southeast Newfoundland. Field data collected during the 1983 field season will form the basis for a Ph.D. thesis by the author at Memorial University of Newfoundland.

PREVIOUS WORK

Regional mapping in the area has been done previously by Bradley (1962), Williams (1971), O'Brien and Nunn (1980), O'Brien et al. (1980a,b) and Dickson (1983).

Subeconomic aplite-pegmatite molybdenum deposits have long been known in the Rencontre area, and occur within the granite at the contact of a fine- to medium-grained porphyritic phase of the Ackley Granite with volcanic rocks of the Belle Bay Formation (Fig. 67.1). The geology, geochemistry and exploration history of these deposits were described in detail by Whalen (1976, 1980, 1983).

Cassiterite-bearing quartz-topaz greisen veins have recently been identified by Esso Minerals Limited, and by the Newfoundland Department of Mines and Energy (Dickson, 1982; Dickson and Howse, 1982) in the Anesty Hill-Sage Pond area (Fig. 67.1). These veins occur within a fine- to medium-grained, porphyritic marginal phase of the Ackley Granite and increase in concentration and size toward the granite contact (Dickson, 1983).

A peralkaline phase of the Cross Hills Plutonic Complex with minor anomalous radioactive zones and anomalous Nb, Zr, Sn and Th has been identified by Saarberg Interplan (Hopfengaertner, 1982).

CURRENT WORK

During the 1983 field season quartz-topaz veins were mapped in detail along the Ackley Granite contact between Rabbit Pond and Gisborne Lake (Fig. 67.2).

Samples were collected from the quartz-topaz veins in the Sage Pond area (Fig. 67.2) and from the molybdenite prospects at Motu, Ackley City, Crow Cliff – Dunphy Brook, and Wyllie Hill for geochemical anlaysis and for fluid inclusion studies (Fig. 67.1). All known molybdenum occurrences in the Ackley Granite were examined and sampled, and samples were collected from the Strouds Hill fluorite prospect at the south end of Long Harbour (Fig. 67.1).

The Cross Hills Plutonic Complex west of Grand Le Pierre, and Precambrian volcanic rocks intervening between the Cross Hills plutonic complex and the Ackley Granite were mapped at a scale of 1:15 000 (Fig. 67.2). Several traverses were made over the Cross Hills Plutonic Complex to the east of Grand Le Pierre.

[1] Contribution to Canada-Newfoundland co-operative mineral program 1982-84. Project carried by the Geological Survey of Canada.

[2] c/o Newfoundland Department of Mines and Energy, Mineral Development Division, P.O. Box 4750, St. John's, Newfoundland A1C 5T7

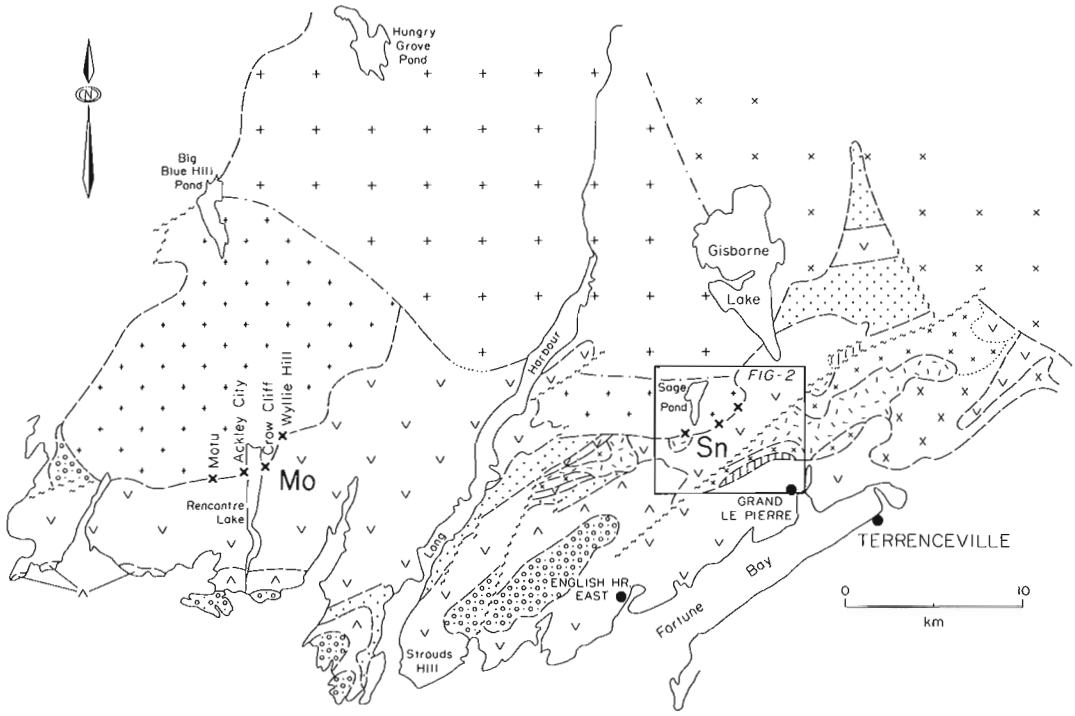

DEVONIAN - ACKLEY GRANITE

- *Massive, porphyritic coarse grained biotite granite.*
- *Massive, uniform coarse grained biotite granite.*
- *Fine to medium grained porphyritic biotite granite.*

DEVONIAN or PRECAMBRIAN - CROSS HILLS PLUTONIC COMPLEX

- *Fine to medium grained peralkaline granite.*
- *Medium to coarse grained hornblende biotite granodiorite.*
- *Fine to medium grained biotite granite (alaskite?).*
- *Gabbro-diabase multiple intrusions.*

PRECAMBRIAN - LONG HARBOUR GROUP

- Rencontre Formation - *red sandstone and conglomerate.*
- Mooring Cove Formation - *felsic tuff, ash flows and massive felsite.*
- Anderson's Cove Formation - *fine to medium grained gray sediment.*
- Belle Bay Formation - *felsic flow and pyroclastic rocks, basalt flows.*

Figure 67.1

General geology north of Fortune Bay, Newfoundland.

GENERAL GEOLOGY

Plutonic rocks to the north of Fortune Bay intrude Precambrian subaerial metavolcanic and metasedimentary rocks of the Long Harbour Group (Williams, 1971; O'Brien and Nunn, 1980) in the Avalon Terrane of the Newfoundland Appalachians (Williams and Hatcher, 1983).

The Long Harbour Group has been subdivided into four separate conformable formations (Bradley, 1962; Williams, 1971; O'Brien and Nunn, 1980). The stratigraphically lowest, Belle Bay Formation, is dominated by felsic ash flow deposits and epiclastic sediment with minor basalt flows, and is overlain by fine- to medium-grained sediments of volcanic derivation belonging to the Anderson's Cove Formation. The overlying Mooring Cove Formation consists of interbedded silicic flows, felsite (commonly with peralkaline affinity; O'Brien, personal communication, 1983) and mafic flows. The Rencontre Formation, a red to purple fining-upward conglomerate to sandstone sequence overlies the Mooring Cove Formation.

The Cross Hills Plutonic Complex intrudes the Belle Bay and Anderson's Cove formations and consists of a complex mixture of diabase, gabbro, granodiorite, alaskite and peralkaline granite, along with abundant xenoliths and roof pendants of silicic volcanic and mafic intrusive-extrusive rocks. The Cross Hills Plutonic Complex has not been dated; however, observation that gabbroic phases are cut by the Ackley Granite and that there is a general lack of deformation and metamorphic effects have led to a consensus that these plutonic rocks are Devonian in age (Bradley, 1962; O'Brien and Nunn, 1980). The peralkaline granite phase of the Cross Hills Plutonic Complex is geochemically comparable to peralkaline silicic volcanic rocks of the Mooring Cove Formation (O'Brien, personal communication, 1983), and an age of Devonian or Precambrian may be inferred for both (Fig. 67.1, 67.2).

The Devonian Ackley Granite occupies an area of 3000 km^2 and has been divided into seven major units based on texture, mineralogy and geochemistry (Dickson, 1983), with the three most differentiated southern units having a silica content of greater than 72 per cent. Fine grained, extremely differentiated marginal granite phases occur along and near the southern contact of the Ackley Granite, and exhibit strong trace element variation trends (Whalen, 1976, 1980, 1983; Dickson, 1983). The marginal phases hosting mineralization are fine grained to porphyritic, miarolitic biotite 'alaskite' granite, and minor occurrences of tuffisite are present. Quartz crystals and quartz-feldspar pegmatite patches are ubiquitous in the fine grained granite of the Rencontre area but are rare to absent in the fine grained granites in the Sage Pond – Gisborne Lake area. In the Fortune Bay area, the Ackley Granite cuts the Belle Bay and

Anderson's Cove formations as well as gabbroic rocks of the Cross Hills Plutonic Complex, and has been dated at about 355 Ma (Bell et al., 1977; Dallmeyer et al., 1983).

GEOLOGY OF THE SAGE POND-GRAND LE PIERRE AREA

Volcanic Complex (units 1 and 2)

The English Harbour volcanics (Bradley, 1962) south of the Cross Hills pluton consist of massive to slightly fractured, light to dark rhyolite flows, welded ash flow deposits, breccias, and tuff (unit 1a).

North of the Cross Hills pluton, rocks mapped as belonging to the Belle Bay and Anderson's Cove formations (Bradley, 1962; O'Brien and Nunn, 1980) consist of a strongly foliated volcanic to volcanic sedimentary sequence (unit 1b) composed of coarse, locally welded rhyolite breccias and tuff, waterlain tuff and sediment, slate, siltstone, quartz-sericite schist, diabase and basalt flows (unit 1c). These rocks exhibit rapid lateral and vertical facies variations. They appear to be in fault contact with a massive banded to brecciated ash flow unit (unit 1d) containing minor (<2%) disseminated and fracture-filling pyrite which occurs along the southern contact of the Ackley Granite. In the western part of the map area, purple-brown ash flow and fine tuff units (unit 2) of the Mooring Cove volcanics (Bradley, 1962) overlie purple, welded to nonwelded massive to layered breccias, banded rhyolite, basalt flows, and minor siltstone.

Moderate to tight chevron folding of the layered tuff and siltstone and the ash flow banding occurs locally. This factor coupled with the massive nature of the rocks makes definitive structural and/or stratigraphic analyses of the volcanic sequence difficult. Bradley (1962) and O'Brien and Nunn (1980) suggested that large scale moderate to tight folding of the volcanic sequence occurred along an east-northeast axis.

The Anderson's Cove Formation is absent from the succession in this area, which suggests a local diconformity or unconformity.

Cross Hills Plutonic Complex (unit 3)

Three main intrusive phases occur in the Cross Hills Plutonic Complex to the northwest of Grand Le Pierre:

Unit 3a. A fine- to coarse-grained diabase-gabbro unit intrudes Precambrian volcanic rocks and is composed of multiple intrusions of diabase and gabbro. Veining by fine to pegmatitic gabbro is common.

Unit 3b. A fine- to medium-grained, orange, 'alaskitic', miarolitic biotite granite intrudes the diabase-gabbro and locally intrudes volcanic country rocks. Extensive stoping of the gabbro-diabase is common and vertical subparallel biotite granite dykes trending 070° to 080° occur near the southern margin of the gabbro-diabase unit.

Unit 3c. A fine- to medium-grained purple-brown, miarolitic, riebeckite peralkaline granite occurs to the south and also above the biotite granite and has intruded the gabbroic and volcanic country rock. The riebeckite granite contains late fine grained veins, and tuffisite breccias related to gas-release from the crystallizing magma. Granophyric texture is common, and small granitic pegmatite patches are locally present. In the western part of the area mapped in detail, a mottled, orange-brown aplite unit ($3c_1$) with sharp vertical contacts occurs between the biotite granite and medium-grained peralkaline granite. In the east the contact between biotite granite and peralkaline granite is marked by a gradual colour change. The northern boundary of the medium grained peralkaline phase is noted by a decrease of 30 to 50 per cent in background total count radioactivity.

Three areas of peralkaline granite to the north and east of the main exposure occur topographically above biotite granite and probably form the upper portion of east-northeast-trending biotite granite dykes. Red-brown aplite (unit 3d) intrudes the Belle Bay Formation east of Deer Park Pond.

West of Grand Le Pierre, the Cross Hills Plutonic Complex appears to mark a phase of south-southeast/north-northwest crustal extension. Initial multiple intrusion of gabbro-diabase occurred, followed by stoping and intrusion of the gabbro and diabase by biotite granite. Differentiation to form a roofward or marginal peralkaline phase may have taken place in the larger silicic magma chambers.

Preliminary investigation of the Cross Hills Plutonic Complex east of Grand Le Pierre indicates a comparable history with diabase being the more abundant mafic intrusive rock stoping into volcanic country rock. East-northeast-trending diabase dykes commonly intrude Precambrian volcanic rocks. Fine- to medium-grained biotite granite is the predominant silicic lithology east of Grand Le Pierre, with minor patches of peralkaline granite noted. A medium- to coarse-grained hornblende-biotite granodiorite with abundant volcanic and diabase xenoliths is confined to the eastern portion of the complex; it has intruded the main diabase unit, and has locally been intruded by gabbro and thin aplite dykes. The relationship between the hornblende-biotite granite and the biotite granite has not been observed. Diabase stoped by granite occurs at the Southeast Bight Hills.

Ackley Granite (unit 4)

The Ackley Granite consists of fine- to medium-grained miarolitic quartz-feldspar porphyritic biotite granite in its southern exposures (unit 4a) and grades northward into a medium- to coarse-grained biotite granite (unit 4). Phenocryst content averages from 10 to 20 per cent. A coarse porphyritic phase with 40 to 50 per cent phenocrysts is host to the greisen veins southeast of Moulting Pond. Topographic relief over the granite is gentle with little exposure, whereas the volcanic country rocks to the south form rugged topographic features and are well exposed.

The granite contact dips from vertical to shallow, with possible roof pendants present west of Anesty Hill and east of Moulting Pond.

MINERALIZATION AND ALTERATION, SAGE POND-GRAND LE PIERRE AREA

Volcanic sequence

Extensive sericite alteration, commonly with 1 to 2 per cent disseminated and fracture-filling pyrite and local zones of up to 5 per cent pyrite, occur throughout the volcanic sequences in the area. Minor alteration with stockwork pyrite is a common feature marginal to the Ackley Granite and has been described from the molybdenite showings in the Rencontre area (Whalen, 1976); it probably resulted from late magmatic-hydrothermal processes associated with emplacement of the Ackley Granite. The pyritic alteration zones in the map area are in part related to the Ackley Granite. However, many of the pyritic zones may have a tectonic and/or synvolcanic origin. No base metal mineralization was observed; however, a potential exists for both gold mineralization and base metal mineralization within the volcanic sequence.

Peralkaline granite – Cross Hills Plutonic Complex

Throughout the peralkaline granite, zones of hematite and limonite stain occur with possible sericitic alteration and about 2 to 5 per cent pyrite, and are developed over an area

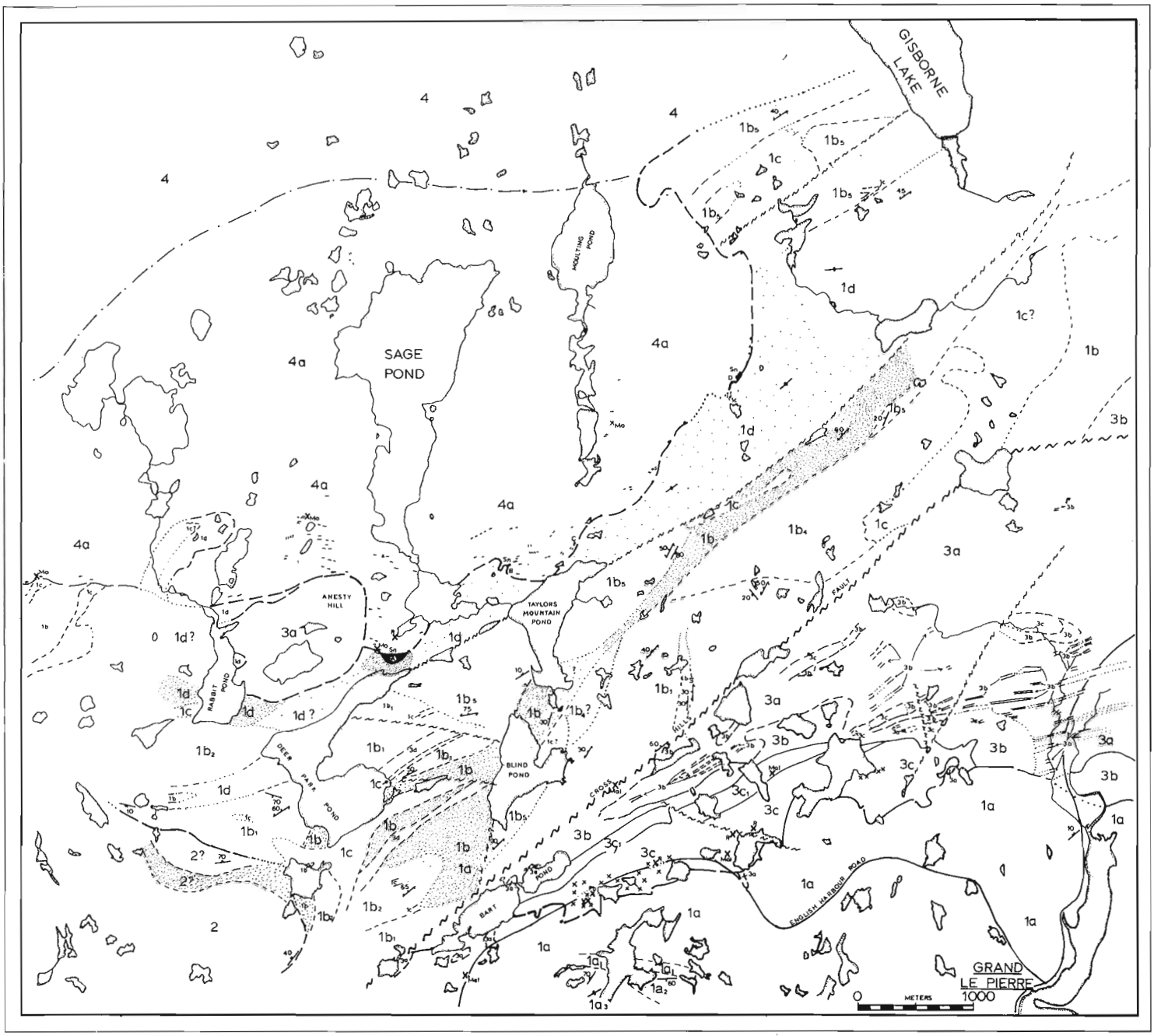

Figure 67.2. *Geology of the Grand Le Pierre-Sage Pond area, Fortune Bay, Newfoundland.*

of 1000 by 200 m along the English Harbour road. Local 'veins' of grey-green intense sericitic alteration have been noted over a strike length of 30 m and a width of 3 m. These veins contain 1 to 5 per cent disseminated and fracture-filling pyrite with trace amounts of galena. The alteration is related to late east-northeast fractures and breccia zones in the pluton.

A zone of anomalously radioactive patches from 2 to 5 times background, trending 070°, was noted in the granite over a strike length of 100 m southeast of Bart Pond. Individual anomalous patches are less than 2 by 0.5 m, and are related to hairline fractures near the granite roof. Several 2 m diameter areas of anomalous radioactivity up to 6 times background were noted elsewhere and are associated with hairline fractures or late aplitic veins in the peralkaline granite.

Traces of chalcocite with minor malachite stain were noted in two separate, late crosscutting quartz veins (maximum width 1 m) in the granitic phases of the Cross Hills Plutonic Complex.

A general metallogenic model would suggest marginal and roofward volatile and ore element concentration in a silicic magma chamber with potential mineralization (Nb, Zr, Sn, Th, F?) at or near the roof contact either as aplite or pegmatite sheets, or as veins in postconsolidation fracture zones. A possibility exists for economic mineralization in late crystallizing differentiates.

LEGEND (Figure 67.2)

PLUTONIC ROCKS

DEVONIAN - ACKLEY GRANITE

c — *Quartz-topaz and/or quartz-muscovite greisen. Less than 10 by 2 m except where lettered.*

4a *Fine to medium grained, orange quartz-feldspar-porphyritic granite.*

4 *Medium to coarse grained equigranular biotite granite.*

DEVONIAN - possibly PRECAMBRIAN - CROSS HILLS PLUTONIC COMPLEX

3d *V ery fine grained, red-brown aplite (?).*

3c *Fine to medium grained, miarolitic red-brown peralkaline granite;* $3c_1$, *orange to red-brown mottled aplite.*

3b *Fine to medium grained biotite (''alaskite?'') granite.*

3a *Diabase-gabbro multiple intrusions; can contain up to 30% veins and stockwork of 3b.*

VOLCANIC AND SEDIMENTARY ROCKS

HADRYNIAN - LONG HARBOUR GROUP

2 Mooring Cove Formation: *fine red-brown tuff and layered welded ash-flow units.*

1 Belle Bay Formation: *felsic pyroclastic and sedimentary rocks, felsic flows, and basalt flow.*

1d *Rheoignimbrite: massive welded and layered ash-flow tuff, breccia, and nonwelded massive tuff.*

1c *Foliated to massive vesicular basalt flow, agglomerate, and/or diabase.*

1b *Foliated felsic breccia, ignimbrite, tuff and flow, minor welded units and sediment:* $1b_1$, *purple breccia and minor welded breccia and massive flow;* $1b_2$, *gray, locally welded breccia;* $1b_3$, *bedded to laminated fine to coarse sediment;* $1b_4$, *dark green, fine to medium grained, massive waterlain tuff or sediment* $1b_5$ *5, laminated to bedded gray, fine silicic tuff, phyllite and sericite schist; minor coarse breccia.*

1a *Massive buff to green, nonwelded polylithic breccia, vesicular and/or feldspar porphyritic flow:* $1a_1$, *welded gray breccia with devitrification textures;* $1a_2$, *massive to bedded, medium to coarse, red and green sediment;* $1a_3$, *welded laminated ash-flow deposits.*

SYMBOLS

2% pyrite, sericite alteration, and gossanous

1-2% disseminated and stringer pyrite, may be gossanous

Hematite-limonite alteration

> 1000 g/t Sn assay; visible molybdenite and galena — X Sn, Mo, Pb

Malachite stain related to minor chalcocite and bornite — X Mal

Anomalous radioactivity, maximum 6 x background — X R

Bedding (tops known, unknown)

Flow layering (inclined, vertical)

Foliation (inclined, vertical)

Quartz-topaz veins in the Ackley Granite

The main concentration of white, medium- to coarse-grained quartz-topaz veins occurs between Rabbit Pond and Gisborne Lake at and near the south contact of a fine- to medium-grained porphyritic marginal phase of the Ackley Granite. Quartz-topaz veins have been noted as far west as Long Harbour and have been observed within the granite up to 3 km from the contact. They increase in concentration and size southward, with the largest quartz-topaz outcrops occuring at convex undulations of the granite contact. Veins are podiform-elongate with a predominant easterly trend (080° to 110°) and are generally less than 10 by 2 m. They form knobs of outcrop or suboutcrop in weathered granite till or in areas of weathered granite subcrop.

Subparallel quartz-topaz ± pyrite ± hematite ± fluorite vein swarms (fracture-fillings to 3 m wide veins) underlie massive quartz-topaz outcrop (50 by 6 m) at the Esso drill site southwest of Moulting Pond. Sericitization and bleaching (± pyrite) of the host orange-red granite quartz-feldspar porphyry is limited to within 1 m of individual veins and is generally narrower than vein width. Grey-green muscovite-quartz-topaz greisen commonly occurs marginal to massive quartz-topaz but can occur as individual veins. Fine fracture networks are common in the unaltered granite host and minor disseminated pyrite may be present in granite near the veins. Intense fracture networks with pyrite coatings are present in the volcanic rocks adjacent to the granite contact.

South of Anesty Hill, massive quartz-topaz rock (± pyrite ± fluorite with occasional grains of molybdenite) outcrops over an area of 200 by 60 m within a convex south lobe of the granite. Gently dipping layering (dipping 20 to 40 degrees south), defined by variation of topaz and quartz content and of grain size, suggests an area where fluorine-rich fluids were ponded near the granite roof. Rhyolite outcropping immediately south and west of the Anesty quartz-topaz body is strongly sericitized, suggesting that the greisen zone plunges to the south and west under the rhyolite.

A generalized model is envisaged in which fluorine ± tin-rich magmatic fluids evolved from a rapidly crystallizing marginal granite phase and rose along east-trending fractures in consolidated granite to collect in embayments at the granite margin and roof (see Dickson, 1983). A potential exists for large tonnage, low grade stockwork deposits in addition to high grade vein and massive greisen deposits.

Comparable mechanisms involving extreme differentiation, roofward migration of molybdenum-rich magmatic fluids, and collection of these fluids in pockets at the granite

roof, have been proposed for the origin of the molybdenite deposits in the Rencontre area (Whalen, 1976, 1980, 1983; Dickson, 1983).

Minor copper occurrences, Grand Le Pierre area

Minor malachite stain associated with chalcocite and/or bornite mineralization in fractures was noted (1) in sheared rhyolite breccia in the Cross Hills fault zone northeast of Bart Pond (Fig. 67.2); (2) in rhyolite breccia approximately 5 m west of the contact of the granodiorite phase of the Cross Hills Plutonic Complex on the Grand Le Pierre – Terrenceville road; and (3) in rhyolite on the west side of the English Harbour road at the southwest limit of the area mapped (Fig. 67.2).

OTHER OCCURRENCES OF ALTERATION AND MINERALIZATION, FORTUNE BAY AREA

i) Several beryl crystals up to 3 by 1 cm were noted in a 50 by 20 cm quartz pocket in the fine grained phase of the Ackley Granite to the southeast of Big Blue Hill Pond (UTM 343 967, 1M/14).

ii) Three molybdenite flakes (up to 1 cm) were noted in a roadside quartz vein on the east margin, and fluorite veinlets were observed near the western margin of the Berry Hill Stock on the Burin Peninsula.

iii) Silicified and/or sericitized zones (in fine grained Precambrian tuff and sediment) with 1 to 5 per cent disseminated and/or stringer pyrite were noted over a width of up to 70 m on the Monkstown road (east of the Burin Highway). Minor fine grained chalcopyrite may be locally present. Other pyrite occurrences are present on the Burin Highway. These may represent synvolcanic hydrothermal exhalative or subvolcanic epithermal processes, and a potential for base metal and/or gold mineralization is evident.

iv) Molybdenite occurrences reported at Hungry Cove Pond and at Spout Brook, and a Mo-Bi showing at Big Blue Hill Pond (Anderson, 1965) could not be located. A vertical quartz vein with maximum dimensions of 1.5 m by 5 cm containing minor pyrite and possible trace wolframite was observed at the Big Blue Hill Pond locality.

v) Swarms of narrow, subvertical quartz-muscovite "greisen?" veins were noted at two localities southeast of Big Blue Hill Pond (UTM 356 937 and 364 948; 1M/14). Veins observed have a maximum dimension of 30 cm by 10 m and trend 060° to 070°. A maximum vein density of 2 to 3 per metre is present.

ACKNOWLEDGMENTS

D.F.G. Taylor is thanked for field and mapping assistance during the past summer. L. Dickson, P. Dean, P. Davenport, D.F. Strong and S. O'Brien are thanked for discussion and encouragement.

REFERENCES

Anderson, F.D.
1965: Belleoram, Newfoundland; Geological Survey of Canada, Map 8-1965.

Bell, K., Blenkinsop, J., and Strong, D.F.
1977: The geochronology of some granitic bodies from eastern Newfoundland and its bearing on Appalachian evolution; Canadian Journal of Earth Sciences, v. 14, p. 456-476.

Bradley, D.A.
1962: Gisborne Lake and Terrenceville map areas, Newfoundland (1M/15 and 10); Geological Survey of Canada, Memoir 321.

Dallmeyer, R.D., Hussey, E.M., O'Brien, S.J., and O'Driscoll, C.F.
1983: Chronology of tectonothermal activity in the western Avalon Zone of the Newfoundland Appalachians; Canadian Journal of Earth Sciences, v. 20, p. 355-366.

Dickson, W.L.
1982: The southern contact of the Ackley Granite, southeast Newfoundland: location and mineralization; in Current Research; Newfoundland Department of Mines and Energy, Mineral Development Division, Report 82-1, p. 99-108.

1983: Geology, geochemistry and mineral potential of the Ackley Granite and parts of the North West Brook and Eastern Meelpaeg Complexes, southeast Newfoundland (parts of map areas 1M/10, 11, 14, 15, 16; 2D/1, 2, 3 and 7); Newfoundland Department of Mines and Energy, Mineral Development Division, Report 83-6, 129 pages.

Dickson, W.L. and Howse, A.F.
1982: Geochemistry of whole rock and stream sediment samples from two mineralized areas of the Ackley Granite: Rencontre Lake molybdenite and Anesty Hill molybdenite – cassiterite prospects; Newfoundland Department of Mines and Energy, Mineral Development Division, Open File Nfld. 1M (203).

Hopfengaertner, D.F.
1982: Assessment report: geology, geophysics, and geochemistry on License 1982. Claim Block 2455, Grand Le Pierre Area NTS 1M/10, Newfoundland. Confidential assessment report to the Department of Mines and Energy, Number 1M/10-205.

O'Brien, S.J. and Nunn, G.A.G.
1980: Terrenceville (1M/10) and Gisborne Lake (1M/15) map areas, Newfoundland; in Current Research, Newfoundland Department of Mines and Energy, Mineral Development Division, Report 80-1, p. 120-133.

O'Brien, S.J., Nunn, G.A.G., and Dickson, W.L.
1980a: Terrenceville (1M/10); Newfoundland Department of Mines and Energy, Mineral Development Division, Map 80-199.

1980b: Gisborne Lake (1M/15); Newfoundland Department of Mines and Energy, Mineral Development Division, Map 80-200.

Whalen, J.B.
1976: Geology and geochemistry of molybdenite showings of the Ackley Granite, Fortune Bay, Newfoundland; unpublished M.Sc. thesis, Memorial University of Newfoundland, St. John's.

1980: Geology and geochemistry of the molybdenite showings of the Ackley City Batholith, southeast Newfoundland; Canadian Journal of Earth Sciences, v. 17, p. 1246-1258.

1983: The Ackley City Batholith, southeastern Newfoundland: evidence for crystal versus liquid-state fractionation; Geochimica et Cosmochimica Acta, v. 47, p. 1443-1457.

Williams, H.
1971: Geology of Belleoram map area (1M/11), Newfoundland; Geological Survey of Canada, Paper 70-65.

Williams, H. and Hatcher, R.D., Jr.
1983: Appalachian suspect terranes; Geological Society of America, Memoir 158, p. 33-53.

68. PRELIMINARY CLASSIFICATION OF CARBONATE BRECCIAS, NEWFOUNDLAND ZINC MINES, DANIEL'S HARBOUR, NEWFOUNDLAND[1]

Contract EMR-MMD-82-0096

Thomas E. Lane[2]

Lane, T.E., Preliminary classification of carbonate breccias, Newfoundland Zinc Mines, Daniel's Harbour, Newfoundland; in Current Research, Part A, Geological Survey of Canada, Paper 84-1A, p. 505-512, 1984.

Also in Current Research, Newfoundland Department of Mines and Energy, Mineral Development Division, Report 84-1, 1984.

Abstract

Zinc ore at Newfoundland Zinc Mines is stratabound in dolomites within the upper third of the Lower Ordovician Catoche Formation (St. George Group) of the Humber Zone in western Newfoundland. Five types of breccias associated with zinc ore are distinguished in a preliminary classification.

Intraformational breccias, stratabound units of the Aguathuna Formation, represent disconformities or early diagenetic dissolution surfaces associated with the transition from subtidal to supratidal lithofacies. Fine rock matrix breccias associated with pre-Middle Ordovician structural depressions are divided into two types: oligomictic breccias, formed by stratabound dissolution and polymictic breccias, accumulated in vertical dilation openings along the margins of structural depressions. White spar breccias that host the zinc ore are characterized by open fracture and cavity systems filled with megacrystalline white dolomite. True spar breccias occur where strata are broken by faulting, veining, or dissolution. Elsewhere, pseudobreccia represents in situ replacement by white dolomite.

Résumé

Le minerai zincifère à l'exploitation de la Newfoundland Zinc Mines est limité à une seule couche de dolomies dans le tiers supérieur de la formation de Catoche de l'Ordovicien inférieur (groupe de St. George), dans la région de Humber située dans la partie ouest de Terre-Neuve. Cinq types de brèches associées au minerai zincifère sont identifiés dans une classification prliminaire.

Les brèches intraformationnelles sont des unités limitées à une seule couche de la formaiton d'Aguathuna; elles représentent des discordances ou des surfaces de dissolution diagénétique précoce associées à la progression d'un lithofaciès subtidal à un lithofaciès supratidal. Les brèches à matrice rocheuse fine, associées à des dépressions tectoniques formées avant l'Ordovicien moyen, se divisent en deux types: les brèches monogéniques, résultat du processus de dissolution se manifestant dans une seule couche, et les brèches polygéniques, accumulées dans des fissures produites par élargissement vertical en bordure des dépressions tectoniques. Les sont caractérisées par Des réseaux ouverts de fractures et de fissures que remplit de la dolomite blanche macrocristalline caractérisent les brèches à spath blanc contenant le minerai zincifère. Les brèches à spath pur se présentent là où les couches sont brisées par la formation de failles et de filons ou touchées par le processus de dissolution. Ailleurs, les pseudobrèches représentent le remplacement in situ par la dolomite blanche.

INTRODUCTION

Zinc deposits of Newfoundland Zinc Mines occur within dolostones of the upper St. George Group (Lower Ordovician) in western Newfoundland (Fig. 68.1). Several types of breccias are related to zinc ore both as gangue and associated rocks, but their nature and interrelationships are poorly understood. An understanding of the genesis of the breccias has direct implications for the origin of this and other Mississippi Valley Type deposits. A preliminary classification of breccias and their relationship to zinc ore is presented as a first step towards this understanding.

The present study is an extension of previous studies that have been carried out at the site. Collins (1971) and Collins and Smith (1975) recognized a variety of features that suggested ground preparation by karst processes. Dillon (1978) analyzed the rock geochemistry. Coron (1982) studied ore genesis from host rock petrography and isotope geochemistry, and developed models for ground preparation by evaporite dissolution, and generation of ore fluids along faults.

REGIONAL GEOLOGY

The Newfoundland Zinc Mines deposit is located within the Humber tectono-stratigraphic zone (Williams, 1979), which is interpreted to be the ancient coastline of North America on the western margin of the Cambro-Ordovician Iapetus Ocean (Fig. 68.1). A Lower Cambrian to Lower Ordovician succession of shallow water siliciclastic and carbonate rocks overlie Grenville basement. The zinc deposit is situated within autochthonous rocks which are partly covered by easterly derived thrust slices of deep water marine strata and ophiolites, which were emplaced during the Taconic (Middle Ordovician) Orogeny. Humber Zone rocks, including those of Newfoundland Zinc Mines, are relatively undeformed and unmetamorphosed. However, strata are displaced up to 1500 m by faults, trending north 20 to 60° east, and tilted into a series of west-dipping monoclines along these faults.

A stable shallow water marine platform existed in the Humber Zone from Early Cambrian to Early Ordovician (Knight, 1977; Levesque, 1977; Pratt, 1979; James and Stevens, 1982). During the late Precambrian-Early

[1] Contribution to Canada-Newfoundland co-operative mineral program 1982-84. Project carried by Geological Survey of Canada.

[2] Department of Earth Sciences, Memorial University of Newfoundland, St. John's, Newfoundland A1B 3X5

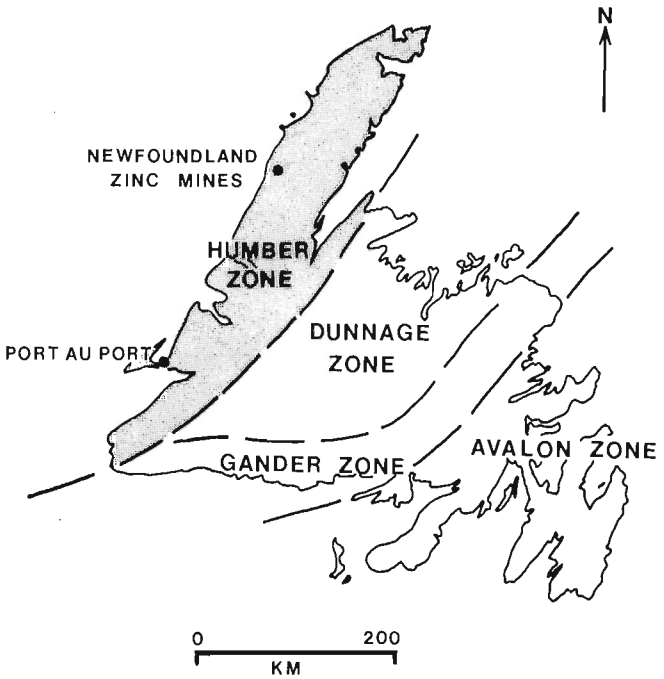

Figure 68.1. Tectono-stratigraphic zones of Newfoundland with the location of Newfoundland Zinc Mines (after Williams, 1979).

Cambrian, the North American continental margin became an area of sediment accumulation following post-rift downwarping. By Middle Cambrian, an extensive shallow water carbonate platform had been established. Middle to Upper Cambrian formations (March Point and Petit Jardin) comprise muddy and sandy carbonates, deposited on tidal flats and sand shoals (Levesque, 1977; Fig. 68.2). During the Early Ordovician, widespread subtidal conditions existed on the platform, resulting in abundant mudstone accumulation (James and Stevens, 1982).

The St. George Group is divided into four formations (Knight and James, personal communication, 1983): the Watt's Bight (80 m) which is overlain by the Boat Harbour Formation (120 m), the Catoche Formation (200 m), and finally the Aguathuna Formation (60 m; see Fig. 68.2). The Boat Harbour and Aguathuna formations are similar lithologically: cycles of intercalated subtidal limestone, mottled dolostone, and supratidal planar laminated, occasionally mudcracked, dolostone (Pratt, 1979). The intervening Catoche Formation consists of thick sections of dark grey, fossiliferous subtidal limestone. Mottled, peloidal mudstones, and wackestones of the upper third of the Catoche Formation mark upward shoaling into an intertidal regime. This upper third of the Catoche Formation is complexly dolomitized, characterized by abrupt diagenetic fronts, breccias, and megacrystalline (1 mm) white dolomite which hosts the zinc ore.

The transition from the Aguathuna Formation to the Middle Ordovician Table Head Group is marked by one or more disconformities. Stouge (1982) used conodonts to recognize a biostratigraphic break and possible lacuna 10 m above the base of the Aguathuna Formation. Another discontinuity with 16 m of erosional relief occurs between the Aguathuna and Table Point formations near Port au Port, Newfoundland (Fig. 68.1). At Newfoundland Zinc Mines, strata above this particular horizon fill paleotopographic depressions generated by solution collapse, faulting, or both (Fig. 68.3, 68.4). These disconformities relate with the Knox-Beekmantown unconformity of the central and southern Appalachians (Rodgers, 1971; Mussman, 1982).

During the Middle Ordovician (White Rock Stage) widespread subtidal conditions were re-established on the platform, recorded by the limestones of the Table Head Group (Klappa et al., 1980). Towards the termination of Table Head Group deposition, the platform rapidly deepened and ribbon limestones, shale, carbonate debris flows, and turbidites were deposited. These were covered by an easterly derived siliciclastic flysch and finally tectonic emplacement of the ophiolitic allochthons. Subsequently, the Grenville basement was uplifted and the cover rock was broken into a series of subparallel fault zones and monoclines.

From this regional overview it is apparent that several environmental conditions may have influenced the formation of the breccias: (1) shoaling on the carbonate platform during St. George deposition; (2) overlying disconformity with a local erosion surface and collapsed paleotopography (the St. George-Table Head break); (3) subsequent tectonic downwarping of the platform prior to allochthon emplacement and (4) faulting during uplift of the Grenville basement.

STRATIGRAPHY AND GEOMETRY OF THE ORE AND HOST ROCKS

Near Newfoundland Zinc Mines the sphalerite ore is stratigraphically and lithologically restricted to mega-crystalline (1 mm crystal size) dolostones of the upper third of the Catoche Formation. This part of the Catoche Formation has been complexly dolomitized, and only 25 per cent of the strata remains as unaltered limestone. The major dolostone types include (1) an assemblage of intercalated strata of megacrystalline (1 to 5 mm) white dolomite and fine crystalline (0.01 mm) grey dolomite and white dolomite veins, comprising 50 per cent of the upper Catoche Formation; (2) 20 per cent pervasive coarse crystalline (0.1 to 1 mm) vuggy grey dolomites; and (3) 5 per cent grey fine rock matrix breccias (matrix size = 0.01 mm, fragment size = 1 mm to 1 m). Fine rock matrix breccias are localized to structural depressions in upper St. George strata (Fig. 68.3). The other dolostones are developed outside the "breccia-depressions". The overlying upper 16 m of the Catoche Formation and the entire Aguathuna are pervasively dolomitized and contain only minor white dolomite. These dolostones are mostly microcrystalline (0.01 mm) and often finely planar laminated (dololaminites). The variety of dolostones of the upper St. George was described by Collins and Smith (1975), Coron (1982), and Haywick and James (1984).

Over one dozen ore bodies, averaging 8 per cent zinc, have been defined to date within the white dolostones. Individual ore lenses are long, narrow, and sinuous: 5 to 15 m (rarely up to 30 m) thick, 7 to 70 m wide by 500 to 4000 m long. The linearity is caused by ore controlling vein systems which in part border structural depressions oriented north 45 to 60° east and north (Fig. 68.3). Though the veins control the orientation of the ore, the majority of mineralization is developed in white dolomite strata peripheral to the veins.

Sphalerite stratigraphy has been employed with some success at other Mississippi Valley Type deposits (McLimans et al., 1980; Craig et al., 1983). At Newfoundland Zinc Mines, as many as four stages of sphalerite precipitation are recognized by colour changes in mineralization lining cavities. Relative ages of brecciation can be tested by presence or absence of these sphalerite stages.

CLASSIFICATION OF BRECCIA ROCK TYPES

Five breccia rock types are differentiated on the basis of macrotexture petrography, and geometry (Table 68.1);

1. Intraformational breccias.
2. Fine rock matrix breccias subdivided into, (2a) oligomictic and (2b) polymictic types.
3. White spar breccias subdivided into, (3a) true breccias and (3b) pseudobreccias.

The stratigraphic, compositional, and geometric relationships of those breccias are summarized in Table 68.1 and Figures 68.4 and 68.5.

Intraformational breccias

The intraformational breccias possess a fine rock matrix, but are distinguished by their stratigraphic characteristics. They are extensive horizons specifically related to primary lithofacies. Stouge's (1982) conodont data indicate that these breccias may overlie disconformities.

Lithology

Angular rotated clasts (1-5 cm in diameter) derived from local, overlying dololaminites are enveloped by a recrystallized sandy to gravelly mud matrix. Green and black clay residues form part of the matrix and are concentrated at the base of breccias. Mud-filled fractures and mosaics of slightly displaced fragments are present where breccias are poorly developed. Chert occurs as clasts within breccias and horizons of nodules in underlying strata.

Geometry

The breccias are tabular bodies, 30 to 50 cm thick, which can be correlated between drillholes for a distance of at least 10 km.

Stratigraphic association

The breccias occur in specific lithofacies successions in the Aguathuna Formation: they abruptly overlie burrow-mottled subtidal dolostones and underlie planar laminated supratidal dolostones (Fig. 68.5). Locally, both breccias and underlying dolostones are recrystallized. This sequence is repeated six times in the Aguathuna Formation.

Genesis

The intraformational breccias are interpreted as synsedimentary or early diagenetic. They mark abrupt breaks between subtidal and supratidal environments, which could be interpreted either as disconformities (e.g. Fischer's (1964) loferites) or postdepositional dissolution surfaces (e.g. Lucia (1972)).

Fine rock matrix breccias

In contrast to intraformational breccias, fine rock matrix breccias are found within and around the structural depressions, and fracture zones. Within these bodies of breccia two major types can be distinguished based on petrography and geometry; oligomictic and polymictic types.

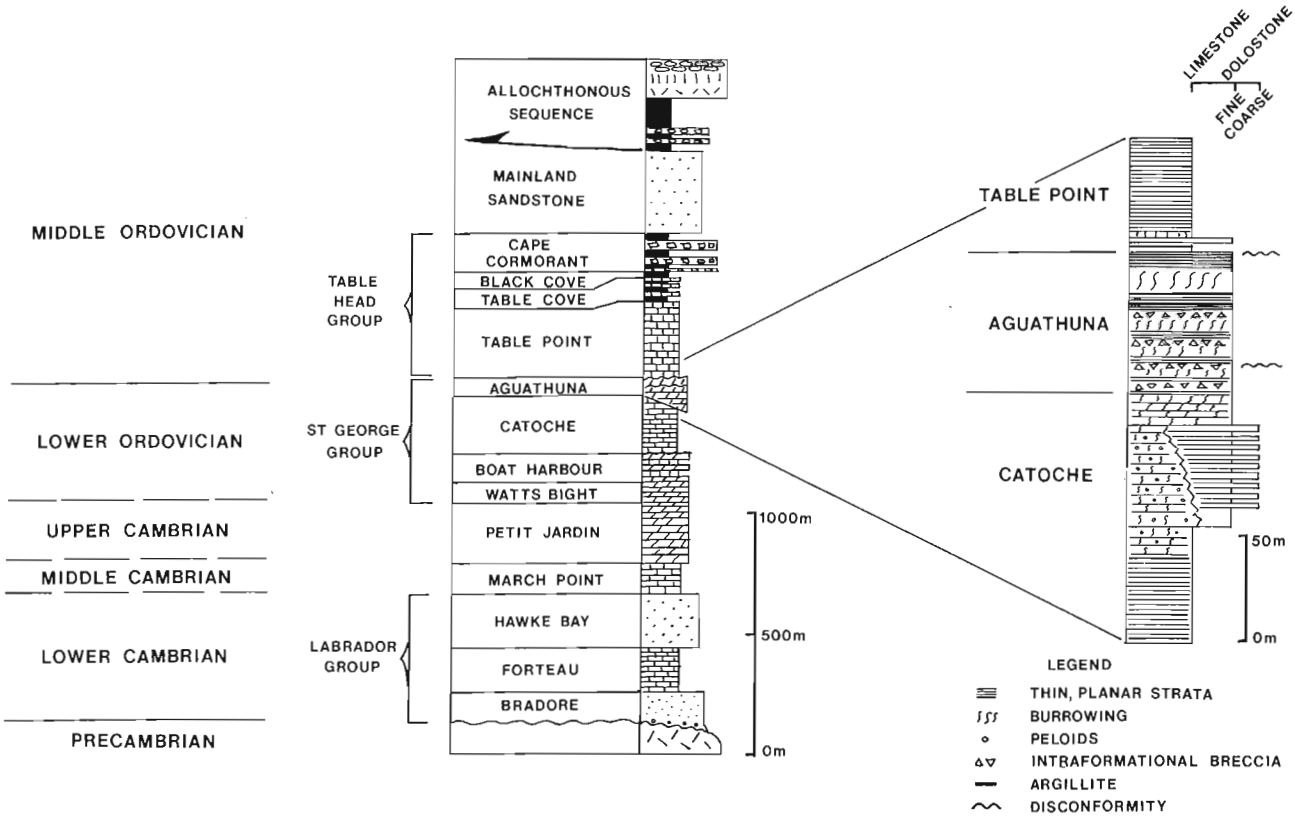

Figure 68.2. Stratigraphy from Newfoundland Zinc Mines set in the Stratigraphy of the Humber Zone Autochthon (adapted from James and Stevens, 1982).

Table 68.1. Summary of stratigraphic, compositional, and geometrical relationships observed within the five breccia rock types at Newfoundland Zinc Mines

Type of breccia		Stratigraphic position	Composition	Geometry
Intraformational		Aguathuna Formation	Local angular dolostone clasts, chert clasts, nodules, sandy mud matrix, clay residues, clast and matrix support	Laterally extensive, stratabound
Fine rock matrix	Oligomictic	Upper Catoche Formation	Local clasts (1-3 cm diameter), subrounded clasts, sandy mud matrix, matrix support; recrystallized clasts and matrix	Laterally continuous in 30 to 3000 m; localized around structural depressions and fracture zones
	Polymictic	Aguathuna and Upper Catoche formations	3 to 4 mixed lithologies of clasts (1 cm to 1 m diameter), gravelly-sandy mud matrix, matrix support, clasts fractured, not recrystallized	Vertically crosscuts pre-existing dolostone; limited lateral extent; common around breccia margins
White spar breccias	True breccias	Upper Catoche Formation	Large angular clasts (up to 1 m diameter) include pseudobreccia, megacrystalline white dolomite matrix	Veins and bodies crosscutting strata; vertical fracture system
	Pseudobreccias	Upper Catoche Formation	Megacrystalline white dolomite replacing 5% to 80% of mottled grey dolomite; partial cavity in filling; minor breccia	Selectively replacing horizontal strata over 1000s of metres

Oligomictic breccias

Lithology

Small fragments (0.1-1 cm diameter) consist of one lithology, mottled dolostone, derived from the same stratigraphic level. These subrounded to subangular clasts are recrystallized to 0.1 mm dolomite. The rock is only partially matrix supported with clasts often bounded and separated by black residue-rich stylolites. The matrix is fine crystalline (0.01 mm), fairly homogeneous and rich in black residues (Fig. 68.5). The residues were identified by Collins (1971) as iron oxides.

Geometry

The breccias are stratigraphically controlled, may be correlated within and slightly beyond the boundaries of the structural depressions, and are laterally continuous up to 200 x 1000 m (Fig. 68.3). In addition, small, 10 m wide, oligomictic breccia bodies occur in association with fracture zones.

Stratigraphic association

The oligomictic types are restricted to the upper Catoche Formation, constituting 60 to 90 per cent of the section. Overlying strata are intact and characterized by common veins healed by grey and white dolostone.

Genesis

The upper Catoche Formation underwent local dissolution and dolomitization during the formation of the structural depressions, prior to the time of deposition of Table Head Group and the later zinc ore emplacement. Dissolution produced the breccias and collapse of strata, causing the veins in overlying strata; and, in part, the major structural depressions. The porous breccias provided permeability for dolomitizing fluids, which produced the pervasive recrystallization.

Polymictic breccias

Lithology

Clasts of three or four lithologies are intermixed, the most distinctive of which are light grey laminated clasts diagnostic of the Aguathuna Formation. The breccias are characterized by a wide range of clast sizes (1 m to 1 cm). The angular, commonly fractured clasts float in 40 to 70 per cent poorly sorted matrix; comprising 1 to 5 mm clasts and 0.1 mm euhedral dolomite crystals enveloped in black residues (Fig. 68.5).

Geometry

These rock bodies crosscut the stratigraphy. One was observed to be 10 m wide with vertical boundaries. Other information indicates irregular widening at specific stratigraphic levels.

Stratigraphic association

The breccias tend to be localized around the margins of the structural depressions and cut across the stratigraphy from the Aguathuna Formation through the upper 60 m of the Catoche Formation. Clasts of the Aguathuna Formation have been displaced up to 60 m below their original stratigraphic position.

Genesis

The origin of polymictic breccias is directly related to structural events at the margin of depressions. Dilation at the rims caused by collapse or downfaulting created sufficient space for rock debris to fall as much as 60 m. The size of openings may have been enlarged by dissolution, forming significant cavities that were subsequently filled with breccia.

White spar breccias

Megacrystalline white dolomite is extensively developed in the mine vicinity; however, it is excluded from areas containing matrix breccias. The white dolomite is considered to be younger than the fine rock matrix breccia, which it locally replaces. Much of the white dolomite was precipitated contemporaneously with the sphalerite.

In this classification, the distinction is made between true spar breccias and pseudobreccias. A true spar breccia contains displaced and rotated grey dolomite fragments surrounded by a matrix of megacrystalline white dolomite. The grey dolomite patches of pseudobreccia often appear to be surrounded by megacrystalline white dolomite; however, they are in situ and interconnected in three dimensions (Fig. 68.5). The white dolomite of pseudobreccia is either open space fill or a recrystallization fabric. Since true breccias and pseudobreccias are overprinted in places, the distinction is not everywhere clear.

True breccias

Lithology

Angular fragments of grey dolomite and pseudobreccia, up to one metre in diameter, are supported by a matrix of megacrystalline white dolomite. These fragments have often only slightly rotated from their original position. A few spar breccias were originally fine rock matrix breccia. In these cases, white spar has selectively replaced grey dolomite matrix.

Geometry

Three types of spar breccia are delineated: (1) veins in grey dolomite strata between pseudobreccia; (2) local breccias within pseudobreccia beds; and (3) linear bodies which crosscut the stratigraphy (10–30 m wide and a 100 or more metres long). Linear breccias are usually a collection of subvertical veins.

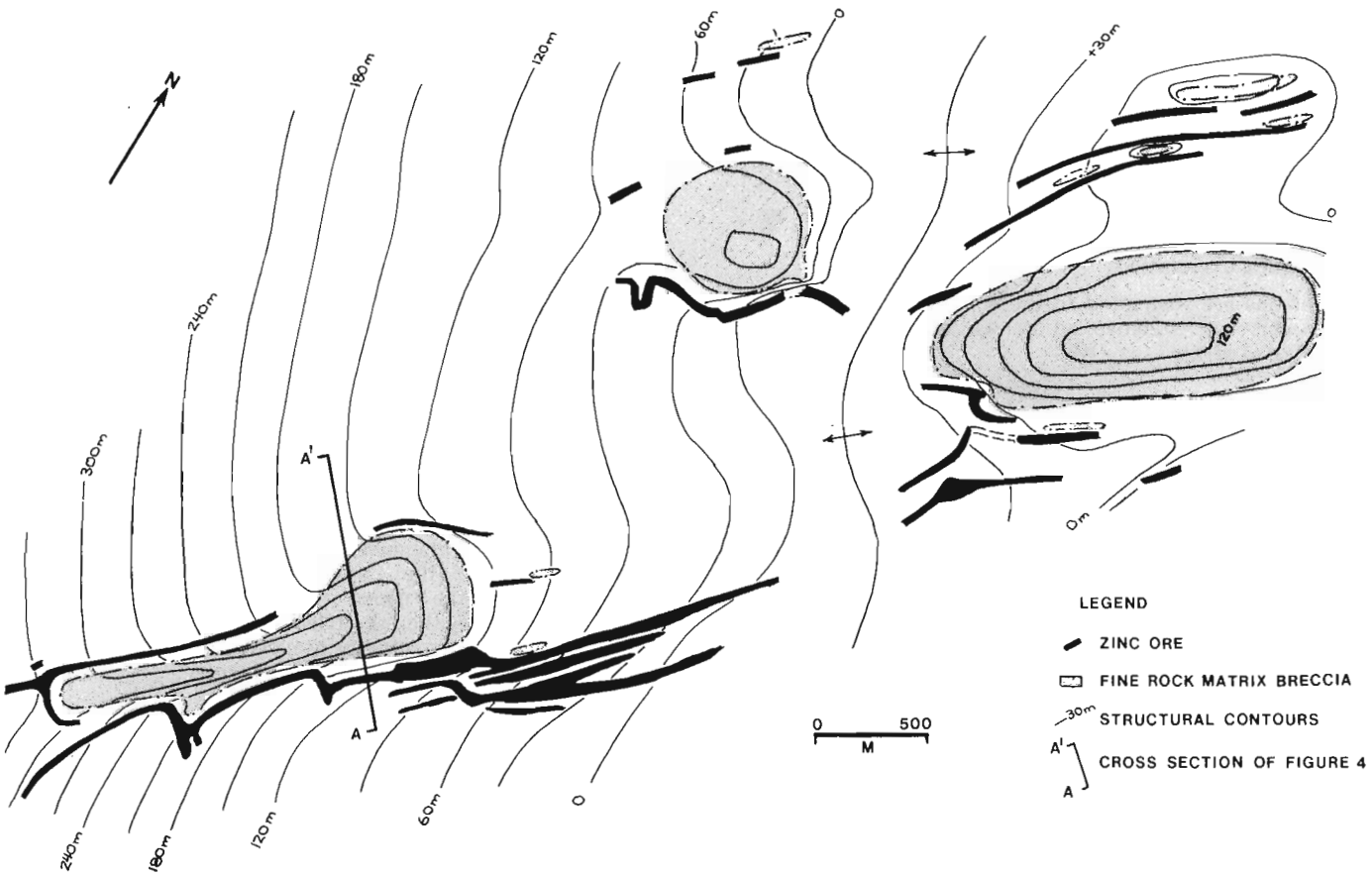

Figure 68.3. *Newfoundland Zinc Mines. A plan view of the upper Catoche Formation, showing the location of zinc orebodies relative to structural depressions and the distribution of fine rock matrix breccias. Structural contours record the depth of an upper Catoche stratum below a datum plane 100 m above sea level (contour interval = 30 m).*

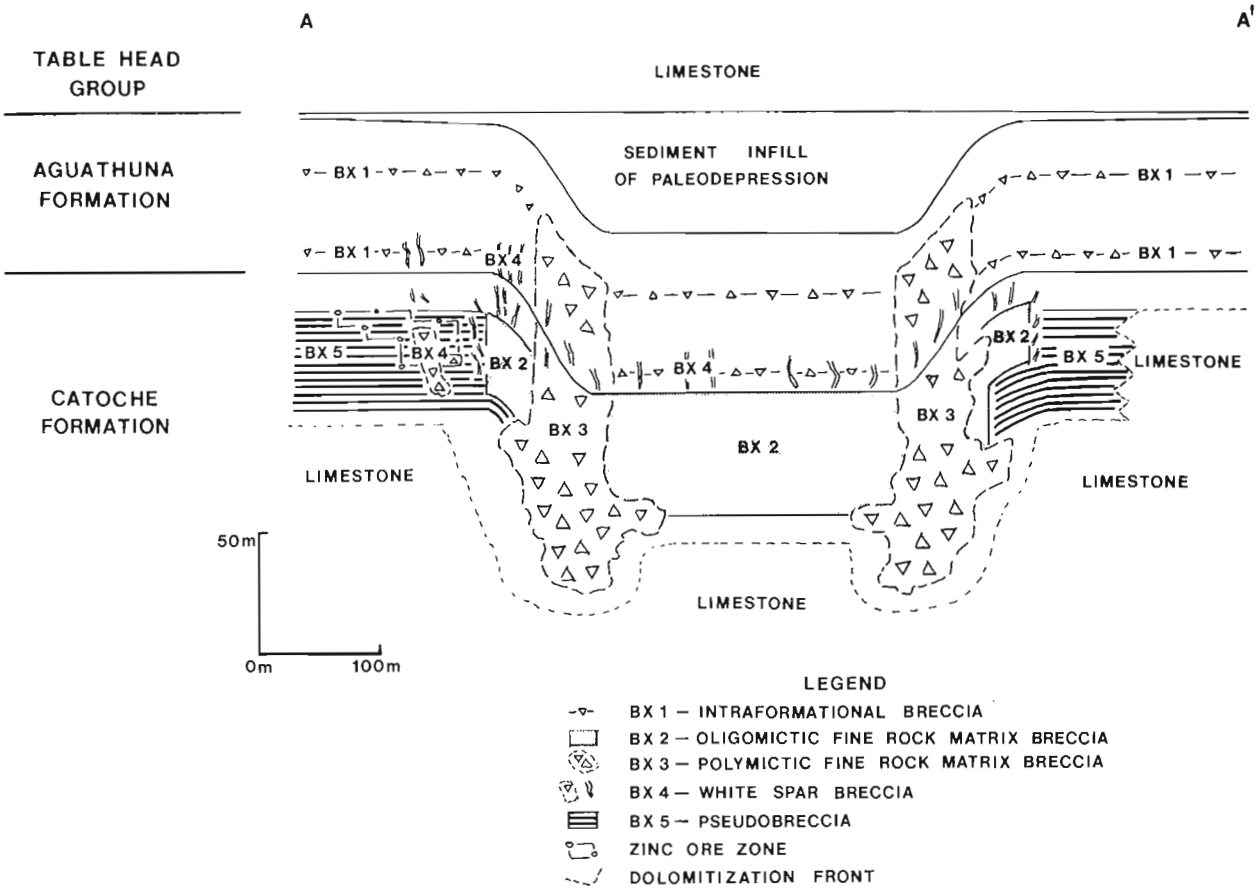

Figure 68.4. Distribution of the five breccia types across an ore zone and a structural depression. Location of the cross-section is indicated on Figure 68.3.

Stratigraphic association

The breccias are restricted to the upper Catoche Formation. Their occurrence is controlled by vein density, faulting, and subsidence of strata.

Genesis

Spar breccias were formed where strata were ruptured by faulting and/or dissolution. Large fragments of these strata were slightly displaced and rotated. Some of these breccias were cogenetic with pseudobreccias; however, the sizeable linear bodies are late structures, associated with vertical movements, after most pseudobreccia development. Only the late stages of ore are found in these dolomites.

Pseudobreccia

Lithology

Megacrystalline white dolomite constitutes 5 to 80 per cent of strata 0.3 to 1.0 m thick. The remainder of the rock consists of dispersed irregular patches of medium crystalline grey dolomite with an internal relict mottled fabric. Intercrystal and vug porosity is abundant. White and grey dolomite alternate in a horizontal, variably developed, "banded" fabric (Fig. 68.5). Breccia fragments of grey dolomite occur locally in veins and cavity fills.

Geometry

Pseudobreccia strata and intercalated grey dolostones are selectively developed according to textural variation in the original limestone resulting in the ability to correlate specific strata over distances greater than 15 km. The highest percentages of white dolomite are concentrated around vein systems; but pseudobreccia development in strata is laterally pervasive over thousands of metres.

Stratigraphic association

Pseudobreccia development is limited to strata 16 to 50 m below the top of the Catoche Formation. The position coincides with the upper limit of limestones and the occurrence of cyclic, mottled, peloidal mudstones and wackestones. In this interval pseudobreccia is excluded from areas of the older fine rock matrix breccia.

Genesis

Pseudobreccia formed by diffusion of dolomitizing fluids into peloidal limestone strata to a depth of 50 m below the top of the Catoche Formation. Linear vein systems were the loci of fluid movement, the area of best spar development, and ore conduits. White dolomite crystallized by selective replacement around early dolomites (Haywick and James, 1984) and filling of vugs and cavities. Sphalerite mineralization occurred prior to and contemporaneous with white dolomite formation.

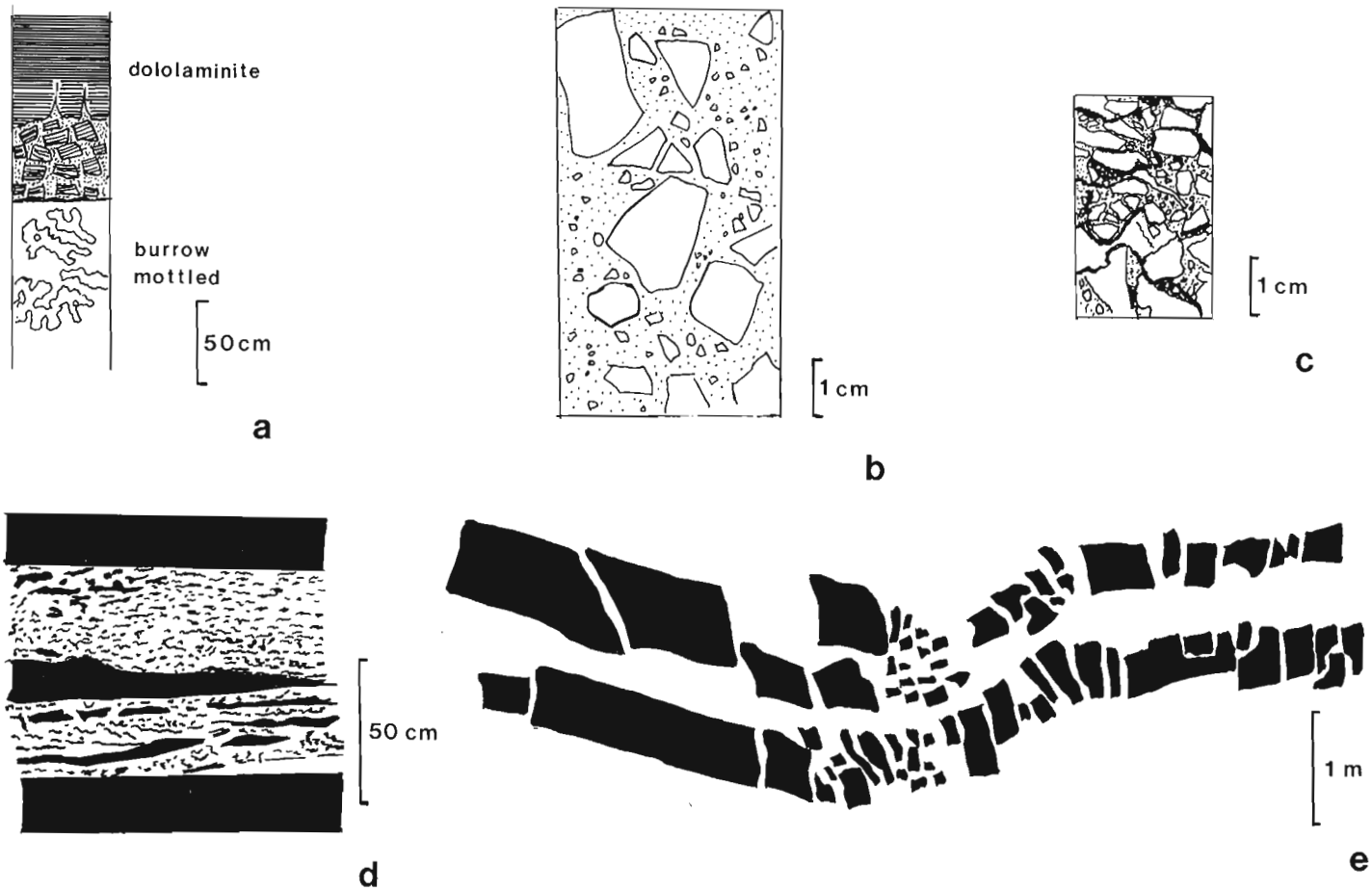

a. *Intraformational breccias relative to dololaminite and burrow mottled lithofacies. Clay residues at the base of the breccia.*

b. *Polymictic fine matrix breccia, with fragments "floating" in matrix.*

c. *Oligomictic fine rock matrix breccia with fragments compacted and black residue in matrix and between clasts.*

d. *Pseudobreccia with horizontal fabric, between grey dolomite strata.*

e. *Grey dolomite strata broken by subsidence and faulting to form a true spar breccia.*

Figure 68.5. *Aspects of breccia macrotextures.*

CONCLUSIONS

Five breccia types occur in association with zinc deposits at Newfoundland Zinc Mines. Differentiation of brecciation styles is essential to the understanding of the permeability, porosity evolution, and subsequent ore deposition. Subaerial exposure of the carbonate platform is suggested by intraformational breccias. Fine rock matrix breccias formed by dissolution and collapse beneath the exposed platform. Early structural dilation along the margins of large depressions (200 x 1000 m) formed the polymictic breccias. Subsequent deformation produced open space fracture systems which were infilled by sphalerite and megacrystalline white dolomite. Peloidal limestone strata was altered to pseudobreccia outward from vein systems. Most ore was precipitated in pseudobreccia strata adjacent to veins. Linear spar breccias formed from vertical tectonic movements during the latest stages of mineralization.

ACKNOWLEDGMENTS

The laboratory phase of this study is funded by EMR-MMD-82-0096 contract to the Geological Survey of Canada. Logistical and financial support for field study has been provided by Newfoundland Zinc Mines. The study is being carried out at Memorial University of Newfoundland. Geologists associated with the mine and Teck Explorations Limited, R.V. Crossley, M. Blecha, J.G. O'Connell, and D. Tiong shared their extensive knowledge with the author. T. Payne served as a valuable field assistant. Stimulating field visits were paid by D.F. Sangster, N.P. James, D.F. Strong, P.W. Choquette, J. Briskey, H. Wedow, M. Coniglio, D. Haywick, and J. Maloney. The manuscript was improved by M. Coniglio, D.F. Strong, N.P. James, and D. Haywick.

REFERENCES

Collins, J.A.
1971: Carbonate lithofacies and diagenesis related to sphalerite mineralization; unpublished M.Sc. thesis, Queen's University, 184 p.

Collins, J.A. and Smith, L.
1975: Zinc deposits related to diagenesis and intrakarstic sedimentation in the Lower Ordovician St. George Formation, Western Newfoundland; Bulletin of Canadian Petroleum Geology, v. 23, p. 393-427.

Coron, C.R.
1982: Facies relations and ore genesis of the Newfoundland Zinc Mines Deposit, Daniel's Harbour, western Newfoundland; unpublished Ph.D. thesis, University of Toronto, 164 p.

Craig, J.R., Solberg, T.N., and Vaughan, D.J.
1983: Growth characteristics of sphalerites in Appalachian zinc deposits; in Proceedings Volume of the International Conference on Mississippi Valley Type Lead-Zinc Deposits, ed. G. Kisvarsanyi, S.K. Grant, W.P. Pratt and J.W. Koenig; University of Missouri – Rolla, p. 317-327.

Dillon, E.P.
1978: Multi-element geochemical study of the pseudobreccia host rock of the Newfoundland Zinc Mine; unpublished M.Sc. thesis, University of Toronto, 31 p.

Fischer, A.G.
1964: The Lofer cyclothems of the Alpine Triassic; in Symposium on Cyclic Sedimentation, ed. D.F. Merriam; Kansas Geological Survey, Bulletin 169, p. 107-149.

Haywick, D.W. and James, N.P.
1984: Dolomites and dolomitization of the St. George Group (Lower Ordovician) of western Newfoundland; in Current Research, Part A, Geological Survey of Canada, Paper 84-1, report 71.

James, N.P. and Stevens, R.K.
1982: Anatomy and evolution of a Lower Paleozoic continental margin, Western Newfoundland; Eleventh International Congress on Sedimentology, Field Excursion Guidebook 2B, 75 p.

Klappa, C.F., Opalinski, P.R., and James, N.P.
1980: Middle Ordovician Table Head Group of western Newfoundland: a revised stratigraphy; Canadian Journal of Earth Sciences, v. 17, p. 1007-1019.

Knight, I.
1977: Cambro-Ordovician platformal rocks of the Northern Peninsula, Newfoundland; Newfoundland Department of Mines and Energy, Report 77-6, 27 p.

Levesque, R.J.
1977: Stratigraphy and sedimentology of Middle Cambrian to Lower Ordovician shallow water carbonate rocks, western Newfoundland; unpublished M.Sc. thesis, Memorial University of Newfoundland, 276 p.

Lucia, F.J.
1972: Recognition of evaporite – carbonate shoreline sedimentation; in Recognition of Ancient Sedimentary Environments, ed. J.K. Rigby and W.K. Hamblin; Society of Economic Paleontologists and Mineralogists, Special Publication No. 16, p. 160-191.

McLimans, R.K., Barnes, H.L., and Ohmoto, H.
1980: Sphalerite stratigraphy of the Upper Mississippi Valley Zinc-Lead District, Southwest Wisconsin; Economic Geology, v. 75, p. 351-361.

Mussman, W.J.
1982: The Middle Ordovician Knox unconformity, Virginia Appalachians: transition from passive to convergent margin; unpublished M.Sc. thesis, Virginia Polytechnic Institute and State University, 121 p.

Pratt, B.
1979: The St. George Group (Lower Ordovician), Western Newfoundland: sedimentology, diagenesis, and cryptalgal structures; unpublished M.Sc. thesis, Memorial University of Newfoundland, 231 p.

Rodgers, J.
1971: The Taconic Orogeny; Geological Society of America, Bulletin, v. 82, p. 1141-1178.

Stouge, S.
1982: Preliminary conodont biostratigraphy and correlation of Lower to Middle Ordovician carbonates of the St. George Group, Great Northern Peninsula, Newfoundland; Newfoundland Department of Mines and Energy, Report 82-3, 59 p.

Williams, H.
1979: Appalachian Orogen in Canada; Canadian Journal of Earth Sciences, v. 16, p. 792-807.

69. GEOLOGICAL SETTING AND VOLCANOGENIC SULPHIDE MINERALIZATION OF THE EASTERN WILD BIGHT GROUP, NORTH-CENTRAL NEWFOUNDLAND[1]

Project 830035
Contract 13SR.23233-3-0325

H. Scott Swinden[2]

Swinden, H.S., Geological setting and volcanogenic sulphide mineralization of the eastern Wild Bight Group, north-central Newfoundland; in Current Research, Part A, Geological Survey of Canada, Paper 84-1A, p. 513-519, 1984.

Also in Current Research, Newfoundland Department of Mines and Energy, Mineral Development Division, Report 84-1, 1984.

Abstract

The Wild Bight Group in north-central Newfoundland is a thick sequence of volcaniclastic, volcanic and related intrusive rocks deposited during the development of an Early-Middle Ordovician island arc. Volcanic flows, which comprise up to 20 per cent of the sequence, are dominantly basaltic and occur at several stratigraphic levels. Rhyolitic flows and pyroclastics are locally developed in the central part of the succession. Volcaniclastic rocks consist of fine grained sandstone, siltstone and chert interbedded with thick volcaniclastic conglomerate units. Sedimentary structures suggest a northerly flow. The environment appears to have been one of quiet sedimentation on the flanks of a volcanic edifice to the south, punctuated by periodic debris flows and local eruptive activity.

Four volcanogenic sulphide deposits are recognized in the Wild Bight Group. The largest of these, the Point Leamington deposit, comprises a massive sulphide body underlain by a zone of pervasive quartz-sericite and chlorite alteration. The Lockport deposit outcrops as a stockwork zone but there is evidence that a small massive cap is present in the subsurface. The Indian Cove and Long Pond prospects are pyrite-chalcopyrite-bearing stockwork zones. All are spatially and stratigraphically associated with felsic volcanism.

Résumé

Le groupe de Wild Bight dans la partie nord-centrale de Terre-Neuve est une épaisse séquence de roches volcaniques et clastiques, de roches volcaniques et de roches intrusives apparentés dont la mise en place date de la période de l'évolution d'un arc insulaire au cours de l'Ordovicien ancien à moyen. Des coulées de lave, surtout de nature basaltique, forment jusqu'à 20 % de la séquence et se manifestent à plusieurs niveaux stratigraphiques. Des coulées rhyolitiques et des débris pyroclastiques se présentent par endroits dans la partie centrale de la séquence. Les roches volcaniques et clastiques se composent de grès fin, de pélite et de chert interstratifiés avec d'épaisses unités de conglomérat volcanique et clastique. Les structures sédimentaires laissent supposer que l'écoulement se dirigeait vers le nord. Le milieu semble avoir subi une phase de sédimentation calme sur les flancs d'une structure volcanique au sud, interrompue périodiquement par des coulées de débris et des éruptions locales.

Quatre gisements de sulfures volcanogéniques sont identifiés dans le groupe de Wild Bight. Le plus gros, soit le gisement de Point Leamington, se compose d'une masse de sulfure massif sus-jacente à une zone de quartzification-séricitisation et de chloritisation pénétrantes. Le gisement de Lockport affleure sous forme d'un stockwerk, mais il appert qu'un petit chapeau massif reposerait vraisemblablement sous la surface. Les venues d'Indian Cove et de Long Pond s'avèrent des régions de stockwerks à pyrite et à chalcopyrite. Toutes ces venues sont associées, des points de vue spatial et stratigaphique, au volcanisme felsique.

INTRODUCTION

The Wild Bight Group comprises a thick sequence of volcanic and sedimentary rocks which outcrop across Notre Dame Bay between Shoal Arm, Badger Bay and Osmonton Arm, New Bay (Fig. 69.1). The sequence is overlain by Caradocian chert and shale and is considered by most workers (e.g. Dean, 1978) to form part of an Early-Middle Ordovician island arc, remnants of which are widely preserved throughout central and southern Newfoundland (Kean et al., 1981; Swinden and Thorpe, in press).

The general distribution of lithologies and their stratigraphic sequence within the Wild Bight Group was first investigated in detail in the 1930s. Heyl (1938) mapped the sequences immediately adjacent to New Bay as part of his comprehensive examination of the stratigraphy of the Bay of Exploits area, and Espenshade (1937) included part of what is now considered to be the western side of the Wild Bight Group in his study of the Pilleys Island area. Each worker erected a local stratigraphic nomenclature in his area, and Espenshade appears to have been the first to coin the term "Wild Bight volcanics" for the sequences exposed in Wild Bight, Badger Bay. Hayes (1951) later mapped part of the western Wild Bight Group outcrop, assigning these rocks to the "Exploits Series" but retaining the term "Wild Bight Formation" for the sequences in Wild Bight.

The "Wild Bight Group" in its present form was first defined by Williams (1963) during his 1:250 000 mapping of the Botwood (2E) map area.

The most detailed published maps of the Wild Bight Group are those compiled by Dean (1978) at a scale of 1:50 000. Wild Bight Group data on these maps was drawn principally from the workers cited above and from unpublished exploration company maps. Dean's (1978) contribution to the geology of the Wild Bight Group was twofold. Firstly, and perhaps most importantly, he provided the first detailed published account of the distribution of

[1] Contribution to the Canada-Newfoundland co-operative mineral program 1982-84. Project carried by the Geological Survey of Canada.
[2] c/o Newfoundland Department of Mines and Energy, Mineral Development Division, P.O. Box 4750, St. John's, Newfoundland A1C 5T7

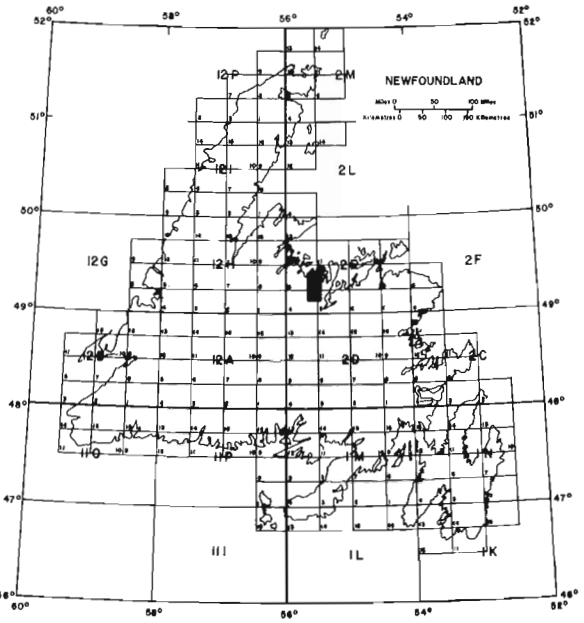

Figure 69.1. Location of the study area. Black square is the area shown in Figure 69.2.

lithologies, particularly volcanic rocks, within the central part of the Wild Bight Group. Secondly, he subdivided the sequence into five informal formations, providing a stratigraphic framework within which the distribution of the various volcanic sequences could be interpreted.

Volcanogenic sulphide mineralization in rocks presently assigned to the Wild Bight Group was first discovered in the late 1800s near Lockport. The deposit there was worked briefly around the turn of the century, yielding the only recorded production from the Wild Bight Group. Since that time, three other deposits of volcanogenic origin have been recognized in the sequence, the Indian Cove and Long Pond Prospects and the Point Leamington deposit (Fig. 69.2).

The present study was designed to investigate the regional geologic and tectonic setting of the Wild Bight Group, with emphasis on the volcanic rocks which occur principally in the eastern part of the group, and the four volcanogenic sulphide deposits which they host.

GEOLOGIC SETTING OF THE EASTERN PART OF THE WILD BIGHT GROUP

Dean (1978) showed that the Wild Bight Group occupies a broad anticlinal structure the axis of which trends approximately north-south through the centre of Seal Bay (the Seal Bay anticline, Fig. 69.2). The base of the sequence is not exposed in this area; the stratigraphic succession becomes younger more or less continuously to the east and west (although crossing numerous minor folds) and eventually passes conformably upward into fossiliferous Caradocian shale and chert of the overlying Shoal Arm Formation. Two virtually complete cross-sections of Wild Bight Group stratigraphy are exposed on the coastline between Shoal Arm and the Leading Tickles peninsula on both sides of the Seal Bay anticline, and well washed exposures display the essential features and critical relationships of the sequence. The author feels that systematic mapping of this area will ultimately result in considerable revision of Dean's (1978) informal stratigraphic nomenclature. Accordingly, this nomenclature will be used sparingly in the following discussions.

In general terms, three rock types are present in the eastern Wild Bight Group: (1) volcaniclastic and sedimentary rocks, (2) volcanic rocks, and (3) mafic intrusive rocks. These are briefly described below; because of the economic significance of the volcanic rocks, they are treated in more detail.

1. Volcaniclastic and sedimentary rocks

Volcaniclastic and sedimentary rocks comprise as much as 80 per cent of the Wild Bight Group succession. In the eastern Wild Bight Group, these are principally of two types: (i) fine grained, planar bedded, laminated greywacke, siltstone, argillite and chert with local conglomerate beds; and (ii) massive, generally unbedded, medium- to coarse-grained volcaniclastic conglomerate. The latter is generally matrix-supported, often poorly sorted, and contains subrounded to angular fragments of locally derived volcanic and sedimentary rocks.

Some general comments can be made concerning the stratigraphic development of sedimentary rocks in the eastern Wild Bight Group. The oldest unit, exposed in the core of the Seal Bay anticline, consists of up to 500 m of fine grained argillite, siltstone and chert with minor amounts of pebble sandstone and rare fine grained conglomerate. This stratigraphic unit, referred to as the Omega Point formation by Dean (1978), is characterized by abundant green to buff chert and particularly by red chert and argillite. It contains a single 6 m thick, black shale horizon exposed on a small island in Seal Bay bottom, and appears to record the most extensive interval of quiet water sedimentation in the Wild Bight Group. Along the eastern shore of Seal Bay, this unit passes upward into a volcaniclastic succession containing increasing amounts of coarse volcaniclastic sandstone and conglomerate horizons. Immediately north of Sparrow Cove Point, these lithologies typically form 0.3 to 5 m beds separated by a similar thickness of fine grained, laminated chert and siltstone. The thickness and abundance of the coarse units increase northward along the east side of Seal Bay (i.e. upsection); in the area north of Locks Harbour individual layers of coarse volcaniclastic conglomerate commonly attain thicknesses greater than 60 m, separated by 1 to 10 m layers of fine grained siltstone and chert. These coarse sediments form a major part of the sequence up to its exposed top on the Leading Tickles peninsula. A similar progression from fine grained, apparently quiet water sedimentation through environments of progressively more coarse deposition by debris flows and turbidite currents is also recorded by sequences on the west side of the Seal Bay anticline, although local structural complications and probable facies changes make detailed correlation difficult.

The environment recorded by the Wild Bight Group succession appears to have changed from initial quiet water sedimentation to quiet sedimentation punctuated by periodic turbidity currents and debris flows. Current ripples, cross-beds and slump structures indicate a generally northerly flow, suggesting a topographic high to the south. The sediments were therefore probably deposited on the middle flanks of a volcanic edifice situated to the south.

2. Volcanic rocks

Volcanic accumulations are present at several localities and various stratigraphic levels within the eastern Wild Bight Group (Fig. 69.2). All volcanogenic sulphide deposits in the Wild Bight Group are hosted by volcanic rocks, although not all volcanic accumulations are known to be mineralized. Each major volcanic sequence is described briefly below; names for these sequences are for convenience only and do not represent formally proposed stratigraphic nomenclature.

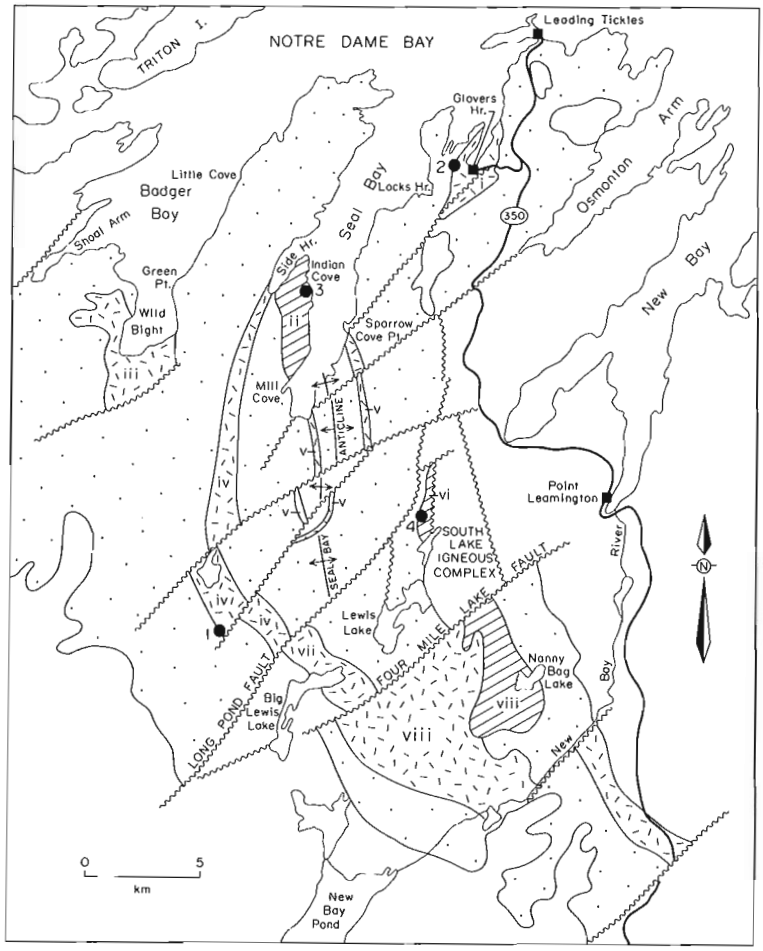

LEGEND

Mainly volcaniclastic and sedimentary rocks.

Mainly mafic volcanic rocks.

Mainly felsic volcanic rocks.

Key to Volcanic Sequences
(see text; most designated names are informal)

i *Glovers Harbour volcanics.*
ii *Indian Cove volcanics.*
iii *Wild Bight, Badger Bay volcanics.*
iv *Side Harbour formation north of Long Pond Fault*
v *Sparrow Cove Point formation.*
vi *Long Pond volcanics.*
vii *Big Lewis Lake basalts.*
viiii *Nanny Bag Lake volcanics.*

Key to Volcanogenic Sulphide Deposits

1 *Point Leamington*
2 *Lockport*
3 *Indian Cove*
4 *Long Pond*

Figure 69.2. *Simplified distribution of lithologies in the eastern Wild Bight Group. Location of volcanogenic sulphide occurrences is indicated by solid circles.*

Descriptions

i) Glovers Harbour volcanics: The Glovers Harbour volcanics, host to the Lockport deposit, were included in the Pennys Brook Formation by Dean (1978). They consist predominantly of pillow basalts which comprise 60 to 70 per cent of the section. The pillows are generally 0.7 to 1.5 m long, bulbous to somewhat flattened and highly vesicular, the vesicles commonly filled with chlorite, calcite or epidote. Most pillows have well developed rinds, and minor hyaloclastic material occurs in the interstices. Well washed coastal outcrops provide good three dimensional exposure of pillows and allow top determinations to be made with confidence.

Most of the remaining lithologies in this unit are volcaniclastic and hyaloclastic. Well bedded volcaniclastic sandstones are locally interbedded with the pillow lavas. The eastern part of the sequence contains a 200 m thick lens of basaltic pyroclastic rock containing abundant fragments of basalt in a chloritic matrix; the lens outcrops on islands and headlands in the central and eastern parts of Glovers Harbour. Pillow breccias are locally developed throughout the sequence.

A single felsic volcanic member outcrops on several rocky hills approximately 700 m south-southwest of the Lockport Mine. This unit consists of grey to bluish, quartz-feldspar crystal tuff and possibly represents a single ash flow. It appears to lie at approximately the same stratigraphic horizon as the Lockport Mine.

Minor amounts of red chert are present in the sequence. One particularly persistent bed up to 1 m thick can be traced for more than 800 m along strike immediately north of the Lockport Mine.

The Glovers Harbour volcanics are faulted against well bedded chert, argillite and sandstone to the west along a fault which is apparently dextral strike-slip. Adjacent to the fault, the basalts are intensely cleaved and hematized, and face northwest. To the east, the volcanics pass conformably upward into coarse volcaniclastic debris-flow deposits; the contact is exposed on the shoreline northeast of Glovers Harbour.

Structural relationships within the volcanics have not been mapped in detail. They appear, however, to occupy a broad anticlinal structure the axis of which trends north-northwest immediately west of Glovers Harbour.

ii) Indian Cove volcanics: The Indian Cove volcanics, host to the Indian Cove Propsect, were assigned to the Seal Bay Brook formation by Dean (1978). They occupy an area approximately 4 km long and 1 km wide between Side Harbour and Mill Cove and consist of a complex assemblage of volcanic flows and pyroclastic rocks. The central and probably oldest part of the Indian Cove volcanics consists of a massive, buff to green rhyolite which outcrops on the north shore of Indian Cove and in the hills west of the cove.

The rhyolite is massive and commonly displays intense hydrothermal alteration characterized by gas brecciation and closely spaced fractures filled with hematite and pyrite. The rhyolite is overlain by various types of felsic to mafic pyroclastic rocks displaying rapid lateral facies changes. These consist mainly of poorly sorted, angular fragments of felsic volcanic rock, chert and minor basalt set in a tuffaceous matrix varying from dark green to buff in colour and mafic to felsic in composition. Spectacular breccias are locally present; they contain red chert fragments up to 5 m across chaotically distributed in a grey to reddish chloritic matrix. These appear to represent debris flows, possibly related to the development of the domal structure represented by the rhyolite. The debris-flow deposits seem to occupy the upper stratigraphic levels of the volcanic sequence and pass conformably upward into well bedded red and green chert, siltstone and sandstone which mark the top of the unit.

A single pillow basalt flow is present in the southern part of the unit. It may occur low in the stratigraphy, but due to structural complications this is uncertain.

The Indian Cove volcanics appear to pass conformably upward into volcaniclastic greywacke and conglomerate to the west, although this contact is not exposed; the eastern contact lies under the waters of Seal Bay.

iii) Wild Bight, Badger Bay volcanics: Mafic volcanic rocks outcropping around the bottom of Wild Bight, Badger Bay, were assigned to the Pennys Brook Formation by Dean (1978). They are composed mainly of basaltic, highly vesicular pillow breccias in which pillow fragments commonly range from 5 to 30 cm in diameter and possess well developed rinds on rounded surfaces. Complete pillows, locally preserved within the breccias, are both clast- and matrix-supported. Interstitial material, consisting of chloritic (probably hyaloclastic) matrix with abundant small angular basalt fragments, generally comprises less than 20 per cent of the rock.

This pillowed flows are present but appear to comprise less than 20 per cent of the sequence. The pillow lava units are 10 to 30 m thick, consisting of 1 to 1.5 m long pillows which generally contain abundant calcite- and chlorite-filled vesicles; they probably represent single flows. Locally, pillow lava can be seen to grade upward into pillow breccia.

The Wild Bight, Badger Bay volcanics are bounded top and bottom by volcaniclastic rocks and apparently lie near the top of the Wild Bight Group; the top is marked by the Caradocian Shoal Arm Formation to the immediate northwest.

Previous maps of this area (e.g. Espenshade, 1937; Dean, 1978) indicated that mafic volcanic rocks also outcropped along the east shore of Badger Bay northeast of Wild Bight, forming a 500 m thick unit from Green Point north to Little Cove, Badger Bay. This unit, in fact, consists of massive, dark green volcaniclastic sandstone with chert and basalt fragments, locally cut by fine grained mafic sills.

iv) Side Harbour formation north of Long Pond Fault: This laterally extensive basaltic sequence hosts Noranda's Point Leamington sulphide deposit. It was assigned to the Side Harbour formation by Dean (1978). It is well exposed in the area immediately south of Side Harbour where it consists mainly of pillow lava, with large (30 to 50 cm), bulbous pillows, commonly quite vesicular.

The Side Harbour formation is relatively thin immediately south of Side Harbour but thickens steadily southward along strike to a maximum of more than 2 km near the Point Leamington deposit. The basalt unit was previously mapped as outcropping in the bottom of Side Harbour (Fig. 69.1). However, outcrops here consist of fine- to medium-grained mafic intrusive rocks which display chilled margins and contain xenoliths of adjacent country rocks. These intrusive rocks are along strike from, and probably represent, a subvolcanic phase of the basalts.

The only felsic volcanics noted are in the immediate vicinity of the Point Leamington deposit where quartz-feldspar crystal tuff forms a lenticular unit approximately 200 m thick which has been traced for more than 1500 m along strike.

The Side Harbour formation is bounded above and below by typical Wild Bight volcaniclastic lithologies. The contacts appear to be conformable, but are not exposed.

v) Sparrow Cove Point formation: This formation consists of a thin (generally less than 100 m) unit of pillowed basalts, originally defined by Dean (1978). The basalts are moderately vesicular and outcrop in a horseshoe-shaped belt around the bottom of Seal Bay. This formation is probably misnamed since it does not appear to outcrop at Sparrow Cove Point where the equivalent stratigraphic level is occupied by volcaniclastic sandstone and chert, and diabase and gabbro dykes and sills. However, the basalt is well exposed south of Seal Bay and generally is thin enough that it could well represent a single flow. The basalt is conformably bounded on both sides by laminated chert, siltstone and greywacke.

vi) Long Pond volcanics: This narrow unit of mainly rhyolite, quartz-feldspar crystal tuff, felsic pyroclastic rocks and red chert outcrops in a narrow, north trending band north of Lewis Lake. It hosts the Long Pond prospect and includes a narrow (30 to 40 m) unit of pillow lava and pillow breccia. The stratigraphic facing direction of this unit is not known; it is conformably bounded to the west by red chert and grey to green argillites which are in turn faulted against volcaniclastic rocks. To the east, the volcanics are faulted against the South Lake Igneous Complex.

vii) Big Lewis Lake basalts: This sequence outcrops between the Long Pond and Four Mile Lake faults, and can be distinguished from the Side Harbour formation basalts which adjoin them across the Long Pond Fault (Fig. 69.2) in two respects: (1) the Big Lewis Lake basalts comprise mainly pillow breccia and basalt-bearing volcanic breccia with relatively little pillow lava; (2) they pass conformably upward into the Caradocian chert-shale interval and are therefore stratigraphically higher in the section. Both lithologically and with respect to their stratigraphic position within the Wild Bight sequence the Big Lewis Lake basalts closely resemble the basaltic sequences in the Wild Bight, Badger Bay section. There are no felsic volcanics in this unit.

viii) Nanny Bag Lake volcanics: Volcanic rocks in this area, assigned by Dean (1978) to the Pennys Brook formation, consist of a felsic volcanic complex centered on the west end of Nanny Bag Lake, bounded to the south and west by basalts which extend south to the New Bay River. The thick basaltic sequence west of the felsic complex comprises mainly massive, unpillowed, generally nonvesicular rocks unlike those anywhere else in the Wild Bight Group. The massive basalts are separated from the felsic complex by a narrow volcaniclastic greywacke and congloemrate unit which passes conformably eastward into the felsic complex. The felsic volcanic complex consists mainly of black to dark blue quartz-eye rhyolite and rhyolitic crystal tuff, but also contains a considerable amount of volcaniclastic material. Detailed traversing is needed to fully define the nature of this complex.

Geologic maps compiled by Dean (1978) show basaltic rocks outcropping southeast and east of the felsic volcanic centre. The present mapping suggests that the south end of this volcanic sequence near the New Bay River is underlain, at least in part, by diorite and gabbro intrusions. To the east of the felsic complex, volcaniclastic turbidites form all the outcrops. North of the Four Mile Lake Fault, mafic rocks east of the volcanic sequence appear to be intrusive and may be related to the South lake Igneous Complex.

Stratigraphic relationships

Volcanic rocks appear to occupy several stratigraphic levels within the Wild Bight Group. In some cases, the relative position of the volcanic rocks can be stated with confidence. In most cases, however, structural disruption and the paucity of outcrops in critical areas render correlations more uncertain. Present evidence suggests the following relationships:

1. The Sparrow Cove Point basalts (v) are the stratigraphically lowest volcanic rocks in the sequence, occurring near the exposed base of the Wild Bight Group in the core of the Seal Bay anticline.
2. The Big Lewis Lake basalts (vii) are the stratigraphically highest volcanic rocks in the sequence and pass directly upward into Caradocian shale and chert. The Wild Bight, Badger Bay basalts are only slightly lower in the sequence, separated from the Caradocian shales of the Shoal Arm Formation by a thin volcaniclastic interval. These two basaltic sequences are very similar lithologically, consisting dominantly of pillow breccia and hyaloclastite with minor pillowed flows. They are probably lateral equivalents.
3. The Side Harbour formation north of the Long Pond Fault (iv) is intermedite in the stratigraphic sequence. It is underlain by volcaniclastic rocks which apparently pass conformably downward into the core of the Seal Bay anticline, and is overlain by similar rocks, the thickness of which is uncertain due to folding but which appear to pass upward into the Wild Bight, Badger Bay basalts. The formation may be more or less equivalent to the Glovers Harbour basalts which appear to lie approximately 2 km stratigraphically below the Caradocian shale at Leading Tickles and to be separated from it by mainly volcaniclastic rocks. The base of the Glovers Harbour volcanics is not exposed. The Nanny Bag Lake volcanics appear to occupy a similar stratigraphic position as they pass upward through approximately 2 km of volcaniclastic rocks into Caradocian shale east of Nanny Bag Lake.
4. The relative position of the Long Pond volcanics is not known as they are fault-bounded on both the east and west. Likewise, the position of the Indian Cove volcanics remains somewhat enigmatic as the upper and lower contacts are not exposed. If the western contact is conformable (suggested by the continuity of planar features across the contact area) then the Indian Cove volcanics are slightly lower in the section than the Side Harbour formation.

In summary, there is evidence for multiple episodes of volcanic activity during deposition of the Wild Bight Group. The units which contain volcanogenic sulphide mineralization are generally intermediate in the stratigraphic sequence but not necessarily at the same stratigraphic horizon. Detailed structural mapping of the units is needed to clarify these relationships.

3. Intrusive Rocks

The Wild Bight Group is extensively cut by mafic sills and, less commonly, dykes ranging from fine grained, locally vesicular diabase to coarse grained, equigranular to somewhat prophryitic gabbro. Fine grained varieties are commonly highly vesicular, locally crosscutting, and some show evidence of intrusion into wet sediments. Most appear to be related to the Wild Bight volcanism and were probably intruded at relatively high levels.

In addition, fine grained lamprophyre dykes are present which cut all lithologic and structural trends and are probably Mesozoic in age (see Strong and Harris, 1974; Dean, 1978).

VOLCANOGENIC SULPHIDE OCCURRENCES

Four principal volcanogenic sulphide occurrences are present in the Wild Bight Group. These were examined in detail on site, and where possible, in drill core. The locations of these deposits are shown on Figure 69.2 and brief descriptions are presented below.

Point Leamington

This is the largest single massive sulphide deposit known in Newfoundland and was discovered in the early 1970s by Noranda Exploration Ltd. Previously published dimensions (Noranda Mines staff, 1974) suggest that more than 20 million tonnes of massive sulphide is present, grading approximately 0.5% Cu and 2% Zn with sporadic precious metal values. The deposit lies at the top of a thick volcanic sequence which is dominantly composed of pillowed basalts (the Side Harbour formation north of the Long Pond Fault, unit iv). In the vicinity of the deposit, the basalts are capped by a 500 m thick unit of felsic quartz-feldspar crystal tuff which has been traced for approximately 1500 m along strike. This unit is the only felsic volcanic member in the Side Harbour formation.

The rocks near the deposit are poorly exposed and the massive sulphide body lies under a bog. A few exposures of highly altered, pyritic, rhyolitic quartz-eye crystal tuff of the footwall outcrop immediately east of the deposit. Similarly altered and mineralized pillow basalt outcrops about 100 m farther east. Unaltered volcaniclastic rocks outcrop in the hanging wall to the west of the deposit.

These outcrops summarize the environment; details of the setting are somewhat better displayed in drill core. The massive sulphide body consists mainly of fine grained pyrite with lesser chalcopyrite and local enrichment of sphalerite which occurs as blebs and discrete beds. The contacts of massive sulphides with both the hanging wall and the footwall are sharp although the footwall displays a zone of pervasive alteration recognizable everywhere below the massive body. The alteration consists mainly of variably intense silicification and sericitization commonly accompanied by veinlets, blebs and disseminations of pyrite and lesser chalcopyrite. This pervasive alteration is locally cut by 5 to 30 cm wide crosscutting zones of intense black chlorite alteration which is generally accompanied by more intense sulphide mineralization. In some drill core, the chlorite alteration can be seen to be most intense in the immediate footwall to the massive sulphides, and locally the lower parts of the massive sulphides have been brecciated, with chlorite introduced between the fragments. The chloritic alteration is believed to represent local zones of more intense fluid flow during the alteration/mineralization episode. Where most intensely developed in the immediate footwall, it may record actual zones of discharge of the mineralizing fluids.

The massive sulphide body has been outlined by diamond drilling to a depth of approximately 260 m, and the nature of the massive sulphides is remarkably uniform from surface to this depth. The total extent of the body is yet to be determined.

The massive sulphides and the host rocks are cut by numerous mafic dykes ranging from fine grained diabase to coarsely porphyritic gabbro similar to those observed in outcrop throughout the Wild Bight Group stratigraphy.

Lockport

The Lockport deposit was discovered in the late 1870s or 1880s. Early workings on the deposit included a series of open cuts on the gossans which marked the original showings, and five shallow shafts from which a limited amount of ore was apparently shipped to the Tilt Cove smelter near the turn of the century. The property received sporadic attention throughout the early 1900s, but the first comprehensive exploration program did not take place until the 1950s when NALCO carried out mapping, geochemistry, geophysics and some diamond drilling on the main prospect. Further diamond drilling has been carried out by other firms from the 1960s to the present; 15 holes totalling 2647 m have been drilled on the deposit. The core from these holes has been lost, although drill logs are on file with the Department of Mines and Energy. Grade and tonnage estimate by Fogwill (1965) suggest the presence of approximately 220 000 tonnes of material grading 1.21% Zn and a further 392 350 tonnes grading 0.75% Cu.

The property was the subject of an M.Sc. dissertation at Memorial University by DeZoysa (1969).

The Lockport deposit occurs near the centre of the Glovers Harbour volcanics, and is partially exposed in the old open cuts and abundant nearby outcrops. The open cuts expose only the western side of the deposit, although the abundant mineralized material on the adjacent dumps may sample material from the unexposed eastern portion as well. The host rocks exposed in the open cuts comprise mainly intensely sheared, silicified pyroclastic rocks and basaltic flows. Felsic quartz-feldspar crystal tuff outcrops 700 m southwest of the deposit approximately on strike with the mineralized horizon. The mineralization exposed in the open cuts is of stockwork type, characterized by intense quartz-sericite alteration and pervasive disseminations and stringers of pyrite and lesser chalcopyrite. The deposit is highly sheared, and lenses up to 10 cm wide of massive pyrite are present, apparently boudins of what were previously relatively large stringers.

There are no exhalative massive sulphides exposed at the prospect; there are, however, numerous large boulders on the dumps which consist of massive, finely laminated pyrite-chalcopyrite with local concentrations of sphalerite. Logs of holes drilled by NALCO in the 1950s suggest that a massive sulphide zone up to 8 m wide was intersected at the eastern margin of the deposit, and that this zone is characterized by markedly elevated zinc grades (the zinc-rich reserves quoted above). It is possible that this zinc-rich zone represents the exhalative cap to the stockwork zone exposed in outcrop and that this zone was also the source of the massive boulders on the dump. According to the NALCO drill logs, this zone appears to have a strike extent of less than 130 m and to pass into massive pyrite at depth (less than 90 m below surface). The distribution of drill holes is inadequate, however, to delineate the body.

A preliminary interpretation of the relationships at the Lockport deposit, therefore, suggests that it represents a proximal-massive sulphide system which faces east and is hosted by basaltic flows and pyroclastic rocks of indeterminate original composition. The mineralization may be related to the felsic volcanic episode represented by laterally equivalent crystal tuffs although this cannot be demonstrated at present.

Indian Cove

The main showing in the Indian Cove volcanics is displayed in a series of outcrops approximately 300 m southwest of Indian Cove. The mineralization is also exposed in several trenches and a small adit. It consists mainly of disseminated and stringer pyrite and chalcopyrite in altered rhyolite and silicic breccia. The mineralized zone is better displayed in drill core from eight holes which were drilled by Texasgulf in 1975. This core is presently stored at the Department of Mines and Energy core storage library in Pasadena.

The mineralization as seen in core comprises a stockwork zone with a small, central, intensely altered chlorite-pyrite-chalcopyrite zone surrounded by less intense sericite-silica alteration containing abundant pyrite-chalcopyrite (sphalerite) stringers. The alteration which accompanies the mineralization is pervasive but uneven in intensity. Quartz-sericite alteration is widely developed and is commonly accompanied by disseminated and stringer pyrite with minor chalcopyrite. Locally, the host rock is almost completely silicified over widths up to 3 m; these zones grade into less altered rhyolite and felsic volcanic breccia in which original textures are preserved. The most intense sulphide mineralization commonly occurs in zones where black chlorite alteration is best developed. These zones are generally 5 to 20 cm wide but locally are as wide as 20 m, and generally contain minor amounts of visible sphalerite as well as the ubiquitous pyrite and chalcopyrite. Grades are commonly low. The best mineralization intersected by diamond drilling assayed 1.04% Cu, 0.78% Zn and minor silver over 10 m.

There does not appear to be any truly exhalative mineralization at the Indian Cove prospect. The showing seems to be a particularly intense facies of the pervasive alteration which is present throughout the felsic flow and pyroclastic sequence of the Indian Cove volcanics, and is interpreted as hydrothermal alteration related to the formation of the rhyolite dome at the base of the sequence. The effects of this hydrothermal activity are well displayed at the previously described locality on the shores of Indian Cove; less intense, although ubiquitous, pyritization and sericitization are evident in the felsic volcanic rocks for several hundred metres along strike from the prospect. The alteration at the main prospect is the most intense yet discovered in the sequence and the only one to contain significant quantities of base metals. This may be partly because most exploration on the property has been in the immediate vicinity of the showing. The hydrothermal system, however, is in evidence over an area considerably wider than the showings, and it may well be that zones of base-metal-bearing stockwork as well as exhalative sulphides related to hydrothermal fluid discharge remain to be discovered.

Long Pond

This prospect lies within a narrow belt of rhyolitic tuff and breccia, but is at least in part hosted by a thin basaltic pillow lava/pillow breccia unit which can be traced for several hundred metres along strike. The mineralization consists mainly of heavily disseminated pyrite and minor chalcopyrite; it is accompanied by chlorite-sericite-silica alteration, and is probably stockwork type. No drilling has been recorded from the prospect. This favourable environment deserves a thorough look for massive sulphide mineralization.

CONCLUSIONS

The information summarized in this report embodies the preliminary phase of a project designed to investigate the geological and tectonic environments of volcanogenic sulphide mineralization in Early-Middle Ordovician island arc sequences of central Newfoundland. Further work in the Wild Bight Group will focus on petrographic, geochemical and isotopic studies of the volcanic rocks and the associated mineralization. Tentative conclusions reached on the basis of field work to date include the following:

1. The Wild Bight Group records a dominantly volcaniclastic environment, punctuated by brief episodes of volcanic activity. It appears to have been deposited on the middle flanks of a major volcanic edifice located to the south of the presently preserved sequence.
2. Volcanic accumulations are present at various stratigraphic levels in the sequence. The accumulations display significant differences in lithology and setting. Volcanism was dominantly mafic, but with development of areally restricted felsic domes and possibly ash flows.
3. Volcanogenic sulphide mineralization accompanied several of the volcanic episodes. Exhalative sulphides are well developed at the Point Leamington deposit and are underlain by stockwork alteration and mineralization. Mineralization exposed on the surface at the Lockport, Indian Cove and Long Pond prospects (and in drill core from Indian Cove) is mainly of stockwork type, although evidence suggests that the Lockport depost has an exhalative cap which does not outcrop. The potential for the existence of related massive sulphide mineralization is good in all cases.

ACKNOWLEDGMENTS

Patrick Carroll provided cheerful field assistance during the course of the field studies. Lillian Luscomb is thanked for help during our stay in Leading Tickles. Bill Hanlon allowed us to camp in his lot at New Bay Pond. Bud James of Noranda Exploration kindly permitted access to drill core from the Point Leamington deposit. Stew Cochrane and Gerrard Humber are thanked for help during sample preparation in Pasadena. The manuscript has benefited from critical reading by B.F. Kean.

REFERENCES

Dean, P.L.
1978: The volcanic stratigraphy and metallogeny of Notre Dame Bay, Newfoundland; Memorial University of Newfoundland, Geology Report 7, 204 p.

DeZoysa, T.H.
1969: Geology and base metal mineralization of Lockport area, Notre Dame Bay, Newfoundland; unpublished M.Sc. thesis, Memorial University of Newfoundland, 99 p.

Espenshade, G.E.
1937: Geology and mineral deposits of the Pilleys Island area; Newfoundland Department of Natural Resources, Bulletin 6, 56 p.

Fogwill, W.D.
1965: Interim report on Lockport copper-pyrite mine; unpublished report for NALCO, 7 p.

Hayes, J.J.
1951: Geology of the Hodges Hill – Marks Lake area, Northern Newfoundland; unpublished Ph.D. thesis, University of Michigan, 163 p.

Heyl, G.R.
1938: Geology and mineral deposits of the New Bay area, Notre Dame Bay, Newfoundland; Newfoundland Department of Natural Resources, unpublished report, 37 p.

Kean, B.F., Dean, P.L., and Strong, D.F.
1981: Regional geology of the central volcanic belt of Newfoundland; in The Buchans Orebodies: Fifty Years of Geology and Mining, ed. E.A. Swanson, D.F. Strong, and J.G. Thurlow; Geological Association of Canada, Special Paper 22, p. 65-78.

Noranda Mines Staff
1974 The Point Leamington sulfide deposit; in A Guidebook to Newfoundland Mineral Deposits, ed. D.F. Strong; Nato Advanced Studies Institute, p. 60-61.

Strong, D.F. and Harris, A.H.
1974: The petrology of Mesozoic alkaline intrusives of central Newfoundland; Canadian Journal of Earth Sciences, v. 11, p. 1208-1219.

Swinden, H.S. and Thorpe, R.I.
– Variations in style of volcanism and massive sulfide deposition in Early-Middle Ordovician island arc sequences of the Newfoundland central mobile belt; Economic Geology. (in press)

Williams, H.
1963: Botwood map area; Geological Survey of Canada, Map 60-1963.

70. SUMMARY OF FIELDWORK IN THE NORTHERN LONG RANGE MOUNTAINS, WESTERN NEWFOUNDLAND[1]

Project 830033
Contract 19SR.23233-3-0191

Philippe Erdmer[2]

Erdmer, P., Summary of fieldwork in the northern Long Range Mountains, western Newfoundland; in Current Research, Part A, Geological Survey of Canada, Paper 84-1A, p. 521-530, 1984.

Also in Current Research, Newfoundland Department of Mines and Energy, Mineral Development Division, Report 84-1, 1984.

Abstract

In preparation for mapping the Precambrian terrane of the northern Long Range Mountains of Newfoundland at 1:100 000 scale, two strips were mapped in 1983, along the western side of White Bay and along the Upper Humber River. The report presents a review of the tectonic nature of the terrane, followed by generalized geological maps and descriptions of the major rock units of the region. A Helikian or older quartzofeldspathic basement gneiss complex, part of which is of sedimentary origin, has been intruded by a gabbro-anorthosite massif and by megacrystic granitic rocks of probable Neohelikian age. Metamorphic grade is generally in the amphibolite facies, with granulite grade rocks occurring locally. A retrograde greenschist event affected the entire eastern portion of the terrane.

Résumé

En prévision du levé au 1/100 000 du terrain précambrien de la partie septentrionale des Monts Long Range de Terre-Neuve, deux coupes ont été effectuées en 1983, l'une, longitudinale, dans la zone côtière de la baie White, et l'autre, transversale, dans la région du cours supérieur de la Humber. Ce rapport comprend une revue de la tectonique régionale, des cartes géologiques généralisées et une description des grandes unités stratigraphiques de la région. Un complexe gneissique quartzofeldspathique de l'Hélikien ou antérieur, dont au moins une partie est d'origine sédimentaire, est recoupé par un massif de gabbro-anorthosite et par des granites mégacrystiques probablement néohélikiens. Les roches sont en grande partie dans le faciès amphibolite, et dans certains cas dans le faciès granulite. Une rétrogression au faciès schistes verts a affecté l'entière bordure orientale de la région.

INTRODUCTION

The Precambrian terrane of the northern Long Range Mountains is a high grade granite-gneiss complex that is generally assumed to be an inlier of the Grenville Province in the miogeoclinal belt of the Appalachian Orogen. It occupies nearly 8500 km^2 of the Great Northern Peninsula of Newfoundland (Fig. 70.1). Of this area, only about 2000 km^2 have been mapped systematically, at 1:125 000 scale (Bostock, 1983); little is known about the remaining portion which extends over parts of fourteen 1:50 000 scale NTS map areas. Mapping of the remaining area at 1:100 000 scale, is to be initiated in the near future. In preparation, a reconnaissance project was carried out in the summer of 1983.

TECTONIC SETTING OF THE PRECAMBRIAN TERRANE

One of the principal aims of future systematic mapping will be to compare the rock types and tectonic framework of the region with those of the Grenville Province in adjacent southern Labrador. Little is known about the rocks underlying the Strait of Belle Isle, which separates insular Newfoundland from Labrador. If the Long Range Mountains constitute an inlier, many similarities to the mainland Grenvillian rocks can be expected. However, if strong contrasts are found to exist or if the similarities are weak, the autochthonous nature of the terrane will be in doubt; the "inlier" may have been displaced from the more interior parts of the Appalachian Orogen during Paleozoic tectonism.

The hypothesis of an overthrust Long Range Mountains terrane was proposed in several early reports of fieldwork at the periphery of the Precambrian rocks. It is also suggested by more recent geophysical observations.

Schuchert and Dunbar (1934) reported that the Precambrian gneiss was thrust over the Paleozoic rocks on the shore of Western Brook Pond. Johnson (1941a,b) concluded that a major east-dipping thrust underlies the entire western boundary of the terrane, carrying it over the Paleozoic platformal assemblage to the west. He showed the apparent dip of this fault to be approximately 60° to the east in two cross-sections, and reported the fault to be "almost flat" in an exposure on St. Pauls Inlet. Oxley (1953) also interpreted the contact as a thrust and reported a dip of 34° to the southeast for the fault plane near Parsons Pond. Similarly, Nelson (1955) suggested the presence of a high-angle thrust fault at the boundary. It appears that none of the outcrops described by these authors has been critically re-examined.

The observation that Paleozoic cover rocks in several localities southwest of the margin of the terrane (in the Bonne Bay – Bonne Bay Big Pond area) contain at least three sets of folds (H. Williams, personal communication, 1983) whereas the Precambrian rocks display no equivalent strain, suggests the presence of a décollement at or near the unconformity surface, and differing structural histories for rocks on either side of the contact. This implies at least a parautochthonous character for some of the cover rocks, and suggests the possibility of basement reworking.

On the basis of a paleomagnetic comparison of rocks in western Newfoundland and mainland eastern Canada, Black (1964) concluded that Newfoundland rotated 30° anticlockwise away from Labrador in the Middle to Late Devonian. Although Deutsch and Rao (1977), together with other workers, considered Black's data inconclusive,

[1] Contribution to Canada-Newfoundland co-operative mineral program 1982-84. Project carried by Geological Survey of Canada.

[2] Newfoundland Department of Mines and Energy, Mineral Development Division, P.O. Box 4750, St. John's, Newfoundland A1C 5T7

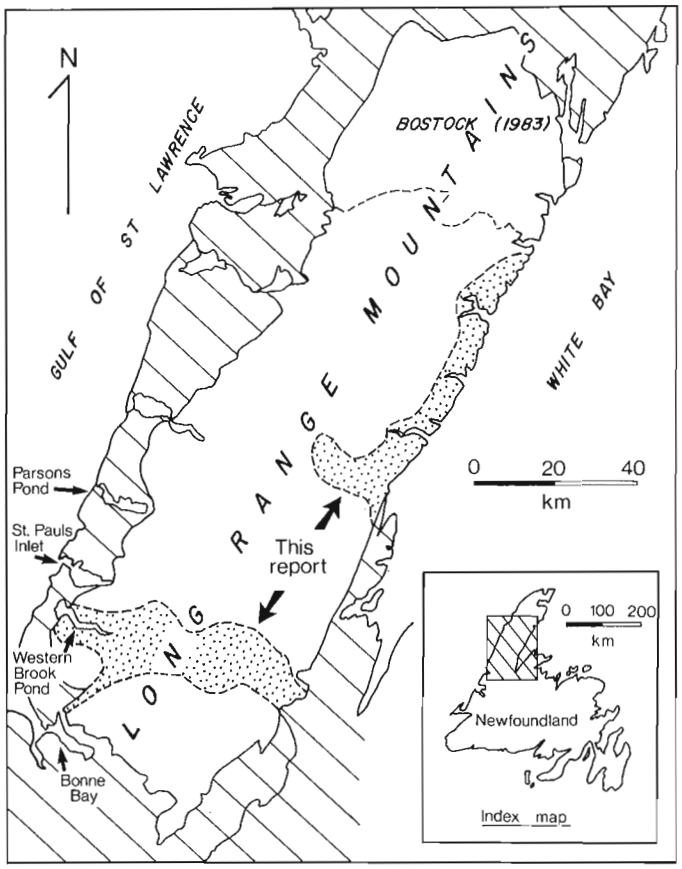

Figure 70.1. *Location of the Precambrian terrane of the northern Long Range Mountains. Paleozoic rocks are shown by hachures. Bostock's (1983) map area and the two strips mapped for the present study (dot pattern) are outlined.*

new measurements led them to conclude that a rotation of 5 to 10° since the Ordovician is possible. Pullaiah et al. (1979), from a reconnaissance study of the Late Hadrynian Long Range dykes, observed that the remanent magnetization of these rocks contains a steeply inclined component that is misaligned with published late Precambrian directions for both Newfoundland and mainland North America; they attributed this discrepancy to a Devonian overprint. However, other interpretations (i.e. terrane displacement) cannot be ruled out until further testing.

A gravity gradient trending diagonally across the area (Haworth et al., 1980) suggests that deep crustal structure is not reflected in the surface distribution of rock types and that the underlying crust may not be entirely sialic. A well defined positive Bouguer gravity anomaly is centred on the southeast portion of the terrane.

To a large extent, the configuration of east-dipping faults beneath the Precambrian rocks can only be determined through deep crustal geophysical measurements similar to those of Cook et al. (1979) in the southern Appalachians. Such a study is being considered as part of a Lithoprobe transect through eastern Canada.

In summary, the physical continuity of the Precambrian rocks of the Long Range Mountains with those of the adjacent Canadian Shield is widely assumed (e.g. Williams and Hatcher, 1983; Keppie, in press), but it has not yet been established. On the basis of the above evidence, the paleogeography of the entire region appears unclear. Further investigation may prove the "inlier" to be either truly autochthonous or a slightly displaced Grenvillian basement.

PREVIOUS WORK AND PRESENT INVESTIGATION

Previous work in the portion of the inlier not covered by Bostock's (1983) study is summarized below.

Murray and Howley (1881, 1918) examined the east coast of the Great Northern Peninsula and reported mainly granitic gneiss intruded by northeast-trending greenstone dykes. Foley (1937) and Fritts (1953) made four traverses across the peninsula, in which they observed various gneissic units of inferred metasedimentary origin, foliated and massive granitic rocks and crosscutting diabase dykes. The British Newfoundland Corporation Ltd. made a reconnaissance survey of the entire terrane in 1954, which resulted in a map at the scale of 1 inch to 2 miles (W. Harrison and F. Johnston, unpublished report, 1955).

On a reconnaissance map at the scale of 1 inch to 4 miles, Baird (1959) indicated the presence of gabbro, anorthositic gabbro and anorthosite, along with various granitoid and mafic gneiss units in the southern portion of the terrane. Clifford and Baird (1962) produced the first comprehensive map of the terrane, at approximately 1:1 000 000 scale. Partly on the basis of data assembled from previous workers, their map shows granitic and basic intrusions of three types within older gneiss, and the extent of the Long Range dyke swarm; they also reported the occurrence of various schist and gneiss units, and quartzite and metaconglomerate. The regional metamorphic grade was considered to be middle amphibolite. Neale and Nash (1963) mapped the distribution of biotite- and hornblende-rich gneiss and granite units and metagabbro along part of the southeastern margin of the terrane at the scale of 1 inch to 4 miles.

Pringle et al. (1971) reported a Rb-Sr age determination of 1130 ± 90 Ma and a K-Ar age of 840 ± 20 Ma for megacrystic granite in the Hawkes Bay – Portland Creek area. Cumming (1973a,b) and Bostock and Cumming (1973) briefly examined the Precambrian rocks of Gros Morne National Park, and reported the presence of granulite facies gneissic rocks and the existence of a large, apparently domal structure at the head of Western Brook Pond. Stukas and Reynolds (1974) studied several of the Long Range dykes west of Great Harbour Deep, for which they determined a $^{40}Ar/^{39}Ar$ age of 605 ± 10 Ma. They also concluded that the apparent range of K-Ar ages from 756 to 865 Ma for samples from a single dyke, within the area mapped by Bostock (1983), reported by Pringle et al. (1971), resulted from excess radiogenic argon and should not be interpreted as the dates of emplacement of the dyke swarm.

In the light of these studies, the main objectives of 1983 fieldwork were to map two strips of the terrane, one along the northeast-trending coastal section on White Bay, and the other centred on the Upper Humber River between Western Brook Pond and Taylor Brook. A secondary objective was the examination of the area scheduled to be flooded in 1984 as part of the Cat Arm hydroelectric development, and of the bedrock exposed during the construction of dams and tunnels for this project. The results presented below are a contribution to the complete study of the inlier, which aims to answer many of the questions raised by the regional geological and geophysical data listed above.

RESULTS OF 1983 FIELDWORK

Coastal section

The geology of the Precambrian rocks along White Bay, between Great Coney Arm and Granite Point, is shown in Figure 70.2. Exposure is excellent along White Bay, and fair to poor inland from the coast.

Map units

Unit 1 includes a variety of rock types that are broadly grouped as quartzofeldspathic gneiss. They are pink to grey, heterogeneous, medium- to coarse-grained, generally well layered but equigranular in places, migmatitic hornblende or biotite granitic gneiss (Fig. 70.3). This gneiss includes abundant layers and lenses of amphibolite, some of which are crosscutting and others conformably interlayered, suggesting the existence of more than one protolith. They are interpreted in large part as relict dykes. Similarly, pegmatite and migmatite veins and segregations either follow the gneissosity or truncate it. Thinly banded layers of quartz-rich gneiss are present in many outcrops within unit 1; this gneiss is differentiated as unit 2 where it is extensive. It is considered to be of metasedimentary origin. Other layers include pink, megacrystic orthogneiss of granitic to monzonitic composition that is correlated with the rocks of unit 3. Unit 1 thus contains rocks of differing protoliths,

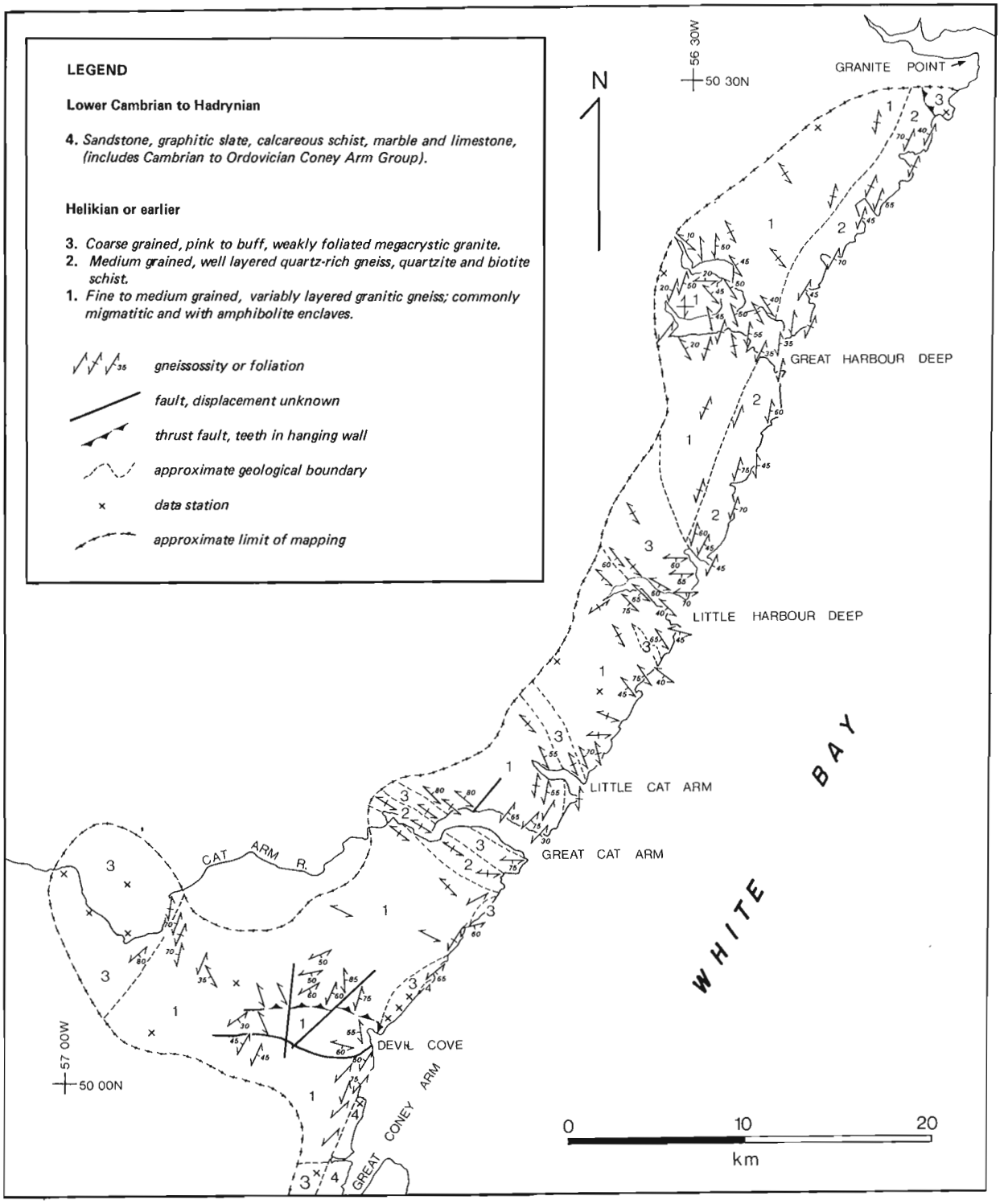

Figure 70.2. *General geology of part of the east margin of the Precambrian terrane along White Bay. Data stations shown as "x" are where no structural observations were made.*

and is likely to have had a prolonged strain history. Pending further subdivision, unit 1 is correlated with the bulk of the old gneiss complex to the northwest (Bostock, 1983), which is of Helikian or older age.

Unit 2 is exposed in two elongate slices several kilometres long which are interlayered with unit 1. It is an assemblage of dominantly medium grained, grey to white, finely banded quartz-rich gneiss (in which quartz forms up to 90 per cent of the rock, and feldspars and biotite the remainder), medium grained quartzite and minor medium- to fine-grained biotite schist (Fig. 70.4). Other minor rock types such as chlorite schist, fine grained amphibolite and transitional layers are present in a few outcrops. A few gossan areas of 10 to 40 m^2 each were noted in layers of unit 2 on the coast. Mineralization appears to be mostly disseminated pyrite, and minor chalcopyrite or hematite and magnetite. A metasedimentary origin is inferred for most of the rocks of unit 2. The unit is correlated with minor rock types (pelitic schist, muscovite-chlorite schist, amphibolite and quartz-rich gneiss) differentiated by Bostock (1983) within the basement gneiss to the northwest, for which a Helikian or older age has been established.

Unit 3 comprises a variety of dominantly coarse grained, megacrystic, massive to weakly foliated granitic rocks exposed in several places along the coast and inland (Fig. 70.5). Their relation to units 1 and 2 appears to be mainly intrusive, although the contact was moderately to strongly modified by later strain and is generally poorly exposed. Where it is exposed, the rocks of unit 3 cut across the main gneissic fabric, and have been involved in a subsequent, less intense deformation. To the west of Great Coney Arm, the rock is generally massive, coarse grained and commonly subporphyritic, buff granite with a characteristic dark green, relatively fine grained groundmass. The body exposed along the upper Cat Arm River is medium- to coarse-grained, almost equigranular, pink, leucocratic granite that is well foliated near its contact with the gneiss of unit 1. Between Devil Cove and Great Harbour Deep, the rocks included in unit 3 are moderately to strongly foliated, pink, megacrystic (K-feldspar) granite to alkali feldspar granite, the protoliths of which may differ in age. The granite near Granite Point is a massive, equigranular, biotite-bearing, leucocratic rock that overlies the gneiss to the west along a shallow dipping mylonite zone (see Structure). The diversity

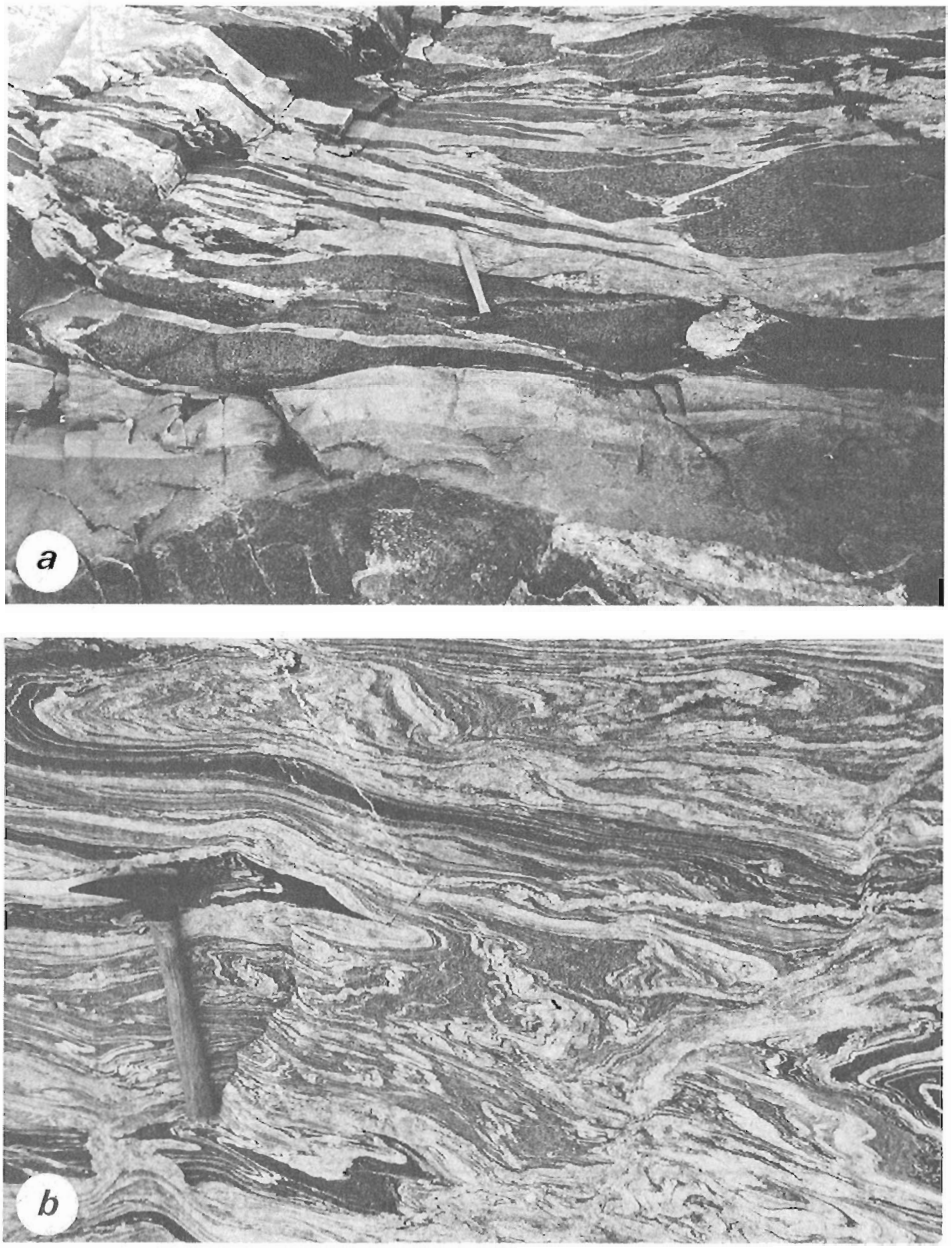

Figure 70.3

(a) Granitic gneiss and interlayered amphibolite of unit 1. (b) Heterogeneous, tightly folded gneiss of the same unit. Both photographs are from outcrops on the shore of White Bay.

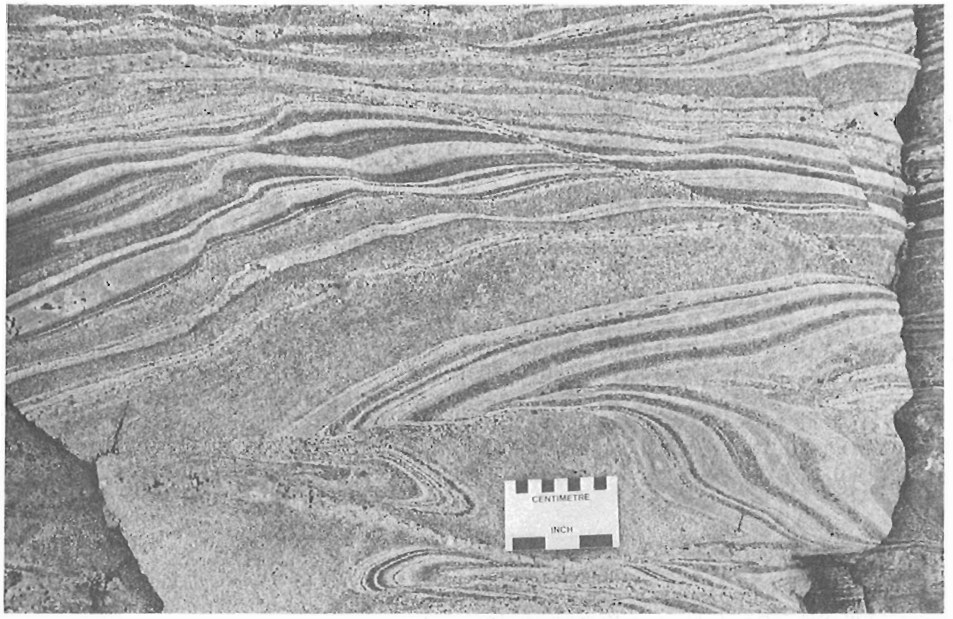

Figure 70.4

Finely layered quartzofeldspathic and quartz-rich gneiss of unit 2, north of Little Harbour Deep.

of rock types within unit 3 suggests that distinct intrusive suites with slightly different compositions are represented. The rocks of unit 3 are correlated with other posttectonic but pre-Grenvillian granite bodies exposed in the region to the north (Bostock, 1983; Pringle et al., 1971).

Units 1 to 3 are cut across by numerous diabase and metadiabase dykes of the late Hadrynian Long Range swarm, that measure a few centimetres to more than 50 m across strike. These dykes invariably strike east-northeast; dips vary from vertical to steep to the southeast or southwest.

Unit 4 includes east-dipping clastic and carbonate strata that lie unconformably on all the above units. The unconformity is exposed at two localities along the coast, 2 km to the south and 3 km to the north of Devil Cove, and in many places along the access road to the Cat Arm Development site. The basal rock type is a thin layer (1 to 20 m) of blue-quartz pebble conglomerate and sandstone of the Beaver Brook Formation (Smyth and Schillereff, 1982), which has been correlated with the Eocambrian Bradore Formation (Schuchert and Dunbar, 1934) exposed around the northern margin of the Precambrian terrane. The Beaver Brook Formation, and the overlying marble, graphitic phyllite and schist, limestone, quartzite and dolomite strata are included in the Cambrian to Middle Ordovician Coney Arm Group, as redefined by Smyth and Schillereff (1982), which is interpreted as an autochthonous Lower Paleozoic platformal assemblage.

Structure

The main fabric of units 1 and 3 is a well developed gneissosity or foliation that is commonly affected in outcrop by irregular, asymmetric tight folds ranging from a few centimetres to several metres in amplitude. Steep dips of the planar fabric are common; a few large (up to 100 m amplitude) overturned to recumbent isoclinal folds are exposed in unit 1 on the coast. Dip variations and reversals over short distances along strike are common.

Shallow north- to northeast-dipping mylonite zones up to 20 m thick, exposed to the west of Devil Cove and south of Granite Point, are the locus of ductile thrust faulting, as suggested by minor structures in at least one locality (D. Besaw, personal communication, 1983). On the basis of the few data available, thrusting appears to have been south-southwesterly directed. Because the granite of unit 3 south of Granite Point is thrust over unit 2 (this relationship confirms Bostock's (1983) observation of a south-dipping fault to the north of Granite Point), the faulting appears to be of Grenvillian age.

Two thrust faults reported by Foley (1937) on the north shore of Great Harbour Deep are small, brittle, east-dipping structures that are probably related to Paleozoic faulting farther east.

Metamorphism

All rocks in units 1 to 3 are pervasively recrystallized. A saccharoidal, friable texture is characteristic of many of the quartzofeldspathic rocks. Migmatite segregations are developed in many outcrops of units 1 and 2. Metamorphic hornblende and biotite are present almost everywhere, but no mineral assemblages diagnostic of a well constrained pressure-temperature field were found. Epidote, chlorite and sericite are present in most outcrops along the coast as retrograde minerals in the gneissic and granitic rocks. The Long Range dykes are locally heavily chloritized; this alteration appears to decrease progressively inland to the west.

Metamorphic grade in the crystalline rocks is thus in the amphibolite facies, with extensive overprinting in the greenschist facies which may be weaker to the west.

Southern transect

The geology of the area between Western Brook Pond and Taylor Brook is shown in Figure 70.6. Exposure in the region is generally fair to poor to the east of Gros Morne National Park, and good within the park.

Map units

Unit 1 includes heterogeneous, leucocratic, pink to grey, medium- to coarse-grained biotite or hornblende granitic gneiss (Fig. 70.7). It is commonly well layered and migmatitic, and includes layers and boudins of amphibolite. Although lack of exposure prevents a firm interpretation, the relations between gneiss and amphibolite are probably similar to those observed along White Bay (i.e. both conformable and crosscutting contacts can be seen). Large (up to 6 m across) boulders of distinctive, finely laminated, fine grained

sillimanite- and muscovite-rich quartzofeldspathic gneiss occur in the bed of the Upper Humber River near 57°10'W. These boulders appear to be of proximal derivation, and are considered to represent fragments of pelitic layers within unit 1. Unit 1 is correlated with the old gneiss exposed along White Bay and in the region mapped by Bostock (1983). The unit is interpreted to be of Helikian or older age and to include rocks of diverse protoliths and various ages.

Unit 2 has most of the characteristics and the overall composition of unit 1, but is distinguished from it by the presence of medium- to coarse-hypersthene grains and the pervasive, waxy, dark olive green of the feldspars in many outcrops. Contacts with unit 1 are mostly gradational, except to the north of Western Brook Pond where a prominent steep northeast-trending fault separates the hypersthene gneiss from the rocks of unit 1. As a difference of metamorphic grade appears to be the only difference between units 1 and 2, their protoliths may have been similar. The granulite facies rocks of unit 2 do not correlate with rocks elsewhere in the Long Range Mountains, but they may be lithologically similar to leucocratic hypersthene gneiss in adjacent Labrador, described by Bostock (1983). The unit is assumed to be Helikian or older.

Unit 3 comprises marble and calc-silicate rocks exposed in two slices within and at the margins of the gabbro-anorthosite body of unit 5. The sliver of unit 3 near the Upper Humber River is mostly white to pale grey, coarsely crystalline, in places graphitic, marble with some grey, impure, quartz-rich layers. In at least two outcrops near the contact with the gabbro, the marble grades into a brown and green (diopside-bearing) fine grained calc-silicate rock a few metres thick. The small sliver of unit 3 within unit 5 is a mottled grey and brown, fine grained, tremolite-rich calc-silicate rock exposed on an isolated knoll within the gabbro massif. It is included in unit 3 on the basis of broad lithological similarity, but its relation to the gabbro and to

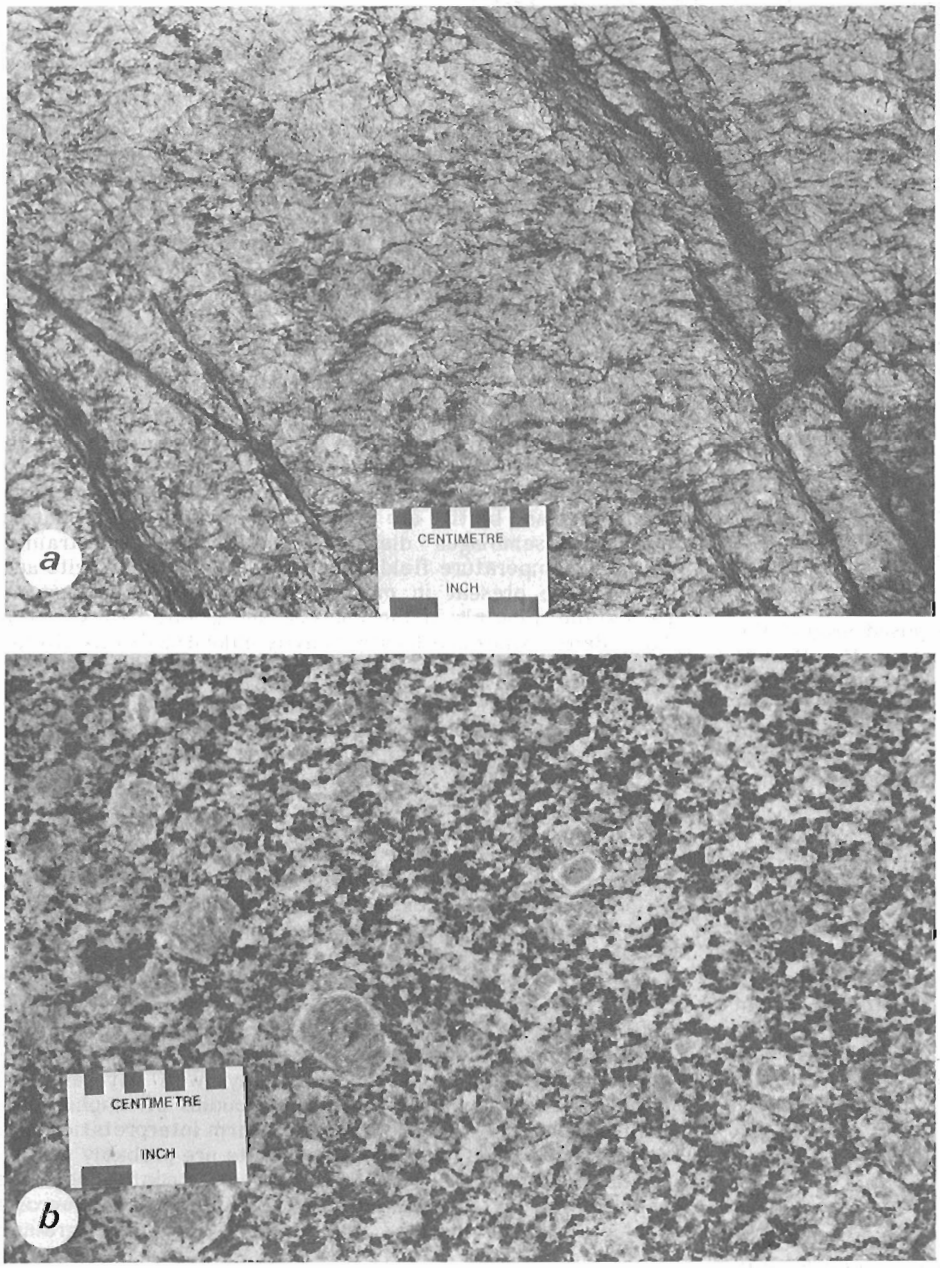

Figure 70.5

(a) Foliated megacrystic granite of unit 3 near Little Harbour Deep. (b) Massive granite of unit 3 north of Devil Cove.

the marble to the west is unclear. It may be similar to bands of tremolite-chlorite-carbonate rocks observed by Bostock (1983) in metagabbro to the north. It may be an intensely altered ultramafic phase or an inclusion within the anorthositic rocks. The marble to the west appears to be interlayered in the gneiss of unit 1, and to have been intruded by the gabbro along with unit 1. Unit 3 is considered to be Helikian.

Unit 4 is coarse grained, in places megacrystic, massive to well foliated hornblende granite exposed south of Gros Morne. Its contact with the gneiss to the east is gradational, and is assumed to be originally intrusive. Unit 4 is correlated with rocks of the posttectonic granitoid suite of Bostock (1983), and with parts of unit 3 in the coastal region. It is inferred to be of pre-Grenvillian age.

Unit 5 comprises a range of gabbroic to anorthositic rocks that occur in a large (at least 15 km across) intrusive complex between the Upper Humber River and Taylor Brook. Rock types include coarse grained (up to 5 cm) equigranular, ophitic gabbro and metagabbro, fine- to coarse-grained, dark anorthosite and gabbroic anorthosite, medium grained hornblende diorite, and medium grained buff monzonitic rocks. The rocks are generally massive; primary layering is outlined by mafic minerals in the gabbroic rocks. Dykes of gabbroic material in the surrounding rocks, and inclusions of granitic gneiss within unit 5 are exposed in several outcrops. Rocks of unit 5 may correlate broadly with rocks of the anorthosite suite recognized in Labrador by Bostock (1983), but they do not appear to have equivalents within the Long Range Mountains. Unit 5 is interpreted to be Helikian or older.

Units 1 to 5 are cut across by numerous diabase dykes of the Long Range swarm, which vary from 1 to 40 m in width, and appear to be generally better preserved here than along White Bay.

Unit 6 is fresh, dark green or pink, fine grained quartz-feldspar porphyry that occurs in several small, low outcrops to the east of Taylor Brook, and is seen as a dyke phase in unit 5 to the west of Taylor Brook. The rocks are not recrystallized and display little strain. They are inferred to be Hadrynian or younger, and to have intruded the Precambrian rocks along the southeast margin of the inlier. They may correlate with parts of the Lower Paleozoic Sops Arm Group mapped on strike to the north by Smyth and Schillereff (1982).

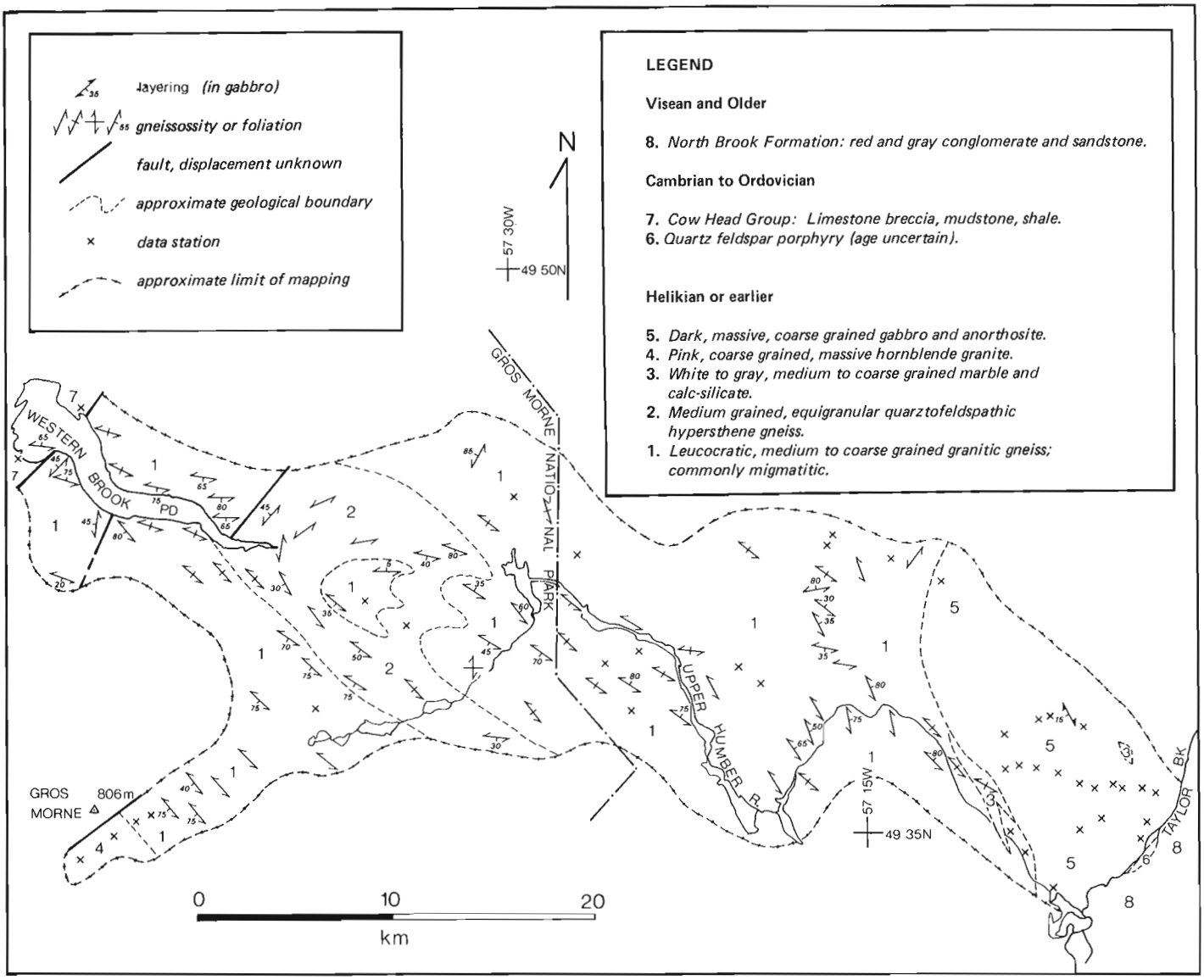

Figure 70.6. *General geology of the Upper Humber River region between Western Brook Pond and Taylor Brook. Data stations shown as "x" are where no structural observations were made.*

Unit 7 is the allochthonous Cow Head Group of Cambrian to Ordovician age (Schuchert and Dunbar, 1934; Oxley, 1953) which comprises interbedded limestone breccia, lime mudstone, calcarenite and shale on the north and south shores of Western Brook Pond. The contact with the gneiss to the east is not exposed; a brief examination of the Precambrian rocks in several localities along the approximate contact reveals extreme brecciation, iron staining and chloritization of the gneiss which suggest that the boundary is a fault.

Unit 8 is the North Brook Formation (Hyde, 1982) of Carboniferous (Visean) age, which includes red to grey, pebble to boulder conglomerate and interbedded red to grey sandstone and siltstone, and grey and pink limestone. The unit forms the margin of the Carboniferous Deer Lake Basin and lies unconformably on the Precambrian and Lower Paleozoic rocks to the west.

Structure

As in most of the rocks of the coastal region, the gneissic rocks of the Western Brook Pond – Taylor Brook area have a well developed planar fabric that is commonly folded in outcrop by irregular, asymmetric folds resulting from highly ductile strain. Banding in marble is inferred to be transposed original bedding.

The large fold structure outlined by unit 2 is well exposed at its western extremity and poorly defined in the east. It appears to be a slightly elongate dome. Discordant dips and the apparent occurrence of lower grade rocks of unit 1 near its centre, however, suggest a more complex structure, such as a nappe of granulite facies rocks infolded with lower grade gneiss into a northwest-plunging antiform with its own planar fabric at the centre. A detailed structural analysis is needed to test this hypothesis.

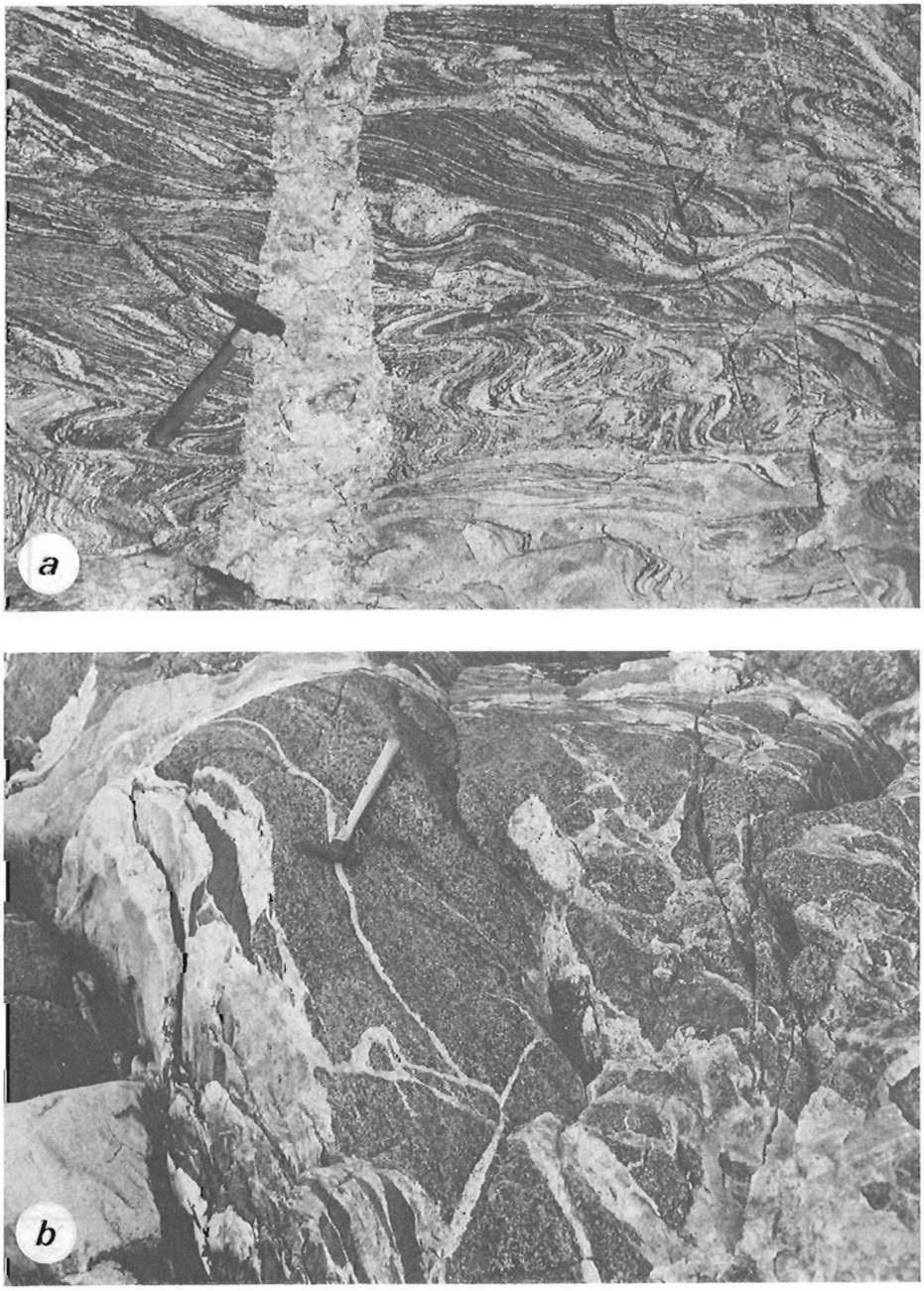

Figure 70.7

(a) Well layered, heterogeneous granitic gneiss of unit 1, near the Upper Humber River. (b) Amphibolite boudin in the same unit.

The faults exposed north and south of Western Brook Pond are large (longer than 10 km, from aerial photographs) and steep structures that are inferred to have been the locus of at least some dip-slip displacement, as the fault on the north side juxtaposes rocks of clearly different metamorphic grade.

The western contact of the Precambrian rocks was examined only briefly; within the brecciated zone (see above), slickensides in the gneiss appear to be variably oriented. Insufficient data are available to speculate on the nature of the fault that crosses Western Brook Pond.

Metamorphism

All rocks in units 1 to 5 of the Western Brook Pond-Taylor Brook area are recrystallized, but they do not appear to have the friable, sucrosic texture noted along White Bay. Migmatite bands and lenses are developed extensively in units 1 and 2. The sillimanite-bearing rocks of unit 1 and diopside-bearing rocks of unit 3 suggest that units 1, 3, 4 and 5 underwent metamorphism in the amphibolite facies; rocks of unit 2 were metamorphosed in the granulite facies, before being emplaced next to the amphibolite facies rocks. No retrogression to greenschist facies conditions is apparent in the region, in contrast to the rocks along White Bay. As noted above, the Long Range dykes are increasingly well preserved toward the west. On Western Brook Pond, several spectacular dykes of this swarm are unaltered, flinty diabase with no sign of alteration (Bostock and Cumming, 1973).

ACKNOWLEDGMENTS

Field assistance was provided by B. Mercer (Department of Earth Sciences, Memorial University). D. Besaw (Cat Arm Consultants) provided guidance at the Cat Arm Development site, and made his geological maps and notes available on several occasions. The existence and location of marble and related rocks was reported by D. Reusch (Department of Earth Sciences, Memorial University; personal communication, 1983). This report has been improved by comments from R.J. Wardle, C.F. Gower and M.J. Murray (Newfoundland Department of Mines and Energy).

REFERENCES

Baird, D.M.
1959: Sandy Lake (West Half), Newfoundland; Geological Survey of Canada, Map 47-1959.

Black, R.F.
1964: Paleomagnetic support of the theory of rotation of the western part of the island of Newfoundland; Nature, v. 202, p. 945-948.

Bostock, H.H.
1983: Precambrian rocks of the Strait of Belle Isle area; in Geology of the Strait of Belle Isle area, northwestern insular Newfoundland, southern Labrador and adjacent Quebec; Geological Survey of Canada, Memoir 400, p. 1-73.

Bostock, H.H. and Cumming, L.M.
1973: Some notes on the Precambrian rocks of the Gros Morne National Park, western Newfoundland; in Report of Activities, Part B, Geological Survey of Canada, Paper 73-1B, p. 109-119.

Clifford, P.M. and Baird, D.M.
1962: Great Northern Peninsula of Newfoundland, Grenville inlier; Canadian Mining and Metallurgical Bulletin, v. 65, p. 95-102.

Cook, F.A., Albaugh, D.S., Brown, L.D., Kaufman, S., Oliver, J., and Hatcher, R.D., Jr.
1979: Thin-skinned tectonics in the crystalline southern Appalachians; COCORP seismic-reflection profiling of the Blue Ridge and Piedmont; Geology, v. 7, p. 563-567.

Cumming, L.M.
1973a: Geology of the proposed Gros Morne National Park, western Newfoundland; in Report of Activities, Part A, Geological Survey of Canada, Paper 73-1A, p. 5-7.

1973b: Geology of Gros Morne National Park, western Newfoundland; Geological Survey of Canada, Regional and Economic Geology Division, manuscript (3 vols.).

Deutsch, E.R. and Rao, K.V.
1977: New palaeomagnetic evidence fails to support rotation of western Newfoundland; Nature, v. 266, p. 314-318.

Foley, F.C.
1937: Geology and mineral deposits of Hawkes Bay – Great Harbour Deep area, northern Newfoundland; Newfoundland Department of Natural Resources, Bulletin no. 10.

Fritts, C.E.
1953: Geological reconnaissance across the Great Northern Peninsula of Newfoundland; Newfoundland Mineral Resources Division, St. John's, Report no. 4.

Haworth, R.T., Daniels, D.L., Williams, H., and Zietz, I.
1980: Bouguer gravity anomaly map of the Appalachian Orogen; Memorial University of Newfoundland, Map no. 3.

Hyde, R.S.
1982: Geology of the Carboniferous Deer Lake Basin; Newfoundland Department of Mines and Energy, Mineral Development Division, Map 82-7.

Johnson, H.
1941a: Newfoundland; in Possible Future Oil Provinces of Eastern Canada; American Association of Petroleum Geologists, Bulletin, v. 25, p. 1558-1562.

1941b: Paleozoic Lowlands of northwestern Newfoundland; New York Academy of Sciences, Transactions, Series II, v. 3, p. 141-145.

Keppie, J.D.
– The Appalachian Collage; in The Caledonide Orogen, Scandinavia and related areas, ed. D.G. Gee and B. Sturt; Wyllie and Sons. (in press)

Murray, A. and Howley, J.P.
1881: Geological Survey of Newfoundland from 1864 to 1880; London, Edward Stanford, 536 p.

1918: Reports of Geological Survey of Newfoundland from 1881 to 1909; St. John's, Robinson & Company Ltd. Press, 725 p.

Neale, E.R.W. and Nash, W.A.
1963: Sandy Lake (East Half), Newfoundland; Geological Survey of Canada, Paper 62-28.

Nelson, S.J.
1955: Geology of Portland Creek – Port Saunders area, West Coast; Geological Survey of Newfoundland, Report no. 7.

Oxley, P.
1953: Geology of the Parsons Pond – St. Pauls area, West Coast; Geological Survey of Newfoundland, Report no. 5.

Pringle, I.R., Miller, J.A., and Warrell, D.M.
1971: Radiometric age determinations from the Long Range Mountains, Newfoundland; Canadian Journal of Earth Sciences, v. 8, p. 1325-1330.

Pullaiah, G., Rao, K.V., Deutsch, E.R., Murthy, G.S., and Morgan, D.
1979: Paleomagnetism of the Late Precambrian Long Range dikes, Newfoundland: an Acadian remagnetization?; Canadian Geophysical Union, Annual Meeting, Fredericton (abstract).

Schuchert, C. and Dunbar, C.O.
1934: Stratigraphy of western Newfoundland; Geological Society of America, Memoir 1, 123 p.

Smyth, W.R. and Schillereff, H.S.
1982: The pre-Carboniferous geology of southwest White Bay; in Current Research, ed. C.F. O'Driscoll and R.V. Gibbons, Newfoundland Department of Mines and Energy, Mineral Development Division, Report 82-1, p. 78-98.

Stukas, V. and Reynolds, P.H.
1974: $^{40}Ar/^{39}Ar$ dating of the Long Range dikes of Newfoundland; Earth and Planetary Science Letters, v. 22, p. 256-266.

Williams, H. and Hatcher, R.D., Jr.
1983: Appalachian suspect terranes; Geological Society of America, Memoir 158, p. 33-53.

71. DOLOMITES AND DOLOMITIZATION OF THE LOWER ORDOVICIAN ST. GEORGE GROUP OF WESTERN NEWFOUNDLAND[1]

Contract 03SU.23233-3-0443

Douglas W. Haywick and Noel P. James[2]

Haywick, D.W. and James, N.P., Dolomites and dolomitization of the Lower Ordovician St. George Group of western Newfoundland; in Current Research, Part A, Geological Survey of Canada, Paper 84-1A, p. 531-536, 1984.

Also in Current Research, Newfoundland Department of Mines and Energy, Mineral Development Division, Report 84-1, 1984.

Abstract

Dolomite makes up approximately one third of the carbonates in the St. George Group of western Newfoundland and six varieties are now recognized.

Dololaminites are ubiquitous, composed of very fine crystals, characteristically laminated and thought to have been formed in shallow marine to supratidal environments. Intramuros dolomite preferentially replaces trace fossil walls as well as certain fossilized shells, is concentrated along stylolites, and is responsible for the dolomitic mottling so prevalent within the St. George Group. Pervasive dolostone is also mottled, but is the result of two different types of dolomite, one with finer crystallinity than the other. Matrix dolomite replaces carbonate mud between allochems and burrows and when extensive, expands to replace the whole rock. Cavity-filling dolostone is finely crystalline and has filled dissolution cavities or voids within pre-existing dolostone and may be related to unconformities. Saddle dolomite fills late stage fractures and voids and in combination with pervasive dolostone, is responsible for "pseudo breccia" beds associated with economic deposits of sphalerite.

Dololaminites are the earliest, probably syn-sedimentary, dolostones whereas saddle dolomite, because it cuts across most other varieties, is clearly the latest. The fact that saddle dolomite is restricted to areas in the northern portion of Great Northern Peninsula implies that this area was affected by a later dolomitization event which did not occur in more southern regions.

Résumé

La dolomite forme environ le tiers des carbonates dans le groupe de St. George de l'ouest de Terre-Neuve; on en reconnaît actuellement six variétés.

Les laminites dolomitiques sont omniprésentes; composées de cristaux très fins, elles ont des laminations caractéristiques et se seraient accumulées dans des milieux marins allant de peu profonds à supratidaux. La dolomite intra-muros remplace de préférence les murs des empreintes fossiles ainsi que certains coquillages fossilisés; elle est concentrée le long de stylolites et cause le mouchetage dolomitique si commun dans le groupe de St. George. La dolomie pénétrante, également mouchetée, est produite par deux types différents de dolomite, l'une plus fine que l'autre. La dolomite matricielle remplace la boue carbonatée entre les allochèmes et les terriers; lorsqu'elle se présente en vastes quantités, elle prend de l'expansion et remplace la roche entière. La dolomie de remplissage est finement cristalline et remplit les trous ou les vides laissés par le processus de dissolution dans les dolomies déjà existantes; elle pourrait être liée à des discordances. La dolomite anticlinale remplit des fractures et des vides récents et, conjugué avec la dolomie pénétrante, est à l'origine des lits de pseudobrèches associés aux gisements économiques de sphalérite.

Les laminites dolomitiques, de nature vraisemblablement synsédimentaires, sont les dolomies les plus anciennes, tandis que la dolomite anticlinale est évidemment la plus récente, puisqu'elle recoupe la plupart des autres variétés. En raison du fait que la dolomite anticlinale est limitée à des régions dans le nord de la Grande presqu'île du Nord, il se peut que cette région ait subi une phase de dolomitisation plus récente qui ne se soit pas produite plus au sud.

INTRODUCTION

The Lower Ordovician St. George Group of western Newfoundland has been extensively studied over the past few years (Levesque, 1977; Knight, 1977a, b, 1978; Pratt, 1979; Smyth, 1982a, b, c) with the result that the stratigraphy, sedimentology, and paleontology of these rocks are relatively well documented. However, little is known about the dolomites which account for approximately one third of the St. George Group. The purpose of the study is threefold; to fully document the various textures exhibited by the dolomites, to determine their stratigraphic and geographic distribution, and to examine possible mechanisms to explain the modes of dolomitization. This preliminary report addresses the first two objectives.

The St. George Group outcrops semi-continuously along the west coast of Newfoundland from the Port au Port Peninsula in the south to Cape Norman in the north. Five sections were studied in the vicinity of the Port au Port Peninsula and a further four sections were studied at specific points along the Great Northern Peninsula during the summer of 1983. In addition, several key locations which contained interesting dolomite relationships, but where sections could not, or were not measured, were also investigated.

ACKNOWLEDGMENTS

This research is in part funded by Contract 03SU.23233-3-0443 to Geological Survey of Canada and in part by NSERC grant number A-9159 to N.P. James and an

[1] Contribution to Canada-Newfoundland co-operative mineral program 1982-84. Project carried by Geological Survey of Canada.

[2] Department of Earth Sciences, Memorial University of Newfoundland, St. John's, Newfoundland A1B 3X5

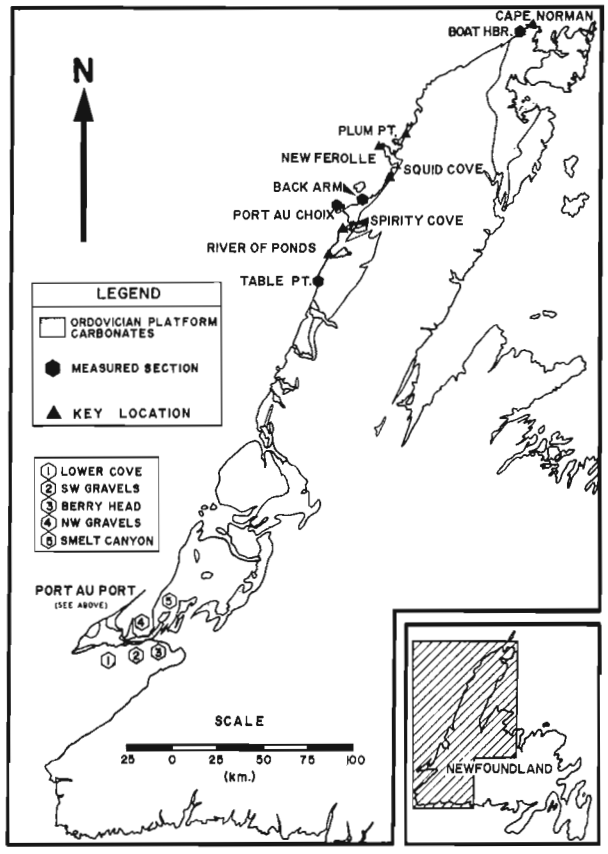

Figure 71.1. Location map of Lower Ordovician platformal carbonate rocks along the west coast of Newfoundland. The position of measured sections and key locations investigated during this study are also indicated.

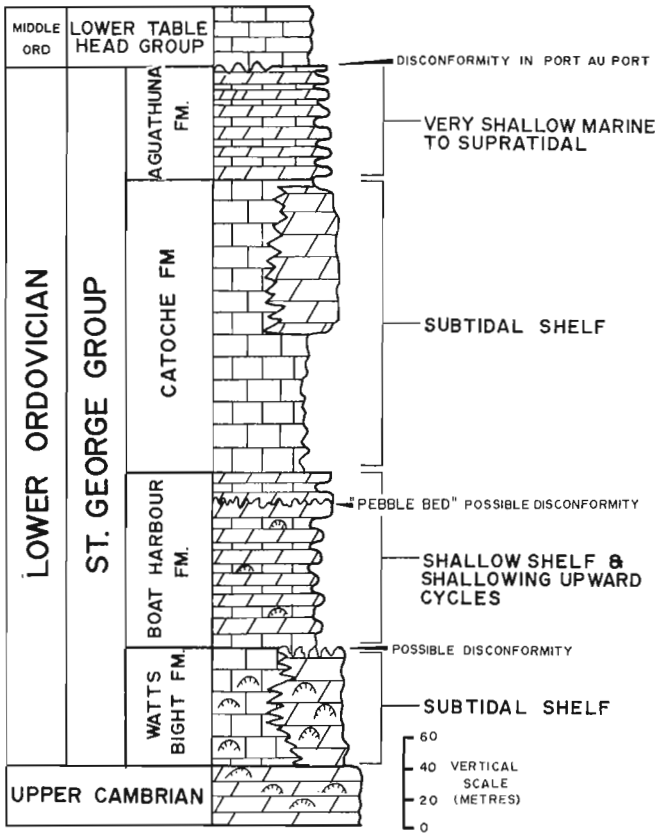

Figure 71.2. Schematic stratigraphic section of the Lower Ordovician St. George Group. Proposed depositional environments (in heavy type) and the locations of disconformities within the St. George Group are summarized on the right side of the section. Coarsely crystalline dolomitization of parts of the Watts Bight and Catoche formations are indicated by the cross hatched pattern. (Data from Knight, 1977b, 1978).

American Association of Petroleum Geologists (AAPG) research grant to D.W. Haywick. S. Scott was the able bodied field assistant. Special thanks are extended to I. Knight, D.F. Sangster, G. Narbonne, and T.E. Lane for many meaningful discussions. D. Bird, J.W. Pickett, and S. Pohler made improvements to the manuscript.

GENERAL GEOLOGY AND STRATIGRAPHY

The Lower Ordovician St. George Group is part of the Cambro-Ordovician platformal sequence (the ancient continental margin of North America) that was assigned by Williams (1978, 1979) to the Humber Zone of the Newfoundland Appalachians (Fig. 71.1). Although the formational nomenclature has been modified extensively since Schuchert and Dunbar's pioneer work published in 1934, it is now generally agreed that the St. George Group can be subdivided into four formations (I. Knight and N.P. James, personal communication, 1983).

The lowermost unit, the Watts Bight Formation conformably overlies upper Cambrian peritidal and stromatolitic dolostones and is characterized by dark grey to black, vuggy and often cherty stromatolitic dolostone (Fig. 71.2). In some regions, particularly Hare Bay and possibly on Port au Port Peninsula, the Watts Bight Formation is a bioturbated and often fossiliferous mudstone to wackestone. This suggests that prior to dolomitization, the rocks of the Watts Bight Formation were subtidal shelf deposits (Knight, 1977a, b, 1978).

A breccia bed, possibly indicating a disconformity, separates the Watts Bight Formation from the overlying Boat Harbour Formation along the Great Northern Peninsula (Knight, 1977b). This breccia bed appears to be somewhat localized as the contact seems conformable where exposed in the Port au Port area.

The Boat Harbour Formation is a series of thick bedded, bioturbated or laminated dolostones and thin- to thick-bedded stromatolitic and/or bioturbated limestones. Levesque (1977), Knight (1977a, b), and Pratt (1979) regarded this formation as being the result of repeated shallowing upward sequences.

A possible break in sedimentation near the top of the Boat Harbour Formation has been suggested by Knight (1978) and Pratt (1979) who cited a layer of chert pebbles and silicified ooids and intraclasts as evidence of an exposure surface. Locally referred to as the "pebble bed", this horizon appears to be of wide extent ranging from the Port au Port vicinity to Cape Norman (Pratt, 1979).

The Boat Harbour Formation is conformably overlain by the Catoche Formation, a bioturbated, fossiliferous mudstone to wackestone of which the faunal content suggests a predominantly subtidal depositional environment (Levesque, 1977; Knight, 1977a, b, 1978; Pratt, 1979).

Table 71.1. Summary of distinguishing characteristics and the proposed paragenetic sequence of the six varieties of dolomite and dolostone observed within the St. George Group

	DOLOMITE TYPE	CRYSTAL SIZE	COLOUR	PERCENT. OF HOST ROCK	DISTINGUISHING CHARACTERISTICS	DISTRIBUTION	
						STRATIGRAPHIC	GEOGRAPHIC
EARLY	1) DOLO-LAMINITES	VERY FINE	BUFF to WHITE	100%	CONTAINS ABUNDANT SHALLOW WATER SEDIMENTARY STRUCTURES (ie. MUDCRACKS, PRISM CRACKS, LAMINATIONS)	AGUATHUNA & BOAT HARBOUR FMS.	WIDESPREAD
	2) INTRA-MUROS DOLOMITE	0.1 mm.	BUFF to DOVE GREY	tr. to 40%	SELECTIVELY REPLACES ICHNOFOSSIL WALLS AND SOME FOSSILIZED SHELLS. CAN BE LOCALIZED ALONG STYLOLITES	WIDESPREAD	WIDESPREAD
	3) MATRIX DOLOMITE	0.1 mm.	BUFF	5 to 100%	REPLACES CARBONATE MUD BETWEEN ALLOCHEMS AND ICHNOFOSSILS.	CATOCHE, BOAT HARBOUR & WATTS BIGHT FMS.	PORT AU PORT
	4) PERVASIVE DOLOSTONE SUB-TYPE (A)	0.1 & 0.3 mm.	MED. GREY	95 to 100%	FINER CRYSTALLINE DOLOMITE IS LOCALIZED IN ICHNOFOSSILS, FOSSILS AND GASTROPOD SHELL WALLS. COARSER CRYSTALLINE DOLOMITE OCCURS IN THE INTERAREAS BETWEEN THESE FEATURES.	WIDESPREAD	WIDESPREAD
	4) PERVASIVE DOLOSTONE SUB-TYPE (B)	0.1 to 0.3 mm. & 1.0 mm.	MED. GREY to WHITE	100%		CATOCHE, BOAT HARBOUR & WATTS BIGHT FMS.	NORTHERN PENINSULA
	5) CAVITY FILLING DOLOSTONE	VERY FINE	BUFF	100%	TYPICALLY GEOPETAL, HAS FILLED DISSOLUTION CAVITIES AND VOIDS IN PRE-EXISTING DOLOSTONE.	BOAT HARBOUR & WATTS BIGHT FMS	LOCALIZED OCCURRENCES PORT AU PORT & NORTHERN PENINSULA
LATE	6) SADDLE DOLOSTONE	0.5 to 15.0 mm.	WHITE to PINK	100%	FILLS IN FRACTURES AND VOIDS WITHIN PRE-EXISTING DOLOSTONE.	CATOCHE, BOAT HARBOUR & WATTS BIGHT FMS.	NORTHERN PENINSULA

North of Table Point (Fig. 71.1), much of the limestone of the Catoche Formation has been replaced by white, sparry dolomite. This dolomite is host to economic sphalerite mineralization in the Daniel's Harbour area.

The Aguathuna Formation conformably overlies the Catoche Formation and is the uppermost division of the St. George Group. A unit of interbedded finely crystalline and laminated dolostones, dolomitic shales and limestones, the Aguathuna Formation was probably deposited in a shallow water to supratidal environment much like the Boat Harbour Formation below (Levesque, 1977; Knight, 1978; Pratt, 1979).

The Aguathuna Formation is extremely variable in thickness. In the Port au Port area, the interbedded limestones and dolostones are a minimum of 50 m thick. Farther north at Table Point, the Aguathuna Formation is exclusively dolostone and is approximately 75 m thick (Levesque, 1977). Still farther north at Port au Choix, the formation is a mere 10 m thick and consists only of a few dolostone beds. The Aguathuna Formation does not seem to be present at all in the Cape Norman area.

This Lower Ordovician sequence is overlain by the Middle Ordovician Table Head Group whose basal limestones are thought to have been deposited in an intertidal to subtidal setting (Klappa et al., 1980). The contact between the St. George and Table Head groups has been well documented as a disconformity on the Port au Port Peninsula along which up to several metres of strata have been removed (Schuchert and Dunbar, 1934; Cumming, 1968). In recent years, however, the importance of this disconformity has been questioned, especially along the west coast of the Great Northern Peninsula where strata appear to be continuous across the boundary.

The basal limestones of the Table Head Group pass upwards into deep water carbonates, shales and finally flysch recording the collapse of the stable continental margin (Klappa et al., 1980).

TEXTURAL TYPES OF DOLOMITE AND DOLOSTONE

The various dolomites and dolostones within the St. George Group can be separated into six distinct types. At this stage of investigation, the principal distinguishing criteria are limited to dolomite crystal size, sedimentary structures and textural relationships. The characteristics of the six varieties of dolomite and dolostone as well as their approximate paragenetic sequence, are summarized in Table 71.1.

Type 1: dololaminites

Dololaminates are dolostones characterized by a very fine crystal size and numerous fine laminations (Plate 71.1) (Wanless, 1979). They contain an abundance of sedimentary structures which include mudcracks, prism cracks, tepees, small-scale crossbedding and flat-pebble breccias. Colourless or white chert is commonly present in dololaminites, either as individual nodules or in discontinuous horizons. Both ichnofossils and body fossils are noticeably absent.

Sedimentologial studies by Levesque (1977), Knight (1977a, b, 1978) and Pratt (1979) have concluded that these dolostones probably formed early in very shallow marine to supratidal environments.

A common component of both the Boat Harbour and Aguathuna formations, dololaminites are widespread and are found in most sections and outcrops examined in this study.

Type 2: intramuros dolomite

The second textural type of dolomite is responsible for the mottling which is so common in most of the limestones within the St. George Group (Plate 71.1). The dolomite is finely crystalline and preferentially replaces trace fossils walls, the shells of some fossils, laminations and/or stylolites. Because of its affinity for burrow walls, this type of dolomite is referred to as intramuros (Latin for "within the walls").

A

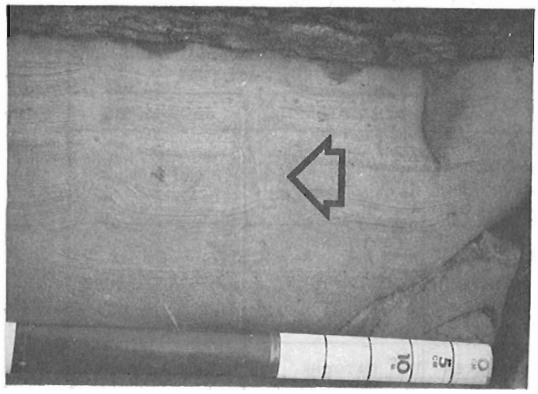

B

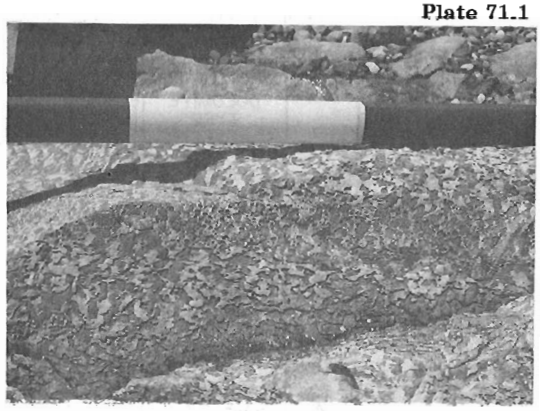

C

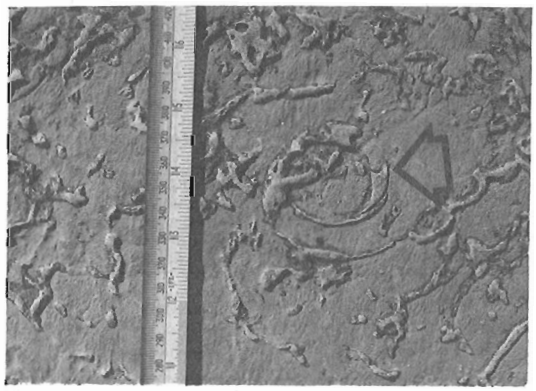

D

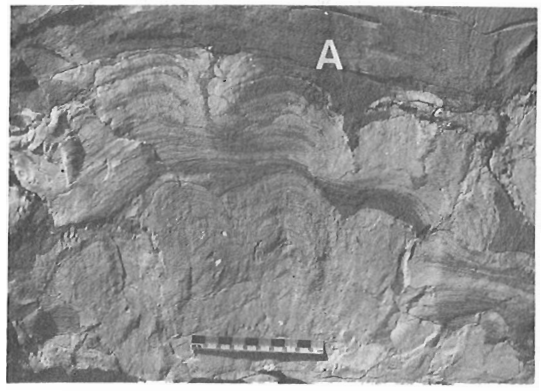

E

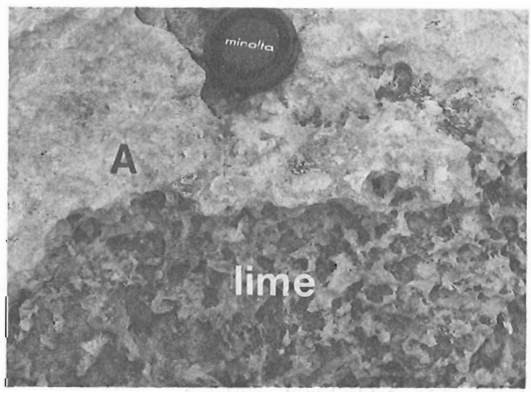

F

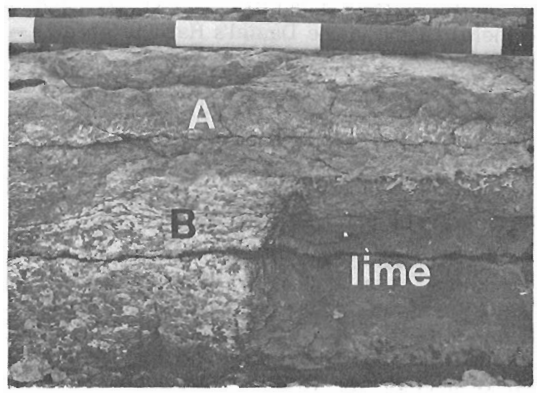

G

H

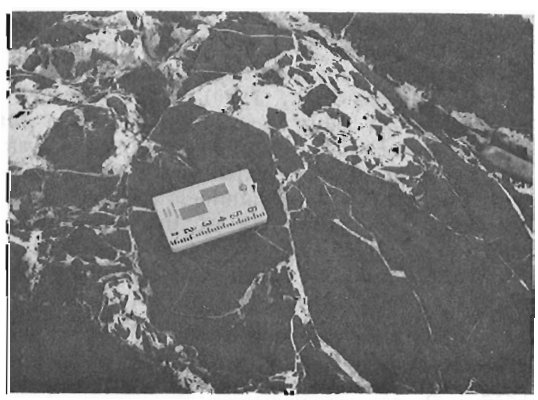

There are variable degrees of intramuros dolomite, ranging from instances of exclusive trace fossil-mottling to instances of exclusive stylolite-mottling. It is tempting to separate out several subtypes to account for the variability observed within this type of dolomite, but even within a single limestone bed, there are zones favouring one "subtype" over another, and consequently a complicated classification scheme for intramuros dolomite would probably cause more confusion than clarification. For the present time, therefore, intramuros dolomite will not be subdivided.

Plate 71.1

Various textures of dolomite and dolostone observed within rocks of the St. George Group

A. Dololaminites are characterized by a very fine crystal size and by shallow water sedimentary structures. This dololaminite from the Boat Harbour Formation on Port au Port Peninsula clearly shows prism cracks (arrow) and fine laminations.

B. Limestone mottled with buff coloured intramuros dolomite from the Boat Harbour Formation, Port au Port. The white portion of the scale bar is 25 cm long.

C. Bedding plane view of the intramuros dolomite displayed in B. The dolomite is localized within gastropod shell walls (arrow) and ichnofossils.

D. Matrix dolomite, unlike intramuros dolomite, does not preferentially replace trace or body fossils so that often the original fabric of the rock is lost. In some instances however, such as this example from the Aguathuna Formation in the Port au Port area, dolomite (labelled A) replaces the matrix between stromatolites but not the stromatolites themselves. As a result, part of the original fabric is preserved.

E. Pervasive dolostone, subtype A (labelled A) in contact with a limestone containing intramuros dolomite (labelled lime) within the Watts Bight Formation, Port au Port. Weak mottling within the dolostone is due to the presence of two crystal sizes; finer dolomite being localized within ichnofossils and coarser dolomite being localized between ichnofossils. The camera lens cap is 6 cm in diameter.

F. Pervasive dolostone, subtype A (labelled A) in contact with pervasive dolostone subtype B (labelled B) and limestone (labelled lime) within the Catoche Formation, Cape Norman. The two subtypes of pervasive dolostone can be distinguished from one another by the appearance and crystal size of the dolomite that occupies the interareas between ichnofossils. The dolomite within the interareas in subtype B is usually much lighter in colour and more coarsely crystalline than that found between ichnofossils in subtype A. Scale bar divisions are 25 cm across.

G. Cavity-filling dolostone (arrow) is typically geopetal and infills voids or cavities within pre-existing dolostone. This example occurs within a stromatolite-rich portion of the Watts Bight Formation near Boat Harbour. The field book is 19 cm across.

H. Saddle dolomite is the latest phase of dolomite observed in the St. George Group. It is localized within fractures and veins that cut across most of the other varieties of dolomite and dolostone. This example is from the Catoche Formation, Table Point.

It is unclear at this time as to the role stylolites have played in the development of intramuros dolomite. Some clearly have acted as zones where dolomitization was initiated (Wanless, 1979), but many also appear to have simply entrapped the more resistant dolomite rhombs during periods of pressure solution. The role that ichnofossils and some shells (especially gastropods) have played is more straightforward. Dolomitization was initiated in the walls of the ichnofossils and shells and spread both inward and outward into the neighbouring limestone once the walls had been completely replaced. This dolomitization occurred relatively early in the diagenetic history of the rock, but probably postdates the event responsible for the dololaminites. This is evidenced by field relationships observed in and between the two dolomite varieties.

The percentage of intramuros dolomite within a host limestone reflects both the intensity of bioturbation and the degree of replacement of the trace fossils. Proportions range from trace quantities to approximately 40 per cent and average overall to approximately 10 per cent.

Intramuros dolomite is widespread, both stratigraphically and geographically. It is present in particularly every limestone bed in every formation of the St. George Group and in all outcrops studied.

Type 3: matrix dolomite

Type 3 is best described as matrix-selective dolomite (Plate 71.1). In packstone and grainstone beds, finely crystalline dolomite rhombs can often be observed replacing the matrix between grains, but not the grains themselves. In the finer grained mudstones and wackestones, dolomite rhombs are randomly distributed over the entire volume of the bed.

Primarily features such as trace fossils are not preferentially dolomitized, and thus commonly a great deal of the original fabric is lost. Occasionally, however, matrix dolomite will selectively replace some parts of a limestone over others with the result that some of the original fabric (usually stromatolitic) is preserved.

Dolomite-mottled stylolites are present in finer grained limestones containing matrix dolomite, but they do not appear to be directly responsible for the dolomitization. They have more likely entrapped dolomite rhombs during a period of pressure solution. Stylolites do, however, tend to mark boundaries between regions of higher and lower proportions of matrix dolomite. This variability can be intense, ranging from approximately 5 per cent to close to 100 per cent within a single bed.

Matrix dolomite probably developed early in the diagenetic history of the rocks. Exact timing is not yet possible, however, on the basis of similar crystal size and field relationships, it is likely that this type of dolomite formed at about the same time as intramuros dolomite.

Matrix dolomite is not abundant in the St. George Group being restricted to the limestones of the Watts Bight, Boat Harbour, and Aguathuna formations in the Port au Port area only.

Type 4: pervasive dolostone

Pervasive dolostone is composed of two generations of dolomite, each generation being characterized by a distinct crystal size. Superficially, this bimodal distribution has resulted in a mottled appearance to the rock.

Two subtypes of pervasive dolostone are recognized within the St. George Group (Plate 71.1). In both cases, finer dolomite is localized within ichnofossils, stylolites and gastropod shell walls, much the same as intramuros dolomite. However, unlike intramuros dolomite where interareas between ichnofossils, stylolites, and gastropod shell walls are undolomitized, the interareas in pervasive dolostone have been dolomitized. The two subtypes of pervasive dolostone can be distinguished from one another by the nature of the dolomite crystals that occupy these interareas. In subtype A, the crystals are medium grey and are finely crystalline. In subtype B, the crystals within the interareas are white to pink and are coarsely crystalline.

Both varieties of pervasive dolostone are common components of the Watts Bight, Boat Harbour and Catoche formations, but differ in their geographic distribution. Subtype B is found only in areas north of Table Point, whereas subtype A is widespread. Textural evidence suggests that subtype B is the result of a dolomitization event later than the one responsible for subtype A. The fact that subtype B is restricted to the Great Northern Peninsula implies that the northern part of the study area was subjected to a late phase of dolomitization which did not affect more southerly areas.

Type 5: cavity-filling dolostone

This dolostone is best described as cavity-filling (Plate 71.1). It occurs in small (less than 30 cm), irregularly shaped cavities within preexisting pervasive dolostone and is finely crystalline, faintly laminated and usually geopetal.

Towards the top of the Boat Harbour Formation on Port au Port Peninsula, cavity-filling dolostone occurs immediately beneath the pebble bed, which has been interpreted as a possible exposure surface (Knight, 1978; Pratt, 1979). There are also several occurrences of cavity-filling dolostone within the pervasive dolostones of the Watts Bight Formation in the Boat Harbour and New Ferolle areas. It is unclear, however, whether or not these occurrences are due to as yet undiscovered disconformities.

Type 6: saddle dolomite

The sixth phase of dolomitization is responsible for the white to pink, very coarsely crystalline and typically saddle-shaped dolomite crystals found exclusively north of Table Point. Saddle dolomite is associated with pervasive dolostone and usually occurs in fractures and veins cutting across the host rock (Plate 71.1). It may also replace the finely crystalline dolomite which marks trace fossils and stylolites in the pervasive dolostone.

In localities where saddle dolomite fractures or veins cut across limestones, there does not seem to be any "dolomite aureole" penetrating the surrounding limestone. It appears then, that this variety of dolomite did not itself cause dolomitization, but simply infilled open fractures. Therefore, saddle dolomite can be thought of as "void-filling."

Saddle dolomite, when associated with the pervasive variety, often develops the texture locally referred to as "pseudobreccia" and it is this pseudobreccia which is associated with sphalerite mineralization in the Daniel's Harbour area of western Newfoundland.

The event, which is responsible for the emplacement of saddle dolomite, is clearly the latest one in the diagenetic history of these rocks. This is evidenced by the fact that saddle dolomite veins cut across most other varieties of dolomite and dolostone. Dololaminites on the other hand are products of the earliest phase of dolomitization. The other varieties formed between the period of time marked by these two end members, probably in the order discussed in this report and summarized in Table 71.1.

REFERENCES

Cumming, L.M.
1968: St. George-Table Head disconformity and zinc mineralization, western Newfoundland; Canadian Institute of Mining and Metallurgy Bulletin, June, p. 721-725.

Klappa, C.F., Opalinski, P.R., and James, N.P.
1980: Middle Ordovician Table Head Group of western Newfoundland: A revised stratigraphy; Canadian Journal of Earth Sciences, v. 17, p. 1007-1019.

Knight, I.
1977a: The Cambrian-Ordovician platformal rocks of the Northern Peninsula; Mineral Development Division, Newfoundland Department of Mines and Energy Report 77-1, p. 27-34.

1977b: The Cambrian-Ordovician platformal rocks of the Northern Peninsula; Mineral Development Division, Newfoundland Department of Mines and Energy Report 77-6, p. 1-27.

1978: Platformal sediments on the Great Northern Peninsula: Stratigraphic studies and geological mapping of the North St. Barbe district; Mineral Development Division, Newfoundland Department of Mines and Energy Report 78-1, p. 140-150.

Levesque, R.J.
1977: Stratigraphy and sedimentology of Middle Cambrian to Lower Ordovician shallow water carbonate rocks, western Newfoundland; unpublished M.Sc. thesis, Memorial University of Newfoundland, 276 p.

Pratt, B.R.
1979: The St. George Group (Lower Ordovician), western Newfoundland: Sedimentology, diagenesis and cryptalgal structures; unpublished M.Sc. thesis, Memorial University of Newfoundland, 254 p.

Schuchert, C. and Dunbar, C.O.
1934: Stratigraphy of western Newfoundland; Geological Society of America, Memoir 1, 123 p.

Smyth, W.R. (Compiler)
1982a: Geology Blanc-Sablon/St. Anthony; Mineral Development Division, Newfoundland Department of Mines and Energy, Map 82-54.

1982b: Geology Port Saunders; Mineral Development Division, Newfoundland Department of Mines and Energy, Map 82-53.

1982c: Geology Sandy Lake; Mineral Development Division, Newfoundland Department of Mines and Energy, Map 82-54.

Wanless, H.R.
1979: Limestone response to stress: Pressure solution and dolomitization; Journal of Sedimentary Petrology, v. 49, p. 437-462.

Williams, H. (Compiler)
1978: Tectonic lithofacies map of the Appalachian Orogen; Memorial University of Newfoundland, Map 1.

1979: Appalachian orogen in Canada; Canadian Journal of Earth Sciences, v. 16, p. 792-807.

72. GEOLOGY OF THE WOLF MOUNTAIN (EAST HALF) AND DOLLAND BROOK (EAST HALF) MAP AREAS, SOUTH-CENTRAL NEWFOUNDLAND[1]

Project 820026

W.L. Dickson[2] and P.W. Delaney[3]

Dickson, W.L. and Delaney, P.W., Geology of the Wolf Mountain (east half) and Dolland Brook (east half) map areas, south-central Newfoundland; in Current Research, Part A, Geological Survey of Canada, Paper 84-1A, p. 537-544, 1984.

Also in Current Research, Newfoundland Department of Mines and Energy, Mineral Development Division, Report 84-1, 1984.

Abstract

The Wolf Mountain (east half) and Dolland Brook (east half) map areas, in south-central Newfoundland, contain metasedimentary and minor volcanic rocks assigned in part to the Lower to Middle Ordovician Spruce Brook Formation(?), Baie d'Espoir Group and Bay du Nord Group. These rocks have been deformed and metamorphosed to greenschist facies, with migmatization of the northern part of the Spruce Brook Formation and all of the Bay du Nord Group. A small area around Dolland Pond contains metasediments of possible Silurian age. The Ordovician units have been intruded by the Silurian-Devonian North Bay Granite, a large batholith composed primarily of massive to very weakly foliated, biotite ± muscovite, K-feldspar porphyritic granite. Some of the smaller, older granitoid units of the North Bay Granite possess a strong foliation. The Burgeo Batholith, within the map area, is strongly mylonitized and forms part of a 100 km long mylonite zone.

Résumé

Les régions cartographiques de Wolf Mountain (moitié est) et de Dolland Brook (moitié est), dans la partie sud-centrale de Terre-Neuve, contiennent des roches métasédimentaires et de petites quantités de roches volcaniques classées en partie dans la formation de Spruce Brook(?), dans le groupe de Baie d'Espoir et dans le groupe de Bay du Nord de l'Ordovicien ancien à moyen. Ces roches ont été déformées et métamorphisées jusqu'au degré du faciès à schistes verts et il y a eu migmatisation de la partie nord de la formation de Spruce Brook et de tout le groupe de Bay du Nord. Une petite région autour de l'étang Dolland contient des métasédiments datant peut-être du Silurien. Le granite de North Bay, gros batholite d'âge silurien à dévonien composé surtout de granite porphyrique à biotite ± muscovite et à feldspath potassique massif à très faiblement feuilleté, a fait intrusion dans les unités ordoviciennes. Certaines des unités granitoïdes plus petites et plus anciennes du granite de North Bay font voir une foliation marquée. Le batholite de Burgeo, situé dans la région cartographique, est fortement mylonitisé et fait partie d'une zone de mylonite longue de 100 km.

INTRODUCTION

Regional setting

The North Bay Granite in south-central Newfoundland is a large (>3000 km^2) composite pluton which intruded Lower to Middle Ordovician sedimentary rocks during the later stages of the Silurian-Devonian Acadian Orogeny. The bathlith is curved in outline and lies in the central part of the Hermitage Flexure, a major structure defined by pronounced swings in the generally northeasterly Appalachian trend of the Lower Paleozoic rocks in eastern and southern Newfoundland (Williams et al., 1970).

The North Bay Granite is economically significant as it is the host of W-Mo mineralization at its northern termination 10 km northwest of Meelpaeg Lake. With mapping carried out by Blackwood (1984) and O'Brien and Tomlin (1984), this work completes mapping and geochemical sampling of the North Bay Granite in south-central Newfoundland (Blackwood, 1983; Colman-Sadd, 1976, 1983; Colman-Sadd et al., 1981; Dickson, 1982; Dickson and Tomlin, 1983). Possible continuations of the North Bay granitoid terrane in central Newfoundland may be examined during 1984 and 1985.

Location and access

The Dolland Pond (11 P/15 E) and Wolf Mountain (12 A/2 E) map areas are located in south-central Newfoundland. The closest, easily accessible settlement is the town of St. Alban's, located 50 km east of the Dolland Brook map area. Access is gained to Meelpaeg Lake in the Wolf Mountain map area by woods roads and access roads to hydroelectric dam sites from Millertown, 80 km to the north. Helicopter support is available from St. Alban's and nearby Milltown.

The area was mapped at a scale of 1:50 000 mainly from helicopter-placed fly camps or by boat and canoe around Meelpaeg Lake. The poorly exposed area between 47°50'N and 47°55'N was surveyed by helicopter.

Previous work

The earliest work in the map area was carried out by the Buchans Mining Company with a survey carried out to the southeast of Meelpaeg Lake (Phendler, 1950) and to the southwest of Dolland Brook (Scott and Conn, 1950; see also Smyth, 1979). The only other major work in the area was by Williams (1970, 1971) who carried out 1:250 000 mapping and outlined the major units.

[1] Contribution to the Canada-Newfoundland co-operative mineral program 1982-84. Project carried by the Geological Survey of Canada and Newfoundland Department of Mines and Energy.

[2] Newfoundland Department of Mines and Energy, Mineral Development Division, P.O. Box 4750, St. John's, Newfoundland A1C 5T7

[3] Department of Earth Sciences, Memorial University, St. John's, Newfoundland A1B 3X5

Lake sediment geochemical surveys in this area indicated that the granitoid rocks were relatively low in Cu, Ag, Mo, U and F (Butler and Davenport, 1978; Davenport and Butler, 1981). However, tungsten values were anomalous over several areas of the North Bay Granite (Davenport and Butler, 1982) including areas of the North Bay Granite with known tungsten mineralization, 10 km northeast of Meelpaeg Lake (Dickson, 1982). A stream sediment and soil survey carried out over the tungsten anomalies (McConnell, 1984) resulted in the discovery of minor scheelite-pyrite mineralization in granite bedrock east of Dolland Brook (Fig. 72.1).

Adjacent map areas to the west, 11 P/15 W and 12 A/2 W, have been surveyed at a scale of 1:50 000 by Blackwood (1984) and Dickson (1982), respectively. The map areas to the east, 12 A/1 and 11 P/16, have also been mapped at 1:50 000 by Colman-Sadd (1984) and Dickson and Tomlin (1983), respectively.

General geology

The Dolland Pond (11 P/15 E) and the western half of Wolf Mountain (12 A/2 E) map areas (Fig. 72.1) are dominated by a variety of granitoid rocks which form the southwestern part of the late Acadian North Bay Granite (Jewell, 1939) which underlies an area in excess of 3000 km^2. To the northeast, in the Wolf Lake – Meelpaeg Lake area, the geology is more complex with much of the area underlain by a variety of metasediments provisionally assigned to the Lower to Middle Ordovician Spruce Brook Formation (Colman-Sadd and Swinden, 1982) and the Baie d'Espoir Group (Jewell, 1939; Colman-Sadd, 1976). To the southwest of Dolland Brook, the North Bay Granite is separated from the highly mylonitized granite of the late Acadian Burgeo Batholith by a narrow belt of migmatite and granite veins assigned to the Lower to Middle Ordovician Bay du Nord Group (Chorlton, 1978).

An elongate belt of highly deformed leucocratic granitoids separates the Ordovician metasediments and smaller granitoid intrusions, mainly within the Wolf Mountain map area, from the main mass of the North Bay Granite to the south. A similar zone of highly deformed granitoids with associated migmatite separates the Ordovician Salmon River Dam Formation in the north from the main mass of the North Bay Granite in the adjacent D'Espoir Lake map area to the east (Dickson and Tomlin, 1983).

In the southern part of the Dolland Brook map area, four quartz-feldspar porphyry dykes intrude the North Bay Granite and represent the last phase of acid magmatism in the area.

The map area is covered with a thick blanket of till in the vicinity of Meelpaeg Lake, Wolf Lake, Dolland Pond and the Dolland Brook area. Glacial striae and stoss and lee surfaces indicate a south-southeasterly direction of ice flow. Eskers are common with an 8 km long esker preserved in the northern half of Wolf Lake.

DESCRIPTION OF UNITS

Lower to Middle Ordovician Spruce Brook Formation(?) (unit 1)

The term Spruce Brook unit was informally introduced by Colman-Sadd and Swinden (1982) for a sequence of Lower to Middle Ordovician quartz-rich turbiditic sandstone and minor conglomerate and shale which had been overthrust by ophiolitic rocks in the Miguels Lake – Pipestone Pond area, 60 km northeast of Meelpaeg Lake. The name has since been changed to Spruce Brook Formation (Colman-Sadd, personal communication, 1983). Subsequent mapping by Colman-Sadd (1983, 1984) has tentatively extended the Spruce Brook Formation to the southwest, outside of the ophiolitic complex, and the unit continues into the Wolf Mountain map area.

Within the Wolf Mountain map area, the Spruce Brook Formation has been divided into four subunits, based on lithology and grade of metamorphism. Subunit 1a is dominantly a biotite ± muscovite psammitic schist with minor interbedded semipelite. Bedding is rarely preserved. Locally the unit consists of 15 to 30 cm thick beds of quartz-rich sandstone with minor crosslaminations. Subunit 1b is dominantly a pelitic sequence with minor interbedded psammite, and probably overlies subunit 1a. Subunit 1c is a coarse clastic unit which comprises orthoquartzite – cobble conglomerate, coarse pelitic-clast breccia and minor interbedded granule conglomerate, coarse sandstone and semipelite. The clast lithologies can be matched to those of underlying subunits 1a and 1b.

Subunit 1d is considered to be the high grade equivalent of subunit 1a, and is dominated by migmatite and biotite psammite which are intruded by abundant granitic veins and pegmatite. Two small basic dykes, now converted to amphibolite schist, intrude the Spruce Brook Formation west of Wolf Lake.

Lower to Middle Ordovician Baie d'Espoir Group (unit 2)

The Baie d'Espoir Group (Jewell, 1939; Colman-Sadd, 1976) lies to the southeast of the Spruce Brook Formation and is separated from it by assumed faults throughout much of the map area. Only in the area east of Meelpaeg Lake is there no apparent evidence for a fault contact between the two units.

The Baie d'Espoir Group is divided into four subunits based on rock type. Subunit 2a consists of thickly bedded, schistose quartz-crystal tuff and coarse tuffaceous sandstone. The subunit may overlie the Spruce Brook Formation in the area southeast of Meelpaeg Lake but the contact is not exposed. A significant geological break is present, however, as the Spruce Brook Formation in the area consists of thinly bedded pelitic, semipelitic and psammitic biotite-muscovite-andalusite schist which is distinct from the tuff. Subunit 2b consists of thinly bedded, graphitic-pyritic, black semipelite and pelite which is interbedded with subunits 2a and 2c in the area southeast of Meelpaeg Lake. About 10 to 15 km east of Wolf Lake, subunit 2b is extensively developed without the other subunits. Subunit 2c consists of very thickly bedded, virtually featureless, brown weathering, grey metasandstone with minor interbeds of pelite similar to subunit 2b. Subunit 2d consists of the grey to green pelitic and semipelitic units which are poorly exposed in a zone around Dolland Pond. About 5 to 8 km north-northwest of Dolland Pond, the unit is reasonably well exposed and consists of brown weathering, parallel bedded (5 to 10 cm thick beds), massive green pelite and semipelite with a poorly developed cleavage. Southwest and west of Dolland Pond, pelite and interbedded pelite and semipelite are exposed. These rocks are tentatively correlated with subunit 2d to the north.

Lower to Middle Ordovician Bay du Nord Group (unit 3)

Unit 3 is exposed in the southwest corner of the map area and consists of a narrow belt of migmatite and foliated granitoid dykes. The migmatites are interpreted to be part of the Lower to Middle Ordovician Bay du Nord Group which is more extensively developed immediately to the west (Blackwood, 1984). The migmatites consist of biotite ± muscovite psammite with a granitic melt fraction, both of which have been intruded by numerous, mainly muscovite-biotite granite and pegmatite veins. Locally, small plugs (<200 m diameter) of foliated, leucocratic, muscovite-garnet granite intrude the migmatite. The unit was post-tectonically intruded by the North Bay Granite.

Silurian(?) sandstone, siltstone and conglomerate (unit 4)

Unit 4 consists of a weakly metamorphosed, deformed and cleaved, medium bedded (30 cm) sandstone, pebble conglomerate and siltstone which is exposed mainly around Dolland Pond (see also Colman-Sadd, 1984). Three km west of Dolland Pond, the unit consists of a thickly bedded, poorly sorted, matrix-supported angular, subangular to subrounded cobble to pebble conglomerate. Clasts are mainly of sedimentary origin with chert and shale fragments being the most abundant. The matrix consists of poorly sorted rock and crystal fragments cemented by pelite. The sandstone and siltstone beds locally display crossbedding and graded bedding, but more commonly only parallel laminations are present. Williams (1970) noted that this unit is similar to the Silurian Goldson Formation in Notre Dame Bay, and Colman-Sadd (1984) notes a similarity to the Silurian Botwood Group exposed to the northeast in the West Gander Rivers area (see Blackwood, 1981; Colman-Sadd, 1980, 1982).

Silurian-Devonian North Bay Granite (unit 5)

The North Bay Granite within the map area has been divided into nine subunits based on mineralogy and degree of deformation. The essential features of each subunit are listed in the legend to Figure 72.1. The numerous smaller intrusions east of Wolf Lake are tentatively included in the North Bay Granite.

The main mass of the North Bay Granite (subunits 5g, 5h, 5i), in the Dolland Brook area, is dominated by very similar granites which vary only in the presence or absence of muscovite. Xenoliths of migmatite and foliated granite are common in subunit 5g within 5 km of the contact with unit 3. A large xenolith of amphibolite schist was found at one locality and is probably derived from the Bay du Nord Group (see Blackwood, 1984).

Subunit 5a is considered to predate subunits 5g and 5i as it usually contains a strong penetrative fabric, generally absent in subunits 5g and 5i.

Subunits 5b and 5b' form a major zone of highly deformed leucocratic granitoids. There is generally an abrupt change in rock type and degree of deformation between subunits 5b and 5b' and the juxtaposed granitoid subunits 5c, 5d, 5f, 5g and 5i and subunit 2d. The contacts are interpreted to be faults and the effects of the faulting are exposed on Dolland Pond, Dolland Brook, southwest of Wolf Lake and west of Wolf Lake where the granite has been injected by abundant quartz veins. In the other areas, the granite is brecciated and strongly sheared.

Subunit 5b' is distinguished from subunit 5b by the presence of abundant xenoliths of foliated diorite and tonalite, migmatite and psammitic schist in subunit 5b', of which the latter two may have been derived from the Spruce Brook Formation. The adjacent Baie d'Espoir Group, to the north, consists mainly of low grade slate and is clearly not the source of the migmatite.

Silurian-Devonian Burgeo Batholith (unit 6)

A small portion of the Burgeo Batholith, which is an extensively developed granitoid unit located to the southwest of the Dolland Brook map area (Chorlton, 1980a,b; O'Brien, 1983; Blackwood, 1984; O'Brien and Tomlin, 1984), occurs in the southwest corner of the map area. The granite is a strongly mylonitized body which forms the northeast margin of the Burgeo Batholith, and forms only a small part of a mylonite zone which extends from Dragon Bay 40 km to the southeast (Blackwood, 1983) into the adjacent Dolland Brook map area (11 P/15 W) (Blackwood, 1984), and beyond into the White Bear River (11 P/14) (O'Brien and Tomlin, 198), Ramea (11 P/11) and Burgeo (11 P/12) map areas where the mylonite zone bisects the Burgeo Batholith. The total length of this mylonite zone, which is about 1 km in width, is more than 100 km. Blackwood (1984) has shown that the mylonite zone bifurcates into zones of nonmylonitic to protomylonitic granitoids and ultramylonitic granitoids. These subdivisions of the mylonitic zone can be traced into the Dolland Brook (east half) map area (Fig. 72.2) where the ultramylonite portions of the mylonite zone are separated by a zone of protomylonitic granite.

The protolith of the mylonitic granitoids may be determined from the less deformed areas of the mylonite zone where the rock is a pink, slightly porphyritic, medium grained biotite granite that is free from xenoliths of migmatite or foliated granitoids.

Devonian or younger quartz-feldspar porphyry dykes (unit 7)

Unit 7 consists of four quartz-feldspar porphyry dykes which intrude subunit 5g and may extend south to intrude subunit 5a (Scott and Conn, 1950). The dykes are straight, parallel sided, up to 15 m in width and more than 200 m long. They contain conspicuous crystals of 2 to 3 mm wide terminated quartz crystals and euhedral to anhedral feldspar in a fine grained, pink matrix. Two of the dykes contain a selvage of grey, very fine grained quartz-feldspar porphyry, up to 1 m wide, along their eastern margin. This may be a separate intrusion, as a similar zone was not observed on the western margin of the dykes.

Similar quartz-feldspar porphyry dykes have intruded the Burgeo Batholith (O'Brien and Tomlin, 1984) and the feldspar in these dykes is sanidine.

STRUCTURE AND METAMORPHISM

The Spruce Brook Formation (unit 1) and Bay d'Espoir Group metavolcanics and metasediments (unit 2) are strongly deformed with a generally northeast trending cleavage or schistosity. This fabric is generally the only fabric present, but locally there is a transposed earlier fabric. Subunit 2b is characteristically highly folded with isoclinal folds plunging to the southwest at about 70 degrees. Overturned folds were found in a few places. The migmatitic Spruce Brook Formation (subunit 1d) commonly contains at least two planar fabrics, the second commonly parallel to the migmatitic layering. The migmatites of the Bay du Nord Group (unit 3) contain tight F_1 folds, which plunge to the west, and an associated axial planar cleavage. This cleavage is commonly transposed by a northwest trending schistosity considered to be S_2.

Unit 4 contains a weak cleavage which is generally parallel to bedding. At Dolland Pond where younging directions are known, an easterly plunging syncline can be defined (see also Williams, 1970).

The grade of metamorphism of the Spruce Brook Formation increases northward from low greenschist facies, south of Wolf Lake, to upper amphibolite and migmatite grade toward Meelpaeg Lake. Andalusite is locally abundant in the amphibolite facies metasediments. The migmatite locally contains conspicuous pre-S_2 cordierite porphyroblasts. East of Wolf Lake, subunit 1a contains andalusite and cordierite porphyroblasts which are post-tectonic and are probably related to contact metamorphism from subunit 5d of the North Bay Granite.

The Baie d'Espoir Group lies generally within the greenschist facies. Close to contacts with the granitoid units, the rock is converted to a hard hornfels with skeletal andalusite in the pelitic units of subunit 2b.

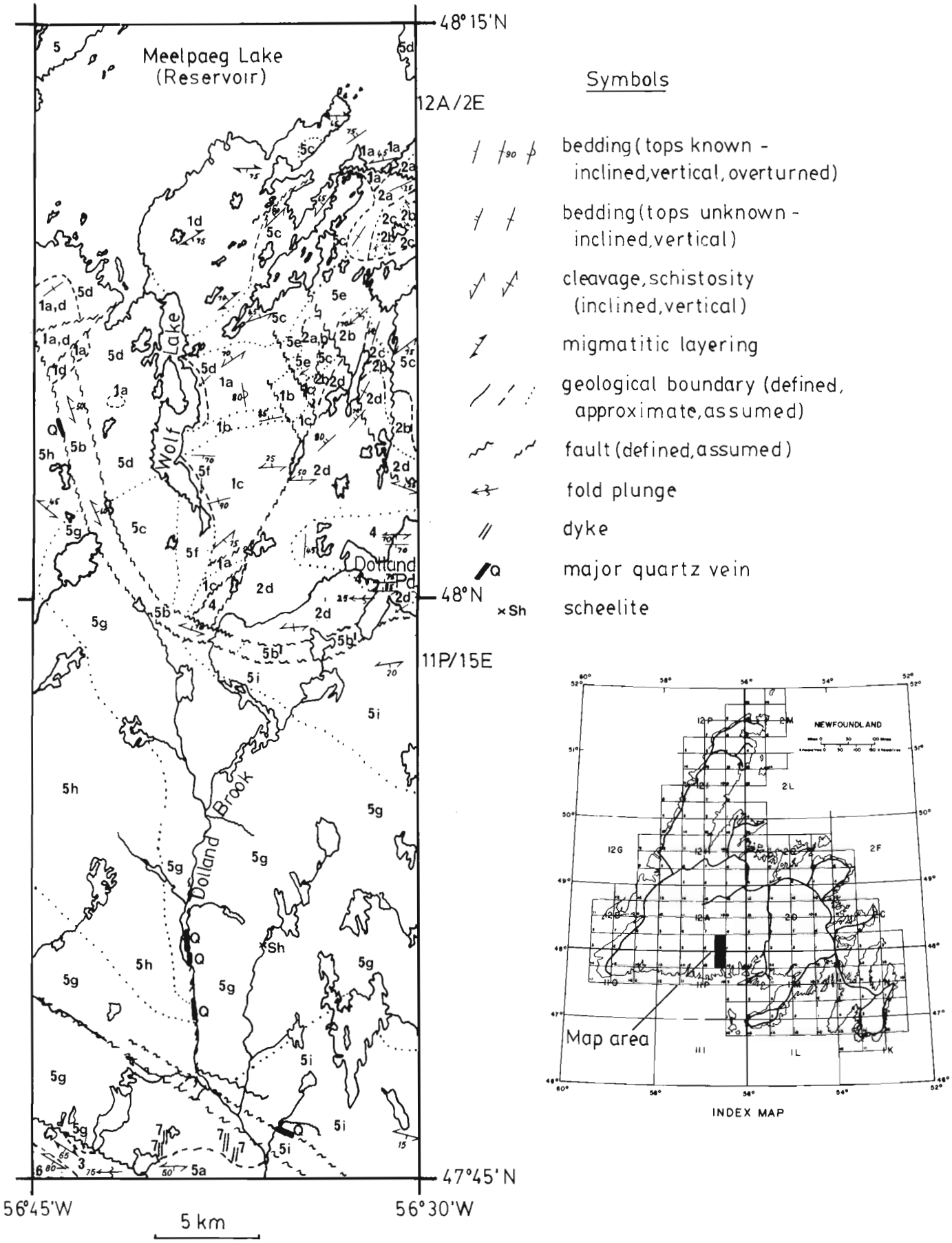

Figure 72.1. *Geological map of the Wolf Mountain (12A/2E) and Dolland Brook (11P/15E) map areas.*

LEGEND

DEVONIAN OR YOUNGER

7 Pink, massive, very fine grained to fine grained, quartz-feldspar porphyritic dykes.

SILURIAN TO DEVONIAN

Burgeo Batholith

6 Pink, protomylonitic to mylonitic, very fine grained to medium grained, locally K-feldspar porphyroclastic, biotite granite.

North Bay Granite (subunits 5a–5b)

5a Pink to buff, foliated, medium grained, equigranular to porphyritic, biotite ± muscovite granodiorite and granite.

5b Pink to white, strongly foliated, medium to coarse grained, equigranular to pegmatitic, muscovite-garnet and muscovite-biotite granite; **5b'** contains numerous xenoliths of migmatite, psammite, and foliated tonalite.

5c Buff to grey, foliated, medium to coarse-medium grained, equigranular, biotite granodiorite and minor tonalite; locally intruded by garnet-muscovite aplite and pegmatite veins.

5d Buff, massive, medium grained, equigranular, biotite granodiorite and granite; granite becomes fine grained and muscovite-bearing southwest of Meelpaeg Lake.

5e Buff, massive, medium grained, equigranular, biotite granite; includes minor biotite-muscovite granite.

5f White to buff, massive, coarse grained, equigranular, biotite-muscovite granite.

5g Pink to buff, massive to weakly cleaved, medium to coarse-medium grained, K-feldspar porphyritic, biotite granite; screens of foliated granite and migmatite common southwest of Dolland Brook.

5h Pink to buff, massive to weakly cleaved, medium to coarse-medium grained, K-feldspar porphyritic, biotite ± muscovite granite

5i Pink to buff, massive to weakly cleaved, medium grained, K-feldspar porphyritic, biotite-muscovite granite.

SILURIAN?

4 Interbedded sandstone, siltstone and pebble conglomerate; minor subangular cobble conglomerate.

LOWER TO MIDDLE ORDOVICIAN

Bay du Nord Group

3 Highly deformed migmatitic metasediments cut by numerous granitoid veins, dykes and small granitoid plugs.

Baie d'Espoir Group (subunits 2a–2d)

2d Grey and green, thinly bedded, cleaved pelite and semipelite.

2c Very thickly bedded, brown weathering, grey massive sandstone, minor interbeds of subunit 2b.

2b Thinly bedded, highly folded black graphitic pelite and semipelite.

2a Thickly bedded, schistose quartz-crystal tuff and coarse tuffaceous sandstone.

Spruce Brook Formation (subunits 1a–1d)

1d Migmatite, psammite, and numerous granitoid dykes; high grade equivalent of 1a, 1b.

1c Orthoquartzite cobble clast-supported metaconglomerate, with minor slate and quartzite matrix-supported breccia and coarse metasandstone.

1b Thinly bedded pelite and minor psammite and semipelite.

1a Dominantly biotite psammite and orthoquartzite with minor semipelite.

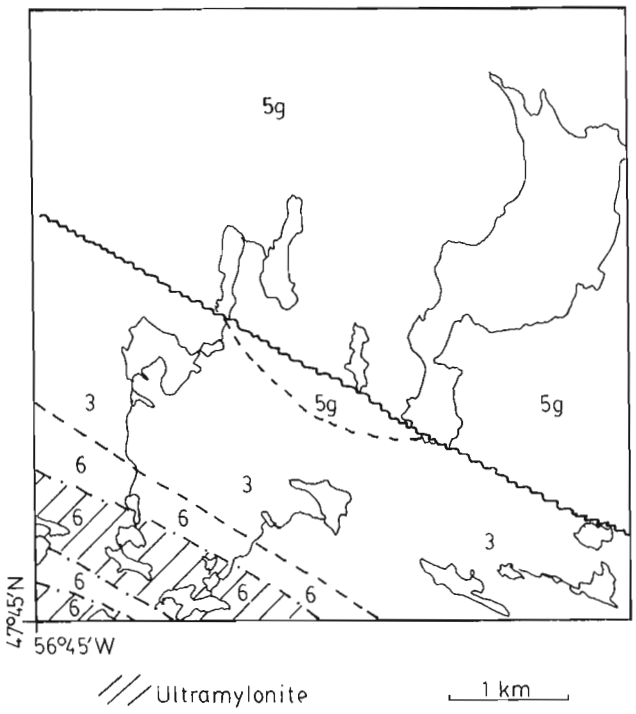

Figure 72.2. *Detailed map of the bifurcation of the mylonite zone in the southwest corner of the Dolland Brook (east half) map area. Legend as in Figure 72.1.*

Unit 4 lies within the lower greenschist facies which is similar to the surrounding pelites of the Baie d'Espoir Group.

The granitoid rocks (subunit 5c), southeast of Meelpaeg Lake, contain a moderately to strongly developed cleavage which is parallel to the main fabric in the metasediments. The fabric is defined by aligned biotite and flattened quartz and feldspar. There is no evidence of recrystallization.

Subunit 5b is deformed throughout its length with a strong fabric parallel to the strike of the subunit, and a relatively constant dip of between 50 and 70 degrees to the northeast. This subunit may represent a major zone of dislocation as it lies along strike from a 1 km wide, 8 km long mylonite zone, well exposed to the northwest between Meelpaeg Lake dam and Granite Lake ditch to the north (Dickson, 1982). The zone of strongly deformed granitoids may be a continuation of the zone of strongly deformed granitoids which form the northern margin of the North Bay Granite in the adjacent D'Espoir Lake map area (Dickson and Tomlin, 1983). In this area, the Ordovician Salmon River Dam Formation is juxtaposed against the granite, and the contact varies from a probable faulted intrusive contact to a possible thrust contact where highly sheared magnesite and limestone slivers are present between D'Espoir Lake and Salmon River (Dickson and Tomlin, 1983). It is, therefore, possible that the granitoids and metasediments between Granite Lake ditch and Salmon River which lie to the north of the zone of highly deformed granitoids are in thrust contact with the North Bay Granite.

MINERALIZATION

Lake sediment geochemical anomaly patterns indicate that the Dolland Brook area shows a potential for tungsten mineralization (Davenport and Butler, 1982). Follow-up work by McConnell (1984), working east of Dolland Brook, resulted in the discovery of minor scheelite-pyrite mineralization in brecciated porphyritic biotite granite.

Several major quartz veins occur along faults which cut subunits 5g, 5h and 5i of the North Bay Granite. Along Dolland Brook a prominent north trending fault scarp contains three large quartz veins. These veins are 10 to 15 m wide and more than 200 m long. They contain several generations of quartz which range from vuggy to massive milky quartz. The veins also contain inclusions of highly altered granite. East of Dolland Brook and southeast of the other quartz veins, another major quartz vein was discovered. This vein also lies along a fault and is similar in all respects to the other quartz veins. The veins will be analyzed for their gold content.

West of Wolf Lake, a large number of thin (5 to 10 cm) parallel quartz veins are injected into highly sheared granite of subunit 5b. During field work, another large quartz vein, similar to those at Dolland Brook, was discovered just to the west of the Wolf Mountain (east half) map area, about 2 km southeast of Meelpaeg Lake dam. These two occurrences both lie along the fault which extends toward the ditch at Granite Lake and contains two large quartz veins (Dickson, 1982).

Examination of all samples from these veins under ultraviolet light did not reveal the presence of fluorescent minerals such as scheelite or fluorite.

GEOCHEMISTRY

Geochemical samples of granitoid rocks and quartz veins were collected using a 2 km by 2 km grid sampling system. Paucity of outcrop over much of the area prevented use of a random sampling technique. Granite samples were collected from 150 sites, and seven samples are from quartz veins. All samples will be analyzed for major and trace elements including W, U, Sn, Mo, Li and F. Samples collected in 1982 have been analyzed for major and trace elements including Li, F and Mo but not as yet for W, Sn and U. No anomalous values are readily apparent from the raw data.

SUMMARY

The area of Wolf Mountain (east half) and Dolland Brook (east half) contains Lower Ordovician to Silurian(?) metasedimentary rocks intruded by a variety of granitoids which form part of the much more extensive Silurian-Devonian North Bay Granite.

The dominantly metasedimentary units 1, 2 and 3 are assigned to the Lower to Middle Ordovician Spruce Brook Formation, Baie d'Espoir Group and Bay du Nord Group, respectively. The Spruce Brook Formation consists of psammite, pelite and a coarse cobble conglomerate. The formation is metamorphosed in the greenschist to upper amphibolite facies, and the northern portion of the formation has been converted to migmatite. The Baie d'Espoir Group is mainly in fault contact with the Spruce Brook Formation and is composed of a lower tuff unit overlain by a thick sequence of interbedded pelitic, semipelitic and psammitic units. The pelitic units are strongly deformed with tight isoclinal folds. The other units are less obviously deformed. Metamorphism is generally in the lower greenschist facies. The Bay du Nord Group (unit 3) is composed of highly deformed and metamorphosed metasediments which are converted to migmatite. This migmatite is intruded by numerous syntectonic granitoid dykes and post-tectonically intruded by the North Bay Granite.

Around Dolland Pond, a poorly exposed unit of siltstone, sandstone and pebble conglomerate (unit 4) is tentatively assigned a Silurian age. The unit contains a weak cleavage and has been metamorphosed in the lower greenschist facies. The unit has a synclinal structure.

The North Bay Granite (unit 5) is a composite intrusion with medium grained, porphyritic, massive, biotite ± muscovite granites (subunits 5d, 5e, 5f, 5g, 5h and 5i) as the dominant rock type. The foliated granitoids (subunits 5a and 5c) contain a moderate to strong foliation which probably developed with the main fabric in the metasediments. Subunit 5b is dominantly leucocratic muscovite ± garnet ± biotite granite and pegmatite which have been strongly deformed possibly as the result of southwesterly overthrusting of the Ordovician units and the granitoids which lie to the northeast.

Unit 6 is a strongly mylonitized granitoid unit which, in the map area, only forms a small part of an intensely deformed, northwest trending zone of mylonites over 100 km in length.

Unit 7 comprises four quartz-feldspar porphyry dykes which post-tectonically intruded the North Bay Granite. These northerly trending dykes are more than 200 m in length and 10 to 15 m in width.

Minor scheelite-pyrite mineralization has been discovered east of Dolland Brook in sheared granite. Several major quartz veins were also found but have no apparent scheelite or fluorite mineralization. The scheelite mineralization corresponds with a lake sediment tungsten anomaly.

ACKNOWLEDGMENTS

This project benefitted greatly from the able assistance of Barry Wheaton and Glen Case. Logistical support from Wayne Ryder and Sidney Parsons of Newfoundland Department of Mines and Energy, and Betty Manning and Gordon Arnold of the Geological Survey of Canada permitted the smooth completion of the field work. Sealand Helicopters at St. Alban's provided its usual competent and skillful services. This report was reviewed and improved by the critical reading of J. Murray, S.P. Colman-Sadd and R.F. Blackwood.

REFERENCES

Blackwood, R.F.

1981: Geology of the West Gander Rivers area, Newfoundland; in Current Research, Newfoundland Department of Mines and Energy, Mineral Development Division, Report 81-1, p. 50-56.

1983: Geology of the Facheux Bay (11P/9) map area, Newfoundland; in Current Research, Newfoundland Department of Mines and Energy, Mineral Development Division, Report 83-1, p. 26-40.

1984: Geology of the west half of the Dolland Brook map area (11P/15), Newfoundland; in Current Research, Newfoundland Department of Mines and Energy, Mineral Development Division, Report 84-1.

Butler, A.J. and Davenport, P.H.

1978: A lake sediment geochemical survey of the Meelpaeg Lake area, Central Newfoundland; Newfoundland Department of Mines and Energy, Mineral Development Division, Open File Nfld. 986.

Chorlton, L.B.

1978: La Poile River map area (110/16), Newfoundland; Newfoundland Department of Mines and Energy, Mineral Development Division, Map 78-168, with marginal notes.

Chorlton, L.B. (cont.)
1980a: Notes on the geology of Peter Snout (11P/13, west half), Newfoundland, and accompanying Map 80-201; Newfoundland Department of Mines and Energy, Mineral Development Division, Map 80-201 with marginal notes.

1980b: Geology of the La Poile River map area (110/16), Newfoundland; Newfoundland Department of Mines and Energy. Mineral Development Division, Report 80-3, 85 p.

Colman-Sadd, S.P.
1976: Geology of the St. Alban's map area, Newfoundland (1M/13); Newfoundland Department of Mines and Energy, Mineral Development Division, Report 76-4, 19 p.

1980: Geology of the Twillick Brook map area, Newfoundland (2D/4); Newfoundland Department of Mines and Energy, Mineral Development Division, Report 79-2, 23 p.

1982: West Gander Rivers (2D/11, west part), Newfoundland; Newfoundland Department of Mines and Energy, Mineral Development Division, Open File Map 82-59.

1983: Geology of the east half of the Cold Spring Pond map area (12A/1), Newfoundland; in Current Research, Newfoundland Deparment of Mines and Energy, Mineral Development Division, Report 83-1, p. 16-25.

1984: Geology of the Cold Spring Pond map area (west part, 12A/1), Newfoundland; in Current Research, Newfoundland Department of Mines and Energy, Mineral Development Division, Report 84-1.

Colman-Sadd, S.P., Dickson, W.L., Elias, P., and Davenport, P.H.
1981: Whole rock analytical data, statistical printouts and maps of plutonic igneous rocks and selected country rocks from southern Newfoundland (1M/10-16; 2D/1-5); Newfoundland Department of Mines and Energy, Mineral Development Division, Open File (Nfld) 1157.

Colman-Sadd, S.P. and Swinden, H.S.
1982: Geology and mineral potential of south-central Newfoundland; Newfoundland Department of Mines and Energy, Mineral Development Division, Report 82-8, 102 p.

Davenport, P.H. and Butler, A.J.
1981: Fluorine distribution in lake sediments in the Meelpaeg Lake area, Central Newfoundland; Newfoundland Department of Mines and Energy, Mineral Development Division, Open file 1222.

1982: Tungsten in lake sediment over granitoids in south-central Newfoundland – a pilot study; Newfoundland Department of Mines and Energy, Mineral Development Division, Open File Nfld. 1302.

Dickson, W.L.
1982: Geology of the Wolf Mountain (12A/2W) and Burnt Pond (12A/3E) map area, Newfoundland; Newfoundland Department of Mines and Energy, Mineral Development Division, Report 82-5, 43 p.

Dickson, W.L. and Tomlin, S.L.
1983: Geology of the D'Espoir Brook map area (11P/16) and part of the Facheux Bay map area (11P/9), south-central Newfoundland; in Current Research, Part A, Geological Survey of Canada, Paper 83-1A, p. 285-290. Also in Current Research, Newfoundland Department of Mines and Energy, Mineral Development Division, Report 83-1, p. 51-56.

Jewell, W.B.
1939: Geology and mineral deposits of the Baie d'Espoir area; Newfoundland Geological Survey, Bulletin 17, 29 p.

McConnell, J.W.
1984: Geochemical surveys over three tungsten anomalies in the North Bay batholith, southern Newfoundland; in Current Research, Newfoundland Department of Mines and Energy, Mineral Development Division, Report 84-1.

O'Brien, S.J.
1983: Geology of the eastern half of the Peter Snout map area (11P/13E), Newfoundland; in Current Research, Newfoundland Department of Mines and Energy, Mineral Development Division, Report 83-1, p. 57-67.

O'Brien, S.J. and Tomlin, S.
1984: White Bear River (11P/14), Newfoundland; in Current Research, Newfoundland Department of Mines and Energy, Mineral Development Division, Report 84-1.

Phendler, R.W.
1950: Geology of the Lake Ebbegunbaeg area; unpublished report, Buchans Mining Company, 5 p.

Scott, H.S. and Conn, H.K.
1950: Preliminary report on the geology of the Buchans Mining Company concession in central and south-central Newfoundland; Photographic Survey Corporation Limited, Geological Division, unpublished report, 12 p.

Smyth, W.R., compiler
1979: Dolland Brook (11P/15), Newfoundland; Newfoundland Department of Mines and Energy, Mineral Development Division, Map 79-54.

Williams, H.
1970: Red Indian Lake (east half), Newfoundland; Geological Survey of Canada, Map 1196A.

1971: Burgeo (east half), Newfoundland; Geological Survey of Canada, Map 1280A, with descriptive notes.

Williams, H., Kennedy, M.J., and Neale, E.R.W.
1970: The Hermitage Flexure, the Cabot Fault and the disappearance of the Newfoundland Central Mobile Belt; Geological Society of America Bulletin, v. 81, p. 1563-1568.

73. THE ARCHEAN-PROTEROZOIC BOUNDARY IN NORTHERN LABRADOR: REPORT 2[1]

Project 820028

A.B. Ryan[2], Y. Martineau[2], J. Korstgård[3], and D. Lee[4]

Ryan, A.B., Martineau, Y., Korstgård, J., and Lee, D., The Archean-Proterozoic boundary in northern Labrador: report 2; in Current Research, Part A, Geological Survey of Canada, Paper 84-1A, p. 545-551, 1984.

Also in Current Research, Newfoundland Department of Mines and Energy, Mineral Development Division, Report 84-1, 1984.

Abstract

The Nain and Churchill structural provinces and the boundary between them have been investigated in the Hebron Fiord area of northern Labrador. The Nain Province comprises migmatized early Archean orthogneiss and interleaved supracrustal gneiss belts intruded by several generations of late Archean tonalite to granite. Diabase dykes intrude all lithologies. Metamorphism of the gneisses and some of the granites reflects granulite facies conditions. The Churchill Province comprises predominantly garnetiferous tonalitic gneisses with lesser mafic and ultramafic granulites, and hypersthene-bearing quartzofeldspathic gneisses, the latter in part derived from Proterozoic reworking of the adjacent Archean complex. Ramah Group supracrustals in the eastern Churchill Province are metamorphosed to amphibolite facies and are structurally interleaved with Hudsonian refoliated Archean basement. The Archean-Proterozoic boundary is defined by a 2 to 5 km zone in which rocks of the Nain Province are progressively modified by Hudsonian thermotectonism upon approaching a sharply faulted boundary with high grade gneisses of the Churchill Province. No minerals of economic importance were detected in the area.

Résumé

Les provinces tectoniques de Nain et de Churchill ainsi que la limite entre ces provinces ont été étudiées dans la région du fjord Hebron, dans le nord du Labrador. La province de Nain comprend de l'orthogneiss et des zones intercalées de gneiss supracortical, le tout ayant été migmatisé et datant de l'Archéen ancien; plusieurs générations de tonalite passant progressivement au granite de l'Archéen récent recoupent ces roches. Des filons de diabase font intrusion dans toutes les lithologies. Le métamorphisme des gneiss et de certains des granites a atteint le stade du faciès des granulites. La province de Churchill comprend surtout des gneiss grenatifères à tonalite avec de plus petites quantités de granulites mafiques et ultramafiques, ainsi que des gneiss quartzofeldspathiques à hypersthène, dérivés en partie du remaniement protérozoïque du complexe archéen voisin. Les sédiments supracorticaux du groupe de Ramah dans la partie est de la province de Churchill ont atteint le degré de métamorphisme caractérisé par le faciès des amphibolites et sont intercalés avec le socle archéen déjà refeuilleté au cours de l'Hudsonien. La limite archéenne-protérozoïque est définie par une zone de 2 à 5 km où les roches de la province de Nain, soumises à un phénomène de thermotectonisme hudsonien, subissent des modifications croissantes à mesure qu'on se rapproche de la limite nettement faillée des gneiss fortement métamorphisés de la province de Churchill. Aucun minéral économiquement important n'a été trouvé dans cette région.

INTRODUCTION

The 1983 season was the second of a two-year program to investigate the nature of the boundary between the Archean Nain Province and the Proterozoic Churchill Province, and to assess the mineral potential of northern Labrador between Saglek and Hebron fiords. The 1982 season concentrated on the Saglek Fiord section of the boundary zone (Ryan et al., 1983); during the 1983 season most of the fieldwork was carried out in the Hebron Fiord area. Heavy arctic pack ice along the northern Labrador coast delayed positioning of helicopter fuel and prevented small-boat work on the coast; hence mapping did not commence until July 28, 1983. Two 1:50 000 map sheets (14 L/2,3; Fig. 73.1) were mapped during the field season which ended on September 1. Ryan, Martineau and Lee were responsible for regional mapping of the Archean terrane covered by 14 L/2; Korstgard concentrated on the Churchill Province and its boundary with the Archean complex within 14 L/3. Much of the area included in Figure 73.2 was ground traversed, but helicopter reconnaissance was also employed, especially to complete coverage of the northwest corner and the southern one-third of 14 L/3.

Studies complementary to the regional mapping program were also conducted during 1983. Some of these are a continuation of investigations begun last year, but new programs were also initiated. D. Bridgwater and L. Schiøtte (Geologisk Museum, Copenhagen, Denmark) have been concentrating on geochronological studies of the early Archean Uivak gneisses and their migmatization in the northern coastal stretch. A. Nutman (Grønlands Geologiske Undersøgelse, Copenhagen, Denmark) conducted detailed studies of the various lithologies that make up the Nulliak assemblage, a series of pre-3.6 Ga supracrustal rocks occurring as rafts in the Uivak gneisses. F. Mengel (Memorial University, St. John's, Newfoundland) has begun a

[1] Contribution to Canada-Newfoundland co-operative mineral program, 1982-84. Project carried by Geological Survey of Canada and Newfoundland Department of Mines and Energy.

[2] Mineral Development Division, Newfoundland Department of Mines and Energy, 95 Bonaventure Avenue, St. John's, Newfoundland A1C 5T7

[3] Geologisk Institut, Aarhus University, Ole Worms Allé, Aarhus, Denmark

[4] Department of Earth Sciences, Memorial University of Newfoundland, St. John's, Newfoundland A1B 3X5

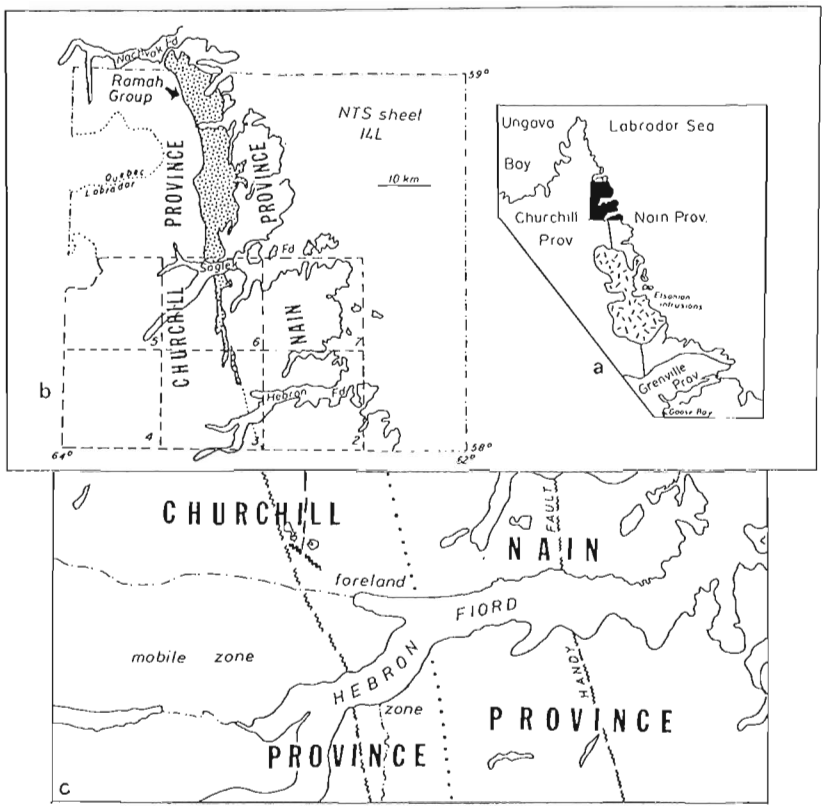

Figure 73.1

Index maps to study area.

a. Shaded area is part of northern Labrador covered by NTS grid 14 L. Major lithotectonic elements of Labrador are after Greene (1972).

b. Outline of 1:50 000 sheet areas at southwest corner of 14 L. Sheets 14 L/2 and 3 were mapped in 1983.

c. Structural subdivisions of the study area. Dotted line represents eastern-most limit of Hudsonian deformed diabase dykes in the Archean terrane, and thus defines the eastern boundary of the Churchill Province foreland zone.

comprehensive mapping and stratigraphic/metamorphic/structural analysis of the southern extension of the Ramah Group, an Aphebian supracrustal belt in the eastern part of the Churchill Orogen. K. Collerson (Australian National University, Canberra) collected material for isotopic investigations of both the Archean and Proterozoic crustal blocks.

GEOLOGICAL SETTING AND PREVIOUS WORK

The study area presents a cross-section of the junction between the Archean Nain Province (Taylor, 1971) and the early Proterozoic Churchill Province (Fig. 73.1). The Nain Province is the western portion of the fragmented Archean North Atlantic Craton (Bridgwater et al., 1973) and contains gneisses older than 3.6 Ga (Hurst et al., 1975; Collerson, 1983); the latest major deformation probably occurred circa 2.7 Ga. The Churchill Province in the study area is part of the southeast projection of an extensive, irregularly shaped Proterozoic orogen which stretches westward and northward into central and Arctic Canada (Davidson, 1972). The Churchill Province comprises rocks which exhibit a strong structural and metamorphic imprint from the Hudsonian Orogeny circa 1.8 Ga, but the majority of the rocks of this younger mobile belt in the study area are probably derived from Archean protoliths.

The major geological elements in northern Labrador were outlined and discussed by Taylor (1969, 1970, 1971, 1979). Joint work by the Geological Survey of Canada and Memorial University of Newfoundland in 1974 and 1975 led to the unravelling of the geological history of the Archean complex in the eastern Saglek Fiord area and the coastal segment directly north of the present study area, cf. Bridgwater et al. (1975), Bridgwater and Collerson (1976), Collerson et al. (1976), and Collerson and Bridgwater (1979). As part of the 1975 Memorial University program, the senior author conducted a study of the eastern half of the peninsula bounded by Iterungnek and Hebron fiords (Ryan, 1977). In addition Barton (1975) and Collerson et al. (1982a) presented discussions of some aspects of the geochronology of the Archean gneisses from the Hebron area. The Churchill Province in this area, however, has received little attention, and apart from Taylor's regional reconnaisance studies, no information is available.

DEFINITION OF ARCHEAN AND PROTEROZOIC TECTONIC ELEMENTS

The definition of Archean and Proterozoic structural elements is relatively straightforward in general terms in the Nain and Churchill provinces of northern Labrador as outlined by Taylor (1971, 1979). However, as Morgan (1975a) correctly pointed out, Hudsonian effects extend beyond the Churchill Province mobile zone into the terrane immediately to the east. This is dramatically illustrated by the thermotectonism which affected the Aphebian Ramah Group, and Morgan therefore assigned the Ramah Group to the Churchill Province. Although he did not define its extent, he recognized that the Hudsonian imprint was also evident in the Archean gneisses east of the Ramah Group and assigned them to the "Hudsonian foreland" zone (Morgan, 1975b, 1978). This designation was also used by Ryan et al. (1983) who noted that where the Ramah Group was not present, the late Archean-early Aphebian diabase dyke swarm could be used to indicate the eastward extent of Hudsonian deformation into the Nain Province. The delineation of Hudsonian effects on the Archean terrane becomes more problematical where these two critical markers are absent. Such is the case for parts of the boundary zone in the Hebron Fiord area. However, we have been able to show that the Hudsonian overprint extends up to 6 km into the Nain Province east of the Churchill Province mobile zone (see below) and we include this area in the foreland zone of the Churchill Orogen (Fig. 73.1c).

NAIN STRUCTURAL PROVINCE

The Archean complex of the Nain Province of northern Labrador has been subdivided into several stratigraphic units of orthogneiss and paragneiss as a result of work in the Saglek area in the mid-1970s (cf. Bridgwater et al., 1975; Collerson et al., 1976; Bridgwater and Collerson, 1976; Bridgwater et al., 1978; Collerson et al., 1981). These lithological and chronological studies have shown that the geological history of the Nain Province (Table 73.1) entails a complex sequence of deposition, igneous activity, metamorphism and deformation. The major aspects of the geology of the Saglek area are summarized briefly below.

The early Archean (pre-3.4 Ga) Uivak gneisses are the oldest regionally distributed gneisses. These comprise a tonalitic to granodioritic suite (Uivak I) which is intruded by, and structurally interleaved with, a more potassic, Fe-rich augen gneiss (Uivak II). Both subgroups contain rafts of older supracrustal rocks (banded iron formation, quartzite, calcareous metasediment, and mafic to ultramafic rocks) termed the Nulliak assemblage, and it can be demonstrated that both the Nulliak assemblage and the Uivak I gneisses had suffered polyphase deformation prior to emplacement of the Uivak II protolith. All the above lithologies were intruded by a suite of massive to feldspar megacrystic basic dykes (Saglek dykes) circa 3.2 to 3.4 Ga. Interleaved with the early Archean orthogneisses is a varied group of rocks termed the Upernavik supracrustals comprising pelitic, psammitic and calcareous metasedimentary rocks, and basic rocks which are interpreted to be of both extrusive and intrusive origin. No Saglek dykes have been observed in the Upernavik supracrustals, and they are interpreted as either an original cover sequence developed on the Uivak gneisses or else an exotic assemblage tectonically juxtaposed against the Uivak gneisses. The intercalation of Uivak gneisses and Upernavik supracrustals probably occurred in the period between 3.2 and 2.8 Ga. Contacts between the two groups are usually marked by podiform ultramafic bodies.

The whole Archean complex was subjected to a period of major crustal reconstitution circa 2.8 Ga. This is manifested in the development of granulite facies assemblages and reworking of the Uivak gneisses to produce a series of migmatites which were termed the Kiyuktok gneisses in the Saglek Fiord area west of the Handy Fault (Kerr, 1980) and the Iterungnek gneisses in the Hebron Fiord area east of the Handy Fault (Ryan, 1977). Equivalent migmatites at amphibolite facies east of the Handy Fault at Saglek were termed "undifferentiated gneisses" by Hurst et al. (1975). This 2.8 Ga event was also accompanied by the emplacement of syntectonic garnet- and orthopyroxene-bearing granites and pegmatites. Intruded late synkinematically with the reworking of the Uivak gneisses were the Ikarut gneiss protolith and the Saglek tonalite-granodiorite sheets which have yielded ages of ca. 2.7 and 2.8 Ga respectively. Pegmatoidal, K-rich granite (termed the Igukshuak granite) cuts all the above units post-tectonically and was emplaced circa 2.5 Ga (Baadsgaard et al., 1979). The final major event in the evolution of the Nain Province was the emplacement of a late Archean to early Proterozoic swarm of diabase dykes.

All the major lithological units identified in the Saglek map area (Ryan et al., 1983) can be traced into the Hebron Fiord sector. However, several differences from the Saglek area are noted:

1. In the Hebron Fiord sector, the gneisses east of the Handy Fault were subjected to a granulite facies event (Ryan, 1977) equated with the 2.8 Ga high grade metamorphism and reworking of earlier crustal material seen west of the Handy Fault at Saglek (Kerr, 1980; Collerson et al., 1981, 1982b). Areas with relict granulite assemblages occur sporadically east of the fault just north of the present study area (Ryan et al., 1983), but the evidence for this high grade reworking is more widespread in the Hebron area, indicating that deeper crustal levels are exposed in the eastern Archean block of this area. This granulite facies metamorphism is not developed to the same degree as in the block west of the Handy Fault, however, so the area probably represents a zone intermediate or transitional between amphibolite and granulite facies.
2. Extensive areas of Uivak gneisses unaffected by younger events are not as common east of the Handy Fault in the Hebron area as in the Saglek area. In the Hebron area the old gneisses are preserved only as small septa on the order of a few tens of metres wide within younger migmatites. These younger migmatites, however, are derived by regional crustal reworking of the Uivak gneisses. These were termed Iterungnek gneisses by Ryan (1977), and their development is considered coeval with that of the Kiyuktok gneisses of Kerr (1980) and Collerson et al. (1982b). However, in contrast to the Kiyuktok gneisses, which are mostly a static reconstitution of the Uivak gneisses, the equivalent rocks east of the Handy Fault at Hebron appear to have developed under structurally dynamic conditions, probably reflecting their slightly higher crustal level of development.
3. South of Hebron Fiord, metasedimentary rocks of the Upernavik supracrustals occupy more than 30 per cent of the granulite terrane west of the Handy Fault, and mafic metavolcanic and intrusive rocks are less abundant than at Saglek. This indicates that significant amounts of metasedimentary supracrustal material were tectonically emplaced to deep crustal levels in the Nain Province in the Archean, and may have implications regarding the origin of a distinctive garnet-rich tonalite gneiss in the adjacent Churchill Province. Granitoid melts in these Upernavik paragneisses are similar in composition to the garnetiferous tonalites, and it is conceivable that the parental tonalite for the Churchill rocks could have been derived by Archean widespread deep crustal melting of continental lithosphere which contained very large amounts of metasedimentary material (Ryan et al., 1983).
4. An extensive unit of coarse grained, undeformed to gneissic tonalite occurs along the western margin of the Nain Province (Churchill foreland zone) north of Hebron Fiord. This unit locally contains xenoliths of

Table 73.1. Simplified geological history of the Nain Province in northern Labrador. Includes data from Collerson (1983)

Emplacement of diabase dyke swarm (ca. 2.3 - 2.4 Ga)
Emplacement of Igukshuak granite (ca. 2.5 Ga)
Emplacement of late synkinematic to postkinematic Saglek sheets and Ikarut tonalite (ca. 2.7 - 2.8 Ga)
Emplacement of synkinematic granites (ca. 2.8 Ga)
Reworking of Uivak gneisses to give Kiyuktok gneisses and Iterungnek gneisses, granulite facies metamorphism (ca. 2.8 Ga)
Intercalation of Upernavik supracrustals and Uivak gneisses
Deposition of Upernavik supracrustals
Intrusion of Saglek dykes (ca. 3.2 - 3.4 Ga)
Deformation and metamorphism
Intrusion of protoliths for Uivak II gneisses (ca. 3.4 Ga?)
Deformation and metamorphism
Intrusion of protoliths of Uivak I gneisses (ca. 3.8 Ga)
Deposition of Nulliak assemblage (pre-3.8 Ga)

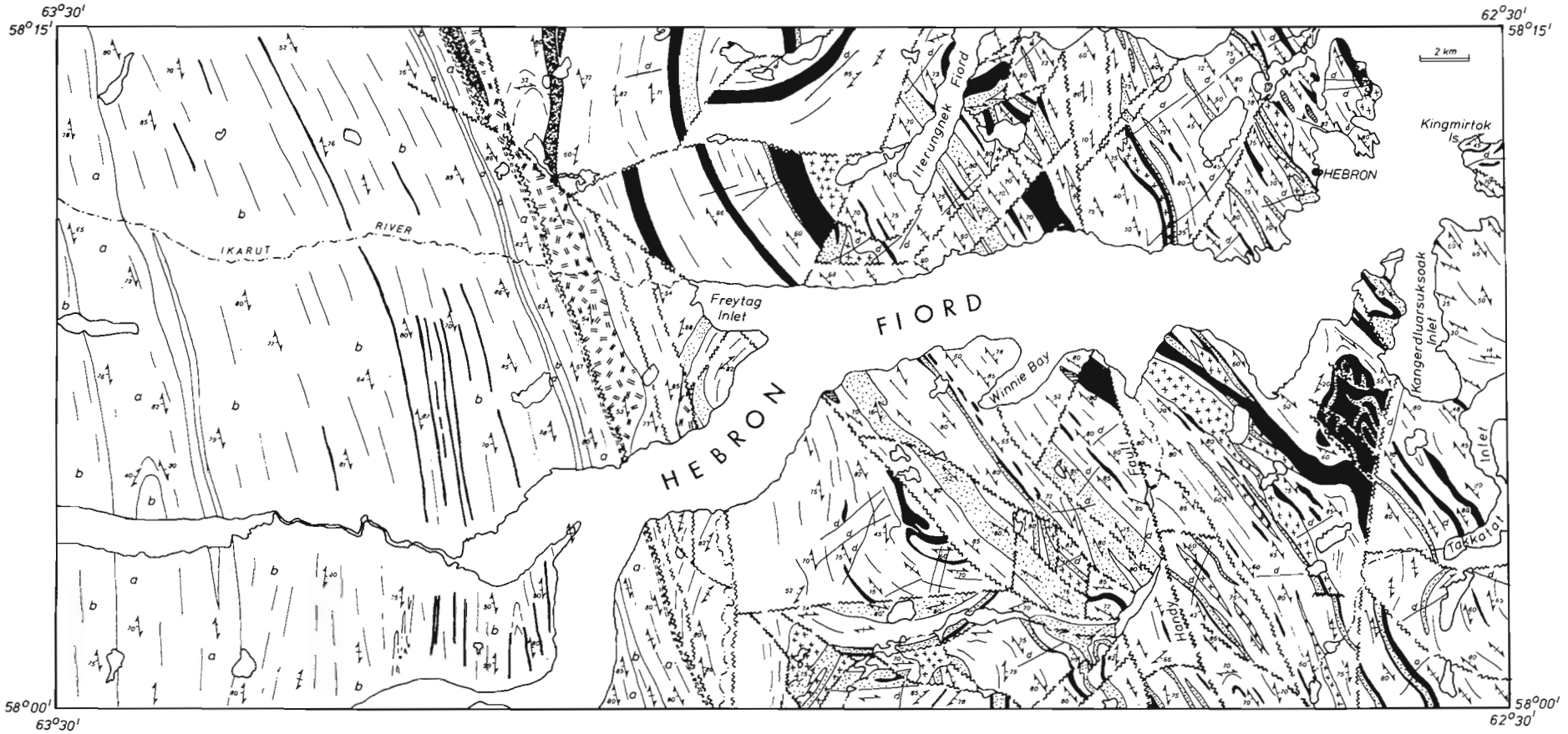

CHURCHILL PROVINCE

APHEBIAN

RAMAH GROUP: *quartzite, pelitic schist.*

ARCHEAN and/or APHEBIAN

Quartz-feldspar-garnet-graphite gneiss; mafic and ultramafic granulite (black).

Hypersthene-bearing quartzofeldspathic gneiss.

NAIN PROVINCE

ARCHEAN - APHEBIAN

Diabase dykes

ARCHEAN

Equigranular to porphyritic, foliated tonalite.

Synkinematic to postkinematic tonalite and granite.

Upernavik supracrustals: metasedimentary rocks (dots), metavolcanic and mafic/ultramafic intrusive rocks (black).

Quartzofeldspathic gneiss: Uivak gneiss and its reworked and migmatized derivatives.

Nulliak assemblage: metasedimentary and mafic/ultramafic rocks.

SYMBOLS

Geological boundary

Fault

Zone of ultramylonite

Trend of gneissic layering (from air photo)

Gneissosity (inclined, vertical, dip unknown)

Figure 73.2. *Geological sketch map of the Hebron Fiord area.*

polydeformed quartzofeldspathic gneiss and mafic pods of diverse origin. It may be correlative with the Ikarut gneiss (Collerson et al., 1982b), an augen gneiss derived from porphyritic tonalite on the north shore of Hebron Fiord southwest of Freytag Inlet. A pre-Proterozoic age is indicated because, although tectonically interleaved with the Ramah Group, it does not intrude the group. It also forms the protolith material for the ultramylonite which defines the eastern boundary of the Churchill mobile zone.

5. Synkinematic to postkinematic granitoid rocks appear to be areally more abundant here than at Saglek. In the northern area, younger granitoid rocks tend to occur only as isolated sheets or as parallel or criss-crossing networks, for instance the Saglek sheets and Igukshuak granite of Collerson et al. (1982b). Here, however, the granitoids are much more conspicuous. They vary from white, medium grained, homogeneous garnet and orthopyroxene-bearing varieties, as found north of Hebron village, to coarser porphyritic charnockites within metasediments 10 km south of Winnie Bay. An extensive unit of grey foliated tonalite to granodiorite, similar to the Saglek sheets, occurs subconcordant to the regional foliation east of the Handy Fault south of Hebron Fiord. Narrow lensoid units of white garnetiferous granite occur in the southern half of this eastern block.

6. The late Archean-early Proterozoic diabase dykes are less abundant in the Hebron area than in the area to the north.

CHURCHILL STRUCTURAL PROVINCE

The dominant rock type in the Churchill Province is a uniform leucocratic, garnet-rich quartzofeldspathic gneiss of tonalitic composition, which can be shown locally to be derived from an igneous protolith (e.g. an equigranular, medium grained tonalite, and white garnetiferous pegmatite). However, rusty garnet-graphite-rich layers appear to be relicts of metasedimentary material. These gneisses occupy a 15 km wide belt trending roughly north-northwest through the central part of 14 L/3. The garnetiferous tonalitic gneiss generally appears coarse grained, but mineral subdomains are polycrystalline and highly elongated due to very strong deformation (Ryan et al., 1983). Even though in most places compositional layering and the conspicuous lenticular quartz fabric are parallel, examples are not uncommon of the quartz fabric oblique to layering, and of small folds of the layering with the quartz fabric as the axial planar foliation and lineation. Minor but persistent and significant components in the garnetiferous gneiss belt in the present study area are garnetiferous mafic and ultramafic granulites, some of which can be traced several kilometres along strike even though they are only 5 to 50 m thick. Their distribution is probably a function of isoclinal folding and repetition of only a few such individual units; such fold patterns can be seen most easily in the gneiss belt in the southern part of the area where macroscopic fold closures are locally preserved (Fig. 73.2).

Hypersthene-bearing, buff to brown weathering, quartzofeldspathic gneisses occur along the eastern and western borders of the white tonalite gneiss. These gneisses contain rare bands of mafic gneiss and garnet-bearing gneiss similar to those described above. At both margins the contact with the white garnetiferous tonalite gneiss is gradational, and in coastal exposures along inner Hebron Fiord, the tonalite is apparently intrusive into the hypersthene gneiss. In this area as well, the easternmost gneiss can be clearly demonstrated to have been derived by pervasive Proterozoic reworking of the Kiyuktok gneisses which occur in the adjacent Nain Province. The origin of the western unit is not as obvious; in fact in places it appears to have been originally a fine grained hypersthene granite which lacks compositional layering but displays the pronounced rodding lineation common to the Churchill Province rocks in this area.

Ramah Group supracrustal rocks occupy two narrow belts north-northwest of Freytag Inlet. The western band comprises strongly deformed quartzite with a single 1 m layer of amphibolite; the eastern band comprises quartzite with a central layer of pelitic (muscovite-biotite) schist. These lithologies are considered to be tectonized members of the basal part of the Ramah Group, the Rowsell Harbour Formation (Knight and Morgan, 1977; Morgan, 1975a), which have been interleaved with reworked Archean basement during the Hudsonian Orogeny. No Ramah Group rocks were found south of the northwest-trending fault through Freytag Inlet.

STRUCTURE AND METAMORPHISM

There is an obvious structural contrast between the Nain Province and the Churchill Province (Fig. 73.2). The Nain is typified by alternating orthogneiss and supracrustal gneiss units with a general northwest grain, locally displaying dome and basin fold patterns which are dissected by faults. Layering and fold axes are commonly steep, with the most obvious exception being a compositionally layered mafic gneiss (metagabbro) with metasedimentary screens which occupies a recumbent structure west of Kangerdluarsuksoak Inlet. The Churchill Province on the other hand lacks this closely alternating polylithological pattern, but instead is typified by broad orthogneiss belts containing only minor amounts of other rock types with a steeply dipping north-northwest trend, and in which the intensity of Hudsonian deformation has destroyed or effectively masked any fold closures. A very prominent feature of the Churchill Province gneisses is a subhorizontal mineral rodding lineation within foliation planes, chiefly defined by grey quartz, but also by graphite smears and minute rutile needles. The Ramah Group in the eastern Churchill Province is structurally interleaved with retrogressed Archean basement. Its distribution seems to be the result of refolding of basement-cover thrust slices (Ryan et al., 1983).

Metamorphic rocks exhibit amphibolite or granulite facies assemblages throughout the study area. The Archean terrane of the Nain Province east of Handy Fault is transitional between amphibolite and granulite facies; the most obvious indicator of this is coarse orthopyroxene grains in pegmatoidal sweats in mafic rocks, and diffuse orthopyroxene- and garnet-bearing pegmatites emplaced syntectonically with the reworking of the Uivak gneisses (cf. Ryan, 1977). Retrogressed quartzofeldspathic rocks in this area have a green "blebby" aspect where orthopyroxene has been replaced by green biotite. West of Handy Fault the granulite aspect of the Archean rocks is more obvious: mafic rocks are friable and the quartzofeldspathic rocks are brownish weathering and are greenish brown on broken surfaces. However, within this terrane there are narrow belts of retrogression to amphibolite facies which have abrupt contacts with the surrounding granulites. Sillimanite and garnet are ubiquitous in paragneisses throughout the map area; cordierite has also been locally identified.

In the Hudsonian foreland zone east of the Ramah Group (Fig. 73.1c, 73.2), the Archean granulite facies gneisses exhibit an amphibolite facies overprint, and the diabase dykes are foliated and converted to amphibolites.

The part of the Churchill Province containing the Ramah Group (Fig. 73.1c, 73.2) exhibits amphibolite facies metamorphism: sillimanite and kyanite have been identified in the pelitic schists just north of the study area, the granulite facies basement is retrogressed to amphibolite facies gneisses and schists, and diabase dykes are transformed into amphibolites and rotated subparallel to an attenuated Archean layering.

In the Churchill Province mobile zone (Fig. 73.1c) the consistent occurrence of orthopyroxene in tonalitic and mafic gneisses clearly demonstrates granulite facies conditions during Hudsonian deformation. It is unclear, however, whether the orthopyroxene was produced by Hudsonian metamorphism or is an Archean paragenesis which was simply modified into the Churchill Province fabric by "dry-reworking" of the Archean terrane during the Proterozoic. Directly adjacent to the western contact of the pseudotachylyte-ultramylonite on the eastern margin of the mobile belt (Fig. 73.2), hornblende is abundant and orthopyroxene rare, indicating transition to amphibolite facies.

NATURE OF THE NAIN-CHURCHILL BOUNDARY

The definition of a discrete boundary between the Nain and Churchill provinces entails all the problems inherent in establishing rigid demarcation lines in juxtaposed orogenic belts (cf. Gower et al., 1980, p. 785). The following features are considered in outlining the Nain-Churchill boundary in this area.

In the easternmost Archean terrane, with the possible exception of the faults there is no mesoscopic indication of penetrative Hudsonian deformation (e.g. the discordant late Archean-early Proterozoic diabase dykes are neither schistose nor metamorphosed) although the isotopic systems are disturbed (Collerson et al., 1982a). In the western part of the Archean block, however, the effects of Hudsonian deformation can be discerned in (i) the transformation of the diabase dykes to "greenstones" and schistose amphibolites, even though they retain their primary discordance with gneissic layering, (ii) the westward retrogression of granulite facies Archean gneisses to amphibolite grade, and (iii) folding and shearing of posttectonic pegmatites in the gneisses. We also tentatively assign the regional deformation of the lenticular grey tonalite west of Freytag Inlet to the Hudsonian Orogeny. Likewise we attribute all the north- to north-northwest-trending faults in this sector to Hudsonian deformation. It is on the basis of these observations that we have outlined the "foreland zone" to the Churchill Orogen shown in Figure 73.1c.

The "Churchill Province mobile zone" (Fig. 73.1c) corresponds to Morgan's (1975a) definition of the "Churchill Province". It comprises two domains: (i) the Ramah Group and its reworked Archean basement, confined to the area northwest of Freytag Inlet, and (ii) the high grade gneisses. The gneisses are separated from the Ramah Group in the north and from the foreland zone in the south of the study area by a major belt of ultramylonite up to 100 m wide. This ultramylonite is a dark grey to black "vitrophyric" rock characterized by large (1 cm) feldspar porphyroclasts and hornblende porphyroblasts in an aphanitic matrix. Later brittle deformation produced abundant pseudotachylyte in this rock and the gneisses immediately west and east of it. On approaching the ultramylonite zone from the gneisses to the west, there is a metamorphic change in the easternmost quartzofeldspathic granulite (Fig. 73.2) so that ortho-pyroxene becomes subordinate to hornblende without any change in structure. Adjacent to the mylonite, however, the subhorizontal linear fabric characteristic of the Churchill Province gneisses is abruptly replaced by steep westerly plunging lineations indicating eastward directed thrust movement.

In summary, the Archean-Proterozoic boundary in the Hebron area can be defined in the same terms as that of the Saglek area to the north, in being a 2 to 5 km wide zone superimposed on the Nain Province in which the Archean and early Proterozoic rocks are overprinted by Hudsonian deformation upon approaching a fault-bordered block of gneisses with pronounced Hudsonian fabrics.

ECONOMIC GEOLOGY

Hand-held scintillometer surveys and limited ultraviolet light investigation failed to reveal radioactive or scheelite mineralization. Pyritic zones are locally present in the metasediments, and graphite seams occur in granulite facies rocks in the Churchill Province, but none appears to be of economic importance.

ACKNOWLEDGMENTS

Ryan, Martineau and Lee thank T. Froude, D. Pollard and R. Wells for cheerful and responsible assistance during a not-so-pleasant field season. Korstgard thanks the Danish Natural Science Research Council for its support, and his assistant, Soren Schaumann, for his help and companionship. We also acknowledge the numerous discussions with A. Nutman, D. Bridgwater and F. Mengel. Ryan and Martineau acknowledge discussions with, and the contributions of, K. Collerson who spent three days navigating the rough and rocky shores of Hebron Fiord with us. W. Tuttle and K. O'Quinn provided logistical support. Phil Faubert and Wayne Murozuk of Verreault Helicopters were an excellent air crew. The staff of Petro-Canada at Saglek again provided their co-operation.

REFERENCES

Baadsgaard, H., Collerson, K.D., and Bridgwater, D.
1979: The Archean gneiss complex of northern Labrador. 1. Preliminary U-Th-Pb geochronology; Canadian Journal of Earth Sciences, v. 16, p. 951-961.

Barton, J.M., Jr.
1975: Rb-Sr isotopic characteristics and chemistry of the 3.6 b.y. Hebron gneiss, Labrador; Earth and Planetary Science Letters, v. 27, p. 427-435.

Bridgwater, D. and Collerson, K.D.
1976: The major petrological and geochemical characters of the 3600 m.y. Uivak gneisses from Labrador; Contributions to Mineralogy and Petrology, v. 54, p. 43-59.

Bridgwater, D., Collerson, K.D., Hurst, R.W., and Jesseau, C.W.
1975: Field characters of the early Precambrian rocks from Saglek, coast of Labrador; in Report of Activities, Part A, Geological Survey of Canada, Paper 75-1A, p. 287-296.

Bridgwater, D., Collerson, K.D., and Myers, J.S.
1978: The development of the Archean gneiss complex of the North Atlantic region; in Evolution of the Earth's Crust, ed. D.H. Tarling; London Academic Press, p. 19-69.

Bridgwater, D., Watson, J.V., and Windley, B.F.
1973: The Archean craton of the North Atlantic region; Royal Society of London, Philosophical Transactions, Series A, v. 273, p. 493-512.

Collerson, K.D.
1983: Ion microprobe zircon geochronology of the Uivak gneisses: Implications for the evolution of early terrestrial crust in the North Atlantic craton; Lunar and Planetary Institute Meeting, August 10-16, 1983, Ottawa, abstract.

Collerson, K.D. and Bridgwater, D.
1979: Metamorphic development of early Archean tonalitic and trondhjemitic gneisses, Saglek area, Labrador; in Trondhjemites, Dacites and Related Rocks, ed. F. Barker; Elsevier, p. 205-273.

Collerson, K.D., Brooks, C., Ryan, A.B., and Compston, W.
1982a: A re-appraisal of the Rb-Sr systematics of early Archean gneisses from Hebron, Labrador; Earth and Planetary Science Letters, v. 60, p. 325-336.

Collerson, K.D., Jesseau, C.W., and Bridgwater, D.
1976: Crustal development of the Archean gneiss complex: eastern Labrador; in The Early History of the Earth, ed. B.F. Windley; John Wiley and Sons Ltd., p. 237-253.

Collerson, K.D., Kerr, A., and Compston, W.
1981: Geochronology and evolution of late Archean gneisses in northern Labrador: an example of reworked sialic crust; Geological Society of Australia, Special Publication 7, p. 205-222.

Collerson, K.D., Kerr, A., Vocke, R.D., and Hanson, G.N.
1982b: Reworking of sialic crust as represented in late Archean-age gneisses, northern Labrador; Geology, v. 10, p. 202-208.

Davidson, A.
1972: The Churchill Province; in Variations in Tectonic Styles in Canada, ed. R.A. Price and R.J.W. Douglas; Geological Association of Canada, Special Paper 11, p. 381-434.

Gower, C.F., Ryan, A.B., Bailey, D., and Thomas, A.
1980: The position of the Grenville Front in eastern and central Labrador; Canadian Journal of Earth Sciences, v. 17, p. 784-788.

Greene, B.A.
1972: Geological map of Labrador; Mineral Resources Division, Newfoundland Department of Mines, Agriculture and Resources, St. John's.

Hurst, R.W., Bridgwater, D., Collerson, K.D., and Wetherill, G.W.
1975: 3,600 m.y. Rb-Sr ages from early Archean gneisses from Saglek Bay, Labrador; Earth and Planetary Science Letters, v. 27, p. 393-403.

Kerr, A.
1980: Late Archean igneous, metamorphic and structural evolution of the Nain Province at Saglek, Labrador; unpublished M.Sc. thesis, Memorial University of Newfoundland, St. John's.

Knight, I. and Morgan, W.C.
1977: Stratigraphic subdivision of the Ramah Group, northern Labrador; Geological Survey of Canada, Paper 75-15.

Morgan, W.C.
1975a: Geology of the Precambrian Ramah Group and basement rocks in the Nachvak Fiord – Saglek Fiord area, north Labrador; Geological Survey of Canada, Paper 74-54, 42 p.

1975b: Geology, Nachvak Fiord – Ramah Bay; Geological Survey of Canada, Map 1469A.

1978: Geology, Bears Gut – Saglek Fiord; Geological Survey of Canada, Map 1478A.

Ryan, A.B.
1977: Progressive structural reworking of the Uivak gneisses, Jerusalem Harbour, northern Labrador; unpublished M.Sc. thesis, Memorial University of Newfoundland, St. John's, 230 p.

Ryan, A.B., Martineau, Y., Bridgwater, D., Schiotte, L., and Lewry, J.
1983: The Archean – Proterozoic boundary in the Saglek Fiord area, Labrador, report 1; in Current Research, Part A, Geological Survey of Canada, Paper 83-1A, p. 297-304.

Taylor, F.C.
1969: Reconnaissance geology of a part of the Precambrian Shield, northeastern Quebec and northern Labrador; Geological Survey of Canada, Paper 68-43.

1970: Reconnaissance geology of a part of the Precambrian Shield, northeastern Quebec and northern Labrador, Part 2; Geological Survey of Canada, Paper 70-24.

1971: A revision of Precambrian structural provinces in northeastern Quebec and northern Labrador; Canadian Journal of Earth Sciences, v. 8, p. 579-584.

1979: Reconnaissance geology of a part of the Precambrian Shield, northeastern Quebec, northern Labrador and Northwest Territories; Geological Survey of Canada, Memoir 393, 99 p.

74. GEOLOGY OF THE DOUBLE MER WHITE HILLS AND SURROUNDING REGION, GRENVILLE PROVINCE, EASTERN LABRADOR[1]

Project 830034

Charles F. Gower[2]

Gower, C.F., Geology of the Double Mer White Hills and surrounding region, Grenville Province, eastern Labrador; in Current Research, Part A, Geological Survey of Canada, Paper 84-1A, p. 553-561, 1984.

Also in Current Research, Newfoundland Department of Mines and Energy, Mineral Development Division, Report 84-1, 1984.

Abstract

The Double Mer White Hills and surrounding region is located near the northern margin of the Grenville Structural Province in eastern Labrador and includes parts of three major crustal segments, namely the Trans-Labrador batholith, the Groswater Bay terrane and the Lake Melville terrane.

The Trans-Labrador batholith comprises two granitoid units, the Walker Lake quartz monzonite and the Crooked River granite, which are inferred to have been emplaced about 1650-1600 Ma. The Groswater Bay terrane comprises muscovite- and kyanite-bearing paragneiss, dioritic, granodioritic and granitic orthogneiss, and foliated to gneissic plutons of muscovite-biotite granite and pyroxene quartz syenite. The Lake Melville terrane is located south of the Groswater Bay terrane and separated from it by thrusts or post-Grenvillian faults. It includes kyanite or sillimanite + K-feldspar paragneiss, granitic orthogneiss and granulite facies gabbroic, monzonitic and granitic rocks. Geochronological ages of these units have not been determined but evidence from adjacent areas suggests that the paragneiss is Aphebian, and remained as remnants after extensive plutonism which probably ceased about 1600 Ma.

The area was subsequently intruded by mafic rocks, probably of several ages, especially the Michael gabbro (ca. 1400 Ma). The Double Mer Formation, which consists of unmetamorphosed arkose and conglomerate, was deposited in a post-Grenvillian half-graben.

Résumé

La région de Double Mer White Hills et la région avoisinante sont situées près de la marge nord de la province de Grenville dans la partie est du Labrador; cette région comprend des parties de trois grands segments de la croûte, soit le batholite Trans-Labrador, le terrain de Groswater Bay et le terrain de Lake Melville.

Le batholite Trans-Labrador comprend deux unités granitoïdes, la monzonite quartzique de Walker Lake et le granite de Crooked River, qui ont vraisemblablement été mis en place il y a de 1 650 à 1 600 Ma. Le terrain de Groswater Bay se compose de paragneiss à muscovite et à cyanite, d'orthogneiss dioritique, granodioritique et granitique et de plutons feuilletés à gneissiques de granite à muscovite-biotite et de syénite à quartz et à pyroxène. Le terrain de Lake Melville est situé au sud du terrain de Groswater Bay et est séparé de celui-ci par des failles chevauchantes ou des failles post-grenvilliennes. Le terrain de Lake Melville comprend un paragneiss à cyanite ou à sillimanite et à feldspath potassique, un orthogneiss granitique et des roches gabbroïques, monzonitiques et granitiques métamorphisées au faciès à granulites. Les âges géochronologiques de ces unités n'ont pas encore été déterminés, mais des indications provenant de régions contiguës permettent de croire que le paragneiss date de l'Aphébien et est demeuré sous forme de résidus après une période de plutonisme étendu qui aurait vraisemblablement cessé il y a environ 1 600 Ma.

Des roches mafiques probablement d'âges variés, notamment le gabbro de Michael, qui a été mis en place il y a environ 1 400 Ma, ont par la suite fait intrusion dans la région. La formation de Double Mer composée d'arkose et de conglomérat non métamorphisés, a été déposée dans un demi-graben post grenvillien.

INTRODUCTION

Systematic 1:100 000 scale geological mapping in Labrador during the past five years by the Newfoundland Department of Mines and Energy has focussed on the northern margin of the Grenville Province. Mapping of the area described in this report during the 1983 field season completes geological coverage along the entire length of the Grenville Front (Tectonic) Zone in Labrador.

The study area (Fig. 74.1), includes six NTS 1:50 000 map sheets (13 J/3, 4, 5, 6, K/ 1, 8), which cover an area of approximately 5500 km^2. Preliminary results from the first year of the Canada-Newfoundland co-operative mineral program in eastern Labrador were reported by Erdmer (1983) who mapped three NTS 1:50 000 map sheets (13 F/16, G/13, 14) immediately south of the present area.

Reconnaissance geological mapping at 1:250 000 scale was carried out by the Geological Survey of Canada; (13 K (east half) by Williams, 1970; 13 J by Stevenson, 1970). Present work has refined the distribution of rock units but, because of the very few outcrops, most geological boundaries and the structural interpretation remain largely conjectural. In contrast, as samples were collected from nearly every outcrop, and have been slabbed, stained (K-feldspar specific) and compared in detail, lithological descriptions and grouping should be more valid.

[1] Contribution to Canada-Newfoundland co-operative mineral program 1982-84. Project carried by Geological Survey of Canada and Newfoundland Department of Mines and Energy.

[2] Newfoundland Department of Mines and Energy, Mineral Development Division, P.O. Box 4750, St. John's, Newfoundland A1C 5T7

REGIONAL SETTING

The study area, which is located within the Grenville province, partly straddles the Grenville Front Zone, as depicted by Gower et al. (1980). The line marking the northern "limit of widespread Grenville deformation" (Gower et al., 1980, p. 787) is indicated in Figure 74.1.

The Trans-Labrador batholith (Wardle et al., 1982) is a belt of granitoid rocks along the northern flank of the Grenville Province across much of Labrador. Rock types include granodiorite, granite, quartz syenite and quartz monzonite. Individual plutons have generally yielded 1650-1600 Ma ages. The Trans-Labrador batholith intrudes felsic volcanic rocks of the upper Aillik Group (ca. 1750-1650 Ma) (Bailey, 1979; Gower, 1981). Elsewhere, the Trans-Labrador batholith is in part unconformably overlain by the Bruce River Group but includes plutons intrusive into the Bruce River Group (ca. 1530 Ma) (Ryan, 1981). The granitoid rocks are regarded as genetically related to felsic volcanic rocks in the upper Aillik Group and to similar rocks in the Bruce River Group (Bailey, 1979; Ryan, 1981). This implies plutonism/volcanism extending over a considerable length of time.

The terms Groswater Bay terrane and Lake Melville terrane refer to two contrasting geological regions recently identified by the author in the Grenville of eastern Labrador. These regions are structurally bounded crustal segments delineated on the basis of lithological associations, structural style and grade of metamorphism. Characteristics of these two terranes are briefly summarized here.

Rock types in the Groswater Bay terrane include tonalite/granodiorite orthogneiss, pelitic/psammitic paragneiss, K-feldspar megacrystic granodiorite, diorite, pyroxene-bearing granitoid intrusive rocks and mafic rocks of various ages. Structural trends, where little modified by Grenvillian deformation, are north to northeast, and are similar to the Makkovik trend in the Makkovik subprovince. There is a metamorphic grade variation southward across the Groswater Bay terrane from greenschist to middle amphibolite facies.

Rock types in the Lake Melville terrane are similar to those in the Groswater Bay terrane, but proportions differ. For example, paragneiss is more extensive, and includes minor calc-silicate layers in the Lake Melville terrane. Mafic rocks, except near the northern flank of the Lake Melville terrane, are less common. In contrast to relatively (deceptively?) simple structural patterns in the Groswater Bay terrane, the Lake Melville terrane shows chaotic structural trends. Also metamorphic grade is generally higher; the broad northern fringe of the Lake Melville terrane is characterized by medium pressure granulite facies rocks which grade southward into middle amphibolite facies assemblages.

The Mealy Mountains Intrusive Suite comprises leucotroctolite, leucogabbro, anorthosite and related rocks, intruded by pyroxene quartz monzonite (Emslie, 1976). It is bounded on its northwest and northeast sides by faults, but a southeast lobe appears to be intrusive.

DESCRIPTION OF ROCK UNITS

Trans-Labrador batholith

The Trans-Labrador batholith within the map area (Fig. 74.2) comprises two contrasting granitoid units. In the north is the Walker Lake quartz monzonite, which is part of the broader Otter Lake-Walker Lake granite (Ryan, 1982). In the south is the Crooked River granite, also defined by Ryan (1982).

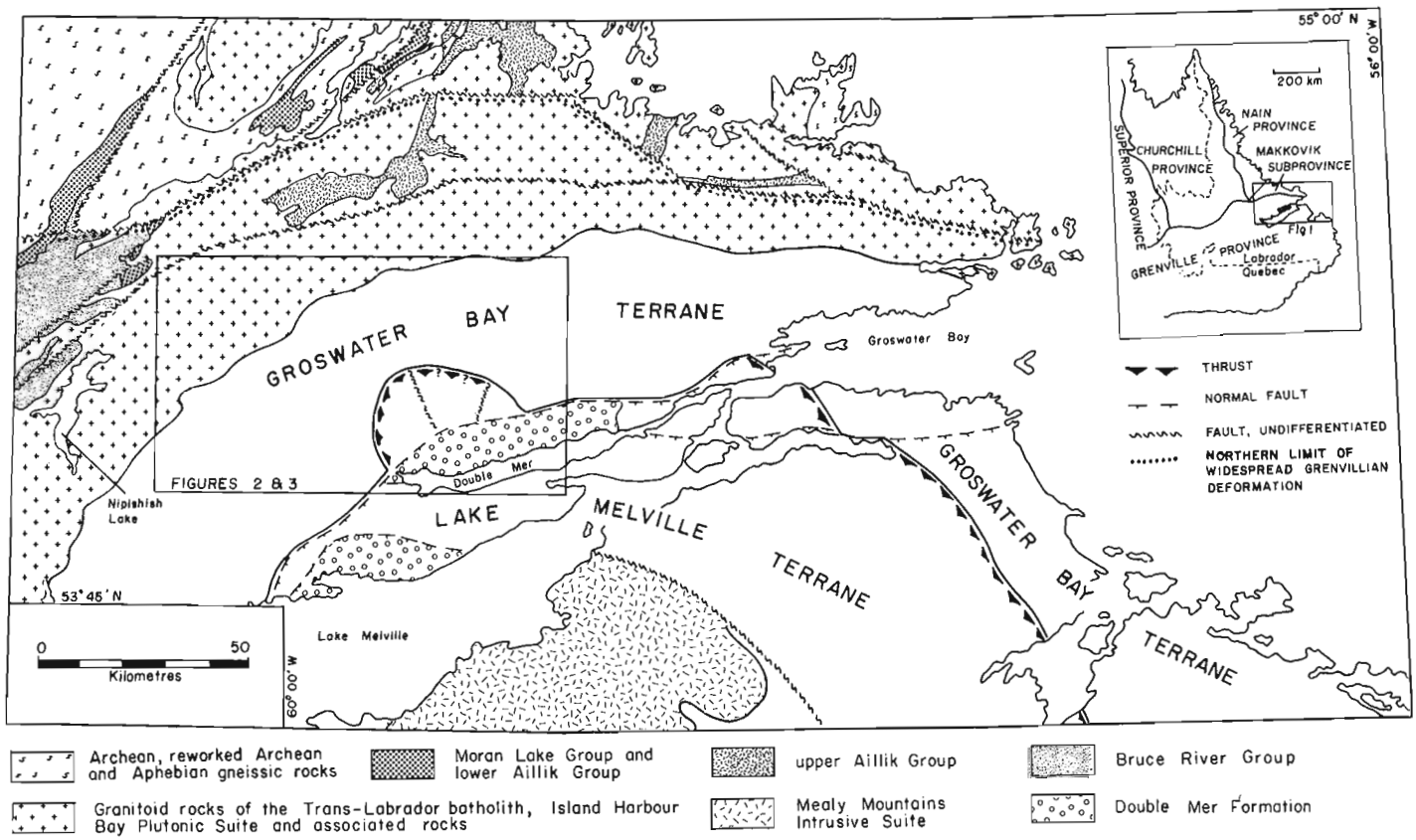

Figure 74.1. Regional geological subdivision of the Grenville structural province in eastern Labrador.

The Walker Lake quartz monzonite is predominantly a coarse grained, seriate textured, biotite-hornblende quartz monzonite, but compositional variations include monzodiorite and granite. Mafic enclaves and minor intrusions are rare. No age dating has been carried out on the Walker Lake quartz monzonite within the map area, and geochronology has not been entirely successful elsewhere. Gower, Flanagan et al. (1982) summarized age data available to the end of 1981, which collectively indicated an age of ca. 1600 Ma. Subsequently Brooks (written communication, 1983) has reported an age of 1628 ± 34 Ma (U-Pb, zircon) for biotite-hornblende quartz monzonite that previously yielded a 1595 ± 34 Ma (Rb-Sr) errorchron. However, some doubt exists whether the quartz monzonite dated by Brooks is the same unit as that underlying the present map area (Ryan, personal communication, 1983).

The Crooked River granite is a homogeneous, fine- to medium-grained muscovite-biotite granite. Quartz veins, hematized fractures, and a lack of mafic enclaves are characteristic. Typically, the rock has a sugary texture, but where deformed takes on a schistose appearance, making it similar to feldspathic metasediment, a previously suggested protolith (Williams, 1970). Lack of bedding, homogeneity over wide areas, and intrusive contacts with other granitoid rocks confirm the plutonic nature of this unit.

A small area of K-feldspar megacrystic granodiorite occurs in the northeast corner of the map area. The rock is strongly foliated with K-feldspar augen up to 4 cm long. It has been included with the Trans-Labrador batholith but could equally well be grouped with the Groswater Bay terrane.

Groswater Bay terrane

The Groswater Bay terrane is underlain by paragneiss, orthogneiss and foliated to gneissic plutons.

The paragneisses, by inference from evidence in adjacent areas, are assumed to be Aphebian, but may be Helikian. Volumetrically, they are a minor rock type in the Groswater Bay terrane. The most common lithologies are grey weathering, medium grained, quartzofeldspathic pelitic and semipeltic schists and gneisses. The gneissose varieties consist of alternating layers of a muscovite + biotite + opaque + garnet 'melanosome' (it is not melanocratic), and a coarser grained quartz + platioclse ± K-feldspar leucosome. Locally the schists are ocherous weathering due to associated sulphides, largely pyrite but also minor arsenopyrite and/or chalcopyrite. Near the southern margin of the Groswater Bay terrane the pelitic rocks have kyanite- and K-feldspar-bearing assemblages. These also contain muscovite but, pending petrographic examination, equilibrium relationships are uncertain. Kyanite was not positively identified in hand samples of pelites from the eastern part of the area, but it occurs in pelitic rocks immediately east of the map boundary (Gower, Gillespie et al., 1983). Other metasedimentary rock types within the Groswater Bay terrane include quartzite, calc-silicate rocks and layered amphibolite.

The orthogneisses include, in order of decreasing colour index, (i) biotite-hornblende granodiorite-diorite gneiss, (ii) biotite granodiorite gneiss, (iii) K-feldspar augen granodiorite gneiss, (iv) biotite granite gneiss, and (v) muscovite-biotite granite gneiss. These gneissic types grade into each other and into more uniform, foliated granitoid units. The latter feature is a major reason for interpreting derivation from the igneous protolith.

Biotite-hornblende granodiorite-diorite gneiss is the most extensive and includes amphibolite enclaves, diorites and hornblende granodiorite gneiss. Particular compositional and textural varieties tend to be grouped in subareas, suggesting that they outline former plutons. The only age data available from the map area was obtained by Wanless et al. (1972) for a rock here included as biotite-hornblende granodiorite-diorite gneiss. The age, 1160 ± 40 Ma (K-Ar, biotite, recalculated using IUGS recommended constants) reflects Grenvillian effects but the gneisses are much older. Krogh (written communication, 1983) reported a U-Pb age of ca. 1680 Ma for similar gneisses in the southwest continuation of the Groswater Bay terrane.

Biotite granodiorite gneiss occurs in two main areas, north and east-northeast of Double Mer White Hills (Fig. 74.2). North of Double Mer White Hills (adjacent to the Crooked River granite), biotite granodiorite gneiss is intermixed with biotite-hornblende granodiorite-diorite gneiss. Included is very sparsely megacrystic biotite granodiorite gneiss and rare muscovite-bearing granodiorite gneiss. The biotite granodiorite gneiss east-northeast of Double Mer White Hills is fine- to medium-grained, garnet-bearing, and grey weathering, and locally shows complex isoclinal folds.

K-feldspar augen granodiorite is interpreted to underlie an arcuate area in the eastern part of the region. The rock is homogeneous apart from a few indistinct, concordant quartzofeldspathic veins and amphibolite enclaves. K-feldspar megacrysts have been flattened and recrystallized to ellipsoidal aggregates.

Biotite granite gneiss is present east of the K-feldspar augen granodiorite. It is a medium grained rock containing minor garnet and, like the adjacent K-feldspar augen granodiorite, it is intensely foliated and lineated.

The muscovite-biotite granite gneiss, which underlies a large part of the south-central map area, is a fine- to coarse-grained, pink weathering rock with biotite schlieren, amphibolite enclaves and pegmatitic segregations. Locally extensive, homogeneous patches of pegmatitic muscovite-biotite-garnet granite are present, which may represent melt which crystallized after the peak of deformation.

The larger of two foliated to gneissic plutons in the Groswater Bay terrane is a pyroxene-bearing quartz syenite to granite recognized during reconnaissance mapping (Eade, 1962; Stevenson, 1970). Its outline has been refined during remapping (see also Erdmer, 1983). Rock types include quartz syenite, granite and alkali feldspar granite, with quartz monzonite and muscovite granite in western and northern border areas respectively. Pyroxene is characteristic, but other mafic minerals include garnet, amphibole and biotite. The rock was originally coarse grained but has been recrystallized to a medium grained texture, especially in gneissic borders of the pluton. Krogh (written communication, 1983) obtained an age of 1632 ± 7 Ma (U-Pb, zircon) from the pluton, south of the present map area.

The muscovite-bearing granite is a medium- to coarse-grained, massive to strongly foliated rock which also contains garnet and biotite. The borders were not observed, and the surrounding granite gneiss may be merely a more deformed equivalent.

Lake Melville terrane

Paragneiss within the Lake Melville terrane occurs as two south-dipping sheets underlying the Double Mer White Hills, and in a third area at the western end of Double Mer. The structurally lower paragneiss sheet, around the west and north flanks of Double Mer White Hills, has more variability than other paragneisses within the map area becuase of a higher porportion of calc-silicate rock and quartzite to semipelite. The semipelitic schist and gneiss are

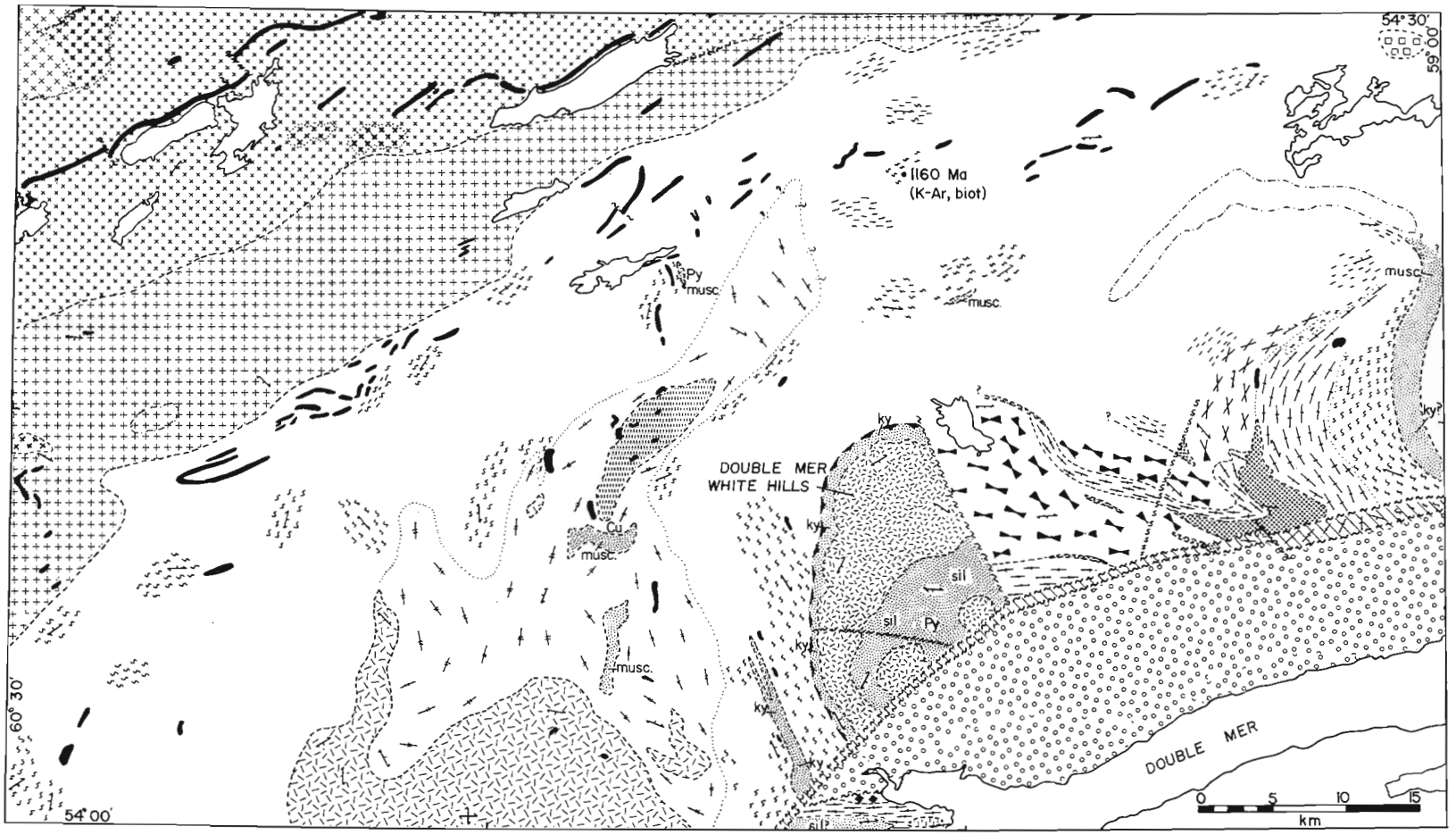

HADRYNIAN

Double Mer Formation: red arkose and minor conglomerate

HELIKIAN

Gabbro, leucogabbro, amphibolite: includes **Michael Gabbro**

TRANS-LABRADOR BATHOLITH

Biot. granite
Biot. hbl. qtz. monzonite
Hbl. monzodiorite
} Otter Lake–Walker Lake Granite

Crooked River Granite: pink, musc. and biot. microgranite

K-fs. megacrystic biot. granite

HELIKIAN (continued)

FOLIATED TO GNEISSIC PLUTONS
GROSWATER BAY TERRANE

Musc.-rich granite
Pyx. qtz. syenite to granite

LAKE MELVILLE TERRANE

Hbl. qtz. monzonite to granite
K-fs. megacrystic biot. granodiorite
Leucomonzonite opx-cpx. granulite

LAKE MELVILLE OR TRANSITIONAL TERRANE

Opx-cpx. monzonite-granite granulite
Pyx.-bearing diorite to gabbro

HELIKIAN AND/OR APHEBIAN?

ORTHOGNEISS: GROSWATER BAY AND LAKE MELVILLE TERRANES

Musc. biot. granite gneiss
Biot. granite gneiss
Biot. granodiorite gneiss
Biot. hbl granodiorite-diorite gneiss
K-fs. augen granodiorite gneiss
Unexposed, assumed underlain by gneiss

APHEBIAN?

Pelitic and psammitic paragneiss, minor calc-silicate rock and quartzite

Fault breccia zone
Fault
Thrust
Geological boundary
approximate, diffuse
Foliation or gneissosity
Marked aeromagnetic anomaly

Cu Malachite
musc Muscovite
sil Sillimanite
Py Pyrite
ky Kyanite

Figure 74.2. *Geology of the Double Mer White Hills and surrounding region.*

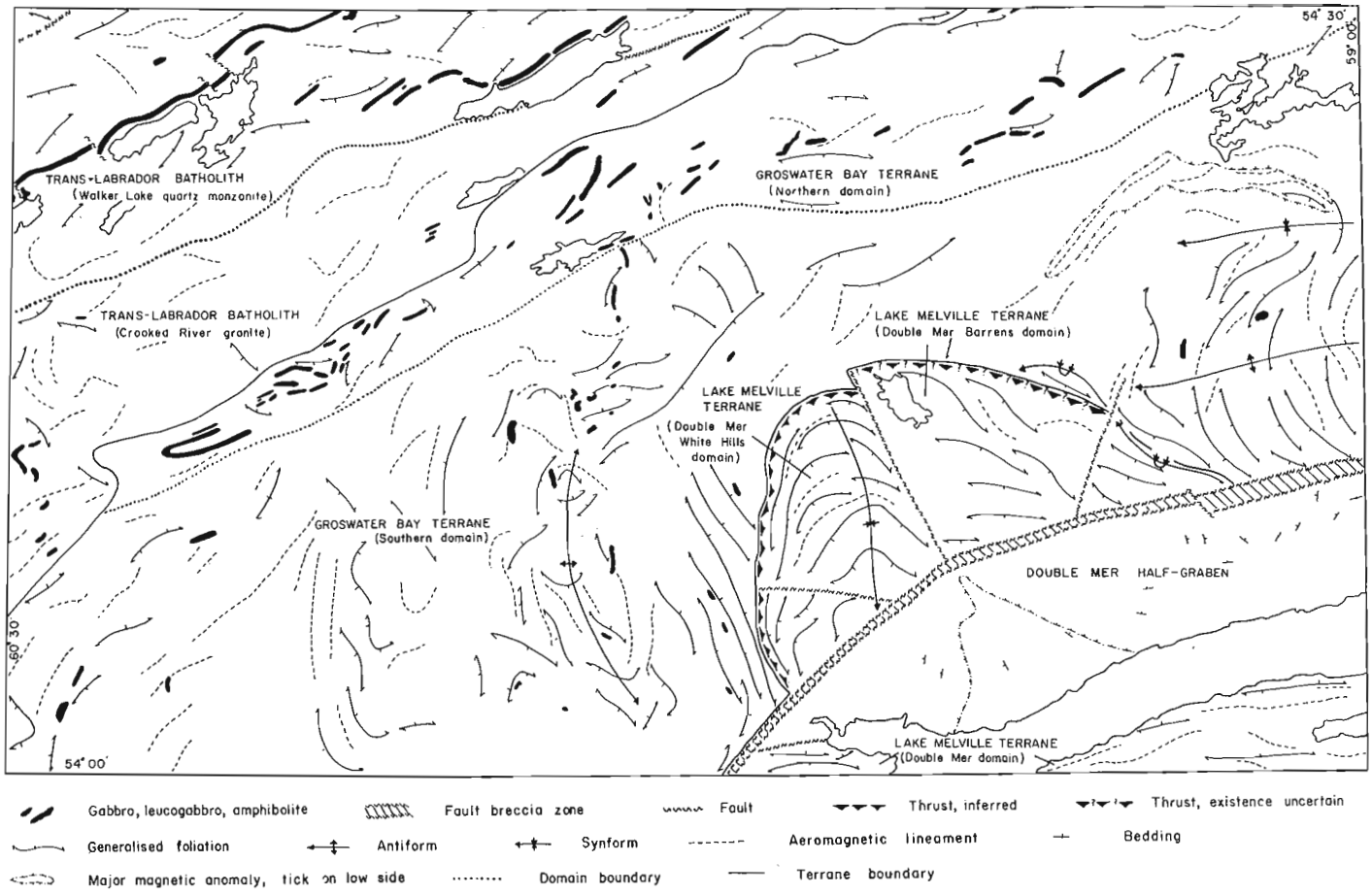

Figure 74.3. *Lithotectonic terranes, domains and other structural features in the Double Mer White Hills and surrounding region.*

characteristically well banded, with abundant kyanite, K-feldspar and garnet. The associated calc-silicate rocks are medium grained, with an alternating green and red banded appearance, due mainly to variation in pyroxene and garnet proportions. Quartzite layers are white or grey weathering and medium grained; both orthoquartzite and impure psammitic quartzite are present.

Paragneiss in the upper sheet comprises ocherous weathering psammitic gneiss with subsidiary pelite and calc-silicate rock. The pelitic rocks differ from those in the lower sheet in having sillimanite- rather than kyanite-bearing assemblages. The garnets are pale mauve, as characteristic of high grade paragneiss.

The small area of paragneiss at the west end of Double Mer is characterized by extensive leucosome, biotite schlieren, mauve garnet, variable grain size and marked compositional contrast between individual layers. Some of the rocks are diatexite. Sillimanite was tentatively recognized at one locality and confirmed identifications have been made in contiguous areas to the southeast.

Apart from granitic geniss, most of the orthogneiss rock types described for the Groswater Bay terrane are not present in the Lake Melville terrane of the map area, but are known in Lake Melville terrane elsewhere (Gower, Gillespie et al., 1983; Gower, Noel et al., 1983). Granitic gniess in the Double Mer Barrens domain (Fig. 74.2, 74.3) is interlayered with monzonite-granite granulite. It is a fine- to medium-grained rock with a strongly foliated, lineated or mylonitic fabric and contains minor garnet and (?)pyroxene. The rock may be simply a lithological variant of the monzonite-granite granulite rather than analogous to other granitic gneisses in the region. Granitic gneiss at the west end of Double Mer is mostly fine grained, homogeneous microgranite closely associated with paragneiss and diatexite. It is possible that this granitic gneiss was derived from a psammitic protolith. Similar rocks are more widespread south of the map area and a comprehensive description is given by Erdmer (1983).

Five units have been grouped as foliated to gniessic plutons in the Lake Melville terrane. These are (i) granulite facies, pyroxene-bearing diorite to gabbro, (ii) monzonite-granite granulite, (iii) leucomonzonite granulite, (iv) K-feldspar megacrystic biotite granodiorite, and (v) hornblende quartz monzonite to granite.

The pyroxene-bearing diorite to gabbro unit is interpreted to have been derived from gabbro, leucogabbro, anorthosite and diorite. These rocks are grouped because of their mutual association, low quartz content and lack of K-feldspar. Although it is tempting to regard these rocks as remants of a former layered mafic intrusion, on present knowledge it is equally possible that entirely genetically disparate rocks have been included.

The monzonite-granite granulite is a medium- to coarse-grained rock containing orthopyroxene, clinopyroxene and abundant garnet. Most outcrops are quartz-poor/K-feldspar-rich monzonite, but the more northerly and easterly areas are underlain by quartz-rich monzonite and granite respectively. Taken at face value, Figure 74.2 suggests equivalence between the granulite facies quartz monzonite and K-feldspar augen gneiss within the Groswater Bay terrane. The rocks indeed have textural similarities. Stained slabs suggest compositional contrasts but these may be interpretable in terms of granulite facies dehydration of biotite to give anhydrous mafic phases and additional K-feldspar. This, however, requires more petrographic and chemical data.

The leucomonzonite granulite underlying the Double Mer White Hills occurs as two separate, lithologically similar sheets. The rocks have been thoroughly recrystallized to a fine- or medium-grained rock with a streaky, layered appearance, due to extreme flattening and stretching. The white weathering appearance of the rock gives a misleading impression that K-feldspar is rare, which staining has demonstrated unfounded. The rock differs from the monzonite-granite granulite farther east because of its finer grain size and much lower garnet content.

The remaining two granitoid units occur at the west end of Double Mer. The K-feldspar megacrystic biotite granodiorite contains elliptical megacrysts up to 8 cm long. This unit correlates with a K-feldspar megacrystic granodiorite sheet farther east mapped by Erdmer (1983) on the south side of Double Mer. The hornblende quartz monzonite to granite is a coarse grained, homogeneous monzonite to granite observed at one locality. It is lithologically comparable to much larger bodies on the southeast side of Lake Melville (Gower, Noel et al., 1983).

Mafic intrusions

Mafic intrusive rocks within the map area are discussed with the following two considerations in mind.

i) Although it has been recognized that mafic intrusive rocks were emplaced at various times in the Grenville of eastern Labrador (Gower et al., 1981; Gower, Owen and Finn, 1982; Owen and Rivers, 1983), it is rarely possible to assign a particular outcrop to a particular intrusive pulse. For this reason, mafic intrusions are not subdivided on the map, and have been collectively grouped as Helikian. Nevertheless, two periods of mafic activity at ca. 1650-1600 Ma (cf. Adlavik Intrusive Suite) and ca. 1400 Ma (cf. Michael gabbro) appear to be of major significance compared to the others.

ii) Mafic intrusive rocks, with some exceptions, show a progressive increase in deformation and/or metamorphism southeastward across the map area.

Within the Walker Lake quartz monzonite, mafic rocks fall into two main groups, both of which are assigned as Michael gabbro. These are a northern, continuous sheet and a southern discontinuous sheet. The northern sheet is a coarse grained, massive olivine gabbro without coronite textures or garnet. K-feldspar is a common interstitial phase. The southern gabbro is mineralogically and texturally similar, but it occurs as a series of elongate, discontinuous bodies. Rarely, double coronas are present (an inner corona of hypersthene and an outer corona of pargasitic amphibole; see Emslie, 1983), and a few rocks contain scattered garnet.

Gabbroid rocks are less abundant in the Crooked River granite. The three mafic bodies closest to the northern border of the Crooked River granite are biotite-bearing amphibolite, locally with relict ophitic textures. In view of the fact that most of the surrounding rocks are only slightly metamorphosed gabbros, these rocks may be the product of an earlier metamorphic event, perhaps related to neither the 1650-1600 Ma suite nor the 1400 Ma gabbros. A cluster of three mafic bodies in the south-central part of the Crooked River granite has very coarse 'appinitic' textures, a feature characteristic of the 1650-1600 Ma suite.

The mafic intrusions at the southwest end of the Crooked River granite are a mixed group of ophitic textured metagabbros, locally with double coronas, grading into amphibolite, especially at intrusion margins. Garnet is present but not in coronas. This group is assigned to the Michael gabbro.

Most of the rocks in the northern domain of the Groswater Bay terrane are fine- to coarse-grained gabbro to leucogabbro, generally massive, with ophitic textures, and best assigned to Michael gabbro. The gabbros are olivine-bearing with well developed double coronas. Locally partial garnet coronas are present, but more typically the garnets are scattered throughout the rock or concentrated near fractures.

Mafic intrusions are much less common in the southern part of the Groswater Bay terrane. The most northerly gabbros contain double coronas and garnet; these grade southward into garnet-coronite gabbros which still retain relict ophitic textures. Some amphibolite and metamorphosed ultramafic rocks are present and, as farther north, they contrast with nearby coronite metagabbros, suggesting that they are genetically distinct. In the most southerly outcrops in the area, ophitic texture is lost, hornblende (which increases in abundnace southward, together with garnet) becomes widespread, and the rocks grade into garnet amphibolite. Hence any textural distinction between the later gabbros and the supposed earlier intrusions is eliminated.

Apart from a few minor mafic intrusions, and the diorite-gabbro unit referred to above, no mafic rocks were mapped within the Lake Melville terrane in the map area. However, it should be noted that mafic intrusions do occur in the Lake Melville terrane farther east and south.

Double Mer Formation

The Double Mer Formation consists of orange, red, pink or maroon weathering, crossbedded arkose sandstone interbedded with shale and conglomerate. These rocks were first named by Kindle (1924) and subsequently mapped by Stevenson (1970). Except for a slight modification at the west end of Double Mer, the present distribution of outcrop shown differs little from that of Stevenson (1970).

STRUCTURE

The area underlain by the Trans-Labrador batholith appears to be structurally simple. The granitoid rocks are massive or show weak east-northeast trending foliation which generally dips within 5 degrees of vertical. All shallower dips are inclined southeast. Foliation directions in the Crooked River granite are less consistent than in the Walker Lake quartz monzonite. The arcuate outline of the gabbro near the western margin of the map area implies folding which must have also affected the host granite. In both granitoid units, but especially the Walker Lake quartz monzonite, foliation is inhomogeneous with large areas of massive quartz monzonite between local foliated zones which may be accompanied by low grade alteration. This feature is attributed to regional inhomogneous Grenvillian strain.

Faulting in two directions is inferred. East-northeast shear zones, accompanied by retrograde alteration, were identified in two places, and northwest trending faults have been interpreted to explain offsets along the northern gabbro.

An important question, especially relevant to the northern domain of the Groswater Bay terrane, is whether the isolated hills of gabbro are part of a subsurface continuous gabbro sheet, with presently unexposed areas having been eroded and covered as a result of glaciation, or else the present outcrop genuinely reflects bedrock gabbro distribution. The former interpretation was adopted by Fahrig and Larochelle (1972) and Emslie (1983), who both depicted the gabbro as anastomosing sheets. In consideration of the opposing viewpoint, the following features are noteworthy: (i) there is a decrease in topographic continuity of exposed gabbro progressively southward, (ii) there is evidence of complex folding (one fold closure has a north trending fold axis), and (iii) many gabbro bodies exposed on the shore of Groswater Bay (outside the map area) exhibit severely deformed and boudinaged margins. Therefore the distribution of gabbro on the sketch map may well reflect bedrock distribution, entertaining the hypothesis that the bodies are 'megaboudins' formed during Grenvillian deformation.

Foliation attitude in the host gneiss is variable, perhaps because many gneiss outcrops are adjacent to gabbro and therefore are influenced by the shape of the adjacent 'megaboudin'. Gneiss remote from gabbro has an east-northeast trend. The poor exposure obscures what is probably a zone of extreme complexity. It is possible that the boundary between the Groswater Bay terrane and the Trans-Labrador batholith is a thrust, a thought endorsed by Ryan (personal communication, 1983) for the comparable boundary farther southwest.

In the southern domain of the Groswater Bay terrane, foliation attitudes and distribution of rock units suggest complex structures resulting from fold interference. The interpretation advanced here is that the pre-Grenvillian structural trend was north to northeast and was subsequently overprinted by east-northeast trending Grenvillian folds.

The nature of the interface between the northern and southern domains of the Groswater Bay terrane is unknown. In the centre of the map area, mafic bodies (and structures in associated gneiss) of the southern domain have a north trend. This appears to be truncated by east-northeast trends in the northern domain, which may mean that the two domains are separated by a 'structural discontinuity', possibly a thrust.

Evidence is strong for a thrust separating the Groswater Bay terrane and the Double Mer White Hills domain of the Lake Melville terrane. In addition to a sharp topographic break, structural trends in the Groswater Bay terrane are truncated by those in the Lake Melville terrane, and the Lake Melville terrane rocks exhibit intense stretching lineations, absent in contiguous Groswater Bay terrane gneisses.

Farther east, the boundary between the Groswater Bay terrane and the Double Mer Barrens domain cannot be delineated using ground features (in contrast to the remainder of the Groswater Bay terrane – Lake Melville terrane interface in Fig. 74.1). However, as the boundary elsewhere includes metamorphic as well as structural contrasts, it is hoped that this problem can be clarified after petrographic studies. In Figure 74.3, the boundary is partly indicated as a thrust and partly located along the axial trace of an interpreted recumbent synform.

The Lake Melville terrane south of Double Mer is characterized by well defined east trending foliations, variable dip directions and small scale isoclinal folds.

The area underlain by the Double Mer Formation is interpreted as a half-graben, bounded on the north by a major fault. The fault is indicated by brecciated, sheared and mylonitized rocks, low grade alteration, a marked topographic scarp and contrasting aeromagnetic patterns. The 'fan' of three faults on the north side probably is a related structure, perhaps formed in response to the change in trend of the Double Mer fault. The presence of both mylonite and low grade alteration/brecciation suggests that the Double Mer Fault was the site of a pre-existing thrust, which was reactivated as a normal fault when the Double Mer half-graben was formed.

The southern contact between the Double Mer Formation and the underlying gneiss is unexposed. If it is a fault, it is certainly not of comparable magnitude to the fault along the northern contact. Aeromagnetic patterns suggest a north sloping base for the Double Mer Formation. An aeromagnetic high near the west end of Double Mer (Fig. 74.3) is interpreted as a basement culmination. Bedding directions in the Double Mer Formation dip away from this high; whether this reflects folding or a pre-Double Mer Formation erosional irregularity is unknown.

METAMORPHISM

The Trans-Labrador batholith is characterized by greenschist facies assemblages. Epidote alteration of plagioclase and chloritization of biotite are widespread. No garnet was observed in either the Walker Lake quartz monzonite or the Crooked River granite, but Ryan (personal communication, 1983) has noted small garnets in thin sections of Crooked River granite farther west. In the granitoid rocks in the Groswater Bay terrane, garnet is more abundant in the south than the north. Some of the dioritic gneisses bear scapolite. Epidote is widespread. The monzonite to granitoid rocks in the Lake Melville terrane north of the Double Mer fault contain common garnet and ortho- and clinopyroxene. In contrast, granulite facies assemblages were noted south of Double Mer.

The metasedimentary gneiss shows a concomitant increase in metamorphic grade in a southeastward direction. Muscovite-bearing assemblages are displaced by kyanite + K-feldspar and then sillimanite + K-feldspar assemblages.

Metamorphic variations in mafic rocks can be summarized as follows. In the northwest, the mafic rocks have entirely igneous mineral assemblages. The first change is the sporadic occurrence of garnet, the distribution of which can be related to avenues of fluid access (i.e. shear zones, fractures and pegmatites). Farther south metagabbro exhibits orthopyroxene – pargasitic amphibole double coronas, and garnet is more common. The garnet at this stage is not necessarily in coronas. There is a progressive change southward to mafic rocks with garnet coronas and common hornblende. The metagabbros retain ophitic textures, except at the southern margin of the map area where some rocks are amphibolite.

ECONOMIC MINERAL POTENTIAL

A thorough assessment of the economic mineral potential of the area has never been undertaken, due in part to inaccessibility and to poorly exposed outcrop. The area was included in reconnaissance mineral exploration by British Newfoundland Corporation Ltd. (BRINCO) (Beavan, 1954, 1955; Morrison, 1957) but results proved unrewarding. However, these surveys entailed very rapid coverage of extremely large areas prior to the availablility of geological mapping, geophysical or geochemical data; therefore assessments made, in my opinion, can no longer be regarded as accurate.

More recently, extensive uranium and molybdenum mineralization has been found (BRINEX Ltd.) in the upper Aillik Group, in particular the Michelin uranium deposit, located only 8 km north of the present map boundary.

Furthermore, uranium mineralization has been discovered (Kerswill and McConnell, 1982) and prospected by Northgate Exploration Ltd. in the Double Mer area, 9 km south of the map area. Thus an additional objective of this study was to determine the relationship between these two areas by examining the intervening ground.

The mineral potential of the area has been further assessed during this project using three approaches, namely (i) background radioactivity, (ii) lake sediment geochemical anomalies, and (iii) mineral occurrences. A scintillometer survey carried out showed that total counts on bedrock decrease from northwest to southeast. The highest values coincide with the Trans-Labrador batholith. This pattern cannot be totally explained by potassium abundance; otherwise higher values would be expected over the monzonites of the Lake Melville terrane.

Lake sediment geochemical anomalies (Geological Survey of Canada/Newfoundland Department of Mines and Energy, 1978) can be divided into two groups. Ni, Co and Fe (locally with Cu and Zn) anomalies are adjacent to mafic intrusions and are unlikely to be of real economic interest. Perhaps more important are U and Mo anomalies (locally also with Cu and Zn), which correlate with areas known, or inferred, to be underlain by paragneiss, or associated muscovite-bearing plutonic rocks.

Three mineral occurrences were located during mapping. The northern pyrite occurrence (Fig. 74.2) and the malachite locality are minor, but it is interesting to note that lake sediment Cu anomalies were detected near both. Nevertheless, the lake sediment geochemistry cannot be relied on to detect all mineral occurrences. For example, the southern pyrite locality is by far the largest, having several pyritic layers up to 50 cm thick and locally containing up to an estimated 15 per cent sulphide, but no lake sediment anomaly has been reported. In this case, no suitable lakes exist down-drainage for sampling.

ACKNOWLEDGMENTS

Peter King and Tony Power were able and cheerful assistants and contributed much to the success of the project. Expediting service from Goose Bay was efficiently carried out by Ken O'Quinn and Wayne Tuttle. Versatile Air Services Ltd. provided excellent helicopter support through their pilots Earl McFarland and Bob Bartlett and engineer Ron Davis. This manuscript was critically reviewed and substantially improved by Philippe Erdmer and Bruce Ryan.

REFERENCES

Bailey, D.G.
1979: Geology of the Walker-Maclean Lake area, 13K/9E, 13J/12, Central Mineral Belt, Labrador; Mineral Development Division, Department of Mines and Energy, Newfoundland and Labrador, Report 78-3, 17 p.

Beavan, A.P.
1954: Report on exploration in Labrador and Newfoundland, 1953; British Newfoundland Corporation Ltd.; unpublished report, 76 p.

1955: Report on exploration in Labrador and Newfoundland, 1954; British Newfoundland Corporation Ltd.; unpublished report with appendices, 35 p.

Eade, K.E.
1962: Geology, Battle Harbour, Cartwright; Geological Survey of Canada, Map 22-1962.

Emslie, R.F.
1976: Mealy Mountains Complex, Grenville Province, Southern Labrador; in Report of Activities, Part A, Geological Survey of Canada, Paper 76-1A, p. 165-170.

1983: The coronitic Michael gabbros, Labrador: assessment of Grenvillian metamorphism in northeastern Grenville Province; in Current Research, Part A, Geological Survey of Canada, Paper 83-1A, p. 139-145.

Erdmer, P.
1983: Peliminary report on the geology north of Upper Lake Melville, Labrador; in Current Research, Part A, Geological Survey of Canada, Paper 83-1A, p. 291-296.

Fahrig, W.R. and Larochelle, A.
1972: Paleomagnetism of the Michael Gabbro and possible evidence of the rotation of Makkovik Subprovince; Canadian Journal of Earth Sciences, v. 9, p. 1287-1296.

Geological Survey of Canada/Newfoundland Department of Mines and Energy
1978: Regional lake sediment and water geochemistry reconnaissance data, Labrador 1977; Geological Survey of Canada, Open File 513.

Gower, C.F.
1981: The geology of the Benedict Mountains, Labrador (13J northeast and 13I northwest); Mineral Development Division, Department of Mines and Energy, Newfoundland and Labrador, Report 81-3, 26 p.

Gower, C.F., Flanagan, M.J., Kerr, A., and Bailey, D.G.
1982: Geology of the Kaipokok Bay – Big River area, Central Mineral Belt, Labrador; Mineral Development Division, Department of Mines and Energy, Newfoundland and Labrador, Report 82-7, 77 p.

Gower, C.F., Gillespie, R.T., Noel, N., Bailey, D.G., and Doherty, R.A.
1983: Rigolet 1:100 000 map-sheet; Mineral Development Division, Department of Mines and Energy, Newfoundland and Labrador, Map 83-42.

Gower, C.F., Noel, N., and Gillespie, R.T.
1981: The geology of the Rigolet Region, Labrador; in Current Research for 1980, Mineral Development Division, Newfoundland Department of Mines and Energy, Report 81-1, p. 121-129.

Gower, C.F., Noel, N., Gillespie, R.T., Finn, G., and Emslie, R.F.
1983: English River 1:100 000 map-sheet; Mineral Development Division, Department of Mines and Energy, Newfoundland and Labrador, Map 83-46.

Gower, C.F., Owen, V., and Finn, G.
1982: The geology of the Cartwright Region, Labrador; in Current Research, Mineral Development Division, Newfoundland Department of Mines and Energy, Report 82-1, p. 122-130.

Gower, C.F., Ryan, A.B., Bailey, D.G., and Thomas, A.
1980: The position of the Grenville Front in eastern and central Labrador; Canadian Journal of Earth Sciences, v. 17, p. 784-788.

Kerswill, J.A. and McConnell, J.W.
1982: Geochemistry and geology of some uraniferous granites in Labrador; in Uranium in Granites, ed. Y.T. Maurice; Geological Survey of Canada, Paper 81-23, p. 171-172.

Kindle, E.M.
1924: Geography and geology of the Lake Melville district, Labrador Peninsula; Geological Survey of Canada, Memoir 141, 71 p.

Morrison, E.R.
1957: Preliminary report on the geological mapping of the Asbestos Corporation Joint Venture – Kaipokok Concession; Asbestos Corporation – Brinex, unpublished report, 19 p.

Owen, V. and Rivers, T.
1983: Geology of the Smokey archipelago, Grenville front zone, Labrador; in Current Research, Part A, Geological Survey of Canada, Paper 83-1A, p. 153-161.

Ryan, B.
1981: Volcanism, sedimentation, plutonism and Grenvillian deformation in the Helikian basins of Central Labrador; in Proterozoic Basins of Canada, ed. F.H.A. Campbell; Geological Survey of Canada, Paper 81-10, p. 361-378.

Ryan, B. (cont.)
1982: Geology of the Central Mineral Belt, Labrador; Department of Mines and Energy, Newfoundland and Labrador, Maps 82-3 and 82-4.

Stevenson, I.M.
1970: Rigolet and Groswater Bay map-area, Newfoundland (Labrador) (13J, 13I); Geological Survey of Canada, Paper 69-48, 24 p.

Wanless, R.K., Stevens, R.D., Lachance, G.R., and Delabio, R.N.
1972: Age determinations and geological studies: K-Ar Isotopic ages, Report 10; Geological Survey of Canada, Paper 71-2, 96 p.

Wardle, R.J. and staff, Labrador Section
1982: The Trans-Labrador batholith; a major pre-Grenvillian feature of the eastern Grenville Province; in Grenville Workshop, 1982, Program with Abstracts, p. 11.

Williams, F.M.G.
1970: Snegamook Lake (east half), Newfoundland; Geological Survey of Canada, Open File 42.

75. THE NEWFOUNDLAND SLOPE AT 49-50°N: NATURE AND MAGNITUDE OF CONTEMPORARY MARINE GEOLOGICAL PROCESSES

Project 780031

Charles T. Schafer
Atlantic Geoscience Centre, Dartmouth

Schafer, C.T., The Newfoundland Slope at 49-50°N: nature and magnitude of contemporary marine geological processes; in Current Research, Part A, Geological Survey of Canada, Paper 84-1A, p. 563-566, 1984.

Abstract

*Survey transects were made across the continental slope and rise near latitude 49°30'N in 1977 (**CSS Dawson**) and 1979 (**CSS Hudson**). Data collected on these cruises have provided new information on the regional marine geology of modern sediment deposits that occur along this section of the continental margin, and on indigenous oceanographic processes that control the textural character of surficial sediments, their geotechnical properties, and the species composition of modern foraminiferal assemblages.*

Résumé

*Des levés ont été effectués le long de lignes déterminées au-dessus du talus continental et du glacis précontinental, près de la latitude 49°30'N en 1977 (**CSS Dawson**) et en 1979 (**CSS Hudson**). Les données recueillies au cours de ces expéditions ont fourni de nouveaux renseignements sur la géologie marine régionale, en ce qui concerne les dépôts de sédiments récents de cette partie de la marge continentale, et sur les processus océanographiques autochtone qui régissent la structure des sédiments de surface, leurs propriétés géotechniques et la répartition des espèces qui composent les assemblages récents de foraminifères.*

INTRODUCTION

This is a summary of a project that was initiated in 1977. Its general objective was to study the role of deep ocean boundary currents flowing off the eastern Canadian margin with respect to: (1) sediment transport and reworking, and (2) their value as indicators of atmosphere-deep ocean circulation coupling effects over the last 20 000-50 000 years. The study area on the continental slope and rise off northeast Newfoundland was selected on the basis of slope morphology (with a view to minimizing the influence of gravitational sedimentary processes) and to provide regional environmental geological information near the site of the first continental slope exploratory oil well (Texaco-Shell, Blue H-28) that was drilled by the **Discover Seven Seas** during the summer of 1979 off northeast Newfoundland (Fig. 75.1).

Milestones established at the start of the project, or subsequently approved, included the determination of modern undercurrent geological and geochemical processes (1977-82), and an assessment of late glacial and Holocene variations of Western Boundary Undercurrent (WBU) intensity and flow characteristics in the Labrador Sea basin (1982-83).

Highlights of the findings observed to date are based on a series of grab and core samples (Fig. 75.3) and are summarized below. These observations form the elements of a semiquantitative descriptive model that has good potential for evaluating the regional interaction of the WBU with bottom sediments and with morphological features throughout the entire Labrador Sea basin. In addition, the model and data base provide an interpretive capability in the study of older undercurrent-reworked sedimentary sequences such as those described by Kenard (1982) for the Flemish Cap area.

SCIENTIFIC RESULTS

Geological processes

Four depositional environments were recognized on the slope and rise off Newfoundland (Carter et al., 1979). Ice rafting processes and some current-reworking of sediment are evident on the upper slope. The middle slope (700-2000 m) is the principal environment of settling depositional processes with some fines transported to the area by the slower-moving upslope edge of the WBU. The lower slope and rise are dominated by undercurrent processes that have reworked older Middle Holocene deposits in addition to drastically reducing the flux of modern fine sediment to the bottom (Fig. 75.2).

At 49°30'N, the undercurrent flows parallel to local bathymetric contours with its high speed core presently situated at about 2600 m (Carter, 1979; Carter and Schafer, in press). Its average velocity is about 8.5 $cm \cdot s^{-1}$; it occasionally reaches velocities of 16 $cm \cdot s^{-1}$ about 1-2 m above the bottom for short periods (Fig. 75.4). The associated bottom water nepheloid layer at 2600 m is comparatively thick and contains the highest proportion of terrigenous sediment found in the 400 to 3200 m interval. Current meter observations indicate that the WBU is capable of transporting bedload; threshold frictional velocities (u*) of about 0.87-1.14 $cm \cdot s^{-1}$ prevail between 1-30% of the time (Carter and Schafer, in press). Staining of gravel clasts by

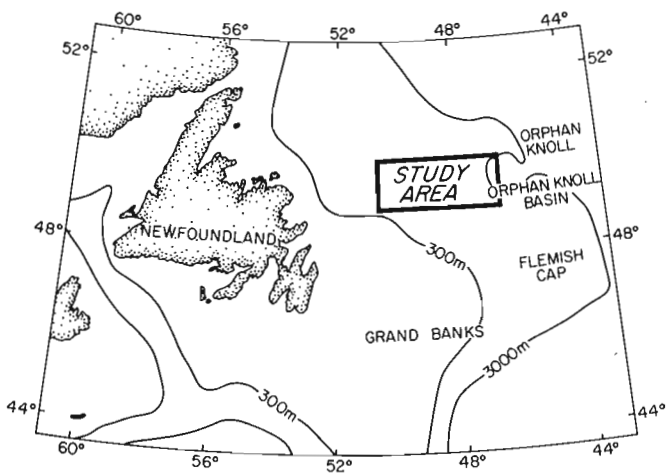

Figure 75.1. Location of the study area on the northeast Newfoundland continental slope and rise showing its position relative to the 300 and 3000 m isobaths.

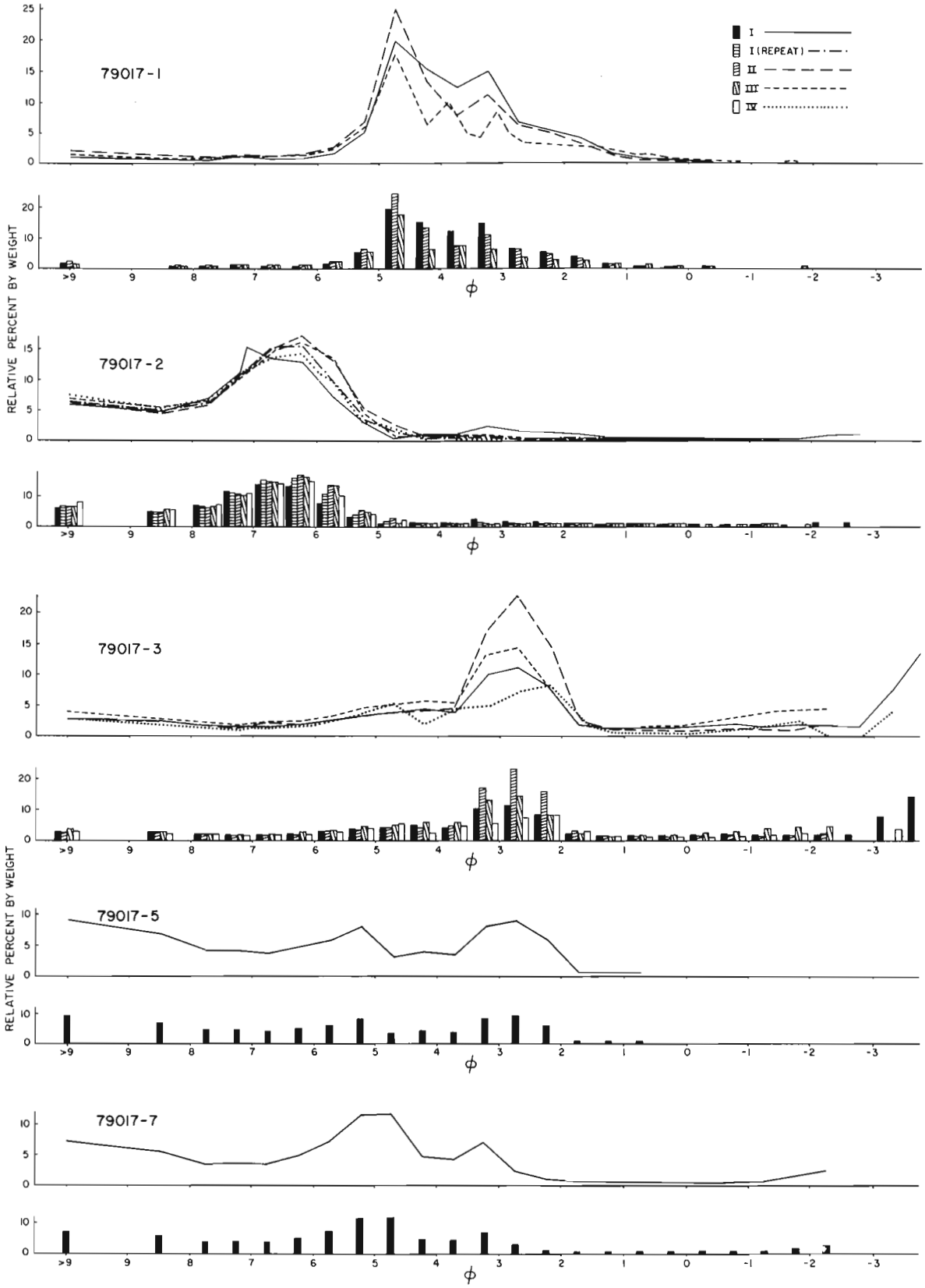

Figure 75.2. *Depth variation of the modal grain size of modern bottom sediment collected with a box corer. Note the distinctive shift from a comparatively fine 6.20 phi mode (79017-2) to the coarse 2.80 phi mode that occurs below the WBU axis (79017-3) at a water depth of about 2750 m. Dashed and solid lines represent grain size distributions from up to 5 replicate box core samples (e.g., 3.1 to 3.4 in Fig. 75.3) that provide a measure of the spatial homogeneity of sediment texture at locations on the upper slope (500 m), middle slope (1500 m) and upper continental rise (2700 m).*

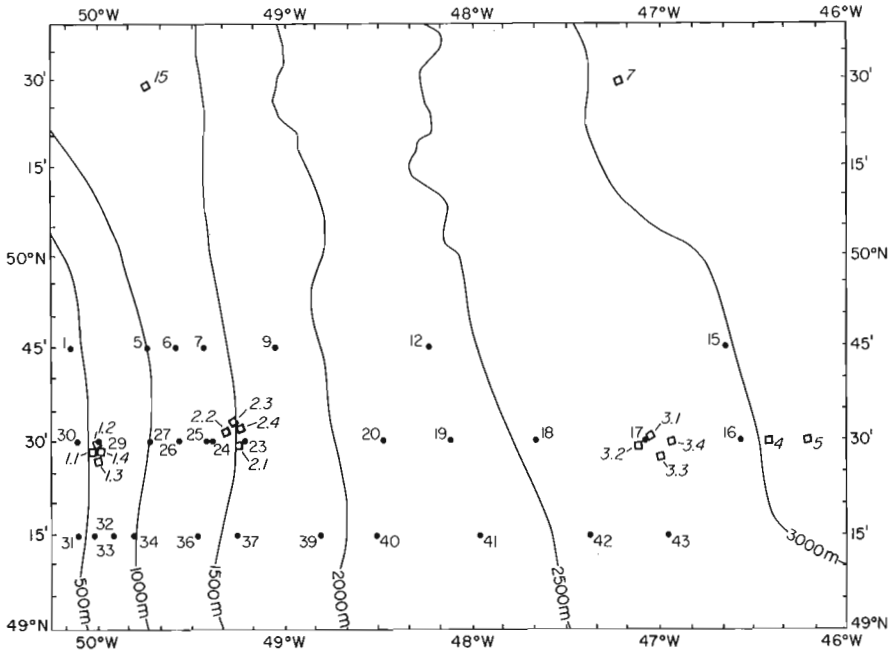

Figure 75.3. *Location of grab/core sampling stations (solid circles) and box core locations (open squares) along several transects between latitudes 49°00'N and 50°30'N.*

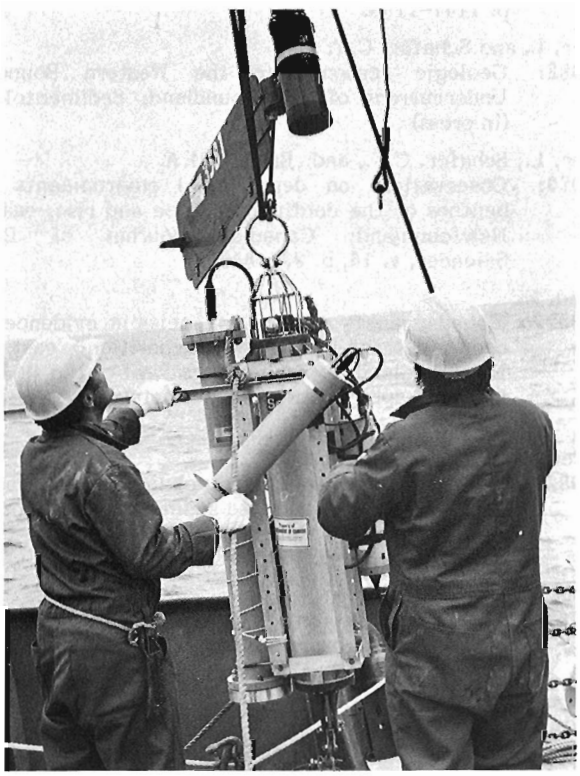

Figure 75.4. *Deployment of a deep sea time-lapse camera/current meter mooring from* ***CSS Hudson*** *that was used to measure velocity variations near the axis of the WBU at station 3.1.*

manganese is a geochemical process that appears to be controlled by the WBU (Fig. 75.5). This process is apparently similar to that documented for ferromanganese nodule fields described in the literature.

Measurements of ^{210}Pb isotope activity distributions in short cores facilitate the differentiation of local bioturbation regimes in this sector of the continental margin. Bioturbation is minimal (2 cm mixing depth) below the WBU because of the inhospitable character of this environment (low food supply and unstable substrate) for the establishment of bioturbating communities. In contrast, the comparatively stable middle slope lithotope is intensely bioturbated with mixing depths in excess of 12 cm.

Bioturbation along with other textural factors control the bathymetric-related variation of sediment shear strength on the slope and rise which ranges between 3.7 to 8.9 kPa on average (Schafer and Asprey, 1982). Sediments deposited on the downslope side of the present WBU axis have comparatively high shear strength gradients throughout their upper 20 cm interval that appear to denote the increased proportion of fine sediment deposition during early to middle Holocene time when the WBU axis may have been located farther upslope than at present.

Paraecology

Compared to the upper slope, the middle slope and rise receive less ice-rafted sediment, support a richer macrofauna (especially the middle slope) and have a higher diversity of foraminifera species (Schafer et al., 1981; Schafer and Cole, 1982). A marked increase in the numbers of both planktonic and benthonic foraminifera tests at about the slope-rise break (≈2500 m) is related primarily to the winnowing capacity of the WBU. Considering the entire slope and rise, the arenaceous foraminiferal genus **Trochammina** is the most abundant and most ubiquitous taxon. **Ammobaculites, Karreriella, Reophax, Hoeglundina,** and **Pullenia** show a strong association to a base-of-slope to rise (2000-3000 m) contour current water mass conditions. **Elphidium** has a distinctive association with the middle slope, low energy fine sediment lithotope. Percentage of living to total specimens of foraminifera (L/T) is highest on the middle slope, a relationship that reflects apparently both the inherent size of the living population and the rate of sedimentation. On the rise, the reduction of predators and the lower sedimentation rate yields intermediate L/T ratios although the living population density per unit area is highest in this environment.

Quaternary paleo-oceanography

Cores collected from the middle slope and rise can be classified into several stratigraphic units (Carter, 1979; Schafer et al., 1980). Unit A-1 forms a thin cover (≈25 cm) that extends from the shelf down to the lower slope and probably represents primarily late Holocene material. The underlying A_2 unit has a higher gravel content that often contains warm water taxa suggesting deposition during the middle Holocene climatic optimum (≈5000 years). Unit B occurs below A_2 and may be about 9000 years. The oldest

recognized Unit (C) contains a depauperate foraminiferal assemblage and a reduction in gravel that is suggestive of late glacial conditions (≈12 000 years). The coarse gravelly sediments observed on the rise are essentially a lag deposit formed by the winnowing of middle Holocene gravel-bearing muds lying below the WBU axis. On the upper rise, the coarsening of sediment, increased percentages of deep bathyal foraminifera species, and the increased proportions of planktonic foraminifera test fragments in the shallower sections of gravity core samples, appear to reflect an intensification of the WBU in this area at about 1000-2000 years. Core studies to date also suggest that surface waters off northeast Newfoundland were comparatively warm between 2500-3000 years. Continuous displacement of a North Atlantic Drift Water eddy from the Newfoundland rise area after about 1500 years by colder Labrador Current Water is suggested by a gradual reduction in abundance of the diatom species **Rhizosolenia styliformis.** Perhaps because of the comparatively gentle slope along this sector of the Canadian margin, slump processes leading to grain and turbidity flows appear to be confined to the pre-Holocene interval where they are characterized by a distinctive hydraulically-sorted allochthonous foraminiferal assemblage.

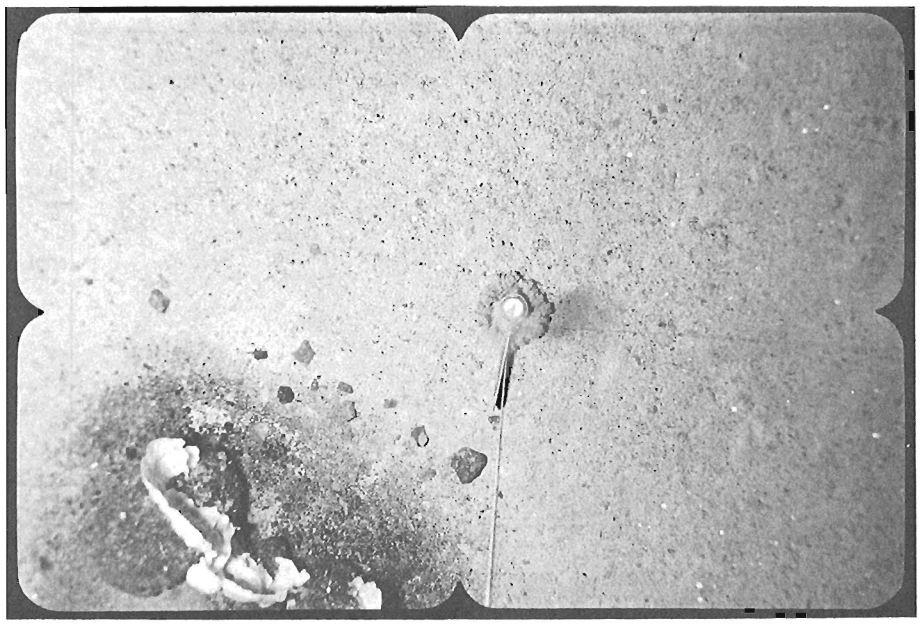

Figure 75.5. Manganese-coated pebbles form halos around large cobble clasts that mark the mean direction of the WBU at 49°30'N.

APPLICATIONS OF THIS STUDY

That part of the continental slope and rise investigated in the study is unique in terms of the intensification of hydrodynamic activity starting at about a depth of 2000 m to about 3000 m. This phenomenon has implications for the transport and dispersal of foreign substances (including oil), and with respect to exploration strategies concerning the prediction of potential reservoir and source formations (the modern WBU reworking zone is about 30 km wide at this latitude). Geotechnical characteristics of the sediment suggest a comparatively high potential for turbidity current development and slumping for the muddy and bioturbated middle slope lithotope given an appropriate triggering mechanism.

The base-of-the-slope to rise biotope is unique in terms of its comparatively high living foraminifera population density and reduced numbers of both infaunal and epifaunal macrofauna. This association suggests a trophic relationship that may be significant in terms of the comparative benthic productivity of this bathyal environment, and thus could be tied indirectly to the autoecology and distribution of certain deep sea commercial species. If this hypothesis is correct, knowledge of regional configuration and biomass of the WBU lithotope would perhaps be useful in predicting the occurrence or yield of certain commercially-valuable fish and/or crustacean populations that are in contact with this environment at some point in their life cycle.

ACKNOWLEDGMENTS

The author wishes to acknowledge the helpful comments and encouragement given by D. Piper and A.C. Grant during the preparation of this report.

REFERENCES

Carter, L.
1979: Significance of unstained and stained gravel on the Newfoundland continental slope and rise; Journal of Sedimentary Petrology, v. 49, p. 1147-1158.

Carter, L. and Schafer, C.T.
1983: Geologic response to the Western Boundary Undercurrent off Newfoundland; Sedimentology. (in press)

Carter, L., Schafer, C.T., and Rashid, M.A.
1979: Observations on depositional environments and benthos of the continental slope and rise, east of Newfoundland; Canadian Journal of Earth Sciences, v. 16, p. 831-846.

Kenard, L.
1982: Mounds, moats and ridges: seismic evidence for deep current-influenced deposition east of Newfoundland; Proceedings of the Joint Oceanographic Assembly (Abstracts), Halifax, N.S., p. 24.

Schafer, C. . and Asprey, K.W.
1982: Significance of some geotechnical properties of continental slope and rise sediments off northeast Newfoundland; Canadian Journal of Earth Sciences, v. 19, p. 153-161.

Schafer, C.T. and Cole, F.N.
1982: Living benthic foraminifera distributions on the continental slope and rise east of Newfoundland, Canada; Geological Society of America Bulletin, v. 93, p. 207-217.

Schafer, C.T., Cole, F., and Carter, L.
1981: Bathyal zone benthic foraminiferal genera off northeast Newfoundland; Journal of Foraminiferal Research, v. 11, p. 296-313.

Schafer, C.T., Smith, .N., and Cole, F.
1980: Record of paleo-oceanographic events in Holocene sediments: Newfoundland Continental slope and rise; Workshop on Research in the Labrador Coastal and Offshore Region, Memorial University, Goose Bay, September 4-6, p. 223-243.

76. SONAR EVIDENCE FOR POSTGLACIAL TECTONIC INSTABILITY OF THE CANADIAN SHIELD AND APPALACHIANS

Project 690095

W.W. Shilts
Terrain Sciences Division

Shilts, W.W., Sonar evidence for postglacial tectonic instability of the Canadian Shield and Appalachians; in Current Research, Part A, Geological Survey of Canada, Paper 84-1A, p. 567-579, 1984.

Abstract

Establishing the timing and location of prehistorical seismic or neotectonic events is important for assessing seismic risk, particularly in the design or location of radioactive waste disposal sites or nuclear power plants. Sonar surveys of lakes of the Canadian Shield and Appalachians have revealed two types of evidence of postglacial (neotectonic) instability: 1) slumping of bottom sediments to form mudflows in response to shaking of the lake basin during a seismic event and 2) fracturing or tilting of glacial and modern sediments by differential movement of underlying bedrock. Large-scale tilting appears to have played a role in the formation of the Lac Deschenes segment of Ottawa River. Fluvial erosional forms appear to be drowned beneath Lac Deschenes by uplift of a bedrock dam at the east end of the lake at some time in the last 10 000 years. Care must be exercised in differentiating paleoseismic or neotectonic features from similar-appearing structures or forms produced by glaciotectonic processes or by nonseismic slope failures.

Résumé

Il est important de situer de façon géographique et temporelle les événements sismiques ou néotectoniques qui ont eu lieu avant l'époque historique, pour évaluer la stabilité à long terme de structures sensibles aux séismes, comme les centrales nucléaires. En effectuant par sonar le levé des lacs du Bouclier canadien et des Appalaches, on a découvert deux types d'indices d'une instabilité postglaciaire (néotectonique) du terrain: 1) le glissement et décollement des sédiments du fond de ces lacs, qui donnent lieu à des coulées boueuses, lorsqu'un séisme secoue le bassin lacustre et 2) la fracturation ou le basculement des sédiments glaciaires et des sédiments récents, par mouvement différentiel du soubassement. Il semble qu'un important basculement ait contribué à former le segment du lac Deschênes, dans la rivière des Outaouais. Il semble que des formes d'érosion fluviatile aient disparu au-dessous du lac Deschênes, le soubassement ayant été soulevé et ayant formé un barrage à l'extrémité est de ce lac à un moment donné au cours des 10 000 dernières années. Il faut user de prudence lorsqu'on cherche à différencier des phénomènes paléosismiques ou néotectoniques de structure ou forme similaires produits par des événements glaciotectoniques, ou des ruptures de pente d'origine autre que sismique.

INTRODUCTION

The numerous small lakes of the glaciated terrain of Canada offer a unique opportunity to study the incidence of late glacial and postglacial tectonic disturbances. The frequency and intensity of seismic activity that accompanies tectonic (or glacioisostatic) adjustments may have an important bearing on the suitability of sites or regions for the construction of structures such as radioactive waste disposal facilities or nuclear power plants. This paper presents selected examples of lake sediment disturbance thought to be related to seismic or neotectonic activity.

Lakes are generally quiet-water settling basins, and they received large amounts of fine grained mineral sediment during the latter stages of deglaciation. They have continued to accumulate fine grained minerogenic and organic sediment at a much slower rate throughout the Holocene. Because of their texture and water saturation, these sediments are particularly prone to disturbance by seismic events, especially where they lie on submerged slopes. The organic nature of the postglacial sediment can allow dating (^{14}C) of disturbed sediment, and the laminated nature of the clastic lacustrine sediment can provide clear visual evidence of offsets, slumping, or channel cutting related to seismic shock or to differential movements of the underlying bedrock floor. In addition, distinctive patterns of acoustical reflections (caused by sediment lamination), where disrupted, can allow age relationships of erosional or slump features to be estimated.

Several seismic studies of lakes and marine environments have been carried out over the past decade in the North American west (eg. Sims, 1975; Otis et al., 1977; Qamar et al., 1982; Field et al., 1982; Prior et al., 1982) and in New York (Wold et al., 1977) in an attempt to estimate paleoseismic conditions and the effect of modern earthquakes. Shilts et al. (1976), Klassen and Shilts (1982), and Shilts and Farrell (1982) have studied glaciotectonic faulting and deformation of glaciolacustrine and late glacial marine beds under modern lakes. Kenny and Balins (1975) have discussed the bathymetry and probable geotechnical properties of unconsolidated sediments of the Lake Timiskaming basin.

SEDIMENTATION AND DISTURBANCE OF LAKE SEDIMENTS

Lakes of the Canadian Shield and Appalachians are generally floored by 1 to 5 m of gyttja, a water-saturated organic sediment composed of autochthonous and allochthonous algal, plant, and animal remains with minor clastic components.[1] Modern sediment in nearshore areas or in areas adjacent to major inflow streams is generally sandy or bouldery. In many lakes, these distinctive modern sediments are underlain by substantial thicknesses of proglacial clastic, laminated, fine grained sediments that rest directly on bedrock or on till.

[1] The physical properties and genesis of lake sediments described in this paper are generally inferred from their acoustic properties as recorded on sonar records. Klassen and Shilts (1982) described the type of coring and comparative studies on which these inferences are based.

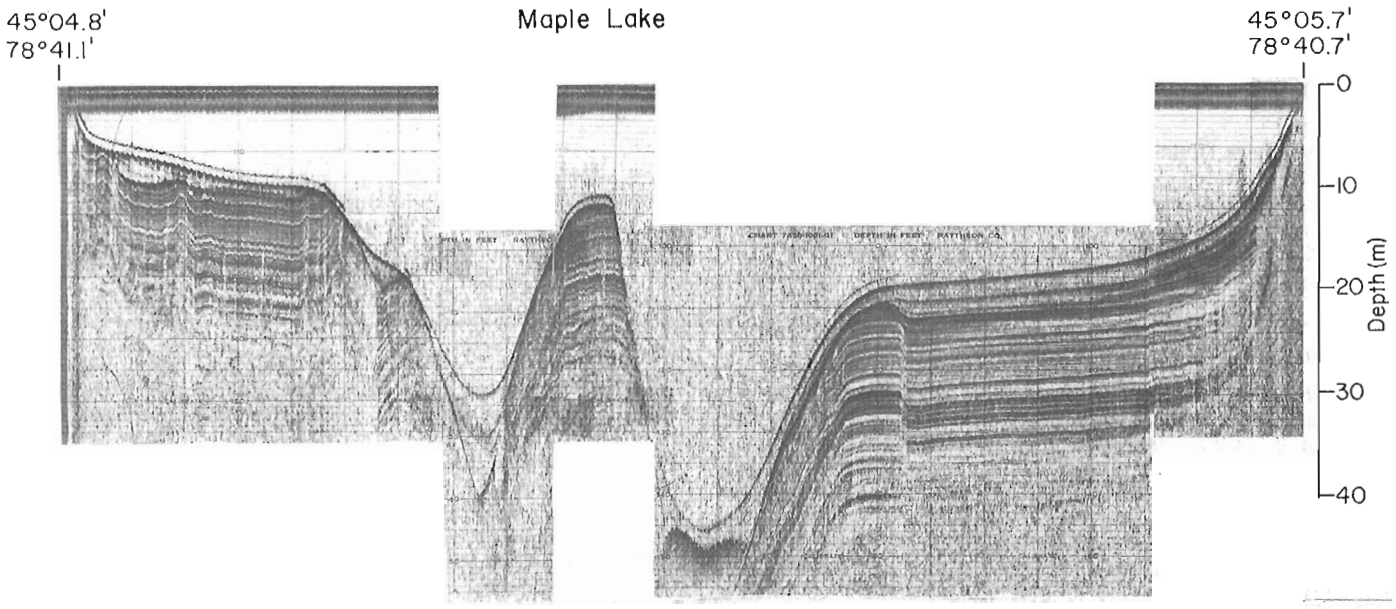

Figure 76.1. *Profile of Maple Lake near Haliburton, Ontario; length of profile is approximately 1750 m. Trenches are "ice-block casts"; slopes cutting the laminae are ice contact in origin. Note the rotational slump block on left-hand slope and the covering of acoustically clear gyttja over proglacial laminated sediment.*

Many glacial and nonglacial processes can trigger or cause slumping or deformation of the various types of unconsolidated sediments that occupy lake basins. Where proglacial lacustrine sediments are thick, they are commonly deformed by diapirism, folding, and faulting (Shilts et al., 1976; Klassen and Shilts, 1982; Shilts and Farrell, 1982) which mark collapse over buried glacial ice. In many places detached remnants of glacier ice were preserved in the hollows now occupied by lakes as the glacier backwasted under conditions that must have caused progressive stagnation of its retreating terminus. The occurrence around many lakes of glaciofluvial sediments, which require a temporary ice floor to allow unrestricted drainage, supports the inference that ice blocks were commonly left in lake basins while active sedimentation was taking place. In some cases the laminated sediments were deposited around more slowly melting ice blocks which persisted until after glaciolacustrine sedimentation ceased, leaving sediment-free holes or "ice-block casts" in the lake bottom, flanked by steep ice-contact faces of thick, laminated sediment. A rotational slump block, probably unrelated to seismic activity, was noted on one of these oversteepened faces (Fig. 76.1).

Slumps and disruption of fine grained sediments also may occur during the late glacial sedimentation phase as a result of various processes associated with rapid deposition of sediment from an ice front within the drainage basin. In postglacial time, sedimentation rates are usually relatively slow, the sediment is generally organic, and chances for slumping are low. Nevertheless, groundwater inflow, floods producing abnormally high sedimentation rates, man's interference with the shoreline or bottom, and other nonseismic processes may account for sediment slumping or deformation.

Although soft-sediment slumping or deformation may be caused by any of the processes mentioned above, certain bottom and subbottom features are best explained as response to postdepositional seismic or tectonic events. The deformed sediments in the Canadian Shield and Appalachian lakes described in this report were probably disturbed by

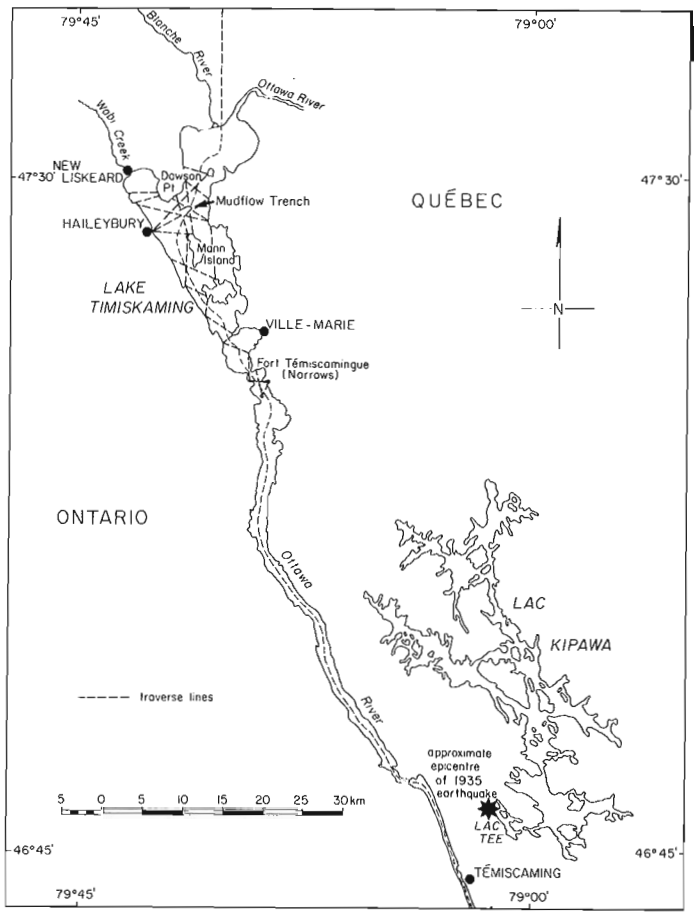

Figure 76.2. *Location map of Lac Tee – Lake Timiskaming region. Mudflow trench is the site of profiles in Figure 76.9. Dashed lines are traces of some of the sonar profiles.*

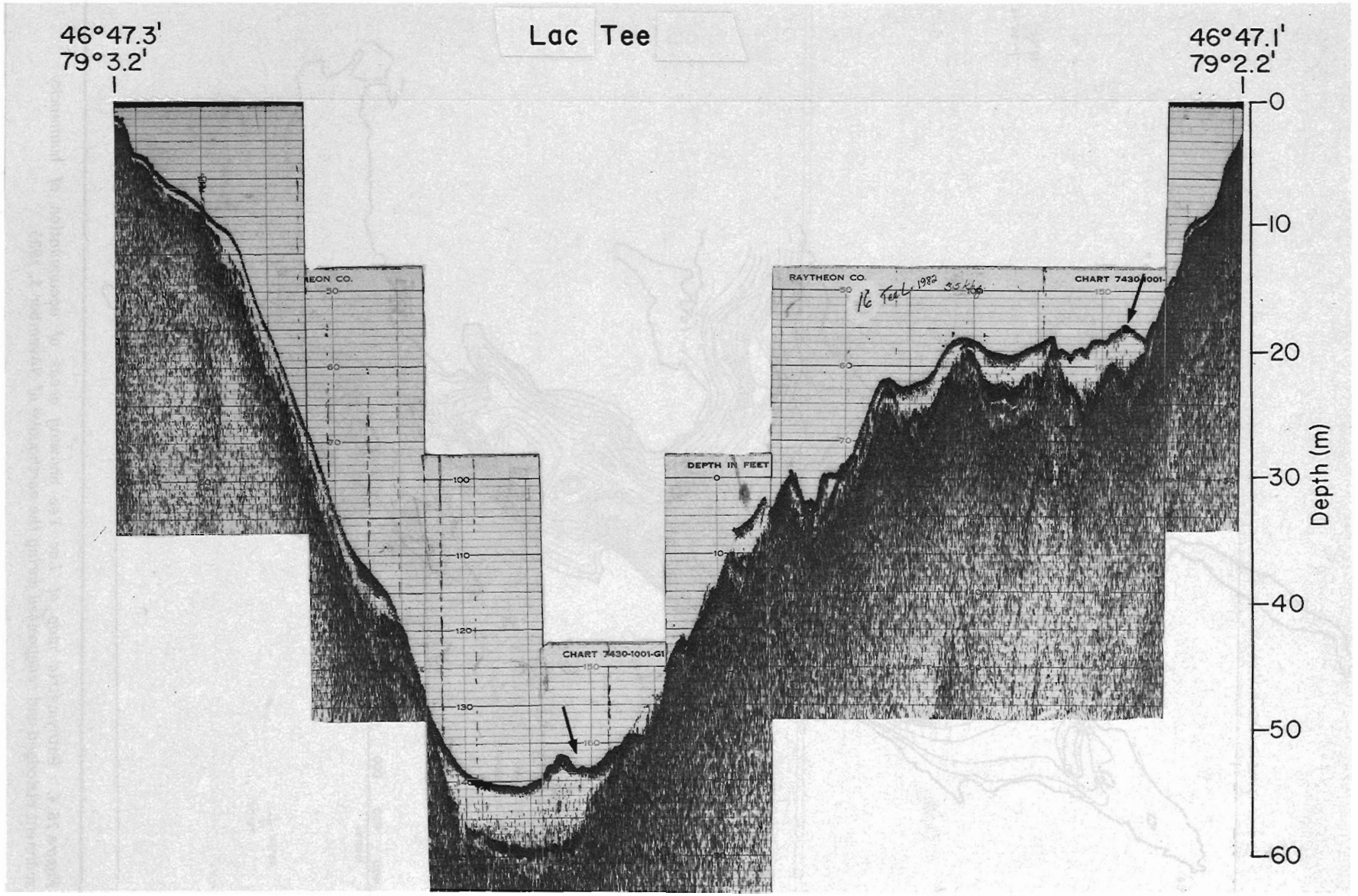

Figure 76.3. *Profile of Lac Tee showing hummocky nature of mudflows composed of gyttja thrown from west-facing (right-hand) side of lake (1200 m long). Arrows indicate slumped sediment.*

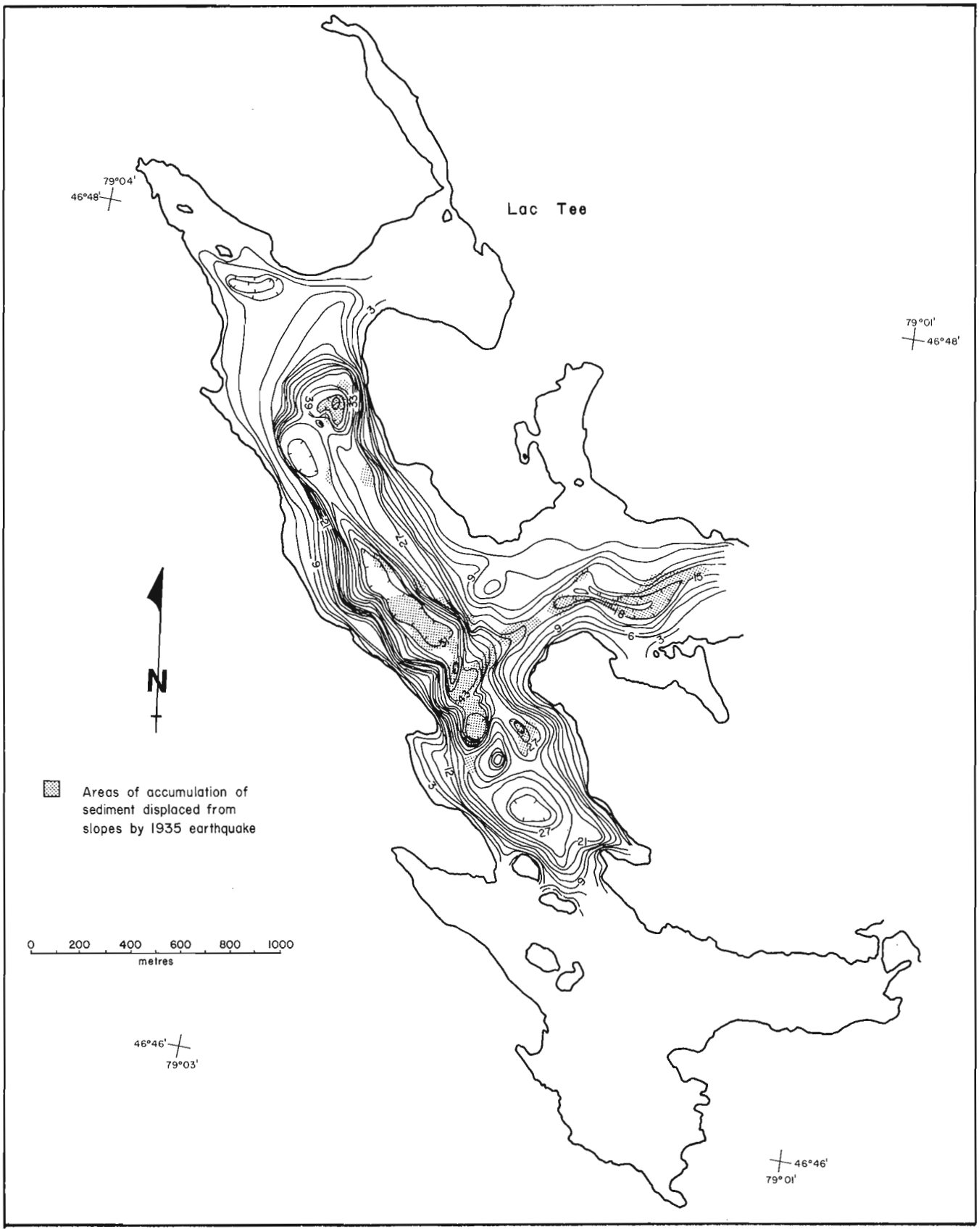

Figure 76.4. *Bathymetric map of Lac Tee showing areas of accumulation of hummocky sediment dislodged and redeposited during the earthquake of November 3, 1935.*

neotectonic processes. It should be borne in mind that they represent only a small proportion of the deformed sediments noted in these and other lakes and that all the rest are more reasonably attributed to nontectonic processes.

Several sediment structures, when interpreted in combination with bathymetric and stratigraphic data, are indicative of seismic or neotectonic disruption:

1. Mudflows, which form distinctive hummocky (or ridged) masses on the normally smooth depositional surface of the lake bottom, are commonly triggered by seismic activity (see also Field et al., 1982). The hummocky surfaces may be associated with trenches eroded by the flow debris into soft sediments upslope from the deposit. Seismically induced slumps are generally unidirectional, that is, they occur only on slopes with similar orientations. They often originate simultaneously from several places or slopes at the same time. Widespread occurrence of contemporaneous multiple slump features in a single basin would be unlikely to be caused by any process other than seismic shock. Where slump deposits are buried by any later sedimentation, sonar profiles can help to establish their contemporaneity.

2. Faulting that penetrates both proglacial and modern sediments, and cannot be related to gravity slumping of a free face, is most likely caused by neotectonic displacements in the underlying bedrock surface. If the faulting can be traced down to bedrock, this is almost certain evidence of neotectonic movement.

3. Subaqueous slump features in lakes known to be in areas of strong, historically documented earthquakes are, of course, easily related to seismic shock.

4. Channels and other features clearly cut into postglacial sediments by fluvial action and now submerged in natural lakes were probably drowned as a result of neotectonic tilting or faulting of the underlying bedrock. Where such topography has been observed, it has the appearance of the bottom of a man-made reservoir.

TECTONIC AND SEISMIC DEFORMATION

Tee Lake

In 1935, a severe (6.2 on Richter Scale) earthquake occurred near the town of Témiscaming, Québec, just east of the south end of Lake Timiskaming (Fig. 76.2). Hodgson (1936) reported that Lac Tee, a small, deep lake located midway between lakes Timiskaming and Kipawa, appeared milky, presumably from soft-sediment disturbance, for several weeks after the earthquake. Sonar profiles of Lac Tee, carried out in 1982, revealed the probable reason for the milky appearance of the water after the earthquake: gyttja on many of the west-facing subaqueous slopes of the lake had slumped from the steeper slopes (>20°) and moved, probably as coalescing mudflows, onto the lake's bottom, forming hummocky deposits (Fig. 76.3). The areas where disturbed sediment was deposited have been mapped and superposed on a preliminary bathymetric map compiled from 35 sonar profiles (Fig. 76.4). The unidirectional displacement agrees well with Hodgson's (1936) deductions that the earthquake's strongest lateral component of movement was eastward. Similar disturbed sediments were found in Lac Kipawa, a few kilometres to the east, particularly in those parts closest to Lac Tee.

Lac Mégantic

A similar hummocky slump deposit was subsequently noted in Lac Mégantic, in the southern Québec Appalachians (Fig. 76.5). Sediment near the top of a steep subaqueous slope flowed down the slope, cutting a trench from which it debouched as a mudflow well out onto the flat, gyttja-covered floor of the lake. Although several other processes could trigger such slumping (rapid sedimentation from inflow streams, groundwater flow, etc.), seismic activity should certainly be considered as a triggering mechanism as none of the nontectonic processes are likely to be important in the vicinity of the slump. Lac Mégantic lies in an area where considerable neotectonic movement has been proposed by Oliver et al. (1970), but little historical seismic activity has been reported in the region.

Lake Doré

Lake Doré, near Eganville, Ontario, occupies a depression in a graben floored by Paleozoic sediments and surrounded by Grenville-age crystalline and metasedimentary rocks. It lies below postglacial marine limit but may have been blocked from the sea because of the configuration of the retreating ice. In any case, it can be seen to be underlain by a thick sequence of fine grained laminated sediments (Fig. 76.6).

Much of the late glacial sedimentary record along the southeast side of Lake Doré is disrupted by a mass (or several masses) of sediment that apparently slumped westward into the basin, disrupting a significant part of the lake bottom (Fig. 76.6). This event(s) occurred before the termination of deposition of laminated sediment, because the slumped mass is overlain by undisturbed laminated sediment which is in turn mantled by postglacial gyttja. The unidirectional slumping is reminiscent of that caused by the Témiscaming earthquake in Lac Tee and may represent a significant late glacial seismic event. Earthquakes are still common in this region of Ottawa valley.

In the profile reproduced here, a series of faults have disrupted almost the entire laminated sediment pile in the central part of the lake, but they clearly postdate the slumping event, the distinctive sequence of beds that overlie the slump deposit being cut by the faults. The faulting is similar to that reported by Qamar et al. (1982) from Flathead Lake, Montana, and appears to extend to bedrock, suggesting that the bedrock surface has risen as much as 5 m under the central part of the lake as a result of some form of postglacial stress. This feature is possibly a "pop-up" structure similar to those documented from quarries in Paleozoic limestones elsewhere in southern Ontario (Adams, 1981).

Lac Deschênes

Lac Deschênes is a ponded section of Ottawa River, lying between Ottawa and Arnprior, Ontario (Fig. 76.7). It is dammed by a low ridge of Paleozoic sedimentary rock at Deschênes Rapids in Ottawa. The profiles that illustrate the subbottom of Lac Deschênes show that the thick fill of fine grained laminated sediment that underlies the north side of the lake is cut on the south side by a channel formed since its deposition (Fig. 76.8). The laminated sediments are interpreted to be of marine origin, deposited between about 12 000 and 10 000 years ago (Richard, 1975), because thick, fine grained sediments exposed on land on either side of Lac Deschênes were deposited in the Champlain Sea. The flat surface of the laminated sediment under the north side of the river is cut by numerous small channels, many of which have an acoustically opaque fill which is interpreted to be sand. East of Aylmer Island, in the broad eastern bay of Lac Deschênes, sediment interpreted to be gyttja directly overlies bedrock and forms a cover 1 to 3 m thick. No trace of the small channels or of the large channel can be found in this part of the lake. The channel can be traced westward to Constance Bay (Canadian Hydrographic Service, 1982); west of Constance Bay, Ottawa River is underlain by laminated sediment that shows only minor evidence of fluvial erosion.

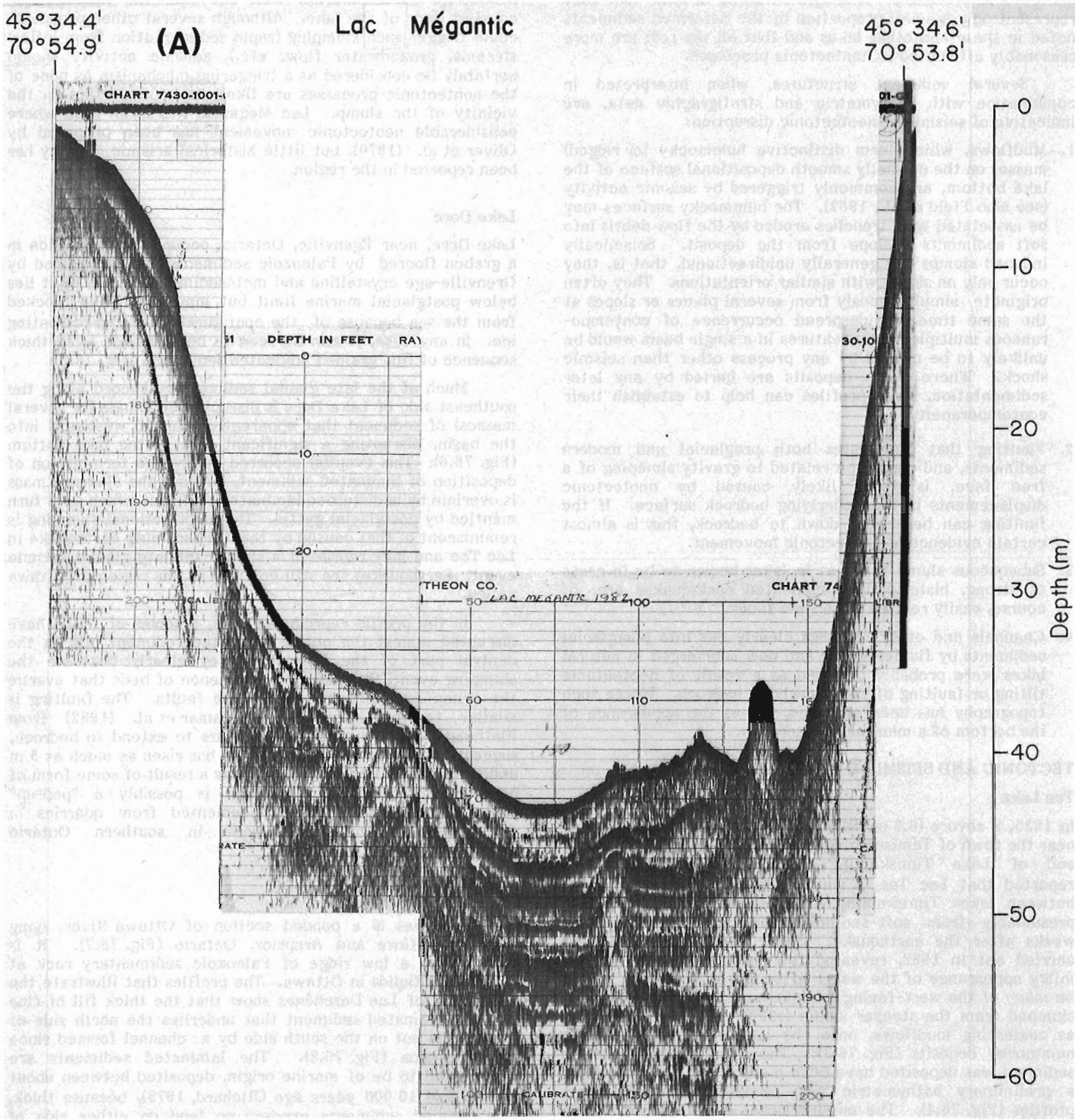
45°34.4'
70°54.9'
(A)
Lac Mégantic
45° 34.6'
70° 53.8'
CHART 7430-1001-
DEPTH IN FEET
THEON CO.
LAC MEGANTIC 1982
CHART 74
CALIBRATE
0
10
20
30
40
50
60
Depth (m)

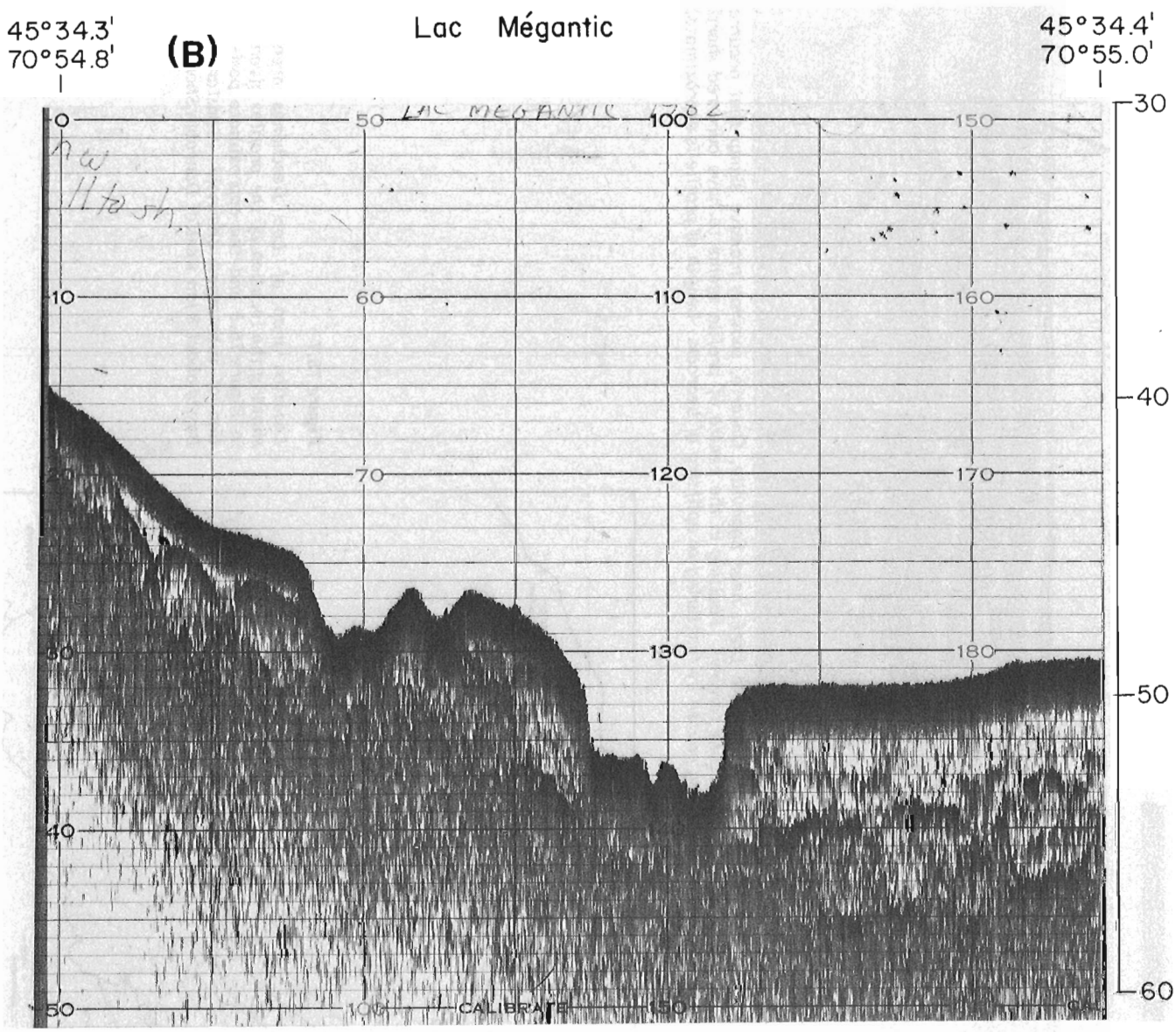

Figure 76.5. *Profiles across Sandy Bay of Lac Mégantic, Québec (A, 2000 m long) and across a mudflow trench parallel to northeast-facing slope of Sandy Bay (B approximately 100 m long). Mounds up to 5 m high on the bottom are flow ridges.*

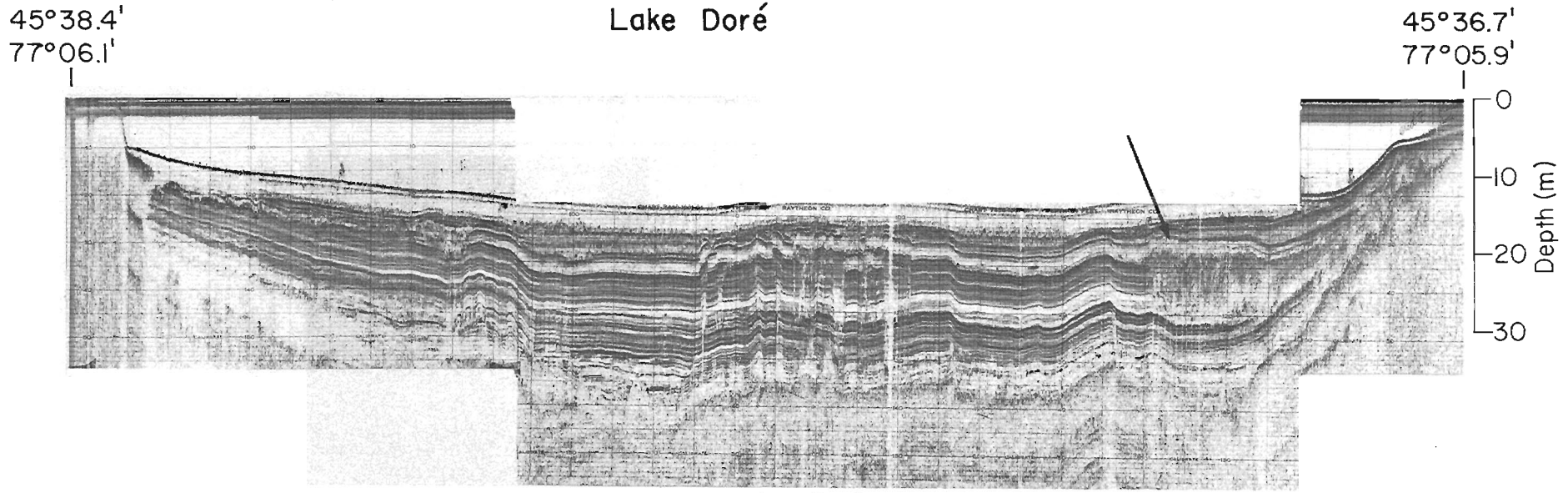

Figure 76.6. *Profile of Lake Doré, near Eganville, Ontario, showing massive slump that occurred early in postglacial time (arrow). Faulting in the centre of profile seems to have occurred shortly thereafter and to be caused by fracturing or uplifting of bedrock. Length of profile is approximately 3000 m.*

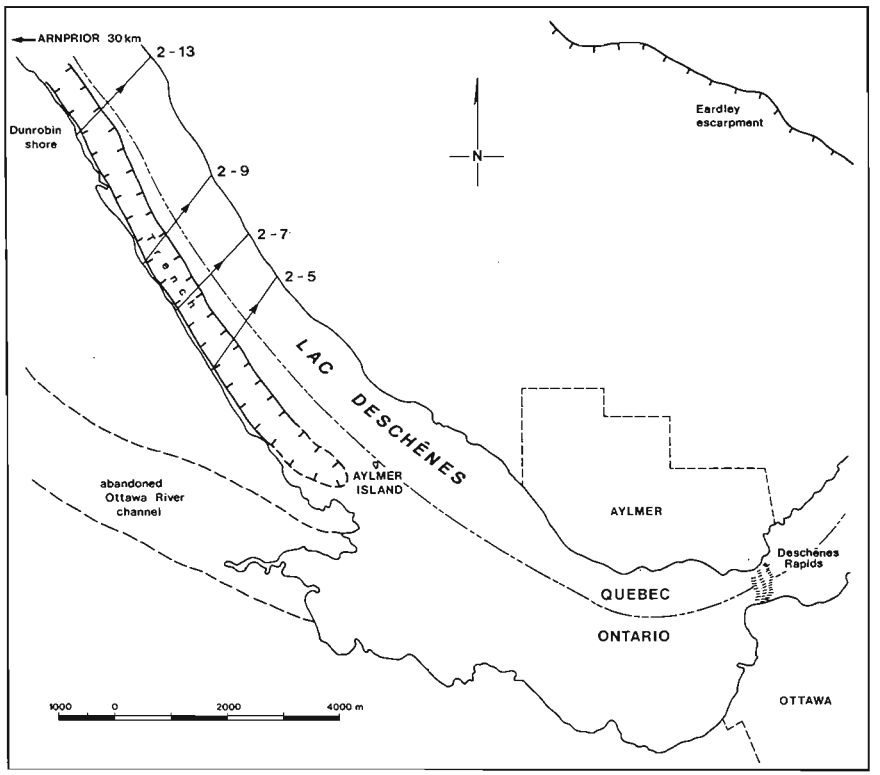

Figure 76.7

Location map of Lac Deschênes area showing the location of the profiles given in Figure 76.8 and the approximate position of submerged channel. Constance Bay is about 8 km west of Dunrobin Shore.

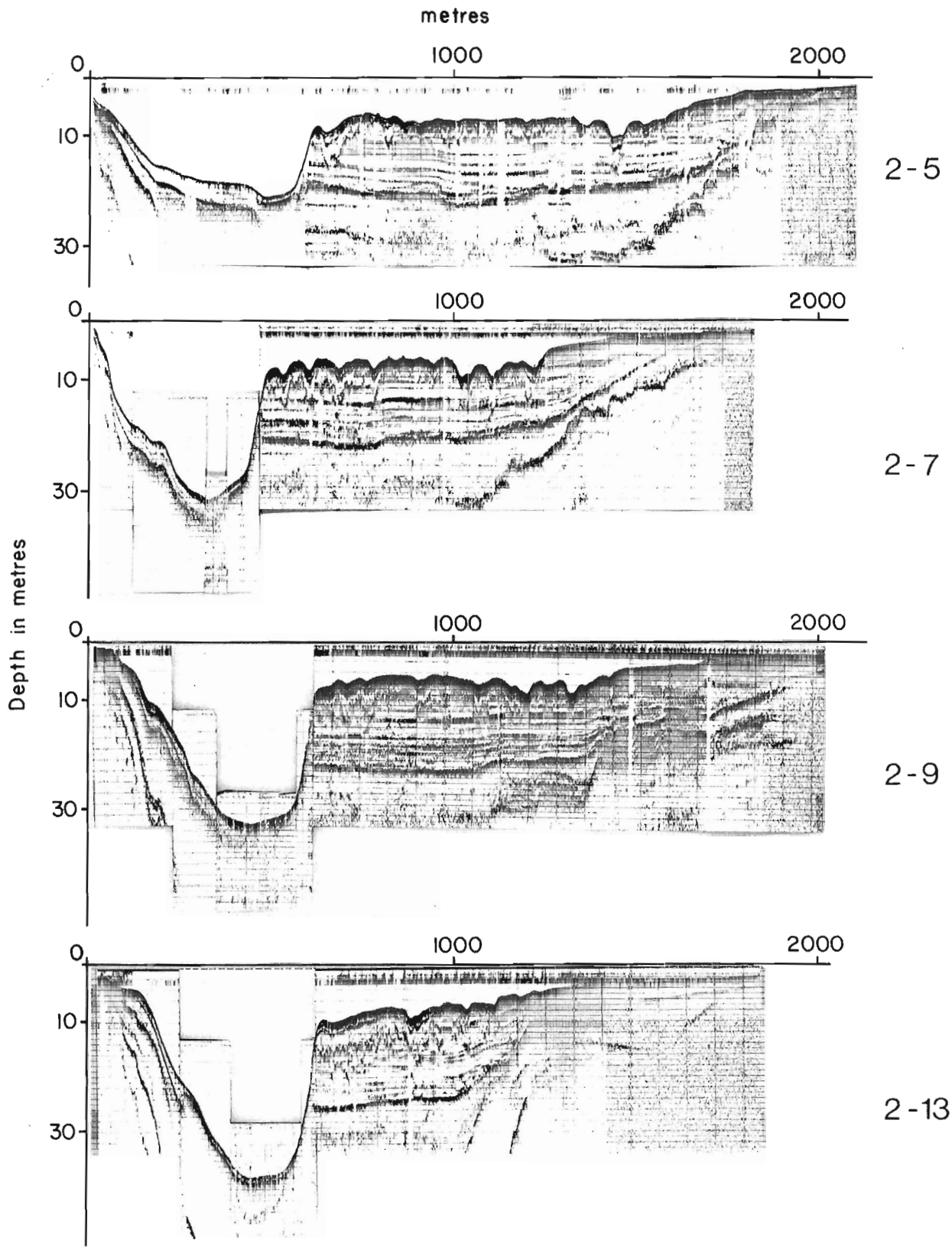

Figure 76.8. *Sonar profiles of Lac Deschênes west of Aylmer Island. Profiles are arranged from southeast (top) to northwest (bottom). (See Fig. 76.7 for locations.)*

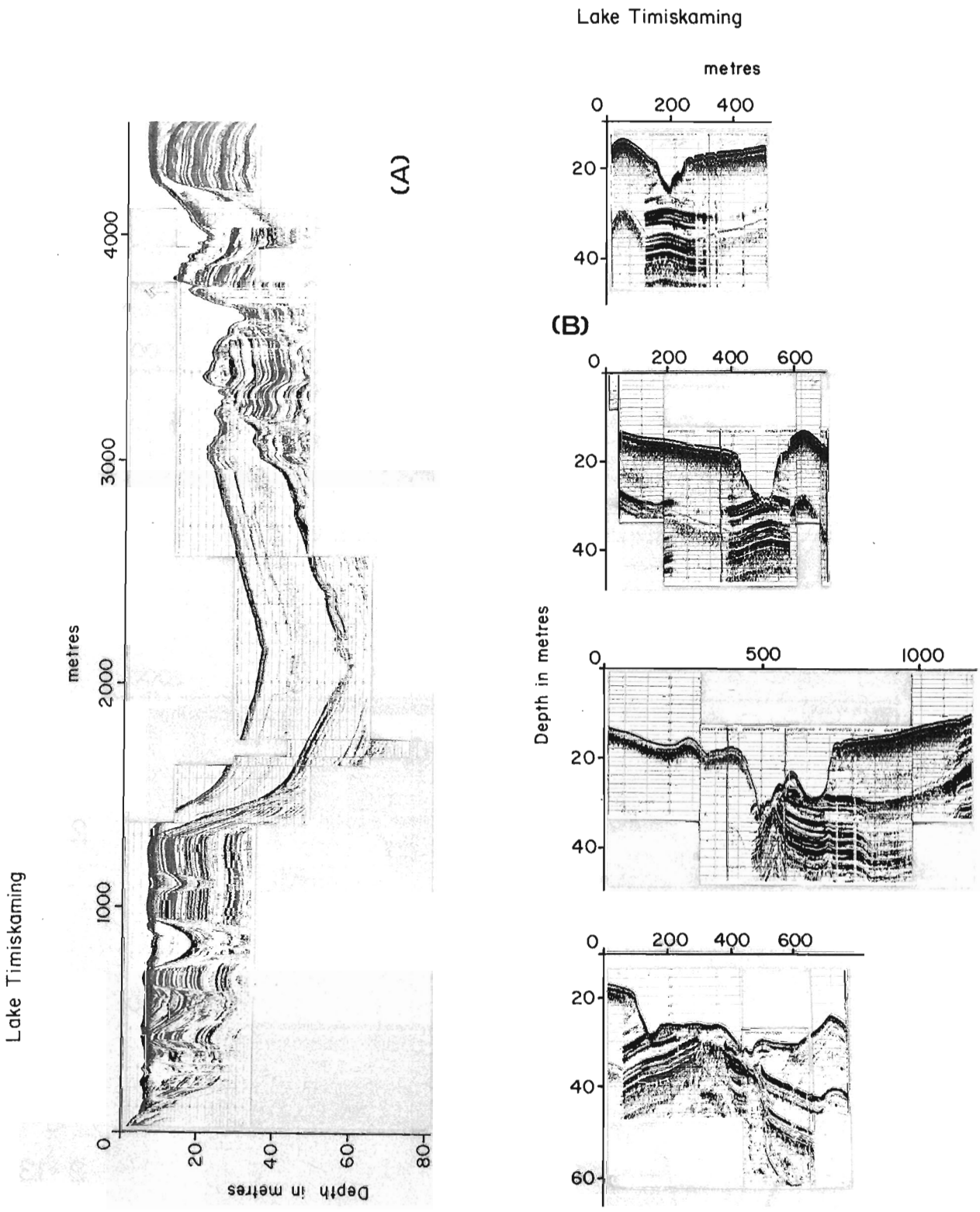

Figure 76.9. *Profiles across a trench created by subaqueous mudflow in the north part of Lake Timiskaming. A. Location of the trench on the profile extending to Mann Island; note surface sediments draped over "pillars" of laminated sediment thought to have been deposited in crevasses in stagnant ice. B. Profiles of the mudflow trench from the east end (top) to the west end (bottom). Note diapirism and general disturbance of older proglacial sediment beneath the trench.*

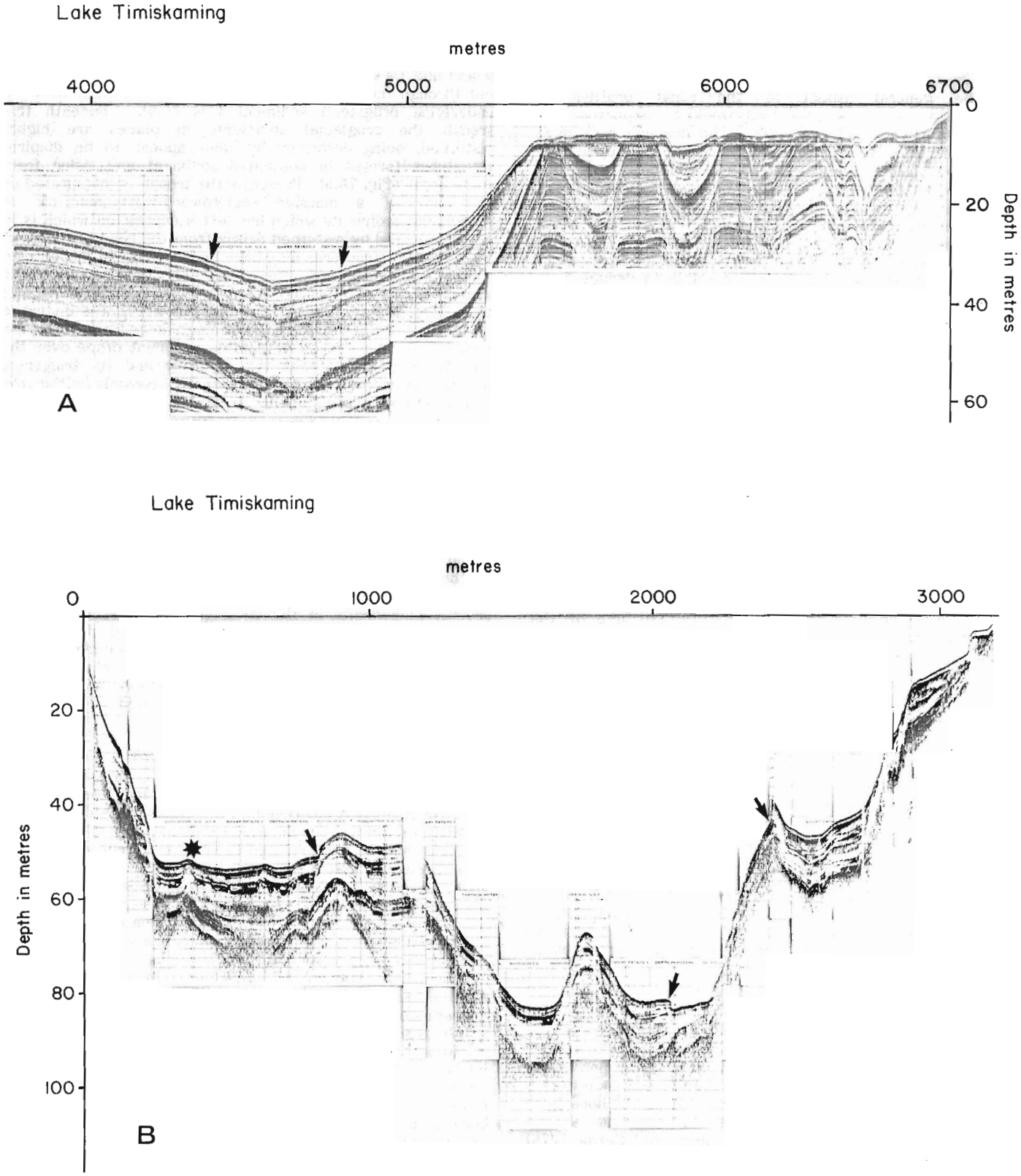

Figure 76.10. *Faulting of modern sediment in Lake Timiskaming. A. Faulting (arrows) in thick, modern sediment just south of the mudflow trench north of Mann Island. B. Faulting (arrows) and possible diapirism (*) in a deep trench near the narrows.*

The large channel is about 13 m deep at its eastern end and deepens westward to more than 40 m west of Dunrobin. It is floored by more than 2 m of sediment that is generally acoustically transparent (fine grained). It is presently a site of deposition rather than erosion. Its southern side is commonly a steep bedrock wall which extends as low cliffs exposing Paleozoic formations for 5 m or more above water level.

The general aspect of the sonar profiles of Lac Deschênes suggests those that would be expected in a lake created by damming a river. The channels may have formed during a period of subaerial exposure before flooding of this part of the valley to form Lac Deschênes. If so, this segment of Ottawa valley has been tilted down to the west, at right angles to the regional pattern of glacioisostatic uplift, since cessation of marine deposition about 10 000 years ago (Richard, 1975). If this conclusion is correct, Ottawa valley has been subjected to major neotectonic movement, but it is impossible to deduce from the information presently available whether such movement occurred during a short period or has been ongoing. The following inferences from the sonar records support the conclusion that this area has been tilted in postglacial time:

1. The major channel is cut into postglacial marine sediments which have bedding that intersects its sides in a horizontal attitude. Marine deposition ceased in this part of the valley about 10 000 years ago.
2. The major channel is cut over 45 m below the present bedrock barrier which ponds Lac Deschênes.
3. The major channel is presently a site of sediment deposition, suggesting that the current that cut it is not presently active.
4. The channel deepens to the west, at a gradient opposite to the flow of the river.
5. The small channels cut into the flat surface of the laminated sediments are of a size and spacing reminiscent of gullies presently being cut into similar sediment onshore.
6. The small channels are draped by a sediment layer similar to that occurring in the large channel, suggesting that the forces that cut them are not presently active.
7. Bedrock in the shallow eastern bay of the lake is covered by a sediment with the acoustical properties of gyttja, a sediment not likely to have been deposited if any strong current existed now or in the past.

Lake Timiskaming

The northern and central parts of Lake Timiskaming were studied in 1983 to determine if a seismic event(s), similar to those that affected Lac Tee and Lac Kipawa near its southern end, had affected Timiskaming. Interpretation of more than 200 km of profiles obtained is incomplete at this time, but some intriguing features were noted and are discussed briefly here.

Lake Timiskaming lies in a graben. The northern part of the lake is underlain by flat-lying Paleozoic limestone, but except adjacent to its northern bays, Precambrian rocks outcrop on shore. Two acoustically distinct sediment facies underlie the lake. The older has strong, generally horizontal internal reflections and is thought to comprise varved sediments of glacial Lake Barlow (Vincent and Hardy, 1979) which cover the lowlands north and east of the lake and which are being actively eroded by Blanche River, Ottawa River, and Wabi Creek. Overlying the proglacial sediments with marked angular unconformity is a thick (10 to >30 m) sequence of clayey, largely clastic sediments with weak internal reflections. This sequence is thought to represent Holocene deposition of sediments derived from erosion of the proglacial sediments exposed around the lake, particularly in the north. The great thickness and clastic character of these Holocene sediments is unique to Lake Timiskaming and contrasts sharply with the 3 to 4 m thickness of organic gyttja that comprises the Holocene sediment of most southern Canadian Shield lakes.

In the north-central part of the lake, between Mann Island and Dawson Point, a 10 to 15 m-deep trench has been cut through the upper sediment down to its contact with the underlying proglacial sediment (Fig. 76.9). Beneath this trench the proglacial sediments in places are highly disturbed, being deformed by what appear to be diapiric structures formed in laminated sediment and rising from some depth (Fig. 76.9). Presently the trench is interpreted as the scar of a massive east-toward-west mudflow of postglacial sediments which has left a depression which is in places covered by disturbed debris from the head of the flow. The diapiric structures may have been formed in response to sudden unloading of the area of the trench with accompanying differential loading by the thick sediments that flank it. Alternatively, but less likely, the disturbed structures may be related to movements in bedrock below the trench. As there is no detectable sediment drape over the trench, it is likely that the mudflow and its triggering mechanism were active quite recently, possibly within the last thousand years, judging from the high sedimentation rates (estimated to range between 0.1 and 0.5 cm/year) elsewhere in the lake. Because of its location in the middle of the lake and the relatively gentle slopes surrounding the trench, it is thought that the triggering mechanism was probably seismic shock or movement on a fault in the underlying bedrock, rather than a nonseismic slope failure.

Faulting and slumping of modern sediments were also noted north of Mann Island and in the steep-walled portions of the Lake Timiskaming narrows just south of Ville-Marie, Québec (Fig. 76.10). The faulting may be related to seismic shocks, movements in the underlying bedrock, differential compaction, or rotational slumping caused by normal subaqueous slope processes. Although the known high level of seismic activity in the region would favour a tectonic origin for these features, until more profiling is carried out in the southern part of the lake, their relationship to seismicity must be regarded as tentative.

CONCLUSION

Sonar profiling with portable, high-resolution, low-frequency acoustic equipment has revealed the effects of a documented earthquake and has documented other bottom and subbottom features thought to be related to seismic or tectonic activity that occurred after the last glaciation. Evidence for neotectonic or paleoseismic activity comprises two groups of features: 1) Seismicity is suggested by slumping and mudflow of both gyttja and fine grained clastic sediments. 2) Postglacial neotectonism or tilting, apparently unrelated to glacioisostatic adjustments, is suggested both by faulting of lacustrine sediments in response to differential movements of their underlying bedrock floor and by the "drowned" appearance of fluvial features that were clearly formed by active fluvial erosion since the last glaciation, but are now submerged in a lake. Caution must be exercised in the interpretation of similar-appearing features, however, because many lake basins contain sediments deformed or faulted as a result of their postdepositional collapse over buried, melting remnants of glacier ice. Slumping also can be induced by nonseismic processes related to sedimentation on steep, subaqueous slopes. A clear differentiation among these types of triggering mechanisms for sediment disturbance can only be made with any degree of certainty where the youngest postglacial sediments are clearly disturbed by the deforming process and the glacial history and late glacial and postglacial sedimentology of the lake basin is understood.

ACKNOWLEDGMENTS

The author was capably assisted in the field by A. Larocque and L. Farrell. The manuscript benefited from discussions with R.N.W. DiLabio and critical reading by J.E. Adams and J.J. Veillette. The author assumes full responsibility for conclusions drawn.

REFERENCES

Adams, J.
1981: Postglacial faulting: a literature survey of occurrences in eastern Canada and comparable glaciated areas; Atomic Energy of Canada, Technical Report TR-142, 63 p.

Canadian Hydrographic Service
1982: Britannia Bay to Chats Falls; Department of Fisheries and Oceans, Hydrographic Chart 1550.

Field, E., Gardner, V., Jennings, E., and Edwards, D.
1982: Earthquake-induced sediment failures on a 0.25° slope, Klamath River delta, California; Geology, v. 10, p. 542-546.

Hodgson, E.A.
1936: The Timiskaming earthquake of November 1, 1935 – the location of the epicentre and determination of focal depths; Journal of the Royal Astronomical Society of Canada, v. 30, no. 4, p. 113-123.

Kenney, T.C. and Balins, J.K.
1975: Bathymetric survey of Lake Timiskaming; University of Toronto, Department of Civil Engineering, Publication 75-11, 20 p.

Klassen, R.A. and Shilts, W.W.
1982: Subbottom profiling of lakes of the Canadian Shield; in Current Research, Part A, Geological Survey of Canada, Paper 82-1A, p. 375-384.

Oliver, J., Johnson, T., and Dorman, J.
1970: Postglacial faulting and seismicity in New York and Quebec; Canadian Journal of Earth Sciences, v. 7, no. 2, p. 579-590.

Otis, R.M., Smith, R.B., and Wold, R.J.
1977: Geophysical surveys of Yellowstone Lake, Wyoming; Journal of Geophysical Research, v. 82, p. 3705-3717.

Prior, D.B., Bornhold, B.D., Coleman, J.M., and Bryant, W.R.
1982: Morphology of a submarine slide, Kitimat arm, British Columbia; Geology, v. 10, p. 588-592.

Qamar, A., Kogan, J., and Stickney, M.C.
1982: Tectonics and recent seismicity near Flathead Lake, Montana; Seismological Society of America Bulletin, v. 72, p. 1591-1599.

Richard, S.H.
1975: Surficial geology mapping: Ottawa valley lowlands (parts of 31G, B, F); in Report of Activities, Part B, Geological Survey of Canada, Paper 75-1B, p. 113-117.

Shilts, W.W. and Farrell, L.E.
1982: Subbottom profiling of Canadian lakes – implications for interpreting effects of acid rain; in Current Research, Part B, Geological Survey of Canada, Paper 82-1B, p. 209-221.

Shilts, W.W., Dean, W.E., and Klassen, R.A.
1976: Physical, chemical, and stratigraphic aspects of sedimentation in lake basins of the eastern arctic shield; in Report of Activities, Part A, Geological Survey of Canada, Paper 76-1A, p. 245-254.

Sims, J.D.
1975: Determining earthquake recurrence intervals from deformational structures in young lacustrine sediments; Tectonophysics, v. 29, p. 141-152.

Vincent, J-S. and Hardy, L.
1979: The evolution of glacial Lakes Barlow and Ojibway, Quebec and Ontario; Geological Survey of Canada, Bulletin 316, 18 p.

Wold, R.J., Isacksen, Y.W., Gerarghty, E.P., and Hutchinson, D.R.
1977: Seismic reflection profiles of Lake George, Adirondack Mountains, New York, as a guide to the neotectonic history of the region (abstract); Geological Society of America, Abstracts with Programs, v. 9, no. 7, p. 1233.

77. GEOLOGY OF THE SKIDDER PROSPECT, BUCHANS, NEWFOUNDLAND[1]

Project 830037
Contract 19SR.23233-3-0434

J. Wayne Pickett[2] and David M. Barbour[3]
Economic Geology Division

Pickett, J.W. and Barbour, D.M., Geology of the Skidder prospect, Buchans, Newfoundland; in Current Research, Part A, Geological Survey of Canada, Paper 84-1A, p. 581-586, 1984.

Also in Current Research, Newfoundland Department of Mines and Energy, Mineral Development Division, Report 84-1, 1984.

Abstract

The Skidder prospect is a volcanogenic massive sulphide deposit hosted in Ordovician mafic volcanic rocks. Three types of sulphide-bearing zones occur in the deposit: 1) a quartz-pyrite stockwork(?) zone that contains very minor amounts of chalcopyrite and sphalerite, 2) a semi-massive to massive, medium to coarse grained pyrite zone with minor chalcopyrite and sphalerite, and 3) a laminated massive sulphide zone consisting of fine to medium grained pyrite with lesser amounts (10-15%) of chalcopyrite and sphalerite. Brecciated, quartz-veined, massive and rarely bedded jasper is associated with the sulphide-bearing zones. Changes in secondary mineral assemblages outline distinct zones of alteration within 100 m of the sulphide-bearing zones. These changes involve a disappearance of epidote and hematite, considerable reduction in carbonate and a large increase in chlorite and quartz contents near the sulphide-bearing zones. The Skidder prospect has more features in common with deposits in ophiolite sequences than to the polymetallic, Kuroko-type massive sulphide deposits typical of the Buchans area.

Résumé

Le gîte possible de Skidder est un gîte sulfuré massif d'origine volcanique contenu dans des roches volcaniques mafiques d'âge ordovicien. On rencontre trois types de zones sulfurées dans le gisement; 1) une zone quartzo-pyriteuse formant un stockwerk (?) et contenant de très faibles quantités de chalcopyrite et de sphalérite, 2) une zone à pyrite semi-massive à massive, de grain moyen à grossier, accompagnée de petites quantités de chalcopyrite et de sphalérite et 3) une zone de sulfures massifs finement laminés, composé de pyrite de grain fin à moyen, qu'accompagnent des quantités moindres (10 à 15 %) de chalcopyrite et de sphalérite. Aux zones sulfurées, est associé un jaspe bréchiforme, à apparence massive, rarement lité, et sillonné de veines de quartz. Les variations des assemblages de minéraux secondaires délimitent des zones distinctes d'altération, dans un rayon de 100 m à partir des zones sulfurées. Parmi ces modifications, on note la disparition de l'épidote et de l'hématite, une réduction considérable des carbonates, et une grande augmentation de la teneur en chlorite et quartz près des zones sulfurées. Le gîte possible de Skidder a davantage de traits en commun avec les gîtes des séquences ophiolitiques, qu'avec les gîtes sulfurés de type Kuroko, à caractère massif et polymétallique, caractéristiques de la région de Buchans.

INTRODUCTION

The Skidder prospect, located approximately 12 km south-southwest of the town of Buchans, central Newfoundland (NTS 12A/10) (Fig. 77.1) is a volcanogenic massive sulphide deposit hosted within mafic volcanic rocks. The prospect was discovered in 1971 by ASARCO Inc. Between 1971 and 1975, ASARCO Inc. and later during 1976 and 1977, Abitibi Price Inc. in a joint venture with ASARCO drilled 38 holes totalling 7795 m of core. The total probable and possible resources indicated by this drilling are approximately 900 000 tonnes, grading about 2% Cu, 2% Zn and containing minor amounts of Pb and Ag (D.M. Barbour, 1977, unpublished company report).

During the summer of 1983, the principal author completed detailed and some regional geological mapping in the vicinity of the deposit and re-logged approximately 50 per cent of the drill core as part of a geological and lithogeochemical study of the deposit. The study will form the basis for a Master of Science thesis. This report concentrates on field aspects of the study, describing macroscopic features of: 1) the regional rock types, 2) the host rocks to the deposit, and 3) the alteration and ore types.

Acknowledgments

The principal author thanks J.G. Thurlow, D.M. Barbour, E.A. Swanson and other staff of Abitibi-Price Mineral Resources and ASARCO Inc. for their generous assistance during the summer of 1983. L. Boone provided able field assistance.

Partial financial support for the study is provided by a fellowship from Memorial University of Newfoundland.

R.V. Kirkham, D.F. Strong and J.G. Thurlow reviewed the paper and made many useful comments.

REGIONAL GEOLOGY

The Skidder area is underlain by submarine mafic volcanic rocks. These rocks have previously been included in the Footwall Basalt unit of the Lower Buchans Subgroup, a calc-alkaline, volcanic and volcaniclastic suite of rocks of island arc affinity (Thurlow and Swanson, 1981a). This Footwall Basalt unit has been described by these authors as "the lowermost unit of the Buchans Group...." consisting of a

[1] Contribution to Canada-Newfoundland co-operative mineral program 1982-1984. Project carried by Geological Survey of Canada.

[2] Department of Earth Sciences, Memorial University of Newfoundland, St. John's, Newfoundland A1B 3X5

[3] Abitibi-Price Mineral Resources, Buchans, Newfoundland A0H 1G0

"thick (approximately 3800 m), laterally continuous sequence composed mainly of basaltic pillow lava and pillow breccia interbedded with lesser pyroclastics and discontinuous lenses of multicoloured, bedded chert".

Field examinations carried out during this study indicated differences between "typical" rocks of the Footwall Basalt unit and the host rocks of the prospect that outcrop in the southern two thirds of the area shown in Figure 77.1. Rocks in the vicinity of the prospect are generally greener in colour and presumably more chloritic than the less altered, dark green-black rocks typical of the Footwall Basalt unit. The flows contain fewer amygdules and the amygdules, where present, are smaller in size than those that occur within mafic flows exposed in other sections of the Footwall Basalt unit. This possibly indicates that these flows were deposited in a deeper water environment than those more typical of the Footwall Basalt unit (Jones, 1969). Pillows with variolitic rims are common in areas near the prospect but not in other areas of Footwall Basalt. Also, the rocks near the Skidder prospect have a higher magnetic susceptibility than those typical of the Footwall Basalt unit. This is evident on hand specimen scale as well as on a regional scale (see GSC Aeromagnetic Map 7049G, Red Indian Lake). On the basis of these differences the rocks in the southern two thirds of the Skidder area are assigned to a new unit, the Skidder Basalt (proposed) (Fig. 77.1). Whether the Skidder basalts are geochemically distinguishable from those of the Footwall Basalt unit will be determined as a part of this study.

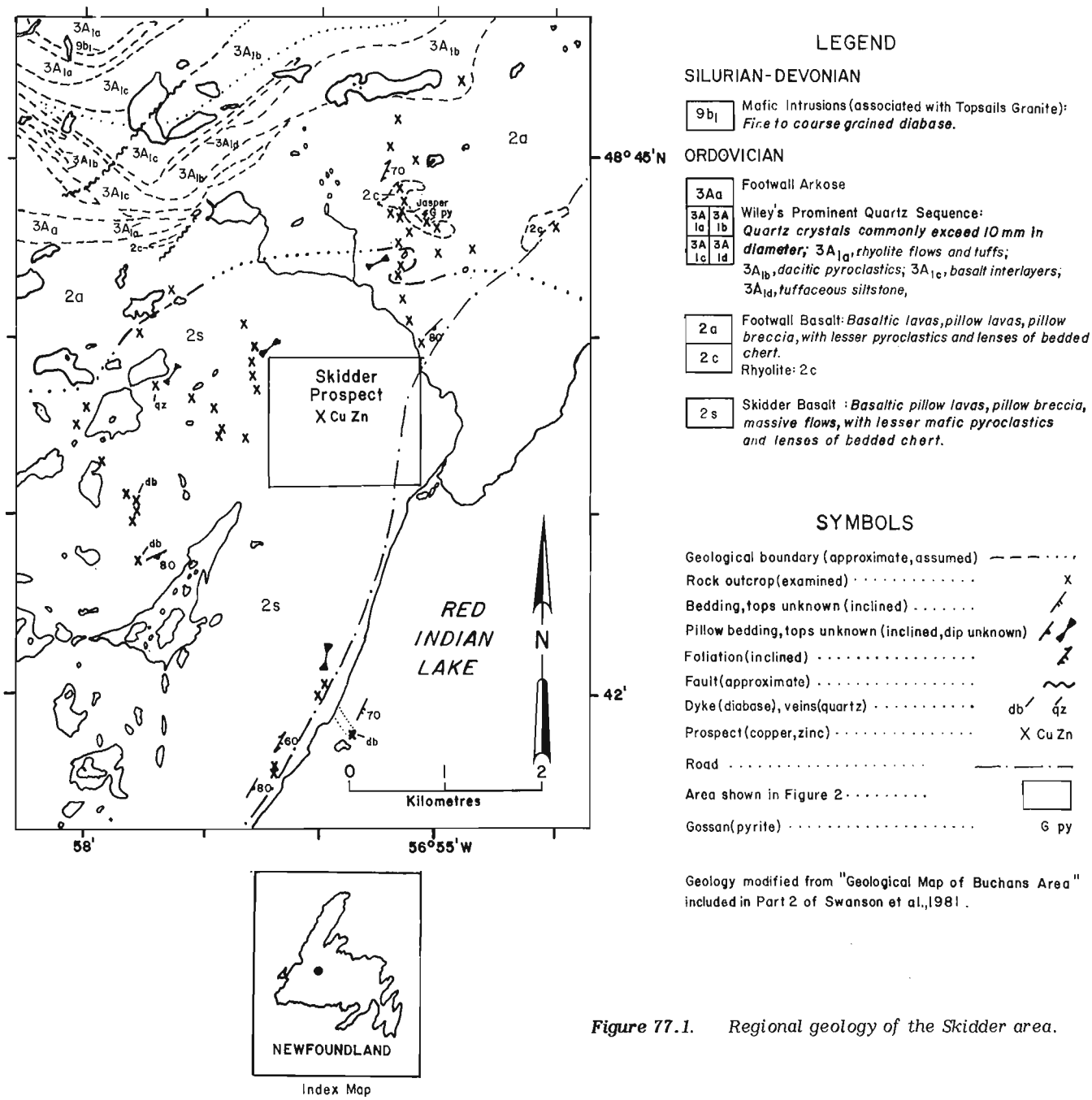

Figure 77.1. Regional geology of the Skidder area.

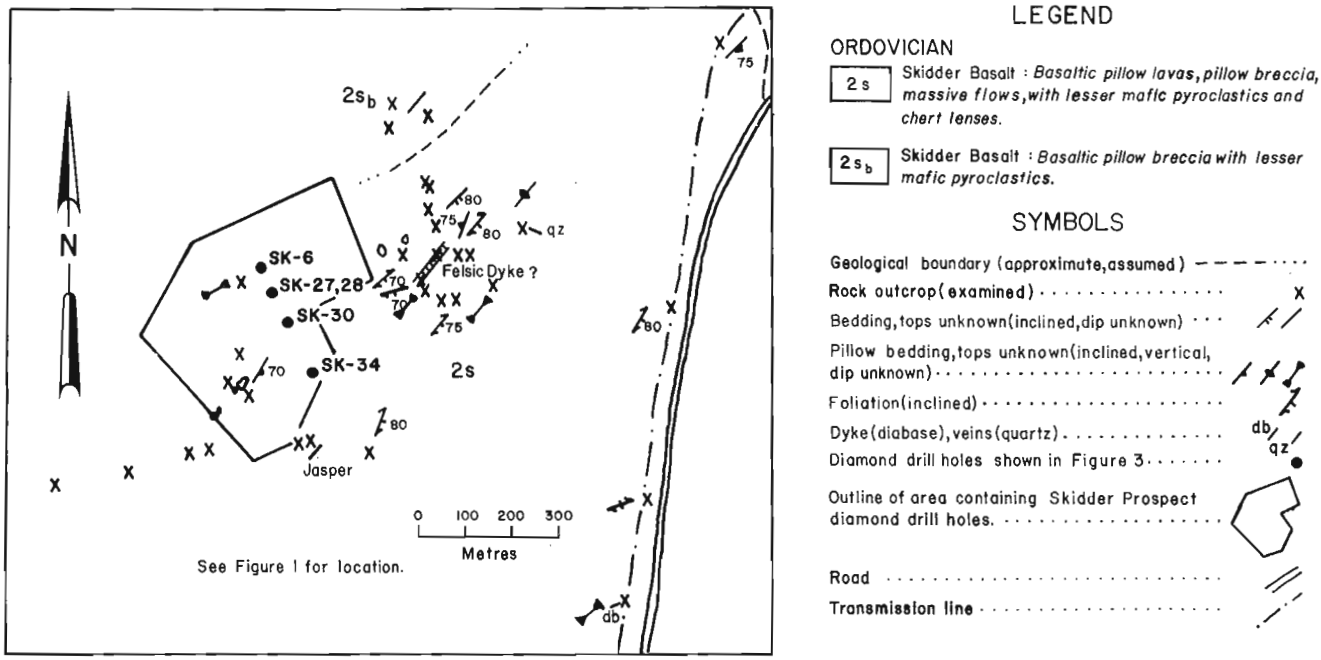

Figure 77.2. Local geology of the Skidder prospect.

Individual flow units plus pyroclastic and sedimentary beds examined within both the Skidder Basalt and Footwall Basalt unit strike generally in a northeasterly direction and dip steeply to the southeast (Fig. 77.1). Pillows predominantly indicate a northwest facing but most pillows are not suitable for determining stratigraphic tops.

Dean (1977), based on general stratigraphic relationships, suggested a Late Ordovician to Middle Silurian age for the Buchans Group. Bell and Blenkinsop (1981) reported a 447 ± 18 Ma whole rock Rb-Sr date for the Buchans Group which supports a Middle Ordovician to Early Silurian age. However, conodonts recovered from carbonate clasts within Buchans Group breccia units are suggestive of slightly older, early Middle Ordovician Llanvirnian age for the carbonate clasts (Nowlan and Thurlow, personal communication). The clasts are considered by these authors to be of local origin and thus their age to be representative of the age of the Buchans Group. The Skidder Basalt appears to conformably underlie the Footwall Basalt unit of the Buchans Group and both are presumed to be of roughly similar age.

LOCAL GEOLOGY

Skidder Basalt

The Skidder Basalt (unit 2s, Fig. 77.1, 77.2) comprises a sequence of basaltic pillow lavas, pillow breccias, massive flows and lesser mafic pyroclastics. The rocks are generally medium green to medium grey and are fine to medium grained.

Pillows in the Skidder Basalt are dominantly small (15-30 cm in diameter) but in certain areas are up to 1 m in diameter and are round but irregular in cross-section. Interpillow material is generally more chloritic than that making up the pillows themselves and in some areas small irregular jasper bodies fill pillow interstices. Some pillows have variolitic rims as characterized by light grey variolites, 3-6 mm in diameter, within a green chloritic matrix. These variolite-rimmed pillows have been noted in drill core structurally beneath the massive sulphide deposit, as well as in outcrop to the south of and presumably stratigraphically below the deposit.

Pillow breccias in the area include angular basaltic fragments within a chloritic and, in many instances, epidote-rich matrix. Other pillow breccias, particularly those noted in drill core, are more characteristic of isolated pillow breccia (Carlisle, 1963). These breccias consist of rounded "mini-pillows" that are 5-20 cm in diameter which are, in most places, within a greener presumably more chloritic matrix. The chloritic matrix generally makes up 30 to 60 per cent of the rock. In many areas, these "mini-pillows" have variolitic rims similar to the variolitic pillow rims described previously.

Massive flows are also medium grey to medium green and fine to medium grained. Locally the flows have been autoclastically brecciated.

An estimated 30 per cent of the massive and pillowed flows are amygdaloidal. These amygdules, dominantly calcite and to a lesser extent epidote and chlorite, are generally 2-4 mm in diameter and, where present, make up less than 10 per cent of the rock.

Mafic pyroclastics consist dominantly of medium green-grey ash-crystal tuffs. These tuffs have an overall massive appearance and are poorly bedded with bedding planes visible only on the weathered surface. The poorly bedded nature and overall massive appearance of these tuffs make them difficult to distinguish from massive flows in drill core. Other mafic pyroclastics include aquagene tuffs (?) that were noted only in core, generally close to the massive sulphide zone. The tuffs consist of angular, olive green, very fine grained "fragments" (locally 1 to 5 cm in length in discontinuous lenses) that occur within a very dark green, fine grained, highly chloritic matrix. One outcrop of matrix-supported lapilli tuff is exposed 400 m northeast

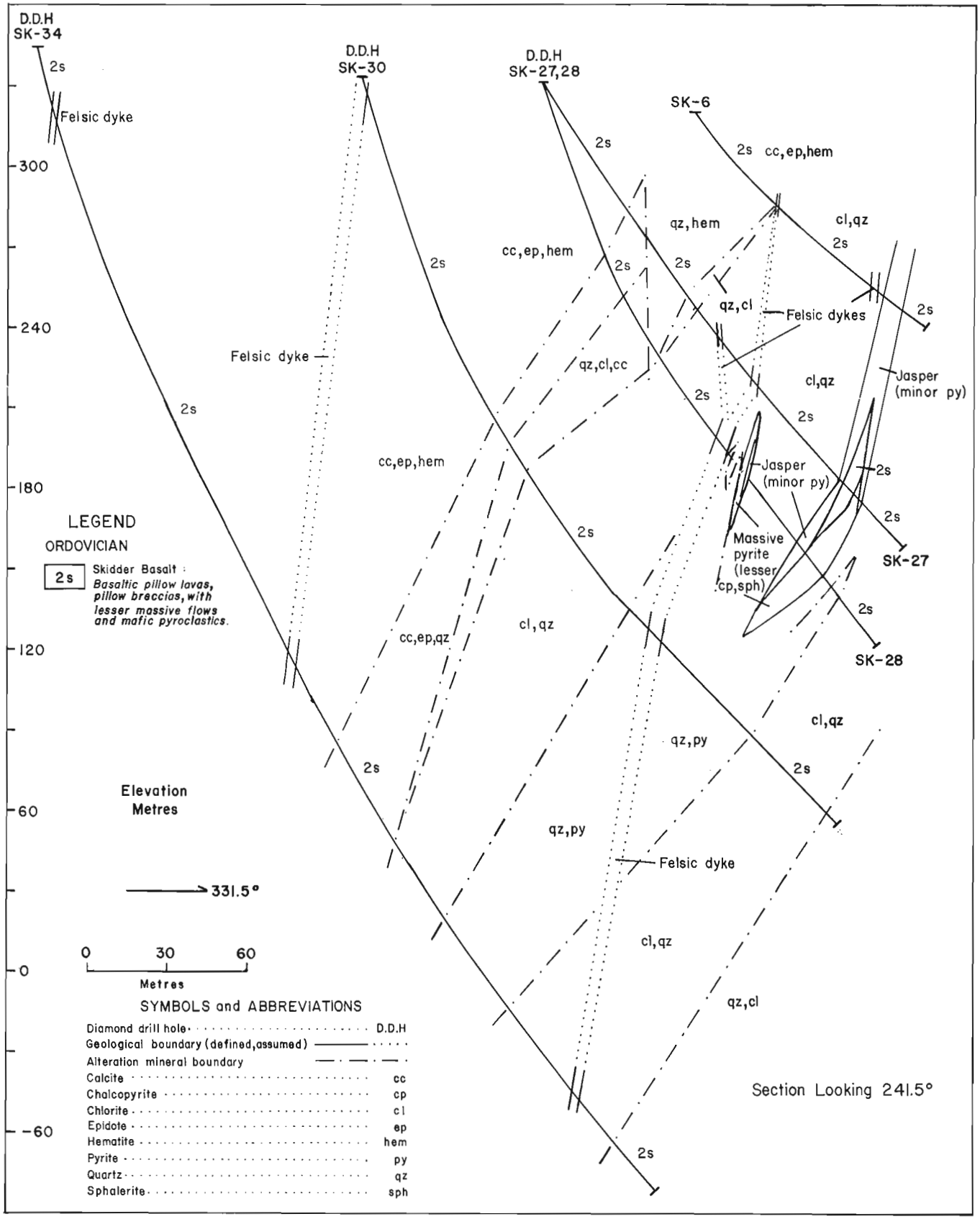

Figure 77.3. *Cross-section through the Skidder prospect showing the alteration zones that flank the sulphide-bearing units. See Figure 77.2 for location of diamond drillholes.*

of the prospect. The lapilli are angular, 2-8 cm in length and make up approximately 10 per cent of the unit. The matrix to the lapilli is chloritic to cherty.

Jasper and red cherty siltstone occur as interpillow material and as discontinuous massive to rare bedded units (Fig. 77.1-77.3).

Mafic intrusive rocks exposed in the area include fine to medium grained diabase dykes and coarser grained gabbroic bodies (dykes?). The latter occur in two outcrops to the west of the Skidder prospect. In hand specimen, these rocks contain visible ophitic intergrowths of plagioclase and pyroxene.

Light grey-green, fine grained felsic dykes were noted in core (Fig. 77.3) and also in two outcrops east of the prospect (Fig. 77.2). The dykes strike approximately parallel to the local stratigraphy and dip steeply to the southeast (Fig. 77.3). In some sections they contain approximately 5 per cent 1 to 3 mm quartz and feldspar phenocrysts that occur in a dense matrix. In many instances, layering is present in these dykes within 30 cm of their contact with adjacent mafic units. This layering is defined by alternating light and dark grey-green to buff-coloured 0.5 to 1 cm wide zones that parallel the dyke contact.

Footwall Basalt

Rocks of the Footwall Basalt unit (unit 2a, Fig. 77.1) examined in the study area are generally basaltic pillow lavas and flow breccias. These rocks are green-black, fine grained and are generally amygdaloidal; the amygdules are usually slightly flatened, 0.5 to 1.5 cm in diameter, calcite-filled and constitute up to 20 per cent of the rock. Pillows are slightly flattened, 0.5 to 1 m in diameter and in some areas contain amygdules arranged in a roughly concentric pattern. The breccia units consist of angular grey-black basalt fragments from 0.5 cm to several centimetres in width that occur in a fine grained, green-black, presumably more chloritic matrix.

Rhyolite(?)

A small body of rhyolite (silicified mafic volcanic rocks?) outcrops approximately 2 km northeast of the Skidder prospect (unit 2c, Fig. 77.1). The rhyolite is grey, fine grained and massive. A 1 m-thick unit of jasper separates the grey rhyolite from the Footwall Basalt in an exposed contact of these units (Fig. 77.1).

Sulphide-bearing zones

The massive and disseminated sulphides are hosted within basaltic pillow lavas, pillow breccias and aquagene tuffs of the Skidder Basalt sequence. The sulphide-bearing units are of three types:

1. The first consists of essentially massive silicified areas and quartz veins that contain 30 to 70 per cent pyrite plus rare chalcopyrite and sphalerite (see qz, py zone, Fig. 77.3). Quartz and pyrite make up approximately 80 per cent of this unit with the remaining 20 per cent consisting of scattered, discontinuous chlorite-rich masses, some of which contain variolites. These masses are presumably altered remnants of the original rock unit. The pyrite is generally medium to coarse grained and occurs as veins, massive bodies and disseminated cubes within the quartz. The chalcopyrite and sphalerite occur typically along the margins of quartz veins.
2. The second type consists of semi-massive to massive, non-bedded medium to coarse grained pyrite with 5-15 per cent quartz and lesser calcite gangue. Rare fine grained chalcopyrite-and sphalerite-rich zones occur within the massive pyrite.
3. Laminated, fine to medium grained pyrite with 10 to 15 per cent interlaminated chalcopyrite and sphalerite constitute the third type.

The massive sulphides (types 2 and 3) occur as two main lens-shaped bodies. The first plunges 37° west with a known length of 380 m along the plunge and has a maximum width of 90 m, a maximum known thickness of 11 m and an average thickness of 4.1 m. The second lens plunges 57° west with a defined length of 243 m, has a maximum width of 68 m, a maximum known thickness of 6.7 m and an average thickness of 3.4 m (D.M. Barbour, 1977, unpublished company report).

Jasper occurs structurally above and in some instances below the massive sulphide lenses (Fig. 77.3). It occurs generally as massive units that are in many areas brecciated and veined by quartz. The units, which in very rare instances show bedding, range from 0.3 to 8 m in thickness.

Regional assemblages

Rocks of the Skidder Basalt examined in outcrop generally contain epidote, calcite and, in places, chlorite as veins and amygdule fillings. In addition, alteration of mafic minerals to chlorite is ubiquitous. Alteration to epidote, particularly in the matrix to pillow breccia fragments, is also pervasive in some areas. Quartz veins are limited in extent and, where observed in outcrops away from the massive sulphide-bearing zones, are present as 1 to 3 cm-wide, subparallel veins, that are probably related to mobilization of silica during regional metamorphism. Basalts exposed in the Halfway Mountain area, approximately 2 km southwest of the prospect, contain fibrous actinolite rosettes as vein fillings in addition to lesser amounts of epidote and carbonate.

Local alteration

A zoned sequence of alteration minerals is present for approximately 100 m structurally above and below the sulphide-bearing zones. Greater than 100 m above and below the sulphide-bearing zones, the first alteration assemblage comprises calcite, epidote and lesser hematite (Fig. 77.3). The calcite and epidote occur as veinlets and amygdule fillings. "Blotches" of epidote, generally 5-15 cm in diameter, are also widely distributed in some areas. Hematite is less abundant than epidote and calcite and is more prevalent in pillow breccia zones. Hematite occurs as veins and, in some areas, is disseminated throughout the unit.

The absence of hematite and the occurrence of quartz alone or with calcite as veinlets and amygdule fillings defines the second alteration assemblage (Fig. 77.3).

An increase in the amount of chlorite, the lack of epidote and presence of fine grained, grey siliceous areas mark the third alteration assemblage (Fig. 77.3). The siliceous sections characteristically have quartz veinlets throughout and range from 5 to 20 cm in length in drill core.

The fourth alteration assemblage is characterized by a marked increase in chlorite and a decrease in calcite relative to zones one and two (Fig. 77.3). In some areas chlorite makes up an estimated 50 to 60 per cent of the rock. Pervasively silicified areas and quartz veinlets, similar to those in the previous zone, are present.

The quartz-pyrite zone (qz, py zone, Fig. 77.3) was the most extensively altered rock noted in the area, with an estimated 80 per cent of the rock replaced by quartz and pyrite.

Discussion of alteration assemblages

Mottl (1983) summarized results of experimental studies of basalt-seawater interaction and the relationship of these results to the alteration minerals in metabasalts and metadiabases dredged from the Mid-Atlantic Ridge. Mottl suggested the following sequences of mineral assemblages to be characteristic of increasing seawater/rock ratios within the temperature range 250°C to 450°C: 1) chlorite-albite-epidote-actinolite, 2) chlorite-albite-epidote-actinolite-quartz, 3) chlorite-albite-quartz and 4) chlorite-quartz. The secondary mineral assemblages that define the alteration zone structurally above and below the sulphide units of the Skidder prospect match reasonably well the assemblages described by Mottl (1983) and indicate that a successively increasing volume of hydrothermal fluid passed through the rocks as the sulphide-bearing unit is approached.

GENERAL DISCUSSION

The Skidder prospect has more similarities to massive sulphide deposits in ophiolite sequences (Franklin et al., 1981; Constantinou and Govett, 1973; Constantinou, 1980) than do other deposits in the Buchans area which are considered similar to the Kuroko ore deposits of Japan (Thurlow, 1973; Thurlow et al., 1975). The similarity to ophiolite-associated massive sulphide deposits is indicated by the following: 1) the sulphides are hosted by mafic pillow lavas and related pillow breccias; 2) pyrite, chalcopyrite and sphalerite are the dominant sulphides with only very minor galena; 3) jasper occurs at the upper and lower contacts of the sulphide-bearing units; and 4) felsic rocks and high barite content characteristic of other Buchans orebodies are lacking.

SUMMARY

The Skidder prospect is a massive sulphide deposit that occurs in pillowed basalts, associated pillow breccias and lesser mafic pyroclastics. The deposit consists of three types of sulphide-bearing units 1) a quartz-pyrite stockwork(?) zone that contains rare chalcopyrite and sphalerite; 2) a semi-massive to massive, non-bedded pyrite zone with minor chalcopyrite and sphalerite, and 3) a laminated massive sulphide zone consisting of fine to medium grained pyrite with lesser amounts of chalcopyrite and sphalerite. Brecciated, quartz-veined, massive and rarely bedded jasper is associated with the massive sulphides. Distinct alteration zones characterized by secondary mineral assemblages occur within 100 m of the sulphide-bearing horizons.

The mafic rocks surrounding the Skidder prospect, including those that host it, are physically different from "typical" rocks of the Footwall Basalt unit. On the basis of these physical differences the rocks surrounding and including the Skidder prospect have been assigned to a new unit called the Skidder Basalt.

REFERENCES

Bell, K. and Blenkinsop, J.
1981: A geochronological study of the Buchans area, Newfoundland; in The Buchans Orebodies: Fifty Years of Geology and Mining, ed. E.A. Swanson, D.F. Strong, and J.G. Thurlow; Geological Association of Canada, Special Paper 22, p. 91-111.

Carlisle, D.
1963: Pillow breccias and their aquagene tuffs, Quadra Island, British Columbia; Journal of Geology, v. 71, p. 48-71.

Constantinou, G.
1980: Metallogenesis associated with the Troodos ophiolite, in Panayioutou, A., ed., Ophiolites: International Ophiolite Symposium, Cyprus, 1979, Proceedings; Cyprus, Ministry Agriculture and Natural Resources, Geological Survey Department, p. 663-674.

Constantinou, G. and Govett, G.L.S.
1973: Geology, geochemistry and genesis of Cyprus sulfide deposits: Economic Geology, v. 68, p. 843-858.

Dean, P.L.
1977: A report on the geology and metallogeny of the Notre Dame Bay Area; Department of Mines and Energy, Government of Newfoundland and Labrador, Mineral Development Division, Report 77-10, 17 p.

Franklin, J.M., Lydon, J.W., and Sangster, D.F.
1981: Volcanic-associated massive sulfide deposits; Economic Geology, 75th Anniversary Volume, 1981, p. 485-627.

Jones, J.G.
1969: Pillow lavas as depth indicators; American Journal of Science, v. 267, p. 181-195.

Mottl, M.J.
1983: Metabasalts, axial hot springs, and the structure of hydrothermal systems at mid-ocean ridges; Geological Society of America Bulletin, v. 94, p. 161-180.

Swanson, E.A., Strong, D.F., and Thurlow, J.G., editors
1981: The Buchans Orebodies: Fifty Years of Geology and Mining; Geological Association of Canada Special Paper 22, 350 p.

Thurlow, J.G.
1973: Lithogeochemical studies in the vicinity of the Buchans massive sulphide deposits, central Newfoundland; unpublished M. Sc. thesis, Memorial University of Newfoundland, 172 p.

1981: Geology, ore deposits and applied rock geochemistry of the Buchans Group, Newfoundland; unpublished Ph.D. thesis, Memorial University of Newfoundland, 305 p.

Thurlow, J.G. and Swanson, E.A.
1981a: Geology and ore deposits of the Buchans area, central Newfoundland; in The Buchans Orebodies: Fifty Years of Geology and Mining, ed. E.A. Swanson, D.F. Strong and J.G. Thurlow; Geological Association of Canada, Special Paper 22, p. 113-142.

1981b: Geological Map of Buchans area, Newfoundland; Part 2 of The Buchans Orebodies: Fifty Years of Geology and Mining, ed. E.A. Swanson, D.F. Strong and J.G. Thurlow; Geological Association of Canada, Special Paper 22.

Thurlow, J.G., Swanson, E.A., and Strong, D.F.
1975: Geology and lithogeochemistry of the Buchans polymetallic sulfide deposits, Newfoundland; Economic Geology, v. 70, p. 130-144.

78. GEOLOGY OF THE SOUTHERN ANTIGONISH HIGHLANDS, NOVA SCOTIA [1]

Project 830031
Contract 19SR.23233-3-0241

J. Brendan Murphy [2]

Murphy, J.B., Geology of the southern Antigonish Highlands, Nova Scotia; in Current Research, Part A, Geological Survey of Canada, Paper 84-1A, p. 587-595, 1984.

Also in Mines and Minerals Branch, Report of Activities, 1983, Nova Scotia Department of Mines and Energy, Report 84-1, 1984.

Abstract

Continuation of mapping in the southern Antigonish Highlands has considerably altered the interpretation of the geological history of the region. Principally, the Keppoch Formation, a sequence dominated by felsic to mafic volcanic rocks and previously thought to be of Cambrian age, is now assigned to the Precambrian. The Keppoch Formation unconformably underlies the James River Formation of the Precambrian Georgeville Group, a sequence dominated by oceanic-type volcanic and sedimentary rocks. The relations of the Keppoch Formation to older formations of the Georgeville Group are unknown and await further mapping.

Within the Antigonish Highlands, rocks formed in an oceanic region to the north (Georgeville Group) adjoin rocks formed in a continental region to the south (Keppoch Formation). The junction between these two zones may be close to the Browns Mountain or Marshy Hope faults.

Lower Paleozoic rocks generally flank the Highlands and within the Highlands adjacent to major faults.

Résumé

La continuation des travaux de cartographie effectués dans le sud des hautes-terres d'Antigonish a mené à la modification considérable de l'interprétation de l'histoire géologique de cette région donnée jusqu'à maintenant. En particulier, la formation de Keppoch, succession dominée par des roches volcaniques de type felsique à mafique et autrefois jugée d'âge Cambrien, est maintenant placée dans le Précambrien. La formation de Keppock repose en discordance sous la formation de James River, qui appartient au groupe précambrien de Georgeville, succession dominée par des roches sédimentaires et des roches volcaniques de type océanique. On ne connaît pas la situation de la formation de Keppoch par rapport aux formations plus anciennes du groupe de Georgeville, et l'on attend la suite des travaux de cartographie.

A l'intérieur des hautes-terres d'Antigonish, des roches formées dans une région océanique au nord du groupe de Georgeville touchent aux roches formées dans une région continentale au sud (formation de Keppoch). Le contact entre ces deux zones se situe peut-être près des failles de Browns Mountain ou de Marshy Hope.

Des roches du Paléozoïque inférieur bordent généralement les hautes-terres, ou se trouvent à l'intérieur de ces dernières, à proximité de grandes failles.

INTRODUCTION

Geological mapping in the Antigonish Highlands during 1983 continued a project, initiated in 1978 by the Nova Scotia Department of Mines and Energy in co-operation with the Canada Department of Regional Economic Expansion, that concentrated on the northern Antigonish Highlands. The purpose of the present study is to map the adjoining northwestern and southern Highlands, to describe the volcanic, sedimentary and plutonic rocks and their stratigrapic and structural relations, to determine their geological history and to examine the potential for mineralization. The Antigonish Highlands comprise about 1500 km^2. To date 650 km^2 have been mapped, 300 km^2 in 1978 and 1979 in collaboration with J.D. Keppie of Nova Scotia Department of Mines and Energy and A.J. Hynes of McGill University, and a further 350 km^2 during 1983.

Stratigraphic and structural relationships described below, when augmented by previous work (Murphy et al., 1982 and in preparation), allow a more comprehensive view of the geological history and tectonic setting of the Highlands. Mineral occurrences observed so far are of rather limited economic interest (see Bourque, 1981); interpretation as to the economic potential has been hindered by lack of stratigraphic control. This report documents interesting new mineral occurrences and provides the stratigraphic and structural field relationships within which they may be investigated.

Geological setting

Rocks of the Antigonish Highlands form part of the Avalon "Composite" Terrane (Keppie, 1983) or "Suspect" Terrane (Williams and Hatcher, 1982) and lie on the southeastern margin of the northern Appalachians. The rocks are bounded to the northwest by the Hollow Fault, to the south by the Chedabucto Fault and to the east by the Devonian-Carboniferous Antigonish Basin (Fig. 78.1). They consist predominantly of Precambrian metavolcanics and metasediments, unconformably overlain by lower Paleozoic strata. In general, most late Precambrian "subterranes" within the Avalon Terrane are characterized by mafic to felsic volcanic rocks with minor associated volcanogenic sediments (see Rast et al., 1976). Parts of this terrane consist of the Jeffers and Warwick Mountain formations in the Cobequid Highlands (Donohoe and Wallace, 1980) and the Forchu Group in southeastern Cape Breton Island (Murphy, 1977).

[1] Contribution to Canada-Nova Scotia Co-operative Mineral Program 1981-84. Project carried by Geologial Survey of Canada.

[2] Department of Geology, St. Francis Xavier University, Antigonish, Nova Scotia B2G 1C0

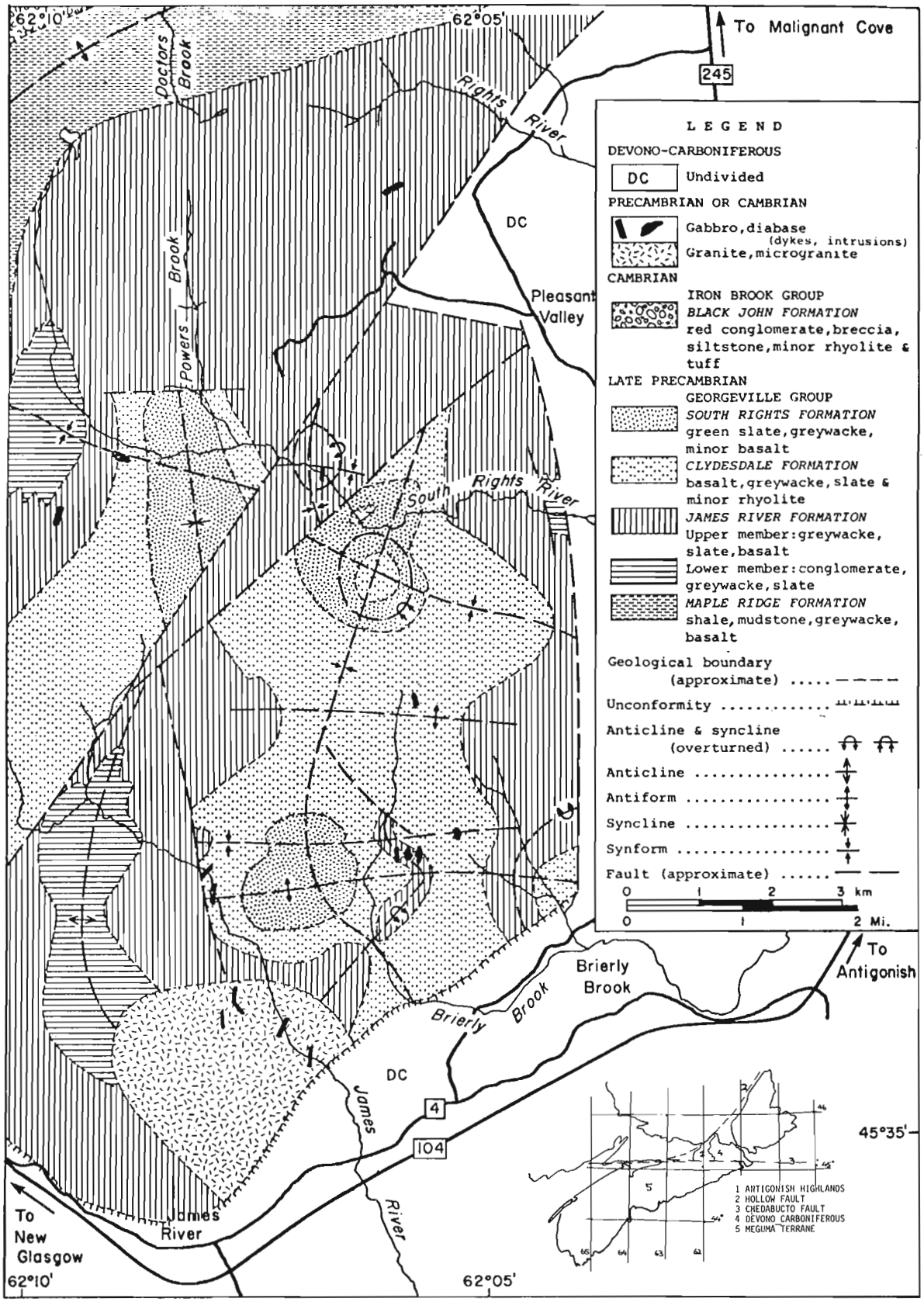

Figure 78.1. *Summary of the geology of the northern Antigonish Highlands. Generalized from Murphy, Keppie and Hynes, 1982.*

Previous work

Benson (1974) interpreted the rocks of the Highlands as "a folded and faulted pre-Silurian eugeosynclinal assemblage of probable Cambro-Ordovician age, overlain by less disturbed Siluro-Devonian sedimentary and volcanic rocks". Reconnaissance work by Keppie (1978) followed by detailed mapping by Murphy et al. (1982) indicated that most rocks of the Antigonish Highlands are of Precambrian age and are unconformably overlain by Cambrian strata. Interpretations of geochronological studies (Cormier, 1979; R.F. Cormier, personal communication, 1980; R.K. Wanless, written communication, 1980) and paleontological studies (Landing et al., 1980) have substantiated these interpretations.

As a result, the term Browns Mountain Group (Benson, 1974), to which these rocks were previously assigned, has been abandoned and replaced by three new groups: the Georgeville Group of Precambrian age and the Iron Brook and the MacDonald Brook groups of Cambrian age. The study showed that Precambrian and Cambrian rocks have distinctly different sedimentary and structural histories, and that their geochemistry indicated they were formed in different paleogeographic and tectonic settings.

The Georgeville Group in the northern Highlands was interpreted to represent a narrow deep-water basinal sequence, probably floored by oceanic crust. The group is dominated by plane, finely laminated mudstones, greywackes, matrix-supported conglomerates, interlayered basalts and associated dykes with minor cherts and limestones. These rocks were polydeformed and post-tectonically intruded by granite (alaskite) and gabbro (appinite) in the latest Precambrian. Cambrian rocks were interpreted as a rift-related succession. The Iron Brook Group consists of fluviatile to shallow-water marine, fossiliferous sediments (red conglomerates and slates, pink limestones, ironstones, and calcareous tuffs). The MacDonald Brook Group consists of red conglomerates, mafic and felsic volcanic rocks with minor interlayered red slates and pink limestones.

Upper Ordovician and Lower Silurian rocks have been described in the Kenzieville area of the Highlands by Maehl (1961) and Smith (1979). The regional extent of these rocks and their tectonic significance are unknown though Smith (1979) suggested that they may be correlatives of the rift-related (Keppie et al., 1978) Dunn Point Formation exposed at Arisaig to the north of the Hollow Fault.

Results of present study

The principal results of the field work during 1983 may be summarized as follows:

1. The Keppoch Formation, considered by Benson (1974) to comprise the lowermost formation of his Cambro-Ordovician "Browns Mountain" sequence, is Precambrian in age.
2. The Keppoch Formation is informally subdivided into members dominated by felsic, intermediate, and mafic volcanic rocks and sediments.
3. Sediments are uncommon in the Keppoch Formation whereas sediments are overwhelmingly dominant in the Georgeville Group.
4. Field relationships indicate that the dominantly volcanic Keppoch Formation is in part a facies variation of the dominantly sedimentary Georgeville Group.
5. The economic potential of the Keppoch Formation, especially members with abundant felsic volcanics, is particularly encouraging. Some interesting, apparently strata-bound pyritic zones were found. Some of these extend discontinuously for about 2 km.
6. Rocks in the northwestern Highlands are an extension of those in the northern Highlands and the stratigraphic units and structural trends continue from one area into the other.
7. The Browns Mountain Fault and the Marshy Hope Fault may approximate the boundary between rocks in the northern Antigonish Highlands deposited upon oceanic crust and rocks in the southern Highlands deposited upon continental crust.
8. Upper Ordovician and Silurian rocks are far more widespread than previously believed. Remnants occur here and there, either flanking the Highlands or in fault-bounded belts. The stratigraphy of these rocks within the Highlands is little known. They consist of red fluviatile arkosic conglomerates, red slates, felsic volcanics and blue-green fossiliferous siltstones. The stratigraphy is similar to that on the northern side of the Hollow Fault, and the sequence represents the oldest rocks that occur on both sides of the Hollow Fault.
9. Plutonic rocks in the present field area may be divided into three categories on the basis of field observations incorporated with geochronological data supplied by Cormier (1979) and Wanless et al. (1967). Appinitic gabbros and granites are probably late Precambrian in age. Some granites are of Devonian age. Other granites of late Precambrian age may be cogenetic with felsic volcanic rocks of the Keppoch Formation.
10. Dykes are generally mafic in composition and probably of several ages. Mafic dykes cut late Precambrian, lower Cambrian, lower Ordovician, Silurian and Devono-Carboniferous rocks. Distinguishing between these dykes is difficult in the field and requires detailed geochemistry.

PRECAMBRIAN

Lithology

The northwestern Highlands are dominated by the Maple Ridge and James River formations (Fig. 78.2). Both formations display similar characteristics to their type areas to the east and have been described in detail by Murphy et al. (in preparation). The Maple Ridge Formation is well exposed in the Vamey Lake and Eigg Mountain areas. It consists of thinly (2-15 mm) plane laminated, poorly cleaved green and black mudstones with relatively subordinate interlayered green graded greywackes. Minor mafic flows may occur. The mudstones show graded bedding, crossbedding and slump structures.

The James River Formation conformably overlies the Maple Ridge Formation and consists of about 1000 m of greywackes. In the northwest, individual units are typically 2-3 m thick (Vamey River in the vicinity of the Hollow Fault) and farther south 1 m thick (east of Bears Brook). Greywacke units grade from a coarse clastic base with load features to a slaty top that may display crossbedding.

The northern section of the Antigonish Highlands is separated from the southern section by the Marshy Hope Fault (which trends subparallel to the Trans-Canada Highway) and by a sequence of Upper Ordovician to Silurian rocks near the fault. Rocks of the Georgeville Group in this section are correlated with the northern section on the basis of lithologic comparison. Greywackes and slates typical of the James River Formation occur adjacent to the contact with the Keppoch Formation.

The South Rights Formation outcrops to the south of the Trans-Canada Highway (e.g. Baxter Brook) and consists predominantly of green, thinly laminated slates and

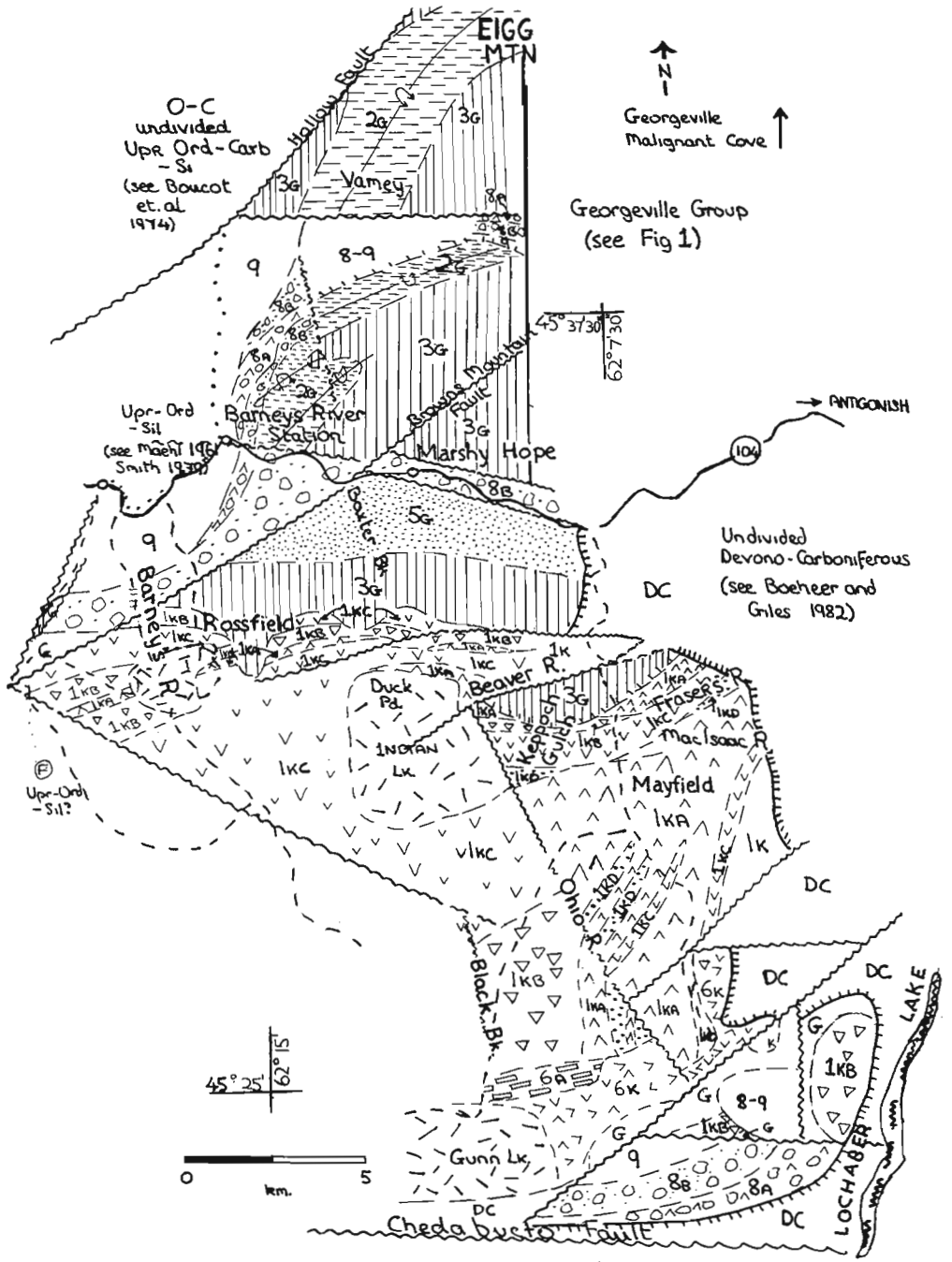

LEGEND

Geological boundary
F_I hinge surface trace
Fault
Unconformity
F Fossil locality (new)
104 Trans-Canada Highway, secondary route

LITHOLOGY*

DC — Devono-Carboniferous (undivided conglomerate, siltstone, limestone, gypsum, sandstone and volcanic rocks). See Boehner and Giles, 1982 for details.

O-C — Upper Ordovician to Carboniferous (undivided blue-grey and red sandstone, siltstone and wacke, mafic and felsic volcanics). See Boucot et. al. 1974.

DEVONIAN — Granite (quartz, microcline, plagioclase, muscovite, biotite, hornblende), minor assimilated host rock.

UPR. ORDOVICIAN -SILURIAN — Beechhill Cove Formation (blue green fossiliferous siltstone)

Bear's Brook Formation (A, rhyolite flow and tuff, B, red conlomerate, arkose and slate) See Maehl 1981, and Smith 1979.

CAMBRIAN-LR. ORD? — A, Macdonald Brook Group* (red conglomerate, slate, basalt, rhyolite)

B, Iron Brook Group* (red conglomerate, slate , limestone, ironstone, tuff). See Murphy et. al. 1982.

LATE PRECAMBRIAN or CAMBRIAN PRECAMBRIAN

K Granite, quartz-feldspar graphic intergrowth.

A Appinite, hornblende-plagioclase porphyrytic and poikilitic gabbro or diorite

G GEORGEVILLE GROUP (see Fig. 1. Formations , 1G Chisholm Brook*, 2G Maple Ridge, 3G James River, 4G Clydesdale*, 5G South Rights).

K KEPPOCH FORMATION (IK, undivided, IKA felsic member IKB intermediate member, IKC mafic member, IKD sedimentary member)

* Note * indicates that the unit is not exposed in the present study area.

Figure 78.2. *Summary of the geology of the central Antigonish Highlands. References are given for available geological maps in adjoining areas. The map is the western and southern extension of the geology shown in Fig. 78.1.*

minor greywackes. In many ways, these rocks are similar to the Maple Ridge Formation and can only be distinguished with confidence on the basis of stratigraphic relationship with the James River Formation.

The Keppoch Formation consists predominantly of volcanic rocks ranging from rhyolite to basalt with very minor interflow sediments. The best exposures occur in the Mayfield area, on Frasers and MacIsaac brooks (Fig. 78.2), on the northern tributary of Beaver Brook and on new logging roads about 1 km east of this tributary. In any given section all of the above lithologies occur interlayered.

Felsic rocks consist of flows, welded to poorly welded ash flow tuffs (ignimbrites), crystal and lithic tuffs, lahars and volcanic breccias. In the field, the rocks are generally pink to dark red and apparently massive. However, the ignimbrites generally display banding defining a primary flattening foliation that is commonly parallel to the regional strike and is assumed to approximate bedding.

True rhyolitic flows are rare in the Keppoch Formation; probably 80 per cent of exposed rocks are pyroclastic. In thin section, flows are aphyric, display crude flow alignment and consist of interlocking grains of plagioclase (now albite), orthoclase, quartz and devitrified glass. Alteration of felsic flows is minor with epidote, chlorite ± calcite occurring as rare secondary phases. Ignimbrites probably account for one-third of the felsic volcanics. The banding visible in hand specimen is defined in thin section by devitrified and partially sericitized pumice imparting a eutaxitic primary foliation. Pumice is also moulded against other fragments, their boundaries are wispy and merge imperceptibly into the felsic matrix. Flattened rhyolitic fragments up to 40 mm long are common in the ignimbrites, as are angular, broken and embayed crystals of quartz, orthoclase and plagioclase (now albite). Much of the brecciation is "in situ". Alteration of ignimbrites is generally minor and consists of small clots rich in chlorite and epidote.

Lithic and crystal tuffs are relatively fine grained and their tuffaceous aspect is commonly not readily visible in the field. They generally consist of variable proportions of angular, moderately well-sorted fragments of felsic volcanics (which themselves commonly display flow textures), quartz (generally embayed), orthoclase (incipiently sericitized) and plagioclase (now albite) in a fine grained quartzofeldspathic matrix. Alteration is minor.

Lahars in hand specimen are reddish green and contain poorly sorted, matrix-supported angular fragments of felsic volcanics, quartz and feldspar with minor intermediate to mafic clasts. Best exposures are along the northern branch of Beaver River, south of the "Duck Pond". In thin section, the matrix is very fine grained and consists of variable proportions of sericite, chlorite, and quartz ± epidote. Sericite-rich lahars generally have a well-defined foliation. Felsic volcanic fragments are generally tuffaceous. Feldspar fragments are commonly strongly sericitized.

Andesites are green to pale green massive rocks, generally containing plagioclase phenocrysts up to 10 mm long. Best exposures are near Rossfield (adjacent to the microwave tower), Beaver River area and west of Lochaber Lake. In thin section, andesites display secondary alteration to varying degrees, but primary textures are preserved. They are dominated by flow-aligned phenocrysts and microphenocrysts of plagioclase (now albite) and augite (partly to completely pseudomorphed by chlorite and/or actinolite). The matrix consists of variable proportions of albite, magnetite, epidote, quartz, chlorite and sphene ± calcite.

Basalts are dark green, chloritic, massive aphyric rocks. More rarely, they contain vesicles, quartz-chlorite filled amygdules, and/or chlorite pseudomorphs of pyroxene phenocrysts. In thin section, the rocks are relatively fresh, consisting of rare but fresh microphenocrysts of augite ± hypersthene. The matrix consists of equant grains of augite and hypersthene, plagioclase laths (now albite) and magnetite-ilmenite intergrowths. Pyroxenes show incipient alteration to chlorite ± actinolite.

Pyritic zones are most commonly found in felsic volcanics. They contain variable amounts of pyrite with traces of copper minerals. Occurrences are generally small and there is one promising occurrence near Callahans Brook. The pyritic zones are apparently stratabound within a rhyolitic tuffaceous volcanic member, 250 m thick and interlayered with mafic volcanics. The mafic volcanics show variable degrees of silicification near their contacts with the rhyolitic tuff.

Contact relations

Precambrian rocks in the map area have been subdivided into two main categories. Sediments are dominant to the north (Maple Ridge, James River and South Rights formations) and volcanic rocks to the south (Keppoch Formation). In the northern region, the Maple Ridge and James River formations can be traced from the eastern Highlands (Murphy et al., 1982) southwards to the Marshy Hope Fault. The contact between these two formations is apparently everywhere conformable and sharply defined by the relative dominance of shales (Maple Ridge) and greywackes (James River).

The Marshy Hope Fault and associated Upper Ordovician and Silurian rocks separate Precambrian exposures to the north and the south. Correlations between northern and southern sequences are based on lithologic comparison and overall stratigraphic considerations of the northern areas. An east-striking formation consisting of greywackes with slaty tops, minor interbedded, matrix-supported conglomerates and volcanic rocks is typical of the James River Formation. These rocks are best exposed in the Keppoch Gulch and Cameron's River areas. They consistently face north and are conformably overlain by a sequence of thinly laminated mudstones with minor greywackes (e.g. Baxters Brook). These rocks are correlated with the South Rights Formation of the northern Highlands (see Murphy et al., 1982, Fig. 1). The Clydesdale Formation (which in the northern Highlands is stratigraphically defined between the James River and South Rights formations and is characterized by a dominance of basaltic volcanics) apparently does not occur in the southern Highlands. In detail, the Clydesdale Formation consists of an ocean island "complex" (Murphy et al., in preparation) of lavas, dykes and sills associated with a strong, linear, positive, vertical-gradient magnetic anomaly (Geologial Survey of Canada, 1982) and are thus likely to be of limited lateral extent.

The contact between the Georgeville Group and the Keppoch Formation is exposed on the Mayfield road. There, slates and greywackes of the James River Formation stratigraphically overlie quartz-eyed rhyolites of the Keppoch Formation. Bedding in the sediments is concordant with the contact; no banding was found in the rhyolites. On a regional scale however, the contact is discordant. Between the road section and the Keppoch Gulch River section to the west (where the river valley separates sediments from volcanic rocks, Fig. 78.2) the James River Formation unconformably overlies the rhyolites to rest upon a predominantly mafic to intermediate volcanic sequence. A screen-type deposit of basal James River in Keppoch Gulch consisting of angular volcanic clasts in a sedimentary matrix occurs at the contact. Furthermore, facing directions obtained in volcanic rocks near this contact consistently face south, in contrast to the north-facing stratigraphically overlying James River sediments. The above relationships indicate that the Keppoch Formation predates the James River Formation of

the Georgeville Group. Further mapping is required to document the relations between the Keppoch Formation and the older formations of the Georgeville Group. However, since the entire Georgeville Group, on the basis of stratigraphic, structural, geochemical, and geochronological arguments, has been interpreted to be of Precambrian age (Keppie, 1978; Murphy et al., in preparation), the Keppoch Formation may now be assigned a Precambrian, probable Hadrynian, age. With the extent of present mapping, it is not possible to establish whether or not the regional unconformity is due to earlier deformation of the Keppoch Formation. Although the Keppoch does have different structural style and trends compared to the Georgeville Group, this could equally be due to primary distribution of the Keppoch and/or to competency differences between the sedimentary and volcanic sequences.

Geochronological data support a Precambrian age for the Keppoch Formation. From reconnaissance work, the Eden Lake "appinitic" Pluton (3 km to the west of the map area) apparently intrudes the Keppoch Formation (see also Benson, 1974) and has been dated at 582 ± 32 Ma (Wanless et al., 1967, K-Ar on hornblende), and thus places a minimum age for the Keppoch Formation. Similar appinites have been found in the Black Brook region in the southwest of the study area and the Greendale Complex to the northeast of the map area dated at 632 ± 10 Ma by P.H. Reynolds (personal communication, 1980, $^{40}Ar/^{39}Ar$ on hornblende).

Zircons for U-Pb age determinations have been collected by W.H. Poole from the felsic rocks of the Keppoch Formation, and the results of this analysis may have significant implications for the geological history of the Highlands rocks.

Further distinction between the Keppoch Formation and Georgeville Group may be gained by comparing their respective environments of deposition. Whereas the stratigraphy of the Georgeville Group (i.e. ocean floor basalts with plane laminated mudstones and greywackes) suggests a basinal environment, welding of ignimbrites and weathered tops to flow units indicates a subaerial environment in the Keppoch Formation. Coarser units of the Georgeville Group contain abundant volcanic clasts of basaltic to rhyolitic composition which may, in part, be derived from the Keppoch. Thus the contact between deep water sediments and subaerial volcanic rocks with no "intermediate" facies suggests that much of the Keppoch volcanic rocks were submerged during James River sedimentation which may have "draped" the Keppoch. This is supported by the apparent restriction of Georgeville-type sediments to the flanks of the Keppoch Formation (Fig. 78.2), and may imply a significant time-gap between Keppoch and James River formations.

However, stratigraphic relations also indicate that minor "late Keppoch-type" volcanism may have occurred during deposition of the James River Formation. Minor mafic and felsic volcanics do occur near the base of the formation. Although the mafic volcanic rocks could also be attributed to distal precursors of Clydesdale ocean island volcanism, felsic volcanics however minor, are in general atypical of Georgeville Group-type volcanics and may represent late-stage distal Keppoch-type activity. This felsic volcanic unit (a distinctive quartz-eyed porphyry) may be a useful marker horizon within the James River Formation. The above relations cannot be attributed to <u>local</u> interlayering of volcanic and sedimentary rocks (i.e. a transitional Keppoch-James River contact) since (1) these formations have apparently opposing facing directions in the vicinity of the contact and (2) it is unlikely that subaerial volcanics and deep water sedimentary rocks would be deposited directly next to one another. Thus, the felsic unit, if related to Keppoch-type volcanism, is considerably younger than Keppoch volcanic rocks adjacent to the Keppoch-James River contact and may indicate that felsic volcanism overlaps in time the deposition of the James River Formation.

Volcanic rocks of the Kepoch Formation have been divided into informal members of the basis of dominance of felsic, intermediate, mafic, and sedimentary rocks (Fig. 78.2). These boundaries either overlap or cut across Benson's (1974) assumed contact between his predominantly felsic Keppoch Formation and his mafic Brierly Brook Formation. The Brierly Brook Formation has been discarded (Murphy et al., 1982) since the mafic rocks they include probably belong to three separate formations, two Precambrian (Chisholm Brook and Clydesdale) and one Cambrian (Arbuckle Brook).

The contacts between members of the Keppoch Formation are defined on a percentage scale though, in a given locality basalt, andesite, and rhyolite may be interlayered. Formal subdivision is not warranted with present data since facing directions are rare. Thus it is not possible at present to evaluate whether, for example, all mafic-dominated volcanic members are part of one stratigraphically continuous unit or whether interlayering of volcanic rocks occurs on a regional scale. This may be resolved by detailed mapping in the vicinity of these contacts.

UPPER ORDOVICIAN AND SILURIAN

Lithology

Upper Ordovician and Silurian rocks that unconformably overlie Precambrian strata in the Antigonish Highlands have been defined as the Bears Brook Formation (Maehl, 1961; Smith, 1979) from the type area north of Bears Brook in the Kenzieville and Barneys River areas. They consist of red conglomerates, arkosic sandstones, felsic crystal and lithic tuffs and minor red slates conformably or disconformably overlain by the fossiliferous lower Silurian Beechhill Cove Formation.

The present study shows they are far more widespread than previously recognized (Fig. 78.2) and that their stratigraphy throughout the Highlands is generally consistent with that determined by the above authors (e.g. in the South Lochaber and College Grant areas).

The conglomerates and arkoses are polymictic and massive, containing subangular to angular clasts of red and green slate, felsic to mafic volcanic rocks, granite, quartz, albitized plagioclase, sericitized K-feldspar, pyrite and hematite. Many of the grains are coated with hematite. The matrix also contains chlorite, sericite and epidote. The best exposures are on the Trans-Canada Highway near Marshy Hope, on McIver Brook (Smith, 1979), and on South Lochaber.

Felsic volcanic rocks are interlayered with, or conformably overlie, the conglomerates and arkoses. They are massive, purple to pale grey rocks composed of lithic and crystal fragments in a fine grained matrix. They are, in part, apparently intrusive (Smith, 1979), but some rocks contain pumice and glass shards and are probably ignimbrites, and others show evidence of flow banding. Crystal and lithic tuffs are generally composed of broken phenocrysts of plagioclase (now albite), sericitized orthoclase, and quartz, with variable abundances of rhyolitic fragments in an ash-sized matrix.

Pumice and glass shards in ignimbrites show evidence of primary flattening imparting a non-penetrative primary foliation. For the present, rhyolitic rocks are undivided, though future mapping may result in the recognition of a systematic distribution of various felsic lithologies.

Rhyolites are overlain, apparently concordantly, by either red conglomerates and arkoses similar to those described above, or by laminated, fossiliferous, blue-green siltstones and slates. In the northern Highlands these siltstones have been placed in the Beechhill Cove Formation (Maehl, 1961; Smith, 1979; Murphy et al., 1982). These rocks are now identified in various parts of the southern and western Highlands (Fig. 78.2). They contain brachiopods, corals, crinoids, and trilobites (Smith, 1979). The Beechhill Cove Formation is thought to define the base of the Silurian (e.g. Boucot et al., 1974) thereby establishing a minimum age for the Bears Brook Formation.

Distribution

Upper Ordovician and Silurian rocks are generally spatially associated with major faults in the area. Thus they occur at the extremities of the Highlands (Fig. 78.2) and also internally in narrow fault-bounded "troughs", e.g. the Hartshorn River adjacent to the Marshy Hope Fault.

INTRUSIVE ROCKS

Plutonic rocks are rare in the northern Antigonish Highlands, especially between the Browns Mountain and Hollow faults. However, in the southern Highlands they may be divided into three categories, (a) appinite, (b) older granites and (c) younger granites, on the basis of lithology, intrusive relations and available geochronological data.

(a) Appinites (i.e. hornblende-bearing gabbros) occur in the Black Brook region in the south of the study area. They consist of roughly equal proportions of hornblende and plagioclase. They are generally fine grained and equigranular, but coarse hornblende-plagioclase pegmatites and quartzofeldspathic sweat pods also occur. Although no contacts are exposed, the appinite apparently intrudes the Keppoch Formation near Black Brook and is in turn intruded by younger granites to the south (Fig. 78.2). They strongly resemble the igenous rocks of the Greendale Complex dated at 632 ± 10 Ma (P.H. Reynolds, personal communication, 1980, $^{40}Ar/^{39}Ar$ on hornblende). The intrusive body at Eden Lake to the west has yielded a 582 ± 32 Ma age (Wanless et al., 1967, K-Ar on hornblende). Thus geochronological data suggests a late Precambrian "appinitic" intrusive event in the Antigonish Highlands.

The older granites pose a problem and in the map area, the best example occurs on the Ohio River. They consist of quartz and sericitized K-feldspar in graphic intergrowth, plagioclase and minor biotite (altered to chlorite). They are similar in texture and mineralogy to the Williams Point Granite east of Antigonish (Dobek, 1983) and to the James River Pluton about 1 km east of the map area. However, some contain aplitic or rhyolitic phases, and are commonly difficult to distinguish from spatially associated rhyolitic volcanic rocks of the Keppoch Formation. Contacts with the Keppoch Formation are not exposed, but the spatial distribution suggests the contact may be both gradational and transitional. On the basis of these field relations, the older intrusives are tentatively interpreted to represent subvolcanic stocks related to Keppoch volcanism. Further evaluation of this interpretation awaits geochemical and geochronological data. Radiometric data available at present yield an age of 533 ± 19 Ma for the Ohio stock (Cormier, 1979). Similar age determinations have been obtained from the James River and Williams Point granites (Rb-Sr whole-rock isochrons, R.F. Cormier, personal communication 1983) and apparently represent a comagmatic suite.

Younger "two-mica" granites intrude all rocks in the map area including the lower Silurian Beechill Cove Formation (Fig. 78.2). They occur at Barney's River, Gunn Lake and Indian Lake. They consist of equigranular coarse grained, anhedral, interlocking crystals of quartz, microcline, plagioclase, biotite and muscovite. They are generally unaltered. The Barney's River Pluton shows evidence of widespread assimilation and magmatic stoping of country rock (mafic volcanic rocks of the Keppoch Formation). The Barney's River and Gunn Lake plutons have been dated at 378 ± 12 Ma and 370 ± 15 Ma respectively (Cormier, 1979).

HISTORY OF DEFORMATION

For the purposes of this discussion, the Precambrian structure of the Highlands may be divided into three regions:

Region 1. north of the Browns Mountain Fault (BMF)

Region 2. between the Browns Mountain Fault and the contact with the Keppoch Formation

Region 3. the Keppoch Formation

Structural styles and deformational history vary considerably from north to south of the mapped area. In general, there are two main factors involved: firstly, the decreasing intensity of F_1 deformation in region 2 relative to region 1 and secondly, the volcanic rocks of the Keppoch Formation display a different structural style relative to the sediments of the Georgeville Group. Although orientations of fold structures appear to have been affected by major faults in the region, fold styles appear to be relatively consistent within each region.

Region 1: North of Browns Mountain Fault the outcrop pattern is dominated by a northeasterly trending F_1 anticlinal fold. The Maple Ridge Formation, in the core of the fold, is flanked by the James River Formation to the northwest and southeast. The structure is the continuation of the F_1 fold mapped to the east (compare Murphy et al., 1982, Fig. 78.1). The fold style is isoclinal as evidenced by comparison with minor F_1 folds, and by S_0 (bedding)/S_1(penetrative cleavage) parallelism on limbs. The locus of the hinge surface trace is defined by localities of high S_0/S_1 angular relations (e.g. east of Vamey River, Fig. 78.2). Cleavage in the hinge zone is typically more strongly developed, generally making bedding less visible than on the limbs. The orientation of the axial plane adjacent to the Hollow Fault is steep to vertical and the fold axis plunges gently to the northeast. This orientation may have been affected by movement along the adjacent northeasterly trending fault. To the west, as the axial trace moves away from the Hollow Fault, the fold axis steepens though it is still northeasterly trending (observe S_0/S_1 relations, Fig. 78.2). The F_1 structure is truncated to the south by the Vamey Fault, and extrapolation is obscured by unconformably overlying Silurian strata. However, a major anticlinal structure is interpreted in the Bears Brook area, where opposing facing directions on a regional scale occur in monoclinal successions.

F_2 northeast- to north-trending upright folds are common in the northeastern Highlands (Murphy et al., in preparation), but regional F_2 hinge zones have not been identified with certainty in Region 1, although one F_2 fold hinge has been tentatively interpreted there (Fig. 78.2). Where they occur in the eastern Highlands, their axial traces generally parallel those of F_1, but they may be distinguished from them in that they fold both S_0 (bedding) and S_1 (penetrative cleavage). The lack of F_2 fold closures may reflect an east to west structural inhomogeneity in the northern Highlands, or more probably, that the present study area is located on one limb of a major F_2 fold.

F_3 folds in the northeastern Highlands are considered to be responsible for the overall change in orientation of F_1 and F_2 folds from northeast trending in the extreme north of the area to north trending farther south. Regional F_3 folds in Region 1 are common (Fig. 78.2) though minor congruous

folds are rare. Folds are generally upright, moderately westerly plunging with broad hinge zones. A weak axial planar fracture cleavage is generally developed. Rarely, S_0/S_3 intersections may also plunge easterly; the change in the sense of plunge may reflect F_3 superposition on opposing limbs of F_2 folds, and may help define F_2 structures.

Region 2: In contrast to generally north structural trends to the north of the Browns Mountain Fault, the area south of the fault is dominated by an east striking monoclinal succession generally dipping and facing to the north. Minor modifications are due to upright folds and/or local faults. Although S_0/S_1 parallelism does occur in this zone it is by no means the rule as in Region 1, and S_0/S_1 intersections commonly occur away from obvious F_1 hinge zones. This relation suggests that the intensity of F_1 folds dies out southwards towards the contact with the Keppoch Formation.

The effects of F_2 and F_3 appear to be minor in Region 2. Fracture cleavages associated with these folds are rare, and the sequence is consistently north facing.

Region 3: Deformation in the Keppoch Formation is difficult to evaluate owing to probable primary distribution of rock units, lack of way-up criteria and penetrative foliation, faults, etc. There is evidence from the map pattern that the competent Keppoch Formation may have controlled structural trends in younger rocks. Trends in the Keppoch Formation are generally east on the north and south of the area and north in the eastern parts of the area (Fig. 78.2). Strikes in younger strata (Precambrian to Carboniferous) generally parallel these trends. This observation generally holds whether the contacts are unconformable or faulted, suggesting that primary distributions of the relatively competent Keppoch volcanic rocks had a significant effect on determining structures. These effects are generally bounded by major faults, whose location is presumably influenced by competence contrast between Keppoch volcanic rocks and adjacent sediments.

The Keppoch Formation is moderately deformed, rarely displays a tectonic fabric and may have behaved in a brittle manner and/or rigid mass during deformation of the Georgeville Group and during subsequent deformations. The map shows that members of the Keppoch Formation can be mapped, but whether their outcrop distribution is governed by primary or deformation considerations awaits further and more detailed analysis.

FAULTING

The Antigonish Highlands are bounded by major transcurrent faults (Fig. 78.1). The northwestern margin is defined by the northeast trending Hollow Fault, and the eastern margin by the Lochaber Lake Fault. The Hollow and Chedabucto faults are considered to be of major regional tectonic significance and have a long history of repeated movements from Precambrian to post-Carboniferous (e.g. Keppie, 1983). The Highlands are caught "in a vice" between these major lineaments and are consequently disected by many northeast trending faults mainly in the northern Highlands and east trending faults in the southern. Most of these faults have limited displacements, and serve only to complicate mapping and stratigraphic interpretation. However, the following points are of interest:

a. Faults apparently control the distribution of post-Precambrian strata. Upper Ordovician and Silurian rocks are generally exposed in fault-controlled river valleys (e.g. the Marshy Hope Fault – Hartshorn River, on the Trans-Canada Highway). At present it is not possible to determine whether these rocks were deposited in active fault troughs or whether the spatial association is due to post-Silurian downthrow and preservation.

b. Many of the faults that displace the Keppoch Formation can be traced into Devono-Carboniferous rocks to the east (cf. Boehner and Giles, 1982) defining a minimum age for latest displacement.

SUMMARY AND DISCUSSION

Mapping in the Antigonish Highlands has resulted in more detailed information on the geological history of the region. The Precambrian rocks may now be divided into at least two successions that are distinct in lithology, stratigraphy, depositional environment, structural history and probably tectonic setting. The Georgeville Group is dominated by intermittent oceanic-type volcanism and a thick basinal-fill sequence of shales and turbidites. The Keppoch Formation to the south, in contrast, consists of a volcanic sequence of interlayered rhyolites, andesites, and basalts and minor interflow sediments. The Keppoch Formation pre-dates the James River Formation of the Georgeville Group and is now assigned a Precambrian age. Its temporal relations to older formations of the Georgeville Group are at present unknown and interpretations await further mapping. Geochronological, geochemical and sedimentological data may also furnish insight into the problem. The absolute age of the Keppoch Formation is critical to understanding the tectonic history of the entire Highlands, especially since the Keppoch Formation has now been assigned a Precambrian age. Geochemical data may help to investigate whether minor felsic volcanism in the James River Formation adjacent to the Keppoch Formation is, in fact, a related late-stage (and distal) Keppoch-type magmatism. Comparative geochemistry between Keppoch volcanic rocks and the volcanic rocks of the Georgeville Group may also be intructive especially in view of the fact that the ocean floor basalts of the Chisholm Brook Formation (the oldest formation identified in the Georgeville Group) also displays the geochemical signature of magma mixing (Murphy et al., in preparation). Detailed geochemistry may establish whether the "diluting" agent is a Keppoch component. Conformation or denial would define a significant contribution to the understanding of the Precambrian history of the Highlands.

Although the contact between the James River Formation and Keppoch Formation is exposed, and has been documented above, it is not considered to be the contact between oceanic and continental tectonic domains in the Highlands. It is thought that these James River sediments draped the submerged Keppoch Formation and are themselves probably floored by Keppoch volcanic rocks. The Browns Mountain and/or Marshy Hope faults are thought to be better candidates in this regard, since they define an abrupt change in the style of F_1 folding in the Georgeville Group with the intensity of F_1 folds diminishing rapidly southwards, and they also define a northern limit of felsic plutonism. It is thus likely that rocks south of these faults are presently floored by continental crust, possibly the upper representatives of this crust being an unexposed part of the Keppoch Formation. Such a crust would account for the relatively reduced intensity of deformation of the "draping" sediments of the James River and South Rights formations compared to the F_1 deformation style to the north. A continental basement may have been the source of felsic plutonism. The study may have implications to the geological history of northwestern Cape Breton Island where Precambrian oceanic-type and continental-type rocks are juxtaposed in the vicinity of the Coolavee Fault (Keppie, 1982).

The presence of oceanic- and continental-type domains in the Precambrian sequences may be reflected to a significant degree in the distribution and type of mineral deposits. Mineral occurrences between the Hollow and Browns Mountain faults are rare. However, a felsic volcanic

unit in the vicinity of the Browns Mountain Fault is mineralized and was mined for silver at the turn of the century. Given the limit of current knowledge, the Keppoch Formation appears to have more potential. Pyritic zones related to felsic volcanism may have considerable strike length. The subdivisions of the Keppoch Formation into felsic, intermediate, mafic and sedimentary dominated members, may provide an essential exploration guide in this regard. The study also illustrates that the stratigraphy of the Keppoch is unknown to the west of the mapped area.

ACKNOWLEDGMENTS

I would like to thank J.D. Keppie, Nova Scotia Department of Mines and Energy, for introducing me to the geology of the Antigonish Highlands. I was fortunate to have the excellent field assistance of M.D. Gurney, St. Francis Xavier University. J.D. Keppie, P.S. Giles, Nova Scotia Department of Mines and Energy, and D.G. Benson, Geological Survey of Canada, provided helpful comments in the field. Office facilities during the course of the study were kindly provided by W.S. Shaw, Chairman of the Department of Geology at St. Francis Xavier University, Antigonish. I thank W.H. Poole, J.G. Arnold and B. Manning of the Geological Survey of Canada for organizational support and C.A. Larocque for critically reading the manuscript. Funding for the project was provided by Geological Survey of Canada.

REFERENCES

Benson, D.G.
1974: Geology of the Antigonish Highlands, Nova Scotia; Geological Survey of Canada, Memoir 376, 92 p.

Boehner, R.C. and Giles, P.S.
1982: Geological map of the Antigonish Basin, Nova Scotia, scale 1:50 000; Nova Scotia Department of Mines and Energy, Map 82-2.

Boucot, A.J., Dewey, J.F., Dineley, D.L., Fletcher, R., Fyson, W.K., Griffin, J.G., Hiskox, C.F., McKerrow, W.S., and Zeigler, A.M.
1974: Geology of the Arisaig area, Antigonish County, Nova Scotia; Geological Society of America Special Paper 139, 191 p.

Bourque, P.D.
1981: A metallogenic study of the Antigonish area, Nova Scotia, with special reference to the copper occurrences of the Ohio-Sylvan Glen belt; unpublished M.Sc. thesis, Dalhousie University, 419 p.

Cormier, R.F.
1979: Rubidium-strontium isochron ages of Nova Scotian granitoid plutons; Nova Scotia Dept. of Mines, Report of Activities, Report 79-1, p. 143-147.

Dobek, G.
1983: Petrology and geochemistry of the Williams Point South Side Harbour Pluton; unpublished B.Sc. thesis, St. Francis Xavier University, 36 p.

Donohoe, H.V. and Wallace, P.I.
1980: Trip 19: Structure and stratigraphy of the Cobequid Highlands, Nova Scotia; in Geological Association of Canada-Mineralogical Association of Canada field trip guidebook, Halifax meeting 1980.

Geological Survey of Canada
1982: Experimental colour compilation (high resolution aeromagnetic vertical gradient, parts of 11E/8, 11E/9, 11F/5, 11F/12, Nova Scotia; Geological Survey of Canada, Map C 40 079G.

Keppie, J.D.
1978: Browns Mountain Group, Antigonish Highlands, Nova Scotia – Preliminary Reassessment; Geological Society of America, Northeast Section, Abstracts.

1982: Tectonic map of the Province of Nova Scotia, scale 1:500 000; Nova Scotia Department of Mines and Energy, Map 82-1.

1983: The Appalachian Collage; International Geological Correlation Program, Caledonide Orogen Volume, Uppsala meeting.

Keppie, J.D., Dostal, J., and Zentilli, M.
1978: Petrology of the Early Silurian Dunn Point and McGillivray Brook formations, Arisaig, Nova Scotia; Nova Scotia Department of Mines, Paper 78-5, 20 p.

Landing, E., Nowland, G.S., and Fletcher, T.P.
1980: A microfauna associated with early Cambrian trilobites of the Callavia Zone, northern Antigonish Highlands, Nova Scotia; Canadian Journal of Earth Sciences, v. 17, p. 400-418.

Maehl, R.H.
1961: The older Paleozoic of Pictou County, Nova Scotia; Nova Scotia Department of Mines Memoir 4, 112 p.

Murphy, J.B.
1977: The stratigraphy and geological history of the Fourchu Group, SE Cape Breton, Nova Scotia, unpublished M.Sc. thesis, Acadia University, 187 p.

Murphy, J.B., Keppie, J.D., and Hynes, A.J.
1982: Geological map of the northern Antigonish Highlands; Nova Scotia Department of Mines and Energy, Map 82-3.

– Geology of the northern Antigonish Highlands, Nova Scotia; Nova Scotia Department of Mines and Energy, Memoir. (in preparation)

Rast, N., O'Brien, B.H., and Wardle, R.J.
1976: Relationships between Precambrian and lower Paleozoic rocks of the 'Avalon Platform' in New Brunswick, the northeast Appalachians and the British Isles; Tectonophysics, v. 30, p. 315-338.

Smith, P.K.
1979: Note on the geology and new Silurian fossil occurrences, south and east of Kenzieville, Antigonish Highlands; Nova Scotia Department of Mines, Report of Activities, Report 79-1, p. 89-94.

Wanless, R.K., Stevens, R.D., Lachance, G.R., and Edmonds, C.M.
1967: Age determinations and geological studies; Geological Survey of Canada, Paper 67-2, part A, p. 125-129.

Williams, H. and Hatcher, R.D., Jr.
1982: Suspect terranes and accretionary history of the Appalachian Orogen; Geology, v. 10, p. 497-560.

79. A TECHNIQUE FOR DETERMINING THE ACID NEUTRALIZING CAPACITY OF TILL AND OTHER SURFICIAL SEDIMENTS

Project 680017

P.H. Wyatt
Terrain Sciences Division

Wyatt, P.H., A technique for determining the acid neutralizing capacity of till and other surficial sediments; in Current Research, Part A, Geological Survey of Canada, Paper 84-1A, p. 597-600, 1984.

Abstract

As part of a study of the sensitivity of surficial sediments to acid precipitation, 8 sediment samples taken from a vertical profile through a sandy till and the soil developed on it were tested to determine their acid neutralizing capacity (ANC). The determination was done by subjecting each sample to a batch titration using small aliquots of 0.1 N H_2SO_4 in a controlled ionic strength environment. Titration results can be plotted as graphs of ANC (meq H^+/100 g sample) versus final pH, making possible the easy comparison of ANC for different sediments and allowing the prediction of ANC for a sediment at different levels of acidification. Results of titrations on the 8 profile samples reveal that in this specific case, sediments containing <2-3% $CaCO_3$ equivalent (<1 mm size fraction) cannot be rated for ability to neutralize acidity by their carbonate content alone. For these sediments the contribution to acid neutralization from cation exchange processes and hydrolysis or dissolution of noncarbonate minerals may be greater than that from the dissolution of carbonate minerals (especially at higher levels of acidification). At solution pH below 4.5, the liberation of Al^{3+} into solution converts hydrogen ion acidity to aluminum ion acidity. Dissolved Al concentrations were controlled by the solution pH level and not availability of reactant.

Résumé

Dans le cadre d'une étude de la sensibilité des sédiments de surface aux précipitations acides, on a prélevé huit échantillons de sédiments dans une coupe vertical traversant un till sableux et l'horizon de sol sus-jacent; l'analyse pour effectuée cherchait à déterminer leur capacité de neutralisation des acides (CNA). On y a procédé en soumettant chaque échantillon à un titrage discontinu, en employant de petits volumes de 0,1 N H_2O_4 dans un milieu de force ionique contrôlée. On peut représenter les résultats du titrage sous forme de graphiques de la CNA (meq H^+/100 g d'échantillon) en fonction du pH final, ce qui permet de facilement comparer la CNA de divers sédiments, et de prévoir celle d'un sédiment à divers degrés d'acidification. Les résultats de titrages effectués sur les huit échantillons indiquent que dans ce cas spécifique, on ne peut évaluer la capacité de neutralisation des sédiments contenant <2-3% d'équivalent de $CaCO_3$ (fraction granulométrique <1 mm) en fonction seulement de leur teneur en carbonates. Dans ces sédiments, les processus d'échange des cations et l'hydrolyse ou la dissolution des minéraux non carbonatés peuvent davantage contribuer à neutraliser l'acide que la dissolution des minéraux carbonatés (surtout à des degrés élevés d'acidification). Si le pH de la solution tombe au-dessous de 4,5, la mise en solution d'Al^{3+} remplace l'acidité de l'ion d'hydrogène par celle de l'ion d'aluminium. Les concentrations d'Al dissous étaient contrôlées par le niveau du pH et non la disponibilité du réactif.

INTRODUCTION

Surface and groundwater reactions with unconsolidated (glacial) sediments involve a variety of mineral weathering reactions. The reactions are promoted by acidification of sediments and their pore waters from sources such as acid precipitation or soil forming processes. These reactions are of significant environmental importance because they determine chemical conditions in the lakes, streams, and aquifers of a watershed in glaciated terrain.

For sediments that have very low carbonate contents, H^+ neutralization is effected essentially by a 2-step process (Kramer et al., 1979; Johnson et al., 1981; Jackson and Patterson, 1982). The process begins when the sediment comes into contact with water of pH <4.5. The H^+ acidity will initially be consumed by the rapid dissolution of soil zone hydrous aluminum and iron oxides and by exchange with cations electrostatically bound to mineral surfaces (especially clay particles). This is followed by a second stage involving the dissolution of trace amounts of calcite and the less rapid dissolution of aluminosilicate minerals.

If the pore water is in contact with the sediment long enough to be involved in the second acid neutralization step (not always the case for sediment above the water table), then the pH may rise enough to cause the dissolved Al and Fe to precipitate back out of solution as hydrous oxides. Indeed, for carbonate-rich glacial sediments and their derived soils, the dissolution of carbonate minerals to produce bicarbonate ions becomes the single most effective acid neutralizing reaction:

$$\text{i.e. } CaCO_3 + H^+ \quad Ca^{2+} + HCO_3^-$$

and raises the pH quickly enough that the other neutralization reactions are largely bypassed. This demonstrates that the contribution of each mineral reaction towards the acid neutralizing capacity (ANC) of a sediment can be dependent on the type, abundance, and size fractionation of each reactant, and the initial pH and residence time of the surrounding pore water.

In order to obtain quantitative data regarding the ANC of a sediment, it is necessary to use a suitable acid titration test.

Kramer et al. (1979) documented the ANC of various sediments subjected to continuous acid titrations. This produced a value for the immediate ANC of the sediment over a range of solution pH.

Jackson and Patterson (1982) modified this technique into a batch titration, wherein separate portions of the same sediment are acidified to varying degrees and allowed to

equilibrate for 24 hours. From this it was possible to determine the capacity of a sediment to neutralize varying strengths of acidity over longer equilibration periods.

A modified version of Jackson and Patterson's (1982) batch titration is used for the experiments presented in this report; this technique allows the determination of metal concentrations in the solution surrounding the sediment being tested.

Acid titrations were performed on 8 till samples taken from a vertical profile through a roadcut along the south shore of Lake Kamaniskeg, near Barrys Bay, Ontario. The UTM coordinates of the sample site are Easting 286728, Northing 502940, in grid zone 18. This location was chosen because the till has a suitable carbonate content and interesting geochemical features. More information regarding the geochemistry of this till is available by checking sample site 80 AR0538 in Kettles and Shilts (1983).

These experiments are presented in order to show one method for determining the ANC of a sediment, and to compare the acid neutralizing properties among sediments of varying carbonate content.

Experimental method

The sediment sample is air dried and sieved to obtain the <1 mm size fraction, i.e., coarse sand size and smaller. This size fraction is used so that several compositionally similar portions of one sample may be obtained. One portion of the sample, approximately 3 g, is accurately weighed into each of four polypropylene 50 mL screw cap centrifuge tubes; 30 mL of 0.01 M NaCl of known pH is then introduced into each tube providing an initial reference condition of ionic strength. Variable amounts of H^+ are added to each centrifuge tube as small aliquots (O µL, 100 µL, 500 µL, 1500 µL) of standarized 0.1N H_2SO_4. The addition of a small volume of acid avoids significantly changing the 1:10 solid solution ratio and ionic strength. The centrifuge tubes are sealed and agitated gently on a shaker for 24 hours to avoid mechanical abrasion of grains and to allow equilibration between the sediment and the hydrogen ions. After 24 hours the tubes are placed in a centrifuge and spun for 15 minutes at about 2000 rpm. The pH of the supernatant is then measured directly in the centrifuge tube using a gel-filled semi-micro combination pH electrode. Centrifuging removes the bulk of suspended clay size particles that may cause electrostatic interference at the pH electrode membrane. The supernatant is decanted into a 50 cm^3 syringe to which is attached a 0.45 µm millipore HA filter. It can then be filtered into a dry clean vessel, acidified with a single drop of concentrated H_2SO_4 and tested by atomic absorption spectrometery to determine the concentration of metals liberated into solution during H^+ neutralization-exchange reactions. This important step makes it possible to calculate the ionic strength more accurately and make corrected pH readings which represent hydrogen ion concentration, not activity.

Table 79.1. Physical and chemical properties for the profile samples

Sample	Depth from surface (cm)	Organic carbon content (%)	$CaCO_3$ equivalent content (%)
SED-1	18	0.88	3.75
SED-2	32	0.72	3.67
SED-3	65	0.34	2.25
SED-4	110	0.22	1.58
SED-5	161	0.24	1.33
SED-6	212	0.14	0.42
SED-7	283	0.13	0.75
SED-8	357	0.12	0.33

Method of calculation

In this experiment, the batch titration of one sediment sample involves 4 separate tubes of sediment solution mixture. For the mixture in each tube we know the initial pH of 0.01 M NaCl ($H^+_{initial}$), the amount of H^+ added as 0.1 N H_2SO_4 (H^+_{added}) and the final solution pH (H^+_{final}). Thus the acid neutralizing capacity (ANC) of each tube mixture is determined as:

$$ANC = H^+_{initial} + H^+_{added} - H^+_{final}$$

where ANC is expressed in units of meq/100 g. Each ANC value represents the amount of H^+ added that the sediment has neutralized, and corresponds to a final pH which itself is a function of the amount of H^+ added that the sediment did not neutralize. The data from a batch titration can be represented graphically by plotting ANC vs pH_{final} for each of the 4 tubes. Thus, over the pH range covered by the titration, one can estimate how many meq H^+ the sediment will neutralize before its solution pH falls to a given value. Calculations for this study were done with the aid of a fortran computer program.

Sediment description

A vertical profile of 8 samples, SED-1 to SED-8, was taken through an exposure of sandy grey till and its overlying soil layer. The exposure is in a 7 m-high roadside borrow pit cut into a moderately sloping hill (10° - 15°) forested with deciduous trees. The upper 11 cm of the exposure is forest litter and decomposing humic material. A layer of fine roots lies between 11 and 15 cm. The depth from surface, equivalent $CaCO_3$ content, and organic carbon content for SED-1 to SED-8 are given in Table 79.1. SED-1 and SED-2 were from the top of the dark brown, oxidized, humus-rich B horizon developed on till. SED-3 and SED-4, also from the B horizon, are sandy, noncompact, and light orange-brown or yellow-brown. SED-5, -6, -7, and -8 were taken in moderately compact, light grey-brown, silty till. SED-5 was taken immediately below the B horizon which is marked at the base by an undulating grey band of precipitated calcareous material. This may account for the higher carbonate content of SED-5 compared to SED-6, -7, and -8.

The trend of decreasing carbonate content with increasing depth is unusual for a temperate humid climate but may reflect a primary compositional feature of the glacial sediment, or more likely, a precipitation (of $CaCO_3$) effect caused by the downslope drainage of near-surface groundwater which evaporates at the vertical exposure surface.

RESULTS AND DISCUSSIONS

ANC graphs

When a sediment-solution mixture is acidified, those hydrogen ions that are not neutralized by reaction with mineral surfaces will then effectively lower the solution pH. Therefore, any point on a curve of an ANC graph (Fig. 79.1, 79.2) represents the amount of H^+ neutralized after acidification of the sediment-solution mixture as a function of the pH level to which the solution falls.

Thus it is evident from the ANC curve for SED-1, that this sample has the greatest capacity to neutralize acidity with the concurrent smallest drop in solution pH. As expected, the ANC curves for SED -2, -3, and -4 each show a

reduced capacity to neutralize acidity corresponding to their lesser $CaCO_3$ contents. The ANC curves for SED-1, -2 are undoubtedly modified somewhat by the exchange properties of humic and fulvic acids (Schnitzer and Khan, 1978). The titration curves for SED-5, -6, -7, and -8 initially show a lower acid neutralization capacity than their counterparts of higher carbonate content. Note that the shape of curves SED-6, -7, -8 (Fig. 79.2) closely match the shape of curve SED-5 (Fig. 79.1). These curves change slope, rising abruptly between pH 4.7 and 4.3, indicating that below this pH level SED-5, -6, -7, and -8 can neutralize more acidity than either SED-3 or -4 (even though SED-3, -4 have higher carbonate contents). This may be due to more effective exchange surfaces being present on minerals in samples SED-5, -6, -7, -8 than those in SED-3, -4 and is an example of how, at lower carbonate levels, dissolution of $CaCO_3$ is no longer necessarily the dominant acid neutralizing reaction.

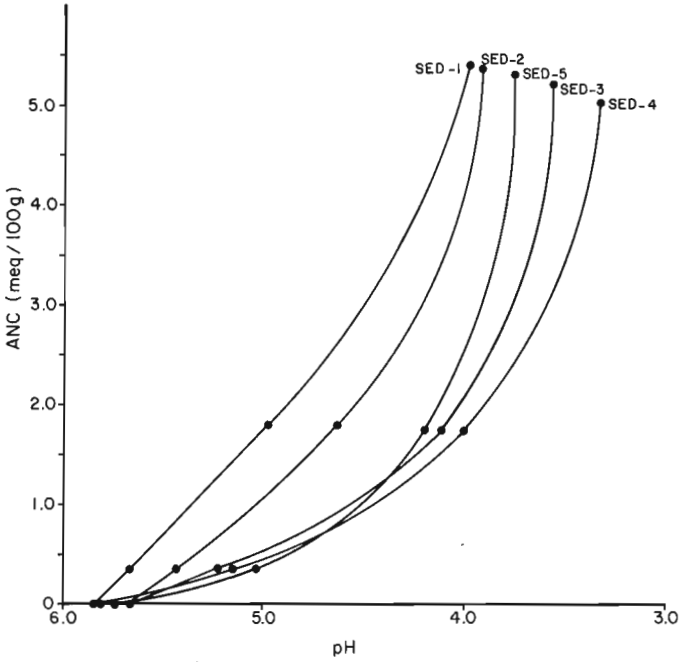

Figure 79.1. H^+ *adsorption (neutralization) isotherm for samples SED-1, SED-2, SED-3, SED-4, and SED-5. The ordinate is the acid neutralization capacity, ANC.*

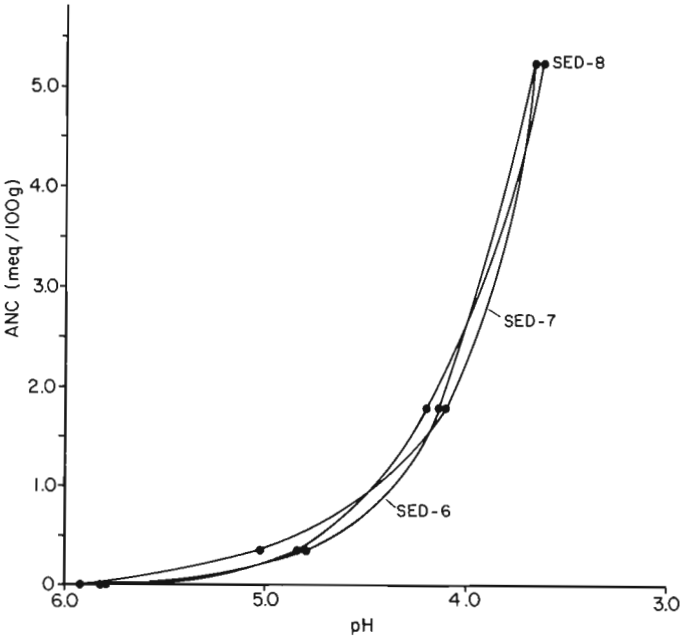

Figure 79.2. H^+ *adsorption (neutralization) isotherm for samples SED-6, SED-7, and SED-8. The ordinate is the acid neutralization capacity, ANC.*

Acidification and cation release

Figures 79.3, 4, 5, and 6 are plots displaying the concentration of Ca^{2+} and Al^{3+} released into solution by a SED sample after 24 hours equilibration at 4 different levels of acidification. No effort is made to determine the speciation of aluminum in solution. The curves representing Ca^{2+} release in Figures 79.3 and 79.4 show that dissolution of

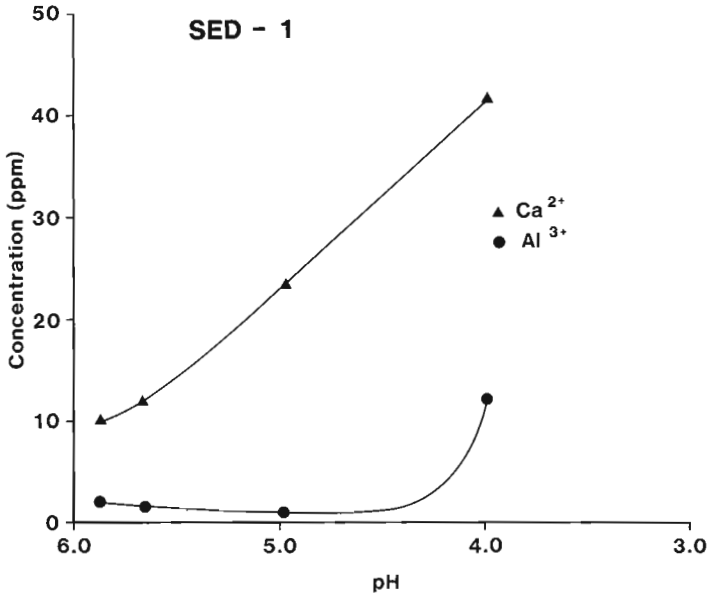

Figure 79.3. *Liberation of* Ca^{2+} *and* Al^{3+} *into solution during acidification of sample SED-1.*

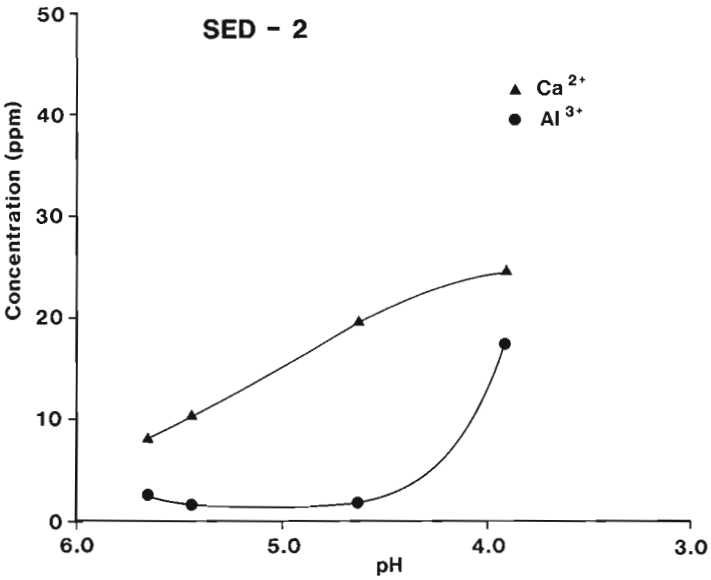

Figure 79.4. *Liberation of* Ca^{2+} *and* Al^{3+} *into solution during acidification of sample SED-2.*

$CaCO_3$ is a major contributor to acid neutralization for SED-1 and SED-2. Comparing these to the same curves in Figures 79.5 and 79.6, it is easy to follow the pattern of decreased Ca^{2+} release for samples of progressively lower carbonate content.

Each SED sample from Figures 79.3-6 underwent the same acid batch titration (0, 100, 500, 1500 µL 0.1 N H_2SO_4 addition). Comparing the 100 µL addition for each SED sample (the second point on each curve), the result is a successively lower equilibrium pH for each sample of lower carbonate content. Thus the low carbonate samples require less acid to drive the solution pH below 4.5 where, under the ionic strength conditions of this experiment, dissolution of hydrous aluminum oxides (amorphous gibbsite) begins:

$$Al(OH)_3 + 3H^+ \; Al^{3+} + 3H_2O$$

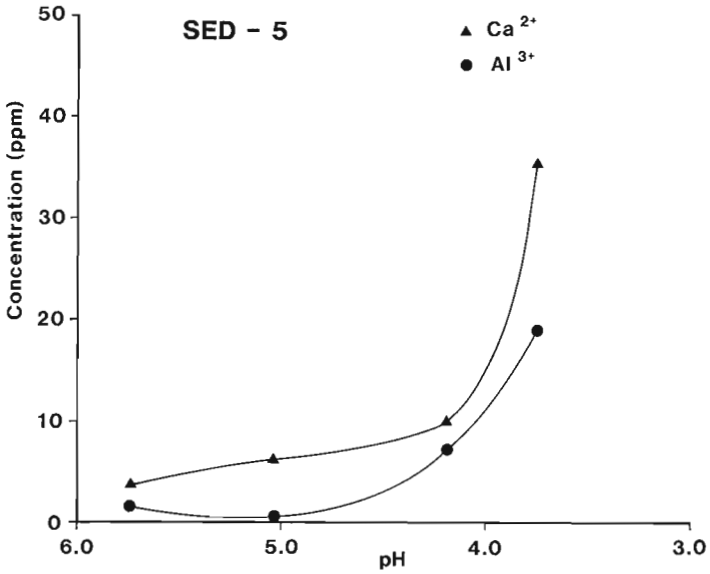

Figure 79.5. Liberation of Ca^{2+} and Al^{3+} into solution during acidification of sample SED-5.

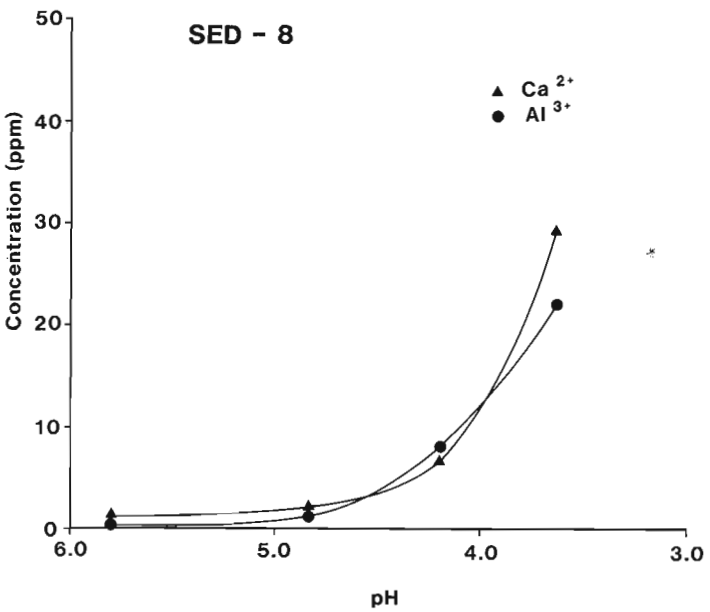

Figure 79.6. Liberation of Ca^{2+} and Al^{3+} into solution during acidification of sample SED-8.

This converts hydrogen ion acidity to aluminum ion acidity. As an example, note that the solution surrounding SED-1, acidified with 1500 µL of acid (corresponding to the fourth point on the curve), dropped to a pH of 4.0 and had an Al^{3+} concentration of 12 ppm (Fig. 79.3). At the same degree of acidification, the solution surrounding SED-8 (lower carbonate content) dropped in pH to 3.6 and had an aluminum concentration of 22 ppm (Fig. 79.6).

The low solubility of $Al(OH)_3$ prevents it from being significantly in solution at pH >4.5 (Johnson et al., 1981). For the titrations presented here it is likely that dissolved aluminum concentrations are much higher immediately after acid addition, before neutralization proceeds sufficiently to buffer pH above 4.5 and reprecipitate the aluminum. Thus it is evident that equilibration time is an important factor in determining the solution chemistry.

Consideration for future work

All parameters of the batch titration – acid strength, soil:solution ratio, equilibration time – can be changed to more closely approximate the chemical conditions that a sediment is subjected to in its site-specific natural environment. Combined with detailed atomic absorption analysis of trace elements in solution, and before/after microprobe analysis of mineral surfaces, the ANC test could provide quantitative data regarding the effects of acid precipitation on surficial sediments.

Acknowledgments

I wish to thank R.E. Jackson of the National Hydrology Research Institute for providing laboratory space, equipment, and valuable guidance; and R.N.W. DiLabio for suggesting improvements to this report.

REFERENCES

Jackson, R.E. and Patterson, R.J.
1982: Interpretation of pH and E_H trends in a fluvial-sand aquifer system; Water Resources Research, v. 18, p. 1253-1268.

Johnson, N.M., Driscoll, C.T., Eaton, J.S., Likens, G.E., and McDowell, W.H.
1981: 'Acid rain', dissolved aluminum and chemical weathering at the Hubbard Brook Experimental Forest, New Hampshire; Geochimica et Cosmochimica Acta, v. 45, p. 1421-1437.

Kettles, I.M. and Shilts, W.W.
1983: Reconnaissance geochemical data for till and other surficial sediments, Frontenac Arch and surrounding areas, Ontario; Geological Survey of Canada, Open File 947.

Kramer, J.R., Booty, W.G., and Stroes, S.
1979: Acid neutralizing capacity of fine soil fractions; in Atmospheric Pollutants in Natural Waters, ed. S.J. Eisenriech; Ann Arbour Science, Ann Arbour, Michigan.

Schnitzer, M. and Khan, S.U.
1978: Soil Organic Matter; Elsevier Scientific Publishing Company, New York, p. 19.

80. SOME OBSERVATIONS ON THE MORPHOLOGY AND ORE TEXTURES OF VOLCANOGENIC SULPHIDE DEPOSITS OF CYPRUS

Project 770063

John W. Lydon
Economic Geology Division

Lydon, J.W., Some observations on the morphology and ore textures of volcanogenic sulphide deposits of Cyprus; in Current Research, Part A, Geological Survey of Canada, Paper 84-1A, p. 601-610, 1984.

Abstract

Field and preliminary laboratory studies reveal features of the volcanogenic sulphide deposits of Cyprus that have not been emphasized in the literature. By analogy, these features offer different perspectives of some features observed in Canadian volcanogenic massive sulphide deposits and processes associated with modern submarine hydrothermal systems and metalliferous deposits. Cyprus-type deposits are not confined to topographic depressions on the seafloor but can also form on the steep slopes of fault scarps. Topographic depressions are therefore not considered a prerequisite for the accumulation of large amounts of sulphides on the modern ocean floor. Ore deposition at the Mathiati deposit was by the accumulation of particulate sulphides and by the infilling of fractures and dissolution cavities in previously deposited sulphides. Some textures of Canadian volcanogenic massive sulphide ores are the metamorphically annealed equivalents of open space filling of a porous and fractured massive sulphide mound. This has significance to the interpretational methods of analytical data which are based on the assumption that coexisting mineral species were coevally precipitated.

Résumé

Des études in situ et études préliminaires en laboratoire ont révélé certains traits des gîtes sulfurés de type volcanogène trouvés à Chypre, sur lesquels n'insiste pas la documentation scientifique. Par analogie, on a observé divers détails, qui pourraient s'appliquer aux gîtes canadiens volcanogènes de sulfures massifs, et aux processus liés aux systèmes hydrothermaux et gîtes métallifères sous-marins actuels. Les gîtes du type de Chypre ne se limitent pas aux dépressions topographiques du fond marin, mais peuvent aussi se former sur les pentes raides d'escarpements de faille. Par conséquent, l'existence de dépressions topographiques n'est pas considéré la condition préalable à l'accumulation de vastes quantités de sulfures sur les fonds océaniques actuels. Dans le gîte de Mathiati, la mise en place du minérai à résulté de l'accumulation de particules sulfurées et du remplissage des fractures et cavités de dissolution apparues dans des sulfures déposés antérieurement. Au Canada, dans certains minerais sulfurés massifs de type volcanogène, la texture correspond à la recristallisation métamorphique des produits de remplissage à l'intérieur d'un amas poreux et fracturé de sulfures massifs. Ces observations présentent un certain intérêt en ce qui a trait à l'interprétation des données analytiques basée sur l'hypothèse selon laquelle les espèces minérales coexistantes ont été précipitées à la même époque.

BACKGROUND

The International Crustal Research Drilling Group, under the leadership of Drs. Paul Robinson and James Hall of Dalhousie University, is currently carrying out an investigation of the Troodos ophiolite complex. The aim of this ICRDG Cyprus Project is, through a combination of deep drilling and surface studies, to provide a three dimensional view of crust formed in suboceanic conditions and to investigate the various geological processes involved. Allied to the scientific program is a training program, designed to allow earth scientists and technicians from developing countries to participate in the scientific and technical aspects of the program under the guidance of experts in the various fields.

The Canadian government, through NSERC and IDRC, has financially supported the Cyprus Project. Other contributing countries include Cyprus, Denmark, the Federal Republic of Germany and the United Kingdom. The Geological Survey of Canada was invited by ICRDG to participate in both the scientific and training segments of the Cyprus Project, and as a result Drs. W.R.A. Baragar, M.B. Lambert, G.R. Bernius and the author visited Cyprus during periods of 1982 and 1983.

Amongst the scientific research projects initiated by Geological Survey of Canada personnel are studies on genetic processes of volcanogenic sulphide deposits. This mineral deposits research is being carried out by the author and Dr. H.E. Jamieson, Queen's University, who visited Cyprus as an ICRDG participant in 1982 and is currently a Visiting Fellow at the GSC, in collaboration with others at Canadian universities and foreign institutions.

INTRODUCTION

The Cyprus deposits are important to students of volcanogenic massive sulphide deposits for several reasons:

1. They are often cited as the classic examples of a distinct type of volcanogenic sulphide deposit, whether the deposits are classified in terms of their tectonic environment as spreading centre- or ophiolite-associated types (Sillitoe, 1973); their mineralogical or chemical characteristics as cupreous pyrite type (Hutchinson, 1973); or petrochemistry/lithology of their immediate host rocks as the mafic volcanic associated type (Solomon, 1976).
2. Observations on the deposits of Cyprus, along with comparable observations on the Kuroko deposits of Japan, provided most of the geological substantiation for, and consequently the widespread acceptance of, the current submarine exhalative theory for the genesis of volcanogenic massive sulphide deposits (Constantinou and Govett, 1972; Clark, 1971; Hutchinson and Searle, 1971; Johnson, 1972).

3. Observations on the hydrothermal alteration of the volcanic rocks of Cyprus provided much of the empirical data to support the currently popular convection cell model for the hydrothermal systems responsible for the formation of volcanogenic massive sulphide deposits (Spooner, 1977; Spooner et al., 1977; Heaton and Sheppard, 1977).

Obviously, a first-hand experience with these classic deposits allows a deeper appreciation of their scientific context, but apart from this scientific curiosity value, the study of the volcanogenic sulphide deposits of Cyprus has two main practical advantages in continuing the development of a genetic model for the deposit type. First, the deposits of Cyprus are relatively young and pristine. Thus, studies are possible on both primary hydrothermal mineralogy, mineral parageneses, textures etc. of the deposits themselves, and also primary geochemical and mineralogical signatures imparted to the stratigraphic substrate by the action of the ore-forming hydrothermal systems. Studies of comparative detail are not possible on Canadian examples of volcanogenic massive sulphide deposits because thermal metamorphism, through the recrystallization and chemical re-equilibration of primary hydrothermal minerals combined with the effects of penetrative deformation, has obliterated microscopic textural features. On a larger scale, the cumulative effects of other crustal processes over as much as 2 billion years has shrouded geochemical signatures of the ore-forming hydrothermal system in the stratigraphic substrate of these older deposits by the superimposition of younger and unrelated geochemical changes. Information on pristine hydrothermal effects is needed to unequivocally identify the processes involved and to quantitatively document the cumulative effects of these processes on the mineral deposits and rocks involved.

The second practical advantage to studying the sulphide deposits of Cyprus stems from the fact that the study of ore deposits alone cannot provide unequivocal interpretations of the dynamic aspects of ore formation. This information is required for the formulation of a truly quantitative genetic model for volcanogenic sulphide ore deposits, and can only be acquired by measurements on active submarine ore-forming systems. An international effort, including Canadian participation, to study submarine hydrothermal systems and metalliferous deposits of the spreading ridges of the eastern Pacific has already begun. However, such research programs are extremely expensive, both in terms of the logistical support required for field operations and in terms of the development of the new technology necessary to make the appropriate observations and sample collections in such a hostile environment. Cyprus is one of the few places in the world where inexpensive land observations can be made of oceanic crust and its mineral deposits that are sufficiently young and pristine to allow direct comparisons to be made with the modern oceanic crust. Studies of the rocks and mineral deposits of the Troodos ophiolite complex therefore have the potential to isolate those specific scientific problems that can only be studied in the modern oceanic crust, and thus, by providing guidance for specific scientific targets, increase the scientific and cost efficiency of submarine investigations.

The objectives of Geological Survey of Canada studies on the volcanogenic sulphide deposits of Cyprus are thus to provide information that will benefit genetic and exploration models for Canadian volcanogenic massive sulphide deposits and to identify criteria that will help guide Canadian scientific investigation of modern submarine hydrothermal systems and metalliferous deposits. The purpose of this and the two accompanying articles is to illustrate the scope of the studies being undertaken at the Geological Survey of Canada, and to present some preliminary results.

SCOPE OF FIELD WORK

Most of the field work on which the current literature on the volcanogenic sulphide deposits of Cyprus is based, was carried out during the 1960s (Searle, 1972) and postdates the peak of mining from these deposits (Bear, 1963). Geological records are very scant, and thus for most of the deposits there is no source for information which current concepts of ore genesis require.

At the present time, access to sulphide mineralization in Cyprus is restricted. Only the (North) Mathiati deposit is being mined to provide a pyrite feed to a fertilizer manufacturing plant. The Mathiati deposit is the only locality at which it is possible to examine and sample fresh exposures of massive sulphide, ochre, and both the central and peripheral parts of the underlying stockwork zone. For this reason, a large proportion of field work was devoted to sampling and mapping in the Mathiati open pit. Access to fresh rocks in other open pits (Fig. 80.1) is limited due to the rapid oxidation of the pyrite since the cessation of active mining and the consequent deep and pervasive acid leaching of surface rock, the flooding of at least the lower benches, and by the landsliding of the pit walls. Limited sampling programs of other pits were concentrated at the Skouriotissa and Limni deposits. All underground mines were inaccessible.

There was no drill core from past exploration or production activities available. Although coring has been used in Cyprus (e.g. Bear, 1963, p. 30), the preferred method for exploration has been churn or percussion drilling. The Hellenic Mining Company Ltd. kindly donated samples of drill chips that will allow whole rock chemical and mineralogical studies of selected deposits, including Agrokipia "B", New Sha, and Limni. In this respect the drill core recovered by the ICRDG Cyprus Project is invaluable, because it provides bulk samples that have not been affected by modern surface processes. To date, drill core has been recovered from the upper part of the Pillow Lava succession (CY-1, 475 m); from near the Agrokipia A deposit (CY-2, 226 m), the Agrokipia B deposit (CY-2A, 690 m); and through the basal part of the Sheeted Dyke Complex into the plutonic rocks below (CY-4, 1850 m) (Fig. 80.1). The drilling program is not yet completed. In addition, river canyons through the volcanic rocks and fresh road cuts provided opportunities for the examination and sampling of relatively fresh material.

The only aspect of the field work which provided a contrast to conditions commonly encountered in Canada was that, because of the pristine nature of the rocks, caution had to be exercised, especially around old mines, to be alert to genuine ocean floor phenomena as opposed to similar effects produced by past mining operations or supergene processes.

MORPHOLOGY OF THE VOLCANOGENIC MASSIVE SULPHIDE DEPOSITS OF CYPRUS

The typical original morphology of the volcanogenic massive sulphide deposits of Cyprus has been described as saucer-shaped and due to the accumulation of the sulphides in caldera-like depressions on the seafloor (Constantinou and Govett, 1972). The maximum horizontal dimension of the deposits is usually one or two hundred metres and their vertical thickness is usually a few tens of metres, though the largest bodies such as at Skouriotissa may have been over 1000 m across and 100 m thick (Bear, 1963). It has been pointed out that the modern sulphide deposits of the eastern Pacific are spatially associated with fault controlled topographic depressions and collapsed lava lakes of about the same dimensions (Malahoff et al., 1983; Ballard et al., 1979; Hekinian et al., 1983; Hekinian et al., 1980), and this association has been used as a point of comparison between the modern sulphide deposits and the massive sulphide deposits of Cyprus (Francheteau et al., 1979).

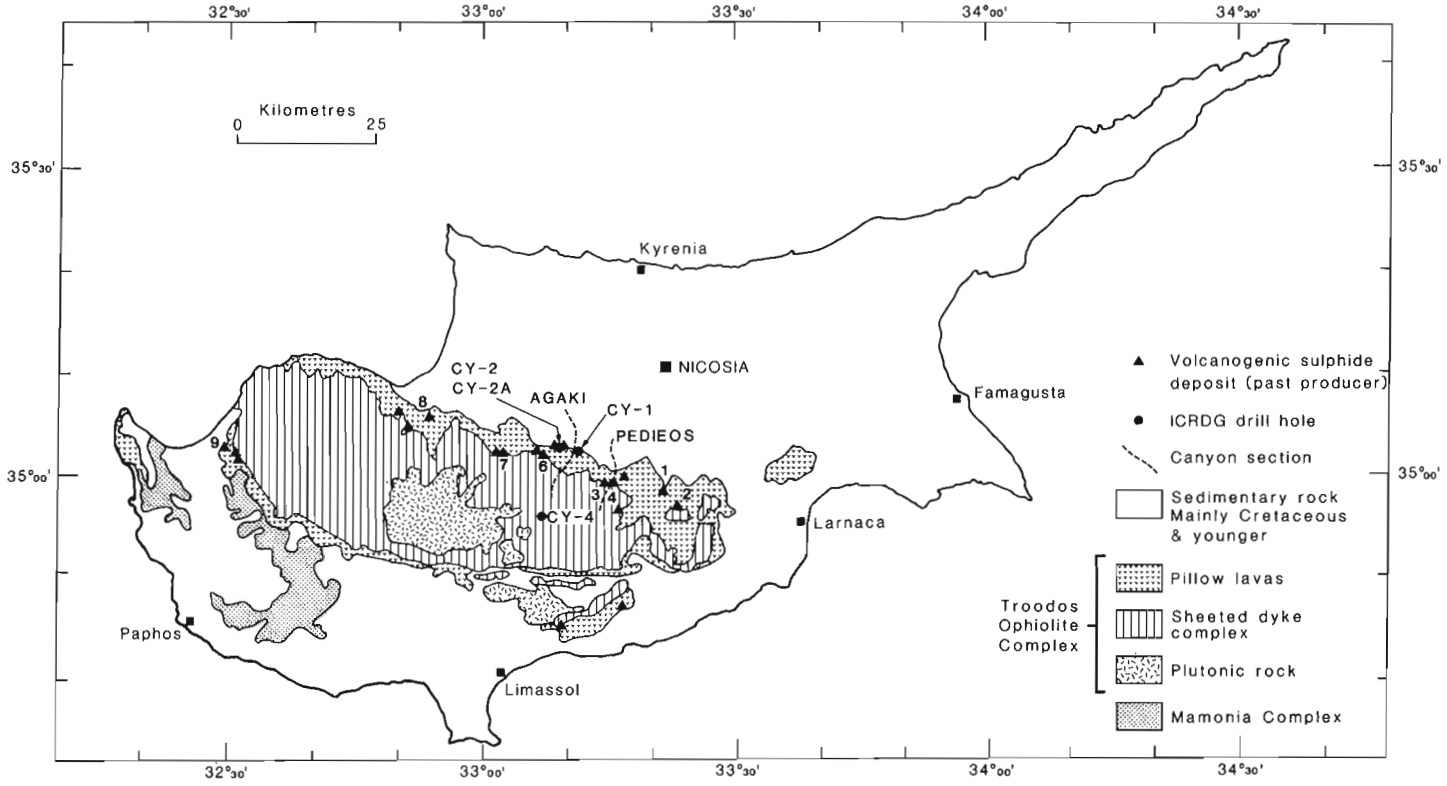

1. *Mathiati,*
2. *Sha,*
3. *Pytharochoma,*
4. *Peristerka,*
5. *Agrokipia A and B,*
6. *Kokkinopezoula,*
7. *Memi,*
8. *Skouriotissa,*
9. *Limni.*

Figure 80.1. *Geological map of Cyprus showing locations of major volcanogenic sulphide deposits, ICRDG drill sites, and canyon sections examined. Numbers refers to sulphide deposits examined.*

However, except for some sulphide occurrences on the Juan de Fuca Ridge (Normark et al., 1982), the sulphide deposits of the eastern Pacific do not actually occur within these depressions but rather on their flanks. The great bulk of metal discharged from the black smoker vents of the East Pacific Rise is dispersed in the overlying water column by the rapidly rising hydrothermal plume (Edmond, 1982). It has been speculated that the local submarine topography may play an important role in the efficiency of the accumulation of sulphides near the hydrothermal vent, and it has been suggested that hydrothermal discharge in a topographic low would be the most favourable for the maximum accumulation of sulphides (Edmond et al., 1979).

Geological mapping at Mathiati suggests that a large component of the present dip of the massive ores (Fig. 80.2, 80.3) reflects the paleoslope, and the deposit itself accumulated on what is interpreted here as a fault scarp. This conclusion indicates that not all volcanogenic massive sulphide deposits of Cyprus accumulated in crater-like depressions, and that the submarine topography is not the primary factor in determining the efficiency of accumulation of the sulphides near the vent site. The submarine topography of the Mathiati deposit would thus be very similar to that of apparently the largest accumulation of sulphides on the modern ocean floor found to date, which Malahoff (1982) describes and illustrates as occurring on a 35 m high fault scarp on the Galapagos Ridge. The conclusion for the steep initial slope to the massive sulphide at Mathiati comes from a comparison of the sediments immediately overlying the massive sulphide on the 268 m level (mapped by the author) at the bottom of the current pit and the 330 m and higher levels (reported by Searle, 1972; Constantinou and Govett, 1972; Hadjistavrinou and Constantinou, 1982) which formed the mining surfaces during the 1960s.

Figure 80.2 shows a plan and section of the Mathiati pit produced at a similar scale and degree of detail as those published by the above mentioned authors. All maps and sections essentially show the same major features in which the mineralization is confined between two northwest-southeast trending major faults forming a structural horst, and the massive sulphide dipping to the north-west at 30-40 degrees. The major difference is that Figure 80.2 shows that on the 268 m level the mineralization is bounded to the northeast by a post-ore dyke. This dyke has chilled and glassy margins on the 268 m level but is difficult to trace up the northwest face of the pit above the 290 m level even though the upward projection of the dyke corresponds to a visible fracture that has no or little vertical displacement across it. It is possible that this dyke is a feeder to the pillow lavas in the hanging wall to the sulphides. The other major difference is in the nature and thickness to the sediments immediately overlying the massive sulphides.

Figure 80.3 shows the details of two sections at the 268 m level that were measured and sampled along the lines indicated on Figure 80.2A. Section I across the floor of the pit shows the configuration of massive sulphide types described as being typical of the Cyprus-type deposits

(Constantinou and Govett, 1972, 1973; Hutchinson and Searle, 1971; Johnson, 1972). Medium to coarsely crystalline "compact ore" (similar to Fig. 80.4A but in this case partly oxidized and impregnated with sulphates) is apparently overlain by fine grained "colloform ore" (Fig. 80.4B) which in turn is overlain by black, unconsolidated, friable "sandy ore". The sandy ore is partly oxidized to ochre. A sample of more consolidated material from near the top of the sandy ore is seen on slabbing with a diamond saw to have a fragmental texture, consisting of unsorted fragments of the colloform type pyrite, stockwork rock types (pyritized, silicified and chloritized volcanics) and jasper (Fig. 80.4D). The western face of the exposure shows a minimum of 30 cm of jasper conglomerate, consisting of subangular to slightly rounded fragments of jasper, usually 3-5 cm, but up to 20 cm in diameter, in a matrix of black sandy pyrite. The immediate hanging wall to the black sandy pyrite and jasper conglomerate had been removed by the mining of waste rock. The bottom part of the western wall to the pit consists of angular to subrounded fragments of vesicular lava ranging in size from less than a centimetre to incomplete pillows over a metre in diameter. This fragmental rock is overlain by pillowed lavas, the contact between the two dipping to the northwest at about 25 degrees. Clearly this fragmental rock occurs in the hanging wall to the sulphides, but because it is probable that a small fault of unknown displacement runs parallel to the western wall between the sulphides exposed in the floor of the pit and the volcanic fragmentals in the western wall, the thickness and nature of any intervening rock types is not known.

Section II (Fig. 80.3) along the eastern wall of the bottom of the pit was obtained by chipping a 50 cm wide channel through a superficial covering of semiconsolidated dust and mud. The stockwork mineralization at the southern end of the section is of the "cobbly" variety which consists of hard, tightly packed cobbles, 5-30 cm in diameter, of normal stockwork mineralization (pyrite, quartz and jasper veins in chloritized and silicified lava) in a soft chloritic matrix, that in turn is cut by pyrite veins. This rock type could be

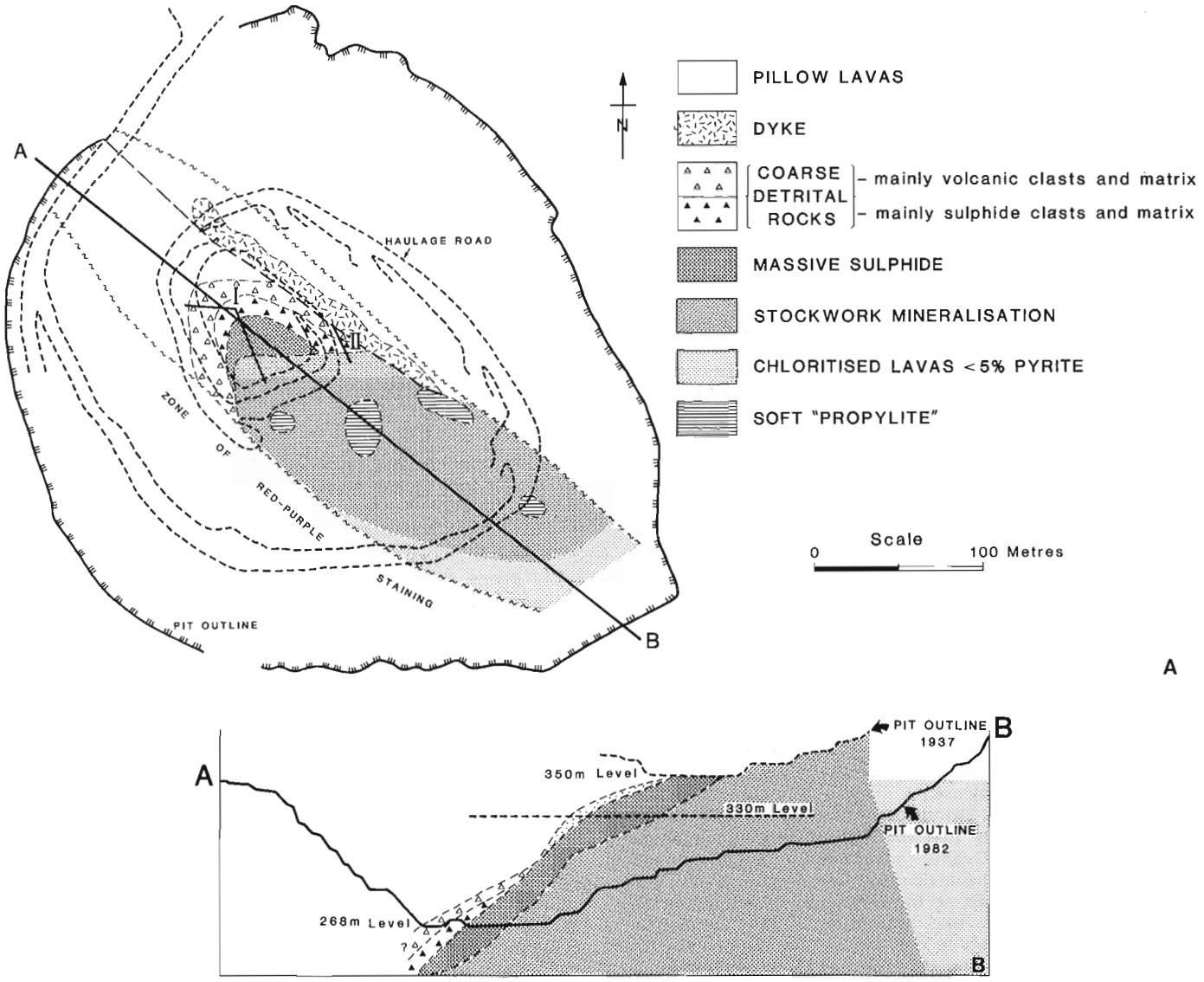

Figure 80.2. *A. Map of the Mathiati open pit showing main geological features. B. Preliminary reconstructed section through the Mathiati deposit along the line A-B shown on Figure 80.2A. Location of massive sulphide at 350 m level from a map first dated 1937 by the Cyprus Mining Corporation (courtesy Hellenic Mining Company Ltd.). Geology at the 330 m from Hadjistavrinou and Constantinou.*

interpreted as a partially "propylitized" (see below) in situ stockwork zone, or a talus breccia derived from stockwork mineralization that has been invaded by later ore solutions (Lydon and Prichard, in preparation). No thick section of compact- or conglomeratic-type massive sulphide, comparable to that seen in Section I is present, though there are zones (veins?) of fine grained massive pyrite up to 30 cm across. The top of the stockwork zone is marked where the matrix changes from soft propylitic material with pyrite veins to black sandy pyrite. Over most of the section in which black sandy pyrite forms the matrix, it contains boulders or fragments (2 cm to 30 cm across) of colloform pyrite and is essentially similar to that rock type occurring immediately above the massive colloform pyrite in Section I. In the central part of Section II, the black sandy pyrite contains angular, decomposed fragment of lava indicating that it is a clastic rock, and thus highly suggestive that the black sandy pyrite with boulders and fragments of colloform pyrite above and below is also of clastic origin. The black sandy pyrite section is succeeded by a fragmental rock in which angular fragments, 3-10 cm across, of lava and pyrite occur in a yellowish argillic matrix, which appears to consist of altered lava particles.

The fragmental rocks of Section II are terminated by the dyke. At the contact the dyke has been chilled to form a glassy margin 2 to 10 cm thick, and, in places, attached and detached, glassy to fine grained, concentrically banded, orbicular aphophyses of the dyke have been injected into the fragmental rock. This indicates that: 1) the fragmental rock is a bona fide seafloor rock and not mining debris; and 2) at the time of the dyke intrusion the fragmental rock was unconsolidated and water-logged. Furthermore, although the dyke is traversed by small northerly trending fractures which form 10 cm to 1 m steps or re-entrants on its surface, because nowhere does it show any major displacement along Section II, the succession from stockwork mineralization to fragmental rocks is a complete and original feature.

Even though Sections I and II are only 30 m apart, the rock types cannot be correlated in detail. This, together with the wide variety of fragments and matrices represented in the fragmental horizon overlying the massive ore, indicates that individual breccia flows were relatively small and derived from local but varied sources. Thus, immediately up the paleoslope from the fragmental rocks there must have been a source of massive sulphide, hydrothermally altered lavas and fresh lavas, which, initially at least, were all synchronously exposed in the source area. The general compositional polarity of the fragmental rocks from mainly sulphides at their base to entirely volcanics at their top indicates that the source area progressively evolved and possibly that the sulphides were entirely buried prior to cessation of the accumulation of fragments. The jasper conglomerate is very interesting, because the only known sources of jasper are veins or inter-pillow fillings of the lavas. The concentration of jasper into a monomict detrital rock implies that the energy level of the source area was sufficiently high to disintegrate the lavas and to winnow the host rock material to leave the mechanically resistant jasper. This may imply that the source area was in part above wave base, which would fit in with the shallow water implications of the large vesicle size of the pillow lavas and the presence of algal filaments in calcareous beds overlying the sulphides at the higher elevations of the mine (Constantinou and Govett, 1972 – see below).

The nature of the rocks immediately overlying the massive ore at the 330 m and higher levels, according to the descriptions and illustrations of Constantinou and Govett (1972, 1973), Searle (1972) and Hadjistavrinou and Constantinou (1982), were completely different from the fragmentals on the 268 m level described above. Searle (1972) described the rocks immediately overlying the ore at the higher elevations as up to 5 m of calcareous and siliceous tuff interbedded with iron rich mudstone containing scattered pyrite, the siliceous and carbonate layer being porous and vuggy, with chalcedonic silica and calcite infilling cavities. Constantinou and Govett (1972) described three types: 1) massive to poorly bedded brown-yellow ochre, which frequently contains blocks of porous pyrite, and thus seems very similar to the ochre seen on the 268 m level (see Fig. 80.3); 2) massive siliceous limestone consisting mainly of calcite, quartz and a goethite infilling of the abundant cavities, containing "abundant algal filaments and mucilage, associated with liquid hydrocarbons" (op. cit. p. B.40); and 3) siliceous calcareous tuff, consisting of "an appreciable quantity of clastic volcanic material cemented with quartz and calcite. Its chief minerals in decreasing order of abundance are quartz, calcite and gypsum" (op. cit. p. B.40). Thus although the sediments immediately overlying the ore at the higher mine elevation contain some fine grained clastic or detrital material, they consist mainly of minerals which in this geological environment would be most reasonably interpreted as being due to chemical precipitation (chalcedonic silica, calcite, siderite, quartz, gypsum) and perhaps in a general sense the equivalent of the "tuffite" or "exhalite" immediately overlying many Canadian massive sulphide deposits.

This contrast in the lithologies of the sedimentary rocks immediately overlying the massive sulphide indicates a contrast in the sedimentary environment between the lower and upper mine elevations. The accumulation of both fragment supported and matrix supported sedimentary breccias of the lower elevations suggest that these rocks were deposited at the foot of a paleoslope down which both grain flows and mudflows took place. The former suggest a slope of at least 18 degrees (Middleton, 1970). The absence of coarse sedimentary breccias at the higher mine elevations suggests that they were also higher, in a paleotopographical sense, than the lower mine elevations, and in the source zone for at least the sulphide fragments (note that sulphide mineralization terminate to the southwest, Fig. 80.2). The direction of the present dip of the Mathiati massive sulphide ores therefore coincides with the direction of dip of the paleoslope. Allowing for the regional tilting of about 15-20 degrees, the average inclination of the paleoslope was 15-20 degrees, with a total drop of at least 50 m. Whether this slope was gradual or stepped is not known for certain, but a possibility exists that it was stepped down along east-west faults which cut the stockwork zone but do not significantly off-set the dyke. As can be seen in Fig. 80.2A, these faults are parallel to, and probably form the contact, between massive and stockwork ores at the 268 m level, and thus probably formed the original ocean floor surface at this site. These faults also probably localized the hydrothermal solutions that formed the "sulphidic mud holes" represented by the massive propylite pipes shown on Fig. 80.2 (Lydon and Prichard, in preparation). It is proposed that these faults were active prior and during sulphide deposition, and formed a stepped fault-scarp on which the sulphides were deposited.

This paleotopographic setting of the Mathiati deposit emphasizes that if Cyprus-type deposits are to be taken as models for the exploration of modern submarine sulphide deposits, topographic depressions are not a prerequisite for the accumulation of large (>3 million tonnes) amounts of sulphide.

ORE TYPES AND ORE TEXTURES

Several types of sulphide mineralization have been recognized in the Cyprus sulphide deposits, which in some cases have direct analogies in Canadian massive sulphide deposits (Hutchinson, 1965). However some contrasting features or significances should also be emphasized.

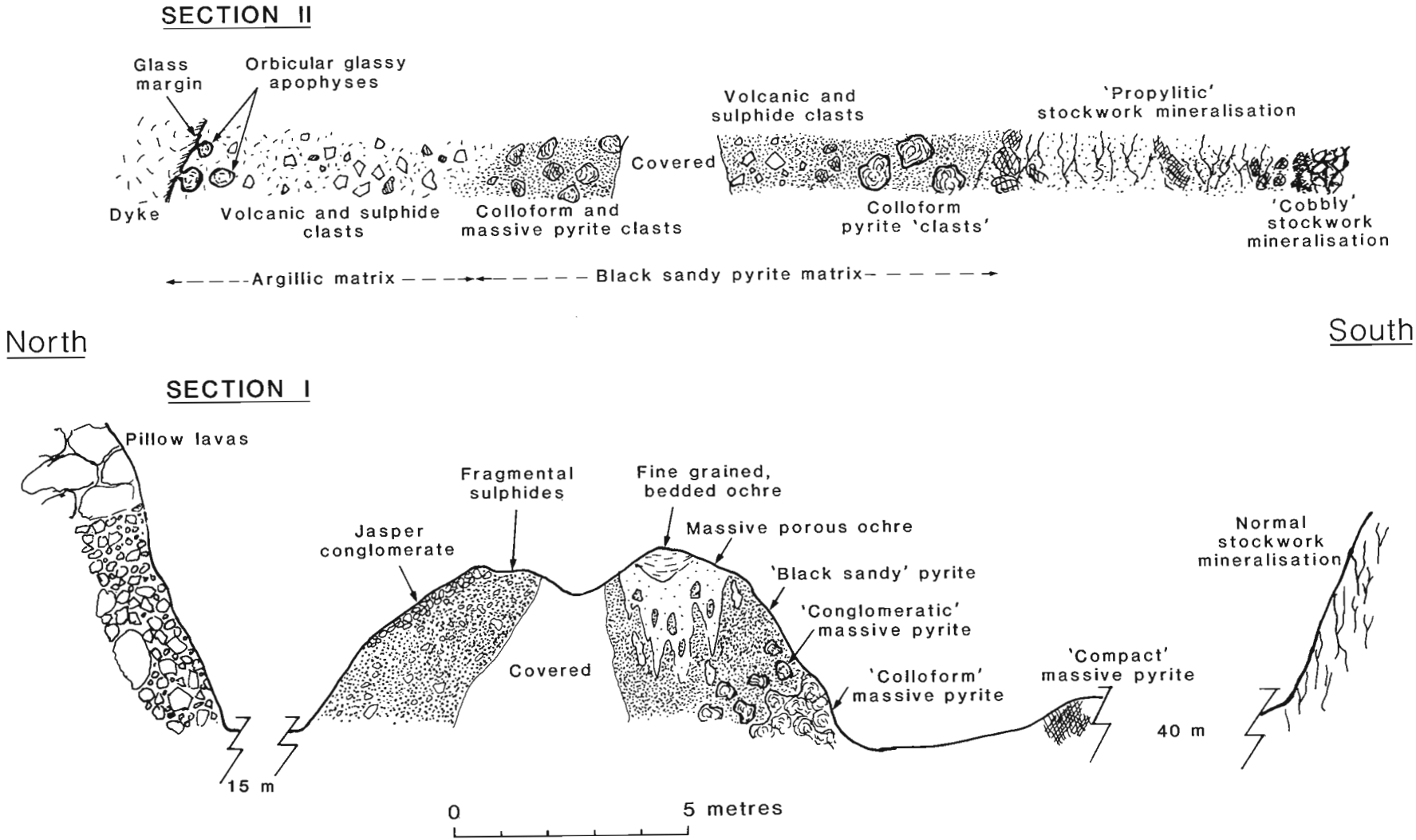

Figure 80.3. *Semi-diagrammatic details of measured sections at the 268 m level of the Mathiati open pit along the lines indicated on Figure 80.2 A.*

The stockwork zone and hydrothermal alteration pipe of the stratigraphic footwall usually show a zonation. Within the outer aureole of the chloritic alteration of the Cyprus deposits, pyrite mainly occurs as vesicle infilling or as disseminations throughout the chloritic groundmass. This alteration type is commonly referred to as "propylite", although in the absence of calcite and epidote in addition to the chlorite, is a scientific misnomer (Bear, 1963) but has become an entrenched mining term for a number of soft, pyritized rock types (Lydon and Prichard, in preparation). Inwards, towards the core of the stockwork zone there is a gradual change in the style of mineralization marked by an increase in the thickness and intensity of pyrite veining. The onset of pyrite and quartz veining is confined to the outlines of pillows and the infilling of their radial and concentric cooling cracks. Closer to the core of the alteration pipe, this veining becomes thicker, due to progressive dissolution and replacement of the host rocks at the vein margins, so that the pillow fragments between veins develop a rounded outline. Accompanying this exaggeration of the primary fracture pattern of the pillows, there is the development of a superimposed network of anastomosing irregular pyrite-quartz veins that are continuous across pillow margins. In this zone a paragenetic sequence of early jasper veins and later sulphide veins with delicate internal growth banding is at its most obvious. In the core of the alteration pipe the shapes of the pillows have largely been obliterated by pervasive chloritization, pyritization and silicification. Examination of polished slabs indicates that a complex history of repeated brecciation and cementation is involved in the process. This mode of the style of stockwork mineralization of the Cyprus deposits contrasts to the style more typical of Canadian Archean deposits, where the gradual increase in intensity and thickness of secondary fracture-controlled polymetallic sulphide veins ultimately gives rise to a breccia of angular altered wall rock fragments cemented by a variety of sulphides, especially pyrite, chalcopyrite and pyrrhotite. This may suggest that explosive hydrothermal discharge was less common in the Cyprus deposits compared to typical Canadian Archean examples, which together with the difference in sulphide mineral ratios, may indicate lower discharge temperatures for the Cyprus deposits.

The amount of vein material in the stockwork ore increases upwards to form a "pyrite-quartz", or "Zone B" (Constantinou and Govett, 1973), or "Zone 2A" (Searle, 1972) ore type. This consists of medium grained pyrite with white silica and jasper, commonly containing large cavities lined with coarse pyrite crystals (Hutchinson and Searle, 1971), and appears to have been formed by open space filling in the substrate (Vokes, 1966). This type of ore, where present, grades upwards into the 'compact ore' of Zone A (Constantinou and Govett, 1972), which consists of massive medium grained pyrite containing irregular cavities of variable distribution intensity and size (Fig. 80.4A). Although in most cases these cavities have remained open, in some cases they have been infilled by later minerals. Fig. 80.4E provides an example of dissolution and infilling in massive sulphide, where a well-defined but irregular network of interconnected dissolution channels is marked by a selvedge of recrystallized pyrite along the dissolution front. These cavities have been subsequently partially filled by colloform sphalerite and later filled to completion by finely banded chalcedonic silica.

Comparison of Figures 80.4A and 80.4B with Figure 80.4C shows that texturally the samples from Cyprus and the Canadian Millenbach deposit are fundamentally similar, the main difference being that whereas the scattered black areas in the Cyprus samples are empty cavities, in the Millenbach sample the dark areas consist of sphalerite or chlorite. This is highly suggestive that the texture of the Millenbach ore owes its origin to the later infilling of a porous massive sulphide by later sphalerite or chlorite. Even more convincing of this mode of origin is a comparison of Figure 80.4F with Figure 80.4E. In these samples both the size and mineralogy of the infilling is identical, though the fine colloform banding of both the sphalerite and chalcedonic silica shown by the Agrokipia example, has been lost by the Millenbach example, due to the recrystallization of both the sphalerite and silica during metamorphism.

A continuation of the analogy leads to the proposal that all monomineralic patches or bands in Canadian Archean massive ores originated by the infilling of cavities or open fractures of a porous sulphide mound. However, in most cases these cavity fillings and veins have been transformed by penetrative deformation into the monomineralic irregular patches, the discontinuous wispy bands, and the schlieren more typical of Canadian volcanogenic massive sulphide ores. The observation in Cyprus that, within a small volume of rock, hydrothermal mineral deposition at any one time is confined to a single mineral species has its repercussions on the methodology of study and interpretation of less well preserved massive sulphide deposits. For example, because co-existing mineral species are probably not coeval, sulphur isotope partitioning ratios between two mineral species may not have any direct relationship to temperatures of formation. Similarly, ratios of different mineral species in a small volume of rock may not bear any direct relationship to the simultaneous solubility of these minerals in a hydrothermal solution.

The compact ore is typically overlain by the colloform conglomeratic ore and black friable sandy ore, as described earlier for Mathiati (see Fig. 80.3). Although Hutchinson (1965) illustrates an example of colloform ore from a Canadian Archean deposit, colloform textures analogous to the size and frequency of occurrence of the Cyprus deposits are not present in most Canadian volcanogenic massive sulphide deposits. It is possible that this colloform texture was once common in the upper part of the massive sulphide lenses of Canadian deposits but like the assumed disappearance of the colloform banding of the sphalerite in Figure 80.4F, has been destroyed by recrystallization during metamorphism. The same might also be true for the black, sandy variety of sulphides observed in the Cyprus deposits.

Constantinou and Govett (1972) and Constantinou (1976) considered the black sandy pyrite and the colloform pyrite to be secondary forms of pyrite produced in the process of submarine oxidation of the massive sulphide bodies to form ochre. However, as seen at Mathiati, black friable sandy pyrite forms the matrix to obviously sedimentary breccias, and there seems to be no evidence to suggest that the black sandy pyrite is other than fine grained detrital rock. This evidence is not confined to Mathiati: Hutchinson (1965, Fig. 7), for example, shows a photograph of similar angular fragmental rocks with a matrix of black sandy pyrite from the Mavrovouni deposit. It is proposed that the black sandy pyrite represents accumulations of particulate sulphide that nucleated within the hydrothermal solutions (presumably in the hydrothermal plume) and settled from suspension near the vent. It would thus be directly analogous to the black sandy sulphidic sediments reported by Rise Project Group (1980) from near vents on the East Pacific Rise at 21°N which is attributed by them to a similar origin. The main difference between the two areas is that, in Cyprus, obviously much more sulphide accumulated near the vent than has happened on the East Pacific Rise, which suggests differences in the composition, rates of discharge or mode of venting of the hydrothermal solutions. If the black sandy pyrite of the Cyprus deposits is detrital, then the colloform conglomeratic ore and the compact ore are best regarded as progressive stages in the recrystallization, annealing, and cementing of

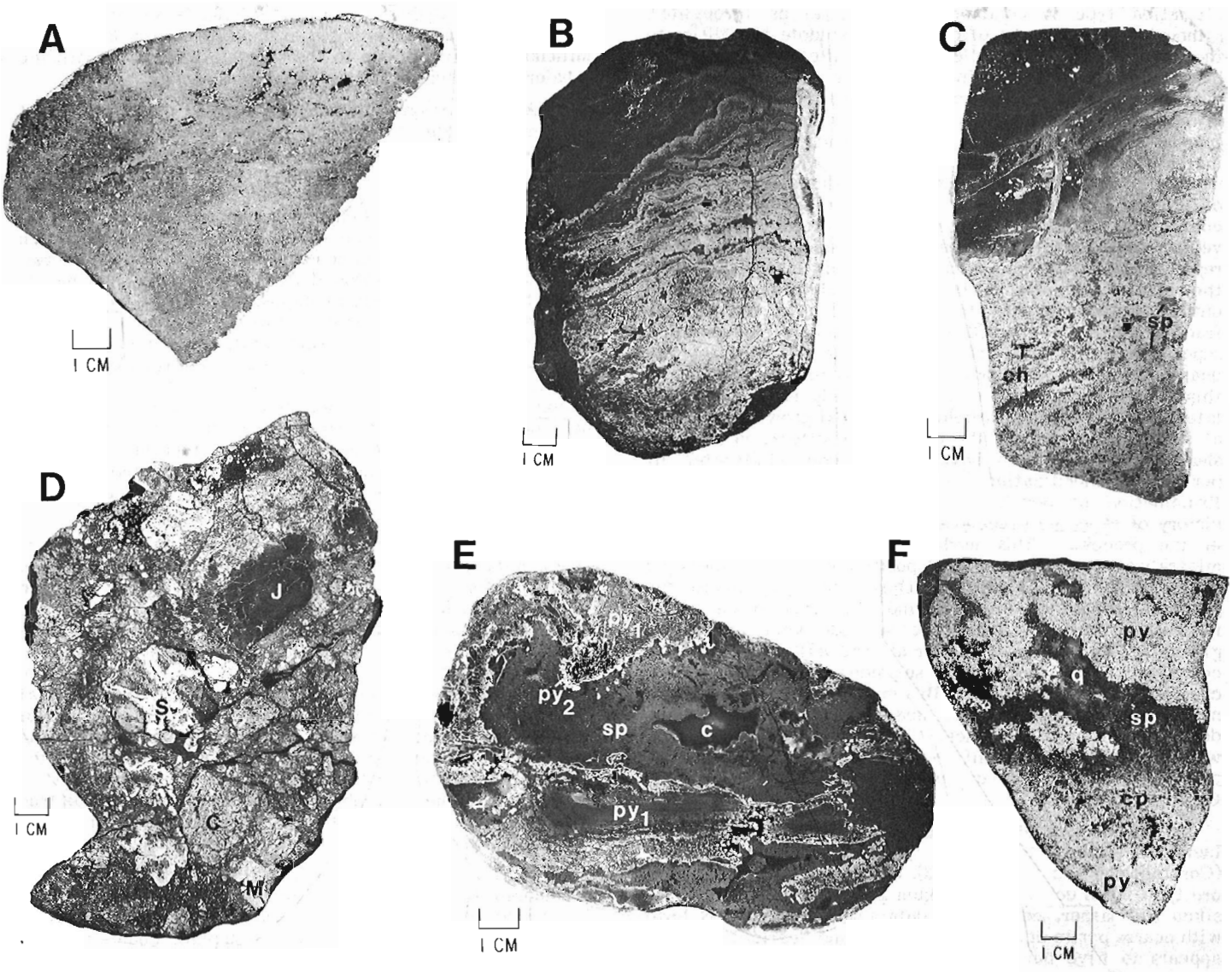

A. *Massive pyrite – "compact ore" – with small open cavities. Loose block, Skouriotissa.*

B. *Massive pyrite – 'colloform ore", Mathiati. Dark area at top of photograph is fine grained, compact "black sandy pyrite".*

C. *Massive chalcopyrite-pyrite with small monomineralic patches of sphalerite (sp) or chlorite (ch), Millenbach. Dark area at top of photograph is hanging wall andesite.*

D. *Detrital sulphide rock, Mathiati. Note fragments of colloform ore (C), compact ore (H), stockwork ore (S) and jasper (J).*

E. *Dissolution and infilling textures in massive sulphides, loose block, Agrokipia. Note early pyrite (py_2) along the dissolution front. Dissolution cavity has been infilled by colloform sphalerite (sp) and later chalcedonic silica (c).*

F. *Textures interpreted, by analogy with E, to be of a disolution-infilling origin in massive sulphide, Millenbach. Original cavities in massive pyrite (py) has been infilled by sphalerite (sp) and quartz. Late chalcopyrite (cp) has pervasively replaced both pyrite and sphalerite. Note that recrystallization during metamorphism fine has obliterated textural details visible in E.*

Figure 80.4 *Polished slabs of sulphide ores from Cyprus and Millenbach deposit, Noranda.*

the black sandy pyrite by the continued flow of hydrothermal solutions through the sulphide mound. In this context, the analogue to the black sandy pyrite of Cyprus deposits in Canadian volcanogenic massive sulphide deposits may be the massive, structureless, more or less homogenously polymetallic, sulphide, which could represent the accumulation of particulate sulphides resulting from the quenching of a polymetallic hydrothermal solution. Where this polymetallic massive sulphide has incorporated coarser grained angular fragments, its detrital nature is more obvious (Sangster, 1972).

CONCLUSIONS

Preliminary results from studies on the relatively pristine volcanogenic sulphide deposits of Cyprus provides some different perspectives that serve to enhance the appreciation of processes associated with the genesis of volcanogenic massive sulphide deposits, and also provides a deeper perception of phenomena that are of interest to the planning of future geological research on modern submarine hydrothermal systems and metalliferous deposits. Perhaps the main conclusion to be reached at this early stage of these studies is that in detail the formation of a massive sulphide deposit is extremely complex, and that great care should be exercised in the interpretation of small scale data of older and metamorphosed deposits which have lost all primary textural and mineralogical details.

ACKNOWLEDGMENTS

The author would like to thank the Hellenic Mining Company Ltd., particularly G. Malliotis and N. Adamides, for their enthusiastic guidance and help in familiarizing the author with the volcanogenic sulphide deposits of Cyprus, and for generously supplying maps, reports and samples of their properties. The author would also like to thank personnel of the ICRDG Cyprus Project for facilitating field work, especially H. Prichard, H. Russell and D. Baide for their help in sample collecting, and C. Xenophontos of the Cyprus Geological Survey Department for ensuring the success of logistical arrangements. H. Poulsen and A. Galley are thanked for their critical review of the manuscript and K. Nguyen and G. Young for drafting the diagrams.

REFERENCES

Ballard, R.D., Holcomb, R.T., and van Andel, T.H.
1979: The Galapagos Rift at 86°W: 3. Sheet flows, collapse pits, and lava lakes of the rift valley; Journal of Geophysical Research, v. 84, p. 5407-5422.

Bear, L.M.
1963: The mineral resources and mining industry of Cyprus; Bulletin Geological Survey of Cyprus, No. 1, 208 p.

Constantinou, G.
1976: Genesis of the conglomerate structure, porosity and collomorphic textures of the massive sulphide ores of Cyprus; in Metallogeny and plate tectonics, ed. D.F. Strong; Geological Association of Canada, Special Paper 14, p. 187-210.

Constantinou, G. and Govett, G.J.S.
1972: Genesis of sulphide deposits, ochre and umber of Cyprus; Transactions of the Institute of Mining and Metallurgy (Section B), v. 81, p. B34-B46.

1973: Geology, geochemistry and genesis of Cyprus sulphide deposits; Economic Geology, v. 68, p. 843-858.

Edmond, J.M.
1982: The chemistry of ridge crest hot springs; Marine Technology Society Journal, v. 16, No. 3, p. 23-25.

Edmond, J.M., Measures, C., Mangum, B., Grant, B., Sclater, F.R., Collier, R., Hudson, A., Gordon, L.I., and Corliss, J.B.
1979: On the formation of metal-rich deposits at ridge crests; Earth and Planetary Science Letters, v. 46, p. 19-30.

Francheteau, J., Needham, H.D., Choukroune, P., Juteau, T., Seguret, M., Ballard, R.D., Fox, P.J., Normark, W., Carranza, A., Cordoba, D., Guerrero, J., Rangin, C., Bougault, H., Cambon, P., and Hekinian, R.
1979: Massive deep-sea sulphide ore deposits discovered on the East Pacific Rise; Nature, v. 277, p. 523-528.

Hadjistavrinou, Y. and Constantinou, G.
1982: Cyprus, in Mineral Deposits of Europe. Volume 2: Southeast Europe, ed. F.W. Dunning, W. Mykura, and D. Slater; Mineralogical Society – Institute of Mining and Metallurgy, London, p. 255-277.

Hekinian, R., Fevrier, M., Bischoff, J.L., Picot, P., and Shanks, W.C.
1980: Sulfide deposits from the East Pacific Rise near 21°N; Science, v. 207, p. 1433-1444.

Hekinian, R., Fevrier, M., Avedik, F., Cambon, P., Charlov, J.L., Needham, H.D., Raillard, J., Boulegue, J., Merlivat, L., Moinet, A., Manganini, S., and Lange, J.
1983: East Pacific Rise near 13°N: geology of new hydrothermal fields; Science, v. 219, p. 1321-1324.

Hutchinson, R.W.
1965: Genesis of Canadian massive sulphides reconsidered by comparison to Cyprus deposits; Canadian Institute of Mining and Metallurgy Bulletin, v. 58, p. 972-986.

1973: Volcanogenic sulfide deposits and their metallogenic significance; Economic Geology, v. 68, p. 1223-1246.

Hutchinson, R.W. and Searle, D.L.
1971: Stratabound pyrite deposits in Cyprus and relations to other sulphide ores; Society of Mining Geologists of Japan, Special Issue No. 3, p. 198-205.

Johnson, A.E.
1972: Origin of Cyprus pyrite deposits; 24th International Geological Congress, Montreal, Section 4, p. 291-298.

Malahoff, A.
1982: A comparison of the massive submarine polymetallic sulphides of the Galapagos Rift with some continental deposits; Marine Technology Society Journal, v. 16, No. 3, p. 39-45.

Malahoff, A., Embley, R.W., Cronan, D.S., and Skirrow, R.
1983: The geological setting and chemistry of hydrothermal sulfides and associated deposits from the Galapagos Rift at 86°W; Marine Mining, v. 4, p. 123-137.

Middleton, G.V.
1970: Experimental studies related to flysch sedimentation; in Flysch sedimentology in North America, ed. J. Lajoie; Geological Association of Canada Special Paper 7, p. 253-272.

Normark, W.R., Morton, J.L., and Delaney, J.R.
1982: Geologic setting of massive sulphide deposits and hydrothermal vents along the southern Juan de Fuca Ridge; United States Geological Survey Open File Report 82-200A.

Rise Project Group
1980: East Pacific Rise: Hot springs and geophysical experiments; Science, v. 207, p. 1421-1432.

Sangster, D.F.
1972: Precambrian volcanogenic massive sulphide deposits in Canada: a review; Geological Survey of Canada, Paper 72-22, 44 p.

Searle, D.L.
1972: Mode of occurrence of the cupriferous pyrite deposits of Cyprus; Transactions of the Institute of Mining and Metallurgy (Section B), p. B189-B197.

Sillitoe, R.H.
1973: Environment of formation of volcanogenic massive sulphide deposits; Economic Geology, v. 68, p. 1321-1325.

Solomon, M.
1976: "Volcanic" massive sulphide deposits and their host rocks – a review and an explanation; in Handbook of strata-bound and stratiform ore deposits, ed. K.H. Wolf; Vol. II, Regional studies and specific deposits, Elsevier, Amsterdam, p. 21-50.

Spooner, E.T.C.
1977: Hydrodynamic model for the origin of the ophiolitic cupriferous pyrite ore deposits of Cyprus; in Volcanic processes in ore genesis; Geological Society of London Special Publication 7, p. 58-71.

Spooner, E.T.C., Beckinsale, R.D., Fyfe, W.S., and Smewing, J.D.
1974: O^{18} enriched ophiolite metabasic rocks from E. Liguria (Italy), Pindos (Greece), and Troodos (Cyprus); Contributions to Mineralogy and Petrology, v. 47, p. 41-62.

Vokes, F.M.
1966: Remarks on the origin of the Cyprus pyritic ores; Canadian Institute of Mining and Metallurgy Bulletin, v. 59, p. 388-391.

81. SOME OBSERVATIONS ON THE MINERALOGICAL AND CHEMICAL ZONATION PATTERNS OF VOLCANOGENIC SULPHIDE DEPOSITS OF CYPRUS

Project 770063

John W. Lydon
Economic Geology Division

Lydon, J.W., Some observations on the mineralogical and chemical zonation patterns of volcanogenic sulphide deposits of Cyprus; in Current Research, Part A, Geological Survey of Canada, Paper 84-1A, p. 611-616, 1984.

Abstract

Sulphur isotopes of gypsum associated with the ochres of the Mathiati deposit suggest that at least some of the ochre was formed by the oxidation of massive pyrite by the circulation of meteoric(?) groundwaters. Oxidized groundwater circulation also appears to have been responsible for the mobilization of copper from the lava host rocks and its deposition as secondary copper sulphide in the uppermost and peripheral parts of the volcanogenic sulphide deposits, resulting, at least at Mathiati, in a reversal to the characteristic copper to zinc zonation of other classic volcanogenic massive sulphide types. The zonation of the hydrothermal alteration pipe of the Mathiati deposit, as is typical of Canadian examples, is from a chloritic core to a potassium enriched periphery, but unlike the Canadian examples, the chloritic core of the Cyprus deposit does not involve significant addition of magnesium.

Résumé

On a analysé les isotopes du soufre que contient le gypse associé aux ocres du gîte de Mathiati. L'analyse indique qu'au moins en partie, l'ocre s'est formé par oxydation de la pyrite massive, due à la circulation d'eaux souterraines d'origine météorique (?). La circulation des eaux souterraines pourrait aussi expliquer la mobilisation du cuivre à partir des roches hôtes (laves), et son dépôt sous forme de sulfures secondaires, au sommet et à la phériphérie des gîtes sulfurés volcanogènes; on observe ainsi, du moins à Mathiati, une inversion de la zonation caractéristique (cuivre-zinc), que montrent d'autres types classiques de gîtes sulfurés volcanogènes. Dans le gîte de Mathiati, la zonation manifestée par la colonne d'altération hydrothermale est, conformément aux exemples typiques canadiens à noyau chloriteux, à pourtour enrichi en potassium; mais, contrairement aux exemples canadiens, le noyau chloriteux du gîte de Chypre ne contient pas de quantités supplémentaires notables de magnésium.

INTRODUCTION

One of the characteristics of volcanogenic massive sulphide deposits is the very pronounced zonation of both the ore and the hydrothermal alteration pipe (Sangster, 1972). In terms of ore metals, Cu:Zn ratios decrease from the core of the massive sulphide lens and hydrothermal alteration pipe upwards and outwards to the periphery. This decrease of Cu:Zn ratios, indicative of a decreasing temperature gradient (Franklin et al., 1982) is accompanied by indications of an increase in fO_2, marked by lower fO_2 mineral assemblages in the core (e.g. pyrhhotite-chalcopyrite) to higher fO_2 mineral assemblages in the periphery (e.g. the hematite-quartz or barite zones of the Kuroko deposits). It is important, for genetic modelling purposes, to distinguish the effects of fO_2 gradients established at the time of ore deposition and the effects of fO_2 gradients established by post-depositional processes. The age of the ochres (dominantly hydrated iron oxides) associated with some Cyprus deposits, has a direct bearing on this problem.

The hydrothermal alteration pipes of many Canadian deposits, especially those occurring in dominantly mafic volcanic successions, is characterized by an Mg-enriched chlorite core to a K-enriched sericitic periphery (Sangster, 1972). Comparable information on the Cyprus deposits has not been well documented in the published literature.

This article presents some preliminary results, obtained from the Mathiati deposit, that pertain to both these problems, and to comment on their significance to general genetic considerations.

ORIGIN OF OCHRES

The rate and extent of ocean floor oxidation of sulphide deposits is of great interest to the exploration of modern submarine sulphides because it places time constraints on limits to the preservation of sulphides left exposed on the ocean floor. Francheteau et al. (1979) and Hekininian et al. (1980) reported that large portions of their sulphide samples obtained from the ocean floor were oxidized and hydrated, and the latter authors predicted that unless the sulphide deposits were buried, they would be altered and dispersed in a relatively short period of time. The process of seafloor oxidation is also of great interest to the study of processes that gave rise to the accumulation and preservation of large quantities of sulphides that form ancient ore deposits. Since evidence of seafloor oxidation in these ancient deposits is rare, the implication may be that anoxic seabottom conditions or rapid burial may be essential to the accumulation and preservation of the ores.

The author does not know what percentage of Cyprus deposits show a significant development of ochre. The Mathiati, Skouriotissa and Moussoulos deposits are cited as having the best development of ochre, with minor development of ochre being reported from the Agrokipia A, Apliki and Maurouvini deposits (Constantinou and Govett, 1972; Constantinou, 1976). Of the ten deposits the author examined, ochres were seen only at Mathiati and Skouriotissa. At Mathiati, the gradational contact between ochre and black sandy pyrite (Lydon, 1984, Fig. 80.3) leaves no doubt that the ochre is an in situ oxidation of the pyrite. However, no ochre clasts were seen in the sedimentary

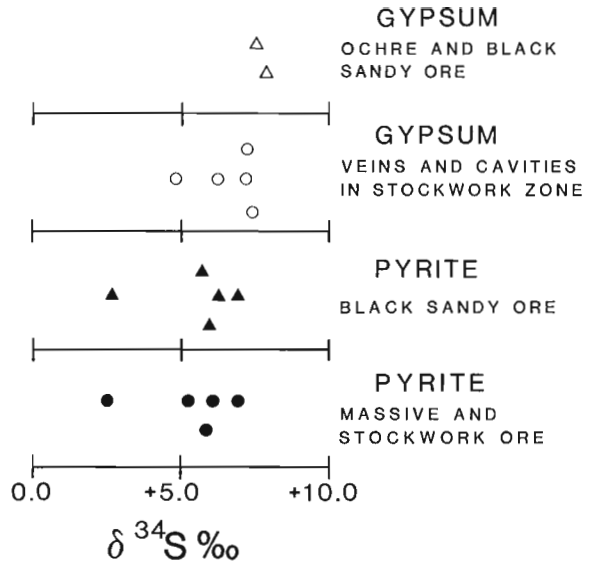

Figure 81.1. *Summary of sulphur isotope results from Mathiati.*

fragmental rocks immediately overlying the ore, suggesting that ochre was not abundantly developed prior to the submarine erosion of the sulphides. To prove through field relationships that the ochre was produced on the ocean floor requires the demonstration that a detrital rock derived from the ochre is stratigraphically overlain by pillow lavas or bona fide primary marine sedimentary rocks.

To the author's knowledge no such a relationship has ever been documented, except that Constantinou (1976) reported that 50 cm of an ochreous sedimentary rock within pillow lavas intersected by a drillhole contained a Cenomanian foraminifer. The prime example of bedded ochres occurs at Skouriotissa. At the small ochre mine to the northwest of the main Skouriotissa pit, the well-bedded ochres are overlain by a fragmental rock. This rock is derived from chalks and marls (although the fragmental nature may be due to the collapse or infilling of old workings because it contains wooden logs near its base), which based on the stratigraphic column described by Constantinou and Govett (1972), are assumed to belong to the Upper Cretaceous-Lower Miocene Lefkara Formation. On the basis of this evidence alone, the author prefers to keep an open mind on the possibility that the bedded ochres at Skouriotissa may be analogous to the "false gossan" at Mathiati, where just to the north of the open pit, sediments described as ochres, umbers and secondary gossan (consisting of hematite, limonite, natrojarosite and a little kaolinite) occupy a basin-like depression in the present erosion surface of hanging wall pillow lavas (Searle and Panayiotou, 1968). The age of the false gossan may be Pleistocene to very recent. At the Agrokipia A deposit, a bed of cream coloured argillic sedimentary rock, locally stained an ochreous colour and containing fragments of sulphide up to 10 cm across, occurs between two lava flows in the immediate hanging wall to the main sulphide body, and would logically seem to be derived from the submarine erosion of exposed portions of this deposit. If this is the case, then the Agrokipia A example, like the fragmental rocks at Mathiati, demonstrates only that erosion, and not oxidation, of the sulphide deposits took place on the ocean floor. The question therefore arises as to why some deposits were oxidized in the submarine environment, as suggested by Constantinou and Govett (1972), while others were not.

The ochre and black sandy pyrite at Mathiati contain up to 20% by weight of gypsum as a poikoilitic impregnation throughout the matrix. As in many of the deposits examined, gypsum also occurs infilling fractures and pores in other massive sulphide ore types and stockwork mineralization. If, as Constantinou and Govett (1972) have suggested, the ochre has been formed by the seafloor oxidation of massive sulphides and the sandy friable pyrite is an intermediate product of the process, it could be expected that the sulphate resulting from the subaqueous oxidation of sulphides would cause seawater to become saturated with respect to gypsum and that this gypsum would be precipitated and perhaps preserved within the ochre and black sandy pyrite. The sulphur isotopes of this gypsum should reflect this mixed parentage of the sulphate.

The result of a preliminary sulphur isotope study of the Mathiati deposit is illustrated in Figure 81.1. Whereas the gypsum from the matrix of the black friable pyrite just below the ochre is isotopically slightly heavier than gypsum from late veins and cavities in the massive and stockwork ore, which in turn is slightly heavier than black sandy pyrite or fresh massive and stockwork pyrite, the gypsum from the black sandy pyrite is significantly lighter than the calculated theoretical minimum value if it formed under submarine conditions. This calculation was carried out assuming that: 1) the composition of Cretaceous seawater was similar to modern ocean water; 2) the precipitation of gypsum was solely because of the addition and immediate homogeneous mixing of sulphate, derived from the isotopically congruent solution of pyrite, with the seawater; 3) the average isotopic composition of the pyrite was $\delta^{36}S = 5.5\%$ and the composition of Cenomanian seawater sulphate was $\delta^{36}S = 17\%$ (Claypool et al., 1980); 4) that Ca^{++} and SO_4^{--} have the same diffusion rates in an aqueous medium; and 5) the dissociation constant for gypsum at 25°C is that reported by Kharaka and Barnes (1973). These calculations predict that the minimum $\delta^{34}S$ value for gypsum precipitated as the result of the submarine weathering of the Mathiati sulphides should be 9.6% or 10.5%, depending on whether the speciation of sulphate in seawater and the activity coefficient of SO_4^{--} is that calculated by the thermodynamic data base and methods used by Garrels and Thomson (1962) or reported by Smith (1974) respectively.

The results illustrated in Figure 81.1 are compatable with the interpretation that all the gypsum at Mathiati was precipitated from aqueous solutions whose only sulphate content was derived from the oxidation of pyrite e.g. groundwater of meteoric derivation. The slight shift in sulphur isotope ratios between the gypsum and the pyrite can be explained by the effective isotopic incongruent dissolution of pyrite, caused by the precipitation of secondary sulphides with light sulphur isotope ratios as a result of Eh fluctuations during the oxidation process. Perhaps the two samples of sulphide with $\delta^{34}S$ values of 2.5 ‰ and 2.7 ‰ respectively contain a significant proportion of this isotopically light pyrite.

Although these sulphur isotope results do not negate the possibility that ochre formed on the ocean floor, they do indicate that the circulation of meteoric groundwaters in the lavas has caused oxidation of the pyrite bodies. At least some iron oxide and hydroxide is therefore not of submarine origin.

ORE METAL ZONATION

There are no published maps showing ore metal zonation of a Cyprus-type deposit. Constantinou and Govett (1972, 1973) emphasized that copper minerals, principally chalcopyrite with subordinate covellite, chalcocite and idaite, are concentrated in the upper portions of the massive ore and are

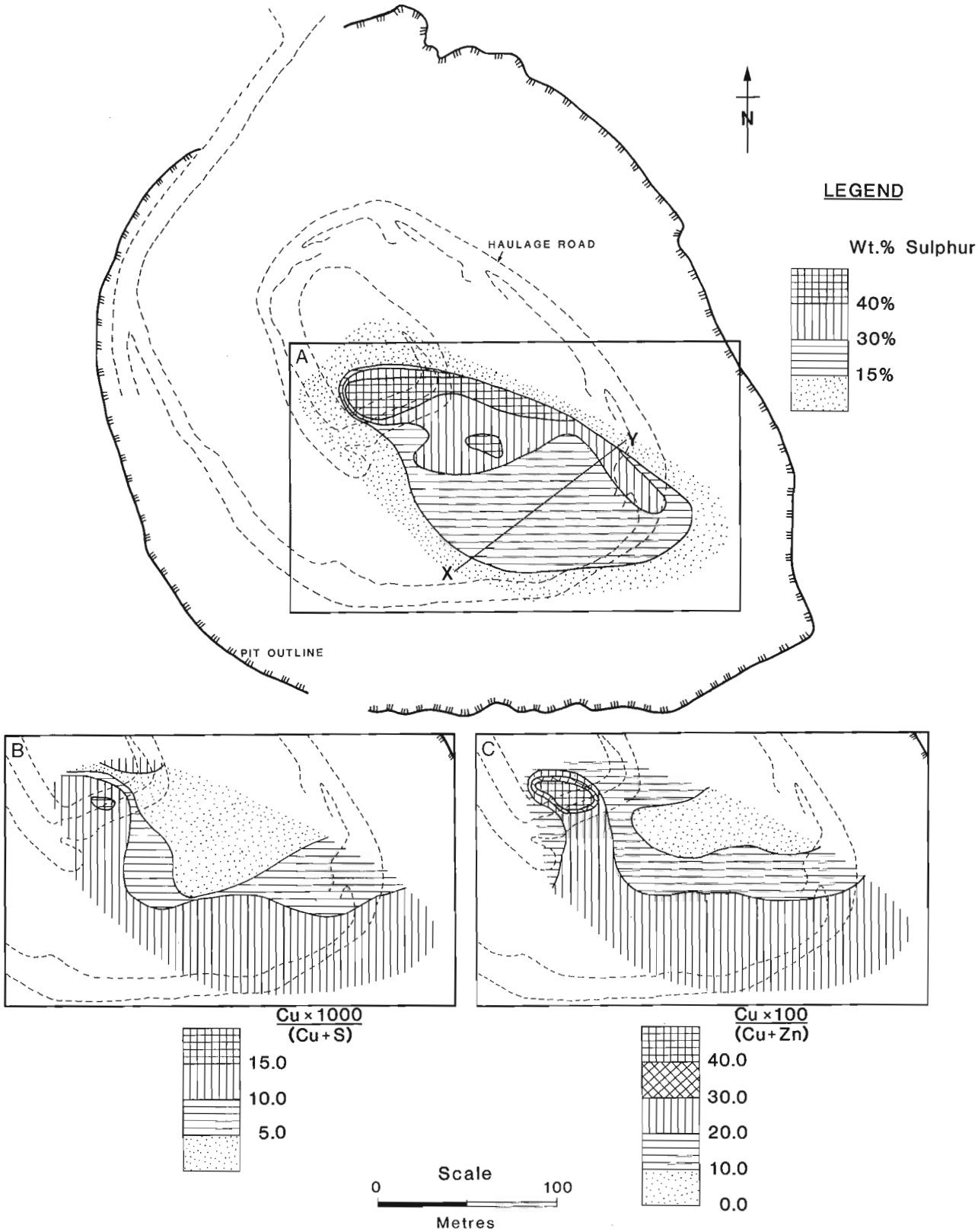

A – Sulphur content, based on 5 foot samples.
B – (Cu x 1000)/(Cu+S) ratios based on 50 foot composite samples.
C – (Cu x 100)/(Cu+Zn) ratios based on 50 foot composite samples.

Figure 81.2. *Chemical zonation patterns at the 330 m level of the Mathiati deposit. Contouring based on assays of samples from underground galleries tabulated on a map dated 1938 by Cyprus Mines Corporation (courtesy Hellenic Mining Company Ltd.). For geological context, compare with Figure 80.2A (Lydon, this volume).*

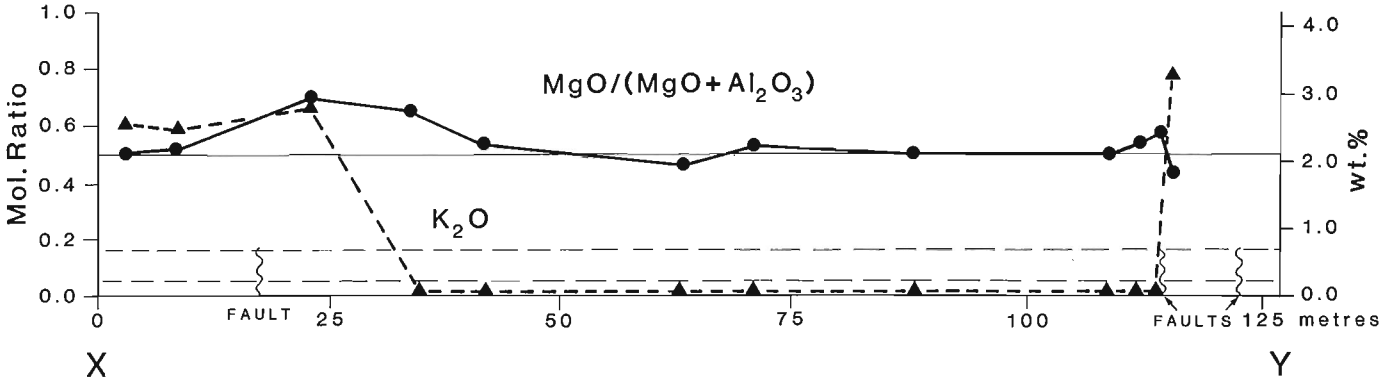

Figure 81.3. Whole rock geochemical traverse across the Mathiati hydrothermal alteration pipe along the X-Y indicated on Figure 81.2, illustration variations in $MgO/(MgO+Al_2O_3)$ mole ratios (thick solid line) and K_2O content (thick broken line). Assumed original valves for unaltered rocks are taken from the average of Lower Pillow Lavas (Desmet et al., 1980) and the average of basaltic glasses (Robinson et al., 1983). $MgO/(MgO+Al_2O_3)$ mole ratios (thin solid line) of both data sets are similar, but average K_2O contents (thin broken lines) are 0.76 and about 0.2% respectively.

paragenetically late. Examination of exploration hole assay data confirms that the highest copper values and the highest Cu/S ratios invariably occur in the uppermost parts of the sulphide deposits, even where they are still covered by 100 m or more of hanging wall lavas. Constantinou and Govett (op. cit.) pointed out that these high copper zones (>1%) are somewhat erratic and do not form a continuous zone over the entire deposit. They attributed this copper enrichment to secondary processes associated with the submarine weathering of the sulphides and the formation of ochre.

Contouring of an assay plan of the 1000 foot (now the 305 m) level underground exploration galleries illustrates that the Mathiati deposit also shows this copper enrichment in its stratigraphically uppermost portion (Fig. 81.2). The average grade of massive and stockwork ore at the 305 m level is 0.23% Cu and 0.99% Zn, and thus has a considerably lower Cu:Zn ratio than the average value of about 12:1 reported by Constantinou and Govett (1972) for 121 samples of both massive and stockwork ore from four different deposits. Based on 50 foot composite sample lengths: both Cu grades (up to 0.6%) and Cu:S ratios are highest in the massive ore; Zn grades are highest (2.0%) in the stockwork zone immediately below the massive ore; Cu:Zn ratios are lowest in the core of the stockwork zone (1:10) and highest in the outer parts of the stockwork zone (1:3) and massive ore (up to 3:1).

This is the reverse to the Cu:Zn zonation pattern so characteristic of volcanogenic massive sulphide deposits of other areas such as the Canadian Archean greenstone belts. This brings up the question as to how much of the present copper distribution pattern of the Cyprus deposits is of primary hydrothermal origin or how much is of secondary origin. Secondary processes involved could be either the remobilization and concentration of copper in the sulphides by submarine weathering (Constantinou and Govett, 1972) or, as the sulphur isotopes of the gypsum at Mathiati suggest, the leaching of copper from the volcanics by circulating oxygenated meteoric(?) groundwaters and its deposition as sulphides in the peripheral parts of the deposits, when these groundwaters encountered this reduction trap.

The Cu:S and Cu:Zn zonation patterns of Mathiati (Fig. 81.2B, 81.2C respectively) suggest that if the relative copper enrichment is because of the late stage introduction of copper by circulating groundwaters, then the direction of flow was from south-west to north-east. This flow direction would also be predicted by field observations of hydrodynamic features of the rocks in the vicinity of the Mathiati deposit. The thick zone of argillic fault gouge along the northeastern side of the deposit would be expected to form an effective barrier to the exchange of groundwaters from this direction. The absence of a comparable barrier on the southwestern side of the deposit would allow maximum groundwater infiltration of the sulphide mineralization to be from this direction. This direction of groundwater exchange is also indicated by the zone of red-purple staining of the lava host rocks along the southwestern side of the mineralization (Lydon, 1984, Fig. 80.2A). Red-purple staining of the host rocks near the contact with stockwork or massive sulphide mineralization is not unique to Mathiati, but was observed in several other deposits e.g. Limni, and is interpreted by the author to represent a redox front established in the zone of exchange between oxidized groundwaters of barren lavas and reduced groundwaters of the sulphide deposits. The red-purple staining at Mathiati is confined to the southwestern side of the deposit, which suggests that this is where maximum groundwater exchange between the host rocks and sulphide deposits took place.

If the copper enrichment of the Cyprus sulphide deposits by groundwater circulation is a common phenomenon, then the idea of a separate cupriferous pyrite type of volcanogenic sulphide deposit (Hutchinson, 1973) may lose much of its validity. From the chemical point of view, the Cyprus-type deposits may best be regarded as a low grade variant of the Cu-Zn type of deposit typical of other dominantly mafic volcanic successions. The particular chemical characteristics of the Cyprus deposits may be because of the unusually pronounced effects of oxygenated groundwater circulation, promoted by the lack of deep burial of the Troodos volcanics and the consequent preservation of their original high porosity.

Mg/K ZONATION OF THE HYDROTHERMAL ALTERATION PIPE

A characteristic of the alteration pipes to the Cu-Zn deposits typical of dominantly mafic volcanic sequences is a zonation from a chloritic core to a sericite margin (Franklin et al., 1981). This represents a metasomatic enrichment of magnesium in the core and potassium in the margin. It has been suggested that the potassium enrichment in the margin is due to the fixing of the potassium liberated by the process of chloritization and potassium depletion in the core zone (Riverin and Hodgson, 1980).

A reconnaissance geochemical traverse across the Mathiati alteration pipe (Fig. 81.3) exhibits the same Mg/K relationships described by Riverin and Hodgson (1980). The chloritic core zone at Mathiati has been depleted in potassium and there is a strong potassium enrichment in the margins. A major difference between the Millenbach deposit, studied by Riverin and Hodgson, and Mathiati is in the apparent mass exchanges involved in the metasomatism. At Millenbach there is a pronounced enrichment of magnesium in the aluminosilicate fraction, expressed by MgO/Al_2O_3 ratio, in the core of the alteration pipe of both the Quartz Feldspar Porphyry and the Millenbach Andesite Unit. In the core of the Mathiati deposit there is no enrichment compared to fresh pillow lavas of the same age. Also, whereas both fresh Quartz Feldspar Porphyry and fresh Millenbach Andesite have enough original potash (2.30% and 1.76% K_2O respectively) to supply the peripheral metasomatic zone of potassium enrichment, order of magnitude calculations for the Mathiati deposit show that the assumed original maximum 0.76% K_2O of fresh Lower Pillow Lavas is insufficient to supply a 25 m plus zone of about 3% K_2O if it is continuous around the alteration pipe.

The lack of a magnesian enrichment in the core of the Mathiati deposit allows a direct analogy to be made between the composition of ore forming solutions responsible for the formation of the Mathiati deposit and the 350°C hydrothermal solutions of the East Pacific Rise, which are magnesium free. By the same token, the magnesium enrichment of the alteration pipes of Canadian Archean greenstone belts deposits suggests that the hydrothermal solutions responsible for their formation were of different chemical composition to the modern submarine hydrothermal systems. Ponderables such as these raise questions as to how much of the chemical metasomatism of the hydrothermal alteration pipes of volcanogenic massive sulphide deposits is because of the primary chemical nature of the hydrothermal solutions or to fortuitous but associated events. For example, a zone of magnesium enrichment does occur at Mathiati coinciding with the inner part of the zone of potassium enrichment (Fig. 81.3). A similar narrow zone of enhanced magnesium enrichment at the inner edge of the zone of relative potassium enrichment has been documented by the author for the Millenbach deposit. Thus MgO/Al_2O and K_2O/Al_2O profiles for the two deposits have similar patterns which suggests a similar genetic process in both cases. However, the amount of magnesian and potassic metasomatism of the host rocks is entirely different. As has been suggested by Roberts and Reardon (1978) for the magnesium of the Canadian Archean Mattagami Lake deposit and by Clark (1971) for the potassium of the Mathiati deposit of Cyprus, it is possible that it is the entrainment of seawater into the hydrothermal discharge zone which supplies the constituents for the observed metasomatism. Thus if seawater is the source for the metasomatic constituents, the amount of metasomatism depends mainly on the amount of seawater entrained, and not the primary composition of the ore fluid.

The disposition of the potassium enrichment at Mathiati may indicate a further complication in the question of the source of metasomatic constituents for the hydrothermal alteration pipes of volcanogenic massive sulphide deposits. As can be seen in Figure 81.3, the zone of potassium enrichment straddles the southwestern fault and is present on the down-throw side of the northeastern fault across from the stockwork zone. This would either imply that both these faults have a small vertical throw of no more than 10 m, which for the northeastern fault at least, conflicts with the assumed volcanic stratigraphy, or that the potassium enrichment is a post-ore, post-faulting metasomatism due to chemical changes imposed by circulating groundwaters in proximity to a sulphide body.

CONCLUSIONS

Preliminary results of the zonation patterns of both the ore metals and main metasomatic elements of the hydrothermal alteration pipe of the Mathiati deposit indicate that the zonation patterns may be strongly influenced by factors other than the effects of the ore-forming hydrothermal solution. Important in this regard is that a volcanogenic massive sulphide deposit may be subject to a variety of modifications to its primary chemical or mineralogical zonation patterns by interaction with circulating groundwaters after burial. These effects must be recognized and compensated for, if they are not to cause confusion in the formulation of a genetic model.

ACKNOWLEDGMENTS

The Hellenic Mining Company is thanked for their cooperation in allowing the work on the Mathiati deposits, especially G. Maliotis, for encouraging the project and supplying maps and other information, and also the mine staff for accomodating mapping and sampling during their mining operations. H. Prichard collaborated on aspects of the research reported here, and also, with H. Russell and B. Diene, provided assistance in mapping and sampling the Mathiati pit. H. Poulsen and A. Galley are thanked for reviewing the manuscript and R. Lancaster and K. Nguyen for drafting the diagrams.

REFERENCES

Clark, L.A.
1971: Volcanogenic ores: comparison of cupriferous pyrite deposits of Cyprus and Japanese Kuroko deposits; Society of Mining Geologists of Japan, Special Issue 3, p. 206-215.

Claypool, G.E., Holser, W.T., Kaplan, I.R., Sakai, H., and Zak, I.
1980: The age curves of sulfur and oxygen isotopes in marine sulphate and their mutual interpretation; Chemical Geology, v. 28, p. 199-260.

Constantinou, G.
1976: Genesis of the conglomerate structure, porosity and collomorphic textures of the massive sulphide ores of Cyprus; in Metallogeny and plate tectonics, ed. D.F. Strong; Geological Association of Canada, Special Paper 14, p. 187-210.

Constantinou, G. and Govett, G.J.S.
1972: Genesis of sulphide deposits, ochre and umber of Cyprus; Transactions of the Institute of Mining and Metallurgy (Section B), v. 81, p. B34-B46.

Desmet, A., Gagny, Cl., Lapierre, H., and Rocci, G.
1980: Organization spatio-temporelle du complexe filonien du Troodos: Son enracinement dans la chambre magmatique; in Ophiolites, Proceedings International Ophiolite Symposium, Cyprus, 1979, ed. A. Panayiotou; Geological Survey Department, Nicosia, p. 66-72.

Francheteau, J., Needham, H.D., Choukroune, P., Juteau, T., Seguret, M., Ballard, R.D., Fox, P.J., Normark, W., Carranza, A., Cordoba, D., Guerrero, J., Rangin, C., Bougault, H., Cambon, P., and Hekinian, R.
1979: Massive deep-sea sulphide ore deposits discovered on the East Pacific Rise; Nature, v. 277, p. 523-528.

Franklin, J.M., Lydon, J.W., and Sangster, D.F.
1981: Volcanic-associated massive sulphide deposits; Economic Geology 75th Anniversary Volume, p. 485-627.

Garrels, R.M. and Thompson, M.E.
1962: A chemical model for sea water at 25°C and one atmosphere total pressure; American Journal of Science, v. 260, p. 57-66.

Hekinian, R., Fevrier, M., Avedik, F., Cambon, P., Charlov, J.L., Needham, H.D., Raillard, J., Boulegue, J., Merlivat, L., Moinet, A., Manganini, S., and Lange, J.
1983: East Pacific Rise near 13°N: geology of new hydrothermal fields; Science, v. 219, p. 1321-1324.

Hutchinson, R.W.
1973: Volcanogenic sulfide deposits and their metallogenic significance; Economic Geology, v. 68, p. 1223-1246.

Kharaka, Y.K. and Barnes, I.
1973: SOLMNEQ – solution-mineral equilibrium computations; United States Department of the Interior, Geological Survey, Computer contribution PB-215899, 75 p.

Lydon, J.W.
1984: Some observations on the morphology and ore textures of the volcanogenic sulphide deposits of Cyprus; in Current Research, Part A, Geological Survey of Canada, Paper 84-1A, Report 80.

Riverin, G. and Hodgson, C.J.
1980: Wall-rock alteration at the Millenbach Cu-Zn mine, Noranda, Quebec; Economic Geology, v. 75, p. 424-444.

Roberts, R.G. and Reardon, E.J.
1978: Alteration and ore-forming processes at Mattagami Lake mine, Quebec; Canadian Journal of Earth Sciences, v. 15, p. 1-21.

Robinson, P.T., Melson, W.G., O'Hearn, T., and Schmincke, H-U.
1983: Volcanic glass compositions of the Troodos ophiolite, Cyprus; Geology, v. 11, p. 400-4.

Sangster, D.F.
1972: Precambrian volcanogenic massive sulphide deposits in Canada: a review; Geological Survey of Canada, Paper 72-22, 44 p.

Searle, D.L. and Panayiotou, A.
1968: Regional geology of the Sha-Mathiati area and the North Mathiati mine; unpublished report of the United Nations Special Fund Project, Cyprus, 22 p.

Smith, F.G.W. (ed.)
1974: Handbook of marine science, Volume 1; CRC Press, Cleveland, Ohio. 627 p.

82. THE GENERATION OF ORE-FORMING HYDROTHERMAL SOLUTIONS IN THE TROODOS OPHIOLITE COMPLEX: SOME HYDRODYNAMIC AND MINERALOGICAL CONSIDERATIONS

Project 770063

John W. Lydon and Heather E. Jamieson
Economic Geology Division

Lydon, J.W. and Jamieson, H.E., The generation of ore-forming hydrothermal solutions in the Troodos ophiolite complex: some hydrodynamic and mineralogical considerations; in Current Research, Part A, Geological Survey of Canada, Paper 84-1A, p. 617-625, 1984.

Abstract

Observations on the extrusive part of the Troodos ophiolite complex suggest a hydrodynamic model different from that of a simple convection cell for the formation of the volcanogenic sulphide deposits of Cyprus. It is suggested that ore solutions were generated by the "gable trapping" of pore waters of the extrusive sequence at the top of the sheeted intrusive complex. The formation of epidote-quartz rock may have particular significance for the diagnosis of the reservoir zones of the ore-forming hydrothermal solutions. At least some of the secondary minerals of the extrusive sequence are due to Tertiary or later circulation of groundwaters. Individual sulphide deposits may have been affected by at least four different types of water circulation, each of different origin and different physico-chemical characteristics.

Résumé

L'observation de la portion extrusive du complexe ophiolitique du Troodos mène à la conception d'un modèle hydrodynamique différent d'une simple cellule de convection, pour la formation des gîtes sulfureux de type volcanogène trouvés à Chypre. Il semble que les solutions minéralisées proviennent du piégeage des eaux interstitielles de la séquence extrusive, au sommet du complexe intrusif stratifié. La formation d'une roche à épidote et quartz pourrait avoir une grande importance, lorsqu'il s'agit d'identifier les zones réservoirs des solutions hydrothermales minéralisantes. Au moins une partie des minéraux secondaires de la séquence extrusive ont été apportés par la circulation d'eaux souterraines au Tertiaire ou plus tard. Chacun des gîtes sulfurés a pu être modifé par au moins quatre types d'eaux souterraines dont l'origine et les caractéristiques physico-chimiques variaient de l'une à l'autre.

INTRODUCTION

Much of the geological evidence for the currently popular convection cell model for the hydrothermal systems responsible for the formation of volcanogenic massive sulphide deposits is based upon observations on the classic volcanogenic sulphide deposits of Cyprus and the upper part of the Troodos ophiolite complex (Spooner et al., 1974; Solomon, 1976; Heaton and Sheppard, 1977; Spooner, 1977). Field and laboratory studies being carried out at the Geological Survey of Canada on aspects of the volcanogenic sulphide deposits of Cyprus provide an excellent opportunity for a first-hand examination of this geological evidence and to make a more knowledgable assessment of the applicability of the convection cell model to Canadian massive sulphide deposits. The purpose of this communication is to point out some pertinent observations on the volcanic part of the Troodos ophiolite complex and comment on their possible significance to the convection cell model.

THE CONVECTION CELL MODEL

The essential features of the convection cell model for the volcanogenic sulphide deposits of Cyprus is illustrated in Figure 82.1. The model itself can be considered to be a refinement of that proposed by Spooner and Fyfe (1973) based on observations on the ophiolites of East Liguria, Italy. Most of the evidence for the circulation of seawater to depths of 3-5 km within the Troodos oceanic crust is based on the interpretation of oxygen, hydrogen and strontium isotope ratios (Spooner et al., 1974; Heaton and Sheppard, 1977; Spooner, 1977), and to some extent ferric/ferrous iron ratios (Spooner, 1977), of hydrously altered rocks of the Pillow Lavas, Sheeted Dyke Complex and the Gabbro divisions of the upper part of the ophiolite complex. It is inferred that hydrothermal solutions that caused this hydrous alteration in the upper part of the ophiolite complex also, on discharge at the ocean floor, precipitated the sulphides and caused the chloritic hydrothermal alteration of their underlying feeder or stockwork zones. The inference is based on the demonstration that oxygen isotope temperatures of the chlorite in the feeder zone are approximately the same as those from the hottest part of the convection cell deeper in the Troodos oceanic crust (Heaton and Sheppard, 1977) and that the salinities of fluid inclusions from quartz veins of the stockwork zone are about the same as seawater (Spooner and Bray, 1977). Solomon (1976) demonstrated that the spacing of the Cyprus sulphide deposits corresponds to those

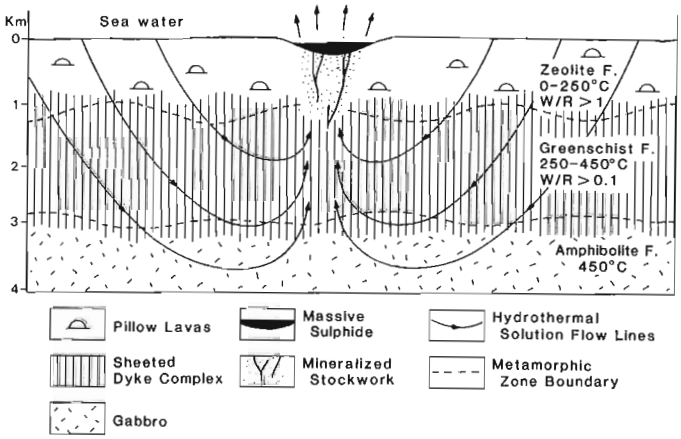

Figure 82.1. *Simple convection cell model for the genesis of the volcanogenic sulphide deposits of Cyprus, after Heaton and Sheppard (1977) and Spooner (1977).*

predicted from simple convection within an homogeneously permeable medium, each cell having a diameter of about 10 km and a depth of 3-5 km. Assuming a metal concentration of 1 ppm Cu and 15 ppm Fe in the hydrothermal solution, Solomon (op. cit.) calculated that even the largest Cyprus volcanogenic sulphide deposit could be formed in 70 000 years.

The convection cell model has found substantiation in observations on the modern oceanic crust. Based on the discrepancy between the theoretical and measured heat flow of oceanic ridges, Palmasson (1967) and Lister (1972) postulated the existence of deep circulating hydrothermal systems. Mathematical models of the heat balance (Wolery and Sleep, 1976; Crane and Normark, 1977) indicated very large volumes of water were involved which penetrated the oceanic crust for depths of up to 5 km. Direct observation of high temperature hydrothermal discharge vents on the East Pacific Rise (Francheteau et al. 1979; Hekinian et al., 1983) confirmed that high temperature (>300°C) hydrothermal activity occurs on spreading ridges and that these hydrothermal systems can give rise to localized sulphide deposits.

Although the convection cell model is an attractive mechanism for generating ore-forming hydrothermal solutions, some points of incompatability exist when it is applied to classic volcanogenic massive sulphide deposits. Amongst these is the frequency of occurrence of volcanogenic massive sulphide deposits: if volcanogenic sulphide deposits are an integral product of submarine convective hydrothermal systems, and submarine hydrothermal convective cells need only a heat source for their generation, then all submarine volcanic sequences might be expected to have associated massive sulphide deposits, which is not the case. There is also the phenomenon that volcanogenic massive sulphide deposits of many mining areas tend to occur within the same small stratigraphic interval, or at the same "favourable horizon", and this interval forms only a fraction of the total stratigraphic range occupied by the volcanic rocks (Franklin et al., 1981). This phenomenon is not a predictable consequence of the simple convection cell model. A more theoretical disadvantage is the limit to the concentration of some ore metals in a convective hydrothermal solution that can be attained by the simple leaching of rock-forming minerals. Maximum concentrations in ore solutions of metals like zinc, lead and silver, which occur mainly as diadochic substitutions in common rock-forming minerals, will be achieved when leaching takes place under conditions of low bulk water:rock ratios, at the time of mineralogical transformations of the reservoir rock, that occur independently of chemical disequilibrium between the hydrothermal solution and the rock-forming minerals e.g. during thermal metamorphism (Lydon, 1981). Cathles (1978) demonstrated that the water:rock ratio of a given volume of rock in a convective hydrothermal system increases with time, and hence the concentration of leached metals in solution can be expected to gradually decrease as convective flow continues. Optimum conditions for achieving maximum metal concentrations in solution therefore occur in a stagnant hydrothermal reservoir.

OBSERVATIONS ON THE EXTRUSIVE PART OF THE TROODOS OPHIOLITE COMPLEX

There are several features of the metalliferous deposits and their host volcanic rocks of the Troodos complex that accord with a convection cell model. By far the dominant metals are iron, in the sulphide and ochre deposits, and manganese, in the umber deposits. Both metals occur in major proportions in the potential reservoir rocks, and therefore the attainment of high concentrations in the hydrothermal solutions are not constrained by the necessity of low water:rock ratios in the reservoir zone mentioned above. The alteration pipe and stockwork mineralization immediately below the massive ore deposits do not exhibit evidence of explosive hydrothermal discharge; the grade of sulphide mineralization decreases very gradually to depths of 700 m or more with no abrupt changes to the sulphide mineral assemblage; and the width of the stockwork zone may increase with depth (Hadjistavrinou and Constantinou, 1982). These characteristics suggest that pressures of the hydrothermal system never rose above hydrostatic (i.e. no over-pressuring usually associated with static reservoir zones) and that temperature decrease or chemical changes to the hydrothermal solutions were uniform and gradual during their ascent to the seafloor through a very permeable substrate. These are characteristics to be expected of a simple convective hydrothermal system.

Within the Pillow Lavas, evidence of hydrous alteration, or of water circulation through the porous pile, is ubiquitous and usually involves the alteration of the igneous minerals to clays, or the infilling of fractures, pillow interstices and vesicles by clays, chalcedonic silica, jasper, zeolites and carbonates. In contrast, the most common expressions of hydrous involvement within the Sheeted Dykes is the weak pervasive alteration towards a greenschist facies assemblage in which actinolite is the main hydrous mineral, with only subordinate amounts of chlorite and epidote (W.R.A. Baragar, personal communication). Patches (50 cm-2 m across) of intense chloritization or veins infilled with chlorite and/or epidote, commonly containing disseminations of pyrite and/or chalcopyrite occur locally, but probably comprise less than 5 per cent of the total rock volume. The transition between zeolite facies and greenschist facies is usually close to the Pillow Lavas-Sheeted Dykes contact (on a scale of hundreds of metres) and can be as sharp as 10-20 m (Gass and Smewing, 1973). Visually, the impression is that water flow has been both more voluminous and more pervasive in the Pillow Lavas than in the Sheeted Dyke Complex, where most water flow has been restricted mainly to small well defined channels. This visual impression is corroborated by the oxygen isotope study of Heaton and Sheppard (1977) who calculated minimum water:rock values >1.0 in the Pillow Lavas but <0.1 for the Sheeted Dyke Complex.

This configuration of water:rock ratios is not compatable with the simple convection cell envisaged by Spooner (1977) for the Cyprus situation, in which flow lines originating at the sea flow penetrate deep into the Sheet Dyke Complex, where they become heated to >300°C before ascending once again to the surface to deposit massive sulphides (see Fig. 82.1). As modelled by Elder (1965) in a Hele-Shaw cell, in simple convection within an homogenously porous medium most of the flow takes place in the lower third of the convection cell, whereas in Cyprus it appears that most water circulation has taken place in the Pillow Lavas which forms the upper third of the convection cell of Figure 82.1. This leads to the suggested modifications of hydrothermal flow patterns for the Troodos oceanic crust illustrated in Figure 82.2.

HYDRODYNAMIC ZONATION OF THE UPPER TROODOS OCEANIC CRUST

Field observations do not indicate any pronounced systematic variation in the style or type of hydrous alteration or secondary mineralogy with depth in the Pillow Lavas unit. Gillis (1983) reported that the occurrence of secondary clay and zeolite minerals strongly correlated with the flow type, in which analcime, natrolite, phillipsite and gmelinite are more typical of pillowed units, whereas heulandite, mordenite and celadonite occur mainly in massive flows. This suggests that the distribution of secondary minerals is related more to the physical properties of the rock, such as porosity, rather

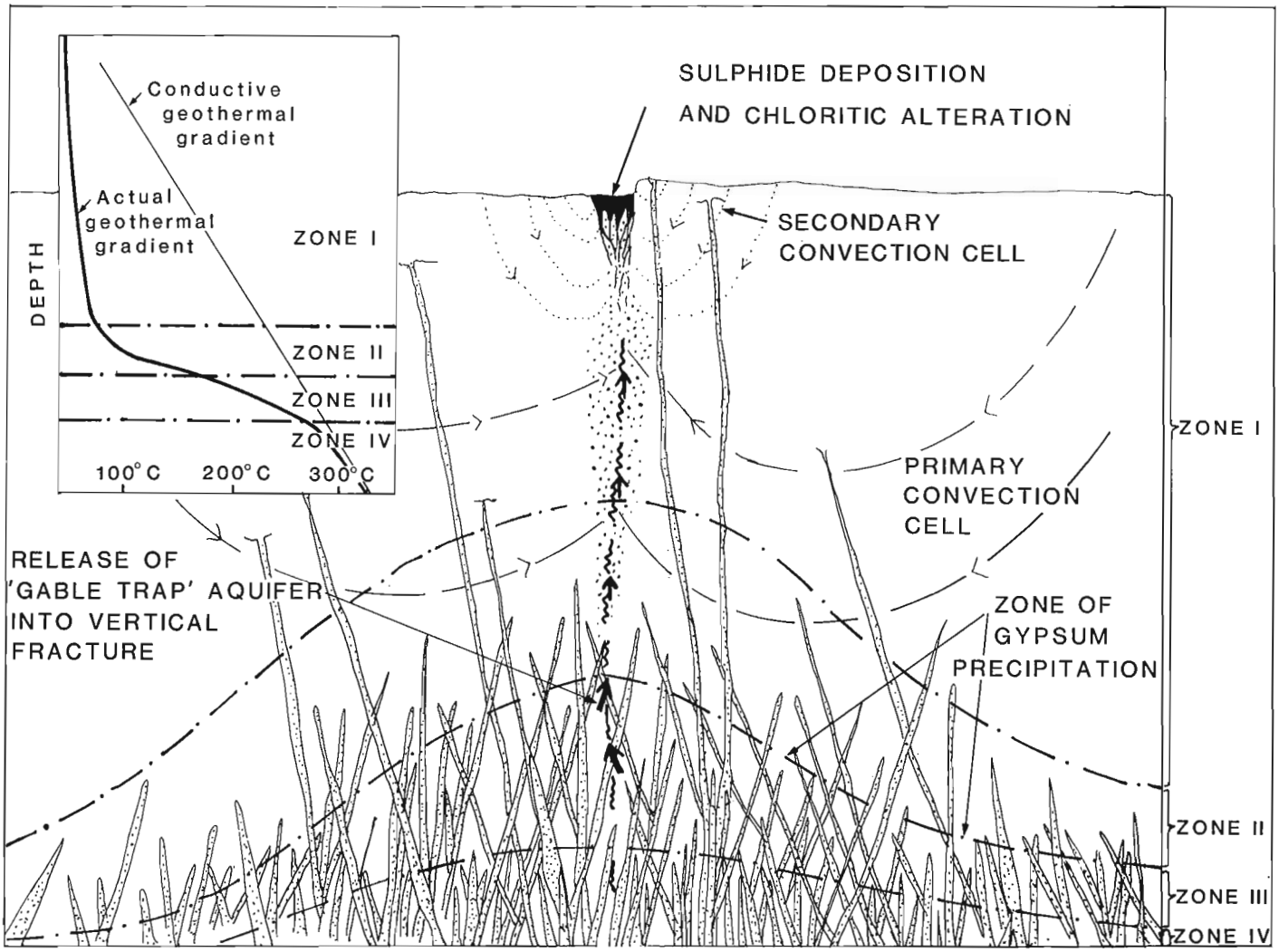

Figure 82.2. *Envisaged hydrodynamic zonation of the Troodos oceanic crust, illustrating the proposed "gable trap" model for the generation of the ore-forming hydrothermal solutions responsible for the volcanogenic sulphide deposits of Cyprus. Note that convection of seawater is largely confined to the Pillow Lavas unit. Inset: comparison of actual and "calculated" conductive geochemical gradients for the different hydrodynamic zones.*

than to the geothermal gradient or to the petrochemistry of the rocks as suggested by Table 2 of Gass and Smewing (1973).

The age of secondary minerals found in the Pillow Lavas is uncertain, although it has been assumed that they resulted from seawater circulation during Cretaceous volcanism. Sulphur isotopes of gypsum collected from fracture and vesicle infillings in the Pillow Lavas, remote from sulphide mineralization, average $\delta^{34}S = 22.6‰$ (7 samples range 21.9‰ to 23.9‰), which is quite different from the assumed value of about 17‰ for Cenomanian seawater sulphate (Claypool et al., 1980), but very close to the average value of 23.8‰ (3 samples, range 23.2‰ to 24.6‰) for gypsum from evaporites of the Miocene Pakhna Formation. This suggests that evaporitic brines of Miocene age, or groundwaters that have re-dissolved the Miocene gypsum, have circulated to depths of at least 1 km into the Pillow Lavas and deposited gypsum in the process. Similarly, the systematic increase in calcite as fracture and vesicle filling in the Pillow Lavas with proximity to the contact of the immediately overlying limestones and marls of the Lefkara Formation, may be attributable to mobilization of the calcium carbonate by relatively young groundwaters. The anomalously D-depleted and ^{18}O enriched average whole rock hydrogen and oxygen isotope values of the Pillow Lavas (Heaton and Sheppard, 1977) may suggest that low temperature waters of meteoric origin have significantly contributed to the hydrous alteration and secondary minerals of the Pillow Lavas sequence.

Lacking any evidence to the contrary it is reasonable to assume that a pronounced geothermal gradient did not exist in the Pillow Lavas sequence during submarine volcanic activity. This in turn implies a very high flux of seawater convection within the Pillow Lavas, which is termed the "primary convection cell" in Figure 82.2. The domain of the primary convection cell forms hydrodynamic Zone I (Fig. 82.2) which is characterized by high porosity, low temperatures (<50°C?) and high bulk water/rock (w/r) ratios. The effective base of Zone I is controlled by the increase with depth in the proportion of the more or less vertical

dykes in the Pillow Lavas, which would tend to act as baffles to lateral water flow and hence decrease the water flux. This decrease in water flux would in turn allow an increase in temperature. This zone at the base of the primary convection cell, characterized by high porosity, restricted water flow, and a rapid rise in rock and water temperatures, is designated hydrodynamic Zone II.

Perhaps a useful way to envisage the development of hydrodynamic Zone III is to consider a dynamic model of Troodos crust development which involves the progressive upward encroachment of the Sheeted Dyke Complex on an accumulating pile of Pillow Lavas. In turn, the Gabbro magma chambers can be considered to gradually stope upwards at the expense of the Sheeted Dyke Complex, such that the thicknesses of Pillow Lavas and Sheeted Dykes units remain relatively constant. This dynamic model is suggested by the consideration that the highly chloritized pillows, which can be found as screens between dykes even deep in the sheeted Dyke Complex, were once on the seafloor and presumably at the top of a pillow lava pile. Most of this upward migration of the Sheeted Dykes or Gabbro fronts, relative to a specific pillow of the Pillow Lavas, would presumably take place while that segment of the oceanic crust is close to the centre of active volcanism near the presumed ridge axis. This introduction of seawater into the Sheeted Dyke Complex by its upward encroachment into porous Pillow Lavas containing interstitial seawater, is an alternative mechanism to that of direct downwards flow of seawater into the Sheeted Dyke Complex of the convection cell model. Thus the observed isotopic shifts of rocks of the Sheeted Dyke Complex or the Gabbros does not necessarily indicate deep hydrothermal convection of seawater.

Individual dykes or dyke swarms of the Sheeted Dyke Complex are not parallel but tend to intersect one another at low angles. New intrusions of dykes at the top of the Sheeted Dyke Complex would therefore form "gables" at their mutual intersections, which would tend to trap the pore waters of the porous Pillow Lavas below them. Hydrodynamically, Zone III is therefore characterized by a zone of individual gable-trapped aquifers, and although free water movement may take place within the permeable Pillow Lavas of an individual aquifer itself, the movement of the trapped pore water from one aquifer to another is restricted or prohibited. Within this zone a range of individual reservoir temperatures can be expected (Fig. 82.2).

The boundary between Zone II and Zone III therefore corresponds to the base of the primary convection cell. The temperature of this boundary is uncertain, but as the onset of widespread chloritization more or less coincides with the Pillow Lava-Sheeted Dykes contact, analogy with temperatures of alteration mineralogy in modern Icelandic hydrothermal systems (Tomasson and Kristmannsdottir, 1972) suggests that a minimum of 200°C would be a reasonable estimate. The rapid rise in temperature at the base of the convection cell is significant for the precipitation of calcium sulphates and carbonates. The heating of modern seawater to >150°C causes the precipitation of calcium sulphate due to its decrease in solubility with increasing temperature (Bischoff and Seyfried, 1978). Similarly the solubility of calcite decreases with increasing temperature in aqueous solutions (Malinin, 1963). Although there are reservations in directly applying these experimental results to the Troodos situation, the probability of calcium sulphate precipitation from convecting seawater is nevertheless greatest in the zone of most rapid temperature increase at the base of Zone II. This precipitation would tend to seal the hydrothermal channelways and help in restricting water flow across the boundary between Zone II and Zone III.

The boundary between Zone III and Zone IV can perhaps be thought of as the change from rocks with a high enough porosity to contain significant volumes of hydrothermal solutions, to rocks with low porosities which are not suitable for significant aquifer systems. In practical terms, this would correspond to the decrease in the relative proportion of pillow lavas, interflow breccias etc. as the proportion of dykes rapidly increases at the top of the Sheeted Dyke Complex.

CRITERIA FOR THE GENERATION OF ORE-FORMING HYDROTHERMAL SOLUTIONS

A genetic model for the volcanogenic sulphide deposits of Cyprus must accomodate the following criteria:

1. Low water:rock ratios and mineralogical transformations in a stagnant reservoir to allow "ore-forming concentrations" of metals and sulphur in the hydrothermal solutions.
2. Solution temperatures high enough to have produced the chloritic alteration of the feeder hydrothermal alteration pipes below the massive sulphide deposits, estimated on the basis of oxygen isotopes (e.g. Heaton and Sheppard, 1977) and fluid inclusions (e.g. Spooner and Bray, 1977) to be about 300°C.
3. The sulphur isotope pattern of the volcanogenic sulphide deposits, (Clark, 1971, Hutchinson and Searle, 1971; Johnson, 1972; Lydon, 1984) which typically shows a range of $\delta^{34}S = +2‰$ to $+7‰$ within a single deposit and averages about $+5‰$.
4. The relatively oxidized state of the ore fluids (compared to other classic examples of volcanogenic massive sulphide deposits) which allowed the jasper veining common in stockwork mineralization; precluded the precipitation of pyrrhotite; and perhaps suppressed the precipitation of chalcopyrite and sphalerite to give the low grades typical of most deposits.

The proposed gable trapped aquifers provide a very convenient explanation for all four criteria (see last section of article). A basaltic mineralogy can be isothermally completely transformed to a greenschist mineral assemblage of chlorite-epidote-actinolite-albite simply by hydration. Therefore, under the conditions of the very low water:rock ratio (1:30) required for the complete alteration of a basalt by simple hydration, very high concentrations of leached metals in the remnant pore water are possible (Lydon, 1981). The weak pervasive hydration of the Sheeted Dyke complex noted above, eliminates these rocks as prime candidates for reservoirs for large quantities of ore-forming hydrothermal solutions. On the other hand, the intensely chloritized screens of Pillow Lavas, most common near the top of the Sheeted Dyke Complex, have the requisite characteristics of ore-forming hydrothermal reservoir rocks. The occurrence of major epidote-quartz zones in intensely chloritized rocks near the base of the Pillow Lavas, corresponding to the envisaged position of Zone III, may have particular significance to the identification of the ore-forming hydrothermal reservoirs for the Cyprus deposits.

FORMATION OF EPIDOTE-QUARTZ ALTERATION

Epidote-quartz alteration has been implicated in the generation of hydrothermal solutions responsible for the formation of massive sulphide deposits elsewhere. MacGeehan (1978) considered epidote-quartz alteration to represent the hydrothermal channelways for the formation of massive sulphide deposits of Mattagami area, and MacGeehan and MacLean (1980) noted that basaltic units containing these epidote-quartz zones were depleted in those elements

(Fe, Mg, Zn and possibly Cu) that formed the metasomatic enrichments in the hydrothermal alteration pipes immediately below the massive sulphide deposits. Similarly Gibson et al. (1983) considered that the quartz-epidote alteration patches within the silicified Upper Amulet Rhyolite of the Noranda area were indicative of the water-rock reactions that produced the constituents of the 'C contact' pyritic exhalite horizon.

The preponderant chemical exchange in the reaction of seawater with basalts at temperatures above 200°C is the gain of magnesium and loss of calcium by the basalt, resulting in an magnesium-rich chloritic rock (Mottl and Holland, 1978). As shown in Figure 82.3, during this metasomatism there is little change in the relative alumina proportion of the whole rock, and hence it can be assumed that alumina is relatively immobile in alteration reactions of this type. The formation of an epidote-quartz rock from a basaltic rock, on the other hand, requires the reverse of this chemical exchange and involves virtually the total loss of magnesium from the rock. To produce an epidote-quartz rock by this mechanism would require a large flux of waters with a high Ca/(Mg + Fe) ratio e.g. seawater that had previously reacted with basalt. The presence of epidote-quartz rocks would therefore indicate high water:rock ratios, which is contrary to the first criterion listed above. The weakness in this high water flux model for epidote-quartz formation is that the composition of evolved seawater in equilibrium with an altered basalt at >200°C is controlled by a chlorite bearing assemblage, and therefore unless changes in pH, PO_2, activity Ca^{++} or temperature (equation 1) are imposed upon the solution, it will not form epidote at the expense of chlorite. It is therefore considered unlikely that major zones of epidote-quartz rock up to several metres across, as observed in Cyprus, formed in an open chemical system of this type.

It is proposed that epidote-rich rocks can form within a closed chemical system as the result of the progressive equilibration of calcium minerals (e.g. calcite, gypsum), previously deposited in veins, with a chloritic host rock. Under these conditions, epidote-rich zones are indicative of mineral transformations under low water:rock ratios and therefore such rocks are potential reservoirs for the generation of metal rich hydrothermal solutions.

Applied to the Troodos situation, calcite and gypsum that were precipitated as veins or open space fillings at the base of the primary convection cell (Fig. 82.2), are trapped along with partially altered lavas and their pore waters in a gabled reservoir. The rise in temperature of the aquifer, as the consequence of the cessation of mass transfer of heat by the primary convection cell, promotes the interaction between the calcium minerals and the chemically evolving pore waters of the basalt. Chemical mass transfer is aided by the internal convection developed by the transfer of heat within the aquifer. The extremes of calcium and magnesium exchange can be represented by the conversion of chlorite to epidote (equation 1) and the chloritization of fresh basalt (equation 2) respectively. The equations are balanced so as to conserve alumina for the reason noted above. Mineral and rock compositions are listed in Table 82.1.

$$2.00\ \text{Chlorite} + 3.48\ Ca^{++} + 10.6H^{+} + 0.30O_2 \rightleftharpoons$$
$$1.89\ \text{Epidote} + 0.78\ \text{Quartz} + 5.00\ Mg^{++} +$$
$$3.78\ Fe^{++} + 10.37\ H_2O \qquad (1)$$

$$.22\ \text{Basalt} + 2.69\ Mg^{++} + 3.68\ Fe^{++} + 10.8\ H_2O \rightleftharpoons$$
$$2.00\ \text{Chlorite} + 4.99\ \text{Quartz} + 2.81\ Ca^{++} +$$
$$0.76\ Na^{+} + 5.60\ H^{+} + .03O_2 \qquad (2)$$

As can be seen by comparing equation (1) and (2), the formation of epidote is promoted by a supply of calcium and hydrogen ion, which are exactly the products of the chloritization of the fresh components of a basalt. Chemical disequilibrium between the two spatially separated parts of the same closed aquifer is maintained by the dissolution of the calcium vein minerals, which thus can be thought of as the driving force of the process (Fig. 82.4). The supply of oxygen for epidote formation is from the calcium minerals,

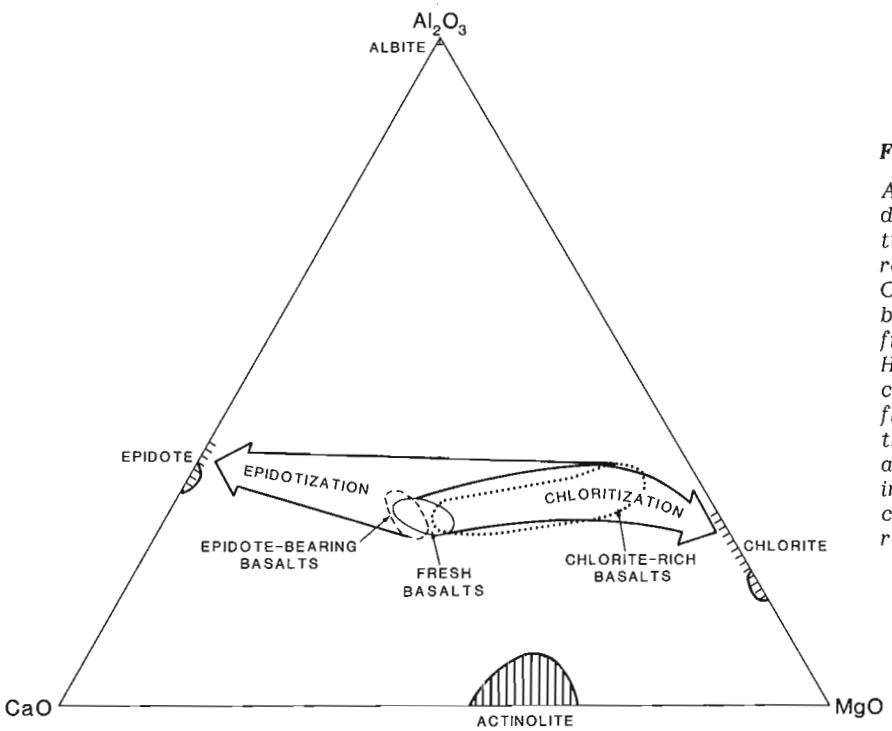

Figure 82.3

Al_2O_3-CaO-MgO mole ratio ternary diagram illustrating the relative variation of these components in a basaltic rock during hydrous alteration. Compositional fields of fresh and altered basalts from the modern ocean floor from Humphris and Thomson (1978). Hatched lines show range of mineral compositions from the modern ocean floor (Humphris and Thomson, 1978) and the Troodos ophiolite complex (Heaton and Sheppard, 1977). Enclosed areas indicate the most common mineralogical compositions from greenschist facies rocks of the Troodos complex.

Table 82.1. Compositions of minerals used in equations. Composition of epidote and chlorite are the idealized averages of samples from the Troodos complex reported by Heaton and Sheppard (1977); actinolite is the idealized average of samples from the modern ocean floor reported by Humphris and Thomson (1978); the Branch unit cell is of the basalt TR-9 from Cyprus analyzed by Robinson et al. (1983)

Actinolite	$Ca_{2.0}Mg_{3.0}Fe_{2.0}Si_{8.0}O_{22}(OH)_2$
Albite	$NaAlSi_3O_8$
Calcite	$CaCO_3$
Chlorite	$Mg_{2.5}Fe_{2.5}Al_{2.0}Si_{3.0}O_{10}(OH)_8$
Epidote	$Ca_{2.0}Fe_{0.7}Al_{2.3}Si_3O_{12}(OH)$
Basalt	$Na_{3.49}Ca_{12.82}Mg_{10.52}Fe^{2+}_{5.46}Fe^{3+}_{0.54}Al_{18.25}Si_{50.13}O_{160.0}$

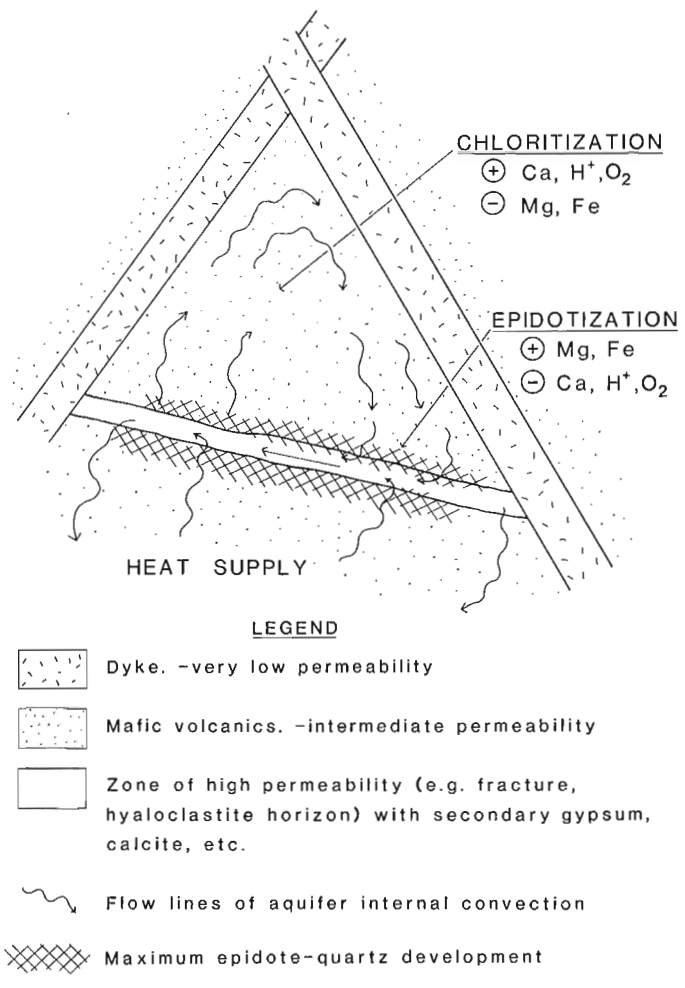

Figure 82.4. *Schematic illustration of the formation of epidote-quartz zones in mafic volcanic rocks of the Troodos complex. Signs indicate changes in the chemical composition of pore waters by the gain (+) or loss (-) of the indicated components during heating of a gable-trapped reservoir. See text for further explanation.*

but the reactions involved depend on the mineral species. For calcite, one can speculate that its dissolution is in response to the supply of hydrogen ion from the chloritization of basalt.

$$CaCO_3 + 2H^+ \rightleftharpoons Ca^{++} + CO_2 + H_2O \qquad (3)$$

Remembering that the fO_2 of a solution in equilibrium with quartz and ferromagnesian minerals is less than that of the CO_2-CH_4 equal fugacity value, the carbon dioxide would be reduced by equilibration with the solution resulting from chloritization of the basalt:

$$CO_2 + H_2O \rightleftharpoons CH_4 + O_2 \qquad (4)$$

In the case of gypsum one can speculate that it is the reduction of the sulphate in solution by equilibration with the low fO_2 solution that causes dissolution:

$$CaSO_4 + 2H^+ \rightleftharpoons Ca^{++} + H_2S + 2O_2 \qquad (5)$$

Regardless of which mineral is predominant, calcium ions and oxygen are the products in both cases, both of which in turn promote the formation of epidote.

This model has some substantiation in mineralogical and textural evidence. Visual inspection indicates that the epidote rich rocks are relatively enriched in pyrite and that the epidote has commonly undergone a late alteration to chlorite. Pyrite would be the expected product of the reaction between the hydrogen sulphide, produced during sulphate reduction (equation 5), with the iron, produced by chlorite alteration (equation 1). The late stage alteration of epidote to chlorite would follow the exhaustion of the reactant calcite or gypsum and the equilibration of epidote with pore waters produced by the chloritization of the larger mass of altered basalt. The same late stage paragenetic relationships could also result, as mentioned below, from the introduction of cooler, magnesium-bearing solutions into the aquifer.

The involvement of gypsum in the reaction is attractive because it offers an explanation for criterion 3 listed above. If it is assumed that the sulphur isotopic composition in the gable-trapped reservoir was the average of the sulphide ores ($\delta^{34}S = 5‰$ approximately), and that this value resulted from the total homogenization of all the sulphur in the hydrothermal reservoir, consisting of igneous sulphide in the basalts (250 ppm and $\delta^{34}S = 0.0‰$) and sulphur from gypsum that had the same isotopic value as coeval marine sulphate ($\delta^{34}S = 17‰$ for Cenomanian seawater – Claypool et al., 1980), then the reservoir rock would have contained about 6 wt. % gypsum. This is a reasonable figure. Furthermore, the quantity of gypsum in the rock would be directly related to the fracture intensity or porosity of the rocks and the amount of temperature increase at the base of the primary convection cell. Since these factors were probably more or less the same at the top of the Sheeted Dyke Complex everywhere, the homogenized sulphur isotope composition of all gable-trapped hydrothermal reservoirs in the Troodos oceanic crust would also be more or less the same. This explanation provides a more controlled mechanism for the similarity in the range of sulphur isotopes for different deposits than does the simple convection cell model, which must rely on similarities in the relative rates of the fractional reduction of seawater sulphate versus dissolution rates of igneous sulphide in open dynamic systems of different convection cells and to produce similar homogenized sulphur isotope ratios. Because this latter model is dependent on many more variables similar isotope ratios for different deposits is much less probable.

Assuming that during the total alteration of a fresh basalt all the calcium and magnesium goes into the formation of epidote and chlorite respectively (compositions as indicated in Table 82.1), approximately equal weight proportions of epidote and chlorite would result in a closed chemical system. If the nucleation energy of epidote is significantly higher than that of chlorite, the distribution of these minerals in the altered rock may not be homogeneous, but, as often observed, would favour epidote distribution as segregated patches of large crystals or crystal aggregates. In a dynamic closed system, this spatial separation of epidote from chlorite may be even more pronounced. As illustrated in Figure 82.4, the pore waters of the bulk rock may become supersaturated with respect to epidote due to the release of calcium from the basalt by the chloritization process. However, precipitation of epidote may be inhibited because the degree of supersaturation is insufficient to overcome the energetics of nucleation. It is only when these pore-waters migrate into the old primary convection cell channelways, where the dissolution of calcium vein minerals locally enhances the activity of calcium in solution that the degree of supersaturation becomes great enough to cause the precipitation of epidote. Once nucleation sites for epidote are established, all excess calcium may be removed from the solution in the growth of large epidote crystals. Thus a precursor calcium mineral may, in a closed system, eventually promote the siting of many times its own weight of epidote or epidote-quartz.

The presence of significant proportions of quartz probably indicates the involvement of the albite component of plagioclase feldspar in the epidotization process:

$$2.3\ \text{Albite} + 2.0\ Ca^{++} + 0.7\ Fe^{+++} + 2.4\ H_2O$$

$$1.0\ \text{epidote} + 3.9\ SiO_2 + 2.3\ Na^{+} + 3.8\ H^{+} \qquad (6)$$

This reaction gives an epidote:quartz weight ratio of about 2:1.

The presence of epidote-quartz zones in mafic rocks may thus be indicative of extensive mineral transformations under conditons of low water:rock ratios and therefore a criterion for the recognition of reservoir zones for ore-forming hydrothermal solutions in a mafic volcanic environment. Studies on the significance of epidote development in the Troodos extrusive volcanic rocks is continuing.

HYDRODYNAMIC MODEL FOR THE FORMATION OF VOLCANOGENIC SULPHIDE DEPOSITS OF CYPRUS

A proposed working model accounting for the known hydrodynamic, mineralogical and chemical constraints of the volcanogenic sulphide deposits of Cyprus is illustrated in Figure 82.2. The intrusion of dyke swarms which form the gable trapped hydrothermal reservoirs produces a local elevation in the geothermal gradient and also a topographic elevation to the effective upper boundary of the Sheeted Dyke Complex. Either of these factors would cause the localization of the upwelling part of the primary convection cell. Any waters reaching the surface from the hottest parts of this convection cell (200°C?) without any substantial decrease in temperature must have flowed upwards along zones of anomalously high cross-stratal permeability, otherwise they would have been cooled by mixing with more slowly ascending pore waters of the main Pillow Lava mass. The surface discharge of the hottest convective waters is therefore localized at the surface intersection of the zone of cross-stratal permeability. It is possible that the paragenetically early jasper veining of the stockwork ores resulted from the near surface cooling of these oxygenated convective hydrothermal solutions.

Subsequent intrusion of dykes or tectonic dislocations in the same volcanically active area, would be expected to cause fracturing of the dykes confining the gable-trapped reservoir. This fracturing would have allowed the escape of the sulphurous, metalliferous hydrothermal solutions of the trapped aquifer, either by release of fluid over-pressure or, more probably, by the convective replacement by waters from the base of the primary convection cell. The entry of cooler magnesium-bearing solutions into the gable-trapped reservoir could be responsible for the late alteration of epidote to chlorite, and also by quenching the hydrothermal solutions of the reservoir, for the precipitation of pyrite.

The upward flow of solutions from the gable-trapped reservoirs likely followed the same zones of cross-stratal permeability as those solutions from the base of the primary convection cell. There was therefore likely to have been mixing of the two different hydrothermal solutions more or less continuously from the gable-trapped reservoir to the surface. This would explain the large vertical extent of the stockwork zone and the relatively high pO_2 nature of the ore solutions (lack of pyrrhotite etc.), compared to other type-examples of volcanogenic massive sulphide deposits. The anomalously wide stockwork zone at depth, often marked by a halo of disseminated pyrite (e.g. Searle, 1972; Vokes, 1966), is attributed to the lateral dispersion of ore solutions away from the main upwelling stream, allowed by the high permeability of the Pillow Lavas. The downwards widening of many stockwork zones may perhaps best be regarded as an upward narrowing, and is attributed here to the confining effects of a secondary convection cell developed in the zone of highest porosities situated at the top of the volcanic pile, and driven by the thermal anomaly created by the hydrothermal discharge. The high temperature hydrothermal flow from the gable trapped reservoirs was likely to have been episodic, as successive separate seismic or volcanic events allowed the expulsion of solutions from adjacent but different reservoirs. On the other hand, flow of the primary convection cell, and perhaps the secondary convection cell, was more likely to have been continuous.

Thus, in detail, the thermal and hydrologic history of the hydrothermal discharge vent, now occupied by a volcanogenic sulphide deposit, is extremely complex. The sulphide deposit may have been affected by the passage of solutions of at least four different origins (the gable-trapped ore-solutions, and solutions of the primary convection cell, the secondary convection cell and post-Cretaceous groundwaters), each with their own temperature and chemical characteristics, and therefore each with their own chemical and mineralogical signatures imparted on the volcanogenic sulphide deposits and host rocks. Studies are continuing to distinguish these effects.

ACKNOWLEDGMENTS

The manuscript greatly benefitted from the critical reading and suggestions of W.D. Goodfellow. K. Nguyen is thanked for drafting the diagrams.

REFERENCES

Bischoff, J.L. and Seyfried, W.E.
1978: Hydrothermal chemistry of seawater from 25°C to 350°C; American Journal of Science, v. 278, p. 838-860.

Cathles, L.M.
1978: Hydrodynamic constraints on the formation of Kuroko deposits; Mining Geology (Japan), v. 28, p. 257-265.

Clark, L.A.
1971: Volcanogenic ores: comparison of cupriferous pyrite deposits of Cyprus and Japanese Kuroko deposits; Society of Mining Geologists of Japan, Special Issue No. 3, p. 206-215.

Claypool, G.E., Holser, W.T., Kaplan, I.R., Sakai, H., and Zak, I.
1980: The age curves of sulfur and oxygen isotopes in marine sulphate and their mutual interpretation; Chemical Geology, v. 28, p. 199-260.

Crane, K. and Normark, W.R.
1977: Hydrothermal activity and crestal structure of the East Pacific Rise at 21°N; Journal Geophysical Research, v. 82, p. 5336-5348.

Elder, J.W.
1965: Physical processes in geothermal areas: American Geophysical Union Minograph Series, No. 8, p. 211-239.

Franklin, J.M., Lydon, J.W., and Sangster, D.F.
1981: Volcanic-associated massive sulfide deposits; Economic Geology, 75th Anniversary Volume, p. 485-627.

Francheteau, J., Needham, H.D., Choukroune, P., Juteau, T., Seguret, M., Ballard, R.D., Fox, P.J., Normark, W., Carranza, A., Cordoba, D., Guerrero, J., Rangin, C., Bougault, H., Cambon, P., and Hekinian, R.
1979: Massive deep-sea sulphide ore deposits discovered on the East Pacific Rise; Nature, v. 277, p. 523-528.

Gass, I.G. and Smewing, J.D.
1973: Intrusion, extrusion and metamorphism at constructive margins: Evidence fromt he Troodos Massif, Cyprus; Nature, v. 242, p. 26-29.

Gillis, K.M.
1983: Low temperature alteration of the extrusive sequence, Troodos ophiolite, Cyprus (abstr). Geological Association of Canada, Mineralogical Association of Canada, Canadian Geophysical Union, Joint Annual Meeting, Victoria, 1983, Program with Abstracts, p. A27.

Gibson, H.L., Watkinson, D.H., and Comba, C.D.A.
1983: Silicification: Hydrothermal alteration in an Archean geothermal system within the Amulet Rhyolite Formation, Noranda, Quebec; Economic Geology, v. 83, p. 954-971.

Hadjistavrinou, Y. and Constantinou, G.
1982: Cyprus; in Mineral Deposits of Europe, Volume 2 Southeast Europe, ed. F.W. Dunning, W. Mykura and D. Slater; Mineralogical Society of London – Institute of Mining and Metallurgy, London, p. 255-277.

Heaton, T.H.E. and Sheppard, S.M.F.
1977: Hydrogen and oxygen isotope evidence for sea water hydrothermal alteration and ore deposition, Troodos Complex, Cyprus; in Volcanic processes in ore genesis; Geological Society of London Special Publication No. 7, p. 42-57.

Hekinian, R., Fevrier, M., Avedik, F., Cambon, P., Charlov, J.L., Needham, H.D., Raillard, J., Boulegue, J., Merlivat, L., Moinet, A., Manganini, S., and Lange, J.
1983: East Pacific Rise near 13°N: geology of new hydrothermal fields; Science, v. 219, p. 1321-1324.

Humphris, S.E. and Thomson, G.
1978: Hydrothermal Alteration of oceanic basalts by seawater; Geochimica et Cosmochimica Acta, v. 42, p. 107-125.

Hutchinson, R.W. and Searle, D.L.
1971: Stratabound pyrite deposits in Cyprus and relations to other sulphide ores; Society of Mining Geologists of Japan, Special Issue No. 3, p. 198-205.

Johnson, A.E.
1972: Origin of Cyprus pyrite deposits; 24th International Geological Congress, Montreal, Section 4, p. 291-298.

Lister, C.R.B.
1972: On the thermal balance of a mid-ocean ridge; Geophysical Journal of the royal Astronomical Society, v. 26, p. 515-535.

Lydon, J.W.
1981: Contributed discussion in Goldie, R. and Bottrill, T.J., Semmar on sea-floor hydrothermal systems; Geoscience Canada, v. 8, p. 93-104.

1984: Some observations on the mineralogical and chemical zonation patterns of Cyprus volcanogenic sulphide deposits; in Current Research, Part A, Geological Survey of Canada, Paper 84-1A, report 81.

MacGeehan, P.J.
1978: The geochemistry of altered volcanic rocks at Matagami, Quebec: a geothermal model for massive sulphide genesis; Canadian Journal of Earth Sciences, v. 15, p. 551-570.

MacGeehan, P.J. and MacLean, W.H.
1980: Tholeiitic basalt-rhyolite magmatism and massive sulphide deposits at Matagami, Quebec; Nature, v. 283, p. 153-157.

Malinin, S.D.
1963: An experimental investigation of the solubility of calcite and witherite under hydrothermal conditions; Geokhimiya, No. 7, p. 631-646.

Mottl, M.J. and Holland, H.D.
1978: Chemical exchange during hydrothermal alteration of basalt by seawater – I. Experimental results for major and minor components of seawater; Geochimica et Cosmochimica Acta, v. 42, p. 1103-1115.

Palmason, G.
1967: On heat flow in Iceland in relation to the mid-Atlantic Ridge; Societas Scientiarum Islandica, v. 38, p. 111-127.

Robinson, P.T., Melson, W.G., O'Hearn, T., and Schmincke, H-U.
1983: Volcanic glass compositions of the Troodos ophiolite, Cyprus; Geology, v. 11, p. 400-4.

Searle, D.L.
1972: Mode of occurrence of the cupriferous pyrite deposits of Cyprus; Transactions of the Institute of Mining and Metallurgy, Section B, p. B189-B197.

Solomon, M.
1976: "Volcanic" massive sulphide deposits and their host rocks – a review and an explanation; in Handbook of strata-bound and stratiform ore deposits, ed. K.H. Wolf; Vol. II, Regional studies and specific deposits: Elsevier, Amsterdam, p. 21-50.

Spooner, E.T.C.
1977: Hydrodynamic model for the origin of the ophiolitic cupriferous pyrite ore deposits of Cyprus in Volcanic processes in ore genesis; Geological Society of London, Special Publication No. 7, p. 58-71.

Spooner, E.T.C., Beckinsale, R.D., Fyfe, W.S., and Smewing, J.D.
1974: O^{18} enriched ophiolite metabasic rocks from E. Liguria (Italy), Pindos (Greece), and Troodos (Cyprus); Contributions to Mineralogy and Petrology, v. 47, p. 41-62.

Spooner, E.T.C. and Bray, C.J.
1977: Hydrothermal fluids of seawater salinity in ophiolitic sulphide ore deposits in Cyprus; Nature, v. 266, p. 808-812.

Spooner, E.T.C. and Fyfe, W.S.
1973: Sub-sea floor metamorphism, heat and mass transfer; Contributions to Mineralogy and Petrology, v. 42, p. 287-304.

Tomasson, J. and Kristmannsdottir, H.
1972: High temperature alteration minerals and thermal brines, Reykjanes, Iceland – Contributions to Minerology and Petrology, v. 36, p. 123-134.

Vokes, F.M.
1966: Remarks on the origin of the Cyprus pyritic ores; Bulletin of the Canadian Institute of Mining and Metallurgy, v. 59, p. 388-391.

Wolery, T.J. and Sleep, N.H.
1976: Hydrothermal circulation and geochemical flux at mid-ocean ridges; Journal of Geology, v. 84, p. 249-275.

A NOTE ON FAULTING IN THE SOUTHERN ROCKY MOUNTAIN TRENCH BETWEEN McBRIDE AND CANOE REACH, BRITISH COLUMBIA

E.M.R. Research Agreement 44/04/83

Donald C. Murphy[1]

Murphy, D.C., A note on faulting in the southern Rocky Mountain Trench between McBride and Canoe Reach, British Columbia; in Current Research, Part A, Geological Survey of Canada, Paper 84-1A, p. 627-630, 1984.

Abstract

The southern Rocky Mountain Trench has been re-examined in the area between Valemount and McBride in order to evaluate the geometry and nature of faulting. Dip-slip displacements have been documented; the possible role of strike-slip movement remains ambiguous. Restoration of the dip-slip displacements implies that the Purcell Fault(?) underlies Miette Group rocks east of the southern Rocky Mountain Trench.

Résumé

Dans la zone comprise entre Valemount et McBride, on a réexaminé la fosse du sud des Rocheuses, afin d'évaluer la géométrie et la nature du faillage. On a étudié les failles de glissement suivant le pendage; le rôle possible des failles de glissement directionnel reste ambigu. La réactivation du faillage de glissement suivant le pendage indique que la faille de Purcell(?) est sous-jacente aux roches du groupe de Miette, à l'est de la fosse du sud des Rocheuses.

The area between McBride and Canoe Reach of McNaughton Lake in east-central British Columbia (Fig. 1, 2) was re-examined in an attempt to clarify the geometry and nature of faulting in the southern Rocky Mountain Trench. Available kinematic indicators between Valemount and McBride are compatible with dip-slip rather than strike-slip fault motion within the southern Rocky Mountain Trench.

Near McBride, outcrops of Cambrian McNaughton Formation are found along both margins of the trench. This formation is faulted against Proterozoic Kaza Group along the southwestern margin, and against Proterozoic middle Miette Group rocks (correlated with the Kaza Group) along the northeastern margin (Campbell, et al., 1973; see Fig. 2, 3). Farther to the southeast, between Shere and Canoe Reach, the southwestern flank of the trench is underlain by a marble of unknown but presumed Cambrian age (Campbell, 1968; see Fig. 2, 3). This marble exhibits sufficient differences is structural style and metamorphic character, compared to both Miette Group rocks along the northeastern margin of the trench and the McNaughton Formation in the trench to the northwest, to infer a fault or faults separating the marble from these units.

The fault separating Kaza Group rocks from McNaughton Formation near McBride is interpreted to be continuous to the southeast with the inferred fault separating the marble from the Miette Group rocks near Valemount (Fig. 2). By connecting these faults, rocks in the Cariboo Mountains, which exhibit a minimum of 7 km of differential uplift between the latitude of McBride and the latitude of Valemount, are separated by a continuous fault from rocks in the Rocky Mountains which show little, if any, differential uplift along the same length. This fault is herein called the Fraser Valley Fault.

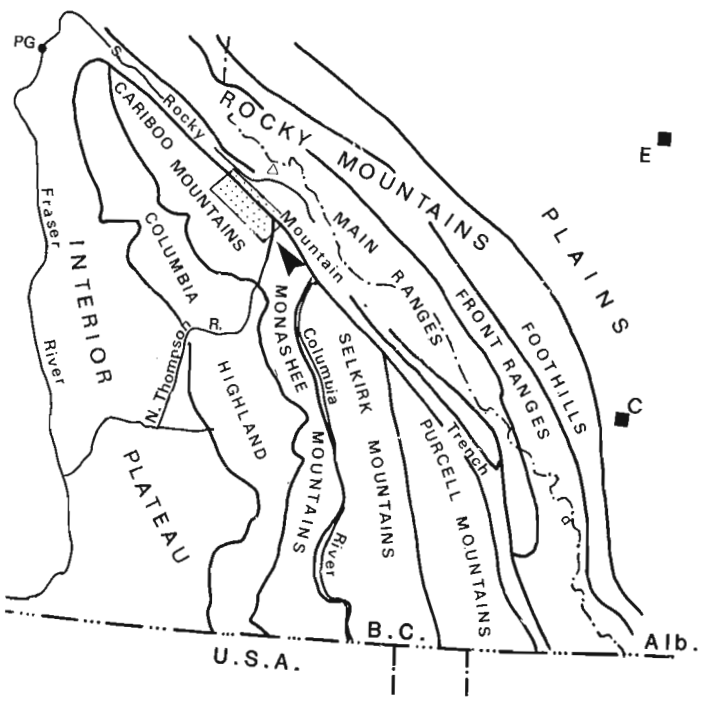

Figure 1. *Physiographic subdivisions of British Columbia. The location of Figure 2 is indicated by the dark arrow.*

[1] Department of Geology, Carleton University, Ottawa, Ontario K1S 5B6

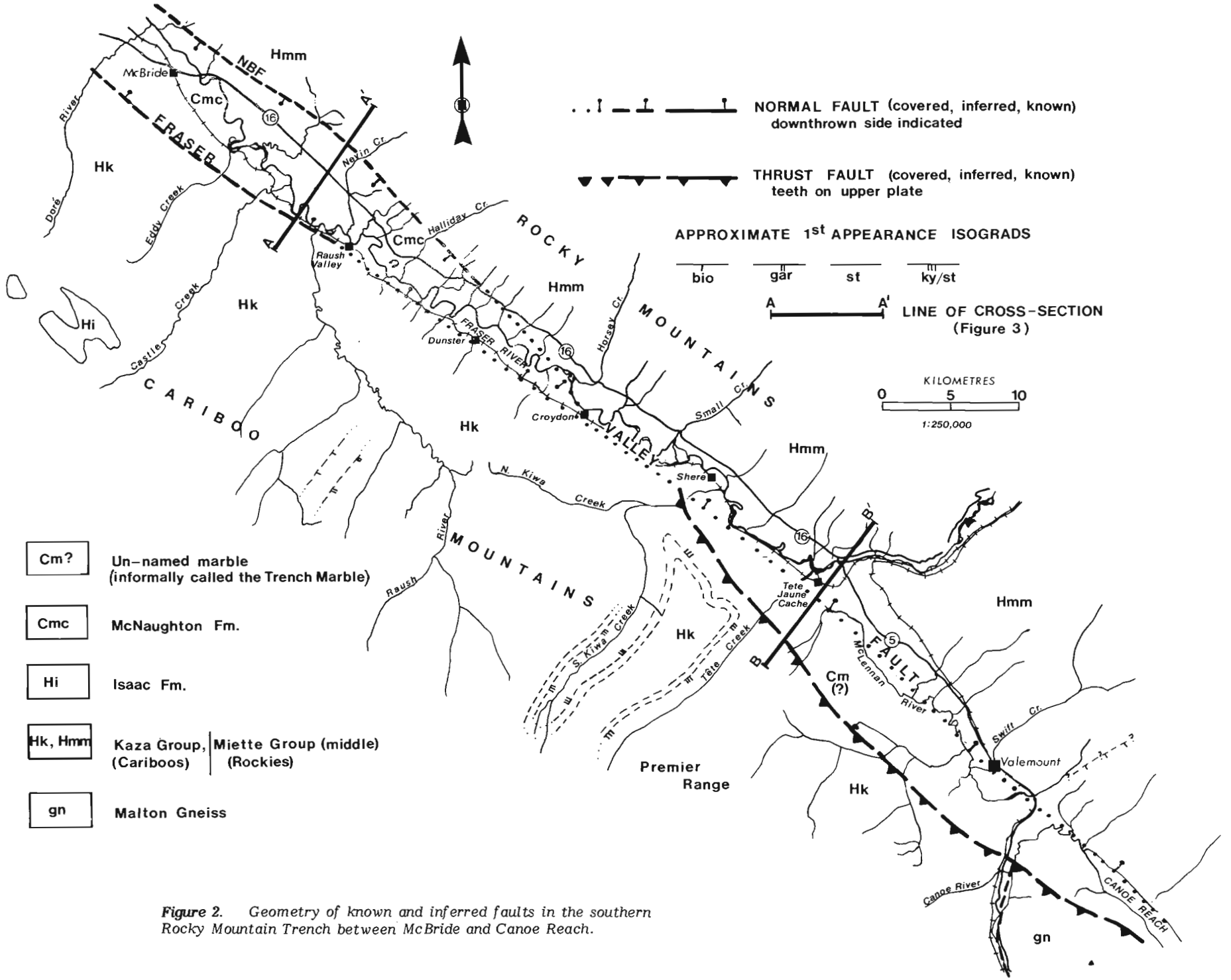

Figure 2. *Geometry of known and inferred faults in the southern Rocky Mountain Trench between McBride and Canoe Reach.*

Lack of exposure within the mapped area precludes direct observation of kinematic features along the Fraser Valley Fault. A large vertical component of displacement (approximately 7 km near Valemount, and substantially less near McBride) is required to produce the observed juxtaposition of rocks of different structural levels; the horizontal component is not known. However, this component is not likely to be large as the fault zone is constrained to a width of less than 100 m (Eddy Creek, Fig. 2). The characteristically wide zone of fault-rock and reoriented bedrock associated with major strike-slip faults is conspicuously absent.

The fault which separates McNaughton Formation from rocks of the Miette Group along the northeastern margin of the trench (Northern Bounding Fault; NBF in Fig. 2) maybe traced as far southeast as Halliday Creek (Fig. 2). Farther southeast at the mouth of Small Creek Valley along Highway 16, and on the west shore of the Fraser River at Tete Jaune Cache, Miette Group rocks appear on strike with rocks of the McNaughton Formation, indicating that the strike of the fault contact between the two units has become more northerly. This change in orientation would cause the fault to intersect the Fraser Valley Fault near Croydon. Because there is no evidence for more than one fault farther to the southeast, it is assumed that the Fraser Valley Fault truncates the Northern Bounding Fault.

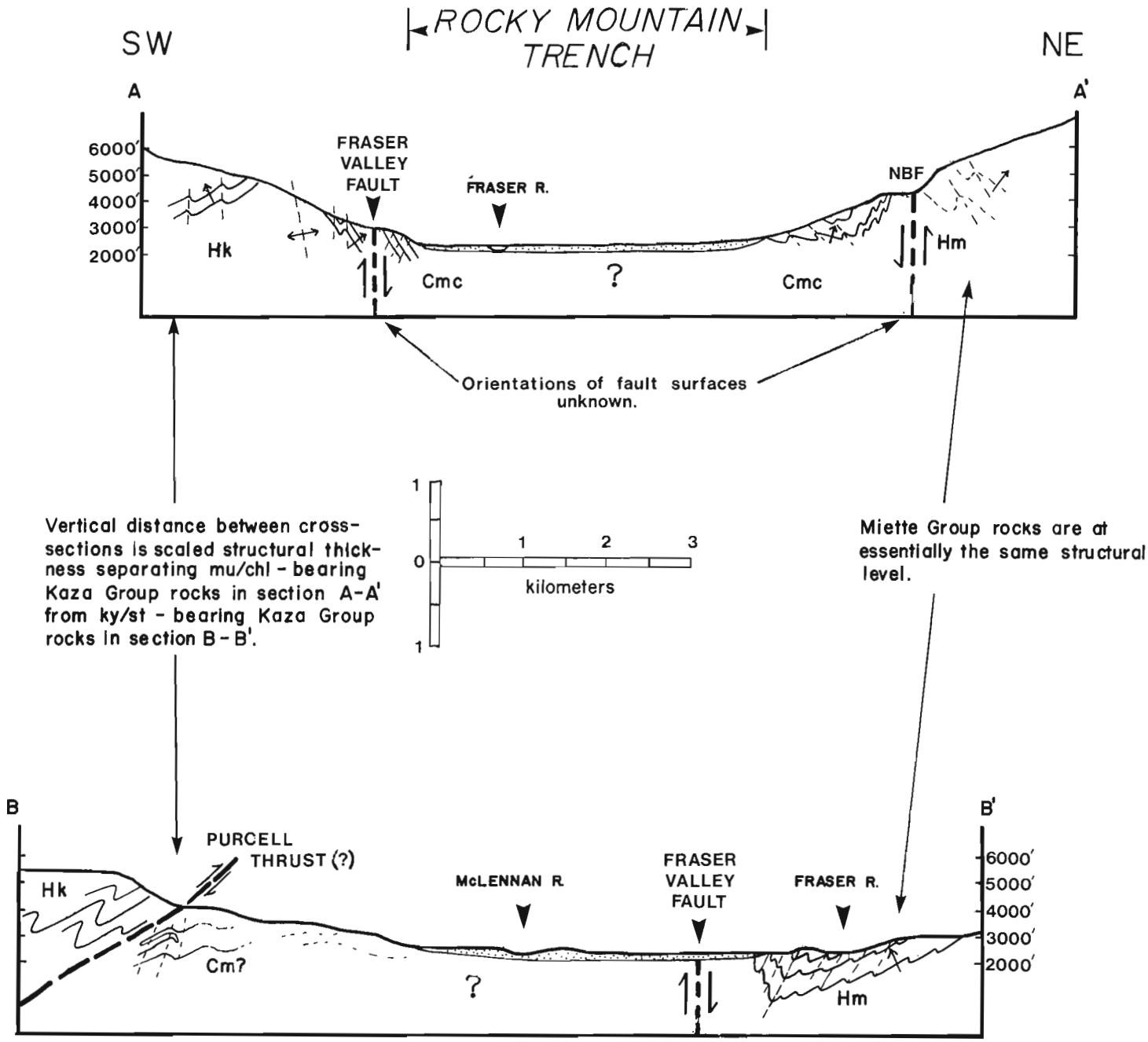

Figure 3. *Cross-sections across the southern Rocky Mountain Trench. The locations of the cross-sections are indicated in Figure 2. Symbols used are the same as in Figure 2.*

Kinematic data from the Northern Bounding Fault were not obtained because of lack of exposure. A minimum of 2.5 km of stratigraphic separation exists between Lower Cambrian rocks in the trench and those above the middle Miette Group in the Rocky Mountains. The width of the fault zone is constrained to less than 30 m on McBride Lookout Road and less than 100 m on the ridge south of the mouth of the Holmes River Valley, again suggesting that major motions were not involved.

The Cambrian (?) marble in the trench (herein referred to as the trench marble) structurally underlies kyanite- and staurolite-bearing rocks of the Kaza Group across a moderately southwest-dipping fault contact. Kinematic indicators from a mylonite zone within the marble, considered to be parallel to, and associated with, the covered fault contact, indicate east-northeasterly-directed thrusting of Kaza Group rocks over the marble (Purcell Thrust?). This thrust appears to be truncated at its northern end by the Fraser Valley Fault; Canoe Reach obscures its southeasterly continuation. Steeply dipping shear fractures oriented parallel to the strike of the trench and commonly containing down-dip fibres and slickensides crosscut the mylonites associated with the thrust, suggesting that high-angle dip-slip faulting postdated thrusting.

If the differential uplift within the Cariboo Mountains, facilitated by displacement along the Fraser Valley Fault, is removed so that only muscovite and chlorite zone rocks are exposed at the surface, stratigraphically equivalent rocks of the same metamorphic grade exist on both sides of the southern Rocky Mountain Trench. Kaza Group rocks on the west side of the trench are in the hanging wall of a thrust that contains presumed Cambrian rocks in the footwall (trench marble). In the pre-uplift configuration, this thrust would project to an approximate depth of 7 km under the trench into the subsurface under the Main Ranges. This reconstruction requires that the Proterozoic rocks along the northeastern margin of the trench, and possibly as far east as the Snake Indian Thrust on the British Columbia-Alberta border, are allochthonous with respect to a footwall containing rocks at least as young as the Cambrian. In other words, the Miette Group rocks presently exposed at the surface structurally overlie rocks at least as young as, and possibly older than, the Cambrian.

ACKNOWLEDGMENTS

This report has been greatly improved by discussions with Richard L. Brown, Gerald M. Ross, and C.J. Rees, all of Carleton University.

REFERENCES

Campbell, R.B.
1968: Canoe River, British Columbia; Geological Survey of Canada, Map 15-1967.

Campbell, R.B., Mountjoy, E.W., and Young, F.G.
1973: Geology of McBride Map Area, British Columbia; Geological Survey of Canada, Paper 72-35, 104 p.

THE AGE OF THE JURASSIC ROSSLAND GROUP OF SOUTHEASTERN BRITISH COLUMBIA

Project 750035

H.W. Tipper
Cordilleran Geology Division, Vancouver

Tipper, H.W., The age of the Jurassic Rossland Group of southeastern British Columbia; in Current Research, Part A, Geological Survey of Canada, Paper 84-1A, p. 631-632, 1984.

Abstract

The Rossland Group of southeastern British Columbia, based on a re-study of fossil faunas collected to date, has a more restricted age range than previously thought. Now, on reasonable grounds, the group is considered to be Early and Late Sinemurian, Early Pliensbachian and Early Toarcian.

Résumé

Selon une nouvelle étude de la faune fossile découverte jusqu'à maintenant, le groupe Rossland de la partie sud-est de la Colombie-Britannique se trouverait dans une fourchette d'âges beaucoup plus restreinte qu'on ne le croyait auparavant. Il est maintenant raisonnable de considérer que ce groupe date du Sinémurien inférieur et supérieur, du Pliensbachien inférieur et du Toarcien inférieur.

Recent work in southeastern British Columbia, involving interpretation of tectonic and plutonic history and radiometric ages related thereto, creates some conflicts with the published paleontological ages of the formations of the Rossland Group. In order to clarify the situation, without entering into a discussion of tectonics, a re-examination of the paleontologial evidence was carried out and the results are presented here. Aside from a brief visit in 1978 to the southern part of the Nelson map area for fossil collecting, the writer is unfamiliar with the area and is relying on the work of H.W. Little and his several publications relating to the topic as the basis for discussion.

In a recent paper, Little (1982, p. 13-21) described the Rossland Group as including three formations, Archibald, Elise and Hall, and the Ymir Group. He recorded the important facts regarding their nomenclatural evolution, lithological features, structural relations, and, most importantly for this paper, their ages and fossil content. Because no fossils have as yet been found in the Ymir Group, its age will not be discussed here. The writer believes there have been some errors in dating because of poor preservation of many specimens and because of inadequate knowledge of Canadian ammonite faunas at the time Little was doing his original mapping in the area. This paper is in no way a criticism of earlier work but a reconsideration of the evidence based on advances in our understanding of Cordilleran tectonics and Canadian Jurassic ammonoid faunas in other areas.

Some important facts about the Rossland Group and its formation follow; the reader is referred to Little's publications (Little, 1950, 1960, 1962, 1963, 1965, 1982) for complete details on the units, particularly GSC Paper 79-26. The oldest formation of the Rossland Group, the Archibald, is characteristically "hard brittle, dark grey to black argillaceous siltstones and arenaceous argillites .... the beds are distinctly laminated". (Little, 1982, p. 15). The sediments are tuffaceous. The Elise Formation, which is predominantly volcanic, overlies the Archibald apparently conformably in one area but in another grades laterally into it (Little, 1982, p. 16). It is mainly flow breccia, lava, agglomerate, tuff, and related intrusives. Feldspar porphyry and augite porphyry predominate. In general the volcanics are andesitic or basaltic. The Hall Formation is characteristically soft, fissile black carbonaceous shale and buff to brown argillaceous sandstone. It is structurally conformable or, in places, erosionally unconformable on the Elise. Frebold (1959; Frebold and Little, 1962) considered that the ammonites in the Rossland Group ranged from Hettangian to younger than Early Bajocian (= Middle Bajocian of Frebold).

Little's most recent interpretations of the internal structural relations indicate much thrust faulting and this, coupled with poor exposures of the Rossland Group, makes it difficult to be confident of the succession at many localities. What had been called the Upper Rossland Group (Frebold and Little, 1962; Little, 1965) he now interprets as an overthrust plate of Elise Formation (Little, 1982, p. 15).

The Archibald Formation has yielded several collections with **Arnioceras** (= **Arniotites**). In the Salmo area Frebold (Frebold and Little, 1962, p. 15) identified **Arnioceras kwakiutlanus** (Crickmay) indicating an Early Sinemurian age. He also identified "**Arnioceras** (**Melanhippites**) sp. indet." (Frebold, 1959, p. 6) which he later recognized as an echioceratid (Frebold and Tipper, 1970, p. 4); it is now thought to be a synonym of **Paltechioceras** sp. Its presence in the Salmo area indicates that part of the Archibald Formation is of Late Sinemurian age. In a collection apparently below a reliable Early Sinemurian locality three genera were found (Frebold and Little, 1962, p. 14), two of which were generically and specifically indeterminable and one was compared doubtfully to **Gyrophioceras?**. Because of its apparent position below an Early Sinemurian locality and a doubtful generic identification, the fauna at the locality was suggested to be of questionable Hettangian age. Many gaps are present in the measured sections and structural complexities may exist. The preservation of the forms is such that no reliable identifications should be attempted but, as both Early and Late Sinemurian forms are now known to occur in the Archibald Formation, the three unidentified forms are more reasonably compared with several Sinemurian genera than with Hettangian genera, particularly as Hettangian fossils are not known with certainty in British Columbia. The only reliable age for the Archibald Formation is Early and Late Sinemurian.

In the Rossland-Trail area, the volcanic Elise Formation has yielded fossils of Sinemurian age. The ammonite **Arnioceras** (= **Arniotites**) is the only genus recognized but, as preservation is poor, other genera may also be present. The presence of **Arnioceras** argues for an Early Sinemurian age. As already stated by Little (1982, p. 18) "The Elise Formation is partly younger, and partly contemporaneous with the Archibald Formation". There is no fossil evidence to suggest it is younger than Sinemurian.

The Hall Formation is entirely sedimentary and rests on the Elise Formation conformably (Little, 1960, p. 70) or with erosional unconformity (Mulligan, 1952, p. 6). In the Salmo area **Harpoceras** cf. **H. exaratum** Young and Bird has been identified associated with aptychi (Frebold and Little, 1962, p. 17, Plate II). In the Rossland-Trail area the Hall Formation has yielded **Dactylioceras** sp. (Little, 1982, p. 19). An Early Toarcian age for the Hall Formation is indicated as stated by Frebold. In addition a Bajocian age and a younger age were suggested for two other collections. The Bajocian age was based on the suggested identification of "**Sonninia**?" but, as the collection is a single, highly distorted imprint specimen, the Bajocian age is questionable. The specimen could as reasonably be compared to **Haugiella** of Late Toarcian age, recently found in the Queen Charlotte Islands but even this is inconclusive. The collection of supposedly younger than Bajocian age was originally identified as several specimens of **Perisphinctes**? sp. indet. A re-examination of this collection indicates the presence of three or more genera, namely **Crucilobiceras, Coeloceras,** and one as yet undetermined. They bear a close resemblance to species of these genera from Oregon (Smith, 1981) and from Queen Charlotte Islands where they are of Early Pliensbachian age. The only reliable age determination for the Hall Formation is therefore Early Pliensbachian and Early Toarcian.

Based on the most reliable faunal evidence available, the Rossland Group is comprised of volcanogenic and partly contemporaneous Elise and Archibald formations of Early and Late Sinemurian age and the overlying sedimentary Hall Formation of Early Pliensbachian and Early Toarcian age. This makes the stratigraphy of the group compatible with the Jurassic stratigraphy of the Quesnellia terrane (Tipper, 1982) with similar Sinemurian volcanics in the Bonaparte Lake, Quesnel Lake, and Aiken Lake areas and possibly others. Totally sedimentary Pliensbachian, Toarcian, and Bajocian strata of this terrane, similar to the Hall Formation, are known near Ashcroft, and in Bonaparte Lake, Quesnel, Quesnel Lake, Prince George, and Fort St. James map areas. It seems reasonable therefore to include the Rossland Group in the Quesnellia terrane.

REFERENCES

Frebold, H.
1959: Marine Jurassic rocks in Nelson and Salmo areas, southern British Columbia; Geological Survey of Canada, Bulletin 49.

Frebold, H. and Little, H.W.
1962: Paleontology, stratigraphy, and structure of the Jurassic rocks in Salmo map-area, British Columbia; Geological Survey of Canada, Bulletin 81.

Frebold, H. and Tipper, H.W.
1970: Status of the Jurassic in the Canadian Cordillera of British Columbia, Alberta, and southern Yukon; Canadian Journal of Earth Sciences, v. 7, no. 1, p. 1-21.

Little, H.W.
1950: Salmo map-area, British Columbia; Geological Survey of Canada, Paper 50-19.

1960: Nelson map-area west half, British Columbia (82F W½); Geological Survey of Canada, Memoir 308.

1962: Trail map-area; Geological Survey of Canada, Paper 62-5.

1963: Rossland map-area, British Columbia; Geological Survey of Canada, Paper 63-13.

1965: Geology, Salmo, British Columbia; Geological Survey of Canada, Map 1145A.

1982: Geology of the Rossland-Trail map-area, British Columbia; Geological Survey of Canada, Paper 79-26.

Mulligan, R.
1952: Bonnington map-area, British Columbia; Geological Survey of Canada, Paper 52-13.

Smith, P.L.
1981: Biostratigraphy and ammonoid fauna of the Lower Jurassic (Sinemurian, Pliensbachian and Lower Toarcian) of eastern Oregon and western Nevada; unpublished Ph.D. thesis, McMaster University, Hamilton, Ontario.

Tipper, H.W.
1982: Jurassic and Lower Cretaceous displaced terranes of the Canadian Cordillera (Abstract); Geological Association of Canada, Cordilleran Section in Rocks and Ores of the Middle Ages – Symposium, Program and Abstracts.

SEDIMENT SAMPLING OF BEACHES ALONG THE MACKENZIE DELTA AND TUKTOYAKTUK PENINSULA, BEAUFORT SEA

Project 720101

M. Lawrence [1], B.R. Pelletier, and G. Lacho [1]
Terrain Sciences Division

Lawrence, M., Pelletier, B.R., and Lacho, G., Sediment sampling of beaches along the Mackenzie Delta and Tuktoyaktuk Peninsula, Beaufort Sea; in Current Research, Part A, Geological Survey of Canada, Paper 84-1A, p. 633-640, 1984.

Abstract

Sixteen representative beaches along the southeastern Beaufort Sea are described and illustrated from the standpoint of morphology, erosion, and sediment transport. This is part of a larger fisheries research program (Department of Fisheries and the Oceans) which is designed to gain information on the sensitivity of these beaches to erosion and oil contamination. Detailed textural analysis on 46 beach samples reveals the undercutting action of waves on shore cliffs that are undergoing thermal degradation and slumping. Fine sediment is removed by the waves and transported easterly by oceanic longshore currents towards Amundsen Gulf or to local sediment sinks lying east or west of the beach source. A strong beach armour of coarse pebbles, cobbles, and a few boulders characterizes most beaches on the mainland. Beaches on the barrier islands are mainly sand. Removal of beach armour should be prevented, and finer granular material should be removed with utmost precaution, particularly in those areas where replenishment is slow or perhaps where the loss cannot be replaced by wave action or longshore currents.

Résumé

On a décrit et illustré, du point de vue de la morphologie, des processus d'érosion et du transport sédimentaire, seize plages représentatives du sud-est de la mer de Beaufort. On a effectué ce travail dans le cadre d'un programme plus vaste (dirigé par le ministère des Pêches et Océans) conçu pour nous renseigner sur la sensibilité de ces plages à l'érosion et à la contamination par le pétrole. Des analyses détaillées des textures effectuées sur 46 échantillons provenant de ces plages, révèlent le travail de sapement exercé par les vagues sur les falaises côtières soumises à des processus d'érosion thermiques et par décollement. Les sédiments fins sont arrachés par les vagues et transportés vers l'est par les courants océaniques littoraux, en direction du golfe d'Amundsen ou de zones de sédimentation situées à l'est ou à l'ouest des plages qui fournissent les sédiments. La plupart des plages bordant le continent ont un solide pavage de galets grossiers accompagnés de quelques blocs. Les plages des cordons littoraux sont principalement sableuses. On doit éviter le retrait du pavage d'estran, et n'enlever les matériaux granulaires fins qu'avec les plus grandes précautions, surtout là où l'engraissement des plages est lent, et où parfois le démaigrissement ne peut être comprensé par l'action des vagues ou des courants littoraux.

INTRODUCTION

As part of a fisheries research program undertaken by the Department of Fisheries and Oceans, Western Region, 54 beaches along the coast of the outer Mackenzie Delta and Tuktoyaktuk Peninsula were visited. Sixteen beaches (Fig. 1), being representative of the area, were sampled at 46 sites between July and September of 1979 and 1980 for the purpose of detailed textural analysis of the sediments. Morphological profiles drawn for five beaches are given in Figure 2.

The purpose of our work was to determine the nature of the sediment being eroded and transported along the coast, and to make preliminary evaluations of the energy involved in the working of the beach environment. This information will be used in the long-term fisheries research study (Lawrence et al., in press) to help to assess the sensitivity and vulnerability of the beach environment to oil contamination (after Gundlach and Hayes, 1978) and to make recommendations regarding the appropriateness and effectiveness of various beach clean-up techniques if ever needed. Through the determination of the organic content of the beach sediments, the contribution of organic matter to the estuarine ecosystems from the terrestrial environment will also be addressed in the long-term fisheries research program.

Biological and oceanographic sampling done in the nearshore environment in conjunction with the beach investigation has been discussed by Lawrence et al. (in press).

Lewis and Forbes (1975) described beach materials, the distribution of sediments, and coastal transport in the study area; much of their information has been included in Worbets (1979). Both these studies relied primarily upon qualitative field observations and photographic interpretation. Most recent coastal investigations include an annotated video tape record of the beaches and foreshore from Herschel Island to Cape Dalhousie (E. Owens, Woodward-Clyde, Victoria, B.C., unpublished data); the beach and longshore current descriptions were made based upon photographic interpretation and observations made from an aircraft.

Comprehensive terrain mapping of the Beaufort coastlands was carried out by Rampton (1974) who provided descriptions and origins of landforms, soils, glacial deposits, and fluvial and coastal sediments. Glaciation and sea level history are further amplified by Forbes (1980) and Rampton (1982). The work of these investigators, together with that of C.P. Lewis, J.R. Mackay, B.C. McDonald, and W.H. Mathews (see Rampton, 1982), has provided us with much of our knowledge of glaciation, thermal history, and sea level movements in the Beaufort-Mackenzie region. Collectively, these workers have constructed the physical and time framework for understanding the interaction of the natural processes and their effects on producing the present coastline and its associated landforms, beaches, and sediments.

[1] Freshwater Institute, 501 University Crescent, Winnipeg, Manitoba R3T 2N6

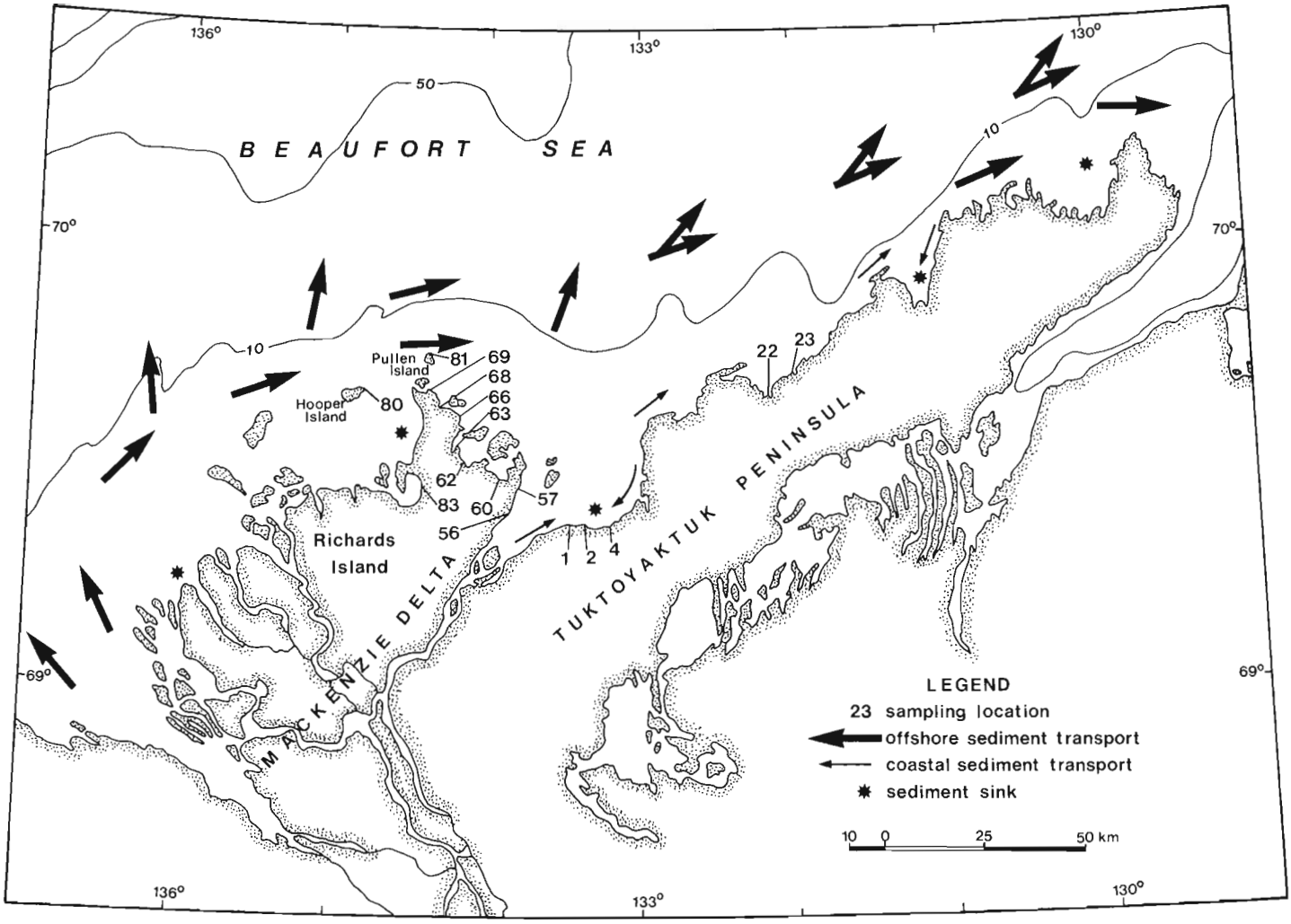

Figure 1. The southeastern Beaufort Sea, showing the beaches studied in the Mackenzie Delta (Richards Island), adjacent barrier islands (Hooper and Pullen), and adjacent Tuktoyaktuk Peninsula. Direction of offshore sediment transport is shown (after Pelletier, 1975; Bornhold, 1975), as well as local inshore movement and locations of sediment sinks (after Lewis and Forbes, 1975).

METHODS

At each coastal location, a transect representative of the surrounding area was extended from the water's edge to the interface between the permanent plant community and the beach. Samples were obtained by combining randomly selected hand-scoops from each of five 20 x 100 cm sectors of 1 m^2 grid laid on the beach (Fig. 3) at points (sites) along the transect (Fig. 4, 5). Grid placement was made to include the following beach zones: subtidal-intratidal interface, intratidal zone, flat beach zone, and supratidal zone. A photographic record was made of each grid site and larger materials such as cobbles and boulders were noted. Samples were frozen to prevent degradation of organic material and shipped to the Freshwater Institute, Winnipeg, for analysis. Beach profiles (Fig. 2) were visually estimated with the aid of a metre stick.

The F.A.S.T. analysis of sediment texture procedure (Rukavina and Duncan, 1970) was used to determine the particle size distribution of the beach grid samples. Organic material was determined by quantifying duplicate subsample weight loss after heating at 500°C for 16 hours.

LOCALITY DESCRIPTIONS

The beach locations sampled varied in their exposure to wind, wave action, and ice of the Beaufort Sea, and the resultant erosional or depositional energies of those forces.

Active slumping as a result of surf energy and probably some ice gouging (scouring) during winter, was observed at locations 57, 60, 62, 63, 68, and 69 on Richards Island (Fig. 1). Where large-size granular material, such as cobble and boulder, was present in the parent mainland material, beach armour of undetermined thickness was present (locations 57, 62, 63, 69). This provided some temporary protection of the beach cliffs against further erosion during the open water season (Fig. 3-6).

Beach material at the barrier island locations (Locations 80, Hooper Island, and 81, Pullen Island) appeared to be transported from the adjacent island landmasses which were actively eroding as a result of thaw and wave processes. Location 1, on the southern shore of Kugmallit Bay, appeared to be a site of active transportation of sediments as evidenced by spit formation. Locations 2 and 4, just east of

location 1, were in sheltered locations and appeared to be sediment sinks (Lewis and Forbes, 1975). The presence of vast quantities of driftwood in these embayments was noted. The fine sand beach at location 22 is a depositional site where sand dunes were observed. Active erosion by surf action of a low, sandy gravel cliff along the coast at location 23 and subsequent transport of fine materials have resulted in an extensive, clean gravel beach.

Locality descriptions are summarized in Table 1.

SAMPLE DESCRIPTIONS

Generally, samples contained sand and gravel, the latter commonly as coarse particles such as cobbles, with minor amounts of silt. Clay occurs in negligible amounts or is absent entirely. The cobbles have not been described petrographically, but their shapes are consistent with those that have been transported by glaciers and rounded by running water. Many are faceted, having a typical flat-iron aspect with rounded edges. Others are ellipsoidal and well rounded.

An inspection of the textural data in Table 2 reveals the abundance of the various classes of sediments. In the beaches of the barrier islands, sand is the most

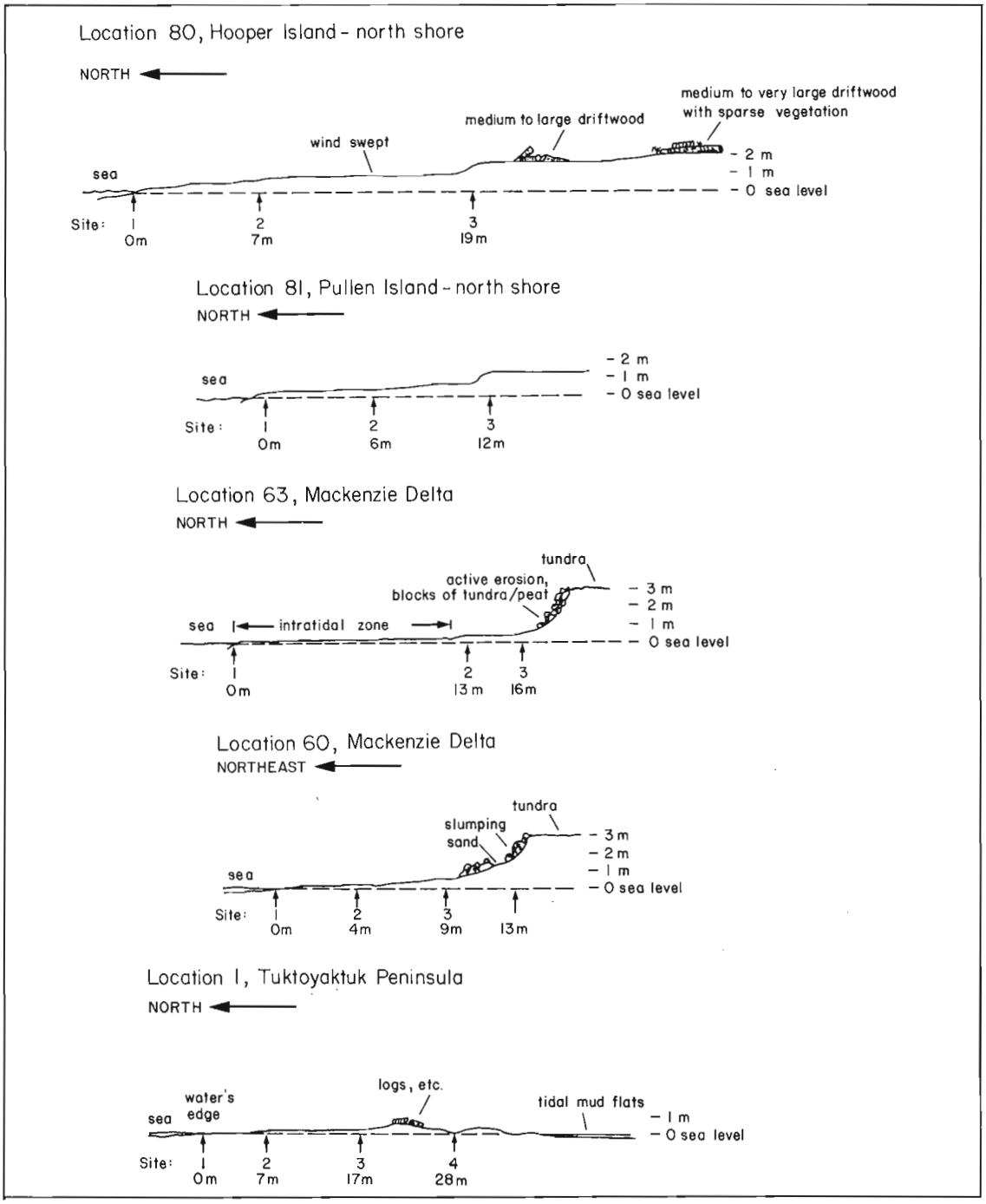

Figure 2. *Morphological profiles of five representative beaches are shown. Except for the eroding cliffs, the general character of these profiles is one of very low relief.*

Table 1. Location and description of beach sampling sites (cf. Fig. 1)

Location	Date	Exposure	Site	Beach description
BARRIER ISLANDS				
80-Hooper Island	7 July 80	North	1	Shoreline; sandy beach with some gravel.
			2	7 m from shoreline; top of 0.7 m rise from shore; medium sand and some gravel.
			3	19 m from shoreline; sand and cobble; medium to large driftwood; no vegetation.
81-Pullen Island	6 Aug. 80	North	1	Shoreline; sandy beach with some gravel.
			2	6 m from shoreline; 0.2 m rise from shore; sand with some gravel.
			3	12 m from shoreline; 1.3 m rise from shore; flat, featureless; no vegetation.
OUTER MACKENZIE DELTA				
69-Richards Island	8 Sept. 80	East	1	Narrow beach at the base of a slumping 6 m-high cliff on the shore of a breached lake; sandy gravel beach with some cobble.
68-Richards Island	8 Sept. 80	Northeast	1	Sandy beach at the base of a slumping shoreline of a breached lake.
66-Richards Island	8 Sept. 80	Northeast	1	Sand/gravel spit; sample taken from exposed side of spit.
63-Richards Island	5 July 80	North	1	Shoreline; mud with some gravel.
			2	Normal high tide line 13 m from shore; wave washed pebble-cobbles, 10 to 70 mm diameter, underlain by sand/mud; no sample taken.
			3	16 m from shoreline; wave and wind eroded beach at the base of a 3 m-high cliff.
62-Richards Island	4 July 80	North	1	Shoreline; sand/gravel.
			2	Intertidal zone; 25 m from shoreline; approximately 0.3 m relief; sand with some gravel.
			3	50 m from shoreline; normal high tide/beach interface.
			4	65 m from shoreline; edge of stream.
			5	Stream edge at base of cliff.
			6	Large cobble beach at base of 8 m-high cliff.
60-Richards Island	3 Aug. 80	North	1	Shoreline; sandy gravel.
			2	4 m from shoreline; top of intertidal, 0.1 m elevation.
			3	9 m from shoreline; at base of 3 m-high eroding cliff.
57-Richards Island	3 July 80	East	1	Shoreline; hard packed sand.
			2	85 m from shoreline; fine sand, some silt; tidal flats.
			3	135 m from shoreline; sand, gravel; tidal flats.
			4	140 m from shoreline; transition between intertidal and beach; coarse sand.
			5	150 m from shoreline; high water line, affected by storm surges; abundant driftwood.
56-Richards Island	2 Aug. 80	South	1	Shoreline; sand/gravel.
			2	5 m from shoreline; 0.5 m elevation above shoreline.
			3	9 m from shoreline; 0.9 m elevation above shoreline; beyond driftwood line; vegetation.
			4	17 m from shoreline; 0.7 m elevation above shoreline; vegetation.
83-Richards Island	6 July 80	South	1	Shoreline; sand/gravel.
			2	10 m from shoreline; 0.8 m elevation above shoreline; coarse sand with cobble pavement.
			3	15 m from shoreline; 1.1 m elevation above shoreline; some vegetation.
TUKTOYAKTUK PENINSULA				
1-Kugmallit Bay	1 Aug. 79	North	1	Shoreline; pebble beach with some cobble and sand.
			2	7 m from shoreline; high tide line; pebble beach with some cobble and sand.
			3	17 m from shoreline; worked by wind and storms; pebble, cobble, sand beach.
			4	28 m from shoreline; beyond driftwood; lower elevation than beach.
2-Kugmallit Bay	28 June 79	North	1	Shoreline; cobble, pebble, sand beach; moss growing on cobbles.
			2	10 m from shoreline; cobble, pebble, sand beach; vegetation present.
			3	26 m from shoreline; high tide line; pebble and very coarse sand; driftwood.
			4	40 m from shoreline; beginning of permanent vegetation cover; medium sand.
4-Kugmallit Bay	28 June 79	North	1	Shoreline; pebble beach.
			2	12 m from shoreline; grassy/mud interface; scattered driftwood.
22-Hutchison Bay	18 July 79	North	1	Shoreline; sand beach.
			2	2 m from shoreline; high tide line; sand beach with some gravel.
			3	4 m from shoreline; sand beach above high tide line.
			4	12 m from shoreline; at edge of sand dunes; bordered by sedges.
23-Tuktoyaktuk Peninsula	18 July 79	North	1	Shoreline; cobble and pebble beach.
			2	5 m from shoreline; pebble beach with some cobble.
			3	9 m from shoreline; pebble beach with some sand; some vegetation present.
			4	14 m from shoreline; near base of eroding gravel/sand cliff.

important constituent. The sand content ranges between 53.3 and 98.8% with specific sites having 72.6, 88.3, and more than 98% sand. Gravel is the chief secondary component of the sediment, with sites containing 46.7, 26.9, 11.6, and less than 2% gravel. The silt/clay component is the least abundant, comprising no greater than 0.5% of the samples at each site.

In the beach sediments of the outer Mackenzie Delta, sand is generally the most important material, although 5 of the 24 sites examined contained gravel as the principal sediment. All other sites were characterized by the secondary abundance of gravel. Only 6 sites contained more than 1% silt/clay, of which one had 29.4% and the other five had contents ranging between 1.3 and 5.6%. The silt/clay content in the remaining 18 sites of the outer delta was less than 1%.

Along the beaches of Tuktoyaktuk Peninsula, gravel is a more important component than on the beaches of the barrier islands or the outer Mackenzie Delta. Of the 16 sites samples, gravel content is high at 10 sites, whereas sand is

Table 2. Size analysis (weight per cent) and per cent organic content of beach sediments. Particulate classification according to the Wentworth scale.

BARRIER ISLANDS

	Location 80 - Hooper Island			Location 81 - Pullen Island		
Particulate (%)	Site 1	Site 2	Site 3	Site 1	Site 2	Site 3
Gravel	0.9	0.7	46.7	1.8	11.6	26.9
Sand	98.8	98.8	53.3	98.1	88.3	72.6
Silt/clay	0.3	0.5	0.2	0.1	0.1	0.5
Organic (% of total)	2.4	3.0	3.1	2.3	2.9	2.2

OUTER MACKENZIE DELTA

	Loc. 69	Loc. 68	Loc. 66	Loc. 63	
Particulate (%)	Site 1	Site 1	Site 1	Site 1	Site 3
Gravel	35.3	9.6	42.3	54.2	53.9
Sand	64.4	89.6	57.6	42.8	46.0
Silt/clay	0.4	0.8	0.1	3.0	0.1
Organic (% of total)	2.6	1.3	2.7	4.4	5.7

	Location 62				Location 60		
Particulate (%)	Site 1	Site 2	Site 3	Site 5	Site 1	Site 2	Site 3
Gravel	75.7	19.6	83.6	0.1	39.5	8.9	0.0
Sand	24.6	79.1	16.3	70.5	60.8	91.0	99.9
Silt/clay	0.7	1.3	0.1	29.4	0.7	0.1	0.1
Organic (% of total)	4.8	1.7	1.2	4.9	3.0	1.7	1.7

	Location 57				
Particulate (%)	Site 1	Site 2	Site 3	Site 4	Site 5
Gravel	0.1	0.2	38.3	2.9	5.0
Sand	99.7	98.4	59.6	97.0	94.4
Silt/clay	0.2	1.4	2.1	0.1	0.6
Organic (% of total)	3.0	3.6	2.9	2.9	1.9

	Location 56				Location 83		
Particulate (%)	Site 1	Site 2	Site 3	Site 4	Site 1	Site 2	Site 3
Gravel	34.0	50.8	35.7	0.1	49.9	82.7	77.3
Sand	65.9	49.1	64.1	94.3	50.0	17.2	22.6
Silt/clay	0.1	0.1	0.2	5.6	0.1	0.1	0.1
Organic (% of total)	2.3	1.6	1.2	1.8	0.7	2.5	1.7

TUKTOYAKTUK PENINSULA

	Location 1			
Particulate (%)	Site 1	Site 2	Site 3	Site 4
Gravel	99.8	97.2	96.7	88.0
Sand	0.2	2.8	3.3	9.8
Silt/clay	<0.1	<0.1	<0.1	2.2
Organic (% of total)				

	Location 2				Location 4	
Particulate (%)	Site 1	Site 2	Site 3	Site 4	Site 1	Site 2
Gravel	70.8	64.1	35.3	0.3	88.7	81.6
Sand	27.0	33.2	64.7	99.7	10.7	17.8
Silt/clay	2.2	2.7	0.0	0.0	0.6	0.6
Organic (% of total)	-	16.8	-	1.1	-	-

	Location 22				Location 23	
Particulate (%)	Site 1	Site 2	Site 3	Site 4	Site 3	Site 4
Gravel	1.3	4.5	0.6	0.0	97.2	97.5
Sand	98.5	95.3	99.4	99.9	2.8	2.4
Silt/clay	0.2	0.2	0.0	0.1	0.0	0.1
Organic (% of total)	1.5	1.0	1.3	2.8	1.5	3.5

high in the remaining 6 sites. Silt/clay varies from less than 0.1% to 16.8%. This is approximately the same proportion described for the delta and barrier islands. The combination of erosive forces, which includes the winnowing action by waves and the removal of fine sediments by currents, is operational on all beaches cited in Tables 1 and 2.

The organic content of site samples ranged from <0.1 to 16.8%, but commonly was between 1.5 and 3.5%. The exceptionally high (16.8%) organic matter content occurred at a beach in a sheltered, sediment-sink embayment (location 2).

DISCUSSION

Most of the local source material is derived from the erosion of adjacent cliffs along the coast. These cliffs comprise glacial drift and glacial outwash material, and are retreating due to the action of wave erosion following thermal degradation and subsequent slumping. This sediment is scoured by waves, and the fine material, such as clay and fine silt, is transported along the shore by marine currents (Pelletier, 1975; Lewis and Forbes, 1975).

Under the influence of the Coriolis force, the main direction of sediment transport over the inner shelf of the southeastern Beaufort Sea is easterly towards the Arctic Archipelago (Fig. 1). This movement is indicated from a study of coastal landforms, such as spits which grow easterly

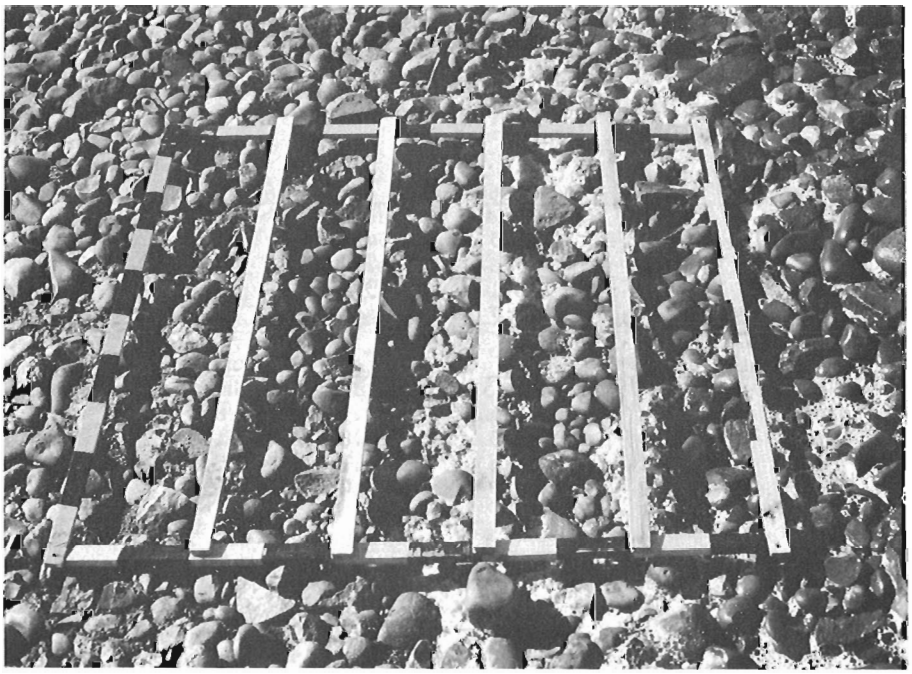

Figure 3

Sampling grid placed over a cobble beach. The 1 m^2 grid is divided into five 20 x 100 cm sectors. Cobbles display faceted aspect and have a waterworn, flat-iron shape. Some cobbles have split due to impact with other cobbles under the action of high energy waves.

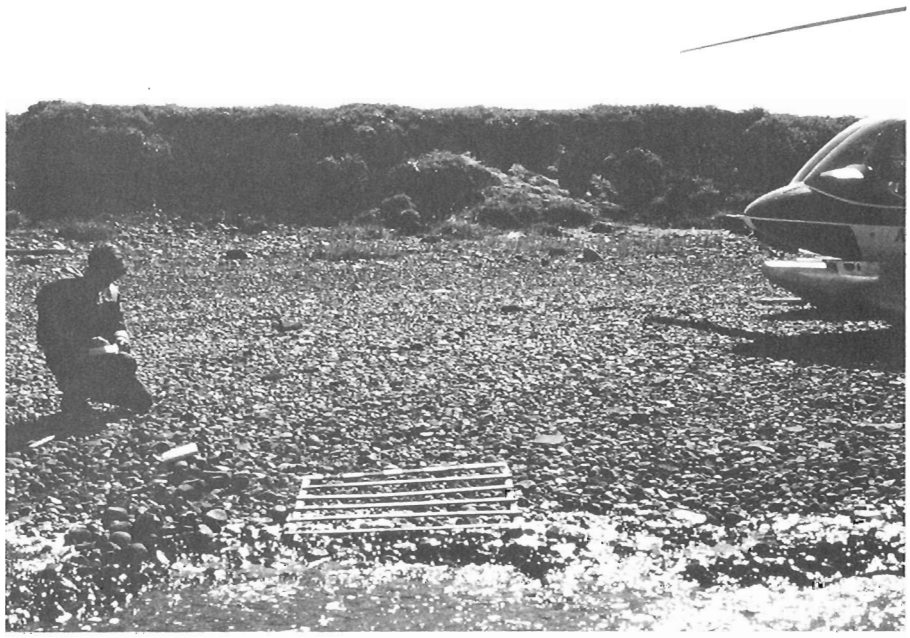

Figure 4

Sampling grid at water's edge of well armoured beach face. A small 3 m-high cliff having slump blocks of vegetation (some tundra) in the background, contains sand and various mixtures of other sediments (Mackenzie Delta).

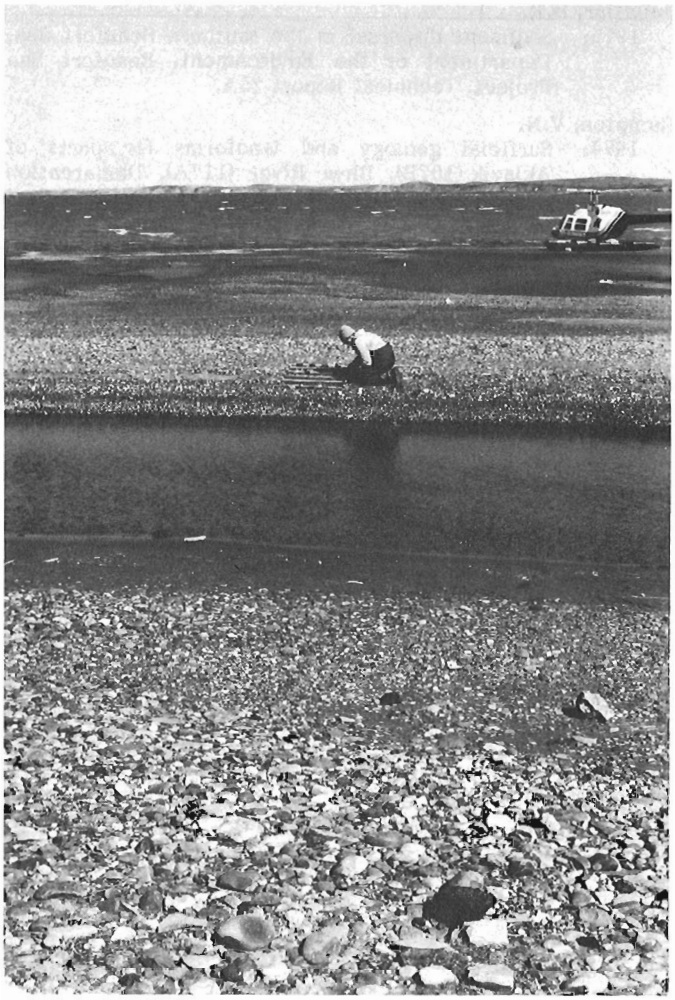

Figure 5. Sampling on Richards Island at the edge of a small stream (site 62, Fig. 1). Sand, coarse gravel, and an armour of heavy cobbles are present.

Figure 6. Beach on Richards Island (site 63, Fig. 1) consists mainly of light armour of pebbles and cobbles; some muddy sand occurs at shoreline. Note the ice eroding the shoreline of Richards Island in background.

from island and mainland points and headlands; it is further supported by the easterly movement of the sediment plume discharged by Mackenzie River, as seen in satellite imagery (Pelletier, 1975). Some coastal landforms, however, are eroded by ice and waves (Fig. 6); some coastal debris may be carried westerly as well as easterly and results in the formation of local sediment sinks (Fig. 1) which are described by Lewis and Forbes (1975).

Protective beaches at the bases of eroding cliffs help to minimize the effect of surf action. The removal of this granular beach material for construction aggregate would hasten cliff erosion with subsequent increases in waterborne particulates. Removal of beach armour from these areas should be prevented. Perhaps more suitable sites for granular material borrowing would be at depositional areas where the loss would eventually be replaced by wave action and longshore currents. In any case, the selection of shore sites for granular material should be done so with the utmost consideration for the long-term downstream effects of removal. Similar precautions have been expressed by McDonald and Lewis (1973) in their study of coastal erosion and sedimentation along the Yukon coast.

ACKNOWLEDGMENTS

We wish to thank the following for their assistance in the field, laboratory, and office: from the Freshwater Institute, B. Fallis and G. McKinnon gave field assistance; N. Strange and R. Erickson performed laboratory analyses; and S. Ahlgren carefully prepared and typed the original tables of data and manuscript. We thank our colleague T.W. Anderson for reviewing the report. Finally we are most grateful to the Polar Continental Shelf Project for providing their fine logistical and helicopter support for the field work.

References

Bornhold, B.D.
1975: Suspended matter in the southern Beaufort Sea; Department of the Environment, Beaufort Sea Project, Technical Report 25b, 30 p.

Forbes, D.L.
1980: Late Quaternary sea levels in the southern Beaufort Sea; in Current Research, Part B, Geological Survey of Canada, Paper 80-1B, p. 75-87.

Gundlach, E.R. and Hayes, M.O.
1978: Classification of coastal environments in terms of potential vulnerability to oil spill damage; Journal of Marine Technology, v. 12, no. 4, p. 18-27.

Lawrence, M.G., Lacho, G., and Davies, S.
– A survey of the coastal fishes of the southern Beaufort Sea; Fisheries and Oceans, Fisheries and Aquatic Sciences, Canadian Technical Report. (in press)

Lewis, C.P. and Forbes, D.L.
1975: Coastal sediments, southern Beaufort Sea; Department of the Environment, Beaufort Sea Project, Technical Report 24.

McDonald, B.C. and Lewis, C.P.
1973: Geomorphic and sedimentological processes of rivers and coast, Yukon coastal plain; Environmental-Social Program, Northern Pipelines, Task Force on Northern Oil Development, Report No. 73-39.

Pelletier, B.R.
1975: Sediment dispersal in the southern Beaufort Sea; Department of the Environment, Beaufort Sea Project, Technical Report 25A.

Rampton, V.N.
1974: Surficial geology and landforms for parts of Aklavik (107B), Blow River (117A), Demarcation Point (117C), Herschel Island (117D); Geological Survey of Canada, Open File 191, scale 1:125 000.

1982: Quaternary geology of the Yukon coastal plain; Geological Survey of Canada, Bulletin 317, 49 p.

Rukavina, N.A. and Duncan, G.A.
1970: F.A.S.T. – Fast analysis of sediment texture; Proceedings of the 13th Conference on Great Lakes Research, International Association for Great Lakes Research, p. 274-281.

Worbets, B.W.
1979: Shoreline oil spill protection and cleanup strategies: southern Beaufort Sea, Manual and Appendix; Arctic Petroleum Operators' Association, Calgary, Alberta, Project No. 136.

QUATERNARY GEOLOGY OF SOUTHWESTERN SASKATCHEWAN

Project 830024

R.W. Klassen
Terrain Sciences Division, Calgary

Klassen, R.W., Quaternary geology of southwestern Saskatchewan; in Current Research, Part A, Geological Survey of Canada, Paper 84-1A, p. 641-642, 1984.

Abstract

Three surface tills occur in the Cypress Hills area of southwestern Saskatchewan. A paleosol in till and loess suggests that the till plain in the east-central part predates the last glaciation, as does a quartzite-rich till on pediments flanking the Cypress Hills in the northwestern part. The youngest till forms a humocky moraine along the northwestern margin of the area.

Résumé

On a identifié trois tills superficiels dans la région de Cypress Hills, dans le sud-ouest de la Saskatchewan. L'examen d'un paléosol formé dans un till et des loess, suggère que la plaine de till du secteur est-central s'est formée avant la dernière glaciation, de même que le till riche en quartzite des sédiments bordant les collines Cypress dans le secteur nord-ouest. Le till le plus récent forme une moraine bosselée le long de la marge nord-ouest du secteur.

INTRODUCTION

Two weeks were spent on field reconnaissance in the Cypress area (Fig. 1) by W.J. Vreeken of Queen's University and the author. This project has been undertaken to map the surficial deposits of the Cypress Hills (72 F) area at 1:250 000 scale and to prepare a regional map at 1:500 000 scale. The Quaternary stratigraphy of the region will be studied with particular focus on establishing criteria for determining relative and absolute age differences of surface tills in this region. Studies concerning soil development and the nature of postglacialsediments in selected parts of the regions will be undertaken by specialists and students. This approach may resolve some of the long-standing controversies concerning the extent of the Late Wisconsin glaciation in this part of Saskatchewan and adjacent parts of Alberta and Montana.

PROGRESS AND RESULTS

A preliminary airphoto interpretation of the Cypress area, plotted on 1:50 000 scale base maps, was field checked in detail in the northwestern part. The transition from the highest part of the unglaciated Cypress plateau to the adjacent glaciated terrain is readily identified on airphotos where relatively young glacial deposits flank the plateau. Where older glaciated terrain occurs, the differences are much more subtle and pediments sloping gently northwards appear hardly modified by glacial deposits.

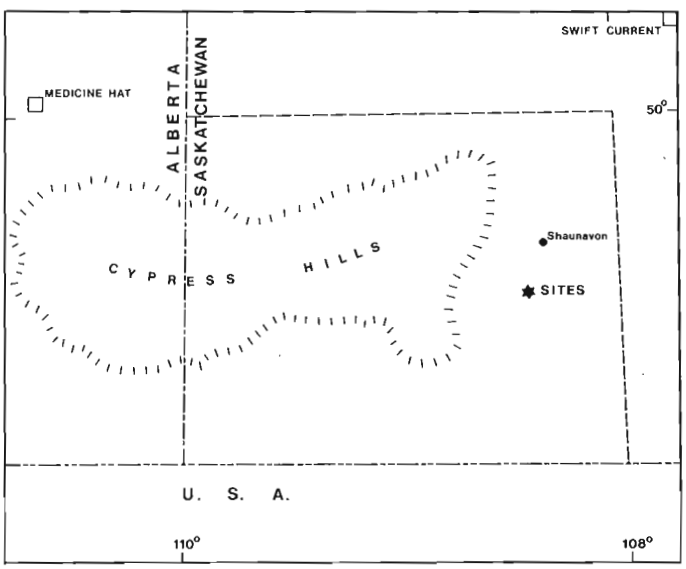

Figure 1. *Location of the Cypress area in southwestern Saskatchewan. The area lies adjacent to Alberta and Montana and is bounded by 50° N to the north and 108° W to the east. Sites indicate location of Figures 2-4.*

Figure 2. *Fresh roadcuts, 1 to 1.5 m deep, across the till plain south of Shaunavon, Saskatchewan (NW 1/4 sec. 25, Tp. 6, Rge. 19, W3). Sites 1 and 2 are described in Figures 3 and 4.*

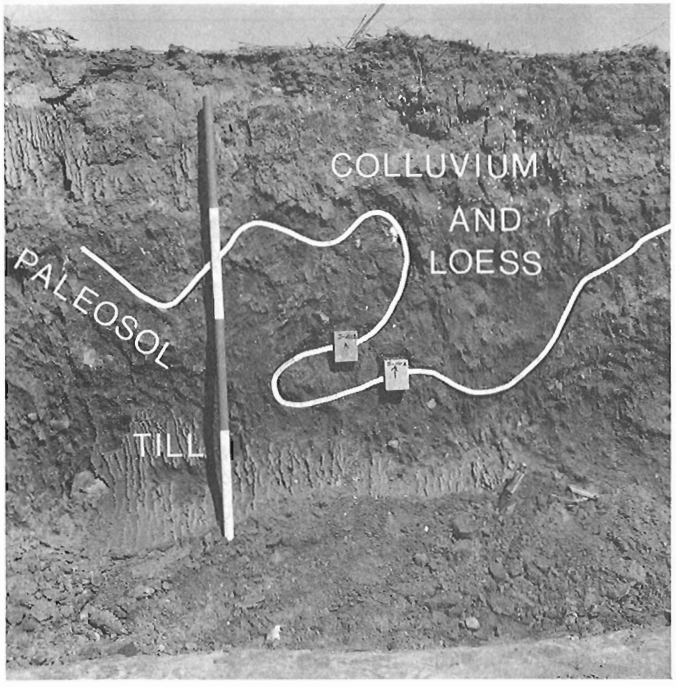

Figure 3. *Roadcut at site 1 (Fig. 2) exposes till overlain by colluvium and loess. Outlined is the convoluted nature of the contact between the till and overlying sediments. Units on rod are 1 foot.*

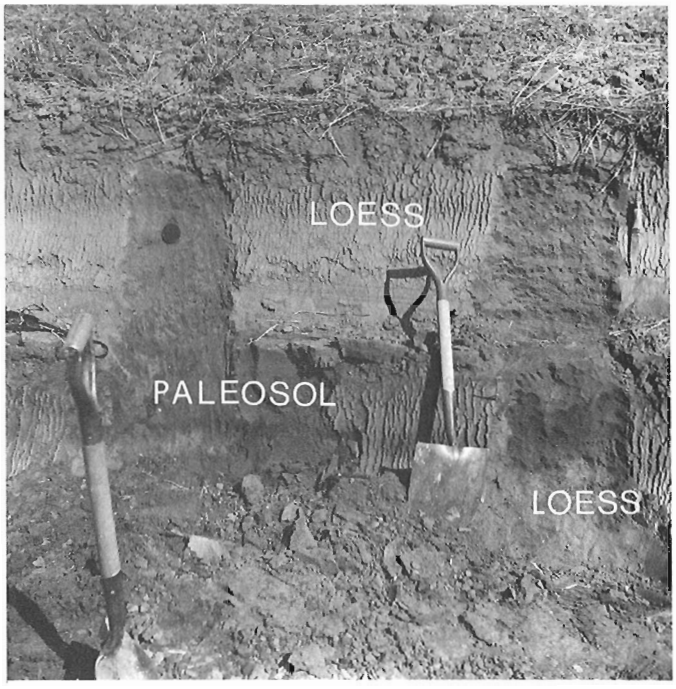

Figure 4. *Roadcut at site 2 (Fig. 2) exposes paleosol in older loess overlain by loess with modern soil development. Shovel is about 1 m long.*

Two distinctive surface tills occur in the northwestern part of the study area north of the Cypress Hills. The oldest surface till occurs along the lower margins of the pediments flanking the Cypress Hills. It typically is dark greyish brown (2.5Y 4/2, moist)* and is high in quartzite pebbles. The youngest till forms a broad belt of hummocky moraine along the northern margin of this part of the area. Its olive brown (2.5Y 4/4, moist) colour and high content of shield and carbonate pebbles is typical of much of the surface till in this region.

The till on the plains surrounding the Cypress Hills appears similar over much of the study area. However fresh roadcuts in a locality in the east-central part expose a paleosol and near-surface structures that suggest that this part of the plain, unlike the belt of hummocky moraine to the north, predates the last glaciation. The paleosol is developed in till and loess (Fig. 2-4). It can be traced from the crest of a low rise where it is developed in dark greyish brown (2.5Y 4/2, moist) till, across a gentle slope and into a shallow depression where it is developed in loess (Fig. 2). Colluvium and loess about 0.5 m thick cover the paleosol on the low rise; loess of about the same thickness covers the paleosol in the depression. Convoluted structures that involve the till, paleosol, and part of the overlying colluvium appear to be cryoturbations (Fig. 3) resulting from post-paleosol periglacial conditions. A higher degree of near-surface weathering than noted in the hummocky moraine to the north is also reflected by the soft, crumbly state of small granitic pebbles in the till and by the noncalcareous nature of the loess. The sediments, structures, and soil development seen in these exposures suggest that glaciation was followed by a sequence of climatic events that entailed loess deposition, the development of a grassland soil, periglacial conditions, loess deposition, and the formation of the modern soil profile.

* Munsell colour chart

PLEISTOCENE-HOLOCENE BASIN SEDIMENTATION, EAST COAST OF CANADA

Project 750038

G. Vilks
Atlantic Geoscience Centre, Dartmouth

Vilks, G., Pleistocene-Holocene basin sedimentation, east coast of Canada; in Current Research, Part A, Geological Survey of Canada, Paper 84-1A, p. 643-646, 1984.

Abstract

Methane is generated in shelf basins that have a high sedimentation rate of fine grained sediment, which leads to reducing conditions a short distance below the sediment-water interface. Foraminifera are well preserved in such environments. Benthic foraminifera in cores from Emerald Basin (Scotian Shelf) and Cartwright Saddle (Labrador Shelf) suggest low salinity shelf water at the time of deglaciation. The transition to more diverse postglacial foraminiferal assemblages is a widely correlated ecostratigraphic boundary.

Résumé

Le méthane se forme dans des bassins de la plate-forme continentale, où la vitesse de dépôt des sédiments à grain fin est rapide, et où apparaissent donc des conditions réductrices à peu de distance au-dessous de l'interface entre les sédiments et l'eau. Les foraminifères sont bien conservés dans ce type de milieu. Les foraminifères benthiques que contiennent des carottes de forage prélevées dans le bassin d'Emerald (plate-forme de Scotian) et sur le bombement de Cartwright (plate-forme du Labrador) semblent indiquer qu'à l'époque de la déglaciation, l'eau recouvrant la plate-forme avait une faible salinité. La transition vers des assemblages de foraminifères post-glaciaires plus diversifiés est une frontière écostratigraphique avec laquelle ont été établies de nombreuses corrélations.

INTRODUCTION

This project was initiated to explore the possibility of using foraminifera to explain sedimentary features in Late Wisconsinan-Holocene piston cores. It was feld that basic paleoenvironmental information on the continental shelf could add to the understanding of sedimentary processes and help establish Quaternary stratigraphy. This would complement acoustic stratigraphy that, with the advent of high resolution seismic surveys, had became a major tool to distinguish glacial from interglacial sediments on the continental shelf. Samples were collected primarily from basins and structural depressions where sediments presumably accumulated in a continuous sequence. The approach to the study was interdisciplinary involving geochemistry, sedimentology and paleoceanography in addition to foraminiferal ecology.

The objectives of this project, as originally defined, were to: 1) describe the Pleistocene-Holocene sedimentary history of the continental shelves of eastern Canada using paleontological and geochemical evidence from sedimentary basins; 2) improve the understanding of the genesis of gaseous hydrocarbons in sediments; and 3) establish the nature of geological environments favourable for the preservation of microfossils (Phase I). The objectives were subsequently modified to: 1) describe Pleistocene-Holocene sedimentary processes, 2) develop Late Quaternary foraminiferal ecostratigraphy; and 3) establish glacial limits and the chronology of deglaciation in the marine environment (Phase II).

During the first phase, processes responsible for the origin and preservation of methane and foraminifera in basin sediments in a subarctic cold-temperate environment were identified. Foraminifera are well preserved in shelf basins that accumulate fine grained sediment and organic matter. The second phase produced paleoceanographic models of Emerald Basin and Cartwright Saddle (Fig. 1) during deglaciation, and established a major Late Glacial/Postglacial ecostratigraphic boundary in the sediments off eastern Canada as well as some areas off Scandinavia.

Although the three objectives of both phases are related to each other, the ensuing work led to the emphasis of the second objective in each phase. The other objectives were followed only to provide environmental setting and better understanding of processes for the main objective.

SCIENTIFIC HIGHLIGHTS

Geochemical processes

Methane in excess of 16 000 ppm was produced and trapped in Late Glacial/Early Postglacial sediments of small basins off eastern Canada (Rashid and Vilks, 1975, 1977; Vilks and Rashid, 1977). The presence of high methane content in these marginal marine to normal marine sediments was not associated with evidence for high rates of organic production or reducing conditions in the water column, or at the sediment-water interface. A fast sedimentation rate of fine debris created a favourable environment for reducing conditions below the sediment-water interface and is the major cause for the presence of methane in this subarctic cold-temperate environment.

Foraminiferal ecology

The foraminiferal species found in the Labrador Shelf sediments occur in much shallower water elsewhere on the North American continental shelf (Vilks, 1980; Vilks et al., 1982). The deeper occurrences reflect the low bottom salinities of the Labrador Current along the inner shelf and support the view that along the continental margins foraminiferal distributions are controlled by salinities rather than depth of water. This is important baseline information for foraminiferal transfer functions describing paleosalinities (Mudie et al., in press).

Paleoceanography

During the time of deglaciation, benthic foraminiferal assemblages suggests that the salinities of bottom waters in Emerald Basin, Scotian Shelf, were lower by approximately 10‰ (Vilks and Rashid, 1975). Evidence for reduced salinities during late glacial time is also found in the Cartwright Saddle, on the Labrador Shelf (Vilks and Mudie, 1978). Most species of late glacial foraminifera in both of these middle shelf basins are similar, suggesting that during the period of deglaciation, an extensive zone of low salinity shelf water was present over most of the continental shelf off eastern Canada.

In Lake Melville, Labrador, foraminiferal assemblages reflect postglacial shallowing of sill depth to the lake (Vilks and Mudie, 1983). Marine maximum is represented by continental shelf faunas, which were replaced by the present-day restricted faunas as the sill depth progressively became shallower. During the last 5000 years, the depth of the sill has been within the halocline, and therefore small changes in sill depth have profound changes in bottom salinity of Lake Melville. Given a sufficient understanding of halocline response to tidal and runoff influences, paleoecological and paleoceanographic changes can be used to estimate post-glacial rebound rates in Hamilton Inlet. Figure 2 shows how Late Holocene uplift rates in the Narrows deduced by Fitzhugh (1972) are extended to the Early Holocene on the basis of paleoceanographic criteria in Lake Melville. Lacking time series oceanographic data, the paleo-ceanographic model has been related only to changing sill depths between the present and 8000 BP. On the basis of these data, a possible isostatic rebound curve at the Narrows in Hamilton Inlet has been extended to the marine transgression maximum around 8000 BP. The isostasy at the Narrows will be readdressed when more time series data on salinity and temperature at the sill are available.

Reworking of shelf sands during changing oceanographic conditions through the late glacial and postglacial has been inferred from surface textures of sand grains (Vilks and Wang, 1981; Wang et al., in press).

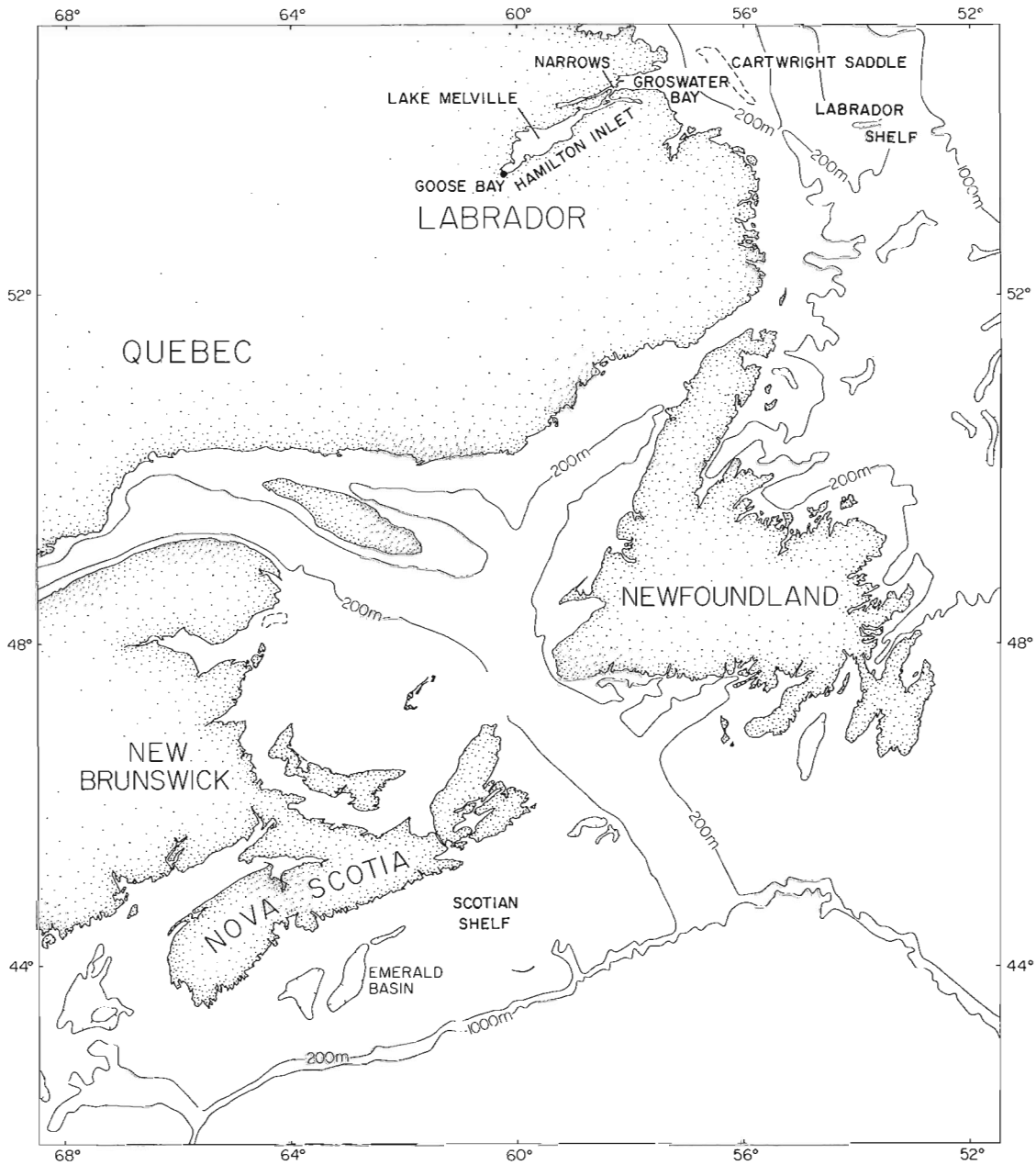

Figure 1. *Location map of areas mentioned in text.*

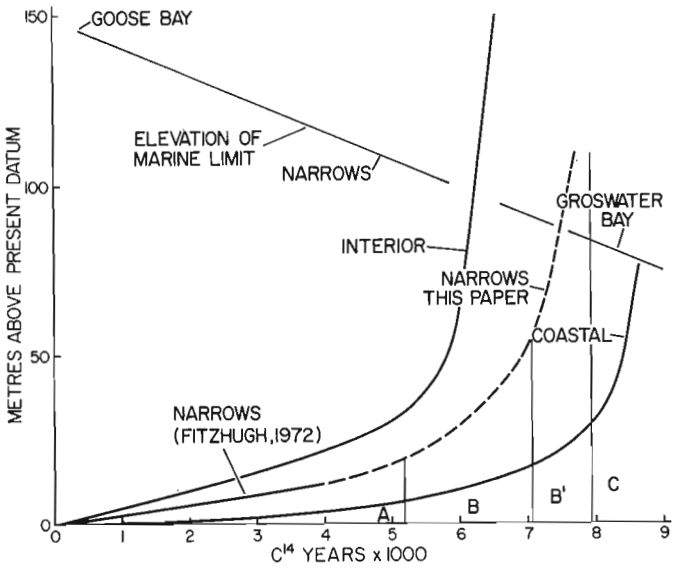

Figure 2. *Elevation of marine limit and approximate relative sea levels (Fitzhugh, 1972; Vilks and Mudie, 1983) during the postglacial time of the Lake Melville area from the coast to the interior. A,B,C, are foraminiferal zones responding to changing salinities in Lake Melville.*

Ecostratigraphy

Synchronous paleoceanographic events that can be deduced from distinct changes in foraminiferal populations are useful stratigraphic markers in sediment cores. Sediment on the Scotian and Labrador shelves and from Late Quaternary borehole samples in Denmark and Norway contain a faunal discontinuity where older foraminiferal assemblages dominated by **Elphidium excavatum f. clavata** change to modern more diverse continental shelf assemblages (Vilks, 1981). In the Scandinavian Late Quaternary borehole samples the faunal discontinuity is dated at 10 000 BP; in the more offshore localities off eastern Canada the boundary is dated between 13 000 and 15 000 BP. This ecostratigraphic boundary is explained by a major change in watermass characteristics related to the retreat of glacial ice from the continental shelf. Although the boundary may be diachronous across large distances, age of local ice retreat is often known from landform evidence, and therefore the ecostratigraphic boundary is useful to estimate depositional age of sediment on the continental shelf.

POTENTIAL APPLIED BENEFITS

Environment of hydrocarbon generation

Hydrocarbons, such as methane, can be generated in sediments that are deposited from a well oxidized water column and moderate organic production, such as the open marine environment of the Labrador and Scotian shelves. The genesis of hydrocarbons is ensured by a constant supply of organics to the seafloor and constant burial rates which are sufficiently rapid to prevent complete degradation of organic matter in the bioturbated zone. Thus sedimentary environment may be more important than total organic production for biogenic methane generation.

Renewable resources on Peru Shelf

During a co-operative investigation of the anchovy fishery on Peru Shelf (a CIDA project involving the Bedford Institute of Oceanography, Dalhousie University and Instituto del Mar del Peru) piston cores and grab samples were collected to try to determine the rate of El Nino reoccurrences, based on planktonic foraminiferal ecostratigraphy. The lack of continuous fossil horizons and a very poor downcore relationship of ^{14}C ages in two piston cores suggested that sediments are constantly redistributed. Although this approach to a study of the paleo-El Nino occurrences failed, the geochemical and paleontological analysis of total samples contributed to the program by showing a relatively rapid breakdown of organic matter, and the exensive sediment redistribution on the continental shelf (Vilks et al., 1981).

REFERENCES

Fitzhugh, W.W.
1972: Environmental archeology and cultural systems in Hamilton Inlet, Labrador; Smithsonian Contribution to Anthropology No. 16, 299 p.

Mudie, P., Keen, C.E., Hardy, I., and Vilks, G.
– Multivariate analysis of benthic foraminifera in seabed samples and Late Quaternary sediment cores, northern Canada; Marine Micropaleontology. (in press)

Rashid, M.A. and Vilks, G.
1975: Geochemical environments of methane-producing subarctic sedimentary basins in Eastern Canada; Proceedings of the 7th International Meeting on Organic Geochemistry, Madrid, Spain, p. 341-356.

1977: Geochemical environment of methane-producing subarctic sedimentary basins of Eastern Canada; in Advances in Organic Geochemistry, ed. R. Campos and J. Goni; Empressia National Adaro de Investigaciones Mineras, S.A. Madrid (Spain), p. 341-356.

Vilks, G.
1976: Foraminifera in an ice-scoured nearshore zone in the Canadian Arctic; Maritime Sediments, Special Publication 1, p. 267-277.

1980: Sedimentary environment off Hamilton Inlet, Labrador; Proceedings of Symposium on Research in the Labrador Coastal and Offshore Regions, Memorial University, Newfoundland, p. 148-166.

1981: Late glacial-postglacial foraminiferal boundary in sediments of Eastern Canada, Denmark and Norway; Geoscience Canada, v. 8, no. 2, p. 48-55.

Vilks, G. and Mudie, P.J.
1978: Early deglaciation of the Labrador Shelf; Science, v. 202, p. 1181-1183.

1983: Evidence for postglacial paleoceanographic and paleoclimatic changes in Lake Melville, Labrador; Arctic and Alpine Research, v. 15, no. 3.

Vilks, G. and Rashid, M.A.
1975: Postglacial paleoceanography of Emerald Basin, Scotian Shelf; Canadian Journal of Earth Sciences, v. 13, no. 9, p. 1256-1267.

1977: Methane in the sediments of a subarctic continental shelf; Geoscience Canada, v. 4, no. 4, p. 191-197.

Vilks, G. and Wang, Y.
1981: Surface texture of quartz grains and sedimentary processes on the southeastern Labrador Shelf; in Current Research, Part B, Geological Survey of Canada, Paper 81-1B, p. 55-61.

Vilks, G., Deonarine, B., Wagner, F.J., and Winters, G.V.
1982: Foraminifera in surface sediments of southeastern Labrador Shelf and Lake Melville, Canada; Geological Society of America, Bulletin, v. 93, p. 225-238.

Vilks, G., Rashid, M.A., and Delgado, C.
1981: Interpretation of paleoceanographic conditions on the Peru Shelf using paleoecology and geochemistry; Boletin Instituto del Mar del Peru, v. Extraordipario, p. 269-273.

Wang, Y., Vilks, G., and Piper, D.J.W.
The surface textures of quartz sand grains from the continental shelf environments: examples from Canada and China; Proceedings of Symposium on Sedimentation on the Continental Shelf, with Special Reference to the East China Sea, Hanzhou, China. (in press)

LONGEST CORE OF QUATERNARY SEDIMENTS FROM QUEEN CHARLOTTE SOUND: PRELIMINARY DESCRIPTION AND INTERPRETATION

Project 790006

K.W. Conway [1] and J.L. Luternauer [1]
Cordilleran Geology Division, Vancouver

Conway, K.W. and Luternauer, J.L., Longest core of Quaternary sediments from Queen Charlotte Sound: preliminary description and interpretation; in Current Research, Part A, Geological Survey of Canada, Paper 84-1A, p. 647-649, 1984.

Abstract

A compilation of the locations, lengths and depths of Quaternary sediment cores from Queen Charlotte Sound is given with a description of the longest core and an interpretation of its lithology.

Résumé

On présente une compilation des localisations, des longueurs et des profondeurs des carottes sédimentaires quaternaires du détroit de Reine-Charlotte; de plus, on donne une description de la plus longue des carottes et on y ajoute une interprétation de sa lithologie.

INTRODUCTION

The main physiographic features of Queen Charlotte Sound (Fig. 1, 2) are shallow banks dissected by troughs. In June 1981, six piston cores were taken from three of the major troughs for a further investigation of the late Quaternary history of the region (Fig. 2). A previous attempt to decipher this history (Luternauer and Murray, 1983) relied mainly on seabed and seismic profiling information. The purpose of this paper is to present a compilation of the locations, lengths and depths of the cores (Table 1), a brief description of the longest of these cores and a preliminary interpretation of its lithology.

METHODS

Cores were taken with a Benthos piston corer on board the **C.S.S. Hudson** from June 6 to 8, 1981. Navigation was accomplished with an integrated BIONAV system employing mainly LORAN C and satellite position fixing (accuracy ± 200 m). Cores were maintained in cold storage prior to opening in June and July, 1983.

Per cent mud, sand and gravel were obtained by wet and dry sieving subsamples on 0.063 and 2.00 mm sieves. Colour of moist sediments was determined using Munsell Soil Color Charts. The internal structure of core #8 was examined by industrial X-radiography (Power source 180-190 KV; exposure time 1.5 minutes, film type – Kodak AA).

B.E.B. Cameron prepared a preliminary compilation of the foraminifera within subsamples selected from major units. Foraminifera were concentrated by washing subsamples on a 0.075 mm sieve.

Molluscan shells were keyed using Keen and Coan (1974) and Smith and Carlton (1975).

RESULTS

The bottom layer in core #8 is 5.77 m thick, massive and composed primarily of mud with scattered granules and pebbles (Fig. 3). It is dark grey (5Y4/1) and both fine shell debris and shells (**Macoma** sp., **Yoldia** sp. and **Nuclana** sp.) are present. There is evidence of bioturbation. Burrows are commonly 1-2 mm in diameter, 1-2 cm long, composed of mud clasts and are blind ending.

The middle unit is a sequence of irregularly bedded sediments 0.51 m thick. It is composed of several layers which enclose abundant shell debris and shells, including gastropods, pelecypods and barnacles. It contains the highest percentage of sand (37.24% at 2.61 m), and is the coarsest and most poorly sorted of the three units. Its colour is olive grey (5Y4/2).

The core is capped by 2.39 m of olive mud (5Y4/3). This unit is massive, shows only slight bioturbation and consists of essentially the same size sediment as that in the lowermost unit.

DISCUSSION

The continental shelf in Queen Charlotte Sound has been extensively modified by Fraser and pre-Fraser glacial episodes (Luternauer and Murray, 1983). The presence of what are probably dropstones, the dark grey colour (indicating a lack of organic material), the fairly uniform grain size and the lack of obvious stratification suggest that the bottom unit in Core #8 was deposited under ice at a

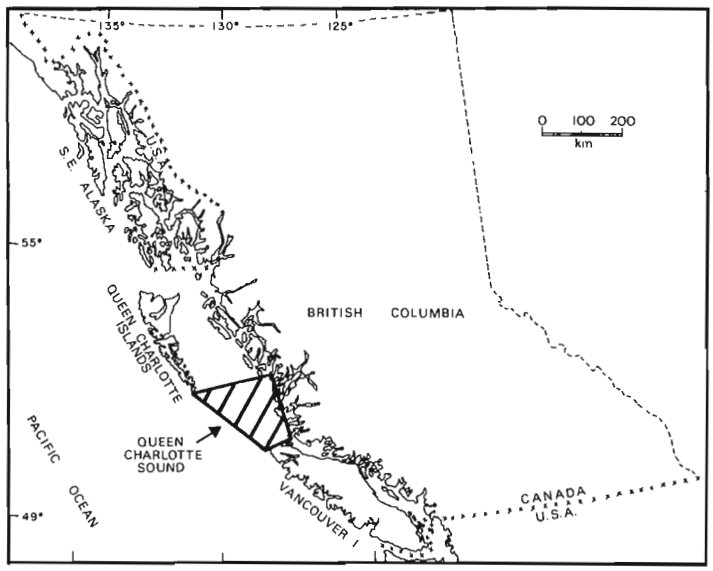

Figure 1. *Location of Queen Charlotte Sound study area.*

[1] Pacific Geoscience Centre, Sydney, B.C.

Table 1. Hudson 81 Phase II Cores

Station	Lat. °N	Long. °W	Core length	Depth
1	51°56.641'	129°29.166'	4.16 m	215 m
2	51°50.912'	129°35.940'	3.74 m	275 m
6	51°14.1'	129°30.8'	3.76 m	284 m
8	51°29.24'	128°29.4'	8.78 m	192 m
12	52°12.92'	130°12.92'	7.63 m	458 m
13	52°09.024'	130°15.635'	6.96 m	458 m

fairly constant rate. The presence of shells and burrows, visible in the X-radiographs indicate that deposition was slow enough to allow a variety of benthic organisms to survive. Species of clam shells obtained, **Macoma nasuta** (Conrad), **Yoldia** sp., and **Nuculana** sp. have been found in units with similar lithologies onshore near Port McNeill, a community 160 km southeast of core site #8 on Vancouver Island. The Port McNeill sediments are considered to have been deposited during deglaciation in a glaciomarine environment (Howes, 1982).

The relative coarseness of the middle unit, the presence of organisms from a variety of environments and the irregular nature of the bedding suggest this may be a slump deposit. The microfauna (Table 2) suggest, however, that if this unit does represent a slump, it was derived from a depth similar to that of the deposit itself. The barnacle shells, which were unattahced but intact, likewise suggest materials were not transported far. The unit may thus represent a deposit formed at a depth similar to that at present, during a period when mud discharge was lower and currents carried in detritus from immediately surrounding areas.

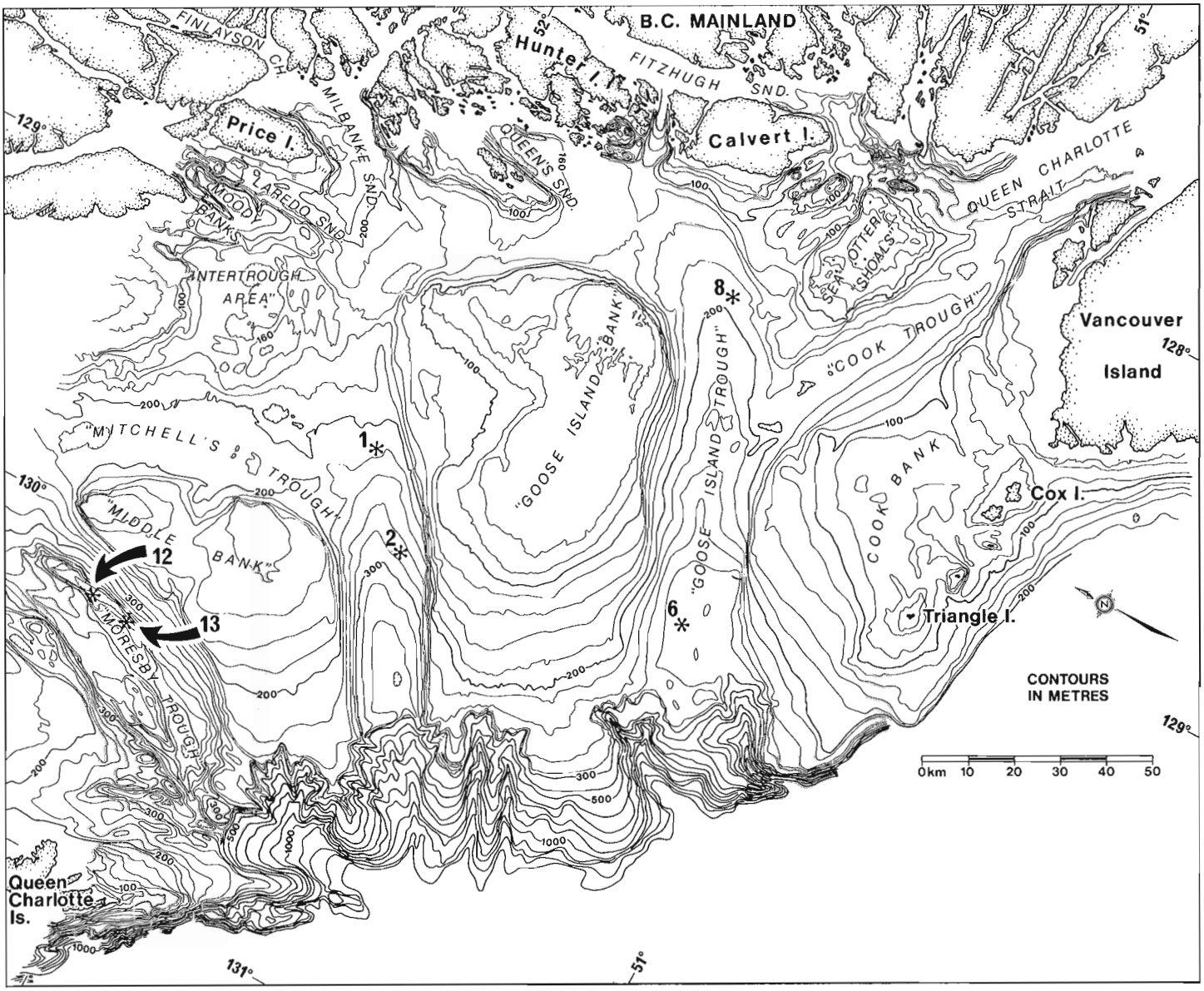

Figure 2. ***Hudson*** *1981 GSC-PGC Phase II piston core locations within Queen Charlotte Sound.*

Table 2. Foraminifera – compiled by B.E.B. Cameron

Depth in core (cm)	Species	Relative abundance	Tentative interpretation
38.5-41.5	Cassidulina teretis	abundant	300-400
	Nonionellina labradorica	common	metres
	Globoquadrina pachyderma	abundant	depth
	Epistominella pacifica	rare	
	Gyroidina sp.	rare	
	Bolivina beyrichi	rare	
	Eilohedra sp.	fairly common	
	Cassidulina sp.	abundant	
	Seabrookia sp.	rare	
254-256	Nonionellina labradorica	relatively rare	150-200
	Elphidium cf. clavatum	relatively rare	metres
	Cassidulina teretis	relatively rare	minimum
	Nonionella stella	relatively rare	depth
	Buccella sp.	relatively rare	
	Vaigerina juncea	relatively rare	
	Uvigerina sp.		
713.5-715.5	Nonionella labradorica	common	approximately
	Elphidium cf. clavatum	common	300-400
	Nonionella sp.	rare	metres
	Globigerina bulloides	rare	depth
	Cassidulina teretis	rare	
	Eilohedra sp.	fairly common	

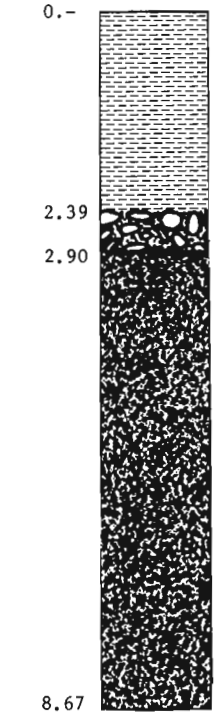

Subsample depth (m)	% mud	%sand	% gravel
0.69-0.70	97.39	2.61	-
1.34-1.35	97.37	2.63	-
1.50-1.51	97.66	2.34	-
1.89-1.90	98.09	1.91	-
2.32-2.33	94.40	5.60	-
2.51-2.52	73.77	26.23	-
2.95-2.96	88.51	11.49	-
3.39-3.40	96.90	3.10	-
4.00-4.01	95.10	4.90	-
4.47-4.58	97.97	2.03	-
5.71-5.72	97.93	2.07	-
6.41-6.42	96.20	3.80	-
7.00-7.01	96.89	3.11	-
7.28-7.29	95.75	4.25	-
7.91-7.92	97.10	2.90	
8.63-8.64	97.59	2.41	-

Figure 3. *Grain size data for core #8. Although gravel was not found in subsamples it was observed within unsampled sections of the lower two units.*

The upper unit of core #8 which, given its colour, appears to have a higher organic content than underlying units (Luternauer and Murray, 1983), is probably postglacial material. The probable sources of this material are the fiords east of Sea Otter Shoals (Luternauer and Murray, 1983).

Chronological control will soon be provided by ^{14}C dating of enclosed shell material within the collected cores. Future laboratory studies will consider organic content, detailed grain size analysis and geochemistry.

REFERENCES

Howes, D.E.
1982: Late Quaternary sediments and geomorphic history of northern Vancouver Island, British Columbia; Canadian Journal of Earth Sciences, v. 20, p. 57-65.

Keen, A.M. and Coan, E.
1974: Marine molluscan genera of western North America: An illustrated key; 2nd Ed., Stanford University Press, Stanford, California.

Luternauer, J.L. and Murray, J.W.
1983: Late Quaternary morphologic development and sedimentation, central British Columbia continental shelf; Geological Survey of Canada, Paper 83-21, 38 p.

Smith, R.I. and Carlton, J.T.
1975: Light's Manual: Intertidal Invertebrates of the Central California Coast; 3rd Ed., University of California Press, Berkeley, Cal.

TILL STRATIGRAPHY AND GOLD DISTRIBUTION, FOREST HILL GOLD DISTRICT, NOVA SCOTIA[1]

Project 830030
Contract 13SR.23233-3-0355

I.J. MacEachern[2], R.R. Stea[3], and P.J. Rogers[3]

MacEachern, I.J., Stea, R.R., and Rogers, P.J., Till stratigraphy and gold distribution, Forest Hill gold district, Nova Scotia; in Current Research, Part A, Geological Survey of Canada, Paper 84-1A, p. 651-654, 1984.

Abstract

Trenches cut to bedrock at a former gold mine provided a unique opportunity to study the three-dimensional dispersal of gold from a bedrock source by glacial and postglacial processes. The till units at all sample locations were panned and profile sampled. Till fabrics, pebble counts and measurements of bedrock and boulder pavement striations were used to reconstruct former ice movements.

Three major surficial units were found. The basal unit is an oxidized and cemented gravel which is restricted to topographically low areas. This is overlain by two till units characterized by a sandy matrix and locally derived granitic and metasedimentary clasts. The lower till is compact and rests upon bedrock with southeastward-trending striations. The upper till is less compact and locally has a strong fabric indicating a southwestward ice movement. These tills are commonly separated by a yellowish-brown alteration zone thought to be a paleosol.

Pan concentrates of the lower till indicate that gold was dispersed southeastward from known veins. Cursory examination of gold and garnet from panned concentrates from the tills provides little evidence of abrasion during transport.

Résumé

Dans une ancienne mine d'or, des tranchées recoupant la roche en place nous ont fourni une occasion unique d'étudier en trois dimensions la dispersion de l'or, à partir d'une roche-source par des processus glaciaires et post-glaciaires. Dans toutes les zones d'échantillonnage, on a lavé à la battée des échantillons d'unités de till et effectué un échantillonnage du profil. Pour reconstruire les anciennes migrations de la glace, on a analysé la texture du till, compté les galets, et mesuré les striations de la roche en place et des blocs.

On a découvert trois principales unités de surface. L'unité basale est un gravier oxydé et cimenté qui se limite aux zones basses. Elle est recouverte par deux autres unités de till, caractérisées par une matrice sableuse, et des roches clastiques granitiques et métasédimentaires d'origine locale. Le till inférieur est compact et repose sur la roche en place; il présente des striations de direction sud-est. Le till supérieur est moins dense, et localement, est caractérisé par la netteté de sa structure, qui indique une migration des glaces vers le sud-ouest. Ces tills sont généralement séparés par une zone d'altération brun jaunâtre, que l'on considère comme un paléosol.

Les produits obtenus par lavage du till inférieur à la battée indiquent que l'or s'est dispersé vers le sud-est à partir de filons connus. Un examen rapide de l'or et des grenats concentrés par lavage des tills n'indique pas qu'il y ait eu abrasion des roches pendant leur transport.

INTRODUCTION

During the summer and fall of 1982, an extensive trenching program conducted at the Forest Hill gold district by Seabright Resources Incorporated exposed several kilometres of excellent 2 to 3 m thick till profiles in 9 trenches which are oriented perpendicular to the strike of both the veins and host strata of the deposit. This afforded the authors a unique opportunity to study the till stratigraphy and the 3-dimensional dispersal of gold and related elements from a bedrock source by glacial and postglacial processes. The project will include an integrated geochemical survey of bedrock, till and soil aimed at developing effective geochemical exploration techniques for locating new gold deposits and re-evaluating old gold deposits in the rocks of the Meguma Group.

Sampling was conducted at 25 m intervals along the trenches. At each sample site the till stratigraphy was described and the section systematically profile-sampled at one metre intervals. Each till unit was panned to obtain a heavy mineral concentrate for analysis. The coarse pebble fraction was removed using a gold pan sifter during the panning process and the pebbles were counted and grouped into principal lithologies. At every fifth site, till fabric measurements were obtained from each sample unit. Till fabrics, pebble counts and measurements of bedrock and boulder pavement striations were used to reconstruct glacier movements at the Forest Hill area.

REGIONAL PLEISTOCENE GEOLOGY

In the eastern meguma Terrane, bedrock striations and roche moutonnées indicate a regional southeastward ice flow (140-160°). The resultant till (Stea and Fowler, 1979) is loose and sandy, and displays rapid transitions in lithological facies southeastward across significant bedrock contacts. Locally an extensive melt-out phase produced hummocky terrain. A regionally consistent striation set trending 180° cuts the southeastward-trending striations. Pebbles of Silurian fossiliferous sandstones and volcanic rocks along the Eastern

[1] Contribution to Canada-Nova Scotia Co-operative Mineral Program 1981-84.
Project carried by Geological Survey of Canada and Nova Scotia Department of Mines and Energy.

[2] Apartment 4, 48 Gebhardt Street, Halifax, Nova Scotia B3M 2X1
[3] Nova Scotia Department of Mines and Energy, P.O. Box 1087, Halifax, Nova Scotia B3J 2X1

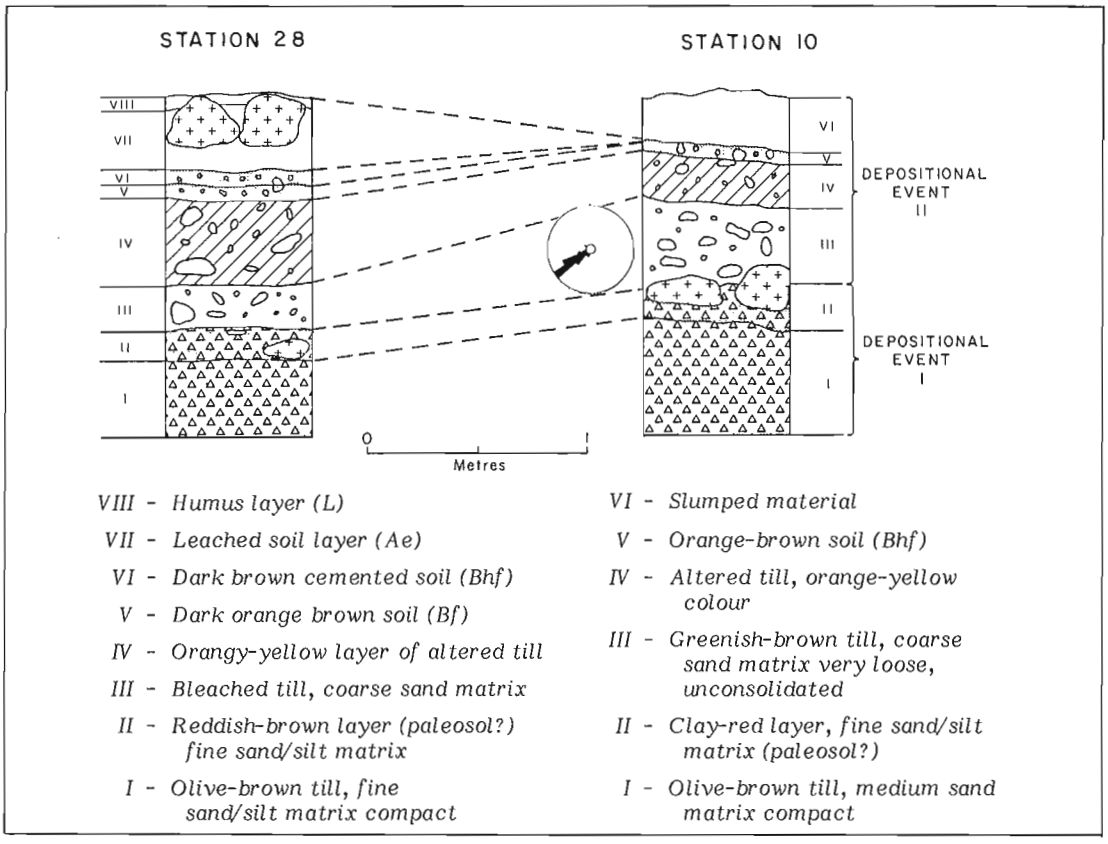

Figure 1. *Stratigraphy and correlation of stations 10 and 28, Forrest Hill gold district, Nova Scotia.*

Shore as well as southwest-trending eskers (Stea and Fowler, 1979) attest to a period of ice flow that crossed or originated in the Antigonish Highlands.

TILL STRATIGRAPHY

The surficial deposits within the Forest Hill area indicate three major depositional events. The earliest episode is represented by a poorly cemented and oxidized gravel observed most commonly in topographically low areas. This is overlain by two till units interpreted as lodgement and/or melt-out phases of deposition. The older till is olive-brown and semicompact, and overlies bedrock inscribed with southeastward trending striations. The younger till is yellowish-brown, loose and sandy; it has a strong fabric striking 250°, and was formed by a southwestward ice movement. Figure 1 illustrates a correlation of stratigraphy in two trenches about 300 m apart (Fig. 2) showing the upper till units and inferred depositional events.

The tills are separated by a widespread but discontinuous 10-15 cm dark yellowish-brown zone tentatively interpreted to be a paleosol. This interpretation implies that the two depositional events were separated by a period of climatic amelioration and ice retreat. The dark yellowish-brown alteration appears to coat the grains and there are many small rootlets within the unit. The results of chemical and grain size analyses (D. Holmstrom, personal communication, 1983) support the paleosol interpretation.

GOLD DISTRIBUTION

Pan concentrates of the tills have shown that gold if present is commonly confined to the till closest to bedrock in topographically high areas and is found in most units including soils in topographically low areas.

The distribution of gold in the lower till generally suggests a southeastward dispersal from gold-bearing quartz veins. Gold-rich till in trenches 1 and 9 (westernmost and easternmost trenches, respectively, in Fig. 2) cannot be explained in this way; postglacial dispersal processes or mechanical dispersal from undiscovered gold-quartz veins may account for these gold-rich tills.

Striations inscribed on bedrock generally record a southeastward ice flow. Striations found on boulders and till fabrics, however, indicate a period of southwestward ice flow (Fig. 2). This ice flow did not appear to redistribute the gold to any great extent as no panned gold was found in the southern part of trench 1.

CHARACTER OF THE GOLD

The gold in the till is present as both small flakes and small nuggets. With a scanning electron microscope the grain surfaces appear rough and pitted (Fig. 3), and exhibit little evidence of deformation indicative of abrasive transport. This is also true of the other heavy minerals.

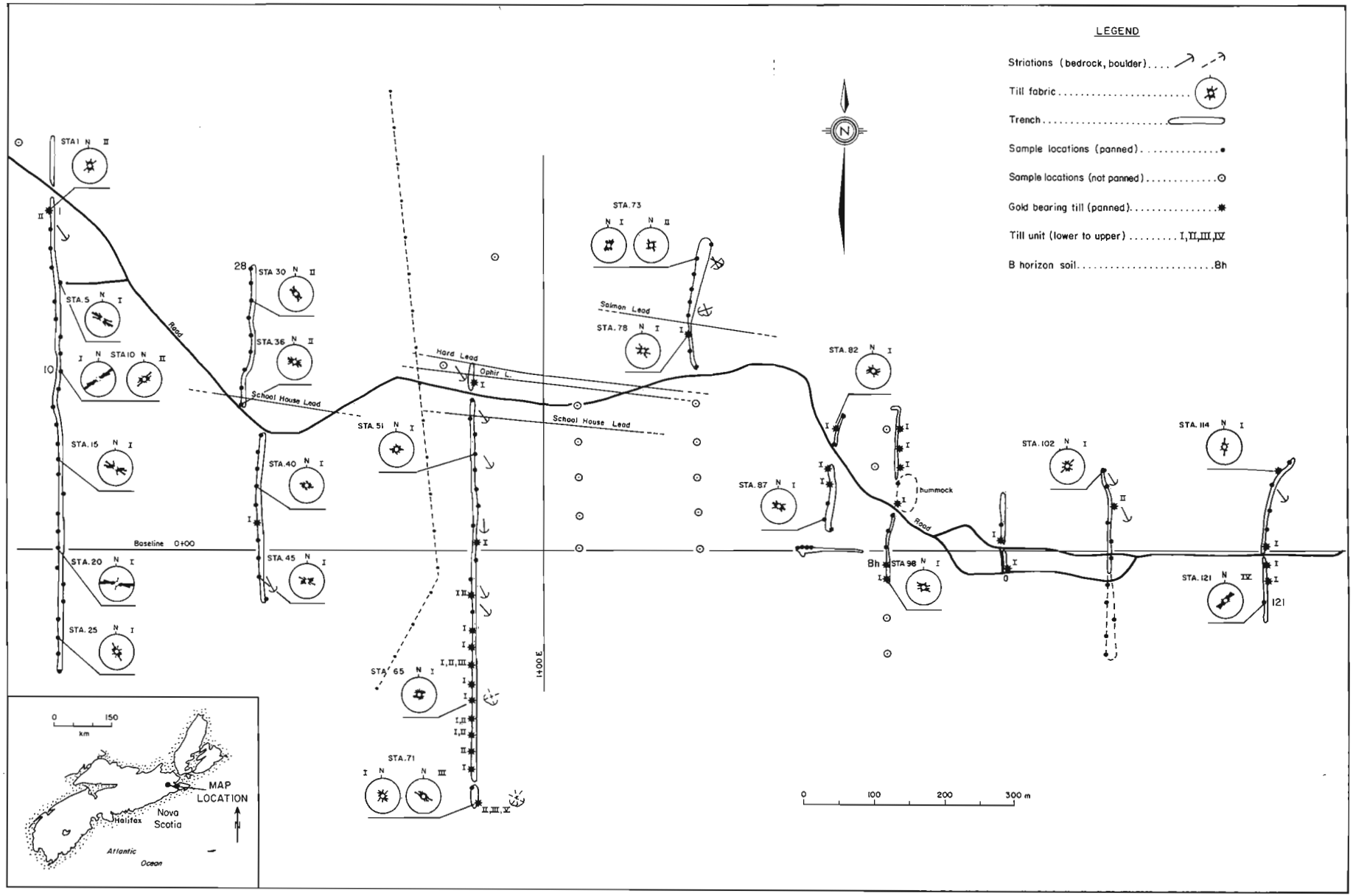

Figure 2. *Map of Forest Hill gold district illustrating trenches, sample locations and preliminary results.*

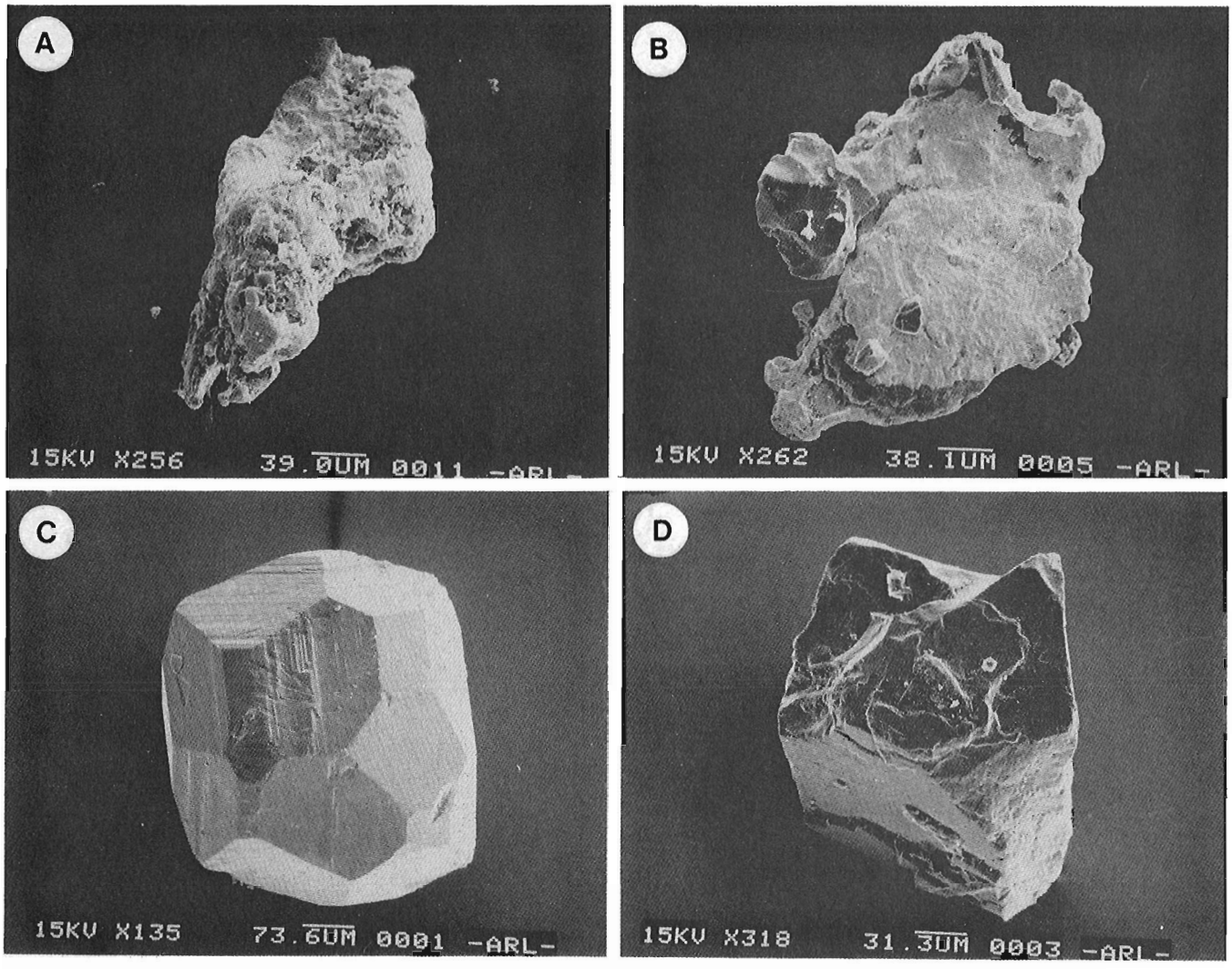

A – Gold nugget.
B – Gold flake. Note slender, delicate extensions at grain edge, indicating minimal deformation during glacial transport.
C – Euhedral garnet crystal. Note the sharp edge between crystal faces, indicating minimal abrasion during glacial transport.
D – Ilmenite.

Figure 3. *Scanning electron microscope photomicrographs of mineral grains recovered from pan concentrates of tills. Magnification and bar scales are shown on each photograph.*

REFERENCE

Stea, R.R. and Fowler, J.H.
1979: Minor and trace element variations in Wisconsinan tills, Eastern Shore Region, Nova Scotia; Nova Scotia Department of Mines and Energy, Paper 79-4, 30 p.

THE 1880 LANDSLIDE DAM ON THOMPSON RIVER, NEAR ASHCROFT, BRITISH COLUMBIA

Project 830016

S.G. Evans
Terrain Sciences Division

Evans, S.G., The 1880 landslide dam on Thompson River, near Ashcroft, British Columbia; in Current Research, Part A, Geological Survey of Canada, Paper 84-1A, p. 655-658, 1984.

Abstract

On October 14, 1880 a sudden landslide (estimated volume 15 x 10^6 m^3) dammed Thompson River, 7.5 km south of Ashcroft. A reservoir quickly formed upstream of the dam and flooded farmland in the valley. Downstream of the landslide dam, the channel of Thompson River was dry for about 35 km. The volume of the reservoir was estimated to be between 42 and 145 x 10^6 m^3. The dam breached after a life of approximately 44 hours after a channel had been cut over the debris. The instantaneous sediment input into the Thompson River channel as a result of the landslide is estimated to be of the order of 4 x 10^6 m^3. This is the first documentation of the landslide damming process in the Canadian Cordillera.

Résumé

Le 14 octobre 1880, un brusque glissement de terrain (qui a déplacé un volume estimé à 15 x 10^6 m^3) a bloqué la rivière Thompson, à 7,5 km au sud d'Ashcroft. Un réservoir s'est rapidement constitué en amont du barrage ainsi formé, et a inondé les terres agricoles de la vallée. En aval de ce barrage, le lit de la rivière Thompson s'est trouvé asséché sur une distance d'environ 35 km. On estime que le volume du réservoir était compris entre 42 et 145 x 10^6 m^3. Après 44 heures environ, le barrage s'est ouvert, après creusement d'un passage au-dessus des débris. L'afflux instantané de sédiments dans le chenal de la rivière Thompson, causé par le glissement de terrain, a été estimé à environ 4 x 10^6 m^3. Ce cas a constitué la première étude documentée de la formation d'un barrage par un glissement de terrain dans la Cordillère canadienne.

INTRODUCTION

The damming of river channels by landslide debris is a little documented process in the Canadian Cordillera. Consideration of the process is important since the secondary effects related to the damming may be of greater consequence than the effects of the landslide itself (e.g. Alden, 1928; Hewitt, 1968). These effects include the flooding of upstream sites during reservoir formation and the damage to downstream sites by the sudden discharge of the contents of the natural reservoir upon breaching of a landslide dam.

This report documents the landslide dam which in 1880 blocked Thompson River, 7.5 km downstream from the present Thompson River bridge at Ashcroft, just above Black Canyon (Fig. 1). The life of the dam was approximately 44 hours.

Information on the landslide dam contained herein has been collated from a number of widely scattered sources, namely, contemporary newspaper accounts (The Victoria Colonist, October 17, 19, 21, 1880; The Inland Sentinel (Yale) October 21, 1880), reports by Gowen (1899), Wade (1979), and Stanton (1898). In passing, it is noted that Stanton (1898) incorrectly gives the year of the landslide as 1881. This information has been augmented by field observations and an examination of current maps and aerial photographs.

THE LANDSLIDE DAM

The damming of Thompson River occurred at approximately 2100 h on Thursday, October 14, 1880 as a result of a sudden landslide (Fig. 2). The landslide was felt and heard in the Ashcroft area and was thought to be an earthquake (Gowen, 1899). The landslide involved Pleistocene glaciolacustrine sediments and is one of the numerous slope movements in these materials along Thompson River between Ashcroft and Spences Bridge (Ryder, 1976, 1981).

The landslide involved an area of approximately 6 x 10^5 m^2, a volume estimated to be of the order of 15 x 10^6 m^3, and dammed a channel which was 160 m wide. The landslide dam was approximately 880 m long along the thalweg of the river. Estimates vary on the maximum height of the dam, but it was probably not less than 45 m with its lowest point between 18 and 25 m above the channel bed.

Although it is beyond the scope of this note to speculate on the cause of the landslide, Stanton (1898) suggested that it was due to the irrigation of the bench in the

Table 1. Historical landslide dams on Thompson River between Ashcroft and the vicinity of Spences Bridge

Date	Location	Effects
August 1, 1880	Spences Bridge	Partial dam
October 14, 1880	Just above Black Canyon	Dammed river for approximately 44 hours
December 31, 1899	Spences Bridge	Partial dam
August 13, 1905	Spences Bridge	Dammed river for approximately 5 hours
August 13, 1921	2.6 km below Spences Bridge	Dammed river

Sources: Wade (1979) and contemporary newspaper reports

area of the failure. The effect of the irrigation may have been increased by the bursting of an irrigation dam, probably at Willard Lake (Fig. 1), some time before the landslide (Stanton, 1898). Waters released by this dam burst rushed down Puckett Creek and spread out over the bench surface near the head of the landslide.

As seen in Table 1 there were five instances of total or partial damming of Thompson River by landslides between 1880 and 1921. In all cases, the cause of the landslides has been given as irrigation.

DOWNSTREAM EFFECTS

The landslide completely blocked the flow of the Thompson. The bed was dry, except for the flow from small tributary channels, from the landslide site south to Nicola River just above Spences Bridge, a distance of 35 km. Dead salmon littered the dry bed and the local inhabitants were quick to harvest this unexpected catch. Others took the opportunity to pan for gold in the gravels of the dry bed. At Lytton, 60 km downstream, the level of Thompson River fell 2.13 m and at Yale, 130 km downstream, the level of Fraser River fell approximately 1.5 m.

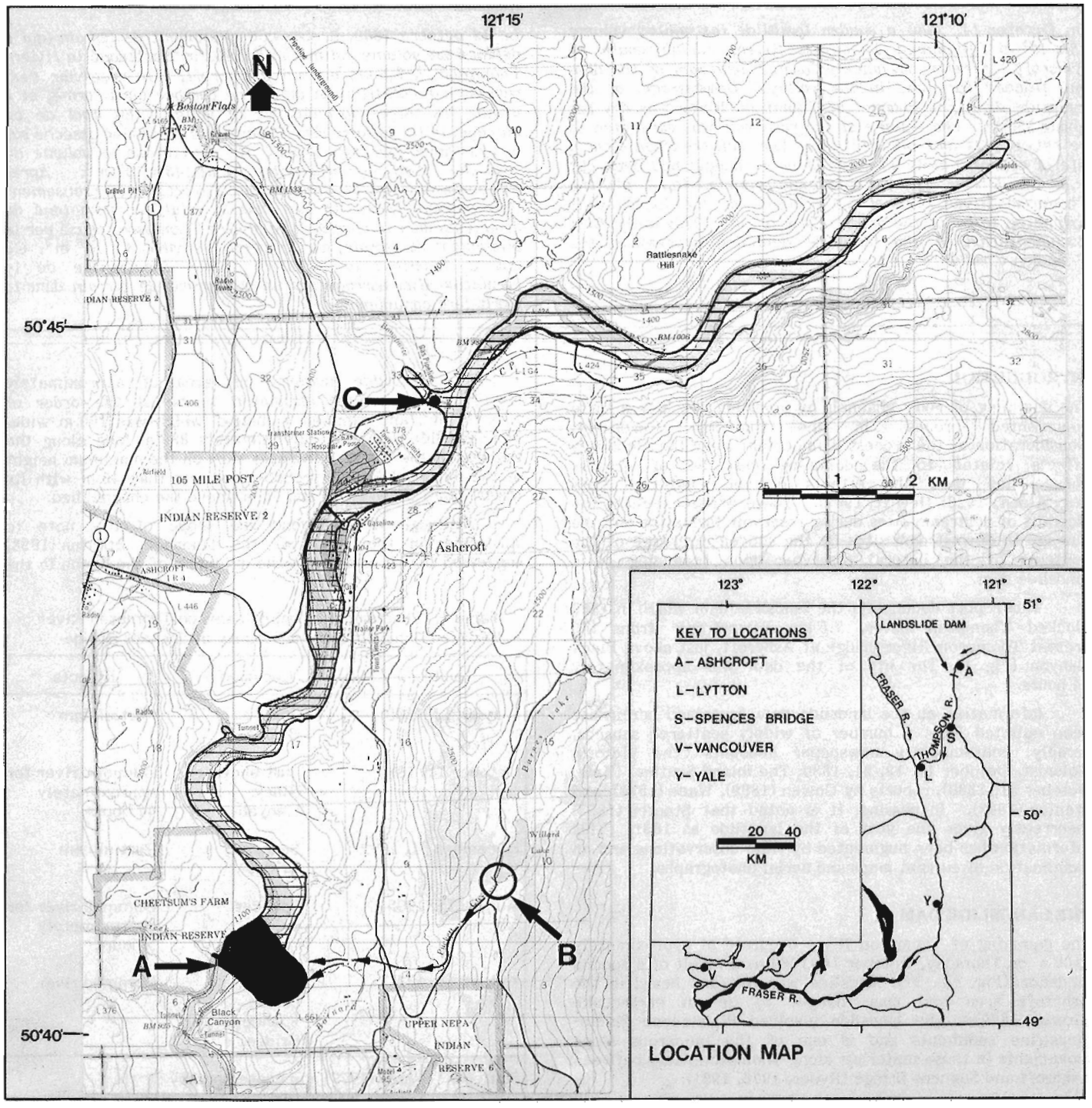

Figure 1. Location of 1880 landslide dam (A) on Thompson River, near Ashcroft, and extent of reservoir (horizontal shading). B is the probable location of irrigation dam burst, suggested by Stanton (1898) as being a possible cause of the landslide at A. Arrows mark the path of water to the head of the landslide. C is the probable location of Figure 3.

UPSTREAM EFFECTS – THE RESERVOIR

A reservoir quickly formed in the valley above the landslide dam. At 0800 h on October 15th, the water level was rising at a rate of 1 m per hour at the mouth of the Bonaparte, 9 km upstream of the dam (Fig. 1). According to Wade (1979), the terrace where Ashcroft now stands was flooded with water to a depth of 40 cm. This would imply that the maximum pool elevation reached by the reservoir was of the order of 306 m a.s.l. (≃ 1004 ft.) Maximum depth of the water at the dam was approximately 18 m (Stanton, 1898; Wade, 1979). At the mouth of the Bonaparte, the rising waters flooded Harper's Mill (C in Fig. 1). Figure 3 shows the pool elevation of the reservoir in the vicinity of the Mill. A house and various outhouses on the Barnes farm floated away and other farmers lost a large quantity of grain in flooded storage buildings. The reservoir was approximately 14 km long and its maximum extent, estimated from the maximum pool elevation noted above, is shown in Figure 1.

The mean monthly discharge for October, measured at Wahlachin (30 km upstream from the dam) between 1932 and 1948 by the Water Survey of Canada, was 405 m^3/s. Maximum and minimum monthly discharges for October during this period were 915 m^3/s and 267 m^3/s, respectively. If the life of the reservoir is taken to have been about 44 hours, these discharge measurements yield approximate volumes for the reservoir of the order 65 x 10^6 m^3 (based on mean monthly discharge for October), 145 x 10^6 m^3 and 42 x 10^6 m^3 (based on maximum and minimum monthly discharges, respectively). These estimates differ substantially from Stanton's (1898) estimate of 198 x 10^6 m^3.

THE BREACHING OF THE DAM

The dam breached at approximately 1700 h on Saturday, October 16, 1880, after a life of approximately 44 hours. A catastrophic breaching had been feared and the inhabitants of Spences Bridge, 35 km downstream fro the dam, had removed all valuables from their houses in the expectation of an outburst flood. A gradual breaching, however, took places after men had been put to work to cut a channel over the dam. The escaping waters gradually enlarged the channel by erosion, until the reservoir was drained and the pre-landslide level was established. In the words of a contemporary account "the dam relieved itself". On the Fraser at Yale on Sunday, October 21, 1880 "very muddy water, floating logs, stumps etc. (were) seen passing down the river all day" (The Inland Sentinel).

A. View upstream of landslide mass, characterized by hummocky topography. The Canadian Pacific Railway traverses the toe region of the landslide. Erosion of debris and local slumping are currently taking place at the channel margin. Note the benchlands at the head of the landslide.

B. View upstream of the channel which was blocked by the landslide dam. Remnants of debris are visible on the right; Canadian Pacific Railway on right, Canadian National Railway on left. Note another landslide on the left.

Figure 2

Oblique aerial photographs of 1880 landslide site taken in July 1983.

Figure 3

Photograph taken in 1930s in the vicinity of the mouth of Bonaparte River, along Canadian National Railway (C in Fig. 1). The sign indicates the maximum pool elevation of the reservoir formed by the 1880 landslide dam. Derelict building behind is probably Harper's Mill mentioned in the text. (Courtesy of Kamloops Museum and Archives, photograph No. 9016).

CONCLUSION

The formation of reservoirs by landslide dams, and their subsequent draining, is a hazard which, hitherto, has not been widely recognized in the Canadian Cordillera. In the example documented above, downstream devastation was probably avoided by the prompt cutting of a channel which served as an enlarging spillway for the noncatastrophic draining of the reservoir.

The geomorphic effects of the dam are also worthy of note. In addition to the movement and modification of the channel in the vicinity of the landslide (Fig. 2), a landslide entering a river channel constitutes an instantaneous sediment input into a river system. In this case the instantaneous sediment input into the Thompson River system was in the order of 4×10^6 m^3.

ACKNOWLEDGMENTS

The assistance of John Stewart, of the Kamloops Museum Association, was invaluable in the assembly of information on the 1880 Thompson River landslide dam. J.A. Heginbottom and R.J. Fulton critically read the manuscript.

REFERENCES

Alden, W.C.
1928: Landslide and flood at Gros Ventre, Wyoming; American Institute of Mining and Metallurgical Engineers, Transactions, v. 76, p. 347-360.

Gowen, H.H.
1899: Church Work in British Columbia; Longmans, Green and Co., London, 232 p.

Hewitt, K.
1968: Records of natural damming and related events in the Upper Indus Basin; Indus: Journal of Water and Power Development Authority, v. 10, p. 11-19.

Ryder, J.M.
1976: Terrain inventory and Quaternary geology, Ashcroft, British Columbia; Geological Survey of Canada, Paper 74-49, 17 p.

1981: Terrain inventory and Quaternary geology, Lytton, British Columbia; Geological Survey of Canada, Paper 79-25, 20 p.

Stanton, R.B.
1898: The great landslides on the Canadian Pacific Railway in British Columbia; Minutes of Proceedings, Institution of Civil Engineers, v. 132, p. 1-20.

Wade, M.S.
1979: The Cariboo Road (Researched, annotated and indexed by E.A. Eastik from an unpublished manuscript); The Haunted Bookshop, Victoria, 264 p.

QUATERNARY DEEP SEA MICROFAUNA IN THE VICINITY OF OFFSHORE SPREADING RIDGES, WEST COAST OF CANADA

Project 690075

B.E.B. Cameron [1]
Cordilleran Geology Division, Vancouver

Cameron, B.E.B., Quaternary deep sea microfauna in the vicinity of offshore spreading ridges, west coast of Canada; in Current Research, Part A, Geological Survey of Canada, Paper 84-1A, p. 659-660, 1984.

Abstract

The benthic microfauna in late Pleistocene and Holocene cores recovered from water depths between 2180 and 3025 m on spreading ridges in the area near the northern end of the Juan de Fuca Ridge are chiefly planktic foraminifera with about 10% benthonic foraminifera and less than 1% ostracodes.

Résumé

La faune benthique, récupérée dans des carottes datant de la fin du Pléistocène et de l'Holocène et prises à des profondeurs variant de 2180 m à 3025 m sur des rides d'expansion d'une zone près de la limite nord de la ride Juan de Fuca, est en grande partie constituée de foraminifères planctoniques contenant 10% de foraminifères benthiques et moins de 1% d'ostracodes.

INTRODUCTION

During the past few years studies of the deep sea spreading ridges off the British Columbia coast by scientists of the Pacific Geoscience Centre and the University of British Columbia have concentrated on the distribution of hydrothermal vents and their related mineralization, spreading rates across the ridge crests, rates and types of sedimentation, and to a lesser extent, the deep sea faunas. Most of the gravity and piston cores (about 150) recovered since 1977, mostly in and around the spreading ridges, will ultimately be incorporated in this examination (Fig. 1).

The present study was initiated to examine the distribution of benthic microfauna relative to the active spreading ridges and vents and especially the distribution of some species in relation to proximity to the vents. In this early phase of the investigation, attention has been concentrated on cores recovered from in and around the ridges. Yet to be examined in detail are cores from similar water depth but well away from the ridge crests.

PHYSICAL CHARACTER AND AGE

Many of the cores studied to the present are from the northern end of Juan de Fuca Ridge and were recovered from water depths varying from 3025 to 2180 m. Sediments, dated by radiocarbon and geochemical methods, indicate a late Pleistocene and Holocene succession of local turbidity and hemipelagic sediments (Cook, 1981; Price, 1981).

PLANKTIC FORAMINIFERA

Planktic foraminifers are by far the most abundant forms recovered. These include:

Globoquadrina pachyderma (Ehrenberg) – abundant
G. hexagona (Natland) – rare
Globorotalia scitula (Brady) – common
Globigerina bulloides d'Orbigny – abundant
G. quinqueloba Natland – common
Globigerinita glutinata (Egger) – common
G. bradyi Wiesner – common
Orbulina universa d'Orbigny – common
"biorbuline" form of **O. universa** d'Orbigny – rare

The species **Globoquadrina hexagona** and **Orbulina universa** ("biorbuline" form) are generally uncommon throughout the study area, but are quite common in localized areas and in particular cores. These species are considered to be deeper planktics, but their absence in adjacent cores of similar depth suggests that their distribution may be influenced by other factors as well as depth.

BENTHONIC FORAMINIFERA

Benthonic foraminifers represent approximately 10% of the total foraminiferal population. Malott (1981) listed 184 benthonic species and suggested perhaps one third of these were undescribed. The present, more extensive study confirms this observation and suggests even greater diversity with the addition of many more new species. Some of the more aberrant and unusual forms include:

Pseudonodosaria sp. – having paired ultimate chambers

Cribrostomoides sp. – selectively agglutinates minute basaltic glass fragments

Dentalina sp. – a species attaining a length of over 7 mm

Uvigerina disrupta Todd – having paired terminal apertures

Cassidulina sp. – having paired divergent ultimate chambers.

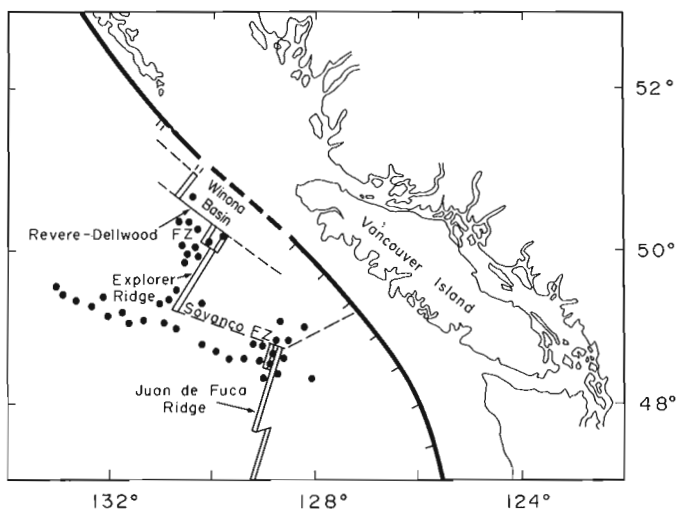

Figure 1. Areal distribution of deep sea cores under study.

[1] Pacific Geoscience Centre, Sydney, B.C.

OSTRACODA

The ostracodes represent less than one per cent of the total microfauna recovered from the cores examined and are difficult to isolate from the dominant planktic foraminifera. A total of forty-five species have been recognized. These include relatively common occurrences of **Krithe, Cytheropteron, Wichmannella, Ambocythere** and a probable new genus of the Rocaleberidinae. Less frequent are representatives of **Poseidonamicus, Munseyella, Argilloecia, Parakrithe, Echinocythereis, Acanthocythereis**?, and **Paracypris.** Rare occurrences of **Eucytherura, Saipanetta, Monoceratina, Bythoceratina, Pseudocythere, Pedicythere, Wolburgia**?, **Xiphichilus, Polycope, Bosquetina**?, **Cytherura** and **Macrocypris** have also been recorded.

Additional ostracodes will be added to the lists as more cores are processed. In addition to several new taxa, it is of interest to note the presence of the psychrospheric genus **Poseidonamicus** which to the writer's knowledge is the most northerly record of the genus in the northeastern Pacific. The healdiacean genus **Saipanetta** has been recovered from the Holocene of Juan de Fuca and Explorer ridges. The genus **Pedicythere,** originally described from the Eocene of Great Britain, is represented in the Holocene cores by two species. This genus has recently been identified from deep sea Quaternary deposits in the Adriatic Sea (Sissingh, 1975).

ACKNOWLEDGMENTS

I wish to thank R.L. Chase of the Department of Geological Sciences, University of British Columbia for providing access to many of the cores. My deep appreciation is extended to M. Johns, Pacific Geoscience Centre, for her patience in preparing much of the material for study.

SELECTED BIBLIOGRAPHY

Be, A.W.H.
1977: 1: An ecological, zoogeographic and taxonomic review of recent foraminifera; in Oceanic Micropalaeontology, v. 1, p. 1-100.

Benson, R.H.
1972: The **Bradleya** problem, with descriptions of two new Psychrospheric Ostracode genera, **Agrenocythere** and **Poseidomanicus** (Ostracoda: Crustacea); Smithsonian Contributions to Paleobiology, no. 12, p. 1-138.

Cook, R.A.
1981: Composition and stratigraphy of late Quaternary sediments from the northern end of Juan de Fuca Ridge; unpublished M.Sc. thesis, The University of British Columbia, 107 p.

Malott, M.L.
1981: Distribution of foraminifera in cores from Juan de Fuca Ridge, northeast Pacific; unpublished M.Sc. thesis, The University of British Columbia, 136 p.

Price, M.G.
1981: A study of sediments from the Juan de Fuca Ridge, northeast Pacific Ocean: with special reference to hydrothermal and diagenetic components; unpublished M.Sc. thesis, The University of British Columbia, 141 p.

Sissingh, W.
1975: A remarkable new species of **Pedicythere** (Ostracoda) from Adriatic Sea; Nederlandse Akademic van Wetenschappen, Proceedings Series B, v. 78, no. 1, p. 62-73.

PRELIMINARY REPORT ON THE GEOLOGY OF THE GLENGARRY HALF GRABEN, CAPE BRETON ISLAND, NOVA SCOTIA[1]

Contract 19SR.23233-3-0362

G.A. Prime[2]

Prime, G.A., Preliminary report on the geology of the Glengarry Half Graben, Cape Breton Island, Nova Scotia; in Current Research, Part A, Geological Survey of Canada, Paper 84-1A, p. 661-663, 1984.

Also in Mines and Minerals Branch, Report of Activities, 1983, Nova Scotia Department of Mines and Energy, Report 84-1, 1984.

Abstract

Intensive exploration in the Glengarry Half Graben area of southeastern Cape Breton Island, Nova Scotia has established economic deposits of lead, celestite, and barite. Because of the importance of this Carboniferous structural basin and the large amount of data available, the present study was undertaken to develop an increased understanding of its stratigraphy and sedimentary history. Surface mapping of all outcrop exposure and logging of selected diamond-drill core were the methods employed.

Preliminary results indicate that the Glengarry Half Graben consists of approximately 2000 m of primarily continental siliciclastics, minor limnic or paralic shales, limestones, and evaporites and very minor marine carbonates. The strata are Viséan to Lake Westphalian in age and occur in an asymmetric syncline. The Half Graben has a similar stratigraphy and sedimentology to the adjacent Loch Lomond Basin. In both areas the strata record a history of progressive onlap. The Glengarry Half Graben may be a remnant of a much larger depositional system.

Résumé

L'exploration détaillée dans la région du demi-graben de Glengarry dans le sud-est de l'île du Cap-Breton, en Nouvelle-Écosse, a établi la présence de gisements économiques de plomb, de célestine et de barytine. Étant donné l'importance de cette cuvette synclinale de nature carbonifère et l'énorme quantité de données disponibles, l'étude a été entreprise afin d'améliorer de contribuer à une meilleure connaissance de la stratigraphie et de l'histoire sédimentaire de la région. Pour ce faire, on a procédé à la cartographie de la surface de tous les affleurements et à la réalisation de diagraphies de certains échantillons de carottage au diamant.

Les résultats préliminaires indiquent que le demi-graben de Glengarry se compose d'environ 2 000 m de sédiments silicieux-clastiques d'origine principalement continentale, de petites quantités de schistes argileux limniques ou paraliques, de calcaires et d'évaporites ainsi que de très petites quantités de roches carbonatées d'origine marine. Les couches datent du Viséen au Westphalien récent et se présentent dans un synclinal asymétrique. La stratigraphie et la sédimentologie du demi-graben s'apparentent à celles du bassin voisin de Loch Lomond. Les strates des deux régions indiquent qu'il y a eu chevauchement progressif. Le demi-graben de Glengarry pourrait être un vestige d'un réseau de sédimentation beaucoup plus vaste.

INTRODUCTION

Description

The Glengarry Half Graben (Salmon River Basin) of Keppie (1982) is a small (125 km^2) elongate structural basin of Carboniferous age (Fig. 1). The Half Graben is located south of the larger Sydney Basin, strikes northeast, and has the structural configuration of a half graben. To the northwest it is bounded by the Lennox Passage Fault, a northeasterly trending high angle fault that separates it from the East Bay Block Hadrynian-Devonian igneous basement. To the southwest, a northwesterly trending, high angle, transverse fault separates it from the structurally similar Loch Lomond Basin. The southeastern boundary is an angular unconformity with the Fourchu Block Hadrynian Devonian igneous basement.

Previous work

Mineral exploration has been recorded in the area for about a century, but has been especially active during the past 20 years. In the late nineteenth and early twentieth centuries, mining operations extracted small amounts of manganese along McCuish Brook and coal at Glengarry. More recently celestite has been mined at Enon (1970-1976) and lead at Silver Mine (1979-1981). Both operations have subsequently closed due to economic problems. An open-pit barite mine is currently in operation at Pine Brook near Loch Lomond. The intensive mineral exploration has provided access to voluminous subsurface information comprising approximately 25 000 m of diamond-drill core.

In addition, several geological maps and reports on the area have been compiled (e.g. Weeks, 1954; Scott, 1978; Boehner, 1981, 1983; Keppie, 1982; Bonham et al., 1982).

Objectives and methods

The principal objective of this study was to examine and describe in detail the stratigraphy and sedimentology of the Glengarry Half Graben. Methods employed included field mapping of all outcrop and logging of selected diamond-drill holes in a series of cross-sections. Data collected included the measurement and description of new lithostratigraphic units, measurement of paleocurrent directions and examination of conglomerate clast lithology. Sandstone was sampled for petrographic examination, shales for palynology and clay mineralogy, and coals for vitrinite reflectance. When complete the project will provide an updated geological map,

[1] Contribution to Canada-Nova Scotia Co-operative Mineral Program 1981-84. Project carried by Geological Survey of Canada.

[2] 12 Cornwall Street, Lower Sackville, Nova Scotia B4C 1J1

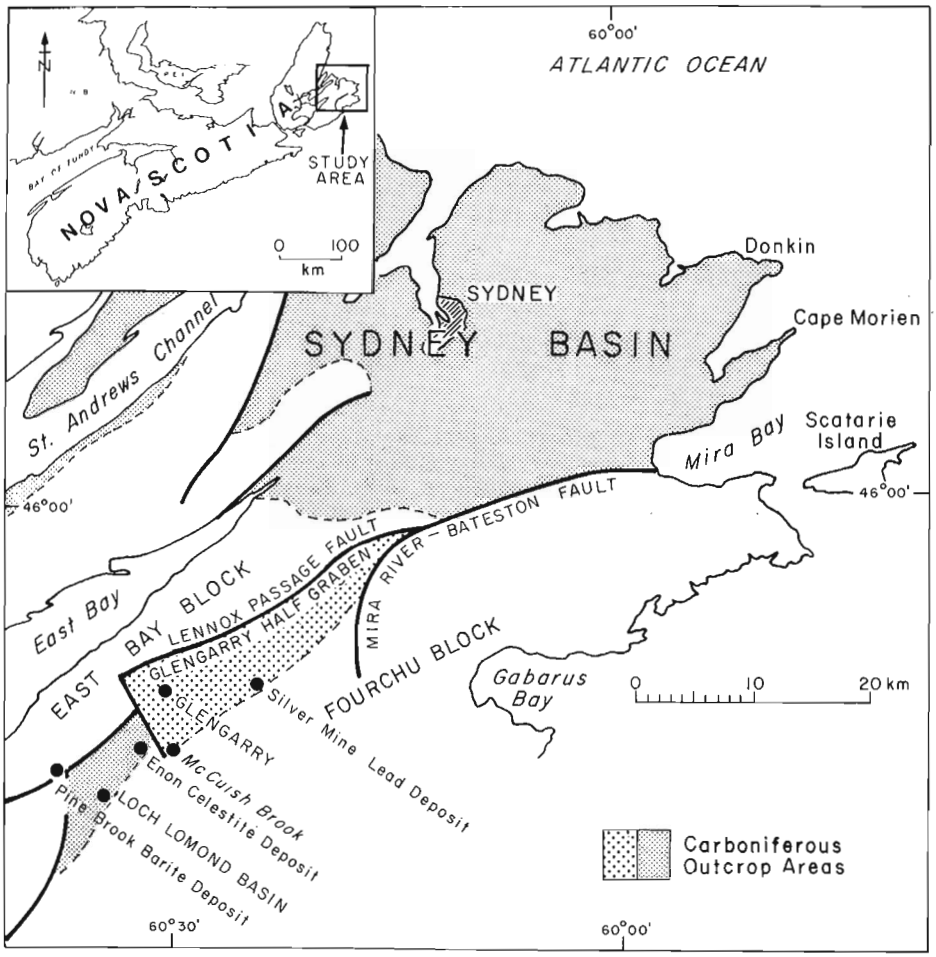

Figure 1

Location map and general geological setting of the Glengarry Half Graben, southeastern Cape Breton Island.

a modern lithostratigraphic framework, and an increased understanding of the sedimentary history of the Glengarry Half Graben.

STRATIGRAPHY AND SEDIMENTOLOGY

The sedimentary sequence within the Half Graben (Fig. 2) consists primarily of fine- to coarse-grained continental siliciclastics and to a lesser extent paralic or limnic shales, limestones, and evaporites and marine carbonates. The age ranges from Visean to Late Westphalian. The strata form an asymmetric syncline with beds generally dipping gently toward the centre where a maximum thickness of 2000 m is projected.

Unconformably overlying the basement on the southeast border is an intermixture of sedimentary breccia and conglomerate with coarse angular to subrounded clasts (92-140 m thick). These represent talus breccia and proximal alluvial fan deposits, respectively. Conformably overlying this sequence and locally interbedded with it is brown, massive, sparsely fossiliferous dolostone (<17 m). Its detailed paleoenvironment is not known, but it is considered to be of marine origin. Conformably overlying the dolostone is a sequence beginning with green and red siltstone (<4 m) at the base followed by interbedded shale, limestone, and gypsum (<78 m) with the gypsum grading upward with fine grained red sandstone and mudstone (<33 m). The sequence indicates that arid conditions in a limnic or paralic environment existed with gradual moderation of the climate followed by replacement of standing water deposition by fluvial sedimentation. A disconformity at the top of the fine grained siliciclastic-evaporitic sequence is represented by a caliche soil. Above this is a thick sequence of medium- to coarse-grained grey sandstone (>225 m) which shows a subtle transition upward into a red, finer grained unit (>335 m) with increased mudstone. This indicates a distal braided river system gradually changing upward to a meandering river system. At the top a coarse sandstone (>60 m) appears again, representing a return of braided river conditions. Overlying the sandstone and transitional with it, is interbedded red conglomerate, sandstone and mudstone (275-700 m) representing either a proximal braided river or a braidplain. At the top of the succession and transitional with the conglomerate unit beneath, is a fine grained green-grey sandstone and shale sequence (210-300 m). This represents a combination of fluvial and limnic or paralic sedimentation.

CONCLUSIONS

The Glengarry Half Graben appears to be a remnant of a much larger sedimentary basin. The limited paleocurrent data gathered suggest that there was a northeasterly oriented trunk stream in the basin throughout much of its development. Comparison of stratigraphic and sedimentological patterns with the Loch Lomond Basin indicates a strong correlation between the two. The Glengarry Half Graben strata appear to represent progressive onlap of stratigraphic units, similar to the Loch Lomond Basin.

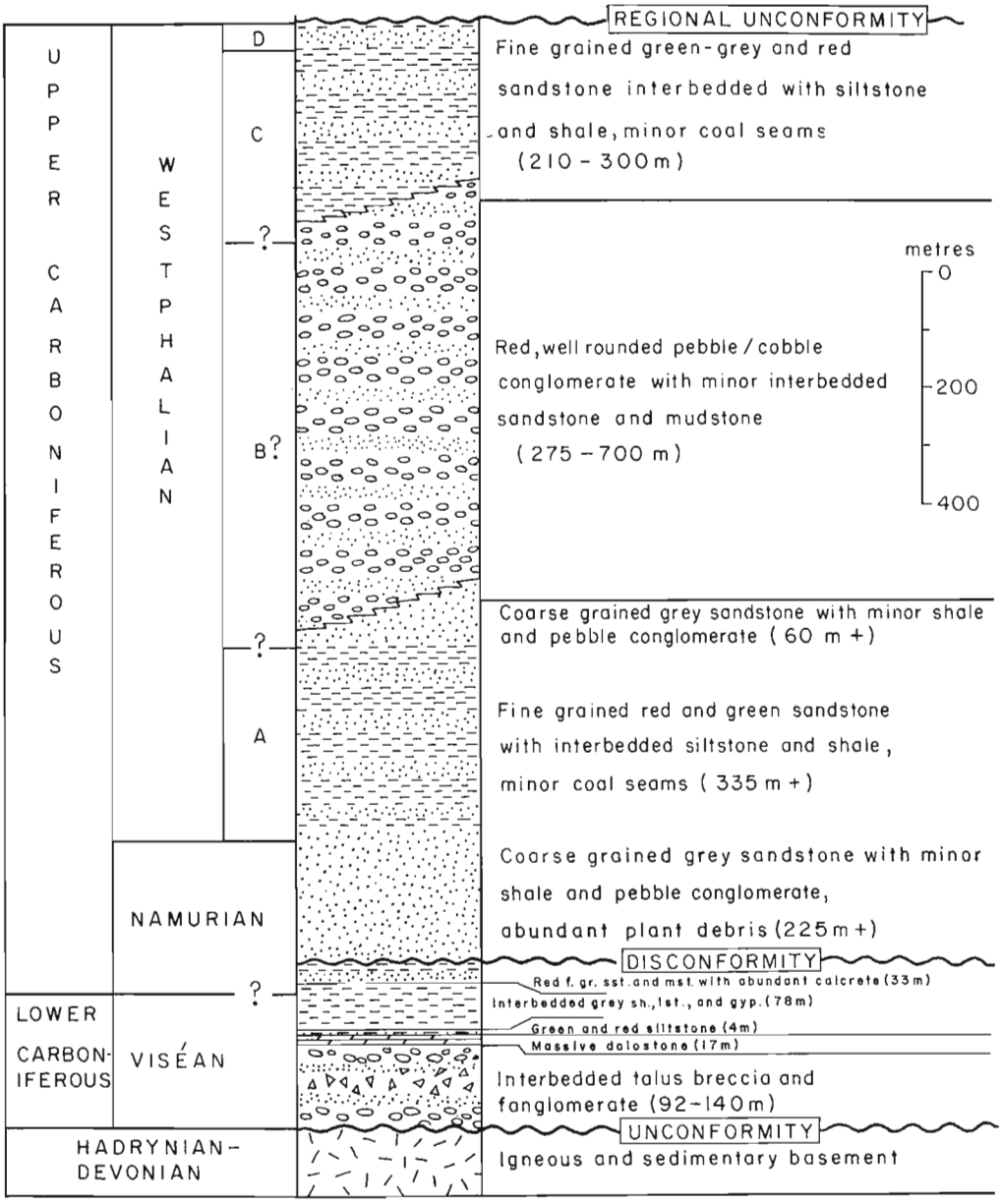

Figure 2

General stratigraphy of the Glengarry Half Graben.

REFERENCES

Boehner, R.C.

1981: Preliminary report on the geology and mineral deposits of the Loch Lomond Basin, Cape Breton Island; in Mineral Resources Division, Report of Activities, 1980, Nova Scotia Department of Mines and Energy, Report 81-1, p. 153-165.

1983: Loch Lomond Basin, Cape Breton Island, Windsor Group Project – An update; in Mines and Minerals Branch Report of Activities, Nova Scotia Department of Mines and Energy, 1982, Report 83-1, p. 97-107.

Bonham, O.J.H., Doucet, N., Johnson, F., and Staff of Nova Scotia Department of Mines and Energy

1982: The Yava lead deposit, Salmon River, Cape Breton, Exploration (1962-1981) and Mining Activities (1979-1981); Nova Scotia Department of Mines and Energy, Open File Report 529, 55 p.

Keppie, D.

1982: Tectonic map of the Province of Nova Scotia; Nova Scotia Department of Mines and Energy, Halifax, Nova Scotia.

Scott, P.

1978: Geochemistry and petrography of the Salmon River lead deposit, Cape Breton Island, Nova Scotia; unpublished MSc. thesis, Acadia University, Wolfville, Nova Scotia, 11 p.

Weeks, L.J.

1954: Southeast Cape Breton Island, Nova Scotia; Geological Survey of Canada, Memoir 277, 112 p.

Erratum

Geological Survey of Canada, Paper 83-1B

Current Research, Part B

Report 29: Structure cross-sections across Asiak Foreland Thrust and Fold Belt, Wopmay Orogen, District of Mackenzie: R. Tirrul, p. 253.

The correct Figure 29.1 is reproduced below:

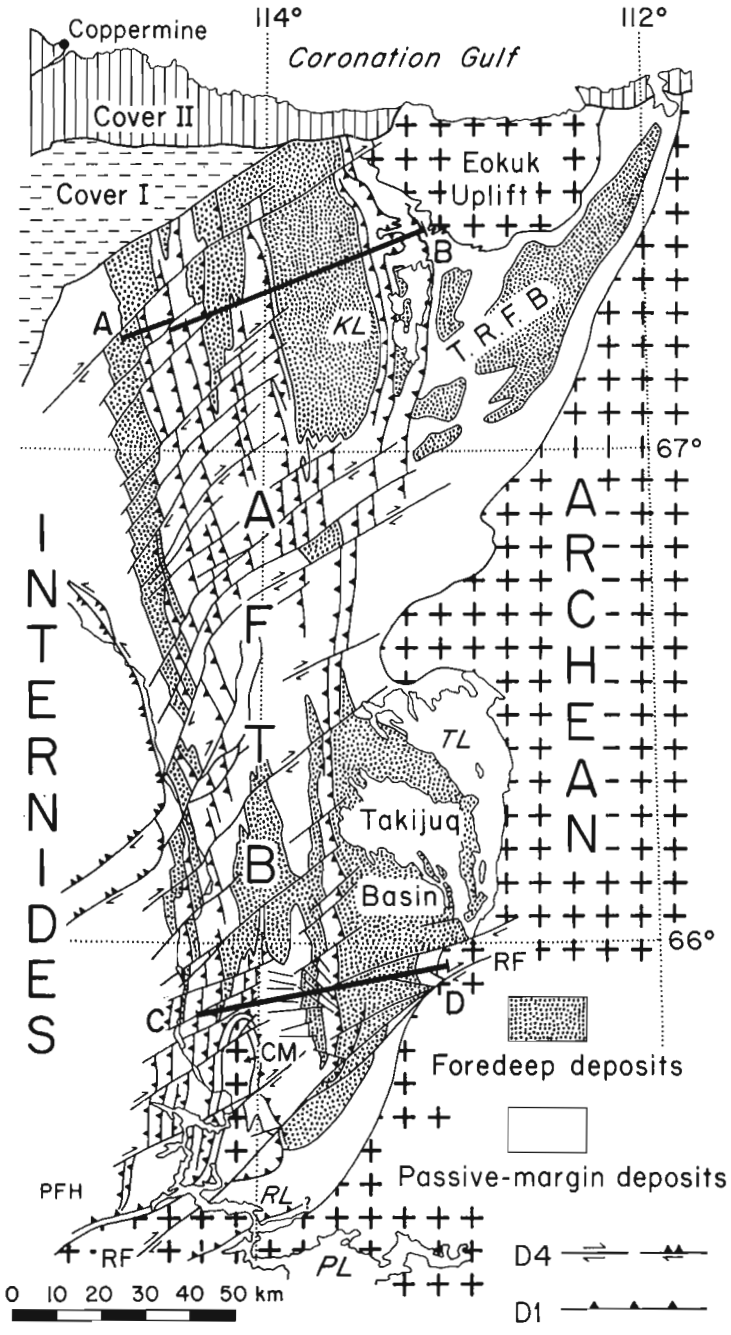

Figure 29.1. *The externides of Wopmay Orogen, showing the location of cross-sections in Figure 29.2.*

Author Index